ZOOLOGICAL SCIENCE

An International Journal

VOLUME 10
1993

published by

The Zoological Society of Japan

ZOOLOGICAL SCIENCE

An International Journal

VOLUME 10
1993

published by
The Zoological Society of Japan

CONTENTS OF VOLUME 10

NUMBER 1, FEBRUARY 1993

NUMBER 2, APRIL 1993

REVIEWS

ORIGINAL PAPERS

Physiology

Biochemistry

Developmental Biology

NUMBER 3, JUNE 1993

NUMBER 4, AUGUST 1993

NUMBER 5, OCTOBER 1993

REVIEWS

ORIGINAL PAPERS

Physiology

Genetics

Immunology

NUMBER 6, DECEMBER 1993

Development
Growth & Differentiation

Published Bimonthly by the Japanese Society of Developmental Biologists
Distributed by Business Center for Academic Societies Japan, Academic Press, Inc.

Development, Growth and Differentiation (ISSN 0012–1592) is published bimonthly by The Japanese Society of Developmental Biologists. Annual subscription for Vol. 35 1993 U. S. $ 191,00, U. S. and Canada; U. S. $ 211,00, all other countries except Japan. All prices include postage, handling and air speed delivery except Japan. Second class postage paid at Jamaica, N.Y. 11431, U. S. A.

Outside Japan: Send subscription orders and notices of change of address to Academic Press, Inc., Journal Subscription Fulfillment Department, 6277, Sea Harbor Drive, Orlando, FL 32887–4900, U. S. A. Send notices of change of address at least 6–8 weeks in advance. Please include both old and new addresses. U. S. A. POSTMASTER: Send changes of address to *Development, Growth and Differentiation*, Academic Press. Inc., Journal Subscription Fulfillment Department, 6277, Sea Harbor Drive, Orlando, FL 32887–4900, U. S. A.

In Japan: Send nonmember subscription orders and notices of change of address to Business Center for Academic Societies Japan, 16–9, Honkomagome 5-chome, Bunkyo-ku, Tokyo 113, Japan. Send inquiries about membership to Business Center for Academic Societies Japan, 16–9, Honkomagome 5-chome, Bunkyo-ku, Tokyo 113, Japan.

Air freight and mailing in the U. S. A. by Publications Expediting, Inc., 200 Meacham Avenue, Elmont, NY 11003, U. S. A.

BRANCHES NOW OPEN IN USA AND EUROPE

Narishige.
The complete range for micromanipulation


MF-83 Patch Clamp Forge

For over 30 years Narishige have been developing their extensive range of precision instruments for Physiology, Pharmacology, Zoology and Psychology research.

This large range includes micromanipulators, microelectrode pullers and microforges, microinjectors, microgrinders and stereotaxic instruments.

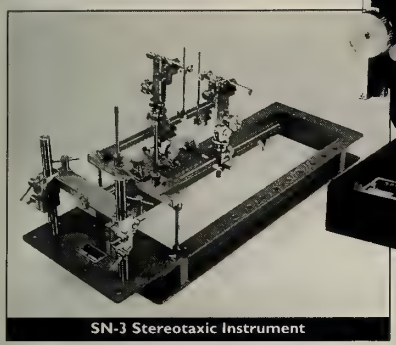
SN-3 Stereotaxic Instrument

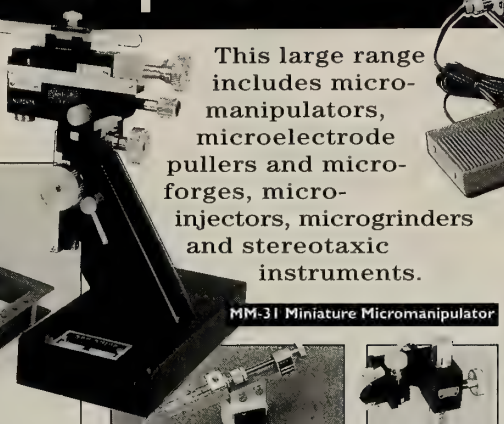
MM-31 Miniature Micromanipulator

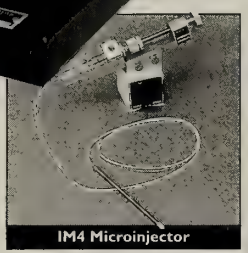
IM4 Microinjector


US-1 Miniature Stand

Shown here is a small selection of instruments from the extensive Narishige range.


Remote Control Hydraulic Micromanipulator

Narishige are pleased to announce that repair facilities have been opened in Europe and the USA.

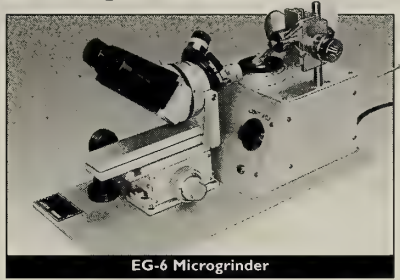
EG-6 Microgrinder

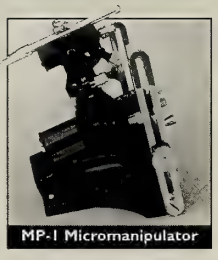
MP-1 Micromanipulator

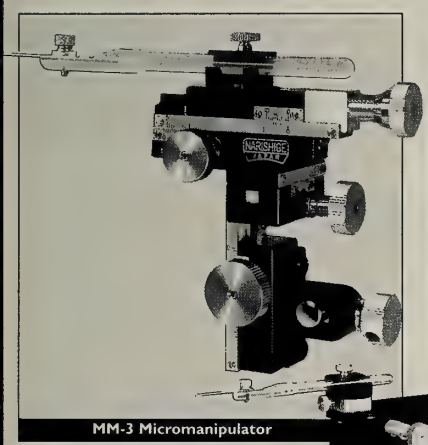
MM-3 Micromanipulator

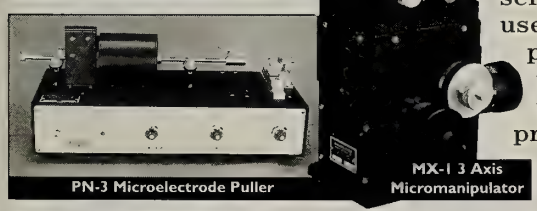
PN-3 Microelectrode Puller

MX-1 3 Axis Micromanipulator

This enables us to provide an improved service to the many users of our quality products throughout the world, including the upgrading of previous types of water filled hydraulic micromanipulators.

PE-2 Microelectrode Puller

Please contact us for more information.

REPAIRS, AFTER SALES SERVICE AND TECHNICAL SUPPORT

JAPAN **Narishige Scientific Instrument Laboratory**
9-28 Kasuya 4-Chrome, Setagaya-Ku, Tokyo 157, Japan. Tel: +81 (0) 3 3308 8233 Fax: +81 (0) 3 3308 2005

EUROPE **Narishige International London Branch**
Unit 7 Willow Business Park, Willow Way, London SE26 4QP U.K. Tel: +44 (0) 81 699 9696 Fax: +44 (0) 81 291 9678

U.S.A. **U.S. Narishige International Inc**
404 Glen Cove Avenue, Sea Cliff, New York 11579 U.S.A. Tel: +1 (516) 759 6167 Fax: +1 (516) 759 6138

NARISHIGE JAPAN

Vol. 10 No. 1 February 1993

ZOOLOGICAL SCIENCE

An International Journal

PHYSIOLOGY
CELL and MOLECULAR BIOLOGY
GENETICS
IMMUNOLOGY
BIOCHEMISTRY
DEVELOPMENTAL BIOLOGY
REPRODUCTIVE BIOLOGY
ENDOCRINOLOGY
BEHAVIOR BIOLOGY
ENVIRONMENTAL BIOLOGY and ECOLOGY
SYSTEMATICS and TAXONOMY

published by Zoological Society of Japan

distributed by Business Center for Academic Societies Japan
VSP, Zeist, The Netherlands

ISSN 0289-0003

ZOOLOGICAL SCIENCE

The Official Journal of the Zoological Society of Japan

The Zoological Society of Japan:
Toshin-building, Hongo 2–27–2, Bunkyo-ku,
Tokyo 113, Japan. Phone (03) 3814–5675
Officers:
President: Hideo Mohri (Chiba)
Secretary: Hideo Namiki (Tokyo)
Treasurer: Makoto Okuno (Tokyo)
Librarian: Masatsune Takeda (Tokyo)

ZOOLOGICAL SCIENCE is devoted to publication of original articles, reviews and communications in the broad field of Zoology. The journal appears bimonthly. An annual volume consists of six numbers of more than 1200 pages including an issue containing abstracts of papers presented at the annual meeting of the Zoological Society of Japan.

MANUSCRIPTS OFFERED FOR CONSIDERATION AND CORRESPONDENCE CONCERNING EDITORIAL MATTERS should be sent to:

Dr. Tsuneo Yamaguchi, Managing Editor, Zoological Science, Department of Biology, Faculty of Science, Okayama University, Okayama 700, Japan, in accordance with the instructions to authors which appear in the first issue of each volume. Copies of instructions to authors will be sent upon request.

SUBSCRIPTIONS. ZOOLOGICAL SCIENCE is distributed free of charge to the members, both domestic and foreign, of the Zoological Society of Japan. To non-member subscribers within Japan, it is distributed by Business Center for Academic Societies Japan, 5–16–9 Honkogagome, Bunkyo-ku, Tokyo 113. Subscriptions outside Japan should be ordered from the sole agent, VSP, Godfried van Seystlaan 47, 3703 BR Zeist (postal address: P. O. Box 346, 3700 AH Zeist), The Netherlands. Subscription rates will be provided on request to these agents. New subscriptions and renewals begin with the first issue of the current volume.

[Publication of Zoological Science has been supported in part by a Grant-in-Aid for Publication of Scientific Research Results from the Ministry of Education, Science and Culture, Japan.]

ZOOLOGICAL SCIENCE 10: 1–11 (1993)

REVIEW

Adaptation Physiology: the Functioning of Pituitary Melanotrope Cells during Background Adaptation of the Amphibian *Xenopus laevis*

Bruce G. Jenks, Hans J. Leenders, Gerard J. M. Martens and Eric W. Roubos

Department of Animal Physiology, University of Nijmegen, Toernooiveld, 6525 ED Nijmegen, The Netherlands

INTRODUCTION

The vertebrate hypothalamo-hypophyseal system is responsible for converting neuronal information into an endocrine output, the release of hormones into the blood. This process is known as neuroendocrine integration. A major source of neural input to the neuroendocrine system comes from sensory information concerning conditions in the environment (e.g. light, temperature, presence of stressors). Neuroendocrine transducer cells of the hypothalamo-hypophyseal system are responsible for integrating the diverse neuronal information to produce and release endocrine signals. These signals in turn coorrdinate the functioning of peripheral organs (e.g. reproductive organs, adrenal glands, thyroid gland) thus allowing the animal to adapt to changes in the environment.

An example of such a neuroendocrine transducer cell is the melanotrope cell of the pituitary pars intermedia. In amphibians this cell is responsible for converting neuronal information concerning color of background into an endocrine output. The cell produces the multifunctional precursor protein proopiomelanocortin (POMC), which is processed to give a number of peptides including melanophore-stimulating hormone (α-MSH). This peptide hormone stimulates the dispersion of the black pigment melanin in dermal melanophores thus causing skin darkening. The hormone is released in animals on a black background. Among amphibians, the South African clawed toad *Xenopus laevis* shows a particularly strong adaptive response to background color. The skin pigment goes very rapidly from the fully aggregated to the fully dispersed state in animals transferred from a white to a black background, and rapidly aggregates upon transfer from black to white background (Fig. 1). The adaptation of *Xenopus* to a black background involves activation of biosynthetic and secretory processes in the melanotrope cells, whereas these processes inactivate during white-background adaptation [17, 22, 32, 65]. Therefore, by simply changing background color, it is possible to manipulate the activity of *Xenopus* melanotrope cells. This ease of manipulation is an attractive feature of these cells for studies aimed at elucidating cellular and molecular mechanisms of cell activation and inactivation. Indeed, *Xenopus* melanotrope cells have been the object of study in a number of laboratories over many years, starting with classic studies of Hogben and Slome (reviewed in [64]). This model system and related topics were extensively reviewed several years ago [23, 31, 39, 60]. The intention of this survey is to examine recent developments in the analysis of *Xenopus* intermediate lobe melanotrope cells, particularly in relation to the physiological functioning of these

Received August 24, 1992

cells.

Dynamics of Background Adaptation: the Demonstration of Short-term and Long-term Adaptive Mechanisms

It has generally been thought that α-MSH is the only factor involved in stimulating pigment dispersion in dermal melanophores of *Xenopus* during black background adaptation. An analysis of events during white to black background transfer, however, has shown that there is a major discrepancy between the degree of pigment dispersion in dermal melanophores and plasma α-MSH levels [67]. The pigment becomes fully dispersed within a few hours of transfer to black background and yet it takes several days for plasma α-MSH to reach its maximum level (see Fig. 1). These results suggested that a factor other than α-MSH must be responsible for the rapid pigment dispersion seen during the early stage of black background adaptation. The discovery that the rapid pigment dispersion can be blocked by the β-adrenergic receptor antagonist propranolol indicates that a β-adrenergic receptor is involved [67]. *In vitro* experiments show that this receptor is working at the level of the dermal melanophore cells in causing pigment dispersion. Denervated skin explants lack the rapid short-term response, which indicates that the short-term mechanism depends on innervation of the skin. Probably, this innervation is a component of the autonomic nervous system releasing (nor)adrenalin in the vicinity of the melanophores [24]. In long-term-adapted animals (several days or longer on black background) the release of α-MSH from the pars intermedia is critical for maintaining pigment dispersion. This is shown by the fact that neurotransmitters such as

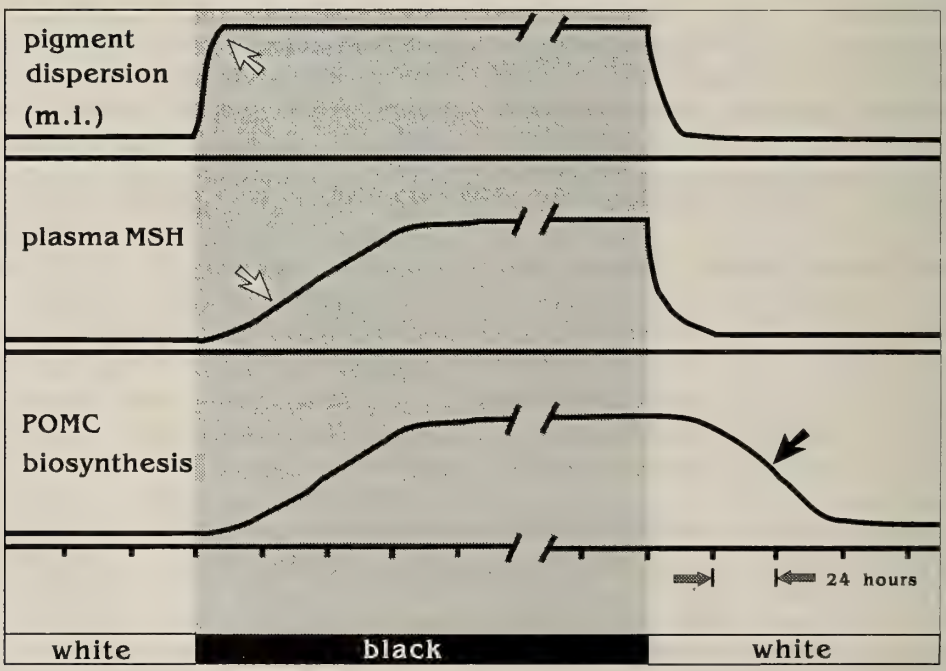

Fig. 1. A summary of the dynamics of various aspects of background adaptation by the amphibian *Xenopus laevis*. Changes in the degree of pigment dispersion in dermal melanophores, in plasma MSH levels and in the level of POMC biosynthesis in pars intermedia melanotrope cells are shown. The discrepancy between the rapid pigment dispersion and slow increase in plasma α-MSH (indicated by white arrows) led to studies that established the involvement of a β-adrenergic mechanism causing pigment dispersion during the early stages of black background adaptation [67]. The relatively slow decrease in POMC biosynthesis (black arrow) in black to white background adaptations is, in part, probably due to the fact that an enzymatic system for the degradation of RNA must first be synthesized [4]. See text for further discussion.

dopamine and GABA, which are known to inhibit *in vitro* release of α-MSH, cause skin whitening when injected into fully black-background-adapted animals [61, 63]. Treatment of long-term black-adapted animals with propranolol has no effect on pigment dispersion, which is in sharp contrast to the effect of this β-blocker in short-term black-adapted animals [67]. The importance of α-MSH in long-term regulation of the melanophores is further illustrated by an analysis of plasma α-MSH levels in animals adapted for several weeks to white, light grey, dark grey and black backgrounds [52, 66]. Grey animals, which have only partially dispersed pigment in dermal melanophores, were found to have plasma α-MSH levels that are intermediate between the low levels found in white-adapted animals and the high levels of black-adapted animals.

Physiological Significance of Short-term and Long-term Mechanisms

It is generally accepted that in most amphibians pigment cells are regulated primarily by the endocrine system (α-MSH) while in fishes the nervous system is a more important regulatory system. This seems to fit the locomotory behavior of these animals as amphibians tend to be more stationary than fish and thus may not need rapid color adaptation. The presence of β-adrenergic receptors on amphibian melanophores, and thus the potential for nervous control of these cells, was established in early studies [14, 15, 30] but the physiological significance of these receptors remained obscure. The idea has been forwarded that the β-adrenergic receptor might be activated as a result of acute handling stress, thus causing transitory darkening, termed "excitement darkening" [6]. It is apparent that, in the species *X. laevis* at least, this receptor is also involved in the regulation of pigment migration during adaptation to a dark background.

In considering the significance of the β-adrenergic regulatory mechanism in *Xenopus* it is important to realize that the capacity of melanotrope cells to synthesize α-MSH is acquired only very slowly, taking a number of days to reach maximum level during adaptation to black background [22, 32, 34, 44]. Hormone stores possessed by animals on white background are, however, depleted within 24 hr during adaptation to black background [22, 62]. For *Xenopus,* the regulation of dermal melanophores must be viewed as a cooperative effort; the β-adrenergic mechanism plays an important role in the short-term, during which time the melanotrope cells of the neuroendocrine system acquire the capacity to produce enough α-MSH to maintain pigment dispersion in the long-term. This cooperation ensures that *Xenopus* is capable of both rapid and sustained pigment dispersion.

Melanotrope Cell Morphology: the Demonstration of Cell Recruitment during Background Adaptations

There have been several studies on the morphology and ultrastructure of melanotrope cells of white- and black-background-adapted *Xenopus* [17, 21, 65]. These studies have shown that cells of white animals are small and inactive when compared to those of black animals. A question that remained was how melanotrope cells meet an intermediate (submaximal) demand for α-MSH, such as in animals on grey background. Two possible physiological mechanisms are: (1) all melanotropes are activated to an intermediate level of secretion to meet the submaximal demand for hormone, or (2) a subpopulation of melanotrope cells becomes fully acitvated to meet this demand, whereas the other cells remain relatively inactive. In the first case, the melanotrope cells act as a homogeneous population whereas in the latter situation they are heterogeneous. The results of an analysis at the light and electron microscopic level showed that the pars intermedia of grey-adapted animals is composed of a mixture of inactive and fully active melanotrope cells [52]. It was therefore concluded that melanotrope cells respond as a heterogeneous cell population to an increased demand for α-MSH, with progressively more cells being recruited to the active state as the physiological demand for α-MSH increases.

Physiological Significance of Recruitment

Two general strategies may be used by endocrine cells to increase the rate of hormone release.

One is a simultaneous activation of the entire population of endocrine cells, the activation of oxytocin-producing neuroendocrine cells being a good example [49]. Here, the strength of stimulation (suckling) determines the degree of activation achieved in the homogeneous cell population. It appears that the heterogeneous response, exemplified by the intermediate lobe melanotrope cells of *Xenopus,* is the more general phenomenon among endocrine cells. Morphometric and biochemical evidence has been given that this mechanism holds for hormone secretion by gonadotropes [47, 48], lactotropes [35], pancreatic β-cells [54] and follicular thyroid cells [11]. There may be an energetic advantage of this mechanism because an increased demand for hormone is met through activation of relatively few endocrine cells.

It appears from studies on mammalian lactotrope and somatotrope cells that the mechanism regulating cell recruitment involves differences in the sensitivity for regulatory factors among the individual endocrine cells. This has been discovered through an analysis of the effects of secretagogues on hormone release from individual cells, measured using the reverse-plaque assay [35, 47, 48] and, more recently, the sequential cell immunoblot assay [1, 26]. Using a modification of this latter assay it has been shown that *Xenopus* melanotropes display different sensitivities to dopamine, one of the α-MSH release-inhibiting factors [50].

Ultrastructure of Intermediate Lobe Nerve Terminals: Coexistence of Dopamine, GABA and Neuropeptide Y

The intermediate lobe melanotrope cells of *X. laevis* are regulated by multiple factors, both stimulatory and inhibitory (see Fig. 2). It had been assumed that each regulatory factor would be present in separate neuronal networks [23]. Analysis at the ultrastructural level, however, has revealed that GABA and NPY are present within

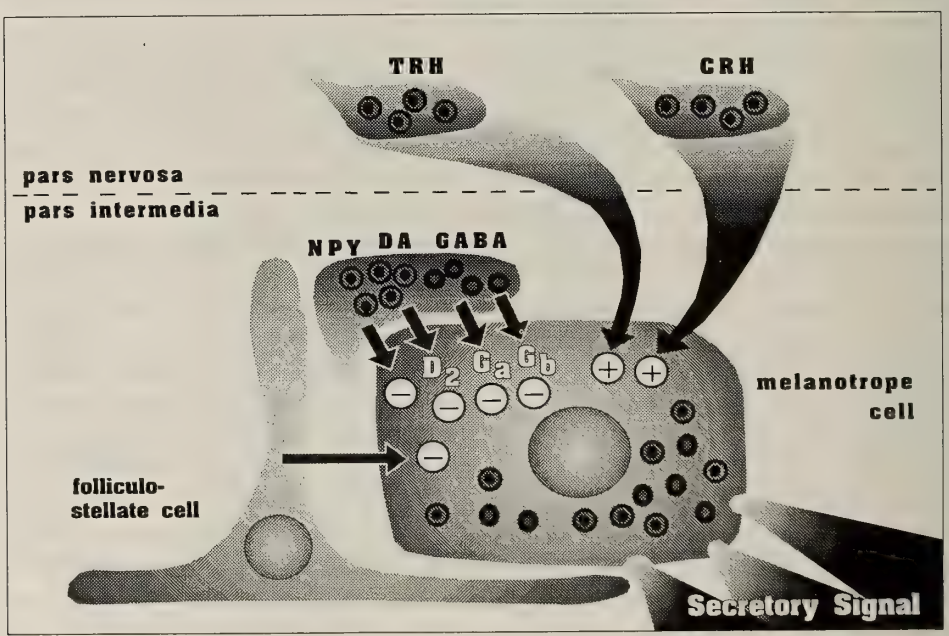

Fig. 2. A summary of the classical neurotransmitters and neuropeptides involved in the regulation of α-MSH secretion from the melanotrope cell of *Xenopus laevis*. Abbreviations: TRH, thyrotropin releasing hormone; CRH, corticotropin releasing hormone; NPY, neuropeptide Y; DA, dopamine; GABA, γ-aminobutyric acid; D_2, dopamine D_2 receptor; G_a, $GABA_a$ receptor; G_b, $GABA_b$ receptor. Stimulatory (+) or inhibitory (−) action on the secretory process is indicated. NPY, DA and GABA coexist in the same nerve terminals [51, 59] with NPY and DA being present within the same secretory vesicle [59].

the same nerve terminals within the intermediate lobe [51]; a recent study showed that these same varicosities also contain dopamine [59]. GABA is confined to small electron-lucent vesicles whereas dopamine and NPY are found in electron-dense vesicles. The varicosities have been shown to make close contact with both the melanotrope cells and the other major cell type of the pars intermedia, the so-called folliculo-stellate cells.

Physiological Significance of Coexistence

At present it is difficult to attribute a functional significance to the fact that the three α-MSH release inhibitory factors occur in the same nerve terminals. In another case of coexistence, that of acetylcholine and vasoactive intestinal peptide (VIP) in autonomic nerve terminals of the cat salivary gland, it has been shown that the transmitter substances involved can be differentially released [36]. Low frequency stimulation leads to release of acetylcholine alone while with high frequency stimulation both the neurotransmitter and the neuropeptide are released. Moreover, it has been shown that VIP potentiates the stimulatory action of acetylcholine on the salivary gland [36]. Concerning the *Xenopus* pars intermedia, the possibility of differential release of the coexisting inhibitory factors has yet to be examined. An analysis of the effect of combinations of these factors on secretion of α-MSH showed only additive effects [27], thus ruling out interactions leading to potentiation. Nonetheless, there is some evidence for differential action of these regulatory factors; inhibitions induced by GABA and dopamine are rapidly reversed when treatment with the factor is terminated whereas recovery from NPY-induced inhibition is achieved only very slowly [28]. Altogether these results suggest that dopamine and GABA are appropriate short-term inhibitors while NPY might be used for long-term inhibition of the melanotrope cell.

The Folliculo-Stellate Cell has an Inhibitory Action on the Release of α-MSH from the Melanotrope Cell

Folliculo-stellate cells are glial-like cells structurally related to the astrocytes of the central nervous system. They are evenly distributed throughout the pars intermedia and constitute about 5% of the cell content of the lobe. These cells possess long extensions that make intimate contacts with virtually every melanotrope cell [53, 56]. The inhibitory action of folliculo-stellate cells on the secretory process of melanotropes was demonstrated in studies with 7-day cultured neurointermediate lobes of *Xenopus* [28]. The cultured tissue is devoid of neuronal influences due to the degradation of nerve terminals, as demonstrated ultrastructurally and confirmed by immunocytochemical analysis showing a complete lack of dopamine, GABA and NPY. Giving such tissue a depolarizing pulse of K^+ in superfusion gives rise to a biphasic response with respect to the secretion of α-MSH. The short duration stimulatory phase could be attributed to a direct K^+-evoked depolarization of the melanotrope cell. The subsequent inhibitory phase, however, can only be attributed to K^+-induced activation of an inhibitory mechanism emanating from another cell type within the cultured lobes. Ultrastructural analyses show that in such tissue the folliculo-stellate cell remains viable and it was therefore concluded that this cell type must be the source of the K^+-induced inhibition. The mechanism of action of the folliculo-stellate cell on the melanotrope cells has still to be established. The stellate cell could release an α-MSH release inhibiting factor. Alternatively, it could inhibit the secretory activity of the melanotrope cells by inducing changes in the extracellular ionic environment of the melanotropes. Precedent for the first option can be found in the literature. Folliculo-stellate cells of the mammalian pars distalis have been reported to produce and secrete paracrine factors that regulate secretory activity of endocrine cells in this organ [5, 12, 13]. In support of the second option is the observation that bovine intermediate lobe folliculo-stellate cells are involved in ion transport [10]. Further, a high level of staining indicative of Na^+/K^+-ATPase activity has been observed between melanotropes and folliculo-stellate cells of the frog pars intermedia [56]. It was suggested that this activity might reflect stellate cell regulation of the extracellular ionic environment of the melanotropes.

Physiological Significance of the Inhibition by Folliculo-Stellate Cells

In view of the structural relationship between folliculo-stellate cells and the melanotropes, activation of an inhibitory mechanism via the folliculo-stellate cell would be expected to affect a number of melanotrope cells simultaneously. Possibly, this indirect mechanism of inhibition is used when a general inhibition of the pars intermedia is required, as opposed to the recruitment mode of regulation where cells are individually activated or inactivated. The question arises as to how the inhibitory mechanism emanating from the folliculo-stellate cell is itself activated and inactivated. While we initially thought that NPY might be of importance in this respect [28], subsequent analyses have shown that NPY can act directly on the melanotrope cell to inhibit α-MSH release. Further research will be required to fully understand the role of the folliculo-stellate cell in the regulation of the secretory process.

Analysis of Secretion: the Demonstration of Fast and Slow Secretory Pathways

The biosynthetic and secretory activity of melanotrope cells of *Xenopus* can be set to a very high level simply by placing the animal for several days on black background. This fact allows the use of *in vitro* pulse-chase labelling methods to follow the biosynthetic and secretory process of *Xenopus* melanotropes. A number of studies have been devoted to an analysis of the release of radiolabelled peptides [27, 33, 43, 57]. In a pulse-chase labelling experiment with *Xenopus* neurointermediate lobes, conducted in combination with tissue superfusion methods to analyze the dynamics of the secretory process, it was shown that there are two phases in the release of radiolabelled products [43]. The first phase comprises a rapid increase (reaching a maximum 3 hr after the pulse) followed by a rapid decrease; the second phase is a low basal secretion that persists for many hours of superfusion. In a subsequent analysis, using dual-labelling protocols to follow simultaneously the release associated with both phases, it was concluded that each phase reflects the functioning of a distinct pathway of secretion [68]. The first, termed the *fast pathway,* concerns peptides that are released within 6 hr of their biosynthesis. The second pathway, designated the *slow pathway,* pertains to peptides remaining in the melanotrope cells for up to 2 days before being released. It was shown that in the presence of dopamine the secretory peptides of the *fast pathway* are shunted to the *slow pathway* and are subsequently released from this latter pathway when the dopamine treatment is terminated.

At present, it is not possible to say whether the two secretory pathways of *Xenopus* melanotrope cells occur in one cell type or, alternatively, reflect the functioning of two different cell types within the tissue. There is morphological evidence for both possibilities. In support of the one cell-type explanation is the observation that there are two types of secretory granules in *Xenopus* melanotropes, electron-dense granules and somewhat larger, fibrous, electron-lucent granules [17]. In the biosynthetically active melanotrope cells of black-adapted animals the dense granules dominate but there also are, within these cells, lucent granules; in the inactive cells of white-adapted animals the granules are almost exclusively of the lucent type. Morphological indication that the pathways might reflect the activity of two cell types is provided by the observation that the melanotrope cell population of the pars intermedia of black-adapted animals is heterogeneous; the tissue possesses both active and inactive malonatrope cells [52].

Physiological Significance of Two Secretory Pathways

The existence of multiple secretory pathways in endocrine cells seems to be a general phenomenon, although the physiological significance of these pathways is unknown. Multiple pathways have been reported for cells producing thyrotropin [25], prolactin [7, 45], somatotropin [7, 8, 58] and parathyroid hormone [16]. An important criterion for attributing physiological significance to such pathways is to establish that they are independently regulated. This would appear to be the case for the pathways in prolactin cells [9] and parathyroid hormone producing cells [16, 46]. In both cases the pathways concern newly synthesized hormone

versus hormone sequestered in mature secretory compartments. For the prolactin cell the mature pathway is cyclic-AMP-dependent while release of newly synthesized hormone is independent of the cyclic nucleotide. A similar situation might exist for *Xenopus* melanotrope cells; the *slow pathway* appears to be more sensitive to stimulation by 8-bromo-cyclic-AMP than the *fast pathway* [68]. Interestingly, in mouse melanotrope cells 8-bromo-cyclic-AMP gives clear differential effects, the cyclic nucleotide analogue being more effective in stimulating mature peptides than newly synthesized peptides [29].

In considering the physiological significance of independently regulated secretory pathways it is worthwhile to focus on cells that produce multifunctional precurgor proteins such as POMC. The existence of independently regulated pathways in POMC-producing cells might endow the cells with the ability to manipulate the peptide composition, and thus the physiological effect(s) of their secretory signal. In this way the cell itself could be multifunctional, responding with different sets of peptides to different physiological demands. Studies with the melanotrope cell of *X. laevis* may help to establish the full potential of POMC-producing cells to participate in multiple regulatory processes.

Analysis of POMC Gene Expression: Regulation is at the Level of both Gene Transcription and mRNA Stability

POMC gene expression in the pars intermedia is 20 to 30 times higher in animals adapted to a black background than in animals adapted to a white background. Using a steady-state kinetic model for mRNA degradation, the half-life of POMC mRNA in *Xenopus* melanotrope cells was determined during the process of background adaptation [4]. During induction of the POMC gene (i.e. following white to black background transfer) the half-life of POMC mRNA was found to be 3- to 4-fold longer than during de-induction of the gene (transfer from a black to a white background). This difference in the stability of POMC mRNA is not sufficient to account for the 20- to 30-fold differences in the steady-state levels of POMC mRNA in fully black- *versus* fully white-adapated animals. Therefore, it seems that background adaptation involves not only changes in the stability of POMC mRNA but also changes in the transcriptional activity of the POMC gene.

Physiological Significance of Dual Control Sites in the Regulation of POMC Gene Expression

The stabilization of POMC mRNA in animals on a black background would seem physiologically relevant. This mechanism will help maintain a high level of POMC mRNA under this environmental condition, and thus would add to the efficiency of the POMC expression system. Likewise, the decreased stability of POMC mRNA in animals transferred from a black to a white background seems a physiologically appropriate response to the new environmental situation. The shutting down of the POMC expression system, viewed at the level of POMC biosynthesis, is a slow process (see Fig. 1). Part of the reason for this may be that in the animals adapting to a white background RNA degrading enzymes must first be synthesized. This is indicated by the fact that treatment of animals with mRNA synthesis inhibitors block the degradation of POMC mRNA observed after black to white background transfers [4].

Analysis using Differential Hybridization: a Battery of Genes is Coexpressed with the POMC Gene

Proper functioning of a peptide-secreting cell requires not only production of precursor proteins for secretory peptides but also expression of genes associated with the secretory function. Such genes include those encoding for precursor-processing enzymes and for structural and regulatory proteins involved in the translocation, sorting, packaging and release of secretory products. To identify genes coexpressed with the POMC gene in *Xenopus* melanotrope cells advantage has been taken of the fact that the transcriptional process is very active in cells of black-adapted animals but inactive in white-adapted animals. The method used, termed differential hybridization, involved screening of a *Xenopus* pituitary cDNA library using single-stranded cDNA probes synthesized from

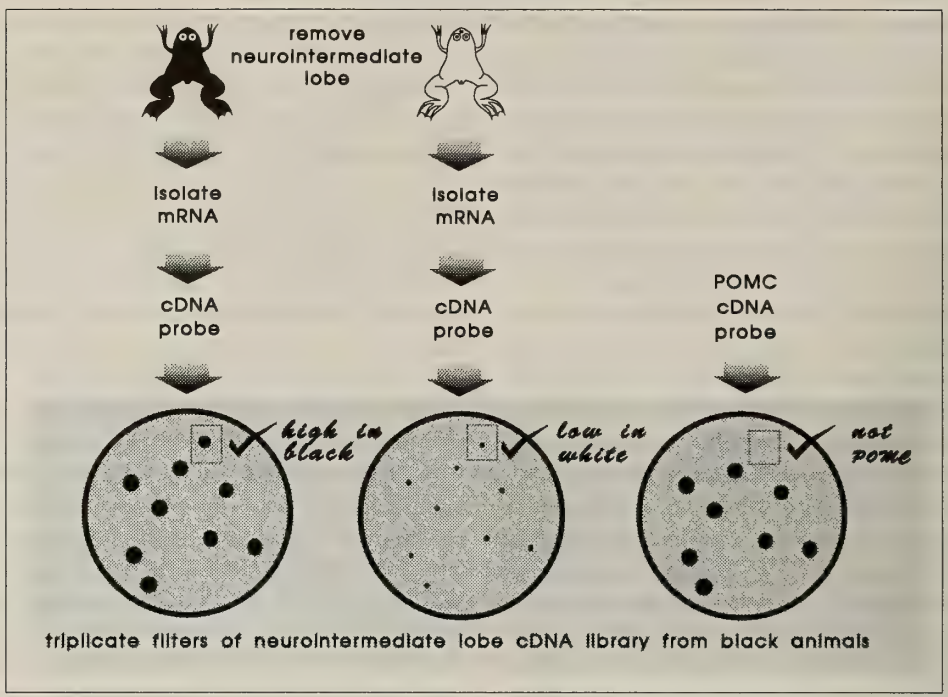

Fig. 3. An overview of the differential screening approach being used to find genes important to the transducer function of the melanotrope cell of *Xenopus laevis*. The approach is based on the premiss that non-POMC genes that are more highly expressed in black- than in white-adapted animals would be important in supporting the regulated secretory pathway leading to the release of POMC-derived peptides.

RNA of biosynthetically active and inactive melanotropes, i.e. from black and white animals, respectively (Fig. 3). Screening approximately 20,000 colonies of the library resulted in the identification of 130 differentially hybridized clones [41]. Of these, 92% were found to be related to POMC mRNA and discarded from further analysis. The 10 remaining clones presumably code for proteins essential for the secretory activity of the *Xenopus* melanotrope cell. Thus far only one of these clones has been fully characterized. It has proved to be highly similar (97% identical) to a partially sequenced porcine and human pituitary protein named 7B2 [18, 55]. The *Xenopus* 7B2 cDNA clone was used to isolated a human pituitary cDNA clone encoding the entire structure of human 7B2 [40]. A comparison of the amino acid sequences of *Xenopus* and human 7B2 shows that the 7B2 protein, and in particular the N-terminal region, is remarkably well conserved during 350 million years of vertebrate evolution. The overall degree of amino acid sequence identity between *Xenopus* and human 7B2 is 83%, with most differences being conservative amino acid substitutions. This degree of conservation is much higher than that between the POMC proteins of these two species (55%) [42].

While POMC and 7B2 are clearly coexpressed, there are some differences in the nature of the expression of these proteins in *Xenopus* melanotrope cells. First, there are large differences in the steady-state levels of mRNA for the two proteins; in black-adapted animals the amount of mRNA coding for POMC in the pars intermedia is about 25-fold higher than that coding for 7B2 [41]. Moreover, the differences in steady-state levels of 7B2 and POMC mRNA between black- and white-adapted animals are about 8-fold and 25-fold, respectively [2]. From an analysis of the time course in the expression of the genes in animals transferred from a white to a black background it is evident that there are also important differences in

the dynamics of the expression of the two genes. The level of POMC mRNA was significantly increased within 16 hours of transfer whereas it took over 40 hours for significant increases in the level of 7B2 mRNA to be detected [2]. It will be interesting to investigate the molecular mechanism(s) underlying the differences in activity between the 7B2 and POMC genes. It could be that the POMC promotor contains elements that are responsible for the very high level of POMC gene expression in the intermediate lobe. Alternatively, it is possible that POMC mRNA contains sequences responsible for a long half-life in this tissue while 7B2 mRNA is less stable because it lacks such sequences.

Biosynthetic studies have revealed that 7B2 is a precursor protein in *Xenopus* [3]. During pulse incubations there was synthesis of a 25 kDa form of 7B2 which was converted, during subsequent chase incubations, to an 18 kDa protein. Chemical cleavage and peptide mapping have shown that processing takes place in the C-terminal region [3], a region that possesses three pairs of basic amino acid residues [40]. Such pairs often function as cleavage sites in the enzymatic processing of precursor proteins. *Xenopus* 7B2 is apparently sequestered in the regulated secretory pathway of the melanotrope cell and is possibly stored within the same granules as the POMC-derived peptides. This is shown by the observation that the 18 kDa form of the protein is released [3] and that this release can be inhibited or stimulated by factors established to inhibit or stimulate, respectively, the secretion of POMC-derived peptides from *Xenopus* melanotrope cells [2]. Therefore, 7B2 is not only coexpressed with POMC but it is also, at the level of secretion, coordinately regulated with POMC-derived peptides. The concept of coordinate regulation can be extended to the level of gene expression. Long-term treatment (3 days) of neurointermediate lobes with apomorphine (D_2 dopamine receptor agonist), GABA or NPY leads to decreases not only in the level of POMC mRNA but also to concomitant decreases in the level of mRNA coding for the 7B2 protein [2].

Physiological Significance of the Coexpressed 7B2 Protein

The function of the 7B2 protein is unknown. In mammalian tissues it has been shown to be present in cells containing secretory granules, such as neurons and endocrine cells [20, 38]. Ultrastructural studies show this protein to be stored within secretory granules [37, 38]. Therefore, it is conceivable that 7B2 has an important function in the secretory pathway of these cells, such as being a component of the exocytotic machinery or a sortase directing secretory proteins to the regulated pathway of secretion. The suggestion has been made that the 7B2 protein is a member of the granin (chromogranin-secretogranin) family [19]. On the other hand, the fact that 7B2-derived products are released makes an extracellular function, i.e. as an endocrine or paracrine factor, also a distinct possibility.

Concluding Remarks

The analysis of the pituitary melanotrope of *Xenopus* shows that this cell, in fulfilling its neuroendocrine integrative function, is extremely complex. The cell acts as a neuroendocrine interface under the control of multiple factors, some of which coexist within the same nerve terminals. The regulatory factors clearly have differential effects on the melanotrope cells, some of these factors stimulating the melanotrope cell secretory process (*viz.* the neuropeptides CRH and TRH) while others (dopamine, GABA, NPY) inhibit secretion (see Fig. 2). Even among the inhibitory factors there appears to be differential action. Dopamine and GABA give rise to rapid and reversible inhibition of secretion, and might thus be appropriate inhibitors for short-term adaptations. Physiological background adaptations have been shown to involve the activation or inactivation of individual melanotrope cells, depending on the demand for α-MSH. Because both dopamine and GABA are delivered to the melanotrope cells via synaptic communication, they could very well be involved in regulating the (de)recruitment of individual cells. NPY, in contrast, may have a more general effect on the pars intermedia. This

neuropeptide acts more slowly than dopamine and GABA in inducing inhibition and, once established, this inhibition is more sustained than that induced by the two classical neurotransmitters.

There are several challenging areas for future research. One area of interest concerns the physiological significance of the multiple secretory pathways of the amphibian melanotrope cell. A first step in examining this will be to determine the peptide content of the pathways. This will give insight into the potential biological activities associated with these secretory signals. Also of immediate interest will be studies on the effect of the various regulatory factors on the pathways, to determine if they are independently regulated. On the molecular front, further characterization of genes co-expressed with the POMC gene in the *Xenopus* melanotrope should ultimately reveal a host of gene products that are essential to the proper physiological functioning of this neuroendocrine transducer cell.

REFERENCES

1 Arita J, Kojima Y, Kimura F (1991) Endocrinology 128: 1887–1894

2 Ayoubi TAY, Jenks BG, Roubos EW, Martens GJM (1992) Endocrinology 130: 3560–3566

3 Ayoubi, TAY (1991) Regulation of proopiomelanocortin and 7B2 gene expression in the pituitary of *Xenopus laevis*. Thesis, University of Nijmegen, Nijmegen, The Netherlands, 89 pp

4 Ayoubi TAY, van Duijnhoven HLP, van de Ven WJM, Jenks BG, Roubos EW, Martens GJM (1990) J Biol Chem 265: 15644–15647

5 Baes M, Allaerts W, Denef C (1987) Endocrinology 120: 685–691

6 Burgers ACJ, Boschman TAC, van de Kamer JC (1953) Acta Endocrinol 14: 72–82

7 Chen TT, Kineman RD, Betts JG, Hill JB, Frawley LS (1989) Endocrinology 125: 1904–1909

8 Chun CC, Hoeffler JP, Frawley LS (1988) Life Sciences 42: 701–706

9 Dannies PS (1982) Biochem Pharmacol 31: 2845–2849

10 Ferrara N, Gospodarowicz D (1988) Biochem Biophys Res Commun 157: 1376–1382

11 Gerber H, Peter HJ, Bachmeier C, Kaempf J, Studer H (1987) Endocrinology 120: 91–96

12 Gospodarowicz D, Abraham JA, Schilling J (1989) Proc Nat Acad Sci (USA) 86: 7311–7315

13 Gospodarowicz D, Lau K (1989) Biochem Biophys Res Commun 165: 292–298

14 Graham JDP (1961) J Physiol (London) 158: 5P–6P

15 Hadley ME, Goldman JM (1970) Am J Physiol 219: 72–77

16 Hanley DA, Wellings PG (1985) Can J Physiol Pharamacol 63: 1139–1141

17 Hopkins CR (1970) Tissue Cell 2: 59–70

18 Hsi KL, Seidah NG, De Serres G, Chretién M (1982) FEBS Lett 147: 261–266

19 Huttner WB, Gerdes HH, Rosa P (1991) Trends Biochem Sci 16: 27–30

20 Iguchi H, Natori S, Nawata H, Kato K, Ibayashi H, Chan JSD Seidah ND, Chretién M (1987) J Neurochem 49: 1810–1814

21 Jenks BG, Martens GJM, van Helden HPM, van Overbeeke AP (1985) Biosynthesis and release of melanotropins and related peptides by the pars intermedia in *Xenopus laevis*. In "Current Trends in Comparative Endocrinology". Ed by B Lofts, WN Holmes, Hong Kong University Press, Hong Kong, pp 149–152

22 Jenks BG, van Overbeeke AP, McStay BF (1977) Can J Zool 55: 922–927

23 Jenks BG, Verburg-van Kemenade BML, Martens GJM (1988) Proopiomelanocortin in the amphibian pars intermedia: a neuroendocrine model system. In "The Melanotropic Peptides: Volume 1" Ed by ME Hadley, CRC Press, Boca Raton, Florida, pp 103–126

24 Jenks BG, van Zoest ID (1990) Melanotrope cell function in the neuroendocrine regulation of dermal melanophores. In "Biology and Physiology of Amphibians" Ed by W Hanke, Gustav Fischer Verlag, Stuttgart, pp 219–228

25 Keith LD, Tam B, Ikeba H, Opsahl Z, Greer MA (1986) Neuroendocrinology 43: 445–452

26 Kendall ME, Hymer WC (1987) Endocrinology 121: 2260–2262

27 Kongsamut S, Shibuya I, Douglas WW (1991) Neuroendocrinology 54: 599–606

28 Koning de HP, Jenks BG, Scheenen WJJM, Rijk de EPCT, Caris RTJM, Roubos EW (1991) Neuroendocrinology 54: 68–76

29 Leenders HJ, Jenks BG, Rêlo AL, Roubos EW (1990) J Neuroendocrinol 2: 563–566

30 Lerner AB, Shizume K, Buding I (1954) J Clin Endocrinol Metab 14: 1463–1490

31 Loh YP, Myers B, Wong B, Parish DC, Lang M, Goldman ME (1985) J Biol Chem 260: 8956–8963

32 Loh YP, Gainer H (1977) J Gen Physiol 70: 37–58

33 Loh YP, Elkabes S, Myers B (1988) Regulation of proopiomelanocortin biosynthesis in the amphibian and mouse pituitary intermediate lobe. In "The Melanotropic Peptides: Volume 1" Ed by ME Had-

ley, CRC Press, Boca Raton, Florida, pp 85–102
34 Loh YP, Jenks BG (1981) Endocrinology 109: 54–61
35 Lucque EH, Munoz de Toro M, Smith PF, Neill JD (1986) Endocrinology 118: 2120–2124
36 Lundberg JM, Hökfelt T (1983) Trends Neurosci 6: 325–333
37 Marcinkiewicz M, Benjannet S, Seidah NG, Cantin M, Chretién M (1987) Cell Tiss Res 250: 205–214
38 Marcinkiewicz M, Benjannet S, Cantin M, Seidah NG, Chretién M (1986) Brain Res 380: 349–356
39 Martens GJM, Jenks BG, van Overbeeke AP (1981) Comp Biochem Physiol 69C: 75–82
40 Martens GJM, Weterings KAP, van Zoest ID, Jenks BG (1987) Biochem Biophys Res Comm 143: 678–684
41 Martens GJM, Bussemakers MJG, Ayoubi TAY, Jenks BG (1989) Eur J Biochem 181: 75–79
42 Martens GJM, Civelli O, Herbert E (1985) J Biol Chem 260: 13685–13689
43 Martens GJM (1988) The pro-opiomelanocortin gene in *Xenopus laevis*: structure, expression and evolutionary aspects. In "The Melanotropic Peptides: Volume 1" Ed by ME Hadley, CRC Press, Boca Raton, Florida, pp 67–84
44 Martens GJM (1988) FEBS Lett 234: 160–164
45 Mena F, Clapp C, Aguayo D, Martinez-Escalera G (1989) Neuroendocrinology 49: 207–214
46 Morrissey TJ, Cohen DV (1979) J Cell Biol 83: 521–528
47 Neill JD, Smith PF, Lucque EH, Munoz de Toro M, Nagy G, Mulchahey JJ (1986) In "Neuroendocrine Molecular Biology" Ed by G Fink, AJ Harmar, KW Kerns, Plenum Press, New York, pp 325–340
48 Neill JD, Frawley LS (1983) Endocrinology 112: 1135–1137
49 Poulain DA, Wakerley B (1982) Neuroscience 7: 773–808
50 Rijk EPC T de, Terlou M, Cruijsen PMJM, Jenks BG, Roubos EW (1992) Cytometry 13: 863–871
51 Rijk EPCT de, Jenks BG, Vaudry H, Roubos EW (1991) Neuroscience 38: 495–502
52 Rijk EPCT de, Jenks BG, Wendelaar Bonga SE (1990) Gen Comp Endocrinol 79: 74–82
53 Rijk EPCT de, Cruijsen PMJM, Jenks BG, Roubos EW (1991) Endocrinology 128: 735–740
54 Schuit FC, In 't Veld PA, Pipeleers DG (1988) Proc Nat Acad Sci (USA) 85: 3865–3869
55 Seidah NG, Hsi KL, De Serres G, Rochemont J, Hamelin J, Antakly T, Cantin M, Chretién M (1983) Arch Biochem Biophys 255: 525–534
56 Semoff S, Hadley ME (1978) Gen Comp Endocrinol 35: 329–341
57 Shibuya I, Kongsamut S, Douglas WW (1991) Proc R Soc Lond 243: 129–137
58 Stachura ME (1986) Mol Cell Endocrinol 44: 37–45
59 Strien FJC van, Rijk EPCT de, Heymen PSH, Hafmans TGM, Roubos EW (1991) Histochemistry 96: 505–510
60 Tonon MC, Danger JM, Lamacz M, Leroux P, Adjeroud S, Anderson A, Verburg-van Kemenade BML, Jenks BG, Pelletier G, Stoeckel L, Burlet A, Kupryszewski G, Vaudry H (1988) Multihormonal control of melanotropin secretion in cold-blooded vertebrates. In "The Melanotropic Peptides: Volume 1" Ed by ME Hadley, CRC Press, Boca Raton, Florida, pp 127–170
61 Verburg-van Kemenade BML, Jenks BG, Smits RJM (1987) Neuroendocrinology 46: 289–296
62 Verburg-van Kemenade BML, Jenks BG, Lenssen FJA, Vaudry H (1987) Endocrinology 120: 62–68
63 Verburg-van Kemenade BML, Tonon MC, Jenks BG, Vaudry H (1986) Neuroendocrinology 44: 446–456
64 Waring H (1963) Color Change Mechanisms of Cold-Blooded Vertebrates. Academic Press, New York
65 Weatherhead B, Whur P (1972) J Endocrinol 53: 303–310
66 Wilson JF, Morgan MA (1979) Gen Comp Endocrinol 38: 172–182
67 Zoest ID van, Heijman PS, Cruijsen PMJM, Jenks BG (1989) Gen Comp Endocrinol 76: 19–28
68 Zoest ID van, Leenders HJ, Jenks BG, Roubos EW (1990) Comp Biochem Physiol 96C: 199–203

ZOOLOGICAL SCIENCE 10: 13–29 (1993)

REVIEW

Vertebrate-type Hormones in Crustaceans: Localization, Identification and Functional Significance

Milton Fingerman, Rachakonda Nagabhushanam and Rachakonda Sarojini

Department of Ecology, Evolution, and Organismal Biology, Tulane University, New Orleans, Louisiana 70118, U.S.A.

INTRODUCTION

In a 1983 review of the literature relating to invertebrate neuropeptides Greenberg and Price [49] referred to invertebrates as having two sets of neuropeptides. One set they called "native neuropeptides." These are the ones that were originally isolated from invertebrates and have been shown to have specific physiological or biochemical roles in these animals. In contrast, the compounds that Greenberg and Price called "naturalized neuropeptides" are those originally discovered in vertebrates and later identified in invertebrates by various techniques, including chromatography, radioimmunoassay, and immunocytochemistry. At the time Greenberg and Price wrote their review very little information had been obtained about what the physiological and biochemical roles of these "naturalized" compounds might be, and for many of them their roles remain obscure. Peptides are now known to be the largest class of neuroregulatory compounds in both invertebrates and vertebrates [92]. The object of this reivew is to present the more recent evidence for the presence in crustaceans of not only vertebrate-type neuropeptides but of all vertebrate-type peptidergic, proteinaceous, steroid, and lipid-derived hormones. However, the classical neurotransmitters, such as norepinephrine and dopamine, are not treated herein because (a) they are so ubiquitious in the animal kingdom that concluding whether one or more of them is vertebrate-type or invertebrate-type does not seem justified and (b) their presence and roles in crustaceans have been extensively reviewed in a recent publication from this laboratory [40]. Where information is available concerning possible physiological roles of these vertebrate-type compounds in crustaceans, that information will be presented also.

In this review we shall use "hormone" as it has been defined by Norman and Litwack [88]. They stated that "any substance that operates at the cellular level, generated either externally or internally, which conveys to that cell a message to stop, start, or modulate a cellular process will come under the purivew of modern endocrinology." Also, Norman and Litwack divided hormones into three classes, based on the distance of action: (a) endocrine hormones, which are the classical hormones such as lutenizing hormone that travel to distant target cells; (b) paracrine hormones, such as the classical aminergic neurotransmitters (e.g. acetylcholine), which travel only a short distance to neighboring cellular targets; and (c) autocrine hormones, such as prostaglandins, that are synthesized and released by the same cell on which they act.

Invertebrate nervous systems, including those of crustaceans, are useful models for analyses of neuronal functioning, including peptidergic

Received September 14, 1992

neurotransmission. Technical improvements in such techniques as high performance liquid chromatography, peptide sequencing and radioimmunoassay have greatly enhanced our ability to identify the vertebrate-type hormones in invertebrate tissues, even when these compounds are present in extremely low concentrations.

ENDORPHINS

Localization and identification

The presence of substances in the mammalian brain that have opiate-like activity was clearly established in 1975 when Hughes *et al.* [57] published the structures of two such endogenous opioids, the pentapeptides methionine enkephalin and leucine enkephalin extracted from the porcine brain. The name "endorphin" is often used, as we have done here, for the entire class of compounds endogenous in mammals that have morphine-like activity [43]. Since 1975, endorphins have been found in several non-nervous organs of vetebrates such as the gut, adrenal medulla, and pancreas [43]. The first demonstration of the presence of an opioid in an invertebrate came from a study with a locust, *Locusta migratoria.* Radioimmunoassays (RIA) showed its nervous system contains both methionine enkephalin-like and leucine enkephalin-like substances [50]. With respect to crustaceans, the first opioid study was done in 1981 by Mancillas *et al.* [75]. Through immunocytochemistry they found leucine-enkephalin-like immunoreactivity in all the retinular cells of the spiny lobster, *Panulirus interruptus.* In addition, such immunoreactivity was also apparent in nerve fibers in chiasm 3 that pass from the medulla terminalis to terminate in the medulla interna. No immunoreactivity against antibodies of another opioid, beta-endorphin, was found. Later, other crustaceans were similarly studied. Jaros *et al.* [58], using the shore crab, *Carcinus maenas,* obtained immunocytochemical evidence for a leucine enkephalin-like substance in the eyestalk, i.e. in the sinus gland, lamina ganglionaris, medulla externa, medulla interna, and medulla terminalis. In addition, high performance liquid chromatography (HPLC) of sinus gland extracts of *Carcinus maenas* revealed the presence of substances that appeared to be methionine enkephalin, leucine enkephalin, and methionine enkephalin-Arg^6-Phe^7 [58]. Likewise, Fingerman *et al.* [39] showed by immunocytochemistry the presence of leucine enkephalin-like and methionine enkephalin-like material in the eyestalk of the fiddler crab, *Uca pugilator.* Immunoreactivity to both substances was apparent in the retinular cells, lamina ganglionaris, sinus gland, optic peduncle, the three chiasms and medulla terminalis. However, in the X-organ of the medulla terminalis, immunoreactivity against only the methionine enkephalin antibodies, but not leucine enkephalin, was seen. Using the mantid shrimp, *Squilla mantis,* Marino *et al.* [77] showed that the subesophageal ganglia contain a peptide that is opioid-like because it is able to displace D-Ala^2-D-Leu^5-enkephalin (DADLE) from rat brain membranes in a receptor binding assay, and gives positive results in the standard guinea pig ileum assay for opioids. In this test, opioids inhibit the twitch response of the electrically stimulated ileum. Furthermore, the action of this opioid-like substance is inhibited by naloxone, an opioid receptor blocker. This peptide, through use of proteolytic enzymes, gave evidence that it is synthesized as part of a larger inactive peptide and subsequently released in the active form. Because this opioid does not coelute with methionine enkephalin or leucine enkephalin, nor does it cross-react with antibodies to methionine enkephalin or give positive results in RIA for methionine enkephalin, leucine enkephalin, or beta-endorphin, Marino *et al.* suggested this peptide from *Squilla mantis* is a "native" neuropeptide. Piccoli *et al.* [91], also using the DADLE receptor binding assay, found opioid-like DADLE displacement with extracts of brain from *Carcinus maenas* and brains plus dorsal organ from *Squilla mantis,* suggestive of the presence of opioid peptides. In an abstract, Dircksen *et al.* [27] reported that leucine enkephalin-like immunoreactivity, as seen by light and electron microscopic immunocytochemistry, was apparent in the pericardial organs and their segmental nerve connections to the thoracic ganglia of *Carcinus maenas* and in the pericardial organs of the crabs *Cancer pagurus, Portunus puber,* and *Maja squinado.*

Carcinus maenas has also been used in other studies involving enkephalins. Amiard-Triquet *et al.* [1] by immunofluorescence showed the presence of methionine enkephalin-like material in the hepatopancreas (midgut gland) of this crab. The immunofluorescent material was located mainly basally in hepatopancreas tubule cells of crabs taken from nonpolluted water. However, in crabs from a polluted site or those exposed to Cd, Pb, Cu or Zn for 1–3 weeks the immunofluorescence was located mainly apically in these tubule cells. No immunoreactivity was seen in the lumina of these tubules, which suggests that this immunoreactive material is either not secreted into the lumen or loses its immunoreactivity upon being secreted. Also with *Carcinus maenas,* Dircksen [26] found by immunocytochemistry that leucine enkephalin-like immunoreactive axons are present in the pericardial organs, neurohemal organs that are cardiostimulatory. These immunoreactive axons enter the pericardial organs *via* segmental nerves 1, 3 and 7. No colocalization of this material with proctolin, FMRFamide or crustacean cardioactive peptide was seen. More recently, both methionine enkephalin and leucine enkephalin were found in extracts of the thoracic ganglion of *Carcinus maenas* [73]. Their presence was established by RIA, HPLC and sequence analysis of the opioids in thoracic ganglion extracts. An immunocytochemical study by Rothe *et al.* [94] of the eyestalks of *Carcinus maenas* revealed immunoreactivity to both methionine enkepahlin and leucine enkephalin in the sinus gland (more leucine enkephalin than methionine enkephalin being present in this neurohemal organ); only leucine enkephalin in the medulla terminalis, lamina ganglionaris, medulla externa and medulla interna; and only methionine enkephalin in the chiasm between the medulla interna and medulla terminalis. In addition, by HPLC analysis a substance that coelutes with leucine enkephalin was identified in sinus gland extracts.

With another crab, the land crab, *Gecarcinus lateralis*, Leung *et al.* [70] by HPLC and RIA analyses found a methionine enkephalin-like substance in the eyestalk, and methionine enkephalin-like and leucine enkephalin-like substances in the brain. Colleti-Previero *et al.* [22] found three peptidases in the hemolymph of the crayfish, *Astacus fluviatilis,* that rapidly degrade leucine enkephalin.

Another opiate first found in mammals is called β-endorphin. It is a 31-amino acid polypeptide. Sephadex G-50 column chromatography of extracts of the hepatopancreas of the red swamp crayfish, *Procambarus clarkii,* revealed three peaks of immunoreactive β-endorphin-like material. These immunoreactive peaks were identified by immunocytochemistry and RIA [52]. Cells of the hepatopancreas of this crayfish contain enzymes capable of degrading β-endorphin [123].

Functions

A *Behavior*

The first study of a possible role of an opioid in any crustaceans was that of Maldonado and Miralto [74] with *Squilla mantis.* They found that the defensive response, rapid flexure of the abdomen, which can be experimentally induced by an electrical shock, can be modified by morphine. This drug increases the threshold current required to elicit the response. The loss of sensitivity is dose-related. Naloxone blocks the action of this opioid; coinjection of morphine and naloxone does not result in a loss of sensitivity.

In a more recent study of locomotor activity of *Gecarcinus lateralis,* Martinez *et al.* [79] found that when the crabs were first placed into the activity monitoring chambers locomotor activity increased. FK 33 824, a stable methionine enkephalin analog, markedly enhances this initial activity; but naloxone blocks this excitatory action of the opioid.

In studies with another crab, *Chasmagnathus granulatus,* Lozada *et al.* [72] found that this crab assumes a defensive posture, with both chelae extended and the body elevated, when an electric shock, 50 Hz, one second duration, and of at least 8 V, is given. Morphine produces a dose-dependent reduction in the sensitivty of this crab to the electrical shock. When naloxone was coinjected with morphine no reduction in sensitivity occured, which suggests that opioid receptors are indeed involved in this reduction of sensitivity to the electric shock. In other behavioral studies with this crab [10, 117], it was found that a danger stimulus in the form of a passing shadow elicits an

escape response that habituates after repeated stimulation, and that this habituation appears to be mediated by endorphins. Support for this suggestion that habituation is the result of endorphin release is the observation that after an habituation session there is an analgesic effect on the defensive response of this crab to an electrical shock.

B *Pigmentary effectors*

Crustaceans have two types of pigmentary effectors: (a) chromatophores which are responsible for color changes and (b) the retinal pigments, which control the amount of light impinging on the rhabdom. Translocation of the pigments in the chromatophores and at least in the distal and reflecting pigments is clearly regulated by neurohormones.

(a) *Chromatophores*

The physiology of crustacean chromatophores has been reviewed recently [38]. In several species dual control of the chromatophores by pigment-dispersing and pigment-concentrating neurohormones has been demonstrated. In this laboratory we have been particulary intersted in identifying the neuroregulators that control the release of crustacean neurohormones. In the fiddler crab, *Uca pugilator,* 5-hydroxytryptamine stimulates release of red pigment-dispersing hormone while norepinephrine stimulates release of black pigment-dispersing hormone, and dopamine stimulates release of red pigment-concentrating hormone and black pigment-concentrating hormone. Methionine-enkephalin, but not leucine-enkephalin, was found to stimulate black and red pigment concentration in intact *Uca pugilator,* but not in isolated legs [93]. Methionine-enkephalin also stimulated the release of black and red pigment-concentrating hormones from isolated eyestalks [13, 93]. The opioid antagonist, naloxone, blocked the effects of methionine-enkephalin in intact crabs and on isolated eyestalks. Methionine enkephalin, like the classical aminergic neurotransmitters, has no direct effect on these chromatophores, as evidenced by the lack of effect on the chromatophores in isolated legs. Presumably, therefore, these compounds exert their effect only indirectly, by stimulating release of the appropriate specific chromatophorotropic neurohormone. However, surprisingly, β-endorphin was found to produce black pigment dispersion in both intact *Uca pugilator* and in isolated legs [93]. Additional evidence for the involvement of opioid-like peptidergic substances in crustacean color changes was provided by Martinez *et al.* [80], who found that although injection of the stable methionine-enkephalin analog FK 33 824 alone into *Gecarcinus lateralis* has no effect on the chromatophores, whereas coinjection of this analog with eyestalk extract strongly potentiates the black pigment-dispersing and red pigment-concentrating actions of the eyestalk extract. This potentiation is blocked by naloxone.

(b) *Distal retinal pigment*

Norepinephrine produces light adaptation of the distal retinal pigment of *Uca pugilator* whereas dopamine induces dark adaptation [62, 64], presumably by stimulating release respectively of the light-adapting and dark-adapting neurohormones. Methionine enkephalin, like dopamine, produces dark adaptation of this pigment, but leucine enkephalin has no effect on this pigment [63].

C *Blood glucose*

The crustacean hyperglycemic hormone (CHH) is found in the sinus gland. In several crustaceans CHH release has been found to be triggered by 5-hydroxytryptamine [40]. Recently Lüschen *et al.* [73] and Rothe *et al.* [94] provided evidence that synthetic leucine-enkephalin, endogenous sequenced leucine-enkephalin isolated from thoracic ganglia of *Carcinus maenas,* and purified leucine-enkephalin-like material (not yet sequenced) from sinus glands of *Carcinus maenas* inhibit CHH release. Injection into intact *Uca puglilator* of synthetic leucine-enkephalin or either the sinus gland or thoracic gland material from *Carcinus maenas* results in a decrease in the hemolymph glucose concentration. Also, eyestalks of *Carcinus* incubated in the presence of synthetic leucine enkephalin release less than the basal level of CHH as compared with eyestalks incubated in saline alone. Injection into intact fiddler crabs of naloxone prior to injection of leucine-enkephalin blocks the hypoglycemic action of this opioid. In contrast, leucine-enkephalin does not affect the hemolymph glucose concentration in eyestalkless fiddler crabs, which is consistent with the hypothesis that the enkephalin is acting by reducing CHH

output from the sinus glands in the eyestalks.

HYPOTHALAMIC AND HYPOPHYSIAL HORMONES AND NEUROPHYSIN

Localization and identification

In what appears to have been the first effort to identify a "naturalized" peptide in a crustacean, Martin and Dubois [78] by use of an immunofluorescence technique demonstrated the presence of a somatostatin-like substance in the brain, subesophageal ganglion, and ventral nerve cord of the isopod, *Porcellio dilatatus*. However, no localization of this somatotropin release-inhibiting hormone-like material was apparent in the sinus glands. Van Herp and Bellon-Humbert [120], using the prawn, *Palaemon serratus*, provided immunocytochemical evidence for neurophysin-like and arginine vasopressin-like substances in the organ of Bellonci, a component of the eyestalk. However, whereas the neurophysin-like material was present at all times, the vasopressin-like substance was present only at ecdysis. Later, Van Deijnen *et al.* [119] did an immunocytochemical study of the eyestalk of the crayfish, *Astacus leptodactylus*, with antibodies against melanocyte-stimulating hormone, vasotocin, and oxytocin. The immunoreactivity they observed to antivasotocin was the most widespread while that to anti-oxytocin was the least widespread. The sinus gland reacts positively to antimelanocyte-stimulating hormone and antivasotocin. In addition, cells or fibers reactive: (a) to antivasotocin are in chiasms 1 and 2, the medulla externa, medulla interna, the medulla terminalis neuropil and X-organ of the medulla terminalis, (b) to antialpha-melanocyte-stimulating hormone are in the lamina ganglionaris, chiasm 1, medulla externa, medulla interna and X-organ of the medulla terminalis; and (c) antioxytocin in the neuropils of the medulla externa and medulla terminalis. In a related study, Mattson and Spaziani [82], using arginine vasopressin antiserum in an RIA with eyestalk extract of the crab, *Cancer antennarius*, found vasopressin-like peptides are indeed present.

Mizuno and Takeda [84] used immunocytochemistry to identify in several crustaceans neurons immunoreactive to arginine vasotocin/arginine vasopressin antibodies. Such neurons were seen in brains of the sea louse, *Gnorimosphaeroma rayi*, and the crab, *Hemigrapsus sanguineus*, but not in the brain or subesophageal ganglion of *Procambarus clarikii* or the crab, *Helice tridens*. Mizuno and Takeda [83] also looked for oxytocin-like immunoreactivity in the nervous systems of these four crustaceans, but none was seen. In a preliminary study done earlier Takeda *et al.* [108] examined only isopod central nervous systems by immunocytochemistry with these neurohypophysial hormone antibodies. Arginine vasotocin/arginine vasopressin immunoreactivity was apparent with *Ligia exotica*, *Porcellio scaber*, and *Armadillidium vulgare*, but no oxytocin immunoreactivity was apparent.

A human somatotropin-like substance was identified by RIA in the hemolymph and extracts of the stomach and hepatopancreas of *Palaemon serratus* [113]. The amounts in the three tissues varied with the molting cycle, being highest in all three tissues during proecdysis.

Functions

Few attempts have been made to identify possible roles in crustaceans of hypophysial compounds. Sarojini *et al.* [99] found that oxytocin elvates the hemolymph glucose concentration in the freshwater crab, *Barytelphusa cunicularis* and the prawn, *Macrobrachium kistnensis*. The glycogen levels in the hepatopancreas, muscles and integument of both species showed concomitant decreases, which suggests that these glycogen stores were hydrolyzed to provide the glucose that appeared in the hemolymph. Later, Mattson and Spaziani [82] reported that lysine vasopressin, arginine vasopressin, vasotocin, and oxytocin mimic the action of molt-inhibiting hormone, inhibiting ecdysteroid production by Y-organs of the crab, *Cancer antennarius*. Charmantier *et al.* [17] found that larval and postlarval lobsters, *Homarus americanus*, grow more rapidly when injected with human somatotropin. This hormone did not bring on precocious molting activity, but the specimens that received the hormone became longer and weighed more than the controls. The hormone appeared to stimulate tissue growth without in-

fluencing the water content of these test individuals.

Zukowska-Arendarczyk [127] tested ovine follicle-stimulating hormone and luteinizing hormone on the sand shrimp, *Crangon crangon*. Both intact and eyestalk ligated females were used. Eyestalk ligation was used to eliminate any influence of the gonad-inhibiting hormone of the sinus gland in the eyestalk. However, the responses when these gonadotropins were injected were qualitatively the same among the ligated and non-ligated individuals, although the ligated individuals did show accelerated vitellogenesis and oocyte growth as compared with the non-ligated shrimp. Follicle-stimulating hormone causes the number of somatic cells in the ovary to increase but does not affect the oogonia or oocytes. In contrast, luteinizing hormone affects only the germinal epithelium; the oogonia increasing in number and size and the oocytes undergoing accelerated vitellogenesis, but the somatic cells are not affected. So, both hormones stimulate this ovary, but in different ways.

Although chorionic gonadotropin is not an hypophysial hormone, in mammals it is functionally similar to luteinizing hormone, and this for this reason is treated here. Bomirski and Klek-Kawińska [9] found that human chorionic gonadotropin stimulates oogenesis in *Crangon crangon*. Similarly, Souty and Picaud [106] found that human chorionic gonadotropin stimulates vitellogenesis by the fat body in the isopod, *Idotea balthica*. Maruo *et al.* [81], using RIA and a radioreceptor assay, found a human chorionic gonadotropin-like substance in the stomach and hepatopancreas of the lady crab, *Ovalipes ocellatus*. However, when these investigators tested this substance from the crab stomach in a mouse uterus bioassay, this substance exhibited no biological activity.

GASTRIN/CHOLECYSTOKININ

Localization and Identification

Gastin and cholecystokinin are peptides that have the same five amino acids at their carboxyl end [68]. Consequently, antisera raised against either of these peptides generally are immunoreactive to both. It is now recognized that both gastrin and cholecystokinin belong to a single peptide family called the gastrin/cholecystokinin (G/CCK) family. Not only do gastrin and cholectystokinin function as vertebrate gastrointestinal hormones, but both are also present in vertebrate nervous systems, probably functioning there as neurotransmitters. By RIA Larson and Vigna [67] showed the presence of G/CCK-like material in the digestive tract of *Cancer magister* (the highest concentration occurring in the stomach), and also in the digestive tract of *Upogebia pugettensis*. This material was not detected in the hepatopancreas of *Cancer* nor in the digestive tracts of two barnacles, *Balanus* sp. and *Pollicipes polymerus*. G/CCK-like material of *Cancer magister* was analyzed by Sepahdex G-50 chromatography [66] from the stomach, hemolymph and carapace. Three immunoreactive molecular forms of G/CCK-like peptides were found.

Scalise *et al.* [102], using immunocytochemistry, provided supporting evidence for the presence of G/CCK-like material in the stomach of *Cancer magister*. This material appears to be synthesized in the gastric epithelial cells and then secreted into the procuticle which lines the stomach lumen. Bellon-Humbert *et al.* [6] reported that by immunocytochemistry and with an antibody to cholecystokinin 8 they observed that neurosecretory cells in the medulla externa and medulla terminalis X-organ of *Palaemon serratus* are immunoreactive to this antibody.

Van Deijnen *et al.* [119] who, as mentioned above, used a wide variety of mammalian antisera to test for "naturalized' peptides in eyestalks of *Astacus leptodactylus* found immunoreactivity against a gastrin (C-terminal) antibody in the medulla externa nd medulla terminalis X-organ. They [119] also used an antibody to cholecystokinin that was raised against the middle portion of the molecule which does not crossreact with gastrin. This anticholecystokinin revealed the presence of reactive cells in the lamina ganglionaris, medulla externa, medulla interna, medulla terminalis (both in the X-organ and the rest of the ganglion), and also in the sinus gland. By immunofluorescence and RIA Turrigiano and Selverston [114] showed G/CCK-like material is in the

input nerve and neuropil of the stomatogastric ganglion, commissural ganglia, brain and eyestalks *Panulirus interruptus*.

Favrel *et al.* [37], by immunocytochemistry, showed the presence of G/CCK-like peptides in the eyestalk and stomach of *Palaemon serratus*. In the eyestalk, cells in the medulla externa and medulla terminalis X-organ and the sinus gland were labelled. In the stomach, epithelial cells and the cuticle were labelled also. Like with *Cancer magister,* Sephadex G-50 fractionation of eyestalks, stomach and hemolymph of *Palaemon serratus* revealed multiple molecular forms of G/CCK-like material. The quantity of G/CCK-like peptides, as measured by RIA, in the eyestalks showed no significant variation with the molting cycle, but in the hemolymph the concentration was highest, during late proecdysis, just before ecdysis; and for the stomach concentration peaks were apparent during postecdysis and during proecdysis. Van Wormhoudt *et al.* [121], using shrimps, *Penaeus japonicus* and *Penaeus stylirostris,* and an RIA for G/CCK-like peptides found, after fractionation on a Sephadex R G-50 SF column, four molecular forms of these peptides in the hemolymph of each shrimp. The amount of each form varies with the species. Four G/CCK-like peptides that cross-reacted with a specific C-terminal G/CCK antiserum were also isolated from extracts of the stomach of the lobster, *Nephrops norvegicus,* by Favrel *et al.* [35]. Their molecular weights are in the range 1000–2000 daltons. These four peptides show very weak crossreactivity with human gastrin, about 0.03%. Amino acid analysis showed none of these peptides has the same five terminal amino acids at the carboxyl end as human gastrin and cholecystokinin, these five being necessary for full immunoreactivity. Instead they had only three or four of the requisite amino acids.

Functions

Because of the established roles of gastrin and cholecystokinin as regulators of digestion among vertebrates, studies of the possible roles of G/CCK-like peptides in crustaceans have centered on similar functions. Larson and Vigna [66] reported that G/CCK-like material from *Cancer magister* does not stimulate secretion of either gastric acid or pancreatic amylase in the rat. This suggests that the crab material while sufficiently like vertebrate G/CCK to react with the antisera is nevertheless sufficiently different so as to be incapable of eliciting a response in the rat. Working with *Palaemon serratus,* Favrel and Van Wormhoudt [36] found that injection of gastrin 17 results in increased incorporation of leucine into proteins of the hepatopancreas.

Turrigiano and Selverston [114] found that electrical stimulation of the stomatogastric input nerve, which contains G/CCK immunoreactive fibers, results in the release of G/CCK-like peptide into the stomatogastric ganglion of *Panulirus interruptus*. Also, application of cholecystokinin to this ganglion results in increases in the spike frequency and number of spikes per burst of the pyloric rhythm and also activates the gastric mill. In view of these results, these investigators suggested that in this lobster G/CCK-like peptide functions as a neuromodulator in the stomatogastric ganglion. When *Penaeus japonicus* and *Penaeus stylirostris* are fed, the amount of G/CCK-like material in their hemolymph increases [121]. This increase indicates that these peptides may help regulate the digestive process. Also, in *Panulirus interruptus* the hemolymph concentration of G/CCK-like peptide increases after feeding (up to fourfold), and the effect lasts about four hours [115]. Concomitant with this increase is an increase in gastric mill activity. Also, the cholecystokinin antagonist, proglumide, when injected within the first two hours after feeding, causes a prolonged decrease in gastric mill activity.

Sedlmeier and Resch [103] tested the efficacy of gastrin and cholecystokinin *in vitro,* using the hepatopancreas of the crayfish, *Orconectes limosus*. Both gastrin and cholecystokinin were found to stimulate release of amylase and proteases into the incubation medium. Favrel *et al.* [35], using three of the four G/CCK-like peptides they isolated from extracts of the stomach of *Nephrops norvegicus,* found that two of the three stimulate protease secretion *in vitro* from the hepatopancreas of *Orconectes limosus*.

INSULIN

Localization and identification

Although early studies [41, 53, 69] showed that injected mammalian insulin does not affect the hemolymph glucose concentration in crustaceans, interest in the possible presence and roles of insulin-like peptides in crustaceans continues. Davidson *et al.* [25] reported that the hepatopancrease of *Carcinus maenas* shows insulin-like activity in a mouse diaphragm glycogen synthesis test, and that some cells in the hepatopancreas, but not in the gut, of *Carcinus maenas* and *Homarus gammarus* have staining characteristics of mammalian insulin-secretory pancreatic islet beta cells. But Davidson *et al.* [25] cautioned about hastily drawing firm conclusions when using light microscopic staining features and histochemical staining reactions devised for mammalian cells on tissues of invertebrates. Likewise, Falkmer [34] had earlier found in a study with the use of light microscopy that such insulin-producing cells are absent from the gut of the blue crab, *Callinectes sapidus,* also.

Sanders [96], using an RIA and guinea pig anti-insulin serum showed that the hepatopancreas, gut and hemolymph of *Homarus americanus* contain insulin-like peptides. The hepatopancreas contains the highest concentration of immunoreactive material while the eyestalk has none. Fractionation of hepatopancreas, hemolymph and gut on a Sephadex G-50 column revealed molecular heterogeneity of the insulin-like material. The hepatopancreas contains the highest proportion of high molecular weight insulin-like material, the gut and hemolymph having relatively more of the lower molecular weight insulin-like material. In view of these results, Sanders [96] hypothesized that a large insulin-like peptide is synthesized in the hepatopancreas, secreted into the gut where it is broken down to smaller units, reabsorbed into the hepatopancreas and then secreted into the hemolymph.

Functions

Sanders [97], using *Homarus americanus,* found that bovine insulin, hepatopancreas extract, and hemolymph induce glycogenesis in abdominal muscle of this lobster *in vitro,* but gut extracts have no such effect. However, injection of these insulin-like peptides from the hepatopancreas does not affect the glucose concentration in the hemolymph of *Homarus americanus* [98]. High glucose concentrations in the hemolymph did not stimulate release of insulin-like peptides into the hemolymph, nor did hepatopancreas extracts speed the rate of glucose clearance from the hemolymph. These findings are consistent with the earlier results from several laboratories mentioned above [41, 53, 69] that mammalian insulin has no effect on the hemolymph glucose concentration in crustaceans. This crustacean insulin-like material presumably functions to regulate glycogenesis in muscle cells, but has no role in hemolymph glucostasis. Insulin does not stimulate release of amylase or proteinase from the isolated hepatopancreas of *Orconectes limosus* [103]. Consistent with the results of Sanders [96, 97] are the observations of Baker and Carruthers [4, 5] that porcine insulin stimulates glucose transport into muscle cells of the barnacle, *Balanus nubilis.* Baker and Carruthers also found with these muscle cells that insulin lowers the cytosolic ionized calcium level, reduces the cyclic AMP content and increases the cyclic GMP content. These observations are consistent with the earlier observations of Bittar *et al.* [7] that insulin stops sequestration of soldium ions in muscle cells of the barnacles, *Balanus nubilus* and *Balanus aquila,* and also increases the activity of the guanylate cyclase system. Insulin injected into these cells produces an increase in the rate of sodium efflux and injection of guanosine triphosphate into muscle cells pre-exposed to insulin also produces an increase in sodium efflux.

SUBSTANCE P

Localization and identification

In the vertebrate central nervous system substance P apparently serves as a neurotransmitter that mediates sensory input, e.g. transmission of pain impulses to the brain. By immunocytochemistry substance P-like material was found in the eyestalk of *Panulirus interruptus* [75]. This immunoreactivity material is in the lamina ganglio-

naris, medulla externa, medulla interna, medulla terminalis (in the X-organ as well as the rest of this ganglion) and sinus gland. In eyestalks of *Uca pugilator,* substance P-like immunoreactivity was seen in the retinular cells, lamina ganglionaris, medulla externa, medulla interna, sinus gland and optic peduncle [39].

Goldberg *et al.* [46, 47] by immunocytochemistry identified cells immunoreactive to substance P antibody in the stomatogastric nervous systems of *Panulirus interruputs, Homarus americanus* and *Cancer borealis.* In these three decapods the neuropil of the stomatogastric ganglion is strongly immunoreactive, but none of the stomatogastric ganglion somata showed any immunostaining. Also, in the connective ganglia some somata and the neuropil were positively immunoreactive. Marder [76] noted that the stomatogastric ganglion of *Cancer irroratus* shows the same pattern of substance P-like immunoreactivity as do the stomatogastric ganglia in these other three decapods studied by Goldberg *et al.* [46, 47].

Sanderman *et al.* [95] by immunocytochemistry demonstrated substance P-like immunoreactivity in cells of the brains of the crab, *Leptograpsus variegatus,* and the crayfish, *Cherax destructor.* Four large neurons in the brain of each of these crustaceans are immunoreactive, two in the protocerebrum and two in the deutocerebrum. These paired immunoreactive protocerebral cells are, more specifically, in the dorsal cell clusters that lie on each side of the median protocerebrum. Each of these cells extends through the ipsilateral and contralateral olfactory lobes to terminate among the lateral somata of the olfactory lobe, not in the neuropil. The cells from each side of the brain are mirror images of each other. Each deutocerebral cell runs only ipsilaterally, terminating within the neuropil of the olfactory lobes.

Functions

Substance P was found to increase the amounts of amylase and proteases released *in vitro* from the hepatopancreas of *Orconectes limosus* [103].

CALCITONIN and CALCITONIN GENE-RELATED PEPTIDE

Localization and identification

Calcitonin is a small polypeptide secreted by the ultimobrachial glands in jawed fishes, amphibians, reptiles and birds; and in mammals by the so-called C cells of the thyroid gland. As a hormone, calcitonin produces hypocalcemia in vertebrates. Calcitonin is also present in the vertebrate central nervous system, presumably functioning there as a neuromodulator. The gene that codes for calcitonin also produces another polypeptide, called calcitonin gene-related peptide (CGRP). This substance is present in central and peripheral nervous systems of vertebrates, where it appears to function as a neuromodulator, and in several other regions of the vertebrate body, including the heart, spleen and urogential tract as well [89].

Bellon-Humbert *et al.* [6] by use of immunocytochemistry and antibodies against human, pig and salmon calcitonins demonstrated the presence of a calcitonin-like substance in the medulla terminalis X-organ of *Palaemon serratus.* Arlot-Bonnemains *et al.* [3] by RIA with anticalcitonin antibodies from salmon showed the presence of a calcitonin-like polypeptide in the hemolymph of *Palaemon serratus.* The amount of calcitonin-like material in the hemolymph varies with the molting cycle, being highest during postecdysis, and lowest during intermolt The hemolymph calcium level, however, was maximal during proecydsis and lowest during postecdysis.

Using RIA, a radioreceptor assay and antisalmon and antihuman calcitonin antibodies, Funchereau-Peron *et al.* [42] found a calcitonin-like peptide in the eyestalks of *Nephrops norvegicus, Homarus americanus, Palaemon serratus,* and *Penaeus vanamei.* In addition, other organs of *Nephrops* were examined. The hepatopancreas of this lobster contains a higher concentration of calcitonin-like peptide than any of the eyestalks examined from these four species. The foregut of *Nephrops* also contains a high concentration, likewise higher than in these eyestalks, but less than in the hepatopancreas. This calcitonin-like material of *Nephrops* that was detected by the antisalmon

calcitonin antibodies exists in two forms. One has a molecular weight of 4500 daltons, somewhat higher than vertebrate calcitonins. Salmon calcitonin is 3432 daltons, and human calcitonin is 3418 daltons. However, in addition to this 4500 dalton molecule, a higher molecular weight calcitonin-like substance was also found. The latter was found by gel filtration to have a molecular weight greater than 5,000 daltons.

Graf *et al.* [48], using extracts of an entire amphipod, *Orchestia cavimana,* in an RIA found a calcitonin-like substance, the concentration of which changes with the molting cycle. The maximum amount is present at ecdysis, while the least is found early in intermolt. The concentration increases markedly late in proecdysis. The least is seen early in intermolt.

Arlot-Bonnemains *et al.* [2] with an RIA and human anti-CGRP antibody found immunoreactive material in several tissues of *Nephrops norvegicus,* including the hepatopancreas, foregut, eyestalk, brain and heart. Of the tissues examined, the hepatopancreas has the highest concentration of this CGRP-like material, followed by the foregut, which led these investigators to suggest the CGRP-like substance may function in crustaceans as a regulator of gastrointestinal function.

Sasayama *et al.* [100] demonstrated by immunocytochemistry with antibodies to salmon calcitonin and rat CGRP the presence of cells immunoreactive to both antibodies in the central nervous system of *Armadillidium vulgare.* CGRP immunoreactive cells are present in the brain and circumesophageal connectives while calcitonin immunoreactive cells are in the brain only. More recently, Cameron and Thomas [14] by use of RIA showed the presence of salmon calcitonin-like material in several tissues, including the hepatopancreas, brain, heart and hemolymph of the blue crab, *Callinectes sapidus.* The hepatopancreas contains the highest concentration of immunoreactive material. The concentration of immunoreactive material in the hemolymph varies with the molting cycle, being highest during proecdysis, but the calcitonin-like material in the other tissues does not vary with the molting cycle. The immunoreactive material in the hemolymph and hepatopancreas consists to a great extent of a 27.2 kilodalton protein with an amino acid composition very similar to those of the 17.5 kilodalton human calcitonin precursor and the 22 kilodalton calcitonin-like molecule isolated earlier from the hemolymph and hepatopancreas of *Nephrops norvegicus* by Van Wormhoudt and Fouchereau-Peron [122]. However, in *Callinectes* there is also some immunoreactive material of relatively low molecular weight. These high molecular weight substances of 22 and 27.2 kilodaltons likely correspond to the one found by Funchereau-Peron *et al.* [42] in *Nephrops* that was larger than 5,000 daltons, whereas the low molecular weight material from *Callinectes* likely corresponds to the 4,500 dalton calcitonin-like compound found by Fouchereau-Peron *et al.* in *Nephrops* [42].

Functions

The roles of calcitonin and CGRP in crustaceans have not been examined extensively. In a study of *Palaemon serratus* by Arlot-Bonnemains *et al.* [3] they found that injection of salmon calcitonin during preecdysis does not alter the hemolymph calcium concentration. Sellem *et al.* [104] investigated the effect of salmon calcitonin on the concentration of calcium in the hemolymph of *Orchestia cavimana.* They found that the calcium level decreased when the calcitonin was injected during intermolt and early proecdysis but had no effect during late proecdysis or during postecdysis. Normally, the hemolymph calcium level is high during proecdysis because of calcium resorption from the old cuticle, and is low during intermolt. As mentioned above, Graf *et al.* [48] found that calcitonin-like material is at its lowest concentration in *Orchestia cavimana* at the start of intermolt and increases rapidly during proecdysis to peak at ecdysis. So, the exogenous salmon calcitonin was effective when the endogenous calcitonin-like activity was low, but ineffective when the endogenous activity was high.

MISCELLANEOUS PEPTIDES

Localization and identification

A few "naturalized" peptides have been the subject of only one or two investigations. These

substances will be treated together in this section. Van Deijnen *et al.* [119], in the immunocytochemical study of the eyestalks of *Astacus leptodactylus* already referred to above, found cells immunoreactive to three antisera in addition to those mentioned earlier. Cells or fibers showing immunoreaction (a) to antisecretin are in the lamina ganglionaris, medulla externa, medulla interna, medulla terminalis and sinus gland; (b) to antiglucagon are in the lamina ganglionaris, medulla externa, medulla interna, medulla terminalis and chiasm 1 and (c) to antiglucose-dependent insulinotropic peptide (antigastric inhibitory peptide) are in the medulla externa, medulla interna, medulla terminalis and chiasm 1.

Charmantier-Daures *et al.* [18] did an immunocytochemical study of the eyestalks of *Homarus gammarus* that involved antibodies against neuropeptide Y and the atrial natriuretic factor. A few cells that are immunoreactive against the atrial natriuretic factor antibody are present in the medulla externa and medulla terminalis whereas the sinus gland and a few cells and numerous fibers in the medulla interna and medulla terminalis react to neuropeptide Y antiserum.

Functions

Turrin *et al.* [116] using an RIA for atrial natriuretic peptide found that the amount of this substance in the hemolymph of the mangrove crab, *Ucides cordatus,* is related to the environmental salinity. When crabs are transferred from 26 parts per thousand sea water, which is isosmotic with the hemolymph of this crab, to 34 parts per thousand sea water the concentration of this peptide in the hemolymph icreases significantly. These investigators suggested that this peptide has a role in the osmoregulation of this crab, perhaps to accelerate sodium excretion under when the crab is in a hyperosmotic environment. Sedlmeier and Resch [103] in a study already referred to above found that glucagon, like insulin, does not produce *in vitro* release amylase or proteinase from the hepatopancreas of *Orconectes limosus* whereas bombesin, like gastrin, cholecystokinin, and substance P does stimulate release of these enzymes *in vitro.*

EICOSANOIDS

Localization and identification

This section will be devoted to those derivatives of fatty acids collectively known as eicosanoids, the best known of which are the prostaglandins. Prostaglandins were first identified in mammalian semen and thought secreted by the prostate gland (hence their name), although it is now clear they are secreted into the semen by the seminal vesicles. However, prostaglandins are by no means limited to the reproductive system. Prostaglandins are produced in virtually all mammalian tissues, and function as chemical messengers. Other eicosanids include the leukotrienes, thromboxanes and such hydroxyunsaturated fatty acids as the barnacle hatching substance.

The barnacle hatching substance is released by adult barnacles into their mantle cavity where it stimulates hatching of nauplii that underwent their early development in the mantle cavity. While several barnacle tissues can synthesize the hatching substance, the epidermis appears to be the major site of synthesis. Preliminary evidence led Clare *et al.* [19–21] to suggest that the hatching substance of *Semibalanus balanoides* is a prostaglandin-like compound. In 1985, the same year as the third publication on the subject by Clare *et al.* [21], Holland *et al.* [56] showed that this hatching substance of *Semibalanus balanoides* is an eicosanoid, but not a prostaglandin. Prostaglandins are cyclic compounds whereas this hatching substance is from the linear, acyclic, pathway of unsaturated fatty metabolism for eicosanoid synthesis, and is therefore more closely related to the leukotrienes. Nevertheless, a histochemical staining technique for prostaglandin synthetase gives positive results with ovaries and developing egg masses of *Semibalanus balanoides,* and extracts of these egg masses have thin layer chromatography characteristics similar to those of the primary prostaglandins [55]. Holland *et al.* [56] proved by thin layer chromatography, gas chromatography, and mass spectrometry that the hatching substance of *Semibalanus balanoides* is 10, 11, 12-trihydroxy-5, 8, 14, 17-eicosatetraenoic acid. Later, Hill *et al.* [54] showed that the hatching substance of another

barnacle, *Elminius modestus,* has a different structure. It appears to be an eicosanoid also, apparently a monohydroxyeicosapenataenoic acid isomer, probably 8-hydroxyeicosapentaenoic acid. Although this substance is different from the hatching substance identified by Holland *et al.* [56] for *Semibalanus balanoides,* the hatching substance of *Elminius modestus* is effective not only with *Elminius* but also with *Semibalanus balanoides.*

Hampson *et al.* [51] found that hemolymph cells of *Carcinus maenas* are capable of synthesizing eicosanoids such as 5-hydroxyeicosatetraenoic acid, prostaglandin E_2 and thromboxane B_2. The calcium ionophore A23187 was used to stimulate this eicosanoid production

Functions

Casterlin and Reynolds [15] used the crayfish, *Cambarus bartonii,* in one study and in another they [16] used *Homarus americanus* and *Penaeus duorarum.* The aim of both studies was to determine whether injection of prostaglandin E_1 would alter the preferred temperatures of these crustaceans. This prostaglandin does indeed evoke an increase in the preferred water temperatures. The test chambers were designed so that each specimen could control the water temperature, thereby revealing its temperature preference. The crayfish showed a 3.4°C increase in temperature preference with 0.5 mg of prostaglandin, the lobster 4.7°C, and the shrimp 4.5°C, the lobster and shrimp receiving 0.1 mg. Prostaglandins may have a role in thermoregulation in these crustaceans, even though it would be minor because they are basically ectotherms, perhaps by stimulating a thermoregulatory control center.

The crab, *Rhithropanopeus harrisii,* produces a rhythmic abdominal flexion during and after copulation. This behavior can be induced by exposing males or females to the crab's semen or homogenates or extracts of the crab's seminal vesicles [44]. This abdominal flexion can also be induced by prostaglandin F_2 and prostaglandin E_2. However, prostaglandins have not yet been identified in crab seminal fluid.

Prostaglandins may have a role in regulating ion transport across crustacean gills. Siebers *et al.* [105] found that indomethacin, an inhibitor of prostaglandin synthesis, produces a decrease of the transbranchial potential across isolated gills of *Carcinus maenas* when applied to the basolateral side of the gills. Concomitantly, the rate of chloride ion influx decreased significantly in the presence of indomethacin.

Spaziani *et al.* [107] incubated ovaries of *Procambarus paeninsulanis,* with the prostaglandin precursor arachadonic acid, and then isolated from these ovaries a newly synthesized compound that comigrated on thin layer chromatography plates with prostaglandin F_{2a}. Synthesis of this prostaglandin was inhibited by indomethacin. The rate of synthesis was higher when ovaries in the early stages of vitellogenesis were used rather than later stages. As suggested by these investigators, prostaglandins may have a normal role in regulating vitellogenesis in this crayfish.

Koskela *et al.* [61], working with the tiger prawn, *Penaeus esculentus,* found that prostaglandin E_2 produces a decrease in the length of the intermolt cycle; but does not stimulate ovarian development. Furthermore, neither 17α-hydroxyprogesterone nor 17β-estradiol affects the duration of the molting cycle or ovarian development of *Penaeus esculentus.*

STEROIDS

Localization and identification

Several steroids that are ordinarliy identified with mammals have been found in crustaceans. Donahue [28], in what appears to have been the first report that a "naturalized" steroid is present in crustaceans, found that the ovaries of *Panulirus argus* contain an estrogenic substance. Ovarian extracts elicited growth of the vaginal epithelium in mature, ovariectomized rats. Later, Donahue [29] by fluorimetric analysis and the rat vaginal assay he used previously [28] showed that eggs of *Homarus americanus,* at the time the eggs attach to the pleopods, contain an estrogenic substance. Donahue [31] identified this estrogenic substance as alpha-estradiol. Lisk [71] later reported that eggs of *Homarus americanus* contain estradiol-17β. Estrone was not found. Whole body extracts

of the euphausiacean, *Euphausia superba,* were found to contain the steroids progesterone, testosterone and esterone [87]. Jeng *et al.* [59] by use of gas chromatography, RIA, and a bioassay based on weight increases of the mouse uterus found that the ovaries of *Parapenaeus fissurus* contain both estrone and estradiol-17β, with estrone being the major estrogen present. In a recent study of the blue crab, *Callinectes sapidus* [101], neither 17β-estradiol nor estrone was detected in males or females. However, a compound similar to estriol is present in the hemolymph, hepatopancreas, ovaries, testes and eyestalks.

Gilgan and Idler [45] found that the testes and androgenic glands of *Homarus americanus* are each capable of converting androstenedione to testosterone. This conversion requires the presence of the enzyme 17β-hydroxysteroid dehydrogenase (oxidoreductase). Blanchet *et al.* [8] showed this enzyme must also be present in the testes and vasa deferentia of male *Carcinus maenas* because extracts of these organs converted androstenedione, dehydroepiandrosterone and estrone respectively to testosterone, androst-5-ene-3β, 17β-diol and estradiol-17β. Burns *et al.* [11] showed that testes of *Homarus americanus* can convert progesterone to 20α-dihydroprogesterone. This conversion requires the enzyme steroid 20-ketone reductase. The same investigators [12] also showed that testosterone is present in the hemolymph and testes of *Homarus americanus.*

Tcholakian and Eik-Nes [109, 110] found that the androgenic gland of *Callinectes sapidus* has the enzymatic capability to convert progesterone to testosterone, 11-deoxycorticosterone, 20α-hydroxyprogesterone, and Δ^4-androstenedione. Also, intact male crabs converted Δ^5-pregnenolone to progesterone, Δ^4-androstenedione, testosterone and 11-deoxycorticosterone.

Teshima and Kanazawa [111, 112] found that the ovaries of the crab, *Portunus trituberculatus,* can convert progesterone to 11-ketotestosterone, 11β-hydroxyandrost-4-ene-3, 17-dione, testosterone, 17α-hydroxyprogesterone and deoxycorticosterone. Kanazawa and Teshima [60] in another study of steroids used *Panulirus japonica.* In this study they injected radioactive cholesterol and then found that the hepatopancreas, ovaries and hemolymph contained newly synthesized progesterone, 17α-hydroxyprogesterone, androstenedione and testosterone, and in addition the hepatopancreas contained deoxycorticosterone and corticosterone. Vitellogenic ovaries of *Penaeus monodon* metabolize progesterone mainly to four 5α-pregnane derivatives (5α-pregnan-3,20-dione, 20α-hydroxy-5α-pregnan-3-one, 3β-hydroxy-5α-pregnan-20-one and 5α-pregnan-3β, 20α-diol) plus two minor metabolites, 20α-hydroxypregn-4-en-3-one and 1,4-pregnadiene-3,20-dione; whereas vitellogenic ovaries of *Nephrops norvegicus* metabolize progesterone to only one metabolite, 20α-hydroxypregn-4-en-3-one [126].

Ollevier *et al.* [90] analyzed the hemolymph of *Astacus leptodactylus* for nonecdysteroid steroids. In both sexes pregnenalone, 17α-hydroxypregnenalone, testosterone and cholesterol were clearly identified, and there was indication that androstenedione, 5α-dihydroxytestosterone, 11-ketotestosterone and 11β-hydroxytestosterone were also present. However, with the techniques they used, dehydroepiandrosterone, progesterone, 17α-hydroxyprogesterone and estrogens could not be detected in either sex, but females alone have 6β-hydroxyprogesterone.

Couch *et al.* [23], using RIA, found progesterone but not testosterone, in mandibular organs of *Homarus americanus.* Later Couch *et al.* [24], again with RIA, and using female specimens reported the presence of estradiol-17β and progesterone in the mandibular organ, green gland, hepatopancreas, ovary and hemolymph of *Homarus americanus.* However, the estradiol was not detectable in any of these tissues if the female had immature ovaries. Progesterone was always present in the mandibular organs; its concentration is unrelated to the state of the ovaries. But in all other tissues progesterone was not detectable or present only in low concentrations when the ovaries were immature.

Van Beek and De Loof [118] analyzed by RIA total body extracts of adult female brine shrimp, *Artemia* sp. Progesterone and pregnenolone were low during vitellogenesis, but high at the beginning and end of each vitellogenic cycle. The amount of 5α-dihydroxytestosterone was very low at the start

of vitellogenesis, peaking at the end of vitellogenesis. The testosterone level was low during the vitellogenic cycle, and highest in nonvitellogenic ovaries. Estrone was higher during vitellogenesis than at other times, but the fluctuation was not large. Estradiol increased during vitellogenesis, peaking at the end of vitellogenesis. Pregnenalone was present in higher concenterations than any of the other steroids.

In a study designed to detect both conjugated and unconjugated steriods Fairs *et al.* [32], using gas chromatography/mass spectrometry, examined tissues of *Nephrops norvegicus*. Found in the ovary in unconjugated form were 5α-dihydroxytestosterone, testosterone, pregnenolone and 20α-hydroxypreg-4-en-3-one. Eggs and hemolymph contained unconjugated 17β-estradiol while the ovary and hemolymph contained conjugated 5α-dihydrotestosterone. Fair *et al.* [33] then analyzed the steroids in the ovary of *Penaeus monodon* by the same techniques. Conjugated pregnenolone, conjugated and unconjugated dehydroepiandrosterone, unconjugated progesterone, conjugated 17β-estradiol and conjugated and unconjugated estrone were present in these ovaries, peaking during mid to late vitellogenesis, but conjugated testosterone was present only in mature ovaries.

Functions

Donahue [30], who showed that eggs of *Homarus americanus* contain an estrogen, looked for a possible role for this substance. Berried females undergo ecdysis only after the larvae have hatched. When he stripped newly laid eggs from the swimmerets, the majority of the lobsters underwent a premature ecdysis. He suggested the eggs contain a moltinhibiting factor. He then proceeded to inject estradiol into male and female lobsters, and found that molting activity was inhibited. Danahue concluded by suggesting that ecdysis of berried females is normally inhibited by egg estrogen and perhaps also ovarian estrogen.

Kulkarni *et al.* [65] found that progesterone stimulates ovarian maturation in the prawn, *Parapenaeopsis hardwickii*. The ovary size, oocyte size, and ovarian fat content all increased. With another species of this prawn, *Parapenaeopsis stylifera*, Nagabhushanam *et al.* [85] found that 17-hydroxyprogesterone induces spawning at 20°C whereas normally spawning does not occur until the water temperature reaches 30°C. Also with male *Parapenaeopsis hardwickii* Nagabhushanam and Kulkarni [86] observed that testosterone injections produce hypertrophy and hyperplasia of the androgenic glands which develop to a functional state only in male crustaceans. There was a concomitant stimulation of testicular development, presumably under the influence of androgenic gland hormone released as a consequence of the effect of the testosterone on the andorgenic gland.

Yano [124] observed, using the greasyback shrimp, *Metapenaeus ensis*, that progesterone injections induce ovarian maturation and spawning of the eggs from these ovaries. Later, Yano [125] using the kuruma prawn, *Penaeus japonicus*, concluded that injection of 17α-hydroxyprogesterone induces vitellogenesis, as evidenced by an increase in the amount of vitellogenin in the hemolymph of the specimens treated with this hormone.

Koskela *et al.* [61], as noted above, reported that injection of prostaglandin E_2 into *Penaeus esculentus* results in a significant decrease in the length of the molting cycle but does not affect ovarian development. However, neither 17α-hydroxyprogesterone nor 17β-estradiol affected the molting cycle or the ovaries of this shrimp.

CONCLUDING REMARKS

Despite the large body of knowledge that has accumulated in recent years concerning the identity of many vertebrate-type hormones in crustaceans, largely as a result of improved immunologic and chromatographic procedures as well as the possibilities offered by recombinant DNA technology/molecular biology, the precise functions and mechanisms of action of these compounds remain to be established. In regard to the vertebrate-type peptides in crustaceans, the biochemical and physiological roles of these peptides (including their receptor systems) in crustaceans need to be firmly established in order to eliminate any doubt as to which ones are normally involved in the vital functions of this large group of

invertebrates.

Similarly, with reference to the vertebrate-type steroids in crustaceans we need to firmly establish their roles, and to determine their relative importance vis-a-vis the "native" steroids, the ecdysteroids, in the regulation of molting and reproduction. Not only are ecdysteroids the crustacean molt-promoting hormones, but there is also evidence that at least in some crustaceans, vitellogenesis is ecdysteroid-dependent.

REFERENCES

1 Amiard-Triquet C, Amiard J-C, Ferrand R, Andersen AC, Dubois M P (1986) Ecotoxicol Environ Safety 11: 198–209

2 Arlot-Bonnemains Y, Fouchereau-Peron M, Chesnais J, Taboulet J, Milhaud G, Moukhtar MS (1991) Gen Comp Endocrinol 83: 1–6

3 Arlot-Bonnemains Y, Van Wormhoudt A, Favrel P, Fouchereau-Peron M, Milhaud G, Moukhtar MS (1986) Experientia 42: 419–420

4 Baker PF, Carruthers A (1980) Nature 286: 276–279

5 Baker PF, Carruthers A (1983) J Physiol 336: 397–431

6 Bellon-Humbert C, Van Herp F, Van Wormhoudt A (1984) Ann Soc Roy Zool Belg 114 (Suppl 1): 164

7 Bittar EE, Schultz R, Harkness C (1977) J Membrane Biol 34: 203–222

8 Blanchet M-F, Ozon R, Meusy J-J (1972) Comp Biochem Physiol 41B: 251–261

9 Bomirski A, Klek-Kawińska, E (1976) Gen Comp Endocrinol 30: 239–242

10 Brunner D, Maldonado H (1988) J Comp Physiol 162A: 687–694

11 Burns BG, Sangalang GB, Freeman HC, McMenemy M (1984) Gen Comp Endocrinol 54: 422–428

12 Burns BG, Sangalang GB, Freeman HC, McMenemy M (1984) Gen Comp Endocrinol 54: 429–432

13 Butler TA, Fingerman M (1985) Amer Zool 25: 102A

14 Cameron JN, Thomas P (1992) J Exp Zool 262: 279–286

15 Casterlin ME, Reynolds WW (1978) Pharmacol Biolchem Behav 9: 593–595

16 Casterlin ME, Reynolds WW (1979) Life Sci 25: 1601–1604

17 Charmantier G, Charmantier-Daures M, Aiken DE (1989) CR Acad Sci Paris 308 Ser III: 21–-26

18 Charmantier-Daures M, Danger J-M, Netchitailo P, Pelletier G, Vaudry H (1987) CR Acad Sci Paris 305 Ser III: 479–483

19 Clare AS, Walker G, Holland DL, Crisp DJ (1982) Mar Biol Letters 3: 113–120

20 Clare AS, Walker G, Holland DL, Crisp DJ (1984) In "Advances in Invertebrate Reproduction, Vol III" Ed by W Engels, Elsevier, Amsterdam, p 569

21 Clare AS, Walker G, Holland DH, Crisp DJ (1985) Proc Roy Soc Lond 224B: 131–147

22 Coletti-Previero M-A, Mattras H, Zwilling R, Previero A (1985) Neuropeptides 6: 405–415

23 Couch EF, Adejuwon CA, Koide SS (1978) Amer Zool 18: 610

24 Couch EF, Hagino N, Lee JW (1987) Comp Biochem Physiol 87A: 765–770

25 Davidson JK, Falkmer S, Mehrotra BK, Wilson S (1971) Gen Comp Endocrinol 17: 388–401

26 Dircksen H (1990) In "Frontiers in Crustacean Neurobiology Advances in Life Sciences" Ed by K Wiese, W-D Krenz, J Tautz, H Reichert, B Mulloney, Birkhäuser Verlag, Basel, pp 485–491

27 Dircksen H, Stangier J, Keller R (1987) Gen Comp Endocrinol 66: 42

28 Donahue JK (1940) Endocrinology 27: 149–152

29 Donahue JK (1948) Proc Soc Exp Biol Med 69: 179–181

30 Donahue JK (1955) Research Bulletin No. 24 State of Maine Department of Sea and Shore Fisheries

31 Donahue JK (1957) Research Bulletin No. 28, State of Maine Department of Sea and Shore Fisheries

32 Fairs NJ, Evershed RP, Quinlan PT, Goad LJ (1989) Gen Comp Endocrinol 74: 199–208

33 Fairs NJ, Zuinlan PT, Goad LJ (1990) Aquaculture 89: 83–99

34 Falkmer S (1969) In "Diabetes Proc Int Diab Fed 6th Congr Stockholm 1967" Ed by J Östman and RDG Milner, Excerpta Med Found Int Congr Ser 172: 55–66

35 Favrel P, Kegl G, Sedlmeier, D Keller R, Van Wormhoudt A (1991) Biochimie 73: 1233–1239

36 Favrel P, Van Wormhoudt A (1986) Bull Soc Zool France 111: 21

37 Favrel P, Van Wourmhoudt A, Studler JM, Bellon C (1987) Gen Comp Endocrinol 65: 363–372

38 Fingerman M (1988) In "Endocrinology of Selected Invertebrate Types" Ed by H Laufer, RGH Downer, ARLiss Inc, New York, pp 357–374

39 Fingerman M, Hanumante MM, Kulkarni GK, Ikeda R, Vacca LL (1985) Cell Tissue Res 241: 473–477

40 Fingerman M, Nagabhushanam R (1992) Comp Biochem Physiol 102C: 343–352

41 Florkin M, Duchateau G (1939) CR Soc Biol 132: 484–486
42 Fouchereau-Peron M, Arlot-Bonnemains Y, Milhaud G, Moukhtar MS (1987) Gen Comp Endocrinol 65: 179–183
43 Frederickson RCA, Geary LE (1982) Prog Neurobiol 19: 19–69
44 Gerhart DJ, Clare AS, Eisenman K, Rittschof D, Forward RB, Jr (1990) In "Progress in Comparative Endocrinology" Ed by A Epple CG Scanes MH Stetson Wiley-Liss, New York, pp 598–602
45 Gilgan MW, Idler DR (1967) Gen Comp Endocrinol 9: 319–324
46 Goldberg D, Nusbaum MP, Marder E (1986) Soc Neurosci Abstr 12: 242
47 Goldberg D, Nusbaum MP, Marder E (1988) Cell Tissue Res 252: 515–522
48 Graf F, Fouchereau-Peron M, Van Wormhoudt A, Meyran JC (1989) Gen Comp Endocrinol 73: 80–84
49 Greenberg, MJ, Price DA (1983) Ann Rev Physiol 45: 271–288
50 Gros C, Lafon-Cazal M, Dray F (1978) C R Acad Sci Paris 287D: 647–650
51 Hampson AJ, Rowley AF, Barrow SE, Steadman R (1992) Biochim Biophys Acta 1124: 143–150
52 Hara M, Kouyama H, Watabe S, Yago N (1985) Zool Sci (Tokyo) 2: 971
53 Hemmingsen AM (1924) Skand Arch Physiol 46: 56–63
54 Hill EM, Holland DL, Gibson KH, Clayton E, Oldfield A (1988) Proc Roy Soc Lond 234B: 455–461
55 Holland DL (1987) In "Barnacle Biology" Ed by AJ Southward Balkema, Rotterdam, pp 227–248
56 Holland DL, East J, Gibson KH, Clayton E, Oldfield A (1985) Prostaglandins 29: 1021–1029
57 Hughes J, Smith TW, Kosterlitz HW, Fothergill LA, Morgan BA, Morris HR (1975) Nature 258: 577–579
58 Jaros PP, Dircksen H, Keller R (1985) Cell Tissue Res 241: 111–117
59 Jeng SS, Wan WC-M, Chang CF (1978) Gen Comp Endocrinol 36: 211–214
60 Kanazawa A, Teshima S (1971) Bull Jap Soc Sci Fish 37: 891–898
61 Koskela RW, Greenwood JG, Rothlisberg PC (1992) Comp Biochem Physiol 101A: 295–299
62 Kulkarni GK, Fingerman M (1986) Comp Biochem Physiol 84C: 219–224
63 Kulkarni GK, Fingerman M (1987) Pigment Cell Res 1: 51–56
64 Kulkarni GK, Fingerman M (1991) Comp Biochem Physiol 99C: 47–52
65 Kulkarni GK, Nagabhushanam R, Joshi PK (1979) Indian J Exp Biol 17: 986–987
66 Larson BA, Vigna SR (1983) Regul Pept 7: 155–170
67 Larson BA, Vigna SR (1983) Gen Comp Endocrinol 50: 469–475
68 Larsson L-I, Rehfeld JF (1977) J Histochem Cytochem 25: 1317–1321
69 Leinen R, McWhinnie MA (1971) Gen Comp Endocrinol 16: 607–611
70 Leung MK, Kessler H, Whitefield K, Murray M, Martinez EA, Stefano GB (1987) Cell Molec Neurobiol 7: 91–96
71 Lisk RD (1961) Can J Biochem Physiol 39: 659–662
72 Lozada M, Romano A, Maldonado H (1988) Pharmacol Biochem Behav 30: 635–640
73 Lüschen W, Buck F, Willig A, Jaros PP (1991) Proc Natl Acad Sci USA 88: 8671–8675
74 Maldonado H, Miralto A (1982) J Comp Physiol 147: 455–459
75 Mancillas JR, McGinty JF, Selverston AI, Karten H, Bloom FE (1981) Nature 293: 576–578
76 Marder E (1986) In "The Crustacean Stomatogastric System" Ed by AI Selverston, M Moulins Springer-Verlag, New York, pp 263–300
77 Marino G, Palmisano A, Di Marzo V, Melck D (1985) Peptides 6 (Suppl 3): 403–406
78 Martin G, Dubois MP (1981) Gen Comp Endocrinol 45: 125–130
79 Martinez EA, Murray M, Leung MK, Stefano GB (1988) Comp Biochem Physiol 90C: 89–93
80 Martinez EA, Vassell D, Stefano GB (1986) Comp Biochem Phsyiol 83C: 77–82
81 Maruo T, Segal SJ, Koide SS (1979) Endocrinology 104: 932–939
82 Mattason MP, Spaziani E (1985) Peptides 6: 635–640
83 Mizuno J, Takeda N (1988) Comp Biochem Physiol 91A: 733–738
84 Mizuno J, Takeda N (1988) Comp Biochem Physiol 91A: 739–747
85 Nagabhushanam R, Joshi PK, Kulkarni GK (1980) Indian J Mar Sci 9: 227
86 Nagabhushanam R, Kulkarni GK (1981) Aquaculture 23: 19–27
87 Nikitina SM, Savchenko ON, Kogan ME, Ezhkova NS (1977) Zh Evol Biokhim Fiziol 13: 443–447
88 Norman AW, Litwack G (1987) Hormones, Academic Press, New York, pp 2–7
89 Okimura Y, Chihara K, Abe H, Kita T, Kashio Y, Sato M, Fujita T (1987) Regul Pept 17: 327–337
90 Ollevier F, De Clerck D, Diederik H, De Loof A (1986) Gen Comp Endocrinol 61: 214–228
91 Piccoli R, Melck D, Spagnuolo A, Vescia S, Zanetti L (1985) Comp Biochem Physiol 80C: 237–240

92 Platt N, Reynolds SE (1988) In "Comparative Invertebrate Neurochemistry" Ed by GG Lunt, RW Olsen, Cornell University Press, Ithaca New York, pp 175–226
93 Quackenbush LS, Fingerman M (1984) Comp Biochem Physiol 79C: 77–84
94 Rothe H, LüSchen W, Asken A, Willing A, Jaros PP (1991) Cmp Biochem Physiol 99C: 57–62
95 Sandeman RE, Sandeman DC, Watson AHD (1990) J Comp Neurol 294: 569–582
96 Sanders B (1983) Gen Comp Endocrinol 50: 366–373
97 Sanders B (1983) Gen Comp Endocrinol 50: 374–377
98 Sanders B (1983) Gen Comp Endocrinol 50: 378–382
99 Sarojini R, Jahagirdar VG, Nagabhushanam R (1980) J Adv Zool 1: 54–61
100 Sasayama Y, Katoh A, Oguro C, Kambegawa A, Yoshizawa H (1991) Gen Comp Endocrinol 83: 406–414
101 Sasser ER, Singhas CA (1992) Aquaculture 104: 367–373
102 Scalise FW, Larson BA, Vigna SR (1984) Cell Tissue Res 228: 113–119
103 Sedlmeier D, Resch G (1989) XIth Inter Symp Comp Endocrinol Malaga Spain Abst P-315
104 Sellem E, Graf F, Meyran J-C (1989) J Exp Zool 249: 177–181
105 Siebers D, Mustafa T, Böttcher K (1991) Biol Bull 181: 312–314
106 Souty C, Picaud J-L (1984) Gen Comp Endocrinol 54: 418–421
107 Spaziani EP, Hinsch GW, Edwards SC (1991) Amer Zool 31: 23A
108 Takeda N, Mizuno J, Fujii K (1986) Abstract Second Symposium on Biology of Terrestrial Isopods Urbino Italy
109 Tcholakian RK, Eik-Nes KB (1969) Gen Comp Endocrinol 12: 171–173
110 Tcholakian RK, Eik-Nes KB (1971) Gen Comp Endocrinol 17: 115–124
111 Teshima S, Kanazawa A (1970) Bull Jap Soc Sci Fish 36: 246–249
112 Teshima S, Kanazawa A (1971) Gen Comp Endocrinol 17: 152–157
113 Toullec J-Y, Van Wormhoudt A (1987) CR Acard Sci Paris 305 Ser III: 265–269
114 Turrigiano GG, Selverston AI (1989) J Neurosci 9: 2486–2501
115 Turrigiano G, Selverston A (1990) In "Frontiers in Crustacean Neurobiology: Advances in Life Sciences" Ed by K Wiese, W-D Krenz, J Tautz, H Reichert, B Mulloney, Birkhaüser Verlag, Basel, pp 407–415
116 Turrin MQA, Sawaya MI, Santos MCF, Veiga LV, Mantero F, Opocher G (1992) Comp Biochem Physiol 101A: 803–806
117 Valeggia C, Fernanadez-Duque E, Maldonado H (1989) Brain Res 481: 304–308
118 Van Beek E, De Loof A (1988) Comp Biochem Physiol 89A: 595–599
119 Van Deijnen JE, Vek F, Van Herp F (1985) Cell Tissue Res 240: 175–183
120 Van Herp F and Bellon-Humbert C (1982) C R Acad Sci Paris 295 Ser III: 97–102
121 Van Wormhoudt A, Favrel P, Guillaume J (1989) J Comp Physiol 159B: 269–273
122 Van Wormhoudt A, Fouchereau-Peron M (1987) Biochem Biophys Res Comm 148: 463–470
123 Watabe S, Hara M, Yago N (1985) Zool Sci (Tokyo) 2: 971
124 Yano I (1985) Aquaculture 47: 223–229
125 Yano I (1987) Aquaculture 61: 49 57
126 Young NH, Quinlan PT, Goad LJ (1992) Gen Comp Endocrinol 87: 300–311
127 Zukowska-Arendarczyk M (1981) Marine Biol 63: 241–247

ZOOLOGICAL SCIENCE 10: 31–37 (1993)

REVIEW

Loss of the Paternal Mitochondrion during Fertilization

CHARLES C. LAMBERT[1] and DAVID E. BATTAGLIA[2]

[1]*Department of Biology California State University Fullerton, CA 92634, and*
[2]*Department of Obstetrics and Gynecology SJ-70 University of Washington Medical School Seattle Washington 98195, U.S.A.*

INTRODUCTION

"If any apology is needed for presenting so strictly a morphological study of such an apparently threadbare subject as the fertilization of the ovum, I might say that the impulse to make it came from an experimental study ...." [22].

Spermatozoa are small cells specialized for the single function of delivering the haploid sperm nucleus to the egg and aiding in inserting this genome into the egg. As a specialized delivery vehicle, the sperm cell loses most of its original cytoplasm during spermatogenesis, leaving us with a basic means of locomotion (generally a tail with a functional axoneme), the nucleus and a means of generating ATP, the mitochondrion or several small mitochondria. Most sperm are divided into three functional regions: head with nucleus and acrosome, midpiece with mitochondria and tail with central axoneme [13, 15, for reviews].

Although the paternal mitochondrion generally makes no genetic or functional contribution to the zygote [5, 8], in most animals the sperm mitochondrion or multiple mitochondria enter the egg along with the nucleus, centriole and tail during fertilization [23 for review]. This occurs even though most of the spermatid mitochondria are shed during spermiogenesis. Here we review the apparently rare cases where the sperm mitochondrion is eliminated during fertilization. Hopefully this will foster additional interest in this area and additional cases will be uncovered. This process which often involves mitochondrial sliding along the sperm tail, occurs sporadically through-out the animal kingdom in such evolutionarily distant organisms as polychaetes and ascidians.

Received September 16, 1992

Annelida

Lillie [22] appears to have been the first to call attention to loss of the paternal mitochondrion during the fertilization of animal eggs. He studied fertilization in the polychaete worm *Nereis limbata* and demonstrated that the sperm mitochondrion remains on the egg surface after sperm incorporation into the egg. The sequence of fertilization in this species begins with sperm binding to the egg vitelline coat (VC) *via* attachment of the tip of the acrosome. The egg reacts to sperm contact within 2–3 min by releasing egg jelly from its cortical granules and forcing supernumerary sperm from the VC surface. Subsequently a fertilization cone forms at the site of contact with the fertilizing sperm. The fertilization cone disappears leaving the sperm on the the egg surface until 40–50 min after insemination when it is rapidly internalized by the egg. The midpiece with its mitochondrion remains on the egg surface (Fig. 1)

A similar process occurs in another polychaete, *Platynereis megalops* [14]. Here fertilization is internal following copulation and the eggs are extruded with sperm attached and the jelly forming. Penetration, as in *Nereis* requires over 30 minutes and results in the midpiece being left on the egg surface after the completion of sperm penetration. However, the large fertilization cone seen during *Nereis* fertilization is not formed in this

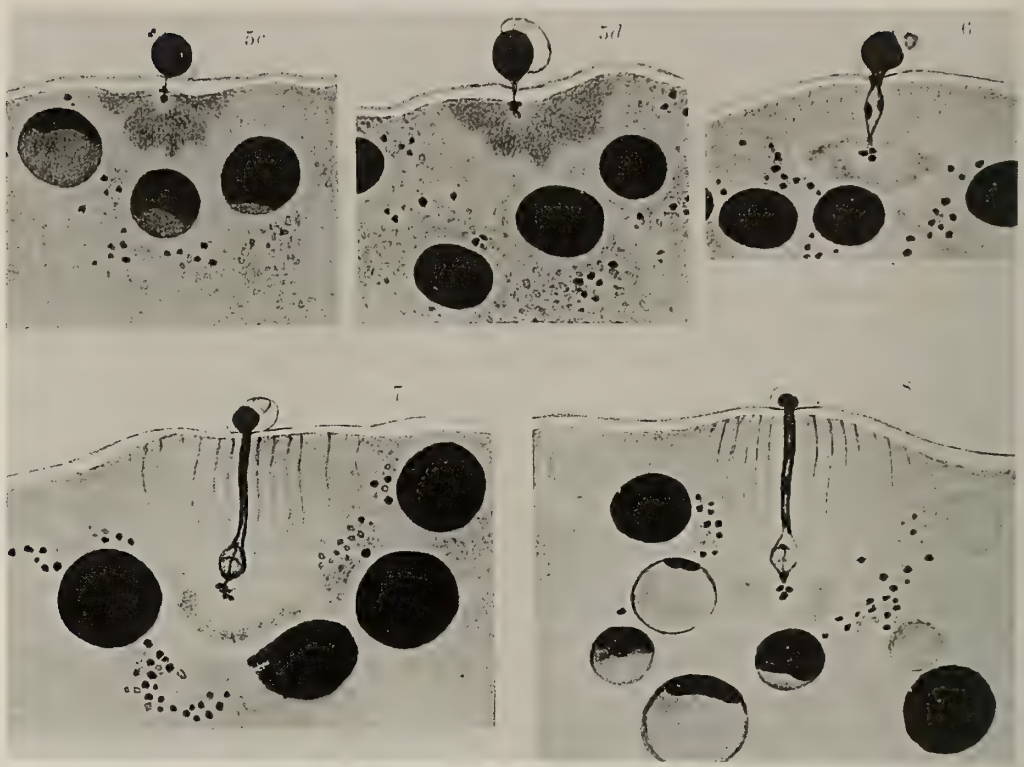

Fig. 1. Fertilization in the polychaete *Nereis limbata* (22) showing the sperm head and tail entering the egg and leaving the mitochondrion on the surface of the vitelline coat.

species.

In all other known cases of fertilization the sperm mitochondrion enters the fertilization cone and is taken into the zygote cytoplasm [23].

Mollusca

During the fertilization of most molluscs the sperm mitochondrion enters the egg and may even persist in the egg cytoplasm [24]. The sperm mitochondrial genome seems to be inherited to a high degree in the bivalve *Mytilus edulis* [10, 35] but this is clearly not the general case in bivalves.

Chitons with their heavily sculptured egg hulls have evolved a unique way to fertilize the egg without forcing the wide midpiece through the VC [1]. Chiton sperm are typical primitive sperm except for the locations of the mitochondria where one lies lateral to the nucleus as in the ascidian sperm and the other encircles the base of the nucleus [1]. In *Tonicella lineata* the sperm passes into cupules in the hull which give the sperm access to the underlying VC. Sperm-egg fusion occurs between the acrosomal membrane and an egg microvillus which penetrates into a pore in the VC. This composite tube formed from the fusion of the two membrane bound cylinders then serves as the connection through which the sperm chromatin mass is injected into the egg without even a nuclear envelope. This leaves the mitochondria and tail behind on the VC surface (Fig. 2).

Laternula limicola is a brackish water bivalve in which a golgi derived "temporary acrosome" moves from the sperm tip to the midpiece during spermatogenesis, finally taking up a position posterior to the mitochondrion in the midpiece [17]. During fertilization, the sperm first encounters a 24 μm thick jelly coat, then penetrates a 7 μm thick metachromatic layer before reaching the VC. The sperm then passes through the VC to the egg interior leaving the midpiece with its mitochondrion and temporary acrosome on the outside (Fig. 3). The temporary acrosome remains unchanged

throughout the entire process [17]. Another bivalve, *Lyonsia ventricosa* also has a temporary acrosome similar to that of *Laternula* [16] but we know of no studies of fertilization in this species.

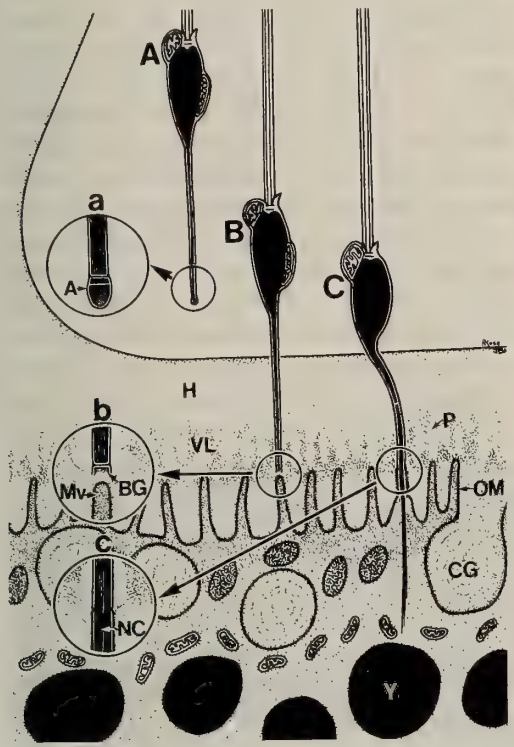

FIG. 2. Fertilization in the chiton *Tonicella lineata* (24). In this mollusc the sperm acrosome fuses with an egg surface microvillus and the nucleus is injected through the composite tube leaving the tail and 3 mitochondria on the egg surface.

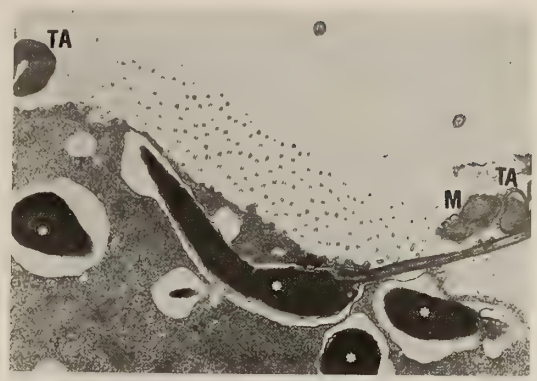

FIG. 3. Fertilization in the bivalve mollusc *Laternula limicola* (10). Here the mitochondrion (M) remains embedded in the vitelline coat with the "temporary acrosome" (TA) as the remainder of the sperm enters the egg cytoplasm.

Bryozoa

Both external and internal fertilization can be found in the bryozoans. In several brooded species fertilization occurs within the ovary during oogenesis. Markus [25] reported that only the nucleus enters the egg in several species, a finding confirmed by Matawari [26]. In a more detailed study, Temkin [31] found that sperm of *Dendrobeania lichenoides, Hippodiplosia insculpta* and *Tricellaria gracilis* leave both the midpiece and tail on the VC surface at fertilization; only the sperm head actually enters the oocyte. In another study [6], both the sperm nucleus and midpiece can be seen within the oocyte of *Chartella papyracea,* a species with precocious intra-ovarian fertilization. Thus there may be interspecific variation of

FIG. 4. Sperm penetration in the asteroid *Pisaster ochraceus* showing the usual pattern with the mitochondrion (arrow) entering the fertilization cone and egg.

whether the paternal mitochondrion is discarded or incorporated during the fertilization of bryozoans [31].

Echinodermata

In most echinoderms the sperm mitochondrion experiences a change in orientation at the time of the acrosome reaction [2, 29] but is generally incorporated into the egg during fertilization. Exceptions to this have been seen in a holothurian and an asteroid which seem to demonstrate facultative rather than obligatory sperm mitochondrial loss during fertilization. Colwin and Colwin [4] report that while the sperm mitochondrion usually enters the egg of the holothurian *Thyone briareus*, occasionally the midpiece remains outside as the sperm is incorporated.

In the asteroid *Pisaster ochraceus* careful observation reveals that there are three patterns of mitochondrial behavior during fertilization to be found among different males in the populations around San Juan Island, Washington [Battaglia, unpublished observations). In the most common pattern the head and midpiece remain intact and pass through the fertilization cone together (Fig. 4). Normally 9–12 min elapse from the time of initial sperm-egg fusion until the entire flagellum enters. The second pattern is seen with the sperm from about 30% of the males where most of their sperm enter the egg jelly, undergo the acrosome reaction, and enter the fertilization cone, but the midpiece becomes separated from the head and remains stationary in the jelly as the sperm moves past this fixed point (Fig. 5). An intermediate pattern is seen in a small number of cases where the midpiece becomes separated from the head and lags behind but is eventually captured by the fertilization cone and incorporated with the rest of

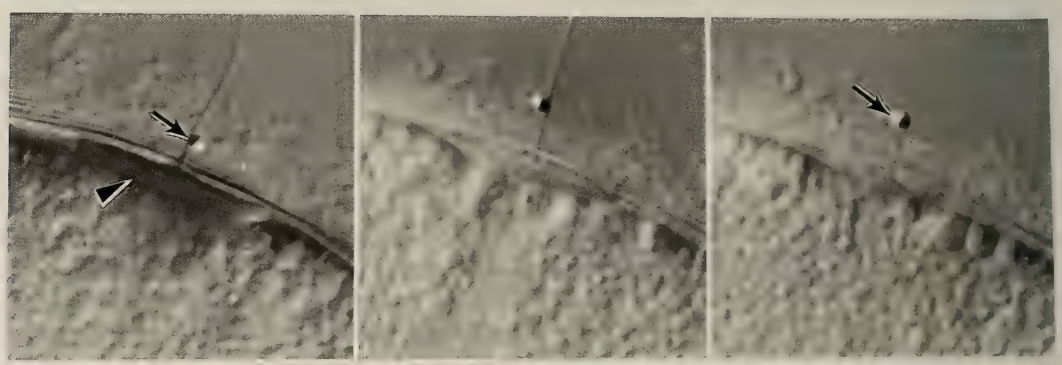

Fig. 5. Sperm penetration in the asteroid *Pisaster ochraceus* showing the case where the mitochondrion (arrow) remains on the surface of the vitelline coat. This pattern was seen in 30% of the males.

Fig. 6. Sperm penetration in the asteroid *Pisaster ochraceus* showing the case where the mitochondrion (arrow) separates from the nucleus but is eventually incorporated in the fertilization cone and taken into the egg cytoplasm.

the sperm (Fig. 6). These patterns were found in the sperm from different males and independent of the source of oocytes. Since these observations were made at the peak of the breeding season and led to perfectly normal development we conclude that they reflect normal modes of fertilization rather than testicular degeneration or some other pathological condition.

Urochordata

The fate of the sperm mitochondrion is now known for several members of the invertebrate complex commonly called the lower chordates. In the cephalochordate *Branchiostoma* the sperm has a well developed acrosome and a single mitochondrion in the midpiece. This mitochondrion clearly enters the egg at fertilization [11]. Although the sperm of the appendicularian tunicates is quite small it also has a well developed acrosome and as in cephalochordates the sperm mitochondrion enters the egg at fertilization (Linda Holland, 1992, personal communication).

Ascidian sperm lack a conspicuous acrosome and midpiece. Instead of a midpiece these sperm have the mitochondrion next to the nucleus in the head [20, for review of sperm structure]. The first detailed account of fertilization in ascidians reported that the mitochondrion entered the egg along with the nucleus and tail [27] but subsequent studies [7, 32, 33] report that sperm between the VC surface and egg surface lack the mitochondrion. Richard Cloney (personal communication, 1975 and 3) first observed the mitochondrion of *Molgula occidentalis* to remain on the VC surface as the sperm moved past this fixed point. This pattern of fertilization was subsequently seen in *Ascidia ceratodes* and other ascidians [9, 18, 19]. Figure 7 shows an *Ascidia ceratodes* sperm head within the inner layer of the VC surface while the mitochondrion remains on the outer surface of this layer between the follicle cells. Mitochondrial sliding can be induced in vitro by a number of treatments including alkaline SW and low Na^+ SW [18, 19]. Mitochondrial migration down the tail results in the sperm moving past this point when the sperm mitochondrion sticks to the cover slip *in vitro*. This sliding occurs at the rate of 6.7 μm/sec *in vitro* but 3.1 μm/sec *in vivo* into the egg and

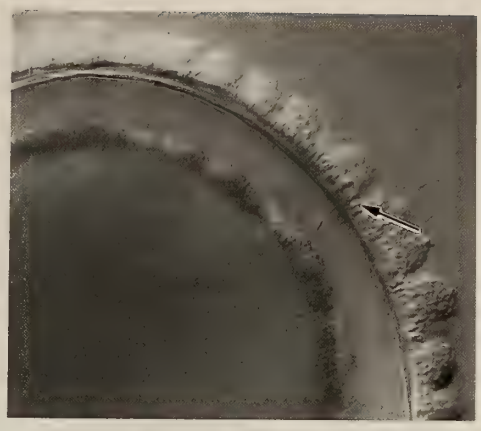

FIG. 7. Sperm penetration in the ascidian *Ascidia ceratodes*. Here the mitochondrion (arrow) remains on the vitelline coat surface between the follicle cells as the remainder of the sperm penetrates through the egg envelopes to reach the egg surface.

appears to be a rate limiting step in fertilization (Yim, Abadi and Lambert, unpublished data). Mitochondrial sliding is thought to drive the sperm through the VC and perivitelline space and into the egg [15, 20 for reviews]. In addition to the mechanical forces generated by mitochondrial sliding, sperm surface proteases are also involved [28 and Koch, Norton and Lambert, unpublished data].

Conclusions

The interplay between the physical and biochemical capabilities of the sperm and egg is instructive as to how the remarkable process of fertilization is accomplished. The management of sperm mitochondria during fertilization is rarely considered in studies of sperm-egg interaction. Generally it may be assumed that all of the mitochondria that survive in the zygote are of maternal origin. Thus, the prevention of paternal mitochondrial replication after fertilization may be a universal feature of all species. The importance of disposing of paternal mitochondria during fertilization is speculative; however, the mechanisms underlying the success of this phenomenon are interesting. Recent evidence suggests that mitochondrial DNA has an extremely high rate of mutation which may be exacerbated by free radical formation [34]. It is

clear that the sperm mitochondrion is a potent source of free radicals due to its extremely high metabolic activity. Thus, oxidative damage to the unprotected mitochondrial genome may be extensive in mature, active sperm. It is conceivable that this could result in inefficient/abnormal zygote mitochondria if the replication of these damaged organelles were allowed to occur after fertilization [12]. Most animal eggs appear to deal with this scenario by inactivating and destroying the sperm mitochondria after they have been incorporated into the egg cytosol. Fertilization in the mammal is a good example of a class of animals where active destruction of sperm mitochondria is mediated by the egg [30]. The complexity of the mammalian midpiece precludes its expulsion during sperm incorporation. It contains many mitochondria which rapidly swell and are destroyed upon entry into the egg cytosol. Thus, all mitochondria in the mammalian embryo are considered to be of maternal origin (although recent evidence suggests that 0.1% of human sperm mitochondria are replicated in the fertilized egg) [34].

However, the mechanisms attendant to the inactivation or destruction of mitochondria within the egg may not exist in all species, particularly in animals where mitochondrial expulsion is observed as described in this review. In these species it is the physical elimination of this organelle that prevents its incorporation into the egg, thereby avoiding any replication of the paternal mitochondrial genome. The results are the same, but the mechanisms that accomplish these phenomena may be different. For example, the ascidian sperm appear to have a complex mechanism that utilizes cytoskeletal elements in the sperm to actively expel the mitochondrial compartment [21]. In contrast, the expulsion of sperm mitochondria in some starfish and polychaetes utilizes a more passive approach; the physical constraints imposed by the egg extracellular matrix aid in holding the mitochondrial compartment in place while the rest of the sperm slides past. One unifying principle to all of these species is that so-called "primitive" sperm are involved, thereby suggesting that mitochondrial expulsion can only be accomplished in species possessing a simple sperm architecture.

REFERENCES

1 Buckland-Nicks J, Ross K, Chia FS (1988) Gamete Research 21: 199–212
2 Christen R, Schackmann RW, Shapiro BM, (1982) J Biol Chem 257: 14881–14890
3 Cloney RR (1989) Urochordata-Ascidiacea. In "Reproductive Biology of Invertebrates Vol IV Part B" Ed by Adiyodi and Adiyodi, Oxford and IBH, New Delhi, pp 391–451
4 Colwin LH, Colwin AL (1956) Biol Bull 110: 243–257
5 Dawid IB, Blackler AW (1972) Dev Biol 29: 152–161
6 Dryrynda PEJ, King PE (1983) J Zool Lond 200: 471–492
7 Ezell SD (1963) Exp Cell Res 30: 615–617
8 Giles RE, Blanc H, Cann HM, Wallace DC (1980) Proc Nat Acad Sci USA 77: 6715–6719
9 Godknecht, A, Honegger TG (1991) Dev Biol 143: 398–407
10 Hoeh WR, Blakley KH, Brown WM (1991) Science 251: 1488–1490
11 Holland LZ, Holland ND (1992) Biol Bull 182: 77–97
12 Hurst LD, Hamilton WD (1992) Proc Roy Soc Lond B 247: 189–194
13 Jamieson BG (1991) Fish evolution and systematics: evidence from spermatozoa Cambidge University Press, Cambridge
14 Just EE (1915) J Morph 26: 217–233
15 Koch RA, Lambert CC (1990) J EM Techniques 16: 115–154
16 Kubo M, Ishikawa M (1978) J Submicr Cytol 10: 411–421
17 Kubo M, Ishikawa M, Numakunai T (1979) Protoplasma 100: 73–83
18 Lambert CC (1989) J Exp Zool 249: 308–315
19 Lambert CC, Epel D (1979) Dev Biol 69: 296–304
20 Lambert CC, Koch RA (1988) Develop Growth Diff 30: 325–336
21 Lambert CC, Lambert G (1984) Dev Biol 106: 307–314
22 Lillie FR (1912) J Exp Zool 12: 413–459
23 Longo FJ (1987) "Fertilization" Chapman and Hall, New York
24 Longo FJ, Anderson E (1969) J Exp Zool 172: 97–119
25 Markus E (1938) Bryozarios marinhos brasieleros II. Univ Sao Paulo Fac Filos Cien Let, Bol Zool 2: 1–196
26 Matawari S (1952) Misc Rep Res Inst Nat Resour (Tokyo) 28: 17–27
27 Meves F (1913) Archiv Mikroschkop Anat 82: 215–260

28 Pinto MR, Hoshi M, Marino R, Amoroso A, De Santis R (1990) Molec Repro Dev 26: 319–323
29 Schroeder TE, Christen R (1982) Exp Cell Res 140: 363–371
30 Szollosi DG (1965) J Exp Zool 159: 367–378
31 Temkin M (1991) Fertilization and early development of gymnolaemate bryozoans Ph D Dissertation University of Southern California
32 Ursprung H, Schabtach E (1965) J Exp Zool 159: 379–384
33 Villa L (1977) Acta Embryol Exp 2: 179–193
34 Wallace DC (1992) Science 256: 628–632
35 Zouros E, Freeman, KR, Ball AO, Pogson, GH (1992) Nature 359: 412–414

ZOOLOGICAL SCIENCE 10: 39–42 (1993)

Immunocytochemical Evidence for the Involvement of RFamide-like Peptide in the Neural Control of Cricket Accessory Gland

Kouji Yasuyama[1], Bin Chen[2] and Tsuneo Yamaguchi[2*]

[1]*Department of Biology, Kawasaki Medical School, Kurashiki 701-01, and*
[2]*Department of Biology, Faculty of Science, Okayama University, Okayama 700, Japan*

ABSTRACT—Using anti-RFamide antiserum, innervation of the accessory gland of the male cricket was investigated. RFamide-like immunoreactive fibers were found over the musculature of this organ, i.e., in the thin muscle winding around each glandular tubule as well as in the thick muscle surrounding the opening of each tubule to the ejaculatory duct. This result suggests that in addition to the previously reported proctolinergic system, another peptidergic system mediated by an RFamide-like substance is involved in regulation or modulation of contractile activity of the accessory gland.

INTRODUCTION

Spermatophore formation in the male cricket requires the rapid release of ingredients produced by the accessory gland at a certain period in the mating cycle [7]. This implies that contraction of the muscles of the accessory gland to extrude the secretions may be directly triggered by neural signals. In our previous morphological and electrophysiological investigations it was shown that the accessory gland is innervated by two types of neurons originating in the terminal abdominal ganglion [5, 11, 12]. The first type is the dorsal unpaired median neuron (DUMR7 neuron), which induces contraction of the accessory gland [5] and has a proctolin-like immunoreactivity [12]. The second type is the ordinary paired neuron (LC neuron), which has an inhibitory effect on the contraction of the accessory gland, and is likely to be serotonergic [5].

Recent investigations indicate FMRFamide immunoreactive fibers innervating the midgut of *Drosophila* larvae [8] and the dual peptidergic innervation of the blowfly hindgut by proctolin, FMRFamide and related peptides [2]. In the locust, FMRFamide and related peptides were shown to have modulatory effects on the oviduct [6], on the heart [3], and on the foregut [1]. In the isolated locust foregut, FMRFamide was reported to potentiate relaxation induced by serotonin and to inhibit the contraction caused by proctolin [1,9].

The present report describes the presence of FMRFamide immunoreactive fibers innervating the glandular tubules of the cricket accessory gland, suggesting that an RFamide-like peptide has an important role in regulation or modulation of contractile activity of the accessory gland.

MATERIALS AND METHODS

Adult male crickets (Gryllus bimaculatus) reared in the laboratory, were used for the experiments. The accessory glands were fixed for 6–12 hr in 4% paraformaldehyde in 0.1 M phosphate buffer at 4°C. Rabbit anti-FMRFamide antiserum (Cambridge Research Biochemical) used for this experiment is specific to the C-terminal (RFamide), and positive reaction to this antiserum demonstrates the existence of RFamide-like peptides. Antiserum was diluted 1 : 2000 in phosphate buffered saline [5] (PBS, pH 7.4) with 0.5% Triton X-100 and 0.5% bovine serum albumin (BSA).

Light microscopic immunocytochemistry was employed using the avidin-biotin-peroxidase complex (ABC, Vector Lab.) method as described by Yasuyama et al [12]. Paraffin sections were incu-

Accepted September 22, 1992
Received September 2, 1992
2* To whom reprint requests should be sent:

bated in primary antiserum for 48 hr at 4°C. The secondary antibody, a biotinylated goat anti-rabbit IgG, was applied to the sections at a 1 : 200 dilution in PBS for 1 hr at room temperature. Incubation in the PBS-diluted ABC reagent (1:100) was for 1 hr at room temperature. Each incubation was followed by three 10 min washes in PBS. The peroxidase activity was visualized by treatment with 0.05 M Tris buffer (pH=7.2) containing 0.025% 3,3′-diaminobenzidine tetrahydrochloride (Sigma) and 0.005% H_2O_2. The sections were dehydrated and mounted in Canada Balsam. For whole mounts, the accessory glands were incubated in the primary antiserum for 72 hr at 4°C. Each of the solutions of the secondary antibody (1 : 200) and the ABC reagent (1 : 100) was applied for 8–10 hr at 4°C. Each incubation was followed by 12–24 hr wash in PBS. After visualization of the peroxidase activity, the preparations were dehydrated and mounted.

For electron microscopic immunocytochemistry, the post-embedding protein A-gold method was employed as described by Yasuyama et al [12]. Ultrathin sections were incubated in primary antiserum for 48 hr at 4°C. The protein A-gold complexes (Janssen Pharmaceutical; particle size 15 nm) were applied at a concentration of 1 : 40 in PBS with 1% BSA. The sections were stained with uranyl acetate and lead citrate, and were examined with a Hitachi H 500 electron microscope.

The specificity of the immunoreactivity was tested by preincubating the anti-RFamide antiserum with synthetic FMRFamide (Funakoshi). The test peptide was added at 10^{-4} M concentration to the working dilution (1 : 2000) of antiserum, and the solution was incubated for 24 hr at 4°C. Immunoreactivity was eliminated by such treatment.

RESULTS AND DISCUSSION

The accessory gland of the male cricket is comprised of more than 600 slender tubules arising from the lobed anterior end of the ejaculatory duct. Single-layered thin muscles wind around most of each glandular tubule's length, and multi-layered thick muscles surround the opening of each tubule to the ejaculatory duct [11]. On the basis of the arrangement of these two types of muscles, it is likely that the antagonistic action of muscles, i.e. the contraction of single-layered muscles and relaxation of multi-layered muscles, causes the release of the secretions into the ejaculatory duct. RFamide-like immunoreactive fibers were found in both single- and multi-layered muscles (Figs. 1 and 2). In the single-layered muscles associated with a glandular tubule, the immunoreactive fibers had many varicosities and ran rather straightly along the tubule's long axis to the distal end. Projection of short thin branches from the thick fibers were observed at rather regular intervals (Fig. 1). In the multi-layered muscles surrounding the opening of each tubule, the RFa-like immunoreactive fibers ran tortuously among the muscle fibers. Figure 2 shows the immunoreactive fibers circularly arranged around the glandular tubule.

Electron microscopic immunocytochemistry revealed the widely distributed RFa-like immunoreactive axons in the accessory gland muscles. RFamide-like immunoreactivity was restricted to large electron-dense granular vesicles with a mean diameter of 141.9 nm (n=56) contained in the axons (Fig. 3). This immunoreactivity was also found in granular vesicles (141.5 nm in mean diameter, n=86) accumulated in the nerve branch (Br3) after ligation ([11]; data not shown). Our earlier investigations have revealed that Br3 carries innervation from the terminal abdominal ganglion to the accessory gland, and ligation of Br3 causes a heavy accumulation of large electron-dense granular vesicles [11, 12]. It is, therefore, suggested that RFa-like immunoreactive granular vesicles found in the accessory gland musculature are transported through the Br3.

Our recent investigation using the protein A-gold method combined with retrograde HRP labeling showed that proctolin-like immunoreactivity is present in the DUMR7 neurons innervating the accessory gland musculature [12]. The RFa-like immunoreactive fibers demonstrated in this experiment are probably derived from neurons which are distinct from the DUMR7 neurons. This conclusion is based on the following facts. First, the size of the vesicles with proctolin-like immunoreactivity found in the axons associated with the acces-

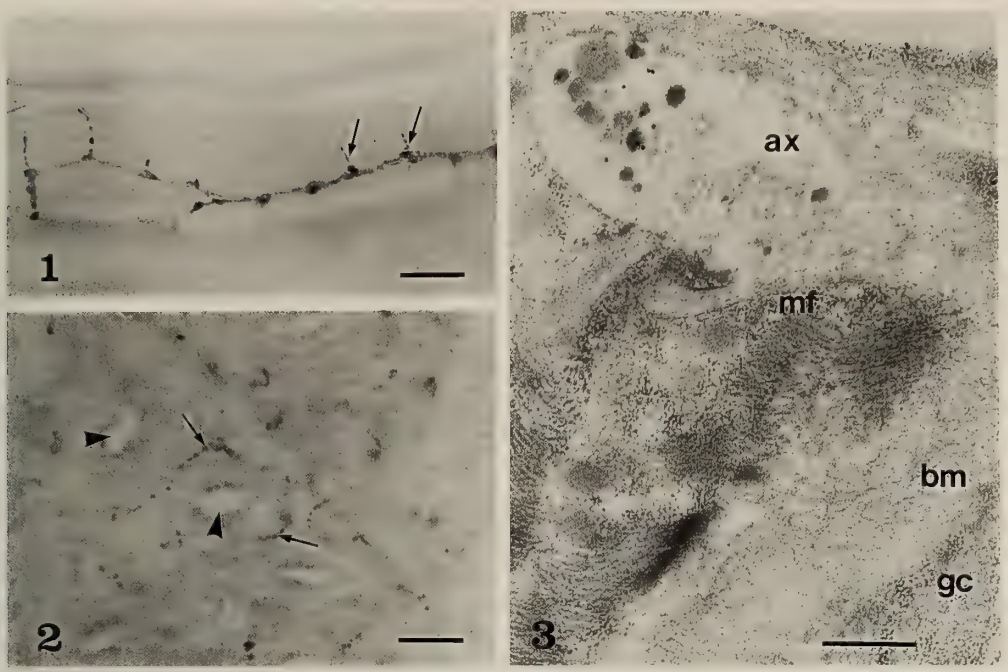

FIG. 1. RFamide-like immunoreactive fibers in a wholemount preparation of a glandular tubule of the accessory gland. Note projection of short thin branches (arrows) from the thick immunoreactive fibers. Scale bar, 20 μm.

FIG. 2. RFamide-like immunoreactive fibers (arrows) within the proximal part of the accessory gland tubule, where multi-layered muscle fibers are located. Arrowheads indicate the lumen of the glandular tubule. Scale bar, 20 μm.

FIG. 3. An axon (ax) containing RFamide-like immunoreactive vesicles and running within the single-layered muscle (mf) which envelops the accessory gland tubule. Immunogold labeling was restricted to the vesicles. bm, basement membrane; gc, glandular cell. Scale bar, 0.5 μm.

sory gland musculature was 100–115 nm in diameter, while the RFamide-like immunoreactivity was restricted to the vesicles with a diameter of about 140 nm. Second, the anti-RFamide antiserum did not stain the DUMR7 neurons, but did stain the bilaterally symmetrical neurons in the terminal abdominal ganglion [10]. These suggest that a separate peptidergic innervation is supplying the accessory gland, and not only proctolin but also FMRFamide-like peptide have important roles in regulation or modulation of neuro- or myogenic activities.

In the locust, Evans and Cournil have described a pair of FLRF-like immunoreactive neurons, which are located in the suboesophageal ganglion and send their axons through the ventral nerve cord to the terminal abdominal ganglion and further, in the male locust, to the genital nerve arising from this ganglion [4]. In the locust there is, also, a possibility that the RFa-like immunoreactivity fibers found in the accessory gland musculature derive from the neurons located in the higher ganglion. Furthermore, a possibility that the RFamide-like peptide is contained in the LC neurons cannot be eliminated, since anti-RFamide antiserum revealed the lateral cluster of neurons around the site where the LC neurons were located in a cluster (Yasuyama, unpublished observation). Further experiments are being carried out both to identify the RFa-like immunoreactive neurons innervating the accessory gland and to elucidate their functional roles in regulation of the mechanical activity of the accessory gland.

ACKNOWLEDGMENTS

This work was supported in part by a Grant-in-Aid from the Ministry of Education, Science and Culture of Japan.

REFERENCES

1 Banner SE, Osborne RH (1989) Modulation of 5-HT and proctolin receptors by FMRFamide in the foregut of the locust *Schistocerca gregaria.* J Insect Physiol 11: 887–892

2 Cantera R, Nässel DR (1991) Dual peptidergic innervation of the blowfly hindgut: a light- electron microscopic study of FMRFamide and proctolin immunoreactive fibers. Comp Biochem Physiol 99C: 517–5251

3 Cuthbert BA, Evans PD (1989) A comparison of the effects of FMRFamide-like peptides on locust heart and skeletal muscle. J exp Biol 144: 395–415

4 Evans PD, Cournil I (1990) Co-localization of FLRF- and vasopressin-like immunoreactivity in a single pair of sexually dimorphic neurones in the nervous system of the locust. J Comp Neurol 292: 331–348

5 Kimura T, Yasuyama K, Yamaguchi T (1089) Proctolinergic innervation of the accessory gland in male cricket (*Gryllus bimaculatus*): detection of proctolin and some pharmacological properties of myogenically and neurogenically evoked contractions. J Insect Physiol 35: 251–264

6 Lange AB, Orchard I, Te Brugge VA (1991) Evidence for the involvement of a SchistoFLRF-amide-like peptide in the neural control of locust oviduct. J Comp Physiol A 168: 383–391

7 Loher, W. (1974) Circadian control of spermatophore formation in the cricket *Teleogryllus commodus* Walker. J. Insect Physiol 20: 1155–1172.

8 White K, Hurteau T, Punsal P (1986) Neuropeptide-FMRFamide-immunoreactivity in Drosophila: development and distribution. J Comp Neurol 247: 430–438

9 Wood SJ, Osborne RH, Casttell KJ, Banner ST (1990) FMRFamide and related peptides modulate the actions of 5-hydroxytryptamine and proctolin on the foregut of the locust, *Schistocerca gregaria.* Biochem Soc Trans 18: 384–385

10 Yasuyama K, Chen B, Yamaguchi T (1992) Comp Physiol Biochem 9: 224

11 Yasuyama K, Kimura T, Yamaguchi T (1988) Musculature and innervation of the internal reproductive organs in the male cricket, with special reference to the projection of unpaired median neurons of the terminal abdominal ganglion. Zool Sci 5: 767–780

12 Yasuyama K, Kimura T, Yamaguchi T (1992) Proctolin-like immunoreactivity in the dorsal unpaired median neurons innervating the accessory gland of the male cricket, *Gryllus bimaculatus.* Zool Sci 9: 53–64

ZOOLOGICAL SCIENCE 10: 43–51 (1993)

Developmental and Pharmacological Studies of Acetylcholinesterase-defective Mutants of *Caenorhabditis elegans*

Y. Kamiya, S. Harada, S. Okoyama[1], H. Yamamoto and R. Hosono[2]

Department of Biochemistry, and [1]Department of Anatomy, School of Medicine, Kanazawa University, Kanazawa, Ishikawa 920, Japan

ABSTRACT—Three genes (*ace-1, ace-2,* and *ace-3*), which code for acetylcholinesterase (class A, B, and C) have been identified in the nematode *Caenorhabditis elegans*. Here we investigate the developmental and pharmacological properties of mutants retaining only one of distinct classes of acetylcholinesterase. Both class A and B acetylcholinesterases share about one-half of the total enzyme activity throughout development and maximum specific activity at the first larval stage, and are sufficient for maintaining normal acetylcholine levels. Although class B acetylcholinesterase is distributed at the head and the body region as seen in the wild type, the class A enzyme is biased towards the head region. Class C acetylcholinesterase occupies only a few percent of the total activity, is mainly distributed in the body, shows maximum specific activity at the late larval stage and is clearly different in pharmacological response from class A and B acetylcholinesterases. We propose that class B is the major acetylcholinesterase, and that classes A and C are supplementary.

INTRODUCTION

Acetylcholinesterases (AChE) have been extensively studied in various organisms (for reviews, see [5, 13]). It has been proposed that the enzyme has roles additional to the hydrolysis of acetylcholine (ACh), such as the regulation of membrane excitability, permeability, general metabolism or the inactivation of neuropeptides. However, many problems remain to be solved, for example, why the enzyme is present in neurons which has neither choline acetyltransferase, the synthetic enzyme for ACh, nor any identified cholinergic input, and in neurons, which use transmitters other than ACh. These findings raise the question of what role AChE would be playing in noncholinergic cells.

Caenorhabditis elegans is a desirable organism for such studies [15]. Because genetic and biochemical properties of AChE are extensively studied [3, 8, 10]. In *C. elegans,* three genes relating to AChE activity have been identified: *ace-1, ace-2* and *ace-3*. These three classes of AChE (A, B, and C) corresponding to the three *ace-1, ace-2,* and *ace-3* genes have been characterized biochemically, molecularly and genetically [9, 12]. Mutations of any of the three *ace* genes do not result in any visible defects. In the *ace-1 ace-2* double mutant, movement is abnormal and the *ace-1 ace-2 ace-3* triple mutant is lethal at the post-embryonic stage [3, 8, 10]. Therefore, any one of the three *ace* genes is sufficient for survival, and *ace-1* or *ace-2* are necessary for normal movement.

Although much is known about the kinetic properties of the three classes of AChE, the developmental or pharmacological differences among them are not understood. To elucidate the functional role of each class of AChE, we studied the developmental changes in AChE activity in relation to enzyme localization and ACh levels. Several organophosphates inhibit *C. elegans* AChE activity but the correspondence between the extent of the enzyme inhibition and the fatal effect is not always coincident [9]. The relationship between enzyme inhibition and pharmacological action has not yet been systematically studied. An organophosphate, trichlorfon {(2,2,2-trichloro-1-hy-

Accepted September 24, 1992
Received August 24, 1992
[2] To whom correspondence should be addressed.

droxyethyl)-phosphonic acid dimethyl ester], is a potent nematocide, which probably functions by inhibiting AChE. We studied the response to trichlorfon of mutants defective in two of three *ace* genes. Our experiments indicate that class A and class B AChE have similar properties but class C AChE is greatly different from the two classes AChE in expression, distribution and response to organophosphates. In addition, we describe that class B AChE is indistinguishable from the wild type in distribution and the staining intensity, suggesting that class B is the major AChE of the three.

MATERIALS AND METHODS

Nematode strains. The following genes and mutations were provided from J.Rand (Oklahoma Medical Research Foundation, USA): *ace-1* (*p1000*) X, *ace-2* (*g72*) I, *ace-3* (*dc2*) II, *ace-1* (*p1000*) *ace-2* (*g72*), *ace-2* (*g72*) *ace-3* (*dc2*), *ace-3* (*dc2*) *ace-1* (*p1000*). *C. elegans* was cultured on NGM agar as described by Brenner [2], except that in some cases, a higher concentration of bactopeptone (20 mg/ml) was added to the medium.

Histochemical staining of AChE. AChE in whole mounts of nematodes was stained by the modified method developed by Karnovsky and Roots [11] and by Culotti *et al.* [3]. Nematodes, permeabilized with 95 % acetone and extensively washed, were suspended in a mixture of 10 mg acetylthiocholine iodide, 65 ml 100 mM malate buffer(pH 6.0), 0.5 ml 100 mM sodium citrate, 1 ml 30 mM $CuSO_4$, 1 ml H_2O and 1 ml 5 mM potassium ferrocyanide, and were shaken at 37°C for 30 min. The reaction was stopped by diluting and washing. A DAB-nickel solution(3,5-diaminobenzoic acid 4 mg, ammonium nickel 60 mg, and 10 ml 10 mM Tris(pH 7.6)) containing 0.003% H_2O_2 were added and shaken for 3 min at room temperature to intensify the staining. The DAB-nickel was removed and the slides were washed several times with 10 mM Tris (pH 7.6).

Acetylcholinesterase assays. Organisms were suspended in two volumes of 50 mM Tris pH 7.6 and 0.03% Triton X-100 and homogenized in liquid nitrogen. The homogenates were mixed with class specific assay mixtures [10] as follows. Wild-type AChE was assayed in 95 mM sodium phosphate buffer (pH 8.0), 0.32 mM 5-dithiobis-2-nitrobenzoic acid and 0.47 mM acetylthiocholine iodide. In addition to this assay mixture, 0.13% deoxycholate for assay of class A AChE and 0.03% Triton X-100 for class B AChE, and 0.03% Triton X-100, 0.013% deoxycholate and 2.5 μM neostigmine bromide for class C AChE were added. The final reaction volume was 1585 μl. The reaction was started by adding the homogenate at 25°C and the absorbance at 412 nm was read [4]. Homogenates from the *ace-1 ace-2* mutants were added to a final concentration of 0.3 mg/ml and from the remaining strains, of 0.03 mg/ml.

Acetylcholine assay. Acetylcholine was assayed by the enzymatic conversion of ACh to [^{32}P] choline in the presence of [γ-^{32}P] ATP, acetylcholinesterase and choline kinase [14].

Assay of paralysis and its recovery. Worms were suspended in M9 buffer containing trichlorfon. Paralysis was followed by measuring the frequency of propagating waves along their bodies as described elsewhere [6]. For recovery, completely paralyzed worms were washed with M9 buffer and resuspended in the buffer.

RESULTS

Developmental changes in AChE activity

Changes in the activity of each class AChE with development were compared (Fig. 1). Class A and B AChE activities were maximum at the first larval (L1) stage and the activity decreased gradually with the progress of development. Class C AChE occupied less than 2% of the total AChE throughout development and reached the maximum activity at the later larval stage. Thus, the synthesis of the class C enzyme might be differently regulated from that of the other two.

Developmental changes in AChE distribution

To determine a more detailed developmental pattern of AChE expression, organisms were

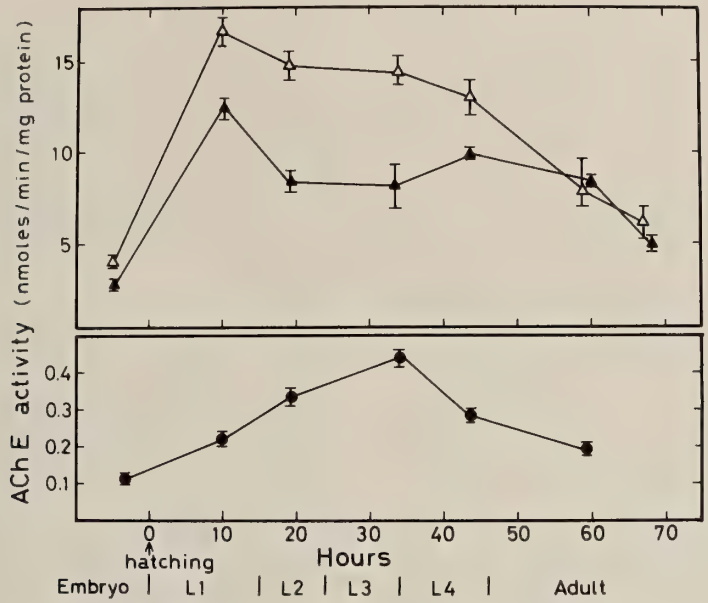

FIG. 1. Changes in AChE activities throughout development. Organisms were homogenized and suspended in the class-specific AChE mixtures [8]. AChE activity was measured at 25°C by the thiocholine method [11]. The embryonic stage is arbitrarily plotted. The mean values of three assays are presented with bar for standard deviation. *ace-2* (*g72*) *ace3* (*dc2*) (▲), *ace-3* (*dc2*) *ace-1* (*p1000*) (△), *ace-1* (*p1000*) *ace-2* (*g72*) (●).

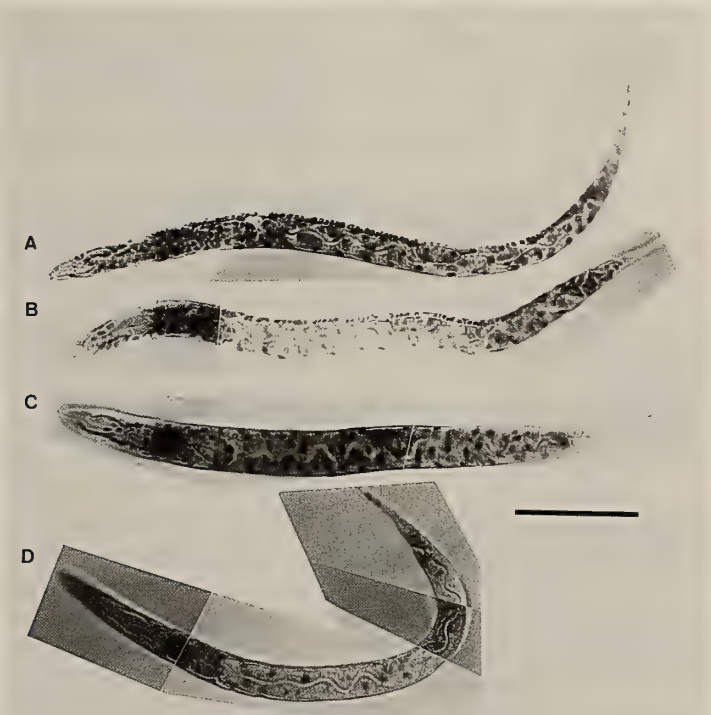

FIG. 2. AChE staining of the second stage larvae. Wild type (A), *ace-2* (*g72*) *ace-3* (*dc2*) (B), *ace-3* (*dc2*) *ace-1* (*p1000*) (C), *ace-1* (*p1000*) *ace-2* (*g72*) (D). Animals are oriented anterior side to the left and the ventral side on top. Bar=100 μm.

stained with acetylthiocholine by the method of Karnovsky and Roots [11]. Culloti *et al.* [3], who pioneered AChE staining with *C. elegans,* found that AChE was abundant in nearly all cells at the early larval stage, then was reduced gradually, but remained mainly in the area of the nerve ring, ventral ganglion, the pharyngeo-intestinal valve and the tail neural region as development progressed. We obtained the same results with the wild-type animal and compared the changes in the staining pattern of the three distinct classes of AChE with the *ace* double mutants from embryo to adult. Representative staining of the second stage larva is shown (Fig. 2). The AChE staining was first detectable on one of two-blastomeres and increased to stable, high levels in all blastomeres at around the 24-cell stage (data not shown). AChE expression in the three double mutants approximately coincided with that of wild type, though the extent of the staining differed. In the newly hatched wild-type larva, nearly all somatic cells and the nerve ring were intensely stained (Fig. 6 A-D). In the *ace-3 ace-1* double mutant, the staining pattern was similar to that of wild type. In the *ace-2 ace-3* double mutant, the head region was stained as in wild type but the body region was less intensely stained. In the *ace-1 ace-2* mutant, the non-neural cells were scarcely stained but the nerve ring and the ventral nerve cord were detectably stained. At the second larval stage in all strains, nonneuronal cells were weakly stained but that of neuronal cells remained intense (Fig. 2). The staining intensity of the positive regions between *ace* mutants was similar to that of the first larval stage.

Developmental changes in ACh levels

At three developmental stages, the ACh levels of three mutants were compared with those of wild-type animals (Fig. 3). The ACh levels in the wild type were high at the larval stage, but decreased to about 25% at the adult stage. ACh levels of the *ace-2 ace-3* and the *ace-3 ace-1* mutants were similar to those of wild-type animals. In the *ace-1 ace-2* mutant, abnormal elevation of ACh was observed at the adult stage, though it was normal at the early larval stage. Therefore, class A and B AChE are sufficient but class C AChE is insufficient for maintaining normal ACh levels.

Inhibition of AChE by trichlorfon

Of the organophosphates tested, trichlorfon was

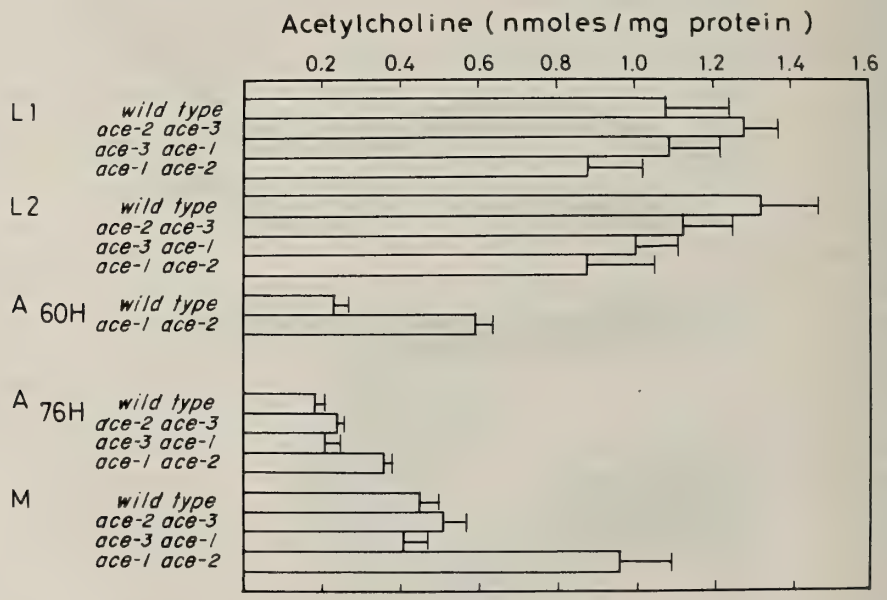

FIG. 3. Changes in ACh levels of wild type and *ace* double mutants. The indicated time at the adult stage means hours after hatching. L1, first stage larva; L2, second stage larva; A, adult; M, asynchronous population. Standard deviations of mean values of three assays are indicated by vertical bars.

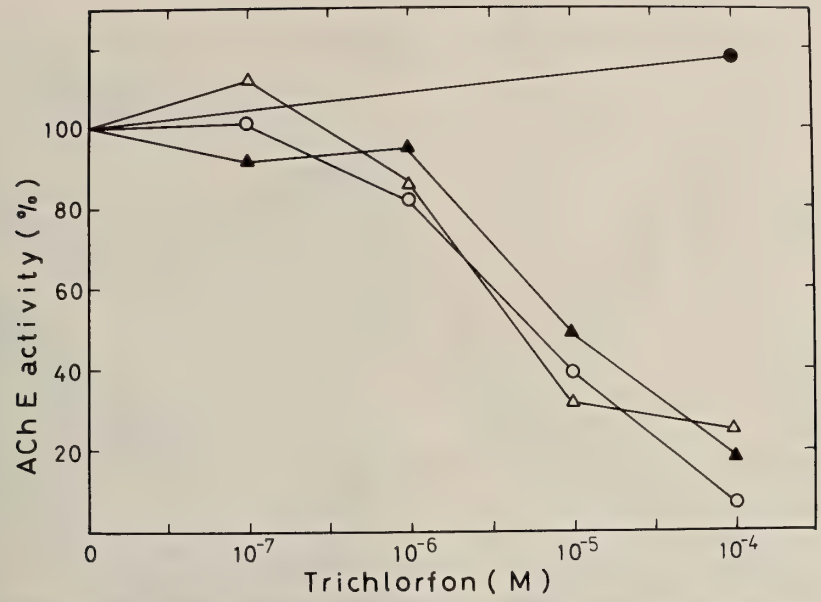

FIG. 4. Inhibition of three classes AChE by trichlorfon. Wild type (○), *ace-2* (*g72*) *ace-3* (*dc2*) (△), *ace-3* (*dc2*) *ace-1* (*p1000*) (▲), and *ace-1* (*p1000*) *ace-2* (*g72*) (●).

the most prominent nematocide [7]. Although several organophosphates have been identified as AChE inhibitors, trichlorfon has not yet been tested [9, 12]. As shown in Figure 4, crude extracts of class A and B AChE were similarly inhibited but class C AChE was not, at the concentrations of trichlorfon tested.

Survival sensitivity of ace *mutants to trichlorfon*

Survival of the *ace* mutants was tested in the presence of trichlorfon (Table 1). Wild-type animals failed to propagate their progeny above 20 μM trichlorfon. Mutation of the *ace-1* or *ace-2* genes did not influence survival. However, mutation of the *ace-3* gene brought about much higher sensitivity to the drug. These results suggest that the trichlorfon sensitivity of wild-type animals is determined by the class C AChE that is encoded by the *ace-3* gene. This hypothesis was tested with mutants preserving one of the three *ace* genes. The sensitivity of the *ace-1 ace-2* double mutant did not differ from that of the wild-type. However, both the *ace-3 ace-1* and the *ace-2 ace-3* mutants were hypersensitive to trichlorfon, supporting the above hypothesis. The *ace-2 ace-3* mutants were slightly but reproducibly more sensitive to trichlorfon than the *ace-3 ace-1* mutants.

TABLE 1. Sensitivity of *ace* mutants to trichlorfon

Mutations	Trichlorfon μM
wild type	20
ace-1 (*p1000*)	20
ace-2 (*g72*)	20
ace-3 (*dc2*)	2
ace-2 (*g72*) *ace-3* (*dc2*)	1
ace-3 (*dc2*) *ace-1* (*p1000*)	2
ace-1 (*p1000*) *ace-2* (*g72*)	40

To determine sensitivity, three fourth stage larvae were put onto NGM agar plates containing various concentrations of trichlorfon (0, 0.4, 1.0, 2.0, 4.0, 10, 20, 40 and 100 μM) and grown at 20°C. The highest concentration of trichlorfon is indicated in which worms, in triple experiments, produced F_2 progeny within ten days.

Paralytic sensitivity of ace *mutants to trichlorfon*

When *C. elegans* was exposed to trichlorfon, the animals gradually became immovable. The pattern of trichlorfon-induced paralysis differed in each *ace* double mutant (Fig. 5). Animals retaining only the *ace-3* genes were slowly paralyzed as

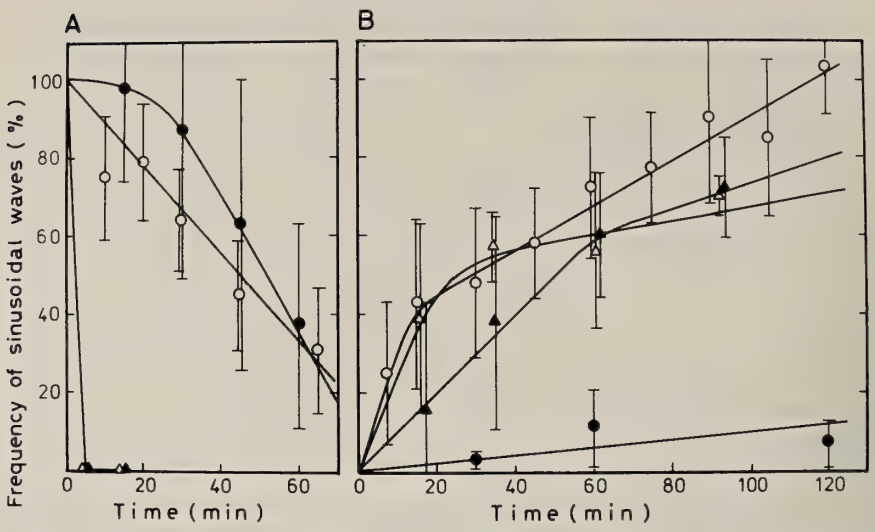

FIG. 5. Paralysis by trichlorfon and recovery. (A) Newly hatched larvae were exposed to 1 mM trichlorfon and changes in the sinusoidal frequency were followed. (B) Recovery from the paralysis was followed after an extensive wash of the completely paralyzed worms. The sinusoidal activity of each strain means a relative value to that prior to trichlorfon exposure. The mean values of seven worms are presented with bar for standard deviation. Wild type (○), *ace-2* (*g72*) *ace-3* (*dc2*) (△), *ace-3* (*dc2*) *ace-1* (*p1000*) (▲), and *ace-1* (*p1000*) *ace-2* (*g72*) (●).

were wild-type animals, but the *ace-3* defective mutants were instantaneously paralyzed (Fig. 5A). Animals preserving either the *ace-1* or *ace-2* gene alone recovered from the trichlorfon-induced paralysis in the same manner as wild-type animals, though a portion of the population did not. On the other hand, animals retaining only the *ace-3* gene had difficulty recovering from paralysis (Fig. 5B). It is likely that the higher concentration of trichlorfon induced a slow but irreversible inactivation of class C AChE, whereas the inactivation of class A and B AChE is completely reversible.

Effects of trichlorfon on the localization of AChE staining

Since trichlorfon principally inhibits AChE activity, the pattern of the AChE staining will diversely change during the paralytic and recovery states after trichlorfon exposure. As described above, newly hatched larvae of wild-type and double mutants of the *ace* genes showed characteristic AChE staining (Fig. 6 A-D). However, the staining was completely lost in any strain during paralysis as shown in the wild-type animal (Fig. 6E). Staining along the ventral nerve cord recovered partially accompanying recovery from the paralysis, but staining at the head region did not recover (Fig. 6F-I). Thus movement recovery does not need complete restoration of the AChE staining.

Effects of trichlorfon treatment on ACh levels

Changes in ACh levels after trichlorfon exposure were also studied (Fig. 7). To prepare animals in the same state of paralysis, each strain was incubated at different concentrations of trichlorfon. At the paralyzed state, the ACh levels were slightly elevated in the *ace-1 ace-3* and *ace-3 ace-2* mutants as seen in the wild type, but greatly elevated in the *ace-1 ace-2* mutant. Therefore, the extent of the paralysis did not apparently correlate with the accumulation of ACh. However, since the ACh level was assayed after washing the animals to remove trichlorfon, it is conceivable that the difference in ACh levels among respective mutants reflects the difference in reversibility of the inactivated enzyme.

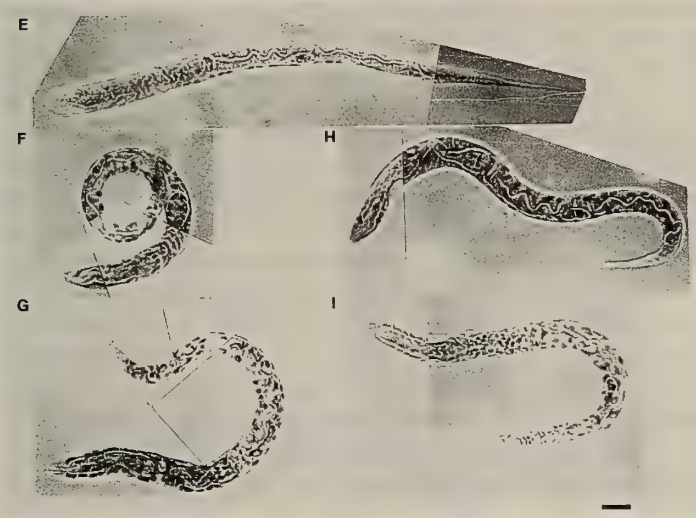

FIG. 6. Changes in AChE staining caused by trichlorfon. Newly hatched larvae became paralyzed, then recovered as in Figure 5. Animals before trichlorfon treatment (A-D). A completely paralyzed wild type (E). Animals recovered from the paralysis (F-I). Wild type (A, E, F), *ace-2* (*g72*) *ace-3* (*dc2*) (B, G), *ace-3* (*dc2*) *ace-1* (*p1000*) (C, H), and *ace-1* (*p1000*) *ace-2* (*g72*) (D, I). Animals are oriented anterior side to the left and the ventral side on bottom. Bar $=200\ \mu$m.

DISCUSSION

To understand the roles that the three classes of AChE may play, we studied the enzyme activity, histochemistry and ACh levels in mutant and wild-type *C. elegans*. Classes A and B AChE have several similar properties. That is, the developmental pattern of the expression of the two enzymes is comparable (Fig. 1) and the inhibitory pattern by trichlorfon is similar (Fig. 4), although both enzymes seem to functionally overlap but are not coincident. For example, mutants retaining class A AChE are more sensitive to trichlorfon than those containing only class B AChE. The staining pattern of AChE of whole mutant animals containing only class B was similar as that of the wild type. However, the staining of animals containing only class A AChE is faint in the body region. Classes A and B AChE differ in Km values [9, 12] and the extent of membrane association [9]. Solubilized class A AChE is as inhibited by trichlorfon as the crude enzyme but solubilized class

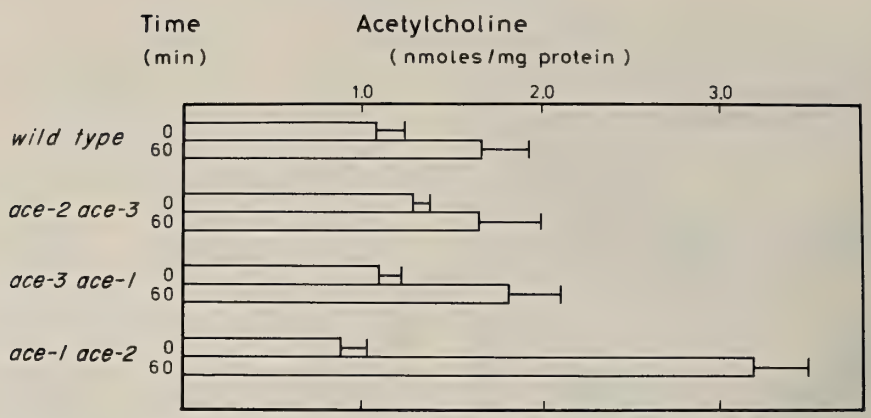

FIG. 7. Changes in ACh levels by trichlorfon exposure. The newly hatched larvae of the wild type and the the *ace-1 ace-2* mutant were exposed to 1 mM, and the *ace-2 ace-3* and the *ace-3 ace-1* mutants to 0.1 mM trichlorfon, respectively. Under these conditions, four strains reached in approximately the same paralyzed state. At 60 min after exposure, animals were collected for the assay of ACh levels. Standard deviations of the mean values of three assays are indicated by vertical bars.

AChE is less inhibited (unpublished results).

Class C AChE was found to be greatly different from classes A and B AChE in expression, distribution and response to trichlorfon. The class C enzyme is resistant to trichlorfon but the strain retaining only the enzyme is hardly recovered from the trichlorfon-induced paralysis. The activity of class C AChE is one-fiftieth lower than the activity of A and B AChE, peaks at the early L4 stage, and distributed in the body rather than in the head region.

For normal locomotion of *C. elegans,* it is essential that either the *ace-1* or the *ace-2* gene is intact, suggesting that a decrease in the total AChE activity rather than in the specific AChE, leads to locomotive abnormalities. In other words, the reduction of ACh hydrolysis and therefore, the accumulation of ACh, results in the movement abnormality. However, the extent of the elevation of the total ACh levels and the movement abnormality is not always correlated because, in the *ace-1 ace-2* mutant, the movement is abnormal throughout development, but the ACh levels are normal at the early larval stage. Also, under the trichlorfon-induced paralyzed states with wild-type animals and *ace* double mutants, the extent of the ACh elevation of the *ace-1 ace-2* mutant greatly differs from those remaining. However, the rule conforms at the adult stage but not at the early larval stage, because, in the *ace-1 ace-2* mutant, ACh levels are normal at the L1 and L2 stage, but are elevated at the adult stage.

The present findings can not fully explain why three types of AChE are present in *C. elegans.* We showed that slight elevation of ACh results in a movement abnormality, indicating that the consequent accumulation of ACh levels leads to lethal over-stimulation of some control and peripheral neurons. The presence of heterogeneous types of AChE, whose localization, expression and abundance differ, is useful for the prompt removal of stagnated ACh. Animals containing only class B AChE are indistinguishable from the wild type in the distribution and the staining intensity. Class A AChE normally presents at the anterior region of the body but is less abundant at the posterior region. Although class C AChE is much less abundant, it is detectable at the posterior region of the body. Therefore, class B AChE may play a major role and class A and C AChE a regionally supplementary role in the hydrolysis of ACh. Thus, the presence of different types of AChE may be useful for regulating the local concentration of ACh in the synapse. The electrical organ of *Torpedo californica* has also structurally distinct molecular forms of AChE [1]. They are differently distributed in the electric organ and suggested that they may play different roles on the hydrolysis of

ACh.

ACKNOWLEDGMENTS

We wish to thank Dr. S.Kuno for suggestions and critical reading of the manuscript. We are grateful to Mrs. R. Kitamura and Mr. S. Matsudaira for technical support. Supported in part by funds for Medical Treatment of Elderly, School of Medicine Kanazawa University, 1990 and Grant in Aid for Special Project Research from the Ministry of Education, Science and Culture of Japan.

REFERENCES

1 Abramson SN, Ellisman MH, Deerinck TJ, Maulet Y, Gentry MK, Doctor BP, TaylorP (1989) Differences in structure of the molecular forms of acetylcholinesterase. J Cell Biol 108: 2301–2311

2 Brenner S (1974) The genetics of *Caenorhabditis elegans*. Genetics 77: 71–94

3 Culotti JG, von Ehrenstein G, Culotti MR, Russell RL (1981) A second class of acetylcholinesterase-deficient mutants of the nematode *Caenorhabditis elegans*. Genetics 97: 281–305

4 Ellman GL, Courtney KD, Andres JV, Featherstone RM (1961) A new and rapid colorimetric determination of acetylcholinesterase activity. Biochem Pharmacol 7: 88–95

5 Greenfield S (1984) Acetylcholinesterase may have novel functions in the brain. Trends Neurosci. 7: 364–368

6 Hosono R (1978) Sinusoidal movement of *Caenorhabditis elegans* in liquid phase. Zool Mag 87: 191–195

7 Hosono R, Sassa T, Kuno S (1989) Spontaneous mutations of trichlorfon resistance in the nematode *Caenorhabditis elegans*. Zool Sci 6: 697–708

8 Johnson CD, Duckett JG, Culotti JG, Herman RK, Meneely PM, Russell RL (1981) An acetylcholinesterase-deficient mutant of the nematode *Caenorhabditis elegans*. Genetics 97: 261–279

9 Johnson CD, Russell RL (1983) Multiple molecular forms of acetylcholinesterase in the nematode *Caenorhabditis elegans*. J Neurochem 41: 30–46

10 Johnson CD, Rand JB, Herman RK, Stern BD, Russell RL (1988) The acetylcholinesterase genes of *C. elegans*: Identification of a third gene (*ace-3*) and mosaic mapping of a synthetic lethal phenotype. Neuron 1: 165–173

11 Karnovsky MJ, Roots L (1964) A "direct-coloring" thiocholine method for cholinesterase. J Histochem Cytochem 12: 219–221

12 Kolson DL, Russell RL (1985) New acetylcholinesterase-deficient mutants of the nematode *Caenorhabditis elegans*. J Neurogenet 2: 69–91

13 Lehmann J, Fibiger HC (1979) Acetylcholinesterase and the cholinergic neuron. Life Sci. 25: 1939–1947

14 McCamann RE, Stetzler J (1977) Radiochemical assay for ACh: modifications for sub-picomole measurements. J Neurochem 28: 669–671

15 Wood WB ed (1988) The nematode *Caenorhabditis elegans*pp. 1–667 Cold Spring Harbor Laboratory, New York

ZOOLOGICAL SCIENCE 10: 53–56 (1993)

Secretion of Mitogenic Factor(s) from Stocks of *Paramecium tetraurelia*, *P. caudatum* and *P. multimicronucleatum*

Yoshiomi Takagi, Kumiko Nimura, Yumiko Tokusumi,
Hiromi Fujisawa, Kazuhiko Kaji[1]
and Hiroyuki Tanabe[2]

Department of Biology, Nara Women's University, Nara 630, [1]*Tokyo Metropolitan Institute of Gerontology, Sakaecho, Tokyo 173,* [2]*Government Industrial Research Institute, Takamatsu 761, Japan*

ABSTRACT—We recently isolated and purified the Paramecium growth factor (ParGF). The starting material (crude sample) was a ca.100-fold concentrate obtained by ultrafiltration of a cell-free medium of an early stationary mass culture of the *jumyo* mutant of *Paramecium tetraurelia*. Its mitogenic function has been assessed from the restoration of the reduced fission rate of the *jumyo* mutant in daily reisolation cultures. To determine whether stocks of *P. tetraurelia* other than the *jumyo* mutant and those of other *Paramecium* species secrete similar substance(s), we assayed crude samples of those stocks for mitogenic function using the *jumyo* mutant. The results obtained were positive for almost all the stocks of *P. tetraurelia*, *P. caudatum* and *P. multimicronucleatum* studied, suggesting that ParGF, or a functional homologue, is common to *Paramecium* and act as a mitogen on "non-self" cells as well as on "self" cells (i.e. those producing the factor).

INTRODUCTION

Paramecium cells divide 3–5 fissions a day at 25°C in bacterized Wheat-Grass-Powder medium. The *jumyo* mutant [3], which was first isolated as a mutant having a short clonal lifespan [4], divides 0.5–1.5 fissions a day in daily reisolation cultures but 3–5 fissions a day in mass culture. This characteristic of the mutant provided the clue that led to the finding of Paramecium growth factor (ParGF) and to a method for its biological assay [5]. ParGF has been collected and purified from a cell-free medium of an early stationary-phase culture of *jumyo* cells and has been assayed in daily reisolation cultures of these cells. We investigated whether the cell-free medium derived from stocks of *P. tetraurelia* other than the *jumyo* mutant and those of other *Paramecium* species can restore the reduced fission rate of the *jumyo* mutant in daily reisolation culture.

Accepted August 21, 1992
Received July 17, 1992

MATERIALS AND METHODS

Stocks

All the stocks except for G3 were from the collections of Y.T. at Nara Women's University. Figure 1 shows the lineages of 12 stocks of *P. tetraurelia* as well as the mating types for some stocks, the genotypes of the *jumyo* locus [3] and the *nd169* locus [1] for all the stocks. Stocks G3 (mating type V) and NK15 (VI) of *P. caudatum* syngen 3 and stocks CH313 (III) and CH312 (IV) of *P. multimicronucleatum* syngen 2 were used. G3 was provided by Dr. M. Fujishima of Yamaguchi University.

Culture

Cells from a given stock were washed and cloned according to the method of Sonneborn [2]. The culture medium was a 1% phosphate-buffered medium of 5 g/l Wheat-Grass-Powder (Pines International, Inc., USA), inoculated with *Klebsiella pneumoniae* 1–2 days before use.

For the mass culture, 1,000 ml flasks, each

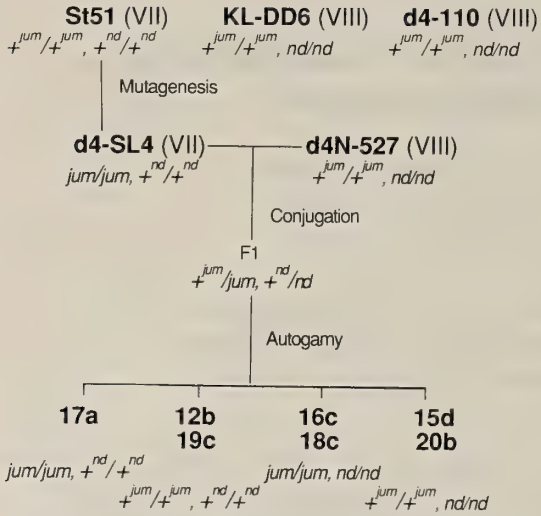

FIG. 1. Lineages of *P. tetraurelia* stocks with their mating types and genotypes of the *jumyo* and *nd169* loci. The two genes are abbreviated *jum* and *nd*. d4-SL4 is the *jumyo* mutant.

containing 400 ml culture medium, were used. After introduction of 1–10 cells/ml, the individual flasks were incubated at 26°C as still cultures. When the culture first became clear, indicating exhaustion of bacteria, it was considered to be at the early stationary-phase of growth.

For the daily reisolation culture, a single cell was placed in 400 μl of culture medium in a well of a depression slide housed in a moist chamber.

Preparation of the crude sample

Cells in the early stationary-phase culture were removed by filtering the medium through two folds of two sheets of filter paper (TOYO). The resulting cell-free fluid was concentrated about 100-fold by ultrafiltration in a Diaflow cell (Amicon) with a Diaflow ultrafiltration membrane YM10 (Amicon) that had a nominal cut-off molecular weight of 10,000. The crude sample obtained was stored in a freezer (−25°C) and thawed in a refrigerator before use.

Assay of the crude sample for mitogenic function

Cells were taken from a clonal culture of the *jumyo* mutant and placed in 12 (or 18) wells of depression slides, each containing 400 μl of culture medium, then cultured as daily reisolation lines for 5 days, half the lines being designated experimental and half control. For each experimental culture, a crude sample was added daily so as to raise concentration 1.5-fold of that in the original cell-free culture medium (when the sample was a 100-fold concentrate, 6 μl was added; an 80-fold concentrate, 7.5 μl was added). When a line died out, it was replaced by one of the other living lines.

Fission rate was compared between two groups of lines for both the daily averages and the total averages on the 5th day. The crude sample was considered effective as a mitogen when the total average of the daily fission rates in the experimental group was significantly higher (*t*-test).

RESULTS

Secretion of mitogenic factor from stocks of P. tetraurelia other than the jumyo mutant

Of the 12 stocks of *P. tetraurelia* with various combinations of mating types and the genotypes of the *jumyo* and *nd169 loci* (see Fig. 1), 11 stocks (except 17a) were examined for the secretion of mitogenic factor, or a functional homologue of ParGF. The crude sample collected from the early stationary-phase culture of each stock effectively restored the fission rate of *jumyo* cells in daily reisolation culture. The results for 6 representative stocks with various combinations of mating types and genotypes are shown in Figure 2. The lines of *jumyo* cells supplemented with the crude sample from the indicated stock showed significantly higher fission rates than unsupplemented control lines, although the restored level of the fission rate was not so high as the wild-type level. The crude sample prepared from bacterized medium that had *not* been inoculated with *Paramecium* cells showed no such effect (data not shown).

These results indicate that the ability to secrete mitogenic factor, probably ParGF or a homologue, has nothing to do with differences in mating types and genotypes of the *jumyo* and *nd169* loci.

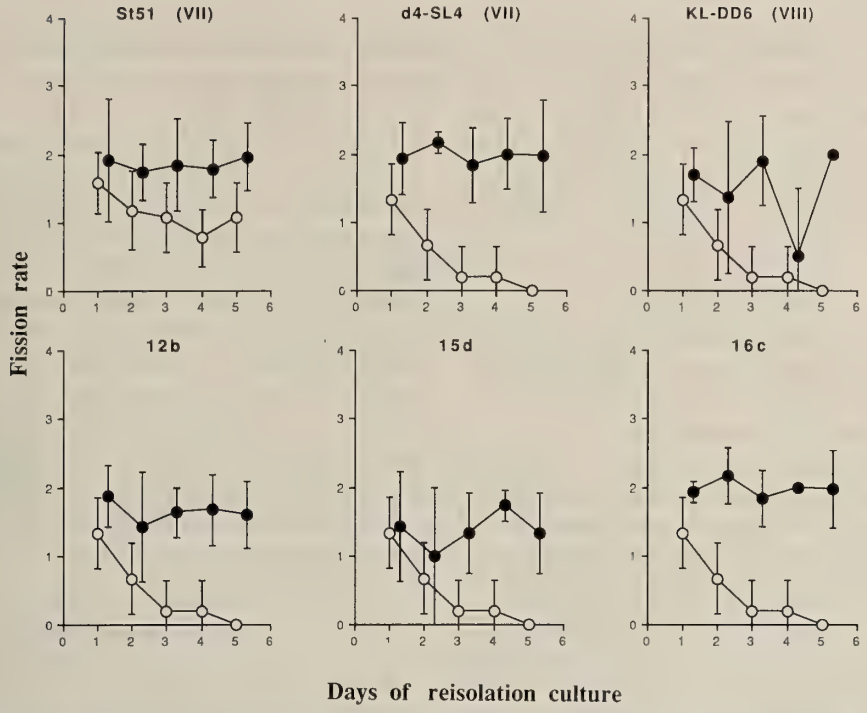

FIG. 2. Mitogenic activity of crude samples prepared from *P. tetraurelia* stocks with various genetic backgrounds (see Fig. 1). Controls (open circles) are for 6 or 9 daily reisolation lines of *jumyo* cells cultured in depression slide wells that contained 400 μl of culture medium. Experiments (closed circles) are for 6 or 9 daily reisolation lines supplemented daily with the crude sample prepared from the stock indicated. Daily reisolation cultures were begun on day 0 and maintained for 5 days. The fission rate is given in $\log_2 N$ where N is the number of cells on the day following reisolation. Bars indicate standard deviations.

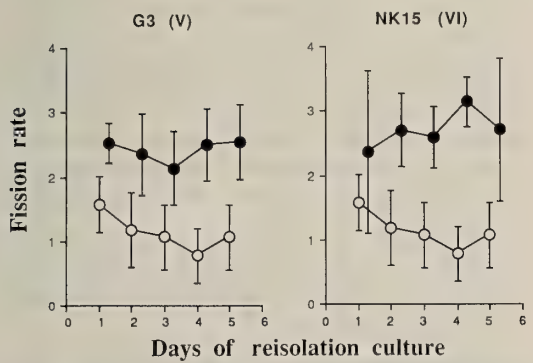

FIG. 3. Mitogenic activity of crude samples prepared from *P. caudatum* stocks of different mating types. Same as in Figure 2.

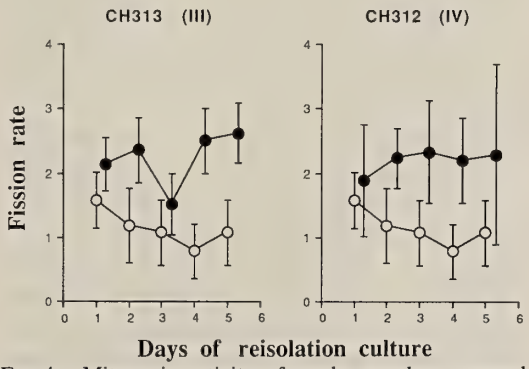

FIG. 4. Mitogenic activity of crude samples prepared from *P. multimicronucleatum* stocks of different mating types. Same as in Figure 2.

restored the fission rate of *jumyo* cells in daily reisolation culture. These results strongly suggest that the mitogenic factor, probably ParGF or a homologue, is secreted into the surrounding medium from every stock of *Paramecium* species.

Secretion of mitogenic factor from stocks of P. caudatum and P. multimicronucleatum

The crude sample collected from the early stationary-phase culture of two stocks of *P. caudatum* (Fig. 3) and two of *P. multimicronucleatum* (Fig. 4), all of different mating types, effectively

DISCUSSION

ParGF first was identified by the use of the *jumyo* mutant both as a donor in mass culture and as a recipient in daily reisolation cultures for the assay [5]. ParGF therefore has been regarded as a substance recognized by "self" cells. This study shows that mitogenic factor(s) is secreted not only by a variety of *P. tetraurelia* cells which are of different mating types and are homozygous dominant and recessive for the *jumyo* locus (Figs. 1, 2), but also by cells with different mating types of *P. caudatum* (Fig. 3) and *P. multimicronucleatum* (Fig. 4). Since what we have tested for the mitogenic activity in this study is not the purified ParGF but crude samples, the restoration of the reduced fission rate of *jumyo* cells is not due to ParGF itself but to interaction of molecules present in the crude samples. However, it is highly probable that a functional homologue of ParGF is secreted by a number of *Paramecium* species and acts on *jumyo* cells; ParGF may be a substance that is recognized by "non-self" cells as well as by "self" cells and all *Paramecium* cells may produce both ParGF and its receptor.

The fact that the *jumyo* mutant divides slowly in daily reisolation culture, where the substances secreted are abandoned daily, but divides rapidly in mass culture, where the substances secreted are accumulated, suggests that the mutant may be slow either in the rate of production of ParGF or in the effectiveness to respond to ParGF, or both. Although we repeatedly prepared crude samples from the same stock and tested their mitogenic activity with the use of this assay method, the levels of the fission rate restored were not consistent and thus comparison of the kinetics among different stocks was impossible. Therefore, the above-mentioned possibilities both remain open. For that, we need the improvement of the assay method that should be accurate enough to compare the quantity and quality of ParGF as well as the use of purified ParGF.

We are so far unsuccessful in developing a new assay method in which wild type cells, not *jumyo* mutant cells, are used. When wild type cells are cultured in a bacterized medium in which Wheat-Grass-Powder is reduced to 1/16 that of the standard, they divide as slowly as *jumyo* mutant cells in daily reisolation cultures. But, this low fission rate can be restored not only by crude samples but also by concentrates of bacterized medium in which *Paramecium* cells had not been inoculated (data not shown). Therefore, the low fission rate induced by nutritional restriction cannot represent the low fission rate of the *jumyo* mutant in daily reisolation culture.

ACKNOWLEDGMENTS

We are grateful to Dr. Masahiro Fujishima of Yamaguchi University for his providing the stock G3 and to Drs. Geoffrey Beale of Edinburgh University, UK, and Donald Cronkite of Hope College, USA, for improving the manuscript. This work was supported by a Grant-in-Aid for Science Research (01540596) and one for Cooperative Research (A) (03304001) to Y.T. from the Ministry of Education, Science and Culture of Japan.

REFERENCES

1 Nyberg D (1978) Genetic analysis of trichocyst discharge of the wild stocks of *Paramecium tetraurelia.* J Protozool 25: 107–112

2 Sonneborn TM (1970) Methods in Paramecium research. In "Methods in Cell Physiology Vol 4" Ed by DM Prescott, Academic Press, New York, pp 241–339

3 Takagi Y, Izumi K, Kinoshita H, Yamada T, Kaji K, Tanabe H (1989) Identification of a gene that shortens clonal life span of *Paramecium tetraurelia.* Genetics 123: 749–754

4 Takagi Y, Suzuki T, Shimada C (1987) Isolation of a *Paramecium tetraurelia* mutant with short clonal life-span and with novel life-cycle features. Zool Sci 4: 73–80

5 Tanabe H, Nishi N, Takagi Y, Wada F, Akamatsu I, Kaji K (1990) Purification and identification of a growth factor produced by *Paramecium tetraurelia.* Biochem Biophys Res Commun 170: 786–792

ZOOLOGICAL SCIENCE 10: 57–64 (1993)

Cytokine-Like Activities of a Humoral Opsonin from the Solitary Urochordate *Styela Clava*

Karen L. Kelly[1], Edwin L. Cooper[1]
and David A. Raftos[2]

[1]*Department of Anatomy and Cell Biology, School of Medicine, University of California, Los Angeles Los Angeles, California 90024, U.S.A and*
[2]*Immunobiology Unit, School of Biological and Biomedical Sciences, University of Technology, Sydney N.S.W. 2007, Australia*

ABSTRACT—Previously, we have identified and purified an opsonin from the plasma of the solitary urochordate, *Styela clava*. Here we show that this opsonin exhibits cytokine-like activies in tunicates. The opsonin enhances incorporation of ^{3}H-thymidine into cultures of pharyngeal tissues from *S. clava* and acts as a powerful chemoattractant. Cytokine-like activity is also indicated by the ability of the *S. clava* molecule to activate tunicate phagocytes. In addition, we show that the opsonin is produced by *S. clava* hemocytes and that its production is stimulated by zymosan. These data suggest that the opsonin characterized here is identical to a tunicate, cytokine-like molecule (tunIL-1β) previously identified by its ability to stimulate mouse thymocyte proliferation.

INTRODUCTION

Opsonins play a key role in invertebrate humoral defense systems. We have previously identified a humoral opsonin in the tunicate, *Styela clava* [8]. Our studies indicate that preincubation of target cells wih *Styela clava* plasma increases the capacity of tunicate hemocytes for phagocytosis. Opsonization is inhibited by the carbohydrates mannan, N-acetyl-D-galactosamine, and galactose, and by the divalent cation chelator, EDTA. Such data suggest that the *S. clava* hemolymph may contain a C-type lectin [6]. This lectin-like activity has recently been isolated from *S. clava* hemolymph [9]. Gel filtration yielded a fraction with strong opsonic activity that was associated with a single, electrophoretically-resolved protein. The fractionated opsonin is sensitive to tryptic digestion and heat denaturation, and its biological activity is dose-dependent. Molecular characterization indicated that the opsonic protein is a 17.5 kDa monomer with a pI of 7.0.

Accepted October 1, 1992
Received June 4, 1992

We postulate that the humoral opsonin from *S. clava* may subserve multiple inducible biological activities during inflammatory reactions. Such a diversity of function is typical of inflammatory proteins in mammals. For instance, the mammalian inflammatory cytokine, IL-1, has multiple activities including the enhancement of IL-2 and IL-2 receptor expression by T-cells, the induction of slow wave sleep, increased thymocyte and fibroblast proliferation and the regulation of chemotaxis and hematopoiesis [5]. IL-1 also appears to be involved with communication between the immune and nervous systems [3, 4].

Similarly, complement components in mammals subserve diverse effector functions. C3 has the capacity to opsonize foreign targets, initiate the subsequent lytic cascade of complement components, release an anaphylatoxin that is both chemoattractive and stimulatory and is involved in the activation of phagocytes and lymphocytes [7].

The propensity of inflammatory protein in mammals to have multiple biological activities may also be reflected in tunicates. Here we test a purified opsonin from *S. clava* for its ability to stimulate cell proliferation, chemotaxis, and cell activation.

MATERIALS AND METHODS

Tunicates

Styela clava was purchased from Marinus Inc., Long Beach, CA. Tunicates were maintained at 15°C in an aerated, sandbed-filtered, 180-liter aquarium filled with artificial sea water (Instant Ocean, Aquarium Systems, Mentor, OH; 3.4% w/v). Approximately 2 ml of Marine Invertebrate Diet (Carolina Biological, Gladstone, OR) were added to the aquarium every two days. Tunicates were allowed to adjust to conditions in the aquarium for one week prior to experimentation.

Hemocyte Suspensions and Plasma

Tunicates were bled by severing the stolon and collecting 1.5 ml of the exuding hemolymph in chilled, polystyrene, centrifuge tubes containing 1.5 ml of sterile-filtered, artificial sea water (ASW) (Instant Ocean; 3.4% w/v). The resulting hemocyte suspensions were allowed to stand for five minutes so that large debris and cell aggregates sank. The upper 2 ml of each suspension were then transferred to fresh tubes. The number of hemocytes in suspension was determined and the volume adjusted with ASW. Hemocytes from individual tunicates were not pooled for any assay.

Plasma was obtained by harvesting hemolymph in the absence of ASW. Cells and debris were removed by centrifugation ($800 \times g$, 15 minutes, twice) and the resulting plasma stored frozen (−20°C).

Proliferation of Pharyngeal Explants

Tunicate Tissue Culture Medium: Tunicate tissue culture medium (T-RPMI) was prepared in sterile-filtered ASW and contained, per liter, 454 mg RPMI 1650 powder (with L-glutamine, without sodium bicarbonate; Sigma Chemicals, St. Lous, MO), 10^5 units penicillin sulfate (Sigma Chemicals), and 100 mg streptomycin sulfate (Sigma Chemicals) [10]. This medium was then sterilized by filtration and stored at 4°C.

Tunicate Tissue Culture Protocol: The stiulatory effects of purified opsonin were tested in cultures of pharyngeal tissue from *S. clava*. Pharyngeal tissue is considered to be a hematopoietic field in tunicates thereby providing an excellent source to study cell proliferation. The procedure used to culture pharyngeal explants was similar to that of Raftos *et al.* [10]. Pharyngeal tissue was diced into $3 \times 3 \times 1$ mm^3 explants and rinsed three times in T-RPMI. Rinsed explants were transferred to 96-well-flat-bottomed culture plates (1 explant/well; Costar, Pleasanton, CA) contianing T-RPMI (200 μl/well). Explants were cultured at 15°C in normal atmosphere.

Incubation of Tunicate Explants with Purified Opsonin: Explants were equilibrated to culture conditions for 3 days prior to adding purified opsonin. After this period, explants were transferred to either fresh T-RPMI or T-RPMI containing 1 μg/ml of purified opsonin (200 μl/well) [9]. Explants were cultured at 15°C in normal atmosphere for a further 3 days.

Quantification of ^{3}H-thymidine Uptake: Explants were removed from tissue culture plates and pooled in 2 ml of the same medium in which they had been cultured. Tissues were then incubated at 15°C with 5 μCi/ml methyl ^{3}H-thymidine (^{3}H-TdR, 20 Ci/mmol; ICN Radiochemicals, Costa Mesa, CA). After 18 hr, excess ^{3}H-TdR was removed by washing the explants three times (1 hr per wash) in 4 ml ASW on a hematology mixer (Fisher Scientific, Pittsburgh, PA). Wahsed explants were transferred to scintillation vials (1 explant/vial) containing 200 μl trypsin (2% w/v in ASW) and digested overnight at 37°C. Two milliliters of scintillation cocktail (Ecolite; ICN Radiochemicals) was added to each vial so that the incorporated radioactivity could be quantified with a Beckman LS 3150P Scintillation Counter. Data are presented as proliferation indexes (P.I.) such that:

P.I. = (counts per minute in experimental trials)/(counts per minute in controls).

Mean values for each trial were calculated from P.I.s for individual trials.

Hemocyte Migration Assay

The migration of tunicate hemocytes was quantified using chemotaxis chambers in which Transwell inserts (6.5mm diameter, 5.0 μm pore size polycarbonate filter, tissue culture treated; Milli-

pore, Bedford, MA) and 24-well tissue culture plates (Costar) formed the upper and lower wells respectively. One hundred microliter aliquots of cell suspensions (2×10^6 cells/ml) were added to the upper wells of the chemotaxis chambers. When required, purified opsonin was added to a final concentration of 1.0 μg/ml to the upper well immediately after the addition of cells. The lower well was filled with 600 μl ASW with or without purified opsonin (1 μg/ml). Cells were allowed to migrate through Transwell membranes for 2 hr (15°C). After incubation, the chemotaxis chambers were agitated vigorously, the Transwell inserts removed, and the plates centrifuged ($200\times g$, 5 min. 4°C). Cells that had migrated to the lower wells were counted in 16 randomly selected 400× fields of view using an inverted (tissue culture) microscope. Data are presented as migration indexes (M.I.) such that:

M.I. = (cells per field of view in experimental trials)/(cells per field of view in controls).

Mean values for each trial were calculated from M.I.s for individual trials.

Zymosan Stimulation of Opsonin Production

Zymosan-treated Hemocyte Cultures: Two hundred microliters of *S. clava* hemocyte suspensions (2×10^6 hemocytes/ml in ASW) were added to 48-well tissue culture plates. The plates were centrifuged ($200\times g$, 5 min.) and the supernatant removed and replaced with 200 μl either T-RPMI or zymosan (50 μg/ml in T-RPMI). The cells were incubated 48 hr at 15°C. Following incubation, the plates were centrifuged ($300\times g$, 5 min.) and the supernatants removed and pooled. Pooled supernatants were centrifuged ($500\times g$, 10 min.) to remove cells and particulate zymosan and then filter-sterilized (0.22 μm; Costar).

Assays of Supernatants: Culture supernatants were analyzed in two ways. First, they were tested for opsonic acitivity as described previously by Kelly, *et al.* [9]. Second, the supernatants were concentrated thirty-fold using Centriprep 10 centrifugal concentration units (Amicon, Danvers, MA) and then assayed for protein content by the Bradford method (Protein Determination Kit, Biorad, Richmond, CA) and subjected to SDS-PAGE (see below).

Activation of Phagocytes by Purified Opsonin

Pre-incubation of Latex Beads: 800 μl aliquots of latex bead (Sigma LB 30, Sigma Chemicals) suspensions were washed ($16{,}000\times g$, 6 min) and resuspended in 200 μl of ASW or purified opsonin. The beads were incubated at room temperature with constant agitation for 1.5 hr. Suspensions were then washed thrice ($16{,}000\times g$, 6 min) and resuspended in ASW to a final concentration of 5×10^6 beads/ml.

Phagocytosis of Latex Beads: Cover glasses (22 mm×22 mm, Gold Seal, Fisher Scientific) were suspended between moistened strips of filter paper in glass petri dishes. Each cover slip was overlaid with 100 μl of hemocyte suspension (3×10^6 cells/ml). Hemocytes were allowed to adhere to cover slips for 2 hr (15°C). Cover slips were then washed thrice (800 μl ASW), and 50 μl of purified opsonin (500 ng/ml) or ASW were added. Cultures were allowed to incubate for 30 min (15°C) before being overlaid with 50 μl of pre-incubated latex beads (5×10^6 beads/ml). These cultures were incubated for a further 30 min at 15°C before excess latex beads were removed by dipping each cover slip in ASW ten times. The cells were then fixed in 200 μl of absolute methanol (15 min, 4°C) and washed in distilled water. Cover slips were inverted onto microsope slides and sealed.

Quantification of Phagocytosis: Phagocytosis was assessed by phase contrast microscopy (1,250 ×magnification, oil immersion). A minimum of 200 hemocytes from at least four fields of view per cover slip were inspected. Data were recorded as the percentage of hemocytes that had phagocytosed any number of latex beads (% phagocytic cells) relative to the total cell population. Data are presented as phagocytic stimulation indexes (PSI) where:

PSI = (% phagocytic cells in experimental trials)/(phagocytic cells in controls).

Mean values for each trial were calculated from PSIs for individual trials.

SDS-PAGE

SDS-PAGE was performed according to the

method of Laemmli [1] using 12% separating gels. Dalton VII-L markers (Sigma Chemicals) were used for calibration. *Styela clava* plasma (total protein concentration 70 μl/ml) and G-50 gel filtration-purifed opsonin (49 μg protein/ml) [9] were diluted 1:1 in 2×SDS/sample buffer with 2% v/v 2-mercapoethanol while tunIL-1β (200 μg protein/ml) [2] and zymosan-stimulated supernatant (260 μg protein/ml) were diluted 1:4 in sample buffer. Gels were silver-stained using an AG-5 kit according to the manufacture's instructions (Sigma Chemicals).

Purification of Opsonin and TunIL-1β

The procedures used to purify opsonin have been described in detail elsewhere [9]. Thirty milliliters of concentrated tunicate plasma was subjected to gel filtration. Plasma was sterilized by filtration (0.22 μm) and concentrated thirty-fold using Centriprep 10 centrifugal concentration units (Amicon). Concentrated plasma was then applied to a gel filtration chromatography column (bed volume 150 ml) packed with Sephadex G-50 (Sigma Chemicals) in phosphate-buffered saline. Hemolymph fractions were eluted with PBS, and fractions of 2.5 ml were collected and immediately sterilized by filtration. The hemolymph fractions were assessed for opsonic activity, and the purity of the opsonic fraction was confirmed by a single band on silver-stained 12% SDS-PAGE gel.

The procedures used to purify tunIL-1β have also been described in detail elsewhere [2]. Tunicate IL-1-like proteins were isolated from 100 ml of tunicate hemolymph. After concentration by ultrafiltration (PM 10 membrane, Amicon, Danvers, MA), hemolymph was applied to a Biogel AcA 54 gel filtration column (Pharmacia, Piscataway, NJ) which was eluted with phosphate buffered saline. Fractions were assayed for IL-1 activity in a mouse thymocyte proliferation assay. Peaks of IL-1 activity were pooled, concentrated and applied to a PBE 84 chromatofocusing column (Pharmacia). The chromatofocusing column was eluted with a linear pH gradient (pH 8.4–pH 4.0) and fractions were assayed for IL-1-like activity as above. Two predominant species, one being tunIL-1β, were isolated. The purity of both species was confirmed on silver-stained 12% SDS-PAGE gels.

Statistical Analysis

Statistical analyses were performed with the *Mystat* software package (Systat, Inc., Evanston, IL). The statistical significance of differences between mean values was determined by the Student's *t*-test [14]. Differences were considered to be significant for probabilities of less than 5.0%.

RESULTS

Effect of Purified Opsonin on ^{3}H-thymidine Uptake

Incubation of pharyngeal explants from *S. clava* with purified opsonin resulted in a significant ($P<0.05$) increase in the level of ^{3}H-thymidine uptake when compared to controls incubated with T-RPMI (Fig. 1). Pharyngeal explants which had been cultured for three days with purified opsonin (1 μg/ml in T-RPMI) followed by 18 hr with ^{3}H-thymidine (5 μCi/ml) exhibited a proliferation index of 39.8±4.8.

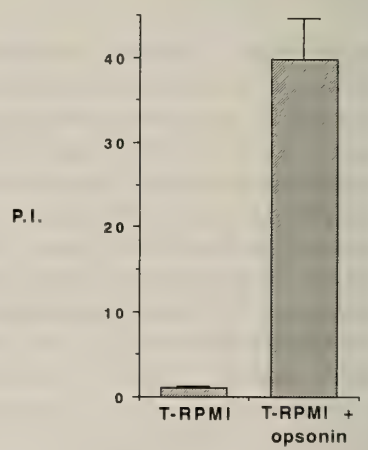

FIG. 1. Proliferation indexes (±SEM, n=20 explants) measured by ^{3}H-thymidine uptake for *S. clava* pharyngeal explants incubated in the presence or absence of purified *S. clava* opsonin.

Purified Opsonin Enhances Hemocyte Migration

When added to the lower wells of chemotaxis chambers, purified *S. clava* opsonin significantly ($P<0.05$) increased the number of tunicate hemocytes migrating through Transwell membranes

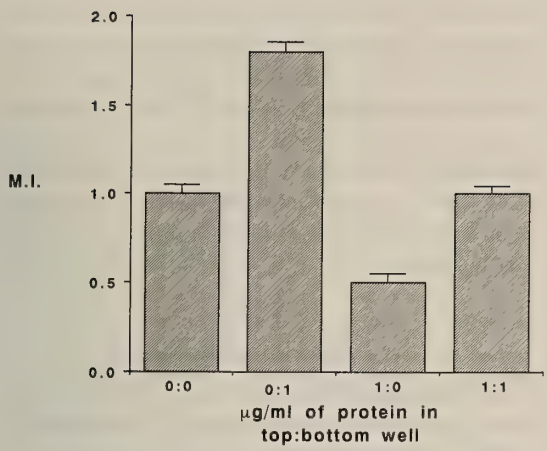

FIG. 2. Migration indexes (±SEM, n=5) for hemocytes incubated in Transwell chambers containing either ASW in both the upper and lower wells, ASW in the upper well and 1 μg/ml *S. clava* opsonin (in ASW) in the lower well, 1 μg/ml *S. clava* opsonin (in ASW) in the upper well and ASW in the lower well, and 1 μg/ml *S. clava* opsonin (in ASW) in both the upper and lower wells.

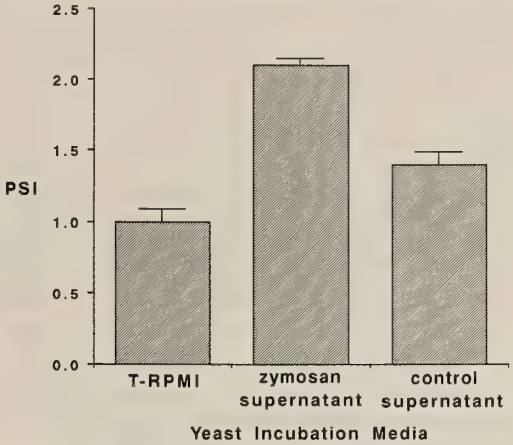

FIG. 3. Phagocytic stimulation indexes (±SEM, n=6) for hemocytes exposed to yeast that had been pre-incubated with either T-RPMI, zymosan-stimulated hemocyte supernatant, or supernatant from cells cultured in the absence of zymosan (control supernatant).

(Fig. 2). Approximately twice as many cells (migration index 1.8±0.05) entered lower wells containing 1 μg/ml of opsonin relative to controls containing ASW alone (migration index 1.0± 0.05). A reciprocal pattern was evident when purified opsonin was added to the upper wells of chemotaxis chambers. The addition of 1 μg/ml of opsonin to the upper wells reduced migration by 50% (migration index 0.5±0.05) relative to ASW-controls ($P<0.05$). The addition of purified opsonin to both the upper and lower wellls ($1\times g$/ml) yielded no significant change ($P>0.05$) in the number of tunicate hemocytes migrating through the Transwell membranes (migration index 1.0± 0.04) compared to ASW-controls.

Effect of Zymosan-stimulated Hemocyte Supernatants on Phagocytosis

Incubation of yeast in supernatants from zymosan-stimulated hemocyte cultures significantly ($P<0.05$) increased their phagocytosis by tunicate hemocytes when compared to yeast incubated in T-RPMI alone (Fig. 3). The phagocytic stimulation index for zymosan-stimulated-hemocyte supernatants was twice (PSI=2.1±0.05) that of T-RPMI controls (PSI=1.0±0.09). Incubation of yeast in supernatants of hemocyte cultures that had not been exposed to zymosan also increased phagocytosis (PSI=1.4±0.09) relative to T-RPMI controls ($P<0.05$). However, this level was signi-

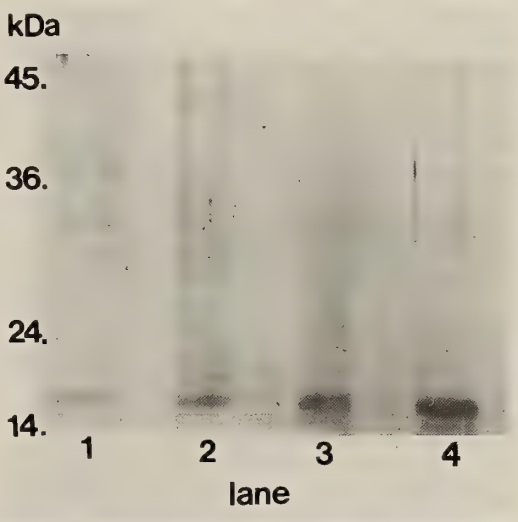

FIG. 4. Silver-stained, reducing SDS-PAGE of *Styela clava* plasma (lane 1), zymosan-stimulated hemocyte supernatant (lane 2), tun-IL 1β (lane 3), and G-50 column purified opsonin from *S. clava* plasma (lane 4). Position of molecular weight markers are shown at the left (kDa).

ficantly lower ($P<0.05$) than that for the phagocytosis of yeast which had been opsonized by zymosan-stimulated hemocyte supernatants.

Characterization of Zymosan-stimulated Hemocyte Supernatant

SDS-PAGE of zymosan-stimulated hemocyte supernatant resolved a number of proteins with a prominent band at 17.5 kDa under reducing conditions (Fig. 4, lane 2). A similar 17.5 kDa protein was evident in whole *S. clava* plasma (Fig. 4, lane 1). The major protein evident in zymosan-stimulated hemocyte supernatant migrated to the same position as both purified *S. clava* opsonin and tunIL-1β (Fig. 4, lanes 4 and 3 respectively).

Activation of Phagocytes by Purified S. clava Opsonin

Pre-incubation of hemocytes with purified *S. clava* opsonin significantly ($P<0.05$) increased their capacity to phagocytose latex beads when compared to hemocytes pre-incubated in ASW (Fig. 5). Hemocytes which had been incubated with purified opsonin had a PSI of 3.0 ± 0.22 in the presence of ASW-incubated latex beads while control (ASW-incubated) hemocytes exhibited a PSI of 1.0 ± 0.15. The addition of latex beads pre-incubated in purified opsonin to ASW-incubated hemocytes did not significantly ($P>0.05$) alter the phagocytic stimulation indexes (1.2 ± 0.14) when compared to controls comprised of ASW-incubated hemocytes exposed to ASW-incubated latex beads.

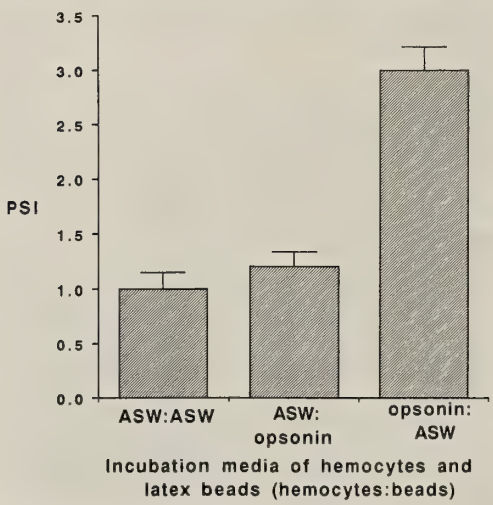

FIG. 5. Phagocytic stimulation indexes ($\pm$SEM, n=5) for tunicate hemocytes exposed to latex beads under the following conditions: ASW-incubated cells with ASW-incubated beads (ASW : ASW), opsonin-incubated cells with ASW-incubated beads (opsonin : ASW), ASW-incubated cells with opsonin-incubated beads (ASW : opsonin). Hemocytes were cultured 30 minutes at 15°C with either ASW or opsonin before the addition of latex beads.

DISCUSSION

We have shown that an opsonin from *Styela clava* exhibits several functional characteristics which are typical of cytokine-like molecules. First, the *S. clava* opsonin stimulates the proliferation of tunicate cells. Differences in cell proliferation between control and experimental cultures of *S. clava* pharyngeal tissue are readily quantified by uptake of ^{3}H-thymidine [11, 12]. Raftos *et al.* [13] have shown that ^{3}H-thymidine incorporation by cultured explants in inhibited by irradiation and competition with non-isotopic thymidine. This suggests that there is a direct relationship between cell proliferation and ^{3}H-thymidine uptake [12]. Hence, the enhanced incorporation of ^{3}H-thymidine in pharyngeal cultures containing *S. clava* opsonin indicates that this molecule can regulate the proliferation of *S. clava* cells *in vitro*.

Purified opsonin also acts as a chemoattractant for *S. clava* hemocytes (Fig. 2). The addition of purified opsonin to the lower well of chemotaxis chambers significantly increased the level of migration of hemocytes to the lower well. Conversely, when opsonin was added to the upper well of the chamber, migration to the lower well was inhibited while no net movement was evident when equal concentrations of opsonin were present in both the upper and lower wells of the chemotaxis chambers. This type of analysis indicates that the *S. clava* opsonin acts as a powerful chemoattractant for tunicate hemocytes.

In addition to its proliferative and chemotactic activities, the *S. clava* molecule activates tunicate phagocytes. Pre-incubation of *S. clava* hemocytes with purified opsonin enchanced the level of phagocytosis of latex beads. This enhanced phagocytic activity cannot be explained by the opsonization

of latex beads by the *S. clava* protein. The *S. clava* protein acts as a carbohydrate specific lectin [8] which, as shown here, is not opsonic for abiotic targets such as latex. Latex beads incubated with opsonin are not ingested at a greater rate than that of untreated controls. Hence, the increased phagocytosis of unopsonized latex beads by hemocytes in the presence of *S. clava* opsonin must reflect the ability of this protein to metabolically activate tunicate hemocytes.

The capacity of *S. clava* opsonin to regulate cellular processes such as proliferation, chemotaxis, and hemocyte activation indicates that it may play a central role in adaptive inflammatory reactions. However, adaptive reactions such as chemotaxis would be dependent upon the differential production of opsonin. To fulfill that prerequisite, we have shown that the secretion of *S. clava* opsonin is induced by antigenic challenge. Assays of supernatants from hemocytes cultured with zymosan revealed an enhanced secretion of opsonic molecules relative to controls cultured in the absence of zymosan. SDS-PAGE indicated that this induced opsonic activity was associated with a 17.5 kDa protein that is of identical electrophoretic mobility to purified *S. clava* opsonin. It is reasonable to conclude that the *S. clava* opsonin is produced by hemocytes in repsonse to stimulation by the target, zymosan.

The functional and physiochemical properties identified here suggest *S. clava* opsonin is identical to a cytokine-like protein, designated tunIL-1β, that has been isolated from the same species [2, 11]. Both the opsonin studied here and tunIL-1β are 17.5 kDa proteins with pI's of 7.0–7.4 [9, 11]. Both molecules are opsonic [13], and exhibit similar sensitivity to inhibition by N-acetyl-D-galactosamine, galactose, and mannose [8]. They enhanced the proliferation of pharyngeal explants *in vitro* above the normal levels [11], act as chemoattractants (D.A. Raftos, personal communication), and activate phagocytic cells [13]. Moreover, production of both *S. clava* opsonin and tunIL-1β by *S. clava* hemocytes is stimulated by zymosan [13]. These data suggest that tunicates express an opsonic protein with cytokine-like activities which can mediate adaptive inflammatory responses.

ACKNOWLEDGEMENTS

We thank Rick Fairhurst and Steve Sarafian for their contributions. This study was supported in part by the National Science Foundation (Grant #DCB 90 05061) and by BRSG funds from the UCLA Schools of Medicine and Dentistry. David A. Raftos was a Fulbright Postdoctoral Fellow and a recipient of a Frederik B. Band Scholarship in Marine Invertebrate Immunology administered by The American Association of Immunologists.

REFERENCES

1 Ausubel FM, Brent R, Kingston RE, Moore DD, Seidman JG, Smith JA, Struhl K (1989) Current Protocols in Molecular Biology section 102 John Wiley and Sons New York

2 Beck G, Vasta GR, Marchalonis JJ, Habicht GS (1989) Characterization of interleukin-1 activity in tunicates. Comp Bioch Physiol 92B: 93–98

3 Berkenbosch J, van Oers J, del Rey A, Tilders F, Besedovsky HO (1987) Corticotoropin-releasing factor-producing neurons in the rat activated by interleukin-1. Science 238: 524–526

4 Besedovsky H, del Rey AE, Sorkin E, Dinarello CA (1986) Immunoregulatory feedback between interleukin-1 and glucocorticoid hormones. Science 233: 652–659

5 Dinarello CA, Cannon JG, Mier JW, Bernheim HA, LoPreste G, Lynn DL, Love RN, Webb AC, Auron PE, Reuben RC, Rich A Wolff SM, Putney SD (1986) Multiple biological activities of human recombinant interleukin-1. J Clin Invest 77: 1734–1739

6 Drickamer K (1988) Two distinct classes of carbohydrate-recognition domains in animal lectins J Biol Chem 263: 9557–9560

7 Fearon DT, Wong WW (1983) Complement ligand-receptor interactions that mediate biological responses. Ann Rev Immunol 1: 243–271

8 Kelly KL, Cooper EL, Raftos DA (1993) A humoral opsonin from the solitary urochordate *Styela clava.* Dev Comp Immunol, 17: 29–39

9 Kelly KL, Cooper EL, Raftos DA (1992) Purification and molecular characterization of a humoral opsonin from the solitary urochordate *Styela clava.* Comp Bioch Physiol, 103B: 749–753

10 Raftos DA, Stillman DL, Cooper EL (1990) *In vitro* culture of tissue from the tunicate *Styela clava.* In Vitro 26: 962–970

11 Raftos DA, Cooper EL, Habicht G, Beck G (1991) Invertebrate cytokines: Tunicate cell proliferation stimulated by an endogenous hemolymph factor. Proc Natl Acad Sci USA 88: 9518–9522

12 raftos, DA, Stillman DL, Cooper EL (1991) Interleukin-2 and phytohaemagglutinin stimulate the proliferation of tunicate cells. Immunol and Cell Biol 69: 225–234

13 Raftos DA, Stillman DL, Cooper EL, Habicht G, Beck G (1992) Invertebrate cytokines II: Release of Interleukin-1-like molecules from tunicate hemocytes stimulated with zymosan. Lymphokine and Cytokine Research, 11: 235–240

14 Sokal RR, Rohlf FJ (1981) Biometry 2nd Ed, WH Freeman and Co, New York, 2nd edition

ZOOLOGICAL SCIENCE 10: 65–72 (1993)

Mouse γ-Casein cDNA: PCR Cloning and Sequence Analysis[1]

Tetsuo Sasaki, Masato Sasaki and Jumpei Enami

Research Laboratory, Zenyaku Kogyo Co., Ltd., 2-33-7, Ohizumi, Nerima, Tokyo 178, Japan

ABSTRACT—A partial amino acid sequence of mouse γ-casein was determined on a gas-phase amino acid sequencer. The N-terminal sequence (23 residues) was obtained using native γ-casein, and the C-terminal sequence (13 residues) was determined with a corresponding peptide. The C-terminal peptide was isolated by affinity chromatography on an anhydrotrypsin agarose column after digestion of γ-casein with *Achromobacter* lysyl-endopeptidase. A cDNA (507 base pairs) encoding the mature protein of γ-casein was produced by polymerase chain reaction (PCR) amplification of lactating mammary gland first strand cDNA with oligonucleotide primers designed from the N-terminal (KHEIKDK-) and the C-terminal (-AHYTRFY) amino acid sequences. The full-length cDNA including 5′- and 3′-noncoding regions (920 base pairs) was cloned by the rapid amplification of cDNA ends (RACE) method of Frohman *et al.* [7]. Comparison of full-length cDNAs of mouse γ-casein and rat γ-casein showed 80% identity at the nucleotide level. The amino acids in the coding region of both γ-caseins were 75% identical.

INTRODUCTION

Caseins are the major milk proteins produced by lactating mammary glands, and their synthesis and secretion are controlled by the coordinated actions of multiple hormones [20]. Tissue- and stage-specific expression of casein genes is regulated by hormones, adipocyte-mammary epithelial cell interactions, and the extracellular matrix [2, 17, 21]. In order to study the specific contributions of elements which play major roles in the control of casein production, casein genes have been cloned and characterized from several species. These include bovine, murine, and rat β-casein as well as bovine alpha-S1 casein [9, 14, 15, 22, 23]. As a further step toward the goal of understanding the molecular mechanisms regulating milk protein gene expression, mouse γ-casein cDNA was cloned and sequenced. Here we present the results including the deduced amino acid sequence.

Accepted July 30, 1992
Received Jyly 8, 1992

[1] The sequence reported in this paper has been deposited in the DDBJ, EMBL and GenBank databases (accession no. D10215).

MATERIALS AND METHODS

Purification of mouse γ-casein

Mouse γ-casein (formerly known as pp22, a phosphoprotein of 22,000 daltons) was purified from SHN mouse skim milk as described previously [5]. Fractions obtained through successive chromatography on Sephadex G-100 and DEAE-cellulose columns were dialyzed against distilled water and freeze-dried. Purified γ-casein was stored at −20°C until characterized.

Amino acid sequence analysis

The N-terminal amino acid sequence was determined using the intact protein. Mouse γ-casein was dissolved in 50% acetonitrile in water to a final concentration of 1 mg/ml. About 150 pmol of γ-casein was applied on a 4-mm square membrane of polyvinylidene difluoride (PVDF; Immobilon-P, Millipore Corporation), and it was oven-dried at 55°C. The sample was placed in the reaction chamber of a Shimazu PSQ-1 automatic gas-phase amino acid sequencer [6], and amino acid sequencing was done by Edman degradation in an automatic mode as recommended by the manufacturer. PTH-amino acids were analyzed with an on-line

HPLC separation system. The C-terminal amino acid sequence was determined using a purified C-terminal peptide fragment [13, 16]. This fragment was purified from lysyl endopeptidase-digested γ-casein by affinity chromatography on a column of anhydrotrypsin agarose (Takara Shuzo, Kyoto), which specifically binds arginyl or lysyl C-terminated peptides under acidic conditions.

Eighteen nmol (400 μg) of mouse γ-casein was incubated at 37°C with 8 μg of lysyl endopeptidase (EC3.4.21.50) from *Achromobacter lyticus* (Wako, Osaka; sample to enzyme weight ratio=50:1) in 25 mM Tris-HCl (pH 8.9) containing 1 mM EDTA. At 0, 18, and 22 hr after starting the incubation, an aliquot of the reaction mixture was applied to a reverse-phase HPLC column (# ODS-2, GL Sciences, Tokyo) to monitor the extent of digestion. Subsequent procedures were done at 4°C. The reaction was stopped by addition of diisopropyl fluorophosphate (DFP) to a final concentration of 0.1 mM. After the pH of the enzyme-digested product was adjusted to 5.0 with acetic acid, 100 μg of the product was applied to a column (10×13 mm) of anhydrotrypsin agarose equilibrated with 50 mM ammonium acetate (pH 5.0) and 20 mM $CaCl_2$. The column was eluted with the same buffer at a flow rate of 0.2 ml/min, and the eluate was collected as the "pass-through" fraction. After the base line stabilized, the elution buffer was changed to 5 mM HCl (pH 2.5). Lysyl C-terminated peptides eluted under these conditions were collected as "bound" fractions.

Since the C-terminal peptide fragment was present in the "pass-through" fraction, this fraction was further purified by reverse-phase HPLC. The "pass-through" fraction was mixed with an equal volume of 0.1% (v/v) trifluoroacetic acid (TFA), and it was applied to a C_{18}-silica column (# ODS-2, GL Sciences, Tokyo) equilibrated with 0.1% TFA. Peptides were eluted with a linear gradient of acetonitrile from 0% in 0.1% TFA at 0 min to 100% in 0.1% TFA at 100 min at a flow rate of 0.5 ml/min. Absorbance was monitored at 215 nm. The fraction corresponding to the major peak was freeze-dried, and the amino acid sequence was determined as described above except that an arylamine-PVDF membrane (Sequelon-AA, Millipore Corporation) was used as a support. The freeze-dried sample was dissolved in 20 μl of 30% aqueous acetonitrile solution, and it was applied to the membrane and heated at 55°C until completely dry. After the membrane cooled to room temperature, 5 μl of 1% (w/v) 1-ethyl-3-(3-dimethylaminopropyl) carbodiimide (EDC) in 15% acetonitrile and 0.1 M 2-(N-morpholino)ethanesulfonic acid (MES), pH 5.0 (supplied in Covalent Attachment Kit from Millipore Corporation), were applied to the membrane, and the reaction was allowed to proceed for 20 min at room temperature. Then the membrane with the peptide coupled at its C-terminal and side chain carboxyl groups was placed in the reaction chamber of the sequencer, and peptide sequence analysis was performed as above.

Alkaline phosphatase treatment of mouse γ-casein

In order to dephosphorylate amino acid residues, mouse γ-casein was treated with alkaline phosphatase as described by Draetta and Beach [4]. Mouse γ-casein (1 nmol; 22 μg) was dissolved in 11 μl of buffer consisting of 100 mM Tris-HCl (pH 8.0), 5 mM $MgCl_2$ and 100 mM NaCl. Then the mixture was incubated with 0.4 unit of calf intestinal phosphatase (Sigma) at 37°C for 2 hr. The amino acid sequence was determined using 400 pmol of the alkaline phosphatase-treated mouse γ-casein as described above.

Reverse transcription

Total RNA was extracted from 10-day lactating BALB/c mouse mammary glands by the acid guanidinium thiocyanate-phenol-chloroform method of Chomczynski and Sacchi [3]. First strand cDNA was synthesized in a 20 μl reaction mixture containing 4.9 μg of total RNA, 800 ng of oligo$(dT)_{12-18}$ primer (Pharmacia) and 200 units of SuperScript™ reverse transcriptase (GIBCO BRL) with a buffer system supplied by GIBCO BRL. After incubation at 45°C for one hr, the mixture was heated at 95°C for 5 min to inactivate the enzyme, and it was rapidly cooled on ice.

Synthesis of oligonucleotides

Oligonucleotide primers for polymerase chain reaction (PCR) and DNA sequencing were synthesized using a Cyclone Plus DNA Synthesizer

(MilliGen/Biosearch).

PCR

The reaction mixture (50 μl) consisted of 0.5 μl of the first strand cDNA and 49.5 μl of PCR cocktail (GeneAmp™ DNA Amplification Kit, Perkin Elmer Cetus) containing 20 pmol each of sense and antisense primers, and 0.2 mM each of dNTPs. Both primers were attached with restriction sites at their 5′ ends for the purpose of cloning into plasmid vectors. The mixture was heated at 95°C for 5 min and rapidly cooled on ice. Then 1.5 units of *Thermus aquaticus* (*Taq*) DNA polymerase (Perkin Elmer Cetus) was added. PCR amplification was carried out for 30 cycles in a DNA Thermal Cycler (Perkin Elmer Cetus) using a step program (50°C, 3 min; 72°C, 2 min; 94°C, 1 min) followed by a 10-min final extension at 72°C. A second amplification reaction was performed in 50 μl of PCR cocktail containing 0.5 μl or 1 μl of the first amplification product and 20 pmol each of the same or internal primers under the same conditions as the first reaction.

Rapid amplification of cDNA ends (RACE) method

The 5′-noncoding region of cDNA was amplified by the RACE method of Frohman *et al.* [7]. First strand cDNA was synthesized using the antisense primer C1 (for sequence, see Fig. 2). Then deoxyadenosine was polymerized to the 3′-end of the first strand cDNA using dATP and terminal deoxynucleotidyl transferase as described below. PCR was performed with an oligo$(dT)_{17}$ primer (U1 as shown in Fig. 2), and a gene-specific antisense primer (N2) located upstream to that used in reverse transcription.

Terminal deoxynucleotidyl transferase treatment

The reaction mixture (20 μl) contained 10 μ l of the reverse transcription product, 100 mM sodium cacodylate buffer (pH 7.2), 8 mM $MgCl_2$, 0.2 mM dithiothreitol (DTT), 0.25 mM dATP, and 10 units of terminal deoxynucleotidyl transferase (Takara Shuzo, Kyoto). After incubation at 37°C for 5 min, the reaction mixture was heated at 65°C for 5 min to denature the enzyme.

DNA sequence analysis

PCR amplification products were cloned into a restriction enzyme- and bacterial alkaline phosphatase-treated pBluescript II vector (Stratagene) using a DNA ligation kit (Takara Shuzo, Kyoto). The plasmid was amplified in XL1-Blue as a host. Plasmid DNA was purified by the alkaline SDS method [1], and plasmid sequencing was performed in both directions by the dideoxy chain termination method using Sequenase Version 2.0 kit (U.S. Biochemical) and alpha-[^{32}P]dCTP (Amersham; 3,000 Ci/mmole) [19].

Data analysis

Protein and DNA sequences were analyzed with PC/GENE software (Release 6.01, IntelliGenetics Inc., California) in an NEC-9801 personal computer.

RESULTS AND DISCUSSION

Analysis of native mouse γ-casein on a gas-phase sequencer determined twenty-three N-terminal amino acid residues. The sequence was Lys-His-Glu-Ile-Lys-Asp-Lys-X-X-X-Glu-Glu-Ser-Ser-Ala-Ser-Ile-Tyr-Pro-Gly-Lys-X-Lys. The letter "X" indicates that the amino acid was not identified during this cycle of sequencing. Since an unidentified "X" amino acid was present as a single peak at the same position in each of these cycles, we hypothesized that the same amino acid was present in modified form in these cycles. In addition, measurement at 322 nm instead of the standard 269 nm revealed the presence of a dehydroserine peak in each cycle where an unidentified peak was present. A dehydroserine peak detected at 322 nm is usually associated with a serine peak at 269 nm [8]. Casein is a well-known phosphoprotein with a high content of phosphoserine. Therefore, the possibility that this amino acid residue was phosphorylated serine was examined. When native γ-casein was treated with alkaline phosphatase [4] and analyzed on a PSQ-1 gas-phase sequencer, serine peaks appeared at the positions where "X" amino acids were found. The height of the unidentified peak diminished correspondingly. Thus, it was concluded that the "X"

amino acid residue was either pure phosphoserine or a mixture of serine and phosphoserine (data not shown).

Determination of the C-terminal amino acid sequence is an important step for obtaining the γ-casein cDNA sequence by the PCR method. Accordingly the C-terminal peptide was purified from the lysyl endopeptidase-digested product using anhydrotrypsin-agarose affinity chromatography. Figure 1A shows the elution profile after affinity chromatography. When the "pass-through" fraction of the affinity chromatography

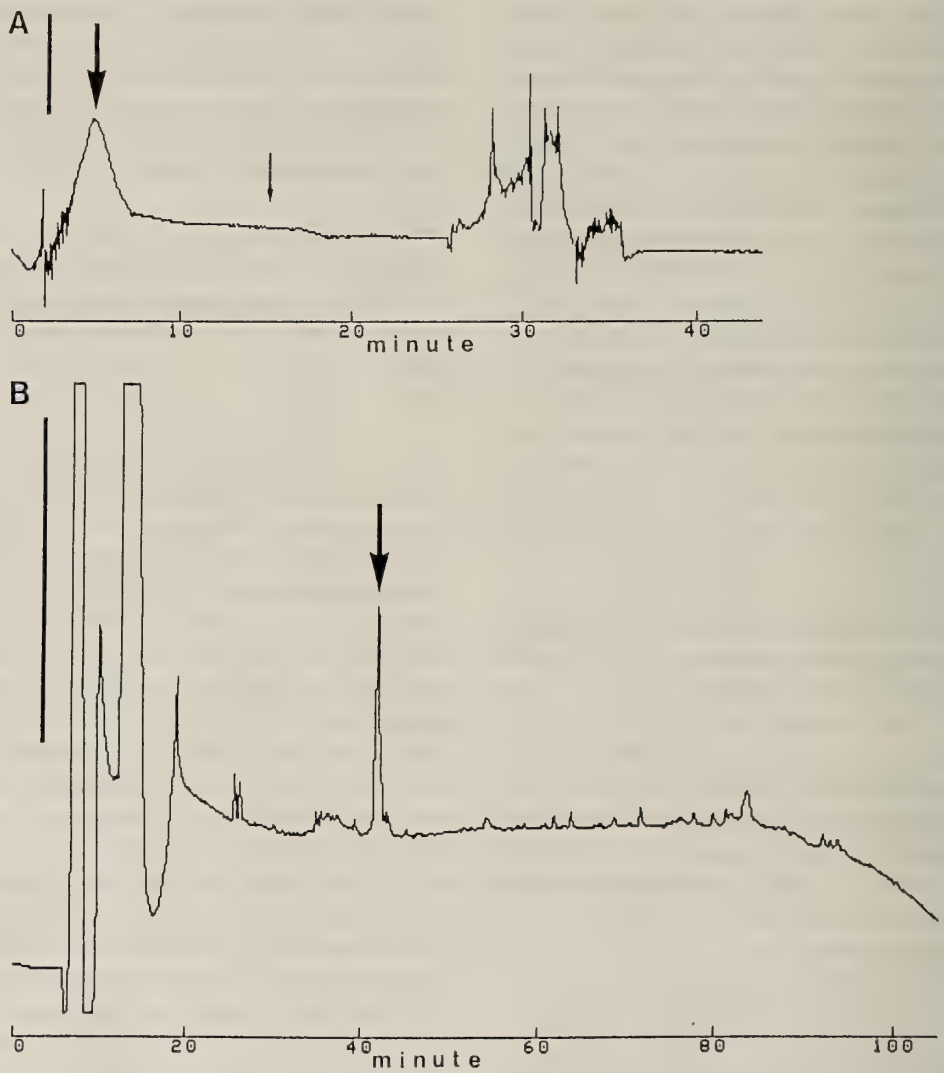

FIG. 1. Isolation of the C-terminal peptide of mouse γ-casein. Lysyl endopeptidase-digested mouse γ-casein (100 μg) was applied to a column of anhydrotrypsin agarose. The C-terminal peptide in the "pass-through" fraction was further purified by reverse-phase HPLC as described in "Materials and Methods." A, Elution profile of lysyl endopeptidase-treated γ-casein from an anhydrotrypsin agarose column. Large arrow points the position of the "pass-through" fraction. Elution buffer was changed to 5 mM HCl at the point indicated by the small arrow. Vertical scale bar represents 1×10^{-4} absorbance unit at 278 nm. B, Separation of the C-terminal peptide. Total "pass-through" fractions were combined and applied to a reverse-phase HPLC column. Elution was performed with a gradient of 0% to 100% acetonitrile in 0.1% TFA. Arrow indicates the position of the major peak. Vertical scale bar represents 0.1 absorbance unit at 215 nm.

was applied to a reverse-phase HPLC column, one major peak was observed (Fig. 1B). To determine the sequence of this peptide, an arylamine-PVDF membrane was selected instead of a PVDF membrane for sample support. An arylamine group can potentially react with both C-terminal and side chain carboxyl groups (aspartic acid and glutamic acid) of peptides via carbodiimide activation. Because the peptide is covalently bound to the membrane, the chance that the progressively shortened peptide will detach is greatly reduced.

Twelve residues distal to the first residue were determined using the arylamine-PVDF membrane. The sequence was ?-Tyr-Thr-Phe-Pro-Asn-Ala-His-Tyr-Thr-Arg-Phe-Tyr. To obtain the internal amino acid sequences, each peptide fragment was purified from the lysyl endopeptidase-digested product, and they were applied to a reverse-phase HPLC column (chromatograms of the HPLC are not shown). Four major peaks were detected, and their amino acid sequences were analyzed. The sequences were Ile-Ile-Asp, Asp-Tyr-Thr-Phe-Pro-Asn-Ala, Asp-Tyr-Thr-Gln, and Tyr-Ile-Gln-Tyr-Gln-Gln-Val-Thr-Ile-Pro-Gln-Leu-Pro-Gln-Ala-Leu-His-Pro-Gln-Ile. Based upon these results, oligonucleotide primers were synthesized for PCR cloning (Fig. 2). The sense primer N1 was an oligonucleotide mixture corresponding to the N-terminal amino acid sequence, and a restriction enzyme site was attached to N1 for cloning. The antisense primer C1 was an oligonucleotide mixture corresponding to the C-terminal amino acid sequence. A restriction enzyme site was similarly attached to C1 for cloning (Fig. 2). After PCR with 20 pmol each of these oligonucleotides primers and first strand cDNA as a template, a DNA fragment of about 500 base pairs (bp) was obtained. The product was then cloned into plasmid vectors, and a partial nucleotide sequence was determined. The sequence

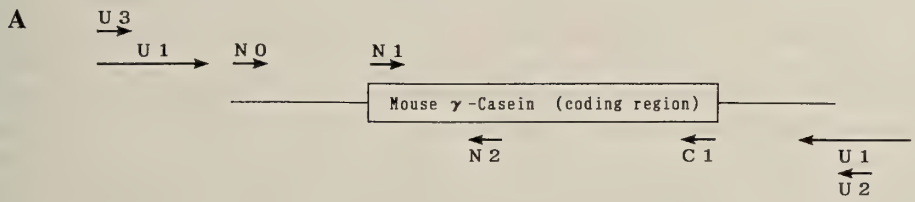

B

Sense Primer

```
                              (LysHisGluIleLysAspLys-)
N1  :   5'-TT-GGATCC-AAACACGAAATAAAAGACAA- 3'
          BamHI     G   T   G   C   G   T
                                T

N0  :  5'-TTT-GGATCC-CTGCAG-GTCTTCCATTTGGGGAGCAAG- 3'
           BamHI     PstI
```

Antisense Primer

```
          (-AlaHisTyrThrArgPheTyr)
C1  :  3'-CGNGTAATATGNGCNAAAAT-GAGCTC-AGATCT-TT- 5'
         G   G   T   G       XhoI    XbaI

N2  :  3'-GATTCGACCTGTTACCG- 5'
```

Universal Primer

```
U1  :  5'-GA-GAATTC-GGATCC-TTT-CTCGAG-TCTAGA-T17- 3'
         EcoRI     BamHI       XhoI     XbaI

U2  :                  5'-CC-TTT-CTCGAG-TCTAGA- 3'
                                XhoI     XbaI

U3  :  5'-GA-GAATTC-GGATCC-TTT- 3'
         EcoRI     BamHI
```

FIG. 2. Primers used for PCR amplification. A, Maps of the PCR primers. Sense and antisense primers are denoted by (→) and (←), respectively. The universal primer U1 was used for both the sense and antisense primer. B, Sequences of primers depicted in Figure 2A. Primers N1 and C1 were mixtures of oligonucleotides corresponding to the N- and C-terminal peptide sequences, respectively. "N" in the sequence of the primer C1 means a mixture of A, C, G and T. Restriction sites attached to each primer also are shown.

closely resembled that of rat γ-casein cDNA, and it was, therefore, concluded that this clone represented part of mouse γ-casein.

The 5′-noncoding region was amplified by the rapid amplification of cDNA ends (RACE) method [7], and poly(dA) was tailed to the first strand cDNA using terminal deoxynucleotidyl transferase. PCR was performed using 1 μl of this poly(dA)-tailed first strand cDNA as a template, 23 pmol of the antisense primer N2, a mixture of 2.2 pmol of the universal primer U1, and 19 pmol of the universal primer U3 (Fig. 2). Subsequently, the product was cloned into plasmid vectors. Sequencing of a clone revealed that the insert consisted of artificial $(dA)_{59}$-tail, 5′-noncoding (57 bp) and coding (54 bp) regions of mouse γ-casein.

For amplification of the full length γ-casein cDNA, the sense primer N0 corresponding to the 5'-noncoding region was synthesized based on the above results (Fig. 2). PCR was done using 20 pmol of the sense primer N0, 20 pmol of the universal primer U2, and 0.5 μl of the first strand cDNA, which was reverse-transcribed using the universal primer U1. A DNA fragment of about 900 bp was obtained, and its size was close to that expected for rat γ-casein cDNA. A second PCR was done with 15 pmol of the sense primer N0, 15 pmol of the universal primer U2, and 1 μl of ten-fold diluted primary PCR product as a template. A DNA fragment of identical size was obtained.

After cloning this fragment into a *Pst*I- and *Xho*I-treated plasmid vector, its nucleic acid sequence was determined in both directions. Analysis of cDNAs obtained from eight independent plasmids revealed that four had an identical sequence. The other four clones differed at several positions. The latter were probably caused by *Taq* polymerase-induced misincorporations of nucleotides during PCR amplification. Figure 3 shows the nucleotide sequence of mouse γ-casein cDNA from the four identical clones. The deduced amino acid sequence is also shown. The size of mouse γ-casein cDNA was 920 bp including the 5′-noncoding region (56 bp), the coding region (552 bp), and the 3′-noncoding region (312 bp). Mouse γ-casein cDNA and rat γ-casein cDNA [12] were 80% identical at the nucleotide level and 75% at the encoded amino acid level. A polyadenylation signal was present near the 3′-end. The amino acid sequences of four internal peptides as well as a C-terminal peptide purified from lysyl endopeptidase-digested product on a gas-phase peptide sequencer were also determined. These were in complete agreement with the amino acid sequence deduced from the mouse γ-casein cDNA. Although the first amino acid residue of the C-terminal peptide was not identified on the gas-phase peptide sequencer, the cDNA sequence showed that it was asparatic acid. This conclusion is reasonable, because asparatic acid cannot be identified on a gas-phase sequencer when peptides are treated with arylamine to fix to the membrane. The total number of deduced amino acid residues is 184 including a signal peptide of 15 residues, and the calculated molecular weight of mature mouse γ-casein is 19,446 daltons.

Although Hennighausen and Sippel [10] isolated a cDNA for mouse γ-casein, the sequence was not reported. The restriction map of their γ-casein cDNA differed from the present γ-casein cDNA. Consequently, their γ-casein cDNA is probably different from ours. They also reported the isolation of a cDNA for mouse δ-casein [10], and a partial amino acid sequence of the δ-casein, Ser-Ser-Ser-Ser-Ser-Glu-Glu-Ser-Ser-Glu-Glu-Val, is identical to the 53rd-64th residues of the present γ-casein [11]. In addition, the restriction map of the δ-casein resembles that of the present γ-casein. Further studies including sequence analysis of δ-casein cDNA are needed to determine whether or not these cDNAs are identical.

In casein phosphoprotein, the common sequence for serine phosphorylation sites (-Ser-Ser-Glu-Glu-) [14], where both serine residues are phosphorylated, is found in three regions in mouse γ-casein (Fig. 3). .In addition, there are three consecutive phosphorylated serine residues near the N-terminal sequence of mouse γ-casein. According to Mercier [18], casein kinase phosphorylates the serine residue in the sequence, Ser-*X*-*Y*, where *Y* is either a phosphorylated serine or an acidic residue, usually glutamic acid. It is likely, therefore, that 16 of 29 serine residues (55%), including the above mentioned three consecutive serine residues, are phosphorylated in

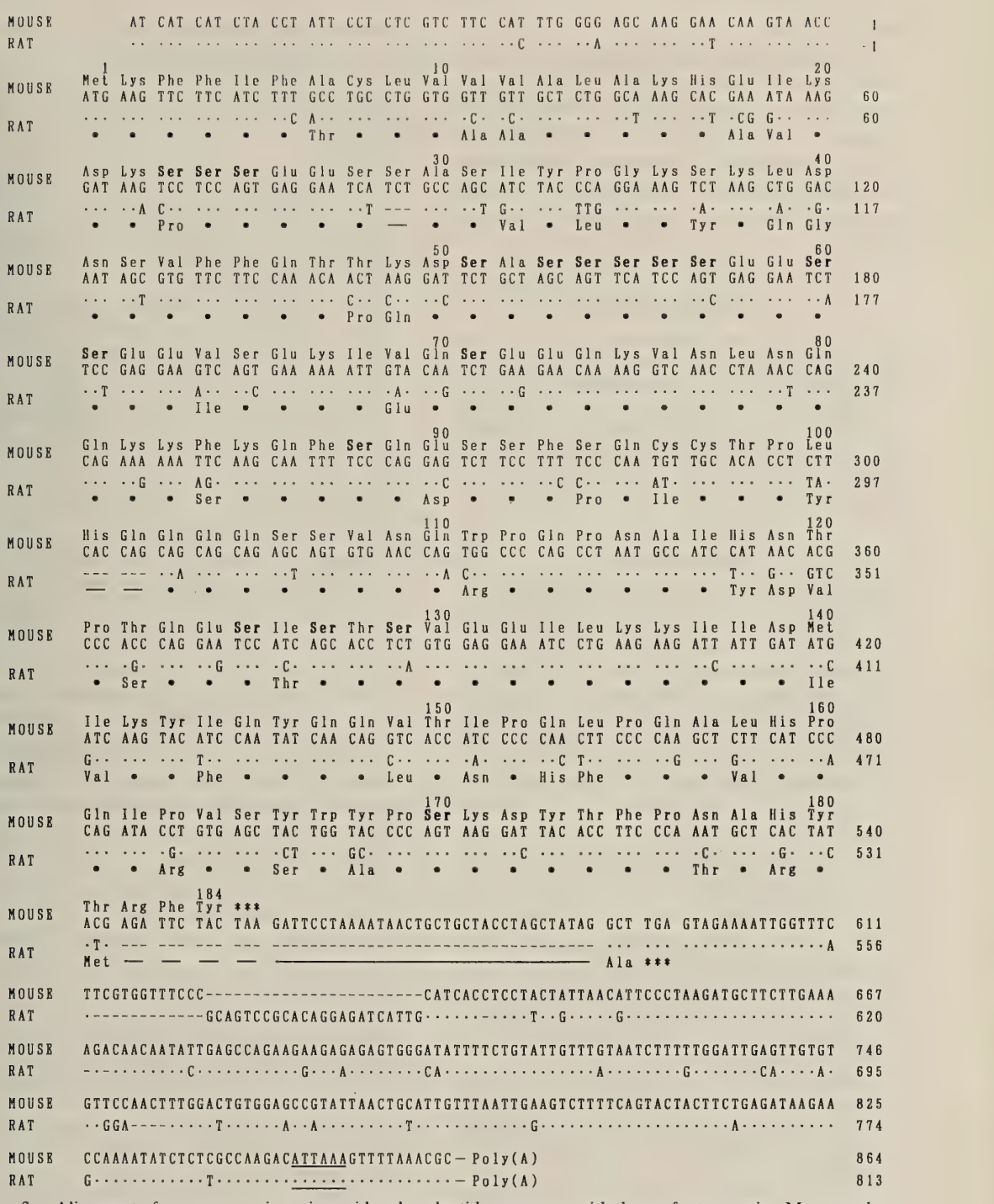

FIG. 3. Alignment of mouse γ-casein amino acid and nucleotide sequences with those of rat γ-casein. Mouse and rat γ-caseins were aligned using the computer software, PC/Gene. Positions of identical residues in both γ-caseins are labeled as (·) for a nucleotide and (●) for an amino acid residue. Amino acids are shown in three-letter code. A sequence gap is marked by (—). Amino acid residues corresponding to the termination codons are indicated by (***). A polyadenylation signal (ATTAAA) is underlined. Potential phosphorylated serine residues are written in bold letters.

mouse γ-casein.

In conclusion, the nucleotide sequence of cDNA encoding mouse γ-casein and the deduced amino acid sequence were presented. Based on this information, cloning of the 5′-flanking region of mouse γ-casein gene is in progress. Identification of regulatory sequences may be useful for understanding transcriptional control of milk protein genes.

ACKNOWLEDGMENTS

We are grateful to Dr. Hideshi Kobayashi, director of this research laboratory, for continuous encouragement. We thank Dr. A. Iwamatsu (KIRIN Brewery Co., Ltd.) for helpful advice on peptide sequencing, Drs. K. Kohmoto and F. Aoki (Department of Agriculture, Tokyo University) for providing information on dephosphorylation, and Dr. R. Shiurba for critically reviewing the manuscript.

REFERENCES

1 Birnboim HC, Doly J (1979) A rapid alkaline extraction procedure for screening recombinant plasmid DNA. Nucleic Acids Res 7: 1513–1523

2 Blum JL, Zeigler ME, Wicha MS (1987) Regulation of rat mammary gene expression by extracellular matrix components. Exp Cell Res 173: 322–340

3 Chomczynski P, Sacchi N (1987) Single-step method of RNA isolation by guanidinium thiocyanate-phenol-chloroform extraction. Analyt Biochem 162: 156–159

4 Draetta G, Beach D (1988) Activation of *cdc2* protein kinase during mitosis in human cells: Cell cycle-dependent phosphorylation and subunit rearrangement. Cell 54: 17–26

5 Enami J, Nandi S (1977) A sensitive radioimmunoassay for a component of mouse casein. J Immunol Methods 18: 235–244

6 Findlay JBC, Pappin DJC, Keen JN (1989) Automated solid-phase microsequencing. In "Protein sequencing" Ed by JBC Findlay, MJ Geisow, IRL Press, Oxford, pp 69–84

7 Frohman MA, Dush MK, Martin GR (1988) Rapid production of full-length cDNAs from rare transcripts: Amplification using a single gene-specific oligonucleotide primer. Proc Natl Acad Sci USA 85: 8998–9002

8 Geisow MJ, Aitken A (1989) Gas- or pulsed liquid-phase sequence analysis. In "Protein sequencing" Ed by JBC Findlay, MJ Geisow, IRL Press, Oxford, pp 85–98

9 Gorodetsky SI, Tkach TM, Kapelinskaya TV (1988) Isolation and characterization of the *Bos taurus* β-casein gene. Gene 66: 87–96

10 Hennighausen LG, Sippel AE (1982) Characterization and cloning of the mRNAs specific for the lactating mouse mammary gland. Eur J Biochem 125: 131–141

11 Hennighausen LG, Steudle A, Sippel AE (1982) Nucleotide sequence of cloned cDNA coding for mouse ε casein. Eur J Biochem 126: 569–572

12 Hobbs AA, Rosen JM (1982) Primary structure of the casein messenger RNA species. Nucleic Acids Res 10: 8079–8098

13 Ishii S, Yokosawa H, Kumazaki T, Nakamura I (1983) Immobilized anhydrotrypsin as a specific affinity adsorbent for tryptic peptides. Methods Enzymol 91: 378–383

14 Jones WK, Yu-Lee L-Y, Clift SM, Brown TL, Rosen JM (1985) The rat casein multigene family: Fine structure and evolution of the β-casein gene. J Biol Chem 260: 7042–7050

15 Koczan D, Hobom G, Seyfert M-H (1991) Genomic organization of the bovine alpha-S1 casein gene. Nucleic Acids Res 19: 5591–5596

16 Kumazaki T, Terasawa K, Ishii S (1987) Affinity chromatography on immobilized anhydrotrypsin: General utility for selective isolation of C-terminal peptides from protease digests of proteins. J Biochem 102: 1539–1546

17 Li ML, Aggeler J, Farson DA, Hatier C, Hassell J, Bissell MJ (1987) Influence of a reconstituted basement membrane and its components on casein gene expression and secretion in mouse mammary epithelial cells. Proc Natl Acad Sci USA 84: 136–140

18 Mercier J-C (1981) Phosphorylation of caseins, present evidence for an amino acid triplet code posttranslationally recognized by specific kinases. Biochimie 63: 1–17

19 Sanger F, Nicklen S, Coulson AR (1977) DNA sequencing with chain-terminating inhibitors. Proc Natl Acad Sci USA 74: 5463–5467

20 Topper YJ, Freeman CS (1980) Multiple hormone interactions in the developmental biology of the mammary gland. Physiol Rev 60: 1049–1106

21 Wiens D, Park CS, Stockdale FE (1987) Milk protein expression and ductal morphogenesis in the mammary gland *in vitro*: Hormone-dependent and -independent phases of adipocyte-mammary epithelial cell interaction. Dev Biol 120: 245–258

22 Yoshimura M, Oka T (1989) Isolation and structural analysis of the mouse β-casein gene. Gene 78: 267–275

23 Yu-Lee L-Y, Richter-Mann L, Couch CH, Stewart AF, Mackinlay AG, Rosen JM (1986) Evolution of the casein multigene family: Conserved sequences in the 5′ flanking and exon regions. Nucleic Acids Res 14: 1883–1902

ZOOLOGICAL SCIENCE 10: 73–83 (1993)

Phosphatidylcholine Is an Endogenous Substrate for Energy Metabolism in Spermatozoa of Sea Urchins of the Order Echinoidea

Masatoshi Mita[1] and Masaru Nakamura[2]

[1]*Department of Biochemistry, Teikyo University School of Medicine, Itabashi-ku, Tokyo 173, Japan and* [2]*Department of Biology, Faculty of Medicine, Teikyo University, Hachioji, Tokyo 192-03, Japan*

ABSTRACT—A study was conducted to examine an endogenous substrate for energy metabolism in spermatozoa of six species of sea urchin, *Anthocidaris crassispina, Echinometra mathaei, Pseudocentrotus depressus, Strongylocentrotus intermedius, Strongylocentrotus nudus* and *Temnopleurus hardwickii,* which belong to the order Echinoidea. These spermatozoa contained cholesterol and several kinds of phospholipids, including phosphatidylcholine (PC), phosphatidylserine, phosphatidylethanolamine and cardiolipin. After dilution of dry sperm from these species in seawater, a rapid decrease in the level of PC was observed, but other phospholipids remained at constant levels. The preferential hydrolysis of PC was related to the properties of phospholipase A_2. Ultrastructural study showed that lipid bodies were present within mitochondria of the sperm midpieces of *A. crassispina, E. mathaei* and *P. depressus.* After incubation in seawater, the lipid bodies became small or disappeared. Thus it is concluded that spermatozoa of sea urchins of the order Echinoidea commonly use PC located in the lipid bodies within mitochondria as a substrate for energy metabolism.

INTRODUCTION

It is known that spermatozoa are stored for months as immotile cells in male sea urchins [7, 24]. After being spawned in seawater, spermatozoa begin movement, and respiration is activated. The energy for swimming is produced by mitochondrial respiration, and ATP is utilized almost exclusively by the dynein ATPase of the flagellar axoneme [4–6]. The transportation of high-energy phosphate from the midpiece to the tail is associated with a creatine-phosphate shuttle [27, 28]. However, it seems unlikely that sea urchin spermatozoa are capable of using an exogenous substrate for energy metabolism, since hardly any nutrients are present in seawater. Previous studies have shown that sea urchin spermatozoa obtain energy for swimming through oxidation of endogenous phospholipids [20–22, 25]. Sperm respiration also supports the phospholipid metabolism [20–22, 25]. Furthermore, it has been shown that following incubation in seawater of spermatozoa from *Hemicentrotus pulcherrimus,* a sea urchin of the order Echinoidea, the content of endogenous phosphatidylcholine (PC) decreases significantly, with no change in the levels of other phospholipids [16, 18, 19]. Thus, *H. pulcherrimus* spermatozoa possibly use PC as a substrate for energy metabolism. It is important to determine whether PC is a common preferred substrate for energy metabolism in sea urchin spermatozoa. For further clarification of energy metabolism using PC, the present study examined the substrate for energy metabolism in spermatozoa of six species of sea urchin of the order Echinoidea; *Anthocidaris crassispina, Echinometra mathaei, Pseudocentrotus depressus, Strongylocentrotus intermedius, Strongylocentrotus nudus* and *Temnopleurus hardwickii.*

Recently, PC has been shown to be abundant in *H. pulcherrimus* sperm midpieces [13]. Following the initiation of motility, the PC content of sperm midpieces decreases significantly, while that in sperm heads and tails does not change [13]. Fur-

Accepted November 4, 1992
Received September 21, 1992

thermore, the sperm midpiece of *H. pulcherrimus* has been shown to contain lipid bodies in the intramembrane space of the mitochondrion [14]. Interestingly, the lipid bodies become small gradually, coincident with a decrease in the level of PC [14]. Therefore, an ultrastructural examination of the sperm midpieces of *A. crassispina, E. mathaei* and *P. depressus* was also carried out.

MATERIALS AND METHODS

Sea urchins

Six species of sea urchin belonging to the order Echinoidea: *A. crassispina, E. mathaei, P. depressus, S. intermedius, S. nudus* and *T. hardwickii,* were collected at Asamushi (Aomori, Japan), Misaki (Kanagawa, Japan), Tateyama (Chiba, Japan) and Kagoshima (Kagoshima, Japan). *E. mathaei* consists of four different types (A, B, C, and D types) which are distinguishable by color pattern of spines, shape of spicules and so on [29, 30]. A type of *E. mathaei* was used in this study. Spermatozoa were obtained by forced spawning induced by injection of either 0.5 M KCl or 0.1 M acetylcholine into the coelomic cavity. Semen was always freshly collected as "dry sperm" and kept undiluted on ice. The number of spermatozoa was counted with a hemocytometer.

Incubation of spermatozoa

Dry sperm were diluted 100-fold in artificial seawater (ASW) consisting of 458 mM NaCl, 9.6 mM KCl, 10 mM $CaCl_2$, 49 mM $MgSO_4$, 10 mM Tris-HCl at pH 8.2. Following dilution and incubation at 20°C, each sample was centrifuged at $3,000 \times g$ for 5 min at 0°C.

Analysis of lipids

Total lipids were extracted from spermatozoa by the method of Bligh and Dyer [13] and analyzed by high-performance thin-layer chromatography (HPTLC), according to the method of Macala *et al* [12] with some modifications as described in previous papers [18, 22]. The amounts of PC, phosphatidylserine (PS), phosphatidylethanolamine (PE), cardiolipin (DPG), cholesterol (Ch), and free fatty acid (FFA) in sea urchin spermatozoa were determined from the standard curves of the respective authentic lipids. The mass of PC in μg was converted to nmol using the relation, 1 μg= 1.27 nmol, based on 1-palmitoyl-2-arachidonyl-PC. Also, 1 μg of FFA was calculated to be 3.27 nmol as arachidonic acid.

Analysis of fatty acid composition of PC

Isolated PC on a thin-layer chromatography (TLC) plate was subjected to methanolysis by heating with 5% HCl-methanol at 85°C for 2 hr, as described previously [16, 17]. The fatty acid methylesters were extracted with *n*-hexane, followed by evaporation under a stream of N_2. The residues were dissolved in a small amount of *n*-hexane and analyzed using a GC-R1A gas-liquid chromatograph (GLC) (Shimadzu Instruments, Kyoto, Japan).

Assays of glycogen and glucose

Before and after incubation of dry sperm in ASW, spermatozoa were homogenized with 0.6 M perchloric acid. The homogenate was used for determination of glycogen by the enzymatic method [8]. The acidified homogenate was centrifuged at $10,000 \times g$ for 10 min at 4°C, and the supernatant was used for estimation of glucose after neutralization to pH 6.5–7.0 with KOH. Glucose was measured enzymatically according to Kunst *et al* [9]. Readings were made at 340 nm at 20°C using a UVIDEC 430B spectrophotometer (Japan Spectroscopic Co., Tokyo, Japan).

Oxygen consumption

Oxygen consumption in a sperm suspension was measured polarographically with an oxygen consumption recorder (MD-1000, Iijima Electronics MFG Co., Aichi, Japan). Twenty-five microliters of dry sperm was incubated in 2.5 ml ASW in a closed vessel of the oximeter at 20°C. The diluted spermatozoa were left exposed to air until determination of oxygen consumption at the desired time. Total oxygen consumption was calculated from the respiratory rate and incubation period, as described previously [20].

Estimation of phospholipase and lipase activity

Dry sperm were homogenized with 10 mM

$CaCl_2$, 10 mM $MgCl_2$, 1 mM dithiothreitol and 50 mM Tris-HCl at pH 7.5. The homogenate was incubated with 4.75 kBq 1-palmitoyl-2-[1-^{14}C]arachidonyl-PC (1.9 GBq/mmol), 4.75 kBq 1-palmitoyl-2-[1-^{14}C]arachidonyl-PE (1.9 GBq/mmol) or 9.25 kBq [carboxyl-^{14}C]-triolein (4.1 GBq/mmol) for 1 hr at 20°C in a total volume of 0.4 ml. The lipids were extracted according to Bligh and Dyer [3]. The radioactivity in the FFA fraction separated by TLC was measured by liquid scintillation spectrometry. The protein content of the homogenate was measured by the method of Lowry *et al* [11], using bovine serum albumin as the standard.

Electron microscopic observation

Before and after dilution of dry sperm in ASW and incubation for 30 min at 20°C, the spermatozoa were prefixed in 2.5% glutaraldehyde-ASW solution for 40–60 min at 4°C; a volume of sperm suspension was mixed with the same volume of cold 5% glutaraldehyde in 80% ASW. The fixed spermatozoa were rinsed with cold ASW and post-fixed with 1% OsO_4 in ASW for 2 hr at 4°C. Samples were washed in distilled water, and then immersed in saturated aqueous uranyl acetate for 4 hr for block staining. After dehydration in a graded series of ethanol solutions, the specimens were embedded in epoxy resin and ultrathin-sections were cut on a Reichert Ultracut ultramicrotome. After staining with lead citrate, they were observed using a Hitachi 7000 electron microscope.

Reagents

The phospholipid, Ch and FFA standards were purchased from Sigma Chemical. 1-Palmitoyl-2-[1-^{14}C]arachidonyl-PC, 1-palmitoyl-[1-^{14}C]-arachidonyl-PE and [carboxyl-^{14}C]triolein were obtained from Du Pont-New England Nuclear. All reagents and solvents were of analytical grade. HPTLC and TLC plates (silica gel 60) were obtained from E. Merck (Darmstadt, Germany).

RESULTS

Lipid content

Previous studies have shown that the lipids in *H. pulcherrimus* spermatozoa are composed of several kinds of phospholipid and Ch [16, 17]. Similar phospholipids and Ch were also detected in *A. crassispina, E. mathaei, P. depressus, S. intermedius, S. nudus* and *T. hardwickii* (Fig. 1). Among the phospholipids, PC, PS, PE and DPG were identified in these spermatozoa. PC was present at high concentrations. Triglyceride and cholesterol ester were present at extremely low levels (less than 1 μg/10^9 sperm).

When dry sperm of *A. crassispina, E. mathaei, P. depressus, S. intermedius, S. nudus* and *T. hardwickii* were diluted 100-fold in ASW and incubated for 1 hr at 20°C, the PC content decreased significantly following the initiation of flagellar movement (Figs. 1 and 2). Although a slight increase in FFA was also observed during incubation, the levels of other phospholipids and Ch remained almost constant. During incubation in ASW for 1 hr, about 11, 9 and 5 nmol PC were consumed by 10^9 spermatozoa of *A. crassispina, E. mathaei* and *P. depressus,* respectively (Fig. 2a). Amounts of FFA accumulated were about 5, 5 and 2 nmol in 10^9 spermatozoa of these species (Fig. 2b).

Fatty acid composition of PC

Fatty acid components of PC in dry sperm of *A. crassispina, E. mathaei, P. depressus, S. intermedius, S. nudus* and *T. hardwickii* were of the unsaturated type for the most part, such as oleic (18:1), eicosamonoenoic (20:1), arachidonic (20:4) and eicosapentaenoic acid (20:5) (Table 1). Polyenoic fatty acids constituted more than 50% of the total fatty acid moiety of PC in these spermatozoa, except that the PC in *T. hardwickii* spermatozoa contained about 35% polyenoic fatty acids. In contrast, the saturated fatty acids in PC were present at only 20–30%, palmitic (16:0) and stearic (18:0) acids being predominant.

Glycogen and glucose content

Glycogen was present in spermatozoa of the six

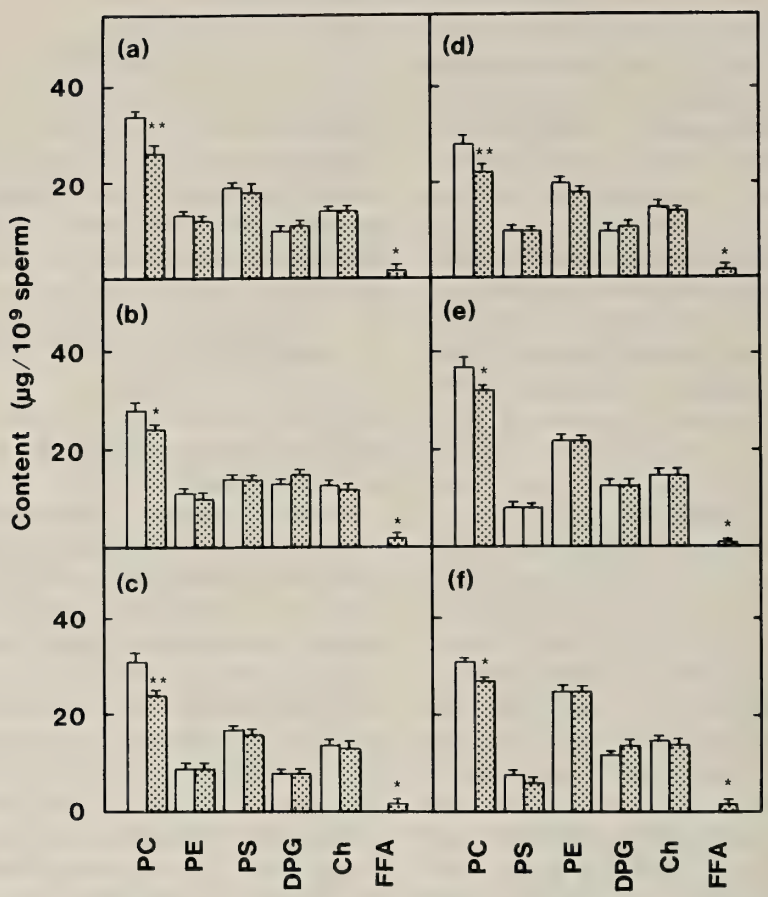

FIG. 1. Changes in lipid levels after incubation of spermatozoa of *A. crassispina* (a), *E. mathaei* (b), *P. depressus* (c), *S. intermedius* (d), *S. nudus* (e) and *T. hardwickii* (f). Before (clear) and after (dotted) 100-fold dilution and incubation of dry sperm in ASW for 1 hr at 20°C, lipids were extracted and analyzed by HPTLC. Each value is the mean of four separate experiments. Vertical bars show S.E.M. *P* values are compared with those prior to incubation by means of Student's *t* test. $^{*}P<0.1$; $^{**}P<0.05$.

species, but at extremely low levels (Table 2). Glucose was present in a trace amount (Table 2). After incubation in ASW for 1 hr, the glycogen content of *T. hardwickii* spermatozoa decreased significantly, but there was little change in spermatozoa of the other species.

Oxygen consumption

Since oxygen is required for oxidation of the lipid, the amount of O_2 consumed by the spermatozoa was measured at various intervals after dilution in ASW (Fig. 3). The rate of O_2 consumption decreased gradually during long-term incubation. About 0.55, 0.40 and 0.20 μmol O_2 was consumed during incubation of 10^9 spermatozoa of *A. crassispina*, *E. mathaei* and *P. depressus* for 1 hr, respectively.

Phospholipase activity

Since hydrolysis of PC in *H. pulcherrimus* spermatozoa occurs *via* the action of phospholipase A_2 [13, 16, 18], an experiment was conducted to examine the properties of the phospholipase A_2 in spermatozoa of the other species of sea urchin. The homogenates of dry sperm from *A. crassispina*, *E. mathaei*, *P. depressus*, *S. intermedius*, *S. nudus* and *T. hardwickii* were incubated with 1-palmitoyl-2-[1-^{14}C]arachidonyl-PC, 1-palmitoyl-

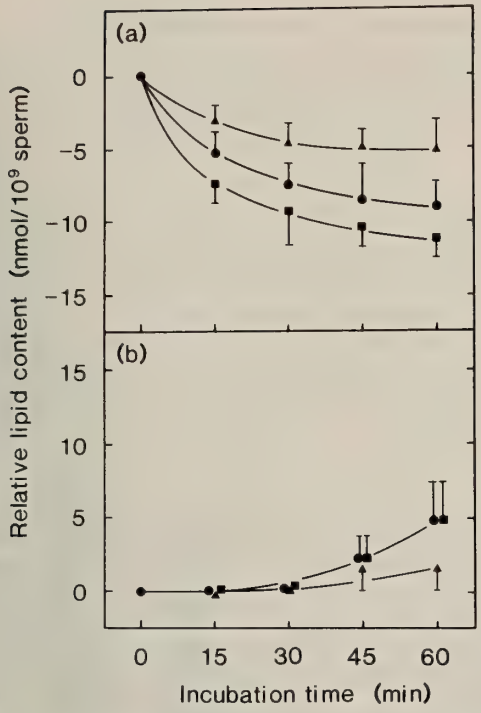

2-[1-^{14}C]-arachidonyl-PE or [carboxyl-^{14}C]-triolein for 1 hr at 20°C, followed by extraction and separation of FFA by TLC. The radioactivity of FFA from PC released by phospholipase A_2 in these species of spermatozoa was 2–3 times higher than that from PE (Table 3), suggesting that the phospholipase A_2 in sea urchin spermatozoa of the order Echinoidea has high substrate specificity for PC. In contrast to phospholipase, there was only a trace amount of radioactivity of FFA from TG released by lipase (Table 3).

Observation of sperm midpieces

The sea urchin spermatozoon consists of a head, a midpiece and a tail. Previous studies have shown

FIG. 2. Changes in levels of phosphatidylcholine (a) and free fatty acid (b) following incubation of sea urchin spermatozoa. Dry sperm of *A. crassispina* (■), *E. mathaei* (▲) and *P. depressus* (●) were diluted 100-fold and incubated in ASW at 20°C. Each value is the mean of four separate experiments. Vertical bars show S.E.M.

TABLE 1. Fatty acid composition of phosphatidylcholine in sea urchin spermatozoa

Fatty acid	Percentage					
	A. crassispina	*E. mathaei*	*P. depressus*	*S. intermedius*	*S. nudus*	*T. hardwickii*
14:0	2.3±0.9	1.1±0.1	1.3±0.2	0.3±0.1	2.1±0.2	2.1±0.4
15:0	n.d.	0.3±0.1	0.1	tr.	1.9±0.2	2.7±0.4
16:0	12.6±0.7	19.6±0.1	12.1±0.5	12.7±0.6	22.8±0.3	18.5±1.5
16:1	4.2±1.0	n.d.	3.4±0.3	2.4±0.3	1.5±0.1	4.1±0.5
18:0	7.9±0.8	9.7±1.1	3.1±0.1	1.1±0.2	6.6±0.7	13.5±2.5
18:1	9.8±0.4	5.1±0.3	8.3±0.9	7.8±0.6	6.7±0.4	15.8±2.5
18:2	1.5±0.2	1.5±0.1	1.1±0.3	0.8±0.1	1.3±0.2	2.3±0.7
18:3	0.3±0.1	1.2±0.3	0.5±0.1	n.d.	0.6±0.1	1.0±0.3
18:4	8.9±0.3	4.5±0.7	14.3±0.5	7.4±0.5	n.d.	n.d.
20:1	4.6±0.2	8.0±0.4	13.4±0.5	8.3±0.3	7.4±0.2	8.4±1.2
20:2	n.d.	2.4±0.7	n.d.	4.9±0.5	2.9±0.1	2.2±0.3
20:3	7.8±0.6	3.2±0.5	6.0±0.6	tr.	2.1±0.6	1.0±0.5
20:4 (n−6)	27.1±0.9	22.5±1.1	23.4±1.5	17.2±0.4	20.0±0.6	7.9±1.1
20:5 (n−3)	12.3±0.2	16.8±1.5	11.2±0.5	32.8±1.3	18.4±0.2	10.6±2.7
22:4	0.5±0.1	0.9±0.1	0.4±0.1	0.9±0.1	0.7±0.2	0.9±0.3
22:5	n.d.	0.7±0.1	0.1	0.2±0.1	1.3±0.2	2.2±0.2
22:6	tr.	2.3±0.6	1.4±0.8	3.2±0.7	3.7±0.3	7.0±0.5
Saturated	22.8±0.8	30.6±0.9	16.6±0.6	14.2±0.7	33.5±0.7	36.6±2.8
Monoenoic	18.6±1.0	13.1±0.2	25.1±1.6	18.4±0.9	15.5±0.4	28.3±2.1
Polyenoic	58.5±1.1	56.2±0.9	58.3±2.2	67.4±1.5	50.8±0.4	35.1±3.2

Each value is the mean±S.E.M. obtained in three separate experiments. tr., trace amount (less than 0.1%); n.d., not detectable.

TABLE 2. Changes in the levels of glycogen and glucose in sea urchin spermatozoa following incubation with seawater

Species	Glycogen (μg/10^9 sperm)		Glucose (nmol/10^9 sperm)	
	dry sperm	incubation for 1 hr	dry sperm	incubation for 1 hr
A. crassispina	0.5±0.1	0.5±0.1	tr.	tr.
E. mathaei	0.6±0.1	0.7±0.1	tr.	tr.
P. depressus	0.3±0.1	0.2±0.1	tr.	tr.
S. intermedius	0.5±0.2	0.4±0.1	tr.	tr.
S. nudus	0.4±0.1	0.3±0.1	tr.	tr.
T. hardwickii	3.7±0.4	2.1±0.5*	tr.	tr.

Dry sperm were diluted 100-fold in ASW and incubated for 1 hr at 20°C. Each value is the mean± S.E.M. obtained from three separate experiments. tr., trace amount (less than 0.1 nmol/10^9 sperm) *P* values are compared with those prior to incubation by means of Student's *t* test. *$P<0.1$.

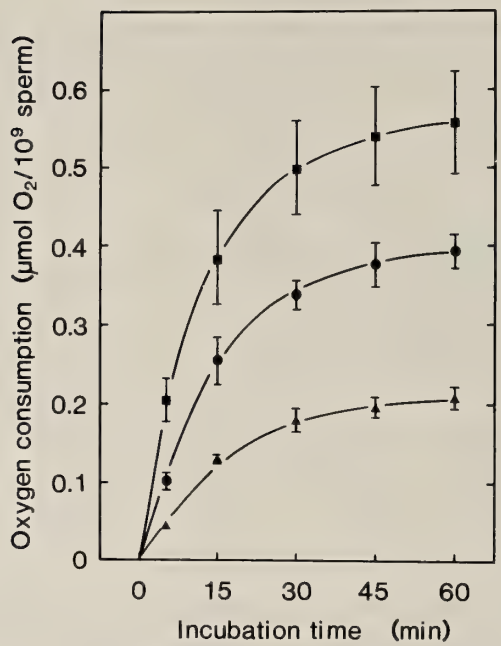

FIG. 3. Oxygen consumption in sea urchin spermatozoa. Dry sperm of *A. crassispina* (■), *E. mathaei* (▲) and *P. depressus* (●) were diluted 100-fold and incubated in ASW at 20°C. Each value is the mean of three separate experiments. Vertical bars show S.E.M.

that the sperm midpiece of *H. pulcherrimus* contains lipid bodies in the intramembrane space of the mitochondrion [14]. In longitudinal sections through the spermatozoa of *A. crassispina* (Fig. 4a), *E. mathaei* (Fig. 4b) and *P. depressus* (Fig. 4c), the lipid bodies were observed within a single toroidal mitochondrion in the midpiece. Although a region between the mitochondrial outer and inner membranes was occasionally empty, the lipid bodies were irregular in profile and low-electron density. After 30 min of incubation in ASW, the lipid bodies in sperm midpieces of *A. crassispina* (Fig. 5), *E. mathaei* (Fig. 6) and *P. depressus* (Fig. 7) had shrunk or disappeared. Although these spermatozoa did not possess the lipid globules which have observed in *Brissopsis lyrifera* [1], *Echinarachinus parma* [26] and *Glyptocidaris crenularis* [15], the midpiece of *A. crassispina* occasionally contained spherical inclusion bodies within mitochondrial matrix (data not shown). However, these inclusion bodies did not change during incubation.

DISCUSSION

This study showed that spermatozoa of *A. crassispina, E. mathaei, P. depressus, S. intermedius, S. nudus* and *T. hardwickii,* sea urchins of the order Echinoidea, contained PC at high concentrations (Table 1). The PC content decreased without any change in the content of other phospholipids following initiation of flagellar movement (Figs. 1 and 2). These spermatozoa contained triglyceride (Table 1) [16, 17], glycogen (Table 2) [20] and glucose (Table 2) [20] at very low levels. Thus it appears that PC is a common endogenous substrate for energy metabolism in spermatozoa of

TABLE 3. Activities of phospholipase A_2 and lipase in sea urchin spermatozoa

Substrate	Activity (nmol hydrolyzed/hr/mg protein)					
	A. crassispina	*E. mathaei*	*P. depressus*	*S. intermedius*	*S. nudus*	*T. hardwickii*
PC	24±3	25±3	21±3	23±2	21±2	29±2
PE	12±1	11±1	6±1	8±1	8±1	15±2
TG	tr.	tr.	tr.	tr.	tr.	tr.

Dry sperm were homogenized with 10 mM $CaCl_2$, 10 mM $MgCl_2$, 1 mM dithiothreitol and 50 mM Tris-HCl at pH 7.5. The homogenate was incubated with 1-palmitoyl-2-[1-^{14}C]arachidonyl-PC, 1-palmitoyl-2-[1-^{14}C]arachidonyl-PE or [carboxyl-^{14}C]triolein for 1 hr at 20°C. Total lipids were extracted following by measurement of the radioactivity in the fatty acid separated by TLC. Each value is the mean±S.E.M. obtained from three separate experiments. tr., trace amount (less than 0.1 nmol hydrolyzed/hr/mg protein).

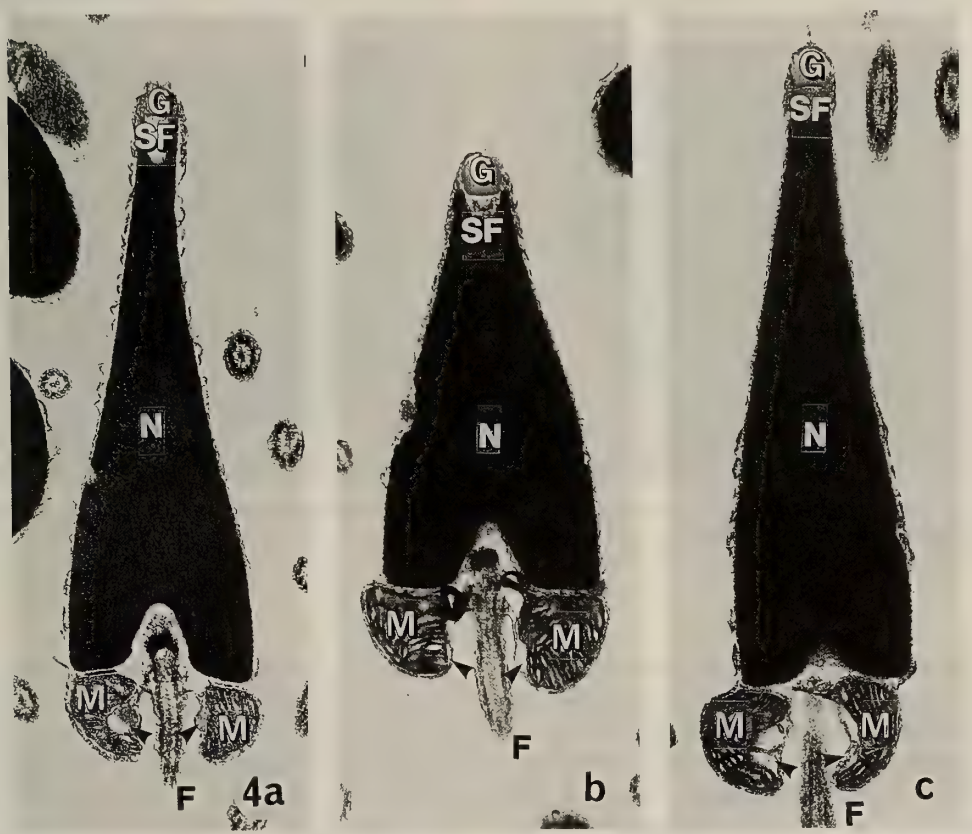

FIG. 4. Longitudinal section through a spermatozoon of *A. crassispina* (a), *E. mathaei* (b) and *P. depressus* (c). Arrow heads show lipid bodies. F: flagullum, G: acrosomal granule, M: mitochondrion, N: nucleus, SF: submitochondrial fossa. ×24,000.

urchins belonging to the order Echinoidea.

The data also showed the presence of phospholipase A_2 activity in spermatozoa of these sea urchin species, but lipase activity was very low (Table 3). The phospholipase A_2 was found to have strict substrate specificity for PC. These results suggest that the preferential hydrolysis of PC among phospholipids is due to the properties of phospholipase

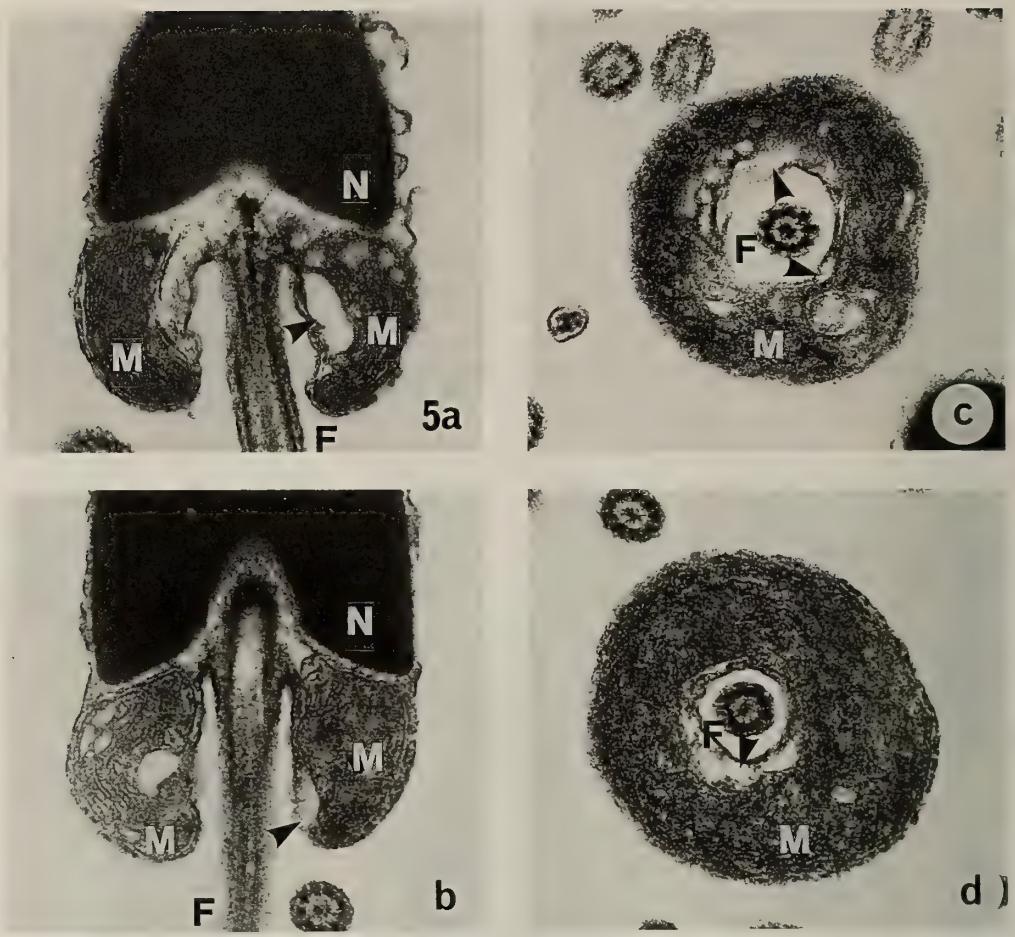

FIG. 5. Longitudinal (a, b) and transverse (c, d) sections through the mitochondrial region of *A. crassispina* spermatozoa before (a, c) and after incubation in ASW for 30 min (b, d). Arrow heads show lipid bodies. F: flagellum, M: mitochondrion, N: nucleus. ×42,600.

A_2. Previous studies have also indicated that *H. pulcherrimus* spermatozoa possess the β-oxidation and tricarboxylic acid cycle system [16, 18, 20], and thus it follows that the fatty acid obtained by hydrolysis of PC is metabolized to produce ATP for flagellar movement in sea urchin spermatozoa.

In this study, about 11 nmol PC was consumed in 10^9 spermatozoa of *A. crassispina* after incubation for 1 hr (Fig. 2a). In *E. mathaei* and *P. depressus*, PC consumption was about 9 and 5 nmol/10^9 spermatozoa, respectively. Since PC is composed of two fatty acid moieties, about 22, 18 and 10 nmol fatty acids/10^9 spermatozoa are produced respectively from PC in *A. crassispina*, *E. mathaei* and *P. depressus* during incubation for 1 hr. However, about 5, 5 and 2 nmol fatty acid remained as FFA following 1 hr of incubation of *A. crassispina*, *E. mathaei* and *P. depressus* spermatozoa (Fig. 2b). Thus it is possible that about 17, 13 and 8 nmol fatty acid/10^9 spermatozoa is utilized, respectively, to produce energy in these species. The chain length of fatty acid in PC of these spermatozoa was generally 20 carbons, as in the case of arachidonic and eicosapentaenoic acids (Table 1). From this, the amount of O_2 required for PC metabolism during incubation for 1 hr was determined to be 0.50 μmol in 10^9 spermatozoa for *A. crassispina*, 0.38 μmol for *E. mathaei* and 0.24

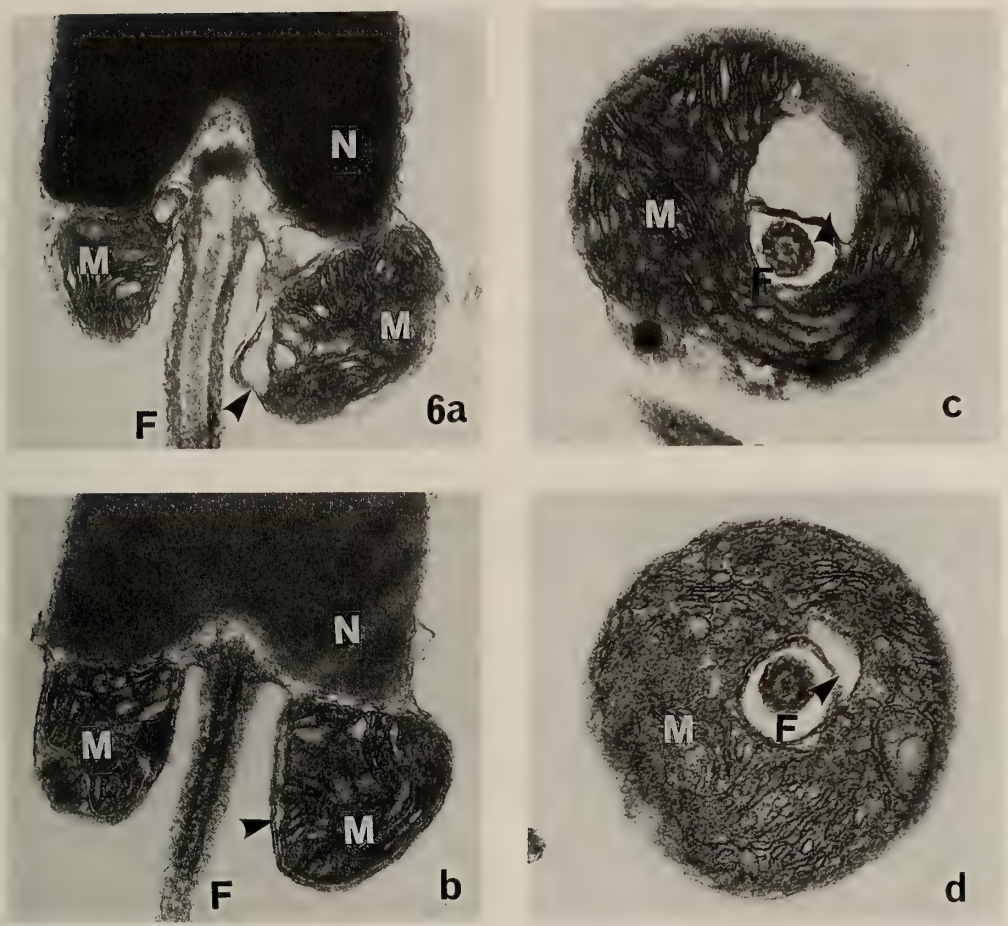

FIG. 6. Longitudinal (a, b) and transverse (c, d) sections through the mitochondrial region of *E. mathaei* spermatozoa before (a, c) and after incubation in ASW for 30 min (b, d). Arrow heads show lipid bodies. F: flagellum, M: mitochondrion, N: nucleus. ×42,600.

μmol for *P. depressus*. These values are quite consistent with those actually determined for O_2 consumption; 0.55, 0.40 and 0.20 μmol O_2 per 1 hr in 10^9 spermatozoa of *A. crassispina, E. mathaei* and *P. depressus,* respectively (Fig. 3).

Upon being spawned in seawater, sea urchin spermatozoa begin flagellar movement and respiration is activated. The initiation of sea urchin sperm motility requires external Na^+ and is associated with Na^+-dependent acid extraction [23]. Following dilution in seawater, the intracellular pH (pH*i*) of sea urchin spermatozoa rises from 6.8 to 7.4 [2, 5, 10]. Internal alkalization leads to activation of dynein ATPase, resulting in initiation of motility [5]. Also, the activation of phospholipase A_2 and fatty acid oxidation have been shown to increase with a rise in pH from 6.5 to 7.5 [19]. Thus, PC metabolism is activated following an increase in pH*i* of spermatozoa, coincident with initiation of motility and activation of respiration.

Our data also showed that several lipid bodies were present within the mitochondria of *A. crassispina, E. mathaei* and *P. depressus* spermatozoa (Fig. 4). Similar lipid bodies located between the mitochondrial outer and inner membrane have been observed in *H. pulcherrimus* spermatozoa [14]. These lipid bodies shrink and disappear after incubation [14], and the present data for spermato-

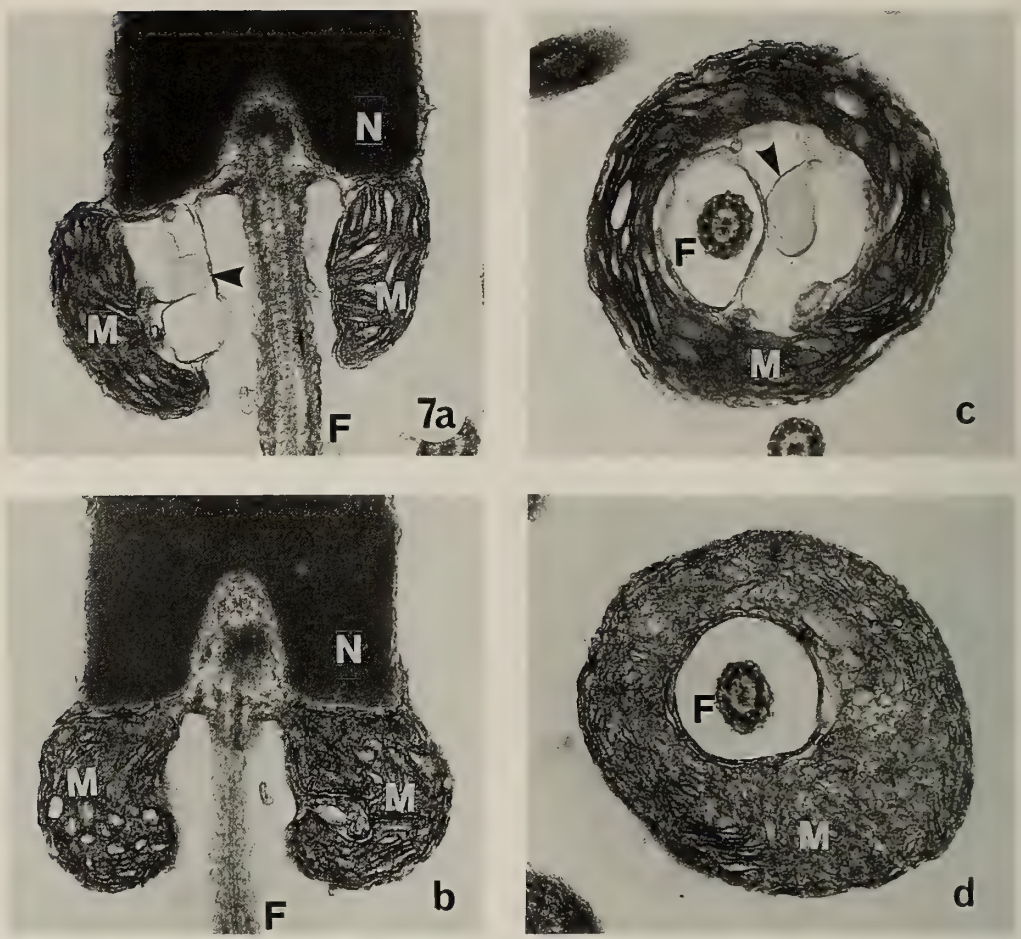

FIG. 7. Longitudinal (a, b) and transverse (c, d) sections through the mitochondrial region of *P. depressus* spermatozoa before (a, c) and after incubation in ASW for 30 min (b, d). Arrow heads show lipid bodies. F: flagullum, M: mitochondrion, N: nucleus. ×42,600.

zoa of *A. crassispina* (Fig. 5), *E. mathaei* (Fig. 6) and *P. depressus* (Fig. 7) confirm this. These findings suggest that the disappearance of the lipid bodies is correlated with the decrease in the level of PC. Presumably, the lipid bodies within mitochondria of echinoid spermatozoa are reservoirs of PC used as an endogenous substrate.

ACKNOWLEDGMENTS

The authors are grateful to Dr. I. Yasumasu, Waseda University, and to Dr. Y. Nagahama, National Institute for Basic Biology, for their encouragement and valuable advice. Thanks are also extended to Dr. K. Osanai and the staff of Asamushi Marine Biological Station, Tohoku University, Dr. K. Inaba and the staff of Misaki Marine Biological Station, University of Tokyo, Dr. S. Nemoto and the staff of Tateyama Marine Laboratory, Ochanomizu University, and Dr. H. Tousuji, Kagoshima University, for affording us the opportunity to utilize their facilities and for their kind assistance in collecting the sea urchins. This study was supported in part by a Grant-in Aid (No. 03740396 to M.M.) from the Ministry of Education, Science and Culture of Japan.

REFERENCES

1 Afzelius BA, Mohri H (1966) Mitochondria respiring without exogenous substrate: A study of aged sea urchin spermatozoa. Exp Cell Res 42: 10–17

2 Bibring TJ, Baxandall J, Harter CC (1984) Sodium-

dependent pH regulation in active sea urchin sperm. Dev Biol 101: 425–435

3 Bligh EG, Dyer WJ (1959) A rapid method of total lipid extraction and publication. Can J Biochem Physiol 37: 911–917

4 Christen R, Schackmann RW, Shapiro BM (1982) Elevation of intracellular pH activates sperm respiration and motility of sperm *Strongylocentrotus purpuratus*. J Biol Chem 257: 14881–14890

5 Christen R, Schackmann RW, Shapiro BM (1983) Metabolism of sea urchin sperm. Interrelationships between intracellular pH, ATPase activity, and mitochondrial respiration. J Biol Chem 258: 5392–5399

6 Gibbons BH, Bibbons IR (1972) Flagellar movement and adenosine triphosphate activity in sea urchin sperm extracted with triton X-100. J Biol Biol 54: 75–97

7 Gray J (1928) The effect of dilution on the activity of spermatozoa. J Exp Biol 5: 337–344

8 Keppler D, Decker K (1984) Glycogen. In "Methods of Enzymatic Analysis Vol 6" Ed by HU Bergmeyer, VCH Publishers, Weinheim, pp 11–18

9 Kunst A, Draeger B, Ziegenhorn J (1984) D-Glucose. In "Methods of Enzymatic Analysis Vol 6" Ed by HU Bergmeyer, VCH Publishers, Weinheim, pp 163–172

10 Lee HC, Johnson C, Epel D (1983) Changes in internal pH associated with initiation of motility and acrosome reaction of sea urchin sperm. Dev Biol 95: 31–45

11 Lowry OH, Rosebrough NJ, Farr AL, Randall RJ (1951) Protein measurement with the Folin phenol reagent. J Biol Chem 193: 265–275

12 Macala LJ, Yu RK, Ando S (1983) Analysis of brain lipids by high performance thin-layer chromatography and densitometry. J Lipid Res 24: 1243–1250

13 Mita M, Harumi T, Suzuki N, Ueta N (1991) Localization and characterization of phosphatidylcholine in sea urchin spermatozoa. J Biochem 109: 238–242

14 Mita M, Nakamura M (1992) Ultrastructural study of an endogenous energy substrate in spermatozoa of the sea urchin *Hemicentrotus pulcherrimus*. Biol Bull 182: 298–304

15 Mita M, Nakamura M (1992) Lipid globules at the midpieces of *Glyptocidaris crenularis* spermatozoa and their relation with energy metabolism. Mol Reprod Develop (in press)

16 Mita M, Ueta N (1988) Energy metabolism of sea urchin spermatozoa, with phosphatidylcholine as the preferred substrate. Biochim Biophys Acta 959: 361–369

17 Mita M, Ueta N (1989) Fatty chain composition of phospholipids in sea urchin spermatozoa. Comp Biochem Physiol 92B: 319–322

18 Mita M, Ueta N (1990) Phosphatidylcholine metabolism for energy production in sea urchin spermatozoa. Biochem Biophys Acta 1047: 175–179

19 Mita M, Ueta N, Harumi T, Suzuki N (1990) The influence of an egg-associated peptide on energy metabolism in sea-urchin spermatozoa: the peptide stimulates preferential hydrolysis of phosphatidylcholine and oxidation of fatty acid. Biochem Biophys Acta 1035: 175–181

20 Mita M, Yasumasu I (1983) Metabolism of lipid and carbohydrate in sea urchin spermatozoa. Gamete Res 7: 133–144

21 Mohri H (1957) Endogenous substrates of respiration in sea-urchin spermatozoa. J Fac Sci Univ Tokyo, Sec IV, 8: 51–63

22 Mohri H (1964) Phospholipid utilization in sea-urchin spermatozoa. Publ Staz Zool Napoli 34: 53–58

23 Nishioka D, Cross N (1978) The role of external sodium in sea urchin fertilization. In "Cell Reproduction" Ed by ER Dirksen, DM Prescott, CF Fox, Academic Press, New York, pp 403–413

24 Rothschild Lord (1956) The physiology of sea urchin spermatozoa. Action of pH, dinitrophenol, dinitrophenol+versene, and usnic acid or O_2 uptake. J Exp Biol 33: 155–173

25 Rothschild Lord, Cleland KW (1952) The physiology of sea-urchin spematozoa. The nature and location of the endogenous substrate. J Exp Biol 41: 66–71

26 Summers DG, Hylander BL (1974) An ultrastructural analysis of early fertilization in the sand dollar, *Echinarachnius parma*. Cell Tiss Res 150: 343–368

27 Tombes RM, Brokaw CJ, Shapiro BM (1987) Creatine kinase dependent energy transport in sea urchin spermatozoa: Flagellar wave attention and theoritical analysis of ~P diffusion. Biophys J 52: 75–86

28 Tombes RM, Shapiro BM (1985) Metabolite channeling: A phosphocreatine shuttle to mediate high energy phosphate transport between sperm mitochondrion and tail. Cell 41: 325–334

29 Tsuchiya M, Nishihara M (1984) Ecological distribution of two types of the sea urchin, *Echinometra mathaei* (Blainville), on Okinawan reef flat. Galaxea, 3: 131–143

30 Uehara T, Shingaki M (1985) Taxonomic studies in the four types of the sea urchin, *Echinometra mathaei*, from Okinawa Japan. Zool Sci 2: 1009 (Abstract)

ZOOLOGICAL SCIENCE 10: 85–92 (1993)

Grafting of Center Cells of Horseshoe Crab Embryos into Host Embryos at Different Developmental Stages

Tomio Itow

Department of Biology, Faculty of Education, Shizuoka University, Ohya 836, Shizuoka 422, Japan

ABSTRACT—The center cells of horseshoe crab embryos at the early gastrula stage induced secondary embryos after grafting into embryos at same stage and into late blastula stages. However, when the center cells of embryos at early gastrula stage were grafted into embryos at the stage of early cleavage, secondary embryos were not formed. Secondary embryos were not induced after grafting center cells into embryos at the late gastrula stage or after. These results indicate that the center cells of the early gastrula cannot induce secondary embryos at stages other than the early gastrula and late blastula.

However, center cells of embryos at stages later than the early gastrula did induce secondary embryos. These center cells of later embryos were grafted into embryos at the early gastrula and late blastula stage, and secondary embryos were induced. This indicates that center cells of embryos after the early gastrula stage retain the ability of embryonic induction.

INTRODUCTION

The mechanism of induction by the primary organizer is now one of the most exciting problems to be analysed in developmental biology [1, 9, 10, 13, 14]. However, reports of the primary organizer in animals except Chordata are sparse [2, 6, 7].

Surface cleavages occur in horseshoe crab embryos as in other Arthropoda, and the blastopore appears at the early gastrula stage. Surface cells migrate toward the blastopore and enter there. A cell mass is formed beneath the blastopore at the early gastrula stage (Fig. 1). The cell mass at the gastrula stage is called the primary cumulus in spider embryos. Morphological observations and previous experimental studies have shown that the germ disc is formed around the cell mass, and that cell mass is later situated at the

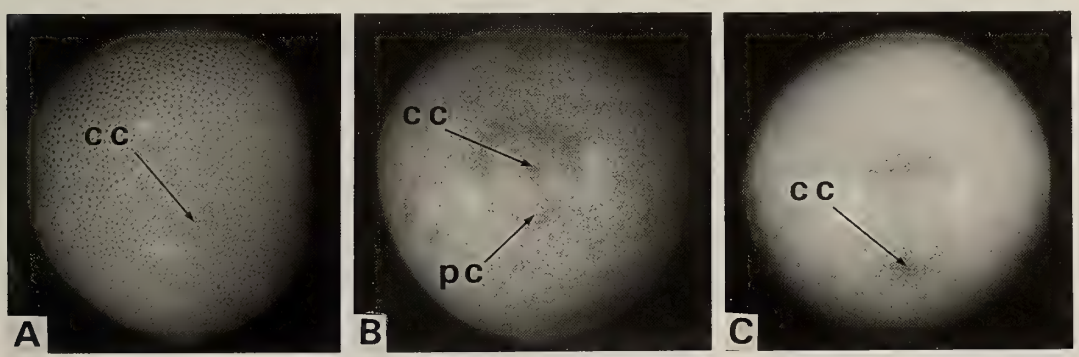

Fig. 1. A: An embryo of horseshoe crab at the early gastrula stage (Stage 7). B: An embryo of horseshoe crab at the late gastrula stage (Stage 10). C: An embryo of horseshoe crab at the early neurula stage (Stage 12). CC; center cells. PC; posterior cumulus.

Accepted March 26, 1991
Received August 29, 1992

posterior end of the ventral plate (the embryonic area) and successively forms segment primordia [3, 4, 5, 12]. The cell mass at the posterior end of the embryonic area is sometimes called the growth zone.

If the cell mass of the embryo at the early gastrula stage is electrically cauterized, the treated embryo cannot develop further. If the cell mass is divided into two or three pieces by electrocauterization or cell dissociation, the treated embryo develops into double or triple embryos [8, 11]. These experiments suggest that the cell mass plays a central role in embryogenesis, and that it is similar to the mesodermal teloblast of Annelida and Crustacea. Therefore the mass is referred to as the center cells. To find out more about the role of the center cells, we attempted grafting experiments [6, 7]. We found that secondary embryos could be induced by interspecific grafts of center cells, indicating that center cells have the capacities of primary induction.

It would be very interesting to know whether the center cells (the primitive cumulus) of the early gastrula can induce secondary embryos in embryos at different stages. Can the center cells (the growth zone) of stages later than the early gastrula induce secondary embryos in embryos at the early gastula stage? This paper deals with this question.

MATERIALS AND METHODS

Adult horseshoe crabs, *Tachypleus* (*Carcinosporpius*) *rotundicauda,* were collected in the Gulf of Siam in Thailand and sent to Japan. *Limulus polyphemus* were obtained from Woods Hole Marine Laboratory in Massachusetts, the Duke University Marine Laboratory in North Carolina, and the Gulf Specimen Company in Florida. They were transferred to Shizuoka University where the present study was conducted. Eggs were fertilized by artificial insemination. The developmental stages were identified according to the normal criteria [12].

For the grafts, a small hole (diameter about 0.05–0.075 mm) was opened in the chorion of host horseshoe crab embryos at the late blastula (Stage 6) and early gastrula stage (Stage 7). The hole was positioned on the side opposite to the center cells. The center cells and other tissues were cut off the donor embryos, and inserted through the hole. In the case of embryos at stages earlier than the gastrula, the surface layer and surface cells of the same volume as the grafted center cells were removed at the early gastrula stage. For the injection of homogenized center cells, center cells of 25–50 eggs at different stages were removed and homogenized in 0.5 ml distilled water or sea water. The concentration of homogenates of center cells from embryos at Stage 7 was about 0.5–5.0 mg (dry weight)/ml. Absorption granules (Collagen, Spongel [Yamanouchi Co., Tokyo]) were added to the resulting homogenates, and the solutions were again homogenized. More than 10^{-6} ml of solution including the granules was then injected into host embryos at different stages, on the side opposite to the center cells. The treated embryos were cultured in a small laboratory dish in about 10 ml sea water containing antibiotics such as 0.5 μg/ml streptomycin and 0.5 unit/ml penicilline.

Normal and treated embryos were vitally stained with 1/20,000–1/400,000 neutral red and observed using a streomicroscope. Secondary embryos were judged to be at stage 20, Stage 21 (the stage of hatching), and the stage after hatching. When the treated embryo had an extra ventral plate (embryonic area), where there were often extra appendages, it was assumed a secondary embryo had been formed.

Some normal and treated embryos were fixed in Bouin's or Carnoy's solution, embedded in celloidin and paraffin and sectioned at 5–10 μm. The sections were stained with Mayer's haematoxylin and eosin.

RESULTS

Grafts of center cells at the early gastrula into embryos at same stage

The grafts of center cells were made in the American horseshoe crab, *Limulus polyphemus* and in the Asian species, *Tachypleus rotundicauda.* The results were similar in both species (Table 1). Although the experiments were performed using mainly *Limulus polyphemus,* the results of experiments using both species are de-

Table 1. Results of transplantation of crude center cells from early gastrulae (Stage 7) into embryos at the same stage

DONOR→HOST	Total number of operated on embryos	No of embryos developed upto St. 20 (percent of the total)	No of embryos with secondary embryos (percent of the developed)
Limulus → *Limulus*	162	83 (51.2)	18 (21.7)
Tachypleus → *Tachypleus*	191	20 (10.5)	4 (20.0)
Limulus → *Tachypleus*	166	22 (13.3)	3 (13.6)
Tachypleus → *Limulus*	211	38 (18.0)	6 (15.8)
Non-center cells → *Limulus* [Control]	107	47 (43.9)	0 (0.0)

Table 2. Results of transplantation of crude center cells and injection of homogenized center cells. The center cells at Stage 7 were grafted into embryos at the same stage

METHODS OF GRAFTINGS	Total number of operated on embryos	No of embryos developed upto St. 20 (percent of the total)	No of embryos with secondary embryos (percent of the developed)
TRANSPLANTATION	1536	188 (12.2)	37 (19.7)
INJECTION	569	243 (42.7)	23 (9.5)
Injection of homogenized non-center cells [Control]	121	72 (59.5)	1 (1.4)

The control for transplantation experiments is shown in Table 1.

Table 3. Grafts of center cells from early gastrulae (Stage 7) into embryos at the late blastula stage (Stage 6) and Stage 7

STAGE OF HOST EMBRYOS	Total number of operated on embryos	No of embryos developed upto St. 20 (percent of the total)	No of embryos with secondary embryos (percent of the developed)
Late blastula (Stage 6)	1878	504 (26.8)	71 (14.1)
Early gastrula (Stage 7)	1503	504 (33.5)	60 (11.9)
Injection of sea water [Control]			
Stage 6	362	137 (37.8)	0 (0.0)
Stage 7	906	373 (41.2)	1 (0.3)

scribed together.

The rate of formation of secondary embryos following the injection of homogenized center cells was lower than that resulting from the transplantation of intact center cells (Table 2). However, as the injection method is simpler, the following section describes the results obtained by this technique.

When the center cells were grafted into embryos at the late blastula stage (Stage 6), secondary embryos were induced at a rate similar to that in embryos at the early gastrula stage (Stage 7) (Table 3 and Fig. 2).

The secondary embryos induced after grafting

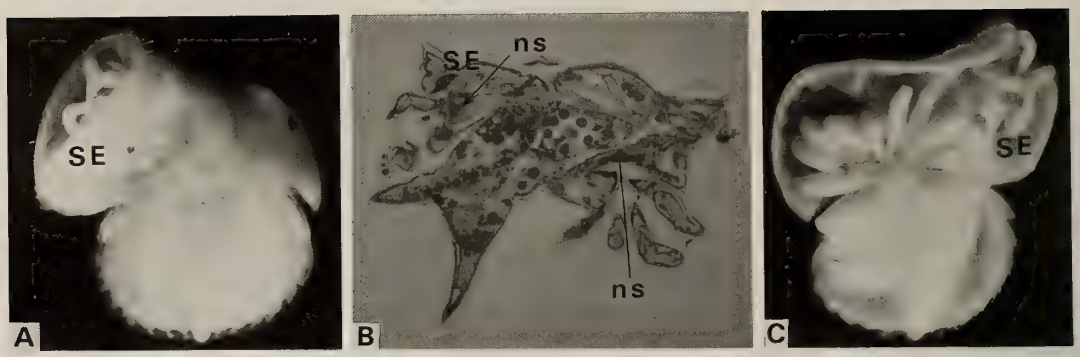

Fig. 2. A: Secondary embryo after gafting of the cortical cytoplasm (surface layer) of an embryo at Stage 3 into an embryo at Stage 7. B: Histological features of the secondary embryo. C: Secondary embryo after grafting of the midgut gland (liver) of an adult into an embryo at Stage 7. SE; secondary embryo. ns; nervous system.

center cells from the early gastrula stage (Stage 7) into embryos at the same stage had the following characteristics. The size and structure of secondary embryos differed. The smaller ones had only a small ventral plate without appendages. The larger ones had the same size and form as the host embryos. The alimentary canals and hearts of secondary embryos often fused with those of the host embryos. The medial body axis of the secondary embryo was sometimes oriented in the opposite direction to that of the host embryo. These characteristics differed from those of double and triple embryos induced by electrocauterization and cell dissociation [11]. In the latter case, the posterior ends of induced double and triple embryos faced towards the point where the center

Table 4. Grafts of center cells from early gastrulae (Stage 7) into embryos at different stages

STAGE OF HOST EMBRYOS	Total number of operated on embryos	No of embryos developed upto St. 20 (percent of the total)	No of embryos with secondary embryos (percent of the developed)
Immediately after fertilization	40	21 (52.5)	2 (9.5)
Early cleavage (Stages 1 & 2)	230	62 (27.0)	0 (0.0)
Late cleavage (Stages 3 & 4)	118	30 (25.4)	1 (3.3)
Early blastula (Stage 5)	149	66 (44.3)	2 (3.0)
Late blastula and early gastrula (Stages 6 & 7)	1005	194 (19.3)	26 (13.4)
Late gastrula and early neurula (Stages 10 to 12)	57	29 (50.9)	0 (0.0)
Later stages (Stages 14 to 17)	26	18 (69.2)	0 (0.0)
Injection of sea water [Control]			
Immediately after fertilization	59	24 (40.7)	2 (8.3)
Stages 1 & 2	113	13 (11.5)	0 (0.0)
Stages 3 & 4	111	41 (36.9)	0 (0.0)
Stage 5	55	26 (47.3)	0 (0.0)
Stages 6 & 7	1268	510 (40.2)	1 (0.2)
Stages 10 to 12	349	231 (66.2)	0 (0.0)
Stages 14 to 17	307	274 (89.3)	0 (0.0)

cells had been. In the secondary embryos resulting from grafting, the clear junction part was often observed in the region between the host embryo and the secondary one. These characteristics were not observed in the double and triple embryos induced by electrocauterization and cell dissociation. More detailed characteristics of the secondary embryos have been described in the previous paper [6].

Grafts of center cells from the early gastrula into embryos at different stages

When the center cells (primitive cumulus) of embryos at the early gastrula stage (Stage 7) were homogenized and injected into embryos at early cleavage stages (Stage 1 and Stage 2), secondary embryos were rarely induced, except in embryos injected immediately after fertilization (Table 4).

For the control experiments, we opened small holes in the chorions of embryos at different developmental stages, without grafting. In these cases, secondary embryos were not induced, except in embryos immediately after fertilization. When the host embryos were operated on immediately after fertilization, 21 of 40 treated embryos (52.5%) developed, and 2 of them (9.5%) had secondary embryos. The proportion of treated embryos which developed secondary embryos did not differ significantly from that of the control embryos with small holes but no grafts.

When the host embryos were in the late cleavage stages (Stage 3 and Stage 4) and the early blastula stage (Stage 5), secondary embryos were induced at a very low rate (Fig. 3). The characteristics of the secondary embryos did not differ from those of secondary embryos induced after grafting center cells of early gastrulae into embryos at the early gastrula stage (Stage 7).

The center cells of early gastrulae (Stage 7) were grafted into embryos at stages later than Stage 7 (Table 4). Secondary embryos were never formed.

Grafts of surface cells at stages earlier than gastrulae into eggs at early gastrula stage

The grafting of cortical cytoplasm (surface layer) and surface cells (blastoderm cells) from unfertilized eggs and embryos at the early cleavage stages (Stage 1 and Stage 2) into the embryos at late blastula and early gastrula stages (Stages 6 and 7) never resulted in the formation of secondary embryos (Table 5). The grafting of center cells of embryos at late cleavage stages (Stage 3 and Stage

Table 5. Grafts of the cortical cytoplasm (surface layer), surface cells and center cells at different stages into late blastulae (Stage 6) and early gastrulae (Stage 7). The whole tissue of larvae and different tissues from adults were also grafted into embryos at the same stages

STABE OF DONOR EMBRYO		Total number of operated on embryos	No of embryos developed upto St. 20 (percent of the total)	No of embryos with secondary embryos (percent of the developed)
Unfertilized eggs		76	25 (32.9)	0 (0.0)
Early cleavage (Stages 1 & 2)		120	113 (94.2)	0 (0.0)
Late cleavage (Stages 3 & 4)		116	66 (56.9)	5 (7.6)
Blastula (Stages 5 & 6)		159	84 (52.8)	3 (3.6)
Early gastrula (Stages 7)		1153	238 (20.6)	28 (11.8)
Late gastrula (Stages 9 to 11)		360	95 (26.4)	9 (9.5)
Later stages (Stages 13 to 20)		629	294 (46.7)	29 (9.9)
1st & 2nd larvae		179	61 (34.1)	9 (14.8)
Tissues of adults	cartilage	238	76 (31.9)	4 (5.3)
	midgut gland	55	14 (25.5)	4 (28.6)
	ovary	110	42 (38.2)	5 (11.9)
	blood	80	39 (48.8)	0 (0.0)

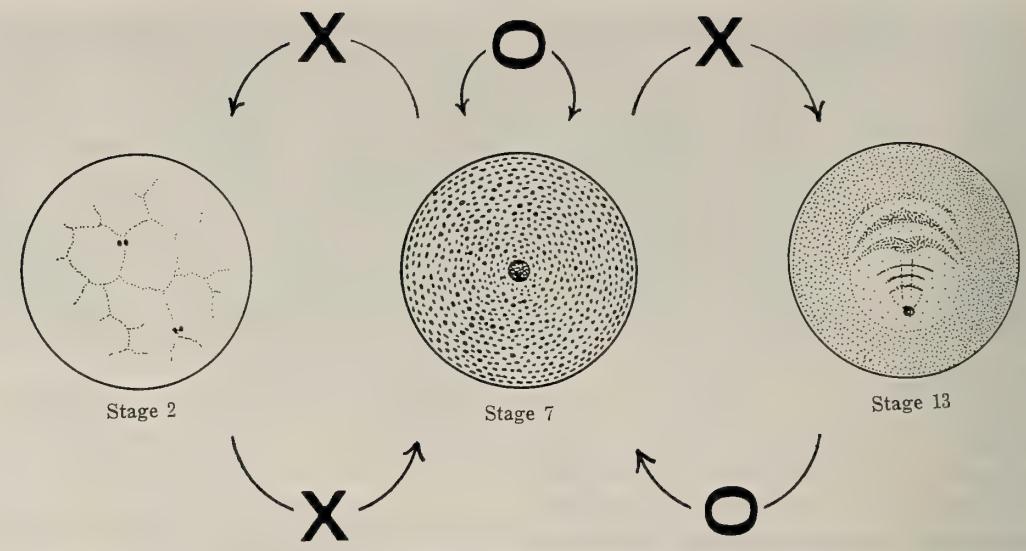

Fig. 3. Summary of results

4) and blastula stages (Stage 5 and Stage 6) into embryos at Stage 6 and Stage 7 resulted in the formation of secondary embryos, but the rate of formation was very low (Table 5). The characteristics of the secondary embryos did not differ from those of secondary embryos induced after grafting center cells of early gastrulae into embryos at the early gastrula stage (Stage 7).

Grafts of center cells of stages later than early gastrulae into embryos at the early gastrula stage

When the center cells (growth zones) of embryos at stages later than early gastrulae were grafted into embryos at the late blastula stage (Stage 6) and early gastrula stage (Stage 7), secondary embryos were induced at a high rate (Table 5). Cells other than center cells did not induce secondary embryos after similar grafting. For example, when the posterior cumulus was grafted into embryos at Stage 6 or Stage 7, 18 of 92 treated embryos developed and none of them had secondary embryos.

The homogenates of whole tissues of larvae induced secondary embryos at a high rate after grafting into embryos at Stage 6 or Stage 7. Several tissues of adult horseshoe crabs were also able to induce secondary embryos, including cartilage (endoskeleton), midgut gland (liver) and ovary. Injection of blood did not induce secondary embryos.

The characteristics of the secondary embryos induced after grafts of tissues of adults, larvae and embryos at stages later than Stage 7 did not differ from those of secondary embryos induced after grafting center cells of early gastrulae into embryos at the early gastrula stage (Stage 7).

The above-mentioned results are summarized in Fig. 3.

DISCUSSION

Secondary embryos were formed at a high rate after grafts of center cells of embryos at the early gastrula stage (Stage 7) into embryos at the late blastula stage (Stage 6) and Stage 7 (Table 1) [6, 7]. The rate of induction of secondary embryos in embryos receiving grafts at Stage 6 was as high as that in grafted Stage 7 embryos. This must mean that the cells of the embryos at the late blastula stage (Stage 6) have the capacity to respond to the signal for embryonic induction.

Secondary embryos rarely developed after grafting center cells of Stage 7 embryos into the embryos at other stages, except Stage 6. This indicates that only embryos at Stages 6 and 7 have the capacity to respond to the signal for embryonic

induction.

When small holes were opened, without grafting, on the chorions of embryos immediately after fertilization, secondary embryos sometimes developed in the treated embryos. I interpret this phenomenon as follows. The chorions of embryos immediately after fertilization are still very soft. The distribution of substances in these eggs is thought not to be stable, and the distribution of cells is determined later, according to the distribution of substances. The shock of opening a hole seems to deragne the normal distribution of substances and cells, and treated embryos may sometimes develop secondary embryos.

When the center cells were grafted into embryos at the stages of late cleavage and early blastula (Stages 3 to 5), secondary embryos were sometimes induced, although at a low rate. I interpret these results as follows. One possibility is that embryos at Stages 3 to 5 have a weak capacity to respond to the signal for embryonic induction. Another posibility is that the grafted center cells or the substance for induction are retained in treated embryos until the latter develop to Stages 6 and 7.

The cortical cytoplasms (surface layers) of unfertilized eggs and embryos at early cleavage stages (Stages 1 and 2) did not induce secondary embryons in embryos at Stage 6 or Stage 7. The cortical cytoplasms of such eggs may not yet possess the induction substance for embryogenesis.

On the other hand, the surface cells of embryos at late cleavage and blastula stages (Stages 3 to 6) induced secondary embryos in embryos at Stage 6 and Stage 7, although the rate of formation of secondary embryos was low. The finding may mean that the surface cells of embryos at Stages 3 to 6 contain the substance for embryonic induction.

When center cells of embryos at the early gastrula stage (Stage 7) were grafted into embryos at the late gastrula stage and after, secondary embryos were never induced. But the center cells (growth zone) of embryos at the late gastrula, or later, stages did induce secondary embryos after grafting into embryos at Stage 6 or Stage 7. This must indicate that the center cells of embryos at stages later than the early gastrula stage (Stage 7) still contain the substance for embryonic induction.

The homogenates of whole tissues of larvae and some tissues of adults induced secondary embryos after injections into embryos at early gastrula. This indicate that the substance for embryonic induction is contained in tissues of larvae and adults.

REFERENCES

1 Cooke J (1989) Mesoderm-inducing factors and Spemann's organizer phenomenon in amphibian development. Development 107: 229–241

2 Holm Å (1952) Experimentelle Untersuchungen uber die Entwicklung und Entwicklungsphysiologie des Spinnen Embryos. Zool Bidrag Uppsala 29: 293–424

3 Itow T (1984) The induction of malformed embryos by inhibition of cell proliferation in the horseshoe crab, *Tachypleus tridentatus*. Acta Embryol Morpho exp NS 5: 177–193

4 Itow T (1985) The effect of Ca^{2+}-free sea water on the body segmentation in the horseshoe crab (Chelicerata, Arthropoda). Acta Embryol Morph exp NS 6: 15–29

5 Itow T (1986) Inhibitors of DNA synthesis change differentiation of segments and increase segment number in horseshoe crab embryos. Roux's Arch Devl Biol 195: 323–333

6 Itow T, Kenmochi S, Mochizuki T (1991) Induction of secondary embryos by intra- and interspecific grafts of center cells under the blastopore in horseshoe crabs. Develop Growth & Differ 33: 251–258

7 Itow T, Mochizuki T (1988) Interspecific transplantation of germ disc cells from the American to the Asian horseshoe crab eggs. Proc Arthropod Embryol Soc Jpn 24: 15–16

8 Itow T, Sekiguchi K (1979) Induction of multiple embryos with $NaHCO_3$ or calcium free sea water in the horseshoe crab. Roux's Arch Devl Biol 187: 245–254

9 Kimelman D, Kirschner M (1987) Synergistic induction of mesoderm by FGF and TGF β and the identification of an mRNA coding for FGF in the early *Xenopus* embryo. Cell 51: 869–877

10 Kintner CR, Dodd J (1991) Hensen's node induced neural tissue in *Xenopus* ectoderm. Implications for the action of the organizer in neural induction. Development 113: 1495–1505

11 Sekiguchi K (1966) Determination in the development of the horse-shoe crab. Jap J Exp Morphol 20: 84–88 (In Japanese)

12 Sekiguchi K (1973) A normal plate of the development of the Japanese horse-shoe crab, *Tachypleus tridentatus*. Sci Rep Tokyo Kyoiku Daigaku, Sec B,

15: 152–162

13 Slack JMW, Darlington BG, Heath JK, Godsave SF (1987) Mesoderm induction in early *Xenopus* embryos by heparin binding growth factors. Nature 326: 197–200

14 Smith JC (1987) A mesoderm-inducing factor is produced by a *Xenopus* cell line. Development 99: 3–14

ZOOLOGICAL SCIENCE 10: 93–101 (1993)

Ultrastructural Observations on Sperm Penetration in the Egg of Elkhorn Sculpin, *Alcichthys alcicornis*, Showing Internal Gametic Association

YASUNORI KOYA[1], KAZUNORI TAKANO[2] and HIROYA TAKAHASHI[1]

[1]*Department of Biology, Faculty of Fisheries, Hokkaido University, Minato-cho 3-1-1, Hakodate 041, Japan, and* [2]*Sesoko Marine Science Center, University of the Ryukyus, Sesoko 3422, Motobu-cho, Okinawa 095-02, Japan*

ABSTRACT—Early fertilization process has been investigated ultrastructurally in elkhorn sculpin, *Alcichthys alcicornis*. In the eggs before immersion in sea water, spermatozoon was seen to be attached to the ooplasmic membrane at the site of an inner opening of the micropylar canal. By 10 sec after immersion in sea water, a fertilizing spermatozoon penetrated the ooplasm for about half the head length, and vesiculation occurred on the fused plasma membrane at the apical region of sperm head. By 30 sec after the immersion, the fertilizing spermatozoon showed a change in the tail axoneme, indicating a loss of its motility. By 1–2 min after the immersion, spermatozoon further penetrated the ooplasm up to its middle piece. It is worthy to note that a portion of ooplasm containing no significant cytoplasmic organelles other than ribosomes appeared around the penetrated sperm head and came to expand during the sperm penetration to form a triangular region surrounding the sperm head. This ooplasmic region may have a role in an active engulfment of immotile spermatozoon into the ooplasm. By 3 min after the immersion, sperm nuclear membrane was separated from chromatin and became vesiculated starting from the anterior region of sperm head caudalwards. Details of the events in early fertilization process were presented.

INTRODUCTION

An extensive work on the ultrastructural level has been accumulated dealing with early events occurring in the course of fertilization in teleosts. Initial stages of sperm-egg fusion and the formation of fertilization cone have been described in mummichog, *Fundulus heteroclitus* [2], and common carp, *Cyprinus carpio* [8]; the process of sperm penetration has been traced, though partially, in several species of teleosts [3, 7, 10, 13, 17, 18, 22, 24]; and changes of sperm nuclear membrane and the formation of the second polar body and blastodisc have been observed in rose bitterling, *Rhodeus ocellatus ocellatus* [18] and the mummichog [3], respectively. However, few studies have so far examined a complete spectrum of these continuous events of early fertilization in any single species of fishes. This seems to be due mainly to a difficulty of determining an actual time of occurrence of these successive events, since these events may proceed rather asynchronously in a mass of eggs after insemination. Only the work of Iwamatsu and Ohta [6] has revealed, using denuded and polyspermic eggs of medaka, *Oryzias latipes*, a series of ultrastructural changes from an initial stages of sperm-egg fusion to the formation of male pronucleus.

Elkhorn sculpin, *Alcichthys alcicornis*, has a unique mode of reproduction called "internal gametic association" [14]. In this teleost species, sperm is introduced into ovarian cavity by copulation and enters the micropylar canal of eggs ovulated into the ovarian cavity, but actual sperm-egg fusion does not occur within the ovary until the eggs have been released into sea water. In eggs freshly stripped from copulated females, sperm remains to be attached to the ooplasmic surface, and an actual fertilization reaction is initiated quite

Accepted October 15, 1992
Received August 5, 1992

synchronously when the eggs are immersed in sea water. Availability of a lot of sperm-associated eggs from a single, copulated female allows samplings of these eggs in accurate time sequences after immersion of the eggs in sea water. Thus the eggs of the elkhorn sculpin appear to provide a useful model system for the time-course studies of early events occurring during fertilization reaction in teleost fishes. In the present study, ultrastructural features were described on gametes in the course of serial changes from "attachment" through "binding" to the early step of male pronucleus formation, with special reference to a characteristic ooplasmic movement having a possible relation with sperm penetration into the ooplasm.

MATERIALS AND METHODS

Adult males and females of the elkhorn sculpin used in the present study were captured by a trammel set along the shore of Usujiri, southern Hokkaido, during spawning season (March–April) in 1989–1991. Mature eggs and sperm were obtained by manually pressing the abdomen of mature fish. Spermatozoa, unfertilized eggs and fertilized eggs sampled at various intervals of time after immersion in sea water at 10°C were fixed with Karnovsky's fixative for 5 hr at room temperature. For transmission electron microscopy, after being washed with cold 0.1 M cacodylate buffer (pH 7.4), the specimens were post-fixed with 1% OsO_4 in 0.1 M cacodylate buffer for 2 hr at 4°C. After dehydration through a graded ethanol series, the specimens were embedded in Epon. Ultrathin sections were prepared with a Reichert-Jung Ultracut E ultramicrotome, stained with uranyl acetate and lead citrate or with lead citrate alone, and examined with a Hitachi H-7000 electron microscope. Epon-embedded eggs were sectioned at about 1 μm in thickness, and stained with toluidine blue for light microscopy. For scanning electron microscopy, the fixed specimens were washed with 0.1 M cacodylate buffer and dehydrated in a graded ethanol series followed by isoamyl acetate. Then the specimens were dried with liquid CO_2 in a critical point drier. The dried specimens were coated with gold and examined with a Hitachi S-2300 electron microscope.

RESULTS

Sperm morphology

The mature spermatozoon of the elkhorn sculpin measures about 37 μm in total length. Its head is of thick spatula-shape, being about 2.9 μm long, 1.4 μm wide and 0.8 μm thick, and is devoid of acrosomal structure (Fig. 1). The sperm nucleus is composed of homogeneously condensed chromatin. On one side of the flattened nucleus, two centrioles are present slightly posterior to the middle of its length. From the distal centriole a groove with an axonema runs posteriorly along the

FIG. 1. TEM micrograph of a sagittal section of the sperm head and middle piece. Numerous mitochondria (m) are seen in the middle piece. Arrow indicats a cytoplasmic sleeve surrounding the proximal portion of the sperm tail. ×15,000.

long axis of the head. A middle piece conjoins the posterior end of the head, with many small-sized mitochondria aggregating compactly. It is noted that, on the centriolar side of the nucleus, several mitochondria extend their distribution anteriorly along the axonema in the head portion. A short, thin cytoplasmic sleeve surrounds the proximal portion of the sperm tail (Fig. 1 arrows). The flagellum has a typical 9+2 arrangement of microtubules.

Micropylar apparatus

The mature egg of elkhorn sculpin is globular in form measuring about 1.2 mm in diameter, and is covered with a vitelline envelope of about 40 μm thick. A micropylar apparatus is located at the animal pole of the egg. The micropyle is composed of a micropylar vestibule forming a shallow depression of about 70 μm in diameter on the chorion, and a micropylar canal which opens in the center of the micropylar vestibule (Fig. 2a). The micropylar canal is about 5.5 μm in diameter at its outer opening, and tapers gradually toward the inner opening of about 1.4 μm in diameter which allows only one spermatozoon to pass through (Fig. 2b). An ooplasmic projection containing a few ribosomes exists just beneath the micropylar canal, and protrudes into the micropylar canal for about 0.6 μm (Fig. 2b).

Morphological changes of the egg after immersion in sea water

In the elkhorn sculpin, sperm is introduced by

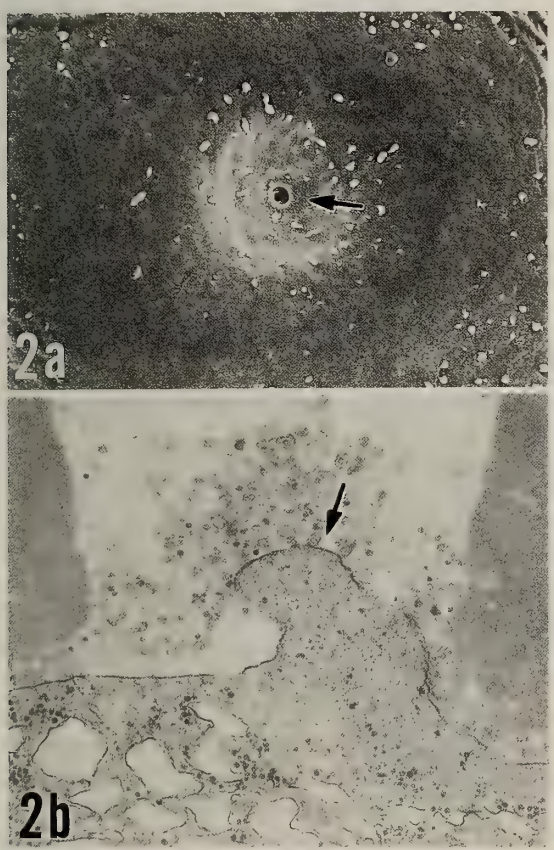

FIG. 2. (a), SEM micrograph of the animal pole of an egg, showing a micropylar apparatus consisting of a vestibule and a canal (arrow). ×285. (b), TEM micrograph of an inner opening of the micropylar canal. Arrow indicates an ooplasmic projection beneath the micropylar canal. ×30,000.

FIG. 3. TEM micrograph of the micropylar canal of an egg before immersion in sea water. A spermatozoon is attached to the ooplasmic projection, but a fusion of its plasma membrane with ooplasmic membrane has not yet occurred. ×20,000.

copulation into the ovarian cavity. In the eggs stripped from copulated females, many spermatozoa had entered the micropylar canal, and a single spermatozoon was seen to be attached to the plasma membrane of ooplasmic projection in the inner opening of the micropylar canal (Fig. 3). However, fusion between sperm and ooplasmic membrane had not yet occurred at this stage, since no spermatozoon remained on the ooplasmic surface around the inner opening of the micropylar canal after the removal of the vitelline envelope from freshly stripped eggs.

Eggs from copulated females were immersed into sea water immediately after stripping. Five sec after immersion, the spermatozoon attached to ooplasmic membrane did not show any change. It was remarked that the ooplasmic projection had disappeared around the attached spermatozoon which came to lie on the flat surface of ooplasm. Membrane fusion between spermatozoon and egg could not be observed yet at that time. Cortical alveoli were distributed closely abutting against the ooplasmic membrane, without showing an actual membrane fusion.

Membrane fusion between spermatozoon and egg had already completed 10–15 sec after immersion. Fertilizing spermatozoon penetrated the ooplasm for about half the head length (Fig. 4), and a vesiculation occurred on the plasma membrane at the apical region of sperm head fused to ooplasmic membrane. As the vesiculation advanced, the sperm plasma membrane disappeared completely to expose the sperm nuclear membrane to ooplasm. In the ooplasm around the penetrated sperm head, there were vesicular membranous structures which appeared to originate in the vesiculated plasma membrane of spermatozoon and egg (Fig. 4). Part of ooplasm came to protrude along the unpenetrated part of sperm head to form the so-called fertilization cone. Furthermore, an ooplasmic region containing no particular cytoplasmic organelles appeared surrounding the penetrating sperm head (Fig. 4). Membranes of cortical alveoli near the micropylar region were fused to the ooplasmic membrane, and the cortical alveoli were broken down to release their contents into the space between the vitelline envelope and ooplasmic membrane.

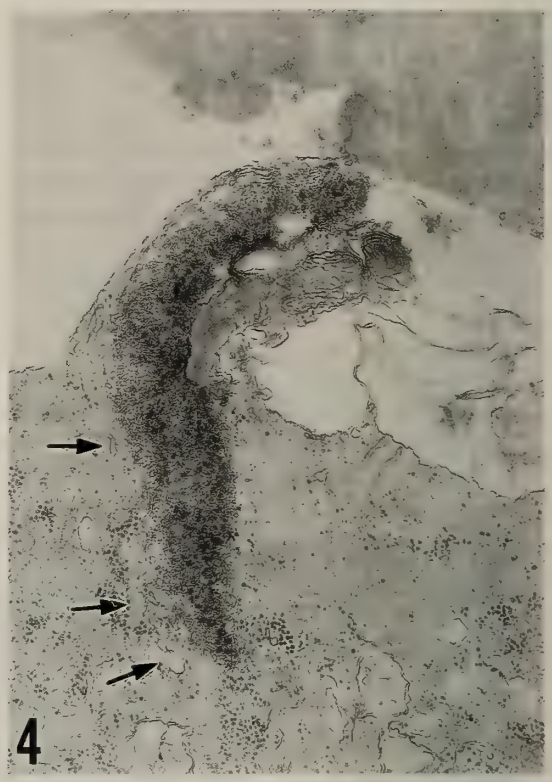

Fig. 4. Electron micrograph of the egg by 10 sec after immersion in sea water. An fertilizing spermatozoon penetrates the ooplasm and membrane fusion between spermatozoon and egg has begun. Several vesiclar structures are seen near the penetrating sperm head (arrows). ×20,000.

Twenty to thirty sec after immersion, the spermatozoon penetrated the ooplasm for more than half the head length. The membrane of sperm head had completely disappeared (Fig. 5). The ooplasm surrounding the penetrating spermatozoon contained few cytoplasmic organelles. At this stage, the sperm tail which remained outside of ooplasm was shown to be completely lacking in the typical 9+2 structure of its flagellar microtubles, and consisted of numerous fibrillar structures running through its length (Fig. 5). Such a structural change of flagellar microtubles seemed to accompany the progress of fertilization reaction in the penetrating spermatozoon. The breakdown of cortical alveoli was advancing further near the micropylar region, but not in other regions of the cortical cytoplasm of the egg.

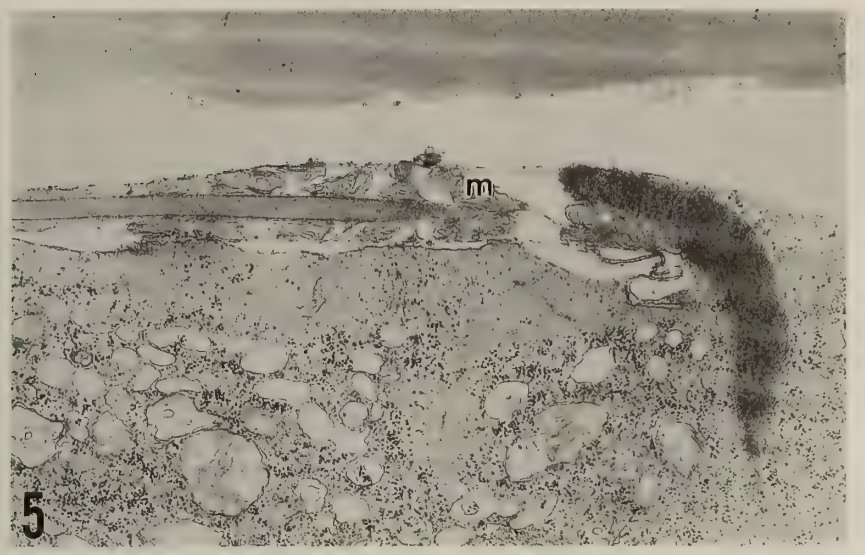

FIG. 5. Electron micrograph of the fertilizing spermatozoon by 30 sec after immersion of the egg in sea water. The flagellar microtubles are degenerated. Sperm mitochondria (m) remain outside the egg. ×15,000.

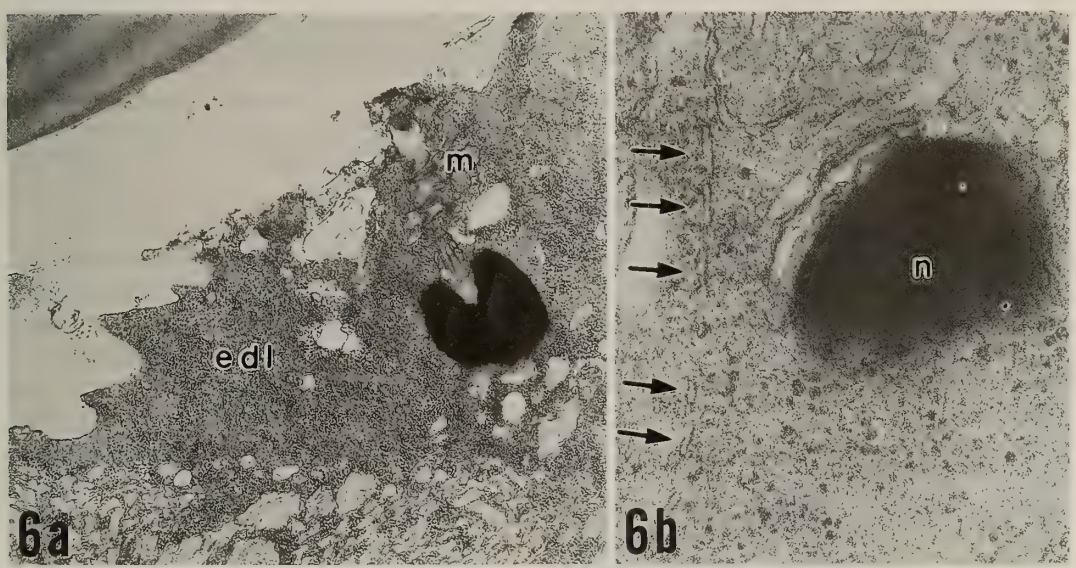

FIG. 6. TEM micrographs of eggs by 2 min after immersion in sea water. (a) Sperm head and mitochondria (m) have penetrated the ooplasm. The ooplasm surrounding the penetrating spermatozoon forms an electron dense, triangular zone (edl) containing lybosomes only. ×12,000. (b) The vesicular structures (arrows) are arranged in a row near the sperm nucleus (n). ×45,000.

One to two min after immersion, the spermatozoon penetrated the ooplasm further up to its middle piece. Sperm mitochondria, the basal part of axial filaments, and sperm nucleus covered with the nuclear membrane were all exposed to ooplasm (Fig. 6a). Several vesicles were seen to be arranged in a row in the ooplasm near the sperm head (Fig. 6b). A portion of the ooplasm containing only ribosomes as a significant cytoplasmic organelles formed a rather electron-dense, trian-

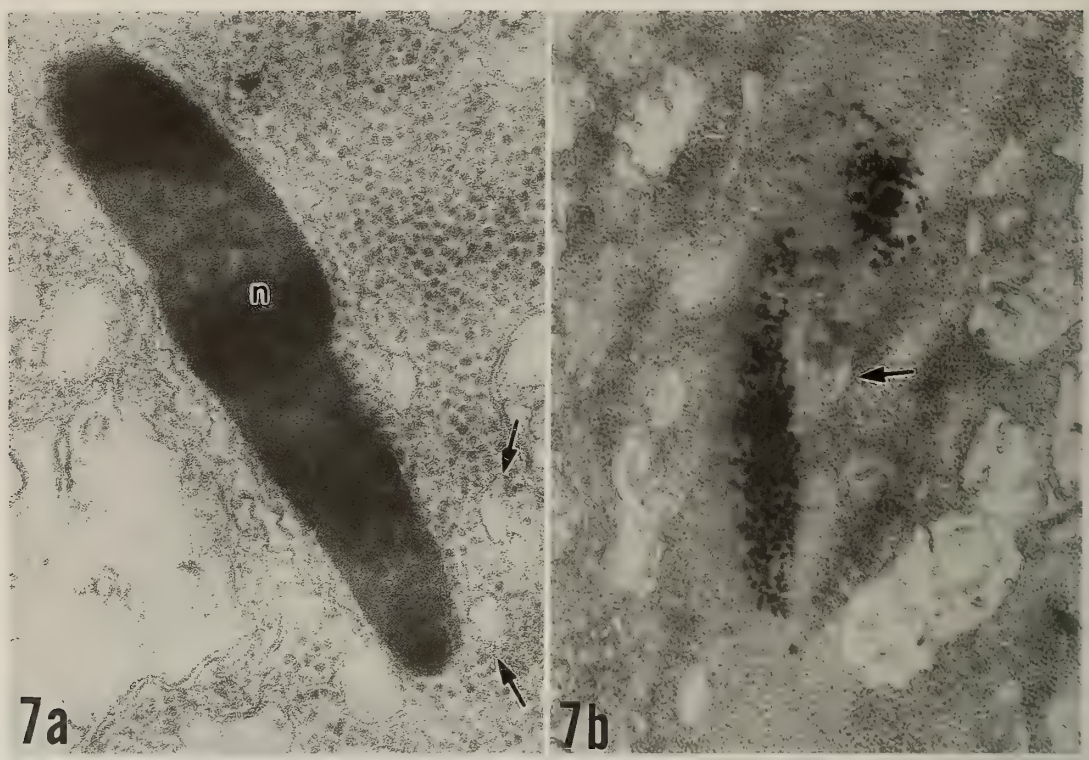

Fig. 7. Electron micrographs of eggs by 3 min after immersion in sea water. (a) The penetrated sperm nucleus (n) in the ooplasm. The nuclear membrane of spermatozoon becomes vesiculated begining from the anterior region of sperm head (arrows). ×60,000. (b) The chromatin of the penetrated sperm nucleus is dispersed. A fragment of nuclear membrane is visible near the centriol (arrow). ×60,000.

gular zone expanding from the apex of sperm head to the associated surface ooplasm (Fig. 6a).

Three min after immersion, the spermatozoon penetrated the ooplasm much deeper, and an electron dense layer was seen over the sperm head. The nuclear membrane of fertilizing spermatozoon was separated from the chromatin aggregation, and became vesiculated beginning from the anterior region of sperm head (Fig. 7a). In that region the chromatin began to disperse into ooplasm, forming a granular structure. In the eggs at this stage of fertilization, granular chromatin, centriole, and the basal part of axial filaments of spermatozoon were seen in the ooplasm. A single

Fig. 8. TEM micrograph of an egg by 5 min after immersion in sea water. The second polar body undergoing second meiotic division is seen in the perivitellin space. Numerous microtubles are present in the cytoplasmic bridge. ×4,000.

vesicle which seemed to be a part of vesiculated nuclear membrane was seen in ooplasm near the spermatozoan centriole (Fig. 7b).

Five min after immersion, fertilizing spermatozoon could not be discerned in ooplasm even by electron microscopy. A second polar body undergoing second meiotic division was seen in the perivitelline space near the micropylar region (Fig. 8). The second polar body was connected with ooplasm by a cytoplasmic bridge in which a number of microtubles ran vertically. The surface of the second polar body was complicatedly crumpled.

DISCUSSION

Fertilization is defined as the fusion of a male and a female gamete followed by nuclear fusion between the two gametes [1]. In the present study on the elkhorn sculpin, it was confirmed that spermatozoa entered the micropylar canal of ovulated eggs and were attached to the ooplasmic membrane without showing any membrane fusion between spermatozoon and egg until after the egg had been released into sea water. It is of significance to refer to such a peculiar reproductive mode as "internal gametic association" in order to distinguish it from the actual oviparity [14].

Spermatozoa of teleostean fishes are different in shape in different species, though they lack an acrosomal structure without exception. Spermatozoon of the elkhorn sculpin has a relatively long middle piece and a long, flattened head. Spermatozoa of a similar shape were reported to occur also in *Oligocottus maculosus* [20], *Cottus hangiongensis* and *C. nozawae* [19], suggesting that such a shape of spermatozoa may be common to fishes belonging to the family Cottidae. However, the spermatozoa of the elkhorn sculpin have a larger number of mitochondria as compared with those of other cottid species. Such a feature may reflect the fact that the spermatozoa of the sculpin can be motile for a very long time in ovarian fluid of the same species (data not shown).

It has been shown in many teleosts that there is a specialized conformation to attach the spermatozoon to the surface of ooplasm beneath the micropylar canal. Kudo [9] showed that the conformation in common carp, Japanese dace, *Tribolodon hakonensis,* and ayu, *Plecoglossus altivelis* was an ooplasmic projection extending up into the micropylar canal and had a function as a receptor for fertilizing spermatozoon. The existence of such a conformation has been demonstrated also in mummichog [2], chum salmon, *Oncorhynchus keta* [12], rose bitterling [18], and zebrafish, *Brachydanio rerio* [5]. The egg of the elkhorn sculpin also had a cytoplasmic protrusion on the egg surface beneath the micropylar canal, and a spermatozoon came to attach to this protrusion after passing through the canal. In the elkhorn sculpin, however, such cytoplasmic protrusion was observed to exist not only just beneath the micropylar canal but in other regions of ooplasmic surface near the micropyle. The present study could not confirm whether the cytoplasmic protrusion has a function of sperm receptor or not. It has been reported that polyslermy occurs in the medaka [6], and the rose bittering [15] when the eggs have been denuded mechanically. If the eggs of the elkhorn sculpin have a similar nature to those of the medaka and rose bitterling, it seems likely that the cytoplasmic protrusion beneath the micropylar canal does not have any special function for fertilization.

In the eggs stripped freshly from copulated female elkhorn sculpin, many spermatozoa have entered the micropylar canal and a spermatozoon have been attached to the egg surface, but the membrane fusion between spermatozoon and egg does not occur yet. The spermatozoon did not remain to be attached to the egg surface after removal of the vitelline envelope when observed by a scanning electron microscope. This indicates that the attachment between egg and spermatozoon in the ovarian lumen is relatively loose. In mammals the egg-sperm association includes two successive steps which are referred to as attachment and binding [21]. The attachment is a relatively loose, nonspecific association, while the binding is a tenacious, species-specific association [21]. Therefore the attachment of spermatozoon and egg in the ovary of the elkhorn sculpin may correspond to the nonspecific attachment of the gametes in mammals.

Membrane fusion between spermatozoon and egg has been studied in various species of animals.

It is known that the inner acrosomal membrane fuses with ooplasmic membrane in several marine invertebrates [4]. On the other hand, in mammals, a fusion between the plasma membranes of sperm head and egg microvilli occurs at the post-nuclear cap region of spermatozoon after the acrosomal reaction has completed [25]. Ultrastructural observations on membrane fusion between spermatozoon and egg in teleosts which is lacking in an acrosome on sperm head have been carried out in the medaka [6], rose bitterling [15, 17, 18], mummichog [3], common carp [11], and zebrafish [22]. However, information about gamete membrane fusion in teleosts has been relatively fragmentary as compared with that in other animal groups, possibly because of the fact that the membrane fusion between spermatozoon and egg in teleosts occurs in a short time after gamete association. As mentioned before, in the case of denuded eggs of the medaka [6], the ooplasmic membrane comes to fuse with the sperm plasma membrane in various regions one min after insemination, giving rise to polyspermy. Ohta [17] demonstrated that, in the rose bitterling, the fusion occurred between the microvillus membrane of a sperm entry site on the egg surface and the sperm head membrane at the portion in front of the centrioles. In the elkhorn sculpin, membrane fusion between spermatozoon and egg began by 10 sec after immersion in sea water. The membrane fusion occurred with a vesiculation of apical membrane of the sperm head and the ooplasmic membrane, and the vesiculation extended successively to the whole surface of the penetrated sperm head, regardless of the location of centrioles existing in the middle region of sperm head. Therefore, the membrane fusion in the elkhorn sculpin seems to occur in a similar manner to that in the medaka, and begins at the portion having no direct relation to the position of sperm centrioles.

By 30 sec after immersion in sea water, a typical 9+2 axonemal structure of the tail of fertilizing spermatozoon had disappeared. Since the microtubles of sperm tail are indispensable for sperm motility, such a change may indicate that the spermatozoon has lost it motility and the sperm tail is undergoing degeneration by this time. The ooplasm surrounding the penetrating spermatozoon was initially lacking in significant cytoplasmic organelles exhibited a relatively uniform structure. As the spermatozoon penetration proceeded, this part of ooplasm continued to expand inside to form a triangular region with accumulating ribosomes. Moreover, several vesicles, which were formed possibly by vesiculations of spermatozoon and ooplasmic membrane, were seen to be arranged in a row near the deeply penetrated sperm head, suggesting that the ooplasm was acting to draw the fertilizing spermatozoon inside into the egg. Such a change of ooplasm was never observed in unfertilized eggs even when they were immersed in sea water. These findings indicate that the ooplasm surrounding a fertilizing spermatozoon may have a role in active engulfment of the spermatozoon which has lost its motility by degeneration of tail axoneme. Wolenski and Hart [23] showed that the treatment of zebrafish eggs with cytochalasin B or D prevented the incorporation of fertilizing spermatozoon into eggs, and suggested the presence of actin-containing filaments in ooplasm which might play a role in the sperm incorporation. In the present study, although the precise mechanism of ooplasmic movement during penetration was not clarified, it is quite possible that ooplasmic microfilaments may be involved in the observed ooplasmic movement.

In medaka egg, sperm nuclear membrane is broken down by vesiculation along the lateral aspect of sperm nucleus by 3 min after insemination [6], while in rose bitterling egg, sperm nuclear membrane disappears first at the apical region of the head by 5 min after insemination [18]. In elkhorn sculpin egg, vesiculation of the outer and inner nuclear membrane occurs by 3 min after immersion of the egg in sea water. The vesiculation of sperm nuclear membrane started at the anterior region of sperm head and finished at the region near the centriole, like in the case of the medaka and the rose bitterling.

The process of formation of the second polar body in teleostean egg has been described in artificially activated eggs of the rose bitterling [16]. In this fish, the second polar body begins to rise by 15 min after activation, and completes its separation from the egg proper by 30 min later. In the

present study, a separating polar body was noticeable ultrastructurally 5 min after immersion of the eggs in sea water. The process of formation of the second polar body was confirmed to be generally similar to that found in the rose bitterling [16].

In present study, we clarified in detail the ultrastructural change of the elkhorn sculpin gametes in early fertilization processes. Moreover, we could suggest an ooplasmic movement for sperm penetration and the destiny of sperm tail during sperm penetration. Information obtained by the present study may be important to solve problems concerning the whole process of fertilization in teleosts.

ACKNOWLEDGMENTS

We wish to thank Dr. H. Munehara, Hokkaido University, for his useful suggestions. For sampling of the specimens, we are greatly indebted to the staff of Usujiri Fisheries Laboratory, Hokkaido University. This work was supported in part by a grant of the Akiyama Foundation.

REFERENCES

1 Balinsky BI (1970) An introduction to embryology. W B Saunders, Co, Philadelphia, Pennsylvania, pp 107–137

2 Brummett AR, Dumont JN (1979) Initial stages of sperm penetration into the egg of *Fundulus heteroclitus*. J Exp Zool 210: 417–434

3 Brummett AR, Dumont JN, Richter CS (1985) Later stages of sperm penetration and second polar body and blastodisc formation in the egg of *Fundulus heteroclitus*. J Exp Zool 234: 423–439

4 Colwin AL, Colwin LH (1961) Changes in the spermatozoon during fertilization in *Hydroides hexagonus* (Annelida). II. Incorporation with the egg. J Biophys Biochem Cytol 10: 255–274

5 Hart NH, Donovan M (1983) Fine structure of the chorion and site of sperm entry in the egg of *Brachydanio*. J Exp Zoo 227: 277–296

6 Iwamatsu T, Ohta T (1978) Electron microscopic observation on sperm penetration and pronuclear formation in fish egg. J Exp Zool 205: 157–180

7 Iwamatsu T, Ohta T (1981) Scanning electron microscopic observation on sperm penetration in teleostean fish. J Exp Zool 218: 261–277

8 Kudo S (1980) Sperm penetration and the formation of a fertilization cone in the common carp egg. Develop Growth & Differ 22: 403–414

9 Kudo S (1982) Ultrastructure of a sperm entry site beneath the micropylar canal in fish eggs. Zool Mag 91: 213–220

10 Kudo S (1983) Response to sperm penetration of the cortex of eggs of the fish, *Plecoglossus altivelis*. Develop Growth & Differ 25: 163–170

11 Kudo S and Sato A (1985) Fertilization cone of carp eggs as revealed by scanning electron microscopy. Develop Growth & Differ 27: 121–128

12 Kobayashi W, Yamamoto TS (1981) Fine structure of the micropylar apparatus of the chum salmon egg, with a discussion of the mechanism for blocking polyspermy. J Exp Zool 217: 265–275

13 Kobayashi W, Yamamoto TS (1987) Light and electron microscopic observation of sperm entry in the chum salmon egg. J Exp Zool 243: 311–322

14 Munehara H, Takano K, Koya Y (1989) Internal gametic association and external fertilization in the elkhorn sculpin, *Alcichthys alcicornis*. Copeia 1989: 673–678

15 Ohta T (1985) Electron microscopic observations on sperm entry and pronuclear formation in naked eggs of the rose bitterling in polyspermic fertilization. J Exp Zool 234: 273–281

16 Ohta T (1986) Electron microscopic observations on the process of the polar body formation in artificially activated eggs of the rose bitterling. J Exp Zool 237: 263–270

17 Ohta T (1991) Initial stages of sperm-egg fusion in the freshwater teleost, *Rhodeus ocellatus ocellatus*. Anat Rec 229: 195–202

18 Ohta T, Iwamatsu T (1983) Electron microscopic observations on sperm entry into eggs of the rose bitterling, *Rhodeus ocellatus*. J Exp Zool 227: 109–119

19 Quinitio GF (1989) Studies on the functional morphology of the testis in two species of freshwater sculpin. Doctoral Dissertation, Hokkaido Univ

20 Stanley HP (1969) An electron microscope study of spermiogenesis in the teleost fish *Oligocottus maculosus*. J Ultrastruct Res 27: 230–243

21 Wassarman PM (1987) The biology and chemistry of fertilization. Science, 235: 553–560

22 Wolenski JS, Hart NH (1987) Scanning electron microscope studies of sperm incorporation into the zebrafish (*Brachydanio*) egg. J Exp Zool 243: 259–273

23 Wolenski JS, Hart NH (1988) Effects of cytochalasins B and D on the fertilization of zebrafish (*Brachydanio*) eggs. J Exp Zool 21: 473–515

24 Wolenski J S, Hart NH (1988) Sperm incorporation independent of fertilization cone formation in the danio egg. Develop Growth & Differ 30: 619–628

25 Yanagimachi R, Noda YD (1970) Physiological changes in the postnuclear cap region of mammalian spermatozoa: a necessary preliminary to the membrane fusion between sperm and egg cells. J Ultrastruct. Res 31: 486–493

ZOOLOGICAL SCIENCE 10: 103–109 (1993)

The Acrosome and Its Differentiation during Spermiogenesis in *Halocynthia roretzi* (Ascidiacea, Tunicata)

Makoto Fukumoto[1] and Takaharu Numakunai[2]

[1]*Biological Institute, College of General Education, Nagoya City University, Mizuho-ku, Nagoya 467, Japan and* [2]*Marine Biological Station, Tohoku University, Asamushi, Aomori 039-34, Japan*

ABSTRACT—The spermatozoa of *Halocynthia roretzi* have architectural features characteristic of ascidian spermatozoa that have been previously described. They have an elongated head (approximately 5.5 μm in length) and a single mitochondrion which is closely applied laterally to the nucleus. They lack a midpiece. An acrosome is present at the apex of the sperm head. The acrosome of *H. roretzi* spermatozoa is a depressed sphere, approximately $125 \times 125 \times 40$ nm.

At an early stage of spermiogenesis a vesicle (about 50 nm in diameter) appears in a blister at the apex of each spermatid. During spermiogenesis this vesicle becomes larger (approximately 100 nm in diameter). The vesicle in the blister contains moderately electron-dense material located along the vesicle membrane. At the completion of spermiogenesis the vesicle is most probably flattened by the elongating nucleus and transforms into an acrosome.

INTRODUCTION

Recent studies have shown that the spermatozoa of ascidians have an acrosome(s), albeit a small one [1, 5, 9]. In spite of various studies on fertilization in *H. roretzi,* there is still a debate over whether or not an acrosome is present in this species.

In *Ciona intestinalis,* the morphological changes in sperm associated with fertilization are becoming clear. An acrosome reaction occurs via vesiculation on the surface of the chorion or after penetration through the chorion. In the perivitelline space, apical processes protrude from the apex of the sperm head. Gamete fusion occurs between these apical processes and egg plasmalemma, resulting in the incorporation of the sperm head into the egg via its anterior region [6–8].

In order to develop a satisfactory understanding of the general mechanism of ascidian fertilization, further studies on morphological aspects of fertilization in other ascidian species are indispensable.

Accepted July 27, 1992
Received June 12, 1992
[1] To whom reprint request should be addressed.

In this paper, the authors describe the acrosome and its differentiation during spermiogenesis as a preliminary step in the analysis of morphological aspects of fertilization in *H. roretzi.*

MATERIALS AND METHODS

The solitary ascidian, *Halocynthia roretzi* (Type C)[13, 14] was collected near Asamushi Marine Biological Station, Aomori, Japan.

For TEM observations on spermiogenesis and on the differentiated spermatozoa, the testes and the sperm duct were prepared for electrom microscopy according to a method described by Fukumoto [2]. Electron micrographs were taken on a Hitachi H-300 electron microscope operated at 75 kV.

RESULTS

The acrosome in Halocynthia roretzi sperm

A fully differentiated spermatozoon of *H. roretzi* is approximately 40 μm length. It consists of a head and a tail. It lacks a midpiece. The head (approximately 5.5 μm long) contains an elon-

gated nucleus and a single mitochondrion which flanks the nucleus (Fig. 1). An acrosome is present at the apex of the head (Fig. 1, arrow).

The fully differentiated acrosome is approximately $125 \times 125 \times 40$ nm (Figs. 2, 3 and 4). At the region where the acrosome is located, the inner and outer nuclear membranes are in extremely close contact with each other and form a "pedestal" for the acrosome (Figs. 2, arrow and 3).

Acrosome Differentiation during Spermiogenesis

The early spermatid is spherical and contains a round nulcues and a single mitochondrion. The chromatin exists as thin strands which are present throughout the nucleus. A fairly well developed Golgi apparatus with its associated vesicles is present in the cytoplasm (Fig. 5, arrow). The vesicle contains moderately electron-dense material (Fig. 6).

In spermatids mid-way through spermiogenesis, the nucleus has undergone some antero-posterior elongation. The future apex of the sperm corresponds to the blister (Fig. 7, arrow) and the future proximal end of the sperm head corresponds to the region where the flagellum extends out. During this stage the chromatin strands begin to become oriented parallel to the antero-posterior axis of the spermatid (Fig. 7). At this stage of spermiogenesis, the blister protrudes out from the apex of the sperm head. Moderately electron-dense material in the vesicle is located along the vesicle membrane (Fig. 8).

In spermatids at later stages of spermiogenesis, the nucleus further elongates antero-posteriorly in a helical configuration. This morphological change of the nucleus is accompanied by a change in the arrangement of the chromatin strands in the nucleus; chromatin strands which were arranged parallel to one another along the longitudinal axis of the nucleus coil up in a definite pattern (Fig. 9). A blister continues to be present in the anterior region (Fig. 9, arrow). A vesicle is present in a blister (Fig. 10). The nuclear membranes at the blister form an indentation, in which both the inner and the outer nuclear membranes are in close contact with each other (Figs. 8 and 10). The plasmalemma enclosing the blister is decorated by fuzzy material on its external surface (Figs. 8 and 10).

At the completion of spermiogenesis, the vesicle in the blister becomes a depressed sphere (Figs. 11 and 12) and transforms into an acrosome. This

FIG. 1. Sagittal section through the head of a differentiated sperm. An acrosome (arrow) is present at the apex between the plasmalemma and the nuclear membranes. Fuzzy material (F) which decorates the outside of the plasmalemma enclosing the apex is thicker than it is on other parts of the head. M, mitochondrion; N, nucleus. The bar indicates 1 μm.

FIGS. 2 and 3. Sagittal and cross sections through the apex of a differentiated sperm head, respectively. An acrosome is present between the plasmalemma and nuclear membrane, where the inner and the outer nuclear membranes make close contact with each other to form a "pedestal" (arrow) for the acrosome. F, fuzzy material. The bar indicates 200 nm, which is also applicable to the Figs. 3 and 4.

FIG. 4. Frontal slightly oblique section through the apex of the head. An acrosome (A) is recognized as a sphere in the central region of the pear-shaped pedestal. F, fuzzy material.

FIG. 5. An early spermatid in which a blister is present (arrow). G, Golgi complex; M, mitochondrion; N, nucleus. The bar indicates 2.5 μm (This is also the magnification for Figs. 7 and 9).

FIG. 6. Enlargement of the blister region. A veiscle which contains electron-dense material is present in the blister. Fuzzy material covers the outside of the plasmalemma enclosing the blister. F, fuzzy material; N, nucleus. The bar indicates 200 nm (This is also the magnification for Figs. 8 and 10).

FIG. 7. Longitudinal section through a spermatid at a middle stage of spermiogenesis. The nucleus has begun to elongate antero-posteriorly. A blister (arrow) is present at the apex. M. mitochondrion; N, nucleus.

FIG. 8. Enlargement of a blister region in a spermatid midway through spermiogenesis. A vesicle with a central electron lucent region is present in the blister. The inner and the outer nuclear membranes are in close contact with each other (arrow). Fuzzy material (F) decorates outside of the plasmalemma enclosing the blister.

FIG. 9. Longitudinal section through a spermatid at a late stage of spermiogenesis where the elongated nucleus has a helical configuration. A blister (arrow) is present at the apex. M, mitochondrion.

FIG. 10. Enlargement of a blister region in a late stage spermatid. The blister projects more than that at early stages of spermiogenesis. A vesicle is present in the blister. Fuzzy material (F) decorates outside of the plasmalemma enclosing the blister.

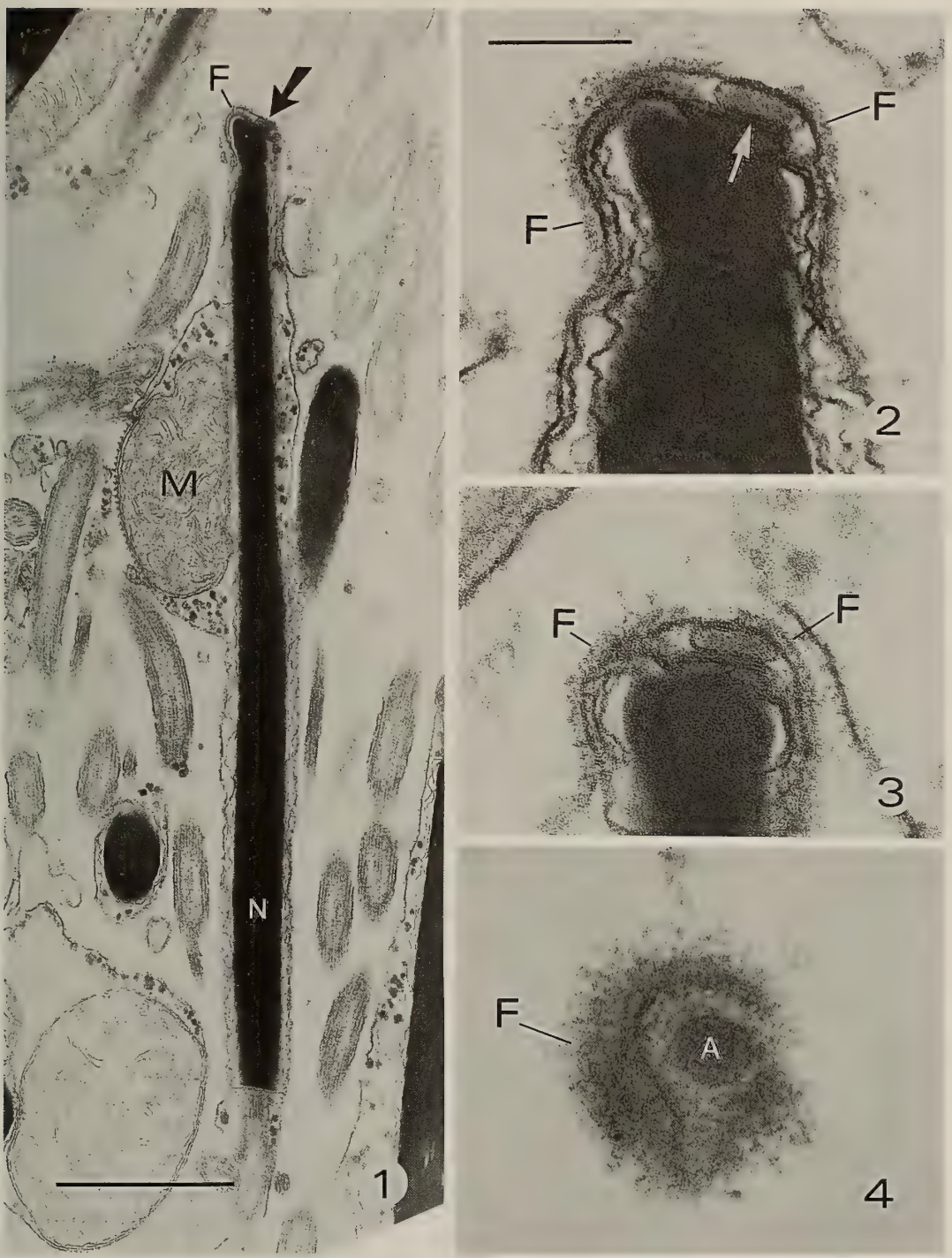
F
M
N
1
F
F
2
F
F
3
F
A
4


G
N
M
5

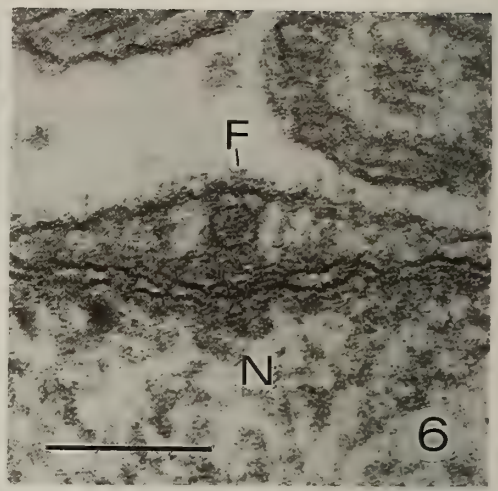
F
N
6


M
N
7

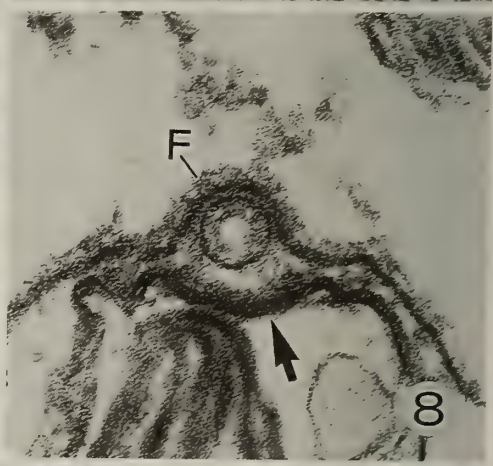
F
8

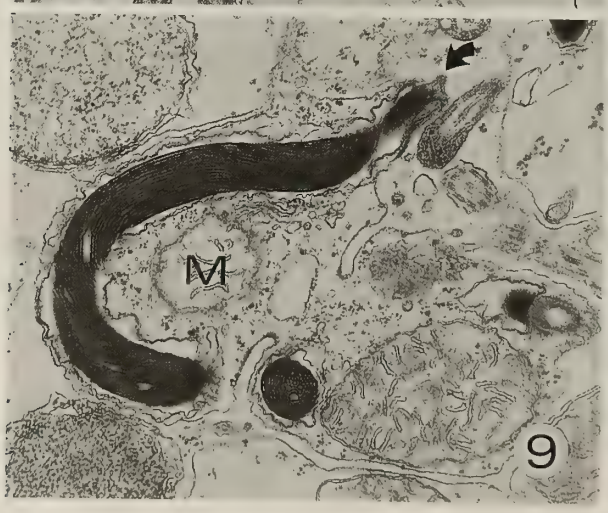
M
9

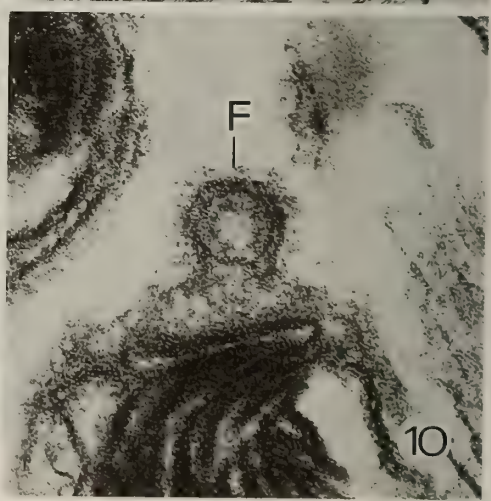
F
10

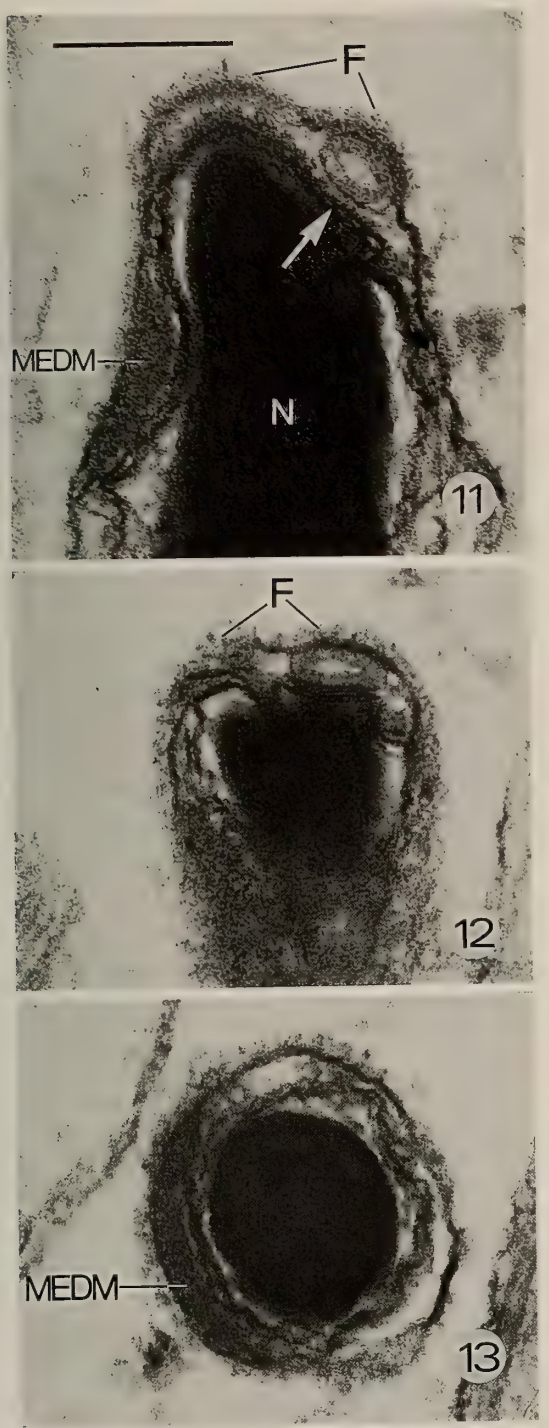

FIGS. 11 and 12. Sagittal and transverse sections through the apex of the head of a sperm that has almost completed maturation. The vesicle in the blister becomes an ellipsoid. Where the vesicle is located, the inner and the outer nuclear membranes come into close contact with each other to form a "pedestal" (arrow) for the vesicle. Moderately electron-dense material (MEDM) is present in the space between the plasmalemma and the uclear membranes near the apex. Fuzzy material (F) covers the outisde of the plasmalemma enclosing the apex. N, nucleus. The bar indicates 200 nm, which is also applicable to Figs. 12 and 13.

FIG. 13. Transverse section through the head at the level of the MEDM. The MEDM occupies almost half of the space around the nucleus.

morphological change of the vesicle most likely occurs as a consequence of the elongation of the nucleus. Moderately electron-dense material (MEDM) is present in the space between the plasmalemma and the nuclear membranes (Fig. 11). A cross section at the level of the MEDM reveals that this material is located at one side of the sperm head (Fig. 13) below the acrosome (Fig. 11).

DISCUSSION

During acrosome differentiation in other animal species, proacrosomal vesicles derived from Golgi complex(es) coalesce to form one acrosomal vesicle. In ascidians, a similar process has been reported. In *Pyura haustor* and *Styela plicata,* two vesicles usually appear in a blister at the apex of these spermatids in an early stage of spermiogenesis. They fuse to form a single acrosome-like structure in the apex of differentiated spermatozoa [3]. In *Molgula manhattensis,* at least three or four vesicles which are moderately electron-dense appear in the blister at the apex of spermatid in early stages of spermiogenesis. They fuse with each other to form an acrosomal vesicle [4]. In *H. roretzi,* in most cases, one vesicle appears in the blister of young spermatids. The vesicle becomes larger during the course of spermiogenesis (compare Figs. 6 and 8). This probably occurs via the coalescence of smaller vesicles. These findings are consistent with reports on acrosome differentiation in other animal species. With respect to the origin of the vesicle in the blister, no direct evidence has been found to show that it is derived from the Golgi apparatus. In view of the fact, however, that early spermatids have a fairly well-developed Gol-

gi apparatus and Golgi-derived vesicles, it seems safe to assume that they are derived from Golgi vesicles.

Recently, Lambert and Koch [12] have argued that the vesicles in ascidian spermatozoa should be called 'apical vesicles' until criteria for their positive identification as acrosomes can be more closely met. However, if a vesicle(s) is present in the proper location for an acrosome, this would be one kind of evidence for the existence of an acrosome, because acrosomes are anteriorly located vesicles in the sperm of other animals. Furthermore the vesicle in ascidian spermatozoa is not an oddity which is only found in one or two species, but a feature of all species examined in the Orders of Pleurogonan and Enterogonan ascidians [5, 9]. These are two good reasons for applying the term "acrosome" to these vesicles. We can conclude that spermatozoa of *H. roretzi* have an acrosome as has been confirmed in other ascidian species [9].

Recently it has been found that caffeine or theophylline induces morphological changes in the acrosome of *Ciona intestinalis* spermatozoa. These morphological changes have been referred to as an acrosome reaction. The acrosome reaction occurs by fusion between the acrosomal outer-membrane and the plasmalemma enclosing the acrosome. The fusion seems to proceed along the peripheral margin of the acrosome, resulting in vesiclulation [8]. Morphological studies on the acrosome reaction in *H. roretzi* are now in progress.

In *H. roretzi,* the egg is enclosed by a relatively thick acellular chorion (vitelline coat). For successful gamete fusion, spermatozoa must pass through the chorion. Sperm might utilize chorion lysin(s) in order to pass through the chorion. Indeed, there is evidence that spermatozoa of *H. roretzi* contain proteases that act as lysins [10, 15]. However, it is not clear where the lysins are located in spermatozoa. Recent studies on fertilization in *H. roretzi* reveal that spermatozoa can pass through the chorion (vitelline coat) with an intact acrosome and have loose their acrosome in the perivitelline space (Fukumoto, in preparation). This suggests that chorion lysin(s) are associated with the surface of the plasma membrane of sperm head. The chemical nature and the precise role of the acrosomal substance remain obscure.

In *H. roretzi,* Kubo *et al.* [11] reported that an acrosome was formed from Golgi-derived vesicles midway through spermiogenesis. They speculated that during further differentiation this acrosome was translocated to the space between the plasmalemma and the nuclear membranes near the apex of the sperm head, where it was recognized as an accumulation of moderately electron-dense material (MEDM). Although the MEDM is not a vesicular structure, they considered it homologous to an acrosome. However, they concluded that the acrosome had dissappeared before the completion of spermiogenesis, because they could not find an acrosome in mature spermatozoa. In this study an MEDM was seen in the same region of spermatids as has been described by Kubo *et al.* [11] during spermiogenesis (Figs. 11 and 13). In contrast to their descriptions, the MEDM is not homologous to an acrosome (Fig. 11). The precise role and fate of the MEDM remains unknown at present. Although Kubo *et al.* [11] found the blister at the anterior tip of spermatid, they did not find the vesicular "precusor of the acrosome" in the blister and the acrosome at the apex of the differentiated sperm head, which are described here.

ACKNOWLEDGMENTS

The authors are grateful to Professor Gary Freeman, of the University of Texas at Austin, for his valuable suggestions and for reading the manuscript. The author (M.F.) wishes to thank Professor Kenji Osanai, the director of the Asamushi Marine Biological Station, for facilities. We also wish to thank Mr. S. Tamura and Mr. M. Yashio, of Asamushi Marine Biological Station, for their help in collecting materials.

This work was supported in part by a Grant-in-Aid from the Ministry of Education, Science and Culture, Japan.

REFERENCES

1 Cloney RA, Abbott LC (1980) The spermatozoa of ascidians: acrosome and nuclear envelope. Cell Tiss Res 206: 261–270

2 Fukumoto M (1981) The Spermatozoa and Spermiogenesis of *Perophora formosana* (Ascidia) with Special Reference to the Striated Apical Structure and the Filamentous Structures in the Mitochondrion. J Ultrastruct Res 77: 37–53

3 Fukumoto M (1983) Fine Structure and Differentiation of the Acrosome-like Structure in the solitary Ascidian, *Pyura haustor* and *Styela plicata*. Develop Growth Differ 25: 503–515

4 Fukumoto M (1985) Acrosome Differentiation in *Molgula manhattensis* (Ascidiacea, Tunicata). J Ultrastruct Res 92: 158–166

5 Fukumoto M (1986) The acrosome in ascidians. I. Pleurogona. Int J Invert Reprod Dev 10:335-346

6 Fukumoto M (1988) Fertilization in ascidians: apical processes and gamete fusion in *Ciona intestinalis* spermatozoa. J Cell Sci 89: 189–196

7 Fukumoto M (1990) Morphological aspects of ascidian fertilization: Acrosome reaction, apical processes and gamete fusion in *Ciona intestinalis*. Invert Reprod Develop 17: 147–154

8 Fukumoto M (1990) The Acrosome Reaction in *Ciona intestinalis* (Ascidia, Tunicata). Develop Growth Differ 32: 51–55

9 Fukumoto M (1990) Review: Morphological Aspects of Ascidian Fertilization. Zool Sci 7: 989–998

10 Hoshi M, Numakunai T, Sawada H (1981) Evidence for participation of sperm proteases in fertilization of the solitary ascidian, *Halocynthia roretzi*: effects of protease inhibitors. Dev Biol 86: 117–121

11 Kubo M, Ishikawa M, Numakunai T (1978) Differentiation of apical structures during spermiogenesis and fine structure of the spermatozoon in the Ascidian *Halocynthia roretzi*. Acta Embryol Exp 3: 289–295

12 Lambert CC, Koch RA (1988) Review: Sperm Binding and Penetration during Ascidian Fertilization. Develop Growth Differ 30: 325–336

13 Numakunai T, Hoshino Z (1973) Biology of the ascidian, *Harocynthia roretzi* (Drasche), in Mutsu Bay. I. Differences of spawning time and external features. Bull Mar Biol Stat Asamushi, Tohoku Univ 14: 191–196

14 Numakunai T, Hoshino Z (1974) Biology of the ascidian, *Halocynthia roretzi* (Drasche), in Mutsu Bay. II. One of the three types which has the spawning season and the time different from two others. Bull Mar Biol Stat Asamushi, Tohoku Univ 15: 23–27

15 Sawada H (1990) Sperm penetration through the vitelline coat in ascidian. In "Advances in Invertebrate Reproduction 5" Ed by M Hoshi, O Yamashita, Elsevier Science Publishers BV (Biomedical Division), pp 111–116

ZOOLOGICAL SCIENCE 10: 111–116 (1993)

Toxicology of Maternally Ingested Carbon Tetrachloride (CCl_4) on Embryonal and Fetal Development and *in vitro* Fertilization in Mice

G. P. Hamlin, S. D. Kholkute and W. R. Dukelow

Endocrine Research Center, Michigan State University
EAST Lansing, MI 48824 U.S.A.

ABSTRACT—Oral administration of carbon tetrachloride (CCl_4) for five consecutive days beginning on either day 1, 6 or 11 of pregnancy in mice had no effect on maternal body weight, liver and kidney weight or pregnancy. The various neonatal parameters e.g. pup weight and crown rump length were also not affected. No malformations were detected in any pup on day 1 post-partum. The development of pups (incisor eruption on day 11 and eye opening on day 14) was normal. CCl_4 at concentrations of 0.05 and 0.5 mM had no significant effect on *in vitro* fertilization while higher doses caused a significant decrease. A significant linear relationship between 1, 2, 5 and 10 mM CCl_4 and a decrease in the fertilization rate were found. Similarly all the doses of CCl_4 (1 to 10 mM) resulted in a significant increase in abnormal ovum forms. A significant linear relationship was found between the dose and percent of abnormal forms. Thus CCl_4 had no *in vivo* reproductive toxic effects following administration of 1/10 and 1/100 LD_{50} dose. However, addition of CCl_4 in culture medium in concentrations found in blood of lethally intoxicated rats, adversely affected the *in vitro* fertilization rate and caused an increased incidence in abnormal ova.

INTRODUCTION

Carbon tetrachloride (CCl_4) is a colorless volatile organic compound commonly used as an industrial solvent, a fumigant and in the manufacture of fluorocarbons. CCl_4 has been detected in ground and municipal water, air, aquatic organisms and food. Thus, it becomes a potential health hazard [7, 17, 21]. CCl_4 is readily absorbed and distributed to all organs following ingestion or inhalation. The liver is the main organ responsible for biotransformation and detoxification [13, 14]. Evidence for a genotoxic or mutagenic action of CCl_4 has largely been negative [9, 10].

Reproduction may be sensitive to a number of environmental factors, physical, chemical or emotional. Studies of reproductive effects of CCl_4 in the past have tended to use varying exposure routes and very high doses resulting in maternal toxicity and conflicting results [3, 4, 11, 15, 16].

The present study reports the effects of oral ingestion of CCl_4 on mice for 5 consecutive days beginning on either Day 1, 6 or 11 of pregnancy in B6D2F1 mice. In this strain the first 5 days of gestation are characterized by sequential cleavage of the fertilized oocytes that generates a hatched blastocyst. Implantation is completed on Day 5. Days 6 to 10 are characterized by organogenesis. Finally, Days 11 to 15 are characterized by growth of the fetus. These time periods were chosen in an attempt to isolate detrimental effects on various stages of development and to determine the most susceptible stage for CCl_4 insult. The effects of CCl_4 on *in vitro* fertilization was also evaluated.

Accepted October 17, 1992
Received July 27, 1992

MATERIALS AND METHODS

Animals

Female B6D2F1 mice were obtained from one of two sources. Six week old females used for *in vivo* experiments were obtained from the Jackson Laboratories (Bar Harbor, ME). In some experiments, mice were bred on site from parental strains. All animals were housed in a 12 hr light:

12 hr dark photoperiod at 27°C. Food and water was available *ad libitum* except where mentioned.

In vivo experiments

Mating procedure: On the evening of their arrival, females were placed with fertile males in a ratio of 1:1 and checked on three subsequent mornings for the presence of vaginal plugs. Most females with plugs were obtained on the third morning as expected from the Whitten effect of induction of estrus [22]. Females were randomly assigned to one of three groups (control, 1/100 LD_{50}, 1/10 LD_{50}) on day 1 of pregnancy (=day of plug) and housed in groups of 5 until day 15 at which time they were separated. A minimum of four animals per group per replicate were housed for the two replicates.

CCl_4 solutions: At room temperature, CCl_4 (catalog number CAS 56–23–5, spectrophotometric grade, Mallinckrodt Int., Paris, KY) was dissolved in corn oil on the first day of treatment and stored at room temperature in light protected, sealed bottles. All solutions were stirred using a teflon coated magnetic bar on each day immediately before use. Animals received either 0.2 ml corn oil day *1* (control), 1/100 LD_{50} (82.63 mg/kg) or 1/10 LD_{50} (826.3 mg/kg) of CCl_4 in 0.2 ml corn oil. The LD_{50} of 8263 mg/kg was obtained from the Materials Safety Data Sheet OH504310 (Occupational Health Servies, Inc., New York, New York). All procedures using CCl_4 were performed in a certified fume hood.

Experimental protocol: *Gavage protocol*: Females were gavaged by placing a curved gavage needle (size 18, Perfektum, New Hyde Park, NY) attached to a 1 ml glass syringe into the stomach through the esophagus. The volume of 0.2 ml was given per animal.

Maternal parameters: Maternal weight (g) was determined on days 1, 8 and 15 of pregnancy and the 22nd day postpartum. On that day the females were sacrificed by cervical dislocation, the kindneys and liver removed, blotted dry, and weighed. A portion of the liver and the kindneys (one sliced longitudinally, the other horizontally) were stored in formalin for histological processing.

Neonatal parameters: On the day of birth, litter size was determined and each neonate was weighed. Crown-rump (C-R) length was measured and individuals were sexed and checked for obvious birth abnormalities e.g. extra/missing digits, cleft palate, exencephaly and spina bifida. After recording these parameters, litter size was reduced to 6, where possible leaving equal numbers of males and females.

Neonatal weight and C-R length were measured again on day 8, 15 and 22. In addition, lower incisor eruption and eye opening was assessed in all pups on day 11 and 15 respectively. On day 22, neonate were weaned and two of each sex allowed to grow to maturity (6 wk), the others were sacrificed by CO_2 asphyxiation. At 6 wk the four remaining youngs were sacrificed by cervical dislocation and the ovaries or testes removed, blotted dry and stored in Bouin's fixative.

Statistical analysis: All *in vivo* parameters were analyzed by one way ANOVA. When statistical significance between control and treatments were found pair-wise analysis of treatment and control was performed using Dunnett's *t* test [6].

In vitro experiments

Culture Medium: Brinster's medium [2] for oocyte culture (BMOC-3, Gibco, Grand Island, New York) was used for incubation of oocytes and sperm in the center well of Falcon organ tissue culture dishes (Becton-Dickinson and Co., #3037, Cockeysville, MD). Alternatively, BMOC medium was prepared in the laboratory and used in the outer well of the tissue culture dishes.

Superovulation: Six to eight-week-old B6D2F1 females were injected s.c. with 8 I.U. pregnant mare serum gonadotropin (PMSG) followed 45–49 hr later with 8 I.U. human chorionic gonadotropin (hCG) s.c. The PMSG and hCG were obtained from Sigma Chemical Co. (St. Louis, MO).

CCl_4: The BMOC and BMOC-3 media were added to the culture dishes 16 hr before IVF. CCl_4 was dissolved in t-butanol (Catalog number B 2138, Sigma Chemical Co.) to a concentration 100 times the final concentration in a total volume of 10 μl to be added directly to the 1 ml BMOC-3 medium at the time stated. Final concentrations of CCl_4 in the center well of organ tissue culture dishes were 0.05, 0.5, 1, 2, 5 or 10 mM.

Gamete recovery and IVF: Twelve hours after

females received hCG, 2 or 3 males of 6–10 months of age were sacrificed by certical dislocation for each IVF experiment and a single epididymis was placed directly into the center well of a organ dish containing 0.5 ml BMOC-3. The cauda epididymis was then repeatedly punctured with a 25 G needle before the dish was returned to the incubator for 1–1.5 hr.

Approximately 45 min after sperm collection the superovulated females were sacrificed by cervical dislocation for collection of the cumulus mass containing the oocytes. One side of each reproductive tract (ovary, oviduct and uterine horn) was placed in the outer well of the organ dishes containing 3 ml of BMOC. The cumulus mass was removed from the oviduct under a dissecting microscope, quickly washed and placed in the center well of a treatment or control organ culture dish. The cumulus masses were randomly placed in either treatment or control across replicates to avoid the same female donating to the same treatment group.

The organ dishes were placed in the incubator after cumulus mass addition while the CCl_4 solutions were prepared. CCl_4 solutions were added to the organ culture dish containing the cumulus mass, with care to avoid directly adding the 10 μl CCl_4 or 10 μl t-butanol (control) on top of the cumulus mass.

Immediately after the addition of the cumulus mass, 50 μl of sperm suspension was added directly to the center well of the dishes taking care that each replicate was inseminated from a different, randomly selected male. All treatment and control dishes were replaced in the incubator for 26 hr before assessment of 2 cell oocytes (which represent fertilized eggs) was conducted.

Statistical analysis: All statistical analysis of IVF experiments used Chi square and Bonferronni Chi square contingency tables [6].

RESULTS

In vivo experiments

Maternal Parameters: Replicate treatement data sets were pooled for tests of statistical significance. A total of 60 female B6D2F1 mice were mated with a pool of fertile male B6D2F1 mice. Thirty-five females were designated as pregnant due to the presence of a plug. Of these 31 were assigned to experimental groups. All 31 treatment females maintained pregnancy to term and a total of 294 pups were delivered. Results are expressed as the mean $\pm$ SEM.

No significant difference ($P>0.1$) in maternal body weight across treatments on the days measured were seen. Dams were sacrificed on day 22 postpartum (day 1 = day of parturition) and liver and kidney weights were recorded, body weight was also recorded to enable calculation of relative organ weights. Relative and absolute liver and kidney weights and maternal weights were not significantly different ($P>0.1$) across treatment groups (data not shown). Tissue samples of liver and kidney were prepared and preserved in formalin for possible histopathological examination at a later date.

Neonatal parameters: Pup weight and C-R length were measured on days 1, 8, 15 and 22 postpartum. A significant difference between control and treated groups was seen on day 15 postpartum (data not shown). No other significant differences were seen across treatment groups in pup weight or C-R length.

No malformations were detected in any pup on day 1 postpartum (observations not presented). The normal development of pups was assessed from observation of incisor eruption on day 11 and eye opening on day 14.

In vitro experiments

CCl_4 was added directly to the center well of organ culture dishes, containing the cumulus before addition of sperm, at concentrations of 0.05, 0.5, 1, 2, 5 and 10 mM. The total number of two cell embryos, total number of ova and percent fertilization for all CCl_4 trials are shown in Table 1.

The vehicle for delivery of CCl_4 was t-butanol and the percent fertilization in 1% t-butanol was not significantly different from the control. CCl_4 at concentrations of 0.05 and 0.5 mM had no significant effect on fertilization while 1, 2, 5 and 10 mM CCl_4 caused a significant decrease in fertilization. A significant linear relationship ($P<0.001$) between 1, 2, 5 and 10 mM CCl_4 and a decrease in

Table 1. Effects of CCl_4 (mM) and t-butanol (v/v) on mouse *in vitro* fertilization

Dose (mM)	2 cell	total ova	% fertilization
Control	298	321	92.8
1% t-butanol	215	240	89.6
0.05	179	197	90.9
0.5	169	186	90.9
1.0	49	109	45.0[a]
2.0	29	94	30.9[a]
5.0	23	75	21.9[a]
10.0	9	75	12.0[a]

[a] significantly different from t-butanol, $P<0.001$

Table 2. Effect of CCl_4 (mM) on ovum morphology in mouse *in vitro* fertilization

Dose (mM)	abnormal	total ova	% abnormal
1% t-butanol	0	175	0
1.0	9	109	8.0[a]
2.0	15	94	16.0[a]
5.0	69	105	65.7[a]
10.0	53	100	53.0[b]

[a] significantly different to t-butanol, $P<0.01$
[b] significantly different to t-butanol, $P<0.001$

fertilization was found.

In the presence of 1, 2, 5 and 10 mM CCl_4 abnormal ovum forms were observed. The number of abnormal forms, total number of ovum and percent abnormal forms are listed in Table 2. All doses of CCl_4 resulted in a significant increase in abnormal ova forms and a significant linear relationship ($P<0.001$) was found to exist between the dose of CCl_4 and percent of abnormal ova forms.

DISCUSSION

The results of the present study demonstrates that oral administration of CCl_4 on days 1 to 5, 6 to 10 and 11 to 15 of gestation had no adverse effects on reproduction of mice. Furthermore, there were no overt signs of maternal toxicity.

Exposure of pregnant mice to 1/10 LD_{50} and 1/100 LD_{50} (which is equivalent to 826.3 mg/kg and 83.63 mg/kg or 0.52 ml/kg and 0.05 ml/kg, respectively) over the first five days of gestation had no effect on fetal mortality and development or postnatal normality and development. The average litter size of all groups was not statistically significant and no stillbirths were observed indicating that CCl_4 had no effect on implantation, resorption or induction of any embryo lethal effects. Average C-R length of pups measured on days 1, 8, 15 and 22 postpartum was not significantly different across treatments. No significant difference in average pup weight was seen across treatments except on day 15 when only the high dose was significantly different from the control. This difference is not interpreted as biologically significant as no other difference in pup weight was seen and the day 15 pup weights within litters were more dispersed than at other times. Also, C-R length is a more sensitive measure of neonatal growth and no differences were seen in this parameter.

Recent reviews [8, 18] have reported that exposure to chemicals during the preimplantation period can lead to teratogenesis. Methyl nitrosourea has been shown to act on preimplantation embryos resulting in teratogenesis visualized at birth [3]. This study provides evidence that maternal exposure during the preimplantation period to CCl_4 at 1/10 LD_{50} or 1/100 LD_{50} does not result in teratogenesis in mice.

In conclusion, this study clearly demonstrates that exposure of maternal mice by oral gavage to 1/10 LD_{50} and the 1/100 LD_{50} of CCl_4 once a day from day 1 through 6 of gestation has no embryotoxic, embryolethal or teratogenic effects. These results agree quite well with the literature in that CCl_4 induction of embryotoxic and or embryolethal effects occur at concentrations where significant overt maternal toxicity is seen [4, 16]. However, this report is significant in that no other studies were found where the effects of CCl_4 were determined during the preimplantation period and most previous studies demonstrated high levels of maternal toxicity.

An additional set of experiments examined the effect of CCl_4 on fertilization utilizing the mouse *in vitro* fertilization system. In these experiments CCl_4 at 0.05 mM and 0.5 mM was found to have no statistically significant effect on the percent of fertilization. While the concentrations of 1 mM through 10 mM had a markedly significant effect

on fertilization. A linear relationship between dose and inhibition of fertilization was established with the lowest effective dose of 1 mM inhibiting fertilization by approximately 50%. Interestingly, the inhibition of fertilization was not just marked by a reduction in 2 cell embryos and an increase in one cell ova. An ovum exhibiting a very dense constricted cellular/nuclear region and a dust like circle of degraded cell constituents surrounding the dense body, was observed. The appearance of these forms was statistically significant at all doses of CCl_4 from 1 mM to 10 mM and a dose-related increase in these forms was established.

The results of this IVF study celarly demonstrate a dosedependent effect of CCl_4 indicating that the effect seen is a direct solvent effect and not a specific one. However, Dahlstrom-King *et al.* [5] studied eight chlorinated hydrocarbons in the isolated rat hepatocyte system and found that toxicity did not relate to physiochemical properties (notably the oil/water partition coefficient) of the chemicals. In fact, the authors found that the *in vitro* toxicity did not correlate well with the *in vivo* toxicity of the eight chemicals. The appearance of the abnormal ovum in this study corresponds well with morphological changes in hepatocytes reported to be due to solvent action [1]. However, it is interesting to note that at 1 mM CCl_4 a 50% reduction in fertilization occurs with only a small highly variable percent of abnormal forms seen, while at 10 mM CCl_4 there is an approximate 80% reduction in fertilization with a more consistent 58% appearance of abnormal forms. This could indicate that at the lower effective levels of 1 mM and 2 mM CCl_4, there are other mechanisms apart from the solvent effect in operation resulting in the inhibition of fertilization.

One of the mechanisms could be a disruption of Ca^{2+} homeostasis which is critical to fertilization and proposed as a mechanism of CCl_4 induced hepatotoxicity [1, 14, 19]. Obviously more research is required to determine the effect of CCl_4 on the IVF system and perhaps some insight into the general mechanism of CCl_4 cytotoxicity may be gained.

Although, our *in vivo* studies failed to reveal any delerious effects of CCl_4 on pregnancy, the dosages employed were low. Nonetheless Kim *et al.* [12] reported that a single oral dose of 25 mg/kg CCl_4 in the rat can result in a plasma concentration of 0.3 mM. Furthermore, Srivastava *et al.* [19] have reported concentrations of 0.5–2.5 mM CCl_4 in the blood of intoxicated animals. Thus a severe decrease in fertilization rate may occur if the ovum were exposed to levels of CCl_4 above 1 mM and this in turn may adversely affect pregnancy following high dose chronic exposure.

ACKNOWLEDGMENTS

This work was supported in part by NIH grants HD07534 and ES04911. Appreciation is expressed to Mrs L. M. Cleeves for preparation of this manuscript.

REFERENCES

1 Berger ML, Sozeri T (1987) Rapid halogenated hydrocarbon toxicity in isolated hepatocytes is mediated by direct solvent effects. Toxicology 45: 319–330

2 Brinster RL (1971) In vitro culture of the embryo. In "Pathways to contraception" Ed. by AI Sherman, CT Thomas, Springfield, IL, pp 245–277

3 Cilman MR (1971) A preliminary study of the teratogenic effects of inhaled carbon tetrachloride and ethyl alcohol consumption in the rat. Diss. Abstr. Int. B32: 2021–2042

4 Clemedson C, Schmid B, Walum E (1989) Effects of carbon tetrachloride on embryonic development studied in the postimplantaion rat embryo culture system and in chick embryos. Toxic. in Vitro 3: 271–275

5 Dahlstrom-King L, Couture J, Lamoureaux C, Vaillancourt T, Plaa A (1990) Dose-dependent cytotoxicity of chlorinated hydrocarbons in isolated rat hepatocytes. Fund Appl Toxicol 14: 833–841

6 Gill JL (1987) Design and analysis of experiments in the animal and medical sciences Vol 1. The Iowa State University Press, Ames, Iowa, pp 117–132

7 Gilli GR, Bono R, Scursatone E (1990) Volatile halogenated hydrocarbons in urban atmosphere and in human blood. Arch Env Health 45: 101–106

8 Iannaccone PM, Bossert N, Connelly C (1987) Disruption of embryonic and fetal development due to preimplantation chemical insults: a critical review. Am J Obstet Gynecol 157: 476–484

9 International Agency for Research on Cancer (IARC) (1987a) Genetic and related effects: an updating of selected IARC Monographs from Volumes 1 to 42. IARC Monogr Eval Carcinog Risk Chem Hum Suppl 6: 136–137

10 International Agency for Research on Cancer (IARC) (1987b) Overall evaluations of carcinogenicity: an updating of IARC monographs Volumes 1 to 42. IARC Monogr Eval Carcinog Risk Hum Suppl 7: 143–144

11 Khominska ZB (1974) Change in function of ovaries and adrenal glands in rats under experimental toxic hepatitis Fiziologicheskii Zhurnal 20: 747–751

12 Kim HJ, Odend'hal S, Bruckner J (1990) Effect of oral dosing vehicles on the acute hepatotoxicity of carbon tetrachloride in rats. Toxicol Appl Pharmacol 102: 34–49

13 Neal RA (1980) Metabolism of toxic substances In "Toxicology: the basic science of poisons" Ed by J Doull, CD Klassen, MO Amdur, 2nd ed, MacMillan Publishing Co Inc, New York, pp 56–70

14 Recknagel RO, Glende E, Dolak J, Waller R (1989) Mechanisms of carbon tetrachloride toxicity. Pharmac Ther 43: 139–154

15 Roschlau VG, Rodenkirchen H (1969) Histologiche Untersuchungen uber die Diaplazentare Wirkung von Tetrachlorkohlenstoff und Allylalkohol auf Mausefeten. Exp Path 3: 255–263

16 Schwetz BA, Leong B, Gehring P (1974) Embryo and fetotoxicity of inhaled carbon tetrachloride, 1, 1-dichloroethane and methyl ethyl ketone in rats. Toxicol Appl Pharmacol 28: 452–464

17 Silkworth JB, McMartin D, Rej R, Narang R, Stein V, Briggs R, Kaminsky L (1984) Subchronic exposure of mice to Love Canal soil contaminants. Fund Appl Toxicol 4: 231–239

18 Spielmann H, Vogel R (1989) Unique role of studies on preimplantation embryos to understand mechanisms of embryotoxicity in early pregnancy. Crit Rev Toxicol 20: 51–64

19 Srivastava SP, Chen N, Holtzman J (1990) The in vitro NADPH-dependent inhibition of CCl_4 of the ATP-dependent calcium uptake of hepatic microsomes from male rats. J Biol Chem 265: 8392–8399

20 Takeuchi IK (1984) Teratogenic effects of methyl nitrosourea on pregnant mice before implantation. Experientia 40: 879–881

21 Wallace LA, Pellizzani E, Hartwell T, Sparacino C, Whitmore R, Sheldon L, Zelon H, Perritt (1987) The TEAM Study: personal exposures to toxic substances in air, drinking water and breath of 400 residents of New Jersey, North Carolina and North Dakota. Env Res 43: 290–307

22 Whitten WK (1958) Modification of the oestrous cycle of the mouse by external stimuli associated with the male. Changes in the oestrous cycle determined by vaginal smears. J Endocrinol 17: 307–313

ZOOLOGICAL SCIENCE 10: 117–125 (1993)

Reproductive Characteristics of Precociously Mature Triploid Male Masu Salmon, *Oncorhynchus masou*

Masaru Nakamura[1], Fumio Tsuchiya[2], Masao Iwahashi[2] and Yoshitaka Nagahama[3]

[1]*Department of Biology, Faculty of Medicine, Teikyo University, Hachioji, Tokyo 192-03,* [2]*Niigata Prefecture Inland Water Fisheries Experimental Station, Koide-cho, Kitauonumagun, 946, and* [3]*Laboratory of Reproductive Biology, National Institute for Basic Biology, Okazaki, 444 Japan*

ABSTRACT—In order to clarify the reproductive characteristics of triploid males, changes in serum steroid hormone levels and testicular development in precociously mature triploid males of masu salmon, *Oncorhynchus masou,* were examined during sexual maturation. Testicular development in triploids differs from that in diploids. The gonadosomatic index (GSI) in triploids in August was high (3.9%), similar to that in diploids (3.0%). Although germ cells at all stages of spermatogenesis were observed in the testes of diploids, the testes of triploids consisted of many cysts of primary spermatocytes and some degenerating germ cells. In the spawning season in October, GSI in triploids dropped suddenly (1.0%), though GSI in diploids increased (4.8%). At that time, a large number of degenerating figures of spermatogenic germ cells were found in the testes of triploids. Very few sperm were seen in the sperm fluid. However, most of the sperm cells revealed abnormalities in morphology, such as two tails, two heads, and heads of various sizes. Changes in serum testosterone (T), 11-ketotestosterone (11-KT) and 17α,20β-dihydroxy-4-pregnen-3-one (17α,20β-diOH) in triploid males were similar to those in mature diploid males. T and 11-KT levels were high in August and October, then they dropped in November after the spawning season. 17α,20β-DiOH levels in both triploid and diploid males were only high in October during the spawning season. From these results, it seems likely that the cause of abnormality of spermatogenesis in triploid males is mechanical difficulty involved in chromosome separation at meiosis I due to triploidy *per se,* rather than the reduced levels of testicular steroid hormones.

INTRODUCTION

Recently it has become possible to manipulate chromosome sets by means of physical or chemical treatment of eggs at an early developmental stage [7, 12]. This technique of chromosome set manipulation is expected to be applicable to practical fish culture in a variety of ways, such as sex determination or improvement of breed [7]. Triploid fish can be induced by retaining the second polar body of eggs just after fertilization. Triploid fish are thought to become sterile as a consequence of having an odd number of chromosome sets. This sterile triploidy may bring about benefits to practical fish culture for the reason that sterile fish avoid the muscle deterioration and death which accompany sexual maturation [10].

Induction of triploidy has been attempted in several fishes so far. However, characteristics of sexually mature triploids depend on sex and species. In a previous paper, we reported the gonadal development and changes of steroid hormones in triploid female rainbow trout, *Oncorhynchus mykiss* [6]. In the present study, we deal with testicular development and changes in steroid hormones in the triploid male masu salmon, *Oncorhynchus masou.*

Accepted November 4, 1992
Received September 18, 1992

MATERIALS AND METHODS

Land-locked masu salmon (Yamame) used in

the present study were obtained from the Niigata Prefecture Inland Water Fisheries Experimental Station. They have been cultivated systematically in ponds. Mature eggs and sperm were obtained from randomely selected 2-year-old females and males. To induce triploidy, just after artificial insemination, eggs were immersed in warm water at 27–31°C for 10–15 min. After this temperature shock, eggs were removed and put into water at about 12°C. Fry were fed on the regular diet for salmon culture from the first feeding.

Precociously mature triploid males (10 to 13 month-old) were autopsied 3 times, August 30, October 22, and November 25, 1986. For each sample, body weight, body size, and testicular weight were measured. To confirm triploidy, a blood smear from each individual was prepared. After staining with 1% Giemsa solution, long diameters of erythrocytes were measured. Testes of triploids were fixed in Karnovsky's solution for 2 hr. Next, they were postfixed in 1% OsO_4 buffered to pH 7.4 with 0.1 M cacodylate buffer for 2 hr. After dehydration, they were embedded in epoxy resin. For histological observations, one micrometer sections were stained with 1% toluidine blue in 0.1 M phosphate buffer.

For the investigation of sperm, sperm fluid was collected in the October spawning season. Smears of sperm fluids were prepared and stained with Delafield's hematoxilin.

For the measurement of steroid hormone levels in serum, blood from each fish was collected by cutting the caudal region. The serum was separated by centrifugation, frozen at −20°C, and stored until use. Serum levels of testosterone (T), 11-ketotestosterone (11-KT) and 17α,20β-dihydroxy-4-pregnen-3-one (17α,20β-diOH) were measured by radioimmunoassay [3, 8, 13, 14].

Precociously mature diploid males were sacrificed in the same manner and at the same time, and they served as the control.

Data were analyzed using Student's *t*-test (erythrocyte diameter) and two-way analysis of variance (ANOVA, GSI and body weight), accepted at $P<0.05$.

RESULTS

Diameter of erythrocytes

Erythrocytes of diploid and triploid males are pictured in Figs. 1A and 1B, respectively. Diameter of erythrocytes of triploids is 19.22 ± 0.81 μm. This value is significantly larger ($P<0.01$) than that of diploids (14.62 ± 0.95 μm). Triploids were distinguished from diploids by the size difference in erythrocytes.

Growth and external view of fish

Body weight and total length of triploid and diploid males is shown in Table 1. Diploid and

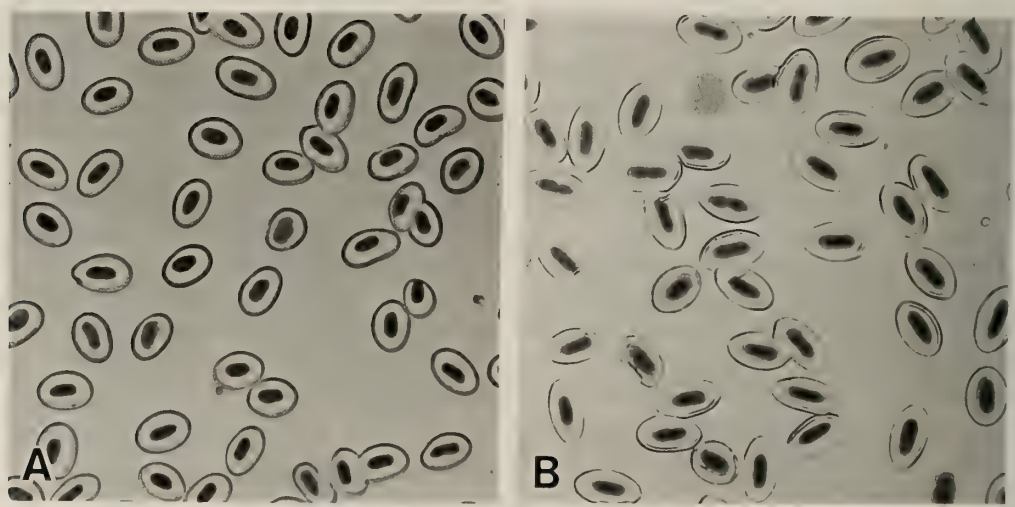

FIG. 1. Erythrocytes of diploid (A) and triploid (B) masu salmon. ×610.

TABLE 1. Comparison of body weight (B.W.) and total length (T.L.) of triploid and diploid males in each sampling time

		Aug. 30	Oct. 22	Nov. 25
Triploid	B.W. (g)	36.7±3.1	48.1±2.3	51.3±3.0
	T.L. (cm)	14.5±0.2	16.7±0.4	17.6±0.3
Diproid	B.W. (g)	32.7±2.5	51.3±3.7	55.4±5.0
	T.L. (cm)	14.7±0.3	17.4±0.3	18.0±0.5

Each value is the mean±SE.

triploid males grew similarly and showed no differences in body weight and total length at any sampling time.

Triploid individuals were not different from diploids in external view (Fig. 2). Male secondary sex characters such as dark color on the skin of body and each fin appeared normally in triploids in the October spawning season, similar to diploid males. About 70% of triploid males matured precociously one year after fertilization. This value was almost the same as that of diploid males.

Changes in gonadosomatic indices (GSI=(gonad weight/body weight)×100)

Changes in GSI in diploid and triploid males are shown in Figure 3. Changes in GSI in triploids differ from those in diploids. GSI in triploids was high, 3.9±0.6%, in August, as was GSI in diploids (3.0±0.9%). In October, GSI in diploids increased further to 4.8±0.8%. In contrast, GSI in triploids dropped markedly to 1.0±0.7%, even in the spawning season ($P<0.01$). GSI in diploids dropped rapidly (1.5±0.2%) in November after the spawning season. GSI in triploids dropped even more (0.2±0.01%) ($P<0.01$).

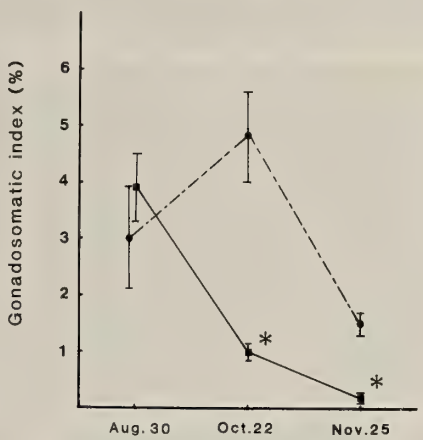

FIG. 3. Changes in the gonadosomatic index (mean± SE) of diploid (---●---) and triploid (—■—) masu salmon. *Significantly different from diploid ($P<0.01$).

FIG. 2. The secondary sex character of dark skin appears in both diploid (D) and triploid (T) male masu salmon.

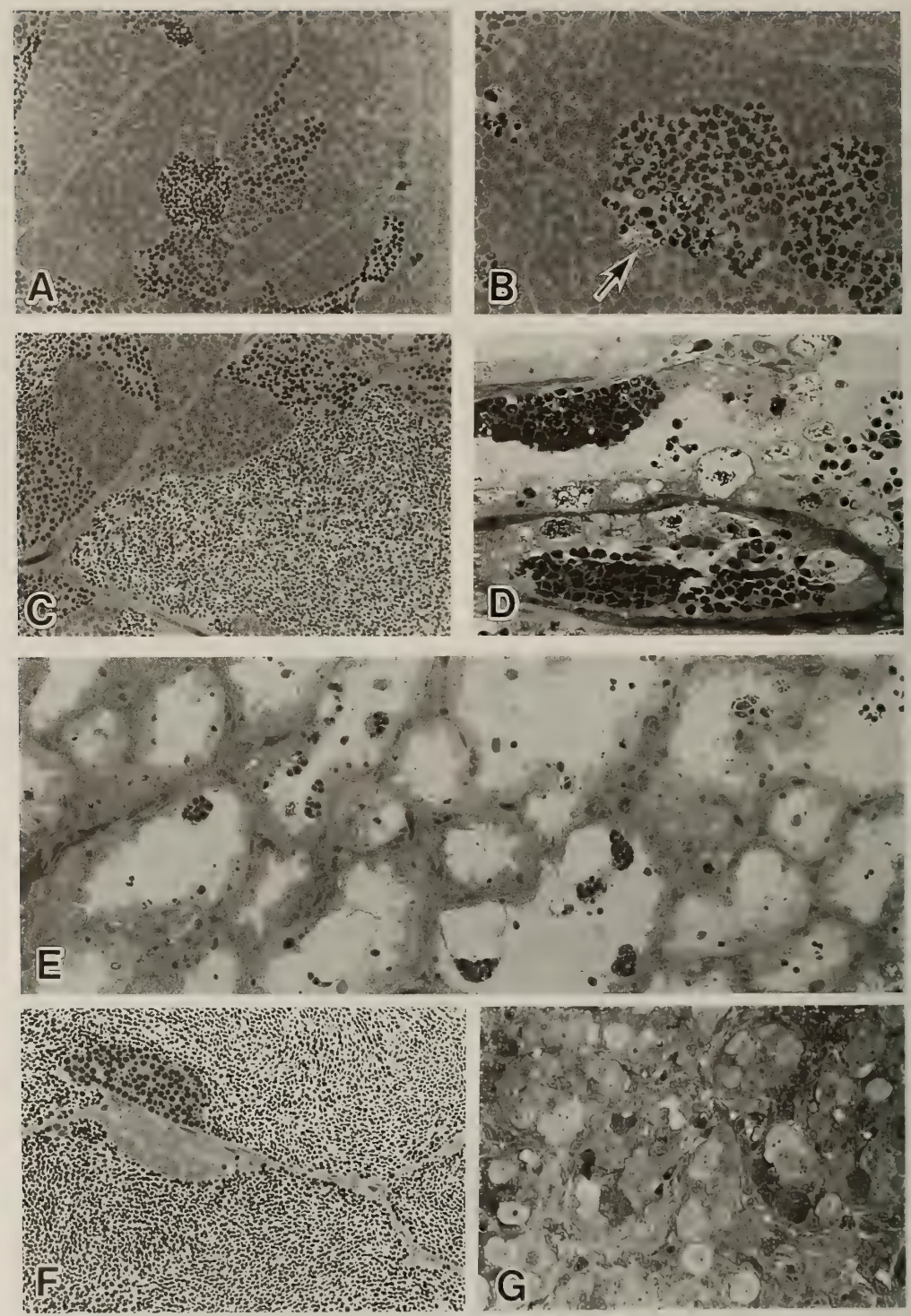

FIG. 4. Photomicrographs of testes from diploid and triploid male masu salmon. Diploid testes in August (A), October (C) and November (F). Triploid testes in August (B), October (D and E) and November (G). ×590.

Testes

Cysts of spermatogenic germ cells at various stages were contained in the testes of diploids in August (Fig. 4A). A small amount of matured sperm had already been seen in the central region of the lumen. Active spermatogenesis was also seen in the testes of triploids (Fig. 4B). However, spermatogenic germ cells consisted mainly of primary spermatocytes (Fig. 4B). Secondary spermatocytes, spermatids, and sperm were not observed in triploids, although some clusters of degenerating spermatocytes were observed in the lumen (Fig. 4B). The testes of triploids in the spawning season in October were noticeably different in size and color from those of diploids (Fig. 5). Testes of diploids were white in color and were packed with matured sperm (Fig. 5). In contrast, those of triploids were semitranslucent. Sperm fluid filled the efferent ducts. The testes of triploids (Figs. 4D and 4E) were also extremely different in histology from those of diploids (Fig. 4C). The amount of spermatogenic germ cells was markedly less in triploids (Figs. 4D and 4E) than in diploids (Fig. 4C). Moreover, these germ cells revealed necrosis. Some necrotic cells were ingested by hypertrophied Sertoli cells lining the inner wall of the lumen (Fig. 4D). Although some sperm were recognized in sperm fluid in triploids (Fig. 6B), they were fewer in number and noticeably different in morphology from those of diploids (Fig. 6A). Sperm of triploids were morphologically abnormal, such as having two heads, two tails, or various sizes of heads. Large amounts of sperm still remained in the testes of diploids in November (Fig. 4F). In the testes of triploids, the inner wall of the lobules contained only some spermatogonia (Fig. 4G).

Changes in serum steroid hormone levels

Changes in T, 11-KT, and 17α,20β-diOH levels in triploids and diploids are shown in Figure 7A-7C. High levels of serum T (diploid, 8.0 ng/ml; triploid, 7.4 ng/ml) and 11-KT (diploid, 5.7 ng/ml; triploid 5.0 ng/ml) were observed when the two groups of males were compared in August. Levels of these steroids rose further in October (diploid, T 37.0 ng/ml and 11-KT 48.1 ng/ml; triploid, T 30.8 ng/ml and 11-KT 33.3 ng/ml). T and 11-KT levels rapidly decreased in November after the breeding season in both diploid (T 0.4 ng/ml and 11-KT, not detectable) and triploid (T 0.5 ng/ml and 11-KT 0.4 ng/ml). Serum 17α,20β-diOH was not detectable in either diploids or triploids in

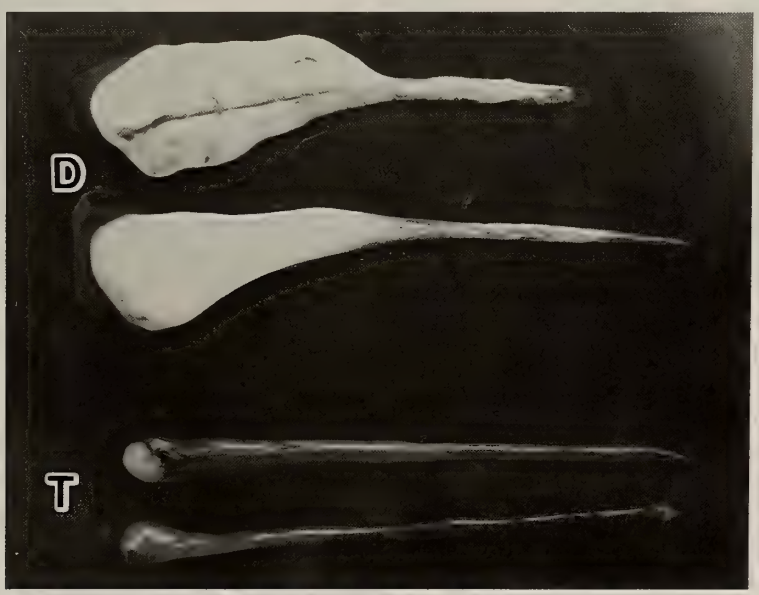

FIG. 5. Testes from diploid (D) and triploid (T) male masu salmon in October.

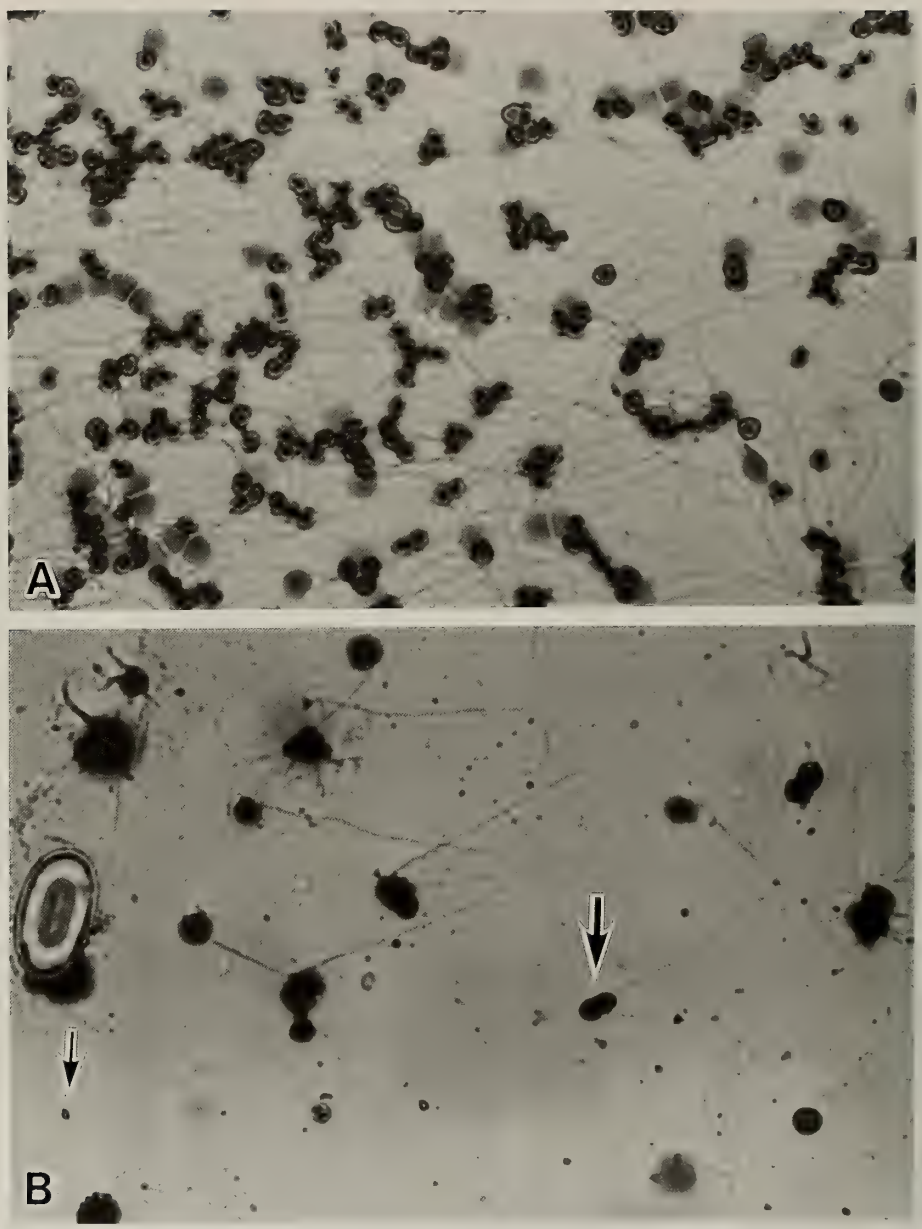

FIG. 6. Photomicrograph of sperm from diploid (A) and triploid (B) masu salmon. Small head (small arrow) and, two heads and two tails sperm (large arrow) are seen. ×1040.

August. A sharp increase of this steroid occurred in October in diploids (8.7 ng/ml) and triploids (15.9 ng/ml). 17α,20β-DiOH dropped in November (diploid 0.7 ng/ml and triploid 0.2 ng/ml).

DISCUSSION

Morphological characteristics of testicular development in triploid males have been reported in several fishes so far. In most cases, abnormalities of spermatogenesis were observed. Despite well-

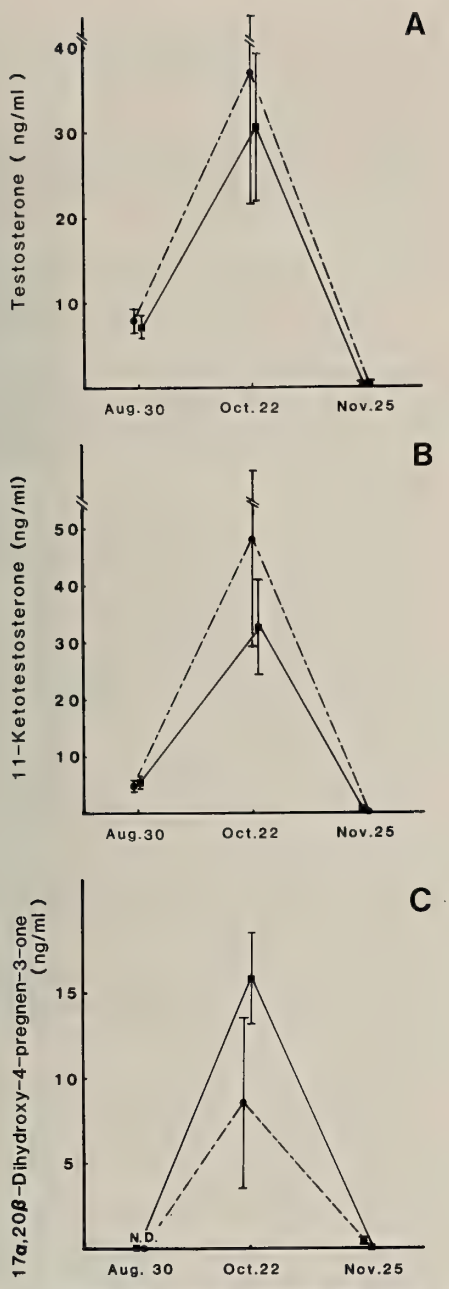

FIG. 7. Changes in serum testosterone (A), 11-ketotestosterone (B) and 17α,20β-dihydroxy-4-pregnen-3-one (C) of diploid (---●---) and triploid (—■—) male masu salmon.

developed testes, matured spermatozoa were not produced in channel catfish (*Ictalurus punctatus*) [17], nor in Atlantic salmon (*Salmo salar*) [2] or in loach (*Misgurnus anguillicaudatus*) [11]. A few sperm were formed in the testes of some species such as Biwa gudgeon (*Gnathopogon caerulescens*) [16], rainbow trout (*Oncorhynchus mykiss*) [4], and Pacific salmonids [1]. The cause of the inability to produce sperm normally in triploids is thought to be the disruption of meiosis due to the odd number of chromosome sets [12].

In the present study, it is clearly shown that the process of testicular development in triploid males is remarkably different from that of diploids. Despite the spawning season, GSI in triploids was markedly low. Sperm in triploids was less in amount and contained cells with morphological abnormalities, such as two heads, two tails, or different sized heads. In addition, secondary spermatocytes and spermatids were not found, though a large number of primary spermatocytes were formed. These facts indicate that the transformation from primary spermatocytes to secondary spermatocytes was suspended. Thus, it seems likely that the large amount of degenerating germ cells that appeared in the testes of triploids in October originated from the primary spermatocytes which failed to be transformed into secondary spermatocytes.

A few papers have dealt with the relationship between testicular development and steroid hormones in triploid fishes [1, 4, 5]. In triploid males, blood steroid hormone levels have been found to be high, just as is the case for mature diploid males. In the triploid males of masu salmon, changes of serum T, 11-KT and 17α,20β-diOH showed no significant differences in comparison with those of mature diploid males. From these results, it is concluded that the production of steroid in triploid males occurs similarly to those in diploid males, even though the development of germ cells is hindered during the process of spermatogenesis. Thus, it is presumed that abnormalities of testicular development in triploids are related to mechanical difficulties involved in chromosome separation at meiosis I due to triploidy *per se*, rather than the reduced level of steroid hormones.

On the other hand, production of steroid hormones and ovarian development in triploid females differs among species. Blood steroid hor-

mone levels in female rainbow trout [4, 6] and female masu salmon (Nakamura *et al.*, unpublished data) were extremely low, even in the spawning season. The ovaries of these female triploids were composed of numerous cysts containing many small oocytes and degenerating oocytes. In contrast, triploid female of tilapia [9] revealed high levels of steroid hormones and had well-developed yolky oocytes in their ovaries. Thus, it is still not known why the reproductive characteristics in triploid fish are different between males and females and among species.

Serum 17α,20β-diOH levels in triploid males increased only in the spawning season. Changes in this steroid are similar to those of diploid males in salmonids [9, 18], but there are no reports on the production of 17α,20β-diOH in triploid males of other species. This steroid is thought to be involved in spermiation [13]. 20β-Hydroxysteroid dehydrogenase (20β-HSD), which is the enzyme essential for the conversion from 17α-hydroxy progesterone to 17α,20β-diOH, was found to be localized on sperm [14]. Thus, it is interesting to note that 17α,20β-diOH production in triploids was as high as it was in diploids, though the amount of sperm in the testes of triploids was reduced. The testes of triploid males may provide a suitable material for the study of 17α,20β-diOH production.

ACKNOWLEDGMENTS

We would like to thank Dr. J. Specker, Department of Zoology, The University of Rhode Island, for reading the manuscript.

REFERENCES

1 Benfy TJ, Dye HM, Solar II, Donaldson EM (1988) The reproductive endocrinology of triploid Pacific salmonids. Western Regional Conference on Comparative Endocrinology p 30

2 Benfy TJ, Shutterlin AM (1984) Growth and gonadal development in triploid landlocked Atlantic salmon (*Salmo salar*). Can J Fish Aquat Sci 41:1387–1392

3 Kagawa H, Young G, Adachi S, Nagahama Y (1982) Estradiol-17β production in amago salmon (*Oncorhynchus rhodurus*) ovarian follicle: Role of the theca and granulosa cells. Gen Comp Endocrinol 47: 440–448

4 Lincoln RF, Scott AP (1984) Sexual maturation in triploid rainbow trout, *Salmo gairdneri* Richardson. J Fish Biol 25: 385–392

5 Nakamura M, Nagahama Y, Iwahashi M, Kojima M (1985) Reproduction of triploid rainbow trout, *Salmo gairdneri*. Proceedings of the 10th Annual Meeting of Japan Society of Comparative Endocrinology p 18

6 Nakamura M, Nagahama Y, Iwahashi M, Kojima M (1987) Ovarian structure and plasma steroid hormones of triploid female rainbow trout. Nippon Suisan Gakkaishi 53: 1105

7 Onozato H (1987) Senshokutai Kougakuteki Shuhouniyoru Ikushu. In: "Kaiyugyo no Seibutugaku" Ed by K Morisawa, K Wada, T Hirano, Japan Science Societies Press, Tokyo, pp 235–251 (in Japanese)

8 Sakai N, Ueda H, Suzuki N, Nagahama Y (1989) Steroid production by amago salmon (*Oncorhynchus rhodurus*) testes at different developmental stages. Gen Comp Endocrinol 75: 231–240

9 Satoh S, Tomita M,Iwahashi M, Nakamura M (1991) Reproduction of triploid tilapia, *Oreochromis niloticus*. Scientific Reports of Niigata Prefecture Inland Water Fisheries Experimental Station. 16: 73–81 (in Japanese)

10 Solar II, Donaldson EM, Hunter G (1984) Induction of triploidy in rainbow trout (*Salmo gairdneri* Richardson) by heat shock, and investigation of early growth. Aquaculture 42: 57–67

11 Suzuki R, Nakanishi T, Oshiro T (1985) Survival, growth and sterility of induced triploids in the cyprinid loach *Misgurnus anguillicaudatus*. Bull Jap Soc Sci Fish 51: 889–894

12 Thorgaard GH (1983) Chromosome set manipulation and sex control in fish. In "Fish Physiology Vol IXB" Ed by WS Hoar, EM Donaldson, Academic Press, New York, pp 405–434

13 Ueda H, Kagawa H, Nagahama Y (1985) Involvement of gonadotropin and steroid hormones in spermiation in the amago salmon, *Oncorhynchus rhodurus*, and goldfish, *Carassius auratus*. Gen Comp Endocrinol 59: 24–30

14 Ueda H, Kambegawa A, Nagahama Y (1984) *In vitro* 11-ketotestosterone and 17α,20β-dihydroxy-4-pregnen-3-one production by testicular fragments and isolated sperm of rainbow trout, *Salmo gairdneri*. J Exp Zool 231: 435–439

15 Ueda H, Young G, Crim LW, Kambegawa A, Nagahama Y (1983) 17α,20β-Dihydroxy-4-pregnen-3-one: Plasma levels during sexual maturation and *in vitro* production by the testes of amago salmon (*Oncorhynchus rhodurus*) and rainbow trout (*Salmo gairdneri*). Gen Comp Endocrinol 51: 106–112

16 Ueno K (1985) Sterility and secondary sexual char-

acter of triploid *Gnathopogon elongatus caerulescens*. Fish Genetics and Breeding Science 10: 37–41

17 Wolters WR, Libey GS, Chrisman GL (1982) Effect of triploidy on growth and gonadal development of channel catfish. Trans Am Fish Soc 111: 102–105

18 Young G, Crim LW, Kagawa H, Kambegawa A, Nagahama Y (1983) Plasma 17α,20β-dihydroxy-4-pregnen-3-one levels during sexual maturation of amago salmon (*Oncorhynchus rhodurus*): Correlation with plasma gonadotropin and *in vitro* production by ovarian follicles. Gen Comp Endocrinol 51: 96–105

ZOOLOGICAL SCIENCE 10: 127–132 (1993)

A case of Intersexuality in the Sea Spider, *Cilunculus armatus* (Pycnogonida; Ammotheidae)

Katsumi Miyazaki[1] and Toshiki Makioka

Institute of Biological Sciences, University of Tsukuba, Tsukuba, Ibaraki 305, Japan

ABSTRACT—An intersexual specimen of the sea spider, *Cilunculus armatus,* having female and male characteristics together with some intermediate ones was collected from Sagami Bay. Eggs are seen through the cuticle of each femoral segment of walking legs. At the same time, cement gland, peculiar to male, is also found on the same segment of each walking leg, but somewhat atrophied and distally shifted. Genital pore opening on the second coxal segment of each walking leg as seen in female is of intermediate size between the sizes of both sexes. Oviger is intermediate in size and shape, and the number and distributional pattern of ovigerous compound spines are also intermediate.

INTRODUCTION

A number of cases of the sexual abnormality, such as the gynandromorphism and the intersexuality, have been reported in arthropods, especially in insects [7], malacostracan crustaceans [3, 4] and spiders [12].

Pycnogonids are dioecious, except for a hermaphrodite species, *Ascorhynchus corderoi* [1]. No intersexuality has been described and gynandromorphs have been known only in the following four cases. Losina-Losinski [9] reported a bilateral gynandromorphic specimen of *Asc. abyssi* from the Greenland Sea. Child [5] examined various grades of gynandromorphism in *Anoplodactylus portus* from the Pacific entrance of the Panama Canal. Child and Nakamura [6] found a gynandromorph of *Ano. gestiens* from Sagami Bay, and described it with a few possible gynandromorphic specimens of *Ano. jonesi* (loc. undescribed).

In the present study, we describe for the first time an intersexual specimen of *Cilunculus armatus,* found among over 1500 specimens newly collected from Sagami Bay.

Accepted July 29, 1992
Received June 22, 1992

[1] Present address: Department of Biology, Keio University, Hiyoshi 4-1-1, Kohoku-ku, Yokohama 211, Japan.

MATERIALS AND METHODS

A specimen of *Cilunculus armatus* (Böhm, 1879) with characters of both sexes was collected by dredge from the sandy bottom at about 40 m in depth off the coast of Shimoda, near the top of Izu Peninsula, Central Japan, 24 March 1990. After fixation with 70% ethanol, the specimen was examined under a stereomicroscope, compared with eight normal male and eight normal female specimens collected by the same dredging.

RESULTS

We newly collected 1535 specimens of *Cilunculus armatus,* and found only one specimen with characters of both sexes. We also reexamined other 1009 preserved specimens which had been collected from the same locality, but could not find any more.

Sexual characters

The present specimen has both ovarian eggs as a female character and cement gland as a male character in the femoral segment of each walking leg, other than the regenerating first right (1R) leg (Fig. 1). There are also some curiosities in several sexual characters of the present specimen especially on morphological features of cement gland, genital pore, oviger, and ovigerous compound

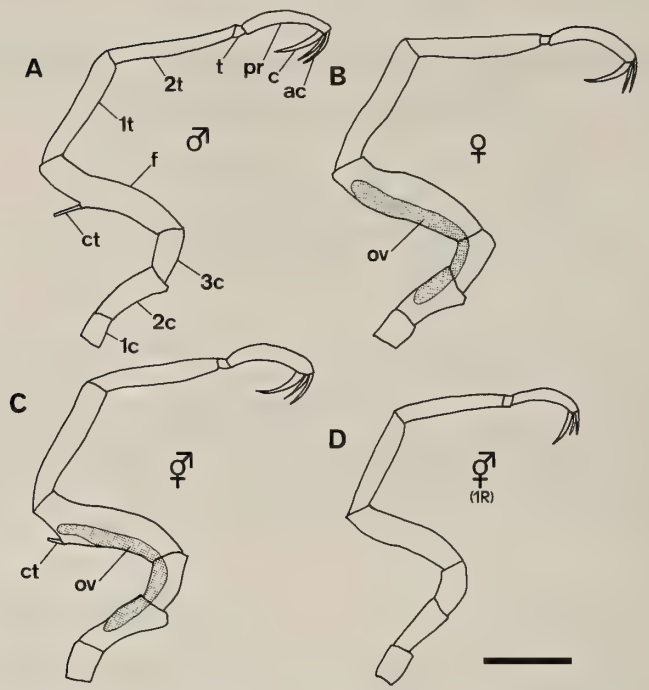

FIG. 1. Walking legs. Setae and spines are omitted. A, Normal male; B, Normal female; C, Intersexual specimen; D, 1R leg of intersexual specimen. ac, accessory claw; c, claw; ct, efferent tube of cement gland; f, femur; 1c, first coxa; 1t, first tibia; ov, ovary; pr, propodus; 2c, second coxa; 2t, second tibia; t, tarsus; 3c, third coxa. Bar=1.0 mm.

TABLE 1. Comparison of some sexual characteristics in an intersexual specimen with those in normal males and females +=present. −=absent

	Normal males	Intersexual specimen	Normal females
Oviger 6–8th	long	intermediate	short
segments	hairy	a little hairy	not hairy
6th seg.	swollen	intermediate	not swollen
Distribution of compound spines	0:2:1:2	3:2:1:2	3:3:1:2
Cement gland	+	+ (somewhat reduced)	−
Genital pore	3rd & 4th legs	all legs (exc. regenerating 1R)	all legs
	small (50×40 μm)	intermediate (75×50 μm)	large (120×100 μm)
Gonad			
Ovary	−	+	+
Testis	+	not visible	−

spine.

Cement gland was found in all the normal males examined and in the present specimen. In normal male, cement gland was well-developed in the femoral segment of each walking leg, and its long external tube with an opening was protruded dorsally at distal one-third of this pedal segment (Fig. 2A). The present specimen had somewhat

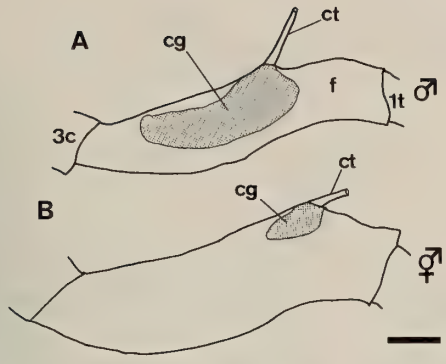

FIG. 2. Comparison of cement glands. A, Normal male; B, Intersexual specimen. cg, cement gland; ct, efferent tube of cement gland; f, femur; 1t, first tibia; 3c, third coxa. Bar=0.25 mm.

atrophied cement gland with shorter tube bearing an opening in the femoral segment of each walking leg other than the 1R leg (Fig. 2B). The tube was shifted more distally than normal one (Fig. 2B).

Genital pore with single cuticular lid was situated on the ventral surface of the second coxae of all the walking legs in female, and on the same position of the third and fourth walking legs in male. The female genital pore was larger than male one (Table 1, Fig. 3A, C). The present specimen had genital pore in all the walking legs other than the 1R leg, whose size was intermediate between that in male and female (Table 1, Fig. 3B).

Male oviger was larger than female one (Table 2, Fig.4A, C), and its sixth segment was prominently stout and hairy (Fig. 5A). Oviger in the present specimen was mostly similar in shape and in size to the female one (Fig.4B, C), but its sixth segment was more hairy than that in female (Fig. 5B). Several apical segments of the oviger had some compound spines (Fig. 5), arranged in different patterns between sexes: In each of normal males, the seventh ovigerous segment had no spines, the eighth two, the ninth one, and the tenth two (0:2:1:2) (Fig. 5A), while in each of normal females, these spines were arranged in 3:3:1:2 (Fig. 5C). In the present specimen, however, they were arranged in 3:2:1:2 (Fig. 5B).

TABLE 2. Comparison of lengths of external body parts in intersexual specimen with those in normal 8 males and 8 females. Mean±SE (Range). measured in mm

	Normal males	Intersexual specimen	Normal females
Proboscis	2.10±0.071 (1.89–2.42)	2.21	2.31±0.060 (2.11–2.63)
Trunk	2.67±0.112 (2.05–3.11)	2.71	2.80±0.092 (2.26–3.05)
Abdomen	1.13±0.061 (0.92–1.39)	1.18	1.15±0.041 (0.95–1.32)
Chelifore	0.44±0.011 (0.39–0.50)	0.47	0.43±0.016 (0.37–0.50)
Palp	2.35±0.075 (1.97–2.68)	2.82	2.59±0.093 (2.21–3.08)
Oviger	3.83±0.085 (3.45–4.13)	2.84	2.40±0.076 (2.13–2.82)
Lateral process	0.39±0.019 (0.32–0.47)	0.37	0.35±0.020 (0.26–0.45)
Leg			
1st coxa	0.46±0.023 (0.37–0.58)	0.45	0.38±0.019 (0.32–0.47)
2nd coxa	0.74±0.038 (0.58–0.92)	0.76	0.69±0.026 (0.58–0.79)
3rd coxa	0.53±0.025 (0.37–0.63)	0.68	0.64±0.023 (0.58–0.76)
femur	1.39±0.039 (1.27–1.53)	1.55	1.53±0.036 (1.37–1.68)
1st tibia	1.36±0.043 (1.18–1.50)	1.47	1.44±0.025 (1.34–1.53)
2nd tibia	1.29±0.054 (1.00–1.50)	1.45	1.47±0.024 (1.42–1.58)
tarsus	0.16±0.010 (0.13–0.21)	0.16	0.17±0.005 (0.16–0.18)
propodus	0.93±0.030 (0.79–1.08)	0.97	0.98±0.015 (0.95–1.05)
claw	0.60±0.019 (0.53–0.68)	0.58	0.62±0.021 (0.55–0.71)
accessory claw	0.34±0.013 (0.29–0.37)	0.26	0.33±0.015 (0.29–0.39)
Cement gland tube	0.35±0.015 (0.26–0.42)	0.18	—

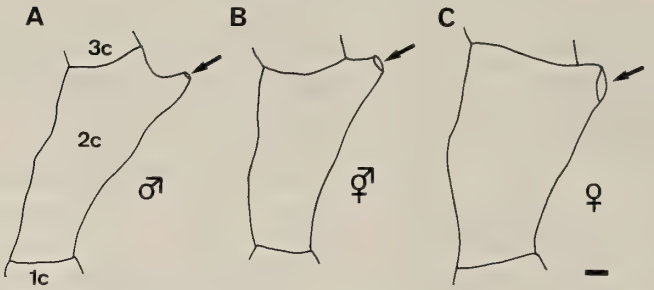

FIG. 3. Comparison of genital pores (arrows). A, Normal male; B, Intersexual specimen; C, Normal female. 1c, first coxa; 2c, second coxa; 3c, third coxa. Bar=0.1 mm.

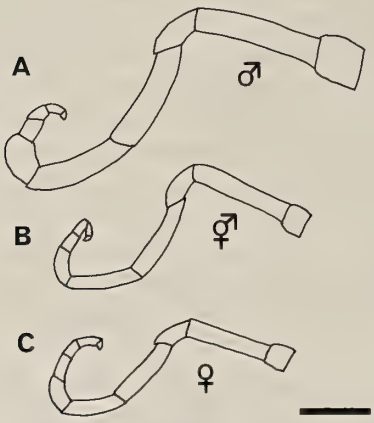

FIG. 4. Comparison of ovigers. Setae and compound spines are omitted. A, Normal male; B, Intersexual specimen; C, Normal female. Bar=0.5 mm.

Any male gonadal element could not be found by the present external observations.

Several sexual characters of the present specimen and normal males and females are summarized in Table 1.

Measurements of external body parts

In *Cilunculus armatus,* females were mostly larger than males (Table 2). Measurements of various parts of the present specimen lay mostly within the female range (Table 2). Normal female leg was stouter than normal male one (Fig. 1A, B). The leg of the present specimen was approximately similar in shape to the female leg (Fig. 1C).

Measurements of some external body parts of the present specimen and normal males and females are summarized in Table 2.

DISCUSSION

In the present specimen, we detected some male, female, and also intermediate characters. Existence of cement glands is a typical male character in *Cilunculus armatus* as in other pycnogonids, but in the present specimen, these glands are somewhat atrophied. The ovarian eggs and the genital pores situated on all the walking legs are female characters. Intermediate sexual characters are seen in size and shape of ovigers and genital pores, and, at the same time, in distributional patterns of ovigerous compound spines (see Table 1).

There are some descriptions incompatible with each other on the distributional pattern of these spines in *Cilunculus armatus.* Ortman [11] noticed compound spines on a probably female oviger; seventh and eighth segments with no spines, ninth with one, tenth with two (0:0:1:2). Loman [8] described the distributional pattern of the spines in both male and female ovigers as 1:2:1:2. Schimkewitsch [13] correctly illustrated female pattern as 3:3:1:2. Utinomi [14] described a female specimen with the 0:1:1:2 spines. Nakamura [10] recognized the difference in male and female patterns as 0:1:1:2 and 3:1:1:2, respectively.

In the present study, we determined correct numbers and distributional patterns of male and female ovigerous compound spines in *Cilunculus armatus,* and found an intermediate pattern in the present specimen.

Bacci [2] defined two main sexual abnormalities; the intersex as "an individual of unisexual species whose reproductive organs and (or) secondary sex characters are partly of one sex and partly of the

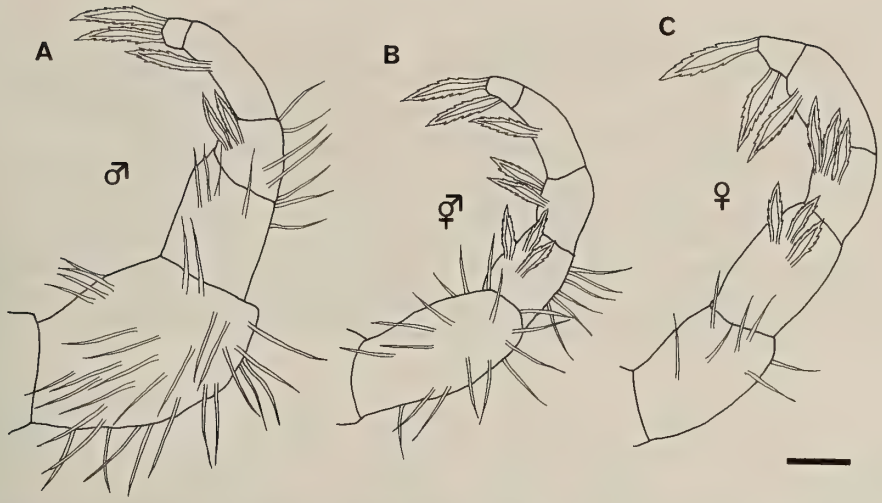

FIG. 5. Comparison of apical parts of ovigers. A, Normal male; B, Intersexual specimen; C, Normal female. Bar= 0.1 mm.

other although it does not show genetically different parts", and the gynandromorph as "an individual of a unisexual species containing a mosaic of genetically male and genetically female cells". According to Bacci's [2] definition, we diagnose the present specimen as an intersexual one.

Child and Nakamura [6] reported a gynandromorphic specimen in other pycnogonid, *Anoplodactylus gestiens*. The specimen had many female characteristics and a few male ones. Existence of the cement gland and the oviger is peculiar to males in *Anoplodactylus* species, but the gynandromorphic specimen has an atrophied cement gland only in the femoral segment of the fourth left leg and the ovigers, the left one being slightly deformed. The gynandromorphic specimen of *Ano. gestiens* has some close resemblances with the present intersexual specimen of *Cilunculus armatus*.

As the intact preservation of the present intersexual specimen is needed, histological, karyological and biochemical details were left untouched.

ACKNOWLEDGMENTS

We gratefully acknowledge Professor Emeritus Jan H. Stock, University of Amsterdam, for his helpful advice and kind encouragement during the present study. Thanks are also due to Mr. Hajime Ueda, Mr. Yasutaka Tuchiya, and Mr. Toshihiko Sato, crew of the collecting ship "Tsukuba", for their constant help in collecting sea spiders, and other staffs of the Shimoda Marine Research Center, University of Tsukuba, for their hospitality. This paper is the Contribution from the Shimoda Marine Research Center, University of Tsukuba, No. 543.

REFERENCES

1 Arnaud F, Bamber RN (1987) The biology of Pycnogonida. Adv Mar Biol 24: 1–96

2 Bacci G (1965) Sex Determination. Pergamon, New York

3 Charniaux-Cotton H (1960) Sex determination. In "The Physiology of Crustacea, Vol. 1". Ed by TH Waterman, Academic Press, New Yolk, pp 411–447

4 Charniaux-Cotton H (1975) Hermaphroditism and gynandromorphism in malacostracan crustacea. In "Intersexuality in the Animal Kingdom". Ed by R Reinboth, Springer-Verlag, Berlin, Heidelberg, New York, pp 91–105

5 Child CA (1978) Gynandromorphs of the pycnogonid *Anoplodactylus portus*. Zool J Linn Soc Lond 63: 133–144

6 Child CA, Nakamura K (1982) A gynandromorph of the Japanese pycnogonid *Anoplodactylus gestiens* (Ortmann). Proc Biol Soc Wash 95: 292–296

7 Lauge G (1985) Sex determination: Genetic and epigenetic factors. In "Comprehensive Insect Physiology, Biochemistry and Pharmacology, Vol. 1, Embryogenesis and Reproduction". Ed by GA Kerkut, LI Gilbert, Pergamon Press, Oxford, New York, Toronto, Sydney, Paris, Frankfurt, pp 295–318

8 Loman JCC (1911) Japanische Podosomata; Beiträge zur Naturgeschichte Ostasiens, herausgeben von F. Doflein. Abh Kaiser Bayersch Akad Wiss Suppl 2: 1–18

9 Losina-Losinsky LK (1964) Pantopoda from the collections of the expeditions of the F Litka in 1955 and the Ob in 1956 Trudy Ark Antarktic Nauchno-Issledov Inst Leningrad 259: 330–339 (in Russian)

10 Nakamura K (1987) The Sea Spiders of Sagami Bay. Ed by Biological Laboratory Imperial Household, Maruzen, Tokyo

11 Ortmann AE (1890) Bericht uber die von Herrn Dr. Doderlein in Japan gesammelten Pycnogoniden. Zool Jahrb (Syst) 5: 157–168

12 Roberts MJ, Parker JR (1973) Gynandry and intersexuality in spiders. Bull Brit Arach Soc 2: 177–183

13 Schimkewitsch W (1929) Pycnogonida (Pantopoda). Fauna SSSR Izdateljstvo Academii Nauk SSSR, Part 1: I-CXV+1-224 (in Russian and Latin)

14 Utinomi H (1955) Report on the Pycnogonida collected by the Soyo-Maru Expedition made on the continental shelf bordering Japan during the years 1926–30. Pub Seto Mar Biol Lab 5: 1–42

ZOOLOGICAL SCIENCE 10: 133–140 (1993)

Metameric Color Pattern in the Bugs (Heteroptera: Lygaeidae, Largidae, Pyrrhocoridae, Rhopalidae): A Morphological Marker of Insect Body Compartmentalization

JAN ZRZAVÝ[1,2], OLDŘICH NEDVĚD[1,2] and RADOMÍR SOCHA[1]

Institute of Entomology, [1]Academy of Science of the Czech Republic and, [2]Faculty of Biological Science, University of South Bohemia, Branišovská 31, 370 05 České Budějovice, Czech Republic

ABSTRACT—Diversity of abdominal color patterns in some coreoid bugs (Heteroptera: Pentatomomorpha: Lygaeidae, Largidae, Pyrrhocoridae, Rhopalidae) is used as a morphological marker to reveal the developmental organization of the abdominal segments. Dominant metameric arrangement of these color patterns is documented by comparison of 160 species, and those results are supplemented by detailed analysis of two model species (*Pyrrhocoris apterus, Dysdercus cingulatus*), including a preliminary clonal analysis of mosaic epidermis in the *P. apterus* mutant strain. This allows the conclusion that (a) the intrasegemental transversal line, marked by contrasting epidermal coloration in the model species, has some properties of the intrasegmental compartmental boundary known in the *Drosophila* segments; (b) this boundary has a considerable role in cuticular color-pattern formation, being hardly exceedable for the cuticular spots established in one half of the segment; and (c) a great majority of the cuticular color patterns, although polyphyletically evolved, follows the same organizational scheme, and their diversity can thus be regarded as constrained by the compartmental boundaries.

INTRODUCTION

The segmentation of the insect body during development have been studied predominantly in *Drosophila,* a species possessing an extremely advanced body plan (for reviews see [1, 6, 8, 14, 18, 25]). The use of *Drosophila* as a model allows us to employ the latest methodologies of molecular genetics and developmental biology. Yet many findings derived from *Drosophila* may pertain only to cyclorrhaphous flies, and may not be sufficient for a general scheme of the insect (or even arthropod and articulate) body plan. A broader comparative survey of the segmentation processes in other insects or arthropods is therefore required. Sander [23] considers spontaneous or experimentally-induced teratological "monsters" a basis for ontogenetic analyses of arthropods which are still unapproachable by genetic methods (i.e., a vast majority of cases). We believe, however, that phylogenetic studies of diversity patterns can also provide a similarly valuable source of evidence.

The studies of Minelli and Bortoletto [19], Emerson and Schram [3], and Nijhout [21] are of particular interest in this respect. These studies deal primarily with morphology rather than genetics or developmental biology, proceeding by three principal steps: (1) description of the diversity pattern, (2) determination of the regularities involved in this diversity, and (3) confrontation of these pattern regularities with presumably relevant developmental processes. The discovery of a convenient morphological trait that would serve as a marker of the sought developmental rules is the critical point in this approach.

Cuticular coloration of some bugs belonging to the superfamily Coreoidea s. lat. (Pentatomonorpha; [24, 29] and references therein) displays conspicuous red-, ochre- or orange-and-black wasp-like patterns on the abdominal segments. The light (non-melanized) and dark (melanized) halves of the individual segments usually alternate regularly. This "half-segment" arrangement of the color pat-

Accepted November 4, 1992
Received July 1, 1992

tern is interesting in terms of the anterior-posterior pattern-formation of the insect body. The coreoid bugs should therefore provide a good model group for developmental studies.

In the present paper, we attempt to examine the color patterns in a variety of species (160 spp.). The results are supplemented by more detailed analysis of the model species [*Pyrrhocoris apterus* (Linnaeus, 1758), *Dysdercus cingulatus* (Fabricius, 1775); both Pyrrhocoridae], including a preliminary clonal analysis of the epidermis in the *P. apterus* mutant strain *mosaic* (*mo*) [20, 26–27].

MATERIALS AND METHODS

Material

The insects used for comparative studies were obtained from the American Museum of Natural History (New York), National Museum (Praha), Moravian Land Museum (Brno), University of Connecticut (Storrs), and Charles University (Praha).

160 species of five higher taxa of the Coreoidea s. lat., viz. Lygaeinae (Lygaeidae: 34 species), Rhyparochrominae (Lygaeidae: 43 spp.), Largidae (9 spp.), Pyrrhocoridae (57 spp.) and Rhopalidae (17 spp.), were examined. Unless otherwise stated, only the adults were studied. Individual variability and sexual dichroism were tentatively checked in approximately 35% of the examined species and found negligible; therefore they were omitted from further analysis.

Two model species, *D. cingulatus* and *P. apterus,* were used for more detailed morphological and ontogenetic analysis. Specimens of both species were obtained from laboratory stock cultures. Besides cuticular color patterns, the epidermal were also examined in all stages of postembryonic development. The coloration of epidermis was either observed through a transparent non-melanized cutile (larvae of both species, adults of *D. cingulatus*), or the animals were beforehand dissected (adults of *P. apterus*).

Morphological analysis and statistical evaluation

The topological distribution of color spots over the abdominal segments was studied. Abdominal segments II to VII were chosen for study, since they are clearly visible and mainly uniform in shape. The abdominal surface was divided into a grid of 120 approximately square-like fields (Fig. 1A), in which the presence vs. absence of melanized cuticle (1 vs. 0) was recorded. An individual field was considered to be melanized if (a) it was completely melanized, or (b) it contained a small melanized spot (a "melanization centre") not exceeding the field borders, or (c) a large melanized spot originating outside the field covered more than 50% of its area. Data obtained by transformation of existing color patterns to the square grid (Fig. 1A) could be compared due to the similar body shapes of the examined species.

The transformed color patterns were tested statistically to reveal regularities in color pattern diversity within the examined taxa. Lygaeinae, Rhyparochrominae, Largidae, Pyrrhocoridae, and Phopalidae were analysed separately. To identify pairs of fields with parallel melanization, the concept of "conjunctions" was introduced. Fields #1 and #2 were in conjunction if #1 was melanized *just when* #2 was melanized. In other words, a conjunction displays a completely concerted melanization of two fields. The fields melanized in less than 10 percent of the examined species within each taxon were excluded from analysis.

The conjunctions fell into four categories: (A) metameric conjunctions between fields on the same (anterior or posterior) halves of different abdominal segments, (B) conjunctions between two fields on the same half of a single segment, (C) conjunctions between two fields on different halves of a single segment, and (D) conjunctions between fields on different halves of different segments (Fig. 1A). Since the number of all possible conjunctions differs for each category (3,000 for A and D, 540 for B, 600 for C), direct comparison of the frequency of the individual categories of conjunctions was not possible. The observed numbers of the conjunctions (N_{obs}) were tested against the expected numbers of the conjunctions (N_{exp}, reflecting 3,000 : 540 : 600 : 3,000 ratio if the probability of all categories of conjunctions was equal) by χ^2 test. The null hypothesis that categories A+B (i.e., those revealing the "half-segment" arrangement) are equal to C+D

was also tested by the χ^2 test (against 3,540 : 3,600 ratio).

Clonal analysis of mosaic epidermis

A laboratory stock of *mosaic* (*mo*) mutant of *P. apterus*, possibly transposon-mediated, was analysed [20, 26–27]. The epidermis of *mo* bugs displays an irregular mosaic of pigmented cells (red anterior, yellow posterior) with transparent (whitish) cell clones lacking pteridine pigments. The distribution of transparent cell clones was considered an apparent marker of normal behaviour of epidermal cell lineages, as the individuals of the *mo* strain do not differ from those of the wild-type in any fundamental morphological, developmental and ecophysiological features. Moreover, when *mo* insects are compared to X-ray-treated animals (for example, [11]), little or no incidence of extraordinary cell deaths should be expected.

Last-instar larvae, whose epidermis is well visible through a transparent cuticle and whose epidermal clones are the best-developed, were studied. Only abdominal segments IV-VI were analysed (both dorsal and ventral surfaces). Since the extent of transparent clones varies considerably in the *mo* strain, only specimens with distinct, sharply outlined patches were anlaysed. Each abdominal segment consists of two distinctly colored areas, red (approximately on the anterior two thirds of the segment) and yellow (the posterior third). A grid of six parallel transversal lines (A, R_1, R_2, RY, Y, P) was superimposed over the segment so that two lines (A, P) fitted the intersegmental boundaries, one (RY) fitted the boundary between the red and yellow parts of the segment, two (R_1, R_2) were laid on the red area, and one (Y) on the yellow area (see Fig. 1B). The distribution pattern of the cell clones was quantified as the number of the patches crossed by the grid lines (see camera lucida drawing in Fig. 1B).

Several hundreds of bugs of both sexes were used for basic screening, and those with suitably distinct clones (10 males, 10 females) were selected for a detailed morphological analysis, which was made on more than 400 uncolored patches.

RESULTS

Development of color patterns in the model species

Postembryonic development of abdominal coloration in *D. cingulatus* and *P. apterus* is summa-

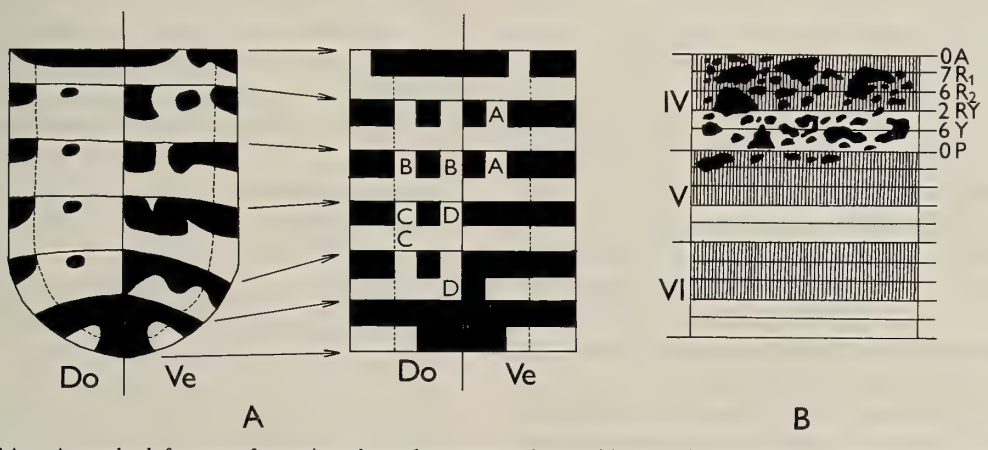

FIG. 1A. A method for transformating the color pattern into grid form (exemplified by *Spilostethus saxatilis* [Lygaeidae]). Do: dorsal, Ve: ventral surface; A-D: categories of conjunctions (A: conjunctions between fields on the same halves of different abdominal segments, B: conjunctions between two fields on the same half of a single one segment, C: conjunctions between two fields on different halves of a single segment, D: conjunctions between fields on different halves of different segments).

FIG. 1B. A method of evaluation of the transparent clones (black) in *mo* mutant of *P. apterus*. IV-VI: abdominal segments; dashed areas: red epidermis; open areas: yellow epidermis; A, R_1, R_2, RY, Y, P: arbitrary grid lines (A, P: intersegmental boundaries; RY: boundary between the red and yellow parts of the segment; R_1, R_2: red area; Y: yellow area); 0, 7, 6, 2, 6, 0: numbers of the clones crossed by the grid lines (in camera lucida drawing).

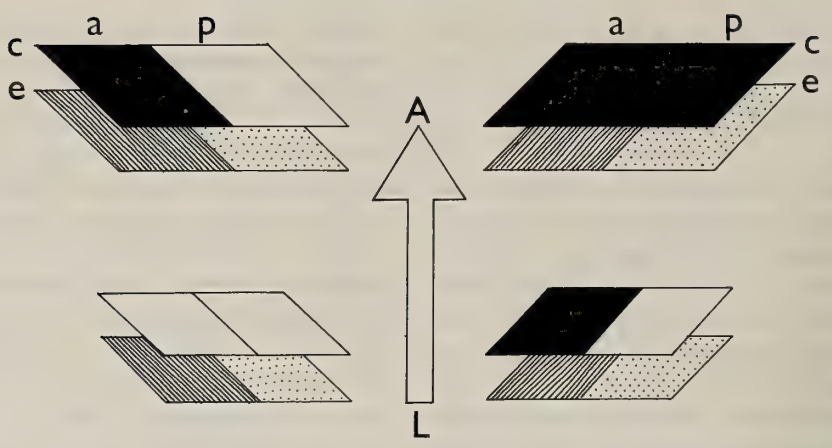

Fig. 2. Postembryonic development of abdominal color patterns in *D. cingulatus* (left) and *P. apterus* (right). L: larvae; A: adults; a: anterior part of a segment; p: posterior part of a segment; c: cuticle; e: epidermis; black areas: melanized cuticle; open areas: transparent cuticle; dashed areas: red epidermis; dotted areas: white or yellow epidermis.

rized in Figure 2. Both species show epidermal color patterns in addition to the cuticular ones. Whereas the epidermis is red or orange-red in the anterior parts of segments, it is either white (*D. cingulatus,* ventral side) or yellow (*P. apterus,* around the entire body) in the posterior parts of segments in both larvae and adults. Posterior boundaries of cuticular melanization in adult *D. cingulatus* completely coincide with the boundaries between red and white epidermal cells (Fig. 2). Similarly, the cuticular melanized spots, which are still distinct in the larvae of *P. apterus,* never reach over the epidermal boundaries from the red to the yellow regions (Fig. 2).

A similar epidermal coloration was previously described by Lawrence [11–12] and Lawrence and Green [15] in *Oncopeltus fasciatus* (Lygaeidae: Lygaeinae). Undoubtedly this subdivision of segment epidermis is widespread among coreoid bugs, especially among the Pyrrhocoridae (Zrzavý, in prep.). In conclusion, cuticular and epidermal color patterns are highly congruent in the model species. A cuticular spot established in one half of a segment usually does not exceed its intersegmental as well as intrasegmental boundaries. The line dividing the segment into anterior and posterior parts (marked by different coloration of the epidermis of the model species) plays an important role in the anterior-posterior arrangement of cuticular coloration.

Clonal restriction in epidermal color pattern formation

As shown in Table 1, no clones seem to lie on the intersegmental boundaries in *P. apterus*; but any intrasegmental line is not an insurmountable barrier.

The red-yellow boundary appears to be the least exceedable, compared to the other lines. We are aware that our simple morphological method is not fully objective since not only the clones but also

Table 1. Distribution of colorless epidermal clones on the abdomen of *mo* mutant of *P. apterus* (10 males, 10 females; c. 7 patches per a segment in average). IV, V, VI: abdominal segments; A, R_1, R_2, RY, Y, P: arbitrary grid lines (A: anterior boundary of a segment; P: posterior boundary of it; R_1, R_2: two lines within the red region of a segment; RY: red/yellow intrasegmental boundary; Y: a line within the yellow region of a segment; see Fig. 1B); +: some number of clones might be overlooked

	A	R_1	R_2	RY	Y	P	Σ
IV	0	61	54	26	34+	1	176+
V	1	37	44	23	28+	0	133+
VI	0	37	31	21	17+	0	106+
Σ	1	135	129	70	79+	1	415+

TABLE 2. General pattern of color conjunctions in Lygaeinae, Pyrrhocoridae and Rhopalidae N_{obs}: total observed number of conjunctions within a taxon; N_{exp}:expected number of conjunctions if the probability of all categories is equal (3,000:540:600:3,000 ratio—see Material and Methods); A, B, C, D: categories of conjunctions (Fig. 1A); χ^2 test—**, ***: significant on the levels of probability $P=0.010$, and 0.001, respectively

	Lygaeinae (34 spp.)		Pyrrhocoridae (57 spp.)		Rhopalidae (17 spp.)	
	N_{obs}	N_{exp}	N_{obs}	N_{exp}	N_{obs}	N_{exp}
A	41	33.2	79	68.9	46	37.0
B	14	6.0	25	12.4	11	6.7
C	6	6.6	20	13.8	15	7.4
D	18	33.2	40	68.9	16	37.0
A+B	55	39.2	104	81.3	57	43.7
C+D	24	39.8	60	82.7	31	44.4
A:B:C:D	***		***		***	
(A+B):(C+D)	***		***		**	

their fragments could be enumerated, while very small transparent (i.e., whitish) clones on the yellow background may be overlooked. Hence, the number of clones within the yellow area (as well as the depth of "RY depression") may have been slightly underestimated.

General organization of color patterns in the coreoid bugs

The color arrangement in the coreoid families is obviously non-random, but organized according to the anterior-posterior polarity of each segment in Lygaeinae (Lygaeidae), Pyrrhocoridae, and Rhopalidae. A significant majority of the color-pattern conjunctions connects either fields lying on the same (anterior or posterior) halves of different segments, or fields lying on the same half of a single segment. Thus, from the four possible categories of conjunctions (see Material and Methods), those marked A and B clearly predominate. On the contrary, the C-category conjunctions connecting fields of the opposite halves of the same segment are less frequent. This data indicates an obviously metameric "half-segment" organization of abdominal color patterns in the taxa studied here (Table 2).

However, the dorsal parts of the abdomen (i.e., those covered by wings in resting position) reveal this metameric color pattern to a much lesser extent. This is because there is, particularly in Rhopalidae, a strong tendency of the abdominal dorsum to display another type of coloration, associated with the aposematic function during flight.

No general metameric arrangement is developed in the Rhyparochrominae (Lygaeidae) and Largidae.

DISCUSSION

Phylogenetic status of the metameric color patterns

Three coreoid taxa examined (Lygaeinae, Pyrrhocoridae, Rhopalidae) apparently tend to generate very similar metameric arrangements of the color pattern. However, each differs from others in some details. For example, the lateral sectors ("connexiva") of both Lygaeinae and Rhopalidae display a clear metamerism, but while the melanized spots usually appear on the anterior halves of the segments in Lygaeinae, they are found on the posterior in Rhopalidae.

It can be assumed that the lygaeines, pyrrhocorids, and rhopalids do not constitute a monophyletic taxon, rather that they represent independent phylogenetic lines of the coreoid bugs. Thus, although our knowledge of phylogenetic relationships among the coreoid bugs is rather scant

[24, 29], and, further, the evolution of their color patterns has never been rigorously analysed, the hypothesis of the homology of their color patterns should be rejected [32]. The majority of the coreoid bugs has cryptic coloration without any conspicuous patterns on the abdominal segments. It appears that the wasp-like abdominal color pattern results from aposematic function of the coloration, which certainly does not belong to the coreoid groundplan. For example, the Rhyparochrominae (a group cladistically related to Pyrrhocoridae, Largidae, Rhopalidae and some other families) and the Largidae (a pyrrhocorid sister group) show complex (but generally cryptic) pyrrhocorid-like color patterns on the pronotum and forewings and generally uniform coloration of abdomen [32].

In conclusion, the wasp-like patterns undoubtedly are not homologous. Instead, the metameric color patterns seem to have arisen independently at least three times during the evolution of the Coreoidea s. lat.—(a) in Lygaeinae, (b) in Pyrrhocoridae, and (c) in Rhopalidae [32]. Yet in spite of the undoubtedly polyphyletic origin of the "wasp-like" color patterns in the Coreoidea s. lat., their diversity is strongly constrained to the formation of a single general organization of color fields, with iteration of the "half-segment" units.

Morphogenetic nature of the color patterns metamerism

The results acquired by clonal analysis of the abdominal epidermis in *P. apterus* are quite compatible with those of Lawrence [11–13] and Lawrence and Green [15]. They showed by clonal analysis of the abdominal epidermis of *O. fasciatus* that (a) segment epidermis is of a polyclonal nature and epidermal cell lineages do not cross intersegmental boundaries; (b) although many clones are sufficiently large to span the entire segment length, no clone comprises both the anterior and posterior margins of the same segment; (c) clones are usually laterally elongated; and (d) clones usually do not cross the intrasegmental boundary between bands of red and white epidermis. Concluding, regions of red and white (or yellow) epidermis in the bugs seem to represent further morphogenetic units within the abdominal segments, and they may represent relatively independent cell lineages (Fig. 3; see Table 1).

These conclusions can, moreover, be applied as well to cuticular color spots of coreoid bugs, which are laterally arranged and do not span the segment

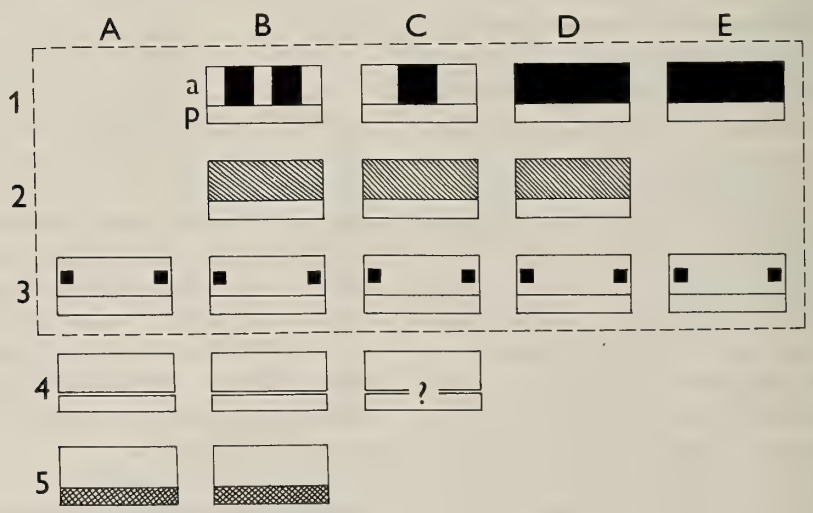

Fig. 3. Comparison of body compartmentalization of the *Drosophila* and coreoid bugs. A: *Drosophila*; B: *O. fasciatus*; C: *P. apterus*; D: *D. cingulatus*; E. coreoid bugs in general; 1: cuticular coloration (orig.); 2: epidermal coloration ([2, 11–13, 15], orig.); 3: position of a spiracle ([7], orig.); 4: clonal restriction [6, 11–16, orig.]; 5: *engrailed* expression pattern [2, 7, 14], a: anterior compartment; p: posterior compartment. Markers available for comparative morphological analysis are boxed.

length. Both color patterns, epidermal and cuticular, seem to be organized with respect to the same line, the "red-white boundary", and the evolution of the aposematic wasp-like coloration only further reveals this basic two-fold organization of the abdominal segment.

This intrasegmental boundary coincides with the line least exceedable by cell lineages, that is, with the possible intrasegmental compartmental boundary, analogous to that of *Drosophila* (Fig. 3) [1, 6–10, 14, 16–18, 25, 30]. The integument of each body segment of *Drosophila* is derived from two cell polyclones, the anterior and posterior compartments, each of which is characterized by a unique combination of active selector genes, and therefore forms a distinct component of the pattern. The compartment seems to be a functional unit for subsequent patterning (including also color-pattern formation: for example, the anterior compartments are melanized, the posterior ones non-melanized).

Using an antibody binding to the product of the segmentation gene *engrailed* (*en*), Campbell and Caveney [2] have shown that *en*-positive cells in *O. fasciatus* form a continuous band localized immediately anterior to the segment border. This pattern of *en* expression is identical to that of posterior compartments in *Drosophila* [7, 9–10, 14], as well as other flies [28], bees [4–5] and locusts [22], and even the crustaceans [22] and centipedes [31]. The size and location of the *en*-positive cell band of the *O. fasciatus* corresponds precisely to a distinct band of white-pigmented epidermal cells [2]. In other words, white pigmentation of the epidermis is a conspicuous morphological marker of the posterior compartment (Fig. 3).

Conclusions

(A) The red-yellow intrasegmental boundary in *P. apterus* seems to display clonal properties similar to the red-white boundary in *O. fasciatus*, and is probably homologous to it (Figs. 3B-C).

(B) The intrasegmental transversal line, marked by contrasting epidermal coloration in the model species, shares the basic properties of the intrasegmental compartment boundary of *Drosophila* segments, and is probably homologous to it (Figs. 3A-C).

(C) The red-yellow boundary takes a considerable role in cuticular color-pattern formation, being hardly exceedable by the cuticular spots established in one half of the segment (Fig. 3).

(D) The great majority of the cuticular color patterns, although independently evolved, respects the same organization scheme. This diversity can be thus regarded as constrained by the compartment boundaries, both inter- and intrasegmental. The uniform organizational scheme of abdominal color patterns in the coreoid bugs seems to serve as a good morphological marker of body compartmentalization.

Consequently, the coreoid bugs can provide a good model for comparative studies of body metamerism, since their compartmentalization seems to be distinctly marked by wild-type body coloration in a large number of species. There is surely some factual bridge between *Drosophila* developmental biology and comparative insect morphology, however careful one must be in making such generalizations.

ACKNOWLEDGMENTS

We are indebted to Prof. C. W. Schaefer and Prof. J. A. Slater (University of Connecticut, Storrs), Dr. R. T. Schuh (American Museum of Natural History, New York), Prof. P. Štys (Charles University, Praha), Dr. L. Hoberlandt (National Museum, Praha), Dr. J. Stehlík (Moravian Land Museum, Brno), Prof. F. Sehnal, Dr. M. Jindra, Dr. V. Novotný, and Dr. P. Švácha (Institute of Entomology, České Budějovice), and Mr. T. Steyskal (University of South Bohemia, České Budějovice) for their kind assistance during preparation of this paper. This study was supported by grants from the Czechoslovak Academy of Sciences and Hasselblad Foundation (Sweden).

REFERENCES

1 Akam M (1987) The molecular basis for metameric pattern in the *Drosophila* embryo. Development 101: 1–22

2 Campbell GL, Caveney S (1989) *engrailed* gene expression in the abdominal segments of *Oncopeltus*: gradients and cell states in the insect segment. Development 106: 727–737

3 Emerson MJ, Schram FR (1990) The origin of crustacean biramous appendages and the evolution

of Arthropoda. Science 250: 667–669

4 Fleig R (1990) *engrailed* expression and body segmentation in the honeybee Apis mellifera. Roux Arch Dev Biol 198: 467–473

5 Fleig R, Walldorf U, Gehring WJ, Sander K (1988) In-situ localization of the transcripts of a homeobox gene in the honey bee *Apis mellifera* L. (Hymenoptera). Roux Arch Dev Biol 197: 269–274

6 García-Bellido A, Lawrence PA, Morata G (1979) Compartments in animal development. Sci Am 241: 102–110

7 Hama C, Ali Z, Kornberg TB (1990) Region-specific recombination and expression are directed by portions of the *Drosophila engrailed* promoter. Gene Dev 4: 1079–1093

8 Kauffman SA, Shymko RM, Trabert K (1978) Control of sequential compartment formation in *Drosphila*. Science 199: 259–270

9 Kornberg T (1981) Compartments in the abdomen of *Drosophila* and the role of the *engrailed* locus. Dev Biol 86: 363–372

10 Kornberg TB, Siden I, O'Farrell PH, Simon M (1985) The *engrailed* locus of *Drosophila*: *in situ* localization of transcripts reveals compartment specific expression. Cell 40: 45–63

11 Lawrence PA (1973) A clonal analysis of segment development in *Oncopeltus* (Hemiptera). J Embryol Exp Morphol 30: 681–699

12 Larence PA (1975) The structure and properties of a compartment border: the intersegmental boundary in *Oncopeltus*. In "Cell Patterning" Ed by S Brenner, Ciba Foundation Symposium 29, Elsevier, Amsterdam, pp 3–23

13 Lawrence PA (1981) The cellular basis of segmentation in insects. Cell 26: 3–10

14 Lawrence PA (1991) The Making of a Fly. Blackwell Scientific Publications, Oxford, pp 228

15 Lawrence PA, Green SM (1975) The intersegmental boundary in *Oncopeltus*. J Cell Biol 65: 373–382

16 Lawrence PA, Green SM, Johnston P (1978) Compartmentalization and growth of the *Drosophila* abdomen. J Embryol Exp Morphol 43: 233–245

17 Lawrence PA, Martinez-Arias A (1985) The cell lineage of segments and parasegments in *Drosophila*. Phil Trans R Soc Lond, B, 312: 83–90

18 Martinez-Arias A, Lawrence PA (1985) Parasegments and compartments in the *Drosophila* embryo. Nature 313: 639–642

19 Minelli A., Bortoletto S. (1988) Myriapod metamerism and arthropod segmentation. Biol J Linn Soc 33: 323–343

20 Němec V, Socha R (1988) Phosphatases and pteridines in Malpighian tubules: a possible marker of the mosaic mutant in *Pyrrhocoris apterus* (Heteroptera, Pyrrhocoridae). Acta Entomol Bohemoslov 85: 321–326

21 Nijhout HF (1991) Development and Evolution of Butterfly Wing Patterns. Smithsonian Institution Press, Washington-London, pp 297

22 Patel NH, Kornberg TB, Goodman CS (1989) Expression of *engrailed* during segmentation in grasshopper and crayfish. Development 107: 201–212

23 Sander K (1988) Studies in insect segmentation: from teratology to phenogenetics. Development 104 (Suppl): 112–121

24 Schuh RT (1986) The influence of cladistics on heteropteran classification. Annu Rev Entomol 31: 67–93

25 Scott MP, O'Farrell PH (1986) Spatial programming of gene expression in early *Drosophila* embryogenesis. Annu Rev Cell Biol 2: 49–80

26 Socha R (1987) Unusual presence of pigmented granules in the Malpighian tubules in a mosaic mutant of *Pyrrhocoris apterus* (Heteroptera, Pyrrhocoridae). Acta Entomol Bohemoslov 84: 241–245

27 Socha R, Němec V (1992) Pteridine analysis in five colour-body mutations of *Pyrrhocoris apterus* (Heteroptera: Pyrrhocoridae). Acta Entomol Bohemoslov 89: 195–203

28 Sommer R, Tautz D (1991) Segmentation gene expression in the housefly *Musca domestica*. Development 113:419-430

29 Štys P, Kerzhner I (1975) The rank and nomenclature of higher taxa in recent Heteroptera. Acta Entomol Bohemoslov 72: 65–79

30 Szabad J, Schüpbach T, Wieschaus E (1979) Cell lineage and development in the larval epidermis of *Drosophila melanogaster*. Dev Biol 73: 256–271

31 Whitington PM, Meier T, King P (1991) Segmentation, neurogenesis and formation of early axonal pathways in the centipede, *Ethmostigmus rubripes* (Brandt). Roux Arch Dev Biol 199: 349–363

32 Zrzavý J (1990) Evolution of the aposematic color pattern in some Coreoidea s. lat. (Heteroptera). Acta Entomol Bohemoslov 87: 470–474

ZOOLOGICAL SCIENCE 10: 141–146 (1993)

N-Terminal Amino Acid Sequences of 440 kDa Hemoglobins of the Deep-sea Tube Worms, *Lamellibrachia* sp.1, *Lamellibrachia* sp.2 and Slender vestimentifera gen. sp.1 Evolutionary Relationship with Annelid Hemoglobins

Tomohiko Suzuki[1], Takashi Takagi[2] and Suguru Ohta[3]

[1]*Department of Biology, Faculty of Science, Kochi University, Kochi 780,*
[2]*Biological Institute, Faculty of Science, Tohoku University,*
Sendai 980, and [3]*Ocean Research Institute,*
University of Tokyo, Tokyo 164, Japan

ABSTRACT—The deep-sea tube worm *Lamellibrachia*, belonging to the phylum Vestimentifera, contains two types of extracellular hemoglobins, a 3,000 kDa hemoglobin and a 440 kDa hemoglobin. The latter hemoglobin is composed of four heme-containing chains with molecular masses of 16–18 kDa. We have collected *Lamellibrachia* sp.1, *Lamellibrachia* sp.2 and Slender vestimentifera gen. sp.1 from the deep-sea cold-seep or hydrothermal areas at a depth of 1100–1400 m. The four constituent chains of the 440 kDa hemoglobin were isolated from each of the three tube worms by reverse-phase chromatography, and the N-terminal amino acid sequences of 16–44 residues were determined by automated protein sequencer. The amino acid sequences of the homologous chains showed high homology (76–85%), suggesting that they are closely related. The sequences also showed 45–49% homology with annelid hemoglobins. A phylogenetic tree constructed from hemoglobin sequences showed that the tube worm *Lamellibrachia*, the polychaete *Tylorrhynchus* and the oligochaete *Lumbricus* diverged from a common ancestor at almost the same time, about 450 million years before present.

INTRODUCTION

The deep-sea tube worms *Riftia* and *Lamellibrachia*, belonging to the phylum Vestimentifera, are found in hydrothermal vent or cold seeps at a depth of 600–2,500 m. These animals are sustained by mutual symbiosis with sulfide-oxidizing bacteria [3], and their blood, containing abundant extracellular hemoglobin, has a function to transport sulfide (H_2S) to internal bacterial symbionts, as well as to facilitate oxygen transport compatible with high oxygen demand [1].

The tube worm *Lamellibrachia* sp.1, referred as *Lamellibrachia* sp. in previous papers [17–20], has two types of giant extracellular hemoglobins, a 3,000 kDa hemoglobin and a 440 kDa hemoglobin. The former hemoglobin is composed of four 16–18 kDa heme-containing chains and two 24–26 kDa linker chains, while the latter consists of only four heme-containing chains. Two of the four heme-containing chains are common to both hemoglobins. So far, we isolated most of the constituent chains of the two hemoglobins by a reverse-phase chromatography, and determined the complete amino acid sequences of a 16 kDa heme-containing chain [18] and a 24 kDa linker chain [19]. The sequence results suggested that the hemoglobin of *Lamellibrachia* sp.1 is closely related to those of annelids.

In this report, we isolated four heme-containing chains of 440 kDa hemoglobin newly from the two tube worms, *Lamellibrachia* sp.2 and Slender vestimentifera gen. sp.1, and determined the N-terminal sequences of all the chains. Phylogenetic relationship among the tube worms and annelids is

Accepted August 18, 1992
Received July 9, 1992

discussed.

MATERIALS AND METHODS

The tube worm *Lamellibrachia* sp.1 and Slender vestimentifera gen. sp.1 (both undescribed) were collected from the cold-seep area located off Sagami Bay at a depth of 1110–1170 m, Japan, by a Japanese submersible *SHINKAI 2000*. *Lamellibrachia* sp.2 (undescribed) and Slender vestimentifera gen. sp.1 were collected from the hydrothermal area of the Okinawa Trough, eastern part of the Iheya Ridge at a depth of 1405 m, Japan.

Hemoglobin was purified from frozen animals as described previously [17]. Two hemoglobin components, a 3,000 kDa hemoglobin and a 440 kDa hemoglobin, were isolated on a gel filtration column of Superose 12 (Pharmacia, 1×30 cm), in 50 mM phosphate buffer (pH 7.2) containing 150 mM NaCl at a flow rate of 0.5 ml/min. The constituent polypeptide chains of the reduced 440 kDa hemoglobin were separated by a Cosmosil $5C_{18}$-300 column (4.6×150 mm, Nacalai Tesque) with a linear gradient of acetonitrile in 0.1% trifluoroacetic acid [17].

The amino acid sequence of carboxymethylated protein was determined directly by use of an automated sequencer (Applied BioSystems 477A Protein Sequencer).

RESULTS AND DISCUSSION

We separated 3,000 kDa and 440 kDa hemoglobins from the three tube worms, *Lamellibrachia* sp.1, *Lamellibrachia* sp.2 and Slender vestimentifera gen. sp.1, by a high-performance gel filtration column of Superose 12. A typical elution profile for the latter species is shown in Fig. 1. The 3,000 kDa hemoglobin is susceptible to dissociation, and its several dissociation products emerge after the 440 kDa hemoglobin as small peaks. The hemoglobins of *Lamellibrachia* sp.1 and Slender vestimentifera gen. sp.1 were isolated mainly in the oxygenated form, but that of *Lamellibrachia* sp.2 was almost in the met (oxidized) form.

The extracellular giant hemoglobins of annelids and tube worms comprise four heme-containing chains, which can be separated into two distinct

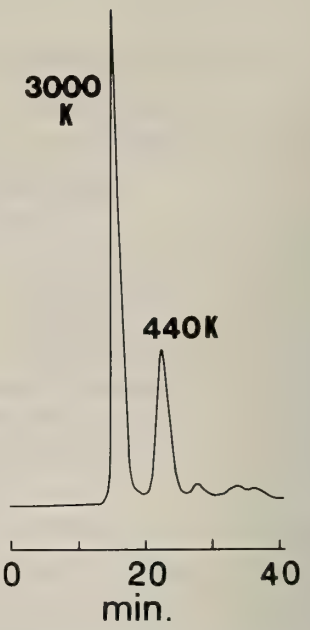

FIG. 1. Separation of the 3,000 kDa and 440 kDa hemoglobins of Slender vestimentifera gen. sp.1 on a gel filtration column of Superose 12. The column was equilibrated and eluted with 50 mM phosphate buffer containing 150 mM NaCl at a flow rate of 0.5 ml/min. Absorbance was monitored at 540 nm.

strains, A and B as suggested by Gotoh *et al.* [7]. However, the nomenclature of the chains is not unified among the researchers, so it is strongly recommended to propose a common name, like alpha and beta chains of vertebrate hemoglobins, for the corresponding chains to make clear their evolutionary relationship. Gotoh *et al.* [8, 9] were the first to propose a common name, a, A, b and B for each chain (see Table 1). But not all of the researchers agreed with the nomenclature, mainly because the difference between capital and small characters is difficult to appreciate in the spoken language [9]. Therefore we modified the nomenclature proposed by Gotoh *et al.* [8, 9], and introduced a new name (A1, A2, B1 and B2) for each of the heme-containing chains, based on the amino acid sequence homology between the chains, in this paper (Table 1).

The four heme-containing chains of the tube worm 440 kDa hemoglobin were separated by a reverse-phase chromatography. A typical elution profile for Slender vestimentifera sp.1 is shown in

TABLE 1. Nomenclature for four heme-containing chains of annelid and tube worm hemoglobins

Source	Chain Name (Earlier Nomenclature)				Reference
	Strain A		Strain B		
Lumbricus	I	II	III	IV	Vinogradov *et al.* [23]
Lumbricus	d	b	c	a	Fushitani *et al.* [5]
Tylorrhynchus	I	IIA	IIC	IIB	Suzuki *et al.* [13]
Lamellibrachia	I	III	IV	II	Suzuki *et al.* [17]
Proposed name	a	A	b	B	Gotoh *et al.* [8, 9]
	A1	A2	B1	B2	This paper

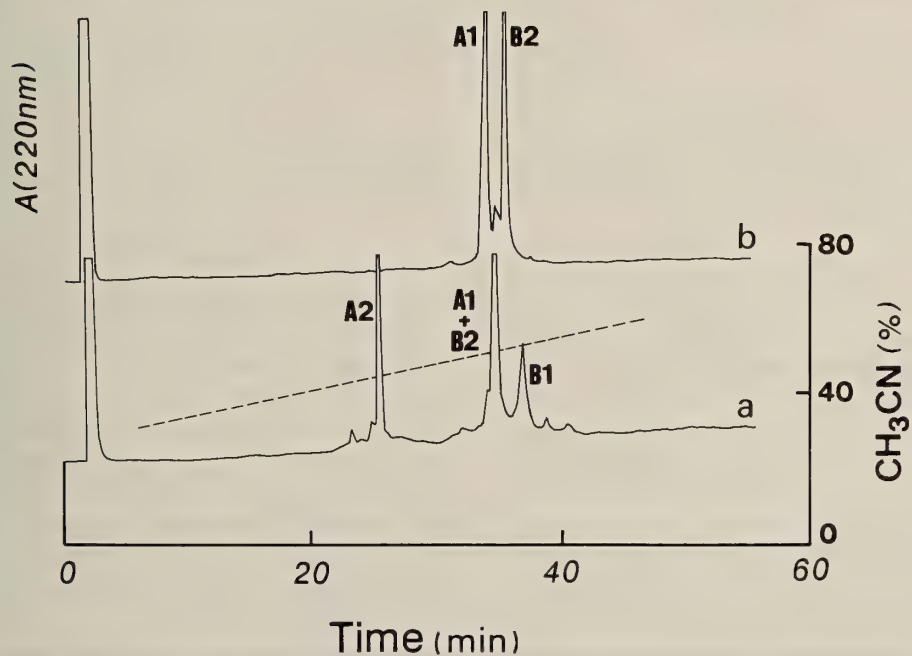

FIG. 2. Separation of the constituent chains of the 440 kDa hemoglobin from Slender vestimentifera gen. sp.1 by reverse-phase chromatography. The column (Cosmosil $5C_{18}$-300) was eluted with a linear gradient of acetonitrile in 0.1% TFA at a flow rate of 1 ml/min. (a), reduced 440 kDa hemoglobin; (b), rechromatography of chains A1 and B2 after carboxymethylation.

Fig. 2. In this case, chains A1 and B2 were not separated (Fig. 2a), but they were separated by rechromatography after carboxymethylation of cysteine residues (Fig. 2b).

The N-terminal amino acid sequences of 16–44 residues of the isolated chains of tube worm 440 kDa hemoglobin were determined by an automated protein sequencer and aligned in Fig. 3 with those of the polychaete *Tylorrhynchus* [13, 14, 16, 21] and the oligochaete *Lumbricus* [5, 12]. The amino acid sequences (total 134 residues compared) of the homologous chains from the three tube worms showed high homology (76–85%) with each other, suggesting that they are closely related. In addition, the sequence of tube worm hemoglobin has significant homology (45–49%) with those of annelid hemoglobins, which is comparable to the homology (43%) between the

```
                          1        10        20        30        40
A1 chain   Lam.sp.1         DcNILQRLKVKMQWAKAYG  FGAERAKFGNSLWTSIFNYAP
           Lam.sp.2        EKcNDLERIKVKMQWAKAYS  FSANRAKFGDALWANVFNYAP
           Ves.sp.1        DNcNILQRIKMKMQWGKAYG  TGAKRAEFGDALWANVFNYAP
           Tyl.            TDcGILQRIKVKQQWAQVYS  VGESRTDFAIDVFNNFFRTNP
           Lum.             EcLVTEGLKVKLQWASAFG  HAHQRVAFGLELWKGILREHP
A2 chain   Lam.sp.1       YEcGPLQRLKVKRQWAEAYG  SGNDREEFGHFIWTHVF
           Lam.sp.2      DHVcGPLQRLKVKRQWAEAYG  SGNRREDFGHYIWAHVF
           Ves.sp.1     DTHVcGPLQRLKVKRQWAEAYG  SGGRREDFGHYIWAHVF
           Tyl.         SSDHcGPLQRLKVKQQWAKAYG  VGHERVELGIALWKSMF
           Lum.          KKQcGVLEGLKVKSEWGRAYG  SGHDREAFSQAIWRATF
B1 chain   Lam.sp.1       SKFcSEGDATIVIKQW
           Lam.sp.2     EASDHcHYEDAEIVMKEW
           Ves.sp.1    TVVSDDcSYEDADIVMKEW
           Tyl.           DTCcSIEDRREVQALW
           Lum.        DEHEHCcSEEDHRIVQKQW
B2 chain   Lam.sp.1        SSNScTTEDRREMQLMWANVWSAQFTGRRLAIAQAVFKDLFA
           Lam.sp.2         SNHcTTEDRREMQLMWGNVWSAQFTGRRLAIAQAVFKDLFD
           Ves.sp.1         SNHcTTEDRKEMQIMWSNVWHAQFTGRRLAIAQAVFNDLFA
           Tyl.             DDCcSAADRHEVLDNWKGIWSAEFTGRRVAIGQAIFQELFA
           Lum.        ADDEDCcSYEDRREIRHIWDDVWSSSFTDRRVAIVRAVFDDLFK
                                *         *
```

Fig. 3. Alignment of N-terminal amino acid sequences of four heme-containing chains of three tube worms with those of *Tylorrhynchus* and *Lumbricus*. Asterisks indicate the invariable residues in all chains. Lam. sp.1, *Lamellibrachia* sp.1; Lam. sp.2, *Lamellibrachia* sp.2; Ves. sp.1, Slender vestimentifera gen. sp.1; Tyl., *Tylorrhynchus*; Lum., *Lumbricus*.

polychaete and oligochaete hemoglobins.

In annelid-like giant hemoglobins, Cys residues play a particularly important role in the subunit assembly of the giant molecule. They are all participating in either intra- or interchain disulfide bridges [5, 15]. All of the chains of the tube worm hemoglobins conserves Cys-7 that would be used for the formation of intrachain disulfide bridge.

The deep-sea tube worms were placed in a new phylum, Vestimentifera, on the basis of their unique outward appearance, such as the very long trunk region and absence of a mouth, gut and anus [10]. Since there is no fossil record on tube worms, it is very hard to get an evolutionary relationship among the tube worms and other invertebrate animals directly. So far both of the 18S ribosomal RNA sequence [4] and hemoglobin sequence [17, 18] suggest that the tube worm and annelid are closely related. In order to get more information on the evolution of the tube worms, we constructed a phylogenetic tree for the hemoglobin sequences by an unweighted pair group clustering method (Fig. 4). Standard errors are given at each branching point, to help evaluation of the tree [11].

Fig. 4a shows a phylogenetic tree constructed from the partial hemoglobin sequences (total 134 residues) of the four chains of the three tube worms and two annelids (see Fig. 3). The tree apparently indicates that the tube worms, polychaete *Tylorrhynchus* and oligochaete *Lumbricus* diverged from a common ancestor at almost the same time, and the radiation of tube worms now examined is a relatively recent event. Judging from the cluster of the tube worms, the Slender vestimentifera gen. sp.1 may be included in the genus *Lamellibrachia*.

We have determined the complete amino acid sequences of the four heme-containing chains of *Lamellibrachia* sp.1 440 kDa hemoglobin, very recently [22]. Fig. 4b shows a phylogenetic tree constructed from the four complete sequences (total 576 residues) of *Lamellibrachia* sp.1, *Tylorrhynchus* and *Lumbricus* hemoglobins. This tree must be more reliable than that of Fig. 4a, but the branching pattern for the two trees was quite similar, supporting the accuracy of the tree in Fig. 4a.

Of great interest is the divergence time of tube worms and annelids. The evolutionary rate of hemoglobins is roughly estimated to be constant in vertebrates, and Goodman *et al.* [6] calculated the

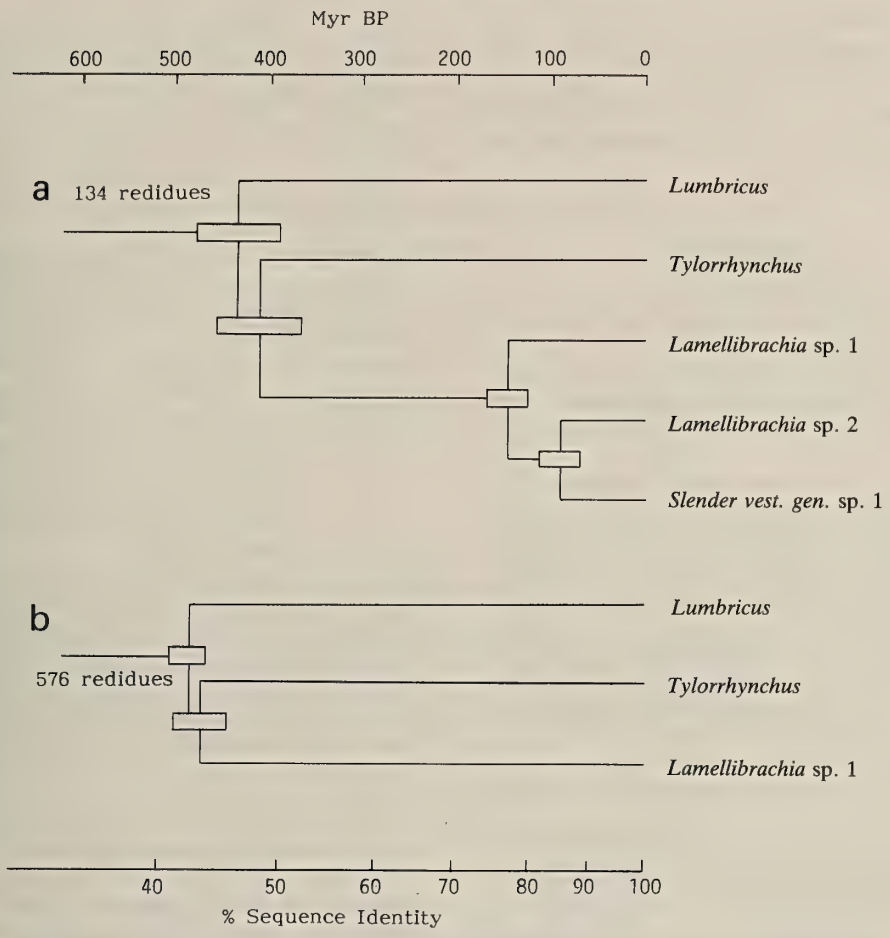

FIG. 4. Phylogenetic trees for the four heme-containing chains of annelid and tube worm hemoglobins. The tree was constructed by an unweighted pair-group clustering method using the Poisson corrected sequence difference matrix. Standard errors at the branching points are indicated as boxes. (a), a tree constructed from the partial amino acid sequences of the four chains compared in Fig. 3 (total 134 residues); (b), a tree from the complete sequences of the four chains consisting of total 576 amino acid residues.

divergence time of human alpha and beta globins with 44% sequence identity to be about 450 million years before present (Myr BP). In addition, the phylogenetic tree constructed from hemoglobin sequences shows a good correlation with that from classical taxonomy [6].

Just as in vertebrates, all of the members belonging to the phylum Annelida expresses abundant hemoglobin, indicating that hemoglobin is a physiologically important molecule. Annelida consists of two major classes, polychaete and oligochaete, but at present it is very difficult to estimate the exact divergence time of the two classes from the poor or incomplete fossil records of annelids. Therefore, to introduce a tentative time scale for the evolution of annelid and tube worm hemoglobins, we used the same evolutionary rate as in vertebrate hemoglobins. Finally, it was estimated that the tube worms, polychaete and oligochaete diverged at almost the same time, about 450 Myr BP, and that the radiation of three tube worms occurred around 100 Myr BP (see Fig. 4). These divergence dates are not unreasonable values, because the fossil records indicate that

most of representatives of the living phyla and classes of invertebrates appeared about 450–500 Myr BP [2]. In addition, Fushitani *et al.* [5] roughly estimated the divergence time of *Lumbricus* and *Tylorrhynchus* to be about 450 Myr BP using hemoglobin sequences.

REFERENCES

1 Arp AJ, Childress JJ (1981) Blood function in the hydrothermal vent vestimentiferan tube worm. Science 213: 342–344

2 Brasier MD (1979) In "The Origin of Major Invertebrate Groups" Ed by MR House MR, Academic Press, New York, pp 103–159 (cited in Ref. 4)

3 Childress JJ, Felbeck H, Somero GN (1987) Symbiosis in the deep sea. Scientific Amer 256: 106–112

4 Field KG, Olsen GJ, Lane DJ, Giovannoni SJ, Ghistelin MT, Raff EC, Pace NR, Raff RA (1988) Molecular phylogeny of the animal kingdom. Science 239: 748–753

5 Fushitani K, Matsuura MSA, Riggs AF (1988) The amino acid sequences of chains a, b, and c that form trimer subunit of the extracellular hemoglobin from *Lumbricus terrestris*. J Biol Chem 263: 6502–6517

6 Goodman M, Moore GW, Matsuda G (1975) Darwinian evolution in the genealogy of hemoglobin. Nature 253: 603–608

7 Gotoh T, Shishikura F, Snow JW, Ereifej K, Vinogradov SN (1987) Two globin strains in the giant annelid extracellular haemoglobins. Biochem J 241: 441–445

8 Gotoh T, Suzuki T (1990) Molecular assembly and evolution of multi-subunit extracellular annelid hemoglobins. Zool Sci 7: 1–16

9 Gotoh T, Suzuki T, Takagi T (1991) Nomenclature of the major constituent chains common to annelid extracellular hemoglobins. In "Structure and Function of Invertebrate Dioxygen Carriers" Ed by SN Vinogradov, OH Kapp, Springer-Verlag, Berlin, pp 279–283

10 Jones ML (1985) On the Vestimentifera, new phylum: six new species, and other taxa, from hydrothermal vents and elsewhere. Biol Soc Wash Bull 6: 117–158

11 Nei M, StephensJC, Saitou N (1985) Methods for computing the standard errors of branching points in an evolutionary tree and their application to molecular data from humans and apes. Mol Biol Evol 2: 66–85

12 Shishikura F, Snow JW, Gotoh T, Vinogradov SN, Walz DA (1987) Amino acid sequence of the monomer subunit of the extracellular hemoglobin of *Lumbricus terrestris*. J Biol Chem 262: 3123–3131

13 Suzuki T, Furukohri T, Gotoh T (1985) Subunit structure of extracellular hemoglobin from the polychaete *Tylorrhynchus heterochaetus* and amino acid sequence of the constituent polypeptide chain (IIC). J Biol Chem 260: 3145–3154

14 Suzuki T, Gotoh T (1986) The complete amino acid sequence of giant multisubunit hemoglobin from the polychaete *Tylorrhynchus heterochaetus*. J Biol Chem 261: 9257–9267

15 Suzuki T, Kapp OH, Gotoh T (1988) Novel S-S loops in the giant hemoglobin of *Tylorrhynchus heterochaetus*. J Biol Chem 263: 18524–18529

16 Suzuki T, Takagi T, Gotoh T (1982) Amino acid sequence of the smallest polypeptide chain containing heme of extracellular hemoglobin from the polychaete *Tylorrhynchus heterochaetus*. Biochim Biophys Acta 708: 253–258

17 Suzuki T, Takagi T, Ohta S (1988) N-Terminal amino acid sequence of the deep-sea tube worm hemoglobin remarkably resembles that of annelid haemoglobin. Biochem J 255: 541–545

18 Suzuki T, Takagi T, Ohta S (1990) Primary structure of a constituent polypeptide chain (AIII) of the giant haemoglobin from the deep-sea tube worm *Lamellibrachia*. A possible H_2S-binding site. Biochem J 266: 221–225

19 Suzuki T, Takagi T, Ohta S (1990) Primary structure of a linker subunit of the tube worm 3000-kDa hemoglobin. J Biol Chem 265: 1551–1555

20 Suzuki T, Takagi T, Okuda K, Furukohri T, Ohta S (1989) The deep-sea tube worm hemoglobin: Subunit structure and phylogenetic relationship with annelid hemoglobin. Zool Sci 6: 915–926

21 Suzuki T, Yasunaga H, Furukohri T, Nakamura K, Gotoh T (1985) Amino acid sequence of polypeptide chain IIB of extracellular hemoglobin from the polychaete *Tylorrhynchus heterochaetus*. J Biol Chem 260: 11481–11487

22 Takagi T, Iwaasa H, Ohta S, Suzuki T (1991) Primary structure of 440 kDa hemoglobin from the deep-sea tube worm *Lamellibrachia*. In "Structure and Function of Invertebrate Dioxygen Carriers" Ed by SN Vinogradov, OH Kapp, Springer-Verlag, Berlin, pp 247–252

23 Vinogradov SN, Shlom JM, Hall BC, Kapp OH, Mizukami H (1977) The dissociation of *Lumbricus terrestris* hemoglobin: a model of its subunit structure. Biochim. Biophys. Acta 492: 136–155

ZOOLOGICAL SCIENCE 10: 147–154 (1993)

Two New Species of the Genus *Staphylocystis* (Cestoda: Hymenolepididae) from the House Shrew, *Suncus murinus*, in Nepal

Isamu Sawada[1], Kazuhiro Koyasu[2] and Krishna Chandra Shrestha[3]

[1]*Biological Laboratory, Nara Sangyo University, Sango, Nara 636,*
[2]*the Second Department of Anatomy, School of Dentistry, Aichi-Gakuin University, 1-100 Kusumoto-cho, Chikusa-ku, Nagoya 464, Japan and* [3]*Department of Zoology, Pri-Chandra Campus, Kathmandu, Nepal*

ABSTRACT—Two new species of the cestode parasite, *Staphylocystis* (*Staphylocystis*) *kathmanduensis* sp. nov. and *S.* (*S.*) *trisuliensis* sp. nov. are described from the house shrews, *Suncus murinus* of Kathmandu and Trisuli, respectively. The former is related to, but different from *S.* (*S.*) *delicata* Sawada et Koyasu, 1991 in the length and number of the rostellar hooks, and the size of the rostellum. The latter is related to, but different from *S.* (*S.*) *dsinezumi* Sawada et Koyasu, 1990 in the rostellar hooks. The house shrew, *Suncus murinus*, one kind of the commensal mammals, are widly distributed in Asia and are found infected with a great number of different cestodes. The difference between the two cestode species infecting *Suncus murinus* collected respectively at Kathamandu and Trisuli is discussed according to the hosts's behavior patterns.

INTRODUCTION

The cestode parasites of the house shrew, *Suncus murinus*, in Nepal are little known except the one reported by Sawada and Koyasu [11], who described a new species, *Pseudhymenolepis nepalensis* from *Suncus murinus* collected at Kathmandu. Since then, no attempts have been made to study the cestode parasites of *Suncus murinus*, although it is quite commonly found in Nepal. This paper reports anothor two new hymenolepidid cestodes obtained from *Suncus murinus* collected at Kathmandu and Trisuli, and discusses the difference between the two new species from the point of view of the host's behavior patterns [1, 3].

MATERIALS AND METHODS

Seven specimens of *Suncus murinus* were collected with traps at Kathmandu and Trisuli in March, 1991, and were examined for cestodes in connection with the previous investigation (Fig. 1). The shrews were autopsied immediately after capture, and their guts were removed and fixed in Carnoy's fluid, and maintained until the investigation in Japan. The methods used have been described in the previous paper [10]. All measurements are given in millimeters unless otherwise stated.

Accepted September 5, 1992
Received March 30, 1992

Staphylocystis (*Staphylocystis*) *kathmanduensis* sp. nov. (Fig. 2–6)

From March 17 to 31, 1991, four house shrews, *Suncun murinus*, were captured at Kathmandu. One of them harbored five mature specimens of this cestode.

Description (based on five specimens): Small-sized hymenolepidid; mature worm length 7.1–8.3 and maximum width 0.8–0.9. Metamerism distinct; margin slightly serrate. Scolex round, 0.221–

Fig. 1. Map of Nepal showing the localities of the house shrews collected.

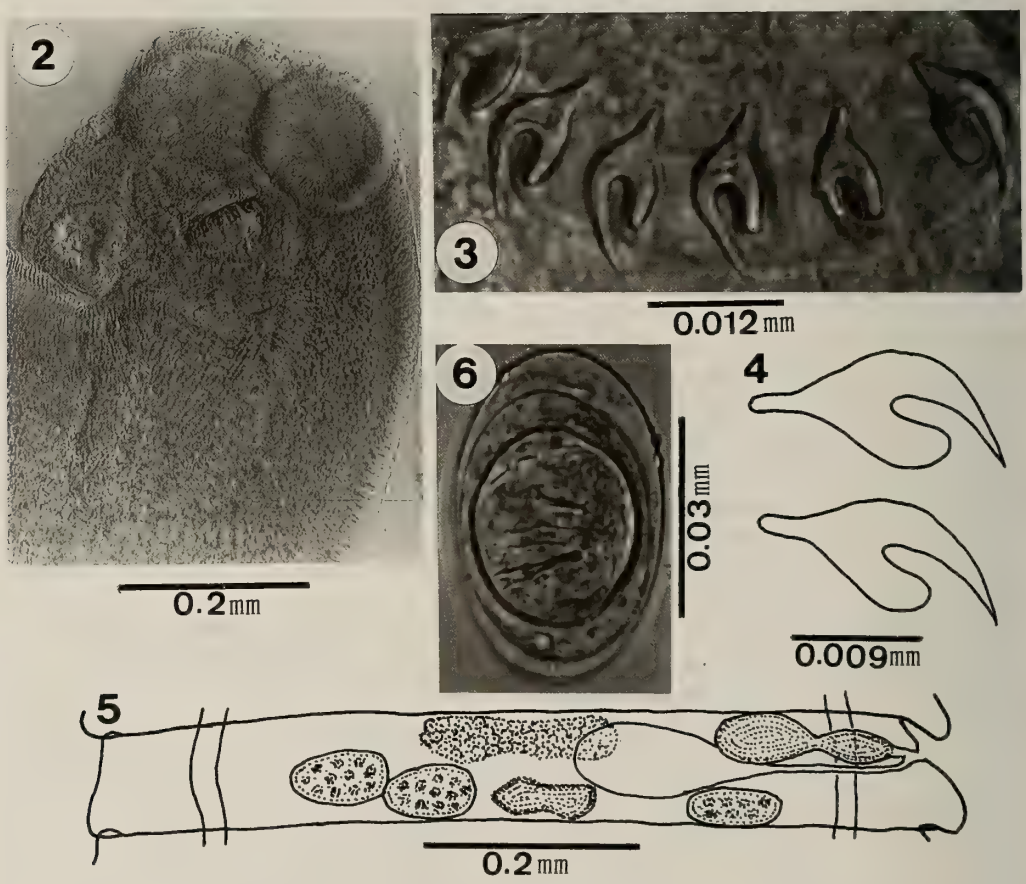

Figs. 2–6. *Staphylocystis* (*Staphylocystis*) *kathmanduensis* sp. nov. 6: Egg.
2: Scolex. 3: Rostellar hooks. 4: Rostellar hooks magnified. 5: Mature segment drawn from a projected microphotographic negative, dorsal view. 6: Egg.

0.235 in length by 0.290–0.456 in width. Rostellum pyriform, 0.056 long by 0.070 wide, armed with a single row of 13 thorn-shaped hooks 0.018 long. Hook handle short; guard bluntly round at its end, shorter than blade; blade slender, sharp at its end, curved toward guard. Rostellar sac slightly elongated, 0.161–0.189 long by 0.119–0.126 wide, extending past posterior margin of suckers. Suckers discoid, 0.111 in diameter.

Genital pores unilateral, situated a little anterior to middle of segment margin. Testes three in number, oval, 0.070–0.084 long by 0.028–0.035 wide, arranged in a transverse row, one poral and two aporal. Cirrus sac pryiform, 0.105–0.126 long by 0.035–0.042 wide, extending beyond longitudinal excretory canals. Internal seminal vesicle 0.049–0.056 long by 0.028–0.035 wide, occupying almost whole of cirrus sac. External seminal vesicle 0.070 long by 0.021–0.028 wide. Ovary transversely elongate, bilobate, 0.105–0.140 wide. Seminal receptacle large, dorsal to ovary, 0.112–0.140 long by 0.035–0.042 wide. Vitelline gland bilobate, 0.049–0.070 long by 0.028–0.035 wide. Eggs elliptical, 0.049–0.053 in major axis and 0.032 in minor axis. Embryophore 0.032 by 0.028. Onchospheres spherical, 0.028 in diameter; embryonic hooks 0.014 long.

Host: *Suncus murinus* (Insectivora: Soricidae).

Habitat: Small intestine.

Locality and date: Kathmandu, Nepal; March 31, 1991.

Type specimens: Holotype, Nara Sangyo Univ. Lab. Coll. No. 9300; paratypes, 9301–9302.

Remarks: About 22 species of *Staphylocystis* (*Staphylocystis*) have been recorded from the Soricidae [9, 10, 12, 13]. Of these, the species armed with 10–15 rostellar hooks ranging in length from 0.015 to 0.021 are: *S.* (*S.*) *minutissima* (Meggitt, 1927) Yamaguti, 1959 [4]; *S.* (*S.*) *pauciproglottis* (Neiland, 1953) Yamaguti, 1959 [6]; *S.* (*S.*) *suncusensis* Olsen et Kuntz, 1978 [8]; *S.* (*S.*) *curiosihamata* Sawada et Koyasu, 1990 [10]; *S.* (*S.*) *naganoensis* Sawada et Koyasu, 1990 [10]; and *S.* (*S.*) *delicata* Sawada et Koyasu, 1991 [12]. The present new species most closely resembles *S.* (*S.*) *delicata* in the shape of the rostellar hooks. However, the species is distinguished from *S.* (*S.*) *delicata* by the larger number (13 against 10) and longer size (0.018 against 0.014) of the rostellar hooks, and the larger rostellum (0.056 by 0.070 against 0.028 by 0.035).

Staphylocystis (*Staphylocystis*) *trisuliensis* sp. nov. (Fig. 7–12)

On March 20 and 21, 1991, three house shrews, *Suncus murinus*, were captured at Trisuli. All of them were found infected with one or two mature cestodes.

Description (based on four specimens): Small-sized hymenolepidid; mature worm 9.2–10.3 long by 0.8–0.9 wide. Mature segment serrate and wider than long. Scolex 0.140–0.175 long by 0.266–0.280 wide, sharply demarcated from neck. Rostellum oval, 0.056–0.070 long by 0.070–0.091 wide, armed with a single row of 21–22 chelate-shaped hooks 0.018 long. Hook handle comparatively long; blade long, slender and pointed; guard shorter than blade and thick. Rostellar sac oval, 0.126–0.161 long by 0.070–0.140 wide. Suckers discoid, 0.119–0.026 in diameter.

Genital pores unilateral, located a little anterior to middle of segment margin. Testes three in number, oval, 0.098–0.105 long by 0.035–0.049 wide, arranged in a transverse row, one poral and two aporal. Cirrus sac pyriform, 0.126–0.140 long by 0.042 wide, extending beyond longitudinal excretory canals. Internal seminal vesicle 0.091–0.105 long by 0.035–0.042 wide, occupying almost whole of cirrus sac. External seminal vesicle 0.105–0.126 long by 0.042–0.049 wide. Ovary transversely elongated, bilobate, 0.154–0.175 wide. Voluminous seminal receptacle measuring 0.119–0.140 long by 0.070–0.098 wide. Vitelline gland irregularly lobate, situated in posterior field of segment, 0.070–0.091 long by 0.035–0.042 wide. Eggs elliptical, 0.039–0.042 in major axis and 0.028–0.032 in minor axis, with at each pole a round projection provided with polar filaments. Onchospheres spherical, 0.025 in diameter; embryonic hooks 0.011–0.014 long.

Host: *Suncus murinus* (Insectivora; Soricidae).

Habitat: Small intestine.

Locality and date: Trisuli, Nepal; March 20 and 21, 1991.

Type specimens: Holotype, Nara Sangyo Univ.

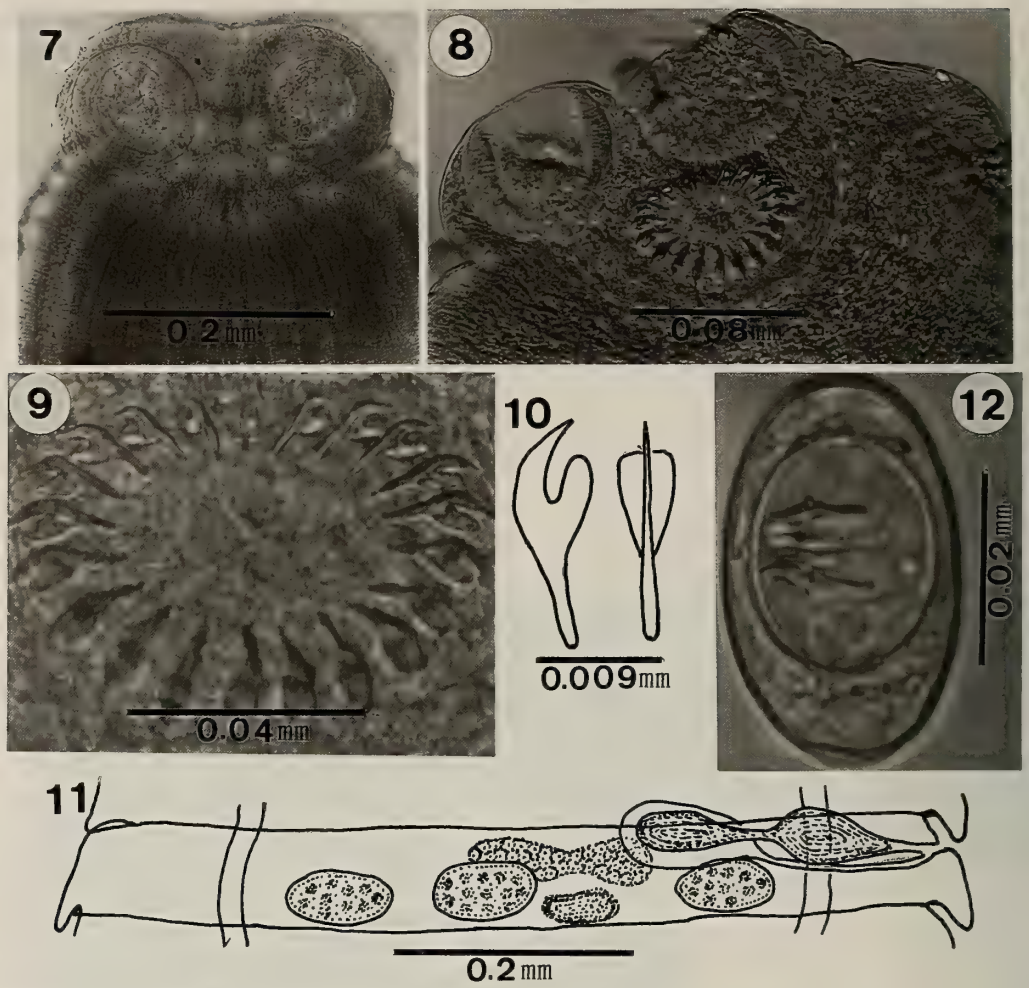

Figs. 7–12. *Staphylocystis* (*Staphylocystis*) *trisuliensis* sp. nov.
7: Scolex 8: Scolex magnified. 9: Rostellar hooks. 10: Rostellar hooks magnified. 11: Mature segment drawn from a projective microphotographic negative, dorsal view. 12: Egg.

Table 1. A comparison of related species of *Staphylocystis* (*Staphylocystis*) armed with 18–24 rostellar hooks ranging in length from 0.020 to 0.029 mm from the Insectivora

Species	Rostellar hooks		Host
	number	length (mm)	
1. *S.* (*S.*) *chrysochloridis* [2]	16–18	0.029	*Chrysochloria capensis* *Ch. aurea*
2. *S.* (*S.*) *furcata* [14]	22–28	0.026–0.028	*Sorex araneus* *Suncus murinus* *Neomys fodiens*
3. *S.* (*S.*) *dsinezumi* [10]	23	0.020	*Crocidura dsinezumi*
4. *S.* (*S.*) *sindensis* [5]	20	0.022–0.023	*Suncus murinus sindensis*

Lab. Coll. No. 9303; paratypes, 9304–9309.

Remarks: Out of the 22 known species of *Staphylocystis* (*Staphylocystis*) from the Soricidae [9, 10, 12, 13], four; *S.* (*S.*) *chrysocholoridis* (Janicki, 1904) Spassky, 1950 [2], *S.* (*S.*) *furcata* (Stieda, 1862) Spassky, 1950 [14], *S.* (*S.*) *sindensis* Nama, 1976 [5] and *S.* (*S.*) *dsinezumi* Sawada et Koyasu, 1990 [10] are armed with 18–24 rostellar

TABLE 2. *Suncus* spp. and their cestode parasites in Asia ([1, 7, 13], the present study)

Locality	*Suncus* spp.	Cestode parasites
Japan		
Kyushu	*Suncus murinus temmincki*	*
Okinawa	〃	*Vampirolepis jakounezumi* Sawada et Hasegawa, 1991
		V. okinawaensis Sawada et Hasegawa, 1991
		V. grascilistrobila Sawada et Harada, 1989
		Staphylocystis (*Staphylocystis*) *suncusensis* Olsen et Kuntz, 1978
		Rodentolepis sp. Uchikawa, Sakumoto et Kinjo, 1981
Taiwan		
Taoyuan Hsien	*S. murinus swinhoei*	*V. sunci* Sawada et Harada, 1989
		V. gracilistrobila Sawada et Harada, 1989
		V. sessilihamata Sawada et Harada, 1989
Nantou Hsien	〃	*S.* (*S.*) *suncusensis* Olsen et Kuntz, 1978
Ping Toung County	〃	*S.* (*S.*) *delicata* Sawada et Koyasu, 1991
		S. (*S.*) *furcata* (Stieda, 1862) Spassky, 1950
		V. microscolex Sawada et Koyasu, 1991
China		
Southern China	*S. murinus*	*
Hainan Dao	〃	*
Vietnam		
Saigon-Cholon	*S. murinus*	*
Nha Trang	〃	*
Con Son Island	〃	*
Bangladesh		
Mymensingh	*S. murinus*	*
Thailand		
Chanthaburi	*S. murinus*	*V. nana* (Siebold, 1852) Spassky, 1954
		Raillietina (*Raillietina*) *madagascariensis* (Davaine, 1869) Fuhrmann, 1920
Pakistan		Syn. *R.* (*R.*) *siriraji* Chandler et Pradatsundarasar, 1957
	S. murinus tytleri	*
	S. murinus sindensis	*V. jacobsoni* (Linstow, 1907) Schmidt, 1986
Karachi	〃	*Hymenolepis mujibi* Bilqees et Malik, 1974
	S. etruscus	*
	S. stoliczkanus	*
Myanmer		
Rangoon	*S. murinus*	*S.* (*S.*) *minutissima* (Meggitt, 1927) Yamaguti, 1959
		S. (*S.*) *furcata* (Stieda, 1862) Spassky, 1954
		S. (*S.*) *solitaria* (Meggitt, 1927) Yamaguti, 1959

Afghanistan		
Jalalabad, Laghman	*S. murinus*	*V. jacobsoni* (Linstow, 1907) Schmidt, 1986
		Hymenolepis sunci Vaucher et Tenora, 1971
Singapore		
	S. murinus	*
	S. etruscus malayanus	*
Malaysia		
Sabah Province	*S. murinus*	*
Sarawak	*S. hosei*	*
Indonesia		
Kalimantan	*S. etruscus*	*
	S. ater	*
	S. murinus	*
Java Island	*S. murinus*	*V. jacobsoni* (Linstow, 1907) Schmidt, 1986
Flores Island	*S. mertensi*	*
India		
Sanchore	*S. murinus sindensis*	*S.* (*S.*) *sanchorensis* Nama et Kichi, 1975
Jadhpur	*S. murinus sindensis*	*S.* (*S.*) *sindensis* Nama, 1979
		V. bhali (Singh, 1958) Schmidt, 1986
Allahabad	*S. murinus*	*V. molus* Srivastava et Capoor, 1979
		V. allahabadensis Srivastava et Pandey, 1982
	S. murinus	*S.* (*S.*) *indicus* Nanda et Malhotra, 1990
Bombay	*S. murinus*	*V. jacobsoni* (Linstow, 1907) Schmidt, 1986
Khrhja	〃	*Pseudhymenolepis guptai* Gupta et Singh, 1987
Lucknow	*S. striatus*	*Pseudhymenolepis suncusi* Gupta et Sinha, 1984
South India	*S. dayi*	*
	S. stoliczkanus	*
Sri Lanka		
Horton Plains	*S. murinus montanus*	*V. montana* Crusz et Sanmugasunderam, 1971
		Pseudhymenolepis eisenbergi Crusz et Sanmugasunderam, 1971
	S. etruscus	*
Nepal		
Kathmandu	*S. murinus*	*Pseudhymenolepis nepalensis* Sawada et Koyasu, 1991
		S. (*S.*) *kathmanduensis* sp. nov.
	S. etruscus	*
Adhabar	*S. stoliczkanus*	*
Trisuli	*S. murinus*	*S.* (*S.*) *trisuliensis* sp. nov.
Philippines		
Palawan Island	*S. murinus*	*
	S. occultidenus	*
	S. palawanensis	*
Luzon Island	*S. luzoniensis*	*
Northern Marianas		
Guam Island	*S. murinus*	*

* Unknown

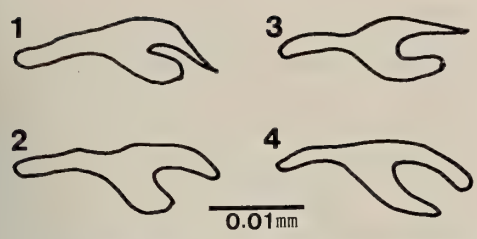

FIG. 13. Comparison of rostellar hook in shape among four related species.
1: *S.* (*S.*) *chrysochloridis* [2] 2: *S.* (*S.*) *furcata* [14] 3: *S.* (*S.*) *dsinezumi* [10] 4: *S.* (*S.*) *sindensis* [5]

hooks ranging in length from 0.015 to 0.025 (Table 1). The present new species most closely resembles *S.* (*S.*) *dsinezumi* in the number and length of the rostellar hooks. However, the shape of the rostellar hooks separates this new species from *S.* (*S.*) *dsinezumi* (Fig. 13).

DISCUSSION

There are quite a number of different cestodes infecting *Suncus murinus* in Asia (Table 2) ([1, 7, 13], the present study). The following is thought to be one of the reasons. Because the behavior patterns of predation displayed by *Suncus murinus* are similar to those of commensal mammals, *Rattus norvegicus* and *Mus musculus* [1, 3], their eating habits are thought to overlap with each other resulting probably in a diversity in the intermediate hosts of the cestodes infecting it. So, varying with the area where *Suncus murinus* lives, the species of cestodes infecting it differ as much.

Even though the areas of Kathmaudu and Trisuli are separated by less than 30 km, the species of tapeworms differ. *Suncus murinus* cannot take low temperature (below 0°C) and the winter in Kathmandu (1350 m) is extremely harsh. The harsh coldness of winter causes their population crash, thus greatly decreasing the number of individuals which can, after surviving the cold season, bear offspring. Nonetheless, when May comes round, they come to appear in various places. This fact suggests, in order to recover the population crash, they represent annually a presence of dramatic fluctuation among the individuals which have survived the winter season. Between the Indian Plains and Kathmandu, and Kathumandu and Trisuli there are ranges of 2000 m plus mountains, so it cannot be presumed that *Suncus murinus* migrates between the three areas (Fig. 14), but in the past there have been numerous cases in which *Suncus murinus* was introduced to each of the areas, so many hereditary changes can be recognized. Evidence for this can be seen in the fact that *Pseudhymenolepis nepalensis* Sawada et Koyasu, 1990 were found infecting *Suncus murinus* in Kathmandu but not those in Trisuli.

Suncus murinus can be found in Kathmandu and Trisuli, wherever there are human dwelling and people often feed them. Looking at this type of

FIG. 14. Topographical map showing the heights above sea level of Kathmandu and Trisuli.

environment, over many years *Suncus murinus* of both areas have formed characteristic population, and since the type of intermediate hosts for cestodes in both areas is fixed, it can be seen that species of cestodes infecting *Suncus murinus* in the two areas differ from each other.

ACKNOWLEDGMENTS

We hereby wish to acknowledge our indebtedness to Mr. A. M. Vaidya, Pension SAKURA, Kathmandu, Nepal, for kind help in collecting shrews.

REFERENCES

1 Corbet GB, Hill JE (1991) A world list of mammalian species. 3rd Nat Hist Mus Publ and Oxford Univ Pres, London and Oxford, pp 243

2 Janicki C (1904) Zur Kenntnis einiger Säugetiercestoden. Zool Anz 27: 770–782

3 Marshall JD, Quy DV, Gibson FL, Dung TC, Cavanaugh DC (1967) Ecology of plague in Vietnam. 1. Role of *Suncus murinus*. Proc Soc Exp Biol 124: 1083–1086

4 Meggitt FJ (1927) On cestodes collected in Burma. Parasitology 19: 141–153

5 Nama HS (1976) On a new species of *Staphylocystis* Villot, 1877 (Cestoda: Hymenolepididae) from *Sunucus murinus sindensis*. Acta Prasitol Pol 24: 19–22

6 Neiland KA (1953) Helminths of Northwestern mammals. Part V Observations on cestodes of shrews with the descriptions of new species of *Liga* Weinland, 1857, and *Hymenolepis* Weinland, 1858. J Parasitol 39: 487–494

7 Ohbayashi M (1985) Helminth parasites of the Soricidae. In "*SUNCUS MURINUS*". Ed by S Oda J Kitoh, K Ohta, G. Isomura Jpn Sci Soc Press, Tokyo, pp 88–93

8 Olsen OW, Kuntz RE (1978) *Staphylocystis* (*Staphylocystis*) *suncusensis* sp. n. (Cestoda: Hymenolepididae) from the musk shrew, *Suncus murinus* (Soricidae) from Taiwan, with a key to the known species of *Staphylocystis* Villot, 1877. Proc Helminthol Soc Wash 45: 182–189

9 Sawada I, Harada M (1990) Cestodes of field micromammalians (Insectivora) from Central Honshu, Japan. Zool Sci 7: 467–475

10 Sawada I, Koyasu K (1990) Further studies on cestodes from Japanese shrews. Bull Nara Sangyo Univ 6: 187–202

11 Sawada I, Koyasu K (1991) *Pseudhymenolepis nepalensis* sp. nov. (Cestoda: Hymenolepididae) parasitic on the house shrew, *Suncus murinus* (Soricidae), from Nepal. Zool Sci 8: 575–578

12 Sawada I, Koyasu K (1991) Further studies on cestode parasites of Taiwanese shrews. Bull Nara Sangyo Univ 7: 131–142

13 Schmidt GD (1986) Handbook of tapeworm identification. CRC Press, Inc., Florida, pp 675

14 Stieda L (1862) Ein Beitrag zur Kenntnis der Taenien. Arch Naturg 28: 208–209

ZOOLOGICAL SCIENCE 10: 155–159 (1993)

Two New Species of *Sabacon* from Sichuan Province, China (Arachnida: Opiliones: Sabaconidae)

Nobuo Tsurusaki[1] and Daxiang Song[2]

[1]*Department of Biology, Faculty of Education, Tottori University, Tottori, 680 Japan, and* [2]*Institute of Zoology, Academia Sinica, 19 Zhongguancun Lu, Haitien, Beijing, China*

ABSTRACT—Two new species of the genus *Sabacon, S. martensi* n. sp. and *S. gonggashan* n. sp. are described based on the specimens collected from Mt. Gong-ga-shan of the Da-xue-shan Mountains, Sichuan Province, southern China. The two species are similar to each other and to some species of the genus from Nepal-Himalayas (*S. chomolongmae, S. dhaulagiri,* and *S. unicornis*) and Japan (*S. dentipalpe* and *S. imamurai*) in having dorsolateral spurs on the fixed fingers of male chelicerae.

INTRODUCTION

The genus *Sabacon* (Sabaconidae, Ischyropsalidoidea, Palpatores) is a group of soil harvestmen, with about 40 species, and is disjunctively found in the Holarctic regions. The distribution covers the eastern (2 spp.) and western areas (5 plus some spp.) of North America (7 described spp. in total [5, 1], Cokendolpher pers. comm., 1992), southern part of Europe (6 spp. [3]), the Nepal-Himalayas (7 spp. [2]), Siberia (2 spp. [4]), and East Asia including Japan (10 spp. [6, 7]). From China, however, only one species, *Sabacon okadai* Suzuki, has been recorded [6].

During an examination of the opilionids collected from the Da-xue-shan Mountains, Sichuan Province, southern China, we found two undescribed species of the genus. Descriptions of the species will be presented here.

All the specimens examined are deposited in the collection of the Institute of Zoology, Academia Sinica, Beijing.

Genus *Sabacon* Simon, 1879

***Sabacon martensi* n. sp.**

(Figs. 1–2)

Material. Male holotype, West slope of Mt. Gong-ga-shan, Kangding, Sichuan Province, China, 2 September 1982, Zhang Xue-zhong leg.

Measurements (in mm). Male holotype: cephalothorax, 0.96 long, total body length 2.3.

Length of palp and legs: Palp (femur/patella/tibia/tarsus; total): 0.88/0.98/1.10/0.50; 3.46. Legs (femur/patella/tibia/metatarsus/tarsus; total): Leg I: 1.75/0.79/1.78/2.40/2.40; 9.12. Leg II: 2.57/0.99/2.80/3.76/4.10; 14.22. Leg III: 1.68/0.78/1.60/2.73/2.80; 9.59. Leg IV: 2.32/0.94/2.24/3.60/3.72; 12.82.

Male. Body (Fig. 1A-B) relatively small, poorly sclerotized. Eye tubercle low, slightly canaliculate, unarmed. Second thoracic tergite with pair of postocular spines. Abdominal tergites represented by small, weakly sclerotized plates (scutum laminatum/dissectum) with few scattered setae. Abdominal sternites poorly sclerotized, with minute black setae. Chelicera (Fig. 1C-E) with basal article flat, dorsally not elevated; fixed finger dorsolateraly with a conspicuous black spur, ventrally with a small knob. Palp (Fig. 1F) relatively slender, patella distally with row of six ventromesal teeth.

Penis (Fig. 2) 2.13 mm long (including glans), 0.16 mm wide at base; pigmented, laterally with a row of several denticles on each side.

Coloration: Venter brownish white, with coxae, abdominal sclerites pale brown; dorsum brownish white with tergites and cephalothorax brown. Eye tubercle dark brown. Chelicerae, palps and legs

Accepted October 15, 1992
Received September 17, 1992

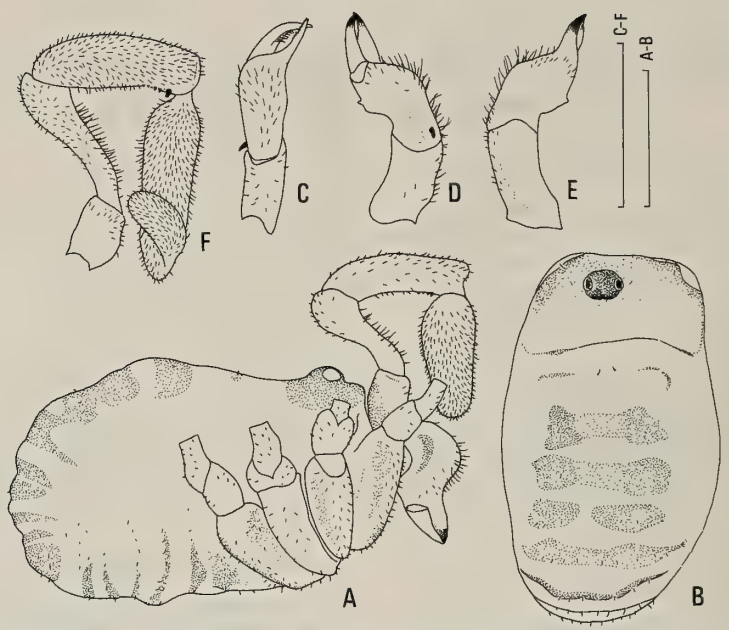

FIG. 1. *Sabacon martensi* n. sp., holotype male. A-B: Lateral (A) and dorsal (B) views of body. C-E: Dorsal (C), ectal (D), and mesal (E) views of left chelicera. F: Mesal view of left palp. Scales=1 mm.

light brown.

Female. Unknown.

Distribution: Known only from the type locality.

Etymology. The specific epithet is given in honor of Prof. Jochen Martens, Mainz, Germany, for his eminent contributions to the systematics of *Sabacon* species.

Remarks. This species has affinities with some species of the genus from the Nepal-Himalayas and Japan (*S. chomolongmae, S. dhaulagiri,* and *S. dentipalpe,* etc.). These species share a dorsolateral spur on both chelicerae and a similar morphology in the penes. The new species, however, can be easily distinguished from any other described species of the genus, by its penis having a row of denticles on both lateral margins of the shaft.

FIG. 2. *Sabacon martensi* n. sp., holotype male. A-B: Ventral and lateral views of penis. C-E: Ventral (C), lateral (D), and dorsal (E) views of distal part of penis. Scales=1 mm for A-B, 0.5 mm for C-E.

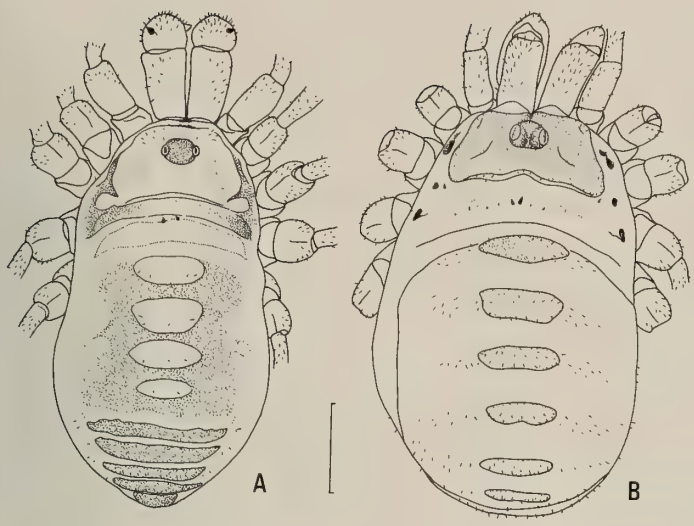

FIG. 3. *Sabacon gonggashan* n. sp. Dorsal view of body. A, holotype male; B, paratype female. Scale=1 mm.

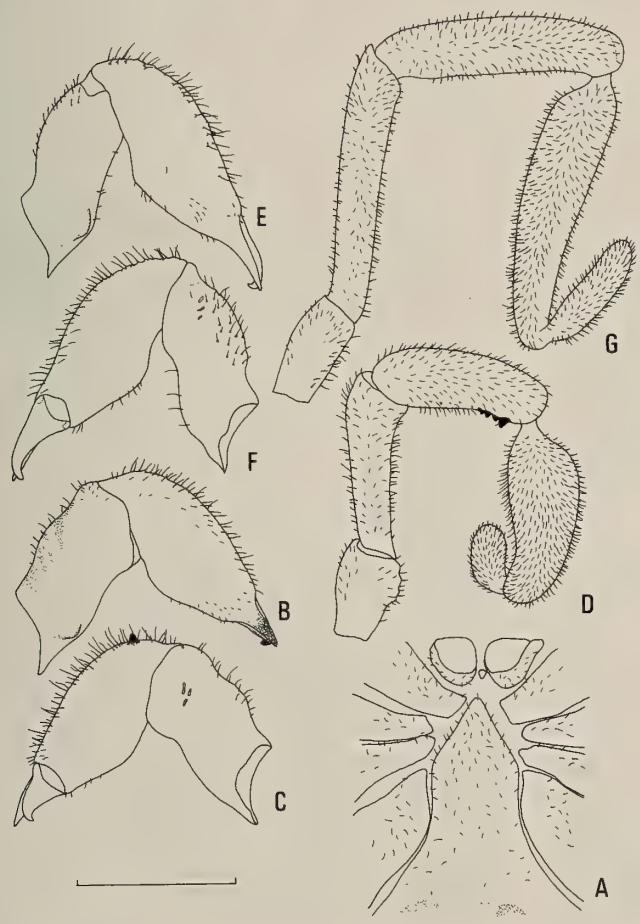

FIG. 4. *Sabacon gonggashan* n. sp. A, Anterior ventral surface of male (holotype) body. B-C: Mesal (B) and ectal (C) views of male left chelicera. D, Mesal view of male left palp. E-F: Mesal (E) and ectal (F) views of female (paratype) chelicera. G, Mesal view of female left palp. Scale=1 mm.

***Sabacon gonggashan* n. sp.**

(Figs. 3–5)

Material. Male holotype, male paratype and two female paratypes, West slope of Mt. Gong-ga-shan, Kangding, Sichuan Province, China, 2 September 1982, Zhang Xue-zhong leg.

Measurements (in mm). Male holotype (one of the female paratypes in parentheses): cephalothorax 1.50 (1.60) long, 2.1 (2.67) wide; abdomen 2.18 (2.82) wide; total body length 4.32 (4.56).

Length of palp and legs: Palp (Fe/Pa/Ti/Ta; total): 1.05/1.06/1.12/0.56; 3.79 (1.52/1.45/1.74/ 0.75; 5.46). Legs (Fe/Pa/Ti/Mt/Ta; total): Leg I: 1.83/0.89/1.66/2.46/2.41; 9.25 (legs I to III of the paratype female measured are absent). Leg II: 2.16/1.00/2.20/3.08/3.88; 12.32. Leg III: 1.80/ 0.80/1.56/ 2.72/2.72; 9.6. Leg IV: 2.40/1.01/ 1.95/3.54/3.90; 12.8 (2.52/0.95/2.16/3.70/ 3.22; 12.55).

Male. Body (Fig. 3A) poorly sclerotized. Eye tubercle low, slightly canaliculate above, unarmed. Second thoracic tergite with pair of postocular spines. Abdominal tergites slightly sclerotized, with few scattered setae, disposed in a manner "scutum laminatum". Abdominal sternites weakly sclerotized, with few scattered setae. Genital operculum pointed anteriorly, set with numerous black setae (Fig. 4A). Chelicera (Figs. 4B-C) with three slit sensilla on ectal surface of basal segment; with a black cone-shaped spur on apico-ectal surface of fixed finger. Palp (Fig. 4D) relatively slender; patella with five large ventromesal teeth followed by a few small denticles. Legs short, with fine setae.

Penis (Fig. 5A-D) 2.87 mm long, simple and slender, laterally with a pair of setae near the apical end of the shaft.

Coloration: Cephalothorax yellowish brown, marked blackish brown near margins, eye tubercle brown, abdominal tergites light brown. Venter yellowish white, lightly mottled brown.

Female. Similar to male but with tergites represented by small median sclerites (Fig. 3B). Chelicera without an apico-ectal spur on fixed finger (Fig. 4E-F). Palp (Fig. 4G) slender, without ventral denticles on patella. Ovipositor (Fig. 5E), 2.09 mm long, elongate, scattered with numerous short setae. Coloration as in male, but with tergites brown.

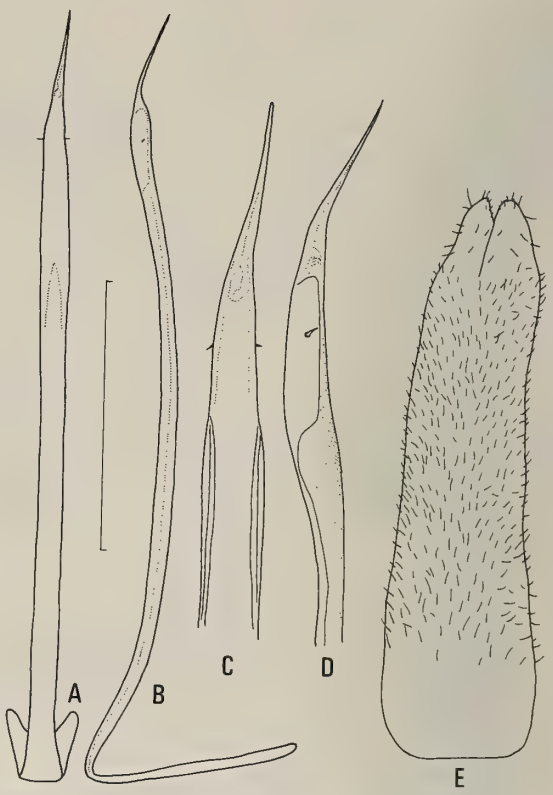

FIG. 5. *Sabacon gonggashan* n. sp. Ventral (A) and lateral (B) views of penis (holotype male). C-D: Ventral and lateral views of distal part of the penis. E, Ventral view of ovipositor (paratype female). Scale = 1 mm for A-B, E, and 0.5 mm for C-D.

Distribution. Known only from the type locality.

Etymology. The specific epithet is a noun in apposition.

Remarks. This species is characterized by its simple and elongate penis. The presence of apico-ectal spurs on the fixed fingers of male chelicerae suggests its close affinity with *S. martensi* from the same mountain; some Nepal-Himalayan congeners, such as *Sabacon chomolongmae, S. dhaulagiri, S. unicornis* [2]; and some Japanese counterparts belonging to the *dentipalpe*-group [7] like *S. dentipalpe* and *S. imamurai*. Phylogenetic proximity to the *dentipalpe*-group, a group which was recognized by Suzuki [7] within Japanese species of *Sabacon*, is also inferred from its elongate oviposi-

tor with numerous setae.Although the present species, as well as *S. martensi,* were found on the west slope of Mt. Gong-ga-shan, it is uncertain if the two species are sympatric.

ACKNOWLEDGMENT

We are grateful to Mr. James C. Cokendolpher, Lubbock, Texas, for his review of the draft.

REFERENCES

1 Cokendolpher JC (1984) A new species of *Sabacon* Simon from Oregon (Arachnida: Opiliones: Sabaconidae). Can J Zool 62: 989–991.

2 Martens J (1972) Opiliones aus dem Nepal-Himalaya, I. Das Genus *Sabacon* Simon (Arachnida: Ischyropsalididae). Senckenbergiana biol 53: 307–323.

3 Martens J (1983) Europäische Arten der Gattung *Sabacon* Simon 1879 (Arachnida: Opiliones: Sabaconidae). Senckenbergiana biol 63: 265–296.

4 Martens J (1989) Sibirische Arten der Gattung *Sabacon* Simon 1879 (Arachnida: Opiliones: Sabaconidae). Senckenbergiana biol 69: 369–377.

5 Shear WA (1975) The opilionid genera *Sabacon* and *Tomicomerus* in America (Opiliones, Troguloidea, Ischyropsalidae). J Arachnol 3: 5–29.

6 Suzuki S (1941) Opiliones from Manchoukuo and North China, with a description of the interesting genus *Sabacon* (Ischyropsalidae). (In Japanese with English description and summary). Bull Biogeogr Soc Jpn 11: 15–22.

7 Suzuki S (1974) The Japanese species of the genus *Sabacon* (Arachnida, Opiliones, Ischyropsalididae). J Sci Hiroshima Univ (B-1) 25: 83–108.

ZOOLOGICAL SCIENCE 10: 161–167 (1993)

Genetic Evidence for the Presence of Distinct Fresh-water Prawn (*Macrobrachium nipponense*) Populations in a Single River System

Kazuo Mashiko[1] and Ken-ichi Numachi[2]

[1]*Biological Laboratory, Teikyo University, Hachioji, Tokyo 192-03, and*
[2]*Ocean Research Institute, University of Tokyo, Minamidai, Nakano-ku, Tokyo 164, Japan*

ABSTRACT—Genetic difference between two groups of individuals in the freshwater prawn *Macrobrachium nipponense,* which exhibit characteristically different egg sizes within a single river system, was examined electrophoretically and morphologically. Out of 16 prospective loci, *PGM* and *MPI-1* were polymorphic and allelic frequencies were significantly different between the two groups in both loci. In addition, rostral tooth count (number of spines on the dorsal margin of rostrum), which is regarded to be genetically controlled on the basis of crossing experiments, varied significantly between the two groups. These facts indicate that the two groups of individuals have genetically differentiated.

INTRODUCTION

A previous study on the freshwater prawn *Macrobrachium nipponense* (de Haan) [14] revealed that egg size remarkably varied from one local population to another, with an apparent relationship between egg size and the hydrogeographic feature of the habitats. Relatively large eggs (approximately 0.10 mm^3 per egg) were associated with freshwater lakes and rivers, small eggs (0.05 mm^3) with estuaries, and intermediate-sized eggs with brackish-water lagoons. Such populations with different-sized eggs were occasionally found even within a single water system, for instance, the Sagami River in central Japan where individuals with large and small eggs were found in the upper basin of the river and in the estuary, respectively [12]. Crossing experiments between these two groups of individuals, where the size of eggs produced by F_1 hybrids was intermediate between those of the parents, suggested that the different egg sizes among local populations of this species are controlled as a quantitative genetic trait [15]. The two groups were also different in larval physiological characteristics [13]. These facts all imply that *M. nipponense* is now differentiating into distinct local populations through modification of some life-history traits.

In the present study, the genetic difference between the two groups of *M. nipponense* in the Sagami River was further confirmed by means of both biochemical and morphological analyses. Electrophoretically different forms of enzyme with the same metabolic function (isozyme), especially at the same gene loci (allozyme), offer very useful information about population structures and systematics [e.g., 19, 23]. Chow and Fujio [4] have attempted this approach to *M. nipponense,* independently of our study without discriminating egg size, among a few local populations. Similarly, several authors [2, 6, 9, 10, 26] have made electrophoretic analyses among conspecific populations or different species in some taxonomic groups of freshwater prawns and shrimps. However, multiple conspecific populations coexisting in the same water system with different life-history traits was beyond the scope of those foregoing investigations, except the study by Chow *et al.* [5] on an inland-water prawn *Palaemon paucidens.* In the present study, in addition to the electrophoretic analysis, a morphological trait (rostral tooth count) was compared between the two groups of *M. nipponense* in the Sagami River with respect to

Accepted October 15, 1992
Received August 24, 1992

its genetic bases.

MATERIALS AND METHODS

Adults were collected from the estuary (station Banyu) and the upper basin (stations Ogura and Lake Tsukui, approximately 35 and 40 km upstream, respectively, from the river mouth) of the Sagami River during the period 1985–1989. Topography of these collecting sites has been described previously in detail with a map [12].

Samples were kept frozen at below −50°C or kept alive in aquaria until electrophoresis. Approximately 0.4 g of abdominal muscle was minced and homogenized in 0.5 ml distilled water containing 25 μg NADP and centrifuged. The supernatant was absorbed into a filter paper wick and inserted into gel blocks. Horizontal starch-gel electrophoresis was run at the constant current of 4 to 5 mA/cm^2 (approximately 30 V/cm) in a cold chamber. During electrophoresis the gel was cooled with a glass-plate pan containing ice water, which was set on the gel. Usually electrophoreses were stopped when the marker of amid black 10B migrated 5 cm from the origin. The enzymes surveyed, along with their buffer systems, are summarized in Table 1. The MES/TEA buffer system (pH 7.0) was newly developed for separation of MPI by one of us (K.N.), where the gel contained 0.6 mg ATP/ml. After electrophoresis, each gel was sliced horizontally into 1 mm-thick sections and stained. The enzyme was detected according to Numachi [21], excepting ACP, HK, AO, MPI and GAPDH which were detected according to Redfield and Salini [22]. In the staining for PGM, MPI, HK, GPI and PEP, agarose solution (final concentration of 0.9%) containing reactants was overlaid on the gel. The stained starch gels were dried and preserved according to Numachi [20] for later analysis. The agarose gel was dried on a gel bond film.

The number of teeth on the dorsal margin of rostrum (excluding the top spine of the rostrum itself) was counted for the two groups of individuals collected from the estuary (Banyu) and the upper basin (Ogura) of the Sagami River. Besides the field-collected individuals, this trait was examined for F_1 individuals by reciprocal crossings between and within the two groups (hybrid and control, respectively). Those F_1 individuals were raised for about 6 months after hatching under nearly identical laboratory conditions. The procedures to obtain the hybrids and rear them have been described previously in detail [15].

RESULTS

In electrophoresis, a total of 17 genic loci were routinely assayed (Table 1). Among them, *PGM* and *MPI-1* showed polymorphic banding patterns according to the definition of polymorphism that frequency of the most common allele was no greater than 0.95 in at least one locality. *HK-1* also appeared to be polymorphic, but its banding pattern was not always definitely scorable. All other loci were judged to be monomorphic, and the proportion of polymorphic loci was 0.13 (excluding *HK-1*).

Phenotypes and interpreted genotypes in *PGM* and *MPI-1* are shown in Figure 1, where one or two bands appeared in each individual, showing monomeric protein structure in both loci. The allelic variants were alphabetically designated in the order of faster anodal migration. Relative mobility of each allele in comparison to the most common one (1.00) was: *a*, 1.84; *b*, 1.47; *c*, 1.00 in *PGM*, and *a*, 1.09; *b*, 1.04; *c*, 1.00; *d*, 0.95; *e*, 0.91 in *MPI-1*. Allelic frequency was not affected by the sex in either locus.

Table 2 shows the observed and expected genotypic frequencies and allelic frequencies of *PGM* and *MPI-1* in individuals collected from the three stations of the Sagami River. All the genotypes of *PGM* and *MPI-1* were at Hardy-Weinberg equilibrium in each station ($P>0.05$ in all, chi-square test). However, allelic frequencies was significantly different between the small-egg (station Banyu) and the large-egg (stations Ogura and Tsukui) groups of individuals for the alleles *b* and *c* in *PGM* and the allele *a* in *MPI-1* ($P<0.05$ in all of them, chi-square test). This means that the two groups of individuals, one with large-sized and the other with small-sized eggs, consist of distinct gene pools. Between the two groups of individuals laying large eggs at Ogura ad Tsukui, on the other hand, no difference in allelic frequency was

TABLE 1. The enzymes and loci surveyed, and corresponding buffer systems. Numerals suffixed to abbreviated enzyme name represent one of multiple banding zones (loci) assigned in the order of faster anodal migration. The abbreviation of enzyme name is based on Shaklee *et al.* [25]

Enzyme (E.C.Number)	Locus	Buffer
Phosphogluconate dehydrogenase (1.1.1.44)	*PGDH*	TBE*
Glycerol-3-phosphate dehydrogenase (1.1.1.8)	*G3PDH*	ibid
Acid phosphatase (3.1.3.2)	*ACP*	ibid
Valyl-leucine peptidase (3.4.—.—.)	*PEPA*	ibid
Esterase (3.1.1.—)	*EST-3*	ibid
Hexokinase (2.7.1.1)	*HK-1*	TME**
Lactate dehydrogenase (1.1.2.7)	*LDH*	ibid
Isocitrate dehydrogenase (1.1.1.42)	*IDHP-1*	ibid
Aldehyde oxydase (1.2.3.1)	*AO*	ibid
Phosphoglucomutase (5.4.2.2)	*PGM*	CAPM***
Asparate aminotransferase (2.6.1.1)	*AAT-1*	ibid
Malate dehydrogenase (1.1.1.37)	*MDH*	ibid
Malic enzyme (1.1.1.40)	*MEP*	ibid
Superoxide dismutase (1.15.1.1)	*SOD-2*	ibid
Mannose-6-phosphate isomerase (5.3.1.8)	*MPI-1*	MES/TEA****
Glucose-6-phosphate isomerase (5.3.1.9)	*GPI-1*	ibid
Glyceraldehyde-3-phosphate dehydrogenase (1.2.1.12)	*GAPDH*	ibid

* Tris-borate-EDTA, pH 8.7 [11]
** Tris-maleate-EDTA, pH 7.4 [8] modified by Numachi [21]
*** Citrate-N-(3-Aminopropyl) morpholine, pH 6.0 [7] modified by Numachi [21]
**** 2-(N-Morpholino)ethanesulfonic acid (MES) 21.32 g, Triethanolamine 16.96 g/1000 ml D.W. for electrode, and its 1/10 dilution for gel, pH 7.0

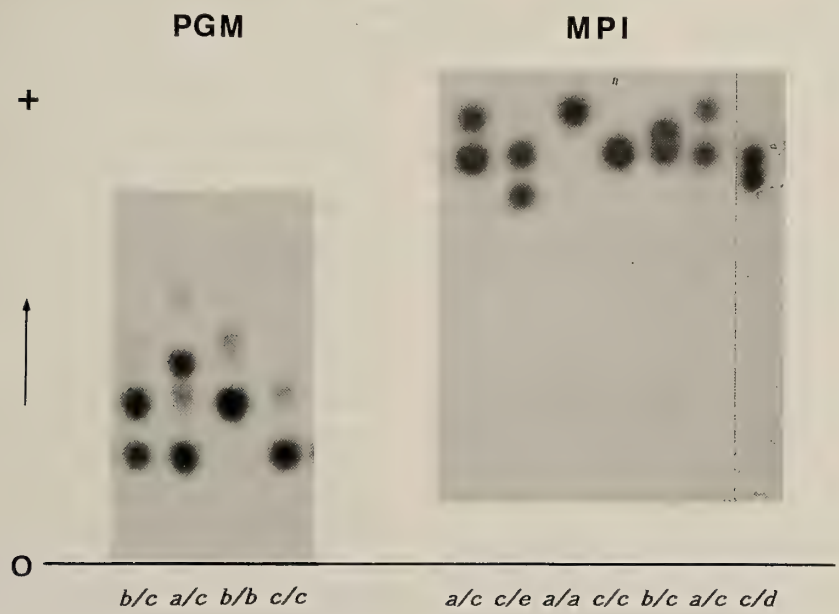

FIG. 1. Banding patterns of Phosphoglucomutase (PGM) and Mannose-6-phosphate isomerase (MPI), with interpreted genotypes for the loci of *PGM* and *MPI-1*. Gels for the reaction of MPI were usually cut off 10 mm toward the anode from the origin.

TABLE 2. Observed *vs.* expected genotypic frequencies and allelic frequencies at the loci of *PGM* and *MPI-1* for small-egg (station Banyu) and the large-egg (stations Ogura and Tsukui) populations of *M. nipponense* in the Sagami River. The expected genotypic frequency is from the Hardy-Weinberg equilibrium. The total number of specimens in each locality is indicated by the symbol n.

Locus	Station		Genotype				Allelic frequency		
			a/c	*b/b*	*b/c*	*c/c*	*a*	*b*	*c*
	Banyu	Obs.	3	19	22	13	0.03	0.53	0.45
	n=57	Exp.	1.3	15.8	26.8	11.4			
PGM	Ogura	Obs.	0	54	16	0	0.0	0.89	0.11
	n=70	Exp.	0.0	54.9	14.1	0.9			
	Tsukui	Obs.	0	32	6	1	0.0	0.90	0.10
	n=39	Exp.	0.0	31.3	7.1	0.4			

			a/c	*b/b*	*b/c*	*c/c*	*c/d*	*c/e*	*a*	*b*	*c*	*d*	*e*
	Banyu	Obs.	14	1	8	33	1	1	0.12	0.09	0.78	0.01	0.01
	n=58	Exp.	10.9	0.5	8.1	35.2	0.9	0.9					
MPI-1	Ogura	Obs.	2	0	13	55	0	5	0.01	0.09	0.87	0.0	0.03
	n=75	Exp.	1.3	0.6	11.6	56.0	0.0	4.0					
	Tsukui	Obs.	1	0	6	32	0	1	0.01	0.08	0.90	0.0	0.01
	n=40	Exp.	0.7	0.5	5.8	32.4	0.0	0.0					

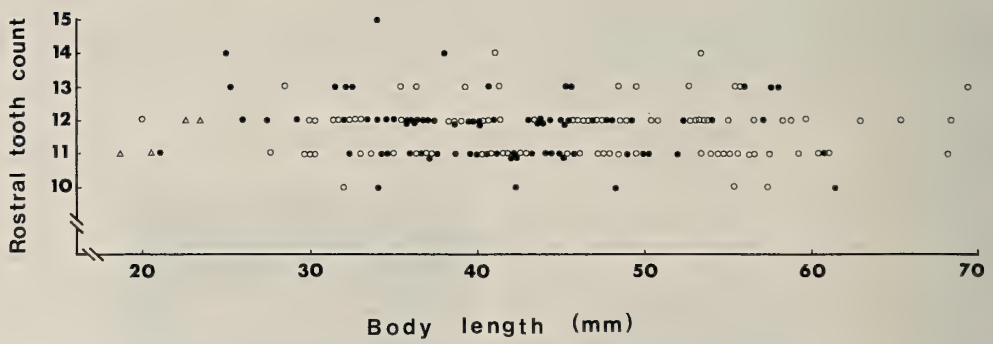

FIG. 2. Rostral tooth counts plotted against body length in individuals collected from station Ogura in the Sagami River. Solid circles, open circles and open triangles indicate males, females and sexually unidentified juveniles, respectively.

observed in both loci. Genetic identity and distance [17] between the large and the small-egg populations of *M. nipponense* in the Sagami River were 0.989 and 0.011, respectively, which were calculated from the results on 16 loci (*HK-1* excluded). The values of average heterozygosity, calculated from actual allelic frequencies, in the large-egg and the small-egg populations were 0.055 and 0.025, respectively.

Prior to analyzing the rostral tooth count, ontogenetic change of this trait was examined using specimens collected from the station of Ogura (Fig. 2). This count fluctuated from 10 to 15 among individuals larger than 20 mm in body length, but was almost independent of the body size of individuals. In the regression equation for this relationship, $Y=12.1-0.0063X$, $r=-0.08$, where X and Y mean the body length (mm) and

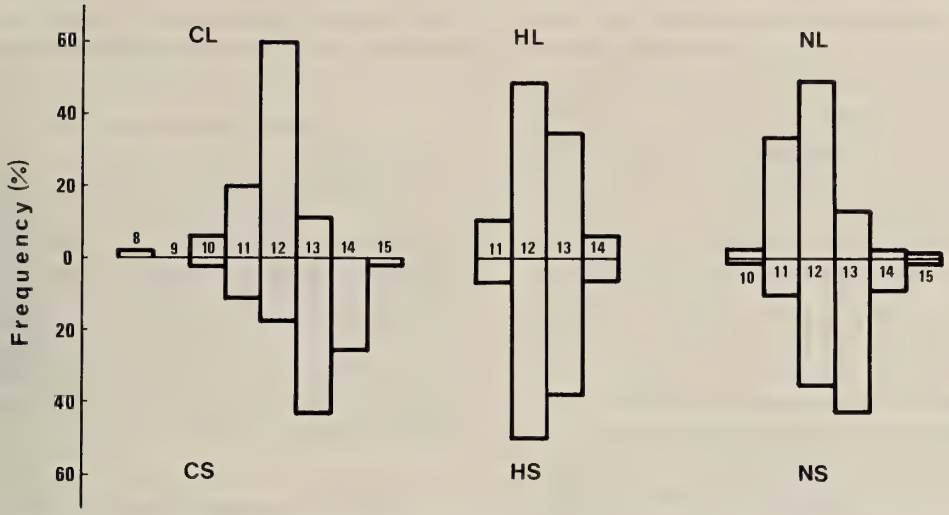

FIG. 3. Frequency distributions of the rostral tooth count in six groups of individuals, NL: natural large-egg population at station Ogura (mean 11.8±SD 0.8, n=93), NS: natural small-egg population at station Banyu (12.6 ±0.9, n=87), HL: F_1 hybrids between females of the large-egg population and males of the small-egg population (12.4±0.8, n=66, HS: F_1 hybrids between females of the small-egg population and males of the large-egg population (12.4±0.7, n=105), CL: control of F_1 individuals by crosses within the large-egg population (11.7± 0.9, n=45), and CS: control of F_1 individuals by crosses within the small-egg population (12.7±1.0, n=46). Numbers on the horizontal axes of histogram represent the ranks of the rostral tooth count.

rostral tooth count, respectively, the slope of −0.0063 did not significantly differ from zero ($P>0.3$, ANCOVA). Moreover, the tooth count did not significantly differ between the two sexes ($P>0.5$, student's *t*-test). Thus, comparison of the mean value of this morphological trait among populations is justified even when the composition of individual body size and sex differ among them.

Figure 3 shows the rostral tooth count in the six groups of individuals, NL: natural large-egg population at Ogura; NS, natural small-egg population at Banyu, HL: F_1 hybrids between females of the large-egg population and males of the small-egg population, HS: F_1 hybrids between females of the small-egg population and males of the large-egg population, and CL and CS: controls of F_1 individuals obtained by crosses within the large-egg and the small-egg populations, respectively. The histogram for F_1 individuals in each type of cross was drawn from the results accumulated for more than three parental females. All individuals examined here were larger than 20 mm in body length. The mean rostral tooth counts for NL and NS, 11.8 and 12.6 (12 and 13 in mode), respectively, were significantly different from each other ($P<0.001$, student's *t*-test). This difference persisted between CL (11.7 in mean and 12 in mode) and CS (12.7 and 13; significant difference in the mean value, $P<0.001$). On the other hand, the mean tooth count was 12.4 (12 in mode) in both hybrids (HL and HS), which was nearly, though not precisely, intermediate between the values of CL and CS, as expected from quantitative inheritance. The differences between HL and CL and between HS and CS were significant ($P<0.001$ and $P<0.05$, respectively). Thus the different rostral tooth counts in the two groups of field-collected individuals (NL and NS) are considered to have a genetic basis as a quantitative trait, like different egg sizes as mentioned at the beginning.

DISCUSSION

Both allozymic and morphological data indicate that the two groups of *M. nipponense* occurring in the Sagami River are genetically different, and these two groups of individuals appear to be more

or less reproductively isolated within the single river system. The reproductive isolation between them has been also suggested from another fact that, while experimentally crossed F_1 hybrids lay intermediate-sized eggs between parental populations, no female carrying such intermediate-sized eggs has been found in the field [15]. Since the two groups of individuals easily intercrossed in the laboratory, and since viability and fertility do not decline significantly in F_1 hybrids [15], any post-mating isolation factor does not seem to work effectively between them. It is likely that, while individuals of this species are apt to move downstream especially during planktonic larval stage, spatial separation of habitats at the estuary and at the upper basin of river plays an important role of the reproductive barrier between the two groups of *M. nipponense* in the Sagami River. However, the detailed mechanism of this reproductive isolation remains to be solved in the future.

It is generally recognized that in natural heterogenous environments a single species consists of genetically diversified local populations or races, fundamentally due to the depression of free gene flow among them [e.g., 1, 24]. For such local populations, Nei's genetic distance is calculated to be, very roughly speaking, no greater than 0.05 in many organisms [18]. This holds also in inland-water prawns and shrimps [e.g., 3, 6, 26]. According to this criterion, the degree of differentiation between the two groups of *M. nipponense* in the Sagami River (genetic distance 0.011) is considered to be within the level of local populations. This suggests that, though the two groups of *M. nipponense* remarkably differ in some life-historical and morphological traits, they have differentiated rather recently. It was presumed previously that the divergence of this species from the presumptive original population with small eggs to those with large and intermediate-sized eggs took place within recent, at most, several thousand years [16]. This consideration comes from the established geological recognition that most of the coastal lagoons in Japan (sea-relict lakes), where the populations with large and intermediate-sized eggs were specifically found [14], were originally formed by alluvial actions after the most recent (Jōmon-period) marine transgression of the Holocene. The electrophoretic data in the present study well coincide with the previous view.

ACKNOWLEDGMENTS

We are grateful to Drs. K. Tatsukawa and T. Kobayashi and other members of the Ocean Research Institute, University of Tokyo for their kind assistance, and also to Prof. M. Peters of Teikyo University for reading the manuscript and improving the English. This work was supported in part by Grants-in-Aid for Scientific Research (Nos. 59740328 and 6074036) to K. M. from the Ministry of Education, Sciences and Culture of Japan, and in part by funds (Cooperative Programs Nos. 89008, 90112 and 9111) provided by Ocean Research Institute, University of Tokyo.

REFERENCES

1 Ayala FJ (1975) Genetic differentiation during the speciation process. Evol Biol 8: 1–78

2 Benzie JHH, Silva PK (1984) The taxonomic relations of the Atyidae (Decapoda, Caridea) of Sri Lanka determined by electrophoretically detectable protein variation. J Crust Biol 4: 632–644

3 Boulton AJ, Knott B (1984) Morphological and electrophoretic studies of the Palaemonidae (Crustacea) of the Perth region, West Australia. Aust J Mar Freshw Res 35: 769–783

4 Chow S, Fujio Y (1985) Population genetics of the palaemonid shrimps (Decapoda: Crustacea) I. Genetic variability and differentiation of local populations. Tohoku J Agri Res 36: 93–108

5 Chow S, Fujio Y (1985) Biochemical evidence of two types in the fresh water shrimp *Palaemon paucidens* inhabiting the same water system. Nippon Suisan Gakkaishi 51: 1451–1460

6 Chow S, Fujio Y, Nomura T (1988) Reproductive isolation and distinct population structures in two types of the freshwater shrimp *Palaemon paucidens*. Evolution 42: 804–813

7 Clayton JW, Tretiak DN (1972) Amine-citrate buffers for pH control on starch electrophoresis. J Fish Res Board Can 29: 1169–1172

8 Gomori G (1955) Preparation of buffers for use in enzyme studies. In "Methods of Enzymology" Ed by SP Colowick and NO Kaplan, Academic Press, New York, pp 138–146

9 Hedgecock D, Stelmach DJ, Nelson K, Lindenfelser ME, Malecha SR (1979) Genetic divergence and biogeography of natural populations of *Macrobrachium rosenbergii*. Proc World Maricul Soc 10: 873–879

10 Ikeda M, Kijima A, Fujio Y (1992) Divergence between two species in *Paratya compressa* (Decapo-

da: Atyidae). Nippon Suisan Gakkaishi 58:819-824

11 Kraus AP, Neeley CL (1964) Human erythrocyte lactate dehydrogenase: Four genetically determined variants. Science 145: 595–597

12 Mashiko K (1983) Differences in the egg and clutch sizes of the prawn *Macrobrachium nipponense* (de Haan) between brackish and fresh waters of a river. Zool Mag 92: 1–9

13 Mashiko K (1983) Evidence of differentiation between the estuarine and upper freshwater populations inhabiting the same water system in the long-armed prawn *Macrobrachium nipponense* (de Haan). Zool Mag 92: 180–185

14 Mashiko K (1990) Diversified egg and clutch sizes among local populations of the freshwater prawn *Macrobrachium nipponense* (de Haan). J Crust Biol 10: 306–314

15 Mashiko K (1992) Genetic egg and clutch size variations in freshwater prawn populations. Oikos 63: 454–458

16 Mashiko K (1992) Laying few large eggs or many small eggs in freshwater prawns of the genus *Macrobrachium*. The Heredity (The Iden), Special issue 4: 7–16 (in Japanese)

17 Nei M (1972) Genetic distance between populations. Am Nat 106: 283–292

18 Nei M (1990) Molecular Evolutionary Genetics, translated into Japanese by T Gojyobori and T Narita. Baifukan Press, Tokyo, pp 180–217

19 Numachi K (1974) Genetic characters of populations. In "Biological Study on Marine Resources" Ed by M Nishiwaki, Tokyo University Press, Tokyo, pp 5–36 (in Japanese)

20 Numachi K (1981) A simple method for preservation and scanning of starch gels. Biochem Genet 19: 233–236

21 Numachi K (1983) Genetic Analysis on the Growth and Survival of Pacific Abalone. Report of Researches (Subject No. 00548050) by the Grant from the Ministry of Education, Science and Culture of Japan. Ocean Research Institute Tokyo University, pp 1–47 (in Japanese)

22 Redfield JA, Salini JP (1980) Techniques of starch-gel electrophoresis of penaeid prawn enzymes (*Penaeus* spp. and *Metapenaeus* spp.). CSIRO Aust Div Fish Oceanogr Rep 116: 1–20

23 Richardson BJ, Baverstock PR, Adams M (1986) Allozyme Electrophoresis: A Handbook for Animal Systematics and Population Studies. Academic Press, New York, pp 271–346

24 Selander R, Smith MH, Yang SY, Johnson WE, Gentry JB (1971) Biochemical polymorphism and systematics in the genus *Peromyscus*. I. Variation in the old-field mouse (*Peromyscus polionotus*). Univ Texas Publ 7103: 49–90

25 Shaklee JB, Allendorf FW, Morizot DC, Whitt GS (1990) Gene nomenclature for protein-coding loci in fish. Trans Am Fish Soc 119: 2–15

26 Trudeau TN (1978) Electrophoretic protein variation in *Macrobrachium ohione* and its implications. Proc World Maricul Soc 9: 139–145

ZOOLOGICAL SCIENCE 10: 169–174 (1993)

Mytilidiphila, a New Genus of Nautiliniellid Polychaetes Living in the Mantle Cavity of Deep-sea Mytilid Bivalves Collected from the Okinawa Trough

Tomoyuki Miura[1] and Jun Hashimoto[2]

[1]*Faculty of Fisheries, Kagoshima University, 4-50-20, Shimoarata, Kagoshima 890, and* [2]*Japan Marine Science and Technology Center, 2-15 Natsushima-cho, Yokosuka 237, Japan*

ABSTRACT—Nautiliniellid polychaetes living in the mantle cavity of deep-sea mytilid bivalves collected from the Minami-Ensei Knoll and the Iheya Ridge of the Okinawa Trough, were studied taxonomically. These polychaetes including two different species were unique in the family in having more than 20 simple hooks per parapodium. They were considered to belong to a single new genus, *Mytilidiphila*. *Mytilidiphila enseiensis* n. sp., found living in the mantle cavity of undescribed mytilid bivalves close to the genus *Adula*, has more than 35 simple hooks per parapodium on middle setigers. *Mytilidiphila okinawaensis* n. sp., found living in the mantle cavity of undescribed deep-sea mussels close to the genus *Bathymodiolus*, has also numerous simple hooks on each parapodium. However, the distal end of simple hook of *M. okinawaensis* is rounded and distinguishable from the pointed one of *M. enseiensis*.

INTRODUCTION

The deep-sea biological community at the Minami-Ensei Knoll of the Okinawa Trough was firstly studied by Japan Marine Science and Technology Center in 1988 and 1989 in a series of surveys using the deep towed camera system and the deep submergence research vehicle (DSRV) *Shinkai 2000* [2]. The community found at the Minami-Ensei Knoll were composed of typical hydrothermal vent organisms including vestimentiferans, mytilid bivalves, vesicomyid clams and lithodid crabs, some of which have been described as new to science [7, 8]. Many specimens of deep-sea mytilid bivalves also were sampled in our recent dives, and during measurement and dissection of these mussels on the research vessel *Natsushima*, we collected nautiliniellid worms living in their mantle cavity. Most nautiliniellid worms attached so stiffly to or penetrated so deeply into the gill filaments of the host mussels that we had to dissect the host tissue for collection.

Accepted October 16, 1992
Received August 6, 1992
[1] To whom all correspondences should be addressed.

The polychaete family Nautiliniellidae has included four genera and five species from both Pacific [4–6] and Atlantic Oceans [1]. These nautiliniellid polychaetes were found living in the mantle cavity of the deep-sea bivalves of hydrothermal vents and cold seeps. Concerned with their commensal or parasitic life, the nautiliniellid worms have simple-structured body with less developed prostomium, numerous similar segments, a few kinds of setae and pygidium lacking anal cirri. However the number of prostomial antennae, the presence of dorsal cirri and/or projected setae on the second segment, the parapodial structure and the setal composition show remarkable interspecific variability. These morphological characters are thus important for their classification at both generic and specific levels. In the previously known species, the Atlantic species, *Petrecca thyasira* Blake is unique in having modified parapodia with elongated notopodia and reduced tentacular segment without dorsal cirri nor setae [1]. The nautiliniellid polychaetes we collected from the Okinawa Trough also have reduced tentacular segment. However they differ from the Atlantic species in the parapodial structure. They also are distinct from the other

nautiliniellid species in the setal composition. Consequently, a new genus and two new species are described in this study. The types are deposited in the National Science Museum, Tokyo (NSMT) and Japan Marine Science and Technology Center (JAMSTEC).

DESCRIPTION

Family Nautiliniellidae Miura & Laubier

Mytilidiphila, new genus

(Japanese name: Igaiyadorigokai-zoku, new)

Type species.—*Mytilidiphila enseiensis*, new species.

Gender.—Feminine.

Diagnosis.—Body long, vermiform, tapering posteriorly with numerous setigers, flattened ventrally and arched dorsally in cross-section. Prostomium short with a pair of antennae, without eyes. Second or tentacular segment well fused with prostomium, having ventral cirri and embedded neuroacicula, with or without setae. Parapodia subbiramous with dorsal and ventral cirri; notopodium supported by a single stout notoaciculum, without setae; neuropodia supported by a single stout neuroaciculum, with numerous simple, hooked setae. Pygidium cylindrical without appendages.

Remarks.—The family Nautiliniellidae is unique in the class Polychaeta, in the combination of one or tow pairs of prostomial antennae, reduced tentacular segment, lack of palps, subbiramous parapodia and simple neuropodial hooks as well as the association with deep-sea bivalves [1, 4–6]. The genus *Mytilidiphila* also is referred to the family, in having these morphological characters and ecological feature.

In the family, the genus *Natsushima* Miura & Laubier has additional simple bifurcate setae and differs from four other genera having only simple neuropodial hooks [5]. The four genera divided into two groups by the thickness of the notoacicula. The genera *Nautiliniella* Miura & Laubier and *Mytilidiphila* have the notoacicula as thick as the neuroacicula [4], while *Shinkai* Miura & Labuier and *Petrecca* Blake have slender notoacicula [1, 5]. The genus *Mytilidiphila* has only a pair of prostomial antennae and differs from *Nautiliniella* with two pairs. The genus *Mytilidiphila* also differs from all other genera of the family in having more than 20 simple hooks on a single parapodium at least in some setigers, instead of up to 10. In other point of view, each nautiliniellid genus is tend to be associated with a certain group of bivalves: *Shinkai* and *Nautiliniella* with *Calyptogena* spp., *Petrecca* with *Thyasira* sp., *Natsushima* with a solemyid bivalve, Mytilidiphila with mytilid bivalves.

Etymology.—The genus name is made by the combination of the family name of the host bivalves, Mytilidae, and a Latinized Greek suffix, *-phila*.

Mytilidiphila enseiensis, new species

(Japanese name: Ensei-igaiyadori, new)

(Fig. 1a-g)

Material.—Minami-Ensei Knoll, Okinawa Trough, DSRV *Shinkai 2000* Dive 616, 1 June 1992, 28° 23.5′N, 127° 38.5′E, 625 m, associated with undescribed deep-sea mytilid bivalves close to the genus

TABLE 1. Measurements of complete specimens of *Mytilidiphila enseiensis* n. sp.

No.	Body Length (mm)	Body Width (mm)	Number of Segments	Notes
2–1	20.8	1.3	121	Holotype
2–2	11.4	1.2	80	caudal end regenerated
2–3	14.1	1.2	81	
2–4	13.5	0.6	79	
2–5	27.8	1.5	164	Largest paratype (ovigerous)
5–1	8.5	1.2	54	caudal end regenerated
5–2	12.8	1.2	77	

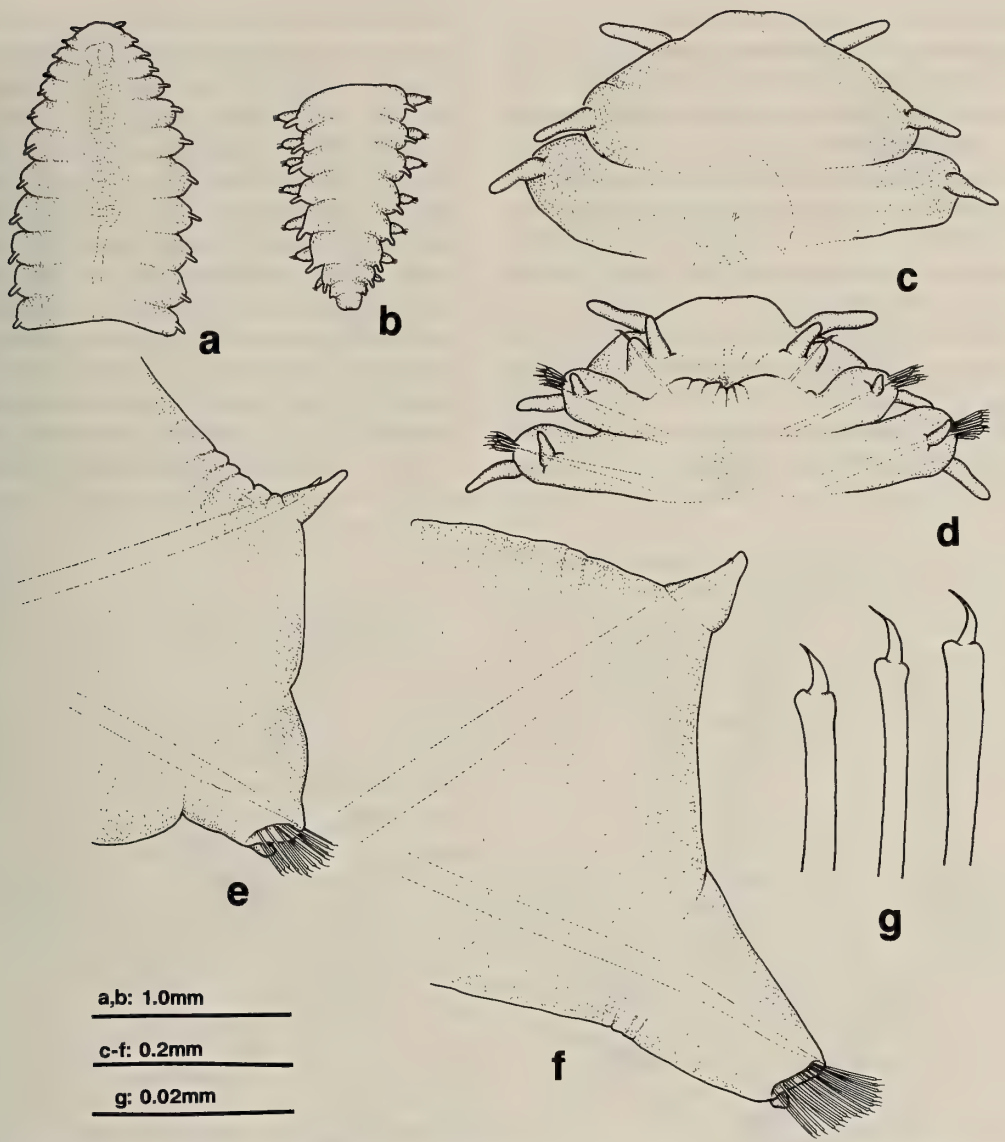

FIG. 1. *Mytilidiphila enseiensis* n. sp. (Holotype): a, Anterior end, dorsal view; b, Posterior end, dorsal view; c, Anterior end enlarged, dorsal view; d, Same, ventral view; e, Parapodium of the 11th segment (or parapodium 10), anterior view; f, Parapodium of the 27th segment (or parapodium 26), anterior view; g, Hooks.

Adula, holotype (NSMT Pol. H-351) and 36 paratypes (JAMSTEC).

Description.—Holotype 20.8 mm long, 1.3 mm wide including parapodia, with 121 setigers. Largest paratype ovigerous, 27.8 mm long, 1.5 mm wide, with 164 setigers (measurement of all complete specimens shown in Table 1). Body flattened ventrally and arched dorsally. Integument smooth. Preserved specimen pale.

Prostomium short, with a pair of short cirriform antennae, without eyes (Fig. 1a, c, d). Second segment well fused with prostomium, defined by embedded acicula and ventral cirri as well as projected simple hooks (Fig. 1d). Mouth opening situated between prostomium and first fully developed setigerous segment. Foregut with well-

developed muscular part (Fig. 1a).

Pygidium simple, without anal cirri (Fig. 1b).

Parapodium subbiramous throughout body; notopodium supported by a single stout notoaciculum; neuropodium well-developed, supported by a single stout neuroaciculum (Fig. 1e, f); dorsal cirrus short, conical, situated distally on notopodium, sometimes distal tip of notoacicula penetrating dorsal cirrus; ventral cirrus very short, conical, situated ventro-posteriorly on neuropodium.

Setae consisting of simple hooks only; number of hooks on each parapodium varying 6-10 on first 3 setigers, reaching more than 35 on parapodium 26. Hooks simple, slender, with inflated subdistal stems and slightly curved, pointed distal ends (Fig. 1g).

Remarks.—*Mytilidiphila enseiensis* differs from most of nautiliniellid species in the absence of dorsal cirri on the second segment and the presence of equally stout noto- and neuroacicula. *Petrecca thyasira* Blake also has less developed parapodia without dorsal cirri on the second segment [1]. However this Atlantic species differs from *M. enseiensis* in having branchia-like long notopodia and occurring of only one or two simple hooks on each parapodium, instead of short conical notopodia and more than 30 simple hooks on a parapodium respectively. *Shinkai longipedata* Miura & Ohta has up to 10 hooks on some anterior parapodia [6] and it has been the maximal number of hooks occurring on a parapodium in the previously known nautiliniellid species.

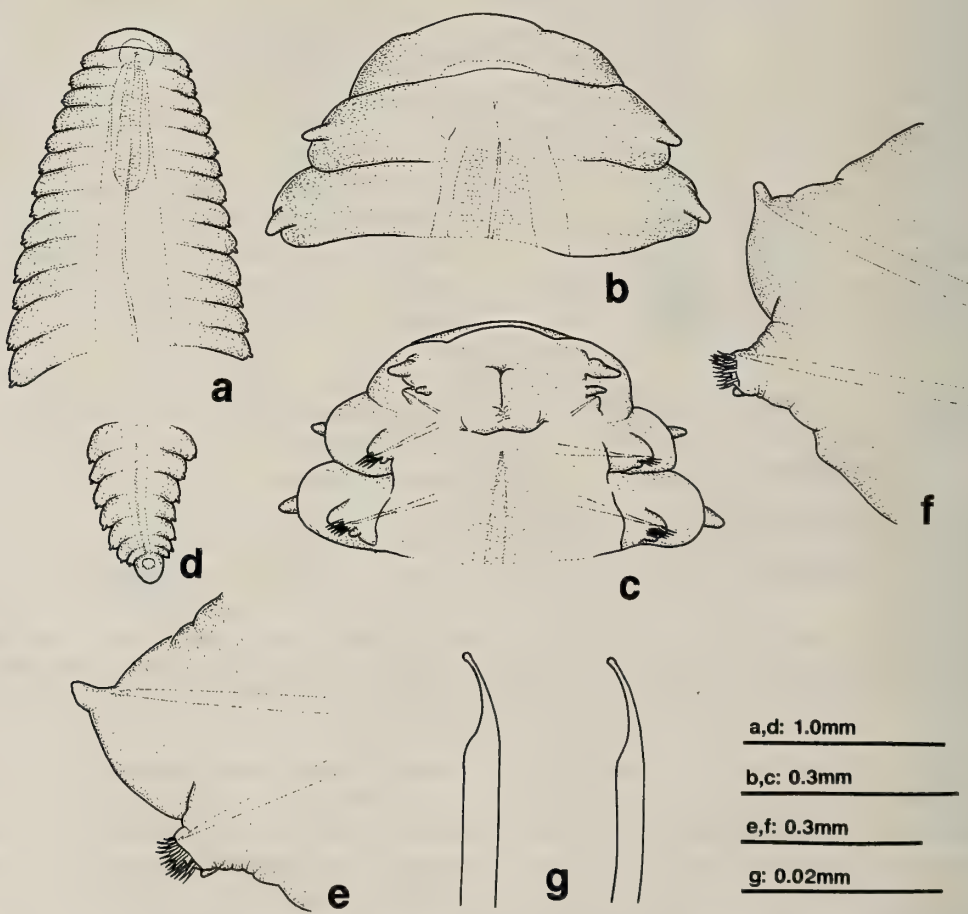

FIG. 2. *Mytilidiphila okinawaensis* n. sp. (Holotype): a, Anterior end, dorsal view; b, Same, enlarged, dorsal view; c, Same, ventral view; d, Posterior end, dorsal view; e, Parapodium of the 11th segment (or parapodium 10), anterior view; f, Parapodium of the 36th segment (or parapodium 35), anterior view; g, Hooks.

Most examined specimens had one or two simple hooks on a single parapodium of the second segment (average number: 0.96 for 37 specimens), though six of them did not have any.

The specimens of *Mytilidiphila enseiensis* were found to harbor all four dissected bivalves from the Minami-Ensei Knoll. The bivalves are ranging from 163 to 175 mm in length. Two of them contained only one nautiliniellid polychaete, while the other two had 16 and 21 individuals. Other than these nautiliniellid polychaetes, two specimens of polynoid polychaetes tentatively identified as *Branchipolynoe pettiboneae* Miura and Hashimoto [3] also were collected from two specimens of the same mytilid bivalve.

Etymology.—The species name is derived from the Minami-Ensei Knoll, the type-locality.

Mytilidiphila okinawaensis, new species
(Japanese name: Okinawa-igaiyadori, new)
(Fig. 2a-g)

Material.—Minami-Ensei Knoll, Okinawa Trough, DSRV *Shinkai 2000* Dive 549, 5 June 1991, 28° 23.5′N, 127° 38.5′E, 701 m, associated with undescribed deep-sea mussel close to the genus *Bathymodiolus,* holotype (NSMT Pol. H-352) and 1 paratype (JAMSTEC); Iheya Ridge, Okinawa Trough, Dive 614, 30 May, 1992, 27° 33.0′N, 126° 58.0′E, 1395 m, associated with undescribed deep-sea mussel, 1 paratype (JAMSTEC).

Description.—Holotype 15.2 mm long, 1.4 mm wide including parapodia, with 95 setigers. Paratype of Dive 549, 9.4 mm long, 1.2 mm wide, with 84 setigers. Body flattened ventrally and strongly arched dorsally. Integument smooth. Preserved specimen pale.

Prostomium short, ventrally with a pair of very short cirriform antennae, without eyes (Fig. 2a-c). Second or tentacular segment well fused with prostomium, achaetous, defined by embedded acicula and ventral cirri (Fig. 2c). Ventral cirri of tentacular segment inserted in front of neuropodium. Mouth opening situated between prostomium and first fully developed setigerous segment. Foregut with well-developed muscular part (Fig. 2a).

Pygidium rounded, without anal cirri (Fig. 2d).

Parapodium subbiramous throughout body, with inflated notopodium supported by a single stout notoaciculum, and smaller neuropodium supported by a single stout neuroaciculum (Fig. 2e, f); dorsal cirrus short, conical, situated distally on notopodium; ventral cirrus short conical, situated ventro-posteriorly on neuropodium.

Setae consisting of simple hooks only; number of hooks on each parapodium varying 4–7 on first 3 setigers, thereafter immediately increasing and reaching to 20 on parapodium 10. Hooks simple, slender; distal end slightly curved, with rounded tips (Fig. 2g).

Remarks.—*Mytilidiphila okinawaensis* differs from *M. enseiensis* in the shape of simple hooks and in the presence of setae on the second segment. The simple hooks of *M. okinawaensis* are gradually tapered with rounded distal ends, while those of *M. enseiensis* have inflated subdistal stems and pointed distal ends. The simple hooks are present on the second segment in most specimens of *M. enseiensis,* but absent in *M. okinawaensis.*

Etymology.—The species name is derived from the Okinawa Trough, the type-locality.

ACKNOWLEDGMENTS

The authors wish to thank Dr. Yoshiyuki Nozaki of Ocean Research Institute, University of Tokyo for his kind offer of a part of the material examined in this study. Thanks are also due to the staff of JAMSTEC for their assistance at the sampling by means of the deep submergence research vehicle *Shinkai 2000.* This work was supported in part by grants-in-aid for the first author from the Ministry of Education, Culture and Science, Japan (No. 03640630) and Kato Foundation for the Promotion of the Bioscience Researches.

REFERENCES

1 Blake JC (1990) A new genus and species of Polychaeta commensal with a deep-sea thyasirid clam. Proc Biol Soc Washington 103: 681–686

2 Hashimoto J, Fujikura K, Hotta H (1990) Observations of deep sea biological communities at Minami-Ensei Knoll. JAMSTECTR Deepsea Res 167–179 (In Japanese with English abstract)

3 Miura T, Hashimoto J (1991) Two new branchiate scale-worms (Polynoidae: Polychaeta) from the hydrothermal vent of the Okinawa Trough and the volcanic seamount off Chichijima Island. Proc Biol Soc

Washington 104: 166–174

4 Miura T, Laubier L (1989) *Nautilina calyptogenicola*, a new genus and species of parasitic polychaete on a vesicomyid bivalve from the Japan Trench, representative of a new family Nautilinidae. Zool Sci 6: 387–390

5 Miura T, Laubier L (1990) Nautiliniellid polychaetes collected from the Hatsushima cold-seep site in Sagami Bay, with descriptions of new genera and species. Zool Sci 7: 319–325

6 Miura T, Ohta S (1991) Two polychaete species from the deep-sea hydrothermal vents in the middle Okinawa Trough. Zool Sci 8: 383–387

7 Okutani T, Fujikura K (1990) A new turbinid gastropod collected from the warm seep site in Minami-Ensei Knoll, West of the Amami-Oshima Island, Japan. Venus (Jap J Malacology) 49: 89–90

8 Takeda M, Hashimoto J (1990) A new species of the genus *Paralomis* (Crustacea, Decapoda, Lithodidae) from Minami-Ensei Knoll in the mid-Okinawa Trough. Bull Natn Sci Mus Tokyo, ser A, 12: 79–88

ZOOLOGICAL SCIENCE 10: 175–178 (1993)

[RAPID COMMUNICATION]

Differential Expression of *Xenopus* BMPs in Early Embryos and Tissues

Atsushi Suzuki, Shin-ichiro Nishimatsu, Kazuo Murakami and Naoto Ueno

Institute of Applied Biochemistry, University of Tsukuba, Ibaraki 305, Japan

ABSTRACT—Expression levels of mRNA for *Xenopus* bone morphogenetic proteins (BMPs) in early embryos and adult organs were examined. Reverse transcription-polymerase chain reaction (RT-PCR) that used specific primers for each BMP subtype revealed that mRNAs for BMP-2 and BMP-4 are distributed in a wide variety of adult tissues including lung, heart, and kideney. Unexpectedly, distribution of mRNA for BMP-7 was found to be limited to ovary and early embryos. The result suggests that *Xenopus* BMP-7 may have a specific role in ovary and early embryos.

INTRODUCTION

A growing body of evidence suggest that peptide growth factors play essential roles in animal development [4]. We have previously isolated genes encoding proteins related to activin, a member of transforming growth factor-β (TGF-β) family proteins from *Xenopus laevis* [12]. Among several activin related genes, one gene was found to code an extremely similar protein to mammalian bone morphogenetic protein-2 (BMP-2) [14], which was originally discovered for its ability to induce bone and cartilage formation *in vivo*. Subsequently, we have cloned cDNAs for BMP-2, -4 and -7 from *Xenopus* oocyte cDNA library using BMP-2 gene as a probe [8]. DNA sequence analysis has shown that their primary structures are highly conserved between amphibian and mammalian.

Accepted August 31, 1992
Received July 17, 1992

In the present study, ontogeny and tissue distribution of these *Xenopus laevis* BMPs were examined by reverse transcription PCR [6] that is a rather sensitive method to detect mRNAs from minute embryonic tissues.

MATERIALS AND METHODS

Xenopus embryos and tissues

Xenopus laevis embryos were obtained by artificial fertilization. The embryos were staged according to Nieuwkoop and Faber [7]. Adult organs are surgically removed from anesthetized male and female *Xenopus laevis*. All embryos and tissues were immediately frozen in liquid nitrogen and kept at −80°C until use.

Reverse transcription PCR

Total RNA was purified from embryos and adult tissues by acid guanidinium thiocyanate-phenol-chloroform extraction (AGPC) method [2] and guanidinium-CsCl method [1], respectively. RNAs from adult tissues were from mixture of several individuals. cDNA was synthesized from total RNA as follows. A 20 μl of reverse transcription mixture containing 500 ng of total RNA, 1× RT buffer (50 mM Tris-HCl, pH 8.3/75 mM KCl/3 mM $MgCl_2$), 100 pmol of random hexamer primers, 0.5 mM of each dNTP, 10 mM DTT, 20 U of RNasin (Promega), and 100 U of MMLV reverse transcriptase (BRL) was incubated at 37°C for 60

min, and heated to 95°C for 10 min. PCR was performed at a final concentration of 1×PCR buffer (10 mM Tris-HCl, pH 8.8/50 mM KCl/1.5 mM $MgCl_2$/0.1% Triton X-100)/0.2 mM each of dNTP/5 μCi of [α-^{32}P]dCTP (3000 Ci/mmol)/5 pmol of each primer/0.225 U of Taq DNA polymerase (Wako Chemical, Japan) in a total volume of 10 μl. The mixture was overlaid with mineral oil and then amplified with a thermal cycler (Perkin-Elemer/Cetus). The amplification profile involved denaturation at 95°C for 30 sec, primer annealing at 58°C for 30 sec, and extension at 72°C for 1 min. A 4 μl of the PCR sample was electrophoresed on 5% polyacrylamide gel and the PCR fragment was visualized by autoradiography. Appropriate bands were cut out from the dried gel and radioactivity was determined by Cerenkov counting. For quantitative analysis, optimal cycle number for each BMP was determined. Cycle of 22 was chosen for all BMPs because it is in the range of exponential increase of PCR products depending on cycle numbers and resulting radioactivities of PCR products are relative to RNA amounts under the amplification condition. Primers used in PCR were as follows: BMP-2 (5′-CAATGGTCGCTGGGATCCAC-3′ and 5′-TCACAACATTTTTGCCAGGCGT-3′), BMP-4 (5′-CATCATGATTCCTGGTAACCGA-3′ and 5′-CTCCATGCTGATATCGTGCAG-3′), BMP-7 (5′-AAGGCCACGAACGCAGA-3′ and 5′-TGTCAGTTCATCTCCAAGT-3′), EF-1α (5′-CCTGAATCACCCAGGCCAGATTGGTG - 3′ and 5′-GAGGGTAGTCTGAGAAGCTCTCCACG-3′).

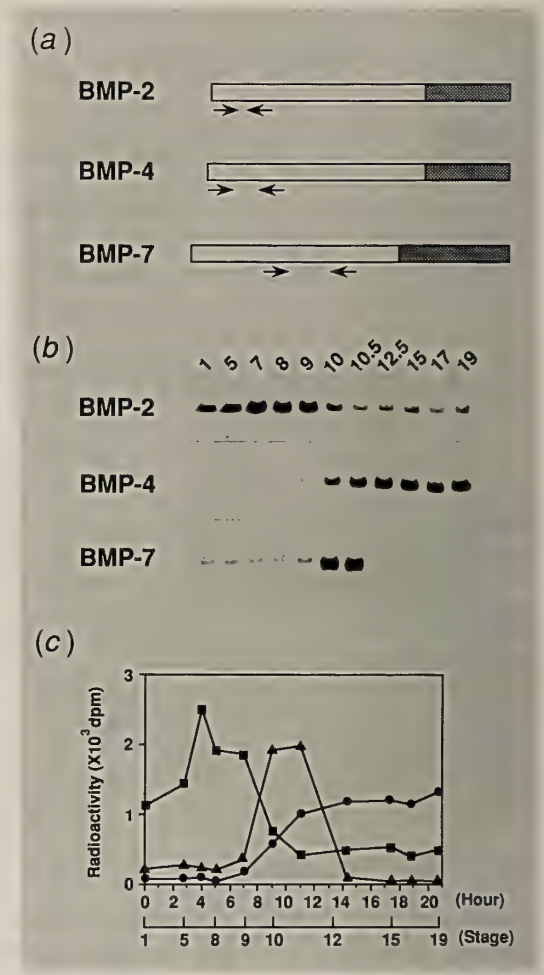

FIG. 1. Levels of BMP mRNAs during early *Xenopus* embryogenesis. (*a*) Primer positions used for RT-PCR. Each primer set was specifically designed to detect each BMP mRNAs and denoted by arrows. The propeptide structures that include mature region (shaded bars) derived from the full-length cDNAs are represented by bars. (*b*) Total RNA from staged embryos was subjected to RT-PCR using specific primers for each BMP mRNA. *Xenopus* embryos were cultured in 0.1× Steinberg's solution at 23°C. Developmental stages are shown to the top of the figure. (*c*) Schematic representation of (*b*). Radioactivity of appropriate band was measured by Cerenkov counting and plotted against hours after fertilization (BMP-2, squares; BMP-4, circles, BMP-7, triangles).

RESULTS AND DISCUSSION

Newly established RT-PCR method enabled us to detect mRNAs in small preparations of embryos and adult tissues compared to conventional methods such as Northern blot analysis and RNase protection assay. In addition, the method has minimized the time required for the assay. Presence of BMP mRNAs in developing embryos were demonstrated by this method using respective specific primers. Figure 1(*a*) schematically represents the precursor structures of BMPs and the regions chosen for designing oligonucleotide primers. Specific nucleotide sequences were chosen for each BMP to prevent the primers from cross-hybridization. Figure 1(*b*) shows the accu-

mulation of mRNA for *Xenopus* BMP-2, -4 and -7 during early embryogenesis. The result shows that all BMP mRNAs are maternally present and that the levels of the BMP mRNAs change drastically during development (BMP-4 transcript in early embryos before stage 9 becomes detectable by longer exposure). It should be noted that genes for BMPs are differentially regulated in early development although their primary structures are closely related to each other. Especially, homology of amino acid sequence of *Xenopus* BMP-2 and BMP-4 are 82% in their predicted mature proteins. Independent gene regulation of BMP genes in early embryos implies that they have distinct functions in embryogenesis. The result is very similar to that obtained by Northern blot analysis of poly(A)+ RNA purified from staged early embryos. This method, however, provided a sharper image of accumulation and decline of the mRNAs by plotting radioactivities of the PCR products (Figure 1(*c*)). Existence of BMP-2 [13] and BMP-4 [9] in embryo was also confirmed by Western blot analysis that used specific antibodies against their respective sequences.

Tissue distribution of BMP mRNAs was also examined. RNA was purified from adult tissues and subjected to RT-PCR assay for BMP mRNAs. As shown in Figure 2, distributions of mRNAs for BMP-2 and -4 are very similar to each other and the transcripts were detected in a wide variety of tissues of not only mesoderm-origin but also ectoderm-orgin. The result is in a good agreement with a previous observation on mammalian BMP-2 and -4 [15]. Interestingly, however, mRNA for *Xenopus* BMP-7 was detected only in ovary. In addition to the presence of MBP-7 mRNA in early embryo before neurula, this observation strongly suggests that BMP-7 has embryo-specific role(s) in *Xenopus* which is as yet unknown. It remains to be examined whether localization of mammalian counter part of *Xenopus* BMP-7 transcript is also limited to ovary and early embryos. It is known that a heterodimer of BMP-2 and -7 (OP-1) subunits is present in mammalian bone extracts [11]. Therefore, BMP-7 may modulate specificity and potency of BMP activities in ovary and early embryos by forming a heterodimer with another BMP peptide.

BMPs are structurally related to gene product of *Drosophila dppc* [10] which is a locus responsible for dorso-ventral specification and formation of imaginal disks in *Drosophila* embryo. Moreover,

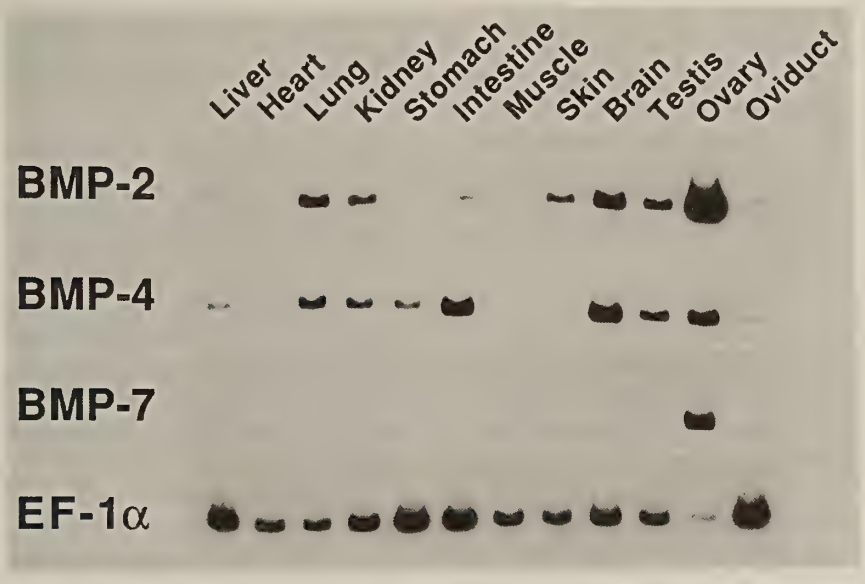

FIG. 2. Distribution of BMP mRNAs in adult *Xenopus* tissues. Total RNA (500 ng) from adult *Xenopus* tissues was subjected to RT-PCR using specific primers for each BMP mRNA and EF-1α mRNA. EF-1α was used to confirm both RNA quality and quantity. RT-PCR for EF-1α mRNA was performed at 19 cycles.

it has been proposed that *Xenopus* BMP-4 may function as a posterior-ventralizing factor in *Xenopus* [3, 5]. The presence of BMP-7 mRNA in "organizer field", dorsal lip of early gastrula (Dr. K. Cho, personal communication) suggests that *Xenopus* BMP-7 whose structure is similar to BMP-4 may also be an essential factor in pattern formation of amphibian development.

ACKNOWLEDGEMENTS

We wesh to thank Dr. R. Makino for technical advice on RT-RCR. This study was supported in part by Grant-in-Aid for Scientific Research (No. 02558017) from Ministry of Education, Science and Culture, Japan and grants from Chichibu Cement Co. and Kowa Foundation for Promotion of Life Sciences.

REFERENCES

1 Chirgwin JM, Przybyla AE, MacDonald RJ, Rutter WJ (1979) Biochemistry 18: 5294–5299
2 Chomczynski P, Sacchi N (1987) Anal Biochem 162: 156–159
3 Dale L, Howes G, Price BMJ, Smith JC (1992) Development 115: 573–585
4 Jessell TM, Melton DA (1992) Cell 68: 257–270
5 Jones CM, Lyons KM, LaPan PM, Wright CVE, Hogan BLM (1992) Development 115: 639–647
6 Makino R Sekiya T, Hayashi K(1990) Technique 2: 295–301
7 Nieuwkoop PD, Faber J (1967) In "Normal Table of *Xenopus laevis* (Daudin) 2nd". North-Holland, Amsterdam
8 Nishimatsu S, Suzuki A, Shoda A, Murakami, Ueno N (1992) Biochem Biophys Res Commun 186: 1487–1495
9 Nishimatsu S, Takebayashi K, Suzuki A, Murakami K, Ueno N (1992) Growth Factors, in press
10 Padgett RW, St Johnston RD, Gelbart WM (1987) Nature 325: 81–84
11 Sampath TK, Coughlin JE, Whetstone RM, Banach D, Corbett C, Ridge RJ, Ozkaynak E, Oppermann H, Rueger DC (1990) J Biol Chem 265: 13198–13205
12 Ueno N, Asashima M, Nishimatsu S, Suzuki A, Murakami K (1991) In "Frontiers in muscle research". Ed. by E Ozawa, T Masaki, Y Nabeshima Elsevier, Amsterdam, pp 17–28
13 Ueno N, Shoda A, Takebayashi K, Suzuki A, Nishimatsu S, Kikuchi T, Wakimasu M, Fujino M, Murakami K (1992) Growth Factors 7: 233–240
14 Wozney JM, Rosen V, Celeste AJ, Mitsock LM, Whitters MJ, Kriz RW, Hewick RM, Wang EA (1988) Science 242: 1528–1534
15 Wozney JM, Rosen V, Byrne M, Celeste AJ, Moutsatsos I, Wang EA (1990) J Cell Sci Suppl 13: 149–156

ZOOLOGICAL SCIENCE 10: 179–182 (1993)

[RAPID COMMUNICATION]

Sperm Behavior in the Micropyle of the Medaka Egg

Sumio Ishijima, Yukihisa Hamaguchi and Takashi Iwamatsu[1]

Biological Laboratory, Faculty of Science, Tokyo Institute of Technology, O-okayama, Meguro-ku, Tokyo 152 and [1]Department of Biology, Aichi University of Education, Kariya 448, Japan

ABSTRACT—Sperm behavior in the micropyle of the medaka egg was examined using videomicroscopy. Spermatozoa swimming near the egg, whose progressive speed was similar to that of spermatozoa freely swimming in a medium, entered the micropylar canal after being trapped in the funnel-shaped micropylar vestibule or entered directly. The spermatozoa stalled in the micropylar vestibule entered the micropylar canal with a time lag of less than 0.5 sec. Proceeding at a fairly high speed for a short time, the spermatozoa gradually slowed down when the flagellar movement of the spermatozoa became obstructed by the surface of the micropylar canal, finally reaching the plasma membrane. The spermatozoa which directly entered the micropylar canal maintained progressive speed until their flagellar movement became obstructed by the surface of the micropylar canal. They reached the plasma membrane through the micropylar canal in the same manner as the spermatozoa experiencing collision with the surface of the micropylar vestibule.

INTRODUCTION

In teleost fish, spermatozoa can reach the egg's plasma membrane only by means of a narrow channel, the micropyle of the vitelline envelope. Since the base of the micropyle is as wide as the diameter of the sperm heads, spermatozoa must pass in single file through the micropyle. This has been thought to be the mechanism for blocking polyspermy [2] because medaka eggs do not show a rapid electrical block to polyspermy [6].

Since observation of sperm entry into the micropyle is difficult, little is known about the exact behavior of spermatozoa in the micropyle. Recent videomicroscopy and the transparency of the medaka egg enabled us to record on videotape the movement of the sperm head in the micropyle of the medaka eggs.

The purpose of the present study is to record and analyze the behavior of spermatozoa in the micropyle of the medaka egg. On the basis of this data, the mechanism for blocking polyspermy in the medaka egg is discussed.

MATERIALS AND METHODS

Medaka oocytes and spermatozoa were prepared by the method described earlier [4] and were kept in Ringer's solution (6.5 g NaCl, 0.4 g KCl, 0.113 g $CaCl_2$ and 0.15 g $MgSO_4 \cdot 7H_2O$ per liter of deionized water, pH=7.3 adjusted with $NaHCO_3$) before use. In each experiment, the gametes were freshly prepared and used within 30 min. The observation chamber was constructed by gluing two strips of silicon rubber (1 mm thick) onto a glass slide parallel to each other. An egg was put in the chamber with a small amount of Ringer's solution, and the chamber was covered with a coverslip after removal of the Ringer's solution around the egg. To observe an oblique view of the egg micropyle, the egg was rotated by sliding the coverslip. Sperm movement was observed using a Nikon Optiphot microscope equipped with a plan 40× objective, 10× eyepieces and a National video camera (WV-1300A, Matsushita Communication Industrial Co., Ltd, Yokohama, Japan). While observing the egg displayed on a

Accepted November 20, 1992
Received October 19, 1992

National TN-96 monitor (Matsushita Communication Industrial Co., Ltd), approximately 0.1 ml of sperm suspension was introduced into the observation chamber from an open end. The image was recorded on video tape with a Panasonic video tape recorder (NV-FS900, Matsushita Communication Industrial Co., Ltd).

For detailed field-by-field analysis, images of the head were traced from the video monitor onto transparent plastic sheets using a fine-point marker. The progressive speed of free-swimming spermatozoa was determined by measuring the distance between the positions of the sperm head at the beginning and the end of a time interval.

RESULTS AND DISCUSSION

Movement characteristics of medaka spermatozoa

Medaka spermatozoa swam at a maximum transverse displacement of the sperm flagella of 5.14± 1.73 μm (mean±S.D., n=16) while rotating about their longitudinal axis at a rate of 3.77 per second as previously reported by Ishijima *et al.* [3]. The progressive speed of medaka spermatozoa swimming near the micropyle was 74.0±14.6 μm/sec (mean±S.D., n=19), whereas that of spermatozoa freely swimming in the medium was 74.9± 31.3 μm/sec (mean±S.D., n=25). No difference was found between them, suggesting that sperm movement, especially progressive speed, is not stimulated by the presence of the micropyle.

The progressive speed of medaka spermatozoa was low as compared to that (191.4 μm/sec) of sea urchin spermatozoa [1], whose flagellum is similar in size to that of medaka spermatozoa. The progressive speed is roughly proportional to the square of the maximum transverse displacement of the flagellum. The ratio of the progressive speed to the square of the maximum transverse displacement of the flagellum does not differ between medaka (2.8; maximum transverse displacement of 5.14 μm) and sea urchin spermatozoa (3.0; maximum transverse displacement of 8.0 μm) [1]. This suggests that the low progressive speed of medaka spermatozoa is mainly due to the narrow amplitude of their flagellar waves. The small transverse displacement of the beating flagella of medaka spermatozoa may be critical for sperm progress in the small diameter of the micropyle (see below).

Progressive speed of medaka spermatozoa in the micropyle

Most spermatozoa attached to the surface of the micropylar vestibule, stayed there for approximately 424 msec (S.D.=243 msec, n=20) and then entered the micropylar canal, although some spermatozoa entered directly. Both the progressive speed of the medaka spermatozoa and the size of the micropyle of the medaka egg varied; the micropyle had a mean diameter (d_v) of 5.30 μm (S.D.=1.25 μm, n=21) at the end of its vestibule and a mean diameter (d_c) of 3.19 μm (S.D.=0.84 μm, n=21) at the base of the micropylar canal (Fig. 1). Thus, the profile of the progressive speed of medaka spermatozoa in the micropyle varied. In general, three phases in the time course of the progressive speed were recognized (Fig. 2). The first phase was a decrease in the progressive speed of the spermatozoa from the free-swimming speed

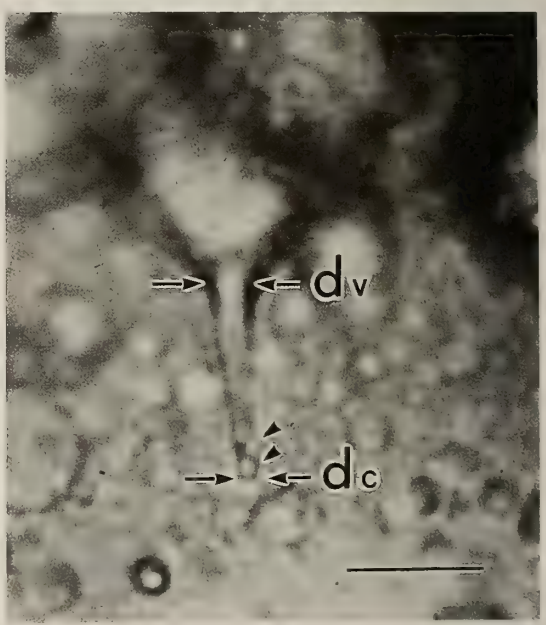

Fig. 1. A phase-contrast videomicrograph of the micropyle of the medaka egg. d_v, diameter of the micropylar vestibule at its base; d_c, diameter of the micropylar canal at its end. Two spermatozoa line up along the micropylar canal (arrowheads). Bar, 20 μm.

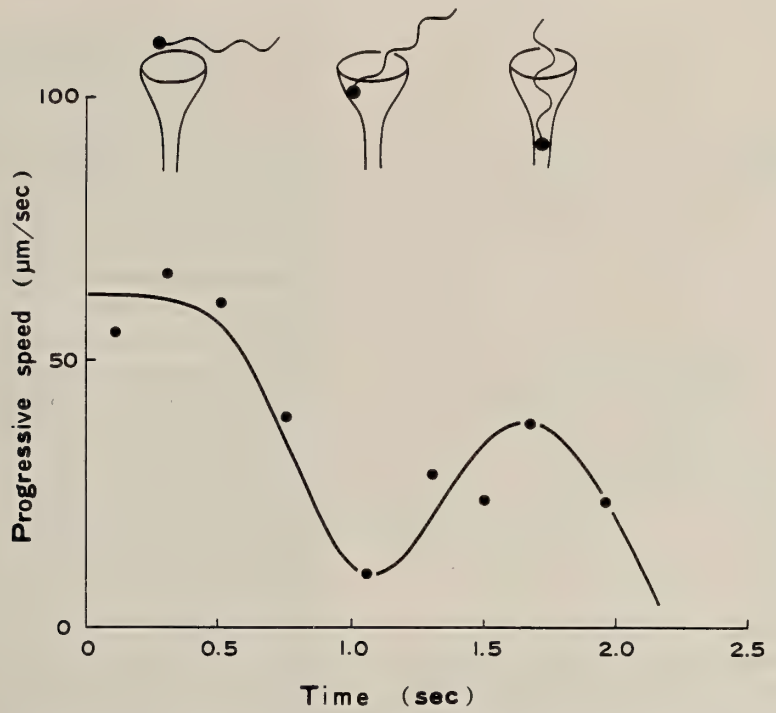

FIG. 2. A typical profile of the time course of the progressive speed of medaka spermatozoa in the micropyle.

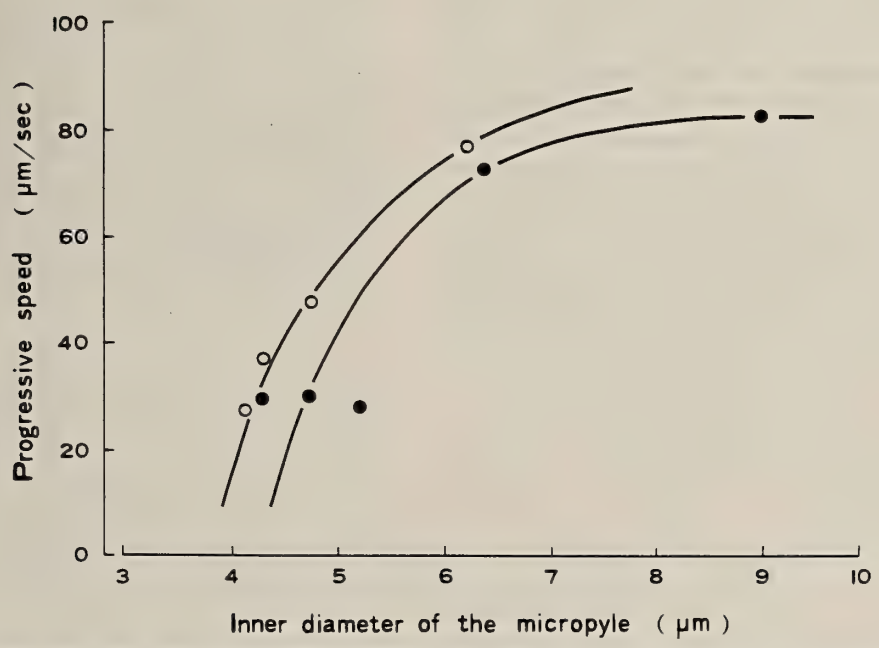

FIG. 3. The relationship between the progressive speed and the diameter of the micropyle. Two examples are shown.

to nearly zero; the spermatozoa which swam freely were trapped in the micropylar vestibule and wandered through it or ceased any progress for less than 0.5 sec as mentioned above. The second phase was the recovery of the progressive speed; the spermatozoa entered the micropylar canal and proceeded without obstruction from the micropylar canal. The final phase was the decrease of the progressive speed until it was reduced to zero; the spermatozoa made their way through the micropyle because the flagellar movement of the spermatozoa was mechanically inhibited by the surface of the micropylar canal, and finally reached the egg's plasma membrane. The inhibitory effect of the micropyle on the progressive speed is shown in Fig. 3. Progressive speed rapidly decreased with a decrease in the diameter of the micropyle. It took 689 ± 428 msec ($n=16$) for the spermatozoa to pass through the micropylar canal (the second and third phases).

No difference was found in the time course of the spermatozoa secondarily entering the micropyle compared to that of the first (data not shown).

Most spermatozoa were trapped in the micropylar vestibule before entering the micropylar canal, suggesting that the micropylar vestibule is very useful in capturing the spermatozoa.

In sperm-egg interaction, there are various mechanisms blocking polyspermy [2]. In medaka, the micropyle plays an important role in blocking polyspermy because only one spermatozoon reached the plasma membrane in our study. The blocking of the polyspermy with the micropyle is probably due to the mechanical inhibition of sperm progression of the surface of the micropyle. The mean diameter of the micropyle at its end (3.19 ± 0.84 μm) is almost the same as that of the head of spermatozoa (3.71 ± 0.60 μm, $n=17$), so that sperm must pass in single file through the micropyle. The decrease in progressive speed (Figs. 2 and 3), especially slow progression of further sperm, may contribute to the effective polyspermy block. There was no difference in sperm behavior in the micropyle between the spermatozoa entering immediately or later. Many spermatozoa could pass through the micropyle which had been isolated from the medaka egg (data not shown). These observations suggest that substances inhibit sperm behavior are not secreted by the plasma membrane and the micropyle.

Most medaka spermatozoa swimming freely in the medium rolled in a clockwise direction on their longitudinal axis when an observer viewed the cell from the anterior ends although some spermatozoa rolled in the other direction [3]. In contrast, the sense of the micropyle is counterclockwise [5]. Therefore, it is unlikely that the chirality of the micropyle is involved in sperm movement when passing through the micropyle.

REFERENCES

1 Gray J, Hancock GJ (1955) J Exp Biol 32: 802–814
2 Hart NH (1990) Int Rev Cytol 121: 1–66
3 Ishijima S, Hamaguchi MS, Naruse M, Ishijima SA, Hamaguchi Y (1992) J Exp Biol 163: 15–31
4 Iwamatsu T (1975) Bull Aichi Univ Educ (Nat Sci) 24: 113–144 (in Japanese)
5 Iwamatsu T, Onitake K, Yoshimoto Y, Hiramoto Y (1991) Develop Growth Differ 33: 479–490
6 Nuccitelli R (1980) Develop Biol 76: 499–504

ZOOLOGICAL SCIENCE 10: 183–187 (1993)

[RAPID COMMUNICATION]

Epidermal Cells of the Tail of an Anuran Larva Are Competent to Transform into the Adult-Type Cells

KATSUTOSHIYOSHIZATO[1], AKIO NISHIKAWA[2], YUMI IZUTSU[1] and MASAYOSHI KAIHO[3]

[1]*Molecular Cell Science Laboratory, Zoological Institute, Faculty of Science, Hiroshima University, Kagamiyama 1-3-1, Higashihiroshima-shi, Hiroshima 724,* [2]*Department of Physiology, Saitama Medical School, Morohongo 38, Moroyama, Iruma-gun, Saitama 350-04, and* [3]*Safety Research Laboratories, Yamanouchi Pharmaceutical Co., Ltd., Azusawa 1-1-8, Itabashi-ku, Tokyo 174, Japan*

ABSTRACT—The epidermis of an anuran tadpole shows the region-specific metamorphic fate: the body epidermis transforms into the adult epidermis, while the tail epidermis commits apoptosis. The only explanation for this difference has been that the tail lacks basal cells which are competent to transform into germinative cells of the adult epidermis. Human blood group antigen A was found to be a specific molecular marker for adult-type epidermal cells. A sharp threshold was apparent at the body-tail junction in expression of the antigen. Utilizing this marker, we succeeded in demonstrating the presence of a specific population of epidermal cells in the tail which can differentiate into the adult-type germinative cells under the direct action of thyroid hormone. This was an unexpected result in that the tail makes provision for the adult life. We propose a hypothesis on the regulation of region-specific metamorphic changes of the anuran larval epidermis.

INTRODUCTION

The metamorphic fate of the epidermis of an anuran tadpole depends on its location in the head-tail axis. Changes in the epidermis of the tail contrast with those in the epidermis of the body (head and body trunk region): the former is to be lost during metamorphosis, while the latter is to survive and transform into the adult type [10]. The present study was carried out to understand the reason for this different metamorphic fate of the two tissues at the cellular level.

The epidermis of a tadpole of bullfrog, *Rana catesbeiana,* is composed of three types of cells: apical, skein and basal cells [8, 10]. Apical and skein cells are larva-specific in that they terminate their life at the metamorphosis. Basal cells are the larva to adult cell in that they transform their characters from the larval type into the adult one. They are most likely the progenitor of germinative cells of the adult skin [8].

The only explanation given hitherto for the region-dependent metamorphic change in the epidermis described above has been the lack of basal cells in the tail and their presence in the body [8]. To verify if this explanation is correct, we looked for a specific probe that detects the adult-type epidermal cells, but not larval cells. We found that the human group A antigen is expressed specifically in the suprabasal cells of postmetamorphic skin and is qualified for the probe. Utilizing this probe, the present study could show the presence of a specific population of epidermal cells also in the tail that can differentiate into the adult-type germinative cells under the direct action of thyroid hormone. These cells are most likely basal cells. We suggest that the tail epidermis is competent to transform into the adult type.

Accepted December 16, 1992
Received November 27, 1992
[1] To whom correspondence should be addressed.

MATERIALS AND METHODS

The bullfrog, *Rana catesbeiana,* was used in the present study. Tadpoles were obtained from a local supplier and staged according to Taylor and Kollros [9].

Epidermal cells were prepared from the tail and the body of tadpole as described previously [6]. Cells were cultured in medium of RPMI-1640 (GIBCO) containing 7% fetal calf serum (Commonwealth Serum Laboratory) which had been treated with charcoal (Wako Pure Chemical Industries LTD.) to eliminate thyroid hormone as described previously [11]. RPMI medium was diluted with distilled water to 70% of its original strength. Cells were maintained at 24°C in a humidified incubator gassed with 5% CO_2 and 95% air. They were precultured for 2 days in the absence of 3,3′,5-triiodo-L-thyronine (T_3, Sigma Chemical Co.) and media were changed (day 0) with fresh medium with (experimentals) or without (controls) T_3. When the culture extended more than 4 days, media were changed at day 4.

Histological studies were performed as follows. The skin was removed from tadpoles, fixed with 10% neutralized formalin, embedded in paraffin and sectioned 4 μm thick. Staining with toluidine blue was performed according to Robinson and Heintzelman [8]. Sections for electron microscopy were prepared according to Kaiho *et al.* [2] and were viewed through a JE-100SX electron microscope. Sections for immunohistochemistry were also processed as described above. Cells for this aim were fixed with 10% neutralized formalin or methanol. The antigen A was detected by the method of Kaiho and Ishiyama [1] using anti-A antiserum (rabbit, Takeda) and Vecstastain ABC kits (Vector Lab.) as an indicator system.

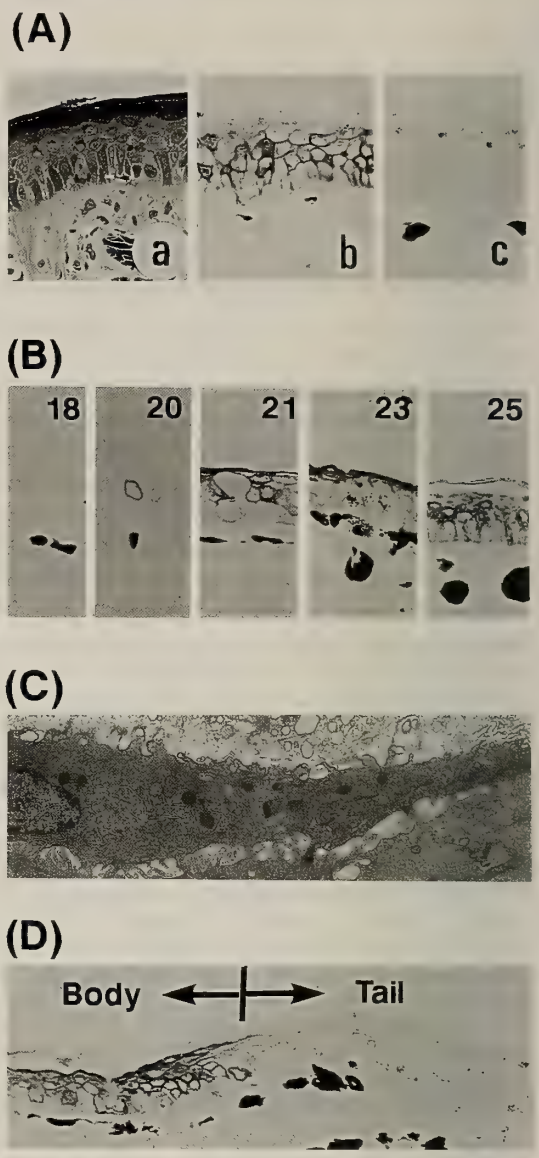

FIG. 1. Immunostaining of the epidermis by antisera against human blood group antigen A. (A) Cross section of the adult dorsal body skin. a, Section stained with toluidine blue, showing a typical five- or six- layered epidermal cells on the dermis. b, Immunostained section, showing that granular cells are positive but outermost keratinized and innermost germinative cells are negative. c, Negative control section stained with the anti-A antiserum which had been immunoabsorbed by human group A blood cells. Black granules in the epidermis were melanins of pigment cells. Magnification: 200×. (B) Immunostaining of the dorsal body skin of tadpoles during spontaneous metamorphosis. The number indicated in each figure shows the metamorphic stage defined by Taylor and Kollros [9]. A few positive cells appeared first at stage XX. The black-colored cells in the dermis are melanocytes. Magnification: 200×. (C) An electron micrograph of a cell which reacts with anti-A antiserum. Magnification: 2000×. (D) A section of the body-tail junction of the skin at stage XXI. The section was immunostained by anti-A antiserum. Black bodies under the epidermis are melanocytes. Note the clear immunological difference of the tail and the body epidermis. Magnification: 150×.

RESULTS AND DISCUSSION

It was found that the human blood group antigen A (A) is a useful probe for the analysis of transition of the epidermis during metamorphosis. Keratinizing cells in the stratum spinosum of the adult body skin of bullfrog were immunostained by the anti-A antiserum (Fig. 1A). This reaction was specifically immunoabsorbed by human A group blood cells. The keratinized outermost layer of the stratum corneum and the innermostlayer of the stratum basale were negative to the antiserum. These indicate that keratinizing daughter cells of basal cells in the germinative layer express human blood group antigen A.

Contrary to the adult skin, we found that there exist no epidermal cells positive to the antiserum in the entire skin of tadpoles at pre- and prometamorphic stages (Fig. 1B). A few positive cells appeared in the epidermis of the body at stage XX, which were flat in shape (Fig. 1C). The presence of A-positive cells at stage XX indicates the appearance of adult-type germinative cells in the body skin at this critical stage of metamorphosis, because they are differentiated daughter cells of germinative cells as shown in Figure 1A. The A-antigen expressing cells increased dramatically in their numbers at stage XXI through stage XXV, when the tail is lost completely, suggesting that basal cells are actively transforming into the germinative cells during climax stages of metamorphosis. It, therefore, can be concluded that the anti-A antiserum is a useful probe for the analysis of the conversion of basal cells from the larval type to the adult one during metamorphosis.

As expected, the tail epidermis did not contain the cells reactive to anti-A antibodies at stage XXI (the climax metamorphic stage) (Fig. 1D), indicating the absence of cells transforming into the adult type. As shown in the figure, the body and the tail epidermis was clearly separated at stage XXI for their reactivity to the antibody.

In vitro studies on epidermal cells clearly demonstrated that thyroid hormone (TH) is directly involved in the conversion of the larva-type epidermis to the adult type. The back skin was treated first with ethylenediaminetetraacetate (EDTA) to remove apical cells. Skein and basal cells were isolated from the EDTA-treated skin by digesting it further with trypsin and EDTA [6]. Cells thus obtained contained skein cells and basal cells with ratios of about 70% and 30%, respectively. They were cultured for 4 days in the presence of T_3 at the concentration of 10^{-8} M. The body cells were induced to express the antigens reactive to anti-A antiserum (Fig. 2, b and d). The identical *in vitro* study was performed for primary tail epidermal cells which were almost a homogeneous population of skein cells. Unexpectedly, tail epidermal cells were also induced to express the adult-type specific antigen as body cells (Fig. 2, a and c). Nishikawa *et al.* [5] recently obtained the similar result utilizing other adult-specific antigen as a prove. Epidermal keratin of *Xenopus laevis* with a molecular weight of 63 K is expressed in the adult but not in the larva. Tail epidermal cells of *X. laevis* were cultured in the presence of TH and shown to express 63 KDa

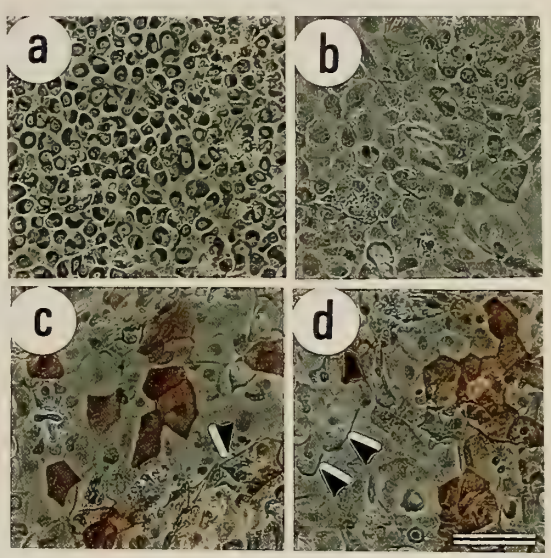

FIG. 2. Induction of anti-A positive cells in cultured epidermal cells. Eight hundred thousand epidermal cells obtained from tadpoles at stage X were cultured in 22-mm dishes at 24°C for 2 days. Media were changed and the culture was continued for additional 4 days in the presence or absence of 10^{-8} M T_3. Cells were immunostained with anti-A antiserum. a and c, tail cells; b and d, body cells; a and b, in the absence of T_3; c and d, in the presence of T_3. Anti-A positive cells are colored brown. Completely keratinized cells are not stained (arrowheads). Bars represent 100 μm.

keratin.

It is reasonable and expectable that the epidermis of the body contains the cells which express adult type characters under the influence of TH. Basal and skein cells in the primary culture seem to respond differently to TH. The former is stimulated to proliferate and then transform into the antigen-expressing adult-type cell, while the latter is fallen into the cell death by the direct action of TH [4]. The result of *in vitro* experiment for body epidermal cells coincides with that of *in vivo* experiment shown in Figure 1.

On the other hand, the *in vitro* result for the tail cells is against expectation in the following four reasons: the tail epidermis apparently need not provide for the adult-type cell, because its life ends up at metamorphosis [10]; the tail epidermis does not express the adult-type character *in vivo* at the climax stage of metamorphosis as shown above in Figure 1D; the tail epidermal primary culture does not contain basal cells as mentioned above; it was shown that the tail epidermis lacks basal cells [8]. However, the result shown in Figure 2 presents clear evidence that the tail contains a population of cells which is competent to convert to the adult type in response to TH.

The cells in the tail that expressed A-antigen in response to TH should be basal cells, because skein cells are to be subjected to the programmed cell death by the direct action of TH [4]. Two possibilities arise to explain the result of *in vitro* experiment of tail cells. One is that basal cells might be present in the tail cell population with so low frequencies as not to be detected micoscopically. This minor population of basal cells is stimulated by TH to proliferate and differentiate into the adult-type cells. The time course experiment on the A-antigen expression was performed. Few cells in the body but not in the tail expressed the antigen at day 0 (Fig. 3). These cells might be contaminated epidermal glandular cells which are known to exist in the body but not in the tail and produce A-antigens (Izutsu and Yoshizato, manuscript in submission). During 4 to 6 days in culture T_3 markedly enhanced the appearance of positive cells in both the tail and the body as in the case shown in Figure 2. It was noteworthy that a few positive cells appeared at day 4 to day 6 depending

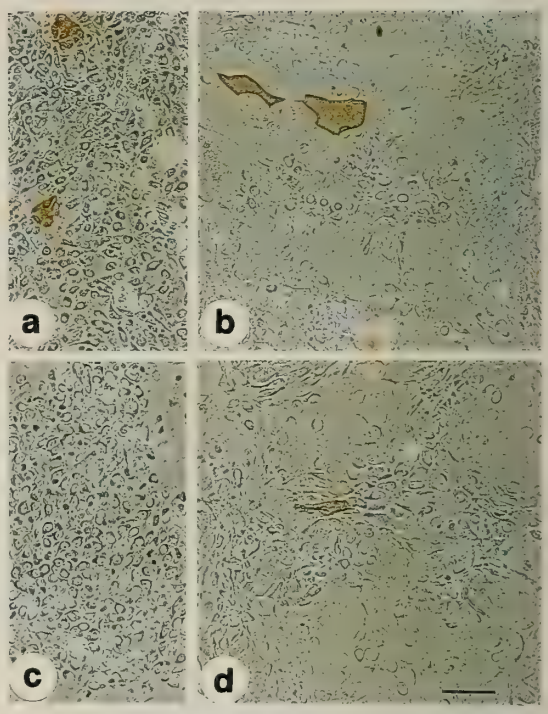

Fig. 3. Appearance of A-antigen expressing cells in tail and body epidermal cells in the absence of TH. Hundred thousand epidermal cells from tadpoles at stage X were cultured in 11-mm dishes for 2 days at 24°C. Media were changed (day 0) and the culture was continued for additional 6 days with a medium change at day 4. Cells were immunostained with anti-A antiserum. a and b, body cells; c and d, tail cells; a and c, day 0; b and d, day 6 without T_3. The bar equals 100 μm.

on experiments in a T_3-free culture of tail cells which contained about 10^5 cells (Fig. 3d). This supports the possibility described above that very few basal cells are included in the tail epidermis. Also a few additional positive cells appeared in T_3-free cultures of body cells, suggesting that the "differentiation" of the larval basal cell into the adult germinative cell could occur spontaneously at a very low level.

The second possibility is described below and is related to the difference between *in vivo* and *in vitro* status of epidermal cells. The reactivity of tail epidermal cells to anti-A antiserum was quite different between *in vivo* and *in vitro* experiments. As shown in Figure 1D, the tail epidermis *in vivo* does not show the positive reactivity even at the

climax stages of metamorphosis in which the plasma level of TH is high enough [7]. There might be some unknown factor(s) *in vivo* which suppresses the expression of A-antigen in the tail epidermis even in the presence of TH.

The character of the epidermis as tail or body seems to be determined by some mesenchymal factor. Utilizing transplantation techniques, Kinoshita *et al.* [3] revealed that the epidermis combined with the tail dermis undergoes degenerative changes during metamorphosis, irrespective of the origin of the epidermis (tail or body), while the tail epidermis combined with the body dermis transforms into the body-type and differentiates into the adult type. Based upon these we propose the second possibility that skein cells are not a homogeneous population: some skein cells could transform into basal cells. The epitheliomesenchymal interaction is postulated for this transformation. The body mesenchyme is required for the epidermal skein cell to "differentiate" into the basal cell. In contrast, the tail mesenchyme inhibits this transformation. When tail epidermal cells are removed from its mesenchyme and are cultured, some of them transform into basal cells because they are free from the influence of the mesenchyme. Thus, the tail epidermal cell in culture is competent to express A-antigens when exposed to TH.

REFERENCES

1 Kaiho M, Ishiyama I (1987) Zool Sci 4: 627–634
2 Kaiho M, Nakamura T, Kumegawa M (1975) Anat Rec 183: 405–420
3 Kinoshita T, Sasaki F, Watanabe K (1986) Cell Tissue Res 245: 297–304
4 Nishikawa A, Kaiho M, Yoshizato K (1989) Dev Biol 131: 337–344
5 Nishikawa A, Shimizu-Nishikawa K, Miller L (1992) Dev Biol 151: 145–153
6 Nishikawa A, Yoshizato K (1985) Zool Sci 2: 201–211
7 Regard E, Taurog A, Nakashima T (1978) Endocrinology 102: 674–684
8 Robinson DH, Heintzelman MB (1987) Anat Rec 217: 305–317
9 Taylor AC, Kollros JJ (1946) Anat Rec 94: 7–23
10 Yoshizato K (1989) Int Rev Cytol 119: 97–149
11 Yoshizato K, Kikuyama S, Shioya N (1980) Biochem Biophys Acta 627: 23–29

ZOOLOGICAL SCIENCE 10: 189–192 (1993)

[RAPID COMMUNICATION]

Kinetics of First Spermatogenesis in Young Toads of *Xenopus laevis*

Tohru Kobayashi[1,2], Yohko Asakawa[1] and Hisaaki Iwasawa[1]

[1]*Biological Institute, Faculty of Science, and* [2]*Graduate School of Science and Technology, Niigata University, Niigata 950-21, Japan*

ABSTRACT—The kinetic profile of first spermatogenesis was examined at 22±1°C in young toads of *Xenopus laevis*. The most progressed spermatogenic stage was primary spermatogonia in newly metamorphosed toads. Secondary spermatogonia were observed 3 days after metamorphosis. First leptotene and pachytene spermatocytes appeared 17 and 20 days after metamorphosis, respectively. Then first diplotene spermatocytes, meiotic division and round spermatids were observed 42 days, and first mature spermatozoa 70 days, after metamorphosis. On the basis of these results, the difference between the time required for first spermatogenesis in young toads and cycling spermatogenesis in adult toads is discussed.

INTRODUCTION

The kinetics of spermatogenesis in amphibians has been studied by several investigators, but the materials used in their studies were mostly subadult and adult animals [2, 4, 9, 17]. The formation of spermatozoa in juvenile frogs has been reported as precocious spermatogenesis in several species [5, 7, 22, 23], but these papers simply describe the phenomenon. Recently, we defined the kinetics of cycling spermatogenesis at 22°C in adult toads of *Xenopus laevis* [2]. In the present study, the time after metamorphosis at which the most rapidly progressed spermatogenic cells appeared at 22°C is examined in young toads of this species, and difference between these results and the kinetics of cycling spermatogenesis in adult toads was discussed.

Accepted August 18, 1992
Received June 8, 1992

MATERIALS AND METHODS

Numerous fertilized eggs were obtained from a few pairs of male and female toads *Xenopus laevis* injected with a human chorionic gonadotropin (Gonatropin, Teikoku Zoki Co., Tokyo). The eggs, embryos, and larvae were kept in dechlorinated tap water at 22±1°C. The larvae and young toads were fed on a commercial diet for carp. These details were previously described [3, 8].

Until the time of the first appearance of spermatozoa after metamorphosis, three to four young toads were decapitated every day, and the testes were fixed in Bouin's solution. The testes were then embedded in Paraplast (Sherwood Medical, St. Louis, U.S.A.), and sectioned serially at 4 μm. The sections were stained with Carazzi's hematoxylin and eosin.

RESULTS AND DISCUSSION

In this study, the average body length just after metamorphosis was 15 mm, and was 20 mm at the end of experiment (82 days after metamorphosis). As previously reported [8], seminiferous tubules were clearly observed in young toads just after metamorphosis. At this time (0 day after metamorphosis), the seminiferous tubules were filled with primary spermatogonia. The days on which

TABLE 1. The most rapidly progressed spermatogenic stage of first spermatogenesis in *Xenopus laevis*

Days after metamorphosis	Stage
0	primary spermatogonium
3–16	secondary spermatogonium
17–19	primary spermatocyte (leptotene)
20–29	zygotene
30–41	pachytene
42–64	diplotene-round spermatid
65–69	elongated spermatid
70–82	spermatozoon

the most rapidly progressed spermatogenic stages were observed are shown in Table 1. The first appearance of spermatocytes and spermatids was observed on 17 days and 42 days after metamorphosis, respectively. Elongated spermatids were seen 65 days after metamorphosis. Seventy days after metamorphosis, the first spermatozoa were observed, though the number is a few (Fig. 1a). When the round spermatids differentiated into the elongated spermatids (from 45 to 70 days after metamorphosis), pycnotic germ cells were frequently observed (Fig. 1b).

From the results shown in Table 1, the duration of each spermatogenic process was calculated. The duration of leptotene, zygotene, and pachytene spermatocytes was 3, 10, and 12 days. The progression from the diplotene spermatocytes to the round spermatids was accomplished within one day. The duration of spermiogenesis was 28 days, whereas the progression of elongated spermatids to spermatozoa was 5 days.

In a previous study, we determined the time required for the progression of cycling spermatogenesis at 22°C in adult *X. laevis* ([2], Kobayashi, unpublished). Although the time required for the progression from elongated spermatids to spermatozoa was similar between young and adult toads (young toads: 5 days, adult toads: 4 days), the present study (Table 1) indicates that the progression from round spermatids to elongated spermatids in young toads was greatly delayed compared with that in adult toads [2] (young toads: 23 days, adult toads: 4 days). In this study, furthermore, during spermiogenesis the degeneration of germ cells, probably round to elongated spermatids, was frequently observed. From these facts, it is suggested that the delay of spermiogenic progression in first spermatogenesis is caused by the failure of nuclear elongation of spermatids. It seems, therefore, that the time required for the progression from round to elongated spermatids in first spermatogenesis is the real time required for the progression from round to elongated spermatids plus the time required for the appearance of round spermatids which could be differentiated into elongated spermatids. Thus, it is calculated that first appearance of round spermatids which

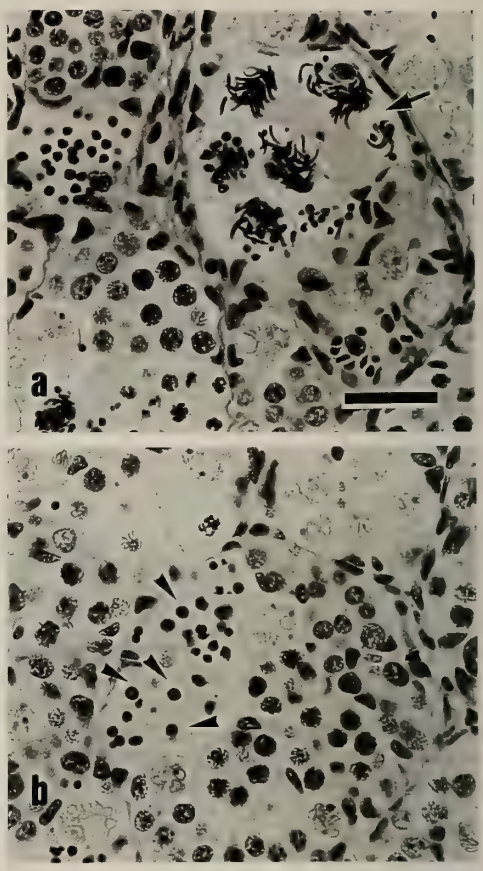

FIG. 1. First spermatogenesis in *X. laevis*. a: First spermatozoa (arrow) are seen 70 days after metamorphosis. b: Pycnotic substances (arrow head) are frequently seen from 45 to 70 days after metamorphosis. Scale bar: 30 μm.

could be differentiated into elongated spermatids is 19 days after the first appearance of round spermatids, if the duration of progression from round to elongated spermatids is similar to that in adult toads as in mice [21]. To define the dynamics in first spermatogenesis, further studies will be necessary.

In *X. laevis* and *Cynops pyrrhogaster,* it is known that in an *in vitro* cell culture system progression from primary spermatocytes to elongated spermatids was accomplished but spermiogenesis failed to be completed [1]. When nuclear elongation proceeds *in vivo,* in *X. laevis,* a few of microtubules contained in spermatids were cast off along with cytoplasm and numerous microtubules in Sertoli cells were situated approximately parallel to the axis of spermatids elongation in the area which immediately surround the spermatids [18]. In *X. laevis* [19], furthermore, progression from premeiotic S spermatogenic cells to mature spermatozoa was accomplished in an *in vitro* organ culture system. Thus, in *X. laevis,* it seems that Sertoli cells play the primary role for the nuclear elongation of spermatids. Therefore, the failure of the progression from round to elongated spermatids may be caused by the lack of functional Sertoli cells and/or abnormality of spermatids, though the functional characterization of Sertoli cells and spermatogenic cells was not clarified in details.

In *Rana esculenta* it was suggested that the completion of spermiogenesis required androgen [15, 16]. Concerning the experiment which dealt with precocious spermatogenesis in *Rana nigromaculata,* we pointed out that androgen was needed for the completion of spermiogenesis [10, 11, 24, 25]. In immature rats, on the other hand, it was reported that an increase of luteinizing hormone binding sites in Leydig cells was induced by prolactin (PRL), though this phenomenon was accompanied by the decrease of PRL-binding sites [12]. On this point, in anurans, it is known that serum PRL levels are high at the climax of metamorphosis [23]. In *X. laevis*, it was reported that gonadotropin- and PRL-producing cells were observed at premetamorphic stages [13, 14]. Furthermore, it was reported that PRL binding sites was present in testes [6]. Although, at present, the information on these pituitary hormonal levels and gonadal steroid levels in young toads of *X. laevis* is few, defined steroid producing cells in the testes were not observed electron microscopically 70 days after metamorphosis (Kobayashi, unpublished). Therefore, it is possible that androgen is involved in spermiogenic process. In this study, however, whether or not the relationship between PRL and androgen production during first spermatogenesis is not known.

In conclusion, the present study indicates in *X. laevis* that the duration of spermatogenesis in first spermatogenesis in young toads is much longer than that of cycling spermatogenesis in adult toads. This delay may be caused by the failure of nuclear elongation of spermatids.

REFERENCES

1 Ábe S-I (1987) Int Rev Cytol 109: 159–209
2 Asakawa Y, Kobayashi T, Iwasawa H (1990) Zool Sci 7: 1088 (Abstract)
3 Asakawa Y, Kobayashi T, Iwasawa H (1991) Biomed Res 12: 269–272
4 Callan HG, Taylor JH (1967) J Cell Sci 3: 615–626
5 Goto G (1940) Acta Anat Nippon 22: 30–43 (Abstract in English)
6 Guardabassi A, Muccioli G, Pattono P, Bellussi G (1987) Gen Comp Endocrinol 65: 40–47
7 Iwasawa H, Kobayashi M. (1976) Copeia 1976: 461–467
8 Iwasawa H, Yamaguchi K (1984) Zool Sci 1: 591–600
9 Kalt MR (1976) J Exp Zool 195: 393–408
10 Kobayashi T, Iwasawa H (1988) Copeia 1988: 1067–1071
11 Kobayashi T, Iwasawa H (1986) Zool Sci 3: 387–390
12 Morris PL, Saxena BB (1980) Endocrinology 107: 1639–1645
13 Moriceau-Hay D, Doerr-Schott J, Dubois MP (1979) Gen Comp Endocrinol 39: 322–326
14 Moriceau-Hay D, Doerr-Schott J, Dubois MP (1982) Cell Tissue Res 225: 57–64
15 Rastogi RK, Iela L, Saxena PK, Chieffi G (1976) J Exp Zool 196: 151–166
16 Rastogi RK, Iela L, Delrio G, diMeglio M, Russo A, Chieffi G (1978) J. Exp Zool 206: 49–64
17 Rastogi RK, Iela L, diMeglio M, Russo A, Chieffi G (1983) J Zool Lond 201: 515–525
18 Reed SC, Stanley HP (1972) J Ultrastruct Res 41: 277–295
19 Risley MS, Miller A, Bumcrot RA (1987) Biol

Reprod 36: 985–997
20 Rosenkilde P (1985) In "Metamorphosis", Ed by M Balls and M Bownes, Clarendon Press, Oxford, pp 221–259
21 Sung WK, Komatsu M, Jagiello GM (1986) Gamete Res 14: 245–254
22 Swingle WW (1921) J Exp Zool 32: 235–331
23 Takahashi H (1971) Zool Mag (Tokyo), 80: 15–21 (Abstract in English)
24 Tanaka S, Iwasawa H, Wakabayashi K (1988) Zool Sci 5: 1007–1012
25 Tanaka S, Iwasawa H (1989) Sci Rep Niigata Univ Ser D 26: 1–11

INSTRUCTIONS TO AUTHORS

ZOOLOCIGAL SCIENCE publishes contributions, written in English, in the form of (1) **Reviews**, (2) **Articles**, and (3) **Rapid Communications** for short reports of timely and unusual interest. A *Review* is usually invited by the Editors. Those who submit reviews should consult with the Editor-in-Chief or the Managing Editor in advance. *Articles* of less than 6 printed pages and *Rapid Communications* less than 3 printed pages will be published free of charge. Charges will be made for extra pages (10,000 yen/page). A *Rapid Communication* cannot exceed 4 printed pages. No charge will be imposed for invited reviews up to 15 printed pages. No free reprints of Articles and Rapid Communications are available. To the author(s) of an invited review 50 reprints are provided gratis. Submission of papers from nonmembers of the Society is welcome. However, page charges (10,000 yen/page) will be made to nonmembers.

A. SUBMISSION OF MANUSCRIPT

The manuscript should be submitted in triplicate, one original and two copies, each including all illustrations. Rough copies of line drawings and graphs may accompany the manuscript copies, but the two copies of continuous-tone prints (photomicrographs, etc.) should be as informative as the original. The manuscript should be sent to:

Dr. Tsuneo Yamaguchi, Managing Editor, Zoological Science, Department of Biology, Faculty of Science, Okayama University, Okayama 700, Japan.

B. CONDITIONS

All manuscripts are subjected to editorial review. A manuscript which has been published or of which a substantial portion has been published elsewhere will not be accepted. It is the author's responsibility to obtain permission to reproduce illustrations, tables, etc. from other publications. Accepted papers become the permanent property of ZOOLOGICAL SCIENCE and may not be reproduced by any means, in whole or in part, without the written consent of both the Zoological Society of Japan and the author(s) of the article in question.

C. ORGANIZATION OF MANUSCRIPT

The desirable style of the organization of an original paper is as follows: (1) Title, Author(s) and Affiliation (2) Abstract (3) Introduction (4) Materials and Methods (5) Results (6) Discussion (7) Acknowledgments (8) References (9) Tables (10) Illustrations and Legends. The author is not obliged to adhere rigidly to this organization. He or she may modify the style when such modification makes the presentation clearer and more effective. In a Rapid Communication, combination of some of these sections is recommended. There is no restriction on the style of review articles.

D. FORM OF MANUSCRIPT

Manuscripts should be typewritten and double spaced throughout on one side of white typewriting paper with 2.5 cm margins on all sides. Abstract not exceeding 250 words, tables, figure legends and footnotes should be typed on separate sheets. All manuscript sheets must be numbered successively. The use of footnotes to the text is not recommended.

1. Title page

The first page of manuscript should contain title, authors' names and addresses of university or institution, abbreviated form of title (40 characters or less, including spaces), and name and address for correspondence, and any footnotes. Authors with different affiliations should be identified by the use of the same superscript on name and affiliation. If one or more of the authors has changed his or her address since the work was carried out, the present address(es) to be published should be indicated in a footnote. In addition, a sub-field of submitted papers to be used as heading of an issue may be indicated in the first page. Authors are encouraged to choose one of the following: physiology, cell biology, molecular

biology, genetics, immunology, biochemistry, developmental biology, reproductive biology, endocrinology, behavior biology, ecology, phylogeny, taxonomy, or others (specify). However, the Editors are responsible for the choice and arrangement of headings.

2. Introduction

This section should clearly describe the objectives of the study, and provide enough background information to make it clear why the study was undertaken. Lengthy reviews of past literature are discouraged.

3. Materials and Methods

This section should provide the reader with all the information that will make it possible to repeat the work. For modification of published methodology, only the modification needs to be described with reference to the source of the method.

4. Results

Results should be presented referring to tables and figures, without discussion.

5. Discussion

The Discussion should include a concise statement of the principal findings, a discussion of the validity of the observations, a discussion of the findings in the light of other published works dealing with the same subject, and a discussion of the significance of the work. Redundant repetition of material in Introduction and Results, and extensive discussion of the literature are discouraged.

6. Statistical analysis

Statistical analysis of the data using appropriate methods is mandatory and the method(s) used must be cited.

7. References

References should be cited in the text at the appropriate places by numbers in square parentheses. All references cited in the text should be listed at the end of the paper on a separate page, arranged in alphabetical order and numbered consecutively. For example:

1 Campbell RC (1974) Statistics for Biologists. Cambridge Univ. Press, London, 2nd ed, pp 59–61

2 Shima A, Ikenaga M, Nikaido O, Takabe H, Egami N (1981) Photoreactivation of ultraviolet light-induced damage in cultured fish cells as revealed by increased colony forming ability and decreased content of pyrimidine dimers. Photochem Photobiol 33: 313–316

3 Takewaki K (1931) Oestrous cycle of female rat in parabiotic union with male. J Fac Sci Imp Univ Tokyo, Sec IV, 2: 353–356

4 Wiersma CAG (1961) Reflexes and the central nervous system. In "The Physiology of Crustacea Vol 2" Ed by TH Waterman, Academic Press, New York, pp 241–279

Titles of cited papers may be omitted in Reviews and Rapid Communications. The source of reference should be given following the commonly accepted abbreviations for journal titles (e,g., refer to 'International List of Periodical Title Abbreviations'). The use of "in preparation", "submitted for publication" or "personal communication" is not allowed in the reference list. "Unpublished data" and "Personal communication" should appear parenthetically following the name(s) in the text. Text citations to references with three or more authors should be styled as, e.g., Everett *et al.* [7].

E. ABBREVIATIONS

Abbreviations of measurement units, quantity units, chemical names and other technical terms in the body of the paper should be used after they are defined clearly in the place they first appear in the text. However, abbreviations that would be recognized by scientists outside the author's field may be used without definition, such as *P*, SD, SE, DNA, RNA, ATP, ADP, AMP, EDTA, UV, and CoA. The metric system should be used for all measurements, and metric abbreviations (Table)

Table. Abbreviations for units of measure which may be used without definition

Length:	km, m, cm, mm, μm, nm, pm, etc.
Area:	km^2, m^2, cm^2, mm^2 μm^2, nm^2, pm^2, etc.
Volume:	km^3, m^3, cm^3, mm^3, μm^3, nm^3, pm^3, kl, liter (always spellout), ml, μl, nl, etc.
Weight:	kg, g, mg, μg, ng, pg, etc.
Concentration:	M, mM, μM, nM, %, g/l, mg/l, μg/l, etc.
Time:	hr, min, sec, msec, μsec, etc.
Other units:	A, W, C, atm, cal, kcal, R, Ci, cpm, dB, v, Hz, lx, $\times g$, rpm, S, J, IU, etc.

should, in general, be expressed in lower case without periods.

F. PREPARATIONS OF TABLES

Tables should only include essential data needed to show important points in the text. Each table should be typed on a separate sheet of paper and must have an explanatory title and sufficient explanatory material. All tables should be referred to in the text, and their approximate position indicated in the margin of manuscript.

G. PREPARATION OF ILLUSTRATIONS

All figures should be appropriately lettered and labelled with letters and numbers that will be at least 1.5 mm high in the final reproduction. Note the conventions for abbreviations used in the journals so that usage in illustrations and text is consistent. All figures should be referred to in the text and numbered consecutively (Fig. 1, Fig. 2, etc.). The figures must be identified on the reverse side with the author's name, the figure number and the orientation of the figure (top and bottom). The preferred location of the figures should be indicated in the margin of the manuscipt. Illustrations that are substandard will be returned, delaying publication. Illustrations in color may be published at the author's expense.

1. Line drawings and graphs

Original artwork of high quality, glossy prints mounted on appropriate mounting card (**less than 25×38 cm**) should be submitted for reproduction. Author(s) may indicate size preference by making on the back of figures, such as "Do not reduce", "Two-column width" (**no wider than 14 cm**), or "One-column width" (**no wider than 7 cm**). Lines must be dark and sharply drawn. Solid black, white, or bold designs should be used for histograms. Xerox or any other copying mean may be used for the two review copies.

2. Continuous-tone prints

Three sets of continuous-tone prints (photomicrographs, etc.) must be submitted. One set for reproduction should be mounted on appropriate mounting card, and the other two for reviewers may be unmounted prints. Xerox or similar copies of photomicrographs are not acceptable for review purposes. The continuous-tone prints should be submitted preferably at the exact magnification which is to be used in the published papers and trimmed to conform to the page size (**in no case should it exceed 14×20 cm**). Press-on numbers should be applied to the lower right corner of individual prints. Letters (a, b, c, etc.) should be used for multiple parts of a single figure. If important structures will be covered by use of the lower right corner, identification may be applied in the lower left corner.

Reproduction of color photographs will have to be approved by the Editors. The extra costs of color reproduction will be charged to the author(s).

3. Figure legends

Each figure should be accompanied by a title and an explanatory legend. The legends for several figures may be typed on the same sheet of paper. Sufficient detail should be given in the legend to make it intelligible without reference to the text.

H. PROOF AND REPRINTS

A galley proof and reprint order will be sent to the submitting author. The first proofreading is the author's responsibility, and the proof should be returned within 72 hours from the date of receipt (by air mail from outside Japan). The minimum quantity for a reprint order is fifty. Manuscript, tables and illustrations will be discarded after the editorial use unless their return is requested when the manuscript is accepted for publication.

I. WORD-PROCESSOR DISKS

The Zoological Science can use your word-processor disks (5 1/4 or 3 1/2 inch). If available, **please send a copy of the disk with your final revised manuscript (two copies of the printout)**. This gives us a substantial decrease in typesetting time and assures you that there are no re-keying errors in the article. Moreover, using word-processor disks helps us to shorten publication times. If you would be willing to lend us the disk, please obey the following instructions.

1. Label the disk with the author's name; the word processor/computer used (e.g., NEC 9801, IBM-PC, Macintosh); the name of program (e.g., WordPerfect, WordStar, MS-Word, MacWrite).

If you have an editor's manuscript number, include it on the label.

2. Send the manuscript as three files; if possible **keep the text, figure legends, and tables in separate files**. File names must clearly indicate the content of each file.

3. Send separate disks if you submit more than one article at a time.

4. A hard copy printout of the manuscript that exactly matches the disk files must be supplied. Special characters and symbols which are not included in the printer used, should be left as blank spaces in the files and these should be correctly written in the printout **in red**.

5. Do not use footnote.

6. Do not justify the right-hand margin.

7. For further information on preparing the disk, please contact the publisher (Daigaku Letterpress Co., Ltd., 809-5, Asakita-ku Kamifukawacho, Hiroshima 739-17, Japan; telephone: (082) 844-7500; fax:(082) 844-7800).

Development
Growth & Differentiation

Published Bimonthly by the Japanese Society of Developmental Biologists
Distributed by Business Center for Academic Societies Japan, Academic Press, Inc.

Papers in Vol. 35, No. 1. (February 1993)

Development, Growth and Differentiation (ISSN 0012–1592) is published bimonthly by The Japanese Society of Developmental Biologists. Annual subscription for Vol. 35 1993 U. S. $ 191,00, U. S. and Canada; U. S. $ 211,00, all other countries except Japan. All prices include postage, handling and air speed delivery except Japan. Second class postage paid at Jamaica, N.Y. 11431, U. S. A.

Outside Japan: Send subscription orders and notices of change of address to Academic Press, Inc., Journal Subscription Fulfillment Department, 6277, Sea Harbor Drive, Orlando, FL 32887–4900, U. S. A. Send notices of change of address at least 6–8 weeks in advance. Please include both old and new addresses. U. S. A. POSTMASTER: Send changes of address to *Development, Growth and Differentiation,* Academic Press. Inc., Journal Subscription Fulfillment Department, 6277, Sea Harbor Drive, Orlando, FL 32887–4900, U. S. A.

In Japan: Send nonmember subscription orders and notices of change of address to Business Center for Academic Societies Japan, 16–9, Honkomagome 5-chome, Bunkyo-ku, Tokyo 113, Japan. Send inquiries about membership to Business Center for Academic Societies Japan, 16–9, Honkomagome 5-chome, Bunkyo-ku, Tokyo 113, Japan.

Air freight and mailing in the U. S. A. by Publications Expediting, Inc., 200 Meacham Avenue, Elmont, NY 11003, U. S. A.

The Ultimate Name in Micromanipulation
Ease of operation, and the most advanced

Can be combined with
New WR & MX series

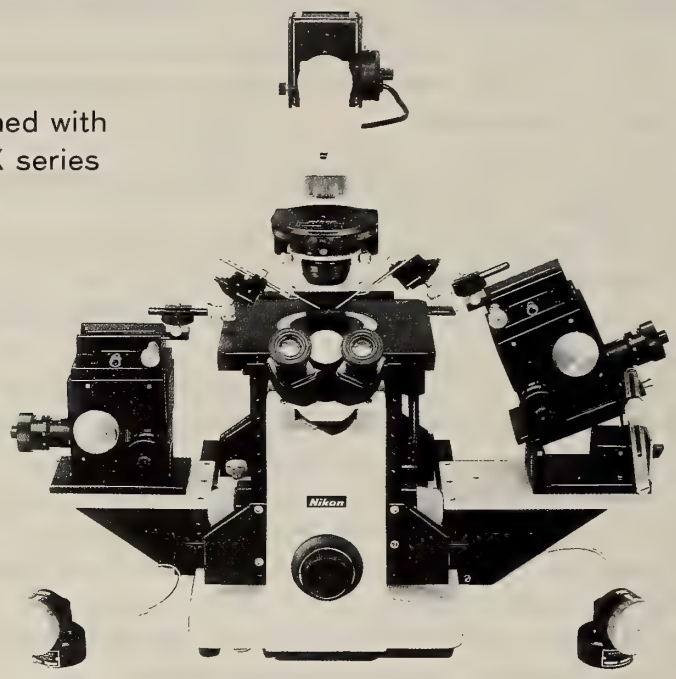

Model MX-1
3-D Micromanipulator

Model MX-2
3-D Micromanipulator

Model WR-87
One Dimensional
Aqua Purificate
Micromanipulator

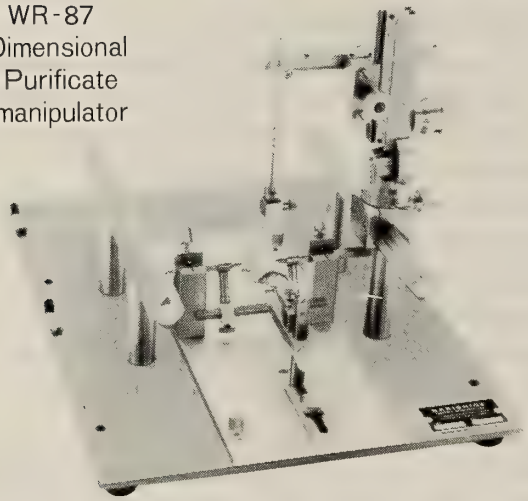

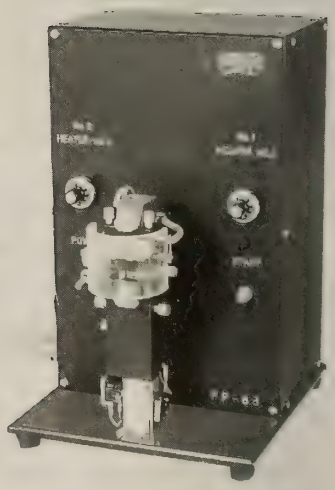

Model SR-6
Stereotaxic Instrument for Rat

Model PP-83
Glass Microelectrode Puller

* * * Send enquiries for request for MODIFICATIONS or IMPROVEMENTS * * *
Physiological, Pharmacological, Zoological & Neurosciences Research Equipments

---

NARISHIGE JAPAN

NARISHIGE SCIENTIFIC INSTRUMENT LAB.

9-28 KASUYA 4-CHOME SETAGAYA-KU, TOKYO 157, JAPAN
PHONE(INT-L)81-3-3308-8233, FAX(INT-L)81-3-3308-2005
CABLE:NARISHIGE LABO, TELEX, NARISHIGE J27781

(*Contents continued from back cover*)

ZOOLOGICAL SCIENCE

VOLUME 10 NUMBER 1 FEBRUARY 1993

CONTENTS

(*Contents continued on inside back cover*)

INDEXED IN:
Current Contents/LS and AB & ES,
Science Citation Index,
ISI Online Database,
CABS Database, INFOBIB

Issued on February 15
Printed by Daigaku Letterpress Co., Ltd., Hiroshima, Japan

. 10 No. 2 April 1993

ZOOLOGICAL SCIENCE

An International Journal

PHYSIOLOGY
CELL and MOLECULAR BIOLOGY
GENETICS
IMMUNOLOGY
BIOCHEMISTRY
DEVELOPMENTAL BIOLOGY
REPRODUCTIVE BIOLOGY
ENDOCRINOLOGY
BEHAVIOR BIOLOGY
ENVIRONMENTAL BIOLOGY and ECOLOGY
SYSTEMATICS and TAXONOMY

published by Zoological Society of Japan

distributed by Business Center for Academic Societies Japan
VSP, Zeist, The Netherlands

ISSN 0289-0003

ZOOLOGICAL SCIENCE

The Official Journal of the Zoological Society of Japan

The Zoological Society of Japan:
Toshin-building, Hongo 2–27–2, Bunkyo-ku,
Tokyo 113, Japan. Phone (03) 3814–5675
Officers:
President: Hideo Mohri (Chiba)
Secretary: Hideo Namiki (Tokyo)
Treasurer: Makoto Okuno (Tokyo)
Librarian: Masatsune Takeda (Tokyo)

ZOOLOGICAL SCIENCE is devoted to publication of original articles, reviews and communications in the broad field of Zoology. The journal appears bimonthly. An annual volume consists of six numbers of more than 1200 pages including an issue containing abstracts of papers presented at the annual meeting of the Zoological Society of Japan.

MANUSCRIPTS OFFERED FOR CONSIDERATION AND CORRESPONDENCE CONCERNING EDITORIAL MATTERS should be sent to:

Dr. Tsuneo Yamaguchi, Managing Editor, Zoological Science, Department of Biology, Faculty of Science, Okayama University, Okayama 700, Japan, in accordance with the instructions to authors which appear in the first issue of each volume. Copies of instructions to authors will be sent upon request.

SUBSCRIPTIONS. ZOOLOGICAL SCIENCE is distributed free of charge to the members, both domestic and foreign, of the Zoological Society of Japan. To non-member subscribers within Japan, it is distributed by Business Center for Academic Societies Japan, 5–16–9 Honkomagome, Bunkyo-ku, Tokyo 113. Subscriptions outside Japan should be ordered from the sole agent, VSP, Godfried van Seystlaan 47, 3703 BR Zeist (postal address: P. O. Box 346, 3700 AH Zeist), The Netherlands. Subscription rates will be provided on request to these agents. New subscriptions and renewals begin with the first issue of the current volume.

[Publication of Zoological Science has been supported in part by a Grant-in-Aid for Publication of Scientific Research Results from the Ministry of Education, Science and Culture, Japan.]

ZOOLOGICAL SCIENCE 10: 197–222 (1993)

REVIEW

Behavior of Exogenously-introduced DNAs in Early Embryos of *Xenopus laevis*

Misaki Asano and Koichiro Shiokawa

Laboratory of Molecular Embryology, Zoological Institute, Faculty of Science, University of Tokyo, Bunkyo-ku, 113 Tokyo, Japan

ABSTRACT—Studies of the behavior of circular and linearized DNAs, injected into fertilized eggs of *Xenopus laevis*, have been reviewed. The review consists mainly of three parts: Formation of nucleus-like structures in the cytoplasm of the DNA-injected eggs, preservation and replication of injected DNAs within embryos, and expression of injected DNAs in the course of early embryonic development. The last part of the review is concerned with the control of the expression of circular and linearized DNAs, and will be discussed in some details, particularly in relation to the timing of the expression in early embryogenesis.

Previously, it has been reported that DNAs injected into fertilized *Xenopus* eggs are activated first at the 12th cleavage (the midblastula stage) along with the changes which are collectively called midblastula transition (MBT). However, this review will focus on our own data, in which it was shown that the nature of the promoter, and not the changes associated with the MBT, determines the timing of the expression of injected DNAs.

INTRODUCTION

Molecular biology of the gene expression in early amphibian embryogenesis started in 1962, when Brown and Caston [9] succeeded for the first time in extracting the RNA from *Rana pipiens* embryos of various developmental stages using phenol methods. In 1964, Brown and Littna [11] extended their study by injecting ^{32}P-orthophosphate into female *Xenopus laevis* and subsequently following the accumulation of the ^{32}P-labeled RNAs in the fertilized eggs during their development. Subsequently, Shiokawa and Yamana [70, 71], and Woodland and Gurdon [87] joined the studies of RNA synthesis in *Xenopus* embryonic cells. Consequently, a general view that in early embryogenesis of *Xenopus laevis* there are at least two characteristically distinct phases with respect to the pattern of RNA synthesis has been obtained [27]: The first phase being that of very active 4S RNA (mainly tRNA) synthesis with no apparent rRNA synthesis (blastula stage) and the second phase being that of the active rRNA synthesis (gastrula and later stages).

In 1981, we surveyed newly labeled 2′-O-methyl groups in high-molecular-weight RNA fractions using a large number of (^{3}H-methyl)methionine-labeled embryos at stages earlier than the blastula stage, and found that rRNA synthesis starts at the late blastula stage and not before that stage [65, 68], approximately 4 hr earlier than the gastrula stage. Subsequent to our studies, it has been proposed that large changes in cellular activities which are collectively termed as "midblastula transition (MBT)" take place in the embryonic cells at the 12th cleavage [52, 53]: The changes include the appearance of G1 phase in cell cycle, acquisition of cell motility, and initiation of the transcription from the nuclear genome.

More recently, however, we have found that expression of heterogeneous mRNA-like RNA takes place during the cleavage stage [51, 61, 64].

Received September 21, 1992

Thus, we proposed that RNA synthesis in early *Xenopus* embryogenesis consists of three different phases: The phase of a low but distinct level of mRNA-like RNA synthesis (cleavage stage), the phase of active tRNA synthesis (the blastula stage), and the phase of active rRNA synthesis (at and after the late blastula stage).

While the studies on gene expression from endogenous DNAs were in progress, Gurdon and Brown [28] went on to study the gene expression from exogenous DNA. They microinjected exogenous genes (5S DNA and rDNA) into fertilized *Xenopus laevis* eggs and followed the expression of these genes throughout the course of their early embryonic development. Following their study, many laborotaries started analysis of the control mechanism of the expression of cloned DNAs that had been introduced into fertilized *Xenopus* eggs (for review of the initial step of the studies, see 26).

Since then, numerous papers concerning the behavior of exogenously-injected DNAs using fertilized eggs of *Xenopus laevis* have been published. In reviewing these studies, we will first describe briefly about the technical aspects of the DNA injection in *Xenopus* system, and then go on to describe the morphological changes which take place in the cytoplasm of DNAs-injected eggs. Then, we will describe the general aspects of preservation and replication of injected DNAs, and compare the results of the experiments carried out to study the expression of the various injected DNAs in the course of embryonic development. We will touch briefly on the experiments which were carried out using coenocytic egg cells, or fertilized eggs whose cleavage was arrested by a low speed centrifugation, then finally compare the behavior of exogenous DNAs introduced into oocytes, unfertilized eggs, and fertilized eggs.

UNIQUE ASPECTS OF DNA-INJECTION STUDIES WHICH UTILIZE FERTILIZED *XENOPUS* EGGS

It may be of an advantage to start with very brief description of the technical aspects of DNA injection experiments which utilize fertilized *Xenopus* eggs. Unlike the microinjection in mouse embryos where exogenous DNAs are injected into the female pronucleus directly, microinjection in *Xenopus* eggs has at least two unique aspects.

Firstly, it is unpractical to inject DNA into the nucleus of *Xenopus* egg, because the egg is not transparent, and therefore cannot visualize its nucleus. Consequently, DNAs must be injected into the cytoplasm of *Xenopus* egg. Secondly, *Xenopus* eggs cleave rapidly (every 30 min), and during the cleavage its nuclear envelope disappears and reappears quickly in each division cycle. Therefore, even if it were possible to inject exogenous DNAs into the egg nucleus, the injected DNAs will be scattered promptly into the cytoplasm. However, this also means that exogenously-injected DNAs could be assembled rapidly in the nuclei together with chromosomal DNAs at each cleavage cycle, even though they were injected into the cytoplasm. Consequently, the cytoplasmic injection of exogenous DNAs in a fertilized *Xenopus laevis* egg may be same in effect as the injection into the nucleus.

Thus, the DNA injection in fertilized *Xenopus* egg clearly differs from those in the mouse, where the division of egg nucleus is very slow (every 24 hr), and in the medaka (*Oryzias latipes*), where DNA is injected into the oocyte nucleus, and the injected oocytes were cultured for 8 hr till maturation and then fertilized *in vitro* [55]. However, similarity can be seen between the DNA injection in *Xenopus* and those in sea urchin [20, 48, 83] (except for the special case of unusually transparent eggs of *Lytechinus variegatus*, where DNA could directly be injected into zygotic nucleus under the microscope; [22]), in zebrafish [77] and in rainbow trout [88].

CYTOLOGICAL CHANGES OBSERVED IN FERTILIZED *XENOPUS* EGGS INJECTED WITH EXOGENOUS DNAS

In *Xenopus laevis*, fertilized eggs undergo rapid and multiple cell divisions in order to increase cell number quickly for future morphogenesis. The first step of the process is the protrusion of second polar body, which is induced by sperm entry, and is accompanied by the assemblage of the female pronucleus. It appears that the formation of the pronucleus depends on the maternal stockpiles

within the egg cytoplasm, since formation of nucleus-like structures is induced even in an *in vitro* system which consists of demembranated sperm nuclei (or naked DNAs) and egg homogenates [35, 44, 54].

It has been shown that when a relatively large amount of exogenous DNA is injected into the cytoplasm of either unfertilized [21] or fertilized [17, 66, 69, 82] eggs of *Xenopus laevis,* large nucleus-like structures are formed in the cytoplasm. Therefore, we shall describe the cytological features of such nucleus-like structures first.

Assemblage of the nucleus-like structures in the animal hemisphere

Unfertilized eggs of *Xenopus laevis* contain metaphase-arrested spindle in the animal-most region of the egg (Fig. 1A). When fertilized, the arrested nucleus completes its nuclear division, and forms a female pronucleus. Uninjected control eggs which were fixed 1.5 hr after insemination contained normal zygotic nucleus of ca. 25 μm in diameter usually in the upper part of the animal hemisphere. When a large amount (24 ng) of bacteriophage lambda DNA was injected into the

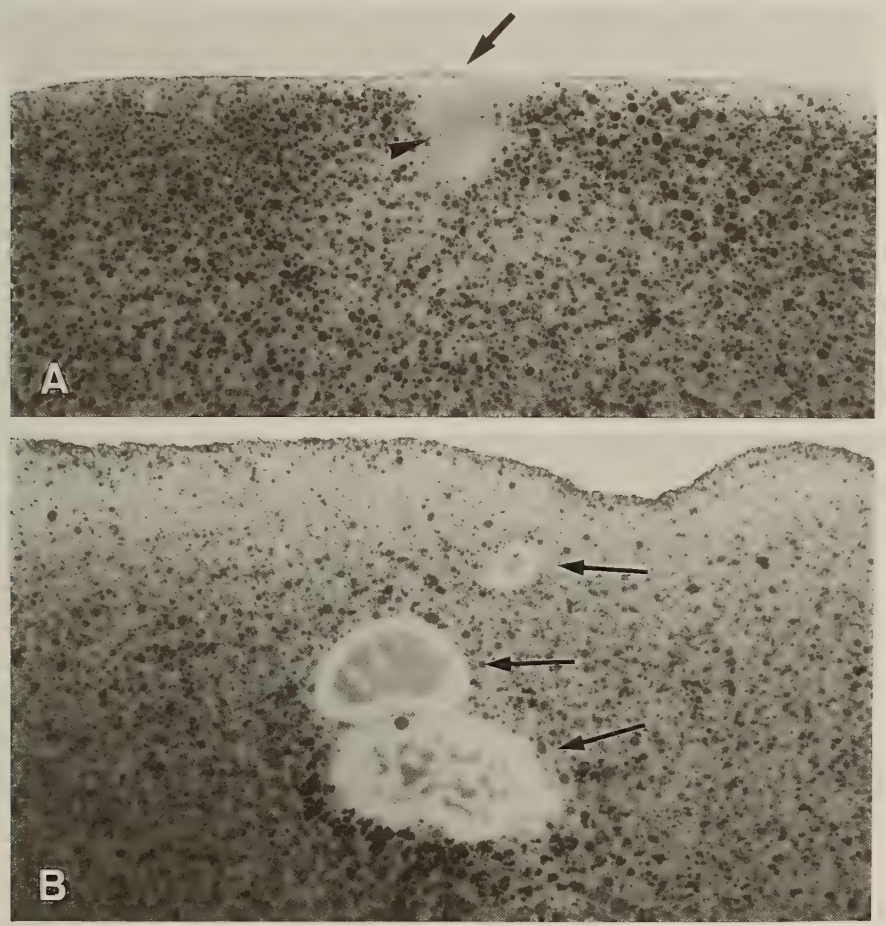

FIG. 1. Light microscopic appearance of nucleus-like structures. (A) Animal pole region of the control uninjected unfertilized *Xenopus laevis* egg. The arrow indicates the metaphase-arrested nucleus. An arrow head indicates the position of equatorial plate. (B) A fertilized *Xenopus laevis* egg was injected with 24 ng of bacteriophage lambda DNA using Narishige microinjector and the was fixed in glutaraldehyde about 1.5 hr after the injection. Arrows indicate cluster of nucleus-like structures. ×330. From Shiokawa *et al.* [69].

fertilized eggs, large nucleus-like structures (ca. 150 μm in diameter) were formed. Figure 1B shows typical nucleus-like structures. Since these nucleus-like structures were not visible in the cytoplasm of the eggs which were injected with a low dose (1 ng/egg) of lambda DNA, the size of the nucleus-like structures appears to depend on the amount of DNAs injected.

Unlike unfertilized eggs which have no perivitelline fluid to permit free egg rotation, fertilized eggs rotate freely within the vitelline membrane, and therefore, their animal-vegetal axis is oriented along the gravity. In such eggs the site of the formation of nucleus-like structures is mostly in the upper part of the animal hemisphere (see, Fig. 1B). The preferential formation of nucleus-like structures in the animal hemisphere also takes place even when DNAs are injected in the vegetal hemisphere. In such cases, it was frequently observed that the shape of the nucleus-like structures resembled a balloon with a tail coming up from the vegetal part of the egg. Therefore, we assume that in fertilized eggs, there are some mechanisms to confine both zygotic nuclei and artificially formed nucleus-like structures in the animal-most region.

The preferencial formation of nucleus-like structures in the animal hemisphere may at least partly explain why telolecithal eggs of amphibia undergo unequal holoblastic cleavage. Recently, it has been reported that the formation of nuclear envelope has important effect on the initiation of DNA replication [7, 43]. Therefore, the constant formation of nucleus-like structures in the animal hemisphere may explain the reason for the recent finding of Hofman *et al.* [33] that exogenously-injected DNA does not replicate in the vegetal hemisphere.

Forbes *et al.* [21], who first observed the formation of large nucleus-like structures in the cytoplasm of *Xenopus* unfertilized egg, demonstrated histochemically that injected lambda DNA itself is assembled into the nucleus-like structures. The nucleus-like structures formed in the cytoplasm of the fertilized egg also appeared to contain the injected DNA, since Hoechst 33258 specifically stained the structures, and furthermore, both biotin-conjugated and ^{3}H-thymidine-labeled DNAs were localized on the nucleus-like structures [69, 74].

In these experiments, especially in the experiment with biotin-conjugated DNA, we detected little DNA signal left in the cytoplasm. Therefore, majority of the injected DNA appears to be assembled within the nucleus-like structures. If so, it follows that *Xenopus* egg cytoplasm contains maternal substances necessary for assemblage of the DNA corresponding to about 4,000 somatic nuclei (see also, [21]), since the DNA injected was 24 ng and a *Xenopus* diploid cell contains 6 pg of nuclear DNA [14].

It has been shown also by Forbes *et al.* [21] that the nucleus-like structures formed in the unfertilized egg contain lamin underneath the "nuclear envelope". By using monoclonal antibody raised against calf thymus histones, we showed that nucleus-like structures contain histones, which must be maternal in nature [74]. Then, it appears that the injected DNAs form nucleosomes before they are assembled in the nucleus-like structures.

Ultrastructural features of the nucleus-like structures

The nucleus-like structures formed by a large amount of exogenously-injected DNA contain homogeneous "nucleoplasm" (Fig. 2A). Inside the "nucleoplasm", however, patches of matrix structures whose electron density is similar to that of the cytoplasm were frequently observed. Furthermore, such matrix structures were seen also at the periphery of the nucleus-like structures, sometimes adjacent to the "nuclear envelope" as shown in Figure 2. These matrix structures consist mainly of particulate components which seem to be glycogen granules and/or ribosomes. Sometimes, lipid droplets were also found in the nucleus-like structures. Therefore, it appears that a part of the cytoplasm is trapped within the large nucleus-like structures during their rapid assemblage.

It has been shown that the giant nucleus-like structures formed in the cytoplasm of unfertilized eggs are surrounded by double membranes equipped with normal-looking nuclear pore complexes [21]. However, more recently, we have shown that the "nuclear envelope" of the nucleus-like structures formed in the cytoplasm of fertilized eggs

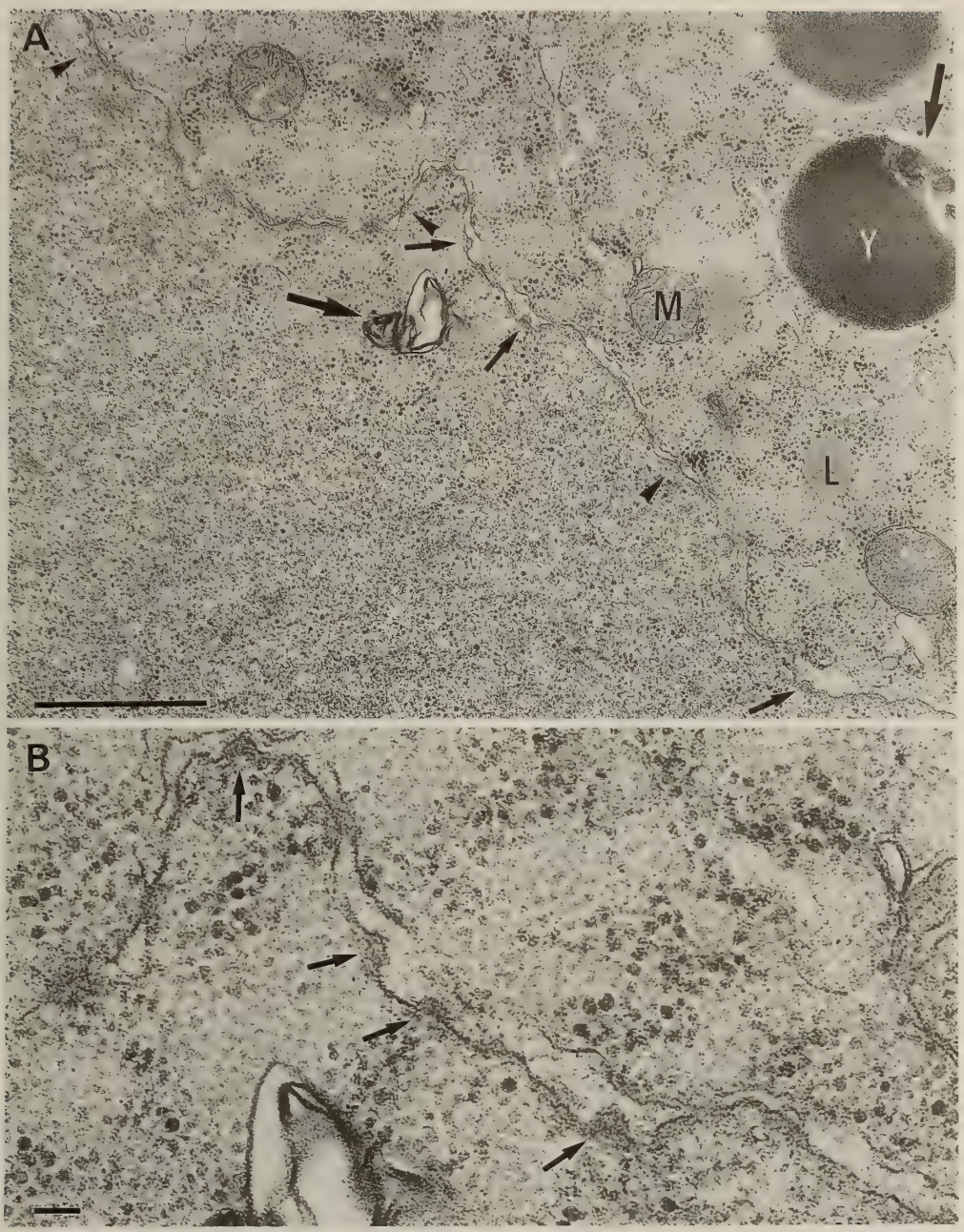

FIG. 2. Electron microscopic pictures of the large nucleus-like structures. (A) Lambda DNA was injected into a fertilized egg at 24 ng/egg and nuclear envelope was examined 1 hr after the injection. Normal (arrow heads) and unusual (small arrows) nuclear pore complexes are seen. M, Mitochondrion; L, lipid droplet. The fibrous structure in the "nucleoplasm" (larger arrow in the nucleus-side) is similar to the one seen on a yolk platelet (Y) in the cytoplasm (larger arrow in the cytoplasm-side). (B) Enlarged picture of the central portion of (A). Arrows show unusual pore complexes which are seen only when a relatively large amount of DNA was injected. The fibrous structure serves as a marker to correlate (B) to (A). Bars, 1 μm (A) and 0.1 μm (B). From Shiokawa *et al.* [74].

carry not only normal-looking pore complexes but also pore complexes of unusual appearance [74]. Such unusual pore complexes are characterized by the occurrence of the blebbing of the inner leaflet, which protrudes into the "perinuclear space" (Fig. 2).

Szollosi and Szollosi [78] observed a similar blebbing in the nuclear envelope of mouse embryonic cells. They concluded that the blebbing represents active nucleo-cytoplasmic transport of nuclear materials through the pore complexes. In the "pore complexes" of the *Xenopus* egg, neither enlargement of the blebbing nor its transformation into cytoplasmic vesicles was observed. Therefore, we assume that the blebbing may simply represent the formation of incomplete nuclear pore complexes, probably induced by the rapid assemblage of abnormally large nucleus-like structures.

So far, it has not yet been clarified what kind of interrelation exists between the normal nucleus and the large nucleus-like structures formed by the injected DNA. When we observed the formation of large nucleus-like structures, we were unable to find the normal nucleus in the cytoplasm. Since both normal nucleus and the large nucleus-like structures are formed in the animal-most region, we assume that the incorporation of the normal nucleus into the large nucleus-like structures may have taken place during their rapid assemblage stage.

Partition of the nucleus-like structures into daughter cells

Nucleus-like structures formed in fertilized eggs are partitioned into descendant cells during cleavage [17, 63, 66, 74, 82]. When fertilized eggs are injected with a relatively large amount (24 ng) of either lambda DNA, circular pBR322, or circular pXlr101A (a plasmid that contains a *Xenopus* rDNA single repeat) [2], the pattern of the cleavage became abnormal. Therefore, the DNA at the dose used is toxic on embryonic development, although there is an experiment in which as much as 50 ng/egg of plasmid DNA was injected, yet no description was made about the toxicity [45].

The abnormal cleavage pattern caused by the exogenous DNA is usually observed in the animal half region. This is probably because the injected DNAs tend to localize in the animal-most region of the egg. Embryos derived from such DNA-injected fertilized eggs often contain blastomeres of abnormally large size especially in the animal hemisphere. Large blastomeres in such DNA-injected embryos often contain large nuclei whose nucleoplasm shows apparent similarity to that of the large nucleus-like structures formed in the fertilized eggs. When the amount of the injected DNA was 2 ng/egg or less, the damage of cleavage was not observed (see also, [85]). It has been reported that when radioactively-labeled DNA is injected, some of the injected DNA becomes associated with chromosomes, and partitioned into daughter nuclei [17].

PERSISTENCE AND REPLICATION OF INJECTED DNAS WITHIN THE DEVELOPING EMBRYO

To understand the basis for the formation of the nucleus-like structures described above, and also to understand the mechanism of the expression of genetic information within the injected DNAs in the developing embryos, it is necessary to know how the injected DNAs are preserved and replicated within the embryonic cells. The behavior of the injected DNAs differs depending upon their molecular forms (circular or linear). We review here mainly the results obtained by Southern blot analysis of the DNAs recovered from the embryos which had been injected with either circular or linearized DNAs.

Changes in the amount and size of circular DNAs injected into the embryo

After the injection of closed circular (c.c.) plasmid DNAs into fertilized eggs, DNAs were extracted from developing embryos and analyzed using Southern blot hybridization techniques without prior treatment with restriction enzymes. Generally, it can be seen that c.c. DNA is immediately converted into open circular (o.c.) form, and soon after that c.c. DNA is reformed. The change usually takes place within an hour and after that the levels of c.c. and o.c. DNAs are kept more or less constant throughout later stages, until sometime during the tailbud to tadpole stages,

where they disappear.

These changes can be seen in our experiments in which we injected a relatively small amount (0.2 ng/egg) of circular forms of pBR322 that carries either an rDNA single repeat (pXlr101A) (15.7 Kb), a *Drosophila* copia gene (cDm2055) (10.3 Kb), a P-element (pπ25.1) (9.1 Kb), or nothing (pBR322; 4.3 Kb) (Fig. 3). In this experiment, both c.c. and o.c. DNAs which were present in embryos an hour after injection were maintained at constant levels, and eliminated at the tailbud stage (in the case of larger plasmids, pXlr101A and cDm2055) or slightly later at the muscular response stage (in the case of smaller plasmids, pπ25.1 and pBR322) [73] (Fig. 3). These results show that the injected circular DNAs did not replicate appreciablly throughout the stages. It was also consistently shown among the four plasmids studied that when these circular DNAs disappear from the embryos, o.c. DNAs do so faster

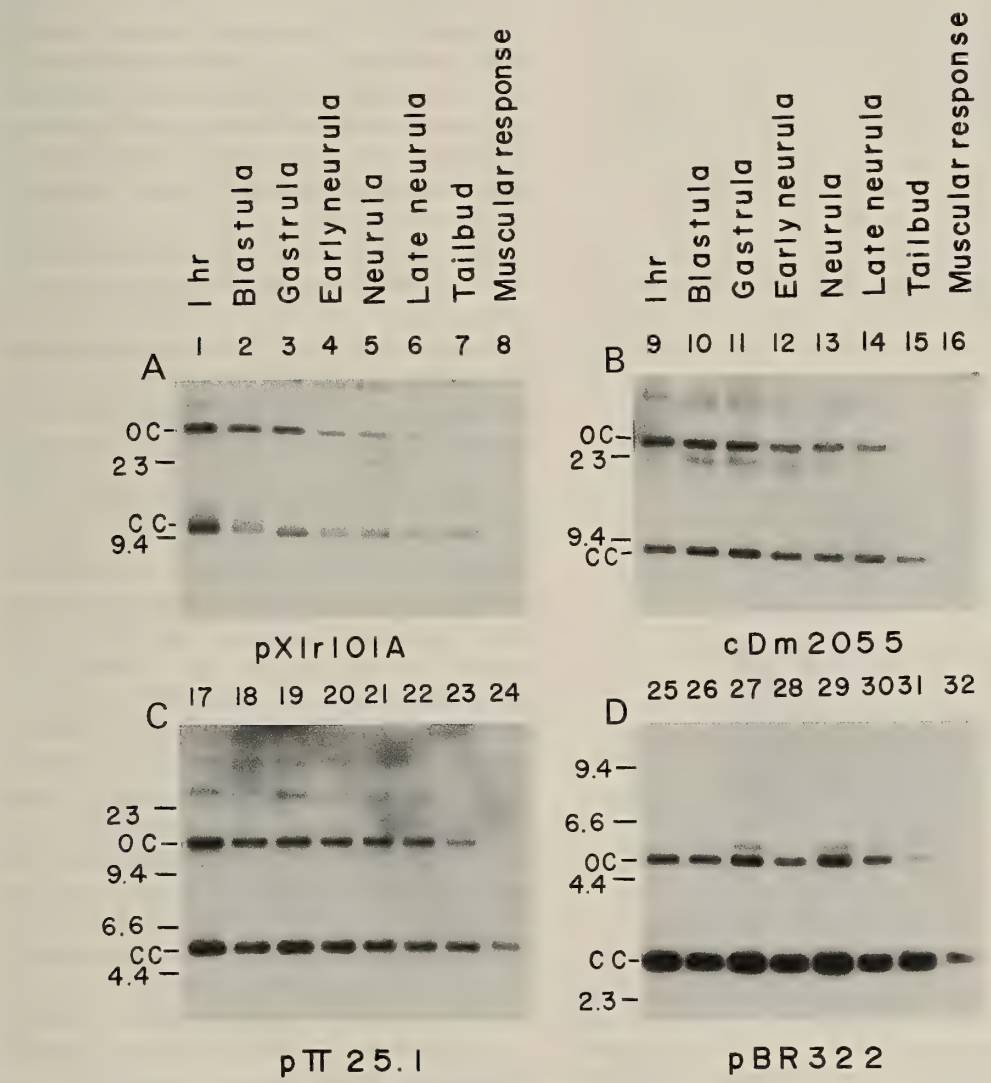

FIG. 3. Southern blot analysis of DNAs from plasmid-injected embryos. Fertilized eggs were injected with 0.2 ng/egg of circular pXlr101A (A), cDm2055 (B), pπ25.1 (C), and pBR322 (D). Embryos were harvested at the indicated stages and subjected to Southern blot analysis without prior enzyme digestion. The positions of open circular (o.c.) DNA, closed circular (c.c.) DNA, and size markers are given. From Shiokawa *et al.* [73].

than c.c. DNAs (Fig. 3). In Figure 3, it is also apparent that most of the injected circular genes are converted to o.c. DNA before they disappear. In the case of the injection of circular form of vitellogenin genes, however, it has been reported that some of the injected DNA are preserved in the nuclei probably as minigenes even after metamorphosis [1].

When circular plasmid DNAs contain viral replication origin in their promoters, they replicate actively after introduction into the embryos. Thus, circular pSV2CAT, which is the bacterial chloramphenicol acetyltransferase (CAT) gene connected to SV40 early promoter (containing viral replication origin), and circular pAd12E1aCAT, which is a circular CAT gene connected to the promoter (that also contains the replication origin) of type 12 adenovirus E1a protein were replicated in the injected embryos quite actively, especially in later stages of development (Fig. 4). In this case, it is apparently shown that only c.c. DNA disappeared at 20 min after injection (Fig. 4, lane 2), then c.c. DNA reappeared 3 hr after injection (lane 3), then both c.c. and o.c. DNAs increased in their amounts through early blastula to gastrula stages.

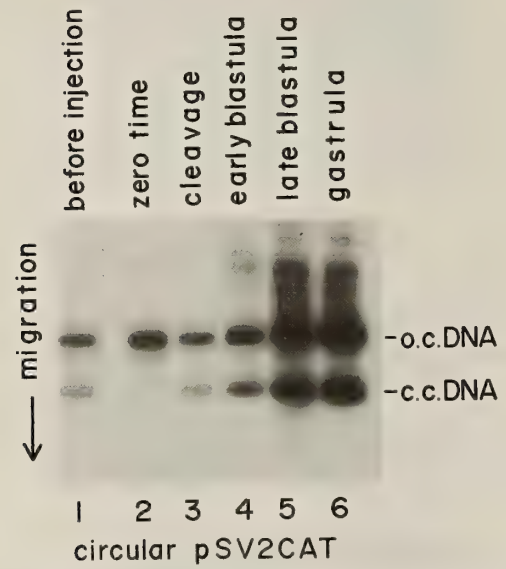

Fig. 4. Southern blot analysis of DNAs from embryos injected with circular pSV2CAT. Fertilized eggs were injected with 1 ng/egg of circular pSV2CAT and DNAs were extracted at the indicated stages and processed as in Figure 3. Zero time and cleavage samples were obtained actually at 20 min and at 3 hr, respectively, after the injection. From Fu *et al.* [23].

In the experiments shown in Figure 3, there were only very small amounts of DNAs which migrated slower than o.c. DNA. However, in the experiment shown in Figure 4, a considerable amount of large-sized DNAs which migrated slower than o.c. DNA appeared in later stages.

We treated these large-sized DNAs with type II topoisomerase, under the conditions in which kinetoplast DNA, as an authentic internal control for catenated DNA, was completely decatenated to the circular DNA of monomer size. However, the amount and size of the large-sized DNA did not change to any appreciable extent. These results show that the large-sized DNAs formed are not catenated DNA.

When we treated the large-sized DNAs with various restriction enzymes, linear DNA of approximately monomer size was obtained in all cases. Then, the large-sized DNA may be either circular form of oligomer of injected DNA or concatemers formed by ligation of DNAs which were linearized after being introduced into the egg.

Factors that affect replication of circular DNAs in developing embryos

Figures 3 and 4 show that the extent of the replication of circular DNA varies considerably depending on the constitution of the plasmid. The general rule may be that the plasmids like pSV2CAT and pAd12E1aCAT which carry viral promoter with replication origin on it replicate actively, whereas other plasmids like pBR322, pXlr101A, cDm2055, and pπ25.1 which do not contain such promoter replicate poorly. Here, it must be noted that, sometimes, especially when the analysis was carried out in early stages of development, even the circular pSV2CAT that carries viral replication origin replicates only poorly (2 to 3-fold). Also, plasmids without eukaryotic replication origin which in most case do not replicate can replicate considerably (at most ca. 2-fold) sometimes in embryos at later stages [18, 73]. Thus, it is still not known why injected circular DNAs sometimes replicate and sometimes not.

It has been reported that supercoiled plasmids

replicate but nicked circular plasmids do not [15]. One report proposes that only a certain fraction of circular DNA can replicate probably by being localized in a special compartment in the cell which is particularly suited for replication [46, 47]. In another paper, it is reported that plasmid DNAs which are injected into the animal half of the fertilized egg, 60–65 min after fertilization, replicate preferentially [33].

In unfertilized egg it has been well established that eukaryotic replication origins are unnecessary for the efficient replication of exogenously-injected DNAs [30, 49]. However, as stated above, the replication is significantly greater in the presence of such origin (pSV2CAT) than in their absence (pBR322, pSV0CAT and others) [23, 73]. Therefore, in developing embryos, the presence of replication origin within the injected circular DNAs may have significant stimulating effects on their replication.

We assume that the presence of the replication origin within the circular DNAs makes little difference in their replication in the cytoplasm of unfertilized egg, where the relative amount of DNA polymerase per DNA is extremely high. By contrast, the presence of the replication origin may have significant stimulating effects on the replication of the circular DNAs in the cytoplasm of embryos, especially in later stages, where the amount of DNA polymerase per cell is very similar to that of the adult-type cells.

Changes in the amount and size of linearized DNAs injected into the embryo

In developing embryos, a great contrast was seen between the behavior of circular DNAs and linearized DNAs: While circular DNAs sometimes replicated but most of time not as already shown in the above section, all the linearized DNAs so far tested (lambda DNA, linearized pSV2CAT, pSV0CAT, and actin-CAT fusion gene) replicated quite actively (by about 50 to 100-fold). Furthermore, the size of the injected linear DNA was increased by 10 to 20-fold. Results in Figure 5 provides a typical example showing such differences. We injected here circular and linearized plasmid DNA known as actin-CAT fusion gene #254 (containing the CAT gene and the promoter

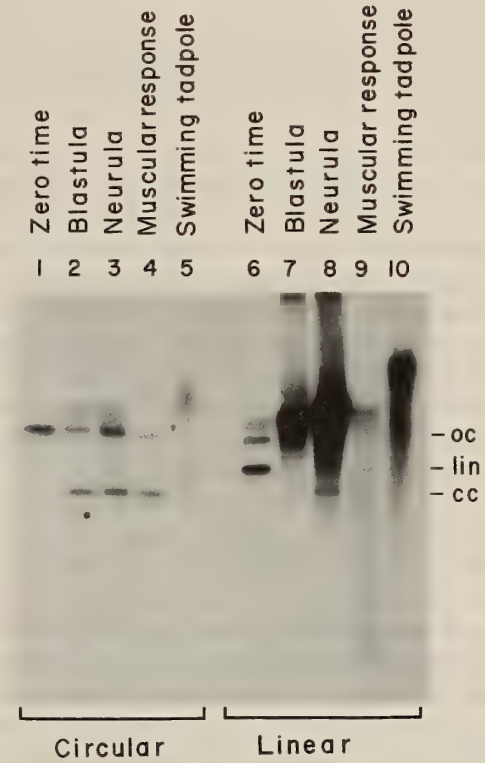

FIG. 5. Southern blot analysis of DNAs extracted from embryos injected with circular or linearized actin-CAT fusion gene. Fertilized eggs were injected with 2 ng of circular or linearized actin-CAT fusion gene #254, and 5 embryos each were harvested at indicated stage and processed as in Figure 3. Zero time (15 min after injection). o.c. (open circular), lin (linear), and c.c. (closed circular) DNA. In lanes 7–9 faint signals are seen at about the position of c.c. DNA, and in lane 6 another signal is seen at the position close to o.c. DNA. However, the nature of these have not been examined. From Shiokawa *et al.* [62].

of *Xenopus* α-actin gene) into fertilized eggs. When linear DNA was injected, a large amount of large-sized DNAs was formed at the blastula and neurula stages of development (Fig. 5, lanes 7 and 8). It is seen here that some DNA is stuck on the gel slots (lanes 7 and 8), probably because of the largeness in the size. However, later at the muscular response stage (lane 9), the majority of the large-sized DNA disappeared [62]. These results are in a remarkable contrast with the practically constant preservation of the circular form of the

fusion gene in the control experiment (Fig. 5, lanes 2 to 5) (note that, c.c. DNA disappeared shortly after injection as in lane 1, but reappeared soon as in lane 2).

We treated the large-sized DNAs obtained by injection of linearized DNAs with type II topoisomerase, under the conditions in which kinetoplast DNA as an internal reference for catenated DNA was completely decatenated to the circular DNA of monomer size. However, we found here again practically no change in the amount and size of the large-sized DNAs before and after the treatment. Therefore, the large-sized DNAs produced by the injection of linearized DNAs are not catenated DNAs.

It was found that such large-sized DNAs were not sensitive to the restriction enzymes which were used to linearize the plasmid DNAs before they were injected. Thus, the large-sized DNA extracted from embryos that had been injected with Acc I-digest of pSV2CAT was not digested with Acc I. Likewise, large-sized DNAs extracted from embryos that had been injected with Hpa I-digest of pSV2CAT, were not digested by Hpa I. However, almost complete conversion of these large-sized DNAs to the DNA of approximately monomer size was seen when they were digested with restriction enzymes that were not used to linearize the injected DNA.

These results strongly suggest that the large-sized DNAs obtained by the injection of linearized DNA are concatemers, formed by ligation of probably all the possible combinations (head to head, head to tail, and tail to tail), as reported previously [3, 4, 60]. The resistance of the large-sized DNAs to digestion with the enzyme which has been used to linearize the injected DNA suggests that distal parts of the injected DNAs are modified probably by exonucleolytic digestion prior to ligation.

Possibility of the integration of the injected linearized DNAs into the host genome

At the beginning of our DNA injection experiment, we injected circular pXlr101A into the fertilized egg of wild-type *Xenopus laevis*, as one of the preliminary experiments to try to rescue anucleolate mutant *Xenopus* embryos which do not synthesize rRNA throughout development. In this

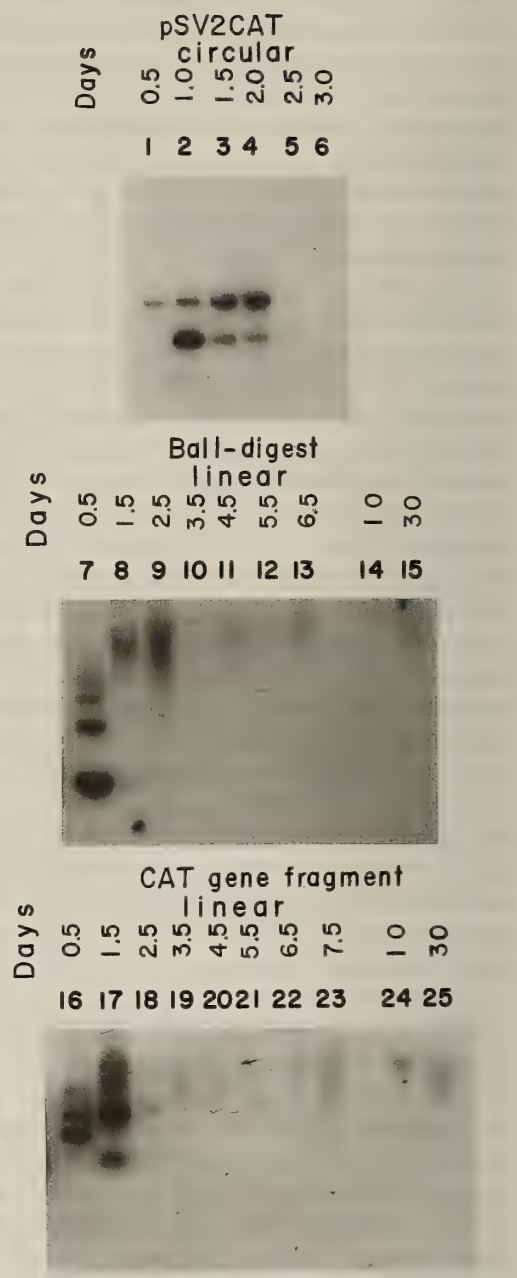

Fig. 6. Southern blot analysis of DNAs obtained from embryos which were cultured for a long period after injection of circular or linearized DNAs. Fertilized eggs were injected with 1 ng each of circular pSV2CAT (top), Bal I digest of pSV2CAT (middle), or CAT gene fragment (bottom), and embryos were harvested at the indicated dates and processed as in Figure 3. From Fu *et al.* [23].

experiment, from the 2 week-old tadpoles, we obtained the evidence that the injected pXlr101A was preserved as chromosome-integrated DNA [80].

However, later, it became clear that linearized DNAs are not only replicated more efficiently [23, 46] but also integrated more frequently into the host genome [17, 19, 23]. Then, we started to inject instead of circular DNA, linearized DNAs, and found in the DNA-injected embryos the formation of a large amount of large-sized DNA that co-migrated with host DNA. In most of such experiments, majority of the large-sized DNA formed at early stages (blastula to neurula stages) always disappeared after about 2 days (during early swimming tadpole stage). However, a small but distinct amount of large-sized DNA was preserved even in 1-month-old tadpoles.

Interestingly, the amount of such long-lasting large-sized DNA varied from preparation to preparation. Figure 6 gives typical results showing the presence of long-lasting DNAs in 1 month-old swimming tadpole, which developed from fertilized eggs injected with either Bal I-digest of pSV2CAT (middle panel) or CAT gene fragment (bottom panel) [23]. The results at the top indicate the DNAs which were recovered from embryos injected with circular pSV2CAT in which we see practically no large-sized DNA. Thus, the long-lasting DNA shown in these 1 month-old embryos (middle and bottom panels of Fig. 6) may be the strong candidates for the chromosome-integrated DNAs.

In *Xenopus laevis,* however, studies which unequivocally demonstrated the integration of the injected gene in host genome are so far very scanty. Only Etkin and Pearman [17] are exceptions, who injected linearized pSV2CAT into fertilized eggs and found that injected DNA persisted in the tissues of 60% of 6- to 8-month-old frogs, exhibiting a mosaic pattern of distribution (2 to 30 copies/cell) among different tissues. Furthermore, they showed that such exogenous DNA sequences were transmitted to the genome of various tissues of offspring through the male germ line.

EXPRESSION OF EXOGENOUSLY-INJECTED DNAS IN THE DEVELOPING EMBRYOS

Expression of exogenous genes in developing embryos has been extensively studied. However, majority of the papers published so far are concerned with the functional characteristics of specific gene cloned by each of the research groups. In addition, experiments are relatively scanty that aimed to elucidate the general control mechanism which regulates the expression of exogenously-injected, as opposed to endogenous (or chromosomal), genes. Therefore, we emphasize here mainly the general aspect of the control mechanisms applicable to various genes introduced into the developing embryo.

Expression of exogenously-introduced ribosomal DNA

One of the most abundant gene products in the early amphibian embryonic cells at RNA level is no doubt rRNA, and naturally, one of the earliest data on the genes introduced into *Xenopus* embryos was concerned with the expression of *Xenopus* rDNA-containing plasmid, pXlr101A. As described above, we have shown that rRNA synthesis from endogenous genes starts at the late blastula stage [65, 68], and furthermore, presented evidence that the initiation of the rRNA synthesis may be regulated at the transcriptional level by decrease at the blastula stage of the intracellular ammonium ion or pH [61, 64].

Shortly after our findings [65, 68], Busby and Reeder [12] injected pXlr101A, a plasmid which contains *Xenopus laevis* rDNA single repeat, into fertilized eggs of *Xenopus borealis.* This "hybrid" combination of *X. laevis* rDNA and *X. borealis* embryo was constructed, because it has been previously shown that the expression of the *X. laevis* rDNA is dominant over that of the *X. borealis* rDNA [34], and it is much easier to detect *X. laevis* new transcript in the presence of a large amount of *X. borealis* maternal rRNA than in the presence of a large amount of *X. laevis* maternal rRNA (4,000 ng/egg). They then tested the effect of the presence of varying lengths of 5′-upstream sequences on the efficiency of the expression of the injected *X. laevis* rDNA, using *X. laevis* specific S1-

protection analysis.

Busby and Reeder [12] have shown that the injected *Xenopus laevis* rDNA is expressed first at the late blastula stage and the efficiency of the expression depends on the lengths of the 5′-upstream sequence [12]. Then, it follows that in developing embryos, the expression of exogenously-injected rDNA begins at the late blastula stage [12], concurrently with the expression of endogenous rDNA [61, 64, 68]. These results suggest that the control mechanism which is intrinsic for the expression of endogenous (or chromosomal) rDNA may also operate on the exogenously-introduced rDNA.

Expression of circular CAT genes which carry viral promoters

In order to obtain the basic data about how protein-coding exogenous genes are expressed in *Xenopus* embryos, we first tested the expression of five different circular plasmid DNAs that carry the CAT gene connected to different viral promoters. Plasmids used here were pSV2CAT containing a CAT gene linked to a relatively strong promoter of SV40 early gene [25], pAl0CAT2 including a part of the SV40 early promoter (the GC-rich 2l-bp repeats and TATA box) but without enhancer sequences (two tandemly repeated 72-bp elements) [59], pAdl2.E1aCAT carrying a relatively strong promoter of E1a protein of type 12 adenovirus [40], pSV0CAT containing no viral promoter [25], and pAl0CAT3m which is a polylinker-containing derivative of pSV0CAT.

We injected a reportedly non-toxic dosage (1 ng/egg) [85] of these plasmid DNAs into the fertilized eggs, and tested the CAT enzyme activity

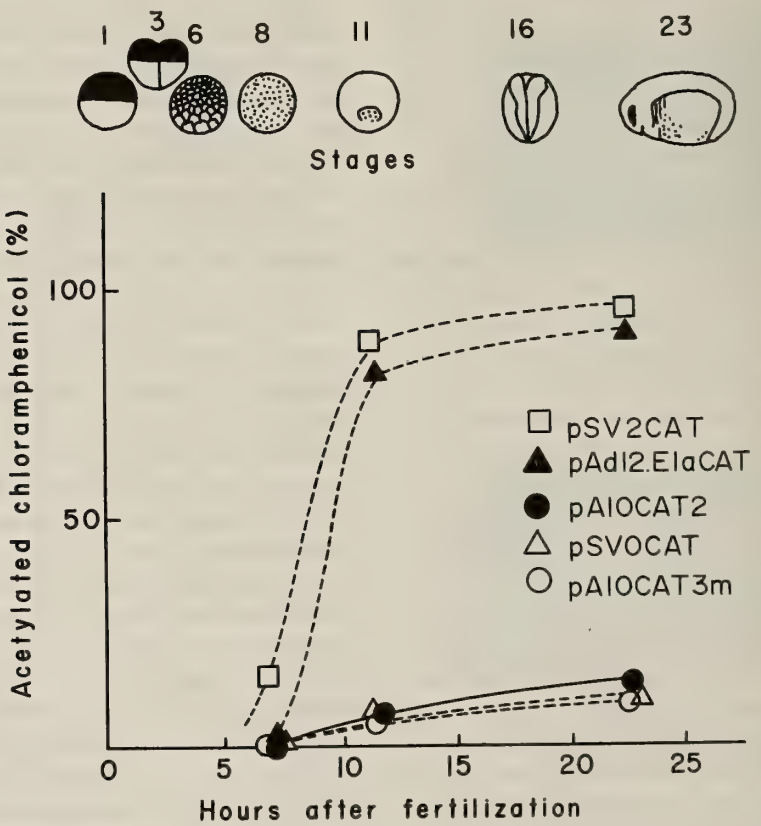

Fig. 7. Kinetics of the accumulation of CAT enzyme activity during development. Following injection of 1 ng of circular plasmids into fertilized eggs, embryos were collected at the blastula, gastrula, and neurula stages. The relative strength of the CAT signal was determined by densitometry and plotted as a function of the time after fertilization. From Fu *et al.* [23].

by autoradiographic exposure of CAT assay samples for 2 weeks. As shown in the summary of the densitometric calibration of these data (Fig. 7), pSV2CAT which contains the strong promoter of SV40 early gene was expressed at as early as the blastula stage. In this case, the CAT enzyme level showed a great increase during the gastrula stage, and then reached a plateau at the late neurula stage. Very interestingly, an extrapolation of the level of the CAT enzyme activity from the gastrula to blastula stages gives us an impression that there might be some CAT enzyme expression even before the blastula stage (we shall discuss this point in detail later on). pAdl2.E1aCAT which also contains a relatively strong promoter was not expressed at a detectable level at the blastula stage, but was expressed at a high level at the gastrula stage and then reached a plateau at the late neurula stage. By contrast, pSV0CAT and pAl0CAT3m which contain no promoter, and in addition, pAl0CAT2 which contains the enhancer-lacking SV40 promoter were expressed only at a background level throughout the stage.

By Northern blot analysis using antisense RNA as a probe, we confirmed that CAT enzyme expression was accompanied by the appearance of 1.6 Kb CAT mRNA. Therefore, in the *Xenopus* embryo system, CAT enzyme level appeared to reflect the transcriptional activity of CAT gene. Therefore, we concluded that the efficiency of the expression of circular DNAs depends mainly on the relative strength of the promoter. For the small amount of background level expression of CAT enzyme activity from promoter-less plasmids, we assume that the cryptic promoters within the plasmid sequence may be responsible for it (cf. [42]).

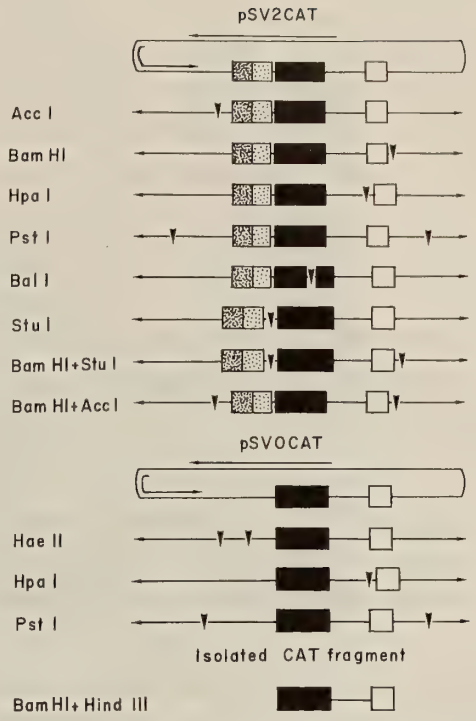

FIG. 8. Plasmids used in the experiment. pSV2CAT and pSV0CAT were digested with restriction enzymes as listed. In circular plasmids, the straight and bent arrows represent gene region for ampicillin and replication origin of pBR322, respectively. Heavily dotted box, enhancer region; lightly-dotted box, promoter region; closed box, CAT coding sequence; open box, poly(A) addition site. Arrowheads show sites of digestion by restriction enzymes indicated. From Fu *et al.*[23].

Expression of linearized CAT genes which carry or do not carry viral promoters

Having selected pSV2CAT and pSV0CAT from the five plasmids used above, we produced variously-linearized forms of these plasmids as shown in Figure 8. We then injected these linearized plasmids at 1 ng/egg into the fertilized eggs, and tested the CAT enzyme expression at various stages of development.

Figure 9 indicate that all of the linearized DNA preparations of pSV2CAT (lanes 6 to 14) were expressed at the levels which were more or less similar to that of circular pSV2CAT (lanes 15 to 17). Furthermore, unexpectedly, all the linearized DNAs of pSV0CAT which did not carry any promoter (Fig. 8) were expressed (not shown in Fig. 9) at levels which were comparable to that of circular pSV2CAT. In addition, a linear CAT coding sequence, which had been prepared from pSV0CAT by double enzyme digestions (Bam HI and Hind III) and freed from the vector sequence prior to the injection (Fig. 8), was expressed at a considerably high level at the gastrula and neurula stages (lanes 4 and 5), albeit the level is lower than that of circular pSV2CAT at the blastula stage

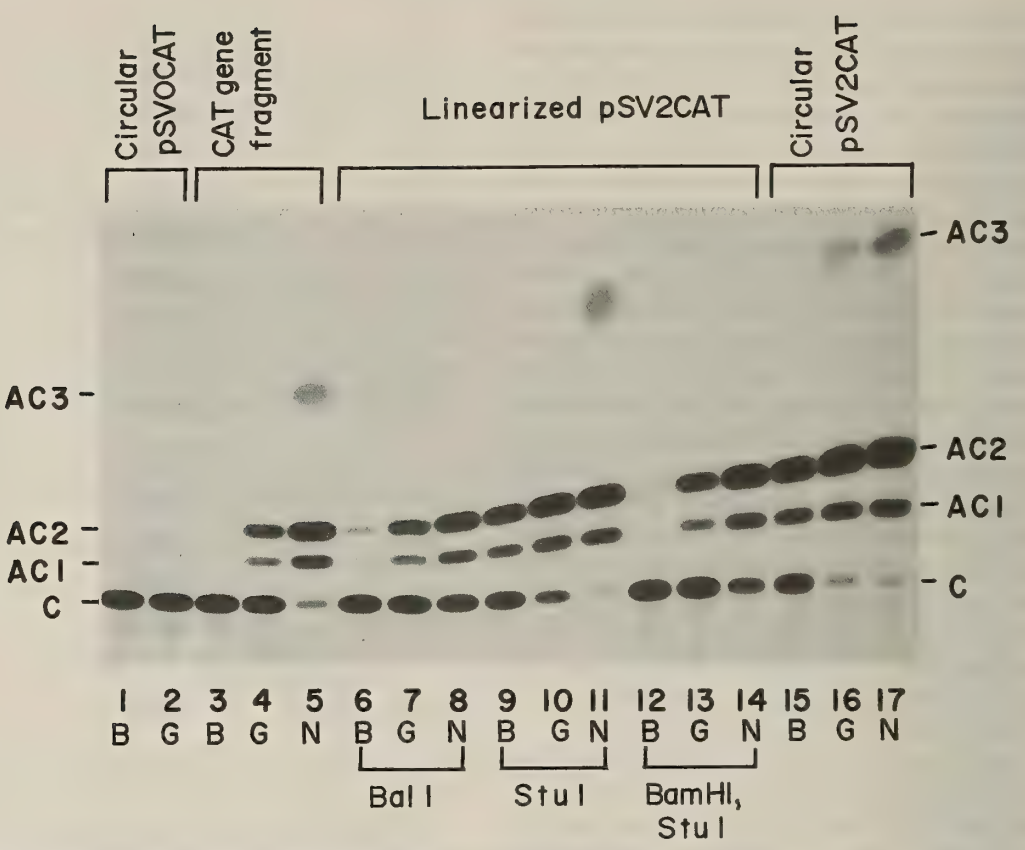

Fig. 9. CAT enzyme assay in embryos following injection of CAT genes. Circular pSV0CAT (lanes 1 and 2), CAT gene fragment (lanes 3–5), linearized pSV2CAT (lanes 6–14), and circular pSV2CAT (15–17) were injected at 1 ng/egg into fertilized eggs. Embryos were collected at the blastula (B), gastrula (G) and neurula (N) stages and used for CAT enzyme assay. The restriction enzymes used were Bal I (lanes 6–8), Stu I (lanes 9–11), Bam HI plus Stu I (lanes 12–14). C, AC1, AC2, and AC3 are chloramphenicol, 1-acetylated chloramphenicol, 3-acetylated chloramphenicol, 1,3-diacetylated chloramphenicol, respectively. From Fu *et al.* [23].

(lanes 15 to 17). Thus, the expression of linearized pSV0CAT (not shown) and CAT gene fragment isolated from pSV0CAT (lanes 4 to 5) makes a great contrast to that of circular pSV0CAT where the expression was almost negligible (lanes 1 and 2).

These results led us to conclude that linearized CAT genes are expressed in embryos by some mechanism which is independent from the promoter. For a DNA to be active as a template, it is necessary for it to have supercoiled domain, and to generate the torsional stress [31, 56]. A possible explanation for the expression of linearized DNA in embryos may be the attachment of the large-sized DNA to some cellular structures such as nuclear matrix.

It may be worth noting here that pSV0CAT digested by Hpa I at the poly(A) addition site and pSV2CAT digested by Bal I within the CAT coding sequence (Fig. 8) were expressed at considerably high levels. A possible explanation for these may be that these broken genes have been re-circularized and thus expressed from the reconstituted coding sequence. However, this explanation is only applicable to the case of the injection of Bal I-digest of pSV2CAT, but not to that of the Hpa I digest of pSV0CAT, since circular pSV0CAT is expressed only at a background level (cf. Fig. 7). Therefore, more likely explanation may be that the genes have been ligated to form

concatemers in every possible combination, and some of the concatemers which happened to reconstitute functionally active CAT coding sequence were expressed.

Expression of the injected circular CAT genes with viral promoters before the midblastula transition (MBT)

Newport and Kirschner [52, 53] proposed that the new gene expression from zygotic genome in *Xenopus* embryogenesis takes place only at and after the 12th cleavage (at and after the timing called MBT). In order to obtain the evidence to support this idea, these authors injected a plasmid containing an yeast leucine tRNA gene (pYLT20) into the *Xenopus* coenocytic egg cell, a fertilized egg whose cleavage has been inhibited by low speed centrifugation. They found that although the tRNA genes were transiently expressed shortly after the injection, the genes became inactive during the cleavage stage, and then re-activated at the 12th cleavage.

Three years later, Etkin and Balcells [16] injected 1 ng/egg (10^7 copies/egg) of pSV2CAT into *Xenopus* fertilized eggs to further confirm the idea of MBT-associated activation of exogenously-injected genes. They reported that injected CAT genes are expressed only during and after the 12th cleavage (MBT). Thus, the MBT theory which maintains that there is no expression of nuclear and exogenously-injected DNAs during the cleavage stage has been much strengthened.

On the contrary, we have shown that even in cleavage stage embryos there is the synthesis of mRNA-like heterogeneous RNA, which is not due to mitochondrial DNA and is sensitive to actinomycin D and α-amanitin [51, 61, 64]. Therefore, we expected that the exogenously-injected DNAs will be actually expressed, and therefore, their expression may be detected during the cleavage stage if sufficiently sensitive methods were applied.

It may be worth pointing out here the difficulty involved in the determination of the gene activity in early *Xenopus* embryos, in which a rapid increase in cell number (or nuclear number) is taking place. For instance, in the experiment of Etkin and Balcells [16] described above, CAT enzyme activity was compared using the samples obtained from the same number of embryos (15 embryos) at all the stages tested. As shown in the above section, DNAs injected into the fertilized eggs are preserved throughout the development, and in this sense, the amount of the injected DNA-templates per embryo is approximately constant throughout their development.

However, under the conditions used, it is not known what percentage of the injected DNA is actually available as templates for transcriptional machinery at each stage of the development. In fact, there is a possibility that only a limited portion of the injected DNA is available as the actual templates at the beginning and the amount of the effective template increases as development proceeds. Then, it would be difficult to detect the expression of the gene in the embryos at early stages using the methods which are sensitive enough to detect the expression of the gene in the embryo at the later stages.

As a method to increase the sensitivity in detecting the gene expression in embryos at the early stages of development, we modified the experiment of Etkin and Balcells [16] by increasing the amount of circular pSV2CAT by 10-fold (10 ng/egg; 10^8 copies/egg) (the number of embryo used was still 10 embryos at all stages) [72]. Under these conditions, development of the DNA-injected eggs was slightly abnormal, especially when embryos reached the neurula stage, although nevertheless, they continued development beyond the neurula stage.

When CAT enzyme assay was carried out using these embryos and autoradiography for the detection of acetylated chloramphenicol was performed for 2 weeks, data similar to those of Etkin and Balcells [16] were obtained; the CAT enzyme signal started to appear at the MBT, and increased thereafter until the late neurula stage. However, when we elongated the autoradiographic exposure time to 2 months, we detected CAT enzyme activity not only at the MBT stage but also at 3 hr (early cleavage stage) and 5 hr (late cleavage stage) after the DNA injection (Fig. 10, left). When measured on a densitometer, the increase in the CAT enzyme signal roughly paralleled to that in cell number per embryo, suggesting the necessity of the increase in the number of nucleus for the

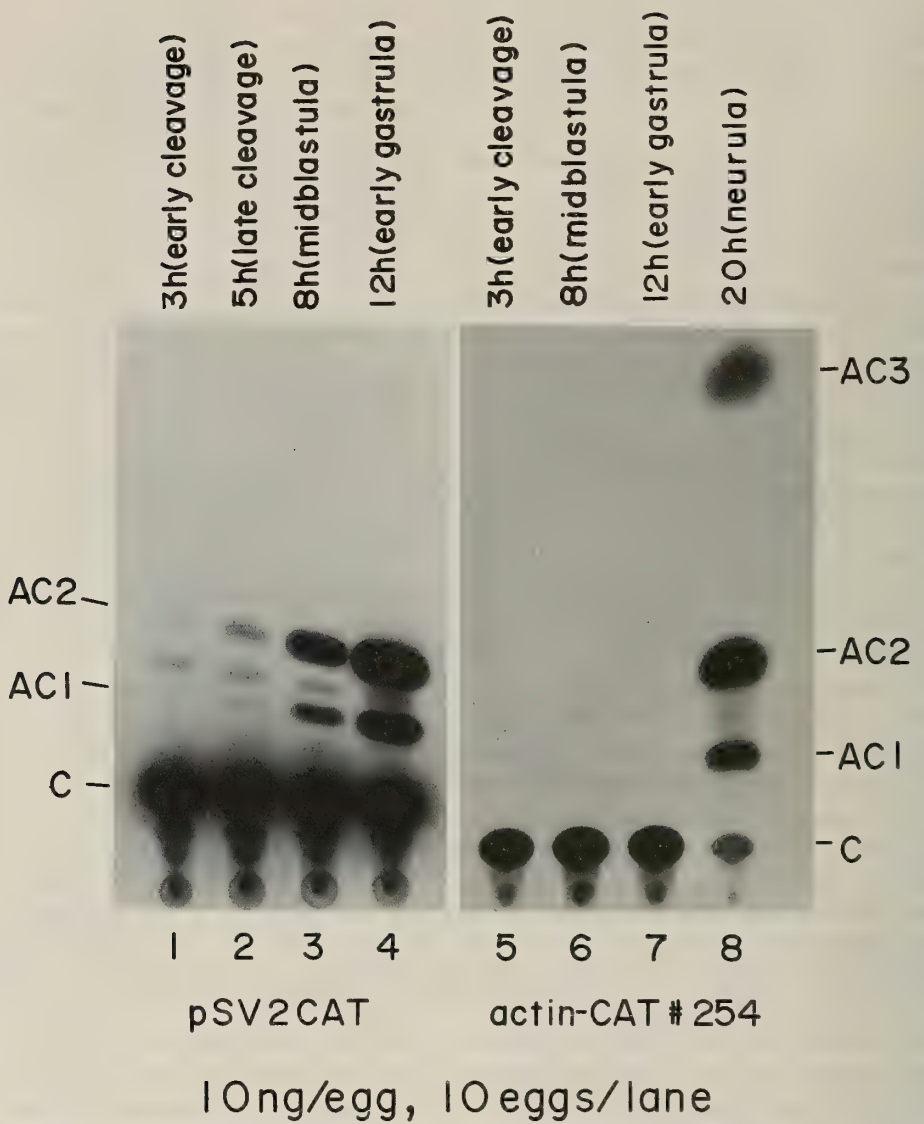

Fig. 10. CAT enzyme assays using embryos injected with circular CAT genes. Fertilized eggs were injected with 10 ng of either circular pSV2CAT (lanes 1 to 4) or actin-CAT fusion gene #254 (lanes 5 to 8), and 10 embryos each were harvested at the indicated stages for CAT enzyme assay as in Figure 9. Autoradiography was carried out for 2 months. A faint signal which appeared between AC1 and AC2 is not due to CAT enzyme expression from the injected genes because it was obtained even in uninjected embryo after long autoradiographic exposure. From Shiokawa *et al.* [62, 72].

increased CAT gene expression.

In the above experiment, we carried out a control experiment using the actin-CAT fusion gene #254 which was also used in the experiment in Figure 5 [50]. Since this CAT gene is connected to the promoter of *Xenopus* α-actin gene and is known to be expressed only after the embryo reached the neurula stage [50], we thought it would be interesting to see how this developmentally-controlled gene is expressed when the gene is injected into the embryo at a high dose.

Then, we injected the fusion gene #254 either

at 1 ng/egg or at 10 ng/egg, and assayed CAT enzyme activity using the samples extracted from 10 injected embryos at four different stages. The results obtained after 2 months of autoradiographic exposure showed that CAT enzyme signal was detected not at the cleavage but at the neurula stage at the two different dosage (Fig. 10, right; only the results with 10 ng/egg are shown). These results indicate that injected fusion gene was expressed in a temporally controlled manner just as its endogenous counterpart. Therefore, it appears that the results obtained using 10 ng/egg of pSV2CAT are not just artifact produced by some toxic effects of the excessive amount (10 ng) of the DNA injected.

However, we thought it may still be possible to argue that the expression of CAT gene during the cleavage stage (pre-MBT stage) (Fig. 10, left) might be due to "aberrant expression" which took place only for the high dose (10 ng/egg) of pSV2CAT for some unknown pSV2CAT-specific reason. Therefore, we repeated the experiment using the dosage (1 ng/egg; 10^7 copies/egg) which is exactly the same as that used by Etkin and Balcells [16]. In doing this experiment, however, we altered the other parameters: We used 10-fold larger number of embryos (100 embryos), and actually, instead of preparing one sample (consisting of 10 embryos), we prepared 5 samples (each consisting of 20 embryos) for two time-points (4 hr; cleavage stage, and 8 hr; blastula stage). Then, the 20 embryo samples were processed separately and at the final step of chromatography, all the samples (100 embryos) were analyzed on one spot.

Even by conducting such a large scale experiment, we were unable to detect CAT enzyme activity during the cleavage stage, when autoradiographic exposure was carried out for 2 weeks. Therefore, again, we extended the exposure time to 2 months. Then, as shown in Figure 11, we were able to detect the presence of the clear signal of acetylated chloramphenicol for the cleavage stage embryos (4 hr after fertilization). In this experiment, plasmid constitutions without viral promoter (pSV0CAT: pSV00CAT) were not active, and pAd12E1aCAT gave a signal significantly weaker than that of pSV2CAT. Therefore, also during the cleavage stage, CAT genes with viral promoters

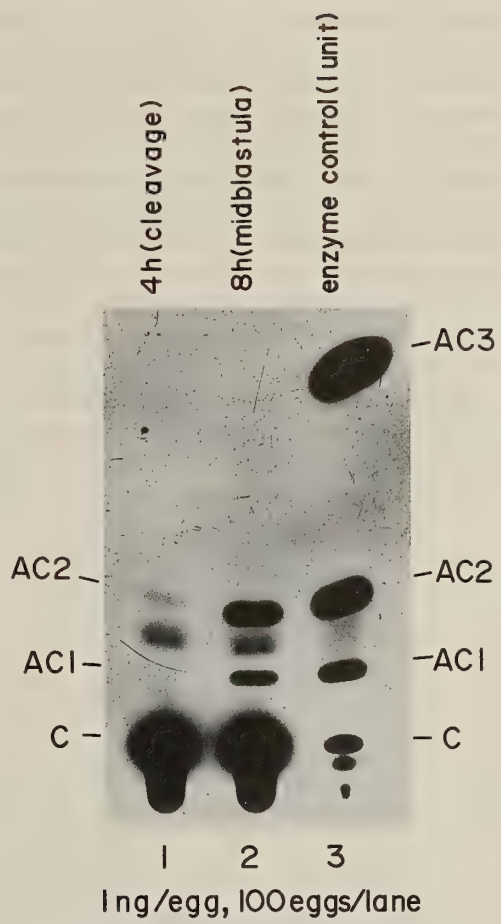

FIG. 11. CAT enzyme assay in embryos from the cleavage stage embryos. Fertilized eggs were injected with 1 ng of circular pSV2CAT and harvested at the indicated stages. Twenty embryos were pooled as a group, and five such groups of embryos were prepared for each sample. Samples were processed separatedly as in Figure 9, but finally pooled and assayed together as one sample at the step of thin-layer chromatography. Thus, each spot is for the sample of 100 injected-embryos. From Shiokawa *et al.* (72).

can be expressed according to the strength of the promoter.

Controlled expression of the exogenous DNAs which carry promoters of Xenopus mRNA-coding genes

It has been shown that the circular DNAs injected into *Xenopus* embryos are transcribed at

correct initiation sites [3, 5, 60]. It has also been reported that the plasmids which carry the promoters for house-keeping functions such as *Xenopus* histone H1 [85] and mouse histone H1° [75] are expressed in almost all cell types. Whereas many genes of so-called luxury function, such as α-actin genes [50, 76, 85], cytoskeletal actin gene [8], and epidermal keratin gene [36] have been reported to be expressed during development not only at correct timing but also at correct embryonic regions (an example for the correct temporal expression for CAT gene connected to α-actin gene promoter is already given in the right panel of Fig. 10).

There have been papers which reported the presence of a promoter whose function is to determine the timing of the expression of the gene during development. One typical example is the promoter of the temporally-controlled gene, GS17 (gastrula-specific gene 17), whose essential part consists of only 74 base pairs localted at 682 bp upstream of its transcription initiation site [39]. Another paper of a special interest is the one which suggested the presence of two different regulatory elements in the promoter of α-actin gene of *Xenopus laevis* skeletal muscle: One for cell-type specific and the other for stage-specific expression of the gene within the embryo [76]. The elucidation of the structure and function of these control elements in developmentally important promoters would help us understand the mechanism of the gene actions in embryogenesis.

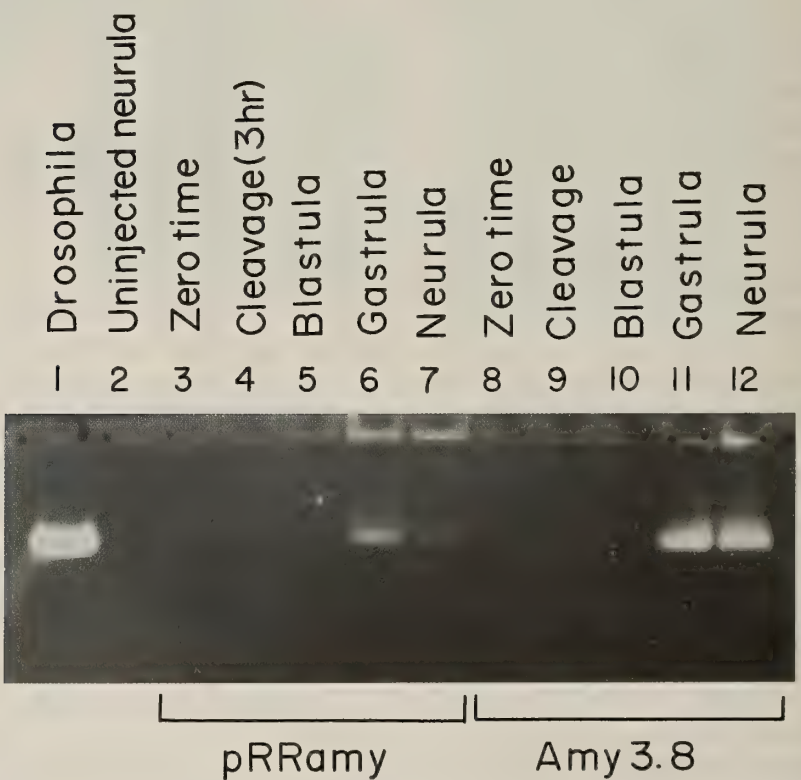

Fig. 12. Expression of *Drosophila* amylase in *Xenopus* early embryos. Fertilized eggs of *Xenopus laevis* were injected with 1 ng/egg of circular pRRamy 1.00 (lanes 3–7) or 2 ng/egg of circular Amy 3.8 (lanes 8–12). Five embryos were harvested at the indicated stages, and homogenized and assayed for amylase by electrophoresis on 3% polyacrylamide gel. Lane 1 shows the authentic amylase extracted from a fly (*Drosophila melanogaster*, Oregon R). Lane 2 shows the sample from control 5 neurulae which were not injected with the plasmid. From Shiokawa *et al.* [73].

Controlled expression in Xenopus embryos of exogenously-injected protein-coding genes from other sources

There have been several papers which report the results of the injection into fertilized *Xenopus* eggs of protein-coding genes derived from materials other than *Xenopus*. For example, we injected *Drosophila* amylase genes (pRRamy 1.00 and Amy 3.8; both code for the same *Drosophila* enzyme amylase, but differ only in the franking sequences) into fertilized *Xenopus* eggs and found that they are expressed at the gastrula and neurula stages (Fig. 12) [73]. The amount of the Amy 3.8 injected was twice that of pRRamy, and the extent of the expression was approximately proportionate to the amount of the injected genes. The formation of functional enzyme whose electrophoretic mobility is exactly the same as that of the fly indicates the correct transcription, processing, and translation of the injected genes as in the *Drosophila* cells. Thus, genes from other sources can also be expressed in a regulated way in *Xenopus* embryos.

In some cases, it has been shown that such regulation takes place in a promoter-dependent manner. The chimeric CAT gene carrying the promoter of *Drosophila* hsp (heat-shock-protein) gene has been shown to be heat-inducible after its introduction into *Xenopus* embryos [41]. Also, the gene for the rat glucose-regulated-protein which is known to be inducible by tunicamycin has been shown to be induced by tunicamycin treatment after its introduction into *Xenopus* embryos [86]. These experiments indicate that the promoters of genes from sources other than *Xenopus* can be recognized in *Xenopus* embryonic cells in specific ways.

Temporally-uncontrolled expression of linearized genes with the promoter which was originally under developmental control

In spite of the considerable amount of data available on promoter-dependent control of gene expression, little attention has been paid to the difference in the mode of expression of injected DNAs in relation to their structures (circular or linear). For instance, in the DNA injection experiments by Etkin and Balcells [16] described above, no clear difference has been detected in CAT enzyme expression between the embryos injected with circular pSV2CAT and the embryos injected with linearized pSV2CAT, even though they found that both forms are expressed. In the experiments by Mohun *et al.* [50] and Wilson *et al.* [85] which studied expression of the genes that contained α-actin promoters, the different modes of the expression of circular and linearized DNAs have not yet been recognized.

We have shown above that the expression of exogenously-introduced CAT genes greatly varies depending on whether they are circular or linear.

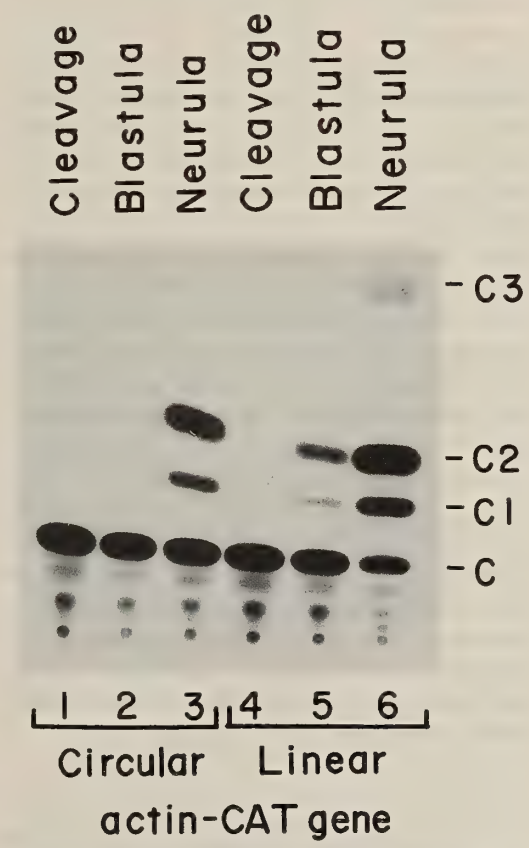

FIG. 13. Earlier expression of linearized actin-CAT fusion gene than circular gene during *Xenopus* development. Ten fertilized eggs were injected with 2 ng of either circular or linearized actin-CAT fusion gene and harvested at the indicated stages. CAT enzyme assay was as in Figure 9. From Shiokawa *et al.* [62].

Therefore, we examined if the expression of CAT gene connected to the developmentally-controlled *Xenopus* cardiac α-actin promoter (actin-CAT fusion gene #254) [50] also varies depending on whether the gene is circular or linearized.

As shown in Figure 10 (right) and in Figure 13 (lanes 1 to 3), the circular form of the fusion gene #254 is expressed only after embryos reached the early neurula stage. However, when we linearized the gene in the vector sequence and injected it into fertilized eggs at 1 ng/egg, the expression of the injected DNA took place as early as at the blastula stage (Fig. 13, lane 5) [62]. These results imply that when linearized, the expression of the fusion gene deviates from the normal temporal control even though the DNA possesses the intact promoter.

The changes in the amount and size of the linearized actin-CAT fusion gene injected here is as shown in Figure 5: while circular gene showed little change in its amount and size, linearized gene was ligated and replicated by about 10-fold at the blastula stage, and about 100-fold at the neurula stage. However, the increase in the amount of the injected DNA template at the blastula stage (by about 10-fold) does not by itself explain why the linearized DNA was expressed at the blastula stage, because the injection of 10 ng/egg of circular fusion gene did not induce the earlier expression of the gene (Fig. 10, right). Therefore, we assume that the temporally-uncontrolled expression of linearized actin-CAT fusion gene in the early embryos must be due to some structural features of the linearized DNA. Probably, the formation of large-sized concatemers would be the reason for their uncontrolled expression, as has been expected from the experiments with linearized pSV0CAT and isolated CAT gene fragment shown in Figure 9 [23].

EFFECTS OF DNA INJECTION ON GENE EXPRESSION IN COENOCYTIC EGG CELLS AND DEVELOPING EMBRYOS

Active cell division takes place in a fertilized *Xenopus laevis* egg and when the cell number is increased to about 4,000 (i.e. blastula stage), the formative movement starts within the embryo. During the process, the content of DNA per embryo increases very rapidly. We have previously carried out experiments to alter the ratio of the DNA to the cytoplasm either by arresting the cell division using colchicine and cytochalasin B [79], or by extracting the cytoplasm from the fertilized egg [67]. In both cases, we found that the change in the ratio (DNA/cytoplasm) did not exert any measurable effect on the timing of the activation of endogenous rDNA.

However, the DNA injection experiment provides more direct and powerful methods to increase the amount of DNA within the embryos. It is of an interest to see whether there is a change in gene expression in fertilized eggs or in developing embryos, when the relative ratio of DNA to cytoplasm, which could be a possible factor to determine the timing of gene expression [53], is changed artificially by the injection of a large amount of exogenous DNA. And so, we will briefly summarize here the experiments carried out on this line using coenocytic egg cells and cleaving embryos.

Experiments using coenocytic egg cells

Coenocytic egg cells which are viable for a relatively long period of time without cell division are prepared by centrifuging fertilized *Xenopus* egg at a low speed for a short time and then removing the spindle apparatus from its normal site. Although these egg cells (or coenocytic egg cells) do not divide, they synthesize DNA to some extent, and produce uncleaved egg cells with increased DNA content.

Newport and Kirschner [53] injected yeast tRNA gene (1 ng/egg; pYLT20) and then after 2 hr a large amount (24 ng/egg) of plasmid (pBR322) DNA into the coenocytic egg cell. They found that the latter injection of DNA (pBR322) which corresponds to the total DNA of an embryo at the MBT stage (cell number; 4,000) caused earlier expression of both previously-injected yeast tRNA genes and endogenous (nuclear) genes. From these observations, Newport and Kirschner [53] proposed a "titration" model, in which they predicted the presence in the egg of a limited amount of DNA-binding inhibitor of transcription. Furthermore, these authors postulated that the decrease in the amount of the inhibitor to a certain

level, which could be caused by the increase in the amount of DNA, triggers the initiation of the transcription from both endogenous and previously-injected DNAs.

Although this titration model has been modified later by Kimelman *et al.* [37] who proposed that events at the MBT are regulated by some changes related to cell cycle, we were still interested in the experiment by Newport and Kirschner [53] and so reexamined whether the second injection of a large amount of DNA is able to modify the timing and the level of the expression of the previously-injected plasmid DNA in coenocytic egg cells. When we first injected pSV2CAT (1 ng/egg) and then after 2 hr rDNA-containing plasmid pXlr101A (12 ng/egg) [2] into the coenocytic egg cells, we observed the faster and enhanced expression of CAT genes by the second injection of pXlr101A [63]. Therefore, in coenocytic egg cells the second injection of a large amount of DNA appears to have stimulating effect on the transcription of the previously-injected DNA.

More recently, however, Lund and Dahlberg [45] have commented on the previous studies made by Newport and Kirschner [53]. They reexamined the macromolecular synthesis in coenocytic egg cells, and found that the increase in the amount of DNA and RNA in these cells is reduced heavily when compared to that of the normal cleaving embryos. They also showed that RNA metabolism including the synthesis of snRNA and tRNA is quite aberrant in such coenocytic egg cells due to the poor replication of these genes. Therefore, Lund and Dahlberg [45] proposed that the previous experiments on transcriptional activation in coenocytic egg cells at the "MBT" must be re-evaluated (in fact, MBT stage or 12th cleavage stage does not exist in coenocytic egg cells).

Experiments in cleaving embryos

We carried out experiments consisting of two consecutive DNA injections using the normally developing embryos in order to compare the sequence of events in the above-described coenocytic egg cells with those in normally developing embryos [63]. We first injected 1 ng/egg of pSV2CAT and immediately after that injected 12 ng/egg of DNAs from different sources, including pXlr101A, total DNA (sonicated) of *Xenopus* tadpoles, and pBR322. As expected, these DNA injections interfered with cleavage in the animal hemisphere to varying extents. However, the injection of the second DNA neither modified the level nor affected the timing of the expression of the CAT genes.

It was confirmed using ^{3}H-labeled lambda DNA that nuclei of most of the blastomeres of the injected embryos contained the label, indicating the wide spreading of the injected DNA during cleavage. Then, the embryos injected with 12 ng/egg of the above DNAs (pXlr101A, lambda DNA, or sonicated *Xenopus* tadpole DNA) were dissociated into cells at the blastula stage and their RNA synthesis was examined by labelling cells with ^{3}H-uridine. We found here on agarose-polyacrylamide gels no appreciable change in the pattern of RNA synthesis between the control and the DNA-injected embryos at later stages (gastrula and early neurula stages).

In developing embryonic cells, it was also shown that 12 ng of secondarily-injected DNAs did not affect the level and the timing of the expression of previously-injected pSV2CAT (1 ng/egg). Therefore, the program of gene expression in the nuclei of developing embryos appears to be constructed in such a way that it is not easily altered by introduction of excess amounts of exogenous DNAs.

EXPRESSION OF EXOGENOUS GENES IN OOCYTES AND UNFERTILIZED EGGS

At first the DNA injection experiments in *Xenopus* system started by introducing the genes into the nucleus (germinal vesicle) of *Xenopus* oocytes. Initially injected were those that did not produce proteins, for example, rDNA [81], 5S DNA (genes for ribosomal 5S RNA) [10, 29], and tRNA genes [13, 38], but later, genes that code for proteins were also injected [56, 84]. The next step seen was to inject DNAs into unfertilized eggs. However, these experiments were mostly to study the mechanism of replication of exogenous DNAs in the egg cytoplasm [30, 32]. It was only after these experiments that the researches to inject exogenous DNAs into developing embryos started.

When considering these historical advancements, it may be important to compare the behavior of DNAs injected into the oocyte nucleus with the behavior of those injected into the cytoplasm of the unfertilized egg, and the cytoplasm of the fertilized egg. Therefore, we summarize here the results of the studies of gene expression from exogenously-introduced DNAs first in oocytes, then in unfertilized eggs.

Gene expression in the oocyte nucleus

We investigated the expression of various CAT gene-containing DNAs after injecting them into the oocyte nucleus. We observed that while circular DNAs were efficiently expressed, linearized DNAs were not expressed appreciably (Table 1) [23, 24], as has been reported previously by Harland *et al.* [31] and Bendig and Williams [5]. The inactiveness of linearized DNAs to serve as the templates in oocyte nucleus may be due to the lack of supercoiled domain and hence the absence of torsional stress, which is assumed to be necessary for efficient transcription [31, 56, 57].

A unique feature of the transcription in oocyte nucleus is that when circular CAT genes are injected, CAT enzyme expression is independent of the presence or absence of the promoter within the plasmid. This feature may be due to the presence of a large amount of DNA dependent RNA polymerase II in the oocyte nucleus (ca. 10^4 times the amount in a differentiated cell) [58], which creates enough chance of the binding of polymerase to the DNA templates. In this connection, it is said that the site of the initiation of transcription on the template DNA in the oocyte nucleus is not necessarily correct (or faithful), even if the circular plasmid contains the appropriate promoter [5].

In relation to this unique feature of the transcription in oocyte nucleus, a very interesting experiment was carried out by Wickens *et al* [84] using circular forms of cDNA and genomic DNA of *Xenopus* vitellogenin. They showed that both DNAs were transcribed into RNA within the oocyte nucleus, a result which is consistent with the above observation that pSV0CAT which does not contain promoter is expressed as strongly as the pSV2CAT which contains SV40 promoter.

In the studies of Wickens *et al* [84], while the transcript from genomic DNA was processed and transported into the cytoplasm as a functional mRNA for translation, the RNA from cDNA, which is by itself completed mRNA, remained in the nucleus and was not transported to the cyto-

Table 1. Expression and molecular structures of CAT genes in *Xenopus laevis* embryos, eggs and oocytes

Stages	CAT gene in circular form	Cat gene in linear form
Embryos	Actively expressed, depending on the strength of the promoter.	Actively expressed, irrespective of the presence or absence of the promoter.
	DNAs replicate moderately or only slightly mostly as DNAs of monomer size.	DNAs replicate actively and form concatemers, and integrated in the host DNA.
	Nucleus-like structures formed.	Nucleus-like structures formed.
Eggs	Very weakly expressed, depending on the promoter.	Very weakly expressed, irrespective of the presence or absence of the promoter.
	DNAs replicate moderately mostly as circular DNAs of monomer size.	DNAs are ligated, and form concatemers and replicated actively.
		Nucleus-like structures formed.
Oocytes	Actively expressed, even when the promoter is missing.	Expression undetectable even when a strong promoter is present.
	DNA stably preserved.	DNAs stably preserved.
	DNAs injected into the cytoplasm are degraded.	DNAs injected into the cytoplasm are degraded.

plasm to be translated into protein. Since the cDNA has neither promoter for correct initiation of transcription nor introns to be spliced out during the processing, it was assumed that nuclear processing may be coupled with nucleo-cytoplasmic transport of the mRNA. Therefore, in conclusion, there may be a limit in using the oocyte nucleus system for the study of the correct transcription of DNA templates.

Gene expression in unfertilized eggs

In unfertilized eggs, changes seen in the amount and size of the injected DNAs are essentially the same as those described above for the DNAs injected into the cytoplasm of fertilized eggs. Thus, in the cytoplasm of unfertilized eggs, c.c. DNA is rapidly converted into o.c. DNA, but c.c. DNA reappears shortly after, and the amount of these circular DNAs increases only to a limited extent during the incubation. Linearized DNAs, on the other hand, actively form concatemers and are replicated extensively [6, 30, 32].

It has been reported that in unfertilized eggs the transcription from circular DNAs starts from the correct initiation point [5], just as in the fertilized eggs [3, 60]. In the unfertilized eggs injected with CAT-containing circular plasmids, such as pSV2CAT and pAd12E1aCAT, CAT enzyme was expressed in a promoter-dependent way, although the extent of the expression was relatively quite low [23, 24]. The expression was observed also for linearized DNAs, but the extent of the expression was extremely low as compared with that observed with circular DNAs.

In the cytoplasm of an unfertilized egg, there is no nucleus but instead metaphase arrested chromosomes are present as has been shown above in Figure 1A. However, the pricking of the egg with a glass needle activates the egg, and then probably induces assemblage of nucleus-like structures [21]. Then, it may be assumed that the low efficiency of the expression of the injected DNA in unfertilized eggs may be due to the assemblage of most injected DNA in the form of chromatin probably in an inactive form. Or, it may be that the scattering of DNA-dependent RNA polymerase II in the egg cytoplasm at the germinal vesicle breakdown (GVBD) has resulted in the presence of only a limited amount of the polymerase in the site of the DNA transcription.

Much higher efficiency of the expression of injected DNAs in embryos as compared with that in unfertilized eggs would be due to the assemblage of a larger amount of injected DNA and RNA polymerase II in nuclei in embryonic cells than that in the unfertilized egg. If so, it follows that the injected DNAs are expressed after they are incorporated into the nuclei, as suggested above in relation to the parallel increase in the CAT enzyme expression and cell number in the experiment in Figure 10.

CONCLUSIONS

Studies of the control mechanism of exogenously-introduced DNAs in *Xenopus* early embryos provide a special opportunity to obtain clues to the understanding in molecular terms of many important aspects of the regulation of zygotic gene expression in animal development, especially in its early phases. When relatively large amount (10 ng/egg or more) of circular or linearized DNAs are injected into the cytoplasm of fertilized eggs, injected DNAs are assembled in the form of giant nucleus-like structures mostly in the animal region of the egg, probably after being complexed with maternal histones. Such giant nucleus-like structures are partitioned into descendant blastomeres, and embryonic development becomes more or less abnormal, especially in the animal half region. However, when relatively small amount (1–2 ng/egg or less) of such DNAs are injected, nucleus-like structures are not seen, and injected embryos show apparently normal development.

In the developing embryos, injected DNAs are replicated and expressed to different extent depending upon their structure. When circular plasmid DNAs are injected, they replicate only to a limited extent mostly as circular DNAs of monomer size, and the expression of the genes included is dependent upon the promoter. Thus, expression of circular form of bacterial CAT genes connected to viral promoter is initiated from the early cleavage stage, and the expression increases as the embryos develop. Also, CAT genes connected to the developmentally-controlled promoter, such as

cardiac α-actin gene, are expressed in both temporally and spatially controlled manner.

By contrast, when linearized DNAs are injected into the fertilized eggs, the injected DNAs are ligated to form large-sized concatemers of probably every possible conbinations (head-to-head, head-to-tail, and tail-to-tail orientation), and replicated extensively to form a large amount of large-sized DNA. Under these conditions, injected linearized DNAs are actively expressed, but the expression is independent on the presence of the promoter within the DNA.

When the linearized DNAs contain the developmentally-controlled promoter such as the promoter of cardiac α-actin gene, their expression takes place in cell-type specific manner in the correct region of the embryo. However, the temporal control of their expression is abolished in such linearized DNAs. Thus, while circular CAT genes with the above *Xenopus* α-actin promoter are expressed at the correct timing at the neurula stage, these genes start to be expressed already from the blastula or even from the early blastula stage if the DNAs were injected in linearized form.

It has been previously proposed that in *Xenopus* embryos the earliest stage of the expression of both endogenous (chromosomal) and exogenously-introduced genes is at the 12th cleavage, or at the stage when so-called midblastula transition (MBT) takes place. However, our data strongly suggest that it is the nature of the promoter contained in the DNA templates, and not the changes associated with the MBT, that determines the timing of the expression of the genes which are exogenously-introduced in circular form into *Xenopus* embryos.

ACKNOWLEDGMENTS

We wish to thank Professor Seiichiro Kawashima for his kind help in editing the manuscript. We are grateful to Professors Kiyotaka Yamana, Keiichi Hosokawa, and Tsuneyuki Yamazaki for their warm encouragements, and also to Drs. Kosuke Tashiro and Yuchang Fu, for their technical helps in doing the studies cited above. Special thanks are also due to Ms. Reiri Kurashima in our laboratory for her kind help in preparing our manuscript. The present work is supported in part by Narishige Zoological Science Award (1992) given to M. Asano.

REFERENCES

1 Andres A-C, Muellner DB, Ryffel GU (1984) Nucl Acids Res 12: 2283–2302
2 Bakken A, Morgan G, Sollner-Webb B, Roan J, Busby S, Reeder RH (1982) Proc Natl Acad Sci USA 79: 56–60
3 Bendig MM (1981) Nature (London) 292: 65–67
4 Bendig MM, Williams JG (1984) Mol Cell Biol, 4: 567–570
5 Bendig MM, Williams JG (1984) Mol Cell Biol 4: 2109–2119
6 Berg CA, Gall JG (1986) J Cell Biol 103: 691–698.
7 Blow JJ, Laskey RA (1988) Nature 332: 546–548
8 Brennan SM (1990) Differentiation 44: 111–121
9 Brown DD, Caston JD (1962) Dev Biol 5: 412–434
10 Brown DD, Gurdon JB (1977) Proc Natl Acad Sci 74: 2064–2068
11 Brown DD, Littna E (1964) J Mol Biol 8: 669–687
12 Busby SJ, Reeder RH (1983) Cell 34: 989–996
13 Cortese R, Harland RM, Melton DA (1980) Proc Natl Acad Sci USA 77: 4147–4151
14 Dawid IB (1965) J Mol Biol 12: 581–599
15 Endean DJ, Smithies O, (1989) Chromosoma 97: 307–314
16 Etkin LD, Balcells S. (1985) Dev Biol 108: 173–178
17 Etkin LD, Pearman B (1987) Development 99: 15–23
18 Etkin LD, Pearman B, Ansah-Yiadom R, (1987) Exptl Cell Res 169: 468–477
19 Etkin LD, Pearman B, Roberts M, Bektesh S (1984) Differentiation 26: 194–202
20 Flytzanis CN, McMahon AP, Hough-Evans BR, Katula KS, Britten RJ, Davidson EH (1985) Dev Biol 108: 431–442
21 Forbes DJ, Kirschner MW, Newport JW (1983) Cell 34: 13–23
22 Franks RR, Hough-Evans BR, Britten RJ, Davidson EH (1988) Development 102: 287–299
23 Fu Y, Hosokawa K, Shiokawa K (1989) Roux's Arch Dev Biol 198: 148–156
24 Fu Y, Sato K, Hosokawa K, Shiokawa K (1990) Zool Sci 7: 195–200
25 Gorman CM, Moffat LF, Howard BH (1982) Mol Cell Biol 2: 1044–1051
26 Gurdon JB, Melton DA (1981) Ann Rev Genet 15: 189–218
27 Gurdon JB (1974) The control of Gene Expression in Animal Development Clarendon Press Oxford
28 Gurdon JB, Brown DD (1977) In "The Molecular Biology of the Genetic Apparatus vol 2" Ed by P T'so, North-Holland Publ Co, Amsterdam, pp 111–123
29 Gurdon JB, Brown DD (1978) Dev Biol 67: 346–

356
30 Harland RM, Laskey RA (1980) Cell 21: 761–771
31 Harland RM, Weintraub H, McKnight SL (1983) Nature 302: 38–43
32 Hines PJ, Benbow RM (1982) Cell 30: 459–468
33 Hofmann A, Montag M, Steinbeisser H, Trendelenburg F, (1990) Cell Differ Dev 30: 77–85
34 Honjo T, Reeder RH (1973) J Mol Biol 80: 217–228
35 Iwao Y, Katagiri C (1984) J Exp Zool 230: 115–124
36 Jonas EA, Snape AM, Sargent TD (1989) Development 106: 399–405
37 Kimelman D, Kirschner M, Scherson T (1987) Cell 48: 399–407
38 Kressmann A, Clarkson SG, Pirrotta V, Birnstiel ML (1978) Proc Natl Acad Sci USA 75: 1176–1180
39 Krieg PA, Melton DA (1987) Proc Natl Acad Sci USA 84: 2331–2335
40 Kruczek I, Doerfler W (1983) Proc Natl Acad Sci USA 80, 7586–7590
41 Krone P H, Heikkila JJ (1989) Development 106: 271–281
42 Langner KD, Weyer U, Doerfler W (1986) Proc Natl Acad Sci USA 83: 1598–1602
43 Leno GH, and Laskey RA (1991) J Cell Biol 112: 557–566
44 Lohka MJ, Masui Y (1983) Science 220: 719–721
45 Lund E, Dahlberg JE (1992) Genes Develop 6: 1097–1106
46 Marini NJ, Etkin LD, Benbow RM (1988) Dev Biol 127: 421–434
47 Marini NJ, Hiriyanna KT, Benbow RM (1989) Nuc Acids Res 17: 5793–5808
48 McMahon AP, Flytzanis CN, Hough-Evans BR, Katula KS, Britten RJ, Davidson EH. (1985) Dev. Biol., 108: 420–430
49 Mechali M, Kearsey (1984) Cell 38: 55–64
50 Mohun TJ, Garrett N, Gurdon JB (1986) EMBO J 5: 3185–3193
51 Nakakura N, Miura T, Yamana K, Ito A, Shiokawa K (1987) Dev. Biol., 123: 421–429
52 Newport J, Kirschner M (1982) Cell, 30: 675–686
53 Newport J, Kirschner M (1982) Cell, 30: 687–696
54 Newport J (1987) Cell 48: 205–217
55 Ozato K, Kondoh H, Inohara H, Iwamatsu T, Wakamatsu Y, Okada TS (1986) Cell Differ 19: 237–244
56 Probst E, Kressmann A, Birnstiel ML (1979) J Mol Biol 135: 709–732
57 Pruitt S, Reeder RH (1984) J Mol Biol 174, 121–139
58 Roeder RG (1974) J Biol Chem 249: 249–256
59 Rosenthal N, Kress M, Gruss P, Khoury G (1983) Science 222: 749–755
60 Rusconi S, Schaffner W (1981) Proc Natl Acad Sci USA 78: 5051–5055
61 Shiokawa K (1991) Develop Growth Differ 33: 1–8
62 Shiokawa K, Fu Y, Hosokawa K, Yamana K (1990) Roux's Arch Dev Biol 199: 174–180
63 Shiokawa K, Fu Y, Nakakura N, Tashiro K, Sameshima M, Hosokawa K (1989) Roux's Arch Dev Biol 198: 78–84
64 Shiokawa K, Misumi Y, Tashiro K, Nakakura N, Yamana K, Oh-uchida M (1989) Cell Differ Dev 28: 17–26
65 Shiokawa K, Misumi Y, Yamana K (1981) Dev Growth Differ 23: 579–587
66 Shiokawa K, Sameshima M, Tashiro K, Miura T, Nakakura N, Yamana K (1986) Dev Biol 116: 539–542
67 Shiokawa K, Takeichi T, Miyata S, Tashiro K, Matsuda K (1985) Cytobios 43: 319–334
68 Shiokawa K, Tashiro K, Misumi Y, Yamana K (1981) Dev Growth Differ 23: 589–597
69 Shiokawa K, Tashiro K, Yamana K, Sameshima M (1987) Cell Differ 20: 253–261
70 Shiokawa K, Yamana K (1965) Exptl Cell Res 38: 180–186
71 Shiokawa K, Yamana K (1967) Dev Biol, 16: 368–388
72 Shiokawa K, Yamana K, Fu Y, Atsuchi Y, Hosokawa K (1990) Roux's Arch Dev Biol 198: 322–329
73 Shiokawa K, Yamazaki T, Fu Y, Tashiro K, Tsurugi K, Motizuki M, Ikegami Y, Araki E, Andoh T, Hosokawa K (1989b) Cell Struct Func 14: 261–269
74 Shiokawa K, Yoshida M, Fukamachi H, Fu Y, Tashiro K, Sameshima M (1992) Develop Growth and Differ 34: 79–90
75 Steinbeisser H, Alonso A, Epperlein HH, Trendelenburg MF (1989) Int J Dev Biol 33: 361–368
76 Steinbeisser H, Hofmann A, Stutz F, Trendelenburg MF (1988) Nuc Acids Res 16: 3223–3238
77 Stuart GW, McMurray JV, Westerfield M (1988) Development 103: 403–412
78 Szollosi MS, Szollosi D (1988) J Cell Sci 91: 257–267
79 Takeichi T, Satoh N, Tashiro K, Shiokawa K (1985) Dev Biol 112: 443–450
80 Tashiro K, Inoue M, Sakaki Y, Shiokawa K (1986) Cell Struct Func 11: 109–114
81 Trendelenburg MF, Gurdon JB (1978) Nature 276: 292–294
82 Trendelenburg MF, Oudet P, Spring H, Montag M (1986) J Embryol exp Morph 97: Supplement 243–255
83 Vitelli L, Kemler I, Lauber B, Birnstiel ML, Busslinger M (1988) Dev Biol 127: 54–63
84 Wickens MP, Woo S, O'Malley BW, Gurdon JB (1980) Nature 285: 628–634
85 Wilson C, Cross GS, Woodland HR (1986) Cell 47: 589–599
86 Winning RS, Bols NC, Wooden SK, Lee AS, Heik-

kila JJ (1992) Differentiation 49: 1–6

87 Woodland HR, Gurdon JB (1968) J Embryol Exp Morph 19: 363–385

88 Yoshizaki G, Oshiro T, Takashima F (1991) Nippon Suisan Gakkaishi 57: 819–824

ZOOLOGICAL SCIENCE 10: 223–234 (1993)

REVIEW

Comparative Aspects of Intestinal Calcium Transport in Fish and Amphibians

Douglas R. Robertson

Department of Anatomy & Cell Biology, State University of New York Health Science Center Syracuse, New York, 13210, USA

INTRODUCTION

One of the features in the transition of vertebrates from an aquatic to a terrestrial environment is the maintenance of a relatively constant cellular ionic calcium concentration of $<1\ \mu M$. Such a level is easily achieved by passive diffusion alone since a gradient exists between the ionic calcium concentration in plasma, usually greater than 1 mM, and the ionic calcium within the cytosol of the cell.

In a marine environment, a gradient also exists between seawater (10–15 mM) and the plasma compartment where the plasma ionic calcium concentration in marine fish is about 1.7–1.9 mM [6, 8]. Thus, for marine animals, calcium can be acquired by passive diffusion across epithelia; i.e. gills [20, 60]. For marine forms calcium homeostasis is concerned primarily with calcium exclusion, rather than acquisition; thus, excess calcium is secreted into the gut lumen and expelled with the feces.

For terrestrial animals, lacking gills, calcium acquisition is obtained by dietary sources, and plasma ionic levels are maintained in a range from 0.9–1.4 mM in frogs [54]; 1.2–1.4 mM in chickens [46] and 1.5 mM in man [31]. With the intestine serving as a primary source for calcium acquisition, it is apparent that movement into the plasma compartment cannot be achieved by passive diffusion alone if gut lumen concentration is below the plasma ionic concentration.

Received October 14, 1992

For fish in freshwater with low environmental calcium (<1 mM) and terrestrial animals, an additional mechanism has been added to allow the gut to "up-regulate", and actively absorb calcium aganist a concentration gradient. This additional capacity is achieved with a vitamin D-dependent calcium binding protein (CaBP) localized in the primary gut absorptive cell, the enterocyte.

MORPHOLOGY

The intestinal epithelium, composed of enterocytes, arise from stem cells found within crypts at the base of villus projections in birds and mammals. These cells are attached to one another via tight junctions situated near the apical region of the cell, with a narrow intermediate junction and wider intervening paracellular space near the basal region of the cell (Fig. 1). Enterocytes have the capacity to move calcium from mucosa to the underlying serosa (Ca_{influx}, $J_{m\rightarrow s}$), or as secretion from serosa to mucosa (Ca_{ouflux}, $J_{s\rightarrow m}$). Both Ca_{influx} by passive diffusion and $Ca_{outflux}$ occur within the paracellular space, and is largely dependent upon the calcium concentration gradient between the two compartments.

On the other hand, transcellular movement of calcium through the enterocyte is energy dependent, and enters via the apical microvillus border, and is extruded across the basolateral membrane to the underlying vascular compartment. Calcium entry into the cell is by passive diffusion, or possibly through specific calcium channels. Once into the cell, calcium movement may be facilitated

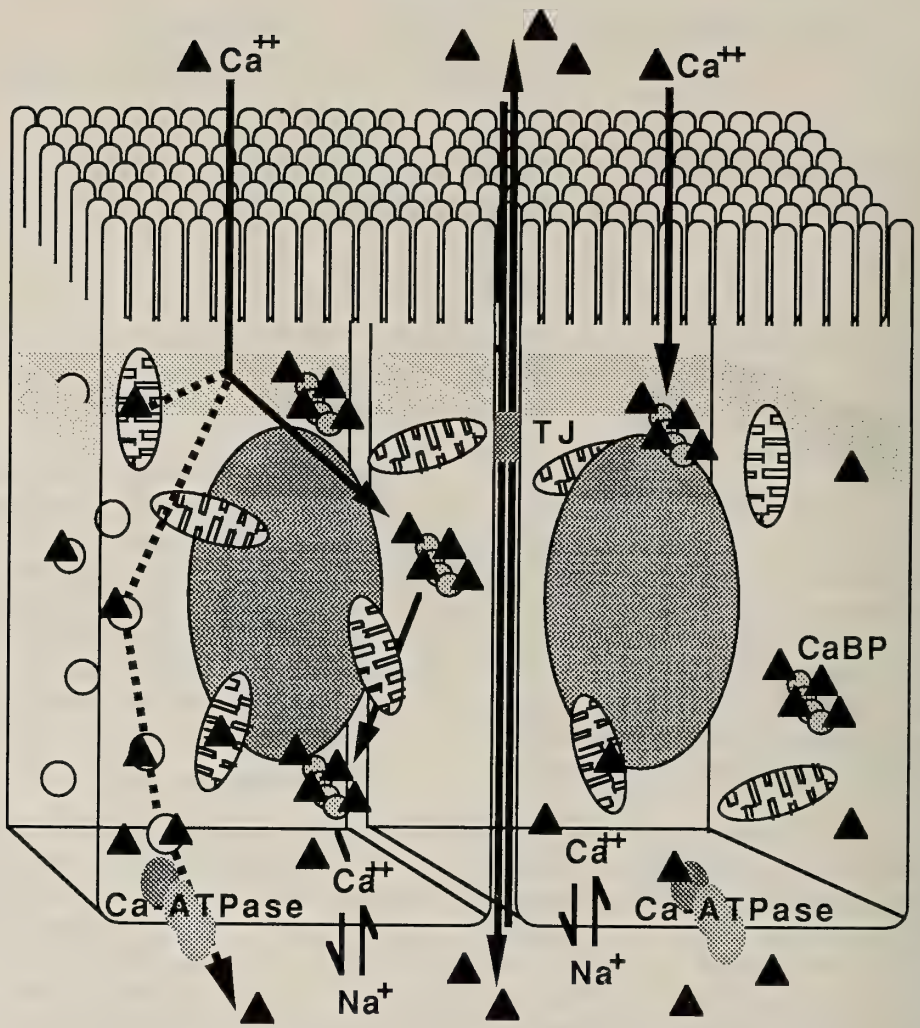

Fig. 1. Schematic representation of calcium movement across gut epithelium. Columnar enterocytes have microvillus apical surface while lateral membranes are attached by apical tight junctions (TJ) with a basal-lateral intervening paracellular space. Ca_{influx} by passive diffusion or $Ca_{outflux}$ (secretion) occurs in paracellular space while active calcium transport is transcellular. Calcium ions entering the enterocytes cross apical border to bind to organelles; cytosolic vesicles or mitochondria, or proteins; e.g. CaBP, to reduce cytosolic ionic calcium and increase diffusion constant. Calcium is extruded across basal membranes *via* Ca^{2+}/Mg^{2+}-ATPase and Na^+/Ca^{2+}-exchange mechanisms.

by enzymes such as alkaline phosphatase, be sequestered into specific organelles; i.e., mitochondria, microtubules, lysosomes, vesicles, or be bound to specific proteins; i.e. calmodulin or a vitamin D-dependent calcium binding protein (CaBP). With movement of calcium into the basal cytosol, calcium is extruded across the basolateral membranes via a Ca^{2+}/Mg^{2+}-dependent ATP ase or by a Na^+/Ca^{2+}-exchange mechanism.

As enterocytes arise from the crypts between intestinal villi, they mature and acquire the capacity to transport calcium with maximal transport in cells isolated near the villus tip [70, 72]. In the rat model, isolation of various populations of cells along the villus axis show high alkaline phosphatase and calcium binding protein (CaBP) acitivity

in those cells at the villus tip, with decreasing amounts in those cells at the villus base and within the crypts. ATP-dependent Ca^{2+} transport is highest just below the villus tip while calmodulin is equally distributed from tip to crypt. In the rat, a Na^{+}/Ca^{2+} exchanger has been found at all villus axis levels, but is of minor importance.

PATTERNS OF CALCIUM ABSORPTION

For marine fish, with a high environmental calcium, acquisition is primarily through the gills [20, 60]; although Sundell and Björnsson [62] concluded that about 30% of whole body influx was contributed by intestinal absorption of calcium in the Atlantic cod, *Gadus*. When placed in 50% seawater the river lamprey, *Lampetra fluviatilis* [48], exhibited both Ca_{influx} and $Ca_{outflux}$ with net calcium secretion. However, in a freshwater environment or during periods of increased need for calcium; e.g. gonadal maturation, intestinal calcium absorption may assume a greater role in calcium acquisition [4]. Intestinal calcium absorption has been identified in freshwater forms such as the trout, *Salmo gairdneri* [33, 58], and goldfish, *Carassius auratus,* [16]; while other studies with the carp, *Cyprinus carpio* [35] have shown no calcium absorption.

In terrestrial animals, the intestine serves as the organ for calcium acquisition; the proximal small intestine (duodenum) has the highest calcium uptake capacity, followed by small intestine with the lowest capacity in the colon. Amphibians as a group have been little studied except for the anurans. Using the everted gut sac technique, higher calcium transport capacity is seen in the proximal duodenum than in distal small intestine of the leopard frog, *Rana pipiens* [52]. Uptake is enhanced 50% in the duodenum after vitamin D_3 administration, indicating the presence of an active, vitamin D-dependent calcium transport mechanism [50]. In *R. esculenta,* uptake of ^{45}Ca injected into the intestinal lumen confirmed that the proximal intestinal segment has a higher uptake capacity than the distal segment [13].

For birds [73] and mammals [14], highest vitamin D-dependent active transport capacity also occurs in the duodenum, and decreases distally along the length of the small intestine as: duodenum>jejunum>ileum. However in some mammals; specifically the rat, segments of the large intestine; i.e. cecum, show a higher uptake in normally fed animals. Vitamin D_2 or D_3 increases calcium uptake in the avian duodenum [67], while vitamin D_3 can also increase uptake in distal ileum [26]. In the rat, vitamin D_3 not only enhances duodenal calcium absorption, but cecum as well [14]. However, in humans no detectable levels of CaBP is found in cecum or colon [61].

MECHANISMS OF CALCIUM ABSORPTION

Passive diffusion.

Passive diffusion, or the nonsaturable uptake of calcium in the gut from mucosal to serosal surface ($J_{m\to s}$), is linear with luminal calcium concentration. Voltage clamp studies on rat ileum [39] indicate that passive diffusion is paracellular and is significant when luminal calcium concentrations are at 10 mM; but negligible at physiological concentrations of 0.05 mM. Nellans [37] also has proposed a translocation pathway that includes negative charged endocytoic vesicles that isolates the bound calcium from cytosolic calcium, mimicking a paracellular route.

Using mannitol fluxes to measure paracellular routes, regional differences in paracellular calcium fluxes have been seen between rat cecum and ileum [38, 39]. Pansu and coworkers [41–43], applying a graded series of calcium concentrations with an *in situ* loop preparation, determined that the diffusion constant (K_d) was relatively constant along the length of the adult rat intestine, where $K_d = 0.20–0.25$/hour (passive diffusion was limited to 20–25% of available luminal calcium).

Sundell and Björnsson [62] using an *in situ* intestinal loop procedure found in the Atlantic cod, *Gadus morhua,* a passive transport component that amounted to about 40% of total calcium absorption at a luminal concentration of about 15mM. In the frog *Rana pipiens,* the passive diffusion component (K_d) in the total small intestine is 0.12–0.15/0.5 hr of available calcium. Thus, at a luminal concentration of 15 mM, 50% of total calcium absorption is derived from passive

diffusion [Robertson, unpublished observations]. A value of K_d=0.16/hr obtained in the adult rat [7] would suggest that the higher diffusional constants in the frog and marine fish may reflect a more permeable mucosa than in the adult rat.

Secretion.

In contrast to passive diffusion of calcium from lumen to plasma, $Ca_{outflux}$, or secretion, represents the movement of calcium from serosa to mucosa ($J_{s\rightarrow m}$), and can effectively reduce net calcium absorption as,

$$Ca_{net}=Ca_{influx}-Ca_{outflux} \quad (1)$$

where Ca_{net} represents the sum of the two unidirectional calcium fluxes. For example, in vitamin D-depleted rats, with a luminal calcium concentration of 0.54 mM, 56% of Ca_{influx} is secreted back into the lumen, with net calcium absorbed representing only 44% of $Ca_{outflux}$. Administration of vitamin D increases net calcium absorption, and reduces secretion ($Ca_{outflux}$) to 31% of Ca_{influx} [76]. While vitamin D up-regulates the duodenum to increase Ca_{influx}, the secretory component can diminish the efficiency of active calcium transport.

Serosal-to-mucosal calcium and mannitol permeability studies indicate that secretion is primarily paracellular [14]. The process is not energy dependent since it is not abolished or reduced by metabolic inhibitors or temperature sensitive [39]. Two routes have been identified; solvent-drag that is dependent on paracellular water flow and diffusional flux, dependent on paracellular permeability [37]. Thus, secretion can be driven by a calcium gradient between plasma and lumen ionic calcium when luminal calcium falls below 1.5 mM.

Some fish such as carp, *Cyprinus carpio,* do not absorb or secrete calcium at any point along the intestine [35]; whereas the Japanese eel, *Anguilla japonica,* kept in freshwater, exhibits secretion of both calcium and magnesium ions into the intestinal lumen. Neither hypophysectomy, stanniectomy or calcitonin administration had any effect on net calcium secretion [36]. In lamprey, in addition to calcium $J_{m\rightarrow s}$ along the length of the intestine, there is a greater calcium $J_{s\rightarrow m}$ at the posterior intestine, resulting in a positive net $Ca_{outflux}$. Rainbow trout, *Salmo,* kept in either fresh water or seawater, exhibit a general increase in calcium concentration of intestinal contents progressing

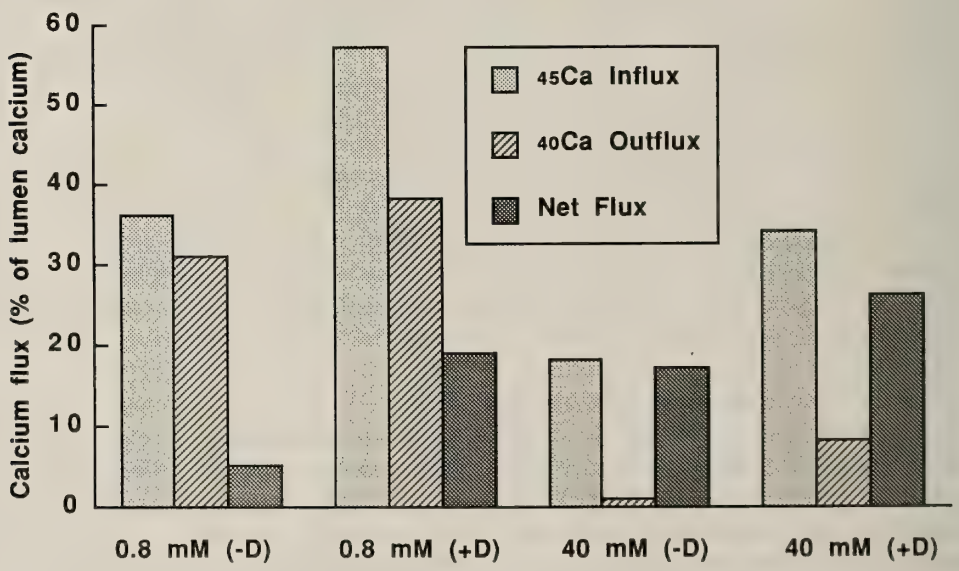

FIG. 2. Histogram depicting calcium movement in duodenum of adult frog (*Rana pipiens*) of control and vitamin D_3 (500 μg) using *in situ* loop preparation with 0.8 and 40 mM calcium in incubation buffer. At 0.8 mM, net Ca_{influx} is reduced by high $Ca_{outflux}$, while at 40 mM $Ca_{outflux}$ is relatively low with resultant high net Ca_{influx}. At both luminal concentrations, vitamin D_3 increases $^{45}Ca_{influx}$ and therefore net Ca_{influx}.

toward the distal segments, indicative of calcium secretion into the feces [12].

$Ca_{outflux}$ or secretion occurs in the frog (*Rana pipiens*) duodenum and is influenced by luminal calcium concentration. At a luminal calcium of <1 mM, Ca_{influx} is about 35% but a high secretion rate reduces the net Ca_{influx} to about 6%; while vitamin D increases Ca_{influx} to elevate net Ca_{influx} to 12% (Fig. 2). At a high luminal calcium (40 mM) with or without vitamin D, net Ca_{influx} is elevated, a result of a decrease in secretion [Robertson, unpublished observations]. For whole animal balance studies, the secretory component should be included, especially at low luminal concentrations when Ca_{net} absorption will be lower than Ca_{influx}, despite the presence of an active calcium uptake mechanism.

Transcellular calcium transport.

In contrast to diffusion mechanisms that are paracellular, active calcium transport occurs within the enterocyte and can be represented as a three step process: 1) transfer across the apical membrane to the cytosol, 2) transfer through the cytosol to the basal region of the cell, and 3) transfer across the basolateral membranes. Since the cell interior has a negative voltage compared to the lumen, calcium movement can cross the apical membrane down the charge gradient. Also, movement is favored by simple diffusion since a concentration gradient can exist from the lumen (1–5 mM) to less than 1 μM within the cytosol [69]. Use of calcium channel blockers, such as verapamil, appears to reduce gut calcium transport, but its effectivness only at high concentrations (1–2 mM) in contrast to concentrations effective at lower concentrations (1–10 μM) in excitable tissues, suggests that the effect may be nonspecific [15, 21, 47, 75].

Transfer within the cytosol is affected by a variety of individual processes. First, calcium may be sequestered into various organelles; i.e., mitochondria, microtubules, lysosomes or vesicles, or bound to specific proteins; i.e. calmodulin. Early studies in the chick recognized that active calcium transport was vitamin D-dependent and was significantly correlated with the presence of a CaBP along the length of small intestine [66] and with the amount of CaBP in the transport tissue [32]; i.e. that CaBP is preferentially localized in duodenum, with a decreasing content at more distal gut segments. Since the degree of active calcium transport, as expressed by the value of J_{max}, varies linearly with the amount of CaBP [7], and the presence of CaBP is vitamin D-dependent, CaBP is viewed as the primary cytosolic "carrier" for movement of calcium within the cytosol. In mammals CaBP is a 9 Kd molecule or a 28 Kd protein in birds (Calbindin). While the specific role of this protein is not completely defined, its capacity to bind calcium lowers the cytosolic free calcium, effectively increasing transcellular calcium diffusion by 60-fold [7]. Thus, it appears as a rate-limited "carrier"; its quantitative presence in intestinal mucosa is linearly proportional to calcium absorption.

For the final transfer across the basolateral membrane, there are two mechanisms of calcium extrusion that are recognized; an ATP-dependent Ca^{2+}/Mg^{2+} transport mechanism [23, 25], and a Na^{+}/Ca^{2+} exchanger [5], both in the same plasma membrane. In mammals, the ATP-dependent calcium transport pump is the dominant mode of calcium extrusion [23, 25, 34], and does not appear to be a rate-limiting step under normal nutritional conditions [7]; while the Na^{+}/Ca^{2+}-exchanger plays a minor role [71].

In fish, where calcium extrusion mechanisms have been examined, there is evidence for both a ATP-dependent calcium transport pump and a Na^{+}/Ca^{2+}-exchanger. In vitamin D-treated goldfish, *Carassius,* chlorpromazine, a Ca^{2+} ATP-ase inhibitor, reduced calcium absorption by 50%, but only 30% in nontreated animals, suggesting that the vitamin D-stimulated transport mechanism was chlorpromazine-sensitive [17]. A similar response was seen in the Atlantic cod, *Gadus,* where chlorpromazine reduced intestinal calcium influx by 45%; however, specificity of the site of action or its role in active transport could not be confirmed [62]. Using isolated basolateral membrane vesicles from the freshwater fish, *Oreochromis* (tilapia), Flik and co-workers [19] identifed both the Na^{+}/Ca^{2+} exchanger and an ATP-ase extrusion mechanism, and noted that calcium extrusion is sodium dependent with the ATP-dependent

Ca^{2+}/Mg^{2+} pump only one-sixth as effective as the Na^{+}/Ca^{2+} exchanger in extruding calcium from the enterocyte.

Viewing all three steps in intracellular calcium transport, evidence indicates that the rate-limting step is cytosolic transfer; e.g., CaBP-dependent. Since CaBP effectively reduces the cytosolic calcium concentration, transfer across the microvilli is facilitated by diffusion; while transfer across the basolateral membranes are by mechanisms that have a higher rate constant than the CaBP-dependent cytosolic transfer.

KINETICS OF CALCIUM ABSORPTION

Active calcium transport is transcellular and operates against an electrochemical gradient. For kinetic studies, uptake can be assessed using either the everted gut sac assay, or the *in situ* intestinal loop preparation. Since active transport (A) is a saturable process that follows Michaelis-Menten kinetics; it follows the equation proposed by Taylor and Wasserman [66]:

$$A=\frac{J_{max}\times[Ca^{2+}]}{K_m+[Ca^{2+}]} \qquad (2)$$

where J_{max} is the maximum saturable flux from lumen to plasma, K_m is the apparent half-saturation constant for J_{max}, and Ca^{2+} is the luminal calcium concentration.

However, since Ca_{influx} also includes a nonsaturable component from passive diffusion (K_d); total Ca_{influx} or $J_{m\rightarrow s}$ is represented by:

$$Ca_{influx}=A+K_d[Ca^{2+}] \qquad (3)$$

and requires the use of the *in situ* loop technique. An idealized model for calcium absorption in a tissue displaying both a saturable and nonsaturable component is illustrated in Figure 3. Following a procedure of Pansu et al., [41], the passive or nonsaturable component (K_d) is represented by a linear uptake profile whose slope is constant; and derived from the uptake data at higher calcium concentrations whose slope is linear, represented by the diagonal line. The remaining component, representing saturable calcium uptake, is used to derive values for J_{max} and K_m. The resulting curvilinear function (equation 3), expresses the uptake profile of the original data.

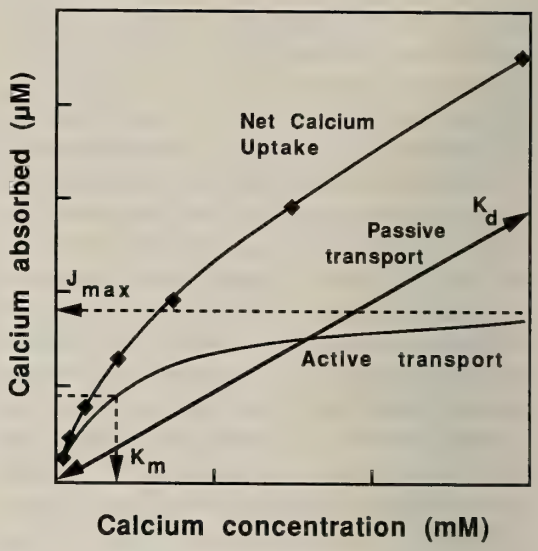

FIG. 3. Idealized model of calcium absorption *in situ* intestinal loop preparation with increasing concentrations of calcium in incubation buffer. Diagonal line, derived from linear uptake at high calcium concentrations, represents uptake by passive diffusion whose slope is K_d. Active calcium transport depicted by lower curvilinear line, calculated for values of J_{max} and K_m, follows Michaelis-Menten kinetics and is derived from uptake data minus contribution from passive diffusion. Upper curvilinear function, connecting data points, is best-fit of uptake data by active transport and passive diffusion.

Using such a procedure, Sundell and Björnsson [62] identified both a saturable and nonsaturable component in the small intestine of Atlantic cod, *Gadus morhua,* where J_{max} was 0.604 μmol/Kg/hr with a K_m=8.41 mM at 10°C. With a luminal calcium concentration of about 15 mM, 60% of uptake was from the saturable component; with the remainder from passive diffusion. In similar studies in the adult male frog, *Rana pipiens,* assayed at 20–22°C, duodenal active uptake (saturable) had a J_{max}=7.0 μmol/0.5 hr/gm wt. tissue compared to the jejunoileum where J_{max}=3.3 μmol/ 0.5 hr/gm. With a luminal concentration of 15 mM, 50% of duodenal uptake was saturable, and 50% by passive diffusion [Robertson, unpublished observations]. In the 30–35 day Wistar rat (assayed at 37°C) active saturable calcium trans-

port in the duodenum had a J_{max}=31 μmol/hr; while jejunum was 12 μmol/hr with no detectable saturable component in more distal ileum [41]. With a duodenal lumen concentration of 15 mM, the saturable component in the rat accounts for 70% of the total calcium absorbed. Although there were differences in assay temperature, the magnitudes of the active, saturable uptake component were similar, with active transport observed in more proximal intestinal segments.

Localization of vitamin D-dependent calcium binding protein.

Assessment of the kinetics of active calcium influx that follow Michaelis-Menten kinetics, specifically the derived value of J_{max}, show a significant correlation with mucosal CaBP. In the growing rat, J_{max} varies with age [42, 68]. Young 3-day old rats that lack CaBP exhibit only calcium uptake by passive diffusion; whereas with older animals, there is a progressive increase in the active, saturable uptake mechanism that is correlated with the presence of CaBP [43]. Evidence presented indicates that CaBP concentration is directly correlated with the quantity of saturable transport (J_{max}) [41] and therefore is related to the total quantity of an available "carrier". Bronner [7] takes this in support of the concept that the rate-limiting movement of calcium within the cytosol is dependent upon CaBP, that acts as a carrier to move calcium from the apical to basal cytosol.

Since intestine of fish and amphibians exhibit an increase in calcium transport in response to vitamin D and its metabolites, there has been interest in localization of vitamin D-dependent CaBP in these forms. Using a ^{45}Ca binding procedure, a heat stable intestinal CaBP was identified in the carp (*Cyprinus cario*) [9]. In another study, CaBP from carp intestine co-migrated with a pig intestinal CaBP; while a frog CaBP co-migrated with CaBP from rat and chick [40]. It is now recognized that there are two different vitamin D-dependent intestinal calcium-binding proteins present in other vertebrates; a 9 Kd protein found exclusively in mammalian intestine, and a more widely distributed 28 Kd molecule found in birds, reptiles and some amphibians. Wesserman and Corradino [74] indicated that frog, toad and turtle intestine showed cross-reactivity to antisera to chick CaBP; however, Parmentier et al., [45] employing antibodies to a chick CaBP (Calbindin 28 Kd), only was able to demonstrate immunocytochemical cross-reactivity in the small intestine of three species of reptiles, but was unable to demonstrate cross-reactivity in the small intestine of four species of amphibian or three species of fish. A slight cross-reaction was apparent in Western blots of gels of gut homogenates of *Xenopus* and *Triturus*. Subsequently, using immunocytochemical and Western blot techniques, Calbindin 28 Kd was localized in the large intestine of the toad (*Bufo bufo*), but was not apparent in the proximal duodenal segment [44]. Thus, the distribution pattern of a 28 Kd CaBP seen in the toad differs from that seen in birds [73], rat [43, 65] or humans [61], that show a direct correspondence to vitamin D-dependent active calcium transport. Recent studies [49] have shown Calbindin 28 Kd to coexist in the intestine of pig and jerboa (a leaping rodent) with the 9 Kd intestinal CaBP; although the presence of both types of CaBP is not observed in rat, mouse or goat. These findings bring to question whether the 28 Kd CaBP is always responsive to vitamin D. The presence of a 28 Kd CaBP in the colon of toads [44], but not in the duodenum that exhibits a vitamin D-dependent increase in calcium transport [50, 52] would suggest that further studies are needed to clarify the molecular species of intestinal vitamin D-dependent CaBP in fish and amphibians.

Endocrine relationships.

An increase in intestinal calcium absorption in response to variations in dietary calcium, growth requirements or reproductive demands, are mediated by changes in enterocyte vitamin D-dependent CaBP. In birds [30] and mammals [29], 1,25-$(OH)_2$-D_3 is the most biologically active form of vitamin D that is a requirement for CaBP synthesis. To become effective, vitamin D must undergo sequential hydroxylations at the 1- and 25-carbon positions. The first conversion is in the liver to form 25-(OH)-D_3; with the second hydroxylation in the kidney by 25-hydroxyvitamin D_3 (25-D_3)-1 alpha-hydroxylase to form 1,25-$(OH)_2$-D_3 [22]. Feedback mechanisms exist to modulate

this conversion. Evidence in rats suggests that 1,25-$(OH)_2$-D_3 inhibits the conversion in the liver by increasing liver cytosolic calcium [2]; an inhibition also seen in man by increasing the dietary calcium [3]. This observation might suggest that an elevation in venous portal blood draining the small intestine, after a high calcium load that flows directly to hepatocytes, can modulate 25-(OH)-D_3 production. In the kidney an additional metabolite, 24,25-$(OH)_2$-D_3, also is formed [28], and may represent a step in a degradative pathway [27]. The renal conversion to 1,25-$(OH)_2$-D_3 is modulated indirectly by plasma ionic calcium mediated by parathyroid hormone (PTH) [22].

Of interest is the phyletic relationship of the metabolites of vitamin D with the appearance of active calcium transport in fish and amphibians and the relationship to parathyroid hormone (PTH). Early studies in the eel (*Anguilla anguilla*) suggested that vitamin D_3 was more effective in stimulating intestinal calcium absorption than the more polar 1,25-$(OH)_2$-D_3 [10]. A somewhat similar response was seen in the marine Atlantic cod, *Gadus* [63] where 25-(OH)-D_3 increases intestinal calcium uptake by 65%; whereas the more polar 1,25-$(OH)_2$-D_3 was without effect; while 24,25-$(OH)_2$-D_3 depressed uptake by 36%. The response to 25-(OH)-D_3 may be direct since the more polar 1,25-$(OH)_2$-D_3, showed no response.

On the other hand, in freshwater fish; e.g. eel and talapia, intestinal calcium uptake is stimulated by 1,25-$(OH)_2$-D_3 [17, 18, 63], or in goldfish, exposed to vitamin D alone [16]. Recently, Takeuchi et al., [64] found 25-hydroxyvitamin D_3-1 alpha-hydroxylase in the liver of carp and halibut. The capacity of some fish to convert vitamin D_3 to the more polar metabolites within the liver, in contrast to birds and mammals, would suggest that the kidney in some fish may not be an essential organ in vitamin D metabolism.

Parathyroid glands are lacking in fish, but with their appearance in the amphibians, an additional mechanism is present that may modulate the formation of 1,25-$(OH)_2$-D_3, and therefore intestinal calcium absorption. Parathyroid removal depresses plasma ionic calcium in the frog *Rana pipiens*, by 20% [55] and duodenal calcium uptake [51]. While vitamin D administration increases duodenal active calcium transport [50, 51]), it is depressed in PTH-depleted frogs after vitamin D_3 administration [51, 53]; suggestive the the PTH-dependent conversion to the active 1,25-$(OH)_2$-D_3 metabolite was inhibited, resulting in depression of the active, saturable component of calcium absorption.

Other factors in calcium absorption.

A variety of factors come into play that can alter intestinal calcium absorption; a major factor is developmental age. Various studies [42, 68] recognized that intestinal calcium uptake in newborn mammals is by passive diffusion alone, with a complete lack of active calcium transport. Pansu and co-workers [42] found in newborn rats that the passive diffusion constant was high (K_d=0.83) with a constant decrease to about K_d=0.33 at 40 days of age, that remained constant at K_d=0.47 thereafter to 160 days of age. During the period of decline, active transport, as expressed by the value of J_{max}, increased to peak at 28–40 days with a gradual decline to about 13% of maximum after 150 days. The appearance of active transport was paralleled by a concomitant increase in the mucosal CaBP. The sequential appearance of 1,25-$(OH)_2$-D_3 receptors on crypt cells by 10 days of age [11] and increasing circulating levels of 1,25-$(OH)_2$-D_3 during the third week [24, 68] indicates the maturation of enterocytes capable of supporting active calcium transport.

Little is known of gut calcium transport at early stages of development in heterotherms. Calcium balance studies with pre-metamorphic anurans (bullfrog tadpoles), indicate that calcium is acquired primarily (70%) by the gills with only 5% attributable to intestinal calcium uptake [1]. However, direct infusion of high calcium (50 mM) into the intestine of bullfrog tadpoles elevates plasma calcium [57], providing a more direct indication that calcium can be absorbed by the gut of pre-adult anurans; although specific mechanisms of absorption are unknown.

Other factors that affect calium absorption include availability of calcium; i.e. complexed or ionically "free", the ionic calcium concentration, and transit time of intestinal contents. A consistent relationship in most terrestrial animals is the

high active calcium transport mechanism in the proximal (duodenal) segment of the small intestine. Stomach contents are typically at low pH (pH <2) resulting in an increased availability of ionic calcium immediately distal to the pylorus. Studies in humans show that pH in the duodenum remains between pH 3–6 and gradually rises toward neutrality near the proximal jejunum [59]. Thus, the kinetics of saturable calcium uptake at low luminal calcium concentration in the duodenum result in high efficiency of Ca influx. On the other hand, calcium food sources are diluted by digestive fluids as they pass along the tract, further reducing the calcium concentration, and passive diffusion becomes less effective. Finally, the lower uptake capacity of the saturable component is compensated by the relatively longer length of the jejunoileum, resulting in almost complete absorption of calcium at the terminus. In mammals with defined segments of large intestine with an active transport mechanism, the longer transit time in this segment, may insure that all available calcium is absorbed.

TOPOLOGY OF CALCIUM ABSORPTION

Of the heterotherms studied, a basic pattern of intestinal calcium absorption is apparent; e.g. passive diffusion occurs along the length of the small (and large) intestine that may be modified by the addition of 1) an active saturable uptake mechanism, and 2) net calcium secretion. These modifications exhibit polarity along the length of the gut; e.g. active uptake is higher in proximal segments; whereas net calcium secretion is found in distal segments. Thus, it is recognized [14] that the intestine exhibits a topology of calcium transport mechanisms with segment-specific net calcium absorption capacity. The presence of an active uptake process, mediated by vitamin D-dependent CaBP, provides a means to up-regulate the intestine when there is a physiological demand. Under conditions of high dietary calcium, passive diffusion will dominate, with down-regulation of active transport. Conversely, with low dietary calcium, passive diffusion is less effective, with up-regulation of active transport. The relative capacity of each intestinal segment is illustrated in figure 4 in normal and vitamin D-treated frogs with a

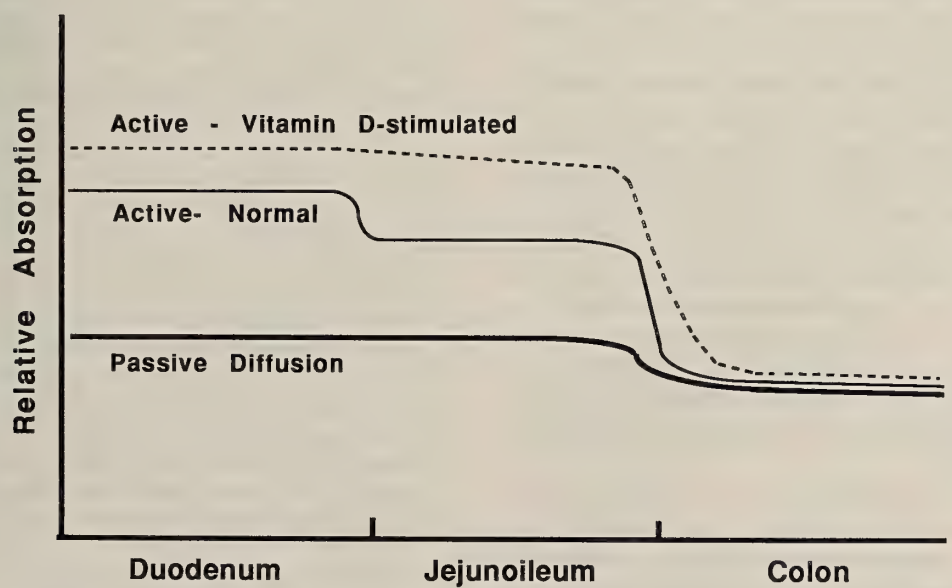

FIG. 4. Diagrammatic representation of topology of calcium absorption in small and large intestine of adult frog. Passive diffusion is relatively constant along the duodenum, jejunoileum and colon; whereas active transport is highest in duodenum and reduced in jejunoileum and absent in colon in normal frogs. After vitamin D_3 (500 μg) adminstation, active transport is elevated in duodenum and jejunoileum but unchanged in colon.

luminal concentration of 15 mM. Paracellular calcium absorption can account for about 50% of all calcium absorbed in duodenum, about 70% in jejunoileum and 100% in large intestine. After vitamin D, calcium uptake is increased in duodenum and jejunoileum, while uptake in colon remains unchanged after 500 μg vitamin D [Robertson, unpublished data]. On the other hand, Rostoff et al., [56] noted that uptake in colon could be increased only with supraphysiological doses of vitamin D.

CONCLUSIONS

Of the heterotherms studied, paracellular calcium transport in the intestine appears to play as important a role as active, transcellular calcium transport; reflecting a more permeable epithelium to passive diffusion, similar to that in newborn mammals. In adult homeotherms, active calcium transport is well established to respond to the demands of increased body and skeletal size, and episodic demand; e.g. egg shell deposition or lactation. The basic patterns and mechanisms identified in birds and mammals are similar to that in fish and amphibians; however, there are some differences that also may reflect basic nutritional needs.

First, is the role of the various vitamin D metabolites in active calcium transport in fish and amphibians. Current evidence indicates that the less polar metabolites of vitamin D; i.e. 25-(OH)-D_3, are effective in stimulating active calcium transport, and may not require the kidneys for further metabolism to the more polar 1,25-$(OH)_2$-D_3, as seen in avian and mammalian systems. On the other hand, since some fish possess the enzyme necessary in the liver to form 1,25-$(OH)_2$-D_3, a tight feed-back loop may exist between the fish proximal intestine and liver via the hepatic portal system.

The appearance of a well defined intestinal topology of active transport in anuran amphibians, and evidence of PTH-sensitive vitamin D-dependent active gut transport indicates that an avian-mammalian pattern is established in the amphibians. What is lacking is characterization of an intestinal CaBP, and its sensitivity to specific vitamin D metabolites. Basic information on gut calcium transport in the more aquatic urodele amphibians and appearance of these mechanisms during metamorphosis of anurans is needed.

The elegant studies of Flik and co-workers [19] on calcium extrusion mechanisms in teleost enterocytes, provides insight into mechanisms that may be more common in the enterocytes of heterotherms than in homeotherms. While fish gills possess an active Ca^{2+}/Mg^{2+}-ATPase extrusion mechanism, the presence of a prominent enterocyte Na^{+}/Ca^{2+}-exchange mechanism hints that intracellular calcium transport in some heterotherms may not be entirely comparable to the avian/mammalian models.

REFERENCES

1 Baldwin GF and Bentley PJ (1980) J exp Biol 88: 357–365
2 Baran DT and Milne ML (1986) J Clin Invest 77: 1622–1626
3 Bell NH, Shaw S and Turner RT (1987) J Bone Min Res 2: 211–214
4 Berg A (1970) Mem. Ist. Ital. Idrobiol. Dott Marco de March 26: 241–255
5 Birge SJ, Gilbert HR and Avioli LV (1972) Science 176: 168–170
6 Björnsson BTh, and Nilsson S (1985) Am J Physiol 248: R18–R22
7 Bronner F, Pansu D and Stein WD (1986) Am J Physiol 250: G561–569
8 Chan DKO, Chester Jones I and Smith RN (1968) Gen Comp Endocrinology 11: 243–245
9 Chartier Baraduc MM (1973) C R Acad Sc Paris, Ser D, 276: 785–788
10 Chartier MM, Millet C. Martelly E, Lopez E and Warrot S (1979) J Physiol, (Paris) 75: 275–282
11 Clark SA, Stumpf WE, Hamstra A and DeLuca HF (1983) J Histochem Cytochem, 31: 1063
12 Dabrowski K, Leray C, Nonnotte G and Colon DA (1986) Comp Biochem Physiol 83A: 27–39
13 El Maraghi-Ater H, Hourdry J, Mesnard J, and Dupuis Y (1987) Reprod Nutr Dévelop 27: 407–412
14 Favus MJ (1985) Am J Physiol 248: G147–G157
15 Favus MJ and Angeid-Backman E (1985) Am J Physiol 248: G676–G681
16 Fenwick JC (1984) Can J Zool 62: 34–36
17 Fenwick JC, Smith K, Smith J and Flik G (1984) Gen Comp Endocrinology 55: 398–404
18 Flik G, Reijntjens FMJ, Stikkelbroeck J and Fenwick JC (1982) J Endocrinol 94: 40

19 Flik G, Schoemnakers Th JM, Groot JA, van Os CH and Wendelaar Bonga SE (1990) J Memb Biol 113: 13–22

20 Flik G, van Rijs JH and Weendelaar Bonga SE (1985) J exp Biol 119: 335–347

21 Fox J and Green DT (1986) Europ J Pharm 129: 159–164

22 Fraser DR and Kodicek E (1970) Nature, New Biol 241: 163–166

23 Ghijsen WEJM, DeJong MD, and van Os CH (1983) Biochem Biophys Acta 730: 85–94

24 Halloran BP, Barthell EN and DeLuca HF (1979) Proc Natl Sci USA 76: 5549–5553

25 Hildmann B, Schmidt A and Murer H (1983) J Memb Biol 65: 55–62

26 Holdsworth ES, Jordan JE and Keenan E (1975) Bio J 152: 181–190

27 Holick MF, Baxter LA, Schraufrogel PK, Tavela TE and DeLuca HF (1976) J Biol Chem 251: 397–402

28 Holick MF, Schonoes HK, DeLuca HF, Gray RW, Boyle IT and Suda T (1972) Biochemistry 11: 4251–4255

29 Kanis JA, Guilland-Cumming DR and Russell RGG (1982) In:Endocrinology of Calcium Metabolism, Ed. JA Parsons, Raven Press, New York pp 321–362

30 Liang CT, Barnes J, Balakir RA and Sacktor B (1976) J Memb Biol 90: 145–156

31 Moore EW (1970) J Clin Inverst 49: 318–334

32 Morrissey RL and Wasserman RH (1971) Am J Physiol 220: 1509–1515

33 Mugiya Y and Ichii T (1981) Comp Biochem Physiol 70A: 97–101

34 Murer H and Hildmann B (1981) Am J Physiol 240: G409–G416

35 Nakamura Y (1985) Comp Biochem Physiol 80A: 17–20

36 Nakamura Y and Hirano T (1986) Comp Biochem Physiol 84A: 595–599

37 Nellans HN (1990) Miner Electrolyte Metab 16: 101–108

38 Nellans HN and Goldsmith RS (1981) Am J Physiol 240: G424–G431

39 Nellans HN and Kimberg DV (1978) Am J Physiol 235: E726–E737

40 Ooisumi K Moriuchi S and Hosoya N (1970) Vitamins Jap 42: 171–175

41 Pansu D, Bellaton C and Bronner F (1981) Am J Physiol 240: G32–G37

42 Pansu D, Bellaton C and Bronner F (1983) Am J Physiol 244: G20–G26

43 Pansu D, Bellaton C, Roche C and Bronner F (1983) Am J Physiol 244: G695–G700

44 Parmentier M (1990) Biol Cell 68: 43–49

45 Parmentier M, Ghysens M, Rypens F, Lawson DEM, Pasteels JL and Pochet R (1987) Gen Comp Endocrinology 65: 399–407

46 Parson AH and Combs GF (1980) Poultry Sceince 60: 1520–1524

47 Pento JT and Johnson ME (1983) Pharmacol 27: 343–349

48 Pickering AD and Morris R (1973) J exp Biol 58: 165–176

49 Pochet R, Blachier F, Gangji V, Kielbaska V, Duée P-H and Résibois A (1990) Biol Cell 70: 91–99

50 Robertson DR (1975) Comp Biochem Physiol 51A: 705–710

51 Robertson DR (1975) Endocrinology 96: 934–940

52 Robertson DR (1976) Comp Biochem Physiol 54A: 225–231

53 Robertson DR (1978) J Endocrinol 79: 167–178

54 Robertson DR (1985) Am J Physiol 249: R290–R295

55 Robertson DR (1986) Comp Biochem Physiol 85A: 359–364

56 Rostoff CJ, Baldwin GF and Bentley PJ (1983) Am J Physiol 245: R91–R94

57 Sasayama Y and Oguro C (1985) In: Current Trends in Comparative Endocrinology. Ed. B Lofts and WN Holmes, Hong Kong Univ. Press pp 838–838

58 Shehadeh ZH and Gordon MS (1969) Comp Biochem Physiol 30: 397–418

59 Sheikh MS, Schiller LR and Fordtran JS (1990) Miner Electrolyte Metab 16: 130–146

60 Simkiss K (1974) In: Ageing of Fish. Ed. by TB Begenal, Univ. Old Working, England, pp 1–12

61 Staun M (1987) Gut 28: 878–882

62 Sundell K and Björnsson BT (1988) J exp Biol 140: 171–186

63 Sundell K and Björnsson BT (1990) Gen Comp Endocrinol 78: 74–79

64 Takeuchi A, Okano T and Kobayashi T (1991) Life Sci 48: 275–282

65 Taylor AN, Gleason WA and Lankford GL (1984) J Histochem Cytochem 32: 153–158

66 Taylor AN and Wasserman RH (1967) Arch. Biochem Biophys 119: 536–540

67 Taylor AN and Wasserman RH (1969) Fed Proc 28: 1824–1838

68 Toverud SU and Dostal LA (1986) J Ped Gastroent Nutr 5: 688–695

69 Tsien RY, Possan T and Rink TJ (1982) J Cell Biol 94: 325–334

70 van Corven EJJM, Roche C and van Os CH (1985) Biochem Biophys Acta 820: 274–282

71 Van Os CH (1987) Biochem Biophys Acta 906: 195–222

72 Walters JRF and Weiser MM (1987) Am J Physiol 252: G170–G177

73 Wasserman RH (1962) J Nutr 77: 69–80
74 Wasserman RH and Corradino RA (1973) Vitamins and Hormones 31: 43–103
75 Wrobel J and Michalska L (1977) Europ J Pharm 45: 385–387
76 Yeh JK and Aloia JF (1984) Endocrinology 114: 1711–1717

ZOOLOGICAL SCIENCE 10: 235–244 (1993)

Physiological Evaluation of the Role of the Liver as a Mediator of the Growth-Promoting Action of Somatotrophin

Nicole L. Schlechter, Larry S. Katz[1], Sharon M. Russell and Charles S. Nicoll[2]

Department of Integrative Biology, The Cancer Research Laboratory and Group in Endocrinology, University of California, Berkeley, CA 94720, USA

ABSTRACT—The role of the liver as a mediator of the somatotrophic actions of GH was investigated in three experiments in hypophysectomized rats. The GH was infused via osmotic minipumps into the hepatic portal vein (HPV) or the external jugular vein (EJV) for 7 days at a constant rate or in 8 pulses of 1 hour each/day. Infusion of rat (r) GH at 1 μg/rat/day into the two vessels in rats hypophysectomized one day after catheterization failed to affect body growth, but it increased their tibial epiphysial plate width (TEPW), and serum IGF-I concentration to the same degree regardless of the site of delivery or the schedule of infusion. When bovine (b) GH was infused at (50 μg/rat/day) starting 12–14 days after hypophysectomy, the EJV route was more effective at stimulating growth and elevating serum IGF-I than was HPV infusion by both modes of delivery, and constant infusion was more effective than pulsed delivery. In the third experiment human (h) GH infusion was started 30 days after hypophysectomy at 50 μg/rat/day. This treatment caused much more striking growth responses than did either of the other two GH preparations, and the EJV route of delivery was again more effective than was infusion into the HPV by both schedules. In addition, the constant mode of delivery was again more effective than was pulsed infusion. These results indicate that effects of GH on peripheral tissues may be more important for growth than effects mediated by the liver. Thus, the hepatic effects of GH may involve maintaining the responsiveness of the liver to other regulators of IGF-I secretion.

INTRODUCTION

The somatomedin hypothesis [1, 2] proposed that growth hormone (GH) acts indirectly to promote growth by stimulatng hepatic production of a mediator, which is now known as insulin-like growth factor-I (IGF-I). Numerous observations support this hypothesis. For example, several groups have reported that GH increases the secretion of somatomedin/IGF-I by the perfused rat liver and by hepatic explants or cells in culture [see reviews in 3]. In addition, *in vivo* studies involving partial hepatectomy [4], cross-hepatic blood sampling [5] and studies of patients with liver disorders [6] demonstrated that the liver produces IGF-I, and that this production is stimulated by GH. Furthermore, Schwander *et al.* [7] estimated that hepatic production of IGF-I in response to GH can account for all of the IGF-I in serum.

Other data indicate that GH can also act peripherally [8–14]. These results raise questions about the relative significance of peripheral *vs* hepatic actions of GH in promoting somatic growth. Mick and Nicoll [15] developed a technique for testing the direct effects of hormones on hepatic functions *in vivo*. Their system involves chronic infusion into the hepatic portal vein, which delivers hormone directly to the liver via one of its two blood supplies. Thus, the direct effect of substances on hepatic functions *in vivo* can be studied in a physiologically meaningful way. In the present study we used their procedure [15] to reevaluate the basic tenet of the somatomedin hypothesis [1, 2].

Accepted September 18, 1992
Received June 16, 1992

[1] Present address: Department of Animal Sciences, Cook College, Rutgers University, New Brunswick, NJ 08903-0231

[2] To whom reprint requests should be addressed.

MATERIALS AND METHODS

Animals

Male rats weighing 120–150 gm were obtained from our own breeding colony or from Simonsen Laboratories (Gilroy, CA, U.S.A.) and maintained as described previously [10]. They were hypophysectomized (Hx) by a transauricular approach [16] either before or after catheterization, depending upon the schedule of the experiment. All procedures used on the rats were described in detail in a protocol that was approved by our Institutional Animal Care and Use committee, and all experiments conformed to the regulations described in the N.I.H. Guide to the Care and Use of Laboratory Animals.

Catheterization

The procedures used to construct the catheters and insert them into either the hepatic portal vein (HPV) or the external jugular vein (EJV) and connecting them to osmotic minipumps were as described [10, 13]. In brief, for constant infusion, Alzet minipumps (2001: Alza Corp, Palo Alto, CA, U.S.A.) were filled with solvent [17] with or without GH, and a 7-cm long catheter filled with solvent containing heparin was attached. For pulsatile delivery, the polyethylene 50 catheter was extended to 70 cm and 1-mm segments of solvent or GH solution were drawn into it. The segments were separted by 2-mm-long air bubbles. By this means the GH solution or solvent was infused in 8 pulses/day of about 1 hour duration with approximately a 2-hour interpulse interval. This mode of delivery should mimic the endogenous GH secretion pattern in adult male rats [18].

Measurements

Changes in body weight were recorded in all three experiments and changes in tail length were measured in two of them. These measurements were made only at the beginning and the end of each experiment. The rats were anesthetized and blood was drawn by cardiac puncture and the tibiae were removed and processed for measurement of the width of the epiphysial cartilage plate [TEPW; 19]. The sellar region was examined carefully using a binocular dissecting microscope for the presence of pituitary remnants. Animals with detectable remnants and/or lack of obvious testicular regression were judged to be incompletely hypophysectomized and were excluded.

Hormones and Assays

Serum from the rats used in the first two experiments was processed for measurement of IGF-I by RIA and the concentration of GH was measured by RIA in the serum samples from the rats that received constant infusion of the (r)GH. Details of these RIA procedures have been published [20, 21]. However, because of the breakdown of a freezer, some of the serum samples from the three experiments were lost and so they could not be assayed for IGF-I, human (h)GH or bovine (b)GH levels. The three preparations of GH used were obtained from the National Hormone and Pituitary Program of the NIH (USA). The rGH (NIH B-9), bGH (NIH B-18), and hGH (NIDDK B-1) had potencies of 1.9, 3.2 and 2.4 I.U./mg, respectively.

Experiments

Three experiments were conducted—one each with rat (r), bovine (b), and human (h) GH. In the first study the rats were Hx one day after catheterization and were killed 6 days later. Thus, this experiment was designed to test the effectiveness of the rGH at maintaining growth after pituitary removal. The dose of rGH of 1 μg/rat/day was selected on the basis of results of our previous study [10] in which rGH was infused into the arterial supply of one hindlimb of Hx rats. A dose of 2 μg/rat/day caused a striking increase in the TEPW in the infused limb but it caused a significant, though lesser growth effect in the contralateral hindlimb. Thus, the 1 μg/day dose given via the HPV should have a significant effect on hepatic secretion of IGF-I and growth while the same dose given into the EJV should have a lesser effect.

In the second experiment, the rats were Hx 12–14 days prior to catheterization and bGH was infused for 7 days at a dose of 50 μg/rat/day to obtain larger responses. In the third experiment, the rats were Hx 30 days before catheterization

and bGH was infused at a dose of 50 μg/rat/day for 7 days. In these experiments with rGH and hGH the rats were killed on the 8th day after the placement of the catheters and minipumps. In the experiments with rGH and hGH control rats received infusion of the solvent that was used to dissolve the GH preparations. In the experiment with bGH the abdomen of the controls was opened to expose the intestines, but no catheter was inserted into an intestinal vein. In all three experiments the rats were killed on the 8th day after the start of infusion.

Significance of differences was determined by the Student's t test or by analysis of variance, as described [10].

RESULTS

In the experiment with rat GH, all of the experimental groups showed an equivalent loss in body weight and reduction in tail growth relative to intact or sham Hx controls. Infusion of the rGH did not affect these changes in body weight or tail length in any of the experimental groups (data not shown). Serum GH was not detectable by RIA (sensitivity of 0.7 ng/ml) in any of the rats that received solvent infusions. In those given constant infusion of the hormone via the EJV or the HPV, the serum GH concentrations were 3.0 ± 0.4 ng/ml (n=7) and 3.2 ± 0.1 ng/ml (n=5), respectively. Thus, the route of administration did not affect the peripheral concentration of GH. Serum GH levels were not measured in the rats that received pulse infusion because meanigful data from these animals could be obtained only by taking multiple samples over an extended period.

Intact rats of the same age as those used in these experiments had a mean TEPW of 314 μm. Thus, the data in Figure 1 show that the TEPW in the rats infused with the solvent had regressed by more

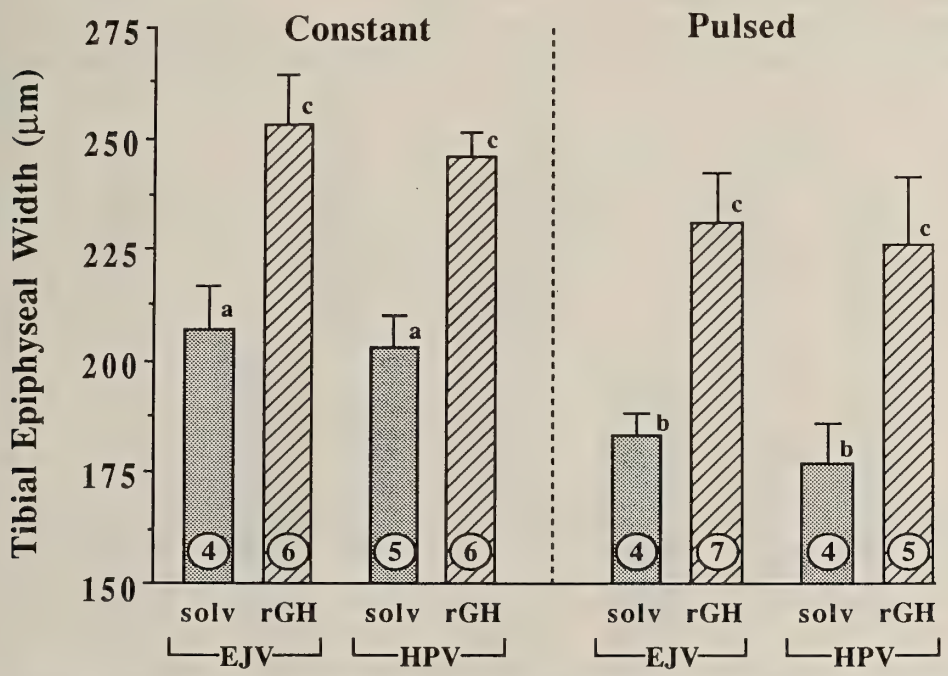

FIG. 1. Effect of infusing solvent (solv) or rGH (1 μg/rat/day) in solvent into the external jugular vein (EJV) or hepatic portal vein (HPV) on the tibial epiphysial plate width of hypophysectomized rats for 7 days. The rats were Hx one day after placement of the catheters and the infusions were either constant or pulsatile (8 pulses of 1 hour each). The number of rats in each group is given within the base of each column. Columns with the same letter superscript are not significantly different from each other. Those with different letters are significant at $P<0.001$. The columns represent the mean$\pm$SEM values for each group.

than 100 μm during the 6 days following hypophysectomy. The TEPW of the rats that received the solvent in pulses was slightly lower than those measured in the animals given constant infusions. This difference is probably due to the fact that the two groups of experiments (constant and pulsed infusions) were done at different times.

The data in Figure 1 show that constant delivery of rGH into the EJV or the HPV increased the mean TEPW over that in the controls given solvent to the same extent [i.e. by 46 μm ($P<0.01$), and 43 μm ($P<0.001$), respectively]. When the rGH was infused in pulses into the EJV or the HPV, the degree of growth stimulation (+48 μm in both groups, $P<0.01$) was similar to that produced by constant infusion. Thus, intrahepatic delivery of the hormone either constantly or in pulses was no more effective than infusing it into the peripheral vessel.

The rats infused with solvent at a constant rate had mean serum IGF-I levels of 55–57 μg/ml, regardless of the site of infusion (Fig. 2). This concentration is less tha 10% of the level measured in intact rats of the same age (i.e. 615 μg/ml). Infusion of rGH into either the HPV or the EJV elevated serum IGF-I concentrations to the same degree over those in the rats that were infused with solvent. Thus, the serum IGF-I levels in these animals are consistent with their equivalent TEPW measurements (Fig. 1) and serum concentrations of rGH.

The effects of infusing bGH at 50 μg/rat/day on changes in body weight and tail length are shown in Fig. 3. The solvent-infused rats lost about 10 gm in body weight during the 7-day experimental period but constant infusion of bGH into either vein prevented this loss. However, constant delivery into the EJV was significantly more effective than was infusion into the HPV. Pulsed delivery of bGH into the HPV did not prevent the loss in body weight. Although pulsed infusion of GH into the EJV was effective in this regard, it was significantly less effective than was constant infusion into that vein. Tail growth was increased significantly only in the groups that received bGH constantly via the EJV.

Only the group that received constant infusion of bGH into the EJV showed a singificant TEPW

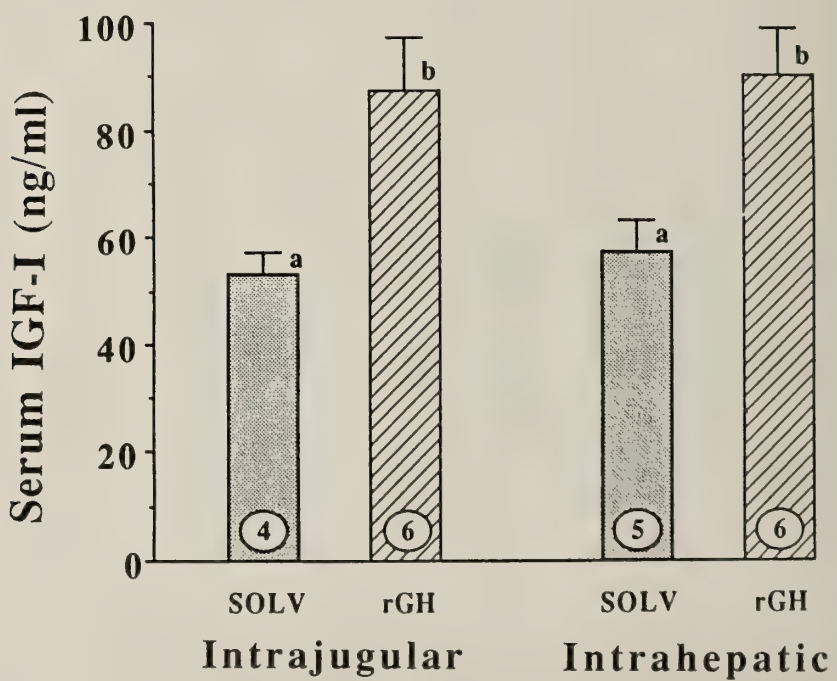

FIG. 2. Serum IGF-I levels in the rats that received constant infusions as described in Fig. 1. Otherwise as in the legend for Fig. 1, but columns with different letters as significantly different at $P<0.01$.

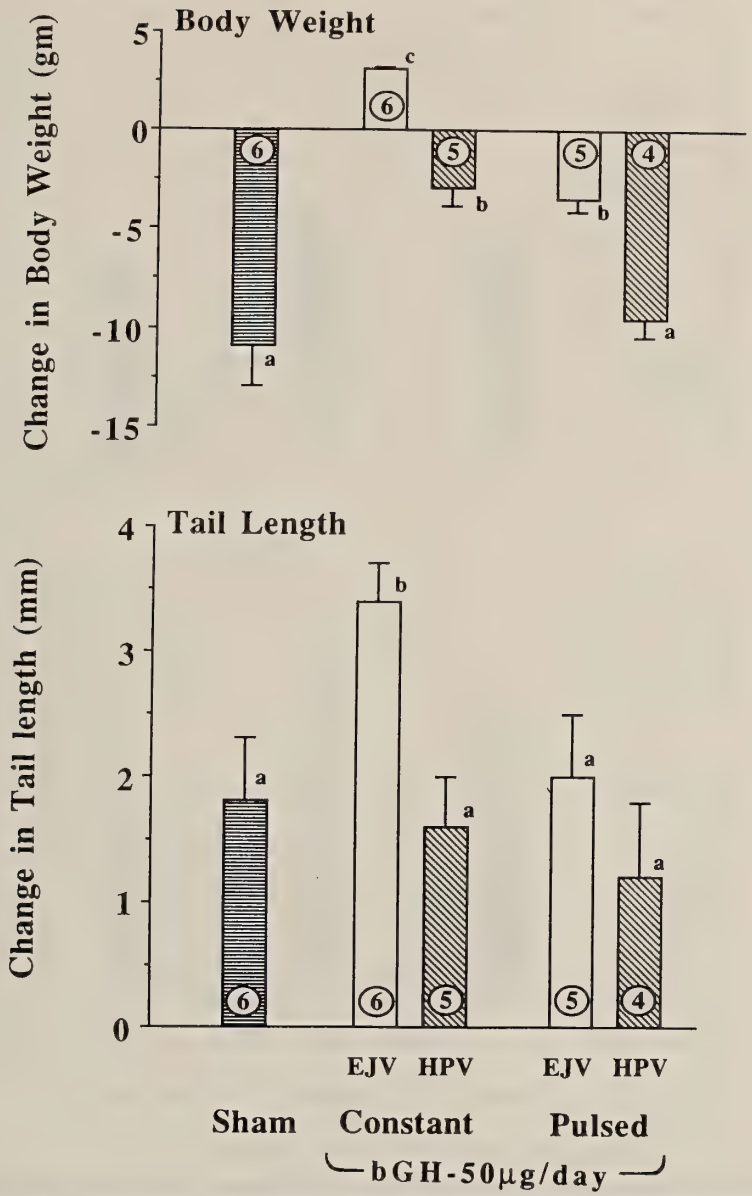

FIG. 3. Effects of infusing bGH at 50 μg/rat/day for 7 days on body weight gain and tail growth of Hx rats. Infusions were started 12–14 days after Hx and the bGH was given constantly or in pulses, as described in Fig. 1. The sham operated rats were subjected to the same surgical procedures as those that were catherized for intrahepatic infusions but without placement of either a catheter or minipumps. Columns with different letters are signicficantly different at $P<0.05$ or better.

response to the hormone (Fig. 4). However, serum IGF-I levels were significantly elevated in the rats given constant infusion of bGH via either the EJV or the HPV (2.5-fold and 2.1-fold, respectivley). Thus, in this study, serum IGF-I levels were not completely consistent with the other growth parameters measured. In the third experiment, the rats that received solvent infusion into either the HPV or the EJV starting 30 days after pituitary ablation lost about 5 gm in body weight

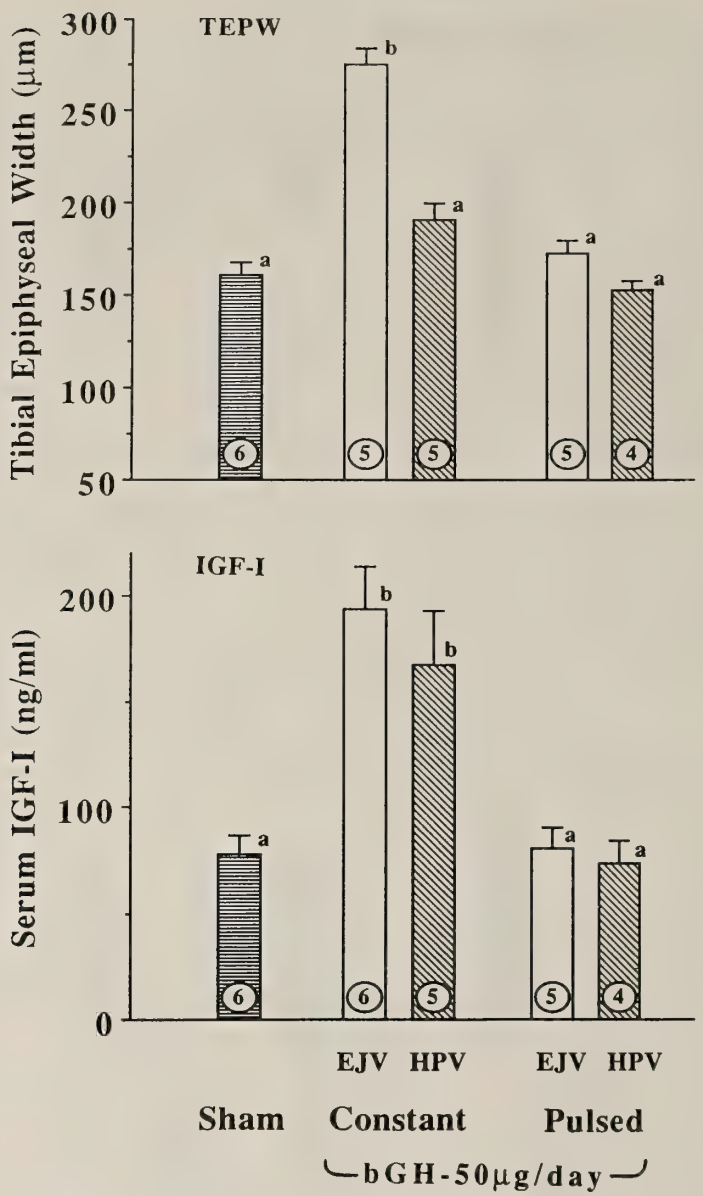

FIG. 4. Tibial epiphysial plate widths and serum IGF-I levels in the rats described in the legend of Fig. 3. Columns with different letter superscripts are significantly different from each other at $P<0.001$.

during the 7-day experimental period (Fig. 5). Constant infusion of hGH into either vein of such Hx rats caused significant increases in body weight gain, but the EJV route was almost 3 times more effective than was the HPV (Fig. 5). Pulsed delivery stimulated significant weight gain only when the hGH was given into the EJV, but it was only about half as effective as was constant infusion into that vessel.

The data on TEPW measurements with hGH infusion are consistent with the body-weight changes (Fig. 5). Infusion into the EJV was more effective than delivery into the HPV by either mode of delivery, and constant infusion into the EJV or the HPV was significantly more effective than pulsed delivery into either vein.

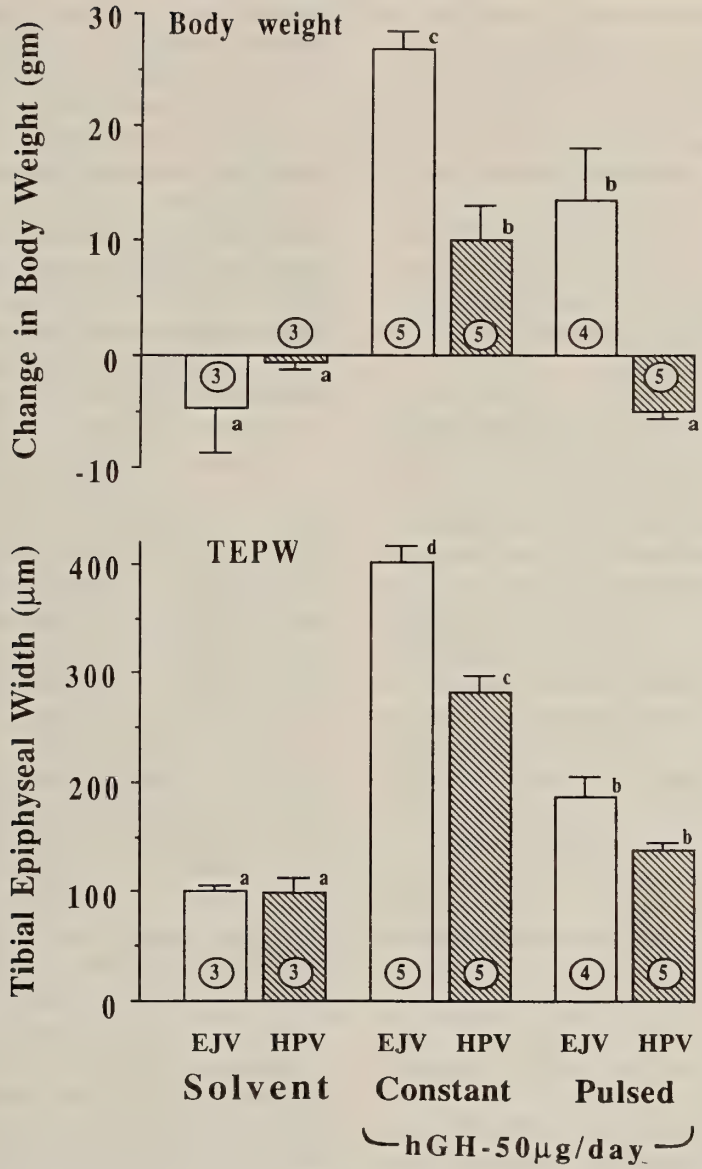

FIG. 5. Effects of infusing hGH (50 μg/rat/day) for 7 days on body weight gain and tibial epiphysial plate width of rats that were Hx 30 days previously. Otherwise as in the legend in Fig. 1. Columns with different letters are significantly different at $P<0.05$ or better.

DISCUSSION

The results presented in this paper show that delivery of a low dose of rat GH directly to the liver via its portal blood supply was no more effective at maintaining growth or elevating serum IGF-I concentration than was infusion at a distant site, regardless of whether the hormone was given constantly or in pulses (Figs. 1 and 2). These findings were unexpected because the liver is generally thought to be the major source of GH-stimulated IGF-I secretion [2, 3], and intrahepatic infusion should have exposed the organ to a concentration of GH that was at least 4 times higher

than that achieved by infusion into the EJV [see 22]. Administration of a higher daily dose of either bGH or hGH gave results that were even more surprising. Infusion of these hormones into the EJV was significantly more effective at stimulating all of the growth parameters measured than was delivery directly into the liver, regardless of whether they were infused constantly or in pulses. Thus, none of these experiments provide data to support the idea that stimulation of hepatic IGF-I secretion by GH is the major means by which the hormone promotes growth.

Another surprising aspect of our studies was the finding that constant infusion of GH was either as effective (with rGH) or more effective (bGH, hGH) than was pulsatile delivery. Several groups have reported that pulsed infusion [23–25] or frequent injections [26–28] of GH are more effective at restoring growth in Hx rats than is constant infusion. However, in one of these studies [23], pulsatile delivery was not more effective than constant infusion during the first week of the treatment; in other experiments [27, 28], the frequency of injections was not related to the magnitude of growth responses until after 5–7 days of treatment. The schedule that we used corresponds to the period when these investigators [23, 27, 28] found that intermittent delivery was not more effective than continuous treatment. Nevertheless, this does not explain our finding that constant infusion of bGH and hGH was more effective than giving pulses of 1-hr duration, while none of the other studies found this effect during the first few days of treatment, and one of them [25] found the opposite result.

By measuring the flow of air bubbles and solvent segments in the catheters, we determined that the minipumps did perform, on average, as expected in terms of delivering the pulses according to the schedule selected [29]. However, there was considerable variation in pulse duration and the interpulse interval. We were unsuccessful in determining the pattern of GH in the blood of the infused animals because of difficulties in collecting a sufficient number of samples serially. Nevertheless, a major difference between our study and those of the others who infused the GH in pulses was in the duration of the pulses. While our system delivered the hormone in square-wave pulses of about 1 hr duration, the other groups used pulse intervals of only a few minutes.

In separate experiments we have investigated the effectiveness of constant vs. pulsed delivery of ovine PRL at restoring lactation in rats in which endogenous PRL secretion was suppressed by bromocriptine [29]. Constant infusion was again found to be consistently more effective than any of several pulse infusion schedules [29], but the difference was not as striking as we observed here with hGH and bGH. In that experiment [29] and in another study [30] we also found that intrahepatic infusion of the PRL was not more effective at restoring lactation than was infusion into the EJV. It is unlikely that downregulation or desensitization of the hepatic GH receptors can account for the lesser effectiveness of intrahepatic *vs* intrajugular delivery of the hormone as constant delivery should be more effective than pulsed infusion at reducing hepatic responsiveness to GH.

When PRL was infused into the HPV of pigeons [15] or rats [31], it was more effective at stimulating growth of target organs of PRL than was infusion of the same dose of the hormone into the EJV. Likewise, infusing insulin into the HPV of diabetic rats was more effective at promoting body growth and normalizing their metabolic status than was delivery into the EJV [32]. It has also been shown that direct delivery of PRL to the liver of bullfrog tadpoles (*Rana catesbeiana*) was more effective at promoting growth and inhibiting metamorphosis than was delivery to the kidney or subcutaneously [33]. These results with PRL [15, 31, 33] and insulin [32] indicate that if GH did have a preferential effect on the liver to promote IGF-I secretion and growth, our infusion system should have allowed it to be manifested. Accordingly, it seems likely that direct hepatic mediation of the growth-promoting effects of GH may be of less significance than is generally considered [1, 2]. Thus, the direct growth-promoting effect of GH on peripheral tissues, which has been well established by recent studies [8–14], may be of greater import for growth than are the hepatic effects of the hormone. This conclusion is supported by the data which show that although intrahepatic delivery of bGH was almost as effective as infusion into the

EJV at elevating serum IGF-I levels (Fig. 4), the HPV route was much less effective at stimulating growth responses (Figs. 4 and 5).

This conclusion does not mean that an effect of GH on the liver is unimportant for growth. Indeed, it has been well established that GH can stimulate IGF-I secretion by liver cells both *in vivo* and *in vitro* [see 3]. However, the significance of the hepatic receptors for GH and the effects that GH may have on liver functions related to growth *via* these receptors may be in maintaining hepatic responsiveness to other factors that can stimulte IGF-I secretion, such as insulin [32] and thyroid hormones [34].

ACKNOWLEDGMENTS

We are indebted to the National Hormone and Pituitary program of the NIH for the GH preparations and for the antiserum to IGF-I, and to Mr. Richard Lin for preparing the figures. Dr. E.M. Spencer, Children's Hospital (San Francisco, CA) kindly supplied us with ^{125}I-labeled IGF-I. This work was supported by NIH Grant HD-14661.

REFERENCES

1 Salmon WD, Daughaday WH (1957) A hormonally controlled serum factor which stimulates sulfate incorporation by cartilage *in vitro*. J Lab Clin Med 49: 825–834

2 Daughaday WH (1989) A personal history of the origin of the somatomedin hypothesis and recent challenges to its validity. Persp Biol Med 32: 194–211

3 Spencer EM (1983) Insulin-like growth factors/somatomedins. de Gruyter, Berlin

4 Uthne K, Uthne T (1972) Influence of liver resection and regeneration on somatomedin (sulphation factor) activity in sera from normal and hypophysectomized rats. Acta Endocrinol (Copenh) 71: 255–264

5 Schimpff RM, Donnadieu M, Glasinovic JC, Warnet JM, Girard F (1976) The liver as source of somatomedin (an *in vivo* study in the dog). Acta Endocrinol (Copenh) 83: 365–372

6 Schimpff RM, Lebrec D, Donnadieu M (1977) Somatomedin production in normal adults and cirrhotic patients. Acta Endocrinol (Copenh) 86: 355–362

7 Schwander JC, Hauri C, Zapf J, Froesch ER (1983) Synthesis and secretion of insulin-like growth factor and its binding protein by the perfused rat liver: dependence on growth hormone status. Endocrinology 113: 297–303

8 Isaksson OGP, Jansson J-O, Gause IAM (1982) Growth hormone stimulates longitudinal bone growth directly. Science 216: 1237–1239

9 Russell SM, Spencer EM (1985) Local injections of human or rat growth hormone or of purified somatomedin-C stimulate unilateral tibial epiphyseal growth in hypophysectomized rats. Endocrinology 116: 2563–2567

10 Schlechter NL, Russell SM, Greenberg S, Spencer EM, Nicoll CS (1986) A direct effect of growth hormone in rat hindlimb shown by arterial infusion. Am J Physiol 250: E231–E235

11 Isgaard J, Nilsson A, Lindahl A, Jansson J-O, Isaksson OGP (1986) Effects of local administration of GH and IGF-I on longitudinal bone gowth in rats. Am J Physiol 250: E367–E327

12 Nilsson A, Isgaard J, Lindahl A, Dahlstrom A, Skottner A, Isaksson OGP (1986) Regulation by growth hormone of number of chondrocytes containing IGF-I in rat growth plate. Science 233: 571–573

13 Schlechter NL, Russell SM, Spencer EM, Nicoll, CS (1986) Evidence suggesting that the direct growth-promoting effect of growth hormone on cartilage *in vivo* is mediated by local production of somatomedin. Proc Nat'l Acad Sci (USA) 83: 7932–7934

14 Nilsson A, Isgaard J, Lindahl A, Peterson L and Isaksson O (1987) Effects of unilateral arterial infusion of GH and IGF-I on tibial longitudinal bone growth in hypophysectomized rats. Calcif Tissue Int 40: 91–95

15 Mick CCW, Nicoll CS (1985) Prolactin directly stimulates the liver *in vivo* to secrete a factor (synlactin) which acts synergistically with the hormone. Endocrinology 116: 2049–2053

16 Gay VLA (1967) A stereotaxic approach to transauricular hypophysectomy in the rat. Endocrinology 81: 1177–1179

17 Patel DG (1983) Rate of infusion with a minipump required to maintain a normoglycemia in diabetic rats. Proc Soc Exp Biol Med 172: 74–78

18 Eden S (1979) Age and sex related differences in episodic growth hormone secretion in the rat. Endcrinology 105: 555–560

19 Geschwind II, Li CH (1955) The tibia test for growth hormone. In "The Hypophyseal Growth Hormone, Nature and Actions" Ed by RW Smith, OH Gaebler, and CNH Long, McGraw Hill, New York, pp 28–53

20 Chiang M, Russell SM, Nicoll CS (1990) Growth-promoting properties on the internal milieu of pregnant and lactating rats. Am J Physiol 258: E98–E102

21 Russell SM (1981) Differential effects of somatosta-

tin on the release of bioactive and immunoactive rat growth hormone *in vitro*. Neuroendocrinology 33: 67–72

22 Goldman H (1966) Catecholamine-induced redistribution of blood flow in the unanesthetized rat. Am J Physiol 210: 1419–1424

23 Clark RG, Jansson J-O, Isaksson O, Robinson CAF (1985) Intravenous growth hormone: growth responses to patterned infusion in hypophysectomized rats. J Endocrinol 104: 53–61

24 Isgaard J, Carlsson L, Isaksson OGP, Jansson J-O (1988) Pulsatile intravenous growth hormone (GH) infusion to hypophysectomized rats increases insulin-like growth hormone messenger ribonucleic acid in skeletal tissues more effectively than continuous GH infusion. Endocrinology 123: 2605–2610

25 Pampori NA, Agrawal AK, Shapiro BH (1991) Renaturalizing the sexully dimorphic profiles of circulating growth hormone in hypophysectomized rats. Acta Endocrinol (Copenh) 124: 283–289

26 Maiter D, Underwood LE, Maes M, Davenport ML, Ketelslegers JM (1988) Different effects of intermittent and continuous growth hormone administration on serum somatomedin insulin-like growth factor I and liver GH receptors in hypophysectomized rats. Endocrinology 123: 1053–1059

27 Jansson J-O, Albertsson-Wickland K, Eden S, Thorngren KO, Isaksson O (1982) Circumstantial evidence for a role of the secretory pattern of growth hormone in control of body growth. Acta Endocirnol (Copenh) 99: 24–30

28 Thorngren K-G, Hansson LI (1977) Effect of administration frequency of growth hormone on longitudinal bone growth in the hypophysectomized rat. Acta Endocrinol (Copenh) 84: 497–511

29 Hebert NJ, Kim JM, Lin RJ, Nicoll CS (1992) Restoration of lactation in bromocriptine-treated rats by prolactin replacement: Comparison of constant vs pulsatile infusion and intrahepatic vs intrajugular routes of delivery. J Endocrinol Invest 16: 29–35

30 Hebert NJ, Kim JH and Nicoll CS (1991) On the possible role of the liver in the galacto-poretic action of prolactin in the rat. Endocirnology 128: 1505–1510

31 English DE, Russell SM, Katz LS, Nicoll CS (1990) Evidence for a role of the liver in the mammatrophic action of prolactin. Endocrinology 126: 2252–2256

32 Griffen SC, Russell SM, Katz LS, Nicoll CS (1987) Insulin exerts metabolic and growth-promoting effects by a direct action on the liver *in vivo*: clarification of the functional significance of the portal vascular link between the B cells of the pancreatic islets and the liver. Proc Nat'l Acad Sci (USA) 84: 7300–7304

33 Delidow BC, Baldocchi RA, Nicoll CS (1988) Evidence for hepatic involvement in the regulation of amphibian development by prolactin. Gen Comp Endocrinol 70: 418–425

34 Ikida T, Fujiyama K, Hoshiro T, Tanaka Y, Takeuchi T, Mashiba M, Tominaga M (1991) Stimulating effect of thyroid hormone on insulin-like growth factor-I release and synthesis by perfused rat liver. Growth Reg 1: 39–45

ZOOLOGICAL SCIENCE 10: 245–256 (1993)

Isolation and Some Characterization of Vitellogenin and Its Related Egg Yolk Proteins from Coho Salmon (*Oncorhynchus kisutch*)

Akihiko Hara[1], Craig V. Sullivan[2] and Walton W. Dickhoff[3,4]

[1]*Nanae Fish Culture Experimental Station, Faculty of Fisheries, Hokkaido University, Nanae, Kameda, Hokkaido 041-11, Japan,* [2]*Department of Zoology, North Carolina State University, Raleigh, North Carolina 27695-7617,* [3]*School of Fisheries, University of Washington, Seattle, Washington 98195,* [4]*National Marine Fisheries Service, Northwest Fisheries Center 2725 Montlake Blvd. East, Seattle, Washington 98112, USA*

ABSTRACT—Vitellogenin (Vg) and its related egg protein 1 (E1) and egg protein 2 (E2) were isolated from serum or eggs of mature female coho salmon by precipitation in distilled water followed by chromatography on Sepharose 6B (Vg) or Sephadex G-200 (yolk proteins). The coho salmon proteins reacted specifically with respective antisera raised against Vg (a-Vg), E1 (a-E1) or E2 (a-E2) purified from chum salmon. Two female-specific proteins were identified in serum from mature coho salmon. Coho salmon Vg had an aparent molecular weight of 540 kDa after chromatography on Superose 6, appeared as a major 240 kDa band and a minor 165 kDa band in SDS-PAGE, and resolved into a major 165 kDa band and several minor 70–150 kDa bands after SDS-PAGE under reducing conditions. It reacted immunologically with a-E1 and a-E2. The other female-specific serum protein, designated coho salmon E2, reacted with a-E2 but not with a-E1. The apparent molecular weight of purified E1 and E2 were 230 and 35 kDa, respectively, after chromatography on Superose 6. E1 appeared as two main bands of 150 and 92 kDa in SDS-PAGE which resolved into two smaller bands (92 kDa and 20 kDa) after reduction. E2 appeared as a 30 kDa band in SDS-PAGE and as a 15 kDa band after reduction. The above immunological and biochemical characteristics and subunit structure of coho salmon Vg, E1, and E2 were found to be nearly identical to the corresponding proteins in several other salmonid species of diverse genera. These properties of Vg have been highly conserved during salmonid evolution.

INTRODUCTION

Vitellogenin (Vg) has been well-characterized in avian and amphibian species as a precursor for egg yolk. Hepatic synthesis of Vg is induced by estrogen in maturing females. The protein is released into the bloodstream from where it is taken up by developing oocytes and chemically modified in the process of yolk formation (for review, [24, 34, 36, 38]). For example, in the amphibian, *Xenopus,* Vg is a lipoglycophosphoprotein complex of precursors to several individual egg yolk proteins including lipovitellin, phosvitin and phosvettes [39].

In teleost fish, there are many reports of the identification of Vg or Vg-like proteins using immunological, electrophoretical and chromatographical methods [1, 3–5, 7–12, 25, 26, 32, 33, 35]. However, there are few reports on the specific biochemical relationship between serum Vg and the egg yolk proteins derived from it. We reported previously that salmonid Vg (female-specific serum protein) from rainbow trout, *Oncorhynchus mykiss* [16], chum salmon, *O. keta* [15] and white-spotted char, *Salivelinus leucomaenis* [17], is a precursor to at least two egg yolk proteins, egg protein one (E1) and egg protein two (E2). E1 was identified as a lipovitellin similar to that of *Xenopus* based on its physicochemical properties such as molecular weight, amino acid composition, sub-

Accepted November 13, 1992
Received September 7, 1992
[1] To whom all correspondence should be addressed.

unit structure and lipid content. Though E2 elutes in size exclusion chromatography in the fraction (mol. wt. 25–30 kDa) where Markert and Vanstone [22] reported two soluble egg yolk proteins that they termed phosvitin and the β'-component, we could identify only one antigenic protein in this fraction (E2). In addition, we identified two distinct female-specific proteins in serum from mature females or estrogen-treated males and immature fish using immunoelectrophoresis with rabbit antiserum raised against female-specific serum proteins from the species mentioned above [15, 17]. One of the mature female-specific serum proteins was identified as a Vg containing both E1 and E2 antigenicity. The other appeared to be a Vg fragment, since it was deficient in E1 antigenicity but had E2 antigenicity. We concluded that the two female-specific proteins found in the serum of maturing female salmonids represent a complex of E1+E2 (Vg) and a free E2.

The present paper describes the identification of coho salmon (*Oncorhynchus kisutch*) Vg by immunological methods using antisera raised in rabbits against chum salmon Vg, E1, and E2, and the isolation and partial biochemical characterization of coho salmon Vg and its related egg yolk proteins.

MATERIALS AND METHODS

Experimental animals, blood and tissue samples

The experimental animals used this study were adult female coho salmon that returned on their spawning migration to the University of Washington experimental fish hatchery where they were sampled for blood and eggs. They were fully mature but had not yet ovulated. Blood samples were collected from the caudal blood vessels using a syringe fitted with a 21 ga needle. The blood samples were held on ice and immediately transported to the laboratory where they were allowed to clot at 0–4°C overnight. The serum was collected after the blood samples were centrifuged at 1000×g for 15 min, and it was stored at −20°C until use.

One year-old immature coho salmon of both sexes were used for experiments in which Vg was induced by estrogen treatment. They were anesthetized in a solution (50 mg/l) of tricaine methane sulfonate (Argent Chemical Lab.) buffered to pH 7.0 with sodium bicarbonate and injected intramuscularly with 1 mg of estradiol-17β per kg of body weight dissolved in 100% propylene glycol. Two weeks after hormone treatment, blood samples were collected from these fish and processed as described above. Ovulated eggs were collected from female coho salmon during their spawning season (November). The eggs were washed twice with 0.9% NaCl and then kept frozen at −20°C until use.

Purification of Vg and egg yolk proteins

Coho salmon Vg and its related egg yolk proteins were isolated using our previously reported procedures [16]. Briefly, 2.5 ml of a sample of serum pooled from several mature females was added to 25 ml of ice-cold distilled-deionized water and the mixture was allowed to stand for 30 min at 0°C. A precipitate formed and was centrifuged at 2,500×g for 15 min at 4°C. The pellet was resuspended in water (25 ml), recentrifuged and dissolved in 0.5 ml of 0.02 M Tris-HCl buffer, pH 8.0, containing 2% NaCl and 0.1% NaN_3. The solution was then applied to a 1.6×60 cm gel filtration column of Sepharose 6B (Pharmacia Inc.) equilibrated with the Tris-HCl buffer. The column flow rate was adjusted to 15 ml/hr and 1.9 ml fractions were collected. The protein concentration in the fractions was estimated by absorbance at 280 nm and the one major peak was collected as the purified Vg. The presense of Vg in the fractions was assessed by single radial immunodiffusion [21] using an antiserum raised in rabbits against chum salmon E1 [15].

Egg yolk was collected from ovulated eggs using a syringe fitted with a 22 ga needle. The yolk was centrifuged at 1000×g for 5 min and the supernatant was collected and added dropwise to a 10× volume of ice-cold distilled-deionized water. The precipitate that formed was sedimented by centrifugation at 1000×g for 30 min and the pellet was redissolved in Tris-HCl buffer. This procedure was repeated twice. The final clear solution in Tris-HCl buffer was applied to a 1.6×60 cm gel filtration column of Sephadex G-200 (Pharmacia

Inc.). The elution buffer, flow rate, fraction volume and assay of protein in the fractions during Sephadex G-200 chromatography were the same as described above for Sepharose 6B chromatography. The elution pattern yielded two peaks, designated as E1 and E2 according to our previously defined criteria [15, 17].

Antisera

Rabbit antisera raised against mature female chum salmon serum proteins, Vg and egg yolk proteins (E1 and E2) were prepared as described previously [15]. An antiserum was also raised in rabbits against the coho salmon egg yolk protein, E1, by intradermal injection with purified E1 (approximately 0.5 mg) emulsified in an equal volume of complete Freund's adjuvant. Injections were done 4 times at 7–10 day intervals.

Electrophoresis and immunological procedures

Immunoelectrophoresis and single radial immunodiffusion [21] and double immunodiffusion [28] were performed using 1.2% agarose gels as described previously [15]. The concentration of serum Vg was determined by single radial immunodiffusion using the antiserum to coho salmon E1 and the purified coho salmon Vg as the reference standard protein. Discontinuous polyacrylamide gradient (3.75–18.75%) gel electrophoresis (PAGE) was carried out with (SDS-PAGE) or without (Disc PAGE) addition of SDS to the gel and samples as described by O'Farrell [27]. Preparation of samples for SDS-PAGE was done as described previously [16]. The marker proteins used for molecular weight determination were lactate dehydrogenase (subunit, 36 kDa), egg albumin (45 kDa), catalase (subunit, 60 kDa), bovine serum albumin (67 kDa), ferritin (subunits, 18.5 and 220 kDa) and thyroglobulin (subunit, 330 kDa).

FPLC chromatography

Chromatography was performed on a Pharmacia FPLC system using a prepacked Superose 6 HR 10/30 column (Pharmacia Inc.). The column was used for determination of the molecular weights of the purified proteins and for observation of the elution pattern of serum proteins. Serum samples were diluted 10×in Tris-HCl buffer and 200 μl of the solution, or about 6 mg of purified protein in 200 μl buffer, was applied to the column and eluted with the same buffer with a flow rate of 0.5 ml/min. The column was calibrated with the marker proteins: trypsinogen (24 kDa), egg albumin (45 kDa), bovine serum albumin (67 kDa), α-amylase (200 kDa), apoferritin (443 kDa) and thyroglobulin (669 kDa).

Comparative studies on salmonid Vg, E1 and E2

Blood serum and eggs were collected as described above from mature females of 10 species of salmonids from the genera Salmo, *Oncorhynchus, Salvelinus* (*Sl.*), and *Hucho,* which were obtained during annual spawning operations at various national, prefectural, university and commercial fish hatcheries in Hokkaido, Japan. These species included sockeye salmon (*O. nerka*), masu salmon (*O. masou*), amago salmon (*O. rhodurus*), rainbow trout, brown trout (*S. trutta*), Japanese huchen (*H. perryi*), brook trout (*Sl. fontinalis*), dolly varden (*Sl. malma*), white-spotted char (*Sl. leucomaenis*), and lake trout (*Sl. namaycush*). The egg yolk proteins, E1 and E2, were isolated as described above from the eggs of each of these species. The mature female serum, E1 and E2 of each species was reacted against the a-Vg, a-E1 and a-E2 antisera generated against the chum salmon proteins, and two additional a-Vg antisera generated against rainbow trout or spotted char vitellogenin [15, 16], in double immonodiffusion assays and immunoelectrophoresis as described above.

RESULTS

Identification of coho salmon Vg

Immunological methods were used for identification of coho salmon Vg. Figure 1 shows immunoelectrophoresis of serum from vitellogenic female coho salmon using the four antisera against chum salmon proteins as follows: antiserum against mature female chum salmon serum proteins (a-S), specific antiserum to chum salmon Vg (a-Vg), and specific antisera to chum salmon egg yolk proteins E1 (a-E1) and E2 (a-E2). With the

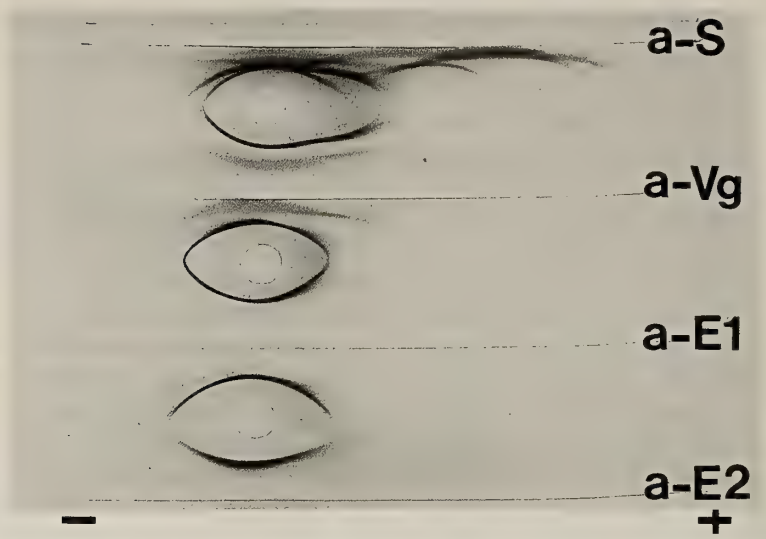

Fig. 1. Immunoelectrophoresis of mature female coho salmon serum using four different antisera against chum salmon. a-S: antiserum to mature female chum salmon serum proteins, a-Vg: antiserum to chum salmon vitellogenin, a-E1: antiserum to egg yolk protein one (lipovitellin) of chum salmon, a-E2: antiserum to egg yolk protein two (phosvitin/β'-component fraction) of chum salmon.

exception of a-S, all the antisera reacted only with serum from vitellogenic females but not with male serum (data not shown). The a-Vg antiserum produced two distinct precipitin lines and the two antisera against egg yolk proteins (a-E1 and a-E2) each produced one precipitin line when reacted against serum from mature female coho salmon in immunoelectrophoresis. Based on our previous studies of salmonid Vg from rainbow trout and chum salmon [13] and white-spotted char [17], the two precipitin lines formed against mature coho salmon female serum by the a-Vg antiserum were considered to be Vg (the inner line formed near antigen well) and a fragment of Vg (the outer line formed near the antiserum trough), respectively. The Vg concentration in serum from mature but unovulated female coho salmon, assayed by single radial immunodiffusion, ranged between 4.68 mg/ml and 15.91 mg/ml (average 13.0 mg/ml).

Purification of Vg and its related egg yolk proteins

The elution pattern in Sepharose 6B chromatography of protein from the water-insoluble fraction of coho salmon serum is shown in Fig. 2. The main peak was found to consist of Vg when assayed by single radial immunodiffusion using the a-E1 antiserum. A single and symmetrical peak was obtained and collected as the purified coho salmon Vg. After immunoelectrophoresis, this preparation of Vg gave rise to only one precipitin line when reacted against the a-S and a-Vg antisera, as shown in Fig. 3. As shown in Fig. 4, the elution pattern of the water-insoluble fraction of coho salmon egg extracts consisted of two distinct peaks, designated E1 and E2, after gel filtration on Sephadex G-200. The relative protein concentrations of E1 and E2, determined planimetrically from charts of gel filtration monitored by absorption at 280 nm, were found to be 13.3 and 1.0 respectively. When adjusted for the estimated molecular weights of E1 and E2 (discussed below), the apparent molar ratio of E1 to E2 is 2 to 1. The peak fractions were tested for their reactivity to the a-Vg, a-E1 and a-E2 antisera by immunodiffusion. The fraction designated coho salmon E1 reacted with the a-Vg antisera and a-E1 antisera, but not with antiserum a-E2. The fraction designated coho salmon E2 reacted with the a-Vg and a-E2 antisera but not with antiserum a-E1 (data not shown). After Disc-PAGE, the preparation of coho salmon Vg displayed a major band and a secondary band which migrated faster than the major band as shown in Fig. 5 (lane e). Some faint bands that migrated more slowly than the major

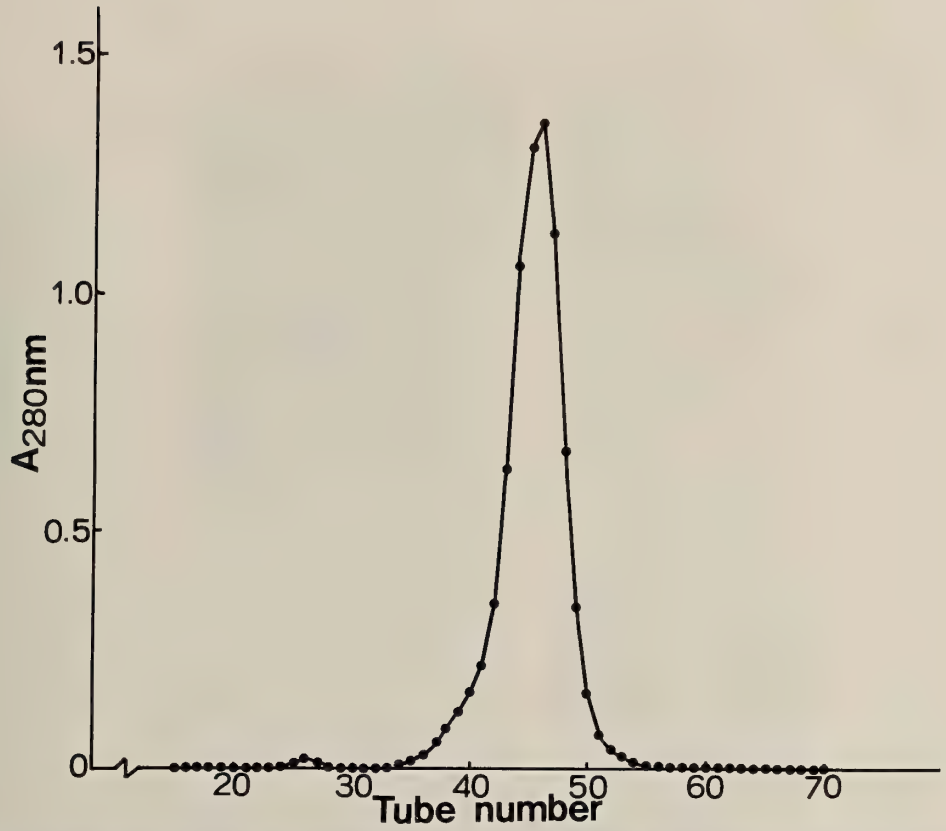

FIG. 2. Elution pattern of the water-insoluble fraction of coho salmon serum chromatographed on Sepharose 6B. The fractions pooled from tube number 43–48 were collected and concentrated as coho salmon vitellogenin for further analysis.

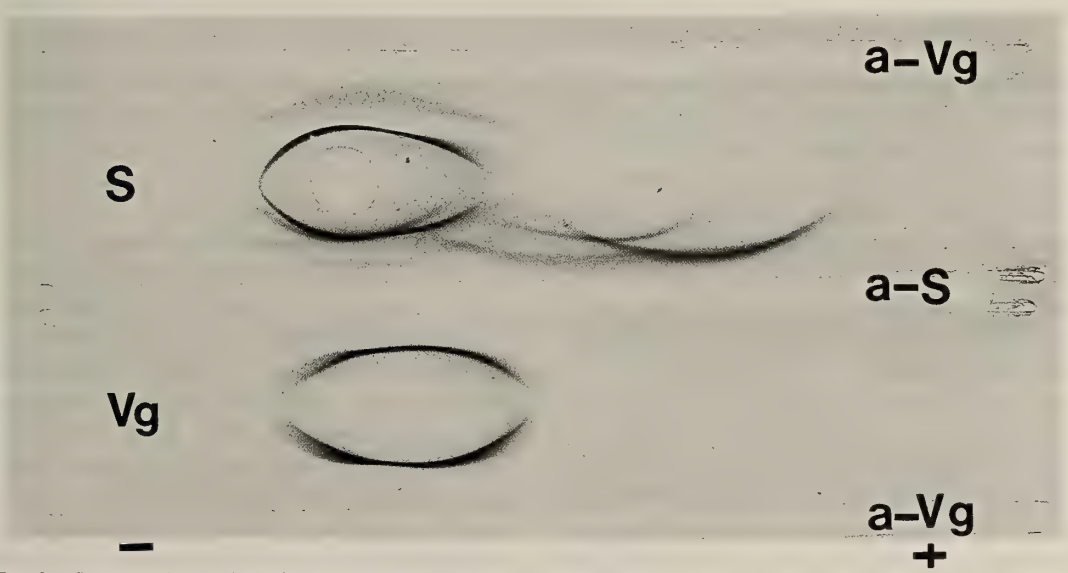

FIG. 3. Immunoelectrophoresis of purified coho salmon vitellogenin. S: mature female coho salmon serum, Vg: purified coho salmon vitellogenin, a-Vg and a-S: same as in Fig. 1.

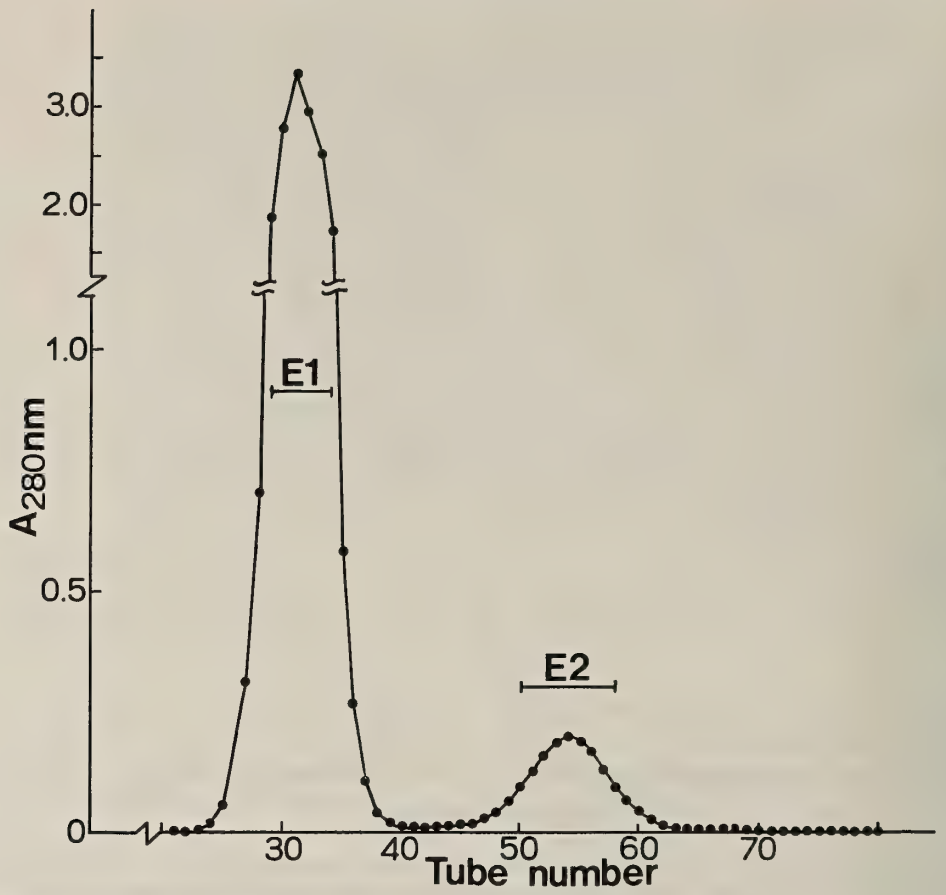

Fig. 4. Chromatography on Sephadex G-200 of water-insoluble proteins isolated from coho salmon eggs. Two major peaks were designated as E1 and E2.

band were also observed. The major band of purified Vg migrated to the position corresponding to the strong band observed only in serum of mature females (lane b) and estradiol-treated fish (lane d). While coho salmon E1 gave a single distinct band in Disc-PAGE (Fig. 5, lane g), coho salmon E2 gave a rather broad band composed of several sharp lines (Fig. 5, lane h). These results are essentially identical to those we reported for chum salmon [15].

In order to compare antigenicity between the three purified coho salmon proteins, double immunodiffusion was performed in 1.2% agarose gels using the a-Vg antiserum. The precipitin line from coho salmon Vg formed a spur over the precipitin lines of the two egg yolk proteins, E1 and E2, and the precipitin lines of each egg yolk protein crossed each other (data not shown), confirming that the coho salmon Vg molecule contains both E1 and E2 antigenicity.

Molecular weight of purified proteins

As shown in Fig. 6, the molecular weights of the purified coho salmon proteins, estimated by FPLC chromatography on the Superose 6 column, were 540 kDa for Vg, 230 kDa for E1, and 35 kDa for E2. The electrophoretic patterns of coho salmon Vg, E1 and E2 after SDS-PAGE ± reduction with 2-mercaptoethanol (2-ME) are shown in Fig. 7. Vg displayed one main band and a minor band coresponding to molecular weights of 240 kDa and 165 kDa, respectively (lane C). Vg reduced with 2-ME showed a main band with a molecular weight of 165 kDa as well as some minor bands of lower

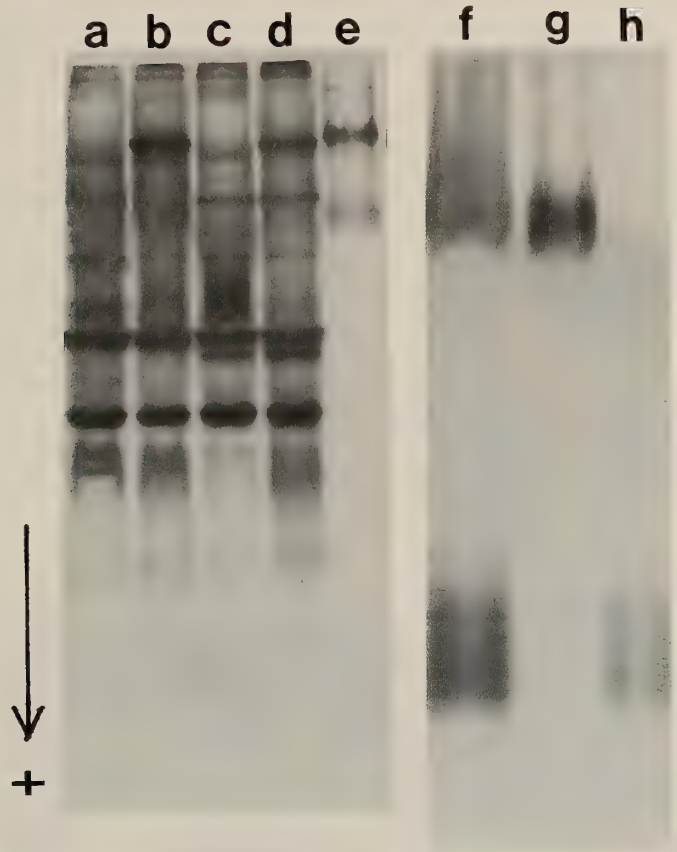

FIG. 5. Gradient Disc-PAGE of purified vitellogenin, E1 and E2 and egg yolk extracts from coho salmon. a: serum proteins from mature male, b: serum proteins from mature female, c: serum from immature male (control fish from estrogen-treatment experiment), d: serum from estrogen-treated immature fish, e: vitellogenin, f: egg yolk extracts, g: E1, h: E2.

(70 to 150 kDa) molecular weight (lane c). E1 showed a main band corresponding to a molecular weight of about 150 kDa and minor 92 kDa band, as well as a faint band migrating near the dye front (lane D). After reduction with 2-ME, E1 appeared as two main 92 kDa and 20 kDa bands, as well as some faint bands of intermediate (70 kDa to 90 kDa) molecular weight. E2 appeared in SDS-PAGE as a single 30 kDa band before reduction, and as a single 15 kDa band after reduction with 2-ME. These results were very similar to those observed Vg, E1 and E2 of rainbow trout and chum salmon [15].

Serum elution profiles in FPLC

Typical patterns of coho salmon serum after chromatography on Superose 6 are shown in Fig. 8. Distinct differences between the sexes were seen in the patterns. The major peak from female serum eluting at effluent volume 13.9 ml (panel b) was not seen in male serum (panel a). This peak was also induced in immature fish by treatment with estradiol-17β (panel c). Purified Vg (see Fig. 6) eluted the same position (arrow, Fig. 8) as the mature female specific and estradiol-inducible peak.

Cross-reactivity of antisera to chum salmon with other salmonid fish

The elution patterns on Sephadex G-200 of E1 and E2 from the 10 species of salmonids were nearly identical to that seen for coho salmon (data

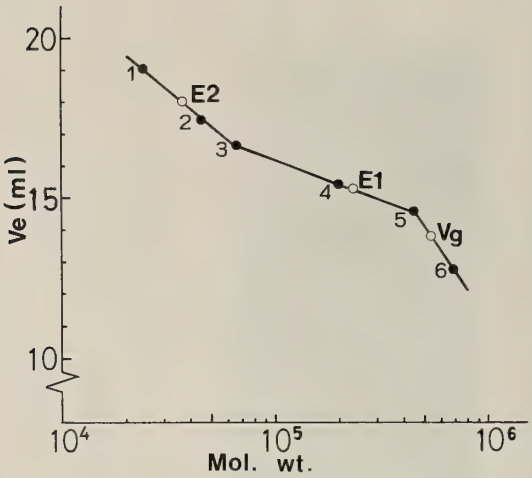

FIG. 6. Estimation of the molecular weight of coho salmon vitellogenin by Supurose 6 gel filtration in the FPLC system. The open circles correspond to the elution volume of purified vitellogenin (Vg), E1 and E2. The marker proteins used for calibration and indicated by the dark circles were, 1: trypsinogen, 2: egg albumin, 3: bovine serum albumin, 4: α-amylase, 5: apoferritin, and 6: thyroglobulin.

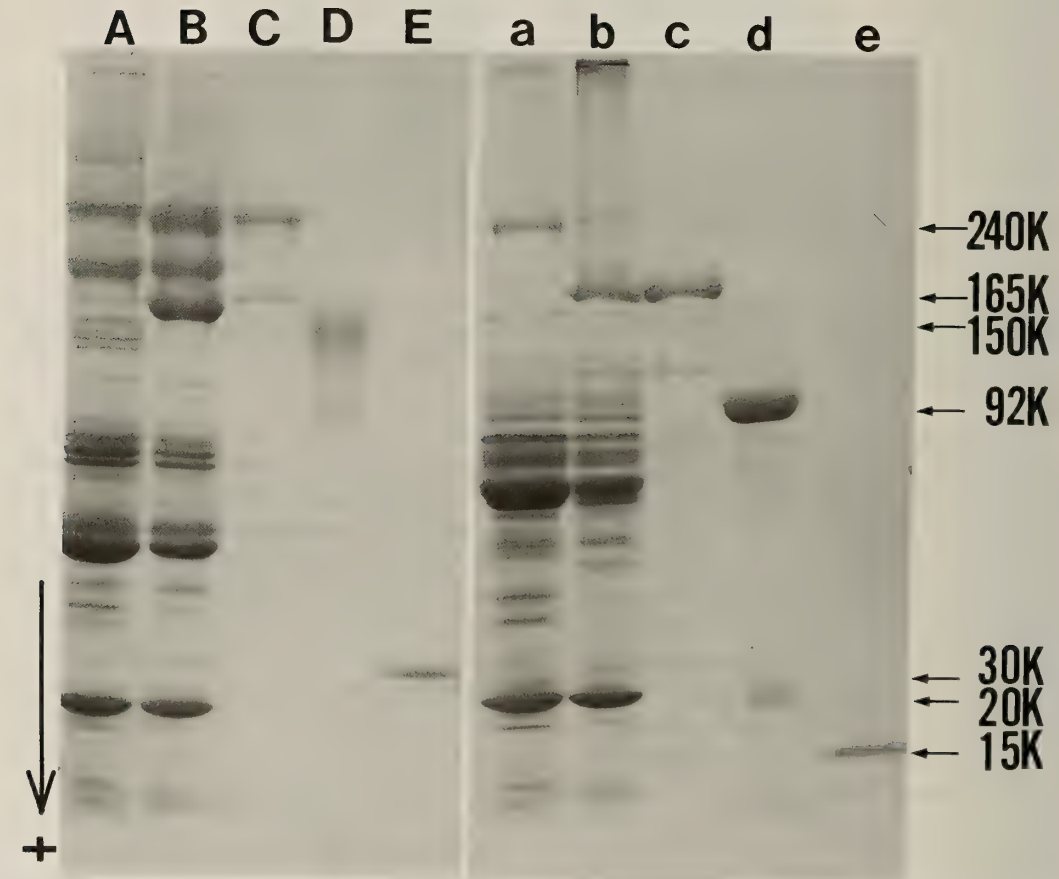

FIG. 7. SDS-PAGE on 3.75–18.75% gradient slab gels of mature male serum (A, a), female serum (B, b), vitellogenin (C, c), E1 (D, d), and E2 (E, e) in coho salmon. Lane A-E represent non-reduced samples and lanes a-e represent samples reduced with 2-mercaptoethanol.

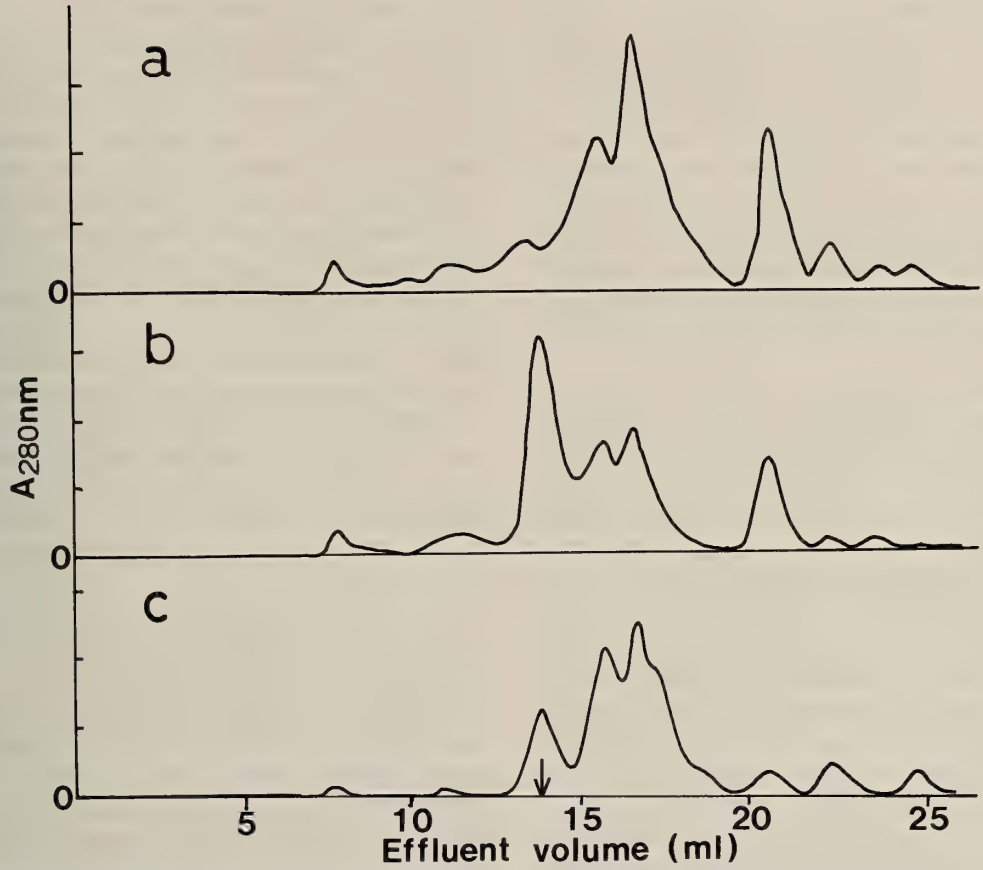

FIG. 8. Elution profiles of mature male (a) and female serum (b), and estrogen-treated male serum (c) in coho salmon on Supurose 6 in the FPLC system. The arrow indicates the elution position of vitellogenin.

not shown). As noted above, the a-Vg, a-E1 and a-E2 antisera raised against chum salmon Vg, E1 and E2, respectively, reacted strongly and specifically to the respective coho salmon proteins. In addition, we found that these antisera, as well as two other a-Vg antisera raised against Vg from rainbow trout and white-spotted char [15, 16], yielded a pattern of immunoreactivity identical to that reported above for coho salmon when they were reacted in double immunodiffusion assays and immunoelectrophoresis against the mature female serum, E1 and E2, from the 10 salmonid species. For each species, two mature female-specific serum proteins were seen in immunoelectrophoresis. One reacted with all of the antisera tested and the other reacted only with the a-Vg and a-E2 antisera. E1's from the various species reacted with all three a-Vg's and with a-E1, but not with a-E2. E2's from the various species reacted with all three a-Vg's and with a-E2, but not with a-E1.

DISCUSSION

In the present study, coho salmon Vg was purified within one day from the serum of mature females by precipitation with distilled water followed by gel filtration on Sepharose 6B. When the gel filtration step was done on a Supurose 6 column using the FPLC system, complete purification of Vg was accomplished within 3 hours, but yields were much reduced (data not shown). The precipitation step with distilled water is a very simple, easy and effective method for purification of sal-

monid Vgs, though its success depends on the starting conditions of the serum and its concentration of Vg. For example, precipitation of coho salmon Vg was not possible using serum containing Vg concentrations below about 5 mg/ml or using serum that was not previously frozen. We have used hydroxylapatite column chromatography to purify Vg from salmonid serum with low Vg concentrations that cannot be precipitated with distilled water, and the purified protein is similar in all respects to that obtained using the precipitation method [14–17].

So far, the detection of teleost Vg has been performed primarily by immunological, electrophoretical and chromatographical procedures. In the present study, in addition to immunological methods, we identified Vg in serum of mature females and estrogen-treated males and immature fish using a Supurose 6 column in an FPLC chromatography system. This method required only one drop of serum for assay and the procedure is simple and rapid. Silversand and Haux [31] recently reported a simiar method for purification of turbot Vg, using a Mono Q column in an FPLC system. Though further studies will be needed to confirm the relation between the concentration of Vg and its peak height or area in FPLC or HPLC chromatography, the method should prove useful for rapid routine assay of fish Vgs.

Vertebrate Vg has been generally confirmed to be the precursor of the major yolk proteins, lipovitellin and phosvitin. Rainbow trout egg yolk proteins can be chromatographically separated into three major components [20]. Phosvitin is a phosphoprotein rich in serine [5, 19, 30], soluble in trichloroacetic acid [5, 30, 37], and poorly stained with Coomassie Blue on electrophoretic gels [18]. Lipovitellin is the main yolk protein of oviparous vertebrates, and it contains a high concentration of lipids and little or no protein phosphorus. In rainbow trout, the lipovitellin has been reported to consist of two subunits of mol. wt. 90 kDa and 15 kDa [16] or 95 and 24 kDa [6] or 92 and 20 kDa [1], or to consist of four subunits from 145–160 kDa (n=2) and from 14–19 kDa (n=2) which can easily dimerize [29]. A third yolk protein, the β'-component [20], is characteristic of the yolk of salmonid eggs [22, 23]. Its amino acid composition is distinct from those of lipovitellin and phosvitin [5]. It can escape precipitation when the yolk is diluted with distilled water [20, 22]. Though the origin of the β'-component remains to be conclusively verified, it has been suggested that it is derived from Vg like lipovitellin and phosvitin [38]. In the present study, the water-insoluble egg yolk proteins of coho salmon were separated into two components, namely, E1 and E2. The molecular weight of E1 and E2 were estimated by gel filtration to be 230 kDa and 35 kDa, respectively. Using SDS-PAGE without reduction by 2-ME, the molecular weights of E1 and E2 were estimated to be 150 kDa and 30 kDa, respectively. Upon reduction with 2-ME, the 150 kDa component of E1 further split into two major polypeptides with molecular weights of 92 and 20 kDa. The 30 kDa E2 split into a single component with a molecular weight of 15 kDa, suggesting that it may be a homodimer. These results are essentially identical to those that we previously reported for rainbow trout egg yolk proteins [16].

Immunological methods using antisera to chum salmon Vg, E1 and E2 revealed two female-specific proteins in the serum of mature coho salmon. One (Vg) was, in part, a complex of E1+E2. The observation that coho salmon Vg contained both the E1 and E2 components of egg yolk proteins is similar to our previously reported results on other salmonid species [15]. The second female-specific serum protein contained only E2 antigenicity. It did not react with antiserum to E1. A relation of these two serum proteins to the coho salmon β'-component and/or phosvitin [23] remains to be established. Our results suggest that an antiserum raised against purified E1 would be preferable to an antiserum to Vg for measurement of Vg concentrations in serum.

Chen et al. [7] developed a rapid sensitive assay for rainbow trout Vg using an antiserum against lipovitellin in rocket immunoelectrophoresis. They reported that their antibody against rainbow trout lipovitellin showed a continuous precipitation arc when reacted against coho salmon lipovitellin in Ouchterlony immunodiffusion and Western immunoblotting assays. These results support our observation that antisera to chum salmon Vg, E1 and E2 strongly react to the

respective coho salmon proteins. We also found that the antiserum to chum salmon Vg, E1 and E2, react fully and specifically with the corresponding proteins of various other species from diverse salmonid genera, including sockeye salmon, masu salmon, amago salmon, rainbow trout, brown trout, Japanese huchen, brook trout, dolly varden, white-spotted char, and lake trout. Benfey et al. [2] also showed that plasma from various salmonid species exhibited parallelism in a coho salmon Vg radioimmunoassay. These results suggest that affinity chromotography on a column containing antibodies against the proteins purified from one salmonid species should be a viable approach to purifying Vg from a variety of other salmonid fishes. They also indicate that Vg and its related egg proteins have been highly conserved during salmonid evolution.

ACKNOWLEDGMENTS

We would express our gratitude to C. V. W. Mahnken, National Marine Fisheries Service, Northwest Fisheries Center, Seattle, Washington, for facilities and finacial support, and to Drs. E. Brannon and W. K. Hershberger, School of Fisheries, University of Washington, Seattle, Washington, for access to fish and samples. Appreciation is extended to Drs. E. Plisetskaya and P. Swanson, School of Fisheries, University of Washington, for their kind advice and valuable suggestions, to M. G. Bernard and Dr. L. Yan for help with fish sampling and care, and to Dr. K. Takano for help collecting samples from the various species of salmonids. This investigation was supported by grant from the National Science Foundation (DCB 8615521) to W.W.Dickhoff, by a grant from the International Exchange Programs Committee of Hokkaido University, Sapporo, Japan, to C.V.Sullivan, and by a Grant-in-Aid for Scientific Research from the Japanese Ministry of Education, Science and Culture (01440014) to A. Hara.

REFERENCES

1 Babin PJ (1987) Apolipoproteins and the association of egg yolk proteins with plasma high density lipoproteins after ovulation and follicular atresia in the rainbow trout (*Salmo gairdneri*). J Biol Chem 262: 4290–4296

2 Benfey TJ, Donaldson EM, Owen TG (1989) An homologus radioimmunoassay for coho salmon (*Oncorhynchus kisutch*) vitellogenin, with general applicability to other Pacific salmonids. Gen Comp Endocrinol 75: 78–82

3 Bradley JT, Grizzle JM (1989) Vitellogenin induction by estradiol in channel catfish, *Ictalurus punctatus*. Gen Comp Endocrinol 73: 28–39

4 Campbell CM, Idler DR (1976) Hormonal control of vitellogenesis hypophysectomized winter flounder (*Pseudopleuronectes americanus* Walbaum). Gen Comp Endocrinol 28: 143–150

5 Campbell CM, Idler DR (1980) Characterization of an estradiol-induced protein from rainbow trout as vitellogenin by the cross reactivity to ovarian yolk fractions. Biol Reprod 22: 605–617

6 Chen TT (1983) Identification and characterization of estrogen-responsive gene products in the liver of rainbow trout. Can J Biochem Cell Biol 61: 802–810

7 Chen TT, Reid PC, Van Beneden R, Sonstegard RA (1986) Effect of Aroclor 1254 and Mirex on estradiol-induced vitellogenin production in juvenile rainbow trout (*Salmo gairdneri*). Can J Fish Aquat Sci 43:169–173

8 Copeland PA, Sumpter JP, Walker TK, Croft M (1986) Vitellogenin levels in male and female rainbow trout (*Salmo gairdneri* Richardson) at various stages of the reproductive cycle. Comp Biochem Physiol 83B: 487–493

9 Covens M, Covens L, Ollevier F, de Loof A (1987) A comparative study of some properties of vitellogenin (Vg) and yolk proteins in a number of freshwater and marine teleosts. Comp Biochem Physiol 88B: 75–80

10 de Vlaming VL, Wiley HS, Delahuntry G, Wallace RA (1980) Goldfish (*Carassius auratus*) vitellogenin: Induction, isolation, properties and relationship to yolk proteins. Comp Biochem Physiol 67B: 613–623

11 Emmersen BK, Petersen IM (1976) Natural occurrence and experimental induction by estradiol 17-β, of a lipophophoprotein in flounder (*Platichthys flesus* L.). Comp Biochem Physiol 54B: 443–446

12 Fletcher PE, Fletcher GL (1980) Zinc- and copper-binding proteins in the plasma of winter flounder (*Pseudopleuronectes americanus*). Can J Zool 58: 609–613

13 Hara A (1976) Iron-binding activity of female-specific serum proteins of rainbow trout (*Salmo gairdneri*) and chum salmon (*Oncorhyncus keta*). Biochim Biophys Acta 427: 549–557

14 Hara A (1978) Sexual differences in serum proteins of chum salmon and the purification of female-specific serum protein. Bull Jap Soc Sci Fish 44: 689–693

15 Hara A (1987) Studies on female-specific serum proteins (vitellogenin) and egg yolk proteins in teleosts:Immunochemical, physicochemical and structural studies. Mem Fac Fish Hokkaido Univ 34: 1–59

16 Hara A, Hirai H (1978) Comparative studies on

immunochemical properties of female-specific serum protein and egg yolk proteins in rainbow trout (*Salmo gairdneri*). Comp Biochem Physiol 48B: 389–399

17 Hara A, Matsubara T, Saneyashi M, Takano K (1984) Vitellogenin and its derivatives in egg yolk proteins of white-spotted char (*Salivelinus leucomaenis*). Bull Fac Fish Hokkaido Univ 35: 144–153

18 Hegenauer J, Ripley L, Nace G (1977) Staining acidic phosphoproteins (phosvitin) in electrophoretic gels. Anal Biochem 78: 308–311

19 Ito Y, Fujii T, Kanamori M, Hattori T, Yoshioka R (1966) Phosvitin of the trout roe. J Biol Chem 60: 726–728

20 Jared DW, Wallace RA (1968) Comparative chromatography of the yolk proteins of teleosts. Comp Biochem Physiol 24: 437–443

21 Mancini G, Carbonara AO, Heremans JF (1965) Immunochemical quantitation of antigens by single radial immunodiffusion. Immunochemistry 2: 235–254

22 Markert JR, Vanstone WE (1968) Egg proteins of Pacific salmon, genus *Oncorhynchus*: Proteins in the soluble fraction. Can J Biochem 46: 1334–1337

23 Markert JR, Vanstone WE (1971) Egg proteins of coho salmon (*Oncorhynchus kisutch*): chromatographic separation and molecular weights of the major proteins in the high density raction and their presence in salmon plasma. J Fish Res Board Can 28: 1853–1856

24 Mommsen TP, Walsh PL (1988) Vitellogenesis and oocyte assembly. In "Fish Physiology Vol XIA" Eds by WS Hoar, DJ Randall, Academic Press, New York, pp 347–406

25 Nath P, Sundararaj BI (1981) Isolation and identification of female-specific serum lipophosphoprotein (vitellogenin) in the catfish, *Heteropneustes fossilis*. Gen Comp Endocrinol 43: 184–190

26 Ng TB, Idler DR (1983) Yolk formation and differentiation in teleost fishes. In "Fish Physiology Vol IXA" Eds by WS Hoar, DJ Randall, Academic Press, New York, pp 373–404

27 O'Farrell PH (1975) High resolution two dimensional electrophoresis of proteins. J Biol Chem 250: 4007–4021

28 Ouchterlony Ö (1953) Antibody-antigen reactions in gels. IV. Types of reactions in coordinated systems of diffusion. Acta Path Microbiol Scand 32: 231–240

29 Riazi A, Fremont L, Gozzelino MT (1988) Characterization of egg yolk proteins from rainbow trout, *Salmo gairdneri* (Rich). Comp Biochem Physiol 89B: 399–407

30 Schmidit G, Bartsch G, Kitagawa T, Fujisawa K, Knolle J, Joseph J, De Marco P, Liss M, Haschemeyer R (1965) Isolation of a protein of high phosphorus content from the eggs of brown brook trout. Biochem Biophys Res Commun 18: 60–65

31 Silversand C, Haux C (1989) Isolation of turbot (*Scophthalmus maximus*) vitellogenin by high-performance anion-exchange chromatography. J Chromatography 478: 387–397

32 So YP, Idler DR, Hwang SJ (1985) Plasma vitellogenin in landlocked Atlantic salmon (*Salmo salar* Quananche): Isolation, homologous radioimmunoassay and immunological cross-reactivity with vitellogenin from other teleosts. Comp Biochem Physiol 81B: 63–71

33 Sullivan CV, Tao Y, Hodson, R.G, Hara A, Bennett RO, Woods III LC (1991) Vitellogenin and vitellogenesis in striped bass (*Morone saxatilis*) broodstock. In "Proceedings of the Fourth International Symposium on the Reproductive Physiology of Fish". Eds by AP Scott, JP Sumpter, DE Kime, MS Rolfe, Sheffield, U.K. pp 315–317

34 Tyler C (1991) Vitellogenesis in salmonids. In "Proceedings of the Fourth International Symposium on the Reproductive Physiology of Fish". Eds by AP Scott, JP Sumpter, DE Kime, MS Rolfe, Sheffield, U.K. pp 295–299

35 Wallace RA (1978) Oocyte growth in nonmammalian vertebrates. In "The Vertebrate Ovary". Ed by RE Jones, Plenum Press, New York, pp 469–502

36 Wallace RA (1985) Vitellogenesis and oocyte growth in nonmammalian vertebrate. In "Development Biology Vol 1" Ed by LW Browder, Plenum Press, New York, pp 127–177

37 Wallace RA, Jared DW, Eisen AZ (1966) A general method for the isolation and purification of phosvitin from vertebrate eggs. Can J Biochem 44: 1647–1655

38 Wiegard MD (1982) Vitellogenesis in fishes. In "Reproductive Physiology of Fish". Eds by CJJ. Richter, HJT Goos, Wageningen, pp 136–146

39 Wiley HS, Wallace RA (1981) The structure of vitellogenin: Multiple vitellogenins in *Xenopus laevis* give rise to multiple forms of the yolk proteins. J Biol Chem 256: 8626–8634

ZOOLOGICAL SCIENCE 10: 257–265 (1993)

Structure and Function of the Molluscan Myoactive Tetradecapeptides

Arata Harada[1], Masayuki Yoshida[1], Hiroyuki Minakata[2]
Kyosuke Nomoto[2], Yojiro Muneoka[1]
and Makoto Kobayashi[1]*

[1]*Physiological Laboratory, Faculty of Integrated Arts and Sciences, Hiroshima University, Hiroshima 730, and* [2]*Suntory Institute for Bioorganic Research, Osaka 618, Japan*

ABSTRACT—Effects of myoactive tetradecapeptides, *Achatina* excitatory peptide 2 and 3 (AEP2 and AEP3) and *Fusinus* excitatory peptide 4 (FEP4), on several molluscan muscles and neurons were investigated. In the penis retractor and radula retractor muscles of *Achatina fulica* (pulmonate), the three peptides enhanced the tetanic contraction elicited by nerve stimulations. The order of potency was AEP2>AEP3>FEP4, although the effects of AEP3 and FEP4 on the radula retractor were somewhat irregular. AEP2 also induced rhythmic bursts of activity in the buccal ganglionic neuron B4 known as a cholinergic motoneuron of the radula retractor. In the radula protractor and retractor muscles of *Fusinus ferrugineus* (prosobranch), FEP4 was most potent in enhancing the contraction. The enhancement was greater in the protractor than in the retractor. It was suggested that myoactive tetradecapeptides modulate mainly the cholinergic transmission in molluscan muscles.

INTRODUCTION

It has been known that the contraction of molluscan muscles is regulated by multiple bioactive substances including neuropeptides [11]. In the African giant snail *Achatina fulica* (pulmonate, mollusc), more than twenty neuropeptides have been purified from the ganglia and hearts [8], and the function of some of them has already been investigated [1, 5]. Two bioactive tetradecapeptides which are highly homologous in structure were isolated from the ganglia of this snail [10]. Further, they appeared to be very close to another tetradecapeptide purified from the ganglia of a prosobranch *Fusinus ferrugineus*. During the process of purification of these peptides, they were found to be active in enhancing the contraction of a few muscles of *A. fulica* [10]. They were named myoactive tetradecapeptides (MATPs) [10].

In the present study, actions of MATPs on several molluscan muscles and neurons were examined and the mechanisms of their action on the neuromuscular systems were studied.

MATERIALS AND METHODS

Two *Achatina* tetradecapeptides and a *Fusinus* tetradecapeptide were isolated from the ganglia of each animal by using the penis retractor muscle of *A. fulica* and the radula retractor muscle of *F. ferrugineus* as a bioassay system, respectively. These isolation procedures have been described previously [10].

Peptides used in the present experiments were synthesized by a solid-phase peptide synthesizer and purified by HPLC. Their structures were confirmed by amino acid sequence analysis and fast atom bombardment mass spectrometric (FAB-MS) measurement.

Bioactivities of the synthesized peptides were examined on the penis retractor muscle, the radula retractor muscle and the buccal ganglionic neurons of *A. fulica,* and the radula protractor and retractor muscles of *F. ferrugineus* and of *Rapana thoma-*

Accepted November 19, 1992
Received October 15, 1992
1* To whom reprint requests should be addressed.

siana (prosobranch). Physiological saline used for the preparation from *A. fulica* consisted of (mM): NaCl 61.0, KCl 3.3, $CaCl_2$ 10.7, $MgCl_2$ 13.0, glucose 5.0 and Hepes-NaOH 10.0 (pH 7.5). In some experiments, saline containing 65 mM $MgCl_2$ (high-Mg^{2+} saline) was used, which was prepared by merely adding $MgCl_2$ to normal saline. Composition of artificial seawater used for the preparation from *F. ferrugineus* and *R. thomasiana* was as follows (mM): NaCl 475.0, KCl 10.0, $CaCl_2$ 10.0, $MgCl_2$ 20.0 and Tris-HCl 10.0 (pH 7.8).

Stimulation of these muscles and recording of the tension were made according to the method previously described by Muneoka and Twarog [9]. Electrical activities of the neurons were recorded by the conventional intracellular microelectrode method [13].

RESULTS

Two *Achatina* peptides were provisionally termed *Achatina* excitatory peptide 2 (AEP2) and 3 (AEP3), and a *Fusinus* peptide was termed *Fusinus* excitatory peptide 4 (FEP4) [10]. The structures of these peptides are as follows:

AEP2: Gly-Phe-Arg-Gln-Asp-Ala-Ala-Ser-Arg-Val-Ala-His-Gly-Tyr-NH_2

AEP3: Gly-Phe-Arg-Gly-Asp-Ala-Ala-Ser-Arg-Val-Ala-His-Gly-Phe-NH_2

FEP4: Gly-Phe-Arg-Met-Asn-Ser-Ser-Asn-Arg-Val-Ala-His-Gly-Phe-NH_2

In the present paper these terms will also be employed.

Figure 1A demonstrates effects of three kinds of peptides on the tetanic contraction of the penis retractor muscle of *A. fulica*. The contraction was

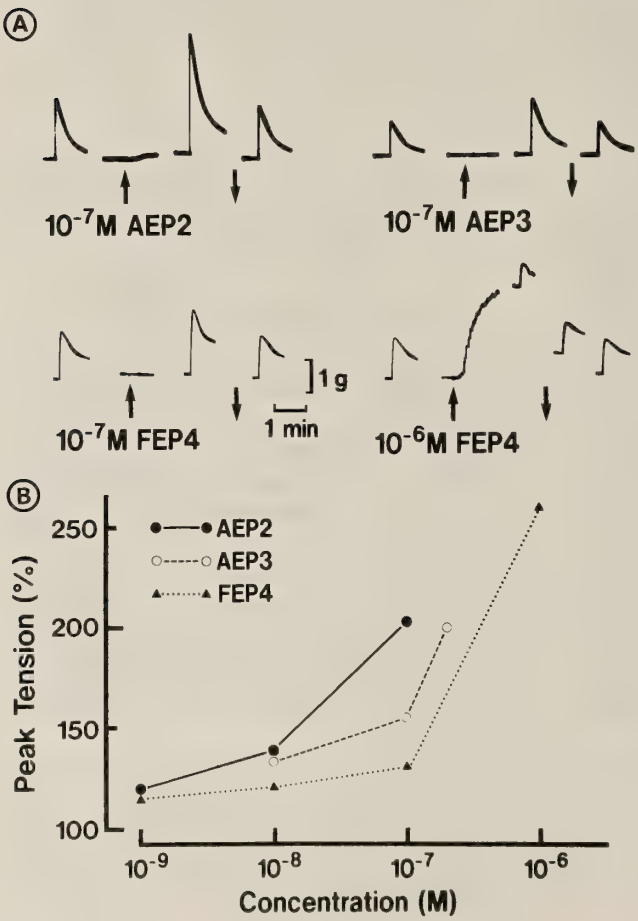

FIG. 1. Effects of three peptides on the tetanic contraction of the penis retractor muscle of *A. fulica*. A. The muscle was stimulated with a train of electrical pulses (0.8 msec, 10 V, 40 Hz) for 1 sec at 10 min intervals. Peptide was applied 8 min before applying the stimulation (upward arrow), and washed out immediately after the recording (downward arrow). B. Dose-response relationships of three peptides. Peak tension was expressed as percent of the control tension.

evoked by applying a train of electrical pulses (0.8 msec, 10 V, 40 Hz) for 1 sec to the muscle. AEP2 remarkably enhanced the contraction with a threshold concentration of 10^{-9} M, and at concentrations more than 10^{-7} M it directly induced a contraction. AEP3 and FEP4 produced similar effects on the penis retractor muscle, although they were slightly less potent than AEP2. Figure 1B illustrates the dose-response relations of the three peptides. As shown in this graph the order of potency in enhancing the muscle contraction was AEP2>AEP3>FEP4.

To test the site of action of the peptides the following experiments were performed (Fig. 2). After confirming that a train of pulses of short duration (0.8 msec, 10 V, 40 Hz) produced a tetanic contraction in normal saline, it was replaced by high-Mg^{2+} saline. In the latter the contraction by electrical pulses of short duration (0.8 msec) was completely blocked, supporting the assumption that short-duration pulses stimulated the muscle indirectly through intramuscular nerve fibers. When pulse duration was increased to 8.0 msec, however, the tetanic contraction of considerable size could be elicited even in high-Mg^{2+} saline. Such long-duration pulses probably stimulated the muscle fibers directly. AEP2 of 10^{-8} M, which potentiated the tetanic contraction by short-duration pulses in normal saline, could also potentiate the contraction in response to long-duration pulses in high-Mg^{2+} saline. Similarly, AEP3 and FEP4 also enhanced the contraction by long-duration pulses in high-Mg^{2+} saline and the efficiency of the three peptides was about the same.

In experiments shown in Fig. 3, effects of the three peptides on the tetanic contraction of the radula retractor muscle elicited by a train of pulses of short duration (0.8 msec, 10 V, 40 Hz) were examined. AEP2 enhanced the contraction in a dose-dependent manner with a threshold concentration around 10^{-9}-10^{-8} M, and at concentrations of 10^{-6} M or more it directly induced a contraction. However, the effects of AEP3 and FEP4 were quite variable with different preparations, and in some preparations inhibition of contraction during application and potentiation after washing of the peptide were observed (Fig. 3). These results may imply that AEP3 and FEP4 act on multiple nerve fibers of inhibitory and excitatory nature.

In applying several kinds of bioactive amine substances such as acetylcholine (ACh), catecholamines, octopamine, serotonin and histamine on the radula retractor muscle, we have found that only ACh at comparatively lower concentrations

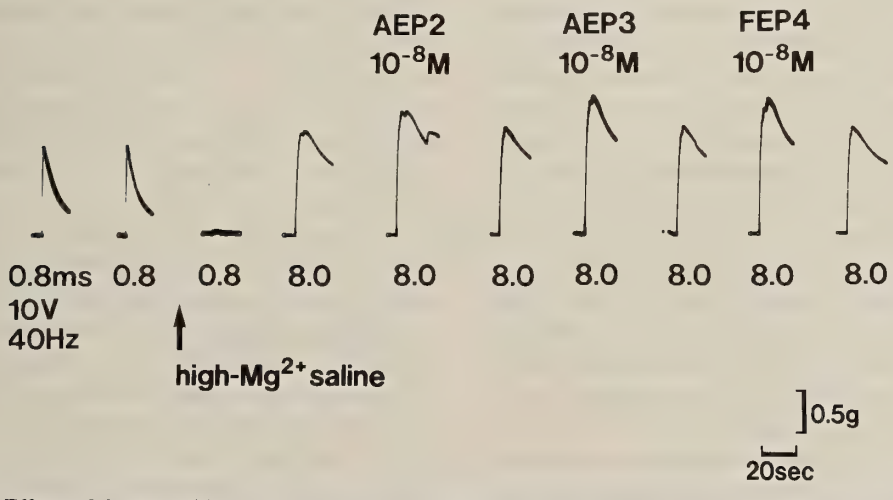

FIG. 2. Effects of three peptides on the tetanic contraction of the penis retractor muscle of *A. fulica* in normal saline and high-Mg^{2+} saline. The muscle was stimulated with a train of short-duration pulses or long-duration pulses at 10 min intervals. Soon after recording the second contraction, high-Mg^{2+} saline was applied (upward arrow). Procedures for applying peptides were the same as in Fig. 1.

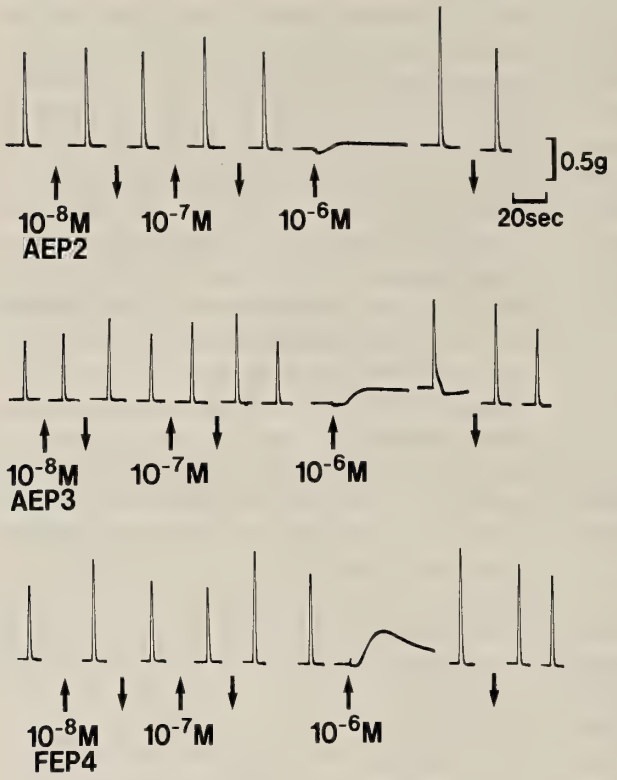

FIG. 3. Effects of three peptides on the tetanic contraction of the radula retractor muscle of *A. fulica*. Procedures for stimulating the muscle and applying peptides were the same as in Fig. 1.

elicited a contraction. Further, an identified motoneuron (B4) of the radula retractor muscle has been shown to be cholinergic [13]. Thus, the modulatory effects of peptides on the contraction in response to ACh were investigated. Figure 4A shows contractions evoked by applying ACh during the period indicated by a horizontal line under each record. AEP2 potentiated the ACh-evoked contraction in a dose-dependent manner, and AEP3 and FEP4 also showed similar effects. The order of efficiency was AEP2>AEP3>FEP4 as shown by dose-response curves (Fig. 4B).

In molluscan neuromuscular junctions, propantheline has been shown to be a cholinergic blocking agent [12, 13]. In the experiments shown in Fig. 5A and B effects of propantheline on the contraction of radula retractor muscle elicited by ACh and by electrical stimulation were compared. ACh-evoked contraction was extremely depressed by propantheline at a concentration of 10^{-5} M and was completely blocked at 10^{-4} M (Fig. 5A). However, the contraction in response to electrical stimulation was inhibited by only 30% of the control during application of 10^{-4} M propantheline. To demonstrate that short-duration pulses (0.6 msec) selectively stimulated the intramuscular nerve fibers the preparation was immersed in high-Mg^{2+} saline. Stimulation of short-duration pulses almost failed to evoke the contraction, but that of long-duration pulses (6.0 msec) elicited a contraction of considerable size, supporting the foregoing assumption. Propantheline of 10^{-4} M did not depress the contraction by long-duration pulses in high-Mg^{2+} saline. From these experiments, the contraction elicited by short-duration pulses during application of propantheline in normal saline is considered to be evoked by the stimulation of nerve fibers other than cholinergic ones. Will this contraction be modulated by peptides? Experiments shown in Fig. 5C were performed to answer this question. AEP2 of 10^{-7} M enhanced the contraction elicited during application of propantheline by only about 14%, in contrast to the contraction without propantheline

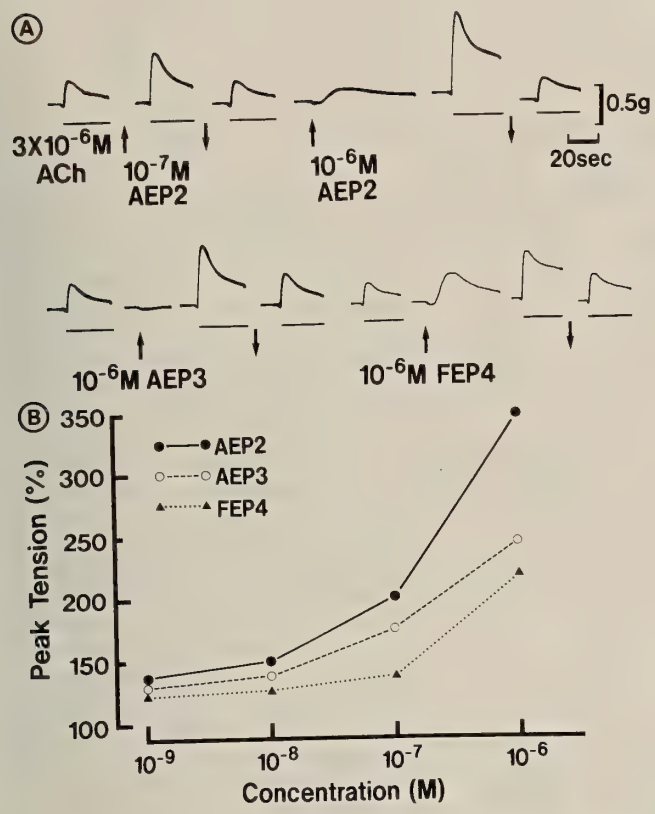

FIG. 4. Effects of three peptides on the contraction of the radula retractor muscle of *A. fulica* induced by ACh. A. ACh was applied during the period shown by a horizontal line under each record. Procedures for applying peptides were the same as in Fig. 1. B. Dose-response relationships of three peptides. Peak tension was expressed as percent of the control tension.

which was enhanced by about 46% by applying the same concentration of AEP2. This seems to imply that AEP2 enhances the contraction of the radula retractor muscle by acting mainly on the cholinergic transmission.

Among the identified neurons in the buccal ganglia of *A. fulica,* six pairs have been known as excitatory motoneurons for the radula retractor muscle [13, 14]. Figure 6 shows effects of the peptides on such identified neurons B1 and B4. AEP2 induced rhythmic bursts of activity in both neurons (Fig. 6A), and AEP3 also elicited several bursts, although they were rather irregular (Fig. 6B). However, FEP4 had no significant effects on these neurons.

In experiments shown in Fig. 7, effects of the three peptides on the twitch contraction of the radula protractor and retractor muscles of *Fusinus ferrugineus* were tested. In these muscles FEP4 showed stronger effects than AEP2 or AEP3 in contrast to their effects on *Achatina* muscles and neurons. FEP4 enhanced the contraction in a dose-dependent manner with a threshold concentration of 10^{-10} M, and at concentration of 10^{-8} M or more it directly induced a contraction. Similar tendency of effects was observed in AEP2 and AEP3, with AEP3 having weaker effects than the others. However, the efficiency of the peptides was different between these two muscles; in the radula protractor 10^{-7} M FEP4 enhanced the contraction by more than 150% of the control, while in the retractor the enhancement was less than 30% of the control (Fig. 7). AEP2 and AEP3 also produced stronger enhancing effects on the contraction of the protractor than the retractor.

Similar experiments were performed by using the radula protractor and retractor muscles of *Rapana thomasiana,* since the mode of excitatory transmission has been shown to be different between these muscles, the protractor being mainly cholinergic and the retractor glutaminergic [6, 7]. As demonstrated in Fig. 8, the three peptides

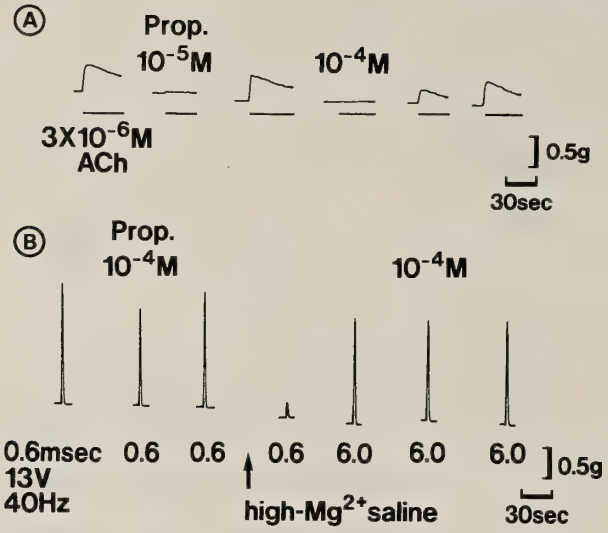

FIG. 5. Effects of propantheline (Prop) on the contraction of the radula retractor muscle of *A. fulica* elicited by ACh (A) and by electrical stimulation (B). Propantheline was applied 8 min before giving ACh or stimulation and washed out immediately after the record. In A, ACh was applied during the period shown by a horizontal line under each record. In B, the muscle was stimulated with a train of short-duration pulses or long-duration pulses at 10 min intervals. Soon after the third record, high-Mg^{2+} saline was applied (upward arrow). C. Effects of AEP2 on the tetanic contraction of the radula retractor muscle of *A. fulica* during and without application of propantheline. The muscle was stimulated with a train of short-duration pulses (0.6 msec, 13 V, 40 Hz) for 1 sec at 10 min intervals. Propantheline was applied 8 min before the fourth record and washed out after the sixth record. Procedures for applying peptide were the same as in Fig. 1.

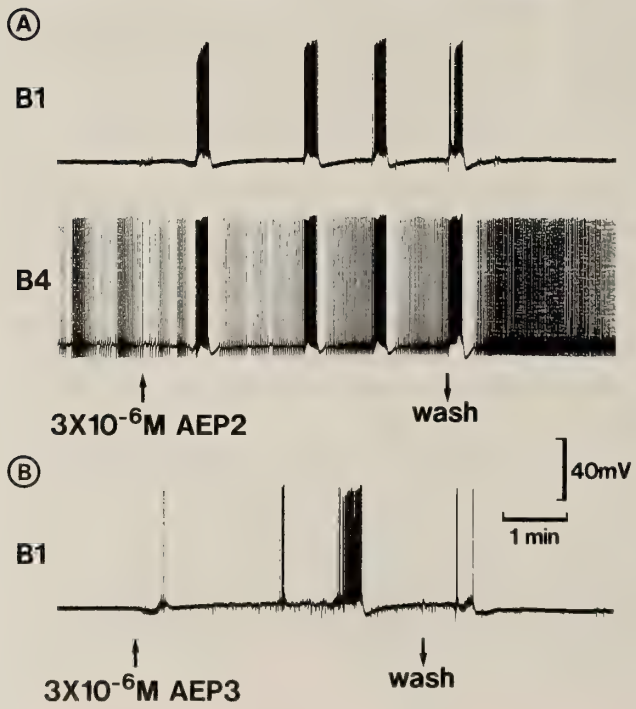

FIG. 6. Effects of AEP2 (A) and AEP3 (B) on the spontaneous activity of identified neurons B1 or B4 in the buccal ganglion.

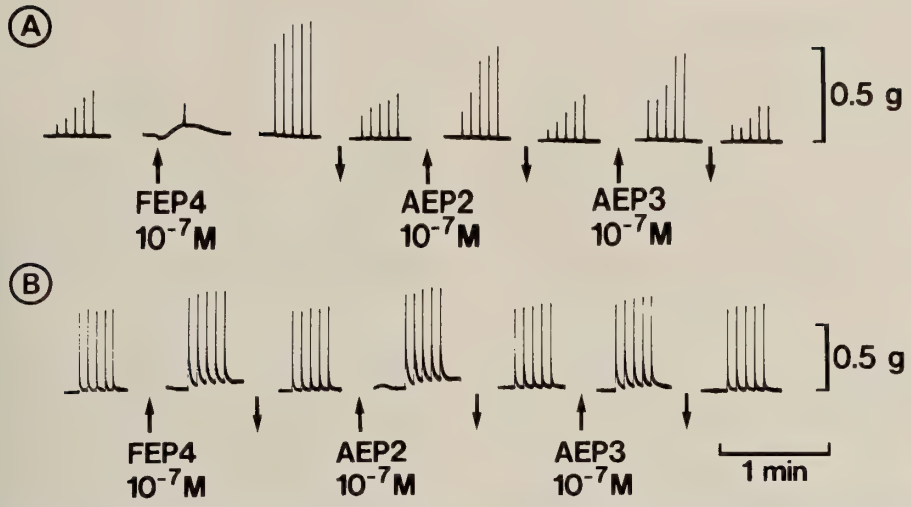

FIG. 7. Effects of three peptides on twitch contractions of the radula protractor muscle (A) and the retractor muscle (B) of *F. ferrugineus*. The muscle was stimulated with a train of electrical pulses (2 msec, 15 V, 0.2 Hz, 5 pulses) at 10 min intervals. Procedures for applying peptides were the same as in Fig. 1.

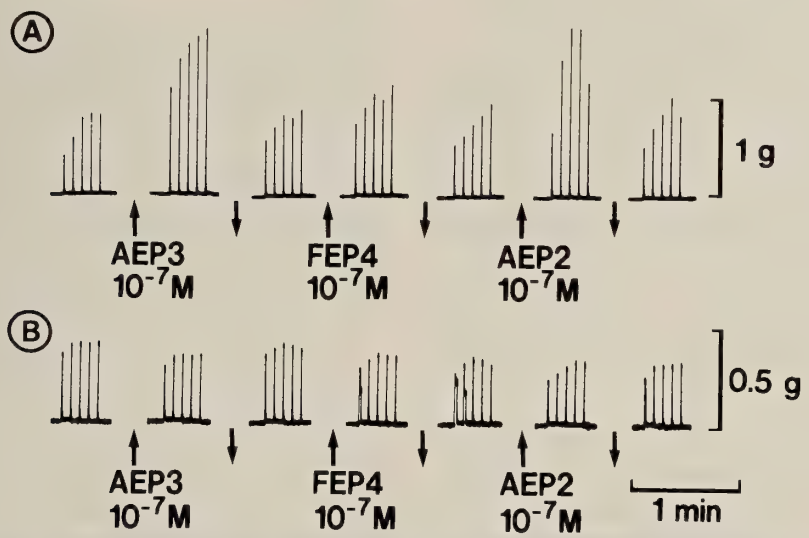

FIG. 8. Effects of three peptides on twitch contractions of the radula protractor muscle (A) and the retractor muscle (B) of *R. thomasiana*. The muscle was stimulated with a train of pulses (1 msec, 15 V, 0.2 Hz, 5 pulses) at 10 min intervals. Procedures for applying peptides were the same as in Fig. 1.

strongly increased twitch contractions of the radula protractor, but they did not show any enhancing effects on the contraction of the retractor. Finally, effects of the peptide AEP3 on the contraction evoked by application of ACh or glutamate were compared between these muscles. In the radula protractor 10^{-7} M AEP3 enhanced ACh-induced contraction prominently, whereas in the retractor it showed no significant effects on ACh-induced as well as glutamate-induced contractions (data not shown).

DISCUSSION

From results obtained in the present experiments the functional mechanisms of myoactive tetradecapeptides (MATPs: AEP2, AEP3 and FEP4) were studied. In the penis retractor muscle of *A. fulica,* the three peptides enhanced the tetanic contraction elicited by nerve stimulations and the order of potency was AEP2>AEP3> FEP4. On the other hand, the enhancing effect of the three peptides on the contraction evoked by muscle stimulations was about the same. These results may well be explained by assuming that actions of the three peptides on the presynaptic sites are different. Molluscan muscles generally receive multiple innervations [2, 11], and it is possible that the three kinds of peptides showed different modulatory actions on the nerve fibers.

In the radula retractor muscle of *A. fulica,* AEP2 enhanced the tetanic contraction in a dose-dependent manner with a threshold concentration as low as 10^{-9} M, suggesting the possibility that this peptide acts physiologically in the regulation of contraction of this muscle. AEP2 also induced rhythmic bursts of activity in the buccal ganglionic neuron B4 which is known as a cholinergic motoneuron of the radula retractor [13]. Furthermore, from the pharmacological examination using propantheline, AEP2 was suggested to act mainly on the cholinergic transmission. Therefore, it is considered that AEP2 regulates contraction of the radula retractor muscle by acting excitatorily on the ganglionic neuron(s) as well as on the muscle.

There are some instances that a kind of peptide regulates the muscle contraction by acting both on the central nervous system and the periphery. Achatin-I isolated from *A. fulica* increased the heart activity by acting excitatorily on the cardio-excitatory neuron PON and on the ventricle of this snail [1]. On the other hand, FMRFamide was shown to act inhibitorily on the central neurons and excitatorily on the myocardium to regulate the heart beat [3].

In the radula muscles of *F. ferrugineus,* on the other hand, FEP4 isolated from this animal showed the most potent activity of the three peptides. FEP4 showed strong enhancing effects on the twitch contraction of the protractor with a threshold concentration of 10^{-10} M, suggesting that FEP4 physiologically regulates the contraction of the radula protractor muscle. It is noteworthy that in *F. ferrugineus* and also in *R. thomasiana* the three peptides showed strong enhancing effects on the contraction of the radula protractor but slight or no effects on the radula retractor. Our previous studies have shown that in the radula protractor of *R. thomasiana* the principal excitatory neurotransmitter is ACh, whereas in the retractor it is glutamate [6, 7, 12]. The same appears to be true in the radula muscles of *F. ferrugineus* (Muneoka, unpublished data). The present results suggest that the three peptides enhanced the contraction of the radula protractor by modulating the transmission mediated by ACh. It is probable that in general MATPs act mainly on the cholinergic transmission in molluscan muscles. Several results obtained in the present experiments appear to support this notion.

We found that the amino acid sequence of a peptide allatotropin purified from the tobacco hornworm *Manduca sexta* [4] is significantly homologous to that of MATPs as shown below.

AEP2	G F R Q D A A S R V A H G Y amide
AEP3	G F R G D A A S R V A H G F amide
FEP4	G F R M N S S N R V A H G F amide
Allatotropin	
	G F K * N V E M M T A R G F amide

Although allatotropin is not a 14-residue peptide but a 13-residue peptide, it shares 36% of residues with AEP3 and 43% with FEP4. Particularly, the N- and C-terminal dipeptide moieties of allatotropin are the same with those of the three molluscan peptides, except the C-terminus of AEP2. Since we have not yet examined the effects of allatotropin on molluscan muscles, the structure-action relationships are not known. However, these results are considered to suggest that MATP-related peptides are distributed not only in molluscs but also in other phyla including arthropods.

ACKNOWLEDGMENTS

This research was supported in part by the Fujisawa Foundation and by Grants-in-Aid for Scientific Research

from The Ministry of Education, Science and Culture of Japan.

REFERENCES

1 Fujimoto K, Kubota I, Yasuda-Kamatani Y, Minakata H, Nomoto K, Yoshida M, Harada A, Muneoka Y, Kobayashi M (1991) Purification of achatin-I from the atria of the African giant snail, *Achatina fulica,* and its possible function. Biochem Biophysic Res Commun 177: 847–853

2 Getting PA (1985) Neural control of behavior in gastropods. In "The Mollusca Vol. 8" Neurobiology and Behavior Part 1. Ed by AOD Willows, Academic Press, New York, pp 269–334

3 Hori K, Furukawa Y, Kobayashi M (1990) Regulatory actions of 5-hydroxytryptamine and some neuropeptides on the heart of the African giant snail, *Achatina fulica* Férussac. Zool Sci 7: 377–384

4 Kataoka H, Toschi A, Li JP, Carney RL, Schooley DA, Kramer SJ (1989) Identification of an allatotropin from adult *Manduca sexta.* Science 243: 1481–1483

5 Kobayashi M, Fujimoto K, Kubota I (1991) Structure and action of novel neuropeptides isolated from a pulmonate, the African giant snail. In "Molluscan Neurobiology" Eds by KS Kits, HH Boer, J Joosse, North-Holland Publishing Company, Amsterdam, pp 260–264

6 Kobayashi M, Muneoka Y (1980) Modulatory action of octopamine and serotonin on the contraction of buccal muscles in *Rapana thomasiana.* I. Enhancement of contraction in radula protractor. Comp Biochem Physiol 65C: 73–79

7 Muneoka Y, Kobayashi M (1980) Modulatory actions of octopamine and serotonin on the contraction of buccal muscles in *Rapana thomasiana.* II. Inhibition of contraction in radula retractor. Comp Biochem Physiol 65C: 81–86

8 Muneoka Y, Kobayashi M (1992) Comparative aspects of structure and action of molluscan neuropeptides. Experientia 48: 448–456

9 Muneoka Y, Twarog BM (1977) Lanthanum block of contraction and of relaxation in response to serotonin and dopamine in molluscan catch muscle. J Pharmacol Exp Therap 202: 601–609

10 Ohta N, Kanda T, Kuroki Y, Kubota I, Muneoka Y, Kobayashi M (1990) Three novel tetradecapeptides isolated from the ganglia of the molluscs, *Achatina fulica* and *Fusinus ferrugineus.* In "Peptide Chemistry 1989" Ed by N Yanaihara, Protein Research Foundation, Osaka, pp 57–62

11 Walker RJ (1986) Transmitters and modulators. In "The Mollusca Vol. 9" Neurobiology and Behavior Part 2. Ed by AOD Willows, Academic Press, New York, pp 279–485

12 Yanagawa M, Takabatake I, Muneoka Y, Kobayashi M (1987) Further pharmacological study on the cholinergic and glutaminergic properties of the radula muscles of a mollusc, *Rapana thomasiana.* Comp Biochem Physiol 88C: 301–306

13 Yoshida M, Kobayashi M (1991) Neural control of the buccal muscle movement in the African giant snail *Achatina fulica.* J exp Biol 155: 415–433

14 Yoshida M, Kobayashi M (1992) Cerebral and buccal neurons involved in buccal motor pattern generation in *Achatina fulica.* Acta Biol Hung 43: 361–367

ZOOLOGICAL SCIENCE 10: 267–273 (1993)

Effects of Proteolytic Digestion on the Control Mechanism of Ciliary Orientation in Ciliated Sheets from *Paramecium*

Munenori Noguchi[1], Ken-ichi Okamoto[2]
and Shogo Nakamura

Department of Biology, Faculty of Science, Toyama University, Toyama 930, Japan

ABSTRACT—Effects of proteolytic digestion on the ciliary response to Ca^{2+} and cyclic nucleotides in ciliated cortical sheets from *Paramecium* were examined. Ciliary orientation toward 5 o'clock (with the anterior of the cell defined as 12 o'clock) in response not only to lowering Ca^{2+} concentration, but also to raising cyclic nucleotides concentrations, was lost by trypsin digestion. Differential sensitivity of cilia, depending on the location of the cell surface to cyclic nucleotides, was also lost by trypsin digestion. The cilia reoriented toward 12 o'clock, which was the ciliary orientation in response to Ca^{2+} above 1 μM before trypsin digestion. Ciliary axonemes lost a large number of outer dynein arms after trypsin digestion. This suggests that the outer dynein arm may contribute to controlling the ciliary beating direction in response to intracellular Ca^{2+} and cyclic nucleotides.

INTRODUCTION

The locomotor behavior of *Paramecium* depends on the ciliary beating direction which is controlled by intracellular Ca^{2+} concentration [3, 7–9] and presumably by cyclic nucleotides concentration [1, 4, 6, 11]. We observed the top view of ciliary orientation controlled by Ca^{2+} and cyclic nucleotides in ciliated cortical sheets from demembranated cell model of *Paramecium*, and found that cyclic nucleotides competed with Ca^{2+} in determining the ciliary orientation [14]. Also, it was revealed that the ciliary sensitivity to cyclic nucleotides depended on the location of the cell surface [14].

We reported that both the change of ciliary orientation and the stable position in response to lowering the Ca^{2+} concentration disappeared by trypsin digestion using Triton-glycerol-extracted *Paramecium* [13]. This seemed to occur as a result of selective digestion of the Ca^{2+}-dependent controlling mechanism of ciliary beating. It is important to examine the changes that proteolytic digestion induces in ciliary orientation on the cortial sheets of *Paramecium*, and the structural changes in ciliary axonemes after proteolytic digestion.

We report here observations of ciliary orientations on cortical sheets of Triton-glycerol-extracted *Paramecium* undergoing proteolytic digestion. Tryptic digestion removed the cyclic nucleotide sensitivity, as well as Ca^{2+} sensitivity, in the ciliary reorientation response on the cortical sheets. After trypsin digestion, the cilia pointed toward 12 o'clock irrespective of cyclic nucleotides and Ca^{2+} concentrations. Electron micrographs showed that a large number of outer dynein arms disappeared after trypsin digestion. The results suggest that the mechanism which controls ciliary orientation, depending on intracellular Ca^{2+} and cyclic nuceotides, may be closely related to the outer dynein arms.

Accepted December 10, 1992
Received August 31, 1992
[1] To whom correspondence should be addressed.
[2] Present address: Department of Biophysical Engineering, Faculty of Engineering Science, Osaka University, Osaka 560, Japan

MATERIALS AND METHODS

Paramecium caudatum (stock G3) was cultured in a hay infusion. Cells were grown to late-logarithmic phase at 25°C.

Preparation of ciliated sheets of permeabilized

cells and reactivation of cilia were essentially the same as the preceding paper [14]. Concentrated and washed cells were extracted with an extraction medium containing 0.1% Triton X-100, 20 mM KCl, 10 mM EDTA and 10 mM Tris-maleate buffer (pH 7.0) for 5 min in an ice bath. The extracted specimens were then washed three times with an ice-cold washing medium which consisted of 50 mM KCl, 2 mM EDTA and 10 mM Tris-maleate buffer (pH 7.0). At that time they were pipetted several times through a glass pipette with a small inside tip diameter to tear or to give a nick to the cell cortex. Then the models were suspended and equilibrated in an ice-cold glycerol-KCl solution which consisted of 30% glycerol, 50 mM KCl and 10 mM Tris-maleate buffer (pH 7.0) prior to experimentation.

A simple perfusion chamber was prepared by placing the sample between a slide and a coverslip. The slide and the coverslip were separated by a thin layer of vaseline applied to two opposite edges of the coveslip. To observe the reactivation of cilia on the sheet of cell cortex, 20 μl of the sample was placed on a slide glass, and a coverslip with vaseline was placed gently on the sample. Solutions were then perfused through the narrow opening at one of the edges of the coverslip while the excess fluid was drained from the opposite end with small pieces of filter paper. During the first perfusion using a reference glycerol-KCl solution, some torn cell cortex adhered flat to the glass surface. The cortical sheets were then perfused successively with reactivation solutions. All the reactivation solutions contained 1 mM ATP, 1 mM $MgCl_2$, 30% glycerol, 50 mM KCl and 10 mM Tris-maleate bufer (pH 7.0) as well as the component(s) noted in the results. Free Ca^{2+} concentration in the reactivation solution was controlled by a Ca-EGTA bufer with 1 mM EGTA [12, 15]. The reactivation was carried out at 22–25°C. The movements of the cilia were observed under a dark field microscope, equipped with a 100 W mercury light source, a heat filter and a green filter, and recorded on video tape using a National WV-1550 TV camera. Pointing directions of cilia which were observed from above were indicated by using a clock face with a definition of the anterior end of the cells as 12 o'clock. The anterioposterior axis of cortical sheets were determined by anterioposterior lines of cilia. Ciliary orientation of cilia were measured as angles to an anerioposterior axis and then converted to an analogue clock face expression using each cilium on the cell surface except for the oral groove. With the definition that the surface area of the anatomical left-hand side is the left-hand field of the cortical sheets, we used the cilia on the left third and the right third for measuring the ciliary orientation of the left-hand field and the right-hand field, respectivley. In the measurement of ciliary orientation after trypsin digestion, we used the cilia on both the left- and right-hand field.

Prepared Triton-glycerol-extracted whole cell models were suspended in a reactivation solution containing 100 μg/ml trypsin (from bovine pancreas, Boehringer, 110 units/mg) or elastase (from porcine pancreas, Sigma type IV, 120 units/mg) in a test tube to make the cellular protein concentration approximately 1 mg/ml. A minute amount of the suspension was placed on a slide glass and the ciliary response to digestion was observed under the dark field microscope. Five minutes after mixing, soybean trypsin inhibitor was added to make the final concentration of 1.0 mg/ml. The samples were fixed with 2% glutaraldehyde in 50 mM sodium cacodylate (pH 7.4) for 1 hr then post-fixed for 1 hr with 1% OsO_4 in the same buffer. They were dehydrated in an ascending series of ethanol to 100% and embedded in epoxy resin following the method of Nakamura [10]. Sections were cut on a Porter-Blum MT-1 ultramicrotome and were stained with uranyl acetate and Reynold's lead citrate. A JEOL 100C electron microscope was used for the observations.

RESULTS

The cilia on the cortical sheets reoriented toward 12 o'clock after trypsin digestion irrespective of Ca^{2+} concentration (Fig. 1). When the Ca^{2+} concentration was low enough to produce ciliary orientation toward 5 o'clock, which corresponded to normal ciliary beat, and consequent forward swimming [14], almost quiescent cilia pointing 5 o'clock began to rotate counterclockwise within a minute after perfusing a reactivation

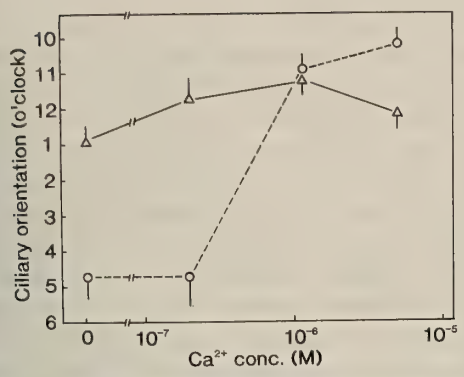

FIG. 1. Ciliary orientation in response to Ca^{2+} concentration after trypsin digestion. Circles and broken lines indicate the ciliary orientations before trypsin digestion. Triangles and solid lines indicate ciliary orientations 3–5 minutes after trypsin digestion. Ciliary orientation measured as angles to an anterioposterior axis and then converted to an analogue clock face expression as indicated in the ordinate. Measurements were performed about cilia on the dorsal area. The data was obtained from four individual preparations. The bars indicate standard deviations.

solution containing 100 μg/ml trypsin. Finally the cilia pointed toward 12 o'clock and stopped within a few minutes (Fig. 1). When the Ca^{2+} concentration was above 10^{-6} M, cilia which oriented toward 10–12 o'clock moving counterclockwise in a circular pattern stopped moving and finally pointed toward 12 o'clock within a few minutes after the perfusion of reactivation solution containing 100 μg/ml trypsin (Fig. 1).

As reported in the preceding paper [8], cAMP induces ciliary orientation toward 5 o'clock and cGMP induces ciliary orientation toward 3 o'clock, even in the presence of Ca^{2+} above 10^{-6} M which induces ciliary orientation toward 11–12 o'clock if cyclic nucleotides are not present. The cilia on the left-hand field of the cell are more sensitive to cyclic nucleotides than those on the right-hand field with the definition that the surface area of the anatomical left-hand side is the left-hand field of the cortical sheets. As shown in Figures 2 and 3, after perfusing a reactivation solution containing 100 μg/ml trypsin, the cilia oriented uniformly toward 12 o'clock irrespective of cyclic nucleotide concentrations and location of the cilia on the cell surface. Also in the presence of cyclic nucleotides without Ca^{2+}, trypsin digestion induces the ciliary orientation toward 12 o'clock (data not shown). Differential response of cilia to cyclic nucleotides in the left- and right-hand field of the cells disappeared by trypsin digestion (middle part of Figs. 2 and 3, and Fig. 4). Elastase which was thought to digest nexin [2], and V8 protease which produced a proteolytic effect different from trypsin on the 21S dynein from sea urchin sperm flagella [5], never produced such a change in ciliary orientation that was found to be induced by trypsin digestion in all cases previously described at concentrations of 100 μg/ml.

The cahnge of ciliary orientation after trypsin digestion in the absence of ATP was also tested to examine whether the changes of ciliary orientation by trypsin digestion were induced by active sliding or induced passively by structural changes of some

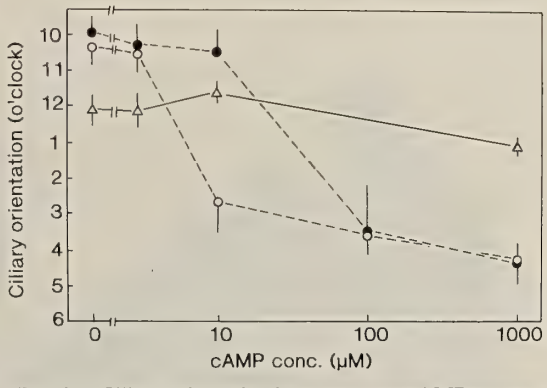

FIG. 2. Ciliary orientation in response to cAMP concentration after trypsin digestion. Ca^{2+} concentration is 5 μM throughout. Circles and broken lines indicate ciliary orientations before trypsin digestion. Open circles and closed circles indicate the ciliary orientations in the left-hand field and in the right-hand field, respectively. Triangles and solid lines indicate the ciliary orientations 3–5 minutes after trypsin digestion. Ciliary orientation of cilia were measured as angles to an anterioposterior axis and then converted to an analogue clock face expression as indicated in the ordinate. In the measurement of ciliary orientation before trypsin digestion, we used the left third and the right third of each cilium for measuring the ciliary orientation of the left-hand field and the right-hand field, respectively. In the measurement of ciliary orientation after trypsin digestion, we used the cilia on both the left- and right-hand field. The data was obtained from five individual preparations. The bars indicate standard deviations.

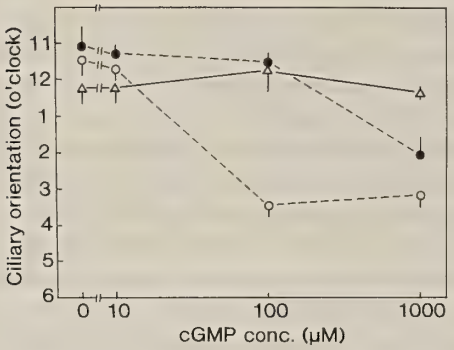

FIG. 3. Ciliary orientation in response to cGMP concentration after trypsin digestion. Ca^{2+} concentration is 1.8 μM throughout. Circles and broken lines indicate ciliary orientations before trypsin digestion. Open circles and closed circles indicate the ciliary orientations in the left-hand field and in the right-hand field, respectively. Triangles and solid lines indicate the ciliary orientations 3–5 minutes after trypsin digestion. Measurements of ciliary orientation were performed as explained in the legend of Figure 2. The data was obtained from four individual preparations. The bars indicate standard deviations.

axonemal components. As shown in Figure 5, the change of ciliary orientation from 5 to 12 o'clock induced by trypsin digestion required ATP. When the ciliated sheets were perfused with a reactivation solution containing EGTA to keep Ca^{2+} concentration under 10^{-7} M, the cilia pointed toward 5 o'clock (Fig. 5a). Following successive perfusions with a solution without ATP and a solution containing trypsin without ATP did not affect the ciliary orientation toward 5 o'clock. Eighty seconds after the trypsin perfusion, a solution containing a trypsin inhibitor without ATP was perfused. Then the reactivation solution con-

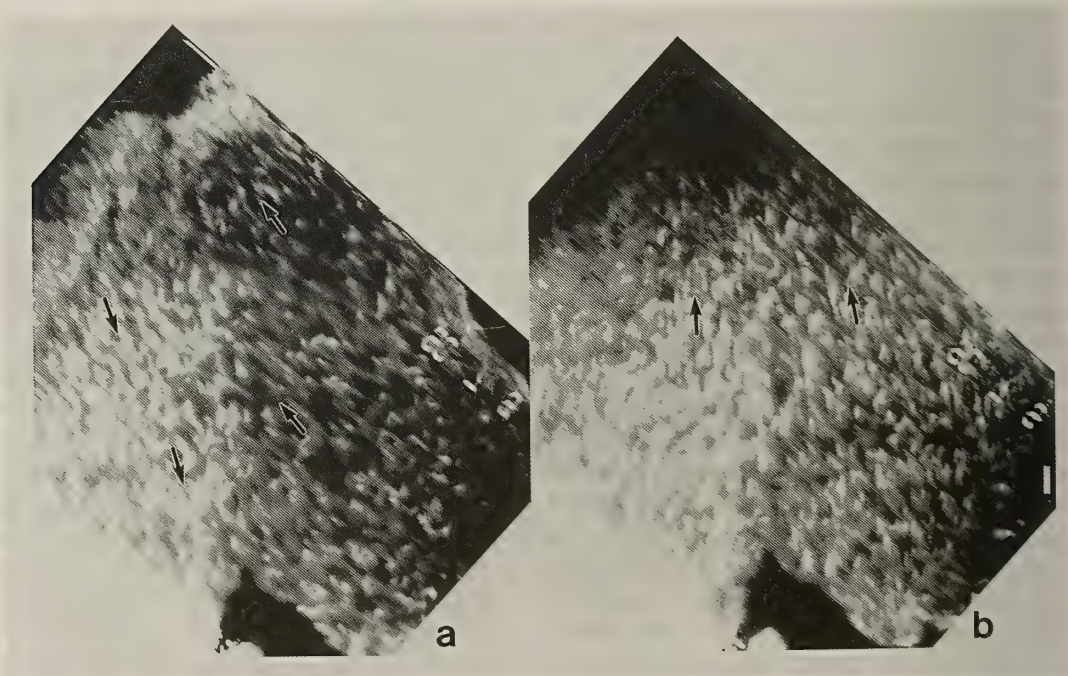

FIG. 4. Ciliary orientations before and after trypsin digestion. The photograph shows a dorsal view of the ciliated sheet. The cortex of a cell model tore along an oral groove. The top of each photograph is the anterior direction of the cell. The sheet was perfused successively with reactivation solutions containing 10 μM cAMP and 5 μM Ca^{2+} (a), and 100 μg/ml trypsin as well as 10 μM cAMP and 5 μM Ca^{2+} (b). Arrows indicate the pointing directions of cilia. Pointing direction of cilia on the left-hand field differed from that on the right-hand field in (a). In (a), as indicated by arrows, ciliary orientation on the left hand field was 5 o'lock, and on the right-hand field was 11 o'clock. On the other hand, ciliary orientation was 12 o'clock uniformly in the whole area of the cortical sheet after trypsin digestion (b). Bar, 10 μm.

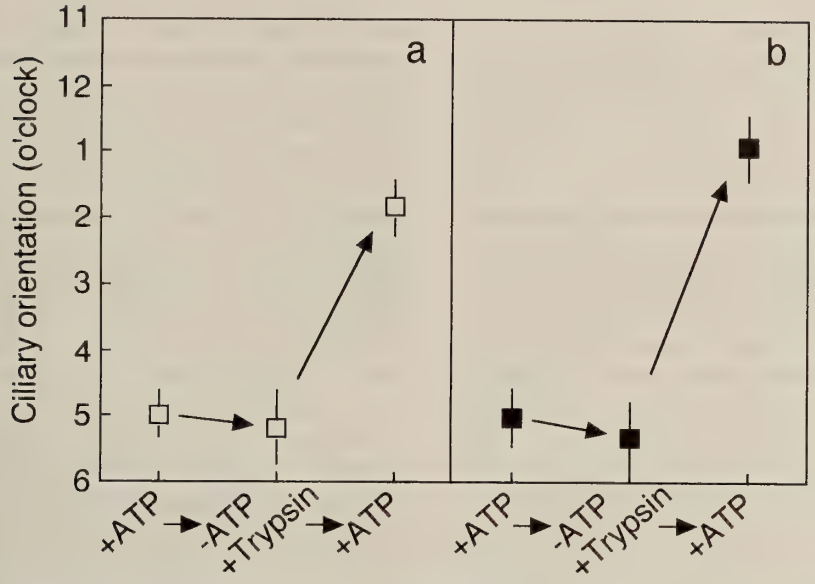

FIG. 5. The effect of trypsin digestion on the ciliary orientation in the absence of ATP. Cortical sheets were perfused successively with solutions fundamentally contained 1 mM $MgCl_2$, 30% glycerol, 50 mM KCl, Tris-maleate buffer (pH 7.0) as well as 1 mM EGTA (a) or 1 μM Ca^{2+} + 100 μM cAMP (b). +ATP indicated under abscissa means the solution contained 1 mM ATP. Trypsin concentration was 50 μg/ml. Cortical sheets were first perfused with solutions containing ATP. In both cases, ciliary orientations on the cortical sheets were not changed by subsequent trypsin digestion in the absence of ATP. After stopping the digestion by the addition of trypsin inhibitor, the solution containing ATP was perfused. The perfusion elicited the change of ciliary orientation from 5 toward 12 o'clock. Trypsin digestion time was 80 sec in (a) and 20 sec in (b). The data presented is a typical example of one of the many series of successive perfusions examined. The bars indicate standard deviations.

taining ATP was perfused. Immediately after the perfusion, the cilia changed their orientation from 5 o'clock to 12 o'clock and never returned toward 5 o'clock. The ciliary orientation toward 5 o'clock induced by cAMP also did not change the orientation by trypsin digestion in the absence of ATP (Fig. 5b). Thus, the change of ciliary orientation from 5 to 12 o'clock after trypsin digestion required ATP, and the trypsin digestion removed the ability to change and to keep the ciliary orientation toward 5 o'clock either in response to cyclic nucleotides or to lowering Ca^{2+} concentration.

We examined the effects of trypsin digestion on the axonemal structures by electron microscopy. The structure which underwent serious break down by trypsin digestion was outer dynein arms

FIG. 6. Cross-sections of the Triton-glycerol-extracted ciliary axonemes before proteolytic digestion (a) and after digestion by 100 μg/ml trypsin (b) and by 100 μg/ml elastase (c). bar, 100 nm.

(Fig. 6b). On the contrary, axonemes treated by elastase in the same condition as that of trypsin digestion kept their outer dynein arms (Fig. 6c).

DISCUSSION

Ciliary orientation on the cortical sheets corresponds to the ditection of the effective stroke of cilia [14]. The ciliary orientation toward 5 o'clock and 12 o'clock correspond to normal beating of cilia and ciliary reversal, respectively. The direction of the effective power stroke is essentially controlled by intracelular Ca^{2+} concentration [3, 7–9]. However, as we reported previously, "ciliary reversal" was induced by trypsin digestion [13] in Triton-glycerol-extracted whole cell model of *Paramecium* even if Ca^{2+} concentration was low enough to produce normal beating. In this paper, we confirmed that the ciliary orientation induced by trypsin digestion was in actual fact 12 o'clock using cortical sheets of Triton-glycerol-extracted *Paramecium* (Fig. 1). This indicates that the Ca^{2+}-dependent controlling mechanism of ciliary beating direction is digested at least in part by trypsin. The part affected by trypsin may be the component which is responsible for switching off the ciliary reversal mechanism when Ca^{2+} concentration is lowered.

The beating direction of cilia is also modulated by cyclic nucleotides [1, 6, 11, 14]. In the cortical sheets, ciliary orientation is controlled by cyclic nucleotides in the competing mode with Ca^{2+}. The cilia on the left-hand field of the cell surface were more sensitive to cyclic nucleotides than those on the right-hand field [14]. Tryptic digestion removed all these ciliary responses to cyclic nucleotides. As indicated in Figures 2–4, ciliary orientations towad 3–5 o'clock in response to cyclic nucleotides together with the differential sensitivity disappeared by trypsin digestion. This indicates that trypsin digestion destroys the component responsible for cyclic nucleotides dependent responses, as well as the Ca^{2+}-dependent component in the controlling mechanism of ciliary beating direction.

Ciliary orientation toward 5 o'clock, induced in the conditions in which Ca^{2+} concentration was low enough, or cAMP concentration was high enough to suppress the Ca^{2+} effect, remained the same after perfusing the solution without ATP. Subsequent perfusions with a solution containing trypsin without ATP, did not induce any change in ciliary orientation. However, the change of ciliary orientation from 5 to 12 o'clock was elicited by the addition of ATP (Fig. 5). This indicates that the change of ciliary orientation induced by trypsin digestion requires ATP and suggests that the change of ciliary orientation requires dynein-microtubul interaction at least to some extent. Thus, the trypsin digestion induced the inabilities to keep the ciliary orientation toward 5 o'clock and to change the ciliary orientation from 12 to 5 o'clock in response to either lowering Ca^{2+} concentration or to cyclic nucleotides.

It has been clarified that ciliary beating is controlled by Ca^{2+} [3, 7–9, 14] and cyclic nucleotides [1, 6, 11, 14]. However, the molecular mechanisms which transmit the signal of the second messengers to dynein-microtubule interaction as a motor system, as well as its localization and structural bases are scarcely known. After trypsin digestion, outer dynein arms disappeared conspicuously in ciliary axonemes (Fig. 6). On the contrary, outer dynein arms remained intact in the axonemes after the digestion by elastase which affected neither Ca^{2+} nor the cyclic nucleotides dependent mechanism as stated previously, whereas axonemes which detached from cell cortex and attached to the glass surface of the perfusion chamber exhibited sliding disintegration within a minute not only by trypsin but also by elastase. Trypsin has been used to produce limited digestion of isolated dynein [5], but how the trypsin affect outer dynein arms within axonemes is not yet known. Although we could not known the exact protein ratio of trypsin to ciliated sheets in perfusion chambers, high concentration of trypsin (above 20 μg/ml) was required to induce the ciliary response by trypsin digestion. This might imply that the quick attack by trypsin on the outside of axonemes is essential to remove selectively the Ca^{2+}-dependent and cyclic nucleotides-dependent controlling mechanism of ciliary orientation. The disappearance of the outer arms after tyrpsin digestion might suggests that outer dynein arms play a key role in Ca^{2+}-dependent

and also in the cyclic nucleotides dependent controlling mechanism of ciliary beating direction in *Paramecium*.

ACKNOWLEDGMENTS

This work was supported in part by a Grant-in-Aid from the Ministry of Education, Science and Culture of Japan. We thank Mr. Takehiko Taneyama and Takumi Shimura for technical assistance. We also thank Miss Sandy Peever and Mercedes Zanon for reading the manuscript.

REFERENCES

1 Bonini NM, Nelson DL (1988) Differential regulation of *Paramecium* ciliary motility by cAMP and cGMP. J Cell Biol 106: 1615–1623

2 Brokaw CJ (1980) Elastase digestion of demembranated sperm flagella. Science 207: 1365–1367

3 Eckert R, Naitoh Y, Machemer H (1976) Calcium in the bioelectric and motor functions of *Paramecium*. Symp Soc Exp Biol 30: 233–255

4 Hamasaki T, Barkalow K, Richmond J, Satir P (1991) cAMP-stimulated phosphorylation of an axonemal polypeptide that copurifies with the 22S dynein arm regulates microtubule translocation velocity and swimming speed in *Paramecium*. Proc Natl Acad Sci USA 88: 7918–7922

5 Inaba K, Mohri H (1989) Dynamic conformational changes of 21S dynein ATPase coupled with ATP hydrolysis revealed by proteolytic digestion. J Biol Chem 264: 8384–8388

6 Majima T, Hamasaki T, Arai T (1986) Increase in cellular cyclic GMP level by potassium stimulation and its relation to ciliary orientation in *Paramecium*. Experientia 42: 62–64

7 Naitoh Y, Kaneko H (1972) Reactivated Triton-extracted models of *Paramecium:* modification of ciliary movement by calcium ions. Science 176: 523–524

8 Naitoh Y, Kaneko H (1973) Control of ciliary activities by adenosinetriphosphate and divalent cations in Triton-extracted models of *Paramecium caudatum*. J Exp Biol 58: 657–676

9 Naitoh Y, Sugino K (1984) Ciliary movement and its control in *Paramecium*. J Protozool 31: 31–40

10 Nakamura S (1981) Two different backward-swimming mutants of *Chlamydomonas reinhardtii*. Cell Struct Funct 6: 385–393

11 Nakaoka Y, Ooi H (1985) Regulation of ciliary reversal in Triton-extracted *Paramecium* by calcium and cyclic adenosine monophosphate. J Cell Sci 77: 185–195

12 Noguchi M, Inoué H, Kubo K (1986) Control of the orientation of cilia by ATP and divalent cations in Triton-glycerol-extracted *Paramecium caudatum*. J Exp Biol 120: 105–117

13 Noguchi M (1987) Ciliary reorientation induced by trypsin digestion in Triton-glycerol-extracted *Paramecium caudatum*. Cell Struct Funct 12: 503–506

14 Noguchi M, Nakamura Y, Okamoto K (1991) Control of ciliary orientation in ciliated sheets from *Paramecium*—Differential distribution of sensitivity to cyclic nucleotides. Cell Motil Cytoskeleton 20: 38–46

15 Portzehl H, Caldwell PC, Rüegg JC (1964) The dependence of contraction and relaxation of muscle fibers from the crab *Maia squinado* on the internal concentration of free calcium ions. Biochim Biophys Acta 79: 581–591

ZOOLOGICAL SCIENCE 10: 275–279 (1993)

The Nucleotide Content of the Octopus Photoreceptor Cells: No Changes in the Octopus Retina Immediately Following an Intense Light Flash

Masatsugu Seidou[1], Kohzoh Ohtsu[2], Zinpei Yamasita[3], Kinya Narita[4] and Yuji Kito[4]

[1]*Aichi Prefectural University of Fine Arts, Nagakute, Aichi 480-11,* [2] *Ushimado Marine Laboratory, Okayama University, Ushimado Oku, Okayama 701-43,* [3]*Isotope Research Center, Osaka University, Suita, Osaka 565,* [4]*Department of Biology, Faculty of Science, Osaka University, Toyonaka, Osaka 560, Japan*

ABSTRACT—The amounts of cyclic-guanosine monophosphate (cGMP) and cyclic-adenosine monophosphate (cAMP) in octopus retina were measured by competitive radioimmunoassay. The amounts of the respective di- and tri-phosphonucleotides, and of visual pigment (as retinal isomers), were determined by high-performance-liquid chromatography (HPLC). Unirradiated octopus retina contained 2.4 ± 0.5 pmol of cGMP and 36 ± 7.0 pmol of cAMP. When 27.6% of the visual pigment in the retina was converted into the meta-form by an intense light flash, the rapidly-frozen retina contained 2.3 ± 0.9 pmol of cGMP and 32 ± 4.0 pmol of cAMP: no significant changes from the unirradiated state. The molecular ratios of cGMP and cAMP to total visual pigment were estimated to be 1/1800 and 1/120, respectively. Assuming that all the cGMP and cAMP were contained only in the rhabdome, it was estimated that there are 1.6 molecules of cGMP and 24 molecules of cAMP per microvillus. The low content of cGMP in the microvillus and the absence of significant change in cGMP content on exposure to light lead us to conclude that cGMP is not the 'intracellular messenger' of phototransduction in octopus photoreceptor cells.

INTRODUCTION

It is known than, in the rhabdomeric photoreceptor cells of cephalopods and arthropods, the cation channels in the plasma membrane are opened by light stimulation, resulting in depolarization of the photoreceptor cell [17]. However, details of the events between photoisomerization of rhodopsin and channel opening are unknown. Cyclic-GMP (cGMP) [12, 15] and inositol trisphosphate (IP_3) [3, 4, 8, 19] are possible candidates for the intracellular messenger, and it is well established that cGMP fulfils this role in vertebrate rod cells [9, 13].

In the ventral photoreceptor cell of *Limulus*, injection of solutions containing cGMP or cAMP does not increase the influx of Na^+ ions [16], but cGMP can depolarize the cell in a similar manner to light stimulation [12]. In the squid retina, it has been reported that (i) light increases the activity of guanylate cyclase [15], and (ii) according to Johnson *et al.* [12], the amount of cGMP in the light-irradiated retina of *Loligo pealei* is up to 1.7 times that in the dark-adapted state. This reported cGMP change in the squid retina would probably be enough to open a cGMP-gated cation channel (cf. the light-stimulated decrease in cGMP to 80 % of that of dark-adapted rods in the frog, *Rana catesbiana,* retina [6]). However, Brown *et al.* [2] reported that light induced no significant changes in the cGMP content of the photoreceptor cells of the squids *Loligo pealei* and *L. opalescens.*

We consider that Johnson's data did not provide sufficient evidence to support the candidacy of cGMP as an intracellular messenger of phototrans-

Accepted January 25, 1993
Received September 9, 1992

duction in cephalopods, and also that Brown's data did not reject a role for cGMP, because both studies were unable to express the content of cGMP as a proportion of the initial content of a single microvillus. In the present study, we compare the amounts of cGMP, cAMP, and their di- and tri-phosphorylated derivatives in octopus retina, before and after light irradiation. Visual pigment content (proportional to the number of microvilli) was determined by HPLC analysis of the chromophore retinal, which was used as an internal standard to normalize the size of the retina and the nucleotide content for each experiment. The cephalopod retina is composed almost entirely of photoreceptor cells (and their axons), which are assumed to be the site of most of the cGMP and cAMP measured in whole retina.

MATERIALS AND METHODS

Small octopuses (30–100 g adult *Octopus fangsiao* d'Orbigny;=*O. ocellatus* Gray [10]), were collected near the Ushimado Marine Laboratory. The animals were kept in the dark for more than 24 hours prior to dissection. All procedures were carried out under infrared light using the noctovision equipment (NEC, Tokyo, Japan). 'Eye-cups' were prepared from enucleated eyes (attached fragments of optic lobe and white body were carefully removed) and the retina was incised radially, flattened sclera-down on filter paper, and mounted on a polystyrene block. The retina was irradiated with white light from an electronic flash unit (5 cm from the retina; 2.5 ms duration, Sunpak Co. Ltd., Tokyo, Japan) and rapidly (within 300 ms) frozen by slamming it against a copper block previously cooled in liquid nitrogen. The frozen retinae with scleral materials were kept below −80°C. Subsequent procedures were carried out under dim red light. Each frozen retina was homogenized in 1.5 ml of ice-cold 6% trichloroacetic acid (TCA) on ice, and centrifuged at 12000 rpm for 30 min. Homogenization and extraction were repeated twice (When a known amount of cGMP was added to an octopus retina, 89.7% of the added amount was recovered by the first extraction). The precipitate was retained for chromophore extraction (see below). The pooled supernatants were washed 3 times with 10 ml diethylether to remove TCA, freeze-dried and dissolved in 2 ml distilled water. A 100 μl of this solution was succinylated and cGMP and cAMP contents were measured by radioimmunoassay (according to the instructions provided with commercial kits; Yamasa Shoyu Co. Ltd., Chiba, Japan).

The amounts of GTP, ATP and ADP were determined by HPLC analysis of the remaining solution, using a SUMIPAX ODS column (6×150 mm, Sumitomo Chem. Co. Ltd., Tokyo, Japan) with a solvent system of 22.5% (v/v) methanol, 4 mM tetra-butyl-ammonium phosphate and 15.5 mM potassium phosphate (pH 5.6) at 30°C. The flow rate was 0.5 ml/min for initial 30 min after sample injection and then 1.0 ml/min. Absorbance at 260 nm was monitored and the amount of each nucleotide estimated using respective molecular extinction coefficients at this wavelength [1].

Visual pigment chromophore was extracted into hexane [11, 18] from the TCA precipitate, applied to a YMC silica gel column (6×150 mm, YMC Co. Ltd., Japan) and eluted with a solvent system of 10% (v/v) ethylacetate and 0.4% (v/v) ethanol in hexane, at a flow rate of 1 ml/min, monitoring absorbance at 360 nm.

The late receptor potential (LRP) of the octopus retina was measured as described in a previous paper [14], with the retina set in an experimental chamber perfused with aerated sea water.

RESULTS AND DISCUSSION

Table 1 shows the amounts of nucleotides and retinal in the octopus retina. The octopus retina

TABLE 1. Contents of chromophore retinal and nucleotides in one retina ($\times 10^{-9}$ mol)

	dark (n=4)	light (n=5)
retinal	4.4±0.7	4.2±0.4
cGMP	0.0024±0.0005	0.0023±0.0009
cAMP	0.036±0.007	0.032±0.004
GTP	11±3	11±4
ATP	17±8	17±6
ADP	4.0±1.3	5.8±1.7

used in this experiment contained about 4 nmol of retinal. The 27.6 % of 11-*cis* retinal was photoisomerized to all-*trans* form by the flash. Significant differences in the amounts of cGMP, cAMP, GTP, ATP and ADP were not found between the irradiated retina and the unirradiated one. It seemed unlikely that the amounts of the nucleotides in the irradiated retina returned to the level in the unirradiated retina before freezing the retina, because the magnitude of the (negative-going) LRP sustained 81.4% of its maximum even at 500 ms after the flash, as shown in Figure 1.

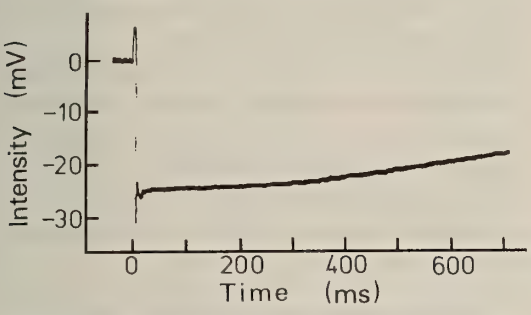

FIG. 1. The late receptor potential of the octopus retina. Flash intensity was attenuated to half that for the determination of cGMP content. The vitreous-side positive signal is upward. The downward spike-shaped signal at zero time is an electrical stimulus artifact.

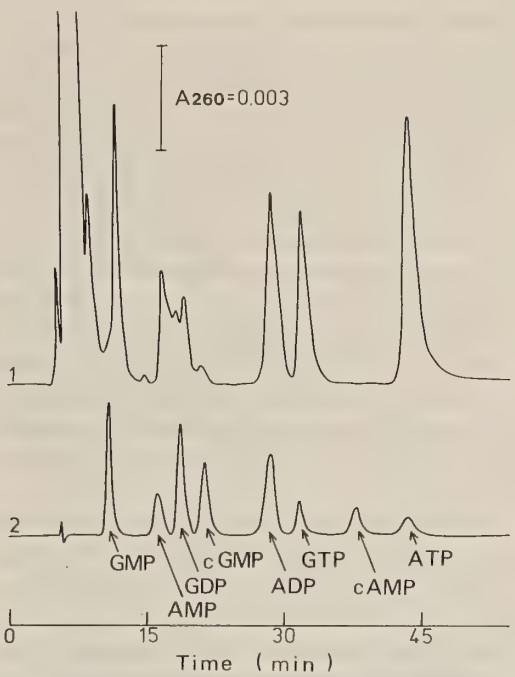

FIG. 2. HPLC analysis of nucleotides in the octopus retina. Trace 1 is a chromatogram of the TCA extract from an octopus retina. Trace 2 is a mixture of the authentic compounds. Flow rate was 0.5 ml/min for first 30 min, then 1 ml/min. A_{260}, absorbance at 260 nm. Other abbreviations as given in Table 1.

Since the ratio of GTP to cGMP was 4600:1 and that of ATP to cAMP 470:1, there were ample amounts of both GTP and ATP in the retina as source materials for both cGMP and cAMP to be produced. The amounts of AMP, GMP and GDP could not be determined accurately due to contamination in the TCA extract, which had some absorbance at the monitoring wavelength 260 nm, as shown in Figure 2.

It has been considered that cGMP may be the intracellular messenger of phototransduction in invertebrate photoreceptor cells as well as in vertebrate rod cells. This was supported by the findings of GTP-binding protein (G-protein), phosphodiesterase and guanylate cyclase in cephalopod photoreceptor cells [5, 7, 20], and by the fact that cGMP injection into the *Limulus* ventral photoreceptor cell could induce a response in a similar manner to the light response [12]. However, our results demonstrated that the amount of cGMP in the octopus retina was not significantly changed by the flash, in agreement with Brown *et al.* [2]. Inability to detect a change in cGMP content is not in itself proof that cGMP is not the intracellular messenger of phototransduction: it is possible that light-induced variation of cGMP occurred but was masked by processes independent of phototransduction. However, this possibility is discounted as follows.

Assuming that all cGMP molecules were localized only in microvilli, the number of cGMP molecules in one microvillus was estimated as follows. The dimensions of *Octopus fangsiao* photoreceptor cells and microvilli were estimated from electron micrographs taken by Prof. M. Yamamoto (Ushimado Marine Laboratory). On average, each photoreceptor cell has a cross-sectional area of $3.9 \times 10\ \mu m^2$. From inspection of

longitudinal sections of photoreceptors, each cell with rhabdomeres of length 150 μm has 3.5×10^5 microvilli. The mean area of the retina used in these experiments was 1.0 cm^2: an estimated total 9.1×10^{11} microvilli. Assuming that all the cGMP exists in the microvilli, then there are about 1.6 molecules of cGMP per microvillus. Of course, if it is assumed that most of the cGMP in the microvillus is concerned with other functions within the cell, less than one molecule of cGMP per microvillus would be available to participate in phototransduction. There is therefore no reason to propose that changes in cGMP have gone undetected because of the presence in the retina of large amounts of cGMP independent of phototransduction.

It is considered that the intensity of the flash used in this experiment was sufficient to activate substantial numbers of visual pigment molecules in all the microvilli, by the following reasoning. (1) About 3000 molecules of visual pigment were contained in each of 9.1×10^{11} microvilli. (2) Assuming that visual pigment was uniformly distributed, only in the rhabdomes, and with mean cross-section of 2.2×10 μm^2 and length of 150 μm, the concentration of visual pigment in the rhabdome is estimated to be 0.5 mM. (3) According to Lambert-Beer's law, the intensity of light passing through the 150 μm rhabdome is reduced to 52% of the incident light. Therefore, with the flash irradiation used in the present study, which converts 28% of the total visual pigment to the meta-form, 36% would be converted in the most distal region of the rhabdome and 18% proximally: i.e. phototransduction occurred in all microvilli.

It is estimated that if phototransduction led to an increase or decrease of only one molecule of cGMP per microvillus, the sum of changes in cGMP over the whole retina would be $\pm60\%$. This would be sufficient for detection by the methods used in the present study, but no such changes were detected. This suggests that there is no change in cGMP content during phototransduction in the octopus retina.

Brown *et al.* [2] discussed the magnitude of the light-induced change in cGMP concentration, estimating that if the dissociation constant of the cGMP-gated channels for cGMP is similar to that reported for vertebrate rods, then the minimum cGMP concentration jump sufficient to saturate all the channels in the microvillar membrane would be 25–225 μM. Assuming that all the measured cGMP was distributed only in the outer segments of the octopus photoreceptor cells, the cGMP concentration estimated from the present study was 0.17 μM in the unirradiated retina. This is 150 to 1300 times less than the magnitude of the concentration jump required, and if this jump happened it would be easy to detect by the methods used here. Since no changes were detected, as shown in Table 1, it is concluded that cGMP is not the intracellular messenger of phototransduction in the octopus retina.

The content of cAMP was 15 times more than cGMP in the retina but no significant change was detected in cAMP content (Table 1). Using arguments similar to those used above with regard to cGMP, it is concluded also that cAMP is not an intracellular messenger during phototransduction in this system.

ACKNOWLEDGMENTS

We wish to express our thanks to Prof. M. Yamamoto of Ushimado Marine Laboratory for the use of his unpublished electron micrographs of the photoreceptor of *Octopus fangsiao*, which were used for calculation of the mean size of the photoreceptor cell and microvillus. We thank Dr. Ian Gleadall for critical reading of this manuscript.

REFERENCES

1 Beaven GH, Holiday ER, Johnson EA (1955) Optical properties of nucleic acids and their components. In "The nucleic acids" Ed By E Chargaff and JN Davidson, Academic press, New York, Vol 1, pp 493–553

2 Brown JE, Faddis M, Combs A (1992) Light does not induce an increase in cyclic-GMP content of squid or *Limulus* photoreceptors. Exp Eye Res 54: 403–410

3 Brown JE, Rubin LJ, Ghalayini AJ, Tarver AP, Irvine RF, Berridge MJ, Anderson RE (1984) *myo*-inositol polyphosphate may be a messenger for visual excitation in *Limulus* photoreceptors. Nature, 311: 160–163

4 Brown JE, Watkins DC, Malbon CC (1987) Light-induced changes in the content of inositol phosphates in squid (*Loligo pealei*) retina. Biochem J

247: 293–297

5 Calhoon R, Tsuda M, Ebrey TG (1980) A light-activated GTPase from octopus photoreceptors. Biochem Biophys Res Commun 94: 1452–1457

6 Cote RH, Biernbaum MS, Nicol GD, Bownds MD (1984) Light-induced decreases in cGMP concentration precede changes in membrane permeability in frog rod photoreceptors. J Biol Chem 259: 9635–9641

7 Ebrey T, Tsuda M, Sassenrath G, West JL, Waddell WH (1980) Light activation of bovine rod phosphodiesterase by nonphysiological visual pigments. FEBS lett 116: 217–219

8 Fein A, Payne R, Corson DW, Berridge MJ, Irvine RF (1984) Photoreceptor excitation and adaptation by inositol 1,4,5-trisphosphate. Nature 311: 157–160

9 Fesenko EE, Kolesnikov SS, Lyubarsky AL (1985) Induction by cyclic GMP of cationic conductance in plasma membrane of retinal rod outer segment. Nature 313: 310–313

10 Gleadall IG, Naggs FC (1991) The Asian ocellate octopuses. II. The validity of *Octopus fangsiao* d'Orbigny. Ann Appl Info Sci, Sendai, Japan 16: 173–180

11 Groenendijk GWT, De Grip WJ, Daemen FJM (1980) Quantitative determination of retinals with complete retention of their geometric configuration. Biochim Biophys Acta 617: 430–438

12 Johnson EC, Robinson PR Lisman JE (1986) Cyclic GMP is involved in the excitation of invertebrate photoreceptors. Nature 324: 468–470

13 Miki N, Keirns JJ, Marcus FR, Freeman J, Bitensky MW (1973) Regulation of cyclic nucleotide concentrations in photoreceptors:an ATP-dependent stimulation of cyclic nucleotide phosphodiesterase by light. Proc Nat Acad Sci USA 70: 3820–3824

14 Ohtsu K, Kito Y (1985) A photoproduct with 13-*cis* retinal generated by irradiation with violet light in the octopus retina. Vision Res 25: 775–779

15 Saibil HR (1984) A light-stimulated increase of cyclic GMP in squid photoreceptors. FEBS Lett 168: 213–216

16 Stern JH, Lisman JE (1982) Internal dialysis of *Limulus* ventral photoreceptors. Proc Natl Acad Sci USA 79: 7580–7584

17 Stieve H (1985) Bumps, the elementary excitatory responses of invertebrates. In "The molecular mechanism of photoreception" Ed By H Stieve, Springer-Verlag, Berlin, pp 199–230

18 Suzuki T, Makino-Tasaka M (1983) Analysis of retinal and 3-dehydroretinal in the retina by high-pressure liquid chromatography. Anal Biochem 129: 111–119

19 Szuts EZ, Wood SF, Reid MS, Fein A (1986) Light stimulates the rapid formation of inositol trisphosphate in squid retinas. Biochem J 240: 929–932

20 Vandenberg CA, Montal M (1984) Light-regulated biochemical events in invertebrate photoreceptors. 1. Light-activated guanosinetriphosphatase, guanine nucleotide binding, and cholera toxin catalyzed labeling of squid photoreceptor membranes. Biochem 23: 2339–2347

ZOOLOGICAL SCIENCE 10: 281–285 (1993)

Effect of Osmolality on the Motility of Sperm from the Lamprey, *Lampetra japonica*

Wataru Kobayashi

Zoological Institute, Faculty of Science, Hokkaido University, Sapporo 060, Japan

ABSTRACT—Lamprey (*Lampetra japonica*) sperm were immotile not only in the seminal plasma but when immersed in an isotonic lamprey Ringer solution. Sperm were also found to be immotile when the semen was diluted with NaCl, KCl, or glucose solution isotonic to the Ringer solution. Sperm became motile, however, after dilution of semen with an hypotonic solution. These results suggest that motility of the lamprey sperm is probably suppressed by the osmolality of the seminal plasma and is initiated by a decrease in osmolality upon dilution into the spawning media (river water).

INTRODUCTION

Sperm of many animal species are quiescent in male reproductive organ and become motile after discharge into spawning media. It has been known that sperm of many species that show external fertilization recognize the difference between their seminal plasma and environmental media as a signal for the initiation of sperm motility [12]. Morisawa and his collaborators reported that hypotonicity induces the initiation of sperm motility in some cyprinid fishes (freshwater spawners) while hypertonicity induces sperm motility in marine teleosts [6, 7]. A change in osmotic pressure is not the sole factor for the initiation of sperm motility; the sperm of some freshwater fish show motility in isotonic media [12]. For example, salmonid sperm move after a decrease in the concentration of surrounding potassium ions even when the seminal plasma is diluted with salt solutions isotonic to it [7, 9]. Knowledge of the external factors that induce sperm motility may offer a basis for understanding the adaptation of gametes to the spawning environments.

I am interested in the fertilization of lampreys, because these animals represent one of the most ancient group of vertebrates. Information obtained from lamprey reproduction may be useful in helping us to understand the evolution of reproductive strategy in vertebrates. However, few studies have focused on the reproductive physiology of lamprey gametes. At spawning, female and male lampreys release their gametes into hypotonic river water (external fertilization). Yamamoto [15] has stated that "artificial activation of the lamprey eggs is possible in an isotonic salt solution (137 mM NaCl, 2.7 mM KCl, 2 mM $CaCl_2$, pH 7.3 with $NaHCO_3$) but fertilization is impossible in the solution". He succeeded in induction of artificial fertilization by immersing the eggs, which had been inseminated with "dry" sperm, into fresh water. These facts suggest that lamprey sperm are immotile in the Ringer's solution and initiate movement after dilution of the seminal plasma with freshwater. The present study was carried out to decide whether decrease in osmolality induces motility in lamprey sperm.

MATERIALS AND METHODS

Adult males of the river lamprey, *Lampetra japonica*, were taken in May (their spawning season) in the Ishikari river at Ebetu, Hokkaido. They were kept without feeding in constant darkness in plastic aquaria containing well water (12°C). In these conditions, they matured within 10 days. Semen was obtained by manual stripping of the animals anesthetized in 0.05% tricaine methanesulfonate (MS-222). The semen from different individuals

Accepted February 2, 1993
Received November 12, 1992

were stored in separate petri dishes at 1°C until use. Care was taken to avoid dehydration during storage. Although the semen retained a capacity for fertilizing the eggs for more than a week, the samples were used within two days after stripping.

Lamprey Ringer (LR) consisted of 137 mM NaCl, 2.9 mM KCl, and 2.1 mM $CaCl_2$ (pH 7.4 with 10 mM Hepes-NaOH) [16]. Test solutions used for the assessment of the initiation of sperm motility were 1/10 strength LR and solutions containing various concentrations of NaCl, KCl, or glucose; they were buffered with 10 mM Hepes-NaOH (pH 7.4). To examine whether external Ca^{2+} ions participate in the initiation of sperm motility, we used 1/10 strength Ca^{2+} free LR containing 13.7 mM NaCl, 2,9 mM KCl, and 10 mM EGTA (pH 7.4 with 10 mM Hepes-NaOH).

For assessment of sperm motility, two μl of the semen was quickly mixed with 198 μl of test solution in a test tube. Ten μl of the mixture was placed on a glass slide without a cover slip within 5 seconds after mixing and examined under a microscope. Sperm movement was observed under a light microscope ($\times$200) and recorded by a video recorder. Sperm represented to be motile when the sperm head showed forward movement. Percentage of moving sperm (more than 50 cells) and swimming speed of the moving sperm (n=10) were monitored by tracing the location of sperm heads on a hard copy of the frame by a video printer. Assessment of sperm motility was carried out in samples from three males. All experiments were performed in triplicate for each sample and performed at room temperature. No significant difference was recognized among these males. Data (mean$\pm$SE, n=3) from a representative fish are therefore presented in the figures. Student's *t*-test was used to determine statistically significant differences, which were considered significant when $P<0.05$.

RESULTS

Lamprey sperm were immotile in the seminal plasma. Upon dilution of semen with full strength LR, less than 1% of sperm began to move within the first few seconds. In the 1/10 strength LR, nearly all sperm immediately showed active forward movement; most of the sperm continued the movement for more than 5 minutes. Sperm initi-

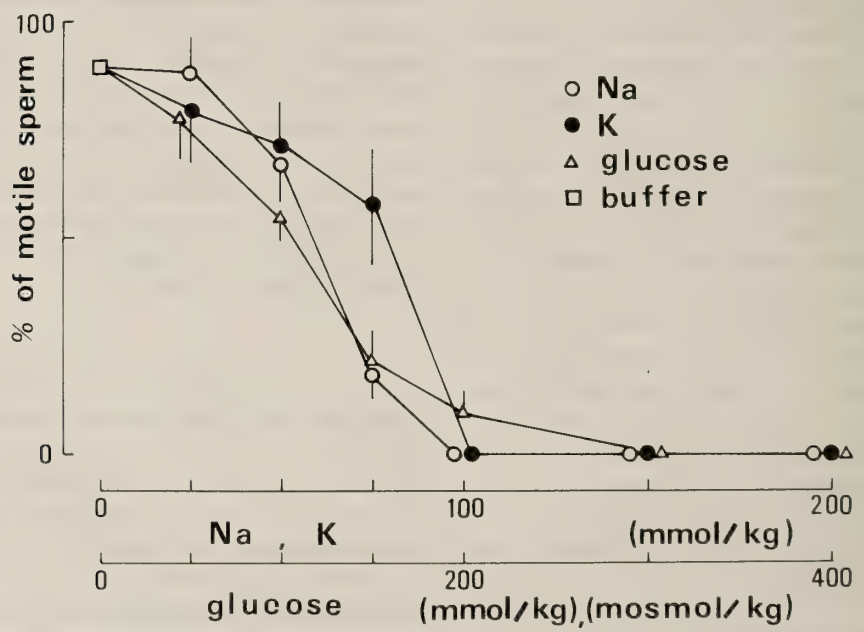

FIG. 1. Effect of NaCl, KCl or glucose on the motility of lamprey sperm. Percentage (mean$\pm$SE) of motile sperm 10 seconds after dilution of semen with the test solutions are presented.

ated similar movement in the 1/10 strength Ca^{2+} free LR. It is clear that the initiation of sperm motility does not require the presence of Ca^{2+} ions in external medium.

Figure 1 clearly shows that sperm were completely immotile in NaCl and KCl solutions at concentrations from 100 mmol/kg (200 mOsmol/kg) to 200 mmol/kg (400 mOsmol/kg). Percen-

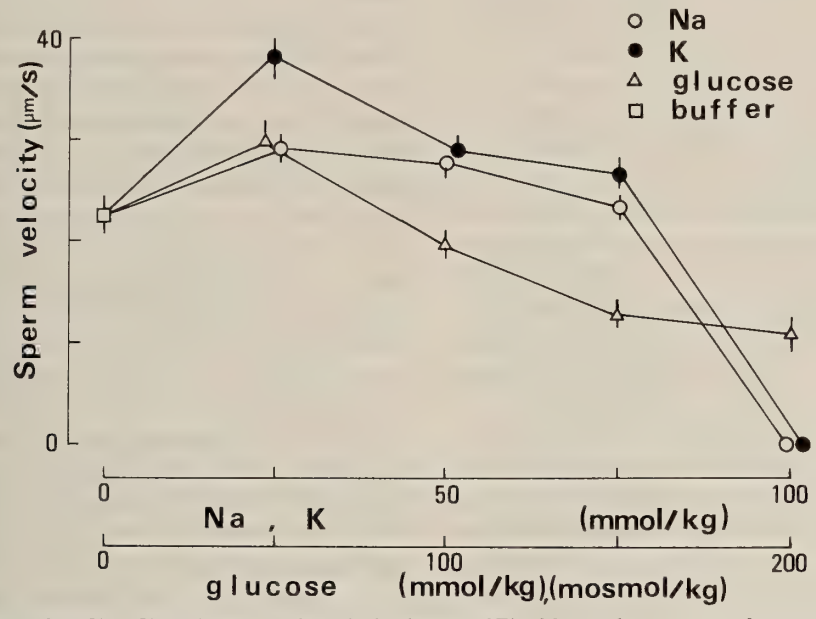

FIG. 2. Effect of NaCl, KCl or glucose on the velocity (mean ± SE) of forward movement of sperm 10 seconds after dilution of semen with test solutions.

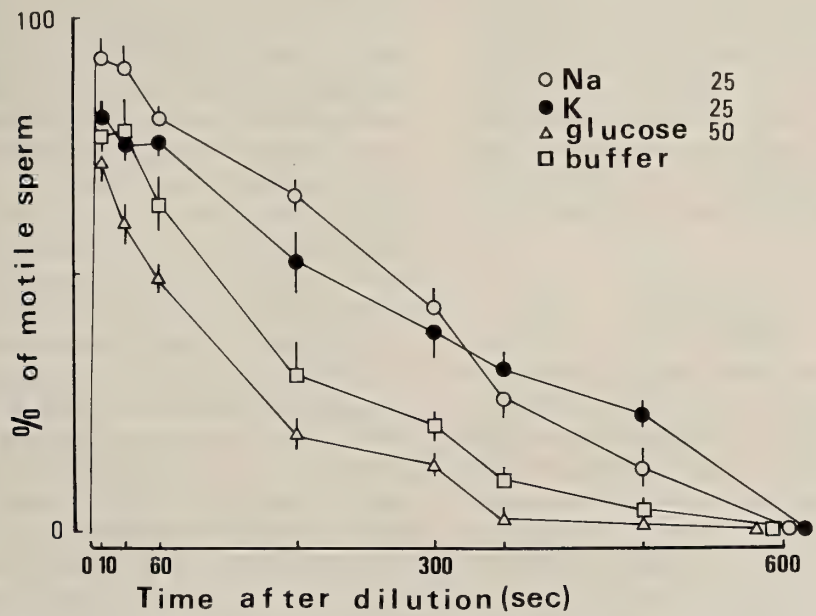

FIG. 3. Effect of the NaCl, KCl or glucose on the duration of the sperm motility. Changes in percentage of motile sperm in the test solutions (50 mOsmol/kg) and in buffer solution alone.

tage of motile cells increased as the concentration of the electrolytes decreased; a maximum value was obtained at a concentration between 0 and 25 mmol/kg (50 mOsmol/kg). A similar lack in the sperm motility in glucose solutions was observed at concentrations between 300 and 400 mmol/kg (mOsmol/kg). The percentage of sperm that showed forward movement increased as the concentration of glucose decreased to less than 150 mOsmol/kg. The value at 150 mOsmol/kg is apparently higher in KCl solution than that in NaCl or glucose solution ($P<0.01$). These results indicate that an isosmotic solution of electrolytes (NaCl, KCl) and nonelectrolytes do not induce forward movement in lamprey sperm, and that a decrease in the osmotic pressure of the extracellular medium is essential for the initiation of lamprey sperm motility.

Velocity of the forward movement was affected by osmotic concentration of the solution; a maximum speed was obtained at 50 mOsmol/kg. At this osmolality, sperm showed faster movement in KCl solution than that in NaCl ($P<0.001$) or glucose ($P<0.005$) solution (Fig. 2). At 100 and 150 mOsmol/kg, sperm velocity in NaCl or KCl solution was higher than that in glucose solution.

The percentage of motile sperm was estimated at 50 mOsmol/kg. Figure 3 shows that about 40% of total sperm were still motile in NaCl or KCl solution 5 minutes after dilution. In these solutions, the percentage of moving cells reached zero at 10 minutes. The life span of sperm was, however, short in a glucose or buffer alone; in these solutions, motile sperm was nearly zero at 6 minutes.

DISCUSSION

This study demonstrates that, although lamprey sperm are immotile in either electrolytes or nonelectrolyte solutions isotonic to blood plasma, they showed active forward movement when the semen is diluted with hypotonic media. These facts suggest that the external signal for the initiation of sperm motility in the lamprey is hyposmolality. Although no data has been reported on the osmolality of lamprey seminal plasma, it is known that in many species the osmolality of seminal plasma is nearly the same as that of blood plasma or isotonic saline solution (Ringer solution) [4, 8]. Osmolality of the seminal plasma is probably involved in the quiescence of lamprey sperm in the semen.

The percentage of motile sperm (at 150 mOsmol/kg) and the velocity of forward movement (at 50 mOsmol/kg) were higher in the solution of KCl in the solution of NaCl or glucose. Similar action of potassium on sperm motility is reported in cyprinid fish [10]. Several investigators have reported that in many vertebrates the seminal plasma contains a high concentration of potassium ions [4, 8, 10, 14]. These facts suggest that the concentration of potassium may be also related to the motility of lamprey sperm when the seminal plasma is diluted in the natural spawning.

Morisawa and Suzuki [7] have reported that some species of freshwater (cyprinids) and marine fish adopt a change in osmolality of the external solution as a signal for the initiation of sperm motility: an external signal for the freshwater species is a decrease in osmolality, while a signal for the marine fish is an increase in osmotic pressure. Amphibian sperm (newt and *Xenopus*) seem to possess a mechanism similar to the freshwater fish [3, 4, 10, 14]. In contrast, the external signal for the initiation of sperm motility in salmonids (primitive type of fish) is the extracellular concentration of potassium ion [9]: motility of salmonid sperm is suppressed by a high concentration of potassium in the seminal plasma and is induced when a decrease in the potassium concentration is caused after dilution of the semen with freshwater at spawning. It is well known that the life cycle of some lamprey species ("parasitic" species) resembles that of some salmonid species [2]. Both groups of animals invariably spawn their gametes in freshwater (river). The embryos hatch there and the young animals migrate to the sea. They grow in the seawater environment and return to freshwater for spawning (anadromous migration). In spite of such a similarity of the life cycle, the external factors that regulate the sperm motility in the two primitive vertebrates, lampreys and salmonids, are quite different. On the other hand, the pattern of the early stages of the embryonic development (cleavage) in the lamprey is very

similar to that of amphibians [13]. Electrophysiological studies of fertilization have further revealed that, unlike the case of fish eggs [11], lamprey eggs as well as anuran amphibians possess a Cl^--dependent fertilization potential that participates in a fast block to polyspermy [1, 5]. These facts, together with the present results, indicate that the physiological properties of lamprey gametes are very similar to those of anuran amphibians. This situation is of interest in relation to the evolution of lower vertebrates and the convergence of reproductive strategy.

ACKNOWLEDGMENTS

I wish to thank Professor T. S. Yamamoto, Hokkaido university, for critical reading of the manuscript.

REFERENCES

1 Elinson RP (1986) Fertilization in amphibians: The ancestry of the block to polyspermy. Int Rev Cytol 101: 59–100

2 Hardisty MW (1979) Biology of the cyclostomes. Chapman and Hall, London.

3 Hardy MP, Dent JN (1986) Regulation of motility in sperm of the red-spotted newt. J Exp Zool 240: 385–396

4 Inoda T, Morisawa M (1987) Effect of osmolality on the initiation of sperm motility in *Xenopus laevis*. Comp Biochem Physiol 88A: 539–542

5 Kobayashi W, Baba Y, Shimozawa T (1991) Fertilization potential in the lamprey, *Lampetra japonica* eggs. Zool Sci 8: 1097

6 Morisawa M (1985) Initiation mechanism of sperm motility at spawning in teleosts. Zool Sci 2: 605–615

7 Morisawa M, Suzuki K (1980) Osmolality and potassium ion: Their roles in initiation of sperm motility in teleosts. Science 210: 1145–1147

8 Morisawa M, Hirano T, Suzuki K (1979) Changes in blood and seminal plasma composition of the mature salmon (*Oncorhynchus keta*) during adaptation to freshwater. Comp Biochem Physiol 64A: 325–329

9 Morisawa M, Suzuki K, Morisawa S (1983) Effects of potassium and osmolality on spermatozoan motility of salmonid fishes. J exp Biol 107: 105–113

10 Morisawa M, Suzuki K, Shimizu H, Morisawa S, Yasuda K (1983) Effects of osmolality and potassium on motility of spermatozoa from freshwater cyprinid fishes. J exp Biol 107: 95–103

11 Nuccitelli R (1980) The electrical changes accompanyingfertilization and cortical vesicle secretion in the medaka egg. Dev Biol 76: 483–498

12 Stoss J (1983) Fish gamete preservation and spermatozoan physiology. In "Fish physiology Vol 9B" Ed by WS Hoar, DJ Randall, EM Donaldson Academic Press, New York, pp 305–350

13 Tahara Y (1988) Normal stages of development in the lamprey, *Lampetra reissneri* (Dybowski). Zool Sci 5:109-118

14 Viljoen BCS, Van Vuren JHJ (1991) Physical composition of the semen of *Labeo ruddi* and *Labeo rosae* (Pisces: Cyprinidae). Comp Biochem Physiol 98A: 459–462

15 Yamamoto T (1961) Physiology of fertilization in fish eggs. Int Rev Cytol 12: 361–405

16 Yamamoto TS (1956) Digestion of egg envelopes and the chemical properties of the lamprey's egg, *Lampetra japonica*. J Fac Sci Hokkaido Univ Ser VI Zool 12: 273–281

ZOOLOGICAL SCIENCE 10: 287–294 (1993)

Identification and Immunological Properties of an Olfactory System-Specific Protein in Kokanee Salmon (*Oncorhynchus nerka*)

Munetaka Shimizu[1,2], Hideaki Kudo[1,3], Hiroshi Ueda[1]*, Akihiko Hara[4], Kenji Shimazaki[2] and Kohei Yamauchi[3]

[1]*Toya Lake Station for Environmental Biology, Faculty of Fisheries, Hokkaido University, Abuta 049-57,* [2]*Research Institute of North Pacific Fisheries, Faculty of Fisheries, Hokkaido University, Hakodate 041,* [3]*Department of Biology, Faculty of Fisheries, Hokkaido University, Hakodate 041, and* [4]*Nanae Fish Culture Experimental Station, Faculty of Fisheries, Hokkaido University, Nanae 041-11, Hokkaido, Japan*

ABSTRACT—An olfactory system-specific protein of 24 kDa (N24) was identified in kokanee salmon (*Oncorhynchus nerka*) by the comparison of proteins restricted to the olfactory system (olfactory epithelium, olfactory nerve and olfactory bulb) with those found in other parts of the brain (telencephalon, optic tectum, cerebellum, hypothalamus) and hypophysis. A polyclonal antibody to N24 was raised in a rabbit, and the specificity of the antiserum was examined by Western blotting analysis; the antiserum recognized only one 24 kDa band in the olfactory system but not in other parts of the brain in kokanee salmon, sockeye salmon (*O. nerka*), masu salmon (*O. masou*) and chum salmon (*O. keta*). Immunocytochemical analysis revealed that positive immunoreactivity occurred exclusively in the olfactory nerve and in some olfactory neuroepithelial cells. Both at the time of imprinting of maternal stream odorants and at the time of homing to the maternal stream, the immunoreactivity of N24 in fish in the maternal stream was stronger than that in seawater fish. The present study indicates that an olfactory system-specific protein may be importantly related to both imprinting and homing mechanisms in salmonids.

INTRODUCTION

The imprinting and homing behaviors of salmon in relation to their maternal stream constitute one of the most interesting phenomena in salmon biology. Since Hasler and Wisby [10] introduced the olfactory hypothesis for anadromous salmonids, olfactory imprinting and homing mechanisms have been studied in many behavioral experiments (e.g., [9, 24]). Several neurophysiological approaches using electrophysiological techniques have also pointed to the olfactory recognition of maternal stream water during spawning migration in several salmonids [8, 26]. It is now widely accepted that in juvenile salmon the olfactory system plays important roles in imprinting of the maternal stream odorants during downstream migration, and that in adult salmon the early olfactory exposure allows recognition of the maternal stream odorants during upstream spawning migration (homing). However, few attempts have been made to investigate biochemical aspects of the olfactory system in any salmonid species.

There are numerous literatures indicating a close relation between olfactory-specific proteins and recognition and discrimination of odorants in higher vertebrates[1, 13, 16]. Several olfactory-specific proteins have been identified and used as molecular markers to study olfactory function, such as the olfactory marker protein in the mammalian olfactory bulb [11, 14], carnosin in tetrapod olfactory systems [3, 15], and olfactomedin in frog olfactory neuroepithelium [23].

The present study was desinged to compare

Accepted February 2, 1993
Received December 14, 1992
* To whom correspondence and reprint requests should be addressed.

proteins restricted to the olfactory system (olfactory epithelium, olfactory nerve and olfactory bulb) with those found in other parts of the brain (telencephalon, optic tectum, cerebellum, hypothalamus) and hypophysis of several salmonid species. In addition, two immunological analyses (Western blotting and immunocytochemistry) were conducted to investigate the possible role of an olfactory system-specific protein in olfactory functions and to evaluate its possible usage as a molecular marker in the study of olfactory mechanisms.

MATERIALS AND METHODS

Fish

Male and female mature kokanee salmon (*Oncorhynchus nerka*; land-locked sockeye salmon), 3 to 5 years old, were caught in Lake Toya from October 22 to November 19, 1991. Mature sockeye salmon (*O. nerka*) of both sexes, 3 to 5 years old, were collected from the Chitose Branch of the Hokkaido Salmon Hatchery on October 29, 1991. Adult chum salmon (*O. keta*) of both sexes, 3 to 6 years old, were captured at sea and in fresh water at two different stages of sexual maturation (pre-spawning fish about 10–20 days before final maturation and spawning fish) on September 25, 1991. Wild one-year-old juvenile masu salmon (*O. masou*) were caught once a month in the Shakotan River from November 21, 1991 to May 25, 1992.

Fish were anesthetized with 10% ethyl p-aminobenzoate, and their heads were removed by decapitation and placed on ice. Under a dissecting microscope, olfactory organs and brains were dissected into olfactory epithelium, olfactory nerve, olfactory bulb, telencephalon, optic tectum, cerebellum, hypothalamus and hypophysis. Each tissue was washed quickly in ice-cold salmon Ringer (0.15 M NaCl, 0.31 mM KCl, 0.03 mM $MgSO_4 \cdot 7H_2O$, 0.34 mM $CaCl_2 \cdot 2H_2O$, 0.4 mM glucose, 0.4 mM Hepes buffer, pH 7.5) containing aprotinin (1 μg/ml), phenylmethylsulfonyl fluoride (PMSF; 1 mM) and ethylenediaminetetraacetic acid (EDTA; 1 mM). The tissue was homogenized in about 1.5 volumes of salmon Ringer and centrifuged at 10,000$\times g$ for 10 min. The supernatant fluid was stored at -30°C and used for gel electrophoresis.

Gel electrophoresis

Sodium dodecyl sulfate polyacrylamide gel electrophoresis (SDS-PAGE) [12] was performed using a Protean II slab gel system (Bio-Rad, South Richmond, CA, USA). Samples containing 50 μg protein, as determined by Lowry's method, were heated at 100°C for 2 min in double volumes of SDS sample buffer containing 2-mercaptoethanol, and applied to slab gels consisting of 7.5–17.5% logarithmic gradient of polyacrylamide and 5% stacking gel. Electrophoresis was carried out at 12.5 mA for stacking gel followed at 25 mA for gradient gel. Molecular weight markers (Pharmacia Fine Chemicals, Uppsala, Sweden) for determination of low molecular weight were run in a separate lane. Gels were fixed and stained for 2 hr in 0.1% Coomassie Brilliant Blue in 5% ethanol-5% acetic acid solution, destained overnight in 10% acetic acid, soaked in 20% ethanol-5% acetic acid-2.5% glycerin, and dried with gel dryer.

Two-dimmensional (isoelectric-SDS) PAGE (2D-PAGE) [19] was also carried out to obtain the evidence whether an olfactory system-specific protein appeared single spot or not.

Antiserum production

A protein band corresponding to an olfactory system-specific protein, designated as N24, was prepared from olfactory bulbs of mature kokanee salmon of both sexes. The band was excised carefully with scissors, and eluted from gel slices using an Electro-Eluter (Bio-Rad, South Richmond, CA, USA) following the manufacturer's instructions. An elution buffer was constituted with 25 mM Tris, 192 mM glycine and 0.1% SDS, and elution was done at 10 mA for 2 hr.

A polyclonal antiserum was raised in a rabbit using lymph node injections. Initial injection of 35 μg eluted N24 was made into inguinal lymph nodes in Freund's complete adjuvant. Subsequent booster injections of 90 μg N24 emulsified with Freund's incomplete adjuvant were made intradermally into the back of rabbit at four weekly intervals. One week after the final booster injection, a test bleeding was taken from the ear vein, and the serum was assayed by Western blotting analysis.

Western blotting

Protein samples were resolved by SDS-PAGE and transferred to Immobilon PVDF membranes (Millipore, Bedford, MA, USA) by the method of Towbin *et al.* [25]. The PVDF membranes were incubated for 1 hr with 1% skim milk in Tris-buffered saline (TBS, pH 7.4) to reduce non-specific protein absorption, and allowed to react for 2 hr with polyclonal antiserum against N24 (working dilution from 1:100 to 1:5000) in a solution of 3% bovine serum albumin and 1% normal goat serum in TBS. After rinsing with TBS, the membranes were incubated for 1 hr with horseradish-peroxidase-labeled goat anti-rabbit IgG (Cappel Laboratories, West Chester, PA, USA) at a dilution of 1:1000 in TBS, and developed in 4-chloro-1-naphthol solution (60 mg in 100 ml TBS containing 0.01% H_2O_2). The reaction was stopped after 3–5 min by washing in distilled water, and the membranes were air-dried.

Immunocytochemistry

The olfactory system and other parts of the brain of mature kokanee salmon were fixed with 4% paraformaldehyde in 0.1 M phosphate buffer (pH 7.3) for 18 hr at 4°C. After rinsing with 0.1 M phosphate buffer containing 10% sucrose, tissues were embedded in Tissue-Tek OCT compound (Miles Laboratories, Elkhart, IN, USA) and stored at −30°C, to be sectioned later at 10-μm thickness in a cryostat. Tissue sections were immersed in 0.3% hydrogen peroxide in methanol for 30 min to eliminate endogenous peroxidase activity. After rinsing with phosphate-buffered saline (PBS), sections were incubated with 1% normal goat serum in PBS for 15 min, and immunoreacted with anti-N24 serum (working dilution 1:2500 or 1:5000) for 2 hr at room temperature. The strepto-avidin-biotin complex (sABC) method (Histofine, Nichirei, Tokyo, Japan) was used for the immunocytochemistry. In order to confirm specificity, normal rabbit serum or PBS was substituted for anti-N24 serum.

RESULTS

Soluble extracts of the olfactory system and other parts of the brain from mature kokanee salmon were resolved by SDS-PAGE (Fig. 1A). Several protein bands were observed in extracts of the olfactory system but not in other parts of the brain or the hypophysis. Among these proteins, the most clearly visible protein band (arrowhead in Figure 1A), which had a molecular weight of 24 kDa, was designated N24, and appeared single spot by the analysis of 2D-PAGE (manuscript in preparation). This protein was eluted from gel slices for antibody generation.

In Western blotting analysis, a polyclonal antiserum to N24 at dilutions of 1:500 and 1:1000 recognized only the band whose position was identical to N24 in extracts of kokanee salmon olfactory bulb. At a dilution of 1:100, presumably weak non-specific reactions were observed in bands of molecular weight around 40 kDa. At a dilution of 1:5000, a faint reaction only was observed in the 24 kDa band. At a dilution of 1:2500, the antiserum reacted with the 24 kDa protein in the olfactory system, which was absent from other parts of the brain and hypophysis in kokanee salmon (Fig. 1B).

Electrophoretic patterns of soluble extracts of the olfactory system and telencephalon of chum salmon, sockeye salmon and masu salmon were similar to those of kokanee salmon, and a similar olfactory system-specific protein of molecular weight 24 kDa was recognized in all these salmonid species (Fig. 2).

During parr-smolt transformation in masu salmon, although there were no distinct changes in electrophoretic patterns of the olfactory system and telencephalon between parr and smolt, the immunoreactivity of N24 to the antiserum was more intense in parr than in smolt (Fig. 3). Similarly, during spawning migration of chum salmon from coastal sea to maternal river, electrophoretic patterns of olfactory nerve, olfactory bulb and telencephalon showed no prominent changes. However, the cross-reactivity of anti-N24 serum was different in fish from the sea and the river; the antigenicity of N24 was more intense in the maternal river fish sample (Fig. 4).

The olfactory rosette of mature kokanee salmon stained with Nissl solution showed olfactory epithelium and several branches of the olfactory

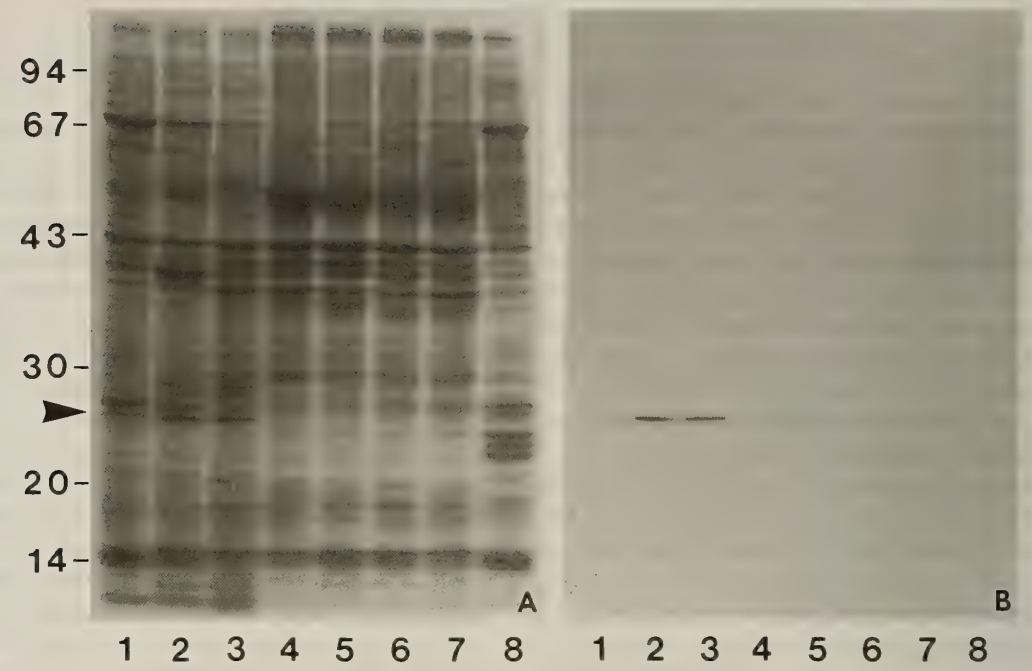

Fig. 1. SDS-PAGE (A) and Western blotting (B) of soluble extracts of the olfactory system (1, olfactory epithelium; 2, olfactory nerve; 3, olfactory bulb), other parts of the brain (4, telencephalon; 5, optic tectum; 6, cerebellum; 7, hypothalamus) and hypophysis (8) from kokanee salmon. Arrowhead in A identifies an olfactory system-specific protein of molecular weight 24 kDa (N24). Anti-N24 serum (1 : 2500) recognizes a band of molecular weight 24 kDa in the olfactory system but not in other parts of the brain. Numbers at left are Mr standards $\times 10^3$.

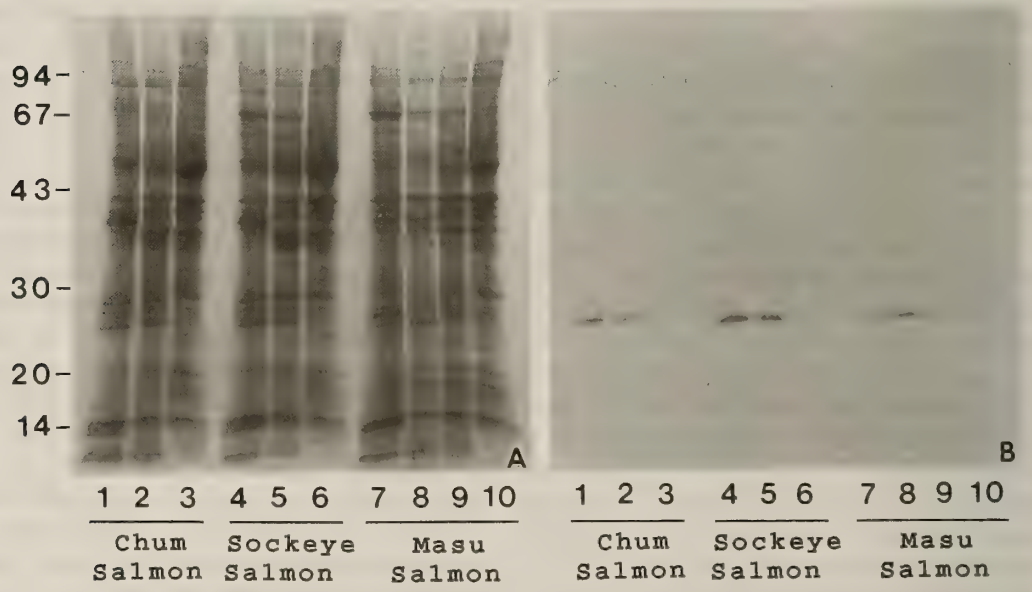

Fig. 2. SDS-PAGE (A) and Western blotting (B) of soluble extracts of the olfactory system (1, 4, 8, olfactory nerve; 2, 5, 9, olfactory bulb; 7, olfactory epithelium) and telencephalon (3, 6, 10) from chum salmon, sockeye salmon and masu salmon. Anti-N24 serum (1 : 2500) recognizes a band of molecular weight 24 kDa only in the olfactory system. Numbers at left are Mr standards $\times 10^3$.

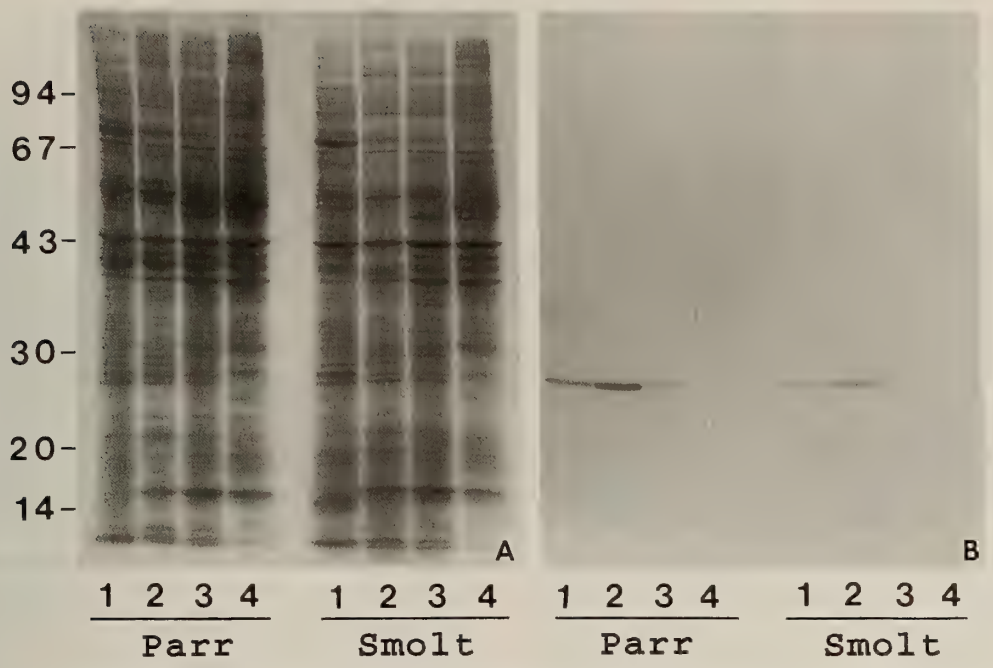

FIG. 3. SDS-PAGE (A) and Western blotting (B) of soluble extracts of the olfactory nerve system (1, olfactory epithelium; 2, olfactory nerve; 3, olfactory bulb) and telencephalon (4) in masu salmon during parr-smolt transformation. The immunoreactivity of anti-N24 serum (1:2500) is more intense in parr than in smolt. Numbers at left are Mr standards $\times 10^3$.

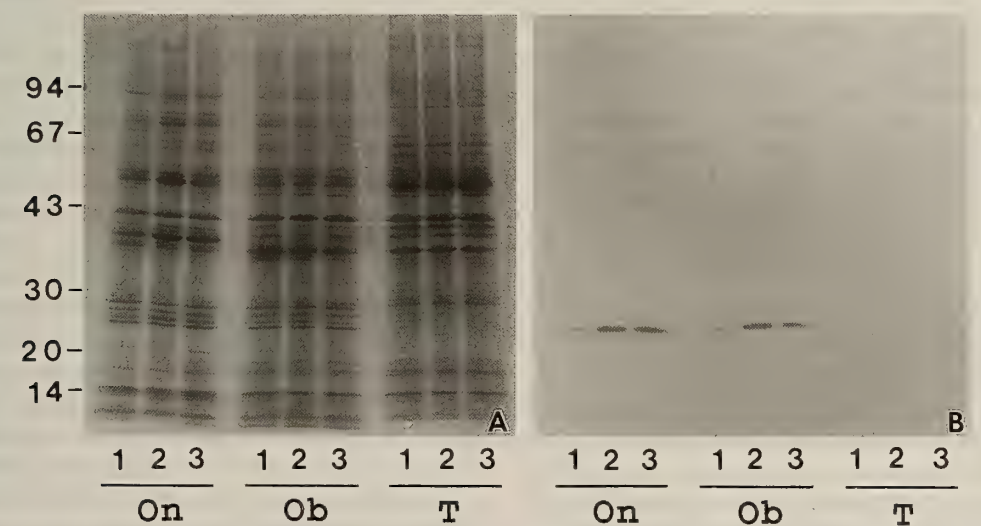

FIG. 4. SDS-PAGE (A) and Western blotting (B) of soluble extracts of the olfactory system (On, olfactory nerve; Ob, olfactory bulb) and telencephalon (T) in chum salmon during spawning migration (1, coastal sea; 2, pre-spawning fish in the maternal river; 3, spawning fish in the maternal river). The immunoreactivity of anti-N24 is more intense in fish from the maternal river than in fish from the coastal sea. Numbers at left are Mr standards $\times 10^3$.

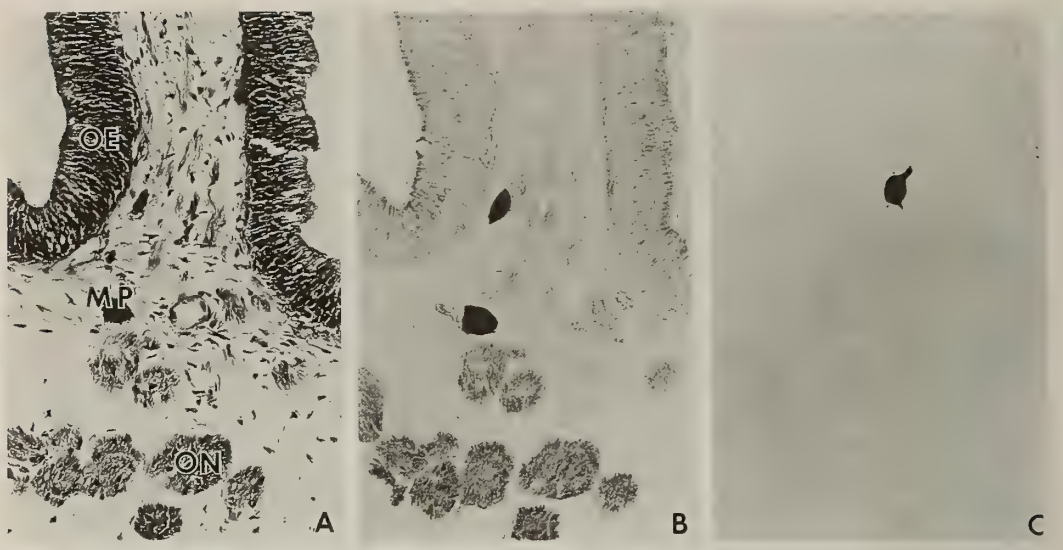

Fig. 5. Adjacent 10-μm thick sections of the olfactory rosette of mature kokanee salmon stained with Nissl solution (A), sABC method with anti-N24 at a dilution of 1:2500 (B), and sABC method with normal rabbit serum at a dilution of 1:2500 (C). N24 immunoreactivity occurs in some olfactory neuroepithelial cells and in branches of the olfactory nerve. MP, melanophore; OE, olfactory epithelium; ON, olfactory nerve. $\times$250.

nerve (Fig. 5A). The sABC method demonstrated that N24 immunoreactivity was localized exclusively in almost all branches of olfactory nerve and in some olfactory epithelial cells, presumably neuroepithelial cells (Fig. 5B). The immunoreactivity of apical portions of the olfactory epithelium was non-specific because the same portions were also stained in control sections, in which anti-N24 serum was replaced with normal rabbit serum (Fig. 5C). Specific immunoreactivity was never observed in other nervous tissues studied.

DISCUSSION

Electrophoretic comparison of proteins restricted to the olfactory system with those in other parts of the brain in kokanee salmon demonstrated the existence of several olfactory system-specific proteins. Among them, the most clearly visible protein designated as N24 based on its 24 kDa molecular weight was used to raise a specific antibody in a rabbit. Western boltting analysis revealed that the antiserum recognized only this 24 kDa band in the olfactory system, which was absent from other parts of the brain not only in kokanee salmon but also in sockeye salmon, masu salmon and chum salmon. However, no cross-reactivity of anti-N24 serum was observed in the olfactory system of carp (unpublished data). Therefore, all salmonids examined to date possess a 24 kDa protein (N24) specific to the olfactory system.

The olfactory sensory cells (olfactory neuroepithelial cells) are bipolar neurons, whose dendrites project to the external environment and axons to the olfactory bulb, which form the olfactory nerve. Preliminary immunocytochemical study showed that positive N24 immunoreactivity occurred exclusively in the olfactory nerve and in some olfactory neuroepithelial cells. The specific immunoreactivity was also found in the olfactory bulb where the olfactory nerve was penetrated (unpublished data). We could not identify types of neuroepithelial cells at the light microscopic level. These observations suggest that N24 has possible roles in neurotransduction from neuroepithelial cells to olfactory bulb; however, further detailed immunocytochemical studies at the electron microscopic level are needed to clarify this point.

A mammalian olfactory marker protein of molecular weight 20 kDa is localized in olfactory sensory neuron cell bodies and axons; its appear-

ance coincides with the establishment of sensory synapses in the olfactory bulb [7]. Although it seems unlikely that the mammalian olfactroy marker protein is identical to N24 because of the difference in their molecular weight, further immunological approaches are necessary. Carnosine is the predominant dipeptide present in the olfactory neurons and nerve in mammals, birds, reptilians and amphibians, but has not been reported in fishes [3]. Olfactomedin, a 57 kDa glycoprotein, is localized exclusively in frog olfactory neuroepithelium [23]. These olfactory-specific proteins may play important roles in chemoreception, however, their precise functions remain uncertain.

Another biochemical approach in higher vertebrates concerns the involvement of olfactory receptor proteins which activate adenylate cyclase [21, 22] *via* a GTP-binding protein [2] leading to the opening of cyclic nucleotide-gated cation channels [5, 18]. A multigene family of GTP-binding protein-coupled receptors expressed uniquely in olfactory tissues has recently been reported [4]. Immunocytochemical studies using monoclonal antibodies against rabbit olfactory bulb have demonstrated subclasses of olfactory nerve fibers and their projections to the olfactory bulb [6, 17]. These aspects need investigation in teleosts.

During downstream migration of masu salmon (at the time of imprinting) and upstream spawning migration of chum salmon (at the time of homing), the immunoreactivity of N24 in fish in the maternal stream was stronger than that in seawater fish. Either qualitative changes (including immunological properties) or quantitative changes of N24 may occur during migration. We found no evident changes in N24 or in other protein bands as judged by their staining properties with Coomassie blue. None the less, the change observed indicates that N24 may have a role in both imprinting and homing mechanisms in salmonids. Inhibitors of RNA and protein synthesis have reported to inhibit olfactory bulbar discrimination in maternal stream water of chinook salmon, as judged by electrophysiological methods [20]. So it is reasonable to consider that some specific proteins must be involved in the homing behavior of salmonids.

In conclusion, the present study identifies an olfactory system-specific protein (N24) in four salmonid species and describes some of its immunological properties. N24 may prove to be good molecular marker for the study of salmonid olfactory functions. Detailed biochemical and cytological analyses of N24 as well as the other olfactory system-specific proteins are now in progress in our laboratory.

ACKNOWLEDGMENTS

We thank Professor Howard A. Bern, University of California, for his interest in the present study and for critical reading of the manuscript. We also thank Dr Osamu Hiroi, Dr Masahide Kaeriyama, Hokkaido Salmon Hatchery, and Mr Hiroshi Kawamura, Hokkaido Fish Hatchery, for providing the chum salmon, the sockeye salmon and the masu salmon, respectively, and Mr Hiroyuki Haruna and Mrs Rirako Yamada, Toya Lake Station for Environmental Biology, for their technical assistance. This study was supported in part by the Special Grant-in-Aid for Promotion of Education and Science in Hokkaido University Provided by the Ministry of Education, Science and Culture of Japan, and by a reseach grant from the Akiyama Foundation to H.U.

REFERENCES

1 Anholt RRH (1989) Molecular physiology of olfaction. Am J Physiol 257: C1043–C1054

2 Anholt RRH, Mumby SM, Stoffers DA, Girard PR, Kuo JF, Snyder SH (1987) Transductory proteins of olfactory receptor cells: identification of guanine nucleotide binding proteins and protein kinase C. Biochemistry 26: 788–795

3 Artero C, Marti E, Biffo S, Mulatero B, Andreone C, Margolis FL, Fasolo A (1991) Carnosine in the brain and olfactory system of amphibia and reptilia: a comparative study using immnocytochemical and biochemical methods. Neurosci Lett 130: 182–186

4 Buck L, Axel R (1991) A novel multigene family may encode odorant receptors: a molecular basis for odor recognition. Cell 65: 175–187

5 Dhallan RS, Yau KW, Schrader KA, Reed RR (1990) Primary structure and functional expression of cyclic nucleotide-activated channel from olfactory neurons. Nature 347: 184–187

6 Fujita SC, Mori K, Imamura K, Obata K (1985) Subclasses of olfactory receptor cells and their segregated central projections demonstrated by a monoclonal antibody. Brain Res 326: 192–196

7 Graziadei GAM, Stanley RS, Graziadei PPC (1980) The olfactory marker protein in the olfactory system of the mouse during development. Neurosci 5: 1239–1252

8 Hara, TJ (1970) An electrophysiological basis for olfactory discrimination in homing salmon: a review. J Fish Res Board Can 27: 565–586

9 Hasler AD, Scholz AT (1983) Olfactory imprinting and homing in salmon. Springer-Verlag, Berlin, pp 1–134

10 Hasler AD, Wisby WJ (1951) Discrimination of stream odors by fishes and relation to parent stream behavior. Am Naturalist 85: 223–238

11 Kott JN, Vickland H, Dong XM, Westrum LE (1992) Development of olfactory marker protein and tyrosine hydroxylase immunoreactivity in the transplanted rat olfactory bulb. Exp Neurol 115: 132–136

12 Laemmli UK (1970) Cleavage of structural proteins during the assembly of the head of bacteriophage T_4. Nature 227: 680–685

13 Lancet D (1986) Vertebrate olfactory reception. Annu Rev Neurosci 9: 329–355

14 Margolis FL (1972) A brain protein unique to the olfactory bulb. Proc Nat Acad Sci USA 69: 1221–1224

15 Margolis FL (1974) Carnosine in the primary olfactory pathway. Science 184: 909–911

16 Margolis FL, Getchell TV (1991) Receptors: current status and future directions. In "Perfumers: Art, Science and Technology" Ed by P Muller, D Lamparsky, Elsevier Applied Science Publishers, Essex, pp 481–498

17 Mori K, Fujita SC, Imamura K, Obata K (1985) Immunohistochemical study of subclasses of olfactory nerve fibers and their projections to the olfactory bulb in the rabbit. J Comp Neurol 242: 214–229

18 Nakamura T, Gold GH (1987) A cyclic nucleotide-gated conductance in olfactory receptor cilia. Nature 325: 442–444

19 O'Farrell PH (1975) High resolution two-dimmensional electrophoresis of proteins. J Biol Chem 250: 4007–4021

20 Oshima K, Gorbman A, Shimada H (1969) Memory-blocking agents: effects on olfactory discrimination in homing salmon. Science 165: 86–88

21 Pace U, Hanski E, Salomon Y, Lancet D (1985) Odorant-sensitive adenylate cyclase may mediate olfactory reception. Nature 316: 255–258

22 Sklar PB, Anholt RRH, Snyder SH (1986) The odorant-sensitive adenylate cyclase of olfactory receptor cells: differential stimulation by distinct classes of odorants. J Biol Chem 261: 15538–15543

23 Snyder DA, Rivers AM, Yokoe H, Menco BPhM, Anholt RRH (1991) Olfactomedin: purification, characterization, and localization of a novel olfactory glycoprotein. Biochemistry 30: 9143–9153

24 Stabell OB (1984) Homing and olfaction in salmonids: a critical review with special reference to the Atlantic salmon. Biol Rev 59: 333–388

25 Towbin H, Staehelin T, Gordon J (1979) Electrophoretic transfer of proteins from polyacrylamide gels to nitrocellulose sheets: procedure and some applications. Proc Nat Acad Sci USA 76: 4350–4354

26 Ueda K (1985) An electrophysiological approach to the olfactory recognition of homestream waters in chum salmon. NOAA Tech Rep NMFS 27: 97–102

ZOOLOGICAL SCIENCE 10: 295–306 (1993)

Development of the Brittle Star, *Ophioplocus japonicus* H.L. Clark. I

Miéko Komatsu and Tomoko Shōsaku

Department of Biology, Faculty of Science, Toyama University, Toyama 930, Japan

ABSTRACT—The entire process of development from eggs to juveniles in the brittle star, *Ophioplocus japonicus*, is described with special attention to external morphology. The breeding of this brittle star in Toyama Bay, Sea of Japan, occurs in August. The eggs are spherical, orange, and 300 μm in average diameter. Cleavage is total and radial. Gastrulation takes place by invagination. Larvae possessing tube-foot buds and ophiuroid rudiments on the posterior part of their bodies, develop into the vitellaria stage. Vitellariae of the present species have transverse ciliary bands, but no larval skeletons. Six days after fertilization at 25°C, metamorphosis is completed and the resulting juvenile is pentagonal in outline and about 400 μm in diameter. The present study shows that ciliary bands are formed in an earlier larval stage than was reported previously.

INTRODUCTION

A considerable number of feeding (planktotrophic) larvae, the ophiopluteus, has been reported in Ophiuroidea [5]. Development of ophiopluteus larvae is generally called an indirect or planktotrophic type [5, 9]. However, ophiuroids with yolky eggs have diverse developmental courses as will be shown below. The developmental pattern was classified into 7 types based on the breeding and brooding styles, the nature of the larvae, and other features [20]. On the other hand, Hendler [5] designated 3 types of development (planktotrophic, direct and abbreviated) based on the egg size, life span, larval size and some other factors. From his view, development of the vitellaria belongs to the abbreviated type. However, the abbreviated type has some heterogeneous larval forms, whereas the planktotrophic and direct types are distinctive. Thus, agreement has not yet been achieved on what are the developmental types and on their nomenclature in Ophiuroidea. This is partly because of the comparative paucity of knowledge available on the development passing through other than typical ophiopluteus larval stages.

At present, 8 species are known to possess vitellaria larvae. They are *Ophiocoma pumila, Ophioderma brevispina, O. cinereum, O. longicauda, Ophiolepis cincta, O. elegans, Ophionereis annulata* and *O. squamulosa* [1, 3, 5, 7, 8, 12, 14, 15, 19]. To date, however, detailed studies on development through vitellaria have been done only in 2 species; *O. brevispina* [1] and *O. squamulosa* [14]. In addition, descriptions on the gastrulation, including formation of the archenteron, are very limited. Indeed, no regular and convenient method, such as KCl and 1-methyladenine which induces spawning in echinoids and asteroids, respectively, has been reported to induce spawning in ophiuroids. However, as the result of several chances of spawning the authors have gotten embryos of this species. The present paper describes the larval development of the brittle star, *Ophioplocus japonicus* through metamorphosis.

MATERIALS AND METHODS

Specimen collection

Ophioplocus japonicus H. L. Clark have their habitat under stones on a sandy bottom. Specimens were collected from the seashores of Uozu,

Accepted February 17, 1993
Received November 13, 1992

Toyama Prefecture, of Tsukumo Bay, Ishikawa Prefecture, and of Sado Island, Niigata Prefecture, all of them facing the Sea of Japan, for nearly every summer between 1980 and 1990. This brittle star is gonochoric. In both sexes, the gonad was arranged in pairs in each interradius. In the breeding season, the body cavity is almost completely occupied with gonads. Ovaries in this season are orange or brown in color and the testes are milky white.

Breeding season

In August 15, 1980, natural spawning occurred in a glass container with small amounts of seawater in which about 20 individuals were kept. They had been en route to a laboratory at Toyama University after they had been collected at Uozu. Natural spawning also occurred in a tank with running seawater at Noto Marine Laboratory, Ishikawa Prefecture, on August 13, 1985, and at Sado Marine Laboratory, Niigata Prefecture, on August 9, 1990, a few days after collection. Specimens, which were held in a glass container containing as much seawater as needed to immerse the dorsal surface of their disk, spawned spontaneously at Noto Marine Laboratory, on August 25, 1983, August 21, 1984, August 6 and 9, 1986, and July 31, 1991. These ova were fertilized using a dilute suspension of spermatozoa from the dissected testes of homologous male specimens.

Culture of embryos and larvae

Temperature in the laboratory culture was approximately 25°C, which is close to the water temperature at the natural habitat in August. The embryos and larvae were taken from the culture dish at appropriate intervals and observed under dissecting and light microscopes. They were measured live with an ocular micrometer. The skeletal system, from fresh squash preparations, was examined under standard and Nomarski differential interference microscopes, and from samples preserved by the following method. Embryos and larvae were fixed in 70% alcohol and then macerated in a 10% aqueous solution of potassium hydroxide.

For histological observation, the embryos and larvae were fixed with Bouin's solution. The fixed material was embedded in paraffin, serially sectioned at a thickness of 6 μm, and stained with Delafield's hematoxylin and eosin. Embryos and larvae were fixed for scanning electron microscopy in 2% OsO_4 in 50 mM Na-cacodylate buffer (pH 7.4); the osmolarity of the fixative was adjusted by the addition of sucrose (final conc. 0.6 M). The fixed materials were dehydrated in an ethanol series and dried with a critical point dryer (Hitachi, HCP-2). They were observed with a scanning microscope (Hitachi, S-510) after being coated with gold-palladium (Hitachi, E101 Ion Sputter).

RESULTS

Annual reproductive cycle

In order to study the annual reproductive cycle, specimens were collected at a fixed locality of the coast of Himi along Toyama Bay, Toyama Prefecture. Sampling of the animals was made once a month during the period from March, 1979 through October, 1981. At each collection, 5 individuals of both sexes and those which were more than 10 mm in disk diameter were selected. Soon after collection, the disk was cut off from the arms and the fresh weight was determined. Gonads were then dissected out and weighed. The gonad index for the gross estimation of the annual reproductive cycle was calculated by the following formula:

$$\text{Gonad Index} = (\text{Fresh Weight of Gonads} / \text{Fresh Weight of Total Disk}) \times 100$$

The annual reproductive cycle was determined in the population of *O. japonicus* at Himi as shown in Figure 1. Although there were some differences throughout the years, the gonad indices of males and females were highest in June, 1981 and July, 1980, while they were lower in August of these 2 years. After September, the value for both sexes increased gradually. According to the transition of the gonad index, and the natural and inductive spawnings, the spawning of this species is presumed to occur in August.

Embryos of cleavage stage

In the present study, the entire process of de-

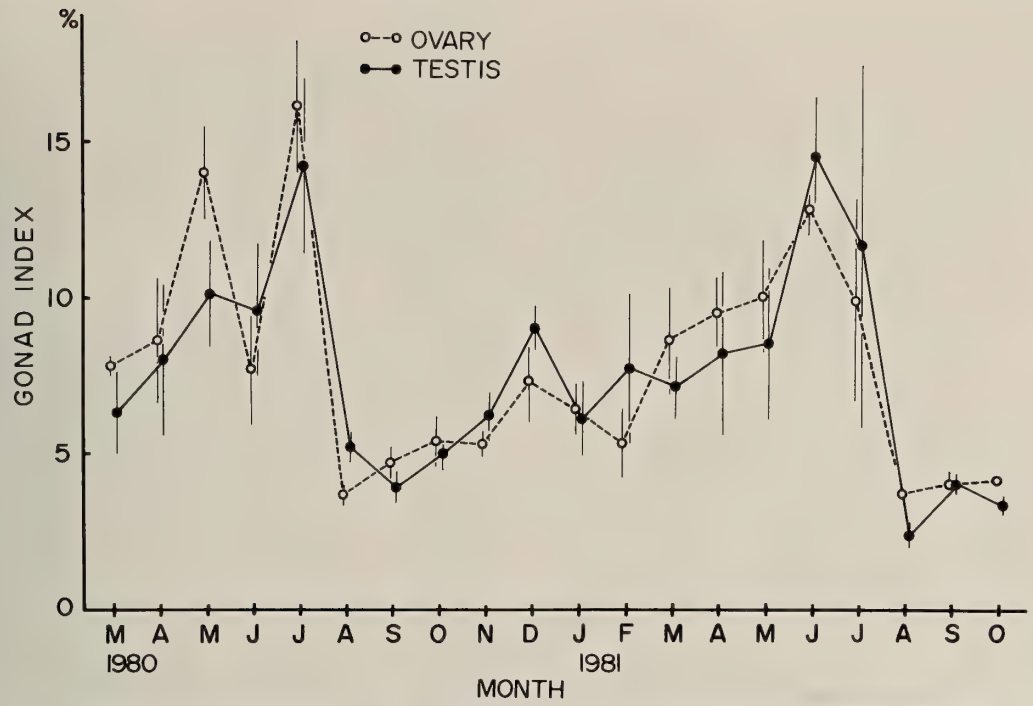

FIG. 1. Monthly variations of the gonad index in *Ophioplocus japonicus*, from March, 1980 through October, 1980. Each point shows an average of 5 individuals and standard error (vertical bar).

TABLE 1. Chronology of development of *Ophioplocus japonicus* (25°C)

Time (after fertilization)	Stage
1 hr	1st cleavage
2 hrs	2nd cleavage
3 hrs	8-cell stage
4 hrs	16-cell stage
5 hrs	32-cell stage
6 hrs	64-cell stage
7.5 hrs	Blastula with blastocoel
12 hrs	Hatching
16 hrs	Gastrulation
20 hrs	Gastrula, 350 μm long and 250 μm wide
30 hrs	Larva with 5 visible hydrolobes
36 hrs	Vitellaria bearing tube-foot buds in hydrolobe, ciliary bands appear
2 days	Terminal tentacles and oral tube-feet present
2.5 days	Vitellaria being rectangular in outline on the posterior potion
3 days	Rudiments of adult skeleton appear as spicules
3.5 days	Vitellaria with 4 distinct transverse ciliary bands on dorsal side, 530 μm long and 350 μm wide
4 days	Preoral lobe begins to be resorbed
5 days	Oral plates are apparent
6 days	Metamorphosis completed, 500 μm diameter
14 days	Juvenile, 600 μm diameter

velopment from fertilization to complete metamorphosis was observed in the laboratrory at 25°C. Naturally spawned eggs lacked the germinal vesicle and were spherical, with an average diameter of 300 μm. They are opaque, grayish brown and heavier than seawater. A transparent jelly coat with a thickness of about 25 μm surrounded the egg surface. The head of the sperm was spherical, about 4 μm in diameter, and the tail was about 50 μm in length.

A chronology of larval development for *Ophioplocus japonica* is presented in Table 1. The fertilized egg had a fertilization membrane with a perivitelline space approximately 10 μm in height. Polar bodies, which direct the animal pole, were visible in the perivitelline space. The lst cleavage occurred through the animal-vegetal axis 1 hr after fertilization and the 2nd followed at about 1 hr later, also through the egg axis but perpendicular to the first plane. Successive cleavages were equal, radial, and total, and occurrd at approximately 1 hr intervals. The resulting blastula was furnished with a large blastocoel in its center at 7.5 hr after fertilization (Fig. 3–1). At this stage, the entire surface of the blastula was furnished uniformly with cilia about 15 μm long. The embryo then began to rotate. Hatching from the fertilization membrane took place 12 hr after fertilization. The hatched larvae were almost spherical in shape, and they swam actively.

Gastrula

Gastrulation occurred by invagination at the vegetal pole about 16 hr after fertilization. The early gastrula was shaped like a pyramid with corners, with a small blastopore at the broad vegetal end. The blastopore became larger as gastrulation proceeded. The 20 hr-old gastrulae were oval, being now 350 μm long and 250 μm wide (Figs. 2–1, 3–2). Their anterior end was round and posterior end was truncate with a blastopore at the center. At this stage, mesenchyme cells were observed in the histological preparations. They were set free from the top of the

FIG. 2. Development of *Ophioplocus japonicus*. Each drawing was made from a living specimen. 1. Twenty hr, gastrula. 2. Thirty hr, early vitellaria larva bearing 5 hydrolobes. 2A; dorsal side, 2B; ventral side. 3. Two and a half days, vitellaria larva with tube-feet and oral tube-feet in a ventral view. 4. Three days, spicules of the rudimental skeletal plate of the adult. 5. More developed spicules than those shown in Fig. 2–4. 6. Three and a half days, vitellaria larva, arrows show transverse ciliary bands. 6A; dorsal side, 6B; ventral side, 6C; spicules of the rudimental skeletal plate of the adult on the dorsal surface of the larva. Dotted lines represent 5 hydrolobes with 2 pairs of tube-feet each. 7. Five days, metamorphosing larva with the absorbed preoral lobe. 7A; dorsal side, 7B; ventral side. 8. Six days, metamorphosed juvenile with a pen-tamerous shape. 8A; aboral side, 8B; oral side. 9. Eight days, juvenile bearing 5 pairs of lateral arm plates in the radius. 9A; aboral side, 9B; oral side. 10. Three months, juvenile with a long arm, 10A; aboral side, 10B; oral side. Symbols: dcp; dorsocentral plate, hl; hydrolobe, lap; lateral arm plate, m; mouth, mpp; madreporic plate, op; oral plate, otf; oral tube-foot, pl; preoral lobe, rp; radial plate, tf; tube-foot, tfp; tube-foot pore, to; tooth, tp; terminal plate, tt; terminal tentacle, vp; ventral plate. Magnification: ca. 65× in all drawings except for 4, 5 and 6C (ca. 200×).

FIG. 3. Development of *Ophioplocus japonicus*. 1 and 2 are micrographs of sections (6 μm) of specimens and others are scanning electron micrographs. 1. Seven and a half hr, blastula with blastocoel (blc). 2. Thirty hr, gastrula showing outer ectodermal layer and inner endodermal layer, same stage as shown in Fig. 2–1. 3. Twenty-four hr, late gastrula. Note a rise (arrows) corresponding to the area of rudiments of a ciliary band. 4, 5 and 6. Thirty-six hr, early vitellaria larva with primary ciliary bands. 4A; dorsal side. Flaglet and arrow show ciliary bands on the preoral lobe and in the posterior portion, respectively. 4B; magnified view of the anterior left lateral part. 5; ventrolateral (left) side showing hydrolobes (hl). Note the ciliary band on the preoral lobe (flaglet), in the middle of the posterior portion (arrow), and below the hydrolobe (arrowhead). 6; ventral side. Note rudiments ( ) of tube-foot on hydrolobe. Flaglet shows ciliary band on the preoral lobe. 7. Two days. 7A; ventral side of a vitellaria larva bearing apparent tube-foot (tf), oral tube-foot (otf) and terminal tentacle (tt) on the hydrolobe, and spiral ciliary band (flaglets) on the preoral lobe, 7B; Magnified view of spiral ciliary band (flaglets) on the preoral lobe. 8 and 9. Two and a half days. 8; dorsal side of vitellaria larva showing 3 parts (arrows) of the upper ciliary band on the posterior portion and the ciliary bands (arrowheads) at the posterior end, 9; magnified view of a posterior part of a specimen. Note ciliary bands (arrowheads) in the future interradius. Each of the hydrolobes in the future radius has a terminal tentacle (✲), 1 pair of tube-feet ( ) and a pair of oral tube-feet (●). Scale; 100 μm in 1–4A, 5–7A and 8, and 20 μm in 4B, 7B and 9.

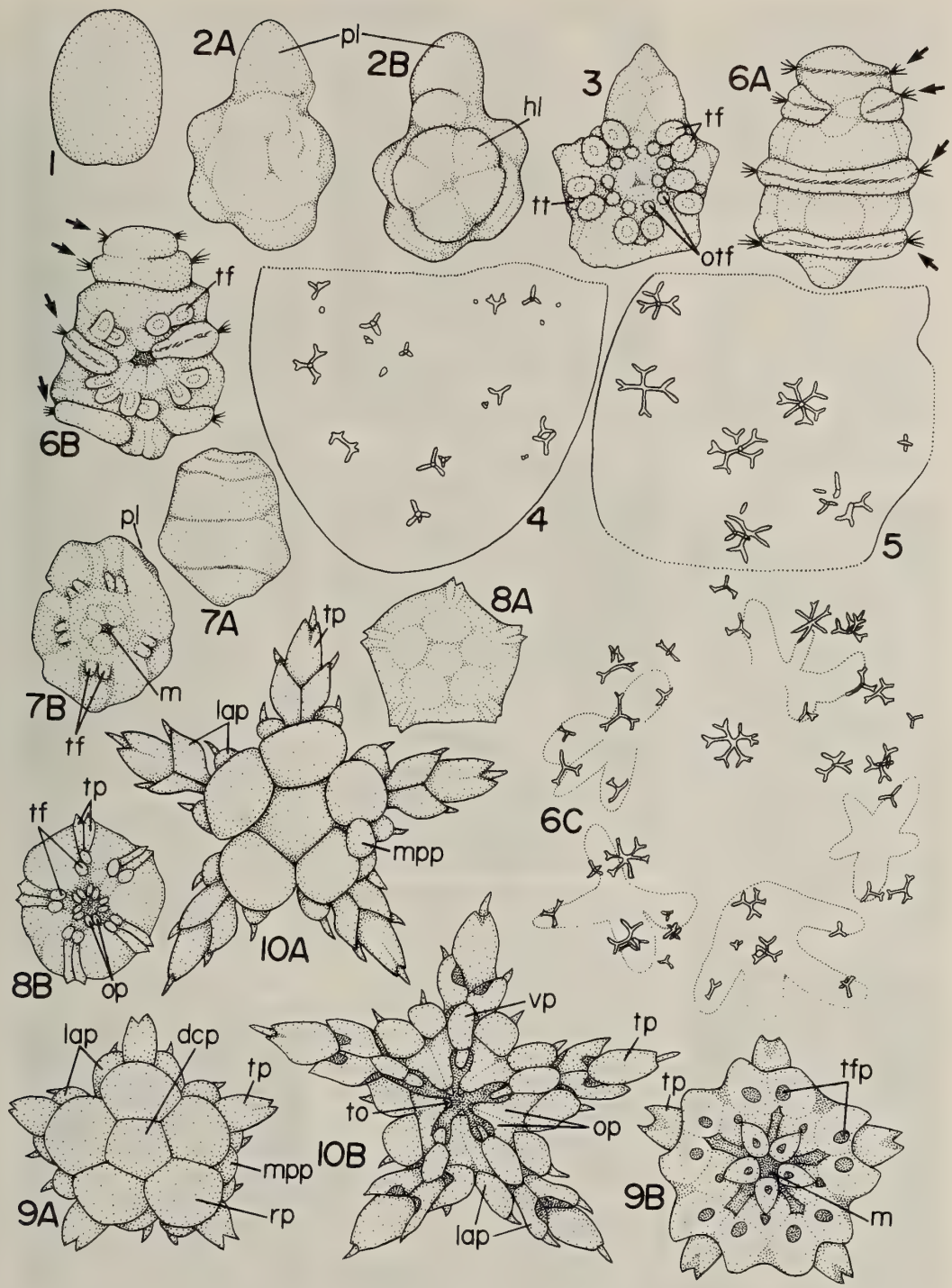
1
2A
pl
2B
hl
3
tf
tt
otf
6A
6B
tf
4
5
pl
7A
8A
7B
m
tf
tp
lap
mpp
6C
tf
tp
8B
op
10A
vp
tp
lap
dcp
tp
to
op
tp
tfp
mpp
10B
9A
rp
9B
m
lap

FIG. 2.

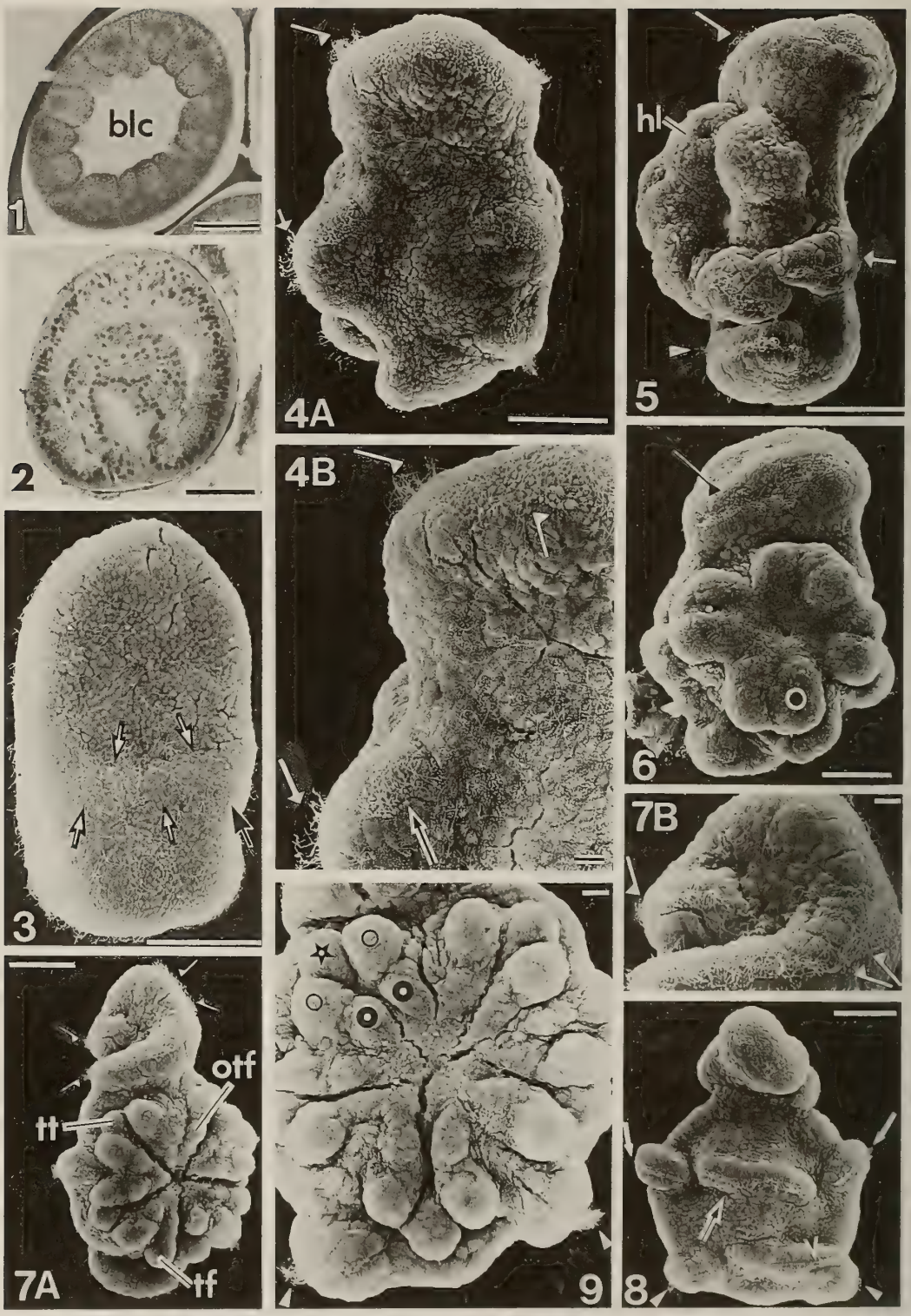

FIG. 3.

archenteron into the blastocoel. Around 25 hrs after fertilization, the area of the middle portion of the body, where the ciliary band will be formed, became apparent as a ridge (Fig. 3–3). The larvae had a distinct constriction which separated the anterior portion from the posterior portion by 30 hr after fertilization (Fig. 2–2A, 2–2B). The anterior portion was seen as tapering and corresponded to the preoral lobe. It disappeared during the metamorphosis into the adult form. The posterior portion, which forms the juvenile body, was more or less pentaradiate in this stage. Projections of the rudiments of the hydrolobes appeared in the future oral side of the larva. In the 1.5 day-old larva, each of the 5 hydrolobes bore one pair of tube-foot buds (Fig. 3–6). The hydrolobes encircled a concave portion, which becomes the oral area of the adult after metamorphosis. At that stage, a ciliary band surrounded the middle part of the preoral lobe (Fig. 3–4A, 3–4B, 3–5, 3–6). In addition to the transverse ciliary band on the preoral lobe, a band encircling the middle of the posterior portion became discontinuous at the ventral and dorsal sides of the body, and could be observed from both lateral sides (Fig. 3–5). On the ventral side, the lateral parts of the ciliary band extended across the hydrolobe (Fig. 3–5), which was situated in the posterior end of the body. There was a transverse ciliary band below the hydrolobes on the ventral side (Fig. 3–5), although it had not yet been formed on the dorsal side. Thus, the larva at this stage should be called a vitellaria, because a transverse ciliary band was now apparent.

Vitellaria

Two days after fertilization, an oral tube-foot appeared in the aboral side of each tube foot (Fig. 3–7A). A terminal tentacle was distinguishable on the peripheral portion of each hydrolobe. At this stage, the ventral parts of the ciliary band on the preoral lobe assumed a spiral form (Fig. 3–7B). The ciliary band below the hydrolobe was displaced to the posterior end of the body and extended to the dorsal side. Two and a half days after fertilization, the posterior portion of the vitellaria larva became clearly rectangular in outline (Fig. 2–3). Because of the change of the vitellaria larval form, the ciliary band of the posterior end became situated in the future interradii of the ventral side (Fig. 3–9). On the dorsal side, each of 2 ciliary bands in the posterior portion were almost continuous (Fig. 3–8). The upper ciliary band consisted of 3 parts: 2 short larval parts and a long median one between them. Three day-old vitellaria larvae had spicules in the posterior portion, as shown in Figure 2–4. These spicules are the rudiments of the adult skeletal plates, some of which later become tetraradiate or hexaradiate, measuring 20–40 μm in diameter (Fig. 2–5).

Three and a half days after fertilization, the vitellaria larvae became dorso-ventrally flattened (Fig. 2–6A, 2–6B). The vitellaria was now 530 μm long and 350 μm wide. By this stage, the juvenile mouth opened. Four transverse ciliary bands were distinct on the dorsal side (Fig. 4–1, 4–2A) and were completely continuous except for the 2nd anterior band, which consisted of small lateral parts (Fig. 4–2B). SEM observation showed that 2 (the 1st and 2nd) anterior bands, which were situated in the preoral lobe, made contact on the ventral side (Fig. 4–3). At this stage, the tube-feet were functional and the vitellariae could either swim freely or creep on the substrata. Figure 2–6C shows spicules viewed from the future aboral side of the juvenile specimen. However, there is no trace of the larval skeleton, in contrast to the findings in the vitellaria of *Ophionereis annulata* by Hendler [8].

Metamorphosis

Four days after fertilization, the anterior portion of the vitellaria, the preoral lobe, began to degenerate (Fig. 4–4A). By this stage, the cilia had disappeared on the oral side and only a trace of ridges of ciliary bands remained (Fig. 4–5A, 4–5B). On the dorsal side, the cilia on the incomplete ciliary bands decreased in number and became short (Fig. 4–4C). On the other hand, 3 transverse ciliary bands were retained (Fig. 4–4B). Absorption of the preoral lobe proceeded rapidly after the commencement of the metamorphosis. The metamorphic stage shown in Figure 4–6 is at approximately half a day after the commencement of metamorphosis. Five days after fertilization,

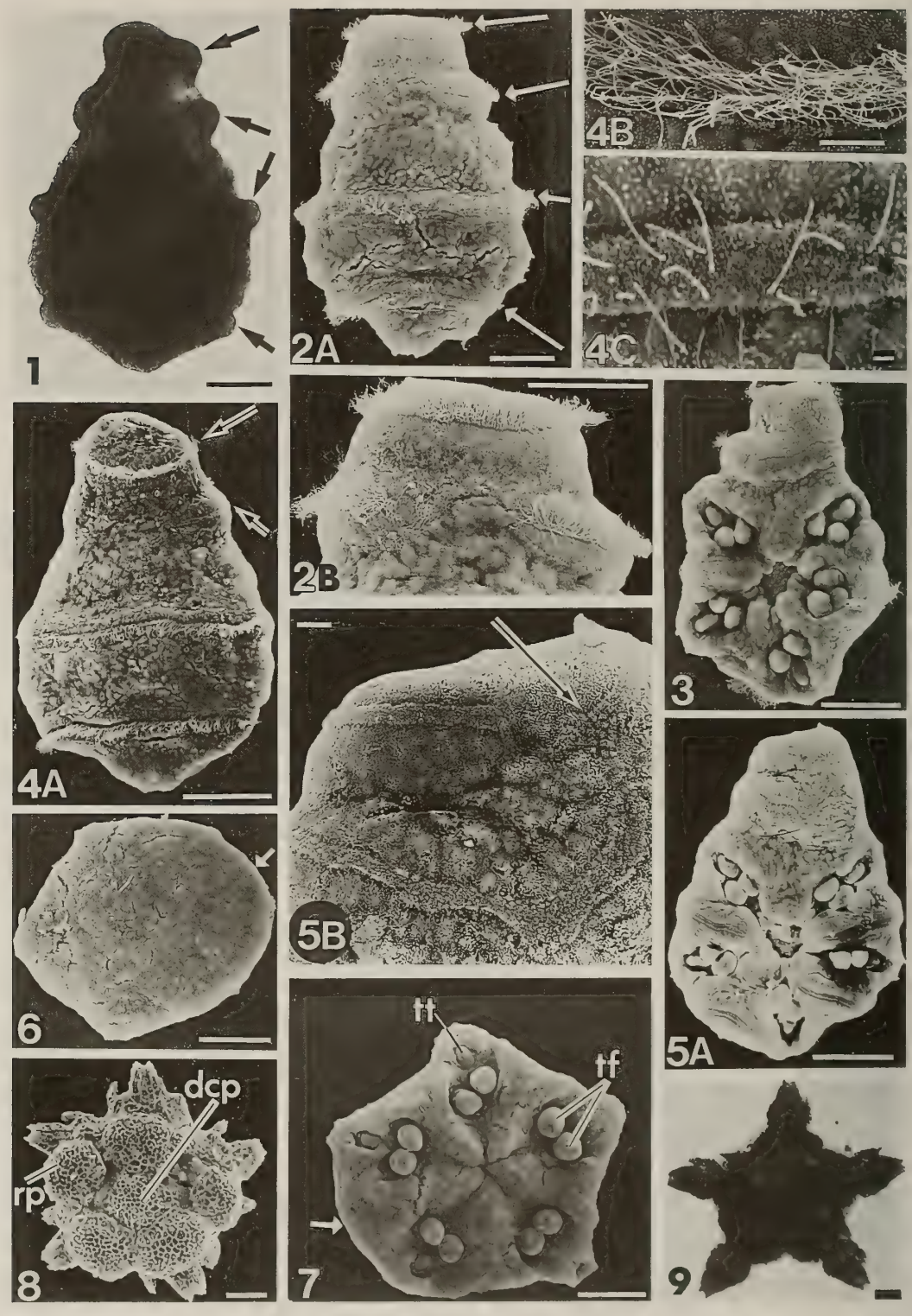
1
2A
4B
4C
2B
3
4A
5B
5A
6
7
tt
tf
8
dcp
rp
9

only a trace of the preoral lobe remained (Figs. 2–7A, 2–7B, 4–7). By this stage, the skeletal system of the adult started to grow and the larval body became more rigid except for the tube-feet. A pair of the oral plate was now apparent in each radius. Six days after fertilization, the anterior portion of the larva disappeared and thus metamorphosis was completed (Fig. 2–8A, 2–8B). Metamorphosed juveniles, 500 μm in diameter, bore 5 rudimental arms, each with a terminal plate at its tip. They were benthonic and moved on the substratum by means of their tube-feet. On the aboral side, rudiments of the skeletal plate were apparent. The aboral side of the disk became convex 1 day later. One dorsocentral plate and 5 radial plates around the former became firm at this stage.

Juvenile

Eight days after fertilization (2 days after the completion of metamorphosis), 1 pair of lateral arm plates each of which bore 1 spine, were formed in both sides of the arm (Fig. 2–9A). The madreporic plate was now recognizable on 1 interradius. Skeletal plates of the oral side of the disk were indistinct except for the oral and terminal ones (Fig. 2–9B). One pair of tube-foot pores were seen to exist in each radius. Ten days after fertilization, the 1st ventral arm plates appeared. Figure 4–8 shows the aboral view of a juvenile at 2 weeks after fertilization. The skeletal plates of the aboral side had many pore-like sieves. The juvenile seen here is 600 μm in diameter. One month after fertilization, juveniles grew to 700 μm in diameter. Although a number of juveniles were kept alive in the laboratory for several months, no further differentiation could be observed. Three month-old juveniles measured 500 μm in disk diameter and 250 μm in arm length (Figs. 2–10A, 2–10B, 4–9). They bore 2 arm segments from the development of the 2nd lateral arm plates. Each arm was furnished with 3 pairs of tube-feet.

DISCUSSION

Detailed studies on the development through metamorphosis are very limited in ophiuroids, although larvae of ophiuroid have been recognized in about 80 species [5].

It was reported that gastrulation takes place by invagination at the vegetal pole [6, 10, 17, 21]. Little is known about the formation of the archenteron in the species with the vitellaria larva. It was reported that the archenteron is formed by splitting of the central core in *Ophioderma brevispina* [1]. On the other hand, judging from the figure by Mortensen ([14], Plate XXXI, Fig. 5) the archenteron seems to be formed by invagination in a 26 hr-old larva of *Ophionereis squamulosa.* In the present species, gastrulation is apparently achieved by an invagination. Thus, formation of the archenteron seems to be diverse in different species in ophiuroids with vitellaria larvae. However, further studies are needed to promote a deeper understanding of the archenteron formation.

Ophioplocus japonicus is the 9th ophiuroid species that has been shown to have vitellaria larvae. The larva of *O. brevispina* was called worm-like larva by Müller [16]. Brooks and Grave [1] described in some detail the larva of *O. brevispina.* Later the term, vitellaria, was proposed by Fell [2] for a distinctive larval type of echinoderm which

FIG. 4. Development of *Ophioplocus japonicus.* 2–8 views are scanning electron micrographs. 1 and 9 are light (regular) micrographs. 1, 2 and 3. Three and a half days, same stage as that shown in Figs. 2–6 and 4–2A. 1; vitellaria larva from the dorsal side with 4 transverse ciliary bands (arrows), 2A; dorsal side, 2B; magnified view of the anterior part, 3; ventral side. 4 and 5. Four days. 4A; dorsal side, vitellaria larva showing the disappearance of cilia on the ciliary band (short arrow). The long arrow indicates a ciliary band on the preoral lobe. 4B; magnified view of the ciliary band (the long arrow shown in Fig. 4–4A) on the preoral lobe, 4C; magnified view of the ciliary band (the short arrow shown in Fig. 4–4A) showing the disappearance of cilia, 5A; ventral side of the vitellaria, 5B; magnified view of the anterior part. Arrow indicates the junction of two ciliary bands on the preoral lobe. 6. Four and a half days, metamorphosing vitellaria with reduced preoral lobe (arrow), view from dorsal side. 7. Five days, metamorphosing vitellaria showing absorbed preoral lobe (arrow), view from ventral side, same stage as that shown in Fig. 2–7. 8. Two weeks, juvenile with a dorsal central plate and 5 radial plates on the dorsal side. 9. Three months, juvenile with arm segments, view from aboral side, same stage as shown in Fig. 2–10. Scale: 100 μm in 1–4A, 5A, and 7–9, 10 μm in 4B and 5B, and 1 μm in 4C.

corresponds to the larva of *O. brevispina*. Occurrence of ciliary rings is one of the characteristics of the vitellaria: the existence of 4 ciliary bands has been reported in the vitellariae of *Ophioderma longicauda* [3] and *O. brevispina* [1]. In fact, Hendler [8] noted that ophiuroid vitellariae generally have 4 transverse ciliary bands. However, the number of the ciliary bands varies in different species. There are 3 ciliary bands in *Ophionereis annulata* because of the lack of the 4th transverse band [8]. Mortensen [15] described that vitellariae of *Ophiolepis cincta* are furnished with a ciliated tuft in addition to 4 transverse ciliary bands. Judging from his figure (Fig. 26, p. 48), the actual number of ciliary bands seems to be 3; the 3rd and the 4th bands are continuous and should be counted as 1. The number of ciliary bands was not described in *Ophioderma cinereum* [7], *Ophiolepis elegans* [19] or *O. squamulosa* [14]. However, it can be determined in the latter 2 species from available figures (Fig. 1c, p. 9; Figs. 2 and 3, Pl. XXXI). Each of these vitellariae is furnished with 3 ciliary bands and 1 ciliated tuft. In the vitellaria of the present species, no ciliated tuft was observed at the anterior portion of the body by both LM and SEM observations. Ciliation of *O. japonica* is, therefore, different from that of *O. cincta, O. squamulosa* and *O. elegans*. Thus, ciliation of the ophiuroid vitellaria differs in different species. The vitellaria larva of *O. japonica* seems to have 4 transverse ciliary bands when observed from the dorsal view. However, the actual number of ciliary bands is 3, since 2 anterior ciliary bands on the preoral lobe are continuous on the ventral side. Therefore, detailed observation of ciliation of the vitellaria should be one of the points to be investigated in the future.

As noted before, the classification of the developmental pattern in ophiuroids seems to be different judging from the literature. Hendler [5] classified the development of ophiuroids into 3 types; planktonic, direct, and abbreviated. According to his view, development that includes vitellariae belongs to the abbreviated development. The abbreviated development category includes *Gorgonocephalus caryi* [18], which develops through only a pear-shaped larva without ciliary bands. Thus, the abbreviated type comprises heterogeneous larval forms. Hendler's proposal was supported by Mladenov [11]. Strathmann and Rumrill [20] later called the abbreviated development a pelagic or demersal development with lecithotrophic larvae.

According to the original proposals by Fell [2], the vitellaria larva is a larval form which bears transverse ciliary bands. Therefore, in terms of abbreviated development, it is reasonable to distinguish development with vitellariae from that with other types of larvae.

The relation between developmental type and egg size in ophiuroids was shown by Hendler [5] and then revised by Mladenov [11]. According to the latter, the ranges of the egg's diameter in the direct and planktotrophic developments are 100–1000 μm and 70–200 μm, respectively. Thus, there is a considerable spread of egg size in these 2 developmental types. On the other hand, the diameter of an egg of the species undergoing the abbreviated development type is greater than 130 μm and less than 350 μm.

It is likely that ophiuroid eggs, being from 200 to 350 μm in diameter, develop through the vitellaria larva. As a matter of fact, egg of *O. japonicus* is approximately 300 μm in diameter. The egg of *Ophiocoma pumila* is very small (73 μm) among the ophiuroids with vitellaria larvae. However, this species is exceptional since *O. pumila* passes through both the vitellaria and the planktotrophic pluteus stages.

In the present species, larva completes metamorphosis 6 days after fertilization at about 25°C. Stancyk [19] reported that in *O. annulata,* metamorphosis is completed 3 days after fertilization at 24°C. The majority of species which have vitellaria larvae were reported to complete metamorphosis within 4 or 5 days, although the temperatures were not indicated [4, 13, 15]. On the other hand, in *Amphipholis kochii* which has planktotrophic development with eight-armed ophiopluteus, metamorphosis is incipient 12 days after fertilization at 23°C [21]. This term seems to be the shortest among planktotrophic developers according to the table by Mladenov ([11], p. 60). Thus, it may be concluded that developments through the vitellaria larva proceed faster than those through the ophiopluteus larva.

In *O. japonicus,* no larval skeleton is present in the vitellariae. No trace of any larval skeleton was observed in either the vitellaria larvae of *O. squamulosa* or *O. brevispina* [1, 14]. On the other hand, occurrence of a larval skeleton was reported in *O. annulata* [8]. Furthermore, an irregular calcareous structure was found in the vitellaria of *O. cincta* [15]. It is, therefore, interesting that there are 2 types of vitellariae, one with a pluteus-like skeleton and the other with no skeleton at all.

O. japonicus is one of the most common ophiuroids in Japan, with its habitat being under the stones of shallow water. In the present study, the larva of this species is demonstrated as being vitellaria, not ophiopluteus, which is thought to be a typical planktotrophic larva of ophiuroids [5, 9, 21]. Twenty-four species of ophiuroids have been known to pass through ophiopluteus larvae. They belong to 5 families of 2 suborders, Gnathophiurina and Chilophiurina. On the other hand, vitellariae have been found in 9 species including the present species, and all belong to 4 families of 1 suborder, Chilophiurina. These families are Ophiodermatidae, Ophiocomidae, Ophiuridae and Ophionereidae. Thus, the occurrence of vitellaria is very limited and this may be phylogenetically significant.

ACKNOWLEDGMENTS

The authors thank Dr. Chitaru Oguro, President of Toyama University, for his valuable advise on this study and critical reading of the manuscript. The present study was supported in part by a Grant-in-Aid from the Ministry of Education of Japan to MK (No. 57740392).

REFERENCES

1 Brooks WK Grave C (1899) *Ophiura brevispina.* Mem natn Acad Sci 8: 79–100

2 Fell HB (1945) A revision of the current theory of echinoderm embryology. Trans Roy Soc New Zealand 75: 73–101

3 Fenaux L (1969) Le développmen larvaire chez *Ophioderma longicauda* (Retzius). Cah Biol Mar 15: 59–62

4 Grave C (1916) *Ophiura brevispina* II. An embryological con tribution and a study of the effect of yolk substance upon development and developmental processes. J Morph 27: 413–453

5 Hendler G (1975) Adaptational significance of the patterns of ophiuroid development. Amer Zool 15: 691–715

6 Hendler G (1977) Development of *Amphioplus abditus* (Verrill) (Echinodermata: Ophiuroidea) I. Larval biology. Biol Bull 152: 51–63

7 Hendler G (1979) Reproductive periodicity of ophiuroids (Echinodermata: Ophiuroidea) on the Atlantic and Pacific coasts of Panamá In "Reproductive Ecology of Marine Invertebrates" Ed by SE Stancyk, Univ of South Carolina Press, USA, pp 145–156

8 Hendler G (1982) An echinoderm vitellaria with a bilateral larval skeleton: evidence for the evolution of ophiuroid vitellariae from ophioplutei. Biol Bull 163: 431–437

9 Hyman L (1955) The Invertebrates VolIV Echinodermata. McGraw-Hill, New York, pp 763

10 MacBride EW (1914) Invertebrate In "Text-Book of Embryology" Ed by W Heape, Macmillan, London, Vol IV, pp 692

11 Mladenov PV (1979) Unusual lecithotrophic development of the Caribbean brittle star *Ophiothrix oerstedi.* Mar Biol 55:55–62

12 Mladenov PV (1985) Development and metamorphosis of the brittle star *Ophiocoma pumila*: evolutionary and ecological implication. Biol Bull 168: 285–295

13 Mortensen Th (1898) Die Echinodermenlarven der Plankton-Expedition nebst neiner systematischen Revision der bisher bekannten Echinodermenlarven. Ergebnis Plankton-Exped Humboldt-Stift 2J: 1–118

14 Mortensen Th (1921) Studies of the Development and Larval Forms of Echinoderms. GEC Gad, Copenhagen, pp 261

15 Mortensen Th (1938) Contributions to the study of the development and larval forms of Echinoderms IV. Kgl Dan Vidensk Selsk Skr, Naturvid Math Afd, Ser 9, 7(3): 1–45

16 Müller J (1850) Ueber die Larven und die Metamorphose der Echinodermen. Dritte Abhandlung Abhandl Konigl Preuss Akad Wiss Berlin, 1849: 35–72

17 Oguro C, Shōsaku T, Komatsu M (1982) Development of the brittle-star, *Amphiolis japonica* Matsumoto In "Echinoderms" Ed by JM Lawrence, AA Balkema, Rotterdam, pp 491–496

18 Patent DH (1970) The early embryology of the basket star *Gorgonocephalus caryi* (Echinodermata, Ophiuroidea). Mar Biol 6: 262–267

19 Stancyk SE (1973) Development of *Ophiolepis elegans* (Echinodermata: Ophiuroidea) and its implications in the estuarine environment. Mar Biol 21: 7–12

20 Strathmann MF, Rumrill SS (1987) Phylum Echi-

nodermata, Class Ophiuroidea In "Reproduction and Development of Marine Invertebrates of the North Pacific Coast" Ed by MF Strathmann, The Univ Was Press, USA, pp 556–573

21 Yamashita M (1985) Embryonic development of the brittle-star *Amphipholis kochii* in laboratory culture. Biol Bull 169: 131–142

ZOOLOGICAL SCIENCE 10: 307–312 (1993)

Maitotoxin Induces Acrosome Reaction and Histone Degradation of Starfish *Asterina pectinifera* Sperm

Tosikazu Amano, Yishihito Okita[1], Takeshi Yasumoto2[2] and Motonori Hoshi[3]

Department of Life Science, Faculty of Bioscience and Biotechnology, Tokyo Institute of Technology, Nagatsuda, Midori-ku, Yokohama 227, Japan [2]Department of Biological Chemistry, Faculty of Agriculture, Tohoku University, Tsutsumidori-Amemiyamachi, Aoba-ku, Sendai 981, Japan

ABSTRACT—Maitotoxin (MTX) is a marine toxin which presumably activates Ca^{2+}-channels and stimulates phosphoinositide breakdown in various mammalian cells. We report here that MTX induces the acrosome reaction of starfish spermatozoa by a cooperative action with a diffusible fraction of the egg jelly. MTX alone does induce the degradation of sperm histones. Both reactions induced by MTX depend on extracellular Ca^{2+}. Verapamil, a Ca^{2+}-channel antagonist, inhibits MTX-induced acrosome reaction but not affects MTX-induced histone degradation. MTX bypasses the blockage by ARIS of the jelly-induced acrosome reaction and histone degradation.

INTRODUCTION

Changes in ion permeability of plasma membrane regulate sperm reactions to extracellular signals [6, 11, 27–29]. Egg jelly, with which spermatozoa interact first in the echinoderms, triggers Na^+- and Ca^{2+}-influx, and K^+- and H^+-efflux in spermatozoa, and eventually induces the acrosome reaction [19, 27, 28]. We have reported that the egg jelly also induces the degradation of sperm histones in the starfish, *Asterina pectinifera* [1]. Both reactions are induced by a cooperative action of homologous ARIS, a fucose sulfate rich glycoprotein having an extremely large molecular weight, and a diffusible fraction of the egg jelly (M8) containing Co-ARIS and sperm-activating peptides (SAP) [2, 14, 15, 17, 20, 22, 24, 26]. The acrosome reaction and the histone degradation induced by the egg jelly depend upon extracellular Ca^{2+} and are inhibited by Ca^{2+}-channel antagonists, suggesting that Ca^{2+}-influx via Ca^{2+}-channels plays important roles in these reactions [1]. However, A23187, a Ca^{2+} ionophore which induces the acrosome reaction of sea urchin sperm is not effective to induce the acrosome reaction and the histone degradation of *Asterina pectinifera* sperm [1]. It induces these reactions only in combinations with monensin or M8 (1; unpublished results). These results suggest that an increase in the intracellular Ca^{2+} concentration ($[Ca^{2+}]i$) is essential but not sufficient to induce the acrosome reaction and histone degradation. Although these reactions of *Asterina pectinifera* sperm are induced by a cooperative action of ARIS and Co-ARIS [3], several lines of evidence indicate that two reactions are regulated by distinct pathways at least partly [1, 2].

Maitotoxin (MTX) has been isolated from a poisonous marine dinoflagellate, *Gambierdiscus toxicus* [23]. MTX stimulates the uptake of Ca^{2+} in various cells [4, 10, 16, 18, 30, 32] and elicits phosphoinositide breakdown in several cell lines [5, 12, 13]. Effects of MTX absolutely depend upon extracellular Ca^{2+}. In most cells, the stimulation of Ca^{2+}-uptake by MTX is blocked by Ca^{2+}-channel antagonists [16, 32], and therefore it

Accepted October 10, 1992
Received September 21, 1992
[1] Present address: Suntory Pharmatech Center, Chiyodamachi, Gunma 370-05, Japan
[3] To whom all correspondence should be addressed.

is proposed that MTX is a direct activator of Ca^{2+}-channels [32]. In contrast to this, the stimulation of phosphoinositide breakdown by MTX is not affected by a variety of organic and inorganic Ca^{2+}-channel blockers [5, 12, 13].

In the starfish, *Asterias amurensis,* it is reported that, in alkaline seawater, MTX triggers only a part of acrosome reaction: it induces acrosomal exocytosis but not the formation of perfect acrosomal process [25].

In this paper, we show that MTX is effective to induce normal acrosome reaction in *Asterina pectinifera* and the effect of MTX on inducing the acrosome reaction is greatly enhanced by M8 and is susceptible to verapamil. MTX also initiates the degradation of sperm histones in a verapamil-insensitive manner.

MATERIALS AND METHODS

Artificial seawater, jelly components and drugs

Normal artificial seawater (ASW) consisted of 450 mM NaCl, 10 mM KCl, 10 mM $CaCl_2$, 30 mM $MgCl_2$, 20 mM $MgSO_4$, 15 mM N-2-hydroxyethylpiperazine-N′-propanesulfonic acid-NaOH, pH 8.2. Ca^{2+}-free seawater (CFSW) was prepared as above except for omitting $CaCl_2$.

Egg jelly, ARIS and M8 were prepared as previously described [1, 3]. Verapamil was dissolved in DMSO to make a 200 mM stock solution. For the control, an equal concentration of DMSO (1%) was run. MTX was dissolved in distilled water at a concentration of 300 μg/ml (87.6 μM), and diluted in ASW or CFSW.

Assays of the acrosome reaction and the histone degradation

Spermatozoa of the starfish, *Asterina pectinifera* were collected "dry" and kept on ice until use. Assays of the acrosome reaction and the histone degradation were performed as previously described [1, 3]. Spermatozoa with an acrosomal process were scored as "reacted". Each experiment was repeated at least two different batches of sperm.

RESULTS

Effects of MTX on starfish spermatozoa: It has been reported that MTX (0.06–0.73 μM) does not induce the acrosome reaction of *Asterias amurensis* spermatozoa in normal seawater, but that it induces only the acrosomal exocytosis in alkaline seawater (pH 9.5) [25]. We examined first the effects of MTX on the acrosome reaction and the histone degradation in *Asterina pectinifera.* MTX (0.6 μM) induced the acrosome reaction considerably, although at the concentration of 0.3 μM its effect was not appreciable (Table 1). Induction of the acrosome reaction by MTX was greatly enhanced by M8 but not by ARIS (Table 1). MTX-induced acrosome reaction was quite normal in the morphology (Data not shown). It required external Ca^{2+} and was completely blocked by 200 μM verapamil (Table 1).

Table 1. Induction of the acrosome reaction by MTX

Treatments	Acrosome Reaction (% Control)*
Jelly	100
ARIS+M8	82
ARIS	9
M8	0
MTX (0.6 μM)	78
+verapamil**	3
MTX (0.3 μM)	12
+ARIS	19
+M8	56
+M8 in CFSW	0
+M8+verapamil**	4

Sperm were treated with egg jelly (100 μg fucose/ml), ARIS (50 μg/ml), M8 (62.5 μg/ml) or combinations of them for 3 min and fixed for microscopic observation. *The percentage of jelly-induced acrosome reaction was referred as 100%. Values are means for two experiments. **Sperm were pretreated with verapamil (200 μM) for 3 min and then MTX plus M8, or MTX, was added to the sperm suspension.

In contrast to the acrosome reaction, the histone degradation was much sensitive to MTX: 0.3 μM of MTX induced the histone degradation as well as

TABLE 2. Induction of the histone degradation by MTX

Treatments	Histone H1 Degradation (%)
Jelly	52
ARIS	9
M8	2
MTX (0.6 μM)	64
+M8	73
+verapamil*	61
MTX (0.3 μM)	42
+ARIS	61
+M8	56

Sperm were treated with egg jelly (50 μg fucose/ml), ARIS (50 μg/ml) or M8 (25 μg/ml) and incubated for 60 min. Reactions were stopped by the addition of an equal volume of sample buffer for SDS-polyacrylamide gel electrophoresis.
* Sperm were pretreated with verapamil (200 μM) for 3 min and then MTX was added to the sperm suspension.

the egg jelly did (Table 2). Neither ARIS nor M8 significantly enhanced the effect of MTX on the histone degradation. MTX-induced histone degradation also required external Ca^{2+}, but it was not blocked by 200 μM verapamil (Table 2).

Sequential treatments of MTX and egg jelly components: It is known that spermatozoa treated with either ARIS or M8 become unresponsive to the egg jelly [2, 14, 21]. We examined whether MTX also showed a similar "pretreatment effect". As shown in table 3, when sperm were pretreated for 3 min with an insufficient concentration of MTX (0.3 μM) to induce the acrosome reaction, they did not undergo the acrosome reaction by the addition of M8. In response to the egg jelly they underwent the acrosome reaction, but much less than intact spermatozoa did (Table 3). ARIS-pretreated spermatozoa, which were unresponsive to the egg jelly, underwent the acrosome reaction in response to a mixture of MTX and M8 (Table 3).

Similarly, ARIS-pretreated spermatozoa did not undergo the histone degradation in response to the egg jelly [2] but they did so in response to MTX (Table 4). Previous study has shown that concanavalin A (Con A) specifically inhibits the jelly-induced histone degradation [1]. Thus, we examined the effects of Con A on the MTX-induced histone degradation. As shown in table 4, Con A (0.2 mg/ml) blocked the jelly-induced histone degradation but did not affect the MTX-induced one.

TABLE 3. Effects of sequential treatments of MTX and jelly components on the acrosome reaction

Treatments 1st	Treatments 2nd	Acrosome Reaction (% Control)*
—	Jelly	100
—	MTX+M8	56
ARIS	Jelly	23
ARIS	MTX+M8	70
MTX	Jelly	38
MTX	M8	6

Sperm were preincubated with ARIS (50 μg/ml) or MTX (0.3 μM) for 3 min and then egg jelly (100 μg fucose/ml), a mixture of MTX (0.3 μM) and M8 (62.5 μg/ml), or M8 (62.5 μg/ml) was added to the sperm suspension. The mixtures were incubated for another 3 min and fixed.
* The percentage of jelly-induced acrosome reaction was referred as 100%. Values are means for two experiments.

TABLE 4. Effects of sequential treatments of MTX and jelly components on the histone degradation

Treatments 1st	Treatments 2nd	Histone H1 Degradation (%)
—	Jelly	52
ARIS	Jelly	11
ARIS	MTX	70
Con A	Jelly	18
Con A	MTX	83

Sperm were treated with ARIS (50 μg/ml) or Con A (0.2 mg/ml) for 3 min, and then egg jelly (50 μg fucose/ml) or MTX (0.3 μM) was added to the sperm suspension. The mixtures were incubated for another 60 min and incubations were stopped by addition of sample buffer for SDS-polyacrylamide gel electrophoresis.

DISCUSSION

External Ca^{2+} is essential for inducing the acrosome reaction and histone degradation by the egg jelly in starfish spermatozoa [1, 21]. Pharmacolo-

gical studies suggest the involvement of voltage-dependent Ca^{2+}-channels in these reactions [1]. We have reported here that MTX (0.6 μM) induces morphologically normal acrosome reaction in *Asterina pectinifera*. This concentration is much higher than effective doses for mammalian cells, but it is comparable to that for the acrosomal exocytosis in *Asterias amurensis* [25]. Echinoderm sperm are generally much less sensitive to various drugs than mammalian cells. The effect of MTX on the acrosome reaction was greatly enhanced by simultaneous addition of M8 but not by ARIS. Similar to the stimulation of Ca^{2+}-uptake by MTX in various cells [16, 32], the acrosome reaction induced by MTX with or without M8 required extracellular Ca^{2+} and was completely blocked by verapamil. This suggests that MTX induces the acrosome reaction by activating Ca^{2+}-channels.

From the present data, we do not know exact roles of M8 in stimulation of MTX-induced acrosome reaction. It seems reasonable to assume that M8 facilitates the opening of Ca^{2+}-channels and/or other intracellular changes that are essential for complete acrosome reaction. The acrosome reaction consists of the acrosomal exocytosis and process formation [7, 8, 33]. Like many other exocytotic events, acrosomal exocytosis probably requires an increase in $[Ca^{2+}]i$. The process formation is thought to be regulated by an increase in intracellular pH (pHi) [31, 34]. Actually, in sea urchin sperm, both Ca^{2+}-uptake and a pHi increase can not be dissociated from the acrosome reaction. It is reported that MTX induces the acrosomal exocytosis significantly, but the process formation slightly, in mussel sperm at normal pH (8.0) and in *Asterias amurensis* sperm at pH 9.5 [25]. A Ca^{2+}-ionophore A23187 did not initiate the acrosome reaction in *Asterina pectinifera* [1]. Thus we think that an increase in $[Ca^{2+}]i$ is essential but not sufficient to induce the acrosome reaction of starfish spermatozoa. It is known in *Asterias amurensis* that ARIS and Co-ARIS induce the acrosome reaction without any detectable pHi increase, and SAP stimulates the reaction by increasing the pHi [14, 20, 22]. Stimulation by M8 of MTX-induced acrosome reaction in *Asterina pectinifera* suggests that M8 induces some other intracellular changes also required for the acrosome reaction, such as a pHi increase.

Pretreatment of sperm with MTX remarkably decreased the egg jelly-induced acrosome reaction suggesting that MTX induces irreversible changes in sperm, which may participate in the jelly-induced acrosome reaction. MTX plus M8 bypassed the blockage of the jelly-induced acrosome reaction in ARIS-pretreated spermatozoa suggesting that ARIS-pretreatment did not irreversibly inactivate MTX-sensitive Ca^{2+}-channels. Two mutually non-exclusive working hypotheses are being considered: (I) ARIS directly makes Ca^{2+}-channels unresponsive to the jelly, but MTX can activate ARIS-modified Ca^{2+}-channels. (II) ARIS acts on a site upstream to the MTX-site(s), which indirectly regulates Ca^{2+}-channels.

MTX was also effective to induce the histone degradation. This effect of MTX was not enhanced by M8 nor affected by verapamil. These results suggest that the action site of MTX for the histone degradation is different from that for the acrosome reaction. This is consistent with the hypothesis that two reactions are controlled by distinct pathways at least partly [1, 2]. It has been proposed that MTX is a potent activator of phosphoinositide breakdown and that Ca^{2+}-channel blockers hardly inhibit this effect [5, 12, 13]. It has been also reported that egg jelly promotes the formation of inositol 1,4,5-triphosphate in sea urchin spermatozoa [9]. Taking these into account, there is a possibility that MTX-induced phosphoinositide-breakdown in sperm cells triggers the histone degradation. Therefore, important questions to be answered are whether phosphoinositide breakdown is induced by the egg jelly also in starfish spermatozoa and, if so, whether it is involved in the induction of histone degradation.

Preincubation of sperm with Con A inhibits jelly-induced histone degradation [1] but it did not affect the MTX-induced one. MTX bypassed the blockage of the jelly-induced histone degradation in ARIS-pretreated sperm. These results suggest that the MTX-sensitive and verapamil-insensitive step in the reaction pathway leading to the histone degradation is later than the action sites of ARIS and Con A, or that MTX induces the histone degradation by a quite different way from the egg jelly does.

It is to be answered how and at which step, the two sperm reactions are linked together.

ACKNOWLEDGMENTS

We thank Dr. Ikegami of Hiroshima University for generous supply of the animals. This work was supported by the Grant-in-Aid for Scientific Research on Priority Areas No. 03207103 from the Ministry of Education, Science and Culture Japan.

REFERENCES

1 Amano T, Okita Y, Hoshi M (1992) Treatment of starfish sperm with egg jelly induces the degradation of histones. Develop Growth and Differ 34: 99–106

2 Amano T, Okita Y, Matsui T, Hoshi M (1992) Pretreatment effects of jelly components on the sperm acrosome reaction and histone degradation in the starfish, *Asterina pectinifera*. Biophys Biochem Res Commun 187: 268–273

3 Amano T, Okita Y, Okinaga T, Matsui T, Nishiyama I, Hoshi M (1992) Egg jelly components responsible for histone degradation and acrosome reaction in the starfish, *Asterina pectinifera*. Biophys Biochem Res Commun 187: 274–278

4 Anderson JM, Yasumoto T, Cronin MJ (1987) Intracellular free calcium in rat anterior pituitary cells monitored by fura-2. Life Sci 41: 519–526

5 Berta P, Sladeczek F, Derancourt J, Durand M, Travo P, Haiech J (1986) Maitotoxin stimulates the formation of inositol phosphates in rat aortic myocytes. FEBS Lett 197: 349–352

6 Collins F, Epel D (1977) The role of calcium ions in the acrosome reaction of sea urchin sperm. Exp Cell Res 106: 211–222

7 Dan J C (1952) Studies on the acrosome. I. Reaction to egg-water and other stimuli. Biol Bull 103: 54–66

8 Dan JC (1954) Studies on the acrosome. III. Effect of calcium deficiency. Biol Bull 107: 335–349

9 Domino SE, Garbers DL (1988) The fucose-sulfate glycoconjugate that induces an acrosome reaction in spermatozoa stimulates inositol 1,4,5-trisphosphate accumulation. J Biol Chem 263: 690–695

10 Freedman SB, Miller RJ, Miller DM, Tindall DR (1984) Interactions of maitotoxin with voltage-sensitive calcium channels in cultured neuronal cells. Proc Natl Accad Sci USA 81: 4582–4585

11 Gonzalez-Martinez M, Darszon A (1987) A fast transient hyperpolarization occurs during the sea urchin sperm acrosome reaction induced by egg jelly. FEBS Lett 218: 247–250

12 Gusovsky F, Yasumoto T, Daly JW (1987) Maitotoxin stimulates phosphoinositide breakdown in neuroblastoma hybrid NCB-20 cells. Cell Mol Neurobiol 7: 317–322

13 Gusovsky F, Yasumoto T, Daly JW (1989) Maitotoxin, a potent, general activator of phosphoiositide breakdown. FEBS Lett 243: 307–312

14 Hoshi M, Matsui T, Nishiyama I, Amano T, Okita Y (1988) Physiological inducers of the acrosome reaction. Cell Differ and Develop 25(suppl.): 19–24

15 Ikadai H, Hoshi M (1981) Biochemical studies on the acrosome reaction of starfish *Asterias amurensis*. I. Factors participating in the acrosome reaction. Develop Growth and Differ 23: 73–80

16 Ikadai H, Hoshi M (1981) Biochemical studies on the acrosome reaction of starfish *Asterias amurensis*. II. Purification and characterization of acrosome reaction-inducing substance. Develop Growth and Differ 23: 81–88

17 Kobayashi M, Kondo S, Yasumoto T, Ohizumi Y (1986) Cardiotoxic effects of maitotoxin, a principal toxin of seafood poisoning, on guinea pig and rat cardiac muscle. J Pharmacol Exp Ther 238: 1077–1083

18 Lebrun P, Hermann M, Yasumoto T, Herchisely A (1987) Effects of maitotoxin on ionic and secretory events in rat pancreatic islets. Biophys Biochem Res Commun 144: 172–177

19 Lee HC, Johnson C, Epel D (1983) Changes in internal pH associated with initiation of motility and acrosome reaction of sea urchin sperm. Develop Biol 95: 31–45

20 Matsui T, Nishiyama I, Hino A, Hoshi M (1986) Induction of the acrosome reaction in starfish. Develop Growth and Differ 28: 339–348

21 Matsui T, Nishiyama I, Hino A, Hoshi M (1986) Acrosome reaction-inducing substance purified from the egg jelly inhibits the jelly-induced acrosome reaction in starfish: An apparent contradiction. Develop Growth and Differ 28: 349–357

22 Matsui T, Nishiyama I, Hino A, Hoshi M (1986) Intracellular pH changes of starfish sperm upon the acrosome reaction. Develop Growth and Differ 28: 359–368

23 Murata M, Iwashita T, Yokoyama A, Sasaki M, Yasumoto T (1992) Partial structures of maitotoxin, the most potent marine toxin from dinoflagellate *Gambierdiscus toxicus*. J Am Chem Soc 114: 6594–6596

24 Nishiyama I, Matsui T, Hoshi M (1987) Purification of Co-ARIS, a cofactor for acrosome reaction-inducing substance from the egg jelly of starfish. Develop Growth and Differ 29: 161–169

25 Nishiyama I, Matsui T, Yasumoto T, Oshio S, Hoshi M (1986) Maitotoxin, a presumed calcium channel activator, induces the acrosome reaction in mussel spermatozoa. Develop Growth and Differ 28: 443–448

26 Okinaga T, Ohashi Y, Hoshi M (1992) A novel saccharide structure, Xyl-3Gal1-(SO_3^-)3,4Fuc-, is present in acrosome reaction-inducing substance (ARIS) of the starfish, *Asterias amurensis*. Biophys Biochem Res Commun 186: 405–410

27 Schackmann RW, Christen R, Shapiro BM (1981) Membrane potential depolarization and increased intracellular pH accompanying the acrosome reaction of sea urchin sperm. Proc Natl Accad Sci USA 78: 6066–6076

28 Schackmann RM, Eddy EM, Shapiro BM (1978) The acrosome reaction of *Strongylocentrotus purpuratus* sperm: Ion movements and requirements. Develop Biol 65: 483–495

29 Schackmann RW, Shapiro BM (1981) A partial sequence of ionic changes associated with the acrosome reaction of *Strongylocentrotus purpuratus*. Develop Biol 81: 145–154

30 Schettini G, Koike K, Login IS, Judd AM, Cronin MJ, Yasumoto T, MacLeod RM (1984) Maitotoxin stimulates hormonal release and calcium flux in rat anterior pituitary cells in vitro. Am J Physiol 247: E520–E525

31 Schroeder TE, Christen R (1982) Polymerization of actin without acrosomal exocytosis in starfish sperm. Visualization with NBD-phallacidin. Exp Cell Res 140: 363–371

32 Takahashi M, Ohizumi Y, Yasumoto T (1982) Maitotoxin, a Ca^{2+} channel activator candidate. J Biol Chem 257: 7287–7289

33 Tilney LG (1985) The acrosome reaction. In "Biology of Fertilization Vol 2" Ed by Metz CB, Monroy A Academic Press, Orlando, pp 157–213

34 Tilney LG, Kiehart DP, Sardet C, Tilney M (1978) Polimerization of actin. IV. The role of Ca^{2+} and H^+ in the assembly of actin and in membrane fusion in the acrosome reaction of echinoderm sperm. J Cell Biol 77: 536–550

ZOOLOGICAL SCIENCE 10: 313–319 (1993)

Reproduction by Overwintering Adults of Water Strider, *Aquarius paludum* (Fabricius)

Tetsuo Harada[1]

Department of Biology, Faculty of Science, Osaka City University, Osaka 558, Japan

ABSTRACT—Overwintering adults of a water strider, *Aquarius paludum* having the macropterous and brachypterous wing forms continued to lay eggs for about 35 days in spring. The oviposition occurred at a high and constant rate under quasi-natural conditions. There was no significant difference between the two wing forms with respect to the number of eggs throughout their most reproductive period. Some of the second generation adults which had overwintered after reproduction in the previous autumn also became reproductively active in the following spring together with the third and diapause generation adults. In early spring, macropterous adults appeared on the water surface later than brachypterous adults, demonstrating the longer distance between diapause sites on land and breeding sites on the water surface in macropterous adults than brachypterous adults.

INTRODUCTION

Among insects, there are many species that are in diapause and overwinter as adults, and the diapause in the adult stage (adult diapause) means that post-emergence development in ovaries does not occur in the female and the ovaries remain small [2]. In most cases of adult diapause, diapause occurs in young and nonparous adults, and the adults became reproductively active after overwintering [2]. Even in reproductive adults, diapause can be induced by suitable cues (e.g., a short-day photoperiod) in a few species of bugs and beetles [6, 9, 11, 16]. However, reproduction after overwintering has never been reported to be induced twice in the same individuals which normally live for less than one year. In some coleopteran species living for several years, adults overwinter in diapause and reproduce repeatedly in successive years in nature, e.g., *Agonum assimile* [10].

Aquarius paludum (Fabricius) is trivoltine and shows alary dimorphism in Kochi, Japan [4, 5]. Although reproductive activity in the first generation continued until death in summer, the females of the second generation entered diapause after a reproductive period in September and October [4]. It is unclear whether the adults of the second generation became reproductively active again in the following spring together with the adults of the third generation.

The present work aims, first, at making this point clear and, second, at studying the appearance on the water surface and the oviposition process by overwintering brachypterous and macropterous adults of *A. paludum* under quasi-natural conditions in spring.

MATERIALS AND METHODS

Overwintering adults of *Aquarius paludum* were collected from a pond in Kochi City (33.3°N, 133.3°E), Japan on the 1st, 4th, 16th, 17th, and 24th of April, and in late September, 1988. The collected water striders were released back into the pond after measurement of wing lengths. Wing length was expressed in terms of the index as per Harada and Taneda [5]. When it was difficult to distinguish macropterous from brachypterous adults by fore-wing lengths, the distinction was made by reference to hind-wing lengths because the two wing forms showed more clear differences

Accepted January 18, 1993
Received October 21, 1992
[1] Department of Biology, Faculty of Science, Kochi University, Kochi 780, Japan

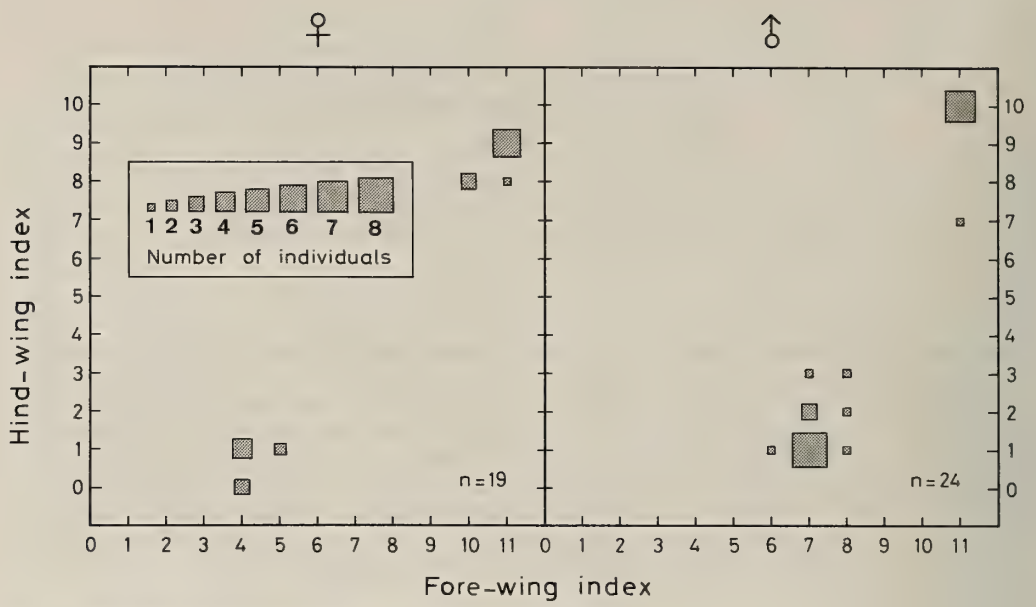

FIG. 1. Fore- and hind-wing lengths of the adults collected from a water way in Kochi in late September, 1988.

in the hind-wing lengths than in the fore-wing lengths (Fig. 1).

Overwintering adults of *A. paludum* were collected in early April, 1991, from the pond. In 1990, fifth instar nymphs of the second generation were collected just before adult emergence from two small canals (A- and B-canal). The water temperature in the A- and B-canal had been higher than 27°C and lower than 22°C, respectively, in the daytime in July and August. Fifth instar nymphs belonging to the third generation were collected from A-canal in mid-October, 1991. Pairs consisting of one male and one female with the same wing form were put just after collection or adult emergence in individual plastic pots, 14 cm in diameter and 5 cm in depth, and reared under quasi-natural conditions in Osaka City (35.0°N, 135.5°E), Japan. Longevity was examined in each pair and the number of eggs was counted every 1–2 days in September, 1990 to May, 1991, and in October, 1991 to May, 1992. The plastic pots were filled with water to a depth of 5–10 mm. A wooden stick, about 10 cm in length and about 1 cm in diameter, was put in each pot for oviposition and resting sites. Water in the pots was replaced daily. Water striders were fed on adult specimens of *Fannia canicularis* or *Lucilia illustris* which were supplied daily at a rate of one fly per two adults.

RESULTS

Overwintering females (mainly the third generation) with either of the two wing forms continued to lay eggs for an average of 36.0 days in spring and then died. Eggs were laid at a constant and high rate (about 60 eggs per 5 days per female) throughout the reproductive period for both wing forms (Fig. 2). The average total number of eggs per female was 386.0 in brachypterous females and 396.7 in macropterous females. Difference in numbers of eggs laid per five days was not significant between the two wing forms (t-test, $P>0.05$) except a period between 16th and 21st May ($P<0.05$). Furthermore, no significant difference was observed between the two wing forms with respect to longevity (t-test, $P>0.05$).

In the second generation, all the reproductive females laid the fertilized eggs in fall. The reproductive females stopped laying eggs between the 21st September and the 31st October, and entered diapause (Fig. 3). None of the pairs in the third generation reproduced in autumn, and all entered diapause (Fig. 3). In early December, the diapause adults of the second and third generations

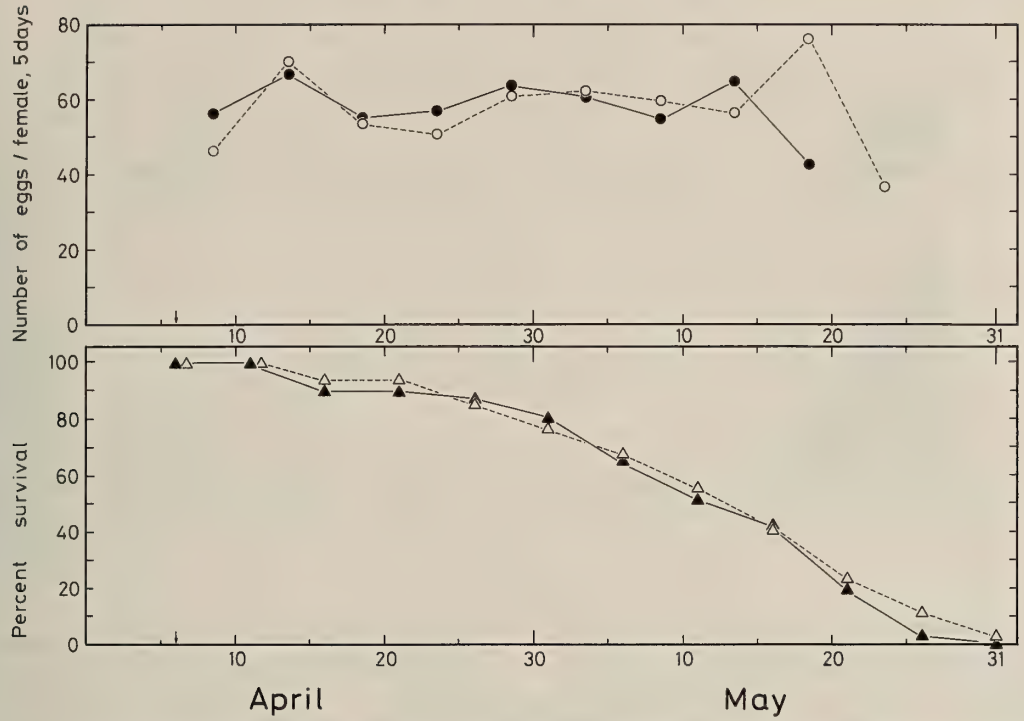

FIG. 2. Survival curves and rates of oviposition for overwintering females (mainly the third generation). Open and solid symbols show brachypterous and macropterous groups, respectively. Arrows show the day on which adults were collected from the pond in Kochi, Japan, 1991. n=34 for brachypterous pairs; n=29 for macropterous pairs.

were transferred onto fallen leaves as overwintering sites. At the beginning of the following March, surviving adults were moved again onto the water surface. For specimens derived from the A-canal, the survival percentage just prior to the move in March was higher in the third generation (females, 84.6%; males, 76.9%) than that in the second generation (females, 21.4%; males, 42.9%) (Fig. 3). In the second generation, when the surviving adults were transferred to the water surface, three pairs were made and the four remaining males were paired with virgin females which had been reared during the nymphal stage under a long-day (14.5L-9.5D) photoperiod at $20\pm2^{\circ}C$. In the third generation, ten pairs were made in early March. The three females in the second generation and surviving five females in the third generation began to lay eggs on average about 2 weeks after the move to the water surface [second generation, 13.3 $\pm$1.5 (S.D.) days; third generation, 15.6$\pm$9.0 (S.D.) days] (Fig. 3). The number of eggs laid after diapause was thought to correlate positively with the number of eggs before diapause, although the correlation could not be inferred statistically because of the insufficient number of samples (Fig. 4A). Both the three overwintering females and the reproductive four females that had been paired with the remaining overwintering males in the second generation laid fertilized eggs in addition to 4 out of 5 females of the third generation.

The proportion of brachypterous adults on the water surface was higher at the beginning than the end of April following overwintering (χ^2-test between 4th and 24th April, $P<0.05$; Fig. 5).

DISCUSSION

Diapause and migration are most closely associated when diapause sites and breeding sites are separated in insects [7]. Water striders are typical examples of this close association. Landin and Vepsäläinen [8] caught many flying long-winged

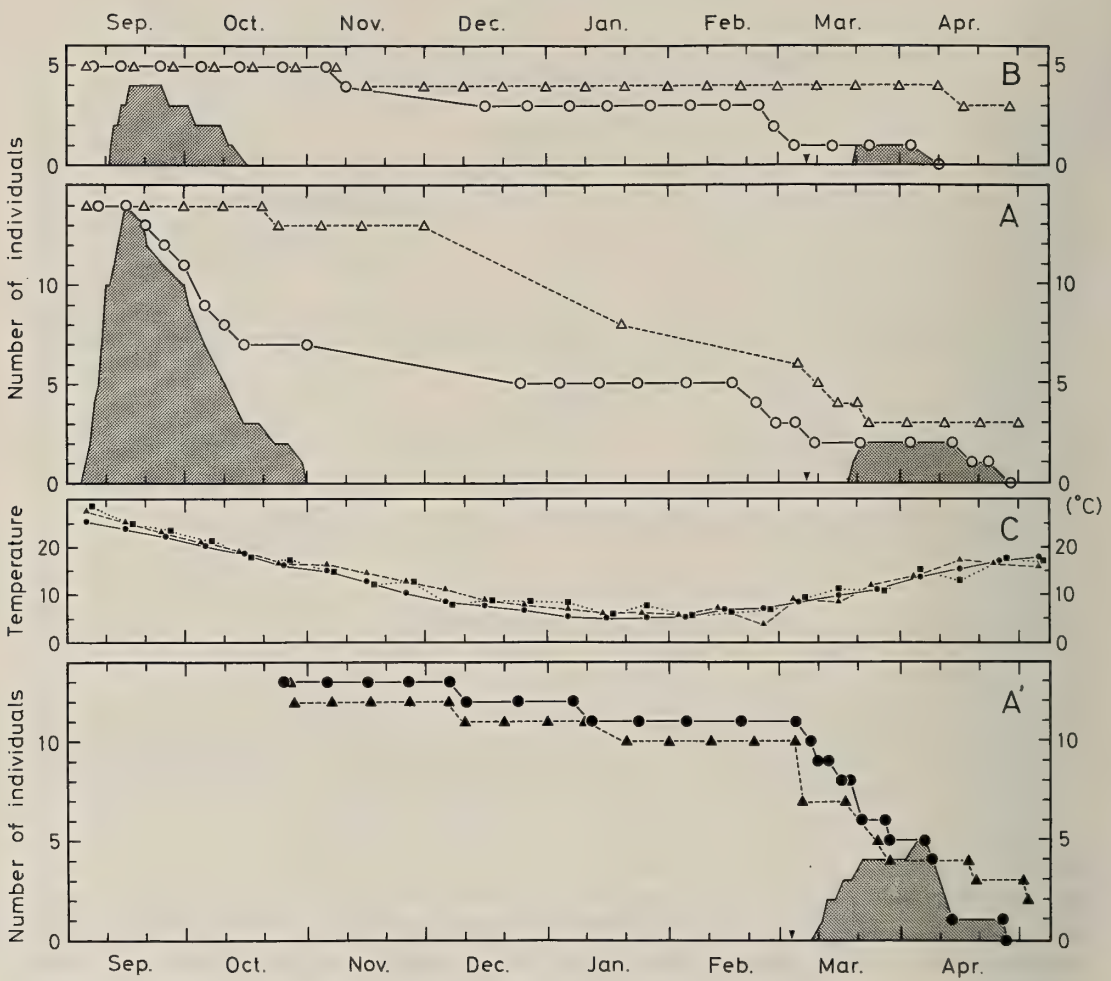

FIG. 3. Survival curves for adults in the second (A, B) and third (A′) generations derived from A- (A, A′) and B-canal (B). All individuals: macropterous. Circles, females; triangles, males. Shaded area shows the number of females which were laying eggs. Arrows indicate the days on which the water striders were transferred from fallen leaves to the water surface in 1991 (A, B) or 1992 (A′). The mean date of adult emergence was 29 August and 15 October in the second and third generations, respectively. C, Seasonal variations in air temperature in Kochi (circles) and Osaka (triangles, squares). The triangles and squares show the means for the first, middle, or last ten days of each month in 1990–1991 and 1991–1992, respectively. The circles indicate the means of the values for 30 years (1961–1990). The data of air temperature were gained by Osaka and Kochi Meteorological observatories.

adults of *Gerris argentatus* on the way from their diapause sites to water surfaces in a meadow on the shore of a lake in Finland. Their capture suggests that the macropterous adults of *G. argentatus* overwintered at sites far from water surfaces. In early spring, no late-awakening from diapause but the long distance between diapause and breeding sites is demonstrated in the case of macropterous adults of *A. paludum* by the following: macropterous adults appear on water surface later than brachypterous adults (Fig. 5), macropterous adults show similar reproductive and survival processes to brachypterous adults (Fig. 2). Moreover, the two facts, the earlier appearance of brachypterous adults (Fig. 5) and the lack of flight ability in the brachyperious having very short hind-wing (Fig. 1), suggest that their diapause sites are near water surface, e.g. under logs or stones on the banks as is the case with *Aquarius remigis* [13].

A high rate of oviposition of more than 60 eggs

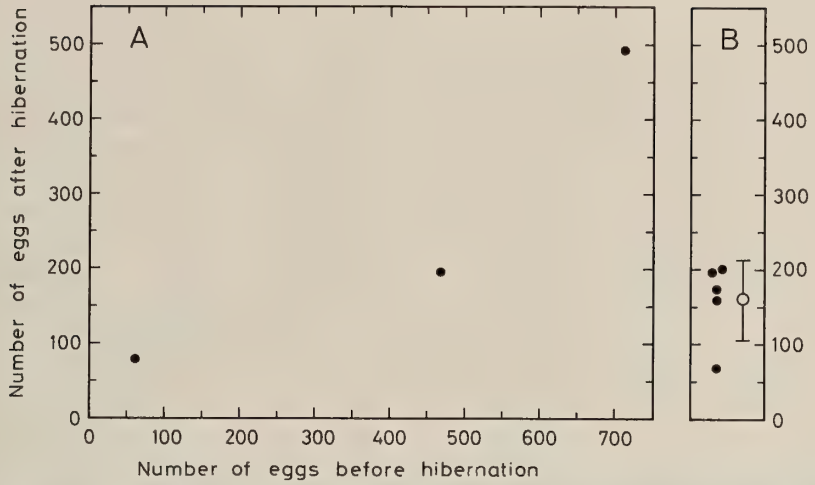

FIG. 4. The total number of eggs laid by each adult before or after overwintering in the second (A) and third (B) generations. The circle and bar in B indicate the mean and S.D., respectively.

per female per 5 days was recorded only during a part of the reproductive period of the first and second generations [4]. However, overwintering adults laid more than 60 eggs per female per 5 days throughout almost their entire reproductive period (Fig. 2). Overwintering adults of *A. paludum* also continue to show strong positive phototaxis for about 50 days in spring [3]. Harada showed experimentally that the experience of overwintering made the adults easy to show the strong positive phototaxis. The overwintering adults of *A. paludum* may be, physiologically, in a specific phase after overwintering. Spence [12] also reported that in some Canadian water striders, *Gerris pingreensis, G. comatus, G. buenoi,* and *Limnoporus dissortis,* diapause breeders showed higher reproductive rates in spring than direct breeders in summer. The experience of overwintering includes the experience of diapause as an internal condition, as well as exposure to low temperature and other winter-related environmental conditions. It is unclear which of these factors is the major one which induces a constant and high rate of oviposition in *A. paludum.*

Spence [12] reported that overwintered macropterous females of *G. pingreensis* had longer pre-oviposition periods than overwintered apterous females, and that their reproductive rate was lower than that of apterous females in early spring. By contrast, there was no difference between the two wing forms in oviposition rates throughout the reproductive period after overwintering in *A. paludum* (Fig. 2). Why do macropterous adults of *A. paludum* continue to lay eggs at the same rate as brachypterous adults, even though macropterous adults seem to expend so much energy during their spring dispersal flight? They may histolyze their wing muscles and their resulting nutrients may be used for the maturation of eggs, as shown in *G. odontogaster* [1], and in *G. lacustris, G. lateralis,* and *G. argentatus* [14].

A high fecundity during the early adult stage was shown in the second generation and that is advantageous for many nymphs of the third generation who can develop into adults before winter comes [4]. The overwintered females of the second generation participated in the reproduction again in the following spring together with third generation females (Fig. 3). The fecundity of the second generation adults was not smaller than that in the third generation (Fig. 4), and moreover the surviving males in the second generation fertilized the eggs in the following spring. Therefore, it seems that diapause after reproduction in autumn and the resulting second reproduction during the subsequent spring are adaptive tactics for the second generation adults to bequeath a larger number of offspring.

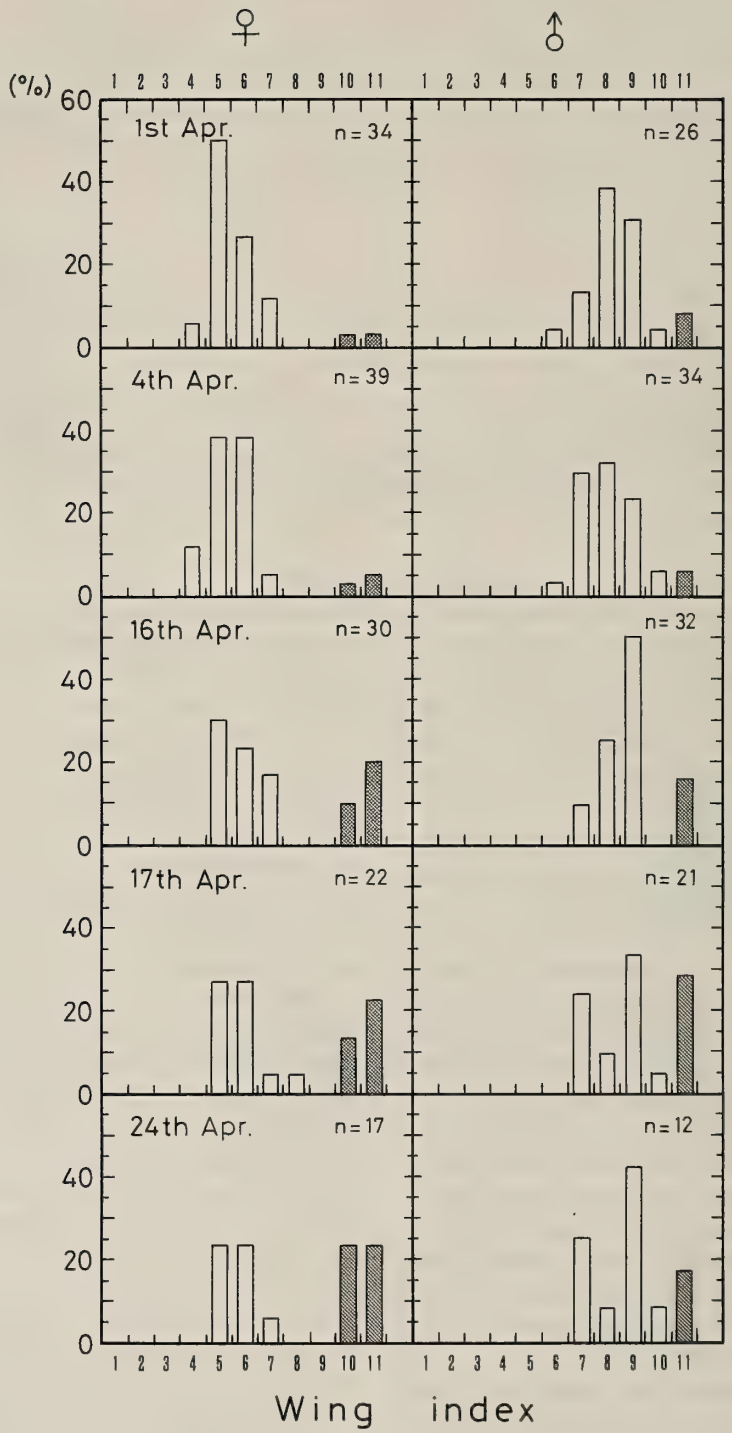

FIG. 5. The appearance of *Aquarius paludum* on the water surface of a pond in Kochi in early spring, 1988. Open bars, brachypterous adults; shaded bars, macropterous adults.

The overwintered (macropterous) adults in both generations laid eggs shortly after the move to water surfaces, although, in our study, the adults were moved to water surfaces earlier than macropterous adults would normally do so in nature (Figs. 3, 5). This earlier reproduction suggests that the water surface as habitat becomes a cue that induces the maturing of the reproductive system. Wilcox and Maier [15] reported that adults of *Aquarius remigis* estivated facultatively during summer in damp areas underneath stream-bed rocks when a pool in a small stream went dry. However, they showed no data on whether the reproductive organs matured or not in the estivated adults. The causal role of the existance of water surfaces in reproductive maturation should be investigated further experimentally on water striders in the future.

ACKNOWLEDGMENTS

I would like to thank Assistant Professor Dr. Hideharu Numata, Osaka City University for his valuable advice.

REFERENCES

1 Andersen NM (1973) Seasonal polymorphism and developmental changes in organs of flight and reproduction in bivoltine pondskaters (Hem. Gerridae). Ent Scand 4: 1–20

2 Danks HV (1987) Insect Dormancy: an Ecological Perspective. Biological Survey of Canada, Ottawa, pp 71–74

3 Harada T (1991) Effects of photoperiod and temperature on phototaxis in a water strider, *Gerris paludu minsularis* (Motschulsky). J Insect Physiol 37: 27–34

4 Harada T (1992) The oviposition process in two direct breeding generations in a water strider, *Aquarius paludum* (Fabricius). J Insect Physiol 38: 687–692

5 Harada T, Taneda K (1989) Seasonal changes in alary dimorphism of a water strider, *Gerris paludum insularis* (Motschulsky). J Insect Physiol 35: 919–924

6 Hodek I (1977) Photoperiodic response in spring in three Pentatomoidea (Heteroptera). Acta Ent Bohemoslov 74: 209–218

7 Kennedy JS (1975) Insect dispersal In "Insects, Science, and Society" Ed by D Pimentel, Academic Press, New York, pp 103–119

8 Landin J, Vepsäläinen K (1977) Spring dispersal flights of pond-skaters *Gerris* spp. (Heteroptera). Oikos 29: 156–160

9 Muraji M, Nakasuji F (1990) Effect of photoperiodic shifts on egg production in a semiaquatic bug, *Microvelia douglasi* (Heteroptera: Veliidae). Appl Ent Zool 25: 405–407

10 Neudecker C, Thiele HU (1974) Die jahreszeitliche Synchronisation der Gonadenreifung bei *Agonum assimile* Payk. (Coleopt. Carab.) durch Temperatur und Photoperiode. Oecologia (Berl.) 17: 141–157

11 Numata H, Hidaka T (1982) Photoperiodic control of adult diapause in the bean bug, *Riptortus clavatus* Thunberg (Heteroptera: Coreidae). I. Reversible induction and termination of diapause. Appl Ent Zool 17: 530–538

12 Spence JR (1989) The habitat templet and life history strategies of pond skaters (Heteroptera: Gerridae): reproductive potential, phenology, and wing dimorphism. Can J Zool 67: 2432–2447

13 Torre-Bueno JR de la (1917) Life-history and habits of the larger waterstrider, *Gerris remigis* Say. Entomol New 28: 201–208

14 Vepsäläinen K, Patama T (1983) Allocation of reproductive energy in relation to the pattern of environment in five *Gerris* species In "Diapause and Life Cycle Strateries in Insects" Ed by VK Brown and I Hodek, Dr W. Junk Publishers, The Hague, pp 189–207

15 Wilcox RS, Maier HA (1991) Facultative estivation in the water strider *Gerris remigis*. Can J Zool 69: 1412–1413

16 Zaslavsky VA (1975) [The distribution of stepwise photoperiod reactions among Insecta and Acari.] Ent Obozr 54: 291–304 (In Russian) [Translation in Ent Rev 54: 36–45]

ZOOLOGICAL SCIENCE 10: 321–328 (1993)

Prostaglandins and Sex Steroids from Reptilian (*Podarcis sicula sicula*) Ovarian Follicles at Different Developmental Stages

Anna Gobbetti, Massimo Zerani, Maria Maddalena Di Fiore[1] and Virgilio Botte[1]

Department of Molecular, Cellular, and Animal Biology, University of Camerino, 62032 Camerino MC, Italy, and [1]Department of Zoology, University of Naples, 80134 Naples, Italy

ABSTRACT—Prostaglandin $F_{2\alpha}$ ($PGF_{2\alpha}$), prostaglandin E_2 (PGE_2), progesterone, androgens, and estradiol-17β *in vitro* basal release by follicles of the oviparous lizard, *Podarcis s. sicula* was studied; in addition, the *in vitro* effect of $PGF_{2\alpha}$ and PGE_2 on sex steroid release was evaluated. Follicles were divided according to the different vitellogenic developmental stages: pre-vitellogenic, early-vitellogenic, mid-vitellogenic and fully-grown. $PGF_{2\alpha}$ and progesterone basal release was highest in fully-grown follicles; PGE_2 and estradiol basal release was highest in early-vitellogenic follicles; androgens basal release was detectable in mid-vitellogenic and fully-grown vitellogenic follicles only. $PGF_{2\alpha}$ increased progesterone release by fully-grown follicles; PGE_2 increased estradiol release by all follicle types, except by early-vitellogenic ones. The present data suggest that $PGF_{2\alpha}$ and PGE_2 exert different roles on follicles: $PGF_{2\alpha}$ seems to induce ovulation through the mediation of progesterone, while PGE_2 seems to be implied in the start and the sustaining of oocyte vitellogenic development through the mediation of estradiol.

INTRODUCTION

In mammals, prostaglandins (PGs) of both F and E series modulate the ovary function, including steroidogenesis [6, 9, 18, 29]. PGs intervene in ovulation and oviduct relax in birds [1, 30]. As regards oviparous reptiles, oviposition is correlated with a dramatic elevation of prostaglandin F (PGF) and prostaglandin E_2 (PGE_2) in the loggerhead turtle, *Caretta caretta* [20] and the tuatara, *Sphenodon punctatus* [19]; $PGF_{2\alpha}$ exhibits luteolytic effects in the lizard, *Anolis carolinensis* [21], and the snapping turtle, *Chelydra serpentina* [24], determining a decline in plasma progesterone. Little is known about the involvement of PGs in the vitellogenic development of follicles in reptiles, and, in particular, nothing is known about the role of PGs on the reproductive processes of the oviparous lizard, *Podarcis sicula sicula,* even if the reproductive cycle of this lizard has been well studied [2, 3, 10].

In this study we have compared the $PGF_{2\alpha}$, PGE_2, progesterone, androgens, and estradiol-17β *in vitro* basal releases by follicles, at different vitellogenic developmental stages, of the lizard, *Podarcis s. sicula*; in addition, the *in vitro* effect of $PGF_{2\alpha}$ and PGE_2 on progesterone, androgens, and estradiol-17β releases by the same follicles has been examined.

MATERIALS AND METHODS

Animals The reproductive cycle of the female lizard, *Podarcis s. sicula,* living in the sourroundings of Naples (Campania, Italy, 25–75 m above sea level) is here briefly described. From the end of summer to the beginning of the next spring (stasis), gonads and genital apparatus are quiescent; then, soon after emerging, the ovary and oviduct undergo recovery and reach their full growth from March to mid-May (recovery period);

Accepted November 9, 1992
Received September 18, 1992

ovulation and egg deposition occur from mid-May to July (ovulatory period); after deposition, gonads and oviduct regress (postovulatory period) [2, 3, 10].

Adult female lizards, *Podarcis s. sicula,* of this population were captured in May and transferred to laboratory terraria, maintained in ambient photothermal conditions (L/D: 15/9; 18°C), and fed with meal worms and fresh vegetables *ad libitum.*

In vitro incubations of follicles The lizards were sacrificed by decapitation, the developmental stage of the reproductive organs was observed and the ovaries rapidly removed. Follicles were freed under dissection microscope and placed in cold Dulbecco's modified Eagle medium (DME, Sigma, USA) containing 10 mM Hepes, 1 mg Penicillin/ml and 2 mg Streptomycin/ml. Follicles were divided according to the different vitellogenic developmental stages: pre-vitellogenic (500–1000 μm ϕ), early-vitellogenic (1500–3000 μm ϕ), mid-vitellogenic (4000–6000 μm ϕ) and fully-grown (>8000 μm ϕ). The follicles were placed in multiple tissue culture plates (Beckton Dickinson, USA); each well contained one follicle. Six follicles of each type were divided into 3 experimental groups (each consisting of 2 wells). The experimental groups were: a) follicle with DME alone; b) follicle with DME plus $PGF_{2\alpha}$ (150 ng); c) follicle with DME plus PGE_2 (150 ng). The final volume of each well was 1 ml. Culture plates were wrapped with aluminium foil and incubated in a shaking water bath (32°C), set at 30 rpm. One well of each experimental group was removed, respectively, after 3 and 6 hr of incubation. The incubation medium samples were immediately stored at −20°C for later hormone determination. In addition, the experiment was repeated without follicles. Tests on 5 parallel incubation sets were carried out. Preliminary evidence led our choosing to the incubation conditions and the $PGF_{2\alpha}$ or PGE_2 minimum effective dose utilized in the present *in vitro* study (data not shown).

$PGF_{2\alpha}$, PGE_2, progesterone, androgens, and estradiol-17β determination $PGF_{2\alpha}$ and PGE_2 were determined in incubation medium samples by radioimmunoassay (RIA) [12, 13]. The determinations were carried out on duplicate incubation medium samples (500 μl) that were extracted with 5 ml of diethyl ether for 4 min. The organic fractions were transferred into glass tubes and evaporated to dryness under a nitrogen stream. The extracts were resuspended with 1 ml of assay buffer and assayed. The recovery of labelled $PGF_{2\alpha}$ and PGE_2 were 83.3±1.3% and 88.8± 1.7%, respectively. Parallelism among the standard curve in buffer, a standard curve in incubation medium (then extracted) and a serial dilution of a single medium sample (extracted) were constant.

Concentrations of progesterone, androgens and estradiol-17β in incubation media were determined by RIA in accordance with methods previously reported [7, 13].

The following sensitivities were recorded: $PGF_{2\alpha}$ 13 pg (intraassay variability: 7.5%; interassay variability: 14.5%); PGE_2, 15.5 pg (intraassay variability: 7.0%; interassay variability: 12.5%); progesterone, 9 pg (intraassay variability: 8.0%; interassay variability: 10.0%); androgens, 7.5 pg (intraassay variability: 6.0%; interassay variability: 11.5%); estradiol-17β, 7 pg (intraassay variability: 8.5%; interassay variability: 13.0%). $PGF_{2\alpha}$, progesterone, testosterone, and estradiol-17β antisera were provided by Dr. G. F. Bolelli and Dr. F. Franceschetti (CNR-Physiopathology of Reproduction Service, University of Bologna, Italy). The PGE_2 antiserum was purchased from Cayman Chemical (USA). Testosterone was not separated from 5α-dihydrotestosterone; therefore, the antiserum used is not specific and the data are expressed as androgens. Tritiated $PGF_{2\alpha}$, PGE_2, progesterone, testosterone, and estradiol-17β were purchased from Amersham International (UK) and non-radioactive $PGF_{2\alpha}$, PGE_2, progesterone, testosterone, and estradiol-17β from Sigma.

Statistics Data relative to each hormone were submitted to analysis of variance (ANOVA) followed by Duncan's multiple range test [8, 31]. Correlation coefficients followed the procedures of Scossiroli and Palenzona [28].

RESULTS

$PGF_{2\alpha}$ basal release was higher ($P<0.01$) in fully-grown follicles with respect to the other follicle types; $PGF_{2\alpha}$ was lower ($P<0.01$) in pre-vitellogenic with respect to early-vitellogenic and mid-vitellogenic follicles (Fig. 1). PGE_2 basal release was higher ($P<0.01$) in early-vitellogenic with respect to the other follile types; PGE_2 was lower in pre-vitellogenic with respect to mid-vitellogenic and fully-grown follicles (Fig. 2). Progesterone basal release was higher ($P<0.01$) in fully-grown with respect to the other follicle types; progesterone was higher ($P<0.01$) in mid-vitellogenic with respect to the pre-vitellogenic and early-vitellogenic follicles; progesterone was higher ($P<0.01$) in early-vitellogenic with respect to pre-vitellogenic follicles (Fig. 3, upper panel).

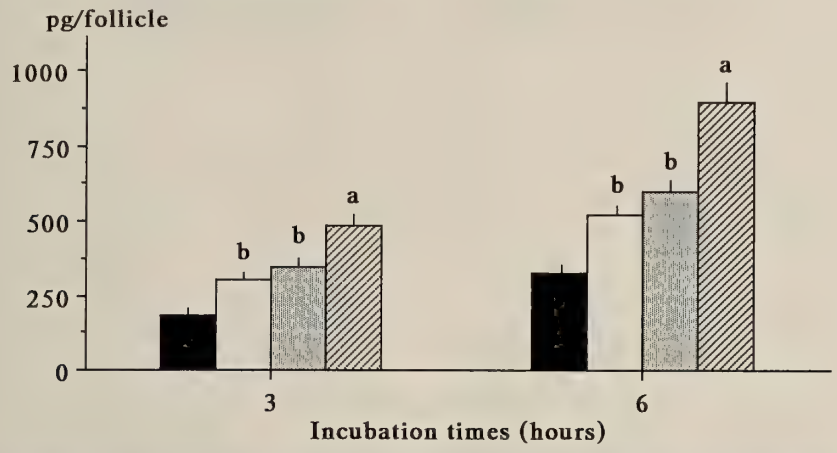

FIG. 1. $PGF_{2\alpha}$ basal release by follicles, at different vitellogenic developmental stages (see Materials and Methods), of the oviparous lizard, *Podarcis s. sicula*. Follicles: pre-vitellogenic (black bars), early-vitellogenic (white bars), mid-vitellogenic (grey bars), fully-grown (hatched bars). Each mean refers to 5 values ± SD. a, $P<0.01$ vs pre-vitellogenic, early-vitellogenic and mid-vitellogenic follicles; b, $P<0.01$ vs pre-vitellogenic follicles (Duncan's multiple range test).

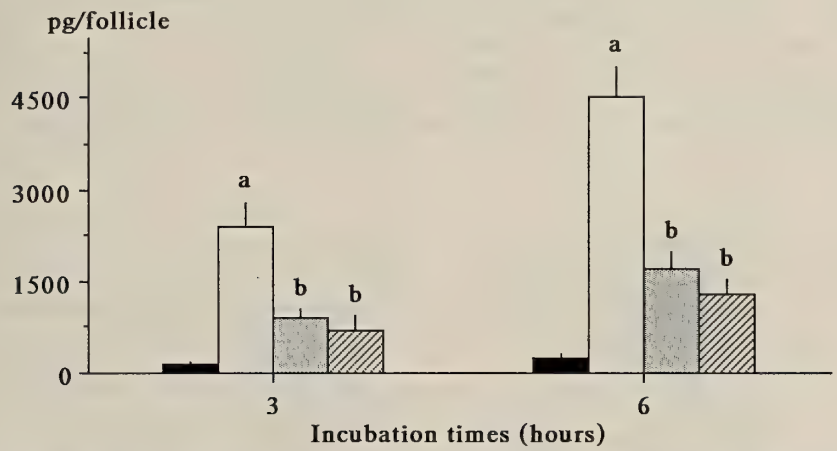

FIG. 2. PGE_2 basal release by follicles, at different vitellogenic developmental stages (see Materials and Methods), of the oviparous lizard, *Podarcis s. sicula*. Follicles: pre-vitellogenic (black bars), early-vitellogenic (white bars), mid-vitellogenic (grey bars), fully-grown (hatched bars). Each mean refers to 5 values ± SD. a, $P<0.01$ vs pre-vitellogenic, mid-vitellogenic and fully-grown follicles; b, $P<0.01$ vs pre-vitellogenic follicles (Duncan's multiple range test).

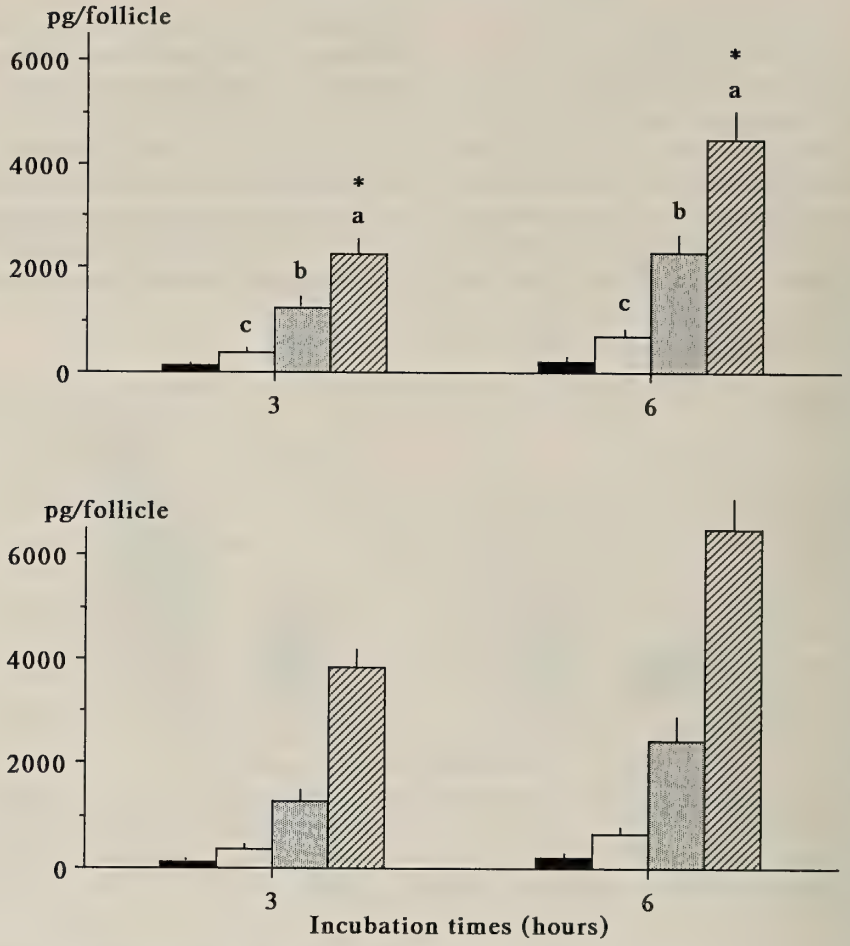

FIG. 3. Progesterone basal release (upper panel) and $PGF_{2\alpha}$ effects (lower panel) on progesterone release by follicles, at different vitellogenic developmental stages (see Materials and Methods), of the oviparous lizard, *Podarcis s. sicula*. Follicles: pre-vitellogenic (black bars), early-vitellogenic (white bars), mid-vitellogenic (grey bars), fully-grown (hatched bars). Each mean refers to 5 values $\pm$ SD. a, $P<0.01$ vs pre-vitellogenic, early-vitellogenic and mid-vitellogenic follicles; b, $P<0.01$ vs pre-vitellogenic and early-vitellogenic follices; c, $P<0.01$ vs pre-vitellogenic follicles; $^*P<0.01$ vs the same follicle type incubated with $PGF_{2\alpha}$ (Duncan's multiple range test).

Androgens basal release was not detectable in pre-vitellogenic and early-vitellogenic follicles; androgens were higher ($P<0.01$) in fully-grown with respect to mid-vitellogenic follicles (Fig. 4). Estradiol-17β basal release was higher ($P<0.01$) in early-vitellogenic with respect to the other follicle types; estradiol was lower ($P<0.01$) in pre-vitellogenic with respect to mid-vitellogenic and fully-grown follicles (Fig. 5, upper panel). $PGF_{2\alpha}$ basal release values were positively correlated

FIG. 5. Estradiol-17β basal release (upper panel) and PGE_2 effects (lower panel) on estradiol-17β release by follicles, at different vitellogenic developmental stages (see Materials and Methods), of the oviparous lizard, *Podarcis s. sicula*. Follicles: pre-vitellogenic (black bars), early-vitellogenic (white bars), mid-vitellogenic (grey bars), fully-grown (hatched bars). Each mean refers to 5 values $\pm$ SD. a, $P<0.01$ vs pre-vitellogenic, mid-vitellogenic and fully-grown follicles; b, $P<0.01$ vs pre-vitellogenic follicles; $^*P<0.01$ vs the same follicle type incubated with PGE_2 (Duncan's multiple range test).

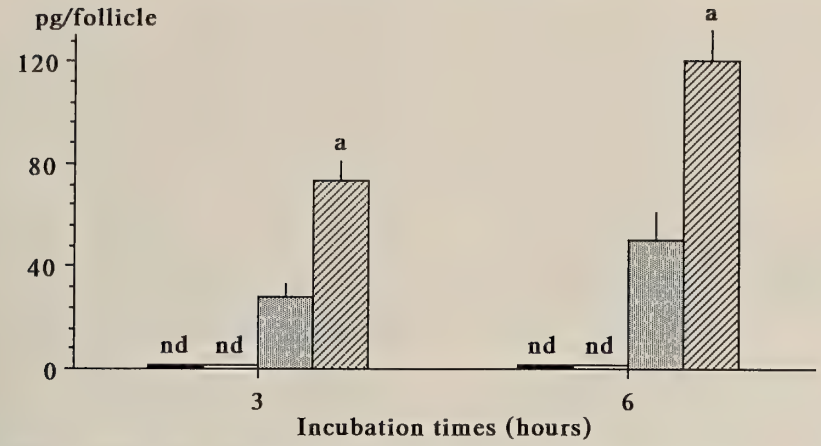

FIG. 4. Androgens basal release by follicles, at different vitellogenic developmental stages (see Materials and Methods), of the oviparous lizard, *Podarcis s. sicula*. Follicles: pre-vitellogenic (black bars), early-vitellogenic (white bars), mid-vitellogenic (grey bars), fully-grown (hatched bars). Each mean refers to 5 values ± SD. a, $P <$ 0.01 vs mid-vitellogenic follicles (Duncan's multiple range test); nd, not detectable.

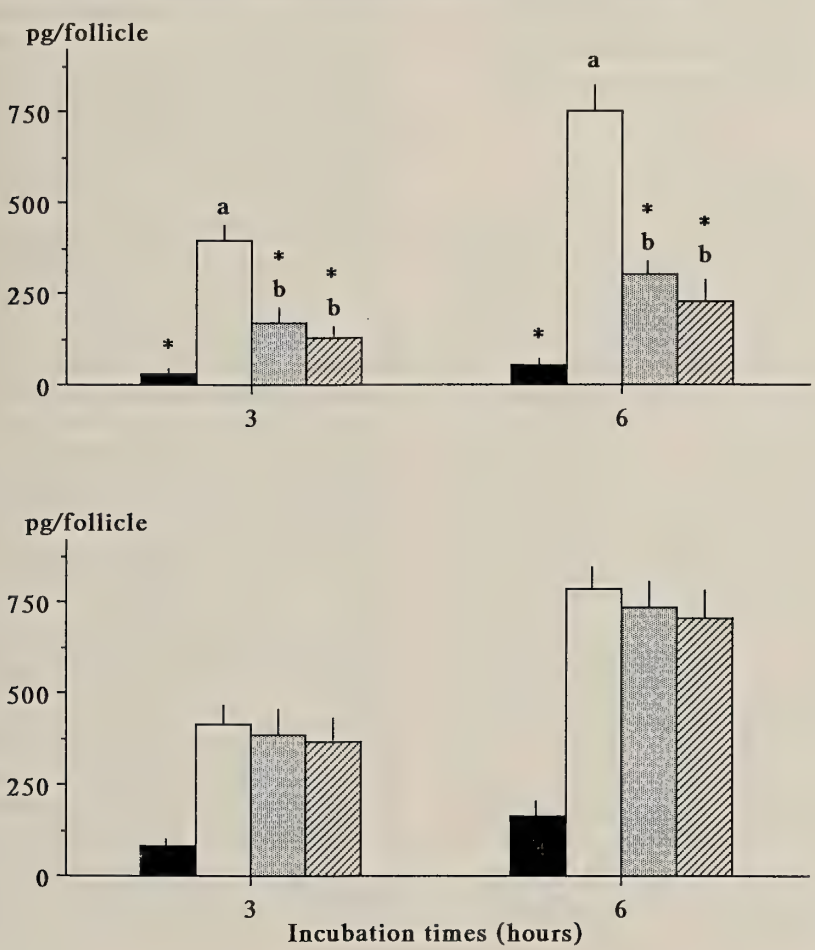

Table 1. Correlation coefficents among $PGF_{2\alpha}$, PGE_2, progesterone and estradiol-17β levels released by follicles, at different vitellogenic developmental stages, of *Podarcis s. sicula*

	Incubation times	
	3 hr	6 hr
$PGF_{2\alpha}$ vs progesterone	0.804	0.814
PGE_2 vs estradiol-17β	0.862	0.911

All correlations show the same level of significance ($P<0.001$); df=18.

($P<0.001$) to those of progesterone (Table 1); PGE_2 basal release values were positively correlated ($P<0.001$) to those of estradiol-17β (Table 1).

$PGF_{2\alpha}$ induced an increase ($P<0.01$) in progesterone release by fully-grown follicles (Fig. 3, lower panel). PGE_2 induced an increase ($P<0.01$) in estradiol release by pre-vitellogenic, mid-vitellogenic, and fully-grown follicles (Fig. 5, lower panel).

DISCUSSION

This is the first study regarding the *in vitro* basal release of PGs and sex steroids by the follicles, kept at different vitellogenic developmental stages, of the oviparous lizard *Podarcis s. sicula.*

$PGF_{2\alpha}$ showed the highest amounts in fully-grown follicle incubation samples; this finding supports the idea that $PGF_{2\alpha}$ could be involved in the stimulation of ovulation; on the other hand, Goetz [15] reported that in several fish species, PGs can induce ovulation; in particular, plasma and ovarian tissue $PGF_{2\alpha}$ levels are higher during ovulation in the yellow perk, *Perca flavescens* [17], in the brook trout, *Salvelinus fontinalis* [16], in the goldfish, *Carassius auratus* [4], and in the pond loach, *Misgurnus anguillicaudatus* [25]. Also in amphibians, $PGF_{2\alpha}$ seems to be implied in ovulation processes, seeing that $PGF_{2\alpha}$ *in vitro* induces ovulation in *Rana pipiens* [27]; more recently Gobbetti and Zerani [14] suggested that $PGF_{2\alpha}$ is implied in the control of ovulation in *Rana esculenta.* The involvement of $PGF_{2\alpha}$ in the ovulatory process of this lizard is also supported by the stimulatory role exerted by this prostaglandin on progesterone increase by fully-grown follicles. Progesterone basal release was higher in fully-grown follicles, if compared with the other follicle types, so suggesting that this steroid is involved in the ovulation of *Podarcis,* as many authors reported for amphibian species [23]; in fact, progesterone, produced by follicle cells, induces ovulation in *Xenopus laevis* [32] and *Rana pipiens* [26].

The early-vitellogenic follicles released the highest values of PGE_2 and estradiol, which both, however, remained still high in mid-vitellogenic and fully-grown follicles. The positive correlation between the basal release values of PGE_2 and estradiol suggests a causal relationship and this hypothesis is validated by the PGE_2 effect in increasing estradiol release. This finding might indicate a possible trigger role for this prostaglandin in the start of the vitellogenic development of the oocytes and also a role in sustaining the following vitellogenic growth of oocytes. In this context we recall that estradiol induces the hepatic vitellogenin synthesis for the development of the follicle, as widely reported for reptiles [5, 22]. The PGE_2 stimulatory effect on estradiol release was detected in all follicle types, except for early-vitellogenic ones. This phenomenon could be due to the refractoriness of this follicle type to an additional stimulation of PGE_2; in fact the early-vitellogenetic follicles released the highest amounts of PGE_2 and estradiol.

Androgens were detected only in the incubation media of mid-vitellogenic and fully-grown follicles in accordance with Fortune [11], who found that only large follicles released these hormones *in vitro* in the amphibian *Xenopus laevis.* The meaning of this last result is unclear; it could be due to the catabolism of progesterone which exhibits the highest values in incubation media of mid-vitellogenic and fully-grown follicles; however, a role for androgens produced by these two follicle types cannot be excluded.

Summarizing, this work suggests different roles for $PGF_{2\alpha}$ and PGE_2 released by *Podarcis s. sicula* follicles: $PGF_{2\alpha}$ could induce ovulation through progesterone mediation, while PGE_2 could be implied in the start and the sustaining of vitellogenic development of oocytes through estradiol mediation.

ACKNOWLEDGMENTS

The authors would like to thank James Burge, of the Camerino University Institute of Linguistics, for help with English. This work was supported by grant from MURST.

REFERENCES

1 Asem EK, Todd H, Hertelendy F (1987) *In vitro* effect of prostaglandins on the accumulation of cyclic AMP in the avian oviduct. Gen Comp Endocrinol 66: 244–247

2 Botte V, Angelini F, Picariello O, Molino R (1976) The regulation of the reproductive cycle of the female lizard, *Lacerta sicula sicula* Raf. Monitore Zool Ital 10: 119–133

3 Botte V, Delrio G (1965) Ricerche istochimiche sulla distribuzione dei 3- e 17-chetosteroidi e di alcuni enzimi della steroidogenesi nell' ovario di *Lacerta sicula*. Boll Zool 32: 191–198

4 Bouffard RE (1979) The role of prostaglandins during sexual maturation, ovulation and spermiation in the goldfish, *Carassius auratus*. M Sc Thesis, University of British Columbia, Vancouver, BC, Canada

5 Carnevali O, Mosconi G, Angelini F, Limatola E, Ciarcia G, Polzonetti-Magni A (1991) Plasma vitellogenin and 17β-estradiol levels during the annual reproductive cycle of *Podarcis s. sicula* Raf. Gen Comp Endocrinol 84: 337–343

6 Dharmarajan AM, Sueoka K, Miyazaki S, Atlas SJ, Ghodgaonkar RB, Dubin NH, Zirkin BR, Wallach EE (1989) Prostaglandins and progesterone secretion in the *in vitro* perfused pseudopregnant rabbit ovary. Endocrinolgy 124: 1198–1203

7 D'Istria M, Delrio G, Botte V, Chieffi G (1974) Radioimmunoassay of testosterone, 17β-oestradiol and estrone in the male and female plasma of *Rana esculenta* during sexual cycle. Ster Lip Res 5: 42–48

8 Duncan DB (1955) Multiple range and multiple F test. Biometrics 11: 1–42

9 Espey LL, Norris C, Saphire D (1986) Effect of time and dose of indomethacin on follicular prostaglandins and ovulation in the rabbit. Endocrinology 119: 746–754

10 Filosa S (1973) Biological and cytological aspects of the ovarian cycle in *Lacerta sicula* Raf. Monitore Zool Ital 7: 151–165

11 Fortune JE (1983) Steroid production by *Xenopus* ovarian follicles at different developmental stages. Dev Biol 99: 502–509

12 Gobbetti A, Zerani M (1991) Gonadotropin-releasing hormone stimulates biosynthesis of prostaglandin $F_{2\alpha}$ by the interrenal gland of the water frog, *Rana esculenta, in vitro*. Gen Comp Endocrinol 84: 434–439

13 Gobbetti, A, Zerani M (1992) $PGF_{2\alpha}$, PGE_2 and sex steroids from the abdominal gland of the male crested newt *Triturus carnifex* (Laur.). Prostaglandins 43: 101–109

14 Gobbetti A, Zerani M (1992) A possible involvement of prostaglandin $F_{2\alpha}$ ($PGF_{2\alpha}$) in *Rana esculenta* ovulation: effects of mammalian gonadotropin-releasing hormone on *in vitro* $PGF_{2\alpha}$ and 17β-estradiol production from ovary and oviduct. Gen Comp Endocrinol 87: 163–170

15 Goetz FW (1983) Hormonal control of oocyte final maturation and ovulation in fishes. In "Fish Physiology Vol IXB" Ed by WS Hoar, DJ Randall, EM Donaldson, Academic Press, New York, pp 117–170

16 Goetz FW, Duman P, Ranjan M, Herman CA (1989) Prostaglandin F and E synthesis by specific tissue components of the brook trout (*Salvelinus fontinalis*) ovary. J Exp Zool 250: 196–205

17 Goetz FW, Theofan G (1979) *In vitro* stimulation of germinal vesicle breakdown and ovulation of yellow perch (*Perca flavescens*) oocytes: effects of 17α-hydroxy-20β-dihydroprogesterone and prostaglandins. Gen Comp Endocrinol 37: 273–285

18 Greenhalgh EA (1990) Luteal steroidogenesis and regression in the rat: progesterone secretion and lipid peroxidation induced in luteal cells by human chorionic gonadotrophin, phospholipase A_2 and prostaglandin $F_{2\alpha}$. J Endocrinol 125: 397–402

19 Guillette LJ, Jr, Bjordal KA, Bolten AB, Gross TS, Palmer BD, Witherington BE, Matter JM (1991) Plasma estradiol-17β, progesterone, prostaglandin F, and prostaglandin E_2 concentrations during natural oviposition in the loggerhead turtle (*Caretta caretta*). Gen Comp Endocrinol 82: 121–130

20 Guillette LJ, Jr, Cree A, Gross TS (1990) Endocrinology of oviposition in the tuatara (*Sphenodon punctatus*): I. Plasma steroids and prostaglandins during natural nesting. Biol Reprod 43: 285–289

21 Guillette LJ, Jr, Lavia LA, Walker NJ, Roberts DK (1984) Luteolysis induced by prostaglandin $F_{2\alpha}$ in the lizard, *Anolis carolinensis*. Gen Comp Endocrinol 56: 271–277

22 Ho SM (1987) Endocrinology of vitellogenesis. In "Hormones and Reproduction in Fishes, Amphibians, and Reptiles" Ed by DO Norris, RE Jones, Plenum Press, New York, pp 145–170

23 Jones RE (1987) Ovulation: insights about the mechanisms based on a comparative approach. In "Hormones and Reproduction in Fishes, Amphibians, and Reptiles" Ed by DO Norris, RE Jones, Plenum Press, New York, pp 203–240

24 Mahmoud IY, Cyrus RV, McAsey ME, Cady D, Woller MJ (1988) The role of arginine vasotocin and

prostaglandin $F_{2\alpha}$ on oviposition and luteolysis in the common snapping turtle *Chelydra serpentina* Gen Comp Endocrinol 69: 56–64

25 Ogata H, Nomura T, Hata M (1979) Prostaglandin $PGF_{2\alpha}$ changes induced by ovulatory stimuli in the pond loach, *Misgurnus anguillicaudatus*. Bull Jpn Soc Sci Fish 45: 929–931

26 Schuetz AW (1967) Effect of steroids on germinal vesicle of oocytes of the frog (*Rana pipiens*) *in vitro*. Proc Soc Ex Biol Me 124: 1307–1310

27 Schuetz AW, Lessman AL (1981) Role of the surface epithelium of the ovarian follicle in the ovulation of frog (*Rana pipiens*) oocytes. J Cell Biol 91: 187a

28 Scossiroli RE, Palenzona DL (1979) Manuale di biometria. Zanichelli Editore, Bologna

29 Sedrani SH, El-Banna AA (1987) Effect of indomethacin on plasma level of vitamin D metabolites, oestradiol and progesterone in rabbit during early pregnancy. Comp Biochem Physiol 87: 635–639

30 Shimada K, Olson DM, Etches RJ (1984) Follicular and uterine prostaglandin levels in relation to uterine contraction and the first ovulation of a sequence in the hen. Biol Reprod 31: 76–82

31 Sokal RR, Rohlf FJ (1981) Biometry. Freeman, San Francisco, 2nd ed

32 Thibier-Fouchet C, Mulner O, Ozon R (1976) Progesterone biosynthesis and metabolism by ovarian follicles and isolated oocytes of *Xenopus laevis*. Biol Reprod 14: 317–326

ZOOLOGICAL SCIENCE 10: 329–336 (1993)

Plasma Steroid Hormone Profiles in HCG-Injected Male Walking Catfish *Clarias batrachus*

Muhammad Zairin, Jr., Kiyoshi Asahina[1], Kiyoshi Furukawa and Katsumi Aida

Department of Fisheries, Faculty of Agriculture, The University of Tokyo, Bunkyo-ku, Tokyo 113, Japan [1]*College of Agriculture and Veterinary Medicine, Nihon University, Setagaya-ku, Tokyo 154, Japan*

ABSTRACT—The present experiment was performed in order to investigate the response of matured male walking catfish to human chorionic gonadotropin (HCG).

Short-term experiment. Mature male walking catfish received a single intramuscular injection of HCG (0.2 and 1 IU/g BW) or saline. Blood samples were taken at 0, 6, 12, 18, 24, 36, 48 and 72 hr. *Long-term experiment.* Mature male walking catfish received a single intramuscular injection of HCG (1 IU/g BW) or saline. Blood samples were taken at 2-day intervals until day 10. In both experiments, plasma testosterone, 11-ketotestosterone (11-KT), 17α-hydroxyprogesterone, 17α,20α-dihydroxy-4-pregnen-3-one and 17α,20β-dihydroxy-4-pregnen-3-one levels were measured by radioimmunoassay, and 17α,20β,21-trihydroxy-4-pregnen-3-one levels were measured by enzyme immunoassay.

Results can be summarized as follows. 1) HCG firstly induces an increase in plasma testosterone and 11-KT levels. 2) Thereafter, 11-KT levels decrease and progestin levels increase. 3) Finally, progestin levels decrease, and 11-KT levels increase again. These results clearly indicate that a shift in the steroidogenic pathway is induced in males in response to HCG.

INTRODUCTION

Walking catfish (*Clarias batrachus*) is a freshwater teleost which is widely distributed throughout Southeast Asia. Although this fish has been commonly cultured for a long period, little information is available on its reproductive physiology, especially regarding males. The reproductive organ of the male tropical walking catfish differs from other teleosts such as cyprinids and salmonids. Walking catfish testes are very small; therefore, milt cannot be obtained by applying pressure to the abdomen in the manner that is commonly employed with other fishes. Male walking catfish reared under 23–25°C start to mature at an age of 9 months, and thereafter maintain conditions of maturity. Plasma testosterone and 11-ketotestosterone (11-KT) in males were always maintained at high levels throughout the year under warm water conditions, but progestin levels were low [26].

It has been proposed that during spermiation and spawning, a shift in the steroidogenic pathway from androgen to progestin production occurs in response to increased gonadotropin secretion in salmonids [6, 12, 24], in cyprinids [5], and in a perciform [9]. Progestins, such as 17α,20β-dihydroxy-4-pregnen-3-one (17α,20β-P), and 17α,20α-dihydroxy-4-pregnen-3-one (17α,20α-P), have been reported to exist in males, and to increase during spermiation and spawning in response to increased gonadotropin secretion. In addition, another progestin, 17α,20β,21-trihydroxy-4-pregnen-3-one (20β-S) has been reported to increase in the female Atlantic croacker [23], in the spotted seatrout [22] and in the walking catfish [25] during final oocyte maturation. However, the presence of 20β-S in male teleosts has not been reported yet.

There still remains a paucity of information on hormonal changes during natural spawning in the male walking catfish; it is generally difficult to follow hormonal changes in individual fish due to

Accepted December 3, 1992
Received August 24, 1992

extreme sensitivity to handling stress. Therefore, in this investigation changes in plasma levels of testosterone, 11-KT, 17α-hydroxyprogesterone (17α-P), 17α,20α-P, 17α,20β-P and 20β-S were monitored in the HCG-treated male walking catfish.

MATERIALS AND METHODS

Fish Walking catfish fingerlings were originally obtained from The Faculty of Fisheries, Bogor Agricultural University, Bogor, Indonesia in 1988. These fish were reared at 23–25°C under 12L12D photoperiod until reaching maturity. Fish began to mature at an age of 9 months and conditions of maturity were maintained thereafter; but under the above stocking conditions, fish were observed not to undergo natural spawning [26].

Short-term experiment Twenty-four 2-year old matured male walking catfish (400–650 g in weight and 35–40 cm in total length) were selected from the stock, and then randomly assigned to three groups, injected with 0.2 IU HCG/g BW, 1 IU HCG/g BW and saline. Each group was kept separately in a $1\times3\times1$ m indoor concrete tank supplied with running fresh water of deep-well origin. Water temperature and photoperiod were maintained at 24 ± 0.5°C, and 12L12D, respectively. Fish did not receive feed during the experiment.

Long-term experiment. Fourteen 16-month old matured male walking catfish (200–275 g in weight and 30–33 cm in total length) were divided into two groups. Eight fish received 1 IU HCG/g BW, whereas the remaining six fish received saline solution. Each group was kept separately in the same manner as in the short term monitoring experiment.

Treatment HCG was purchased from Teikoku Zoki Pharmaceutical Company, Japan. In order to meet the required dosage, the original hormone was diluted with 0.6% saline solution into 0.2 IU/μl and 1 IU/μl solution.

HCG treated groups received a single intramuscular injection of HCG, whereas the saline group received an equal volume of saline solution. Injection was done just below the beginning of the dorsal fin at 6 a.m.

Blood sampling Initial blood samples were taken from all fish before administering hormone solution or saline. Sampling was carried out at 6, 12, 18, 24, 36, 48 and 72 hr in the short-term experiment. In the long term experiment, sampling was carried out 2, 4, 6, 8, and 10 days after HCG injection (at 10 a.m.). Fish were sacrificed for the measurement of gonadosomatic index (GSI) at the termination of the experiments.

Approximately 0.8 ml of blood was drawn from the caudal vasculature with a heparinized syringe fitted with a 24-gauge, 1 inch needle after anesthetizing fish with 600 ppm of 2-phenoxyethanol (Wako, Japan). Blood samples were centrifuged at 3000 rpm, and plasma was stored in 1.5 ml polypropylene tubes at −20°C until analysis by radioimmunoassay (RIA).

RIA In this experiment, plasma testosterone, 11-KT, 17α-P, 17α,20α-P and 17α,20β-P were determined by RIA. Details of RIA for each steroid have been described previously [1, 13, 25]. Validation of the assay system for testosterone, 17α-P, 17α,20α-P and 17α,20β-P has also been previously reported [25].

Validation of the 11-KT assay system for walking catfish plasma was carried out in the same manner as has been reported previously [8]. Intraassay coefficients of variation at binding rates around 25%, 50% and 75% were 6.3, 4.0, and 4.5, respectively. Interassay coefficients of variation at binding rates around 25%, 50% and 75% were 18.6, 9.1, and 19.8, respectively.

EIA Plasma 20β-S levels were measured using a specific enzyme immunoassay system (EIA). Validation for this EIA was reported previously [25].

Statistics The Student-t test, and the Duncan's multiple range test and the Kruskal-Wallis test were used for statistical analysis.

RESULTS

Short-term experiment

Changes in plasma testosterone levels following HCG injection are presented in Figure 1. Plasma testosterone levels in 0.2 IU HCG-treated group became elevated at 6 hr ($P<0.01$; 0 hr *vs* 6 hr), reaching a peak at 18 hr (207.4 ng/ml), and thereafter remained higher than initial levels (5.2 ng/ml) until the end of the experiment ($P<0.01$; 0 hr *vs* 72 hr). Testosterone levels in 1 IU HCG-treated group showed changes similar to those of the 0.2 IU HCG-treated group. No significant changes occurred in the control group.

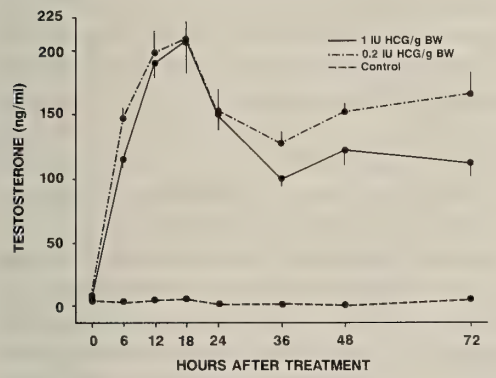

FIG. 1. Plasma testosterone levels of male walking catfish following HCG injection in short-term experiment. Each point represented as mean±SEM (n=8 for each treatment).

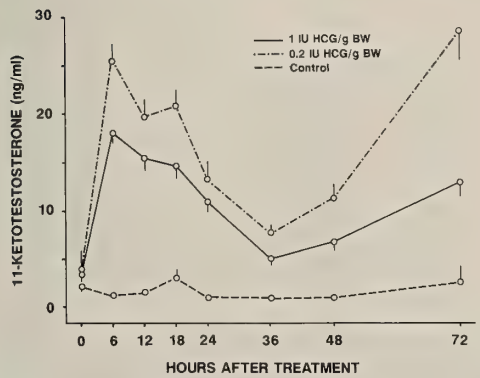

FIG. 2. Plasma 11-KT levels of male walking catfish following HCG injection in short-term experiment. Each point represented as mean±SEM (n=8 for each treatment).

Changes in plasma 11-KT levels are shown in Figure 2. Plasma 11-KT levels in 0.2 IU HCG-treated group peaked at 6 hr (25.6 ng/ml; $P<0.01$; 0 hr *vs* 6 hr), and then decreased until 36 hr (7.6 ng/ml; $P<0.01$, 18 hr *vs* 36 hr), and thereafter increased again until the end of the experiment (28.6 ng/ml). Plasma 11-KT levels in the 1 IU HCG-treated group showed a similar pattern of changes. 11-KT levels in the control group were maintained at low levels during the experiment.

Changes in plasma 17α-P levels are presented in Figure 3. Plasma 17α-P levels increased from 36 hr until 72 hr in both 0.2 and 1 IU HCG injected groups ($P<0.01$; 24 hr *vs* 72 hr). Levels at 72 hr for 0.2 and 1 IU HCG/g BW were 13.6 ng/ml and 26.2 ng/ml, respectively. On the other hand, no significant changes were observed in the control group.

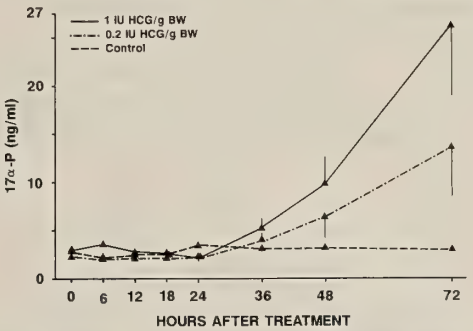

FIG. 3. Plasma 17α-P of male walking catfish following HCG injection in short-term experiment. Each point represented as mean±SEM (n=8 for each treatment).

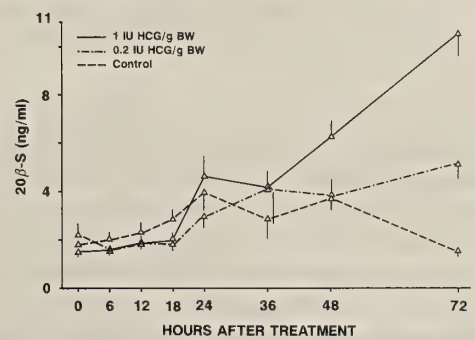

FIG. 4. Plasma 20β-S levels of male walking catfish following HCG injection in short-term experiment. Each point represented as mean±SEM (n=8 for each treatment).

Changes in plasma 20β-S levels are presented in Figure 4. Plasma 20β-S levels in the 1 IU HCG/g BW-treated group started to increase at 24 hr ($P<$ 0.01; 18 hr *vs* 24 hr), and reached 10.5 ng/ml at 72 hr. Plasma 20β-S levels in the 0.2 IU HCG/g BW-treated group increased in the same manner as those of 1 IU HCG/g BW group, but levels for 48 and 72 hr were lower. Plasma 20β-S levels in the control group slightly increased during 24–48 hr ($P<0.01$; 0 hr *vs* 24 hr), and then decreased ($P<0.01$; 48 hr *vs* 72 hr).

Changes in plasma 17α,20α-P levels are presented in Figure 5. Injection of 1 or 0.2 IU HCG/g BW caused a parallel increase in 17α,20α-P levels, starting from 6 hr ($P<0.01$; 0 hr vs 6 hr) continuing until 72 hr (levels for 0.2 and 1 IU HCG/g BW treated groups were 1.7 and 3.0 ng/ml, respectively). Levels in the control group were always under the detectable limit throughout the experiment.

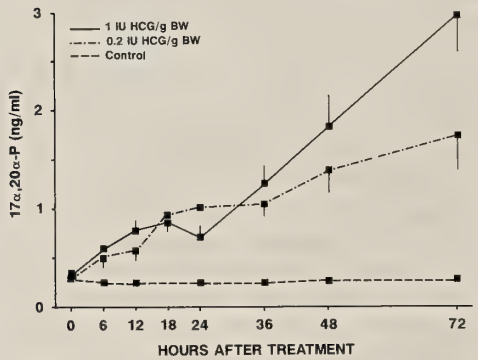

FIG. 5. Plasma 17α,20α-P of male walking catfish following HCG injection in short-term experiment. Each point represented as mean$\pm$SEM (n=8 for each treatment).

Changes in plasma 17α,20β-P levels are presented in Figure 6. Injection of 1 and 0.2 IU HCG/g BW caused a similar increase ($P<0.01$; 6 hr *vs* 72 hr) in 17α,20β-P levels, starting from 6 hr. This trend continued until 72 hr (2.8 and 4.6 ng/ml for 0.2 and 1 IU HCG/g BW, respectively). Except for values at 24 and 36 hr, plasma levels were higher in the 1 IU HCG/g BW treated group than in the 0.2 IU treated group. Levels in the control group were always under the detectable limit.

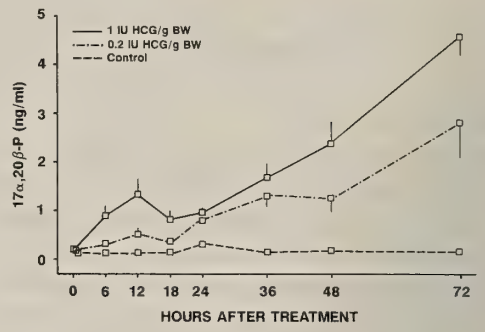

FIG. 6. Plasma 17α,20β-P levels of male walking catfish following HCG injection in short-term experiment. Each point represented as mean$\pm$SEM (n=8 for each treatment).

GSI values at the end of the short-term experiment are presented in Figure 7a. GSI increased significantly from 0.15 % to 0.22% in 0.2 IU HCG/g BW treated group, and to 0.20% in 1 IU HCG/g BW treated group.

Long-term experiment

Changes in plasma testosterone, 11-KT, and 17α-P levels are presented in Figure 8.

Plasma testosterone levels increased sharply from 9.9 ng/ml to 77.6 ng/ml on day 2 ($P<0.01$; day 0 vs day 2), and then decreased but remained high until day 10 (34.1 ng/ml). Testosterone levels on day 10 were still significantly higher than initial and control levels. No significant changes occurred in the control group.

Plasma 11-KT levels decreased from 5.7 ng/ml

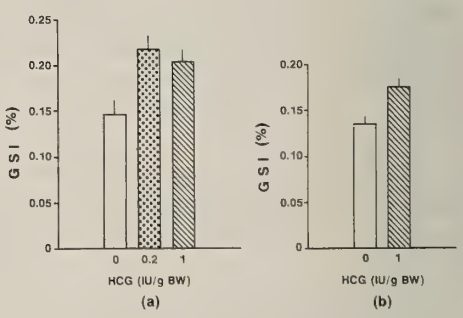

FIG. 7. Changes in GSI values following HCG injection in short-term (a) and long-term (b) experiments. Each bar represented as mean$\pm$SEM (n=8 for each treatment in short-term experiment, and n=8 and 6 for HCG and control group, respectively in long-term experiment).

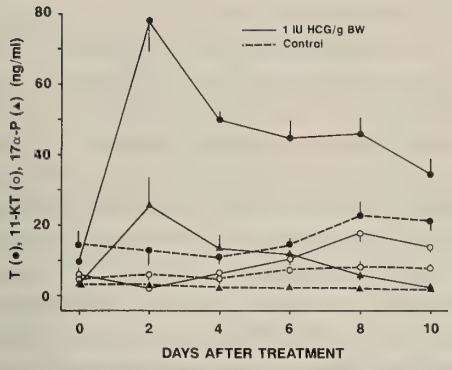

FIG. 8. Plasma testosterone, 11-KT, and 17α-P levels following HCG injection in long-term experiment. Each point represented as mean $\pm$ SEM (n=8 and 6 for HCG and control group, respectively). Solid line is HCG treatment, dotted line is control.

to 1.8 ng/ml on day 2 ($P<0.01$; day 0 *vs* day 2). Thereafter levels increased, peaking on day 8 (17.6 ng/ml; $P<0.01$; day 2 *vs* day 8) and decreasing on day 10. No significant changes occurred in the control group.

Plasma 17α-P levels peaked on day 2 (25.4 ng/ml; $P<0.01$; day 0 *vs* day 2), and then decreased to initial levels on day 10 (2.2 ng/ml). No significant changes occurred in the control group.

Changes in plasma 20β-S, 17α,20α-P, and 17α,20β-P levels are presented in Figure 9. Plasma 20β-S levels started to increase on day 2 (7.4 ng/ml), peaking on day 4 (9.1 ng/ml; $P<0.01$; day 0 *vs* day 4) and returning to initial levels on day 10.

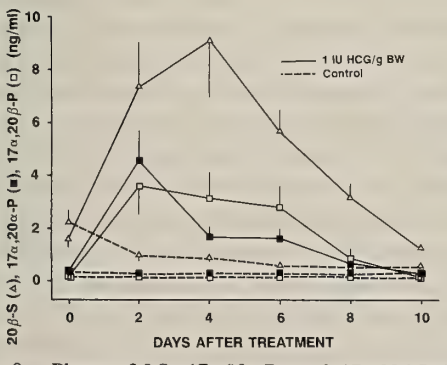

FIG. 9. Plasma 2β-S, 17α,20α-P, and 17α,20β-P levels following HCG injection in long-term experiment. Each point represented as mean $\pm$ SEM (n=8 and 6 for HCG and control group, respectively). Solid line is HCG treatment, dotted line is control.

Meanwhile, levels in the control group decreased gradually ($P<0.01$; day 0 *vs* day 10).

Plasma 17α,20α-P levels in the HCG-treated group peaked on day 2 (4.5 ng/ml; $P<0.01$; day 0 *vs* day 2) and then returned to basal levels on day 10. No significant changes were observed in the control group.

Plasma 17α,20β-P levels in the HCG-treated group also peaked on day 2 (3.8 ng/ml; $P<0.01$; day 0 *vs* day 2), and remained high until day 6, returning to the initial levels on day 10. No significant changes occurred in the control group.

Changes in GSI values following HCG injection in the long-term experiment are presented in Figure 7b. HCG injection caused significant increase in GSI from 0.14% to 0.18%.

Summary of the changes in levels of the six plasma steroids following HCG injection, both in short-term and long-term experiments are presented in Figure 10. 1) HCG firstly induces an increase in plasma testosterone and 11-KT levels. 2) Thereafter, 11-KT levels decrease and progestin levels increase. 3) Finally, progestin levels decrease, and 11-KT levels increase again.

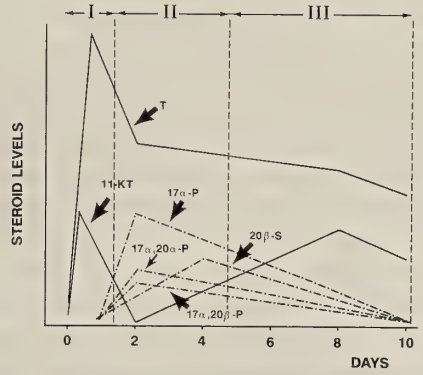

FIG. 10. Changes in levels of the six plasma steroids following HCG injection shown schematically for both the long- and short-term experiments. Lines represent trends, not absolute values. I: Androgen increase; II: Androgen decrease and progestin increase; and III: Progestin decrease and 11-ketotestosterone increase.

DISCUSSION

A single injection of HCG in mature male tropical walking catfish caused significant changes

in all of the steroids monitored. HCG injection also caused enlargement of the testes.

HCG injection in both the 0.2 and 1 IU HCG-treated groups caused rapid increases in testosterone levels peaking at 18 hr. Thereafter, levels decreased but remained high. This suggests that the enzymes which are involved in testosterone synthesis are activated by HCG injection. In rainbow trout, gonadotropin has been suggested to stimulate the activity of two enzymes: C_{17-20} lyase which converts 17α-P to androstenedione, and 17β-HSD which converts androstenedione to testosterone [11, 15].

The function of testosterone in teleosts is still unclear, but is present in appreciable amounts during maturation in both males and females. Testosterone is regarded as an intermediate androgen product in the biosynthesis of 11-KT. However, based on replacement therapy in hypophysectomized catfish [17], it has been found that testosterone is able to maintain all stages of spermatogenesis, except spermatogonia mitosis. In addition, it has been shown also that testosterone isobutyrate crystals induce *in vitro* completion of spermatogenesis in undeveloped testes of goldfish [18]. In the present experiment, HCG injection elevated levels of testosterone which were much higher than those of 11-KT. This is in contrast to eel, in which the testosterone peak was lower than that of 11-KT [16]. These results suggest that the function of testosterone in male walking catfish is not merely to serve as a precursor to 11-KT synthesis.

The fluctuation pattern of 11-KT following HCG-injection in the present experiment is particularly interesting, since it showed two peaks. 11-KT levels peaked at 6 hr, decreased to initial levels at 36 hr, and then peaked again on day 8. The first peak was perhaps induced by the stimulatory effect of HCG on the conversion from testosterone to 11-KT, which is also observed in other fishes. The decreases, as will be discussed later, may be caused by the inhibitory effect of the progestin, as the decrease coincided with the increase in progestin levels. The fact that second peak occurred when progestin levels had already decreased, and that its magnitude was smaller than that of the first peak, suggests that the increase in the second peak was probably due to the elimination of the inhibitory effects of progestin. On the other hand, injection of HCG in dab [8] and goldfish [14], or salmon gonadotropin in brown bullhead [19] did not induce increases in 11-KT. One possible explanation is that these fish are annual spawners in which the sensitivity of testes to HCG or gonadotropin varies with time. However, under our stocking conditions, since plasma testosterone and 11-KT fluctuated at high levels throughout the year [26], male tropical walking catfish may possesses all developmental stages of the testes, so that fish can readily respond to HCG injection.

Plasma 17α-P levels increased slowly after HCG injection and peaked at 72 hr, then decreased and returned to initial levels on day 10. This indicates that HCG treatment stimulates the testes to produce 17α-P. Increased 17α-P is converted into androstenedione by C_{17-20} lyase, and testosterone production is increased as a result. However, it is considered that when lyase activity has been used to its maximum capacity, the conversion to progestin formation occurs, resulting the decrease in androgen production and the increase in 17α,20α-P, 17α,20β-P, and 20β-S. This is in contrast to dab [8] in which HCG did not increase 17α-P levels.

One of the interesting findings in the present experiment is the simultaneous increase in the levels of three progestins, 20β-S, 17α,20α-P and 17α,20β-P, following HCG injection. Levels of 20β-S were highest, followed by 17α,20β-P and 17α,20α-P. The occurrence of more than one progestin for example, 17α,20α-P and 3β,17,20α-P-5β in dab [8], and 17α,20α-P and 17α,20β-P in carp [4] during spermiation in males has been reported. Progestin types seem to vary with species.

Little is known about the function of 20β-S in male fish. Our results show that HCG injection can elevate plasma 20β-S levels. Levels of this progestin were higher than those of 17α,20α-P, and 17α,20β-P. The role of this hormone in the reproductive system of male walking catfish is still unknown. In HCG-injected female walking catfish as well, this hormone increases prior to ovulation [25].

17α,20α-P level increased due to HCG injection, and peaked at the day 2. High levels were main-

tained until the day 8. This increase suggests the presence of 20α-HSD in the male walking catfish. In the other teleosts, activity of this enzyme has been detected in spermatozoa of carp [2], dab and plaice [7]. The real function of this hormone in male walking catfish is yet unknown. In carp, however, this hormone has been suggested to be a spermiation regulator [2] as this hormone possessed an inhibitory effect on androgen production as did its isomer [3]. The fact that 17α,20α-P is produced at high levels by mature spermatozoa suggest that it is released into the environment at the time of spawning, and could therefore play an important behavioral/pheromonal role [2].

In this investigation, HCG injection possibly enhanced the activity of 20β-HSD which converts 17α-P to 17α,20β-P production. In the short-term experiment, 17α,20β-P levels started to increase after HCG injection, peaking at 72 hr. However, in the long-term experiment, this hormone peaked on day 2. Several roles have been proposed for 17α,20β-P. Based on an *in vitro* study in carp, it has been suggested that this hormone inhibits androgen production [4]. The hormone was reported to induced spermiation in amago salmon, *Oncorhynchus rhodurus* [24], and change the K^+/Na^+ ratio of rainbow trout seminal fluid [20]. Furthermore, pheromonal effects of this hormone have been reported to occur in the goldfish, *Carassius auratus* [21]. Recently, 17α,20β-P has been suggested to be a steroidal mediator in the spermiation of eel [16].

In the present experiment, HCG injection caused long-term changes in elevation of levels in all of the steroids monitored. These results were in contrast to those corresponding to females of the same species, in which HCG effects lasted only 24 hr [25]. The duration of steroid elevation following HCG injection in the present experiment is longer than the reported value during natural spawning or GtH treatment in other fishes. These differences may be due to the high dose and/or slow clearance of HCG in the male walking catfish. In goldfish, small doses of GtH (0.2 pg/g body weight) are cleared within 1 hr [10]. This has also been shown in *Ictalurus nebulosus* [19] injected with sGtH 5 to 500 ng/g body weight. The reason may be that the dosage used here is relatively high and that HCG is not an endogenous GtH.

In the short-term experiment, androgen levels were higher in the low dose group, whereas progestin levels were higher in high dose group. Lower levels in androgen and higher levels in progestin in the high dose group were probably caused by the conversion shift from androgen to progestin, since it is reported that high dose of gonadotropin induces the shift in salmonid [15]. Inhibition of androgen synthesis by increased progestin, which was found in carp [3], may also decrease androgen levels in catfish.

In summary, HCG injection increases testosterone production which is further converted to 11-KT. As a result, 11-KT production increases several hours after injection. Meanwhile, steroidogenic pathways favoring progestin production gradually become active. Increased progestin production possesses an inhibitory effect on 11-KT production. At this point, GSI increases and probably more sperm is produced. Consequently, 11-KT production decreases during progestin peaks, and increases again when progestin levels decrease.

ACKNOWLEDGMENTS

We express our thanks to colleagues in the Fisheries Laboratory, The University of Tokyo, Maisaka, Shizuoka Prefecture,for allowing use of facilities for field experiments. We thank Marcy N. Wilder for correcting the English. This study was partially funded by a Grant-in Aid for Scientific Research from the Ministry of Education, Science and Culture.

REFERENCES

1 Aida K, Kato T, Awaji M (1984) Effects of castration on the smoltification of precocious male masu salmon *Oncorhynchus masou*. Bull Japan Soc Sci Fish 50: 565–571

2 Asahina K, Barry TP, Aida K, Fusetani N, Hanyu I (1990) Biosynthesis of 17α,20α-dihydroxy-4-pregnen-3-one from 17α-hydroxyprogesterone by spermatozoa of the common carp, *Cyprinus carpio*. J Exp Zool 255: 244–249

3 Barry TP, Aida K, Hanyu I (1989) Effect of 17α,20β-dihydroxy-4-pregnen-3-one on the *in vitro* production of 11-ketotestosterone by testicular fragments of the common carp, *Cyprinus carpio*. J Exp Zool 251: 117–120

4 Barry TP, Aida K, Okumura T, Hanyu I (1990) The shift from C-19 and C-21 steroid synthesis in spawning male common carp, *Cyprinus carpio*, is regulated by the inhibition of androgen production by progestogen produced by spermatozoa. Biol Reprod 43: 105–112

5 Barry TP, Santos AJG, Furukawa K, Aida K, Hanyu I (1990) Steroids profiles during spawning in male common carp. Gen Comp Endocrinol 80: 223–231

6 Baynes SM, Scott AP (1985) Seasonal variations in parameters of milt production and in plasma concentration of sex steroids of male rainbow trout (*Salmo gairdneri*). Gen Comp Endocrinol 57: 150–160

7 Canario AVM, Scott AP (1989) Synthesis of 20α-hydroxylated steroids by ovaries of the dab (*Limanda limanda*). Gen Comp Endocrinol 76: 147–158

8 Canario AVM, Scott AP (1991) Levels of 17α,20α-dihydroxy-4-pregnen-3-one, and 3β,17α,20α-trihydroxy-5β-pregnane, and other sex steroids, in blood plasma of male dab, *Limanda limanda* (marine flatfish) injected with human chorionic gonadotropin. Gen Comp Endocrinol 83: 258–264

9 Colombo L, Belvedere PC, Simontacchi C, Lazzari M (1987) Shift from androgen to progesterone biosynthesis by the testes of the northern pike, *Esox lucius* L., during transition from spermatogenesis to spermiation. Gen Comp Endocrinol 66: 18 [Abstract 48]

10 Cook AF, Peter RE (1980) Plasma clearance of gonadotropin in goldfish, *Carassius auratus*, during the annual reproductive cycle. Gen Comp Endocrinol 42: 76–90

11 Depeche J, Sire O (1982) *In vitro* metabolism of progesterone in the testis of the rainbow trout, *Salmo gairdneri* Rich., at different stages of spermatogenesis. Reprod Nutr Develop 22: 427–438

12 Hunt SMV, Simpson TH, Wright RS (1982) Seasonal changes in the levels of 11-oxotestosterone and testosterone in the serum of male salmon, *Salmo salar* L., and their relationship to growth and maturation cycle. J Fish Biol 20: 105–119

13 Kobayashi M, Aida K, Hanyu I (1985) Radioimmunoassay for silvercarp gonadotropin. Bull Japan Soc Sci Fish 51: 1085–1091

14 Kobayashi M, Aida K, Hanyu I (1986) Effects of HCG on milt amount and plasma levels of steroid hormones in male goldfish. Bull Jap Soc Sci Fish 52: 755

15 Le Gac F, Loir M (1988) Control of testis function in fish: *in vitro* studies of gonadotropic regulation in the trout (*Salmo gairdneri*). Reprod Nutr Develop 28: 1031–1046

16 Miura T, Yamauchi K, Takahashi H, Nagahama Y (1991) Involvement of steroid hormones in gonadotropin-induced testicular maturation in male Japanese eel (*Anguilla japonica*). Biomed Res. 12: 241–248

17 Nayyar SK, Keshavanath P, Sundararaj BI, Donaldson EM (1976) Maintenance of spermatogenesis and seminal vesicles in hypophysectomized catfish, *Heteropneustes fossili* (Bloch): effects of ovine and salmon gonadotropin and testosterone. Can J Zool 54: 285–292

18 Remacle C (1976) Actions hormonales sur les cellules germinales males de *Carassius auratus* L. en culture oranotypique. Gen Comp Endocrinol 29: 480–491

19 Rosenblum PM, Callard IP (1987) Response of male brown bullhead catfish, *Ictalurus nebulosus* Lesueur, to gonadotropin-releasing hormone and gonadotropin. J Exp Zool 243: 189–199

20 Scott AP, Baynes SM (1982) Plasma levels of sex steroids in relation to ovulation and spermiation in rainbow trout (*Salmo gairdneri*). Proc Second Int Symp on the Reprod Physiol of Fish, Wageningen, The Netherlands, pp 103–106

21 Stacey NE, Sorensen PW, Dulka JG, Van der Kraak GJ, Hara TJ (1987) Teleost sex pheromone: Recent studies on identity and function. Proc Third Int Symp on the Reprod Physiol of Fish, St John's, Newfoundland, pp 150–153

22 Trant JM, Thomas P (1989a) Evidence that 17α,20β,21-trihydroxy-4-pregnen-3-one is a maturation inducing steroid in spotted seatrout. Fish Physiol Biochem 7: 185–191

23 Trant JM, Thomas P (1989b) Isolation of a novel maturation-inducing steroid produced *in vitro* by ovaries of Atlantic croaker. Gen Comp Endocrinol 75: 397–404

24 Ueda H, Young G, Crim LW, Kambegawa A, and Nagahama Y (1983) 17α,20β-dihydroxy-4-pregnen-3-one: Plasma levels during sexual maturation and *in vitro* production by the testes of amago salmon (*Oncorhynchus rhodurus*) and rainbow trout (*Salmo gairdneri*). Gen Comp Endocrinol 51: 106–112

25 Zairin M Jr; Asahina K, Furukawa K, Aida K (1992) Plasma steroid hormone profiles during HCG induced ovulation in female walking catfish *Clarias batrachus*. Zool Sci 9: 607–617

26 Zairin M Jr (1993) Endocrinological studies on maturation and spawning in the walking Catfish, *Clarias batrachus*. Doctoral thesis, The University of Tokyo, pp 1–90

ZOOLOGICAL SCIENCE 10: 337–351 (1993)

Annual Patterns of Testicular Development and Activity in the Chinese Bullfrog (*Rana rugulosa* Wiegmann)

YUNG-HSI KAO[1,2], PAUL S. ALEXANDER[2], VIVIAN V. CHENG YANG[2] and JOHN YUH-LIN YU[1,3]

[1]*Endocrinology Laboratory, Institute of Zoology, Academia Sinica, Nankang, Taipei, Taiwan 115, R.O.C. and* [2]*Department of Biology, Tunghai University, Taichung, Taiwan 407, R.O.C.*

ABSTRACT—Annual patterns of testicular development and of testicular and plasma androgen levels in the Chinese bullfrog, *Rana rugulosa* Wiegmann, are reported. The animals were collected from a frog culture farm from November of 1986 through November of 1987, at monthly intervals or more frequently during the breeding season. Proliferation of primary spermatogonia was observed in November-December. In January-February, the number of primary spermatogonia decreased while secondary spermatogonia increased. Primary and secondary spermatocytes showed little changes until February when their number rose sharply. Although every stage of spermatogenesis was present year around, spermatozoa were massively formed in April-June. Thus, the spermatogenetic cycle of *R. rugulosa*, inhabiting subtropical Taiwan, is of continuous type. Leydig cells began to proliferate in late March and were abundant from April through July. Testicular androgen content showed basal values in January-February and August-December, began to increase in late March, peaked in April, and dropped markedly in May. The pattern of plasma androgen levels was similar to that of testicular androgen content, except peaking in middle April-early May and dropped in late June. The unimodal pattern of seasonal changes in plasma androgen levels parallels Leydig cell proliferation, spermatogenesis, testicular androgen content, and reproductive activities. In addition, the testicular weight was negatively correlated with liver weight, but not with fat body weight during an annual reproductive cycle of *R. rugulosa*.

INTRODUCTION

The patterns of reproductive cycle have been investigated in many species of anurans. The annual spermatogenetic pattern in anurans varies from discontinuous spermatogenesis in the temperate zone to continuous spermatogenesis in tropical species [22]. Earlier studies have shown that ranids, one of the major groups of anurans, display a diverse type of spermatogenesis: such as *Rana temporaria, R. arvalis,* and *R. dalmatina* exhibiting the discontinuous spermatogenesis; *R. tigerina, R. esculenta,* and *R. perezi,* the potencially continuous spermatogenesis; and *R. hexadactyla, R. cyanophlyctis,* and *R. catesbeiana,* the continuous spermatogenesis [6, 22, 43, 44, 58].

The secretion patterns of the pituitary gonadotropins in relation to testicular development and activity during a reproductive cycle of anurans have been relatively less studied [13, 19]. It was demonstrated that the circulating luteinizing hormone (LH) and follicle-stimulating hormone (FSH) were highly correlated, respectively, with the changes in plasma androgen levels and in testicular weight during an annual cycle of male toad, *Bufo japonicus* [13]. On the other hand, seasonal changes in testicular and/or circulating androgen levels in relation to spermatogenetic and/or reproductive activity have been established in several anurans, such as *R. esculenta* [7, 38, 43, 56], *R. perezi* [6], *R. catesbeiana* [19, 58], *B. japonicus* [13], *B. mauritanicus* [48], *Pachymedusa*

Accepted December 3, 1992
Received August 18, 1992
[3] Reprint requests should be sent to: Dr. J.Y.L. Yu, Endocrinology Laboratory, Institute of Zoology, Academia Sinica, Nankang, Taipei, Taiwan 115, R.O.C.

dacnicolor [41], *R. ridibunda* [55], and *Rana occipitalis* [17]. However, the annual patterns of circulating androgen levels in anurans exhibit a great variation of species specificity.

The Indian bullfrog (*R. tigerina* Daudin) was reported to show a potentially continuous spermatogenetic cycle [1, 45]. Correlations of the androgen levels in testis and in blood with spermatogenesis and reproductive activity during an annual cycle of this species were, however, not investigated.

The Chinese bullfrog, *R. rugulosa,* is phylogenically closely related to the Indian bullfrog, *R. tigerina* [9, 20, 39]. Little information has been available in male *R. rugulosa,* inhabiting subtropical Taiwan, and central and southern China, with respect to its patterns of reproductive cycle: spermatogenetic cycle, androgen levels, breeding activity, secondary sexual characters, and changes in various organs in association with reproduction, such as liver and fat body. We have conducted a series of studies investigating the annual reproductive patterns of *R. rugulosa* in both males and females. We report here the annual patterns of male *R. rugulosa* with respect to: 1) the changes in the sizes of body, testis, liver, and fat body; 2) the spermatogenetic cycle, and the changes in the proliferation of Leydig cells; 3) the androgen levels in testis and plasma; and 4) the correlation of plasma and testicular androgen levels with spermatogenesis and other reproductive activity.

MATERIALS AND METHODS

Study site

Rana rugulosa were collected from a frog culture farm located in Tungshih (23°40′N, 120°15′E), Yunlin County, Central Taiwan. Briefly, the frogs were raised in an open pond which was surrounded with fishing nets. They were fed with "frog food" manufactured by Fu-Shou Food Co., Taichung, and the natural preys as well. During hibernation, the frogs were dormant under digged earth caves or the hayricks of rice and woody box.

Chorussing of male frogs was heard from March through July at the frog culture farm, and was occasionally heard in August and September. Young tadpoles with external gills were first observed in late May, and metamorphosing froglets were first observed in early June.

Data on rainfall, temperature, and photoperiod at Tungshih, are summarized in Fig. 1. The period between March and September, 1987 was the rainy season. The lowest monthly mean air temperature was 15.4°C in January and the highest was 28.5°C in August. Monthly minimum air temperature averaged about 5°C in January and February. The photoperiod was shortest in December and longest in June. Shortest and longest days had about three hours difference in photoperiod.

Collection of blood and tissues

Monthly samples of 12–25 sexually mature male frogs (hatched in April, 1986) were collected from November, 1986 through November, 1987, except for sampling at weekly or biweekly intervals during the breeding season from March through early July. Frogs, after collection, were imediately placed into a wet fishing net and were anesthetized with ether. Blood (0.8–2.0 ml) was drawn from the conus arteriosus with a 2-ml heparinized syringe, and centrifuged at 1000 G for 10 min at 8°C; and plasma (0.4–1.0 ml) was collected and stored at −20°C until androgen assay. Both right and left testes of each frog were removed and their lengths and weights were measured. One testis was fixed in Bouin's fluid for histological observations, and the other was stored at −20°C for androgen assay. Liver and fat bodies were removed and weighed as well.

Histological examination

Bouin's-fixed testes were wax-embedded, sectioned at 7 μm, and stained with Harris' hematoxylin and eosin. We determined spermatogenetic cycle by two phases: spermatogenesis, and spermiogenesis. The stages of spermatogenesis were identified according to the method used by Rastogi *et al.* [43]: stage 1, primary spermatogonia (ISPG); stage 2, secondary spermatogonia (IISPG); stage 3, primary spermatocytes (ISPC); stage 4, secondary spermatocytes (IISPC); and stage 5, spermatids (SPT). Spermiogenesis was recorded by the extent of spermatozoa present in the seminiferous tubules. Both spermatogenesis and sper-

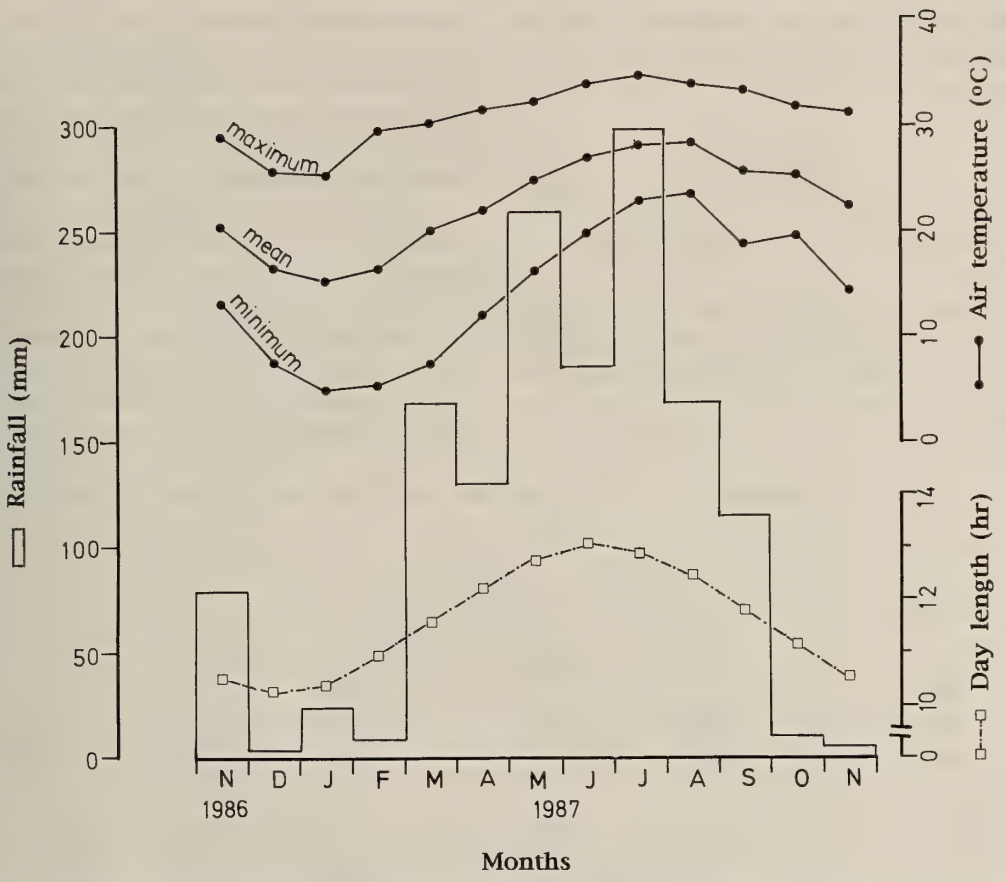

FIG. 1. Monthly cahgnes in the rainfall, photoperiod (day length), and air temperature in Tungshih, Yunlin County, Taiwan.

miogenesis of each animal were determined from twenty cross-sectioned seminiferous tubules representing four different cross-sections of each testis. The proliferation of Leydig cells in the interstitial tissues was recorded.

Radioimmunoassay of androgen in plasma and testis

Androgen concentrations in blood plasma and testis were measured by the radioimmunoassay described previously by Chen *et al.* [4]. The steroids in samples were extracted with diethyl ether. The average recoveries of the added steroids were 70.2% and 83.3% for plasma and testicular androgen, respectively, and individuals recoveries were run with each sample. The cross reactivities of the antiserum with various androgens, in relative to testosterone (100%), were: 5α-dihydrotestosterone (74%), androstenedione (1.23%), and androstenediol (0.59%) [59]. Thus, the data are expressed as "androgen" which mainly representing testosterone and dihydrotestosterone.

The coefficient of variation (CV) of the interassay was 11.0% (N=5) and that of intraassay was 6% (N=6) for plasma androgen. The CV of interassay was 9.2% (N=8) and that of intraassay was 2.4% (N=6) for testicular androgen.

Statistical analysis

Analysis of variance (ANOVA) and Duncan's multiple range tests were used to examine differences among the numerous means. Linear correlations were performed for all variables. Probability

levels of 0.05 and 0.01 were used to indicate significance in comparison of means and correlations [49].

RESULTS

Annual changes in the sizes of body, testis, liver and fat body

Changes in body weight and body length are shown in Table 1. During the annual reproductive cycle of *R. rugulosa,* body weights ranged from 30–82 g; and body lengths from 70–92 mm. The body weights were greater during May–November than those during December–April. The weight of paired testes increased during Dcember–February, peaked in March, sharply declined in April–May, and remained at low levels in June–October (Table 1). Differential changes in the weights and lengths of left and right testes were observed (Fig. 2). The mean weight of the left testis was 20% higher than that of the right testis; while, the mean length of the left testis was 40% higher than that of the right testis. The shape of left testis was less uniform than that of right testis. In addition, the annual changes in lengths of both testes were not as great as those of testicular weight although the lengths of both testes rose in February–April.

Table 1. Changes in the sizes of body, testis, liver, and fat body during an annual reproductive cycle of *R. rugulosa*

Months[1]		N[2]	Body[3]		Organ weights[3]		
			length	weight	testes	liver	fat bodies
			(cm)	(g)	(mg)	(g)	(g)
1986							
Nov	21	21	78.5±1.0	46.9±1.4	86.4±5.9	1.33±0.06	2.40±0.20
Dec	28	12	80.1±1.4	40.9±2.0	88.5±8.7	0.89±0.05	1.63±0.18
1987							
Jan	23	20	78.8±0.9	42.5±1.3	117.4±9.2	1.05±0.06	1.38±0.15
Feb	26	20	80.4±0.7	43.0±1.3	132.8±10	0.97±0.05	1.52±0.14
Mar	12	16	80.2±0.8	42.7±1.0	133.2±9.7	0.78±0.03	1.10±0.17
	26	16	82.8±0.6	47.9±1.2	131.3±4.8	0.85±0.03	1.28±0.16
Apr	2	15	79.2±0.6	38.5±0.9	115.7±8.2	0.66±0.02	0.82±0.11
	9	19	79.2±0.6	39.2±0.9	107.6±4.8	0.59±0.03	0.61±0.09
	16	14	79.4±0.7	39.4±1.2	122.1±10	0.62±0.03	0.51±0.01
	23	17	77.6±0.7	37.7±3.9	102.5±5.3	0.62±0.03	0.34±0.10
	30	16	77.5±0.7	36.2±1.0	110.6±5.2	0.58±0.03	0.29±0.06
May	7	11	78.3±1.0	39.1±1.5	109.8±6.5	0.65±0.04	0.29±0.06
	21	17	80.5±1.3	44.8±2.0	85.0±4.6	0.88±0.06	0.14±0.07
Jun	4	19	79.9±0.6	49.2±1.5	71.5±5.7	1.36±0.09	0.14±0.03
	28	21	81.3±0.7	55.1±1.9	72.6±4.2	2.07±0.14	0.19±0.03
Jul	29	25	81.3±0.8	43.8±1.2	79.4±7.1	1.28±0.07	1.07±0.22
Aug	29	22	84.8±0.7	56.6±2.5	60.8±6.3	3.14±0.28	1.35±0.17
Sep	24	17	81.6±0.9	52.8±1.2	65.0±7.4	3.40±0.28	2.96±0.25
Oct	30	12	80.6±0.6	51.1±1.9	67.3±9.4	3.00±0.27	2.42±0.14
Nov	23	17	81.3±0.7	50.7±2.0	99.0±6.4	1.68±0.11	2.39±0.26

[1] The frogs were collected monthly, or more frequently during the active breeding season from march through June.

[2] Number of animals

[3] The data are expressed as the means±SE.

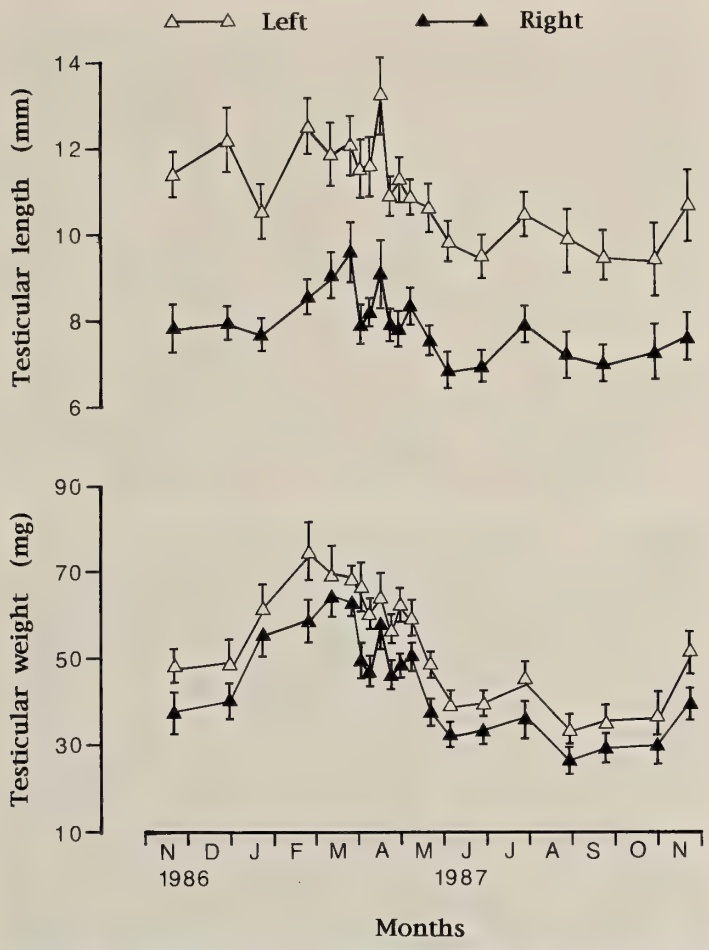

FIG. 2. Changes in the weights and lengths of the left and right testes during an annual reproductive cycle of *R. rugulosa*. The data are expressed as the means ± SE, and the number of animlas as indicated in Table 1.

Annual pattern in the weights of liver and fat body are shown in Table 1. The liver and fat body weights decreased in November–February, reached the minimal sizes in early May and late June, repsectively, and increase in early June and late July, repsectively. In September, both organs attained the maximal sizes, and then began to decrease in late October. Highly significant correlation was observed between liver and fat body weights ($r=0.60$, $p<0.01$). As shown in Fig. 3, an inverse relationship existed between the hepatosomatic index and the gonadosomatic index ($r=-0.828$, $p<0.01$). The correlation between fat body-somatic index and the gonadosomatic index was, however, not significant.

Testicular development and spermatogenesis

Proliferation of Leydig cells changed with season (Fig. 4). In November–December and January–February, Leydig cells were sparse and difficult to distinguish from other connective tissue (Fig. 4-A). The Leydig cells began to proliferate in late March and were abundant in the broad intertubule space in April–July (Fig. 4-B) after which they rapidly decreasd between the decreasing intertubular space (Fig. 4-C).

Seasonal changes in histological observations of the spermatogenetic cycle in the testis of *R. tigerina rugulosa* are also representatively shown in Fig. 4. The spermatogenetic cycle showed every

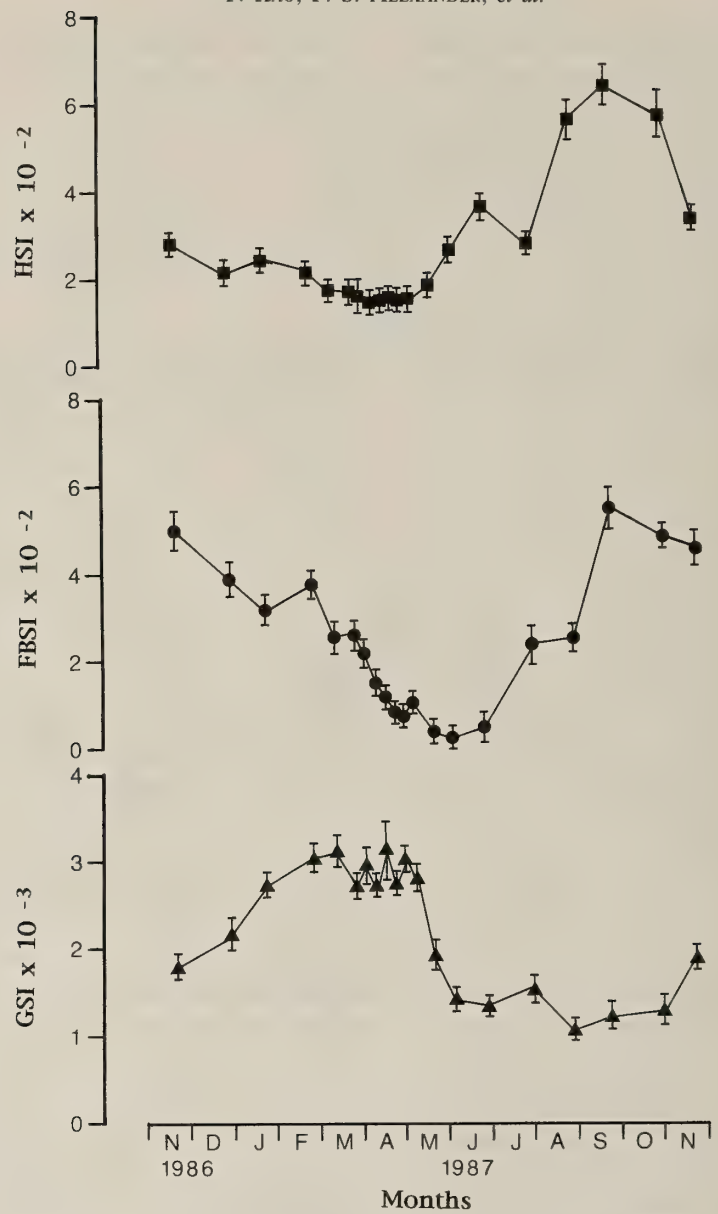

FIG. 3. The relations of liver and fat body weights to the testicular weights during an annual reproductive cycle of *R. rugulosa*. The data are expressed as mean ± SE, and the number of animals as indicated in Table 1. GSI, testes weight/body weight; HSI, liver weight/body weight; FBSI, fat body weight/body weight.

FIG. 4. Seasonal changes in the spermatogenetic cycle and the proliferation of Leydig cells of *R. rugulosa*. **a**, the nest of primary spermatogonia; **b**, the nest of secondary spermatogonia; **c**, the nest of primary spermatocytes; **d**, the nest of secondary spermatocytes; **e**, the nest of spermatids; **f**, spermatozoa; **g**, Leydig cells. A. Hibernation (December). Primary and secondary spermatogonia were the most numerous spermatogenetic cells in this period. A few clusters of spermatozoa were produced. Leydig cells existed in sparse between the seminiferous tubules. B. Breeding Season (May). Massive spermatozoa were formed in this period. Leydig cells were abundant in the intertubular space. C. Postbreeding Season (August). Cell nests of all stages of spermatogenetic cycle were existent. Few spermatozoa occurred in this period. Leydig cells were greatly reduced in number in the intertubules.

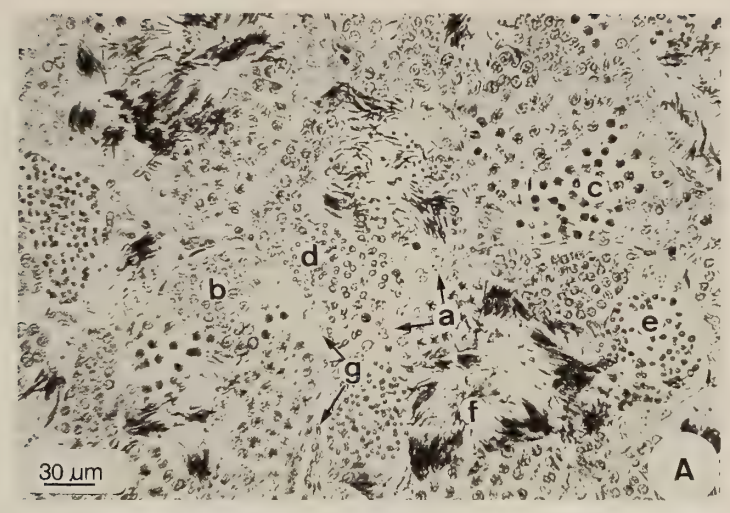
a
b
c
d
e
f
g
30 µm
A

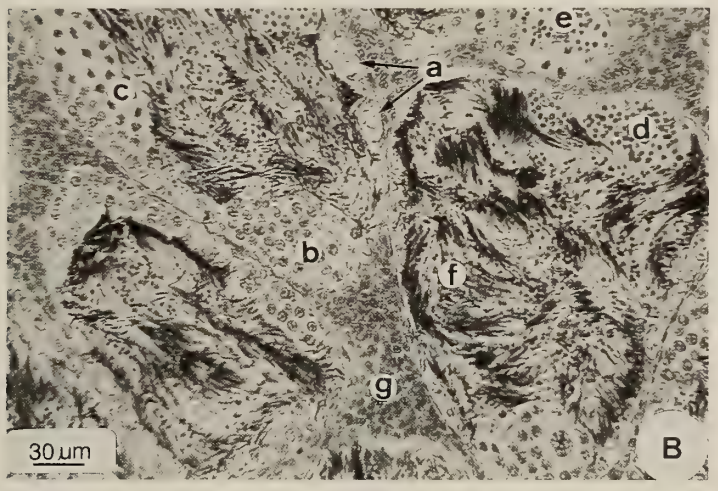
a
b
c
d
e
f
g
30 µm
B

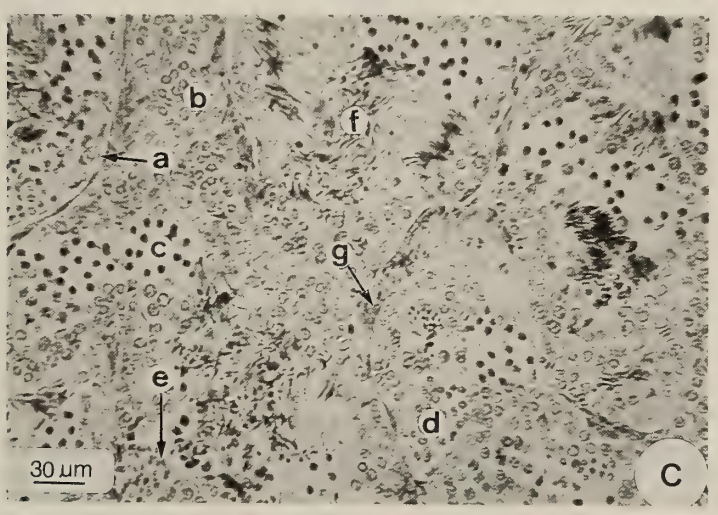
a
b
c
d
e
f
g
30 µm
C

stage of spermatogenesis year around. Only a few clusters of spermatozoa were found in the seminiferous tubules during hibernation (November–February) (Fig. 4-A). Massive formation of spermatozoa occurred during the active breeding season mainly in April–June (Fig. 4-B). Spermatozoa were greatly reduced in number during postbreeding in August–October (Fig. 4-C).

Significant annual changes occured in the spermatogenetic cycle (ANOVA, $p<0.01$) based on the estimate of the number of various stages of cell nests from primary spermatogonia to spermatids (Fig. 5). In November–December of 1986, ISPG were most numerous, accounting for 48% of the

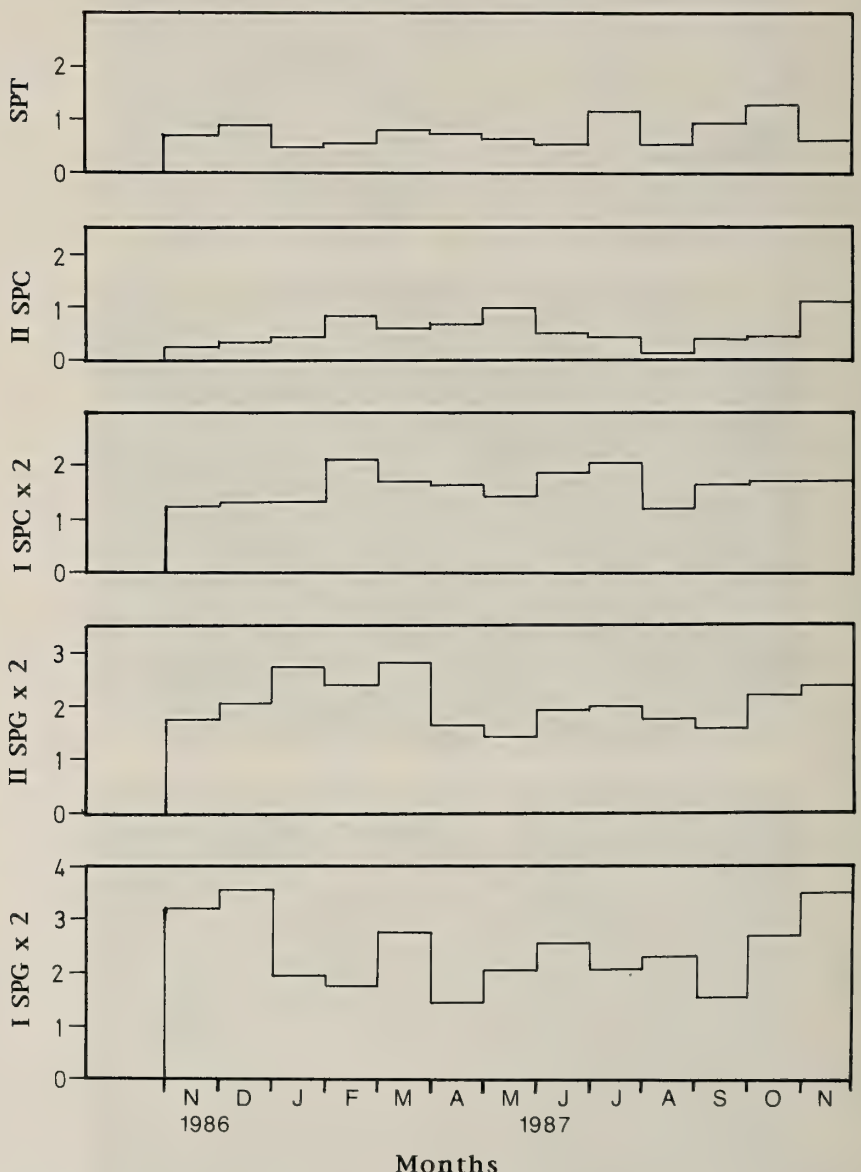

Fig. 5. Quantitative changes in different stages of spermatogenesis during an annual reproductive cycle of *R. rugulosa*. Values are expressed as the average number of cell nests of various spermatogenetic stages per seminiferous tubule. ISPG and IISPG, primary and secondary spermatogonia; ISPC and IISPC, primary and secondary spermatocytes; SPT, spermatids.

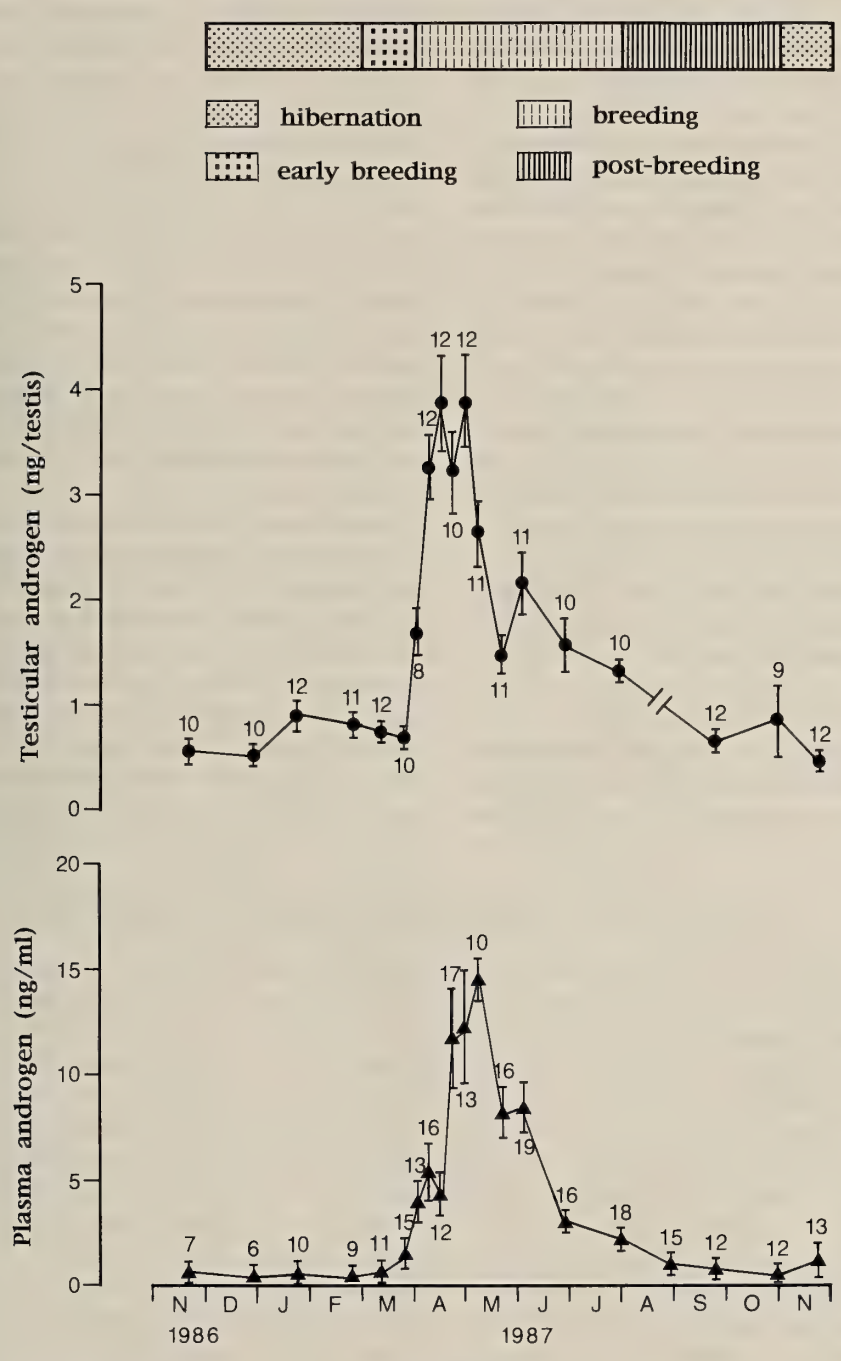

FIG. 6. The unimodal patterns of changes in testicular androgen content and plasma androgen levels during an annual reproductive cycle of *R. rugulosa*. The annual reproductive cycle was divided into four periods: hibernation, early breeding, breeding, and post-breeding. The data are expressed as the means ± SE, and the number of animlas as indicated with Arabic numerals.

total germinal cell nests; other stages of germ cells began to multiply in December. In January and February, the number of ISPG and SPT declined, but those of IISPG, ISPC, and IISPC increased with the rise in ISPC and IISPC lagging behind that of IISPG. In March there were increases in the ISPG and IISPG followed by sharp decreases in April. ISPG then exhibited a slight increase with some fluctuations in May–August; it decreased again in September, followed by sharp increases in October and November. IISPG remained virtually constant from May through September, and then increased in October. ISPC decreased in March–May, and increased again in June–July; by contrast, a reverse pattern existed for IISPC in March–July. At this period (March–July), the cell nests of SPC (the sum of ISPC and IISPC) became the most numerous. During the breeding season (March–July), spermatozoa were massively formed from SPT. ISPC, IISPC, SPT, and spermatozoa all reduced in August, and increased in September–October.

Plasma and testicular androgen levels

Plasma and testicular androgen levels showed significant seasonal changes (ANOVA, $p<0.05$, Fig. 6). Plasma androgen levels were very low (<1 ng/ml) during hibernation (November–February), increased in late March, peaked in early May (14.50 ± 1.05 ng/ml), decreased sharply in late May and June, and reached basal levels afterwards (from July through October). Testicular androgen content was also low during hibernation period (<1 ng/testis), increased rapidly in early April (3.28 ± 0.28 ng/testis) and peaked in middle (3.88 ± 0.45 ng/testis) and late April (3.90 ± 0.44 ng/testis); the androgen levels were decreased markedly in May, followed by a gradual drop afterwards, and reached basal values in September (0.7 ± 0.07 ng/testis). During the annual reproductive cycle of *R. rugulosa,* the difference between maximal and minimal values in testicular androgen content was 10 fold, while that in plasma androgen was 50 fold.

Correlations of plasma androgen concentration with testicular development, liver, and fat body are summarized in Table 2. Highly significant correlations were observed between plasma androgen levels and testicular androgen content. There were significant negative correlations of plasma and testicular androgen levels with liver weight and fat body weight respectively, as well as with two stages of spermatogonia (the number of nests of primary spermatogonia, ISPG, and of

Table 2. Correlation coefficients (r) of plasma and testicular androgen levels with spermatogenetic cell types, and liver and fat body weights of male *R. rugulosa* during an annual reproductive cycle

	Plasma androgen	Testicular androgen
Testicular androgen	0.734**	1.0
Testicular weight	0.087	0.188
GSI	0.288	0.426
Liver weight	−0.438†	−0.460*
HSI	−0.448†	−0.466†
Fat body weight	−0.702**	−0.696**
FBSI	−0.719**	−0.707**
Primary spermatogonia	−0.515†	−0.628*
Secondary spermatogonia	−0.499†	−0.403
Primary spermatocytes	0.025	0.139
Secondary spermatocytes	0.389	0.141
Spermatids	−0.074	−0.019

Correlation coefficients (r) were analyzed from the monthly means of those parameters. GSI, gonadosomatic index=testis weight/body weight; FBSI, fat body weight/body weight; HSI, liver weight/body weight; †, $p<0.10$; *, $p<0.05$; **, $p<0.01$.

secondary spermatogonia, IISPG). The rising phases of both plasma and testicular androgen levels were synchronized with active spermiogenesis (Figs. 4-B and 6).

DISCUSSION

Annual patterns of testis, liver, and fat body

A unimodal pattern of annual variation exists in the testicular weight of *R. rugulosa*. There are significant differences between the maximal and minimal mean values of both testicular weight (2 fold) and GSI (3 fold) during the annual cycle. Such annual changes in GSI of this species are similar to those of *R. tigerina* [44], *B. marinus* [44], *R. esculenta* [21, 43], and *B. japonicus* [13, 30], but are different from those of *R. perezi* [6] and *R. catesbeiana* [19, 58], showing little variation of GSI. The annual change in the testicular weight of *R. rugulosa* also shows a positive correlation with secondary spermatogonia ($r=0.625$; $p<0.05$). Thus, the rising phase of testicular weight in January–March is presumably due to the increases in the secondary spermatogonia even though other factors, such as water reabsorption and cellular hypertrophy, may be involved. On the other hand, the observations that the testicular weight of *R. rugulosa* exhibited some fluctuations during the entire breeding season (March–July) and sharp decreases in the late breeding season (June–early July) may be attributed to the evacuation of spermatozoa. We observed that both lengths and weights of left testis were greater than those of right testis during an annual cycle of *R. rugulosa*. Such findings are similar to those of *B. bufo* and *R. nigromaculata* reported by other investigators [53].

In male anurans, the roles of liver in the reproductive cycle include the formation of sex steroid-binding proteins, the formation and storage of lipids and carbohydrates for the metabolic activity of the gonads, the degradation of gonadal steroid hormones and others [23, 26, 29, 35, 47]. we demonstrated that a unimodal pattern of annual change in liver weight exists in male *R. rugulosa*. This finding is similar to those of *A. crepitans* [23], *B. woodhousei* [23], *B. canorus* [29], and *R. esculenta* [47], but is different from that of *R. nigromaculata* [27], a temperate species, which showing no significant difference in the liver weight during the annual cycle. We also found that the annual change in liver weight of *R. rugulosa* positively correlates with that of the body weight ($r=0.877$, $p<0.01$), but negatively with that of the testicular weight. Such findings are in disagreement with those reported for *R. ridibunda* [24], which displaying high positive correlations among the weights of body, liver, and testes.

The functions of fat body on reproduction in male anurans are likely the supply of metabolic energy for the maintenance of testicular activity during hibernation, and for androgen production during the breeding season, as demonstrated in *R. esculenta* [28, 43], and in *Acris crepitans* and *B. woodhousei* [23]. Male *R. rugulosa*, as observed in the present study, exhibits a unimodal pattern of annual change in the fat body weight, which being positively correlated with liver weight, but not with the body weight ($r=0.421$, $p>0.05$). The annual change in the fat body weight is not correlated with that in the testicular weight, but is negatively correlated with androgen levels in testis and plasma (Table 2). These results are similar to those of *R. perezi* [6] and *B. japonicus* [30] thus support the proposals that the fat bodies serve as a major lipid nutrient for metabolic energy in general and in the testis in particular [5, 8].

Spermatogenetic cycle

The annual spermatogenetic cycles in anurans have been classified into three types: discontinuous, potentially continuous, and continuous [22]. Discontinuous spermatogenesis is commonly found in temperate and cold zone species such as *R. temporaria* [22]; while continuous spermatogenesis is characteristic of the spermatogenetic cycle of tropical and subtropical anurans [22]. Some anuran species such as *R. esculenta* and *R. tigerina* are classified as "potentially continuous cycle" where the primary spermatogonia never become refractory to gonadotropin and continue to undergo multiplication until the lowering temperature of autumn and winter causes a retardation [1, 22, 34, 44, 45]. In the present study, we observed that *R. rugulosa* inhabiting subtropical Taiwan exhibits a continuous spermatogenetic

cycle with germ cells of all stages found throughout the year, although massive spermatozoa being existed in April–May.

Androgen patterns

Annual changes in plasma androgen levels have been studied in many species of male anurans: seven temperate species, *R. perezi* [6], *R. catesbeiana* [19], *B. japonicus* [13], *R. esculenta* [7], *B. mauritanicus* [48], *R. ridibunda* [55], and *R. nigromaculata* [51]; three subtropical species, *P. dacnicolor* [41] and *B. bufo gargarizans* and *B. melanostictus* [12]; a tropical species, *D. occipitalis* [17]. These male anurans exhibit either unimodal or bimodal types of annual patterns in plasma androgen characterized by a single peak or two peaks, respectively, of annual circulating androgen levels [13]. Studies have demonstrated that subtropical male anurans show an annual unimodal pattern of plasma androgen levels [12, 41], while temperate male anurans show both unimodal and bimodal patterns of androgen levels [6, 7, 13, 19, 48, 51, 55]. However, *D. occipitalis* [17], a tropical anura, displays a bimodal pattern of annual plasma androgen level. We have demonstrated in the present study that male *R. rugulosa,* inhabiting subtropical Taiwan, displays a unimodal pattern of circulating androgen levels during an annual reproductive cycle. This pattern is comparable with those of subtropical anurans reported by other investigators [12, 41].

In vitro studies of testicular androgen biosynthesis in Amphibia indicate that dihydrotestosterone (DHT) is the major androgen in Anura and that testosterone (T) is the major androgen in Urodele [15]. Such a conclusion is supported by *in vivo* investigations of the circulating androgens in Anurans, *R. catesbeiana* [19], *R. nigromaculata* [51], *R. pipiens* [57], *Eleutherodactylus coqui* [54], and in Urodeles, *Necturus maculosus* [2], *Salamandra salamandra* [18], *Pleurodeles waltl* [10], and *Ambystoma tigrinum* [33]. However, in several anuran species, such as *B. japonicus* [13], *R. esculenta* [38], *B. mauritanicus* [48], and *P. dacnicolor* [41], T is more predominant than DHT in circulation. Whether T or DHT is the predominant androgen in the male Chinese bullfrog, *R. rugulosa,* requires further investigations. In mammals, DTH is identified to be primarily a metabolite of T in peripheral target tissues. DTH is considered to be directly formed by testis of anuran amphibians [11, 15, 16, 31, 32, 36, 37], while it has not been identified in the testis of urodel amphibians [15, 25, 29, 50, 52]. The physiological role of DHT in amphibians is not yet clearly defined, and thus needs further studies.

Androgen secretion is regulated by the interactions of hormonal and environmental factors [43, 44]. Rastogi *et al.* [43] reported that androgen in *R. esculenta* shows a negative feedback interaction with gonadotropins by a study of hypophysectomic implantation with homoplastic pituitary extract; on the other hand, in *R. catesbeiana,* plasma gonadotropins and steroids are simultaneously elevated throughout most of the reproductive cycle, as well as LH levels exhibit a weak correlation with androgen levels [19]. In *B. japonicus,* Itoh *et al.* [13] reported that plasma LH levels, but not FSH levels, were highly correlated with circulating androgen levels.

Correlation of androgen patterns with spermatogenetic cycle

The hormonal control of spermatogenesis in anurans has been investigated [6, 40, 41, 43, 44, 58]. It was demonstrated that FSH stimulates the spermatogenesis on the basis of the studies with mammalian hormones [40, 44]. On the other hand, the controversial results of the effect of androgen on spermatogenesis have been reported in anurans: such as in *R. hexadactyla, R. esculenta* and *R. tigerina,* where androgen exhibiting suppression of spermatogenesis (mainly at the secondary spermatogonia stage); and in *B. fowleri* and *B. arenarum,* where androgen showing the stimulation of spermatogenesis [1, 40, 44]. In male *R. rugulosa,* as observed in this study, androgen levels in both testis and plasma show a weakly reverse correlation with spermatogenetic stages of primary and secondary spermatogonia, but parallel with changes in the number of spermatozoa. The role which androgen plays on different stages of spermatogenesis in *R. rugulosa* needs further investigation.

Relations of androgen patterns to breeding activity

In male *R. rugulosa,* we observed that the pattern of androgen secretion parallels with breeding activity; the circulating androgen peak occurring in early May was found to be coincident with the active breeding period in April–June. Such patterns are similar to those of *P. dacnicolor* [41], but different from those of *R. perezi* [6], *B. japonicus* [13], *R. esculenta* [38], and *R. ridibunda* [55] which showing a peak of plasma androgen level prior to breeding season. The patterns of testicular activity and androgen secretion observed in male *R. rugulosa* were synchronized with the patterns of ovarian maturation and estradiol secretion of the females, which were simultaneously investigated in a parallel study at the same frog culture farm [3].

The role of androgen in induction and subsequent maintenance of male reproductive behavior, has been established in several anurans [14, 48, 54, 57]. For example, *B. Mauitanicus* [48] and *E. coqui* [54] both show a high androgen level during the amplexing behavior; while, *B. japonicus* [14] shows a high androgen level during the migration behavior. We also observed in the present study that high androgen levels in plasma of *R. rugulosa* are paralleled with its reproductive activity such as chorussing and spermiation, as well as with nuptial pad development in relation to amplexing behavior. These observations support the proposal that androgen plays a role in maintenance of the male reproductive behavior in this species.

Association of environmental factors with reproductive cycle

Effects of environmental cues on male anuran reproductive cycle have been studied [6, 22, 42, 43, 44, 46]. It was reported that, in most subtropical and tropical species, rainfall is the most important factor associated with initiation of breeding activity since temperature changes little with seasons in these areas [11]. However, the mechanisms of rainfall in the regulation of anuran reproductive cycle are not clear [46]. On the other hand, temperature is the primary factor in temperate species, which exhibiting a cyclic reproductive pattern with season. The role of temperature in the regulation of anuran spermatogenetic cycle has been investigated in many speices [6, 22, 43, 46]. In *R. esculenta,* the proliferation of primary spermatogonia is available in low temperature; in addition, the formation of secondary spermatogonia, and primary and secondary spermatocytes occurs with increasing temperature [42, 43]. It was subsequently demonstrated in this species that the temperature plays a major role in the spermatogenesis via stimulation of the release of pituitary gonadotropins and testicular androgen secretion [43]. Rastogi *et al.* [43] also demonstrated that photoperiod serves as a permissive role on temperature influence upon spermatogenesis of *R. esculenta.* In the present study, we found that the rising phases of climatic factors (rainfall, temperature, and photoperiod) parallel temporally with active testicular development and spermatogenesis, the rising androgen levels in plasma and testis, and breeding activity during the annual reproductive cycle of *R. rugulosa.* Regulatory mechanisms of environmental factors on a reproductive cycle of anurans are highly complex, and are presumably mediated by a pathway of optic or other transmissions to the hypothalamo-hypophysial-gonadal axis.

ACKNOWLEDGMENTS

We are grateful to the Department of Biology, Tunghai University, Taichung, and Institute of Zoology, Academia Sinica, Taipei, Taiwan, R. O. C., for the grants supporting this study. Thanks are also due to Mr. Shen San-tai, Miss Chen Chao-yin, Miss Chern Jyun-rur, and Miss Su Huey-min for assistance during various periods of this study.

REFERENCES

1 Basu SL (1962) A study of the spermatogenesis of common Indian frog (*Rana tigerina*) treated with testosterone. Naturwissenschaften 49: 188

2 Bolaffi JL and Callard IP (1979) Plasma steroid profiles in male and female mudpuppies, *Necturus maculosus* (Rafinesque). Gen Comp Endocrinol 37: 443–450

3 Chen CY (1988) Seasonal changes in ovarian activity and plasma sex steroids levels in the Chinese bullfrog, *Rana tigerina rugulosa* Wiegmann. Master's Thesis, Tunghai University, Taichung, Taiwan, ROC

4 Chen RH, Lin JY, Yu YL and Cheng HY (1987) Annual changes in plasma and testicular androgen in relation to reproductive cycle in a Japalura Lizard in Taiwan. Zool Sci 4: 323–329

5 Chieffi G, Rastogi RK, Iela L and Milone M (1975) The function of fat bodies in relation to the hypothalamohypophyseal-gonadal axis in the frog, *Rana esculenta.* Cell Tiss Res 161: 157–165

6 Delgado MJ, Gutierrez P and Alonso-Bedate M (1989) Seasonal cycle in testicular activity in the frog, *Rana perezi.* Gen Comp Endocrinol 73: 1–11

7 D'Istria M, Delrio G, Botte V and Chieffi G (1974) Radioimmunoassay of testosterone, 17β-oestradiol and oestrone in the male and female plasma of *Rana esculenta* during sexual cycle. Steroids Lipids Res 5: 42–48

8 Fitzpatrick LC (1976) Life history patterns of storage and utilization of lipids for energy in amphibians Amer Zool 16: 725–732

9 Frost DR (1985) Amphibian Species of the World. Lawrence, Kansas: Assoc Syst Coll pp 512–518

10 Garnier DH (1985) Androgen and estrogen levels in the palsma of *Pleurodeles waltl,* Michah, during the annual cycle. I. Male cycle. Gen Comp Endocrinol 58: 376–385

11 Gavaud J (1975) Etude experimentale du role des facteur externes sur la spermatogenese et la steroidogenese des male de *Nectophrynoides occidentalis* Angel J Physiol (Paris) 70: 549–559

12 Huang, WS (1991) Male reproductive cycles of two sympatric toads, *Bufo bufo gargarizas* and *Bufo melanostictus.* Master's Thesis, Tunghai University, Taichung, Taiwan, ROC

13 Itoh M, Inoue M and Ishii S (1990) Annual cycle of pituitary and plasma gonadotropins and plasma sex steroids in a wild population of the toad, *Bufo japonicus.* Gen Comp Endocrinol 78: 242–253

14 Itoh M and Ishii S (1990) Changes in plasma levels of gonadotropins and sex steroids in the toad, *Bufo japonicus,* in association with behavior during the breeding season. Gen Comp Endcrinol 80: 451–464

15 Kime DE (1980) Comparative aspects of testicular androgen biosynthesis in nonmammalian vertebrates. In "Steroids and Their Mechanism of Action in Nonmammalian Vertebrates". Eds by G Delrio and J Brachet, Raven Press, New York pp 17–32

16 Kime DE and Hews EA (1978) Androgen biosynthesis *in vitro* by testes from amphibia. Gen Comp Endocrinol 35: 280–288

17 Kuhn ER, Gevaerts H, Vandorpe G and Jacobs GFM (1987) Plasma concentrations of testosterone and thyroxine in males of the giant swamp frog, *Dicroglossus occipitalis* at the equator. Gen Com Endocrinol 68: 492–493

18 Lecouteux A, Garnier DH, Bassez T and Joly J (1985) Seasonal variations of androgens, estrogens, and progestorone in the different lobules of the tesits and in the plasma of *Salamandra salamandra.* Gen Comp Endcrinol 58: 211–221

19 Licht P, McCreery BR, Barnes R and Pang R (1983) Seasonal and stress related changes in plasma gonadotropins, sex steroids, and corticosterone in the bullfrog, *Rana catesbeiana.* Gen Comp Endocrinol 50: 124–145

20 Liu CC (1950) Amphibians of Western China. Fieldiana: Zoology Memoirs 2: 1–400

21 Lofts B. (1964) Seasonal changes in the functional activity of the interstitital and spermatogenetic tissues of the green frog, *Rana esculenta.* Gen Comp Endocrinol 4: 550–562

22 Lofts B (1974) Reproduction. In "Physiology of the Amphibia". Ed by B Lofts, Academic Press, New York Vol 2 pp 107–218

23 Long DR (1987) A comparison of energy substrates and reproductive patterns of two anurans, *Acris crepitans* and *Bufo woodhousei.* Comp Biochem Physiol 87A (1): 81–91

24 Loumbourdis NS and Kyriakopoulou-Sklavounous P (1991) Reproductive and lipid cycles in the male frog *Rana ridibunda* in northern Greece. Comp Biochem Physiol 99A: 577–583

25 Lupo di Prisco C, Basile C, Delrio G and Chieffi G (1972) *In vitro* metabolism of cholesterol-4-C^{14} and testosterone-4-C^{14} in testes and fat bodies of *Triturus cristatus carnifex.* Comp Biochem Physiol 41B: 245–249

26 Martin B (1980) Steroid-protein interactions in nonmammalian vertebrates: distribution, origin, regulation, and physiological significance of plasma steroid binding proteins. In "Steroids and Their Mechanisms of Action in nonmammalian Vertebrates". Eds by G Delrio and J Brachet, Raven Press New York pp 63–73

27 Maruyama K (1979) Seasonal cycles in organ weights and lipid levels of the frog, *Rana nigromaculata.* Annot Zool Japon 52(1): 18–27

28 Milone M, Chieffi G, Caliendo MF and Pierantoni R (1984) Effect of the removal fat bodies on lipid biosynthesis in frog testis. Boll Zool 51: 75 (Abstract)

29 Morton MC (1981) Seasonal changes in total body lipid and liver weight in the Yosemite toad. Copeia 1981(1): 234–238

30 Moriguchi Y and Iwasawa H (1987) Annual changes in male reproductive organs in *Bufo japonicus formosus*: Histological observation. General Endocrinol 6: 115–120

31 Muller CH (1975) *In vitro* steroidogenesis by bullfrog testis. Soc Study Reprod 8th Ann Meeting pp 95–96 (abstract 104)

32 Muller CH (1976) Secretion of 5α-dihydrotestosterone by bullfrog testis. Prog Abstr 58th Ann Meet-

ing Endocrine Soc p 286 (abstract 423)

33 Norris DO, Norman MF, Pancak MK and Duvall D (1985) Seasonal variations in spermatogenesis, testicular weights, vasa deferentia, and androgen levels in neotenic male tiger salamanders, *Ambystoma tigrinum*. Gen Comp Endocrinol 60: 51–57

34 Oordt PGWJ van (1960) The influence of internal and external factors in the regulation of the spermatogenetic cycle in amphibia. Symp Zool Soc London 2: 29–52

35 Ozon R (1972) Androgens in fishes, amphibians, reptiles, and birds. In "Steroids in Nonmammalian Vertebrates". Ed by DR Idler, Academic Press, New York pp 329–389

36 Ozon R, Breuer H and Hisboa BP (1964) Etude du metabolisme des hormones steroides chez les vertebre inferieurs. III Metabolisme *in ivtro* de la testosterone par l'ovaire et la testicule de la grenouille *Rana temporaria*. Gen Comp Endocrinol 4: 577–583

37 Ozon R and Stocker C (1974) Formation *in vitro* de 5α-dihydrotestosterone par le testicular de *Discoglossue pictus*. Gen Comp Endocrinol 23: 224–236

38 Pierantoni R, Iela L d'Istria M, Fasano S, Rastogi RK and Delrio G (1984) Seasonal testosterone profile and testicular responsiveness to pituitary factors and gonadotrophin-releasing hormone during two different phases of the sexual cycle of the frog (*Rana esculenta*) J Endocrinol 102: 387–392

39 Pope CH and Boring AM (1940) A survey of Chinese Amphibia. Peking Nat Hist Bull 15: 49–50

40 Rastogi RK and Iela L (1980) Steroidogenesis and spermatogenesis in anuran amphibia: A brief survey. In "Steroids and Their Mechanism of Action in Nonmammalian Vertebrates". Eds by G Delrio and J Brachet, Raven Press, New York pp 131–146

41 Rastogi RK, Iela, L, Delrio G and Bagnara JT (1986) Reproduction in Mexican leaf frog, *Pachymedusa dacnicolor* II. male Gen Comp Endocrinol 62: 23–35

42 Rastogi RK, Iela L, Delrio G, Dimeglio M, Rosso A and Chieffi G (1978) Environmental influence on testicuiar activity in the green frog, *Rana esculenta*. J Exp Zool 206: 49–64

43 Rastogi RK, Iela L, Saxena PK and Chieffi G (1976) The control of spermatogenesis in the green frog, *Rana esculenta*. J Exp Zool 196: 151–166

44 Saidapur SK (1983) Patterns of testicular activity in Indian amphibians. Indian Rev Life Sci 3: 157–184

45 Saidapur SK and Nadkarni VB (1975) Seasonal variation in the structure and function of testis and thumb pad in the frog *Rana tigerina* (Daud.). Indian J Exp Biol 13: 432–438

46 Salthe SN and Mecham JS (1974) Reproductive and courtship patterns. In "Physiology of the Amphibia". Ed by B Lofts, Academic Press, New York Vol 2 pp 309–521

47 Schlaghecke R and Blum V (1978) Seasonal variations in liver metabolism of the green frog *Rana esculenta* (L). Experientia 34: 456–457

48 Siboulet R (1981) Variations saisonnieres de la teneur plasmatique en testosterone et dihydrotestosterone chez le crapaud de mauritanie (*Bufo mauritanicus*). Gen Comp Endcrinol 43: 71–75

49 Steel RGD and Torrie JH (1980) In "Principles and Procedures of Statistics", 2nd ed McGraw-Hill Book Company

50 Tajima H, Arai R, Tomaoki B-I and Hanaoka K-I (1969) *In vitro* steroidogenesis in testicular homogenates of the Japanese newt, *Cynops Pyrrhogaster* (Boie). Gen Comp Endcrinol 12: 549–555

51 Tanaka S, Iwasawa H and Wakabayashi K (1988) Plasma levels of androgens in growing frogs of *Rana nigromaculata*. Zool Sci 5: 1007–1012

52 Tanaka S and Takikawa H (1983) Seasonal changes in plasma testosterone and 5α-dihydrotestosterone levels in adult male newt, *Cynops pyrrhogaster pyrrhogaster*. Endocrinol Japon 30(1): 1–6

53 Ting HP and Boring AM (1939) The seasonal cycle in the reproductive organs of the Chinese toad *Bufo bufo* and the pond frog *Rana nigromaculata*. Peking Nat Hist Bull 14: 49–80

54 Townsend DS and Moger WH (1987) Plasma androgen levels during parental care in a tropical frog (*Eleutherodactylus*). Horm Behav 21: 93–99

55 Vandorpe G, Jacobs GFM and Kuhn ER (1987) Seasonal changes of the 5′-monodeiodination activity in kidney and skin homogenates of male *Rana ridibunda*: relation to plasma thyroxine (T4) and testosterone. Gen Comp Endocrinol 68: 163–169

56 Varriale B, Pierantoni R, Matteo LD, Minsucci S, Fasano S, D'Antonio M and Chieffi G (1986) Plasma and testicular estradiol and plasma androgen profile in the male frog *Rana esculenta* during the annual cycle. Gen Comp Endocrinol 64: 401–404

57 Wada M, Wingfield JC and Gorbman A (1976) Correlation between blood level of androgens and sexual behavior in male leopard frogs, *Rana pipiens*. Gen Comp Endocrinol 29: 72–77

58 Yoneyama H and Iwasawa H (1985) Annual changes in the testis and accessory sex organs of the bullfrog, *Rana catesbeiana*. Zool Sci 2: 229–237

59 Yu JYL, Liaw JJ, Chang CL, Lee SN and Chen MC (1988) Seasonal changes in circulating levels of gonadal steroids during an estrous cycle of holstein-friesian cows Bull Inst Zool Academia Sinica (ROC) 27(2): 133–143

ZOOLOGICAL SCIENCE 10: 353–360 (1993)

Prolactin Binding Sites in Normal Uterus and the Uterus with Adenomyosis in Mice

Tippawan Singtripop, Takao Mori, Min Kyun Park,
Koichi Shiraishi, Toshio Harigaya*
and Seiichiro Kawashima

*Zoological Institute, Faculty of Science, University of Tokyo, Tokyo 113, and *Laboratory of Functional Anatomy, Faculty of Agriculture, Meiji University, Kawasaki 214, Japan*

ABSTRACT—Radioreceptor assay for mouse prolactin (mPRL) was developed in the mouse uterus. The specific binding of [^{125}I]-mPRL to the uterine preparations was demonstrated and the binding was found to have a similar affinity to that in the liver preparations. The specific PRL-binding to the uterine preparations tended to increase after estrogen treatment, while the differences among the three groups, diestrous intact, ovariectomized, and ovariectomized and estrogen-treated mice, were statistically not significant. Immunohistochemical staining of PRL revealed that PRL immunoreactivity was preferentially localized in the myometrial cells. Pituitary grafting into the uterus induced a high incidence of adenomyosis associated with the increase in plasma PRL levels. Furthermore, the PRL-binding activity in the uterus with adenomyosis was significantly higher than that in normal uterus. These results indicate that the elevation of PRL binding in the uterus, hyperprolactinemia, and the development of adenomyosis are interrelated.

INTRODUCTION

Prolactin (PRL) is known to act on various organs, such as the brain, mammary gland, liver, ovary, testis and some reproductive tracts in mammals [1, 6, 20, 21, 26]. Evidence of PRL effects on these target organs involves the presence of specific PRL-binding sites. Estrogens have been found to increase the specific PRL-binding sites in the liver of rats in the presence of intact pituitary glands [22, 24]. In mice, however, Marshall *et al.* [9] reported that ovariectomy increased the number of liver PRL-binding sites, and exogenous estrogen administration resulted in a decrease in the number. By contrast, estrogen administration increases the number of PRL-binding sites in the mouse mammary gland [29]. Therefore, the regulation of the number of PRL-binding sites is variable among different organs.

Previous studies have revealed that the specific PRL-binding sites are detected in the uteri of rat [34], rabbit [4], pig [36], sheep and cow [23], mink [27] and human [5] by means of radioreceptor assay. In mice, PRL-binding sites have been found in the brain, mammary gland, liver and kidney [3, 25]. However, the presence of PRL receptors in the uterus has not yet been reported in this species, in spite of evident synergistic effect of PRL with estrogen on the mouse uterus.

While long-term exposure to estrogen is known to induce uterine adenomyosis, a pathological disorder of endometrial tissues defined as the outgrowth of endometrial glands and stroma into the myometrium in some animal species [14, 15, 17, 32], our experiments have demonstrated that in mice isologous anterior pituitary transplantation into the uterine lumen induces an early and a high incidence of uterine adenomyosis associated with the elevation in blood PRL levels [11, 13]. Furthermore, we have found the accelerative effect of dopamine antagonist which stimulates PRL release from the pituitary [30], and the inhibitory effect of danazol which suppresses pituitary PRL release

Accepted November 20, 1992
Received December 11, 1992

[31] on the development of adenomyosis. From these findings, we have proposed that PRL plays an important role for the development of adenomyosis, and have claimed that the uterus is one of the target organs of PRL, suggesting the presence of PRL receptors in the mouse uterus.

In the present study, radioreceptor assay of PRL binding to the mouse uterus and liver was developed. In addition, the relationship between the development of adenomyosis and the PRL-binding ability of the mouse uterus was examined.

MATERIALS AND METHODS

Animals and treatment

Experiment I Five-week-old female mice of the ICR/Jcl strain were purchased from Japan CLEA Inc. (Tokyo, Japan) and kept in light(12 hr/day)- and temperature($25 \pm 0.5^{\circ}C$)-controlled animal room. Forty-five mice were ovariectomized at 8 weeks of age. One day after ovariectomy, 20 out of the 45 mice were given a subcutaneous injections of 5 μg estradiol-17 $\mu\beta$ in 0.1 ml sesame oil daily for 7 days at 9:00 AM and killed by decapitation one hour after the last injection. Remaining 25 ovariectomized mice given no steroid injections were also killed at 9 weeks of age. In addition, 25 intact mice at estrus were killed in the early morning at 9 weeks of age.

Experiment II Fifty adult female mice of the SHN strain were used in this experiment. The experimental group of 24 mice was given transplantation of the anterior pituitary gland (AP) into the uterine lumen at 6 weeks of age and killed by decapitation at 20 weeks of age. The AP donors were age-matched male littermates. The AP-grafted mice which were at diestrus and marked subserosal nodules visible on the outer surface of the uterus, an advanced state of adenomyosis [13] were chosen for further analysis, and the AP-grafted mice which showed no sign of the development of nodules were discarded. Twenty six intact mice which were killed by decapitation at diestrus at 30 days or 20 weeks of age and showed no sign of the development of nodules were used as controls.

Experiment III Female mice of the ICR /Jcl strain purchased from Japan CLEA Inc. were used in this experiment. Three intact mice at diestrus were killed by cervical dislocation at 50 days of age and used for PRL immunohistochemical staining.

Animal handlings were carried out in accordance with the NIH Guide to the Care and Use of Laboratory Animals.

Receptor preparations

Receptor samples were prepared essentially following the method of Kelly *et al.* [7, 8] and Young *et al.* [37]. Immediately after autopsy, the uteri and liver from about 10–15 mice were separately pooled on ice. Pooled tissues were weighed and rinsed in 5 ml of ice-cold homogenizing buffer (pH 9.0) composed of 100 mM Tris, 150 mM NaCl, 50 mM ethyleneglycol-bis-(B-aminoethyl ether)-N, N-tetraacetic acid (EGTA), 50 mM ethylenediaminetetraacetic acid (EDTA), 300 mM sucrose, 1 mM phenyl-methylsulfonyl fluoride (PMSF) and aprotinin (400 kallikrin inhibitory units/ml), and were chopped by a razor blade for 5 min on an ice-cold teflon plate. The chopped-tissues were homogenized in cold homogenizing buffer (4 ml/g tissue fresh weight) by using a Polytron PT 3000 homogenizer for three times at 20,000 rpm, 20 sec each, in a glass tube in ice bath. After centrifugation of the tissue homogenates at 3,750 rpm for 15 min at 4°C, the precipitate was discarded and the supernatant was recentrifuged at 33,000 rpm for 120 min at 4°C. The second precipitate was used as the receptor preparation and was resuspended in 500 μl of cold assay buffer (pH 7.4), containing 25 mM Tris, 10 mM $MgCl_2$, 0.1% bovine serum albumin and 0.02% sodium azide. Protein measurement was performed in 10 μl of the resuspension by micro BCA protein assay reagent kit (Pierce Co., U.S.A). Remaining receptor preparations were stored at $-80^{\circ}C$ until radioreceptor assay for PRL.

Iodination of mPRL

Mouse PRL (mPRL) (AFP6476C, donated by Dr. A. F. Parlow) was radioiodinated with ^{125}I ($Na^{125}I$, Radiochemical Centre, Amersham, UK) in the presence of lactoperoxidase (Boehringer Mannheim GmbH, Germany) and hydrogen peroxide according to the method of Miyachi *et al.*

[10] with minor modifications. After the reaction, the radio-labeled hormone was separated from free radioiodine by gel filtration using a Sephadex G-50 column (disposable plastic column; Whale Sci. Inc. U.S.A). The specific activity of labeled mPRL was about 50 μCi/μg.

Procedures for PRL-binding assay

The procedures were basically the same as the methods of Kelly *et al.* [7, 8] and Young *et al.* [37]. For routine PRL-binding assay of liver samples of ICR mice, 500 μg of protein of the second precipitate of liver homogenates in 100 μl of assay buffer was incubated with [^{125}I]-mPRL (*ca* 55,000 cpm, 0.5 ng/100 μl) at 25°C in an assay tube (12×75 barosilicate glass tube) in the presence or absence of an excess amount (5 μg) of unlabeled ovine PRL (oPRL, Sigma) for 18 hrs. Incubation was terminated by addition of 3 ml of cold assay buffer. Unbound hormone was separated by centrifugation at 4,000 rpm for 30 min at 4°C. After aspiration, the radioactivity of precipitates was counted by an autowell gamma counter (Aloka ARC-300). Each assay was composed of triplicate determinations. In some experiments, recombinant mPRL (5 μg/tube) raised by Yamamoto *et al.* [35] was used as the competitor instead of oPRL.

The specificity of the binding was analyzed by competitive displacement experiments. Specific binding of [^{125}I]-mPRL was calculated as the difference between the binding in the absence and presence of various concentrations of unlabeled oPRL (5, 50, 500, 5,000, 50,000 ng). All the reaction tubes contained 500 μg of protein in 300 μl assay buffer and 55,000 cpm of [^{125}I]-mPRL (100 μl). The affinity of binding (Ka) and the dissociation constant (Kd) were determined from the Scatchard plots constructed from the binding displacement experiments [28].

In some experiments, the receptor samples were pretreated with 4 M $MgCl_2$ to dissociate endogenously bound PRL from its binding sites before assay following the method of Kelly *et al.* [8]. However, routine assays were carried out without $MgCl_2$ pretreatment, because $MgCl_2$ treatment was not effective in increasing PRL binding in either uterus or liver preparations (data not shown). PRL-binding assays at each point were repeated twice in pooled samples of two groups consisting of 10–15 mice each.

Radioimmunoassay (RIA) of serum PRL

In Experiment II in SHN mice, blood was collected at autopsy by decapitation and allowed to clot at room temperature for one hour. After centrifugation at 3,000 rpm for 20 min, the serum was stored at −80°C. Serum PRL levels were determined by homologous RIA using mPRL RIA kit (reference preparation AFP6476C; rabbit anti-mPRL serum, AFP131078; and mPRL, AFP6476C, [^{125}I]-labeled) donated by Dr. A. F. Parlow. Assay reaction mixture was incubated overnight at room temperature. PRL-antibody complexes were separated from unbound PRL by centrifugation after the incubation for 3 hr at room temperature with goat anti-rabbit immunoglobulin serum, donated by Dr. K. Wakabayashi. The PRL concentrations assayed in 100 μl serum were expressed in terms of ng AFP6476C/ml.

Immunohistochemistry of PRL

In Experiment III, the uterus and kidney were dissected out and fixed in 4% paraformaldehyde in phosphate buffer(pH 7.3) at 20°C overnight. Tissues were dehydrated in alcohol, embedded in paraffin, sectioned at 5 μm, and mounted on glass slides previously coated with gelatin. The sections were deparaffinized and rinsed with 0.1 M phosphate-buffered saline (PBS). Immunohistochemical demonstration of PRL was carried out by Histofine SAB-PO (Nichirei Co. Tokyo) method. The sections were preincubated with goat normal serum diluted with PBS 10 times for 10 min and washed briefly with a fresh PBS solution. Rabbit anti-mPRL (AFP6476C) at various dilutions (1:2,500, 1 : 10,000 and 1 : 50,000) in PBS was used as the primary antiserum. After incubation with the primary antiserum overnight at room temperature, the sections were washed with 0.1 M PBS containing triton X-100 (PBST), and then incubated with biotinylated anti-rabbit IgG for 15 min, followed by incubation with peroxidase-conjugated streptavidin for 20 min. Following 15 min washing with PBST, the sections were incubated for 15 min with 0.05 % 3,3′-diaminobenzidine (DAB) tetrahydrochloride solution contain-

ing 0.01% hydrogen peroxide and lightly counterstained with hematoxylin. All these steps were performed at room temperature. The specificity of the method was examined by the use of diluted normal rabbit serum 1:50,000 or PBS instead of primary antiserum. For another test for the antigen specificity, primary antiserum (1:500 dilution) was added with mPRL (400 ng/ml antiserum), stirred for one hour at room temperature, and incubated at 4°C overnight. To eliminate the resolubilization of the antibody-antigen complexes, the mixture was centrifuged at 4,000 rpm for 15 min, and the supernatant was used. The sections incubated without primary antiserum or with adsorbed antiserum showed no immunostaining.

Statistical analysis

The significance of differences between any two groups was evaluated by Student's t-test, where $P < 0.05$ was considered as statistically significant.

RESULTS

In order to determine the optimum incubation time, 500 μg of liver protein and 55,000 cpm of [^{125}I]-mPRL were incubated with or without 5 μg of unlabeled hormone (oPRL) for 3, 6, 12, 18 and 24 hrs. Incubation for 18 hrs resulted in the maximum specific binding of [^{125}I]-mPRL to 500 μg of protein of liver preparations. When various amounts of liver protein (125, 250, 500, 1,000, 2,000 μg) and 55,000 cpm of [^{125}I]-mPRL were incubated in the presence or absence of 5 μg of unlabeled of oPRL, the specific binding increased as a function protein concentration.

Figure 1 shows Scatchard plots drawn from the data of displacement experiments in liver and uterine preparations. From the plots, the equilibrium constant of dissociation (Kd) and the affinity constant (Ka) were calculated: for liver $Kd = 0.048 \times 10^{-8}$ M, $Ka = 2.08 \times 10^{9}$ M^{-1}; for uterus $Kd = 0.054 \times 10^{-8}$ M, $Ka = 1.8 \times 10^{9}$M^{-1}.

Thus, in this study the binding assays in both liver and uterine preparations were routinely carried out under the following conditions; 500 μg of protein for a one assay sample; 55,000 cpm of [^{125}I]-mPRL, with or without 5 μg unlabeled oPRL to obtain specific binding and 18 hrs of incubation at 25°C.

Ovariectomy increased [^{125}I]-mPRL binding to the mouse liver preparations compared to that in intact control mice at estrus (Fig. 2). Estrogen treatment to ovariectomized mice tended to decrease the binding to the liver preparations (Fig. 2), while the differences among the three groups

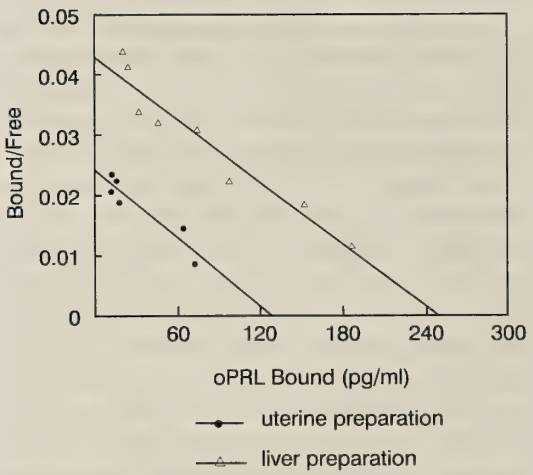

FIG. 1. Scatchard plots of binding of [^{125}I]-mPRL to ICR mouse liver and uterine preparations, based on the data of the binding of [^{125}I]-mPRL to the liver and uterine preparations of ICR mouse under various concentrations of unlabeled oPRL.

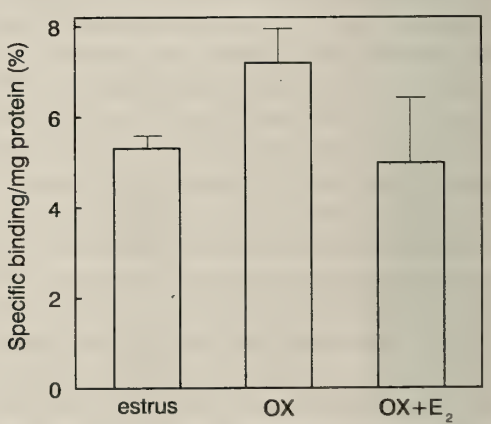

FIG. 2. The specific binding of [^{125}I]-mPRL (% of total radioactivity added) to liver preparations 500 μg of ICR mice at estrus, 7 days after ovariectomy (OX) and 7 days of estrogen treatment following ovariectomy (OX+E_2). Five μg unlabeled oPRL was used to assess non-specific binding. The bars and vertical lines denote mean of two pooled samples.

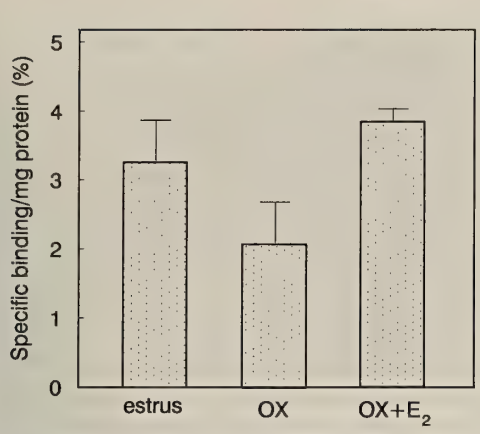

FIG. 3. The specific binding of [^{125}I]-mPRL (% of total radioactivity added) to uterine preparations (500 μg protein) of ICR mouse at estrus , OX and OX+E_2. Five μg unlabeled oPRL was used to assess non-specific binding. The bars and vertical lines denote mean of two pooled samples. For explanation of abbreviations, refer to legend of Fig. 2.

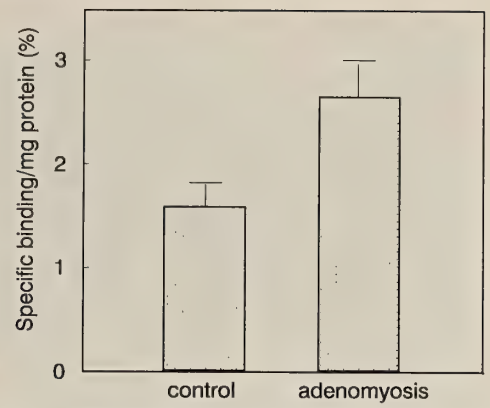

FIG. 4. The specific binding of [^{125}I]-mPRL (% of total radioactivity added) to uterine preparations of intact control SHN mice and the 20-week-old mice with adenomyosis. Five μg unlabeled oPRL was used to assess non-specific binding. The bars and vertical lines denote mean of two pooled samples.

were not statistically significant.

In the uteri of ovariectomized mice, the specific binding of [^{125}I]-mPRL was lower than that in intact mice at estrus (Fig. 3). Daily injections of 5 μg estradiol for 7 days induced a slight increase in the binding activity as compared to the preparations from ovariectomized mice. However, the differences among the groups were again statistically not significant (Fig. 3).

The specific binding of [^{125}I]-mPRL to the uterine preparations from 20-week-old SHN mice at diestrus with adenomyosis tended to be higher than that in age-matched control mice at diestrus, where 5 μg oPRL were used as the competitor to assess nonspecific binding. However, the difference was not statistically significant (Fig. 4). When 5 μg of unlabeled recombinant mPRL was used in

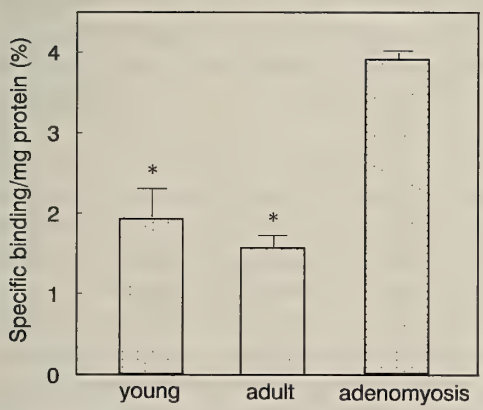

FIG. 5. The specific binding of [^{125}I]-mPRL (% of total radioactivity added) to uterine preparations of intact control 30-day-old or 20-week-old SHN mice and the 20-week-old mice with adenomyosis. The recombinant mPRL was used as competitor to assess non-specific binding. The bars and vertical lines denote mean of two pooled samples. *$P<0.05$ (vs. young & adult controls).

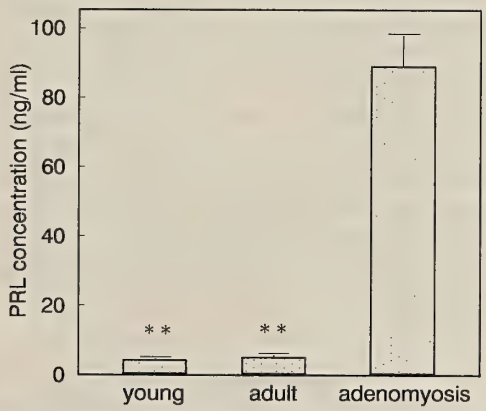

FIG. 6. Plasma PRL levels (ng AFP6476C) in intact control 30-day-old or 20-week-old SHN mice at diestrus and 20 week-old SHN mice with adenomyosis in their uteri. The bars and vertical lines denote means±S.E.M. (n=4–9). Significantly different from both intact controls: **$P<0.01$.

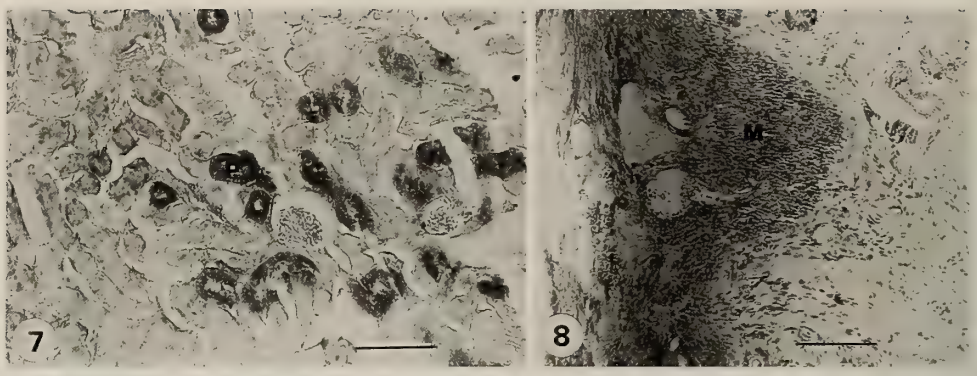

FIG. 7. Immunohistochemical localization of mPRL in paraffin sections of the mouse kidney. PRL is detected in the proximal convoluted tubules (P). Anti-mPRL (AFP6476C) at ×2,500 dilution. Bar represents 100 μm.

FIG. 8. Immunohistochemical localization of mPRL in paraffin sections of the mouse uterus. PRL is detected in the muscle layer (M). Anti-mPRL (AFP6476C) at ×2,500 dilution. Bar represents 100 μm.

place of oPRL, the specific binding of [^{125}I]-mPRL to uterine preparations in mice with advanced state of adenomyosis (3.90±0.13%) was significantly higher than that in 30-day-old or 20-week-old normal mice ($P<0.05$, in either comparison) (Fig. 5).

The serum PRL level is significantly higher in pituitary-grafted 20-week-old mice bearing adenomyosis in their uteri than those in normal 30-day-old or 20-week-old mice, ($P<0.01$, in either comparison) (Fig. 6).

The specificity of antibody and immunohistochemical reaction was tested by the sections of mouse and rat kidneys, since the influence of PRL on the kidney was well established [13, 16, 32]. Immunoreactivity to mPRL was localized in some proximal convoluted tubules and the medulla of mouse kidneys (Fig. 7). In the uterus, immunoreactivity to anti-mPRL serum (in either dilutions, ×2,500, ×10,000 or ×50,000) was preferentially localized in the muscle layers, and the reactivity of other areas of the uterus was negligible (Fig. 8).

DISCUSSION

In the present experiments, optimum conditions for the specific PRL-binding assay were determined by using mouse liver, because the assay methods in the liver have been well established. Assay data from the present experiments revealed that maximum binding of [^{125}I]-mPRL to its receptors occurred at 18 hrs of incubation at 25°C. In addition, 500 μg of sample protein and 55,000 cpm of [^{125}I]-mPRL with or without of 5 μg unlabeled oPRL were found to be the optimum condition for the binding assay. These conditions were basically similar to those reported by previous investigators using rat liver preparations [4, 5, 7, 23, 27, 34, 36]. According to Marshall *et al.* [9], ovariectomy increased [^{125}I]-mPRL binding to the liver preparations of female mice, and estrogen treatment decreased the binding, indicating the manifestation of down-regulation in the binding of PRL to the liver by estrogen. In the present study, the same tendency was observed in the PRL-binding to the liver samples.

The present results indicate that specific PRL receptors were present in the uterus of mice. Scatchard plot analysis revealed that the affinity of binding of mPRL to mouse uterine preparations was similar to that to liver preparations.

The level of specific PRL-binding in the uterus was low in ovariectomized mice and tended to increase after estrogen treatment, although these differences were not statistically significant. The present results that the changes in the PRL-binding activity were very slight under various hormonal conditions may be due to the insufficiency in estrogen stimulation. Treatment by greater doses of estrogen for longer period might be needed. However, the present immunohistochem-

ical observations revealed that the target cells of PRL in the uterus were preferentially myometrial cells, confirming our previous suggestion [11, 16]. Because the amount of myometrial tissue in the uterus constitutes only a small portion of the organ, any hormonal influence on the number of PRL receptors in the myometrium might be too meager to get a significant difference.

In these experiments, oPRL was routinely used to obtain non-specific binding. When recombinant mPRL was used, significant increase in PRL receptors was observed in the uterine preparations of mice with adenomyotic changes. Therefore, recombinant mPRL might be a better competitor for future study.

PRL plays a key role in the development of adenomyosis [11–13, 15, 16, 30, 31]. The present results showed that the specific binding of PRL in the uterus and plasma PRL level were significantly higher in pituitary-grafted mice with adenomyosis than in normal age-matched controls. Previous reports indicated that changes in the endometrial PRL receptors in the pig are regulated by exogenous estrogen administration and circulating levels of PRL during gestation and lactation [36, 37]. The specific binding of PRL to the mouse mammary gland was increased by treatment with various doses of estrogen associated with elevated serum PRL levels in ovariectomized mice [19, 29]. These results suggest a possible direct effect of estrogen to increase the specific binding of PRL and/or indirect effect of estrogen through its action on the pituitary prolactin release. Thus, it is most likely that statistically significant increase in the specific binding of PRL may be due to the longterm hyperprolactinemia in the pituitary-grafted mice bearing uterine adenomyosis.

In conclusion, this is the first report to demonstrate the presence of specific PRL-binding sites in the mouse uterus. Immunohistochemical findings suggest that PRL binds to the myometrial cells. In addition, the present results strongly support our hypothesis that the development of adenomyosis in mice with pituitary grafting is related to the increase in both blood PRL level and PRL-binding activity in the uterus.

ACKNOWLEDGMENTS

This study was supported by Grants-in-Aid for Fundamental Scientific Research from the Ministry of Education, Science and Culture, Japan. to T.M. and S.K., and Research Grants from Takeda Foundation to T.M. and from Zenyaku Kogyo LTD. to S.K.. T. Singtripop is a recipient of the fellowship from Hitachi Scholarship Foundation.

The authors thank Dr. K. Kohmoto and Dr. S. Sakai (Department of Animal Breeding, Faculty of Agriculture, University of Tokyo) for their technical advice. We are grateful to Dr. A. F. Parlow (Pituitary Hormones and Antisera Center Harbor-UCLA Medical Center, California) for his generous gift of mouse PRL RIA kit, and Dr. K. Wakabayashi (Institute of Endocrinology, Gunma University, Gunma, Japan) for providing us goat anti-rabbit IgG serum.

REFERENCES

1 Bern HA, Nicoll CS (1968) The comparative endocrinology of prolactin. Rec Prog Hormone Res 24: 681–720

2 Dube D, Kelly PA, Pelletier G (1980) Comparative localization of prolactin-binding sites in different rat tissues by immunohistochemistry, radioautography and radioreceptor assay. Mol Cell Endocrinol 18: 109–122

3 Frantz WL, Macindole JH, Turkington RW (1974) Prolactin receptors: Characteristics of the particulate fraction binding activity. J Endocrinol 60: 485–497

4 Grissom FE, Litteton GK (1988) Evolution of lactogenic receptors in selected rabbit tissue during pregnancy. Endocrinol Res 14: 1–19

5 Healy DL (1984) The clinical significance of endometrial prolactin. Aust NZJ Obstet Gynecol 24: 111–116

6 Hermanns U, Hafez ESE (1981) Prolactin and male reproduction. Arch Androl 6: 95–125

7 Kelly PA, Posner BI, Friesen HG (1975) Effects of hypophysectomy, ovariectomy, and cycloheximide on specific binding sites for lactogenic hormone in rat liver. Endocrinology 97: 1408–1415

8 Kelly PA, Leblanc G, Djiane J (1979) Estimation of total prolactin-binding sites after *in vitro* desaturation. Endocrinology 104: 1631–1637

9 Marshall S, Bruni JF, Meites J (1978) Prolactin receptors in mouse liver: Species differences in response to estrogenic stimulation. Proc Soc Exp Biol Med 159: 256–259

10 Miyachi Y, Vaitukitis JL, Nieschlag, Lipset MP (1972) Enzymatic radioiodination of gonadotropins. J Clin Endocrinol Metab 34: 23–28

11 Mori T, Nagasawa H, Takahashi S (1981) The

induction of adenomyosis in mice by intrauterine pituitary isografts. Life Sci 29: 1277–1282

12 Mori T, Nagasawa H (1983) Mechanisms of development of prolactin-induced adenomyosis in mice. Acta Anat 116: 46–56

13 Mori T, Nagasawa H (1984) Alteration of the development of mammary hyperplastic alveolar nodules and uterine adenomyosis in SHN mice by different schedules of treatment with CB-154. Acta Endocrinol 107: 245–249

14 Mori T, Nagasawa H, Ohta Y (1989) Prolactin and uterine adenomyosis in mice In "Prolactin and Lesions in Breast, Uterus and Prostate" Ed by H Nagasawa, CRC Press, Florida, pp 123–129

15 Mori T, Nagasawa H (1989a) Multiple endocrine syndrome in SHN mice: Mammary tumors and uterine adenomyosis In "Comparative Aspects of Tumor Development" Ed by HE Kaiser, Kluwer Academic Pub, Netherlands, pp 121–130

16 Mori T, Nagasawa H (1989b) Causal analysis of the development of uterine adenomyosis. Zool Sci 6: 103–112

17 Mori T, Kawashima S, Nagasawa H (1991a) Induction of uterine adenomyosis by pituitary grafting and retardation of its development by bromocriptine-mesilate (CB-154) in Balb/c mice. In vivo 5: 107–110

18 Mori T, Singtripop T, Kawashima S (1991b) Animal model of uterine adenomyosis: Is prolactin a potent inducer of adenomyosis in mice. Am J Obstet Gynecol 165: 232–234

19 Muldoon TG (1981) Interplay between estradiol and prolactin in the regulation of steroid hormone receptor levels, nature, and functionality in normal mouse mammary tissue. Endocrinology 109: 1339–1346

20 Nagasawa H (1979) Prolactin: Its role in the development of mammary tumors. Med Hypoth 5: 1117–1121

21 Nicoll CS, Bern HA (1972) On the action of prolactin among the vertebrates: Is there a common denominator? In "Lactogenic Hormones" Ed by GEW Wolstenholme and J Knight, Churchill Livingstone, London, pp 299–324

22 Posner BI, Kelly PA, Friesen HG (1974a) Induction of lactogenic receptor in rat liver: Influence of estrogen and the pituitary. Proc Natl Acad Sci USA 71: 2407–2410

23 Posner BI, Kelly PA, Shiu, RPC, Friesen HG (1974b) Studies on insulin, growth hormone and prolactin binding: ontogenesis effects of sex and pregnancy. Endocrinology 96: 521–531

24 Posner BI (1976a) Regulation of lactogen specific binding sites in rat liver: Studies on the role of lactogen and estrogen. Endocrinology 99: 1168–1177

25 Posner BI (1976b) Characterization and modulation of growth hormone and prolactin binding in mouse liver. Endocrinology 98: 645–654

26 Reddi AH (1969) Role of prolactin in the growth and secretory activity of the prostates and other accessory glands of mammals. Gen Comp Endocrinol 2, Suppl. 81–96

27 Rose J, Stormshak F, Adair J, Oldfield JE (1983) Prolactin binding sites in the uterus of the mink. Mol Cell Endocrinol 31: 131–139

28 Scatchard G (1949) The attraction of proteins for small molecules and ions. Ann NY Acad Sci 51: 660–672

29 Sheth NA, Tikekar SS, Ranadive KJ, Sheth AI (1978) Influence of bromocriptine on estrogen-modulated prolactin receptors of mouse mammary gland. Mol Cell Endocrinol 12: 167–176

30 Singtripop T, Mori T, Park MK, Sakamoto S, Kawashima S (1991) Development of uterine adenomyosis after treatment with dopamine antagonists in mice. Life Sci 49: 201–206

31 Singtripop T, Mori T, Sakamoto S, Sassa S, Park MK, Kawashima S (1992) Suppression of the development of uterine adenomyosis by danazol treatment in mice. Life Sci 51: 1119–1125

32 Squire RA, Goodman DG, Valerio MG, Fredrickson T, Strandberg JD, Levitt MH, Lingeman CH, Harschbarger JC, Dawe CJ (1978) Female Reproductive System In "Pathology of Laboratory Animals Vol 2" Ed by K Benirschk, FM Garner, TC Jones, Springer-Verlag, New York, p 1172

33 Sternberger LA, Pertrali JP, Joseph SA, Meyer HG, Mill KR (1978) Specificity of the immunocytochemical-luteinizing hormone-releasing hormone receptor reaction. Endocrinology 102: 63–73

34 William GH, Hammond JM, Weisz J, Mortel R (1978) Binding sites for lactogenic hormone in the rat uterus. Biol Reprod 18: 697–706

35 Yamamoto M, Harigaya T, Ichikawa T, Hoshino K, Nakashima K (1992) Recombinant mouse prolactin: Expression in Escherichia coli, purification and biological activity. J Mol Endocrinol 8: 165–172

36 Young KH, Bazer FW (1989) Porcine endometrial prolactin receptors detected by homologous radioreceptor assay. Mol Cell Endocrinol 64: 145-154

37 Young KH, Kraeling RR, Bazer FW (1990) Effect of pregnancy and exogenous ovarian steroids on endometrial prolactin receptor ontogeny and uterine secretory response in pig. Biol Reprod 43: 592–599

ZOOLOGICAL SCIENCE 10: 361–366 (1993)

Juvenile Hormone Analogue, S-31183, Causes a High Level Induction of Presoldier Differentiation in the Japanese Damp-Wood Termite

Kimihiro Ogino, Yoshiyuki Hirono[1], Tadao Matsumoto[1] and Hajime Ishikawa[2]

Zoological Institute, Faculty of Science, University of Tokyo, Bunkyo-ku, Tokyo 113, and [1]Department of Biology, College of Arts and Sciences, University of Tokyo, Meguro-ku, Tokyo 153, Japan

ABSTRACT—The effect of a juvenile hormone analogue, 2-[1-methyl-2(4-phenoxyphenoxy)ethoxy]pyridine (S-31183), on differentiation of the presoldier was tested with the Japanese damp-wood termite, *Hodotermopsis japonica*. Sixth and 7th instar larvae were reared on filter papers impregnated with various amounts (10–1000 μg/filter paper) of the analogue for 3 weeks. While presoldiers were induced, with some mortality, under all the conditions tested, the rate of induction was significantly higher (>90%) with lower mortality (<10%) than under the other conditions when 10 μg or 30 μg of S-31183 were administered to the 6th instar larvae. The length of the premolt interval of larval-presoldier molt was about 5.5 days, equal to that of larval-larval molt.

INTRODUCTION

The society of termites is characterized by polymorphism and polyethism, which, like other social insects, are based on the caste system. Termites usually consist of several castes: primary reproductives, supplementary reproductives, soldiers, and workers or pseudergates. In addition, replacement reproductives appear after the death of primary reproductives. The set of castes and scheme of postembryonic pathway producing castes vary with species.

The caste of the termite is not genetically, but epigenetically determined: the first instar larva can become any caste. It is well established that juvenile hormone (JH) is a key factor controlling the caste differentiation and regulation [12]. Yin and Gillot [23] proposed the following relationship between the titer of JH and the outcome of molts in a primitive termite, *Zootermopsis angusticollis* (Termopsidae). A high titer of JH in hemolymph at a specific stage leads to the formation of soldier via presoldier, and a low titer to the production of alata, which will shed the wings and become primary reproductive. An intermediate titer induces the molts without differentiation, or stationary molts.

While many studies have shown that the artificial increase of JH titer in larvae of termites by exposing them to exogenous JHs or their analogues (JHAs) causes an increase in the number of presoldier [5, 14], its production at the rate of 100% has never been observed. Luescher [9] explained this by the concept of competence in asserting that termite can respond to stimulus only at a specific period ("sensitive" or "competence" period) within the intermolt. This explanation was confirmed for some termites in several studies [11, 15, 18]. In the meantime, Lenz [8] emphasized the influence of nutrition and caste composition on the differentiation of soldiers. For example, the presence of soldiers in an experimental colony will tend to inhibit the differentiation of larvae to presoldiers. The actual JH titer in a termite is supposed to be influenced by these environmental factors. Lenz suggested that continuous contact

Accepted November 6, 1992
Received September 4, 1992
[2] To whom offprint request should be addressed.

and exchange of food among termites bring about the transfer of pheromones. Although Luescher [10] hypothesized the existence of pheromone which is involved in the termite caste regulation, no actual substance has been identified yet.

In spite of its decisive role, little is known about the mechanism of JH action in the caste regulation [17]. This is mainly due to the difficulty in performing biochemical and molecular biological analyses on termites. In order to overcome the difficulty, it is desirable to control the caste differentiation artificially. If larvae are successfully induced into presoldiers synchronously at a high rate, we will be able to obtain much important information about the physiological, biochemical, and molecular biological mechanism underlying the caste determination in termites.

The Japanese damp-wood termite, *Hodotermopsis japonica* Holmgren is a lower termite species whose differentiation of caste occurs at a late stage of development. Even the last (7th) instar larvae are capable of differentiation into either of nymphs, neotenics and soldiers. Soldiers also derive from either the 6th instar larvae or nymphs [13]. Since 2-[1-methyl-2(4-phenoxyphenoxy)ethoxy]pyridine (S-31183) displayed higher hormonal activity than that of a well-known JHA, methoprene on some insects [1, 22], it was expected that the JHA would also induce the differentiation of presoldiers of termite at a high rate. To determine the conditions that induce differentiation of larvae into presoldiers at the highest rate, we have examined the effects of the amount of S-31183, group size, instar of larvae, and locality of original colony on the presoldier production in *H. japonica*.

MATERIALS AND METHODS

Termites

Hodotermopsis have been known from Sichuang, Guizhou, Hunan, Guangxi, Guangdong, Zhejiang, Fujian, Jiangxi, Vietnam on the continent, and also from the Hainan and Taiwan islands. In Japan, *H. japonica* have been found from the Nansei archipelago and the Capes of Seta and Ashizuri [21]. Colonies of *H. japonica* were collected in the natural forest at Onoaida in the Yaku-shima island and at Takamoto in the Nakano-shima island of the Nansei archipelago, Japan. They were brought back to the laboratory and kept in plastic cases in an incubator at 25°C in the constant darkness.

Juvenile hormone analogue

2-[1-Methyl-(4-phenoxyphenoxy)ethoxy]pyridine, S-31183 was kindly offered by Sumitomo Chemical Company, Osaka, Japan. Technical grade (98.1%) of S-31183 was used in this study.

Treatments

Dark-colored 6th and 7th instar larvae were picked up from stock colonies, and groups of 10 or 20 individuals were placed in glass petri dishes (70 mm diam.) containing filter paper disks (approx. 33 cm^2). Generally, newly-molted termite larvae are light-colored and gradually become darker. Preliminary studies suggested that the light-colored larvae do not have the competence to differetiate into presoldiers under the influence of JHA. Six experimental groups, each consisting of either 10 or 20 6th instar larvae, were kept with filter paper disks containing 0 (control), 10, 30, 100, 300, and 1000 ug of S-31183, respectively. The disks had been uniformly impregnated with 150 μl of the acetone solutions of S-31183 and then air-dried, on which insects fed instead of wood. The same procedures were used for the experiments with the 7th instar larvae. Equal numbers of males and females were included in each experimental group. Insects were supplied with water daily and the treated filters were renewed weekly. All experimental groups were kept at 25°C in the constant darkness.

Experimental groups were observed daily for three weeks. Each experimental series was triplicated. Larvae from the stock colony collected in the Yaku-shima island were used in one series, and larvae from the Nakano-shima island were used in two other series. The data were evaluated by multiple-way of variance and Tukey's multiple comparison.

Determination of the length of premolt interval

At the premolt stage, larvae empty the hindgut

and become white, which is called "whitening". We observed the larvae every about 12 hours and labeled individuals which began to whiten with the date and time by attaching sticker on the back. In the following days, the number of newly-molted larvae and presoldiers were counted. We estimated the length of premolt interval of each individual based on the duration between the whitening and molting. Larvae which did not molt and died after whitening were counted in mortality, and not subjected to post-mortem examinations. Larvae which died a few days after molting were counted in both mortality and those molted.

RESULTS

It was obvious that S-31183 impregnated in filter paper disks caused superfluous production of presoldiers and some mortality of larvae (Table 1). In control group with no JHA, no presoldier was produced while a few larvae underwent larval-larval molt with little mortality. Significantly more presoldiers were produced with all the amounts tested (10–1000 μg) compared with the controls ($P<0.01$). Regardless of other factors, with 10 or 30 ug of S-31183, about 90% of larvae differentiated into presoldiers within 3 weeks from the start of experiment. The three higher doses (100, 300, 1,000 μg) led to significantly fewer ($P<0.01$) production of presoldiers than the above two. As shown in Fig. 1, with higher amounts of S-31183, the level of presoldier production attained the maximum on earlier days.

As the amount of S-31183 was increased, the mortality increased. The mortality of the larvae treated with 300 or 1,000 μg of S-31183 was significantly higher than with the lower dosages ($P<0.01$), which was incurred mainly as a result of incomplete ecdysis (Table 1). The dosage of JHA also effected the larval-larval molting ($f=9.37$, $P<0.01$). Throughout all the experimental groups except control, only a few larvae underwent larval-larval molt.

With the 6th and 7th instar larvae, results were significantly different on the rate of presoldier production ($f=15.34$, $P<0.01$) and mortality ($f=11.03$, $P<0.01$). In the 7th instar larvae, the rate of presoldier production was lower and mortality

Table 1. Differentiation and mortality of *H. japonica* exposed to various doses of S-31183 for 3 weeks

6th-instar larvae				7th-instar larvae			
JHA dose	% molted to		% mortality	JHA dose	% molted to		% mortality
	Larvae[a]	Presoldiers[a,b]			Larvae[a]	Presoldiers[a,b]	
Groups of 10 larvae				Groups of 10 larvae			
0	10.0±5.8	0.0± 0.0	6.7± 3.3 (0.0±0.0)	0	3.3±3.3	0.0± 0.0	6.7±3.3 (0.0±0.0)
10	0.0±0.0	96.7± 3.3	3.3± 3.3 (0.0±0.0)	10	6.7±3.3	90.0± 0.0	3.3±3.3 (0.0±0.0)
30	0.0±0.0	96.7± 3.3	3.3± 3.3 (0.0±0.0)	30	0.0±0.0	93.3± 3.3	6.7±3.3 (0.0±0.0)
100	00.0±0.0	83.3± 8.8	10.0± 5.8 (0.0±0.0)	100	0.0±0.0	70.0±10.0	13.3±8.8 (0.0±0.0)
300	3.3±3.3	76.7± 3.3	30.0± 5.8 (6.7±6.7)	300	0.0±0.0	63.3± 8.8	43.3±8.8 (13.3±3.3)
1000	0.0±0.0	56.7± 6.7	23.3± 8.8 (16.7±8.8)	1000	0.0±0.0	46.7± 8.8	40.0±0.0 (30.0±0.0)
Groups of 20 larvae				Groups of 20 larvae			
0	11.7±1.7	0.0± 0.0	5.0± 2.9 (0.0±0.0)	0	8.3±4.4	0.0± 0.0	3.3±1.7 (0.0±0.0)
10	3.3±3.3	93.3± 1.7	3.3± 1.7 (0.0±0.0)	10	0.0±0.0	90.0± 2.9	16.7±1.7 (0.0±0.0)
30	0.0±0.0	91.7± 1.7	3.3± 3.3 (0.0±0.0)	30	0.0±0.0	93.3± 1.7	3.3±1.7 (0.0±0.0)
100	1.7±1.7	85.0± 2.9	16.7± 3.3 (0.0±0.0)	100	0.0±0.0	63.3± 6.0	20.0±2.9 (0.0±0.0)
300	0.0±0.0	70.0±10.0	30.0±10.4 (11.7±6.7)	300	3.3±1.7	48.3± 6.0	35.0±2.9 (25.0±2.9)
1000	0.0±0.0	55.0±15.0	33.3±12.0 (25.0±7.6)	1000	0.0±0.0	40.0± 2.9	50.0±2.9 (35.0±7.6)

Values are means±SE of % initial 10 or 20 larvae of three replicates of experimental group. Values in parentheses are means±SE of mortality due to incomplete molt.

[a]: including individuals died after complete molting.

[b]: not including individuals died due to incomplete molts into presoldiers.

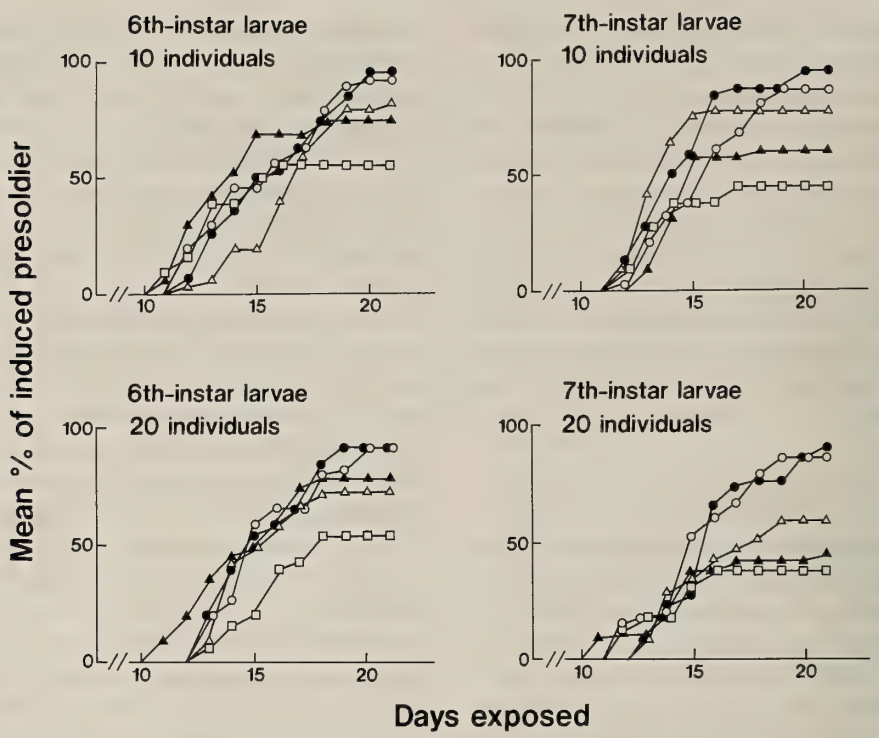

Fig. 1. Induced presoldiers in experimental groups exposed to various amounts of S-31183. Cumulative rates of induced presoldiers against initial number of larvae were plotted. Values represent means of triplicated experimental groups. Amount of S-31183 impregnated into each filter disk: ○, 10 μg; ●, 30 μg; △, 100 μg; ▲, 300 μg; □, 1,000 μg.

Table 2. Timing of premolt interval for various types of molt

Types of molt / Length of premolt stage (days)	6th-instar larvae to				7th-instar larvae to			
	Larvae		Presoldiers		Larvae		Presoldiers	
	Molting %	total	Molting %	total	Molting %	total	Molting %	total
4.5	2	4.7	8	6.9	3	5.9	5	4.6
5	9	20.9	25	21.6	7	13.7	14	13.0
5.5	25	58.1	71	61.1	35	68.6	66	61.1
6	6	14.0	10	8.6	4	7.8	21	19.4
7	0	0.0	1	0.9	1	2.0	0	0.0
Total	43	100.0	116	100.0	51	100.0	108	100.0
Mean (SD)	5.44 (0.39)		5.39 (0.40)		5.46 (0.42)		5.50 (0.38)	

was higher than in the 6th instar larvae (Table 1).

Group size and locality of original colony did not influence the rate of induction of presoldiers or mortality (Table 1). As shown in Table 2, there was no significant difference between the length of premolt interval of larval-larval molt and that of larval-presoldier molt with either the 6th or 7th instar larvae (Mann-Whitney's U-test, $P>0.05$). In both cases, the length of premolt interval was about 5.5 days with little variance irrespective of instar. However, the 6th instar larvae became presoldier earlier than the 7th instar larvae (Mann-

Whitney's U-test, $P<0.05$).

DISCUSSION

In a preliminary experiment, it was shown that the lower amounts of S-31183 (1 and 3 μg) caused just a few presoldier production accompanied with intercaste production. As shown in Table 1, with 10 and 30 μg of S-31183, the rate of presoldier production was over 90%. Moreover, the intercaste production, which has inevitably accompanied the presoldier production even under the most ideal conditions so far, was not observed in this study.

The successful induction of presoldier in this study will be due to several factors. Among others, one important factor is strong JH activity of S-31183. While S-31183 is structurally different from other well-known JHAs such as methoprene and hydroprene, it exerts a higher activity than others in some insects [1, 22]. In *Musca domestica,* its activity in inducing supernumerary larvae is 50 times higher than methoprene [1]. High chemical stability of S-31183 [22] probably accounts, in part, for the strong activity of this JHA.

In the meantime, it is likely that the successful induction of presoldier by S-31183 in *H. japonica* is not only due to the strong JH activity of the analogue, but also due to the high sensitivity of this species of termite to S-31183. Actually, while in *Coptotermes formosanus* S-31183 is not as effective as methoprene in inducing the presoldier differentiation [2], our preliminary experiments have suggested that in *H. japonica* the effects of the two JHAs are just the reverse. Su and Scheffrahn demonstrated also that *C. formosanus* and *Reticulitermes flavipes* show different sensitivity to S-31183 [20].

High rate of the presoldier induction in this study may be also due to our experimental procedures employed, in which we examined experimental groups composed entirely of larvae instead of natural colonies including soldiers, considering that some termite species with lower population density of soldier are more sensitive to JHAs [8]. In addition, relatively low population density of soldier in the natural colony of *H. japonica* (<8%) [13] may also account for its high sensitivity to S-31183.

As shown in Fig. 1, presoldier production was saturated earlier in the experimental groups treated with higher amounts (100, 300, 1,000 μg) of S-31183. This may indicate that when the concentration of JHA in the filter paper is higher, the level of JHA in the insect reaches the threshold earlier. Alternatively, this is a reflection of the difference of amount received by termites. Although, with these concentrations of S-31183, the rate of overall presoldier production was relatively low, this was not because of low induction to presoldier but because of high mortality under these conditions. Indeed, many of the termites that had survived under these conditions differentiated to presoldiers (Table 1). Toxic effects of excess amount of JHA were reported by many investigators [2, 4–7, 14, 15, 19, 20].

In the 6th instar larvae, the rate of presoldier production was higher and mortality was lower than in the 7th instar larvae. This suggests that the 6th instar larvae are more resistant to the toxic effect of S-31183 and have more potentials for differentiation to presoldiers.

Presoldiers induced by S-31183 appeared 11–21 days after the first treatment (Fig. 1). It has been known that the timing of molting depends on not only the titer of JH during the intermolt period, but also many other factors such as the titer of ecdysteroid [16]. We demonstrated that both the premolt interval of larval-larval molt and larval-presoldier molt are fixed on about 5.5 days (Table 2). In addition, when the larvae treated with S-31183 underwent larval-larval molt, it always took place during the first 9 days from the first treatment. In other words, all the larvae that whitened on day 6 or later did not become larvae but presoldiers after molting 5.5 days later. This enables us to predict the fate of larvae at intermolt stage, and analyze the events underlying molting to presoldier.

ACKNOWLEDGMENTS

We are grateful to Sumitomo Chemical Company for supplying the JHA S-31183. This work was supported by a Grant-in-Aid for Scientific Research on Priority Areas ("Symbiotic Biosphere: Ecological Interaction Network Promoting the Coexistence of Many Species"

[03269102]) from the Ministry of Education, Science and Culture of Japan.

REFERENCES

1 Hatakoshi M, Agui N, Nakayama I (1986) 2-[1-methyl-2-(4-phenoxyphenoxy)ethoxy]pyridine as a new insect juvenile hormone analogue: Induction of supernumerary larvae in *Spodoptera litura* (Lepidoptera; Noctuidae). Appl Entomol Zool 21: 351–353

2 Haverty MI, Su NY, Tamashiro M, Yamamoto R (1989) Concentration-dependent presoldier induction and feeding deterrency: Potential of two insect growth regulators for remedial control of the Formosan subterranean termite (Isoptera; Rhinotermitidae). J Econ Entomol 82: 1370–1374

3 Hirono Y (1990) Histological and ecological studies on the caste differentiation of the Japanese dampwood termite *Hodotermopsis japonica*. Ph.D. thesis, University of Tokyo

4 Howard RW (1983) Effects of methoprene on binary caste groups of *Reticulitermes flavipes* (Kollar) (Isoptera; Rhinotermitidae). Environ Entomol 12: 1059–1063

5 Howard RW, Haverty MI (1979) Termites and juvenile hormone analogues: A review of methodology and observed effects. Sociobiol 4: 269–278

6 Jones SC (1984) Evaluation of two insect growth regulators for the bait-block method of subterranean termite (Isoptera; Rhinotermitidae) control. J Econ Entomol 77: 1089–1091

7 Lebrun D (1990) Termite control: Biological basis. Sociobiol 17: 115–127

8 Lenz M (1976) The dependence of hormone effects in termite caste determination on external factors In "Phase and caste determination in insects: Endocrine aspects" Ed by M Luescher, Pergamon Press Inc. New York, pp 73–89

9 Luescher M (1952) Die Produktion und Elimination von Ersatzgeschlechtstieren bei der Termite *Kalotermes flavicollis* Fabr. Z Vergleich Physiol 34: 123–141

10 Luescher M (1961) Social control of polymorphism in termites In "Insect polymorphism" Ed by JS Kennedy, Symp R ent Soc, London pp 57–67

11 Luescher M (1974) Die Kompetenz zur Soldatenbildung bei Larven (Pseudergaten) der Termite *Zootermopsis angusticollis* Rev Suisse Zool 3: 710–714

12 Luescher M (1976) Evidence for an endocrine control of caste determination in higher termites In "Phase and caste determination in insects: Endocrine aspects" Ed by M Luescher, Pergamon Press Inc. New York, pp 91–103

13 Matsumoto T, Hirono Y (1985) On the caste composition of a primitive termite *Hodotermopsis japonica* Holmgren (Isoptera; Termopsidae). Sci Pap Arts and Sci univ Tokyo, 35: 211–216

14 Okot-Kotber BM (1980) The influence of juvenile hormone analogue (ZR515, methoprene) on soldier differentiation in *Macrotermes michaelseni* (Isoptera; Macrotermitinae) Physiol Entomol 5: 407–416

15 Okot-Kotber BM (1980) Competence of *Macrotermes michaelseni* (Isoptera; Macrotermitinae) larvae to differentiate into soldiers under the influence of juvenile hormone analogue (ZR-515, methoprene). J Insect Physiol 26: 655–659

16 Okot-Kotber BM (1985) Mechanisms of caste determination in a higher termite, *Macrotermes michaelseni* (Isoptera; Macrotermitinae). In "Caste differentiation in social insects". Ed by JAL Watson, BM Okot-Kotber, Ch Noirot, Pergamon Press, Oxford, pp 267–306

17 Okot-Kotber BM, Prestwich GD (1991) Juvenile hormone binding proteins of termites detected by photoaffinity labelling: Comparison of *Zootermopsis nevadensis* with two Rhinotermitids. Arch Insect Biochem Physiol 17: 119–128

18 Springhetti A (1972) The competence of *Kalotermes flavicollis* pseudergates to differentiate into soldier. Monitore Zool Ital (NS) 6: 97–111

19 Su NY, Tamashiro M, Haverty MI (1985) Effects of three insect growth regulators, feeding substrates, and colony origin on survival and presoldier production of the Formosan subterranean termite (Isoptera; Rhinotermitidae). J Econ Entomol 78: 1259–1263

20 Su NY, Scheffrahn RH (1989) Comparative effects of an insect growth regulators S-31183 against the Formosan subterranean termite (Isoptera; Rhinotermitidae). J Econ Entomol 82: 1125–1129

21 Wang J, Masuko K, Kitade O, Matsumoto T (1992) Allozyme variation and genetic differentiation of colonies in the damp wood termite *Hodotemopsis* of Japan and China. Sci Pap Arts and Sci Univ Tokyo, 42: 95–109

22 Wimmer Z, Romanuk M (1989) Insect juvenile hormones and their bioanalogues. Collect. Czech Chem Commun 54: 2302–2329

23 Yin CM, Gillot C (1975) Endocrine control of caste differentiation in *Zootermopsis angusticollis* Hagen (Isoptera). Can J Zool 53: 1701–1708

ZOOLOGICAL SCIENCE 10: 367–373 (1993)

A New Species of the Genus *Pasiphaea* (Crustacea, Decapoda, Pasiphaeidae) from the North Pacific

Tomoyuki Komai and Kunio Amaoka

Laboratory of Marine Zoology, Faculty of Fisheries, Hokkaido University, Hokkaido, Japan

ABSTRACT—A new pasiphaeid shrimp, *Pasiphaea oshoroae* sp. nov., is described based on material collected from scattered localities in the northern North Pacific Ocean. It differs from the closely allied congeners in having the short rostrum with regularly concave anterior margin, the telson being shorter than the sixth abdominal somite, the merus of the first pereopod armed with 0–3 (mostly 1) spines, the basis of the first pereopod rounded ventrodistally, and the dactylus of the second pereopod being shorter than the palm. The new species seems to be a mesopelagic inhabitant and to be widely distributed in the northern North Pacific Ocean.

INTRODUCTION

The caridean genus *Pasiphaea* now contains about 50 species from the world oceans, and most of the members are known as pelagic inhabitants. In 1988, T/S *Oshoro-Maru* of Hokkaido University made a collection of the pelagic organisms using a 2.0×2.5 m non-closing rectangular midwater beam trawl net [7] in the eastern part of the northern North Pacific Ocean during the "Cruise 23"; six specimens of a caridean shrimp belonging to the genus *Pasiphaea* were captured from four stations (Table 1). Detailed examination proved that these specimens represent an undescribed species. In addition, a single specimen collected from east of the Cape Erimo, Hokkaido, Japan, was showed to be identical with the eastern Pacific specimens. In this paper we describe these specimens as a new species.

The specimens were preserved in 75% ethyl alcohol. Drawings were made with a camera lucida mounted on a WILD 308700 stereomicroscope. The holotype was deposited in the National Science Museum, Tokyo (NSMT), and the paratypes were deposited at the Laboratory of Marine Zoology, Faculty of Fisheries, Hokkaido University (HUMZ). Postorbital carapace length (CL) (measured from the orbital margin to the posteromedian margin of the carapace) is used for indication of measurements.

Accetped December 15, 1992
Received September 28, 1992

DESCRIPTION

Family Pasiphaeidae
Genus *Pasiphaea* Savigny, 1816

Pasiphaea oshoroae sp. nov.
(Figs. 1–3)

Type series. Holotype: NSMT-Cr 11117, female, 12.3 mm CL, off Aleutian Islands, OBT8822. Paratypes: HUMZ-C 750, 1 female, 12.4 mm CL, Gulf of Alska, OBT8811; HUMZ-C 751, 1 female, 13.8 mm CL, Gulf of Alaska, OBT 8816; HUMZ-C 752, 1 female, 11.1 mm CL, Gulf of Alaska, OBT8821; HUMZ-C 753, 2 youngs, 8.6 and 8.7 mm CL, OBT8822; HUMZ-C 935, 1 female, 12.0 mm CL, east of Cape Erimo, eastern Hokkaido, Japan, OST8901. Sampling data are summarized in Table 1.

Diagnosis. Rostrum directed upward, falling short of anterior margin of carapace, with regularly concave anterior margin. Carapace bluntly carinate dorsally in anterior three-quarters; branchiostegal sinus obscure. Abdomen rounded, unarmed dorsally. Telson slightly shorter than sixth abdominal somite, with posterior margin deeply notched. Merus of first pereopod armed with 0–3

Table 1. Sampling data of *Pasiphaea oshoroae* sp. nov.

Station	Position	Towed depth	Time	Date
OBT8811	54°32.1′N 151°54.5′W	0–400 m	20:36–21:31	9 July 1988
OBT8816	54°58.7′N 139°55.6′W	0–400 m	20:53–21:50	16 July 1988
OBT8821	52°01.2′N 154°34.6′N	0–400 m	22:02–23:06	31 July 1988
OBT8822	49°59.9′N 176°55.4′W	0–400 m	21:08–22:12	4 Aug. 1988
OST8901	42°24.0′N 144°02.3′E	0–720 m	11:00–13:31	5 Sept. 1988

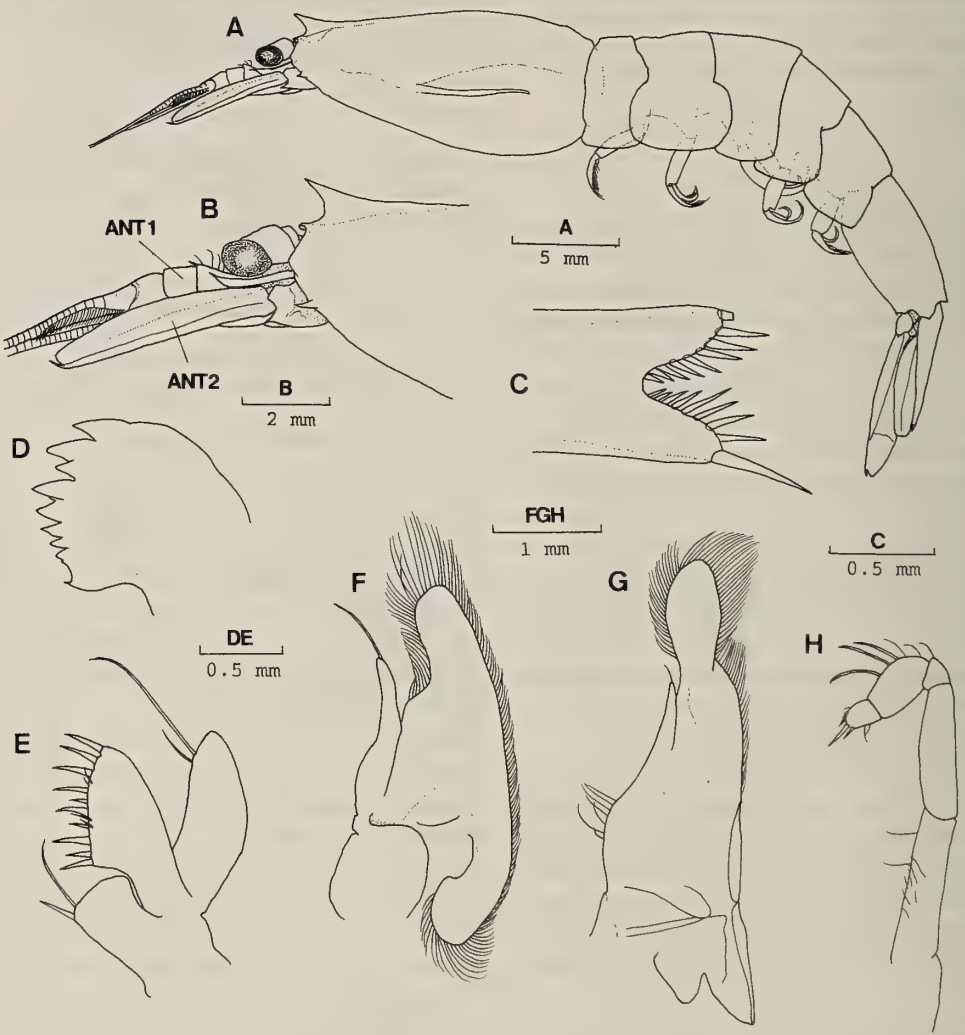

Fig. 1. *Pasiphaea oshoroae* sp. nov., holotype, female (NSMT-Cr 11117): A, entire animal in lateral view (thoracic appendages removed); B, anterior part of carapace and cephalic appendanges; C, posterior part of telson in dorsal view; D, left mandible; E, left maxillule; F, left maxilla; G, left first maxilliped; H, left second maxilliped. ANT1=antennule; ANT2=antenna.

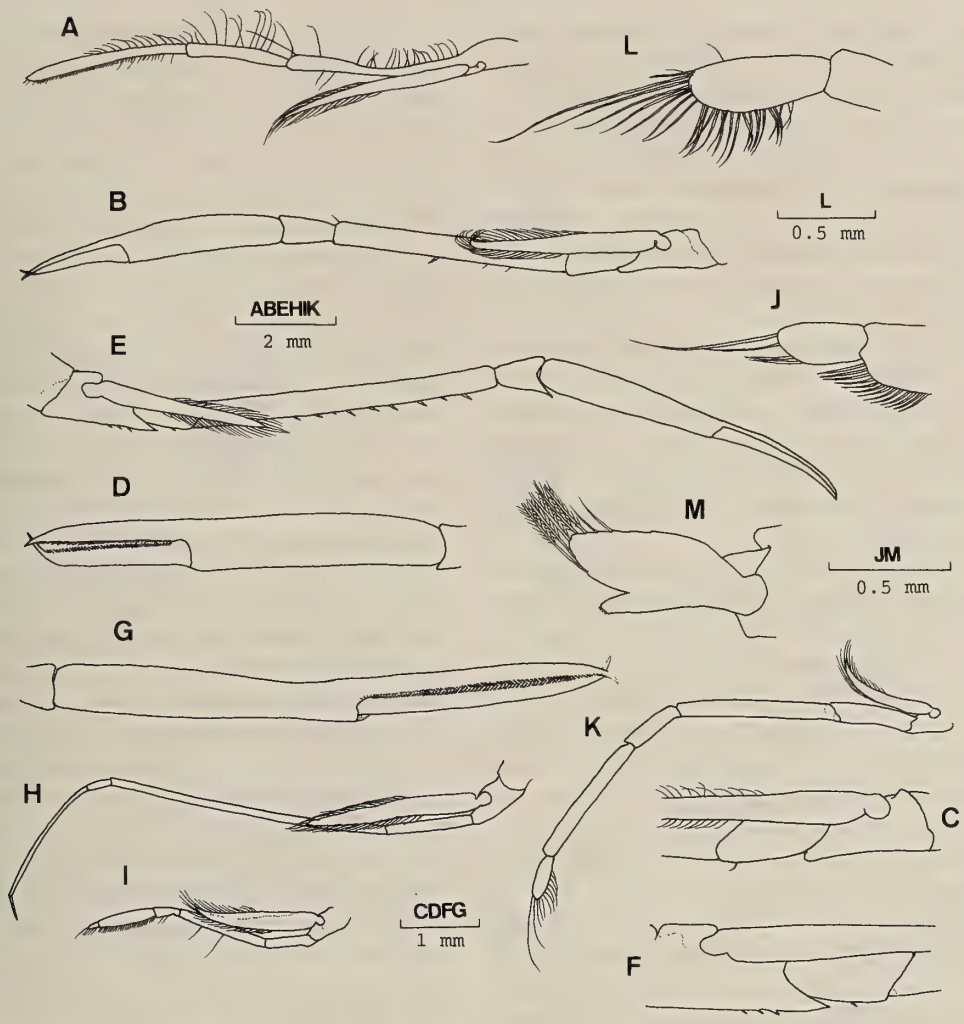

FIG. 2. *Pasiphaea oshoroae* sp. nov., holotype, female (NSMT-Cr 11117): A, left third maxilliped; B, left first pereopod; C, same, basis and ischium; D, same, chela; E, right second pereopod; F, same, basis and ischium; G, same, chela; H, left third pereopod; I, left fourth pereopod; J, same, dactylus; K, left fifth pereopod; L, same, dactylus; M, endopod of left first pleopod.

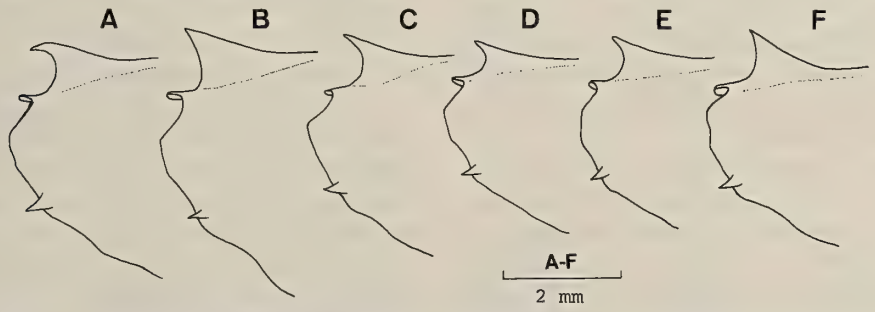

FIG. 3. *Pasiphaea oshoroae* sp. nov., paratypes, variations of rostral shape: A, HUMZ-C 750; B, HUMZ-C 751; C, HUMZ-C 752; D, E, HUMZ-C 753; F, HUMZ-C 935.

spines; basis with rounded ventrodistal angle. Merus of second pereopod armed with 9–11 spines or spinules; ischium with 0 or 1 spine; basis with 0–3 spines; dactylus slightly shorter than palm.

Description of holotype. Body (Fig. 1A) strongly compressed. Integument thin, glabrous.

Rostrum (Fig. 1B) slightly falling short of anterior margin of carapace, directed obliquely upward, anteriorly narrowed into acute tip, anterior margin regularly concave. Carapace (Fig. 1A) bluntly carinate dorsally in anterior three-quarters, posterior quarter rounded; hepatic groove shallow; lower branchial ridge blunt, falling far short of posterior margin of carapace; branchiostegal tooth arising just posterior to anterolateral margin of carapace, supported by short buttress; branchiostegal sinus obscure.

Abdomen (Fig. 1A) dorsally rounded over entire length, all somites lacking posterodorsal tooth. Pleuron of first somite straight ventrally, those of second to fifth somites rounded ventrally. Sixth somite about 0.5 times as long as carapace; posteroventral angle pointed; posterolateral process obliquely truncate. Telson (Fig. 1A, C) 0.9 times as long as sixth somite, dorsally grooved; posterior margin deeply notched, with 9 pairs of spines.

Cornea of eye (Fig. 1B) darkly pigmented, almost as wide as eyestalk.

Antennule (Fig. 1B) with peduncle reaching three-fifths of scaphocerite; stylocerite twisted, distally acute, falling considerably short of proximal segment of peduncle; intermediate segment less than half length of proximal segment; outer flagellum somewhat thickened proximally, ventral excavation filled with aesthetascs.

Antenna (Fig. 1B) with basicerite bearing moderate ventrolateral tooth; scaphocerite with lateral margin slightly convex, distolateral tooth distinctly reaching beyond blade; carpocerite slightly reaching beyond distal end of proximal segment of anternnular peduncle.

Mouthparts typical of genus. Mandible (Fig. 1D) with 10 sharply pointed teeth on mesial margin of incisor process; palp absent. Maxillule (Fig. 1E) with palp bearing 2 subapical setae on mesial margin, distal portion broadly rounded; distal endite armed with 10 stout spines on cutting edge; proximal endite truncate, with 2 setae at posterior angle. Maxilla (Fig. 1F) with endites vestigial, without marginal setae; palp with apical seta. First maxilliped (Fig. 1G) reduced to large elongate lamina, with palp rudimentary; central part of mesial margin with sparse setae; distal lobe ovate, not articulated, fringed with setae; posterior half of lateral margin somewhat thickened, separated into two lobes by shallow, but distinct notch. Second maxilliped (Fig. 1H) five-segmented, pediform, lacking both of epipod and exopod; propodus with sparse setae but no spinules on extensor margin; dactylus armed with 2 spines distally. Third maxilliped (Fig. 2A) overreaching scaphocerite by distal part of ultimate segment; ultimate segment 1.6 times as long as penultimate segment.

All pereopods with well-developed expod (Fig. 2B, E, H, I, K). First pereopod (Fig. 2B) overreaching scaphocerite by length of fingers and one-third of palm; basis (Fig. 2C) with rounded ventrodistal angle; merus bearing 1 or 3 spines on ventral margin; carpus unarmed; dactylus (Fig. 2D) 0.6 times as long as palm, cutting edges of both fingers pectinated with minute spinules. Second pereopod (Fig. 2E) exceeding scaphocerite by length of fingers and half of palm; basis (Fig. 2F) armed with 3 spines on ventral margin; ischium (Fig. 2F) with 1 or 2 spines on ventral margin; merus bearing 11 spines including some minute ones on ventral margin; carpus with ventrodistal spine; dactylus somewhat curved inward (Fig. 2G), 0.8 times as long as palm, cutting edges with minute numerous spinules. Third pereopod (Fig. 2H) very thin, overreaching anterolateral margin of carapace by length of dactylus and distal two-thirds of propodus. Fourth pereopod (Fig. 2I) much shorter than other pereopods, reaching level of slightly anterior to middlength of carapace by tip of dactylus; propodus with flexor face densely setose; dactylus (Fig. 2J) ovate, with setae on distal and flexor margins, 0.25 times as long as propodus. Fifth pereopod (Fig. 2K) falling slightly short of level of branchiostegal tooth of carapace; dactylus (Fig. 2L) ovate, 0.3 times as long as propodus, fringed with setae increasing in length distally on flexor to distal margin.

Branchial formula as shown below. Epipods absent from pereopods; arthrobranchs on first to

third pereopods well developed.

	Maxillipeds			Pereopods				
	1	2	3	1	2	3	4	5
Pleurobranch	—	—	—	1	1	1	1	1
Arthrobranch	—	—	—	1	1	1	—	—
Podobranch	—	—	—	—	—	—	—	—
Epipods	—	—	—	—	—	—	—	—
Exopods	1	—	1	1	1	1	1	1

Endopod of first pleopod (Fig. 2M) roughly ovate, with short, stout appendix interna. Endopod of uropod (Fig. 1A) exceeding apex of telson by about distal one-fifth; exopod overreaching apex of telson by about distal one-third, distolateral tooth reaching beyond blade.

Coloration. In fresh, entire animal reddish translucent, densely with fine red dots over body; fingers of chelae deep red. Cornea of eye brown.

Variations. The paratypes agree well with the holotype, but show some variations. The anterior margin of the rostrum varies from weakly concave to strongly concave, as depicted in Fig. 3.

In two small specimens with CL 8.6 and 8.7 mm CL, the dorsal carina on the carapace is rather obscure.

The merus of the first pereopod bears 0 or 1 spine. The merus of the second pereopod is armed with 7–12 spines on ventral margin; ischium with 0 or 1 spine; basis with 0–3 spines. It is found that the number of spines on the ventral margin of the merus and ischium of the second pereopod increases with age in the present new species, as well as in other congeners [4, 5].

Determination of sex. In all of specimens examined, the second pleopod lacks the appendix masculina. Four specimens with CL more than 11.1 mm (holotype, paratypes: HUMZ-C 750; 751; 752) had a small, but distinct ovary containing ova, clearly visible posterodorsally through the transparent cuticle of the carapace. A specimen with CL 12.0 mm (HUMZ-C 935) is seriously damaged in the internal structure of the cephalothorax, but this specimen is probably female judging from its size. In two small specimens with CL 8.6 and 8.7 mm (HUMZ-C 753), the gonad was too poorly developed to determine the sex.

Etymology. Named after T/S Oshoro-Maru of Hokkaido University, which collected the present new species.

Distribution. Known with certainty only by the type series: Gulf of Alaska; Pacific off Aleutian Islands; Pacific off eastern Hokkaido.

DISCUSSION

The carinated carapace, rounded abdomen, and deeply notched posterior margin of the telson distinguish the new species from all but four species of the approximately 50 described and recog-

TABLE 2. Comparison of characters among *Pasiphaea oshoroae* sp. nov. and four allied species

Items	*P. oshoroae* sp. nov.	*P. alcocki*	*P. corteziana*	*P. liocerca*	*P. rathbunae*
Anterior margin of rostrum	concave	vertical and sinuous	inclined forward, without concavity	concave	convex and sinuous
Dorsal carina of carapace	blunt	sharp	blunt	sharp	sharp
Branchiostegal sinus	obscure	distinct	distinct	distinct	dustinct
Ventrodistal corner of ischium of first pereopod	blunt	acute	blunt	blunt	blunt
Number of meral spines of first pereopod	0–3, mostly 1	—	3 or 4	0	9
Dactylus of second pereopod	shorter than palm	equal to palm	longer than palm	shorter than palm	shorter than palm
Distribution	northern North Pacific	Bay of Bengal Indian Ocean	California Eastern Pacific	Bermuda Western Atlantic	Antarctic
Reference	present study	[1]	[9]	[2]	[8]

nized species of the genus *Pasiphaea*. These four species are as follows: *P. alcocki* (Wood-Mason, 1891) from the Bay of Bengal, Indian Ocean; *P. corteziana* Rathbun, 1902 from off California, eastern Pacific; *P. liocerca* Chace, 1940 from Bermuda, Western Atlantic; *P. rathbunae* (Stebbing, 1914) from the Antarctic.

The differences that help to separate the new species from the four allied species are given in Table 2. The anterior margin of the rostrum is regularly concave in the new species and *P. liocerca,* though the rostrum of the latter is considerably smaller than that of *P. oshoroae* [2]. In *P. alcocki,* it is vertical and sinuous [1]. In *P. corteziana,* it is inclined forward and upward without concavity or convexity [9]. In *P. rathbunae,* it is convex and sinuous [8].

The dorsal carina on the carapace of the *P. oshoroae* is blunt as in *P. corteziana* [9], while sharply ridged in the other three species [1, 2, 8].

The branchiostegal sinus is very obscure in *P. oshoroae,* while it is more distinct in the other four species [1, 2, 8, 9].

The number of spines on the merus of the first pereopod is useful in separating these species: the spines are 0 to 3 in the new species, 3 to 4 in *P. corteziana* [9], 9 in *P. rathbunae* [8], and 0 in *P. liocerca* [2]. Unfortunately, this character has been remained uncertain in *P. alcocki.*

P. alcocki appears to be unique among these five species in having the basis of the first pereopod armed with ventrodistal spine [1]. In the other species, the ventrodistal angle of basis of the first pereopod is rounded [2, 8, 9].

In *P. oshoroae* the dactylus of the second pereopod is slightly shorter than the palm as in *P. liocerca* and *P. rathbunae* [2, 8]. On the other hand, the dactylus is equal to the palm in *P. alcocki* [1], and it is distinctly longer than that in *P. corteziana* [9].

Recently, Hayashi [6] enumerated five Japanese species of *Pasiphaea*. Thus, *P. oshoroae* represents the sixth species of the genus from the Japanese waters.

The present specimens strongly suggest that *P. oshoroae* is widely distributed in the northern North Pacific Ocean. Like the other members of this genus as well as related genera [3], the present new species seems to be a pelagic inhabitant. Unfortunately, the bathymetric range could not be determined satisfactorily, since all of the specimens were collected by oblique tow of open net. All but one of the type series were collected from mesopelagic zone shallower than 400 m where the bottom depth greater than 2000 m. One specimen from the eastern Hokkaido (HUMZ-C 935) was captured by the bottom trawl, but it was entangled in the wing net together with other pelagic organisms such as *Bentheogennema borealis* (Rathbun, 1902) (Dendrobranchiata, Benthesicymidae) or myctophiid fishes.

ACKNOWLEDGMENTS

We are grateful to Dr. Y. Sakurai and Mr. O. Yamamura of Research Institute of North Pacific Fisheries, Hokkaido University, for the opportunity to examine and report upon this interesting shrimp. We thank Dr. B. Kensley of the National Museum of Natural History, Smithsonian Institution for reading the manuscript and helpful advice.

REFERENCES

1 Alcock A (1901) A descriptive catalogue of the Indian deep-sea crustacea decapoda macrura and anomala in the Indian Muserum. Being a revised account of the deep-sea species collected by the Royal Indian Marine Survey Ship "Investigator". Indian Museum, Culcatta, pp 286, pls 3

2 Chace FA Jr (1940) Plankton of the Bermuda Oceanographic Expedition. IX The bathypelagic caridean Crustacea. Zoologica 25: 117–209

3 Crosnier A Forest J (1973) Les crevettes profondes de l'Atlanticque oriental tropical. Faune Tropicale 19: 1–409

4 Figueira AJG (1957) Madeiran decapod crustaceans in the collection of the Museu Municipal do Funchal. I On some interesting deep-sea prawns of the family Pasiphaeidae, Oplophoridae and Pandalidae. Bol Mus Municipal Funchal 10: 22–51, pls 1–4

5 Iwasaki N (1989) Pasiphaeid shrimps from the eastern North Atlantic and the Caribbean Sea with the description of a new species of *Pasiphaea* (Crustacea: Decapoda: Pasiphaeidae). Zool Meded 63: 187–203

6 Hayashi K (1990) Prawns, shrimps and lobsters from Japan (54). Family Pasiphaeidae-Genera *Parapasiphae* and *Pasiphaea*. Aquabiol 69: 304–307 (in Japanese)

7 Nakatani T (1987) Sampling techniques for fish eggs, larvae and juveniles and their food organisms.

Aquabiol 49: 108–110 (in Japanese)

8 Stebbing TRR (1914) Stalk-eyed Crustacea Malacostraca of the Scottish National Antarctic Expedition. Trans R Soc Edinburgh 50: 253–307, pls 23–32

9 Rathbun MJ (1904) Decapod crustaceans of the northwest coast of North America. Harriman Alaska Exped 10: 1–190, pls 1–10

ZOOLOGICAL SCIENCE 10: 375–379 (1993)

[RAPID COMMUNICATION]

Immunocytochemical Localization of Troponin I and C in the Muscles of *Caenorhabditis elegans*

Hiroki Nakae[1] and Takashi Obinata[2]

[1]*Advanced Research Laboratory, Research and Development Center, Toshiba Corporation 1, Komukai Toshiba-cho, Saiwai-ku, Kawasaki 210, and* [2]*Department of Biology, Faculty of Science, Chiba University, 1-33 Yayoi-cho, Inage-ku, Chiba 263, Japan*

ABSTRACT—Troponin-I (TNI) and troponin-C (TNC) in muscle tissues of a nematode, *C. elegans*, were investigated using antibodies against the respective troponin-components of *Ascaris*. Immunoblot analysis demonstrated that these antibodies recognize the troponin components of *C. elegans* that have the same molecular masses as the corresponding troponin components in *Ascaris* body-wall muscle. In the immunocytochemical staining of the serial cryosections of *C. elegans*, the anti-TNI antibody stained both the pharyngeal and the body-wall muscles. On the other hand, the anit-TNC antibody reacted with the body-wall muscle but not with the pharyngeal muscle. These results suggest that variants of troponin components exist between the pharyngeal and body-wall muscles, and troponin is involved in the actin-linked regulatory system of *C. elegans*.

INTRODUCTION

Caenorhabditis elegans is an eligible system for studying morphogenesis of muscle. Various protein components in the *C. elegans* muscles have been identified and investigated genetically and biochemically. Especially, contractile proteins, for example, actin, myosin, and paramyosin, have been studied intensively (for review, [19]). The existence of actin- and myosin-linked calcium regulatory systems for muscle contraction was suggested in *C. elegans* [8]. The myosin regulatory light chains of 18 kDa which may be responsible for the myosin-linked regulation have been characterized (for review, [1]). However, only limited attempts have so far been made to clarify the actin-linked Ca^{2+}-regulatory proteins in *C. elegans*.

Troponin, a Ca^{2+}-dependent regulatory protein, is localized on actin filaments and plays a significant role together with tropomyosin in the Ca^{2+}-dependent regulation of muscle contraction [3, 4]. In the previous study, troponin composed of three components, namely troponin-T (TNT), troponin-I (TNI), and troponin-C (TNC), was detected in the muscle of a nematode, *Ascaris lumbricoides*, and the components were isolated and characterized [9]. Although it is known that some invertebrate troponin, for example in ascidian [5] and molluscan [16] muscles, activates actin-myosin interaction in a Ca^{2+}-dependent manner, the *Ascaris* troponin inhibited actomyosin ATPase in the absence of Ca^{2+}, but did not activate it in the presence of Ca^{2+}. Moreover, the polyclonal antibodies against TNI and TNC were prepared by immunizing rabbits with each troponin component and location of troponin components along this filaments at constant periodicity was demonstrated by immunoelectron microscopy [9]. In this study, the existence of the troponin components in *C. elegans* has been ascertained,

Accepted December 21, 1992
Received November 20, 1992
[1] To whom correspondence should be addressed.

and their immunocytochemical localization has been investigated, using the cross-reactivity of the antibodies against *Ascaris* troponin components.

MATERIALS AND METHODS

Caenorhabditis elegans ver. Brisol (strain N2) was grown at 20°C on NG agar plates with *Escherichia coli* OP50 as feed, described by Brenner [2].

The affinity-purified polyclonal antibodies against *Ascaris* TNI and TNC were prepared as described [9]. The antibodies were absorbed with acetone-dried liver powder. Fluorescein (FITC)-labeled goat anti-rabbit IgG antibody (GAR) was purchased from Cappel Laboratories.

For all studies with nematodes, worms on agar plates were washed in M9 buffer (6.0 g Na_2HPO_4, 3.0 g KH_2PO_4, 5.0 g NaCl and 0.25 g $MgSO_4 \cdot 7H_2O$ in 1 l H_2O), and collected by incubating at 4°C for 1 hr. For SDS-polyacrylamide gel electrophoresis (PAGE), an SDS-sample buffer (2% SDS, 2 mM β-mercaptoethanol, 40 mM sodium-phosphate buffer, pH 7.0) was added to the pellet of worms, and then the mixture was frozen in liquid nitrogen. The frozen mixture was dissolved immediately by incubating at 95°C for 3 min, and applied for SDS-PAGE. SDS-PAGE was carried out using 13.5% polyacrylamide gel according to Laemmli [10]. Peptides were transferred electrophoretically from electrophoretic gel to nitrocellulose paper according to Towbin *et al.* [18], and the paper was reacted with the antibodies against *Ascaris* TNI or TNC. Immunoglobulin bound to the paper was detected with ^{125}I-labelled protein A.

Squash preparation was performed basically according to Miller *et al.* [13]. A small droplet of the collected adult worms was placed between two 3% gelatin-coated glass slides, squashed by gentle pressure, and then immersed directly in liquid nitrogen until frozen. The slides were pried on dry ice with a razor blade. The slides were treated with ethanol cooled at −20°C for 10 min, and air-dried.

To prepare specimens for cryosections, the pellet of adult worms in M9 buffer was mixed with Tissue Tek-II O.C.T. compound (Miles Lab. Inc.), then immersed in liquid nitrogen-cooled isopentane. Serial cryosections were cut at 8 μm, and rapidly air-dired.

Immunostaining was performed as follows. The squashed specimens and the sections were fixed with phosphate buffered saline (PBS) containing 3.5% formalin for 5 min. After washing with PBS, the specimens were treated with PBS containing 1% bovine serum albumin. They were then exposed to the antibodies against TNI or TNC, and the antibody binding was detected with FITC-GAR. Each antibody incubation was performed for 1 hr at room temperature followed by thorough wshing in PBS. The antibody-treated specimens were mounted in 90% glycerol-10% 0.2 M carbonate buffer (pH 8.6), and the fluorescence was observed and photographed by using a fluorescence and phase contrast microscope.

RESULTS

At first, immunoblotting was performed to

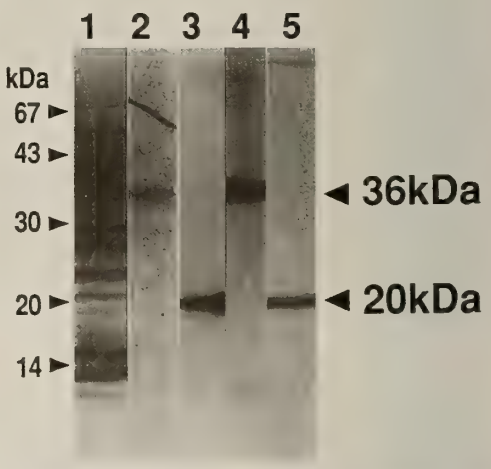

FIG. 1. Cross-reactivity of the antibodies against *Ascaris* TNI and TNC with a whole protein extract of *C. elegans*. The protein extracted with an SDS-sample buffer from *C. elegans* (1, 2, 3), purified *Ascaris* TNC (4), TNC (5) were electrophoresed on 13.5% polyacrylamide gels. The extract was transferred on nitrocellulose paper, and then reacted with the anti-TNI (2) or the anti-TNC (3) antibodies. Lane 1 shows the Amide black stainign of the extract on the nitrocellulose paper. The anti-TNI and anti-TNC antibodies reacted with the protein bands having approximately same molecular masses to *Ascaris* TNI (36 kDa) and TNC (20 kDa), respectively.

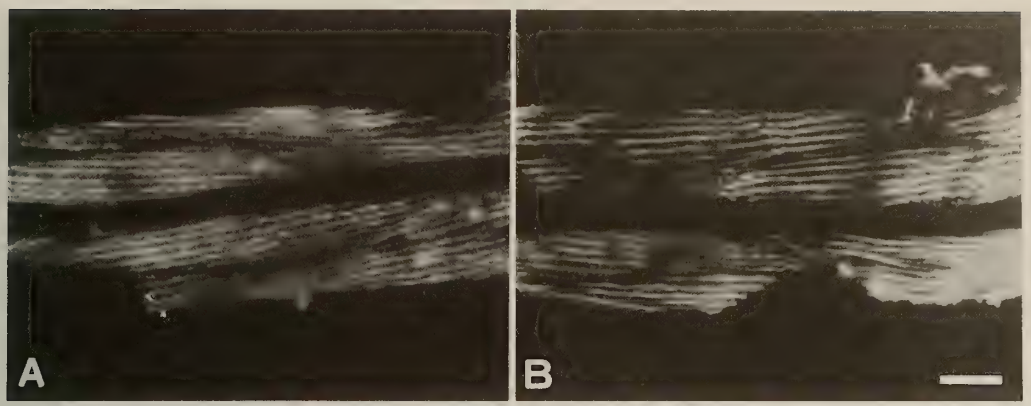

FIG. 2. Indirect immunofluorescent stainig of squashed specimens of *C. elegans*. Bar: 10 μm. The squashed specimens were treated with anti-TNI (A) and the anti-TNC (B) antibodies.

examine whether the antibodies prepared by immunizing *Ascaris* TNI and TNC cross-react with the corresponding proteins in *C. elegans*. Figure 1 shows the results of the immunoblotting. Each antibody reacted with a single peptide band in the whole extract of *C. elegans*. Moreover, the apparent molecular masses of the proteins of *C. elegans* which were recognized by the anti-*Ascaris* TNI and TNC were almost equivalent to those of the respective troponin components of *Ascaris* which were described previously [9]. Therefore, it is reasonable to conclude that the antibodies against *Ascaris* TNI and TNC also recognize TNI and TNC in *C. elegans*, respectively.

Using the antibodies, the immunocytochemical localizations of TNI and TNC in *C. elegans* were examined by staining the squashed specimens (Fig. 2) and the serial cross-sections in the head region (Fig. 3). As shown in Figure 2, antibodies stained the squashed specimens of the animal to give striated patterns. The positively stained regions probably correspond to I-band of myogibrils in body-wall muscle, because the spots of reduced staining, which seemed to correspond to the positions of dense-bodies, were observed in the striation of the staining. Further, anti-TNI and TNC exhibit different reactivity to the muscles of nematode. The sections shown in Figure 3 contained two kinds of muscles namely body-wall and pharyngeal muscles. Body-wall muscles were stained positively with both antibodies. On the other hand, pharyngeal muscle exhibited the different reactivity to anti-TNI or anti-TNC antibodies. As shown in Figure 3 anti-TNI antibody stained the pharyngeal muscle clearly, while anti-TNC antibody failed to react with this muscle.

DISCUSSION

The immunoblot analyses showed that the antibodies which were prepared against the *Ascaris* TNI and TNC, recognize the protein bands of *C. elegans*, whose molecular masses are equivalent to TNI and TNC in *Ascaris* muscles. It has been also ascertained by immunocytochemical methods that the respective antigens are localized in the I-bands of the body-wall muscles of *C. elegans*. Considering these results together with the close phylogenetic relationships between *Ascaris* and *C. elegans*, we have concluded that the troponin regulatory system functions in *C. elegans* muscles as in *Ascaris*, and both animals contain troponin components of identical size. In this study, we could not examine the other troponin component, TNT, but it is likely that TNT also exists in the muscle of *C. elegans*.

We further observed that the pharyngeal muscle and the body-wall muscle exhibit different immunoreactivity to the anti-troponin antibodies. The anti-TNI antibody exhibited positive reaction with both body-wall and pharyngeal muscles, while anti-TNC antibody reacted only with body-wall muscle. These results may potentiate three interpretations. First, pharyngeal muscle may not have

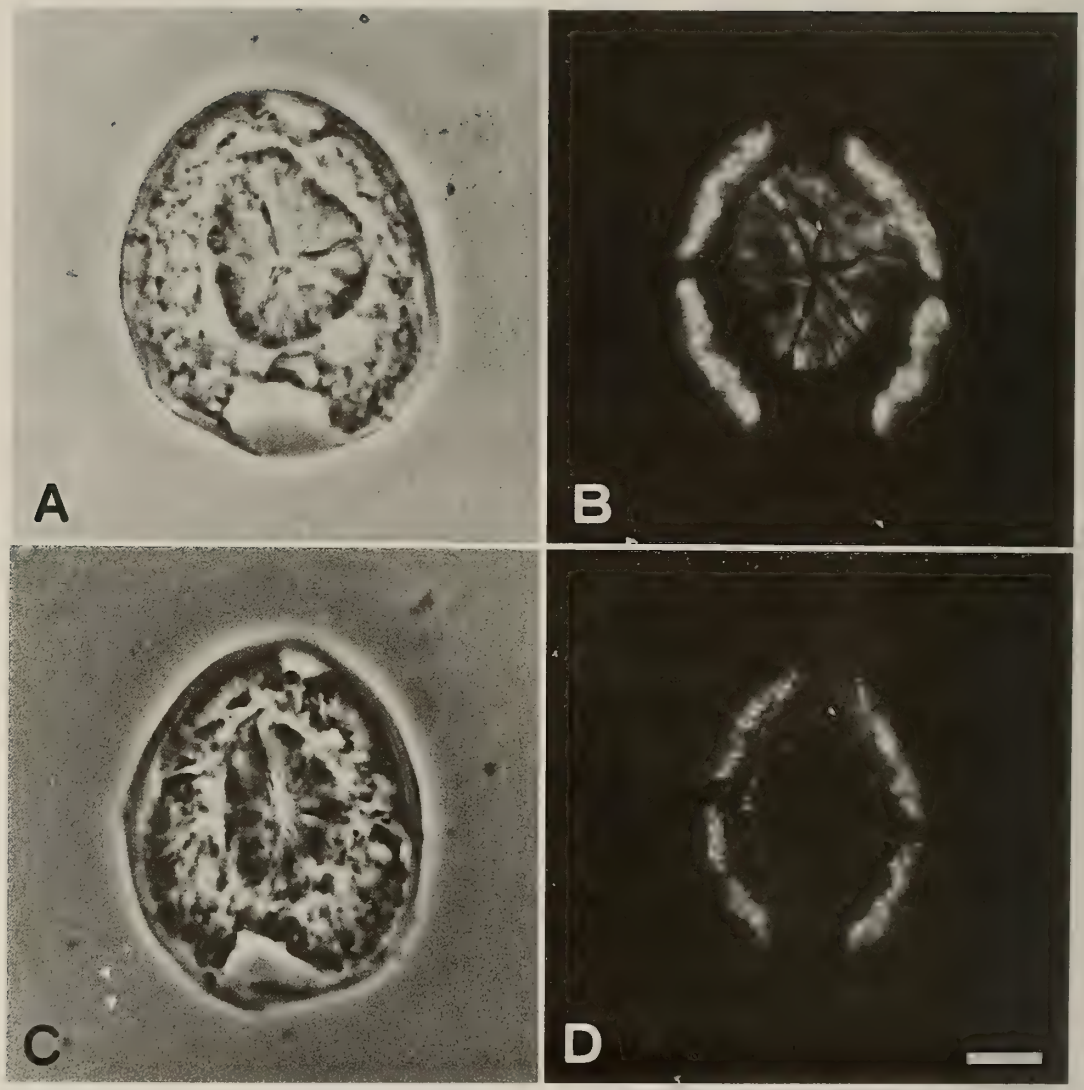

FIG. 3. Immunocytochemical localization of the TNI and TNC in the muscles of *C. elegans* head region. Bar: 10 μm. Serial cross sections of worms were treated with anti-TNI (A, B) and the anti-TNC (C, D) antibodies. Florescent images (B, D) were corresponded to the phase-contrast micrographs (A, C).

TNC. Secondly, the TNC in pharyngeal muscle may be too small in amount to be detected. Thirdly, pharyngeal muscle may have the other TNC isoform(s) with different antigenicity. Previous comparative biochemical studies have demonstrated that three troponin components mostly exist roughly in equimolar ratio in various invertebrate animals [5, 12, 16], although they vary in size and sometimes exist in multiple isoforms [15]. Therefore, it is most likely that body-wall and pharyngeal muscles of nematodes contain different TNC isoforms, although further investigation is needed to reach a definit conclusion. We can not eliminate the possibility that TNIs in the two muscles share common antigenic site(s) but differ somehow in moecular structure.

Besides the troponin conponents, it is konwn that pharyngeal muscle differs from body-wall muscle in several points. Differences in myosin isoforms between these muscles are particularly

remarkable. It has been demonstrated that four myosin heavy chain isoforms, named myoA, myoB, myoC and myoD, are distinguishable electrophoretically in the wild-type *C. elegans,* and the pharyngeal muscle possesses myoC and myoD, while the boyd-wall muscle contains myoA and myoD [6, 14, 17, 20]. Obliquely striated myofibrils have been observed in the body-wall muscle [7], but the pharyngeal muscle exhibits different structural organization [for reivew, 1]. The pharyngeal muscle seems to be functionally distinct somewhat from the body-wall muscle. Previous studies suggested that nematode muscle may be controlled dually by actin-linked and myosin-linked regulatory systems [8, 11]. Contractile activity of the two muscles of the nematode could be altered by the difference in myosin and troponin isoforms.

In conclusion, we have demonstrated that the body-wall muscle contain the troponin components, TNI and TNC, of approximately the same size as the counterparts of *Ascaris.* Thus, it is obvious that the contraction of body-wall muscle is under the control of the actin-linked troponin regulatory system. In addition, it is very likely that pharyngeal and body-wall muscles possess distinct troponin components. It is a matter of interest for furture studies how these protein variants are derived, whether encodered by different genes or generated from a single gene.

ACKNOWLEDGMENTS

Caenorhabditis elegans N2 was provided by the Caenorhabditis Genetic Center, which is funded by the NIH National Center for Research Resources (NCRR), through Dr. Joji Miwa of NEC Fundamental Research Laboratories. The authors thank Dr. H. Takano-Ohmuro for technical advice about the immunoblot analyses. One of the authors (H.N.) also thanks Drs. K. Ando, H. Nakanishi, and Y. Ishimori for advice in many phases of this work, and Ms. M. Sugano and Mrs. K. Nakae for helpful comments on the manuscript. This work was partially supported by research grants from the Ministry of Education, Science and Culture of Japan.

REFERENCES

1 Anderson P (1989) Annu Rev Genet 23: 507–525
2 Brenner S (1974) Genetics 77: 71–94
3 Ebashi S, Ebashi F (1964) J Biochem Tokyo 55: 604–613
4 Ebashi S, Endo M (1968) In "Progress in biophysics and molecular biology" Ed by JAV Butler and D Noble, Vol 18, Pergamon Press, Oxford, New York, pp 123–183
5 Endo T, Obinata T (1981) J Biochem Tokyo 89: 1599–1608
6 Epstein HF, Waterston RH, Brenner S (1974) J Mol Biol 90: 291–300
7 Francis GR, Waterston RH (1985) J Cell Biol 101: 1532–1549
8 Harris HE, Tso M-YW, Epstein HF (1977) Biochemistry 16: 859–865
9 Kimura K, Tanaka T, Nakae H, Obinata (1987) Comp Biochem Physiol 88B: 399–407
10 Laemmli UK (1970) Nature, Lond 227: 680–685
11 Lehman W, Szent-Györgyi AG (1975) J Gen Physiol 66: 1–30
12 Lehman W, Regenstein JM, Ransom AL (1976) Biochim Biophys Acta 434: 215–222
13 Miller DM III, Ortiz I, Berliner GC, Epstein HF (1983) Cell 34: 477–490
14 Miller DM III, Stockdale FE, Karn J (1986) Proc Natl Acad Sci USA 83: 2305–2309
15 Ohshima S, Komiya T, Takeuchi K, Endo T, Obinata T (1988) Comp Biochem Physiol 90B: 779–784
16 Ojima T, Nishita K (1986) J Biol Chem 261: 16749–16754
17 Schachat FH, Harris HE, Epstein HF (1977) Cell 10: 721–728
18 Towbin H, Staehelin T, Gordon J (1979) Proc Natl Acad Sci USA 76: 4350–4354
19 Waterston RH (1988) In "The nematode *Caenorhabditis elegans*" Ed by WB Wood and the community of *C. elegans* Researchers, Cold Spring Harbor Lab., New York, pp 281–335
20 Waterston RH, Moerman DG, Baillie DL, Lane TR (1982) In "Disorders of the motor unit", Ed by DM Schotland, John Wiley, New York, pp 747–760

ZOOLOGICAL SCIENCE 10: 381–383 (1993)

[RAPID COMMUNICATION]

Biosynthesis of 17α,20α-dihydroxy-4-pregnen-3-one from 17α-hydroxyprogesterone by Goldfish (*Carassius auratus*) Spermatozoa

Kiyoshi Asahina[1], Katsumi Aida[2] and Teizo Higashi[1]

[1]*College of Agriculture and Veterinary Medicine, Nihon University, Setagaya-ku, Tokyo 154, and* [2]*Department of Fisheries, Faculty of Agriculture, The University of Tokyo, Bunkyo-ku, Tokyo 113, Japan*

ABSTRACT—Goldfish (*Carassius auratus*) spermatozoa were incubated with 4-^{14}C-labeled 17α-hydroxyprogesterone at 22°C for 60 min. After extraction of the steroids from the incubation medium, they were separated by thin-layer chromatography (TLC). Radioactive steroids were localized on the TLC-plates by autoradiography. The major metabolite showed an *Rf* value lower than that of 17α,20β-dihydroxy-4-pregnen-3-one (17α,20β-P) but co-migrated with 17α,20α-P, the isomer of 17α,20β-P. The TLC behaviour of the metabolite was identical with authentic 17α,20α-P after both acetylation and oxidation. The identity of the metabolite with 17α,20α-P was finally confirmed by repeated crystallization to constant specific activity. These results indicate that goldfish sperm cells show 20α-hydroxysteroid dehydrogenase activity.

INTRODUCTION

The mature sperm cells of the rainbow trout (*Oncorhynchus mykiss*) produce very high levels of the steroid 17α,20β-dihydroxy-4-pregnen-3-one (17α,20β-P) when incubated with 17α-hydroxyprogesterone (17α-P) *in vitro* [11, 14]. In contrast, it was recently found that spermatozoa of the common carp (*Cyprinus carpio*) produce 17α,20α-dihydroxy-4-pregnen-3-one (17α,20α-P), the isomer of 17α,20β-P, when incubated with 17α-P [1]. In the present study we investigated which 17α-P metabolites were formed by spermatozoa of another cyprinid fish, the goldfish (*Carassius auratus*).

Accepted February 12, 1992
Received December 21, 1992

MATERIALS AND METHODS

Chemicals

4-^{14}C-Labeled 17α-hydroxyprogesterone (*17α-P; specific activity, 1.85 GBq/mmol) was obtained from Du Pont (UK). All organic solvents were of special grade and were obtained from the Tokyo Kasei Chemical Co. (Tokyo, Japan). 17α,20α-Dihydroxy-4-pregnen-3-one (17α,20α-P), and other non-radioactive steroids and chemicals were obtained from the Sigma Chemical Company (St. Louis, U.S.A.).

Fish

Male goldfish were kept with females in 5×0.8×0.6 m tanks under natural temperature and photoperiod conditions at the University of Tokyo; they were fed with commercial trout pellets. In April, 1991, five spermiating males were selected from the tank. Milt samples were collected in glass tubes from their genital pores by applying gentle pressure to the abdomen. Milt from all five fish was pooled and transported on ice to the department of fisheries, faculty of agriculture and veterinary medicine, Nihon University.

Incubation

Sperm cells were washed twice with carp Ringer

and collected with centrifugation at 2000 rpm for 15 min. The incubation was carried out in 5 ml of carp culture medium [8] containing 240 mM NADPH, *17α-P (1×10^5 cpm), and approximately 100 mg wet weight of washed spermatozoa. They were incubated in a 50 ml round-bottomed flasks for 1 hr at 22°C. The incubation was stopped by adding 15 ml dichloromethane and shaking vigorously for one minute.

Extraction and TLC

The procedures were the same as described previously [2]. In short, the incubation medium containing the spermatozoa was extracted twice with dichloromethane. The extracts were pooled and dried with anhydrous Na_2SO_4. After evaporation of the solvent, the residues were subjected to thin-layer chromatography (TLC) with six unlabeled steroids for standards; progesterone, 17α-P, androstenedione, testosterone, 17α,20β-P and 17α,20α-P in a benzene: acetone (4:1, v/v) solvent system. After development, the standard steroids were detected under UV light and radioactive spots on the chromatograms were detected autoradiographically by exposing the TLC plate to a sheet of medical X-ray film for one week. Each spot was then separately scraped off the plate. Radioactive compounds were eluted from the silica gel with a mixture of chloroform and ethanol (1:1, v/v), and aliquots were used to determine the radioactivity by liquid scintillation counting. The metabolites were identified on the basis of the following criteria:

(1) Isopolarity with authentic steroids on TLC developed in two systems of the following solvent mixture: benzene:acetone, 4:1 (v/v) and dichloromethane:diethyl ether, 5:2 (v/v).

(2) Identical chemical behaviour of the radioactive metabolites with the authentic preparations after acetylation [15] and oxidation [10].

(3) Constant specific radioactivity of crystals after repeated crystallization of the radioactive metabolite with the corresponding authentic preparation.

RESULTS

In the initial thin-layer chromatogram developed in a benzene: acetone (4:1, v/v) system, only one clear band ($Rf.=0.24$) corresponding to authentic 17α,20α-P was detected, in addition to the unchanged radioactive substrate, *17α-P. Following scintillation counting it was found that the conversion of radioactivity to 17α,20α-P was approximately 34 times greater than that obtained from the area of authentic 17α,20β-P (Table 1). The mobility of the metabolite was also identical with authentic 17α,20α-P on TLC using dichloromethane:diethyl ether (5:2, v/v) as solvent system. Furthermore, it behaved identically with authentic 17α,20α-P after both acetylation and oxidation. The identity of the metabolite was finally confirmed by repeated crystallization to constant specific activity with authentic 17α,20α-P (Table 2).

TABLE 1. *In vitro* conversion of 17α-hydroxyprogesterone by goldfish (*Carassius auratus*) spermatozoa

Metabolite	Yield
Unchanged substrate (17α-hydroxyprogesterone)	753.1*
17α,20α-dihydroxy-4-pregnen-3-one	64.6
17α,20β-dihydroxy-4-pregnen-3-one**	1.9

* pmol of steroid/100 mg tissue/60 min
** Tentatively identified.

TABLE 2. Recrystallization of the radioactive metabolite with the authentic preparation of 17α,20α-dihydroxy-4-pregnen-3-one for identification

	Specific radio activiry (cpm/mg)
Before recrystallization	371
After recrystallization	
1st (dichloromethane-*n*-hexane)	333
2nd (dichloromethane-*n*-heptane)	361
3rd (chloroform-*n*-hexane)	350

DISCUSSION

Our results indicate that mature sperm cells of the goldfish contain the enzyme 20α-hydroxysteroid dehydrogenase (20α-HSD) and produce

significant levels of 17α,20α-P when incubated with 17α-P for one hour *in vitro*. In addition, low levels of radioactivity co-migrated with authentic androstenedione. However, there was too little radioactivity for further analysis.

17α,20α-P is reported to be synthesized *in vitro* in the ovarian tissues of a marine teleost, the dab [5]. In the dab, high levels of this steroid were detected after hCG treatment of both female [4] and male fish [3]. Because the 20α-HSD activity was suggested to reside in dab spermatozoa [5], the sperm cells may be responsible for the synthesis of plasma 17α,20α-P. Recently, 17α,20α-P was also shown to be synthesized by goldfish ovary *in vitro* [6].

We did not detect a clear 20β-HSD activity in goldfish spermatozoa after 60 min of incubation. However, increased plasma levels of 17α,20β-P were detected with radioimmunoassay in male goldfish in relation to spawning behaviour [7] and after the administration of GTH [12]. Since a low 20β-HSD activity was detectable after a long term (18 hr) incubation of common carp spermatozoa [1], it cannot be ruled out that goldfish sperm cells also show low 20β-HSD activity. This, however, was almost undetectable after our short term incubation.

17α,20β-P has been reported to be effective by inducing spermiation in amago-salmon and goldfish [13], and the acquisition of sperm motility in salmonid fish [9]. From our results, however, it is reasonable to hypothesize that 17α,20α-P also has some role in regulating spermiation in the goldfish. Recently we have found that during spawning the 17α,20α-P plasma levels increase to almost the same levels as those of 17α,20β-P in both male and female goldfish (Asahina *et al.*, unpublished results). The reason(s) for the discrepancy between the *in vitro* production and the plasma levels of these two steroids is currently under investigation.

ACKNOWLEDGMENTS

We are grateful to Dr. R. Schulz at University of Utrecht for critical reading of the manuscript.

REFERENCES

1 Asahina K, Barry TP, Aida K, Fusetani N, Hanyu I (1990) J Exp Zool 255: 244–249
2 Asahina K, Suzuki K, Aida K, Hibiya T, Tamaoki B (1985) Gen Comp Endocrinol 57: 281–282
3 Canario AVM, Scott AP (1991) Gen Comp Endocrinol 83: 258–264
4 Canario AVM, Scott AP (1990) Gen Comp Endocrinol 77: 177–191
5 Canario AVM, Scott AP (1989) Gen Comp Endocrinol 76: 147–158
6 Kime DK, Scott AP, Canario, AVM (1992) Gen Comp Endocrinol 83: 258–264
7 Kobayashi M, Aida K, Hanyu I(1986) Gen Comp Endocrinol 62: 72–79
8 Kobayashi M, Aida K, Hanyu I (1986) Nippon Suisan Gakkaishi 52: 1153–1158
9 Miura T, Yamauchi K, Takahashi H, Nagahama Y (1992) J Exp Zool 261: 359–363
10 Poos GI, Arth GE, Beyler RE, Sarett LH (1953) J Amer Chem Soc 75: 422–429
11 Sakai N, Ueda H, Suzuki N, Nagahama Y (1989) Biomed Res 10: 131–138
12 Suzuki Y, Kobayashi M, Aida K, Hanyu I (1988) J Comp Physiol B 157: 753–758
13 Ueda H, Kambegawa A, Nagahama Y.(1985) Gen Comp Endocrinol 59: 24–30
14 Ueda H, Kambegawa A, Nagahama Y (1984) J Exp Zool 321: 435–439
15 Zaffaroni A, Burton RB (1951) J Biol Chem 193: 749–767

Development
Growth & Differentiation

Published Bimonthly by the Japanese Society of Developmental Biologists
Distributed by Business Center for Academic Societies Japan, Academic Press, Inc.

Papers in Vol. 35, No. 2. (April 1993)

Development, Growth and Differentiation (ISSN 0012–1592) is published bimonthly by The Japanese Society of Developmental Biologists. Annual subscription for Vol. 35 1993 U. S. $ 191,00, U. S. and Canada; U. S. $ 211,00, all other countries except Japan. All prices include postage, handling and air speed delivery except Japan. Second class postage paid at Jamaica, N.Y. 11431, U. S. A.

Outside Japan: Send subscription orders and notices of change of address to Academic Press, Inc., Journal Subscription Fulfillment Department, 6277, Sea Harbor Drive, Orlando, FL 32887–4900, U. S. A. Send notices of change of address at least 6–8 weeks in advance. Please include both old and new addresses. U. S. A. POSTMASTER: Send changes of address to *Development, Growth and Differentiation,* Academic Press. Inc., Journal Subscription Fulfillment Department, 6277, Sea Harbor Drive, Orlando, FL 32887–4900, U. S. A.

In Japan: Send nonmember subscription orders and notices of change of address to Business Center for Academic Societies Japan, 16–9, Honkomagome 5-chome, Bunkyo-ku, Tokyo 113, Japan. Send inquiries about membership to Business Center for Academic Societies Japan, 16–9, Honkomagome 5-chome, Bunkyo-ku, Tokyo 113, Japan.

Air freight and mailing in the U. S. A. by Publications Expediting, Inc., 200 Meacham Avenue, Elmont, NY 11003, U. S. A.

OLYMPUS®

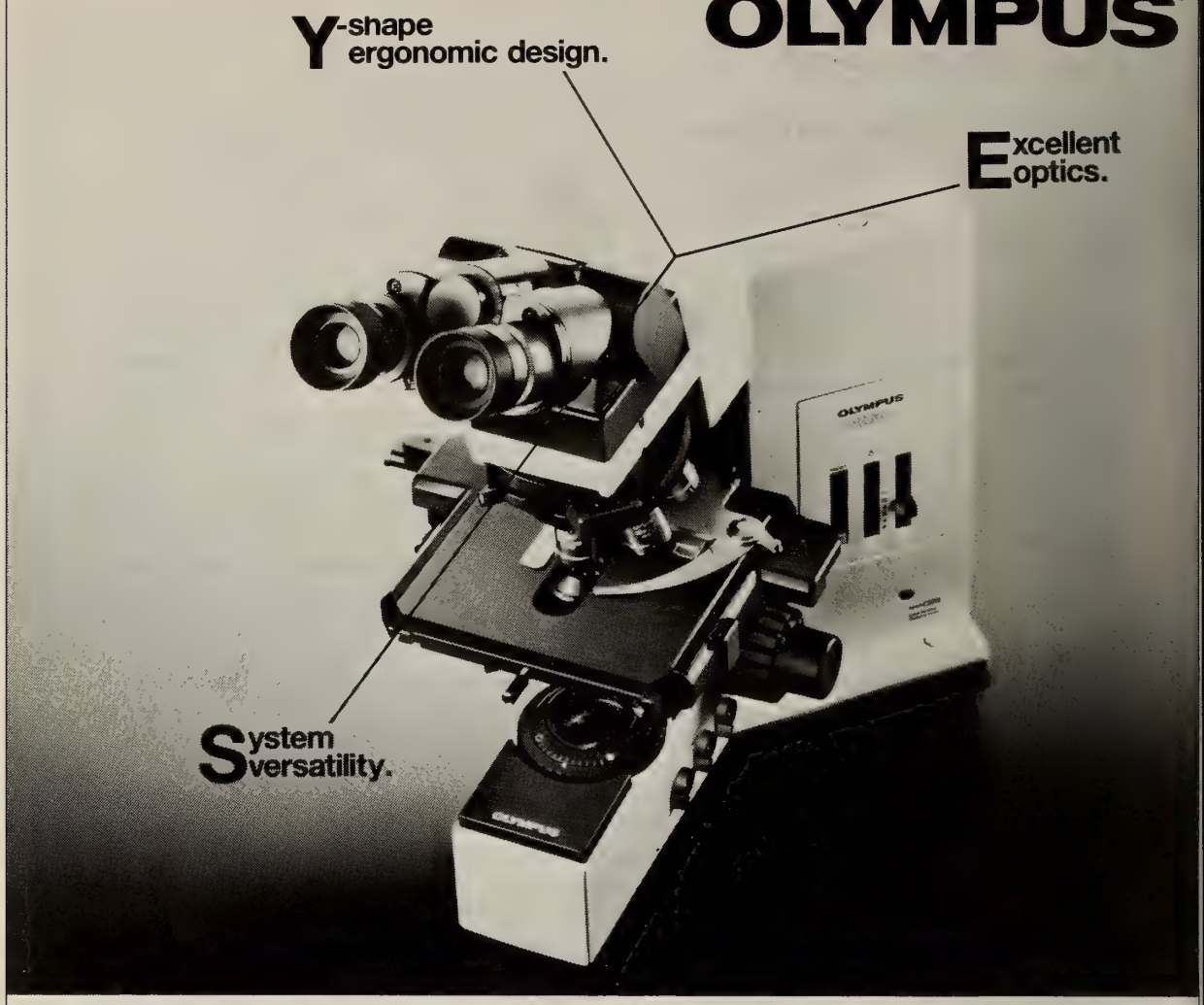

Y·E·S is the answer.

The BX Series was developed with your needs and our ideals in mind.

Y-shaped ergonomic design ensures maximum comfort.
Easy operation. Easy recognition. And fatigue-free use. To the question of what constitutes the ideal microscope from the user's point of view, our answer is a unique Y-shaped design. We invite you to discover unprecedented operational ease and comfort.

Excellent optics provide superior image quality.
Developed through the application of more than 70 years of experience and what the latest technology has to offer, Olympus' own UIS (Universal Infinity System) infinity-corrected optical system assures exceptional image quality. You benefit from both higher contrast and outstanding flatness throughout the field of view.

System versatility answers diverse research requirements.
Frame rigidity and stability have been increased dramatically through use of computer simulation (FEM analysis). You'll find that reliability has been enhanced, too, when the time comes for system expansion, via devices for image processing, microscopic light metering, photography and so on.

SYSTEM MICROSCOPE
BX
BX40/BX50

N E W

OLYMPUS OPTICAL CO.,LTD. OLYMPUS (JAPAN) CO.,LTD.
For free catalog, please contact: OLYMPUS (JAPAN) CO.,LTD. Ryumeikan Bldg., 3-4, Kanda-surugadai, Chiyoda-ku, Tokyo Tel. (03) 3251-8971

The Ultimate Name in Micromanipulation
Ease of operation, and the most advanced

Can be combined with
New WR & MX series

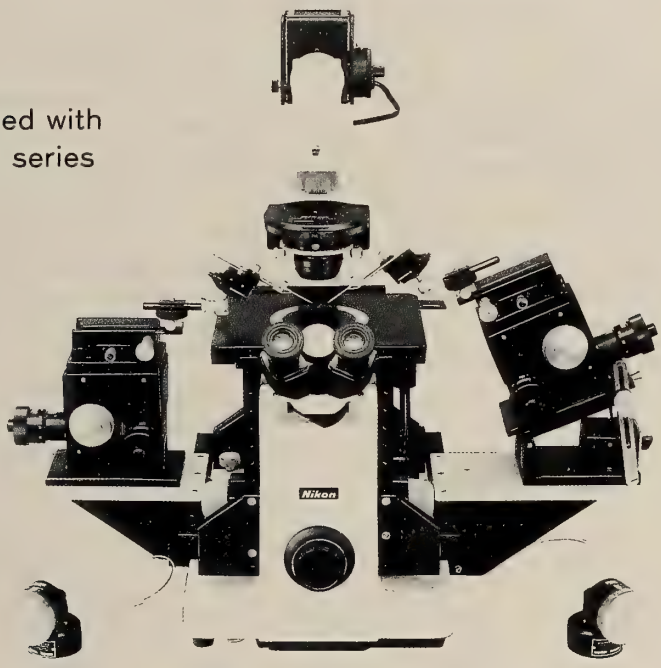

Model MX-1
3-D Micromanipulator

Model MX-2
3-D Micromanipulator

Model WR-87
One Dimensional
Aqua Purificate
Micromanipulator

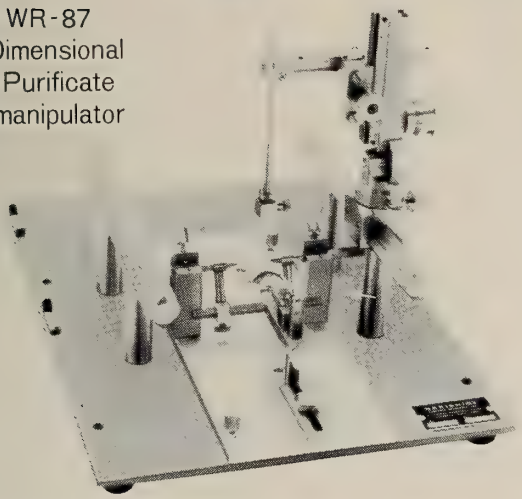

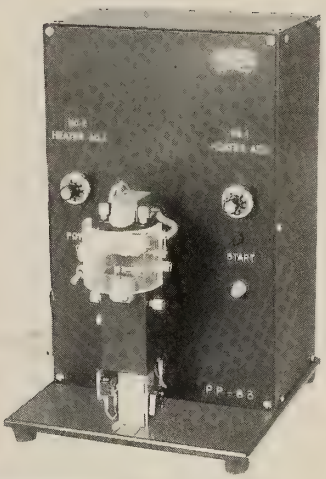

Model SR-6
Stereotaxic Instrument for Rat

Model PP-83
Glass Microelectrode Puller

* * * Send enquiries for request for MODIFICATIONS or IMPROVEMENTS * * *
Physiological, Pharmacological, Zoological & Neurosciences Research Equipments

---

NARISHIGE JAPAN

NARISHIGE SCIENTIFIC INSTRUMENT LAB.

9-28 KASUYA 4-CHOME SETAGAYA-KU, TOKYO 157, JAPAN
PHONE(INT-L)81-3-3308-8233, FAX(INT-L)81-3-3308-2005
CABLE:NARISHIGE LABO, TELEX, NARISHIGE J27781

(*Contents continued from back cover*)

ZOOLOGICAL SCIENCE

VOLUME 10 NUMBER 2 APRIL 1993

CONTENTS

(*Contents continued on inside back cover*)

INDEXED IN:
Current Contents/LS and AB & ES,
Science Citation Index,
ISI Online Database,
CABS Database, INFOBIB

Issued on April 15
Printed by Daigaku Letterpress Co., Ltd.,
Hiroshima, Japan

l. 10 No. 3 June 1993

ZOOLOGICAL SCIENCE

An International Journal

PHYSIOLOGY
CELL and MOLECULAR BIOLOGY
GENETICS
IMMUNOLOGY
BIOCHEMISTRY
DEVELOPMENTAL BIOLOGY
REPRODUCTIVE BIOLOGY
ENDOCRINOLOGY
BEHAVIOR BIOLOGY
ENVIRONMENTAL BIOLOGY and ECOLOGY
SYSTEMATICS and TAXONOMY

published by **Zoological Society of Japan**

distributed by Business Center for Academic Societies Japan
VSP, Zeist, The Netherlands

ISSN 0289-0003

ZOOLOGICAL SCIENCE

The Official Journal of the Zoological Society of Japan

The Zoological Society of Japan:
Toshin-building, Hongo 2–27–2, Bunkyo-ku,
Tokyo 113, Japan. Phone (03) 3814–5675
Officers:
President: Hideo Mohri (Chiba)
Secretary: Hideo Namiki (Tokyo)
Treasurer: Makoto Okuno (Tokyo)
Librarian: Masatsune Takeda (Tokyo)

ZOOLOGICAL SCIENCE is devoted to publication of original articles, reviews and communications in the broad field of Zoology. The journal appears bimonthly. An annual volume consists of six numbers of more than 1200 pages including an issue containing abstracts of papers presented at the annual meeting of the Zoological Society of Japan.

MANUSCRIPTS OFFERED FOR CONSIDERATION AND CORRESPONDENCE CONCERNING EDITORIAL MATTERS should be sent to:

Dr. Tsuneo Yamaguchi, Editor-in-Chief, Zoological Science, Department of Biology, Faculty of Science, Okayama University, Okayama 700, Japan, in accordance with the instructions to authors which appear in the first issue of each volume. Copies of instructions to authors will be sent upon request.

SUBSCRIPTIONS. ZOOLOGICAL SCIENCE is distributed free of charge to the members, both domestic and foreign, of the Zoological Society of Japan. To non-member subscribers within Japan, it is distributed by Business Center for Academic Societies Japan, 5–16–9 Honkomagome, Bunkyo-ku, Tokyo 113. Subscriptions outside Japan should be ordered from the sole agent, VSP, Godfried van Seystlaan 47, 3703 BR Zeist (postal address: P. O. Box 346, 3700 AH Zeist), The Netherlands. Subscription rates will be provided on request to these agents. New subscriptions and renewals begin with the first issue of the current volume.

[Publication of Zoological Science has been supported in part by a Grant-in-Aid for Publication of Scientific Research Results from the Ministry of Education, Science and Culture, Japan.]

ZOOLOGICAL SCIENCE 10: 385–392 (1993)

REVIEW

Proliferation of Anterior Pituitary Cells in Relation to Aging and Longevity in the Rat

Hiroshi Ooka

Department of Cell Biology, Tokyo Metropolitan Institute of Gerontology, 35-2 Sakaecho, Itabashi-ku, Tokyo 173, Japan

ABSTRACT—Some of the hormones secreted from the anterior pituitary are related to the potency of survival during the aging process. The proliferation of thyrotrophs affects the lifespan of the rat through the activity of the thyroid gland. Adrenocorticotropic hormone promotes the deterioration of brain function in aged rats. Average prolactin levels and the incidence of prolactinoma increase in aged rats. A longitudinal study showed that the increase in prolactin levels represents the precancerous state for a prolactinoma. Culture experiments indicate that the proliferation of acidophils is regulated by hypothalamic growth hormone-releasing factor and other hormones, which are possibly responsible for the age-related change in acidophil populations.

ANTERIOR PITUITARY CELLS AND THE RATE OF AGING IN THE RAT

Theories on the biological mechanisms of aging include the alteration of the humoral regulatory system in which the hypothalamo-pituitary axis has central importance. In this chapter I will deal only with the role of the anterior pituitary in the aging of structures and functions related to the survival of individuals. The anterior pituitary is deeply concerned in age-related changes in the reproductive system. With regard to these aspects, other review articles can be consulted [2, 20, 28, 77].

In his series of research on surgically hypophysectomized rats, Everitt [19] has shown that several cirteria for aging (hardening of tail tendon collagen, increase in protein excretion in urine, renal and cardiac hypertrophy, etc.) are prevented by hypophysectomy. Despite the retarded rate of aging in these criteria, hypophysectomy shortens the duration of life. Later work showed, however, that replacement therapy with cortisone acetate prolongs the lifespan of hypophysectomized rats to even longer than the lifespan of intact rats, thereby suggesting that adrenocorticotropic hormone (ACTH) is an essential life-maintaining factor in survival [21]. From these results he concluded that the pituitary secretes "aging hormone(s)" which accelerate the rate of aging processes.

Chronic food restriction has been the most effective means for prolonging the lifespan of rats [30, 46]. The onset of various kinds of age-associated disease is also delayed by food restriction. Some studies have shown that food restriction inhibits the secretion of pituitary hormones [13, 48], suggesting that the anti-aging effect of food restriction may partly be ascribed to the reduced secretion of "aging hormone(s)".

One candidate for such an aging factor is the pituitary-thyorid axis. A very early study showed that mice fed desiccated thyroid throughout their liver had shorter lifespans than controls [67]. Exposure to low temperature (9°C), which was expected to induce the secretion of thyroxine (T_4), shortened the lifespan compared to control rats maintained at 28°C [35]. The periodic acid—Schiff (PAS) stainability of the anterior pituitary decreased in tryptophan-deficient rats, which also showed retardation of aging. The concentrations of T_4, 3,3′,5-triiodothyronine (T_3), and thyrotropic

Received December 25, 1992

hormone were lower in these tryptophan-deficient animals than in control rats [57].

More direct and precise experiments were carried out using the neonatally T_4-treated hypothyroid rats of both sexes. Thyrotrophs in the anterior pituitary of neonatal rats proliferate actively and increase rapidly in number [55]. When rats were injected intraperitoneally with 1–2 μg T_4 per g body weight 5 times during the first 10 days of life, the division of thyrotrophs was suppressed by the exogenous T_4. There was almost no increase in the number of thyrotrophs in rats at 10 days of age. The capacity to increase the number of thyrotrophs was restored after discontinuation of T_4 injection; the pituitaries in adult rats treated neonatally with T_4 contained almost the same density of thyrotrophs as the controls [55]. The levels of T_4 in the treated rats were lower than in control rats, as reported in previous studies [3, 5], throughout almost the whole lifespan, indicating that the function of the thyroid gland was impaired by the inhibition of thyrotroph proliferation during neonatal T_4-treatment. The levels of T_3 were also lower than controls in young rats. These artifitial hypothyroid rats of both sexes lived longer than control rats [56]. On the other hand hyperthyroid rats, produced by continuous administration of T_4 in the drinking water, had shorter lifespans than controls [58]. The life-shortening effect of T_4 was observed even when the rats were treated with T_4 during only the first or second half of life. T_4 treatment was not effective, however, when treatments were confined to the senescent period (more than 26 months old). These results indicate that T_4 does not directly induce the senescent diseases that are the causes of death, but accelerates the aging rate during the young and middle-aged periods [58].

The aging factors suggested by the experiments of Everitt seem not to include ACTH, because he supplied glucocorticoid to hypophysectomized rats that showed aging retardation. However, it has been reported that the ACTH-adrenal cortex axis accelerates some aspects of the aging process. Wexler [91] has reported the premature aging of the cardiovascular system and many other tissues in hyperadrenocorticoid rats produced by repeated breeding. Recent evidence indicates that some aging phenomena in the hippocampus and other brain regions are modulated by glucocorticoids [23]. Sapolsky [71] emphasized that the hippocampus is a primary CNS target for glucocorticoids which induce neuronal loss in the aged hippocampus. Minimal damage in the hippocampus was observed in adrenalectomized rats after microinjection of toxins (kainic acid or 3-acetylpyridine). Enhanced damage was induced in corticosterone-treated rats. Adrenalectomy appears to protect the brain against age-related reductions in neuronal density and age-related increases in glial density [44]. However, part of the effect of adrenalectomy seems to be due to prolonged neural stimulation resulting from elevated ACTH, rather than to a reduction in steroids *per se*, since the morphologic correlates of brain aging were reduced and maze learning was improved by treatment with a non-steroidogenic ACTH analog.

AGE-ASSOCIATED DEVELOPMENT OF HYPERPROLACTINEMIA AND PROLACTINOMA

The concentration of prolactin (PRL) in the blood of female rats increases with age [78, 84]. The incidence of spontaneous prolactinoma also increases in the pituitary of aged rats, but there is a wide variation among strains [93]. High tumor incidence in one strain is generally associated with age-related hyperprolactinemia, not only in the individuals which have pituitary hyperplasia, but also in the rats with histologically normal pituitaries [89]. Although aged male rats of many strains also have high PRL levels, the magnitude differs depending on the strain [7, 65, 70, 90]. In mice, C57BL/6J females over 14 months of age have a high tumor incidence [22], but PRL levels are not elevated in male mice at ages up to 28 months [17].

Even in strains in which aged female rats have very high average PRL levels, the individual variations are very large with some rats showing low PRL values at advanced ages [89]. Therefore it is impossible to determine any chronological pattern for the development of hyperprolactinemia or prolactinoma in individual rats from the cross-sectional data. A longitudinal study on PRL levels in female Wistar rats by serial sampling of blood

from the same individuals was useful for such purpose [59]. A prolactinoma inevitably develops within 3 months in rats with blood PRL levels higher than 70 ng/ml. On the other hand, rats with no tumors at the time of death showed very low PRL levels throughout life (Fig. 1). These facts indicate that moderate hyperprolactinemia is the precancerous state prior to the development of prolactinoma. The duration of tumor growth is 2–3 months (Fig. 1). The highest generation of new tumors is observed at around 27 months of age. Some rats with a large tumor survive for more than 10 months, indicating that prolactinoma is not always a direct cause of death for rats [59]. This finding may have some relation to a report that increased immunoreactive PRL molecules show low biological activity when assayed for proliferation-inducing potency on Nb_2 lymphoma cells [12]. Moreover, we can expect anti-aging effects of PRL since the administration of PRL prevents an age-related decrease in dopamine receptors in the rat striatum [68]. PRL-treated rats recovered from motor dysfunctions.

As with many other aging criteria, the age-associated increase in PRL levels is suppressed in rats by food restriction [81]. Synthesis of PRL messenger RNA is also reduced in energy-restricted C3H/SHN F_1-hybrid mice [41]. These suppressions might be due to direct inhibition of the production or secretion of pituitary hormones by underfeeding, since the level of growth hormone (GH), which decreases with age, is remarkably reduced by food restriction [62]. Measurements of PRL levels in rats refed after 24 months of food restriction by an intermittent food supply, however, showed that low PRL levels are maintained for more than 9 weeks, indicating that the prevention of PRL increase in food-restricted rats is not due to a direct effect of underfeeding, but represents a retardation of aging in the hypothalamo-pituitary axis (Fig. 2).

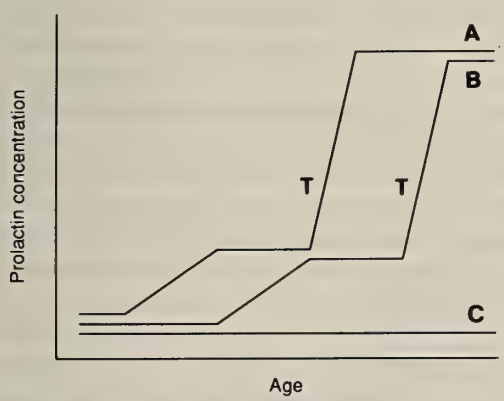

FIG. 1. Schematic representation of the longitudinal changes in the PRL levels of female Wistar rats with large tumors (A), small tumors (B), and no tumors (C) at the time of death. The time of tumor development was accompanied by a sudden rise in PRL level (T). Prolactinomas always developed in hyperprolactinemic rats within 3 months. When the period between tumorigenesis and examination of the pituitary was less than 2 months, the pituitary had a small tumor (less than 1 mm), indicating that the duration of tumor growth is about 2 months.

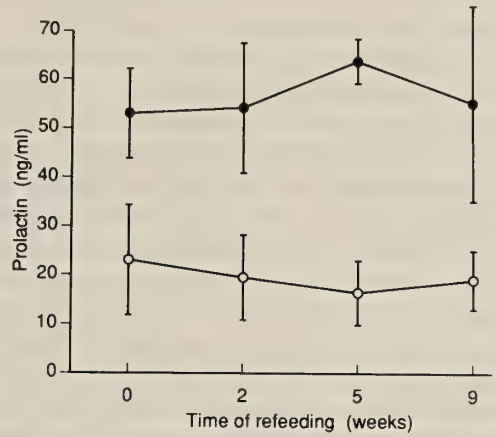

FIG. 2. PRL levels in food-restricted and refed male Fischer 344 rats. Experimental rats (open circles) were fed every other day from 1 to 24 months of age, with a total food intake approximately 60% that of controls (closed circles). Radioimmunoassay for PRL was performed on serially sampled blood from the same individuals. Protection against hyperprolactinemia continued for more than 9 weeks of *ad libitum* refeeding.

The close association of hyperprolactinemia with prolactinoma suggests the possibility that the number of mammotrophs increases in the pituitary of hyperprolactinemic rats. The volume fraction occupied by the mammotrophs in the pituitary increases with age [89]. The ratio of mammotroph number to total secretory cells also increases in the

pituitary of hyperprolactinemic rats [15], although no increase was observed in aged individuals with low PRL levels [59]. Moreover, many previous studies have shown that the synthesis and secretion rate of PRL in each mammotroph do not increase, or rather decrease in the pituitary of aged rats [86]. These results indicate that changes in the regulation of cell number, besides the regulation of hormone secretion [6, 18, 27, 33, 37, 40, 53, 54, 82], are important in the mechanism for the development of hyperprolactinemia.

REGULATION OF ACIDOPHIL PROLIFERATION IN AGING AND TUMORIGENESIS

Mammotrophs in the pituitary of adult animals can increase through cell proliferation, or by conversion from somatotrophs [38]. The possibility of transdifferentiation of mammotrophs and somatotrophs is suggested by the presence of cells which secrete both PRL and GH (mammosomatotrophs) [29, 75]. Estrogen induces the production of PRL in somatotrophs, and increases the number of mammosomatotrophs in primary pituitary cell culture obtained from adult male rats [10] and in a clonal pituitary cell line, GH_3 [9]. Insulin and IGF-1 stimulate the secretion of PRL, and inhibit the secretion of GH, in GH_3 cells [49, 61]. On the other hand, cortisol antagonizes insulin in the secretion of PRL by GH_3 cells [61]. Cortisol also increases the number of both somatotrophs and mammosomatotrophs in cultured bovine pituitary cells by transdifferentiation [39]. More detailed informations about mammosomatotrophs are available in a recent review [86].

The increase in mammotrophs by cell proliferation, however, is most likely in age-related hyperprolactinemia, since tissue hyperplasia is a general feature of the precancerous state. The proliferative activity of mammotrophs is stimulated by estrogen, which also enhances the secretion of PRL [32, 47, 78]. Both the mitotic index and the number of cells in S-phase increase after *in vivo* estradiol treatment of rats [34, 60, 87]. Prolonged administration of natural or synthetic estrogen induces prolactinomas in rats and mice [11, 92]. The sustained plasma estradiol levels associated with persistent vaginal cornification in middle-aged rodents are suspected by some authors to be a factor responsible for both the elevated PRL levels and the high incidence of prolactinoma in females [23]. In constant estrous Long-Evans rats older than 25 months, moderately high estrogen levels are accompanied by high PRL concentration in the blood [45]. However, plasma estrogen levels are rather lower in constant estrous C57BL/6J mice than in the estrous and diestrous stages of cyclic young in which estrogen levels are very high in the proestrous stage [22]. Moreover, only a small portion of rats older than 25 months are in constant estrus [1, 45], while many rats show an increase in PRL levels and prolactinoma development between 25 and 30 months [59]. In some strains of rats, for example, Wistar and Fischer 344 rats, age-related hyperprolactinemia and prolactinoma are observed even in males [7]. These facts suggest the presence of other factors involved in the increase in mammotroph number.

Hypothalamic dopamine is a well-known inhibitor of PRL secretion. Sulpiride, a dopamine antagonist, activates both DNA synthesis and the mitosis of mammotrophs *in vivo*, and bromocriptine, a stable dopamine agonist, suppresses them [34, 87]. The content of dopamine in the hypothalamus decreases in aged rodents [16, 80]. Old female rats with spontaneous prolactinomas, as well as young females with prolactinomas induced by prolonged estrogen treatment, show damaged tuberoinfundibular dopaminergic neurons [72–74]. These reports suggest that dopamine plays an important role in the regulation of mammotroph proliferation. However, the sensitivity of mammotroph DNA synthesis to amantadine, a compound that causes an increase in dopamine synthesis, seems to be lower than that ot PRL secretion [42]. Dopamine concentration in the hypophyseal portal blood has been reported to decrease with age in both male [26] and female [64] rats, but a more recent study has shown that the rate of dopamine secretion is markedly elevated in aged rats [31]. Dopamine content in the anterior pituitary is also higher in aged rats than in young rats [63].

Among secretory cells in the anterior pituitary of adult rats, mammotrophs are the only cells to

proliferate actively in culture with ordinary basal medium containing no hypothalamic factors [4]. Recent studies on cultured anterior pituitary cells have revealed the direct influence of hormones, especially hypothalamic peptides, on the proliferation of these cells. Billestrup *et al.* [8] reported that DNA synthesis in cultured somatotrophs is stimulated by the addition of growth-hormone releasing factor (GRF), and suppressed by somatostatin. Frawley and Hoeffler [24] studied the effects of various hypothalamic hormones on the number of mammotrophs and somatotrophs in 5-day-old rats by a reverse-plaque assay. They reported that the relative number of mammotrophs to somatotrophs increases in cultures containing GRF or luteinizing hormone-releasing hormone (LHRH). The proliferation of both cell types is stimulated by corticotropin-releasing factor (CRF), but thyrotropin-releasing hormone (TRH) stimulates the proliferation of other cell types. Treatment of pituitary reaggregate cell culture from immature (14-day-old) rats with LHRH or neuropeptide Y increased ^{3}H-thymidine incorporation into mammotrophs and corticotrophs, whereas these peptides decreased the number of labeled somatotrophs [88]. The actions of these peptides were suggested to be mediated by specific paracrine growth factors released from gonadotrophs.

The effects of various hypothalamic hormones on the proliferation of pituitary cells from adult rats were examined in culture using 8-month-old female Wistar rats [79]. In a basal medium consisting of Eagle's MEM and 10% fetal bovine serum, mammotrophs proliferated actively, and no increase in the number of somatotrophs was observed. The proliferative situation was completely reversed by the addition of GRF (Fig. 3). This result suggests that the relative number of acidophils is regulated by hypothalamic GRF through inverse responses of mammotrophs and somatotrophs to GRF. GH and PRL belong to the same gene family, and both secretory cells differentiate from the same precursor cells [38]. The mechanism by which the expression of one gene changes the characteristics of cell proliferation is worth investigating. Another possibility is that GRF suppresses the proliferation of mammotrophs indirectly through an unknown inhibitor secreted by somatotrophs or other cell types under the stimulation of GRF. Failure to detect GRF binding sites on the mammotroph surface suggests this possibility [51]. If this assumption is correct, the postulated inhibitor should be specific to mammotrophs since the proliferation of somatotrophs is not suppressed. In contrast with the effect of dopamine, GRF does not inhibit the secretion of PRL [14, 76, 83].

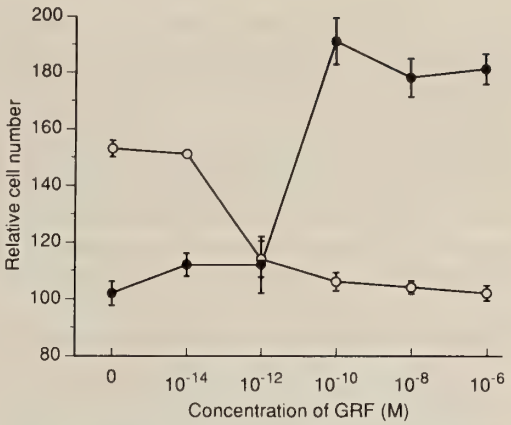

FIG. 3. Changes in the numbers of mammotrophs (open circles) and somatotrophs (closed circles) from adult rats during a 6 days in culture with varying concentration of GRF. Relative cell number represents the percentage of cells at the start of culture period.

The content of GRF in the median eminence decreases markedly with aging in the rat [52]. This is not conclusive evidence that GRF secretion into the protal blood is reduced, since a decreased content of a substance in the median eminence could occur with either increased or decreased secretion. However, the fact that the secretion of GH [62] decreases with aging, while total volume of GH cells does not change [86], suggests a decrease in GRF secretion in aged rats. It is possible that a decrease in GRF secretion plays a role in the change in the relative number of acidophils in aged rats.

The addition of LHRH into the culture accelerates the rate of mammotroph proliferation (submitted for publication). It has been reported that the content [69] and secretion rate [85] of LHRH increase gradually in middle-aged and old rats. High luteinizing hormone (LH) levels in the blood

of aged mice also suggest an increase in LHRH secretion in these animals [25]. On the other hand, no increase is observed in the blood LH levels of aged female rats [45]. However, a decrease in the responsiveness to LHRH may prevent the increase in LH release in aged rats, since the density of LHRH receptor is reduced in the pituitary cells of aged rats [50]. From these data it can be assumed that LHRH also contributes to the age-related increase in the number of mammotrophs.

Although the proliferation of mammotrophs in adult rats is activated by LHRH, the stimulation of PRL secretion by physiological doses of LHRH seems to be restricted to very young animals [66]. In older rats, the PRL-secreting response to high, nonphysiological doses of LHRH has been reported, and this phenomenon is suggested to be mediated by angiotensin II produced by paracrine secretion [36, 43]. But angiotensin II had no distinct effect on the proliferation of mammotrophs in culture experiments.

The suppressive effect of bromocriptine on mammotroph proliferation has been confirmed *in vitro* (unpublished data). TRH stimulates the secretion of PRL [27, 33], but showed no effect on the proliferation of mammotrophs.

The effects of hypothalamic and ovarian hormones on the proliferation of acidophils, as shown by *in vitro* studies, are summarized in Fig. 4. Age-related changes in the production and secretion of these hormones probably cause the changes in the acidophil populations of the anterior pituitary in aged rats, the increase in mammotrophs and the decrease in somatotrophs.

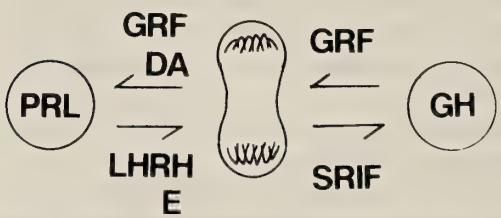

Fig. 4. Regulation of the proliferation of mammotrophs (PRL) and somatotrophs (GH) by GRF, LHRH, dopamine (DA), somatostatin (SRIF), and estrogen (E).

ACKNOWLEDGMENTS

The author is grateful to Dr. T. Shinkai, Department of Cell Biology, Tokyo Metropolitan Institute of Gerontology, for his cooperation in the preparation of this review. Hormones and antibodies for radioimmunoassay and immunostaining were kindly supplied by the National Institute of Diabetes and Digestive and Kidney Diseases, USA, and Gunma University, Japan.

REFERENCES

1 Aschheim P (1976) In "Hypothalamus, Pituitary, and Aging" Ed by AV Everitt, JA Burgess, Charles C. Thomas, Springfield, pp 376–418
2 Aschheim P (1983) In "Neuroendocrinology of Aging" Ed by J Meites, Plenum Press, New York, pp 73–101
3 Azizi F, Vagenakis AG, Bollinger J, Reichelin S, Braverman LE, Ingbar SH (1974) Endocrinology 94: 1681–1688
4 Baker BL, Reel JR, Van Dewark SD, Yu YY (1974) Anat Rec 179: 93–106
5 Bakke JL, Lawrence N, Wilber JF (1974) Endocrinology 95: 406–411
6 Bernton EW, Beach JE, Holaday JW, Smallridge RC, Fein HC (1987) Science 238: 519–521
7 Bethea CL, Walker RF (1979) J Geront 34: 21–27
8 Billestrup N, Swanson LW, Vale W (1986) Proc Natl Acad Sci USA 83: 6854–6857
9 Boockfor FR, Hoeffler JP, Frawley LS (1985) Endocrinology 117: 418–420
10 Boockfor FR, Hoeffler JP, Frawley LS (1986) Am J Physiol 250: E103–105
11 Brawer JR, Sommerstein C (1975) Am J Anat 144: 57–87
12 Briski KP, Sylvester PW (1990) Neuroendocrinol 51: 625–631
13 Campbell GA, Kurcz M, Marshall S, Meites J (1977) Endocrinology 100: 580–587
14 Casanueva FF, Brorras CG, Bruguera B, Lima L, Muruais C, Tresguerres JAF, Devesa J (1987) Endocrinology 27: 517–523
15 Chuknyska RS, Biackman MR, Hymer WC, Roth GS (1986) Endocrinology 118: 1856–1862
16 Damarest KT, Riegle GD, Moore KE (1980) Neuroendocrinol 31: 222–227
17 De vellis JS, Swerdloff RS (1977) Endocrinology 101: 1310–1318
18 Dymshitz J, Laudon M, Ben-Jonathan N (1992) Neuroendocrinol 55: 724–729
19 Everitt AV (1976) In "Hypothalamus, Pituitary, and Aging" Ed by AV Everitt, JA Burgess, Charles C. Thomas, Springfield, pp 68–85

20 Everitt AV, Meites J (1989) J Geront 44: B139–147
21 Everitt, AV, Seedman NJ, Jones F (1980) Mech Ageing Dev 12: 161–172
22 Felicio LS, Nelson JF, Finch CE (1980) Exp Geront 15: 139–143
23 Finch CE, Landfield PW (1988) In "Handbook of the Biology of Aging" Ed by CE Finch, EL Schneider, Van Nostrand Reinhold, New York, pp 567–594
24 Frawley LS, Hoeffler JP (1988) Peptide 9: 825–828
25 Gee DM, Flurkey K, Finch CE (1983) Biol Reprod 28: 598–607
26 Gudelsky GA, Mansel DD, Porter JC (1981) Brain Res 204: 446–450
27 Hanna S, Shin SH (1992) Neuroendocrinol 55: 591–599
28 Harman SM, Talbert GB (1985) In "Handbook of the Biology of Aging" Ed by CE Finch, EL Schneider, Van Nostrand Reinhold, New York, pp 457–510
29 Hashimoto S, Fumagalli G, Zanini A, Meldolesi J (1987) J Cell Biol 105: 1579–1586
30 Holeman AM, Merry BJ (1986) Biol Rev 61: 329–368
31 Hotta H, Ito H, Matsuda K, Sato A, Tohgi H (1991) Jap J Physiol 41: 317–325
32 Huang HH, Marshal S, Meites J (1976) Biol Reprod, 14: 536–543
33 Hyde JF, Murai I, Ben-Honathan N (1987) Endocrinology 121: 1531–1539
34 Jahn GA, Machiavelli GA, Kalbermann LE, Szijan I, Alonso GE, Burdman JA (1982) J Endocrinol 94: 1–10
35 Johnson HD, Kintner LD, Kilber HH (1963) J. Geront 18: 29–36
36 Jones TH, Brown BL, Dobson RPM (1988) J. Endocrinol 116: 367–371
37 Karanth S, McCann SM (1991) Proc Natl Acad Sci USA 88: 2961–2965
38 Karin M, Castrillo JL, Theill LE (1990) Trends Genet 6: 92–96
39 Kineman RD, Faught WJ, Frawley LS (1992) Endocrinology 130: 3289–3294
40 Kochman K, Kowatch MA, Roth GS, Blackman MR (1987) Gerontologist 27: 147A
41 Koizumi A, Tsukada M, Masuda H, Kamiyama S, Walford RL (1992) Mech. Ageing Dev 64: 21–35
42 Krawczyk Z, Lyson K, Stawowy A, Pisarek H, Stepien H (1990) Neuroendocrinol 51: 632–636
43 Kubota T, Judd AM, McLeod RM (1990) J Endocrinol 125: 225–232
44 Landfield PW, Baskin RK, Pitler TA (1981) Science 214: 581–584
45 Lu KH, Hopper BR, Vargo TM, Yen SSC (1979) Biol Reprod 21: 193–203
46 Masoro EJ (1988) J Geront 43: B59–64
47 Meites J (1980) Neurobiol Aging 1: 141–143
48 Meites J, Goya R, Takahashi S (1987) Exp Geront 22: 1–15
49 Melmed S (1984) J Clin Invest 73: 1425–1433
50 Miyamoto A, Maki T, Blackman MR, Roth GS (1992) Exp Geront 27: 211–219
51 Morel G (1991) Endocrinology 129: 1497–1504
52 Morimoto N, Kawakami F, Makino S, Chihara K, Hasegawa M, Ibata Y (1988) Neuroendocrinol 47: 459–464
53 Nagy GM, Frawley LS (1990) Endocrinology 127: 2079–2084
54 Nikolics K, Masoro AJ, Szonyi E, Ramachandran J, Seeburg PH (1985) Nature 316: 511–517
55 Ooka H (1986) In "Pars Distaris of the Pituitary Gland—Structure, Function and Regulation" Ed by F Yoshimura, A Gorbman, Elsevier Science Publishers, Amsterdam, pp 29–35
56 Ooka H, Fujita S, Yoshimoto Y (1983) Mech Ageing Dev 22: 113–120
57 Ooka H, Segall PE, Timiras PS (1978) Mech Ageing Dev 7: 19–24
58 Ooka H, Shinkai T (1986) Mech Ageing Dev 33: 275–282
59 Ooka H, Shinkai T (1992) Arch Geront Geriat Suppl 3: 287–293
60 Perez RL, Machiavelli GA, Romano MI, Burdman JA (1986) J Endocrinol 108: 399–403
61 Prager D, Yamashita S, Melmed S (1988) Endocrinology 122: 2946–2952
62 Quigley K, Goya R, Nachreiner R, Meites J (1990) Exp Geront 25: 447–457
63 Reymond MJ, Donda A, Lemarchand-Beraud J (1989) Hormone Res 31: 32–38
64 Reymond MJ, Porter JC (1981) Brain Res Bull 7: 69–73
65 Riegle GD, Meites J (1976) Proc Soc Exp Biol Med 151: 507–511
66 Robberecht W, Andries M, Denef C (1992) Neuroendocrinol 56: 185–194
67 Robertson TB (1928) Aust J Exp Biol Sci 5: 69–88
68 Roth GS, Joseph JA (1988) Gerontol 34: 22–28
69 Rubin BS, Elkind-Hirsh K, Bridges RS (1985) Neurobiol Aging 6: 309–315
70 Saksena SK, Lau IF (1979) Exp Aging Res 5: 179–194
71 Sapolsky RM (1987) Trends Neurosci 10: 346–349
72 Sarkar DK, Gottschall PE, Meites J (1982) Science 218: 684–686
73 Sarkar DK, Gottschall PE, Meites J (1983) In "Neuroendocrinology of Aging" Ed by J Meites, Plenum Press, New York, pp 353–376
74 Sarkar DK, Gottschall PE, Meites J (1984) Endocrinology 115: 1269–1274

75 Sasaki F, Iwama Y (1988) Endocrinology 123: 905–912
76 Schally AV (1978) Science 202: 18–28
77 Schneider EL (1978) "The Aging Reproductive System" Raven Press, New York
78 Shaar CJ, Euker JS, Riegle GD, Meites J (1975) J Endocrinol 66: 45–51
79 Shinkai T, Ooka H, Noumura T (1991) Neurosci Lett 123: 13–16
80 Simpkins JW, Mueller GP, Huang HH, Meites J (1977) Endocrinology 100: 1672–1678
81 Snyder DL, Wostmann BS, Pollard M (1988) J Geront 43: B168–173
82 Spangelo BL, Judd AM, Isakson PC, McLeod RM (1989) Endocrinology 125: 575–577
83 Stachura ME, Tyler JM, Farmer PK (1988) Endocrinology 123: 1476–1482
84 Steger RW (1981) Neurobiol Aging 2: 119–123
85 Steger RW, De Paolo LV, Shepherd AM (1985) Neurobiol Aging 6: 113–116
86 Takahashi S (1992) Zool Sci 9: 901–924
87 Takahashi S, Kawashima S (1987) Zool Sci 4: 855–860
88 Tilemans D, Andries M, Denef C (1992) Endocrinology 130: 882–894
89 Van Putten LJA, Van Zwieten MJ, Matheij JAM, Van Kemenade JAM (1988) Mech Ageing Dev 42: 75–90
90 Van Putten LJA, Bonga SEW, Van Kemenade JAM (1988) Mech Ageing Dev 45: 253–276
91 Wexler BC (1976) In "Hypothalamus, Pituitary and Aging" Ed by AV Everitt, JA Burgess, Charles C. Thomas, Springfield, pp 333–361
92 Yokoro K, Furth J, Haran-Ghera N (1961) Cancer Res 21: 178–186
93 Yokoro K, Ito A (1981) In "Hormone Related Tumors" Ed by H Nagasawa, K Abe, Japan Scientific Society Press, Tokyo/Springer Verlag, Berlin, pp 3–21

ZOOLOGICAL SCIENCE 10: 393–410 (1993)

REVIEW

The Peculiar Case of the Giants of *Oxytricha bifaria* (Ciliata, Hypotrichida): a Paradigmatic Example of Cell Differentiation and Adaptive Strategy

Nicola Ricci and Rosalba Banchetti

Dipartimento di Scienze dell'Ambiente e del Territorio
Via A Volta, 6-56100 PISA, Italy

INTRODUCTION

In a stage of biological research such as today's, characterized by the extreme specialization of each scientist, in turn due to the need of obtaining ever new information about Life, the quantity of new reports available daily, even within a relatively "restricted" area such as protozoology is so large and evergrowing, that most of us cannot study and master much of the recent knowledge, even in the field of their own specific interest. It is our opinion that every day it becomes more and more practically urgent and culturally necessary for all of us to make all possible attempts to reconsider each of our results in a double perspective, if we want to avoid the danger of creating isolated, limitedly useful pieces of Science. On one hand, we must place them correctly in the wider context of Nature, but try to interpret them in the general light of evolutionary biology on the other. This is the rational of the present review article, in which the whole story of the giants of *Oxytricha bifaria* will be described overall and then discussed (and the relative implications examined) in its double-faced valence, namely both as an example of cell differentiation and of reversible carnivorism.

The idea of a review article about nature and biology of the giants of *Oxytricha bifaria* (Ciliata, Hypotrichida) arose when the overall picture of the process became sufficiently exhaustive and selfstanding as a consequence of a complex round of experiments recently carried out [59, 60, 65, 66, 69, 71]: it now lends itself to be rationalized in terms of a general model which, in turn, can be used fruitfully to penetrate further into the general adaptive strategies which shaped the history of life.

Protozoa are as unique and peculiar as they are precious, for approaching many of the most fundamental problems of biology with ever new investigation tools and a fresh mind. What makes them unique among the other organisms is their double sided nature: each single protozoon is indeed a perfect eukaryotic cell ("a physiological unit") and a complete organism ("a selective unit") at the same time. This character of theirs enables us to pass from the cellular to the organismic-adaptive level directly, without approximations. Protozoa, moreover, were the first eukaryotes to appear in the primeval Ocean: they are very ancient organisms, 2.2 billion years old [47]. This trait of Protozoa is a highly relevant one, once we consider that they reached first, the eukaryotic organization, exploiting then all its potentialities and realizing the widest range of variations on the theme "eukaryotic cell", adapting their morphology and physiology to match very different environmental challenges. We could say that Protozoa reach the highest peaks of complexity at the cellular level, in much the same way as metazoa do at that of the organismic level [3]. This consideration, then, should urge us to make a sort of "Copernican revolution" in Biology, leading us to recognize their primigenial nature and to use them more correctly than to date. From this point of view,

Received January 5, 1993

indeed, it was Protozoa which first found the correct solutions of most general adaptive problems (regulation of differentiative processes, exchange of information through cellular interactions, cell locomotion as behaviour capable of reaching optimal conditions of environmental factors), so that we should learn to study and to understand them according to the characters of their own biology, instead of continuing to consider them as just "simple metazoa" or even as sort of "simple" free-living lymphocytes, neurons, etc. This thought will prove to be quite a relevant one in section III, when the cell differentiation aspects of the process object of this article will be discussed.

In our opinion Protozoa are among the best biological material for a wide interdisciplinary investigation enabling us to collect information which can be compared and integrated directly and immediately. The clearest tendency illustrating this theory of ours is the eco-ethological approach recently proposed for protozoa by Ricci [57]: he tends to link the study of their behaviour [54], with that of their ecology [16] in an attempt to comprehend their general adaptive philosophy. The first line of research has its roots in the studies of cell locomotion [33, 34], but draws new strength and perspectives when the electrophysiological studies [40, 41] are brought in [56]. The second half of this study, namely the ecological one was suggested by Fenchel in his masterpiece [16], and it led to a new understanding of the importance of the protozoa's microbial loop in aquatic environments, of their totally antiintuitive world [53, 62, 63, 64], of their usefulness in monitoring the environmental conditions [7, 17, 55].

This example shows how powerfully these rather disregarded organisms can be investigated by means of widely different technical approaches to achieve very useful results in widely different fields of Biology: what we would like to do in the present paper is to describe the complete picture of the morpho-functional steps leading a normal *Oxytricha bifaria* to differentiate into a gigantic organism, to discuss then this story in the more general context of "cell differentiation" problematics, on one hand, and in that of the different secondary consumer adaptive strategies, on the other.

I The giant of O. bifaria: a multi-step adaptation

The data henceforth described as a single body of information, were published in six papers [59, 60, 65, 66, 69, 71] as the results of partial rounds of experiments carried out from 1982 to 1990, in which all the technical and methodological details can be found concerning both the culturing of *O. bifaria* and the various experimental approaches. The steps in the story of the giant in *O. bifaria* will be discussed in series, putting together all the available information, each indicated by one of the above numbers, to facilitate bibliographic consultation.

O. bifaria is a freshwater hypotrich ciliate [8], with a typical ellipsoidal body ($\sim 110 \times 60\ \mu m$) differentiated into a convex dorsal surface and into a more or less planar ventral one, where all the composed ciliary organelles are placed: they can be distinguished into (a) somatic locomotory organelles (namely the fronto-ventral, transverse and marginal cirri) and (b) peristomial organelles (namely the anterior-left Adoral Zone Membranelles, AZM, and the mid-ventral Undulating Membranelles (UM) (Fig. 1). The nuclear apparatus is formed by one macronucleus divided into two pieces and by two micronuclei, each close to either macronuclear envelope. *O. bifaria* lives in freshwater canals, springs, creeks, rivers, ponds, lakes, typically feeding on bacteria: its cell cycle [12, 58] usually lasts about 7–8 hr at about 20°C. As to its life cycle it is characterized by quite a long immaturity period (~180 binary fissions, Ricci & Cetera, unpublished results), following a sexual phenomenon (conjugation), by a maturity period (which lasts no longer than 2–3 years, under laboratory conditions, Ricci & Banchetti, unpublished results) and by a rather short senescence, (progressive loss of the mating competence) unfailingly leading to the death of the clone. The general description of *O. bifaria's* biology cannot be considered complete, without taking into account the nature of its habitat; in the natural environment where we find this species, indeed, we measured very different conditions at different times as to temperature (−2°C to 36°C), to pH (5.7–7.5) and dissolved oxygen (3.5 mg solved oxygen/ml), not to speak of the water itself,

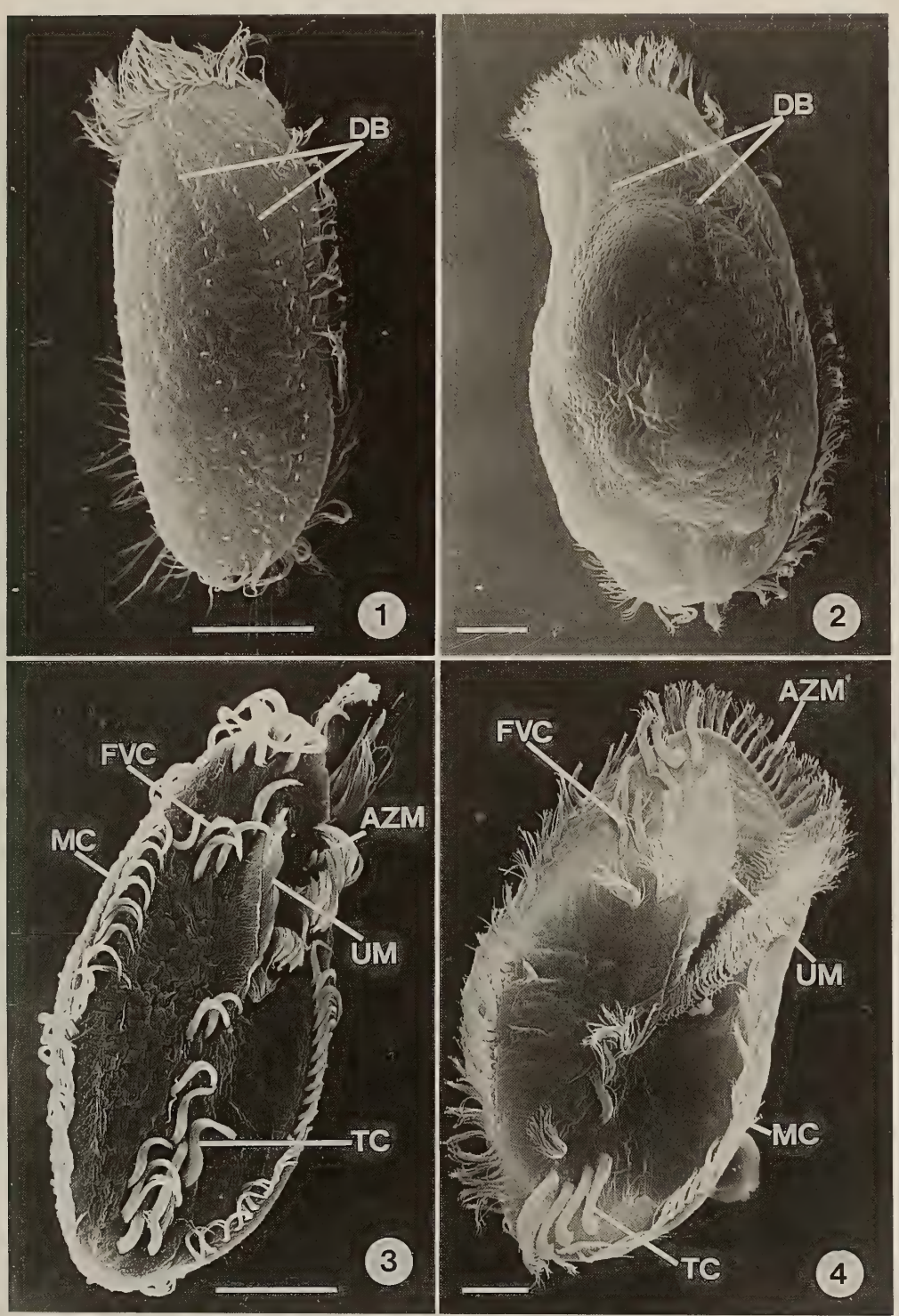

FIG. 1. The normal *Oxytricha bifaria*, in dorsal (1) and ventral (3) views; the giant of the same species, in dorsal (2) and ventral (4) views. AZM: Adoral Zone Membranelles; UM: Undulating Membranelles; MC: Marginal Cirri; FVC: Fronto-Ventral Cirri; TC: Transverse Cirri; DB: dorsal bristles. The bar represents 50 μm.

which, quite frequently in the summer, can disappear completely (Ricci & Banchetti, unpublished results). We could say that the environment of *O. bifaria* (that of inland, often impermanent waters) is characterized by the widest (and wildest) variations of the physical, chemical and biological parameters describing it: in agreement with such an extreme environmental variability, the species we have been studying since 1972, shows a similarly extreme adaptability, being capable of changing dramatically both its shape and its physiology as it is required to withstand the challenges periodically met in such an environment. Although more than 95% of its life span is spent in the normal morpho-physiological state, three other states are possible and actually found in our samples collected in nature in different periods of the year (Fig. 2).

The conjugating pair is a peculiar morpho-functional state formed by two oxytrichas united side by side, which carry on their sexual processes,

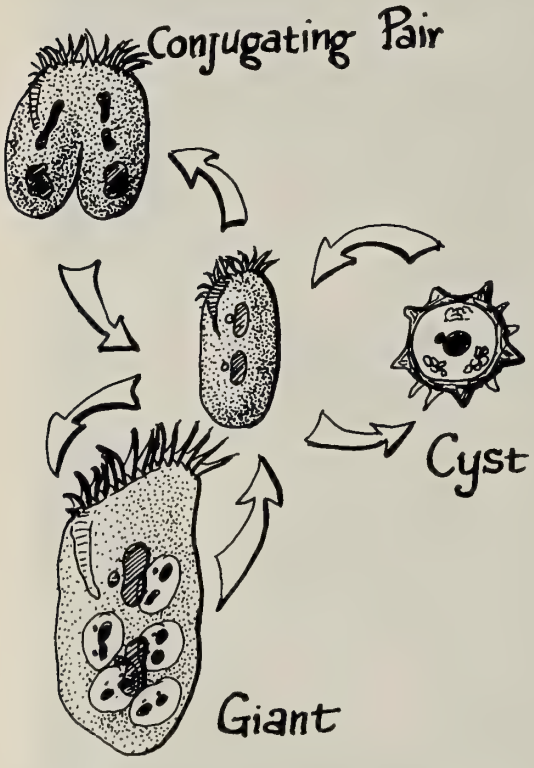

Fig. 2. *O. bifaria* spends ~95% of its lifetime as normal organisms, capable of differentiating conjugating pairs, cysts and giants, according to the internal/external conditions of the system.

through a complex cascade reaction: (a) two-step cell interactions leading to (b) cell membrane fusion, (c) trigger of micronuclear meiosis, actual (d) meiotic divisions of micronuclei, (e) exchange of pronuclei (=cross fertilization), (f) separation of the partners [52]. Such a complex sexual process mediates the rejuvenation of the population: it can be adaptively interpreted as the periodical solution (triggered by proper environmental conditions) found by the species to the problem of overcoming its main biological bottleneck, namely the absolute need of producing genetic recombinants and of fighting progressive ageing.

Cysts represent the second possibility *O. bifaria* evolved to match the challenges periodically met in its widely changing environment: they represent a sort of life-boat for the species when severe, prolonged environmental stresses (drought in summer, for instance) affect natural populations. The dramatic morpho-physiological changes a cell undergoes to produce the sophisticated structure that a cyst is, were studied mainly from ultrastructural [75], cytochemical [68] and adaptive *s.l.* points of view [67].

On the basis of the above integrated results concerning the nature and story of both pairs and cysts, a thorough, specific giant formation was then undertaken.

A Normal populations

This is the phase preceding the onset of any specific induction of the phenomenon "giant-formation".

O. bifaria is a species whose natural populations can produce gigantic organisms: only 1–2% of the strains collected in nature, however, show such a capability. A certain strain, which proves to be capable of differentiating giants, under proper conditions, tends to maintain such a trait steadily in time.

Many strains have been collected and stocked in Lab cultures and each clone has its own giant producing potentiality, which can be measured by two parameters: (i) number of giants produced and (ii) time lag before the appearance of the first giant. According to these two traits, the clones we used in the last 8 years can be ordered as it follows:

C9>S9>S6, C9 being the strain producing the largest number of giants in the shortest time. No exhaustive theory has been proposed so far to account for the nature of the character "giant formation": no clear-cut genetic inheritance of this trait has yet demonstrated, for any clone, isolated and cultured in our Lab. Only very few cells can produce giants *ex-novo* even in the richest population of *O. bifaria* belonging to a giant-producing strain: these few cells have such a capability only for a relatively short time, being then substituted by other individuals, in turn only temporarily predisposed for such an adaptive task (Ricci and Pelamatti, unpublished results). It has been found, indeed, that although hundreds of giants can be observed in the experimental populations, by far the largest part of their number is produced through binary fission of preexisting giants, while only very few (2–3 per day) are differentiated *ex-novo* from normal individuals, even in cultures as dense as 1600 cells/ml. While the problem of the nature of this labile predisposition to produce giants seems today far from being accounted for, both at clonal and at individual level, it might be simpler to answer to the question "why can so few, and so frequently changing oxytrichas differentiate a giant?" In our opinion, a certain degree of loss of fitness *s.l.* is to be expected for the "ready-to-differentiate" organisms, while a clear advantage is evident for the gigantic forms. If this is true, the labile determination of only few oxytrichas to differentiate giants might be considered as the best solution to limit the reduction of fitness within the population (due to the acquisition of such a potential state which only very rarely actually leads to the advantageous giantic form) without missing the adaptive convenience brought to the population by the occurrence of such a differentiated gigantic state. The temporal lability of the determination to produce giants could have been acquired to avoid the risks of a progressive reduction of genetic variability in time, if only a few cells (and only they) should be destined to become giants: all the possible genomic combinations of a certain genetic pool, indeed, have the same, although small, probability of undergoing the gigantic adventure.

This general hypothesis seems to us supported and strengthened by the finding that, as the individuals of a certain population are periodically determined to undergo gigantic differentiation, there is no convenience for any population to have a large number of organisms predisposed to cell differentiation: the need of producing a large population of giants, whenever a proper rich *pabulum* should exist, is matched by the cell-binary-fission-mechanism, a fairly convenient and fast asexual reproductive process.

Terminological foreward: (i) the time lag between the onset of the conditions suitable for the formation of giants and the actual formation of the first giant has been defined "induction period" and indicated "Δt FG"; (ii) the induction period is formed by an "activation period", followed by the successive "predation", namely the actual feeding of activated cells on the potential preys: (iii) within the activation, two successive periods have been distinguished: the "Early-Activation Window" (= EAW, roughly corresponding to the first third of Δt FG) and the "Late-Activation Window" (= LAW, occurring during the second third of the Δt FG): the last third of the Δt FG corresponds to predation. All these concepts are illustrated in Fig. 3.

B The Early Activation Window (EAW)

Giants of *O. bifaria* form whenever favourable conditions are created [1], namely whenever an overcrowded population is obtained. Different strains have different thresholds for the occurrence of the phenomenon. "Threshold" can be defined as the lowest cell density capable of producing a First Giant in that strain within 12 hr from the onset of the overcrowding conditions: as an example #C9 had a threshold of 340 cells/ml, while #S9 and #S6 had thresholds of 390 and 500 cells/ml, respectively (Ricci & Cifarelli, unpublished results).

Starvation, on the contrary, has been shown to play only a minor, disturbing role in giant formation. A clearcut, statistically significant, positive linear correlation has been found to occur between the cell density of an overthreshold population and the number of giants formed in time: only beyond extreme values of cell densities (>40,000 cells/ml for #C9) this tendency shows a clear reversal, very likely due to the strong disturbance of the

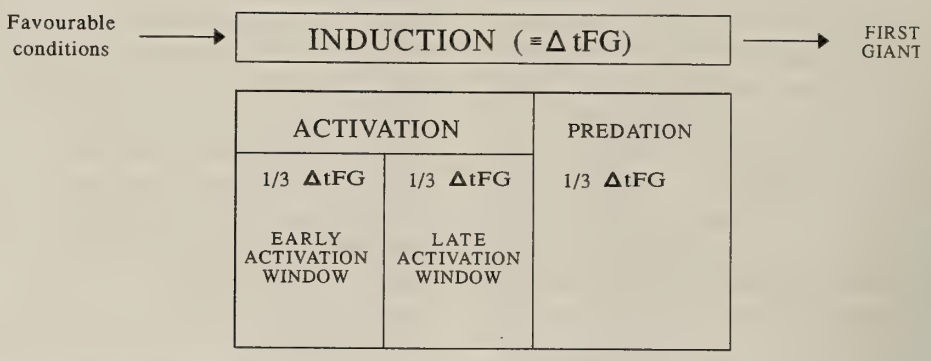

Fig. 3. The temporal succession and the various relative correspondances of the phases of the process leading on *O. bifaria* from its normal state to the production of the first giant.

locomotory behaviour of the potential giants, in turn induced by the continuous, unavoidable cell-against-cell bumps [66].

It has been found also that there is a clear, significant, negative, linear correlation between the number of cells/ml and the Induction Period (Δt FG): optimizing the number of cells/ml, their biological state and growing conditions, it has been found that a minimum, non reducible, Δt FG exists and that it lasts approximately 45 min [65]: thus, we can say that the higher the cell density of the overthreshold population, the shorter the induction period, the larger the total number of the giants produced.

The biological phenomenon controlling the beginning of the story of the differentiation of giants in *O. bifaria* (and guiding its development later on) is a really interesting contact-dependent cellular interaction, demonstrated by using Con-A as a specific inhibitor of the process [59]: no soluble factor plays any role, as shown by the lack of the slightest effects of both the Cell Free Fluid of giant-producing populations and the perfusion microchamber experiments, using top quality cultures [59]. The adaptive reasons of this choice (the choice of using short range signals to trigger the differentiation of giants rather than long range soluble factors, as happens for the conjugation of the same *O. bifaria,* [52]) seems to us to reside in the nature itself of the giants of *O. bifaria,* which are true, opportunistic, all-devouring carnivores, rather than cannibals: direct contact seems to us more effective than soluble factors in informing a potential giant about the number of the preys living in the water volume surrounding it, namely about the possible convenience of differentiating into an actual giant.

Several things must be said to characterize the kind of cell contacts required by this differentiation. First of all they must occur between normally behaving cells: neither frozen-thawed nor mildly $K_2Cr_2O_7$ fixed ciliates ever induce any kind of activation [65]: according to these results we can expect a mechanism very likely relying on a certain activation energy which enables *O. bifaria* to distinguish living (=food) from inert (=no food) objects and, therefore, to avoid senseless, quite expensive differentiations of giants [65]. Thus, it seems to us more appropriate to speak of active contacts, or bumps, which must occur among different cells, to trigger the process, rather than of simple, cellular contacts. By the way, quite a similar recognition mechanism seems to occur also in the story of *Litonotus,* a specific, a very efficient predator feeding on *Euplotes* (Ricci & Verni in prep.).

A second trait characterizes the bumps activating induction: they are not species-specific bumps. It has been demonstrated that many different species of ciliated protozoa can bump fruitfully against an oxytricha, activating it to differentiate into a giant, provided that it has such a potentiality. In our experiments *Paramecium aurelia* perfectly succeeded in activating *O. bifaria,* the only difference being that the threshold for giant formation induction was a little higher than with conspecific individuals: ~1,000 paramecia/ml are required to trigger the process, while only 340

oxytrichas/ml are sufficient for the same effect [59]. The adaptive meaning of the giant of *O. bifaria* is clearly demonstrated by such a finding: we cannot speak of cannibals [66] any more, while we have to look at this heteromorphic state as a true carnivorous gigantic form [59]. The basic nature of the giant of *O. bifaria* is well described by several elements characterizing the differentiation: (a) the choice of direct interactions: (b) their non species-specificity; (c) the prompt answer (Δt FG $\sim 40'$) induced by favourable conditions. This way of understanding the biological significance of the giants of *O. bifaria* is of the highest relevance to interpret the giant itself properly in the context of this species' adaptive biology: not any more a form by which the species escapes environmental stress conditions feeding the few at the expenses of the many conspecific organisms, but a form through which it opportunistically shifts from its normal diet (bacteria) to a new, temporarily richer *pabulum* (other ciliates). In so doing, *O. bifaria* changes its trophic niche, shifting from its normal one (primary consumer) to a new one, that of a secondary consumer. The general interpretation is very likely to be found in the attempt of this bacterivorous species to prolong opportunistically its existence in a certain spatial spot growing at first at the expenses of bacteria ("minimum", ever present food), and later feeding on the ciliated population supported by the bacteria themselves: by producing the giants, *O. bifaria* reaches at least four very convenient goals: (a) it reduces the intraspecific competition for bacterial food; (b) it reproduces at the expenses of different species; (c) by predating the bacterivorous species it reduces the interspecific competition for bacterial food; (d) it survives in the first favourable micropatch for a longer period, the peak of primary consumers being reached later than that of bacteria [16].

One surprising thing must be added with regard to the nature of the bumps triggering the giant formation: they can occur even with organisms not lending themselves as preys [65]! *Blepharisma japonicum* ($\sim 300\ \mu$m long) induces giants in *O. bifaria* populations, whose cells are activated, although having no possibility of predating those large organisms! This kind of experiment is the only one so far enabling us to separate the inducing stimuli (cell-cell bumps) from the presence of preys: this possibility is a truly important one for further investigations about the nature of the molecular aspects of this part of the story. The finding that organisms not suitable as preys induce the giant formation demonstrated that "activation" truly exists as a biological step in the process leading to giant formation. The occurrence of these peculiar bumps in the first third of the Δt FG is a prerequisite for the process to continue [60]: thus, the objective existence of an Early Activation Window (=namely a short period during which, and only during which, something conditioning the occurrence itself of the whole process has to happen!) has been shown clearly by simple, successive dilutions of experimental populations. The conclusion to draw is therefore that, if proper bumps occur at the right moment, they cannot but trigger the physiological steps of the next phase, the Late Activation Window [60].

Before concluding this chapter about the nature of the phenomena leading to giant formation in *O. bifaria,* the so called "Labile Memory Counter" (LMC) working hypothesis [65] must be briefly described and discussed: the LMC is supposed to be a cellular device somehow capable of counting the cell bumps activating the cortical keys, of recording them for a while (labile memory) and of adding the new contacts to the total: when the sum reaches a certain threshold value (within a certain period of time?) the initial processes of activation period are triggered. Although nothing can be proposed about the basic nature of the LMC, it accounts for several of the observations so far made about the giant differentiation story: the different, strain specific "thresholds" for instance, may be explained in terms of (a) different strain specific number of cortical activating keys, (b) different strain specific number of bumps necessary for the activation, (c) different forgetting velocities, (d) different key activation energy.

C The Late Activation Window (LAW)

The second half of the Activation (roughly corresponding to the second third of the induction period) has been found to be characterized by the occurrence of a specific protein synthesis triggered by the LMC when the threshold is reached. While

the use of Act-D had demonstrated the relevance of the role played by some protein synthesis, specific low dosage-short term pulses of cycloheximide demonstrated the temporal occurrence of that synthesis [60]. It was also found that higher dosages of Chx induce longer Δt FG and smaller number of giants formed: this seems to indicate that the Chx action is a fairly specific one, inducing just quantitative, absolutely physiological effects. It will be of great interest to ascertain the nature of the specific protein synthesized during the LAW, also in attempting to understand the nature of its action, which, in turn, very likely represents the basic meaning of LAW.

D Predation

Both the EAW and the LAW proved to be necessary, but not sufficient steps for the differentiation of giants of *O. bifaria*: the actual engulfment of several/many preys is necessary (as shown by the induction by *Blepharisma* [65] to make the potentialities triggered by the activation real, namely to change the gross cell morphology, thus producing the First Giant. Activated, morphologically normal oxytrichas feed successfully on casually encountered preys because of their peculiar behaviour. Although specific ethological studies of the problem are not yet available (being in progress in our Lab at the present moment): however, we can say that in a creeping oxytricha activation induces periodical, violent, forward jerks, which enable it to engulf any suitable (=of the right size) prey (Ricci & Riggio, unpublished results). Although only very few things can be said about this step in the induction of giants of *O. bifaria,* a sort of working hypothesis can be proposed, to orientate our future research: does activation affect the bioelectrical state of the temporarily predisposed cells? What is the role played by the specific protein(s) synthetized during the LAW in this change of the electrical properties of the membrane? Answers to these two guide-questions will help us in further penetrating the nature of the biological processes constituting that complex phenomenon called induction period.

E The First Giant (FG)

The end of the induction period is represented by the appearance of the First Giant, namely of that organism easily and unfailingly distinguishable from the other cells for its clearly altered morphology: it must be noted that it is exactly the same as that of the Steady State Giants that will appear later on in the population. The most typical traits of the FG are the strikingly irregular morphology, which is due to the large number of preys engulfed within roundish food vacuoles, together with darker cytoplasm, larger dimensions of the body and of macronuclear pieces as well. Only very recently has it been possible to measure both micro- and macronucleus DNA content. As far as these two very important parameters are concerned the FG definitely presents no significant difference at all from normal cells. This finding cannot but suggest that the first morphological alterations of the giants are induced by the relatively extraordinary diet, the true, nuclear regulation of the process occurring only later.

We must recall here that only a very small percentage (1–2%) of *O. bifaria* can differentiate directly into FG, while most of the giants of a population (>98%) are produced by transverse binary fissions of preexisting giants [59]. An important, still unsolved problem related to the formation of the FG is represented by its widened peristomial area, namely that lying between the AZM and the UM ($\sim 30^\circ$ in width vs the 15° in normal organisms [66]): is it a feature of the temporarily determined cells? Is it acquired during activation? Is it the consequence of the many successive predatory events?

F The binary fission of the FG

When the FG recovers from the phase of dramatic cellular changes undergone to begin its own existence, a binary fission occurs, which gives rise to the first generation of Steady State Giants (SSG): during this division the macro- and micronuclear DNA content increases heavily, reaching the quantitative strain-specific values characterizing the SSG. The reason why this value for the macronucleus is ~ 3.7 times the normal value in #C9 [69], and of ~ 1.9–2.1 times the normal value in #S9 [6], is still to be ascertained, as well as the origin of the extra-DNA itself: is it synthesized ex novo, or does it come from a recycling of that of

the preys?

As to the micronucleus, both #C9 and S9 SSG show the same DNA content, about 1.9 times the normal quantity. The reasons why in different strains different increases of DNA content occur in the macronuclei and not in the micronuclei are not yet understood. The most relevant result, however, is the finding itself; it is a well established topic among ciliatologists that the micronucleus is a sort of unchangeable, diploid genetic memory in each species. That of the *O. bifaria* giant is therefore quite a rare exception to the general rule, and it cannot but deserve to be investigated further, for instance from a cytological point of view: could any chromosomal alteration be detected in comparison with what is described for normal cells [32]?

G The Steady State Giant (SSG)

SSG are those giants regularly undergoing a series of cell cycles, thus reproducing regularly through apparently regular binary fissions: their cell cycle is about twice as long as the normal one. The general kinetics of their growth is described by a logistic curve, where the log period is represented by the *ex novo* dedifferentiation of the few First Giants, the log period is the expression of their intensive binary fissions, while the plateau is reached when the available preys become rarer and scattered through progressively wider spaces [66].

To describe such an interesting heteromorphic form thoroughly, the general morphology has been studied at the cytological [66] and ultrastructural levels [67]. The general shape of a normal *O. bifaria* (the upper half of a rotation ellipsoid) becomes more irregular in the SSG, due to the widening of the peristomial funnel at the anterior end of the giant (already mentioned in the paragraph about the First Giant) and to the preferential accumulation of the food vacuoles in the posterior two thirds of the body, which assumes roughly the shape of half a pear. While all the particulars are described elsewhere [67], three major results deserve particular attention: (i) the normal 8 frontoventral cirri become 10–12 in SSG; (ii) the paraoral external (of the Undulating Membranelles) from a double ciliary array passes to a triple or multiple ciliary array; (iii) the AZM strikingly increase the number of membranelles, exactly doubling the number of cilia per single membranelle: 3, 16, 22, 22 in normal cells, 3, 32, 44, 44 in a SSG.

These alterations well describe the change of the trophic niche of *O. bifaria*'s SSG, an organism which in fact needs wider peristomial and stronger "predating" organelles, being specialized in feeding on large, sturdy preys. The digestive system of a SSG, generally studied in [66], proved to be particularly interesting, being formed by many vacuoles, each containing either one single prey or a large amount of bacteria, the two foods being never mixed together within the same, single vacuole [67]; it seems likely, that in this way, different enzymatic batteries can be activated around different vacuoles, thus making the two digestive strategies more effective.

The last and perhaps the most important cytological trait of an SSG is its already mentioned higher degree of micro- and macro-nuclear DNA content [60, 69], a biological trait actually characterizing the differentiating process.

Moreover the SSG proved to depend upon continuous active cellular contacts (=bumps) to maintain its differentiated state. The bumps must occur continuously between cortically normal cells: Con-A used separately either on SSG or on preys can interrupt this flux of information about the presence of preys, thus removing the continuous trigger maintaining the gigantic state or, in other words, initiating the process of dedifferentiation. Experimentally to interrupt the normal reproduction cycle of the SSG, it is sufficient also to isolate the giants in cell-free media: this clearly imitates the natural conditions at the end of a ciliate bloom in a certain volume. This shows that the maintenance of the gigantic state is continuously controlled opportunistically by a sort of feedback, capable of promptly revealing the progressive exhaustion of the specific *pabulum* (other ciliates): as soon as this situation occurs, the processes leading a SSG back to the normal state of the species are triggered.

To conclude about the nature of the SSG, we can well state that it represents a reversibly differentiated phase, specifically acquired by the spe-

cies, to exploit a new, predatory niche: specific traits facilitating such a role are developed by this primarily bacterivorous species: (a) wider peristomial funnel, (b) stronger ciliary organelles, and (c) non-oriented (=blindly casual) prey detecting system.

H The Dedifferentiation

In absence of a sufficient number of bumps, a SSG undergoes 4 binary fissions which specifically lead it back to its normal morpho-physiological state. Body size, nuclear size and DNA content have been measured during this process, and found to decrease progressively; in particular, the size and the DNA content of macronuclear apparatus pass from 220 μm and 371 arbitrary units (AU), respectively, to 200 μm and 380 AU after the 1st division, to 160 μm and 257 AU after the 2nd, to 100 μm and 177 AU after the 3rd division, to 102 μm and 108 AU after the 4th: being $\sim$100, the control values of macronuclear size and DNA content, it becomes evident that, while the normal size is acquired after 3 cell divisions, the normal DNA content is established again only after the 4th division. Bacterized medium, autoclaved lettuce medium and SMB (Synthetic Medium for *Blepharisma,* [44]) were used as dedifferentiating conditions: it was found that dedifferentiation occurs according to different kinetics, that in bacterized medium being capable of inducing the fastest dedifferentiation, the second being the autoclaved lettuce medium, the third the SMB [60]. Overall these results seems to indicate that this process clearly depends upon some energetical energy input, but more precise experiments are required before drawing conclusions from this story. We are at present carrying out a series of experimental sessions to draw the ethogram of these ex-giants, to test the general hypothesis [16] about the meaning of the newly "normal" individuals as a sort of exploration shuttles (cf. the *Tetrahymena*'s swarmers), by which the species, after such a differentiation, quickly and efficiently spreads through the environment to find out new possible favourable conditions, where new populations can settle and grow.

II The Protozoa and the "invention" of cell differentiation

First of all, we must recall the mental "Copernican revolution" invoked in the Introduction section: we must keep it clearly in mind that protozoa were the first eukaryotic living entities to colonize the primeval ocean for hundreds of millions of years before the pluricellular organization was reached: "All the pluricellular eukaryotes evolved from unicells, in which the fundamental traits of development appeared" [22]. Such a statement must guide our culture in approaching many biological problems correctly: with regard to "cell differentiation" we must recall that, though representing a typical aspect of the biology of metazoa from a cultural point of view, it is actually one of the brightest "inventions" of protozoa, which used it to face several, dramatic survival problems. The definition itself of development has "developed" over recent years, passing from "the growth from one embrional stage to the next" (typically given for metazoa) to "the progress of an organism through its life cycle", a general concept perfectly fitting the case of protozoa and of *Oxytricha,* as well, once we consider its life cycle as represented in Fig. 2.

If we proceed in this attempt to establish terminological parallelisms, which in turn underly substantial similarities between protozoa and metazoa, we can consider now the main, three classical steps characterizing the development of a multicellular organism: (i) cell differentiation, i.e. the process leading from one single stem cell to many different types; (ii) pattern formation (the process leading the different types of different cells to congregate in a certain, well defined organ); (iii) morphogenesis, i.e. the mechanical process underlying organism shaping and tissue generation. According to the most commonly given definition of cell differentiation ("cells with one single genotype give rise to definitely different phenotypes"), there can be very little to debate, about the fact that the production of cysts and giants by *O. bifaria* actually are cell differentiations: strikingly different morphological and physiological states are generated, not through any casual abortive process (as has been suggested for the doub-

lets of *O. bifaria*, [2]), but rather through genetically encoded clearcut cytoplasmic reorganization(s) and specific protein synthesis.

This parallel holds further, if we consider that in the cell differentiation of the metazoan developmental processes two basic strategies have been described [28]: (a) long-range interactions mediated by soluble inductors (messages) such as those involved in the metamorphosis of Amphibians [37] and Insects [23, 26]; (b) short-range interactions (cell-cell contacts), as those described by Jacobson [32] and Muthukkaruppan [45], for mouse lens development, Grobstein [27] for mouse metanephros development, Slavkin & Bringas [74] for odontogenesis, Cutler & Chaudhry [10] for rat submandibular gland development, Lehtonen *et al.* [38] for kidney tubules formation. Quite similar is the case of cell interactions described for protozoa, whose differentiative biology is controlled by soluble factors (*Blepharisma*'s preconjugation,

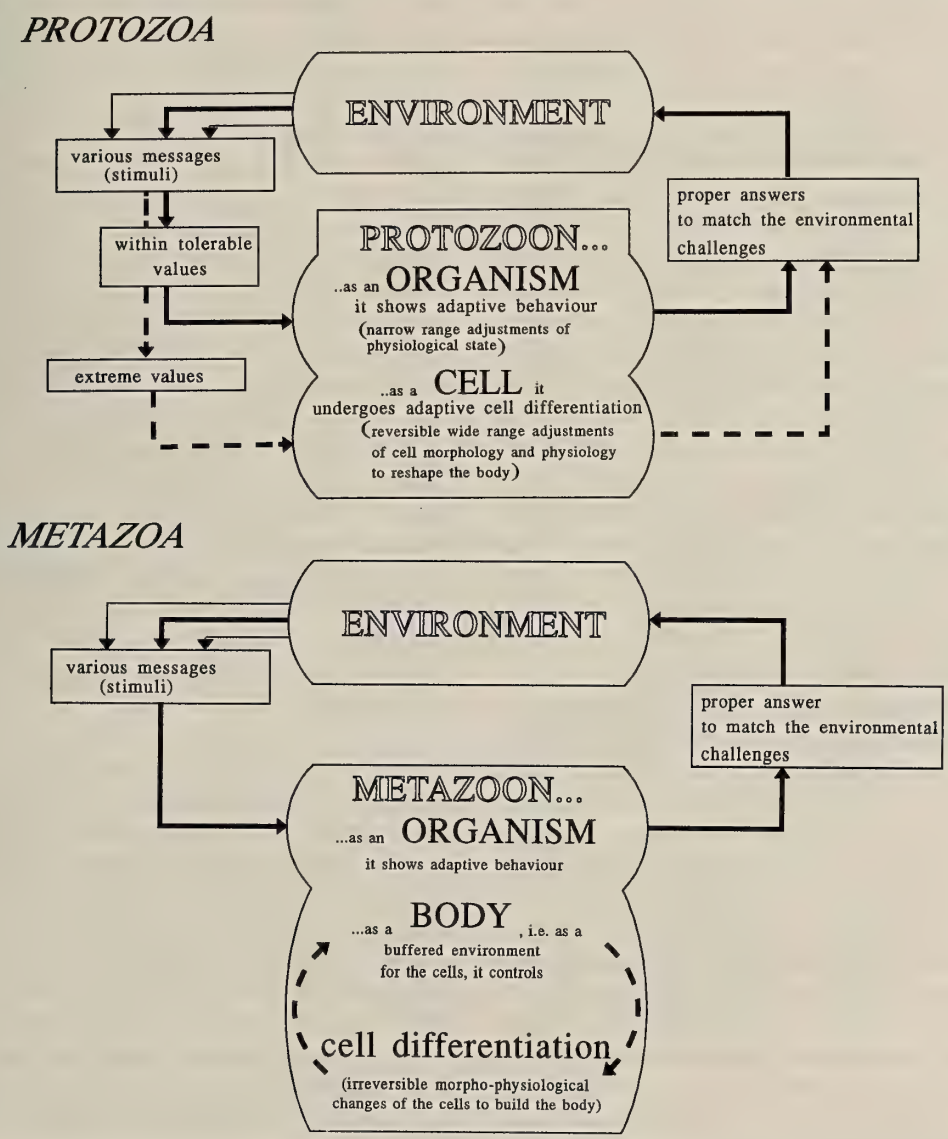

FIG. 4. The parallelisms and the differences occurring between cell differentiation in Protozoa and Metazoa.

Miyake [44], *Volvox carteri*'s, Kochert [36] and *Dictyostelium discoideum*'s development, O'Day & Lewis [49]) or by direct cell-cell contacts (*Chlamydomonas,* Goodenough [24], *Paramecium*'s, Hiwatashi [31]).

Among the other models, *O. bifaria*'s preconjugative story is particularly interesting, inasmuch as the potential partners rely on a peculiar two step interaction process [52]: *O. bifaria* indeed releases the mating type specific soluble factors (gamones) to mediate the first-step cellular interactions between potential partners occurring from a distance [15], while it uses a cell-bound-gamone strategy to guide the partners along the last, critical steps of the interactions leading to membrane fusion, meiosis, pronuclear exchanges etc. [61]: the species, in other words, is capable of using both these different strategies! Why does it use only cell contacts to trigger and to control the differentiation of giants? The opportunistic, highly convenient species-non-specificity of preys discussed above seems to us the evolutionary clue, possibly accounting for such an interactive strategy.

Coming back to the basic problem (can we speak of cell differentiation in the protozoan world?), the classic examples of *Acetabularia* [29, 35, 84] and of *Naegleria* [18] should cancel any doubt. On the other hand most of the efforts spent to convince zoologists working in the field of development that our attempt to make a terminological extrapolation actually represented quite a convenient (and perfectly correct) cultural jump, often came up against two major obstacles.

The first one was that the developmentalists have always said that "Cell differentiation is an irreversible phenomenon among metazoa": in our opinion on the contrary the primigenial cell differentiation on the contrary was a reversible phenomenon (like that found in protozoa), while irreversibility was added only later when multicellularity was reached. There would be no advantage for a protozoon in being capable of skipping environmental stresses by encysting, if it could not resume normal morphology and physiology on the return of favourable conditions. It is obviously true, moreover, that a concept like "irreversibility of the cell differentiation" could not be imagined except for a metazoon, which is a multicellular organism capable of spending even millions of cells for just one function (electrical conducibility, contractility, distribution, *etc.*), not needing at all any dedifferentiation! This point of view seems well supported by the finding that whenever such a cellular "expendibility" is obtained by protozoa too, the same irreversibility is also realized: the case of *Volvox* seems paradigmatic!

The second objection to our efforts to establish strong parallelisms between protozoan and metazoan cell differentiation was somehow less critical, on the one hand, and yet more complicated to answer, on the other: the trigger and the control system of cell differentiation is "internal" in Metazoa, but "external" in Protozoa! If we consider the scheme in Fig. 4, the meaning of this observation is perfectly evident: in the case of protozoa, the environment modulates the behaviour of an organism to induce the proper adaptive answers to the environmental changes under normal conditions, while it stimulates cell differentiation under extreme conditions, as a sort of deep morpho-physiological adjustment of the entire body to the environmental challenges. In the case of metazoa, on the contrary, the same environment, although acting clearly on the organism at the level of its adaptive behaviour, does not exert any direct effect on the cell differentiation itself, which relies upon specific messages released by another very peculiar and buffered "environment", namely the whole body, which ends up by playing the role of a sort of fairly complex interface between the cells and the external environment.

Before concluding this part of the discussion, we should like to recall also "pattern formation" and "morphogenesis", the other two stages of development after cell differentiation: if one considers the complex life cycle of *V. carteri* [36] and the sophisticated one of *D. discoideum* [49], it seems to us that also as far as these two stages of development are concerned, protozoa show quite complex behaviour and unexpected capabilities. Therefore it seems to us perfectly appropriate and justified to use the biological concepts (not only the terminology) of cell differentiation *etc.* also when speaking of protozoa.

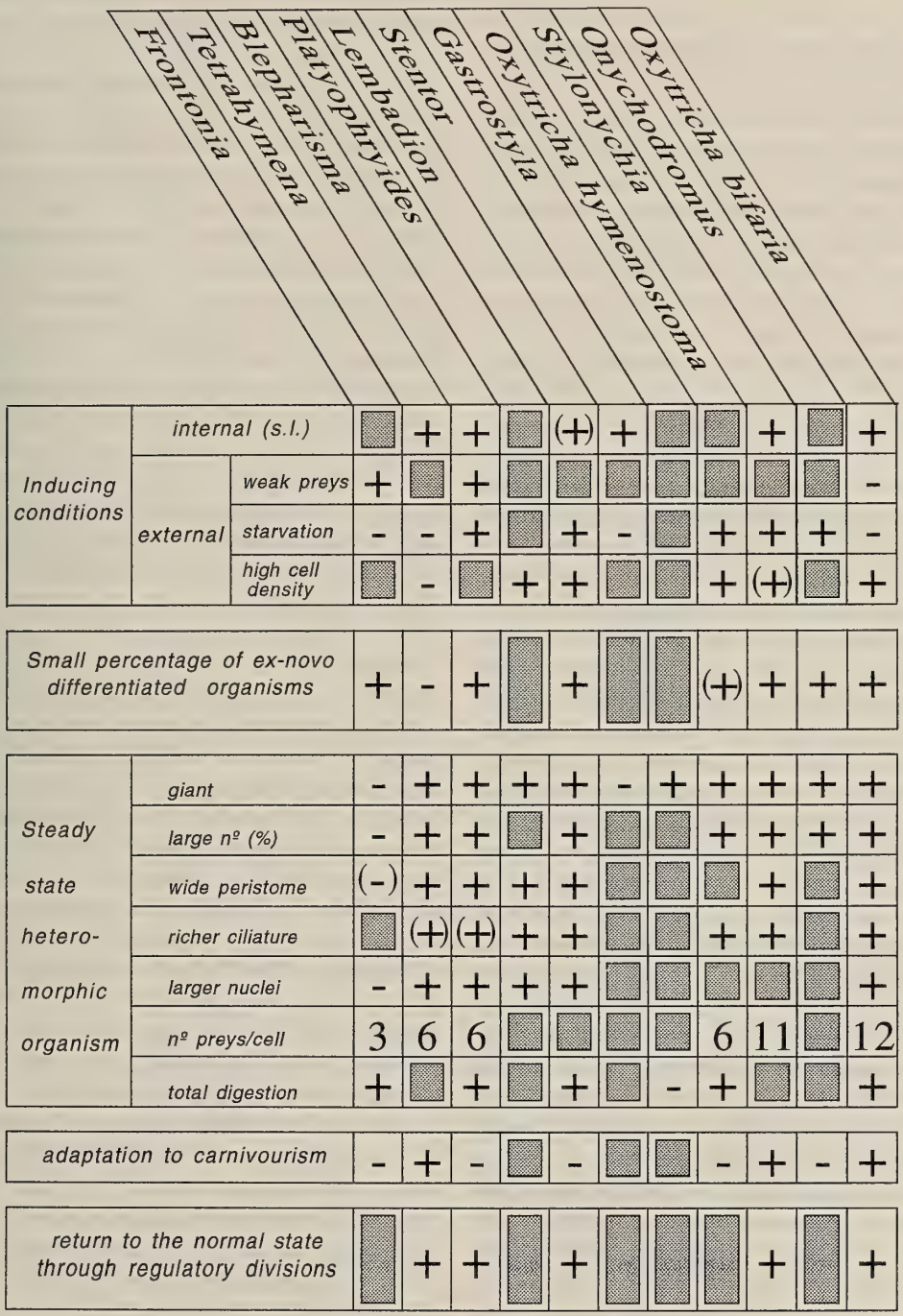

FIG. 5. A comparative, synoptic scheme of what reported in bibliography about the reversible cannibalism-gigantism-carnivourism in ciliates; ▒ = information ignored by the authors; (+) = reported by the authors as a minor observation; + = yes!; − = no!

III The Protozoa and the "invention" of the "consumers": new ways of exploiting environmental resources.

There can be no doubt that modern protozoa represent the descendants of the first eukaryotes: they appeared in a primeval ocean completely colonized by prokaryotes, which represented a potentially limitless *pabulum,* for any organism capable of feeding on them [25]. This concept introduces to us the idea that the first protozoa found themselves literally "embedded" in a "full-food" substrate: the primary consumers, seen as new exploiters of the environmental resources, appeared therefore quite early in the evolutionary hystory of protozoa, which, due to both their "superior", eukaryotic design and the endless food source (prokaryotes), underwent a tremendous adaptive radiation, concerning them so deeply and dramatically, that the widest morpho-physiological variations on the theme "eukaryotic cell" were realized. Of all the new adaptive solutions one in particular is to be considered in the context of our present paper, namely the conquest of the trophic niche of the secondary consumer, as a consequence of that evergrowing, as yet ungrazed *pabulum* represented by the protozoa themselves. This second step made by the primitive eukaryotic unicells in the recent world of the consumers represented quite an important achievement, because it completed the first food chain ever: deep and extensive studies of the classic examples of protozoan predation [1, 13, 43, 77] might guide us to a more correct comprehension of the phenomenon "carnivorism" in its general lines, in its essential, basic traits. The study of *Litonotus lamella* which predates specifically *Euplotes crassus* [68] led us to show that, although very simple and primitive, this organism had already realized an almost perfect carnivore: *Litonotus,* indeed, has specific systems to recognize and locate its prey (Ricci & Verni, in prep.), to kill it [73], to ingest and to digest it [74]; with respect to the more renowned wolves or lions, *Litonotus* lacks only the social dimension of the hunting pack.

In our opinion, the correct approach to the phenomenon of the reversible cannibalism-giantism-carnivourism (CGC) in protozoa is to consider it as a very peculiar phenomenon, somehow representing an intermediate trophic niche, for the ciliate capable of behaving as herbivour or as carnivour organism. A hypothesis might even be put forward, concerning the possibility that the phenomenon CGC could represent, and somehow tetstify, that intermediate stage of evolution, when ciliates were neither fully primary consumers nor fully secondary consumers: could the advantage of being an active predator in the proper conditions lead a bacterivorous species to acquire the reversible capability of becoming carnivorous, before becoming a fully irreversible carnivorous species?

We tried to reconsider as many bibliographic items as possible dealing with the CGC study: although a large number of reports is available in the field, it must be stressed, however, that they are only relatively useful in drawing a complex picture of this problem for several reasons: (a) the total number of the ciliate species studied for their CGC is very small, no more than fifteen out of thousands, characterized by extreme diversity and heterogeneity; (b) they belong to widely different systematic groups, so that any possible similarity among them might actually be due to different phylogenetic evolution and/or to different adaptive strategies, thus making it impossible to unify interpretations, in terms of homologies/analogies, possibly accounting for the observed CGC process; (c) the reports range in time from 1853 [30] to 1993 [37]: this extremely wide span makes most of the papers only partially comparable, due to the different minds, cultures, attitudes the researchers had not only toward the problem, but also toward the way of reporting the data: simple, direct, descriptive, naturalistic the earlier (roughly up to the sixties), eminently technical, elaborate and mainly focussed on cell biology aspects, the most recent.

Bearing all these considerations in mind, however, we tried to put the things together, in an attempt to identify, where possible, common features and elements, indicating to us, at least tentatively, the basic fundaments of the adaptive logic of CGC phenomenon, in order to be able to propose a unifying working hypothesis to guide future research in this field toward more ordered, more comparable and more interpretable results.

The papers we studied deal with *Frontonia* [81],

Tetrahymena [4–6, 14, 42, 73, 83], *Blepharisma* [20, 48, 50, 77], *Platyophryides* [51], *Lembadion* [37], *Stentor* [19, 39, 76], *Gastrostyla* [85], *Oxytricha hymenostoma* [11], *Stylonychia* [21], *Onychodromus* [86], *O. bifaria* [59, 60, 65, 66, 67, 69]. The results just described led us to put together a sort of patchwork (Fig. 5) describing the main characters (horizontal lines) known for the different species (vertical columns). The first consideration is that a very large number (58) of the 154 possibilities are black (="unknown"), and that 7 more refer to information not reported directly by the Authors, but just found as small, secondary observations. In other words ~40% of the possible, basic information is not yet available even for the few species considered! In spite of all the handicaps so far mentioned, however, a sort of Common Denomenator, formed by several basic elements, seems to emerge from the scheme of Fig. 5.

A The induction conditions (internal and external)

Independently from the different single, species-specific solutions, this general character well indicates a basic adaptive value of the CGC phenomena in ciliates: a physiological, internal, very likely epigenetic (*sensu* Nanney, [46]) predisposition is controlled and determined by environmental modulations (proper, weak preys-starvation-high cell densities).

B The number of the ex-novo produced heteromorphic CGC organisms

With the only exception of *Tetrahymena* (which evolved the quite singular stomatin-induction of giants) the other species seem to share the same adaptive strategy: very few heteromorphic organisms differentiated *ex-novo* undergo intense cell binary fissions, for producing massively CGC. This finding seems to represent one of the clearest traits shared by most of the species studied. Why, on the contrary, should they prefere this solution (few changed FG reproduce many heteromorphic SSG instead of the *Tetrahymena*'s strategy (many changed SSG) is quite a complex question, far from being resolved, on the basis of the data so far available.

C The body size

Only *Frontonia* and *Stentor* do not enlarge the body to fulfill the new adaptive tasks, while the other 9 genera produce overdimensional individuals. The sub-characters, namely wider peristomial structure, richer ciliary organelles and larger nuclei seem to follow unfailingly (automatically) the shift in body size, as possibly confirmed also by the case of *Frontonia*, where normal sized organisms have also normal peristome, ciliature and nuclei. The adaptive meaning of this deep, morphological reshaping seems to be quite clear, once the CGC nature of the heteromorphic phase is considered. It can be easily observed that (a) normal size cannibals (*Frontonia*), (b) gigantic cannibals (*Blepharisma, Lembadion, Onychodromus*) and (c) gigantic carnivores (*Tetrahymena, Oxytricha bifaria*) are described, while (d) no small carnivore has been found so far. If this element should be confirmed by future research, it might represent an important clue to the penetration of the intimate nature of a predator, which it is to be expected should be considerably larger and stronger than its preys, to work as an efficient carnivore. The case of *Frontonia*, in this context, seems to us the clearest example of a purely cannibalistic species, according to three major characters: (i) short lasting tendency to produce cannibals; (ii) small size cannibals; (iii) three preys per cannibal, at maximum.

A final remark must be made with regard to the change in the body shape, when a giant is produced: while all the ciliates seem just to "inflate" their body, regulating them isometrically (="the giant is just a larger-normal individual), Hypotrichs, on the contrary, seem to have a highly conservative, untouchable portion of their body (namely their ventral surface, with all the locomotory organelles) and an extremely plastic, dorsal one, which, on the contrary, can undergo extensive variations (cf. the *O. bifaria*'s case, as the most paradigmatic in this sense.

D The adaptive meaning

As to the adaptive strategy actually applied by a CGC producing species we must be extremely cautious: many authors, indeed, speak of cannibals

merely because they only experienced that situation in their experiments, without trying to check whether those forms could also be capable of predating non conspecific preys (carnivorous *vs* cannibal behaviour). According to our data, only the case of *Lembadion*'s giant was specifically tested in this sense and found to be a true, cannibalistic form. In general, the two strategies are followed by the different species, roughly in a 1:1 ratio: their basically different meanings have been already discussed in section I and II. To conclude this paragraph which deals with the possible adaptive meaning of these heteromorphic stages in the biology of ciliates, a special word must be said about the *Tetrahymena* example: *T. vorax* specifically undergoes cell differentiation whenever it perceives the substances released by *T. pyriformis*. In our opinion, this seems to indicate that the species has chosen an extremely specialized form of carnivourism, feeding on only one species. This, in turn, cannot but remind to us the case of all those species of ciliates specifically predating only one prey (cf. the cases above mentioned). The finding that also among the temporarily, reversibly differentiated predators, a similar strategy has been chosen not only extends the number of those cases, but seems to us moreover to strengthen Fenchel's [16] hypothesis about the significant general advantages of such feeding behaviour, which enables many different species of predators to survive also in one single habitat, without such a wide species diversification.

E The return to the normal state

The way by which the different species return to their normal morphology and physiology once the proper CGC conditions are over, namely the series of regulating fissions, represents another apparently univocal solution found by quite different species to solve the same problem. The explanation of the reasons why this solution actually represents such a convenient dedifferentiation path for the species studied could represent a strong contribution to a deeper understanding of the cell differentiation in general.

On the basis of the data already published and of the considerations so far made, we would like to recall how difficult and delicate the correct study of these phenomena can be even for the most brilliant scientists [9, 87]: therefore it seems to us an absolute necessity, if we extend our knowledge of this theme, to carry on widespread new research, not only to complete what reported in Fig. 5, but also to extend it by adding new species and new elements: only after such a basic investigation phase, will any seriously indicative conclusion become possible.

CONCLUSIVE REMARKS

The data and the arguments above reported demonstrate that, as stated in the first part of this paper, protozoa actually help us in penetrating not only their biology and life philosophy, but also at least some of the most hidden aspects of the general adaptive strategies of Life: their peculiar, unique, double-sided nature, indeed, enables us to put together different fields of Biology, interpretating the same phenomenon according to the ideas and concepts typical of diverse areas. As a simple example, we cite Fig. 6, where the successive steps of the process "*O. bifaria* giant formation" are read as successive phases of a "cell differentiation" and as serial states of an "adaptive strategy", as well.

In other words, Protozoa lend themselves as precious material in biological investigation, representing a solid, polyhedric bridge between cell biology and whole organism adaptive biology: in protozoology, in fact, two quite different and basic aspects of biology (cell *vs* organism) become directly the two faces of the same coin and, in these conditions, both contribute to define the nature of the coin itself.

In our opinion, this is the most important thesis of the present review.

REFERENCES

1 Balbiani EG (1873) Arch Zool Exper 2: 363–394
2 Banchetti R, Ricci N (1986) Protistologica 22: 161–168
3 Bradbury P, Hausmann K (1993) Ciliates: cells as organisms. Ed. by P Bradbury and K Hausmann, Springer Verlag
4 Buhse HEJr (1966) J Protozool 13: 429–435
5 Buhse HEJr (1967) J Protozool 14: 608–613

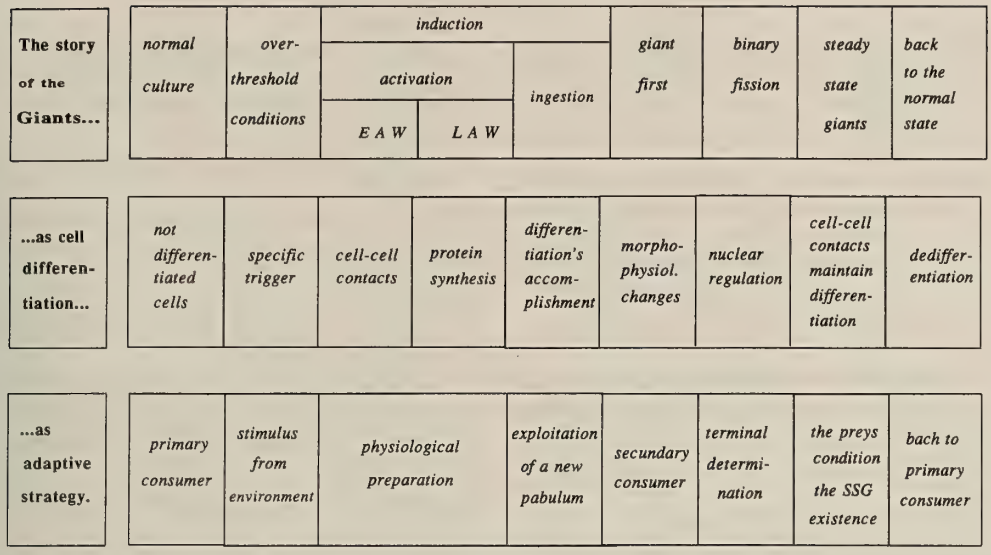

FIG. 6. The three levels of the story of the giants of *O. bifaria*: the story itself, the cell differentiation, the adaptive strategy.

6 Butzel HM, Fisher J (1983) J Protozool 30: 247–250
7 Cairns JJr (1991) Environm Auditor 2: 187–195
8 Corliss JO (1979) The Ciliated Protozoa. Pergamon Press, Oxford
9 Curds CR (1966) J Protozool 13: 155–164
10 Cutler LS, Chaudhry AP (1973) Dev Biol 33: 229–240
11 Dawson JA (1919) J Exp Zool 29: 473–513
12 Dini F, Bracchi P, Luporini P (1975) Acta Protozool 14: 59–66
13 Dragesco J (1962) Bull Biol Fr Belg 96: 123–167
14 Dupy-Blanc J, Metenier G (1975) Protistologica 11: 159–167
15 Esposito F, Ricci N, Nobili R (1976) J Exp Zool 197: 275–282
16 Fenchel T (1987) Ecology of Protozoa. The Biology of Free-living Phagotrophic Protists. Science Tech. Publishers. Madison, WI
17 Foissner W (1987) In "Progress in Protistology Vol 2" Ed. by JO Corliss and J Patterson, Biopress Ltd, pp 69–212
18 Fulton C, Walsh C (1980) J Cell Biol 85: 346–360
19 Gelei J (1925) Arch Protistenkd 52: 404–417
20 Giese AC (1973) *Blepharisma*. The Biology of a light-sensitive Protozoan. Stanford Univ. Press, Stanford, California, pp 123–134
21 Giese AC, Alden RH (1938) J Exp Zool 78: 117–134
22 Gilbert LI (1988) Developmental Biology. Sinaver Associates, Inc, Sunderland, Massachusetts, U.S.A., pp 1–635
23 Gilbert LI, Goodman W (1981) In "Metamorphosis: a problem in developmental biology" Ed. by LI Gilbert and E Frieden, Plenum, New York, pp 139–176
24 Goodenough UW (1977) In "Receptors and recognition Vol 3" Ed. by JL Reissig, Ser. B, Chapman & Hall, London, pp 323–351
25 Gould SJ, Raup DM, Sepkoski JJJr, Schopf TJM, Simberloff DS (1977) Paleobiology 3: 173–181
26 Granger NA, Bollenbacher WE (1981) In "Metamorphosis: a problem in developmental biology" Ed. by LI Gilbert and E Frieden, Plenum, New York, pp 105–138
27 Grobstein C (1955) J Exp Zool 78: 539–547
28 Grobstein C (1956) Exp Cell Res 10: 424–440
29 Haemmerling J (1934) Wilhelm Roux Arch Entwicklungsmech Org 131: 1–81
30 Haime J (1853) Ann Sci Nat Zool 19: 109–134
31 Hiwatashi K (1969) In "*Paramecium*" Ed. by CB Metz and A Monroy, Academic Press, New York, pp 255–293
32 Jacobson AG (1966) Science 152: 25–34
33 Jahn TL, Bovee EC (1967) In "Research in Protozoology" Ed. by TT Chen, Pergamon Press, Oxford, pp 41–200
34 Jennings HS (1906) Behaviour of the Lower Organisms. Indiana Univ. Press, Bloomington, IN
35 Kloppstech K, Schweiger HG (1975) Differentiation 4: 115–123
36 Kochert G (1975) Symp Soc Dev Biol 33: 55–90
37 Kuhlmann HW (1993) Arch Protistenkd in press

38 Lehtonen E, Wartiovaara J, Nordling S, Saxen L (1975) J Embryol Exp Morphol 33: 187–203
39 Lennartz DC, Bovee EC (1980) Trans Am Microsc Soc 99: 310–317
40 Lueken W, Krueppel T, Gaertner M (1987) J Exp Biol 130: 193–202
41 Machemer H (1988) In "*Paramecium*" Ed. by HD Goertz, Springer Verlag, Berlin, pp 185–215
42 Metenier G (1981) Eur J Cell Biol 24: 252–258
43 Miller S (1968) J Protozool 15: 313–319
44 Miyake A (1968) Proc Jpn Acad 44: 837–841
45 Muthukkaruppan VR (1965) J Exp Zool 159: 269–288
46 Nanney DL (1958) Proc Natl Acad Sci 44: 712–717
47 Nanney DL (1980) Experimental Ciliatology. Wiley and Sons, New York, pp 67–75
48 Nilsson JR (1967) Compt Rend Trav Lab Carlsberg 36: 1–24
49 O'Day DH, Lewis KE (1975) Nature 254: 431–432
50 Padmavathi PB (1961) Arch Protistenkd 105: 341–344
51 de Puytorac P, Kattar MR, Groliere CA, da Silva Neto I (1992) J Protozool 39: 154–159
52 Ricci N (1981) In "Sexual interactions in Eukaryotic Microbes" Ed. by PA Horgen and DH O'Day, Academic Press, New York, pp 319–350
53 Ricci N (1989) Limnol Oceanogr 34: 1089–1097
54 Ricci N (1990) Anim Behav 40: 1048–1069
55 Ricci N (1991) Mar Pollut Bull 22: 265–268
56 Ricci N (1992) Proc 3rd Int Congr Neuroethology, August 9–14, 1992, Montreal, Canada, pp 79–80
57 Ricci N (1992) Acta Protozool 31: 19–32
58 Ricci N, Banchetti R (1981) Acta Protozool 20: 153–164
59 Ricci N, Banchetti R, Pelamatti R (1989) Hydrobiologia 182: 115–120
60 Ricci N, Bravi A, Grandini G, Cifarelli D, Gualtieri P, Coltelli P, Banchetti R (1991) Eur J Protistol 27: 264–268
61 Ricci N, Cetera R, Banchetti R (1980) J Exp Zool 211: 171–183
62 Ricci N, Erra F, Russo A, Banchetti R (1989) J Protozool 36: 567–571
63 Ricci N, Erra F, Russo A, Banchetti R (1991) Limnol Oceanogr 36: 1178–1188
64 Ricci N, Erra F, Russo A, Banchetti R (1992) J Protozool 39: 521–525
65 Ricci N, Erra F, Russo A, Banchetti R (1991) Eur J Protistol 27: 127–133
66 Ricci N, Riggio D (1984) J Exp Zool 229: 328–337
67 Ricci N, Rosati G, Verni F (1985) Trans Amer Microsc Soc 104: 70–78
68 Ricci N, Verni F (1988) Can J Zool 66: 1973–1981
69 Riggio D, Banchetti R, Seyfert HM, Ricci N (1987) Can J Zool 65: 847–851
70 Robinson H, Chaffee S, Galton VA (1977) Gen Comp Endocrinol 32: 179–186
71 Rosati G, Giari A, Ricci N (1988) Eur J Protistol 23: 343–349
72 Rosati G, Verni F, Ricci N (1984) Protistologica 20: 197–204
73 Ryals PE, Smith-Sommerville HE (1985) J Protozool 33: 382–387
74 Slavkin HC, Bringas PJr (1976) Dev Biol 50: 428–442
75 Smith HE (1982) J Protozool 29: 616–627
76 Tartar V (1961) The Biology of *Stentor*, Academic Press, New York, pp 1–413
77 Tulchin N, Hirshfield, HI (1962) J Protozool 9: 200–203
78 Verni F (1985) Zoomorphol 105: 333–335
79 Verni F, Ricci N (1986) Symp Biol Hungar 33: 213–216
80 Verni F, Rosati G, Ricci N (1984) Protistologica 20: 87–95
81 Vimala Devi, R (1964) J Protozool 11: 304–307
82 Visscher JP (1924) Biol Bull 45: 19–27
83 Williams NE (1961) J Protozool 8: 403–410
84 Wilson EB (1896) The Cell in Developmental Inheritance, Mac Millan, New York
85 Weyer G (1930) Arch Protistenkd 71: 139–228
86 Wicklow BJ (1988) J Protozool 35: 137–141
87 Yanbin P, Zuoren Z (1981) Acta Zool Sinica 27: 7–11

ZOOLOGICAL SCIENCE 10: 411–415 (1993)

The Defective Color Vision in Juvenile Goldfish Does Not Depend on Used Training Task as the Measure of Discrimination: A Two-choice Response Measure

KEN OHNISHI

Department of Physiology, Nara Medical University, Kashihara, Nara 634, Japan

ABSTRACT—Color discrimination ability of juvenile goldfish (*Carassius auratus*) was measured using a Y-maze training technique to test whether the defective color vision in juveniles found in a previous study [10] would be similarly observed using another training paradigm. The discrimination ability of juveniles was compared with that of adults that had been previously obtained with the same training paradigm [9]. Although the juveniles trained with green and red discriminative stimuli (colored papers) showed good discrimination ability comparable to that of the adults, the juveniles had great difficulty in discriminating blue from both green and red while the adults did not. These results are in agreement with findings in the previous study [10] using a "go/no-go" task. The defective color vision of juveniles is clearly not task-dependent but is rather a general property originating from the developmental process of blue vision.

INTRODUCTION

A previous study [10] on the development of color vision in goldfish has clearly shown that juveniles have defective color vision, specifically for color blue, when it is examined with a "go/no-go" training technique. It may be possible, however, that they can process blue information normally and discriminate blue from other colors as do adults when they are confronted with another training paradigm. The neural pathway (especially the blue information processing pathway) in juveniles that produces avoidance responses might not yet have developed fully compared with other neural pathways subserving other types of behavior. It is still unclear whether or not the defective color vision observed in the previous study [10] is task-specific. Many behavioral studies on spectral sensitivity indicate that the property of any spectral sensitivity depends on the training task. For example, the reflex-like startle response tends to be triggered predominantly by long-wavelengths [2, 13]. A more complex behavior, such as a two-choice discriminative response, is produced by short- and mid-wavelengths as well as long-wavelengths [6, 15, 16]. Yager [15] reported that short-wavelengths are most effective for the two-choice type of response. It seems that a definite spectral region is dominantly processed in a neural pathway when a certain type of behavioral pattern is used as the measure of a discriminative response.

In addition to such task-dependency, the color vision of goldfish also depends on the intensity levels of background illumination and discriminative lights. The vision for red is defective under low levels of background illumination when the fish are trained on a "dark" test field [7, 8]. The color vision disappears in wavelength discrimination performed at a low intensity of discriminative lights when trained on an "illuminated" test field [8]. In this condition, the fish use a "brightness" cue but not a "color" one. Considering the lighting-condition dependence of color vision as well, in this study, the discriminative colored papers were presented under a relatively high intensity level of background illumination (about 1000 lx) compared with that in the previous study (15 lx; [10]).

Accepted March 1, 1993
Received January 25, 1993

MATERIALS AND METHODS

The same size juvenile goldfish (3–5 cm, age of <1 year) as those used in the previous study [10] were trained to discriminate between three types of paired colored papers, blue *vs.* green, red *vs.* blue and red *vs.* green, using the same Y-maze instrumental conditioning technique employed and described in detail in another former study [9]. In brief, juvenile fish were rewarded with food when they chose a correct stimulus in such a way that they swam into one of the choice chambers. For brightness control, the colored papers which had been adjusted to be of equal subjective brightness were adopted in this study as well. The maxima of reflectance (λ_{max}) of the colored papers was 480 nm in blue, 520 nm in green and 660–700 nm in red. In the two cases of blue/green and blue/red discriminations in juveniles, the blue papers of higher brightness (about 5% higher in relative brightness than for adults) were used, taking into account the juveniles' lower blue sensitivity [10].

RESULTS

Juveniles, unlike adults, showed very poor abilities in color discrimination between blue and green and red and blue as shown in Figure 1 and 2a. In particular, in the discrimination between blue and green, the percentages of correct responses for the juveniles (n=11) were very low and not incremental (they did not increase over 60% in later sessions), whereas those for the adults (n=6) reached about 90% by later sessions: all data on the adults' color discrimination used in this study were taken from a previous study [9]. Significant differences between the correct responses were observed in the two groups (for statistical analysis, a three-way analysis of variance was used: Groups, $F(1, 15)=52.18$, $P<0.01$; Days, $F(7, 105)=8.33$, $P<0.01$; Groups×Days, $F(7, 105)=3.90$, $P<0.01$). Similarly, in the discrimination of blue/red, those for juveniles (n=23) were not as high as for adults (n=6; Groups, $F(1, 27)=8.80$, $P<0.01$; Days, $F(7, 189)=24.42$, $P<0.01$; Groups×Days, $F(7, 189)=0.93$, $P>0.05$). Some juveniles (n=10), however, showed adult-like color discrimination ability (Fig. 2b). No significant differences

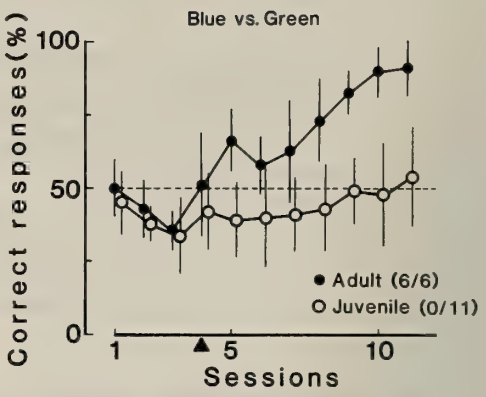

FIG. 1. Learning curves in juveniles (○, n=11) and adults (●, n=6) trained with the blue vs. green stimuli. The fish were rewarded only when they responded to a correct stimulus (a stimulus less frequently responded to during the pretraining trials) during the training trials. The filled triangle indicates the start of the training trials. The numbers in the parentheses indicate learners/trained fish. Vartical bars, ±SD.

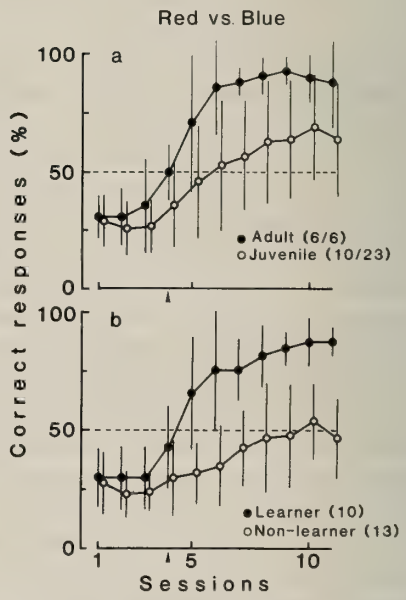

FIG. 2. Learning curves in juveniles (○, n=23) and adults (●, n=6) trained with the red vs. blue stimuli (a) and those in learners (●, n=10) and non-learners (○, n=13) of the juveniles (b). Significant differences were observed in (a) but the juvenile learners showed a very similar learning curve to that of adults as shown in (b). See Figure 1 for further explanations.

were observed between the correct responses of the juvenile learners (the fish which showed over 75% correct responses for at least 3 days successively: all trained adults fulfilled this criterion) and adults (Groups, $F(1, 14)=1.65$, $P>0.05$; Days, $F(7, 98)=24.54$, $P<0.01$; Groups×Days, $F(7, 98)=0.30$, $P>0.05$). The percentages of correct responses of non-learners (n=13) in this task of discrimination were very low (Fig. 2b); they did not increase over 50% in later sessions like those of juveniles in the discrimination between blue and green. Contrarily, in the discrimination between red and green (Fig. 3), the juveniles (n=12) showed a good, adult-like color discrimination ability. Their correct responses were not significantly different from those of adults (n=7; Groups, $F(1, 17)=1.61$, $P>0.05$; Days, $F(7, 119)=9.37$, $P<0.01$; Groups×Days, $F(7, 119)=0.50$, $P>0.05$). When the juveniles had acquired the learned responses, the tasks of discriminating between the reinforced colored papers and gray papers with various brightnesses were performed to make sure that the fish did not discriminate among the colored papers on the basis of brightness. The fish correctly discriminated the reinforced colored papers from the gray ones, showing similar percentages of correct responses to those for color discrimination. Thus, the juveniles clearly used a color cue, but not a brightness cue, in the color discriminations.

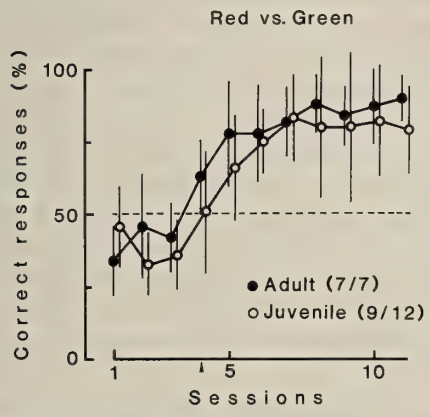

FIG. 3. Learning curves in juveniles (○ n=12) and adults (●, n=7) trained with the red vs. green stimuli. No significant differences were observed between the curves. See Figure 1 for further explanations.

To test whether another type of visual discrimination ability is normal in juveniles, brightness discrimination was performed using white and black papers. Figure 4 shows that juveniles (n=12) could normally discriminate differences in brightness. Their correct responses clearly increased with the increment of training sessions as did those of adults (about 80% correct responses in later sessions) and were not significantly different from those of adults (n=6; Groups, $F(1, 16)=0.33$, $P>0.05$; Days, $F(7, 112)=20.29$, $P<0.01$; Groups×Days, $F(7, 112)=1.16$, $P>0.05$). This indicates that brightness discrimination ability is normal in juveniles.

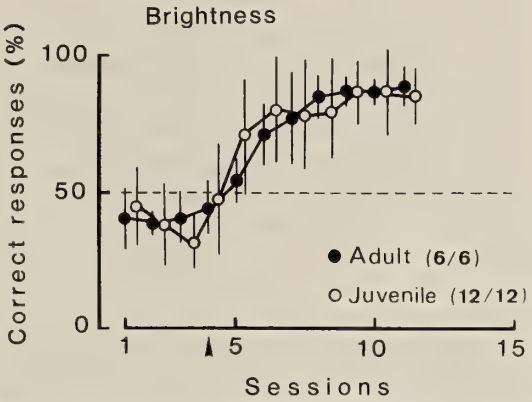

FIG. 4. Brightness discrimination in juveniles (○, n=12) and in adults (●, n=6). All trained juveniles showed adult-like clear learned responses. See Figure 1 for further explanations.

TABLE 1. Percentages of learners in the 3 types of color discrimination measured with 2 training techniques

	blue *vs.* green	red *vs.* blue	red *vs.* green
Two-choice			
Juveniles	0 (0/11)	43 (10/23)	75 (9/12)
Adults	100 (6/ 6)	100 (6/ 6)	100 (7/ 7)
Go/No-go*			
Juveniles	0 (0/10)	0 (0/ 9)	70 (7/10)
Adults	33 (4/12)	50 (6/12)	70 (7/10)

The numbers in the parentheses indicate learners/trained fish. *The data (10 training periods) are from [10].

The percentages of learners in this study, together with those measured in the previous study [10], are shown in Table 1. No juveniles trained to discriminate between blue and green could fulfill the criterion defining "learner" (0%), but some juveniles (43%) showed clear learned responses in the discrimination between red and blue. In the discrimination between red and green, many more juveniles (75%) could acquire the learned responses. The brightness discrimination was easy for all trained juveniles to learn (100%). All trained adults fulfilled the criterion defining "learner" in the three types of color discrimination as well as the brightness discrimination.

DISCUSSION

There are several important differences in the training methods used in this study and those of the previous one [10]. The correct responses of the fish were reinforced with a reward (food) and motivated by appetite in this study while they were reinforced with punishment (electro-shock) and motivated by fear in the previous study. The discriminative stimuli were presented simultaneously using colored papers under a 1000 lx background illumination in this study, while they were presented successively using monochromatic lights under a 15 lx background illumination in the previous study. It has been reported that the intensity level of background illumination considerably afftects the color vision of goldfish. The tetrachromatic color vision becomes trichromatic and, furthermore, the spectral sensitivity function becomes the luminosity function with the decrease in its intensity [7, 8]. Moreover, the fish seem to use a brightness cue at a low intensity (detectable level) of discriminative lights but they use a color cue for high intensity (about 1.0 log unit higher than the dectable level) of discriminative lights for wavelength discrimination when they are trained on an "illuminated" test field [8]. The evidence led to the assumption that the previously observed defective color vision in juvenile goldfish [10] may be due to the low intensity of background illumination. Such a possibility, however, can be rejected because this study, which was performed under a high intensity (about 1000 lx) of background illumination, also demonstrated defective color vision. Thus, the defect in color vision of juveniles is thought to originate from the developmental process of the neural system of blue vision.

Another aspect of interest in this study is that some juveniles showed an adult-like discrimination ability in the discrimination between red and blue but none for the discrimination between bule and green (Table 1: The training task of the present study was probably more easy for the fish to acquire discriminative responses than that of the previous study [10]. The numbers of adult learners in the present study were relatively large compared with those in the previous study [10].). This difference in the discrimination ability between blue *vs.* green and red *vs.* blue may be due to the different quantal absorption ratio of the mid-wavelengths to the long-wavelengths sensitive cones among "blue", "green" and "red" spectral regions. The quantal absorption ratio of the mid-wavelengths to the long-wavelengths sensitive cones in "blue" spectral region is more similar to that in "green" spectral region than that in "red" spectral region [1]. In "blue" and "green" spectral regions, the quantal absorption of the long-wavelengths sensitive cones is not ignorable. Contrary to this, in "red" spectral region, the quantal absorption of the mid-wavelengths sensitive cones seems to be insignificant. Thus, the discrimination between blue and green is probably more difficult than that between red and blue for juveniles who may have not the functionally matured short-wavelengths sensitive cones (The quantal absorption of the ultraviolet sensitive cones is insignificant in visible spectra [1].). Although this explanation is based on the immatureness of the receptor level, the possible immatureness of the post-receptor level should keep in mind. If the short-wavelengths sensitive cones have matured, some juveniles may have already developed a matured blue/red opponent processing pathway but not yet a blue/green one at the same stage of growth.

It is unknown, at present, whether the poor blue vision of juveniles originates from receptoral or post-receptoral elements. However, as already discussed before [10], some possible explanations of the poor blue vision of juveniles can be propo-

sed, considering the morphological studies on the development of the retinal neurons [3–5, 11, 12, 14]. Those neurons of goldfish are very unique in such a respect that they continue to grow and further are added newly beyond larval stages into adult life, while in most vertebrates this neurogenesis is completed during early postembryonic stages. Such unique neurogenesis may have a relation to the prolonged development of blue vision.

REFERENCES

1 Bowmaker JK, Thorpe A, Douglas RH (1991) Ultraviolet-sensitive cones in the goldfish. Vision Res 31: 349–352

2 Cronly-Dillon JR, Muntz WRA (1965) The spectral sensitivity of the goldfish and the clawed toad tadpole under photopic conditions. J Exp Biol 42: 481–493

3 Johns PR (1981) Growth of fish retinas. Amer Zool 21: 447–458

4 Johns PR, Easter SS (1977) Growth of the adult goldfish eyes. J Comp Neurol 176: 331–342

5 Meyer RL (1978) Evidence from thymidine labeling for continuing growth of retina and tectum in juvenile goldfish. Exp Neurol 59: 99–111

6 Neumeyer C (1984) On spectral sensitivity in the goldfish: evidence for neural interactions between different "cone mechanisms". Vision Res 24: 1223–1231

7 Neumeyer C, Arnold K (1989) Tetrachromatic color vision in the goldfish becomes trichromatic under white adaptation light of moderate intensity. Vision Res 29: 1719–1727

8 Neumeyer C, Wietsma JJ, Spekreijse H (1991) Separate processing of "color" and "brightness" in goldfish. Vision Res 31: 537–549

9 Ohnishi K (1991) Goldfish's visual information processing patterns in food-reinforced discrimination learning between compound visual stimuli. J Comp Physiol 168: 581–589

10 Ohnishi K (1993) Development of color vision in goldfish: selective delayed maturation of blue vision. Vision Res 33: 1665–1672

11 Peng YW, Lam DMK (1991) Organization and development of horizontal cells in the goldfish retina, I: The use of monoclonal antibody AT101. Visual Neurosci 6: 357–370

12 Peng YW, Lam DMK (1992) Organization and development of horizontal cells in the goldfish retina, II: Use of monoclonal antibody MH1. Visual Neurosci 8: 231–241

13 Powers MK (1978) Light-adapted spectral sensitivity of the goldfish: a reflex measure. Vision Res 18: 1131–1136

14 Raymond PA (1990) Horizontal cell axon terminals in growing goldfish. Exp Eye Res 51: 675–683

15 Yager D (1967) Behavioral measures and theoretical analysis of spectral sensitivity and spectral saturation in the goldfish *Carassius auratus*. Vision Res 7: 707–727

16 Yager D (1969) Behavioral measures of spectral sensitivity in goldfish following chromatic adaptation. Vision Res 9: 179–186

ZOOLOGICAL SCIENCE 10: 417–424 (1993)

Cardiotoxic Effects of Adrenochrome and Epinephrine on the Mouse Cultured Myocardium

Keiko Mikami[1], Shigeru Sato[2], Minoru Otokawa[3], Anna Palumbo[4] and Kiyoaki Kuwasawa[5]

[1]*Department of Legal Medicine,* [2]*Central Institute for Electron Microscopic Researches, Nippon Medical School, Tokyo 113,* [3]*Laboratory of Biology, Hosei University, Tokyo 194-02, Japan,* [4]*Stazione Zoologica, Napoli, Italy, and* [5]*Department of Biology, Tokyo Metropolitan University, Tokyo 192-03, Japan*

ABSTRACT—Effects were studied on cultured mouse ventricular myocardial cells of 10^{-6}–10^{-3} M epinephrine and adrenochrome, a metabolite of epinephrine. Single ventricular myocardial cells in culture had negative chronotropic responses to adrenochrome (10^{-4} M) and positive responses to epinephrine (10^{-6} M). However, cultured ventricular myocardial cells in confluent sheets had positive chronotropic responses to adrenochrome (2×10^{-4} M) and epinephrine (10^{-6} M). Cumulative LDH leakage from ventricular myocardial cells in confluent sheets increased remarkably after application of 10^{-3} M adrenochrome but only somewhat after application of 10^{-3} M epinephrine. Both adrenochrome and epinephrine (10^{-6} M) induced mitochondrial fusion and an increase of atrial specific granules, in ventricular myocardial cells in confluent sheets. Epinephrine induced an increase in size of myofibrils. In cultured ventricular myocardial cells, adrenochrome at 2×10^{-4} M induced mitochondrial damages, as shown by a swollen appearance, but epinephrine never induced such necrotic changes even at concentrations up to 10^{-3} M. The role of adrenochrome and epinephrine in catecholamine cardiotoxicity is discussed.

INTRODUCTION

Myocardial necrosis which occurs during reperfusion following myocardial ischemia might be, at least in part, due to excessive release of catecholamines in the heart [17, 21, 26]. Administration of excessive concentrations of epinephrine, norepinephrine or isoproterenol has been shown to induce myocardial necrosis in experimental animals [4, 5, 20, 22]. Furthermore, adrenochrome is known as one of the non-physiological products of epinephrine [8, 19], but the *in vivo* formation of adrenochrome has been demonstrated in pathological conditions [1, 14, 15]. Yates and his coworkers [29] assumed that in isolated perfused rat hearts the drug produced cell membrane injury and contractile impairment and might be partly responsible for necrogenesis in catecholamine-induced cardiomyopathy. On the contrary, Wheatley and his colleagues [28] insisted that the catecholamine-induced myocardial cell damage in isolated rat hearts and papillary muscles was the result of epinephrine and norepinephrine stimulation, but not due to adrenochrome, since 10^{-4} M of adrenochrome was required in order to produce a cardiotoxic effect, while the physiological peak concentration of epinephrine was 10^{-8} M.

The cultured myocardium has not been employed to evaluate the effects of adrenochrome and epinephrine on myocardial cells in catecholamine-induced cardiotoxicity. In the present study, we used mouse cultured myocardial single cells and confluent sheets to examine the effects of the drugs on beat rates and ultrastructure in the preparations. We also examined the cumulative leakage of lactate dehydrogenase (LDH) from the cells in the confluent sheets to the culture medium, as an index of cellular damage [18].

Accepted March 8, 1993
Received February 1, 1993

MATERIALS AND METHODS

Mouse ventricular myocardial cells were prepared as reported previously [16]. Single myocardial cells were prepared by seeding cells in plastic dishes (Falcon, ϕ35 mm) at concentrations of 2.5–5$\times10^4$ cells/dish. Myocardial cells in a confluent monolayer were prepared by seeding cells in a 4 Well Multidish (Nunclon, Nunc) at concentrations of 1$\times10^5$ cells/well or, for an ultrastructural study, in MicroWell Modules (Nunc) at concentrations of 1.6$\times10^4$ cells/well.

Adrenochrome was synthesized at the University of Naples, as described by Sobotka and Austin [25]. Adrenochrome and epinephrine bitartrate (Sigma) were applied to the myocardial cells after cultivation for 5 days. The culture medium was replaced with Eagle's minimum essential medium (MEM) containing 10% fetal bovine serum (FBS) buffered with 10 or 20 mM BES (pH 7.3) 1–2 hr prior to the application of the drugs and the myocardial cells were then placed at 37°C in a CO_2-free environment. Adrenochrome (10^{-6}, 10^{-5}, 10^{-4}, 2$\times10^{-4}$ and 10^{-3} M) or epinephrine (10^{-6}, 10^{-5}, 10^{-4} and 10^{-3} M) dissolved freshly in the MEM was applied to the myocardial cells by replacing the normal MEM.

Beating rates of cultured single and confluent myocardial cells were obtained by counting beats in the screen image of individual myocardial cells recorded by a television microscope (a phase contrast inverted microscope: Nikon, TMD; a color camera: Hitachi, DK-7001N) coupled to a video system (Panasonic, AG-6720A). Statistical analyses were performed using the unpaired Student's *t*-test. Activity of LDH in the culture medium was measured spectrophotometrically according to Vassault [27]. An ultrastructural study was performed by a conventional electron microscopic method previously reported [16].

RESULTS

Chronotropic effects on single ventricular myocardial cells

Most of the single ventricular myocardial cells beat spontaneously at a variety of rates ranging from about 50 to 350 per min. Adrenochrome (10^{-6} and 10^{-5} M) did not induce chronotropic

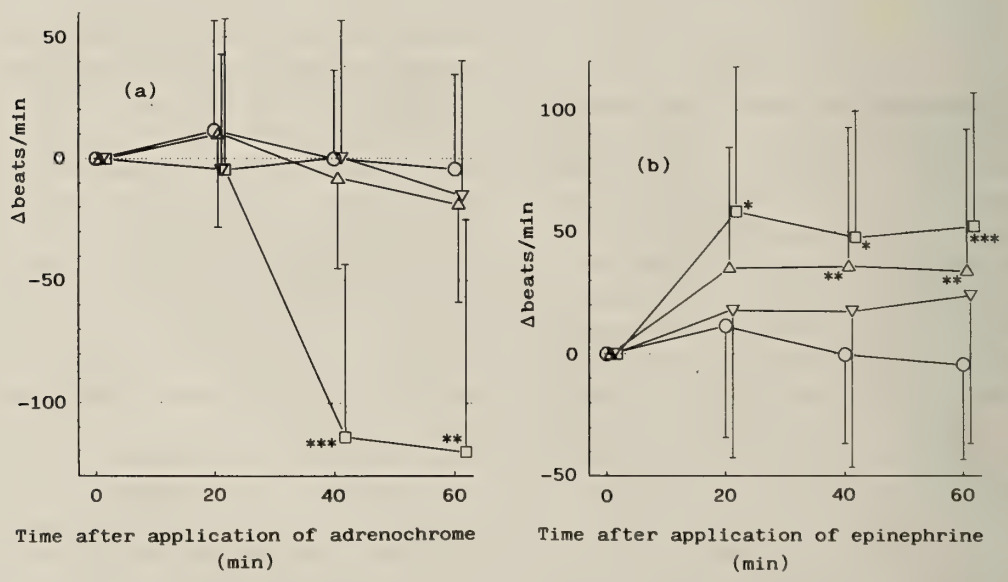

FIG. 1. Chronotropic effects of adrenochrome (a) and epinephrine (b) on single ventricular myocardial cells in culture. Graphs express changes in beat rates per min of the cells from the values before applying the drugs (means±S.D.). ○, control (a normal medium); △, 10^{-6} M; ▽, 10^{-5} M; □, 10^{-4} M. *, $P<0.01$; **$P<0.02$; ***$P<0.001$.

effects on single ventricular cells in a 60 min period after the onset of drug applications (Fig. 1a), though about half of the cells ceased beating in the normal medium after a 60 min exposure to a dosage of 10^{-5} M. A dosage of 10^{-4} M adrenochrome clearly exerted negative chronotropic effects at 40 min and 60 min after the onset of the application, but not at 20 min. At 40 min some cells ceased beating or died, and the beat rates of the beating cells decreased, statistically significant by Student's *t*-test (Fig. 1a, $P<0.001$ *vs.* control). At 60 min about half of the cells ceased beating or died, and the remaining cells beated weakly and slowly ($P<0.02$ *vs.* control). All of the cells died even when they were returned in the normal medium after a 60 min exposure to 10^{-4} M adrenochrome.

Epinephrine (10^{-6}, 10^{-5} and 10^{-4} M) induced positive chronotropic effects (Fig. 1b). There were statistical significances between the control value and the beat rates at 40 min ($P<0.02$) and 60 min ($P<0.02$) after the onset of application at a dose of 10^{-6} M, and at 20 min ($P<0.01$), 40 min ($P<0.01$) and 60 min ($P<0.001$) after the onset of application at a dose of 10^{-4} M. We never observed inhibitory effects of the dosages on the cells such as bradycardia or beat arrest.

Chronotropic effects on myocardial cells in confluent sheets

Ventricular cells in the confluent sheets appeared to beat synchronously and regularly. Adrenochrome (10^{-6} and 10^{-5} M) induced transient slightly positive chronotropic effects on the ventricular cells in confluent sheets at 1 hr after application (Fig. 2a). Adrenochrome at 2×10^{-4} M maintained the positive chronotropic effects over a period of 3 hr (Fig. 2a), the reverse of the case for single ventricular cells (Fig. 1a). The difference from the control value at 2 hr after application was statistically significant ($P<0.05$). At a higher dose (10^{-3} M) beats ceased immediately and completely.

Epinephrine (10^{-6}–10^{-3} M) effects on ventricular cells in confluent sheets had a tendency to shift the whole configuration of the graph toward the area of chronotropic positivity (Fig. 2b). Epinephrine induced no negative chronotropic responses up to 3 hr after the application.

LDH leakage

Cumulative LDH leakage from beating ven-

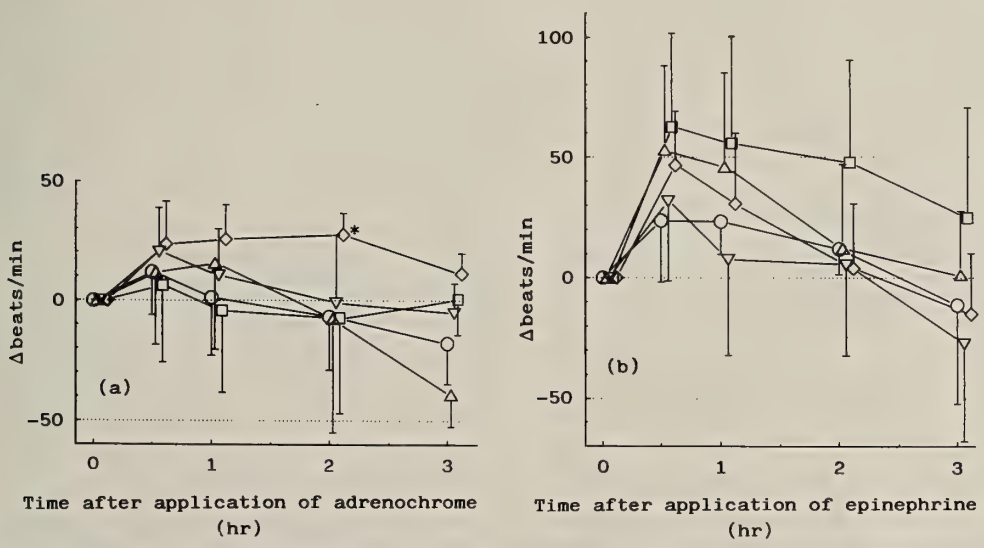

FIG. 2. Chronotropic effects of adrenochrome (a) and epinephrine (b) on cultured ventricular myocardial cells in confluent sheets. Graphs express changes in beat rates per min of the cells from the values before applying the drugs (means±S.D.). ○, control; △, 10^{-6} M; ▽, 10^{-5} M; □, 10^{-4} M; ◇, 2×10^{-4} M (a) and 10^{-3} M (b). *: $P<0.05$.

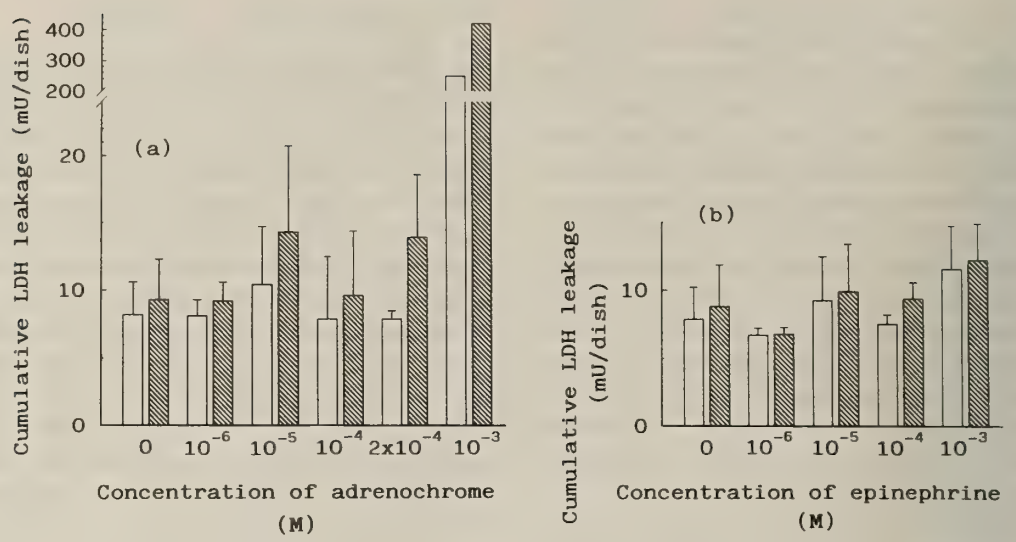

FIG. 3. Cumulative LDH leakage from cultured ventricular myocardial cells in confluent sheets after application of adrenochrome (a) and epinephrine (b) (means±S.D.). □ : 1 hr after application, ▨ : 2 hr after application.

tricular cells in confluent sheets was almost the same in a control experiment, 1 hr after application of 10^{-6}–2×10^{-4} M adrenochrome. However, LDH leakage was somewhat increased 2 hr after application of 10^{-5} and 2×10^{-4} M adrenochrome (Fig. 3a). Application of 10^{-3} M induced a significant increase of LDH leakage at 1 hr and 2 hr after the onset of the dosage (Fig. 3a), but not at 30 min (data not shown). These responses corresponded to the observation of the cell death accompanied with destruction of the cell membrane, as observed under a phase-contrast microscope.

Epinephrine (10^{-6}–10^{-3} M) induced no significant increase of LDH leakage from confluent ventricular cell sheets, though a dose of 10^{-3} M appeared to induce increase of the leakage somewhat (Fig. 3b). Indeed, we never observed cell death in epinephrine (10^{-6}–10^{-3} M) under a phase-contrast microscope.

Ultrastructure

At 30 min after application of adrenochrome (10^{-6}–10^{-4} M) to ventricular cells in confluent sheets, mitochondria were already fusing (Fig. 4a). Atrial specific granules (atrial natriuretic peptide, [3, 12]) had increased, even among myofibrils, as well as in perinuclear regions (Fig. 4b). After a dosage of 2×10^{-4} M, mitochondria having more electron-lucent matrix and parallel cristae appeared abundantly (Fig. 4c; arrows). Furthermore, some mitochondria were markedly swollen and had electron-lucent matrix, vesicular cristae and amorphous deposits (Fig. 4c; arrow head). But, the specific granules were scarcely seen at this point (Fig. 4c). Glycogen granules and rough endoplasmic reticulum had increased in number around mitochondria (10^{-5}–2×10^{-4} M; Fig. 4a-c).

Application of epinephrine (10^{-6}–10^{-3} M) for 30 min induced mitochondrial fusion (Fig. 4d, arrows), giant mitochondria (Fig. 4d, arrow head), an increase in number of the atrial specific granules in perinuclear regions and among myofibrils (Fig. 4e, f, arrows) and an increase in size of myofibrils (Fig. 4e) in a dose-dependent manner, but no mitochondrial changes such as seen after the application of 2×10^{-4} M adrenochrome (Fig. 4c).

DISCUSSION

The response of single ventricular myocardial cells to adrenochrome was different from that of the ventricular cells in confluent sheets; first, the

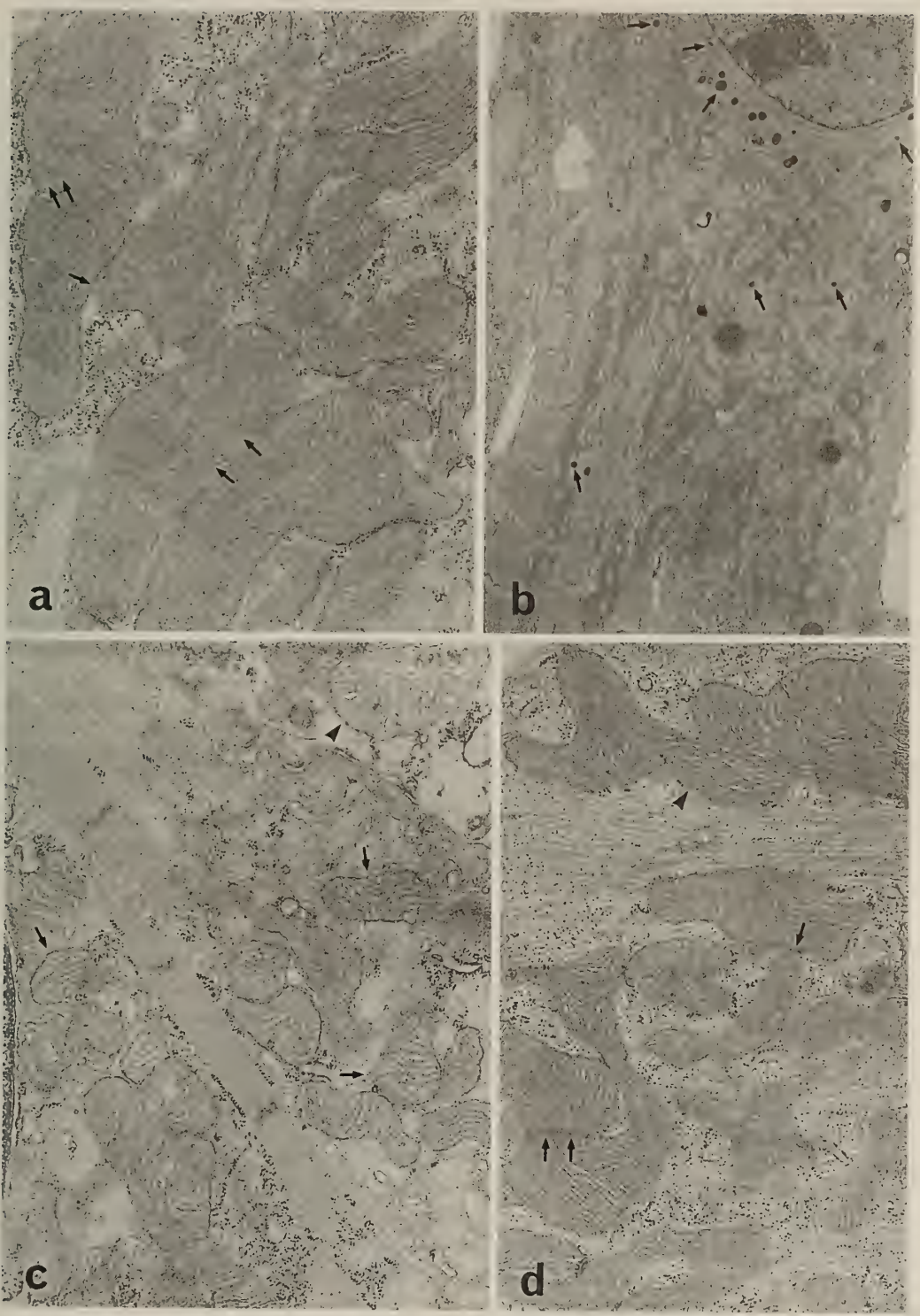
a
b
c
d

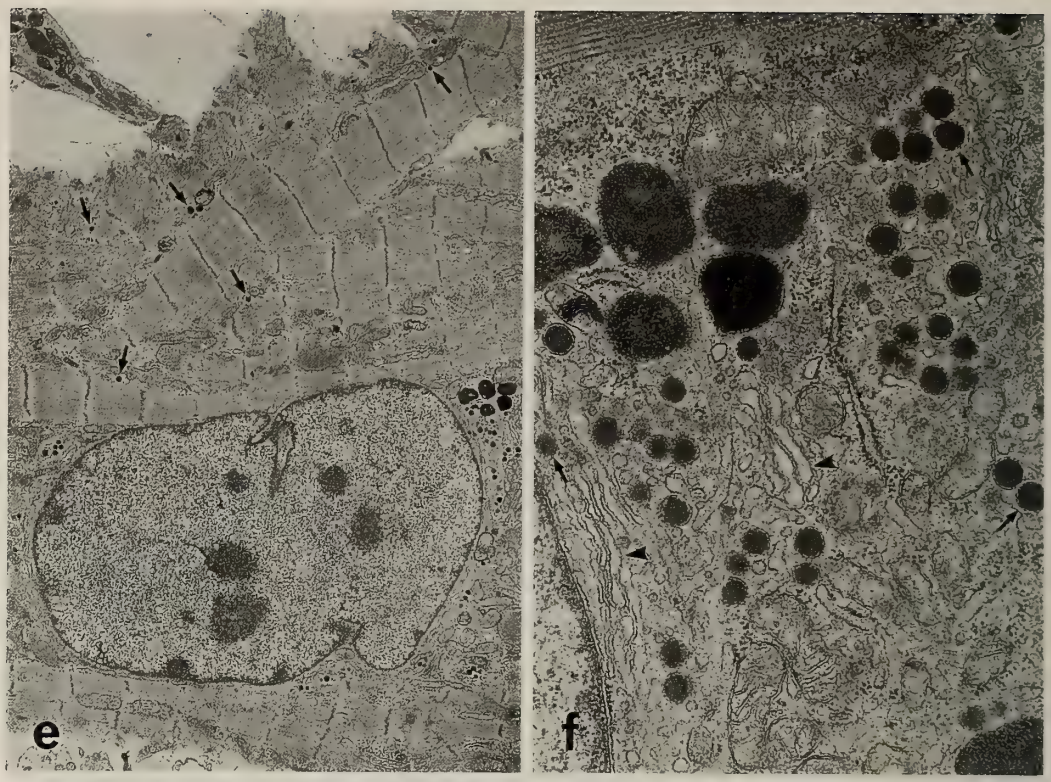

Fig. 4. Electron micrographs of cultured mouse ventricular myocardial cells in confluent sheets at 30 min after the onset of application of adrenochrome or epinephrine. (a) Mitochondrial fusion (arrows). 10^{-4} M adrenochrome. ×23,500. (b) Atrial specific granules (arrows) appeared. 10^{-4} M adrenochrome. ×4,700. (c) Almost all mitochondria became slightly swollen (arrows), and occasionally some revealed ischemic appearances (arrow head). 2×10^{-4} M adrenochrome. ×18,900. (d) Mitochondrial fusion (arrows) and giant mitochondrion (arrow head). 10^{-6} M epinephrine. ×18,900. (e) Atrial specific granules increased in number and appeared even among myofibrils (arrows). Thickness of myofibrils was increased, compared with figure 4b (where myofibrils were of normal size). 10^{-3} M epinephrine. ×3,900. (f) Many atrial specific granules (arrows) appeared in the perinuclear region and there was abundant Golgi apparatus (arrow heads). 10^{-3} M epinephrine. ×23,500.

former response was negative chronotropic one (Fig. 1a) but the latter positive one (Fig. 2a). Secondly, the dose inducing a necrotic response was also different between the two culture systems; single cells often revealed beat arrest in adrenochrome at a relatively low concentration, 10^{-5} M, and cell death at 10^{-4} M. But the cells in the sheets did not have such responses even at 2×10^{-4} M up to 2 hr after application (Fig. 3a) and had at a higher dose, namely 10^{-3} M, although mitochondrial swelling had already appeared 30 min after the onset of application of 2×10^{-4} M adrenochrome (Fig. 4c). In general, grouped cells may be more resistant to various attacks than single cells, probably due to intercellular cooperation by transporting various substances through gap junctions [6, 7], and it is possible that this mechanism can function in setting up the differential chronotropic responses of these culture systems.

Mitochondrial swelling was observed after application of 2×10^{-4} M adrenochrome (Fig. 4c), which was in agreement with the finding of Dhalla and his co-workers using perfused isolated hearts and intact hearts [23, 24, 29]. However, the dose of adrenochrome required to induce necrotic responses was different between the isolated or intact hearts and the present cultured myocardial

cells in sheets; in the former preparations intracellular edema, swelling of sarcoplasmic reticulum, contracted sarcomeres and dissolution of myofibrils were observed with application of adrenochrome at a 10^{-4} M order of concentration. However, these changes were not observed in the cultured myocardial cells at a dose of 2×10^{-4} M, and necrogenic responses were detected only at a higher dose, 10^{-3} M (Fig. 3a). We observed that LDH leakage from non-beating fibroblast-like cell clusters did not increase till 3 hr after application of 10^{-3} M adrenochrome (data not shown). This observation may indicate that cell membrane injury responsible for an increase of LDH leakage might be aggrevated by contractile movements. Since the contractile movement of the cultured myocardium in sheets should be less active than that of isolated or intact hearts, it is likely that the necrogenesis of adrenochrome might be less potent in cultured ventricular cells in sheets.

The *in vivo* production of a high concentration of adrenochrome, such as an order of 10^{-4} M, might not be predicted from the physiological serum peak concentration of 10^{-8} M of epinephrine [28] except in limited myocardial loci, such as subneuronal terminals which could be exposed to high concentrations of epinephrine. It is unlikely that adrenochrome plays an important role *in vivo* in inducing catecholamine cardiotoxicity, although there remains a possibility that even a low concentration of adrenochrome exhibits a synergic cardiotoxic action in the presence of an additional cell injury factor such as other drugs, oxygen lack, and so on.

Epinephrine induced positive chronotropic effects on both single ventricular cells (Fig. 1b) and cells in sheets (Fig. 2b). The drug failed to induce necrogenic responses even at 10^{-3} M, as confirmed by enzyme leakage (Fig. 3b) and ultrastructural studies (Figs. 4d-f). This differs from the results with myocardial enzyme leakage of Wheatley *et al.* [28] using perfused isolated hearts, when the perfusion pressure was high, and also differs from the ultrastructural results of Ferrans *et al.* [4], using intact hearts. In our experimental model, a hypoxic effect could not be supposed to take place, since myocardial cells were soaked in oxygen-rich media. This is different from isolated perfused hearts or intact hearts, which might be subjected to oxygen lack due to insufficient coronary circulation or to metabolic acceleration [9, 22].

Mitochondrial fusion was observed after application of either adrenochrome or epinephrine (Figs. 4a, d). This mitochondrial change seems to be a common characteristic of cultured myocardial cells subjected to ethanol attack, as previously reported [16]. The number of atrial specific granules increased in the vicinity of the nucleus and also slightly among myofibrils, after application of either adrenochrome or epinephrine (Figs. 4b, e, f). Some occasions are known in which atrial specific granules are produced in cultured ventricular myocardial cells [2, 10, 16]. The granules often appeared in hypertrophied [28] and volume-overloaded [13] rat ventricles *in vivo*. Both mitochondrial fusion and an increase in the granules may indicate that the drugs have had a common pathway for induction of the effects, as in the case of some metabolic alterations.

There is a difference in the ultrastructural effects of epinephrine and adrenochrome; epinephrine induced an increase in size of myofibrils, but adrenochrome did not. This may suggest that metabolic acceleratory action of epinephrine causes myocardial hypertrophy. Consequently, it is likely that epinephrine *per se* up to 10^{-3} M is not able to induce cardiotoxicity in cultured myocardial cells, since fatal damages to cell membrane and mitochondria have not been perceived in cells to which epinephrine has been applied.

ACKNOWLEDGMENTS

The authors wish to thank Dr. R. B. Hill for revising the manuscript.

REFERENCES

1 Bindoli A, Rigobello MP, Galzigna L (1989) Toxicity of aminochromes. Toxicol Let 48: 3–20

2 Bloch KD, Seidman JG, Naftilan JD, Fallon JT, Seidman CE (1986) Neonatal atria and ventricles secrete atrial natriuretic factor via tissue-specific secretory pathways. Cell 47: 695–702

3 Cantin M, Gutkowska J, Thibault G, Milne RW, Ledoux S, MinLi S, Chapeau C, Garcia R, Hamet P, Genest J (1984) Immunocytochemical localization of atrial natriuretic factor in the heart and

salivary glands. Histochem 80: 113–127

4 Ferrans VJ, Hibbs RG, Cipriano PR, Buja LM (1972) Histochemical and electron microscopic studies on norepinephrine-induced myocardial necrosis in rats. In "Recent Advances in Studies on Cardiac Structure and Metabolism" Ed by E Bajusz, G Rona, University Park Press, Baltimore, pp 495–525

5 Ferrans VJ, Hibbs RG, Weily HS, Weilbaecher DG, Walsh JJ, Burch GE (1970) A histochemical and electron microscopic study of epinephrine-induced myocardial necrosis. J Mol Cell Cardiol 1: 11–22

6 Goshima K (1977) Ouabain-induced arrhythmias of single isolated myocardial cells and cell clusters cultured *in vitro* and their improvement by quinidine. J Mol Cell Cardiol 9: 7–23

7 Goshima K, Wakabayashi S (1981) Inhibition of ouabain-induced arrhythmias of ouabain-sensitive myocardial cells (quail) by contact with ouabain-resistant cells (mouse) and its mechanism. J Mol Cell Cardiol 13: 75–92

8 Green DE, Richter D (1937) Adrenaline and adrenochrome. Biochem J 31: 596–616

9 Gremels H (1939) Über Potentialstoffe. Ergeb Physiol 42: 53–106

10 Hassall CJS, Wharton J, Gulbenkian S, Anderson JV, Frater J, Bailey DJ, Merighi A, Bloom SR, Polak JM, Burnstock G (1988) Ventricular and artial myocytes of newborn rats synthesise and secrete atrial natriuretic peptide in culture: Light- and electron-microscopical localisation and chromatographic examination of stored and secreted molecular forms. Cell Tissue Res 251: 161–169

11 Izumo S, Lompre A-M, Nadal-Ginard B, Mahdavi V (1987) Expression of the genes encoding the fetal isoforms of contractile proteins and atrial natriuretic factor (ANF) in the hypertrophied adult ventricles. J Am Coll Cardiol 9: 1A

12 Jamieson JD, Palade GE (1964) Specific granules in atrial muscle cells. J Cell Biol 23: 151–172

13 Lattion A-L, Michel J-B, Arnauld E, Corvol P, Soubrier F (1986) Myocardial recruitment during ANF mRNA increase with volume overload in the rat. Am J Physiol 251: H890–H896

14 Matthews SB, Hallett MB, Henderson AH, Campbell AK (1985) The adrenochrome pathway: A potential catabolic route for adrenaline metabolism in inflammatory disease. Adv Myocardiol 6: 367–381

15 Matthews SB, Henderson AH, Campbell AK (1985) The adrenochrome pathway: The major route for adrenalin catabolism by polymorphonuclear leucocytes. J Mol Cell Cardiol 17: 339–348

16 Mikami K, Sato S, Watanabe T (1990) Acute effects of ethanol on cultured myocardial cells: An ultrastructural study. Alcohol Alcohol 25: 651–660

17 Muntz KH, Hagler HK, Boulas J, Willerson JT, Buja LM (1984) Redistribution of catecholamines in the ischemic zone of the dog heart. Am J Pathol 114: 64–78

18 Murphy MP, Hohl C, Brierley GP, Altschuld RA (1982) Release of enzymes from adult rat heart myocytes. Circ Res 51: 560–568

19 Palumbo A, d'Ischia M, Misuraca G, Prota G (1989) A new look at the rearrangement of adrenochrome under biomimetic conditions. Biochim Biophys Acta 990: 297–302

20 Pearce RM (1906) Experimental myocarditis: A study of the histological changes following intravenous injections of adrenalin. J Exptl Med 8: 400–409

21 Rona G (1985) Catecholamine cardiotoxicity. J Mol Cell Cardiol 17: 291–306

22 Rona G, Chappel CI, Balazs T, Gaudry R (1959) An infarct-like myocardial lesion and other toxic manifestations produced by isoproterenol in the rat. Arch Pathol 67: 443–455

23 Singal PK, Yates JC, Beamish RE, Dhalla NS (1981) Influence of reducing agents on adrenochrome-induced changes in the heart. Arch Pathol Lab Med 105: 664–669

24 Singal PK, Dhillon KS, Beamish RE, Kapur N, Dhalla NS (1982) Myocardial cell damage and cardiovascular changes due to I.V. infusion of adrenochrome in rats. Br J Exptl Pathol 63: 167–176

25 Sobotka H, Austin J (1951) Betaine hydrazone of aminochromes. J Am Chem Soc 73: 3077–3079

26 Symes J, Poirier N, Michelborough L, Sniderman A (1977) Catecholamine release in ischemic cells: a mechanism of reperfusion necrosis. Clin Res 25: 673A

27 Vassault A (1984) Lactate dehydrogenase: UV-method with pyruvate and NADH. In "Methods of Enzymatic Analysis Vol 3" Ed by HU Bergmeyer, Verlag Chemie, Weinheim, 3rd ed, pp 118–126

28 Wheatley AM, Thandroyen FT, Opie LH (1985) Catecholamine-induced myocardial cell damage: Catecholamines or adrenochrome. J Mol Cell Cardiol 17: 349–359

29 Yates JC, Beamish RE, Dhalla NS (1981) Ventricular dysfunction and necrosis produced by adrenochrome metabolite of epinephrine: Relation to pathogenesis of catecholamine cardiomyopathy. Am Heart J 102: 210–221

ZOOLOGICAL SCIENCE 10: 425–430 (1993)

Immunochemical Detection of GTP-binding Protein in Cephalopod Photoreceptors by Anti-peptide Antibodies

Tatsuo Suzuki[1], Kinya Narita[2], Kazuo Yoshihara[3], Kazuo Nagai[1] and Yuji Kito[2]

[1]*Department of Pharmacology, Hyogo College of Medicine, Nishinomiya, Hyogo 663,* [2]*Department of Biology, Faculty of Science, Osaka University, Toyonaka, Osaka 560,* [3]*Suntory Institute for Bioorganic Research, Shimamoto, Osaka 618, Japan*

ABSTRACT—We prepared polyclonal antibodies (Pab) against the following peptides: partial sequences of bovine transducin α subunit including the ADP-ribosylation sites sensitive to cholera toxin (CTX) and pertussis toxin (PTX) and the N-terminus of *Drosophila* GTP-binding protein qα (DGqN) ; Pab CTX, Pab PTX and Pab DGqN, respectively. These antibodies were specific to the peptides used as antigen and no crossreactivity was observed. Pab CTX and Pab PTX reacted with bovine transducin α subunit and the reactivity was lost by preincubation with the specific antigen peptide. Proteins of 41–42 kDa in octopus and squid photoreceptor membranes were recognized by Pab DGqN but not by Pab CTX or Pab PTX. Anti-α antibody (GA/1) reacted with the same bands as Pab DGqN recognized. These results suggest that the major GTP-binding protein in cephalopod photoreceptors is a Gq-type, similar to *Drosophila* Gq.

INTRODUCTION

Signal transduction of vertebrate photoreceptors has been well studied and the main sequence of events at the molecular level is well established [16, 20]. Light triggers rhodopsin to activate GTP-binding protein (G-protein), transducin, which in turn activates an effector enzyme, phosphodiesterase, resulting in a decrease of cyclic guanosine monophosphate (cGMP) and the closure of cGMP-dependent cation channels.

In invertebrate photoreceptors, electrophysiological studies have suggested that, besides cGMP, inositol trisphosphate (IP_3) and/or calcium are candidates for intracellular second messengers [2, 6, 16]. Biochemical studies have shown light-dependent binding of non-hydrolysable GTP analogues to the photoreceptor membrane [17, 23] and light-dependent GTPase activity [3, 4, 13, 23], which indicate involvement of G-protein in phototransduction in invertebrate photoreceptors.

Accepted March 18, 1993
Received January 4, 1993

Transducin, the key molecule in vertebrate phototransduction, is susceptible to modification (ADP-ribosylation) both by cholera and pertussis toxins [1, 24]. ADP-ribosylation by bacterial toxins had been applied to identify G-proteins of invertebrate photoreceptors (mainly in cephalopods) but the reported results were contradictory [7, 17, 22, 23], so the type of G-protein, as identified by the ADP-ribosylation, has remained uncertain.

Recently, G-protein was partially purified from squid photoreceptor membrane and its partial sequence was suggesting a Gq-type G-protein [15]. Genes encoding the α subunit of G-protein coupling to phosphoinositide-specific phospholipase C have been cloned and amino acid sequences were deduced from cDNAs in both vertebrates and invertebrates (Gqα, $G_{11}\alpha$, DGqα) [12, 18]. These three Gq-type proteins have some unique sequences which are not found in other G-proteins so far reported. In the present study, we prepared anti-peptide antibodies which react specifically with the N-terminus of *Drosophila* Gqα subunit (DGqα) and with peptides including ADP-

ribosylation sites of transducin α subunit. The G-protein of cephalopod photoreceptors was investigated using these anti-peptide antibodies.

MATERIALS AND METHODS

Preparation of anti-peptide antibodies

We synthesized three peptides: EQDVLRSRVKTTGI (residues 167–180) and DIIIKENLKDCGLF (337–350), corresponding to amino acid sequences around the ADP-ribosylation sites of bovine transducin [8]; and CLSEEAKEQKRINQE (4–19) of the N-terminal region of *Drosophila* Gqa [18]. The synthetic peptides were purified by reversed phase HPLC (C4 column), and amino acid composition was confirmed by amino acid analysis of each purified peptide. Each peptide of 5 mg was conjugated to 10 mg of bovine serum albumin (BSA, Sigma) using 1 mg of *m*-maleimidobenzoic acid N-hydroxysuccinimide ester (MBS, Sigma) as a cross-linker.

Japanese white rabbits were immunized with 1 ml emulsion of 1 mg BSA-peptide conjugates mixed with Freund's complete adjuvant. Three weeks later, the rabbits were boosted with the same amount of conjugates and Freund's incomplete adjuvant, and after two weeks antisera were obtained. The immunoglobulin fraction was purified by ammonium sulfate fractionation and DEAE-column chromatography. BSA-Sepharose complex was made by coupling BSA to CNBr-activated Sepharose 4B (Pharmacia) according to the manufacturer's instruction, and anti-BSA antibodies were removed by the BSA-Sepharose column. The antibodies against peptides around the ADP-ribosylation sites of transducin, sensitive to cholera and pertussis toxins, and against the N-terminus of *Drosophila* Gqα were named Pab CTX, Pab PTX and Pab DGqN, respectively.

Activities and specificities of the anti-peptide antibodies were determined by the method of enzyme-linked immunosorbent assay (ELISA), using the above three peptides as adsorbed antigens (each 0.5 μg/well). Antibodies diluted serially were reacted with adsorbed peptides. The bound antibodies were determined by anti-rabbit IgG (goat)-peroxidase (Wako Chemicals) by the standard method with *o*-phenylenediamine/hydrogen peroxide as substrates; absorbance at 492 nm was determined with a microplate reader.

Preparation of photoreceptor membranes and transducin

Outer segment membranes of octopus (*Octopus vulgaris*), squid (*Todarodes pacificus*) and bovine photoreceptors were prepared by the method of sucrose-density-gradient centrifugation [10]. Membranes floated on 32% sucrose were diluted with 50 mM Tris-HCl buffer (pH 7.4) and precipitated by centrifugation. The membrane preparations were used for sodium dodecyl sulfate-polyacrylamide gel electrophoresis (SDS-PAGE) without further treatment.

Bovine transducin was prepared by the method of Kuhn [11]. Outer segment membranes were illuminated and washed three times with hypotonic buffer (5 mM Tris-HCl, pH 7.4), and once with 100 mM Tris-HCl buffer (pH 7.4). The membranes were then washed three times with the hypotonic buffer containing 200 μM GTP, and soluble fractions, containing transducin, were combined and concentrated.

SDS-PAGE and immunoblotting

The photoreceptor membranes were solubilized with sample buffer, subjected to SDS-PAGE and transferred to nitrocellulose sheet. The sheet was blocked with 1% gelatin/casein solution. Anti-peptide antibodies were diluted with 1% gelatin/casein in phosphate buffered saline (PBS) containing 1% BSA and preincubated at room temperature for 1 hr (1/500 dilution for Pab CTX and Pab PTX, 1/1000 for Pab DGqN), and then incubated with the nitrocellulose sheet at 4°C overnight. The sheet was then treated with anti-rabbit IgG (goat)-peroxidase, and immunoreactive proteins were visualized with 3,3′-diaminobenzidine tetrahydrochloride (DAB)/hydrogen peroxide solution.

Anti-α antibody (GA/1; specific to the GTP/GDP-binding site, GAGESGKSTIVK; common to Gt, Gs and Go) and anti-β antibody (SW/1, specific to the C-terminus of common β) were purchased from Daiichi Chemicals Co., and immunoblot analyses were performed as above (1/300 dilution for GA/1 and 1/500 for SW/1).

RESULTS

The specificity and reactivity of the anti-peptide antibodies are shown in Fig. 1. Each antibody preparation reacted specifically with the peptide used as antigen, with no crossreactivity. The reactivities to BSA were 1/500–1/1000 of those to the specific peptides.

The transducin fraction extracted from bovine outer segment membranes was subjected to SDS-PAGE, transferred to nitrocellulose sheet and treated with the anti-peptide antibodies. The main components of this fraction were transducin α and β subunits (Fig. 2a). Pab CTX and Pab PTX recognized the transducin α subunit: apparent molecular mass 39 kDa (Fig. 2b). The reactions were completely inhibited by preincubation of Pab CTX and Pab PTX with respective peptide antigen.

Immunoblot analyses of octopus, squid and bovine photoreceptor membranes were performed using the three anti-peptide antibodies, as shown in Fig. 3b. Pab DGqN recognized a 41 kDa protein of octopus and a 42 kDa protein of squid membranes but no bovine protein. The reactivity of Pab DGqN against the 41–42 kDa proteins was significantly reduced by preincubation with the N-terminal peptide of DGqα (data not shown). Pab CTX and Pab PTX did not recognize the 41–42 kDa proteins of octopus and squid membranes, though unknown 35 kDa bands were weakly stained by Pab CTX. The results of analyses with anti-α antibody (GA/1) and anti-β antibody (SW/1) are shown in Fig. 3c. GA/1 reacted with the same 41–42 kDa proteins in octopus and squid membranes as Pab DGqN recognized, although the reactivity was lower than with transducin α. The bands with apparent molecular mass of about 35 kDa were equally recognized by anti-β antibody (SW/1) in the membranes of three species. These results show that cephalopod photoreceptor membranes contain Gq-type G-protein and no transducin-like G-protein.

DISCUSSION

The antibodies, Pab CTX and Pab PTX, were proved to be good tools for detection of G-proteins

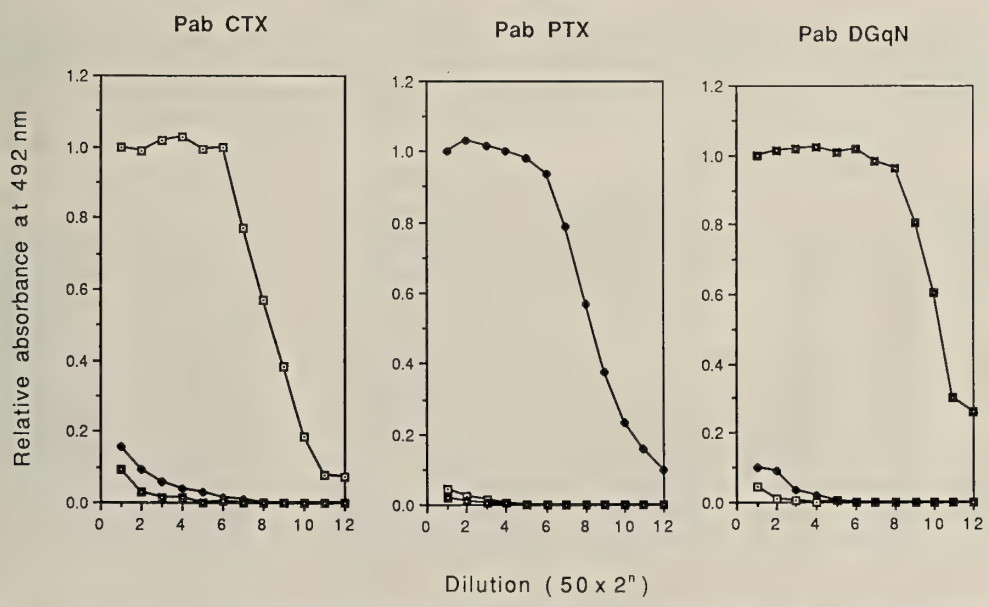

FIG. 1. Reactivities and specificities of anti-peptide antibodies determined by ELISA. Three peptides corresponding to: bovine transducin sequences around ADP-ribosylation sites sensitive to cholera toxin (EQDVLRSRVKTTGI, □), and pertussis toxin (DIIIKENLKDCGLF, ◆); N-terminus of Drosophila Gqα (CLSEEAKEQKRINQE, ■), were used as adsorbed antigens.

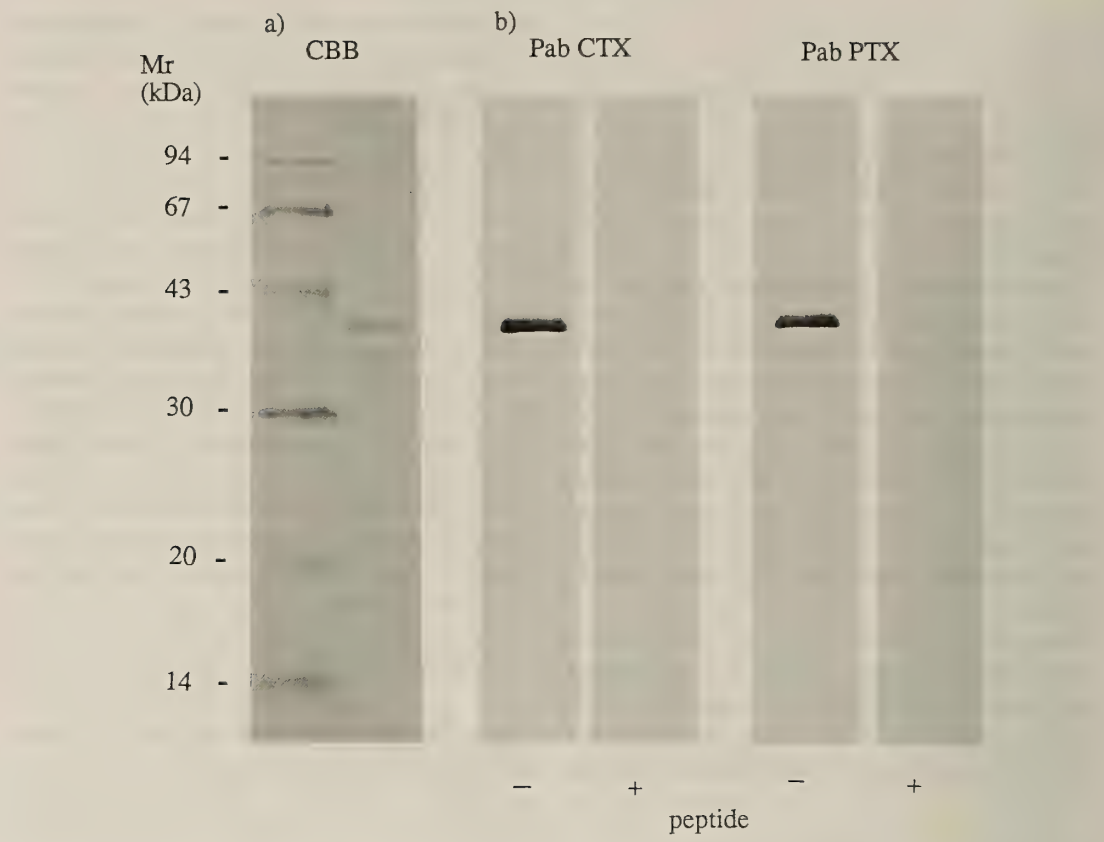

FIG. 2. Specificities of immunoreactions of Pab CTX and Pab PTX against bovine transducin α subunit. a) Coomassie brilliant blue stain (CBB). 14% polyacrylamide gel. b) Immunostains by Pab CTX and Pab PTX (1/500 dilution). Pab CTX preincubated with (+) or without (−) 20 μg/ml peptide (EQDVLRSRVKTTGI), and Pab PTX with (+) or without (−) 20 μg/ml peptide (DIIIKENLKDCGLF) at 25°C for 1 hr.

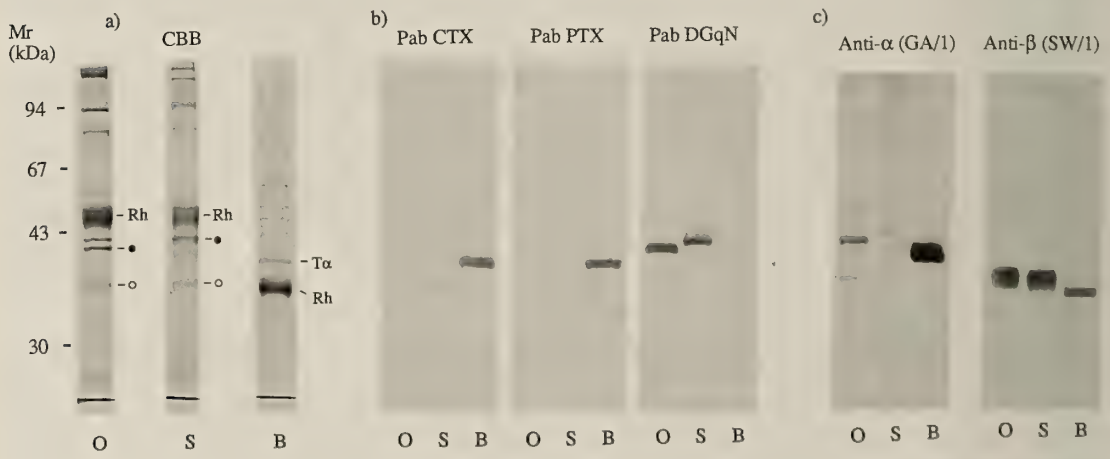

FIG. 3. Immunoblotting of octopus, squid and bovine photoreceptor membranes.a) Coomassie brilliant blue stain (CBB). 12.5% polyacrylamide gel. O, octopus; S, squid; B, bovine. The bands stained by Pab DGqN (●) and by anti-β antibody (○) are indicated. The broad bands around 45 kDa in octopus and squid and 35 kDa in bovine samples are the rhodopsins (Rh). b) Immunostains by Pab CTX, Pab PTX (1/500 dilution) and Pab DGqN (1/1000 dilution). c) Immunostains by anti-α antibody (GA/1, 1/300 dilution) and anti-β antibody (SW/1, 1/500 dilution).

having ADP-ribosylation sites similar to bovine transducin. The peptide sequence corresponding to the N-terminus of *Drosophila* Gqα is highly conserved among Gqα, $G_{11}\alpha$ and DGqα, and has low homology with other G-protein α subunits. The antibody Pab DGqN, therefore, is considered to be specific to these three members of Gq-class G-proteins. When these three antibodies were applied to immunoblot analyses, only Pab DGqN strongly reacted with the 41–42 kDa proteins in cephalopod rhabdomeric membranes.

Reports on ADP-ribosylation of cephalopod rhabdomeric photoreceptor membrane proteins by bacterial toxins have shown that proteins with apparent molecular weight around 40–42 kDa are ADP-ribosylated by pertussis toxin [7, 17, 22], 44–45 kDa proteins by cholera toxin [7, 23] and some others by both bacterial toxins [17, 22]. The results of our present work show that cephalopod photoreceptor membranes contain no transducin-like G-protein which is detectable by both Pab CTX and Pab PTX (Fig. 3b). The sequence around the ADP-ribosylation site by pertussis toxin in Gi-type G-proteins (Gi_1 and Gi_2) is very similar to that in transducin (12 of 14 residues are identical) [8]. Pab PTX did not react any proteins of squid and octopus membranes. This suggests that a Gi-type G-protein, if any, is below the detectable level. Gq-type G-protein lacks the cysteine residue of the ADP-ribosylation site [18] and so is not a substrate for ADP-ribosylation by pertussis toxin [14, 20]. The protein ADP-ribosylated by pertussis toxin, reported previously [7, 17, 22], is not Gq-type G-protein but may be minor component of G-proteins; Gi or Go. The proteins reported to be modified by cholera toxin [7, 23] are probably Gs-like G-proteins. The results in Fig. 3b, showing no Pab CTX-positive 44–45 kDa proteins, do not necessarily exclude the possibility that Gs-type G-protein is involved in rhabdomeric photoreceptors, because the amino acid sequence around ADP-ribosylation site by cholera toxin in transducin is considerably different from that in Gs [8].

The proteins recognized both by Pab DGqN had apparent molecular weight of 41–42 kDa, which is consistent with the reported molecular weight of α subunit of Gq, 42 kDa [14, 18, 21]. Anti-α antibody (GA/1) reacted with the same proteins as Pab DGqN recognized. The reactivity of GA/1 with 41–42 kDa proteins was lower than with transducin α (Fig.3c), suggesting that the sequence of GTP/GDP binding site of cephalopod Gα is slightly different from the common sequence recognized by GA/1. The Coomassie blue stain of the SDS-PAGE gel in Fig. 3a shows that the 41–42 kDa protein is a substantial component of cephalopod photoreceptor membranes, and that its ratio to rhodopsin is nearly the same as that of transducin α subunit to rhodopsin in bovine photoreceptor membrane. These results suggest that the major G-protein in cephalopod photoreceptors is a Gq-type, similar to *Drosophila* Gq. Our results are consistent with those of Pottinger *et al.* [15] suggesting that G-protein of squid photoreceptor is Gq-type.

The biochemical pathway of signal transduction is still obscure in invertebrate rhabdomeric photoreceptors. Both IP_3 and cGMP induce a depolarizing response mimicking light stimulation in *Limulus* ventral photoreceptor [2, 6, 9, 16]. Recent biochemical studies provide evidence suggesting that cGMP is not a second messenger in rhabdomeric photoreceptors [5, 19]. Our results suggesting that Gq-type G-protein is predominant in rhabdomeric photoreceptors strengthen the IP_3 hypothesis for invertebrate phototransduction.

ACKNOWLEDGMENTS

We thank Drs Komatsu and Okamura (Hyogo Coll Med) for technical suggestions in preparing anti-peptide antibodies and Dr Gleadall (Tohoku Univ) for reading the manuscript.

REFERENCES

1 Abood ME, Hurley JB, Pappone MC, Bourne HR, Stryer L (1982) Functional homology between signal-coupling proteins: Cholera toxin inactivates the GTPase activity of transducin. J Biol Chem 257: 10540–10543

2 Bacigalupo J, Johnson E, Robinson P, Lisman JE (1990) Second messengers in invertebrate phototransduction. In "Transduction in biological systems" Ed by C Hidalgo, J Bacigalupo, E Jaimovich and J Vergara, Plenum, New York, pp 27–45

3 Blumenfeld A, Erusalimsky J, Heichal O, Selinger Z, Minke B (1985) Light-activated guanosinetriphosphatase in *Musca* eye membranes resem-

bles the prolonged depolarizing afterpotential in photoreceptor cells. Proc Natl Acad Sci USA 82: 7116–7120

4 Brown JE, Combs A, Ackermann K, Malbon CC (1991) Light-induced GTPase activity and GTP[γS] binding in squid retinal photoreceptors. Vis Neurosci 7: 589–595

5 Brown JE, Faddis M, Combs A (1992) Light does not induce an increase in cyclic-GMP content of squid or *Limulus* photoreceptors. Exp Eye Res 54: 403–410

6 Frank TM, Fein A (1991) The role of the inositol phosphate cascade in visual excitation of invertebrate microvillar photoreceptors. J Gen Physiol 97: 697–723

7 Fyles JM, Baverstock J, Baer K, Saibil HR (1991) Effects of calcium on light-activated GTP-binding proteins in squid photoreceptor membranes. Comp Biochem Physiol 98B: 215–221

8 Gilman AG (1987) G proteins: Transducers of receptor-generated signals. Ann Rev Biochem 56: 615–649

9 Johnson EC, Robinson PR, Lisman JE (1986) Cyclic GMP is involved in the excitation of invertebrate photoreceptors. Nature 324:468–470

10 Kito Y, Seki T, Hagins FM (1982) Isolation and purification of squid rhabdoms. In "Methods in Enzymology" Ed by L Packer, Academic Press, New York, Vol 81, pp 43–48

11 Kuhn H (1980) Light- and GTP-regulated interaction of GTPase and other proteins with bovine photoreceptor membranes. Nature 283: 587–589

12 Lee Y-J, Dobbs MB, Verardi ML, Hyde DR (1990) *dgq*: A Drosophila gene encoding a visual system-specific Gα molecule. Neuron 5: 889–898

13 Nobes C, Baverstock J, Saibil H (1992) Activation of the GTP-binding protein Gq by rhodopsin in squid photoreceptors. Biochem J 287: 545–548

14 Pang I-H, Sternweis PC (1990) Purification of unique α subunits of GTP-binding regulatory proteins (G proteins) by affinity chromatography with immobilized $\beta\gamma$ subunits. J Biol Chem 265: 18707–18712

15 Pottinger JDD, Ryba NJP, Keen JN, Findlay JBC (1991) The identification and purification of the heterotrimeric GTP-binding protein from squid (*Loligo forbesi*) photoreceptors. Biochem J 279: 323–326

16 Rayer B, Naynert M, Stieve H (1990) Phototransduction: Different mechanisms in vertebrates and invertebrates. J Photochem Photobiol 7: 107–148

17 Robinson PR, Wood SF, Szuts EZ, Fein A, Hamm HE, Lisman JE (1990) Light-dependent GTP-binding proteins in squid photoreceptors. Biochem J 272: 79–85

18 Strathmann M, Simon MI (1990) G protein diversity: A distinct class of α subunits is present in vertebrates and invertebrates. Proc Natl Acad Sci USA 87: 9113–9117

19 Seidou M, Ohtsu K, Yamashita Z, Narita K, Kito Y (1993) The nucleotide content of the octopus photoreceptor cells: no changes in the octopus retina immediately following an intense light flash. Zool Sci 10: 275–279

20 Stryer L (1986) Cyclic GMP cascade of vision. Ann Rev Neurosci 9: 87–119

21 Taylor SJ, Smith JA, Exton JH (1990) Purification from bovine liver membrane of a guanine nucleotide-dependent activator of phosphoinositide-specific phospholipase C. J Biol Chem 265: 17150–17156

22 Tsuda M, Tsuda T (1990) Two distinct light regulated G-proteins in octopus photoreceptors. Biochim Biophys Acta 1052: 204–210

23 Vandenberg CA, Montal M (1984) Light-regulated biochemical events in invertebrate photoreceptors. 1. Light-activated guanosinetriphosphatase, guanine nucleotide binding, and cholera toxin catalyzed labeling of squid photoreceptor membranes. Biochemistry 23: 2339–2347

24 Van Dop C, Yamanaka G, Steinberg F, Sekura RD, Manclark CR, Stryer L, Bourne HR (1984) ADP-ribosylation of transducin by pertussis toxin blocks the light-stimulated hydrolysis of GTP and cGMP in retinal photoreceptor membranes. J Biol Chem 259: 23–26

ZOOLOGICAL SCIENCE 10: 431–438 (1993)

Serum Induced Cell Death

Takeshi Kurita and Hideo Namiki[1]

Department of Biology, School of Education, Waseda University, Shinjuku-ku, Tokyo 169-50, Japan

ABSTRACT—In the culture system of human fetal lung fibroblasts (TIG-1) using Eagle's MEM containing various proportion of fetal bovine serum (FBS), FBS stimulated cell growth within the range below 40%. FBS at 60% and above inhibited cell growth in a dose-dependent manner and also induced cell death. As well as TIG-1, several types of cells presently tested also exhibited cell death in high concentration FBS. Bovine plasma also showed the same type of cytotoxicity as FBS. As a first step toward identifying the molecular basis of serum toxicity, FBS was divided into high and low molecular weight fractions by ultrafiltration and these were tested at various concentrations on variety of cell lines including TIG-1 human-fetal lung fibroblast, HeLa human epithelioid carcinoma cells, CPAE bovine aorta endothelial cell, FR Rat skin fibroblast, B16 mouse melanoma, and rat embryo primary cultures. When the macromolecular fraction was supplemented with inorganic salts and nutrients and its osmolarity was adjusted with Eagle's MEM, it showed no toxic effects over a blood range of concentrations. By contrast, a high concentration of low molecular- weight fraction induced cell death. These data suggest FBS contains low molecular-weight (<1,000) factor(s) which cause cell growth inhibition and cell death.

INTRODUCTION

When cells are cultured *in vitro*, serum is commonly added to defined basal media as a source of nutrients and macromolecules essential for growth. As serum is complicatedly constituted of numerous types of biologically active substances, it's roles in culture is also complex and difficult to clearly defined. A proposal that hormonally defined media could be substituted for serum-containing media [5] gave the concept of serum-free media. During the progress of development of the serum-free media, a number of factors such as growth factors, hormones, or cell attachment factors have been identified as essential factors for the cell culture. Despite the efforts, serum is generally still the best additive and many types of cells especially normal cells can survive for long period only with serum, implying the existence of other unknown factors in serum. Some of possible function of serum were postulated [4, 5]. Ever since Carrel and his co-workers reported in 1920's that sera from adult animals inhibit cell growth [1, 2], serum from young animals especially fetal bovine serum (FBS) has been most commonly used for cultures. Adult sera are known to contain much more immunoglobulins, complement, hormones, and lipids at higher concentrations than those from fetal and early animals, and these are thought to inhibit growth. In addition, some reports suggest that neoplastic transformation and chromosomal abnormalities occur less frequently in medium containing FBS as opposed to horse serum [3]. Nevertheless it is well known that FBS occasionally shows cytotoxicity [6], the cause of which is unclear. Since there are relatively few studies of this phenomenon, we began an investigation of its molecular basis. Initially, we found that cells cultured in high concentration of FBS appended to undergo cell death. When the macromolecular fraction (>M.W. 1,000) was separated from FBS by ultrafiltration and the low molecular weight fraction was substituted by Eagle's MEM, this macromolecular FBS stimulated growth of TIG-1 human fetal lung fibroblast and some other cell types of cultures in a dose-depended manner without causing cell death. By contrast the low molecular weight fraction (<M.W. 1,000) caused

Accepted April 2, 1993
Received February 12, 1993
[1] To whom all correspondence should be addressed.

cell death of TIG-1 cell. These results suggested that the FBS low molecular weight fraction contained cytotoxic factor(s). Serum, a product of blood coagulation, is formed at sites of tissue injury *in vivo* and may contain many factors in addition to those in plasma. Thus we also conducted a comparative experiment between serum and plasma in cytotoxicity, showing no practical difference.

MATERIALS AND METHODS

Cell cultures

Human fetal lung fibroblasts TIG-1, human epithelioid carcinoma HeLa, mouse melanoma B16 were obtained from JCRB. Mouse fetal skin FR was from ATCC. All cells were maintained in Eagle's MEM containing 10% FBS. Cell cultures were observed and photographed using Nicon Diaphot phase-contrast inverted microscope. Rat whole-embryo primary culture (RWEC) was established as follows. Wistar-lamichi rat (Japan Crea co.) embryos at 16 days of age were collected and minced in 60 mm petri-dishes. After digestion in 0.1% trypsin, 0.02% EDTA CM-PBS at 37°C for 30 min, the tissue was minced again and dispersed in MEM+10% FBS. Undigested tissue clumps were removed with a nylon-mesh, and cells were collected by centrifugation. Cells were seeded in a 35 mm petri-dish/one embryo (Corning) in MEM+10% FBS, and cultures were washed to remove cell debris and red blood cell. Medium was changed everyday, and when the cultures reached confluence, the cells were harvested and used for experiments.

Serum

We preliminarily tested 14 lots of obtained from several commercial sources (Hyclone, Salmond Smith Biolab Ltd., GIBCO BRL, Boheringer Mannheim, Bio cell, IRVINE) with TIG-1. All showed almost identical cytotoxicity. Heat treatment (57°C, 30 min) had no effect on serum toxicity. Accordingly, we used FBS from Boheringer mannheim (Lot 562044) for all experiments without heat treatment.

Medium

Eagle's MEM "Nissui" (Nissui Pharmaceutical Co., Ltd.) was used as the basal medium for all the experiments. Hanks solution "Nissui" (Nissui Pharmaceutical Co., Ltd.) was used for washing the cell.

Ultrafiltration of FBS

Ultrafiltration of FBS was performed using ultrafiltration membrane YM2 (M.W. 1,000) (Amicon Co.). FBS was concentrated 10-fold and diafiltrated with a 10-fold volume of deionized water to remove the low-molecular-weight fraction. The resultant macromolecular fraction of FBS (MM-FBS) was again concentrated 10-fold then MM-FBS was diluted to the original FBS volume with 10/9 concentrated Eagle's MEM, and the pH and osmolality were adjusted to 7.2 ± 0.2 and 290 ± 10 mosmol/Kg·H_2O, as the ultrafiltrated FBS (UF-FBS). The FBS filtrate (<M.W. 1,000) was freeze-dried and dissolved in 90% volume of deionized water, and the insoluble fraction was removed by centrifugation. The pH of supernatant was adjusted to be pH 7.4 with 150 mM HCl, and MM-FBS was diluted 10-fold with this supernatant to prepare recombined FBS (RC-FBS). The osmolarity of RC-FBS was slightly higher than that of FBS (298–306 mosmol/Kg·H_2O). The ultrafiltrate, low molecular fraction of FBS, was adjusted to pH 7.4 with 0.15 M HCl, almost equivalent to FBS in osmotic-pressure. This prepared ultrafiltrate was used as medium for culturing cells.

Preparation of plasma

Fresh bovine carotidal blood obtained from a local slaughterhouse was immediately added with sodium citrate (final conc. 0.5%) and kept at 15°C. The blood was centrifuged at 6,800 g from 30 min in a continuous centrifuge to remove the hemocyte fraction. The supernatant was stepwise microfiltered and finally passed through a 0.22 μm filter. After the keeping at 4°C for about 1 week, the supernatant was divided into three fractions and processed just before experiments as follows: 1. fibrin was simply spinned out (crude plasma), 2. treated with 1% of 100 unit/ml thrombin (Sigma) at 37°C for 16 hr and contrifuged (thrombin-

treated plasma), and 3. incubated at 37°C for 16 hr without thrombin treatment and centrifuged (incubated plasma).

Measurement of Serum effect

Cells were harvested from confluent 25 cm^2-culture flasks (Corning) after treatment with 0.25% trypsin and 0.02% EDTA in CMF-PBS. An appropriate number of cells in 100 μl/well MEM+10% FBS were seeded into 96 well culture plates (Corning). The cell number used resulted in 1/20–1/5 confluence in each well, and they were as follows; TIG-1 4×10^3/well, CPAE 3×10^3/well, FR 4×10^3/well, HeLa 3×10^3/well, B16 6×10^3/well, RWEC 6×10^3/well, and 6×10^4/well.

After overnight incubation at 37°C in 5% CO_2, the culture medium was removed. The wells were washed with Hanks balanced solution and 100 μl of test medium was added. After 6 days of culture, the cell number in each well was determined using a Coulter Counter ZM (Coulter Electronics).

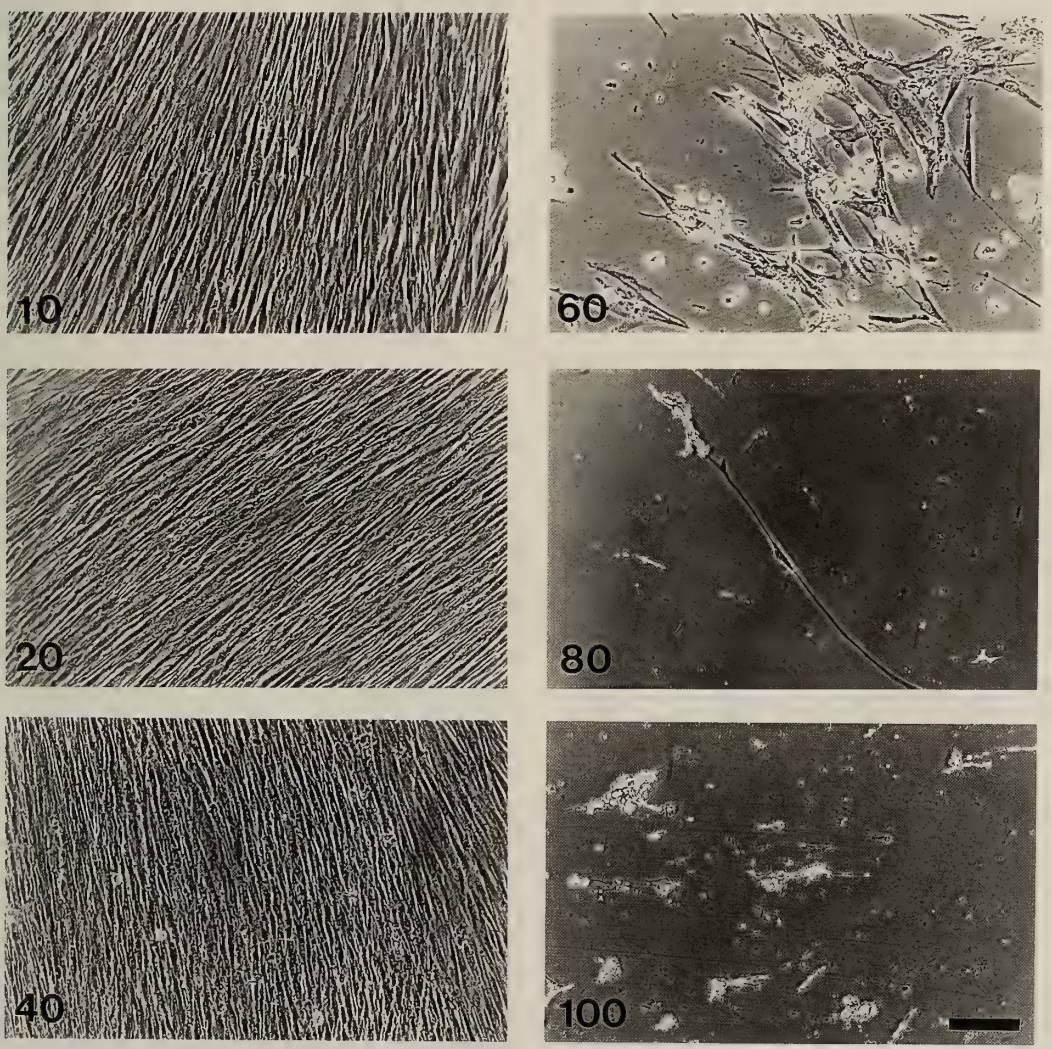

FIG. 1. Effect of FBS on TIG-1 human fetal lung fibroblasts. Human fetal lung fibroblast TIG-1 cells were seeded at 1.0×10^4 cells/well in a 24-well plate, and after 24 hr incubation at 37°C the medium was changed to MEM containing the indicated concentrations of FBS. Six days later photographs were taken. Bar=100 μm.

RESULTS

TIG-1, human fetal lung fibroblasts, were cultured in Eagle's MEM containing various proportion of FBS. FBS stimulated cell growth within the range below 40%. FBS at 60% and above inhibited cell growth in a dose-dependent manner and also induced cell death (Fig. 1, 2). The time required for the cell death was 2–3 days at 60% FBS during which slight cell growth was observed. On the other hand FBS at 80% and above induced complete cell death within 24 hr accompanied with no cell growth. FBS from several different commercial sources had essentially the equal effects on TIG-1 cells. Figure 1 shows the morphologices of TIG-1 cells cultured for 6 days in media containing several different concentrations of FBS. FBS cytotoxicity was dependent upon cell density affected for the degree of the cytotoxicity of FBS. The higher density, the slower the death of the TIG-1 cells (data not shown).

In order to estimate the molecular-weight of the cytotoxic factor(s), we separated FBS into a macromolecular fraction and a low molecular weight fraction by ultrafiltration, and pH and osmolarity were then adjusted. Cytotoxicity was not retained above ultrafilter (Amicon Co.) of the following sizes: YM10 (M.W. 10,000), YM5 (M.W. 5,000), YM2 (M.W. 1,000) (data not shown). Accordingly we used ultrafilter YM2 for the experiments. UF-FBS showed no cytotoxicity and stimulated cell growth dose-dependently (Fig. 2). Recombined FBS (RC-FBS) promoted cell growth more effectively, but the cytotoxicity was comparable to intact FBS. These results indicated that the low molecular-weight fraction of FBS is necessary for the cytotoxicity.

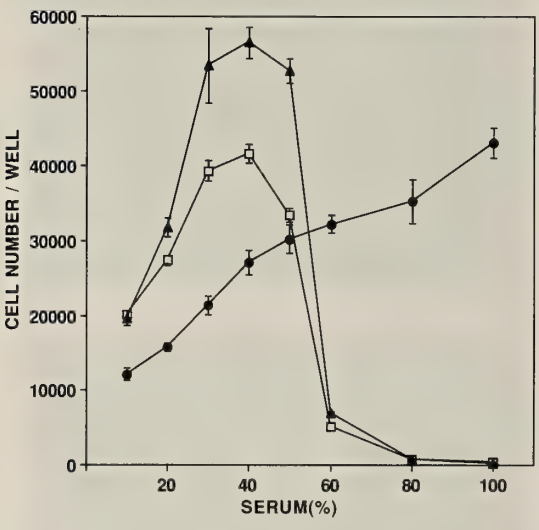

FIG. 2. Effect of serum concentration of TIG-1 cell growth. □: FBS, ●: UF-FBS, ▲: RC-FBS. Human fetal lung fibroblast TIG-1 cells were seeded at 4.0×10^3 cells/well in a 96-well plate, and after 24 hr incubation at 37°C medium was changed to MEM containing the indicated concentrations of FBS. Six days later, cell number was determined with a Coulter Counter.

To determine whether the low-molecular-weight fraction is sufficient for cytotoxicity, TIG-1 cells were cultured in various concentration of FBS-filtrate (from 10% to 100%). Cell death was maximal in 80% filtrate (Fig. 3). The FBS filtrate had cytotoxic activity, but it was slightly less than intact FBS. Thus most of the activity was able to pass through the filter.

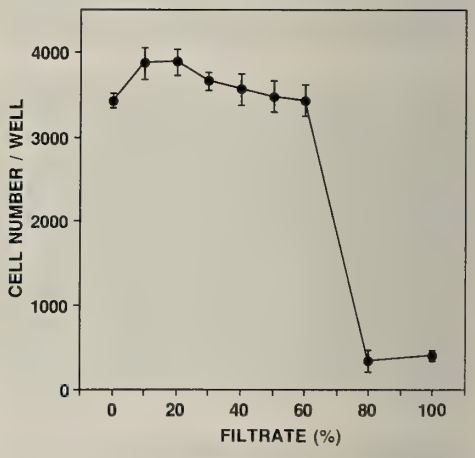

FIG. 3. Cytotoxicity assay of the FBS ultrafiltrate. Human fetal lung fibroblasts (TIG-1) were seeded at 4.0×10^3 cells/well in a 96-well plate, and after 24 hr incubation at 37°C the medium was changed to MEM containing the indicated concentrations of FBS ultrafiltrate. Six days later, cell number was determined with a Coulter Counter.

The cell death induced by FBS is not a specific phenomenon for TIG-1 human fetal lung fibrlblasts. We observed that several other types of cells also ceased to grow and died in FBS. Figure 4 shows cultures of TIG-1 and HeLa cells in media

containing FBS or UF-FBS. Figure 5 depicts the growth patterns of four types of cells cultured in media containing 10–100% of FBS. Though the cells were variously sensitive, all of the type showed cell death in FBS. Interestingly, growth of B16 mouse melanoma was inhibited by a high concentration of UF-FBS. This suggests that growth inhibitor remains in UF-FBS, although it is possible that a small amount of low molecular weight cytotoxic material did not pass completely through the filter. B16 melanoma was very sensitive to the cytotoxicity of FBS, and the cytotoxicity of the ultrafiltrate was less than FBS. In addition to TIG-1, HeLa, B16, CPAE, and FR cells, we tested human adult dermal fibroblasts (HDF) and Bovine carotid artery endothelial cells (HH). These culture also showed cell death in high concentration FBS.

It is possible all of the cell lines examined lost their resistance to cytotoxic substances during long term culture in media containing 10% FBS. We, therefore, tested rat whole-embryo primary cultures (RWEC) (Fig. 6), but the results were similar. All of the cells died in FBS. When the cells from embryos were cultured in 100% FBS, we couldn't observe any growing cells (data not shown). In the case of RWEC, cell-density was related to cell sensitivity to FBS cytotoxicity. Low density cultures were more sensitive than high density cultures. It is possible that cell-cell interactions or cell adhesion conditions affected cell tolerance to FBS cytotoxicity.

Cytotoxicity of plasma as compared with serum was studied upon cultures using medium supplemented either with the crude plasma, thrombin treated plasma or incubated plasma (Fig. 7). As the result, paractically non of three kinds of plasma was different in cytotoxicity from FBS, and TIG-1 cells also exhibited cell death when cultured with high concentration of those plasma.

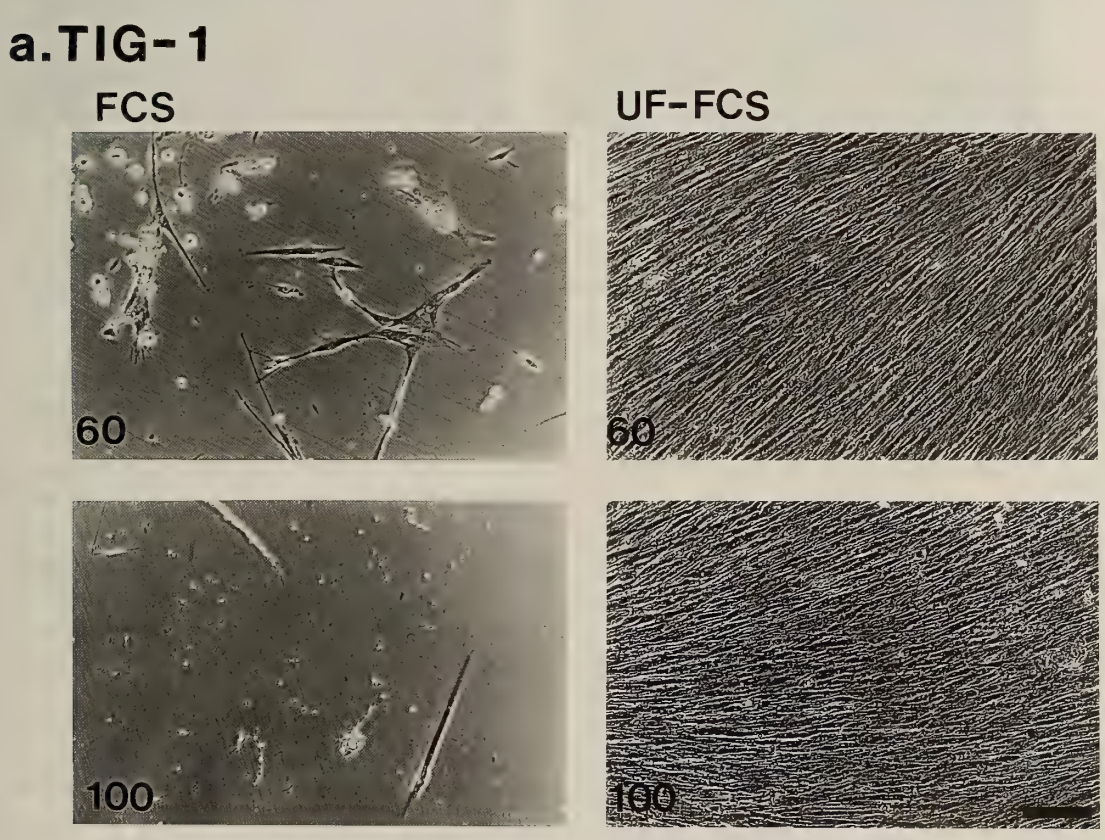

FIG. 4. a

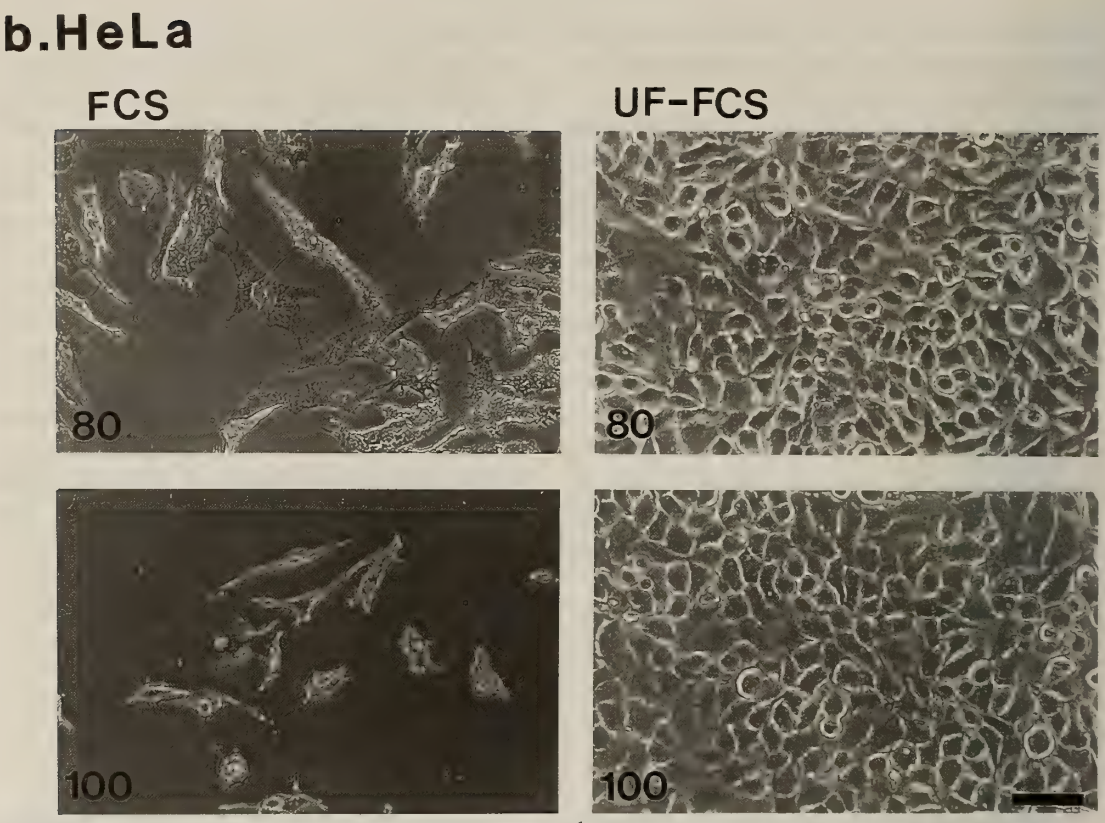

FIG. 4. b

FIG. 4. Effect of FBS on TIG-1 cells and HeLa cells. **a**. TIG-1 cells were seeded at 1.0×10^4 cells/well in a 24-well plate, and after 24 hr incubation at 37°C the medium was changed to MEM containing the indicated concentrations of FBS (left) or UF-FBS (right). Six days later photographs were taken. Bar=100 μm. **b**. Human epithelial carcinoma cells (HeLa) were seeded at 1.0×10^4 cells/well in a 24-well plate, and after 24 hr incubation at 37°C the medium was changed to MEM ontaining the indicated concentrations of FBS (left) or UF-FBS (right). Six days later photographs were taken. Bar=50 μm.

DISCUSSION

Based upon these results, it is likely that endogenous cytotoxic factors exist among the low molecular weight components of serum. FBS ultrafiltrate caused cell death, and the greater part of the cytotoxic factor(s) could pass through the YM2 filter (M.W. $<$1,000). The cytotoxicity, however, was slightly weaker than that of FBS. When the FBS fractions separated by ultrafiltration were recombined, the resultant mixture was more effective for cell growth but was no less cytotoxic than intact FBS. It may be hypothesized that there may exist a macro-molecular co-factor(s) that increases toxicity or amplifies the signal for cell death. It also possible that some of the toxic factor(s) was retained above ultrafilter by binding to macromolecules. Furthermore, we found that in some cases small amounts of high molecular-weight of proteins ($>$M.W. 3000) leaked through the membrane ($<10\ \mu$g/ml) (data not shown). It is also possible that low concentration of proteins play an important role in inducing cell death. At this point it is not possible to conclude with certainly that cell death was exclusively caused by low molecular weight factor(s). It is, however, clear that these factors are necessary for the cytotoxicity.

In answer to the question that the serum cytotoxicity might extraordinarily be produced only at blood coagulation and, if so, plasma might not exhibit such the toxicity, the present data of Fig. 7 that non of preparations of plasma differed from

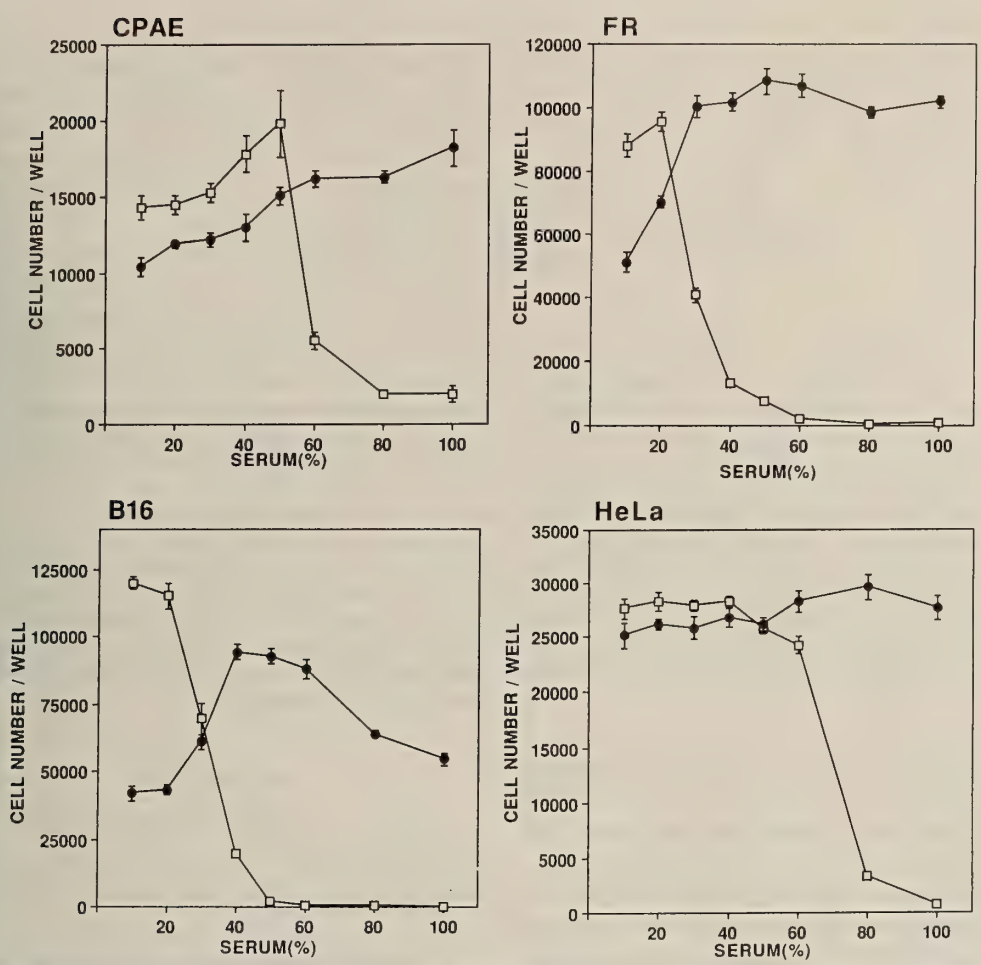

FIG. 5. Effect of serum concentration of growth of CPAE, FR, HeLa, and B16 cell lines. □: FBS, ●: UF-FBS. Cells were inoculated at the following densities in 96-well plates; CPAE 3×10^3/well, FR 4×10^3/well, HeLa 3×10^3/well, B16 6×10^3/well. After 24 hr incubation at 37°C the medium was changed to MEM containing the indicated concentrations of FBS. Six days later, cell number was determined with a Coulter Counter.

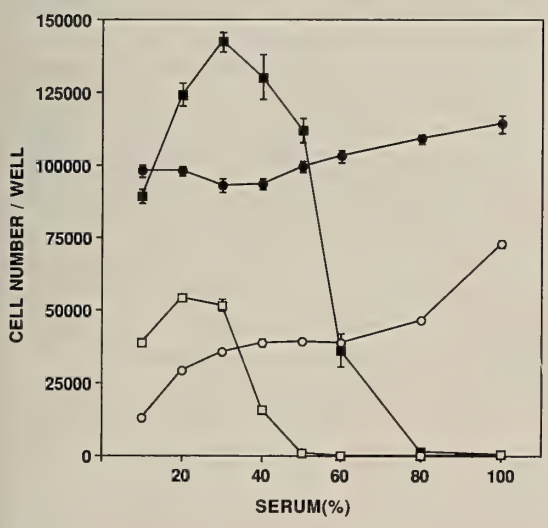

FIG. 6. Serum effect on the primary culture of a rat whole-embryo. A primary culture of a rat whole embryo cells was seeded 6.0×10^3 (□: FBS, ○: UF-FBS) and 6.0×10^4 (■: FBS, ●: UF-FBS) cells/well in a 24-well plate. After 24 hr incubation at 37°C the medium was changed to MEM containing the indicated concentrations of FBS. Six days later, cell number was determined with a Coulter Counter.

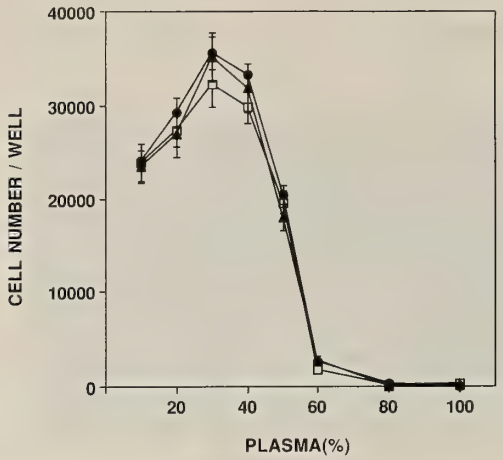

FIG. 7. Effect of plasma concentration on growth of TIG-1 fibroblast. ●: crude plasma, □: thrombin-treated plasma, ▲: incubated plasma. Human fetal lung fibroblast TIG-1 cells were seeded at 5.0×10^3 cells/well in a 96-well plate, and after 24 hr incubation at 37°C medium was changed to MEM containing the indicated concentrations of bovine plasma. Six days later, cell number was determined with a Coulter Counte.

FBS suggested the cytotoxicity existed normally in blood.

As to the question of why the toxic factor(s) do not cause cell death *in vivo*, one explanation may be that the cells are not exposed to the same high concentrations of these factors that are present *in vitro*. Most tissues are protected by an endothelial barrier and are not exposed to blood directly. If so, endothelial cells *in vivo* may be less sensitive to FBS cytotoxicity. CPAE bovine aorta endothelial cells showed cell death in FBS, however (Fig. 4B), it may be that the CPAE cell line lost this property during long-term culture. In a preliminary experiment we have that bovine aorta endothelial cells in the primary culture survived and even grew in 100% FBS (data not shown). By contrast, rat whole-embryo primary cultures did not grow and almost all the cells died in FBS (Fig. 6). It seems that most cell types except vascular endothelial cells can not survive in FBS *in vitro*.

The molecular identity of the cytotoxic factor is still unclear, but cells cultured in either Hank's balanced salt solution and Dulbecco's PBS did not showed cell death (data not shown). This suggests that cell death is not caused by simple starvation, nutritional imbalance, or a defect of physicochemical conditions of culture.

In vivo, all normal cell growth is well controlled, but once cells are transplanted *in vitro*, they start to rapidly proliferate in serum containing media. Vigorous cell growth may reflect the response at a site of injury. Therefore it is possible that cytotoxic factor(s) is a negative growth regulator or an inducer of cell death in tissue injured *in vivo*.

ACKNOWLEDGMENTS

TIG-1 was provided by Japanese Cancer Research Resources Bank (JCRB). This work was supported in part by a donation from KIRIN brewery Co. LTD. Authors are also grateful to Dr. Robert, A. Shiurba, Mitsubishi-Kasei Institute of Life Sciences, for critical reading of the manuscript.

REFERENCES

1 Baker LE, Carrel A (1925) Lipids as the growth-inhibiting factor in serum. J Exp Med 42: 143–154

2 Carrel A, Ebeling AH (1921) Age and multiplication of fibroblasts. J Exp Med 34: 143–154

3 Evans JV, Jackson LJ, Andersen WF, Mitchell JT (1967) Chromosomal characteristic and neoplastic transformation of C3H mouse embryo cells *in vitro* in horse and fetal calf serum. J Nat Cancer Ins 38: 761–769

4 Ham RG, Mckeehan WL (1978) Nutritional requirement for clonal growth of nontransformed cell. Japan Sci Soc Press Tokyo, pp 63–115

5 Hayashi I, Sato G (1976) Replacement of serum by hormones permits growth of cells in defined medium. Nature 259: 132–134

6 Sato G (1981) A working hypothsis for cell culture Hormones and cell regulation. INSERM Europ Symp, Elsevier/North-Holland Biomedical Press, Amsterdam, 5: 1–13

ZOOLOGICAL SCIENCE 10: 439–447 (1993)

Effect of the Oesophageal Mesenchyme on the Differentiation of the Digestive-tract Endoderm of the Chick Embryo

Susumu Matsushita

Department of Biology, Tokyo Women's Medical College, Tokyo 162, Japan

ABSTRACT—The endoderm of various regions of the digestive tract of 6-day chick embryos was cultured *in vitro* in recombination with the oesophageal or other digestive-tract mesenchymes of 6-day chick embryos, and the differentiation of the epithelium was examined with attention given to the appearance of the stratified squamous epithelium characteristic of the mature oesophageal epithelium.

The oesophageal endoderm developed stratified squamous epithelium in high frequency in the presence of the oesophageal mesenchyme, but in low frequency when recombined with the other mesenchymes, which suggested the supporting action of the oesophageal mesenchyme on the proper differentiation of the oesophageal endoderm. Among the other endoderms of digestive tract, only the proventricular endoderm developed stratified squamous epithelium, when cultured in recombination with the oesophageal mesenchyme. The squamous cells of this epithelium contained numerous tonofilaments as those of the stratified squamous epithelium of the intact oesophagus. The ability to elicit stratified squamous epithelium in the proventricular endoderm was shown to be confined to the oesophageal mesenchyme. Thus, the oesophageal mesenchyme was likely to induce oesophagus-type differentiation at least in the proventricular endoderm.

INTRODUCTION

It is well known that the epithelial-mesenchymal interaction is prerequisite for the development of the digestive tract of the Aves [1, 14, 24]. Numerous studies have shown that the mesenchyme of the digestive tract can induce some endoderms to differentiate in a mesenchyme-dependent fashion. The duodenal mesenchyme of the young chick embryo was reported to elicit, in the gizzard endoderm associated to it, the intestine-like simple columnar epithelium forming villus- or previllous ridge-like structures, which developed brush-border structure and its enzymes [2, 5–7]. The proventricular mesenchyme induced the associated gizzard or oesophageal endoderm to form compound gland and to produce embryonic pepsinogen or pepsinogen mRNA, which was specific to the differentiated proventricular epithelium [3, 18–20]. Recently, it was demonstrated that the gizzard mesenchyme could induce the duodenal endoderm to become an epithelium forming tubular glands with prominent mucus production, which resembled the intact gizzard epithelium [12], though it is not yet proved whether the chemical nature of the mucus produced in the recombinates was the same as that of the gizzard mucus. Thus, it may be possible that the mesenchymes of most regions of the digestive tract of the young chick embryo possess the ability to induce the region-specific differentiation at least in some endoderms.

The effect of the oesophageal mesenchyme on the differentiation of the endodermal epithelium was also studied so far. The undifferentiated allantoic endoderm was reported to become pluri-stratified epithelium showing some resemblance to the embryonic oesophageal epithelium when recombined with the oesophageal mesenchyme of the young avian embryo and cultured *in vitro* or *in vivo* on the chorioallantoic membrane of the chick embryo [21, 22], but it became intesinal epithelium with sucrase as well as cloacal epithelium when cultured long enough to achieve full differentiation in the coelomic cavity of the chick embryo [11]. The oesophageal mesenchyme was also reported

Accepted March 30, 1993
Received December 28, 1992

to elicit the yolk sac endoderm to become pluristratified epithelium [9], but the intestinal epithelium with brush border and its enzyme activities also developed in the same type of recombination [9, 10]. The recombination study using the epithelia and mesenchymes of digestive tract demonstrated the heterotypic differentiation of some endoderms cultured in recombination with the oesophageal mesenchyme [23]. Thus, it is still obscure whether the oesophageal mesenchyme has the inductive ability of mesenchyme-dependent differentiation. The present study intended to examine whether the oesophageal mesenchyme has the region-specific inductive influence or not, by the recombination experiment carried out under *in vitro* culture condition. As for the marker of oesophageal differentiation, appearance of the stratified squamous epithelium was examined, since this epithelium was the characteristics of the fully differentiated oesophageal endoderm and was far from being mistaken for other types of epithelium. Though histological is the marker of oesophageal-type differentiation adopted in this study, the stratified squamous epithelium could be regarded as closely related to the cytodifferentiation of the oesophageal epithelial cells, since it appears only in the terminally-differentiated oesophagus of the chick near and after hatching [4, 8, 15, 16].

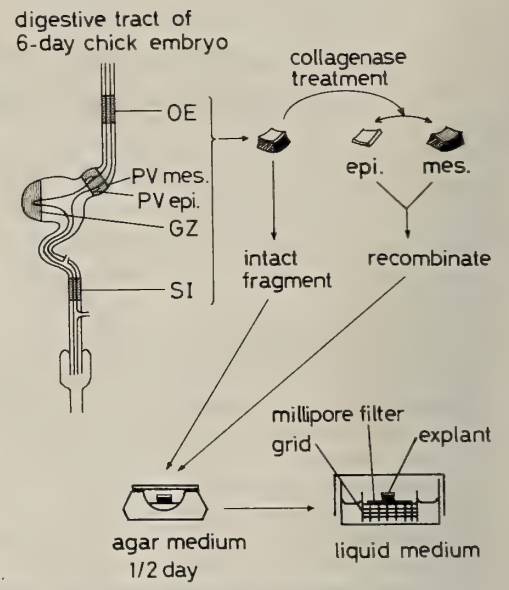

FIG. 1. Diagram showing the mode of combination of epithelia and mesenchymes of the digestive tract. OE, oesophagus; PV, proventriculus; GZ, gizzard; SI, small intestine; epi., epithelium; mes., mesenchyme.

MATERIALS AND METHODS

Animal

Embryos of the White Leghorn chick were used throughout the experiments.

Preparation of tissue fragments

The middle portion of the oesophagus and of the small intestinal fragment between the bile duct entrance and the yolk stalk, and the apex of gizzard body were removed from 6-day-old chick embryos (Fig. 1), and the endodermal epithelium and mesenchyme were separated with the aid of collagenase (Worthington, Code CLS, 0.03% in Tyrode's solution at 38°C for 1 h). Whole portion of the proventriculus was taken from 6-day chick embryos for the proventricular mesenchyme, while only the posterior part was used for the proventricular endoderm or the intact proventricular fragment, for the purpose of eliminating the possible contamination of the apparent oesophageal tissue (Fig. 1). For the oesophageal mesenchyme of older stages, the fragment just anterior to the crop was taken from 8-day, 10-day and 12-day embryos. The isolated endoderm and mesenchyme were recombined after washing in serum-supplemented (50%) Tyrode's solution and then in Tyrode's solution.

In Vitro culture technique

After cultivation on an agar medium for about half a day at 38°C to ascertain the coherence of endoderm and mesenchyme [23], the recombinates were transfered onto a millipore filter (Nihon Millipore Kogyo K. K., pore size 0.8 μm). The filter with the recombinate was placed on a stainless-steel grid in a small culture dish containing a liquid medium up to the level of the membrane filter, and the recombinate was cultured at 38°C in 95% air and 5% CO_2. The intact fragments of digestive tract were also cultured in the same way.

The culture medium consisted of 75% Medium 199 with Earle's salt (Nissui Seiyaku), 20% 12-day chick digestive organ- and eye-free embryo extract (50% in Tyrode's solution), 5% fetal bovine serum (GIBCO Lab.), and antibiotics (penicillin 100 units/ml, streptomycin 100 μg/ml). The medium was changed every third day. Since the stratified squamous epithelium was shown in a preliminary experiment to appear in the intact oesophageal explant after 12 days' cultivation in a liquid medium, explants were cultivated for 12 days or longer up to 18 days.

Histology

After cultivation, the explants were fixed with ice-cold 95% ethanol for 4 hr. Six μm paraffin sections were stained with alcian blue (AB)-hematoxylin. Some explants were fixed in 2.5% glutaraldehyde in 0.1 M sodium cacodylate buffer at 4°C for 2 h and then in 1% O_sO_4 in the same buffer at 4°C for 1 h. They were dehydrated with ethanols and embedded in Embedding Resin (TAAB). Ultra-thin sections were stained with methanolic solution of uranyl acetate and with lead citrate.

RESULTS

Appearance of stratified squamous epithelium in the digestive-tract endoderm in the intact digestive-tract fragments and in the recombinates with the oesophageal mesenchyme

In the explants of intact digestive-tract fragment, the stratified squamous epithelium appeared only in the explants of oesophageal fragment cultured for 12 or 18 days (Table 1, Fig. 2). Columnar epithelium producing AB-stained mucus that might probably correspond to the oesophageal mucous gland epithelium was also found in the oesophageal explants (Fig. 2). In the proventricular explants, columnar epithelium with apical AB-staining differentiated, part of which occasionally developed glandular invagination (Fig. 3). Gizzard explants often formed lots of tubularglandlike structures or intra-epithelial invaginations, which were lined with AB-positive mucus-secretory epithelium. In the small-intestinal explants, simple columnar epithelium with goblet cells appeared. Thus, the appearance of the stratified squamous epithelium was confirmed to be specific to the oesophageal-type differentiation.

When cultured in the presence of the oesophageal mesenchyme, the proventricular endoderm as well as the oesophageal endoderm developed the stratified squamous epithelium after 12 days' cultivation (Table 1). It appeared in the recombinates with the oesophageal endoderm in wide area, while in those with the proventricular endoderm it appeared in various degree, which varied from only a small number of a tiny focus consisting of several squamous cells to a rather wide area (Figs. 4, 5). Transmission electron microscopy showed that numerous tonofilaments were contained in the squamous cells of this stratified squamous epithelium, and ciliated cells were often found (Figs. 6a, b). These were characteristics found in the intact oesophagus during normal development [4, 15] and in the explants of intact oesophagus in the present study (Figs. 7a, b). The possibility that the stratified squamous epithelium found in these recombinates originated from the

Table 1. Appearance of stratified squamous epithelium in the digestive-tract endoderm in the intact digestive-tract fragments and in the recombinates with the oesophageal mesenchyme cultured *in vitro*

Origin of endoderm	Grafts developing stratified squamous epithelium	
	Intact fragments	Recombinates
Oesophagus	16/17 (94%)	7/ 9 (78%)
Proventriculus	0/17 (0%)	20/21 (95%)
Gizzard	0/11 (0%)	0/11 (0%)
Small intestine	0/15 (0%)	0/12 (0%)

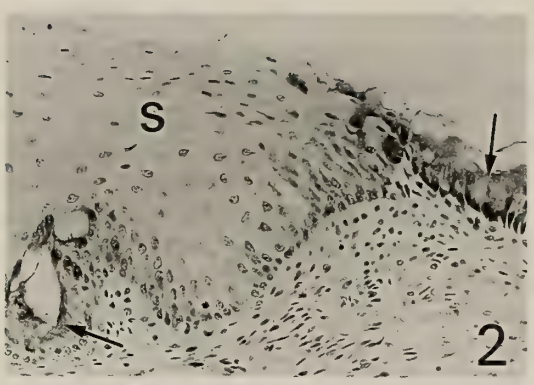
s
2


g
3

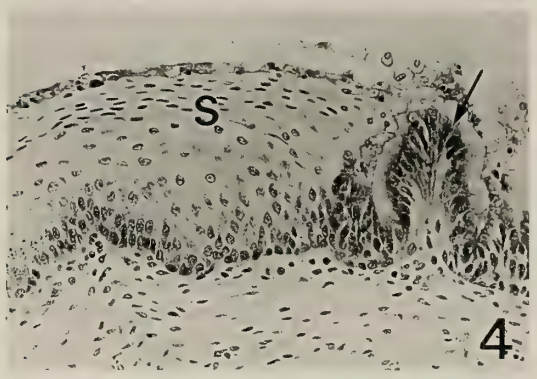
s
4


5


t
n
6a

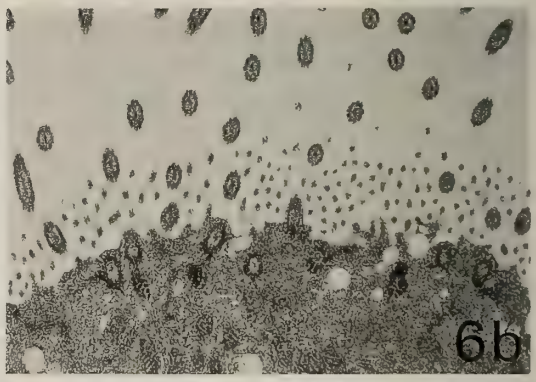
6b

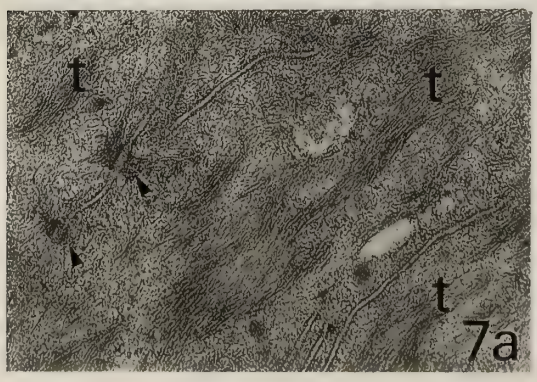
t
t
t
7a

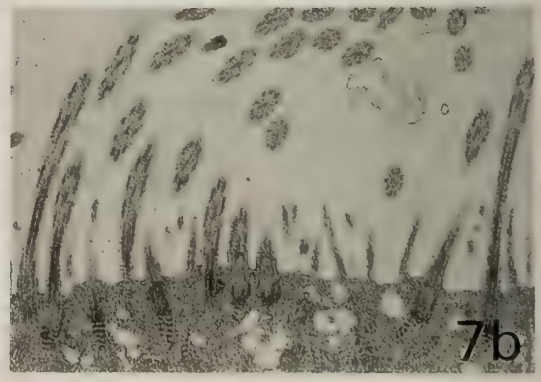
7b

oesophageal epithelial cells contaminated in the oesophageal mesenchyme was denied by the following findings. Serial sections of the isolated oesophageal mesenchyme revealed the absence of oesophageal epithelial cells, and the cultivation of the mesenchyme alone for 12 days or longer never developed stratified squamous epithelium. In rare cases (1 out of 12), the isolated mesenchyme contained a small epithelial vesicle of unknown origin in the presumptive adventitial tissue outside of the muscular layer, and this epithelial cells did not become stratified squamous epithelium after cultivation. In the other region of the recombinates with the proventricular endoderm and in the recombinates with the gizzard endoderm, mucus-secreting epithelium with abundant undulations or short invaginations appeared (Figs. 4, 5, 8). These epithelial cells may be regarded as the differentiated proventricular or gizzard mucous cells, but discrimination from the oesophageal mucous cells was impossible in the present study. The small-intestinal endoderm became simple columnar epithelium with goblet cells. In a few explants, non-goblet mucous cells were also found.

Effect of various digestive-tract mesenchymes on the differentiation of the proventricular and oesophageal endoderm

The proventricular and oesophageal endoderms were found to develop stratified squamous epithelium in the presence of the oesophageal mesenchyme. Then, the effect of other mesenchymes on these endoderms was analyzed.

As shown in Table 2, the proventricular endoderm developed stratified squamous epithelium only in the recombinates with the oesophageal mesenchyme, in which AB-positive mucous epithelium also appeared. The AB-stained epithelium with occasional glandular invagination differentiated in the presence of the proventricular mesenchyme, and the mucus-secretory epithelium forming intra-epithelial invaginations or tubular gland-like structures developed in the presence of the gizzard mesenchyme. In the recombinates with the small-intestinal mesenchyme, AB-positive epithelium was less frequently found.

The oesophageal endoderm developed stratified squamous epithelium in high frequency in the presence of the oesophageal mesenchyme. In the presence of other digestive-tract mesenchymes, stratified squamous epithelium was found in low frequency (Table 2). In the recombinates with the proventricular mesenchyme, AB-positive epithelium with occasional glandular invagination differentiated but even a small focus of stratified squamous epithelium rarely developed (Table 2, Fig. 9). In the recombinates with the gizzard mesenchyme, AB-positive stratified or simple epithelium and stratified squamous epithelium appeared (Fig. 10). In the recombinates with the small-intestinal mesenchyme, AB-positive columnar epithelium appeared. Stratified squamous epithelium was found only in small areas of a few recombinates.

Fig. 2. An explant of intact oesophageal fragment cultured for 18 days. Stratified squamous epithelium (s) and mucous epithelium (arrows) differentiated. ×230.

Fig. 3. An explant of intact proventricular fragment cultured for 18 days. A glandular invagination (g) is formed, and the epithelium is often stained with alcian blue in the apical portion (arrowheads). ×230.

Fig. 4. A recombinate of proventricular endoderm and oesophageal mesenchyme cultured for 18 days. Typical stratified squamous epithelium (s) and mucous epithelium (arrow) are seen. ×230.

Fig. 5. Small foci (arrows) of stratified squamous epithelium that appeared in the mucous epithelium found in a recombinate of proventricular endoderm and oesophageal mesenchyme cultured for 18 days. ×230.

Fig. 6. Transmission electron microscopy of an epithelium of a recombinate of proventricular endoderm and oesophageal mesenchyme cultured for 18 days. a. Cells in the middle layer of the stratified squamous epithelium, which are interconnected with each other by desmosomes (arrowheads) and contained abundant tonofilaments (t). n, nucleus. ×24000. b. A ciliated cell. ×12000.

Fig. 7. Transmission electron microscopy of an epithelium of an explant of intact oesophageal fragment cultured for 18 days. a. Cells in the middle layer of the stratified squampous epithelium. Desmosomes (arrowheads) and numerous tonofilaments (t) are seen. ×24000. b. A ciliated cell. ×12000.

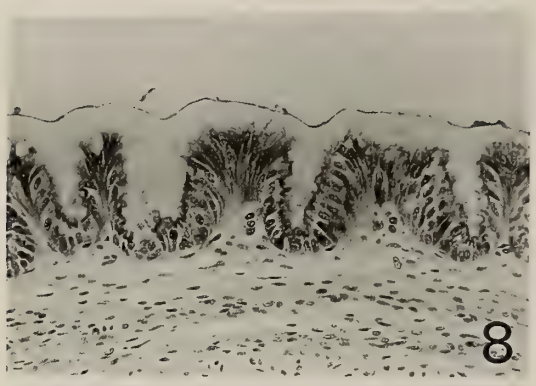

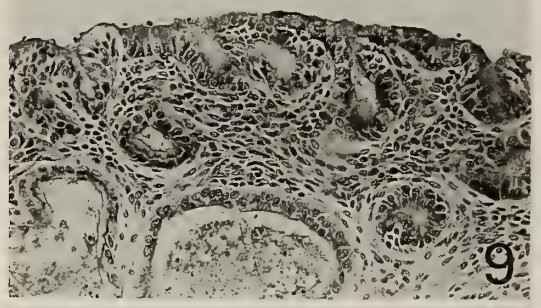

Effect of the oesophageal mesenchyme of aged embryos

As shown in Table 3, the stratified squamous epithelium appeared only in the presence of the oesophageal mesenchyme of 6-day embryos and not in the presence of the mesenchyme of older embryos, suggesting that the inductive ability of the oesophageal mesenchyme declined rather quickly after 6 days of incubation. The epithelium in the recombinates with the mesenchyme of older embryos became mucus-secreting epithelium with abundant undulations or short invaginations.

TABLE 3. Appearance of stratified squamous epithelium in the 6-day proventricular endoderm cultured in the presence of oesophageal mesenchyme of various developmental stages

Stage	Grafts developing stratified squamous epithelium
6-day	20/21 (95%)
8-day	0/10 (0%)
10-day	0/ 8 (0%)
12-day	0/ 6 (0%)

FIG. 8. A recombinate of gizzard endoderm and oesophageal mesenchyme cultured for 18 days. Mucus-secreting epithelium with abundant undulations or short invaginations appeared. ×230.

FIG. 9. A recombinate of oesophageal endoderm and proventricular mesenchyme cultured for 18 days. Columnar epithelium with apical alcian blue-staining forming glandular invaginations appeared. ×230.

FIG. 10. A recombinate of oesophageal endoderm and gizzard mesenchyme cultured for 18 days. A small area of stratified squamous epithelium (s) is seen. × 230.

TABLE 2. Appearance of stratified squamous epithelium in the proventricular and oesophageal endoderms cultured in the presence of various digestive-tract mesenchymes

Origin of mesenchyme	Grafts developing stratified squamous epithelium	
	Proventricular endoderm	Oesophageal endoderm
Oesophagus	20/21 (95%)	23/26 (88%)[a]
Proventriculus	0/21 (0%)[a]	1/18 (6%)
Gizzard	0/11 (0%)	6/11 (55%)
Small intestine	0/12 (0%)	3/11 (27%)

[a], Explants of the intact fragments as well as the recombinates were included.

DISCUSSION

The present study clearly showed that the stratified squamous epithelium appeared in high frequency in the proventricular endoderm cultured in recombination with the oesophageal mesenchyme, demonstrating the ability of the oesophageal mesenchyme to induce the differentiation of stratified squamous epithelium. The previous study [23] also reported an occasional appearance of the stratified squamous epithelium in the same type of recombination, but in the present study the stratified squamous epithelium appeared in much higher frequency, which might be due to a better culture condition or a longer cultivation period. The ultrastructural features of the stratified squamous epithelium found in the recombinates were shown to resemble those of the stratified squamous epithelium of intact oesophageal explants, suggesting that both epithelia might represent the same cytodifferentiated state. As shown in the present study, the appearance of stratified squamous epithelium in the proventricular endoderm was confined to the recombinates with the oesophageal mesenchyme. Thus, it was likely that the oesophageal mesenchyme had the region-specific mesenchyme-dependent inducing ability to elicit the oesophagus-like differentiation at least in the proventricular endoderm. The small focus of stratified suamous epithelium would have developed from a single induced cell or a group of a few induced cells in the recombined proventricular endoderm. The inductive ability of the oesophageal mesenchyme to elicit stratified squamous epithelium in the proventricular endoderm was shown to decline rather quickly after 6 days of incubation, while the ability to elicit pluristratified epithelium in the allantoic endoderm was reported to be retained until the 11th days of incubation [21]. This discrepancy might be due to the difference in the responding tissue and/or to the difference in the examined histological marker in the two experiments.

Regional difference in the responsiveness of the digestive-tract epithelium to the inductive stimuli of the mesenchyme was repetitively reported [3, 5, 20, 23]. The responsiveness to the oesophageal mesenchyme also showed regional difference in the digestive-tract endoderms, and was found to be confined to the endoderm of the proventriculus, which situated next to the oesophagus, at least in the 6-day-old chick embryo. That the competence for the inductive action of the mesenchyme was high in the endoderm of its neighboring region(s) was reported also in the case of intestinal differentiation induced by the duodenal mesenchyme [5] or of the induction of pepsinogen or pepsinogen mRNA by the proventricular mesenchyme [3, 20]. As for the high responsiveness of the proventricular endoderm, the following three possibilities may be considered; 1) some of the proventricular endodermal cells might be induced to change their fate and to become oesophageal-type epithelium; 2) undifferentiated cells capable to adopt oesophageal or proventricular fate according to the influence of the mesenchyme might be contained in the proventricular endoderm; 3) a small number of oesophageal cells which are to be lost through some selective mechanism(s) during normal development in the proventriculus might be distributed even in the posterior part of the proventriculus. It needs further extensive analysis to know which is the case.

The present study also showed that the differentiation of the oesophageal endoderm was influenced by the mesenchyme. The appearance of stratified squamous epithelium was low in the oesophageal endoderm cultured in recombination with the mesenchyme other than that of the oesophagus. Thus, the other mesenchyme might provide only an inappropriate condition for the differentiation of the stratified squamous epithelium or exert an inhibitory effect on its differentiation. The proventricular mesenchyme was known to possess an ability to induce proventricular differentiation [3, 20], and this effect may have contributed to rare appearance of the stratified squamous epithelium in the recombinates with the proventricular mesenchyme. On the contrary, the oesophageal mesenchyme provided a suitable condition for the normal differentiation of the oesophageal endoderm. Whether this effect of the oesophageal mesenchyme on the oesophageal endoderm may be a nutritional one or be related to the inductive influence as exerted over the proventricular endoderm is not known. The appearance

of the stratified squamous epithelium even in the recombinates with the mesenchyme other than the oesophageal one, though in a rather low frequency, suggests that the oesophageal endoderm of the 6-day chick embryo has already been determined to some extent, as suggested by the presence of self-differentiation potency in the oesophageal endoderm of this stage [17].

At least at 6 days of incubation and probably at later stages during normal development, the oesophageal mesenchyme would interact mainly with the oesophageal endoderm likely to be endowed with the oesophageal fate. Since the oesophageal endoderm of 6-day embryos has also a potency of heterotypic differentiation into proventricular-type [3, 20], the inductive effect of the oesophageal mesenchyme might play, in concert with its probable supporting action that provides the approprtiate condition(s), an important role in assurring the correct differentiation of the oesophageal endoderm, as suggested by Mizuno (1975) [13].

ACKNOWLEDGMENTS

The author wishes to express his deep gratitude to Professor Kazuo Utsugi of Tokyo Women's Medical College.

REFERENCES

1 Haffen K, Kedinger M, Simon-Assmann P (1987) Mesenchyme-dependent differentiation of epithelial progenitor cells in the gut. J Ped Gastroenterol Nutr 6: 14–23

2 Haffen K, Kedinger M, Simon-Assmann PM, Lacroix B (1982) Mesenchyme-dependent differentiation of intestinal brush-border enzymes in the gizzard endoderm of the chick embryo. In "Embryonic Development, Part B: Cellular Aspects" Ed by MM Burger and R Weber, Alan R Liss, New York, pp 261–270

3 Hayashi K, Yasugi S, Mizuno T (1988) Pepsinogen gene transcription induced in heterologous epithelial-mesenchymal recombinations of chicken endoderms and glandular stomach mesenchyme. Development 103: 725–731

4 Hinsch GW (1967) Ultrastructural differentiation of the epithelium and mucous glands of the esophagus in the chick embryo. J Morph 123: 121–132

5 Ishizuya-Oka A, Mizuno T (1984) Intestinal cytodifferentiation *in vitro* of chick stomach endoderm induced by the duodenal mesenchyme. J Embryol Exp Morphol 82: 163–176

6 Ishizuya-Oka A, Mizuno T (1985) Chronological analysis of the intestinalization of chick stomach endoderm induced in vitro by duodenal mesenchyme. Roux's Arch Dev Biol 194: 301–305

7 Ishizuya-Oka A, Mizuno T (1992) Demonstration of sucrase immunoreactivity of the brush border induced by duodenal mesenchyme in chick stomach endoderm. Roux's Arch Dev Biol 201: 389–392

8 Ivey WD, Edgar SA (1952) The histogenesis of the esophagus and crop of the chicken, turkey, guinea fowl and pigeon, with special reference to ciliated epithelium. Anat Rec 114: 189–211

9 Masui T (1981) Differentiation of the yolk-sac endoderm under the influence of the digestive-tract mesenchyme. J Embryol Exp Morphol 62: 277–289

10 Masui T (1982) Intestinalization of the area-vitellina endoderm cultured in association with digestive-tract mesenchymes. J Embryol Exp Morphol 72: 117–124

11 Matsushita S (1984) Appearance of brush-border antigens and sucrase in the allantoic endoderm cultured in recombination with digestive-tract mesenchymes. Roux's Arch Dev Biol 193: 211–218

12 Matsushita S (1988) Effect of the mesenchyme on the differentiation of the duodenal and gizzard epithelia of the chick embryo. Zool Sci 5: 1264

13 Mizuno T (1975) Une hypothèse sur l'organogenèse du tractus digestif. C R Soc Biol 169: 1096–1098

14 Mizuno T, Yasugi S (1990) Susceptibility of epithelia to directive influences of mesenchymes during organogenesis: Uncoupling of morphogenesis and cytodifferentiation. Cell Differ Develop 31: 151–159

15 Mottet NK (1970) Mucin biosynthesis by chick and human oesophagus during ontogenetic metaplasia. J Anat 107: 49–66

16 Romanoff AL (1960) The digestive system. In "The Avian Embryo", Macmillan, New York, pp 429–531

17 Sumiya M (1976) Differentiation of the digestive tract epithelium of the chick embryo cultured in vitro enveloped in a fragment of the vitelline membrane, in the absence of mesenchyme. Roux's Arch Dev Biol 179: 1–17

18 Takiguchi K, Yasugi S, Mizuno T (1986) Gizzard epithelium of chick embryos can express embryonic pepsinogen antigen, a marker protein of proventriculus. Roux's Arch Dev Biol 195: 475–483

19 Takiguchi K, Yasugi S, Mizuno T (1988) Developmental changes in the ability to express embryonic pepsinogen in the stomach epithelia of chick embryos. Roux's Arch Dev Biol 197: 56–62

20 Takiguchi K, Yasugi S, Mizuno T (1988) Pepsinogen induction in chick stomach epithelia by reaggregated proventricular mesenchymal cells *in vitro*. Develop Growth & Differ 30: 241–250

21 Yasugi S (1979) Chronological changes in the inductive ability of the mesenchyme of the digestive organs in avian embryos. Develop Growth & Differ 21: 343–348

22 Yasugi S, Mizuno T (1974) Heterotypic differentiation of chick allantoic endoderm under the influence of various mesenchymes of the digestive tract. Wilhelm Roux's Arch 174: 107–116

23 Yasugi S, Mizuno T (1978) Differentiation of the digestive tract epithelium under the influence of the heterologous mesenchyme of the digestive tract in the bird embryos. Develop Growth & Differ 20: 261–267

24 Yasugi S, Mizuno T (1990) Mesenchymal-epithelial interactions in the organogenesis of digestive tract. Zool Sci 7: 159–170

ZOOLOGICAL SCIENCE 10: 449–454 (1993)

Immunohistochemical Expression of Inhibin-α Subunit in the Developing Rat Gonads

Satoshi Koike[1] and Tetsuo Noumura

Department of Regulation Biology, Faculty of Science, Saitama University, Urawa, Saitama 338, Japan

ABSTRACT—In order to investigate the roles of inhibin for rat gonadal differentiation, the expression of inhibin-α subunit in the developing rat gonads was determined. Sprague-Dawley rat gonads from the gestational day (GD) 13 through the postnatal day (PD) 21 were fixed in Methacarn solution and immunohistochemically stained with a polyclonal antibody against [Tyr^{30}] porcine inhibin α-chain (1–30)NH_2 subunit raised in the goat. During fetal period, inhibin-α subunit was detected only in male gonads: slight or moderate staining was observed in Sertoli/supporting cells on GDs 14 and 15, and moderate or marked staining in Leydig cells from GD 17 to 20. Reactivity was negative in female gonads and in the Müllerian and Wolffian ducts in both sexes during fetal period. After birth, inhibin-α subunit was moderately expressed in Sertoli cells and slightly in Leydig cells on PD 21 for males, and markedly in the granulosa cells for females. These results indicate that the expression of inhibin-α subunit is stage- and cell-specific during the gonadal development and the inhibin may participate in rat testicular differentiation.

INTRODUCTION

Inhibin is a gonadal glycoprotein which regulates pituitary FSH secretion [3, 16, 24] and synthesis [27, 29]. The purification, cloning and sequencing of inhibin cDNA showed that inhibin is a heterodimer comprised of an α-subunit (18 KD) and one of two related β-subunits (14 KD, βA and βB) joined by a disulfide bond [2, 5, 8, 10, 19, 23]. After the purification of inhibin protein, it has been obvious that inhibin plays a variety of types of roles as hormone, paracrine and autocrine regulators of cellular proliferation and functions in some mammals [for reviews, 4, 7, 14, 28, 30].

Expressions of inhibin α- and β-mRNAs were seen by using *in situ* hybridization in the gonads of embryonic rats from gestational day (GD) 14 to birth [22]. Inhibin-subunits mRNAs were localized by the stage-specific and tissue-specific manners in the developing rat gonads: α-mRNA was seen in the seminiferous tubules and interstitial tissue from GD 14, βA-mRNA only in the interstitial tissue just before birth and βB-mRNA over the tubules from GD 14. Immunohistochemical localizations of α- and β-subunit proteins were exhibited in the germ, Sertoli and Leydig cells in fetal rat testes and the germ cells in the fetal ovaries [20]. These results indicate that inhibin may play roles for gonadal cell proliferation and differentiation, like the cases of immature and adult gonads.

In the present study, immunohistochemical expression of inhibin-α subunit was chronologically clarified in the fetal and prepubertal rat gonads from gestational day 13 to postnatal day 21.

MATERIALS AND METHODS

Experimental animals

Crj: CD (Sprague-Dawley) rats in 13 to 20 weeks of age were housed in constant temperature ($22 \pm 2^{\circ}C$), relative homidity ($55 \pm 10\%$) and light-dark cycle (lights on 7:00–19:00). The animals fed purina chow and took the tap water *ad libitum*. Cohabitation was done in the evening in the 1:1 basis of male:female. In the next morning, copulation was checked by the presence of sperm in the vaginal smear. The day when sperm-positive

Accepted December 10, 1992
Received August 31, 1992

[1] Present address: Upjohn Pharmaceuticals Limited, Wadai, Tsukuba, Ibaraki 300-42, Japan

smear was found was designated as GD 0, and the day when litter was found was designated as postnatal day (PD) 0.

Preparation of tissues for immunostaining

Dams were sacrificed from GD 13 to 21 and neonates on PD 5, 11 and 21 by carbon dioxide. The gonads and genital ducts dissected from the fetuses and pups were fixed in Methacarn solution consisting of methanol, chloroform, and acetic acid, 6:3:1 in volume for a few hours to overnight. The sexes of fetuses were determined as described by Agelopoulou et al. [1]. Then, the tissues were dehydrated through a series of graded concentrations of ethanol and xylene, embedded in paraffin and sectioned in 5 μm thickness.

Immunohistochemistry

Sections were deparaffinized with xylene and hydrated in decreasing concentrations of ethanol, and incubated in 6 M urea (ICN Biomedicals Inc.) at room temperature for 30 min and to block endogenous peroxidases with 0.5% periodic acid (Sigma Chemical Co.) for 15 min. Sections were subsequently rinsed with 10 mM phosphate buffered saline (PBS, pH 7.4, Sigma Co.) for 20 min, blocked non-specific staining with 1.5% normal rabbit serum in 10 mM PBS including 0.5% casein (Wako Pure Chemical Industries Ltd.) for 20 min and then incubated with avidin and biotin blocking solution (Vector Laboratory Inc.) for 15 min, each at room temperature. After that, sections incubated overnight at 4°C with the polyclonal antibody against [Tyr^{30}] porcine inhibin α-chain (1–30)NH_2 raised in the goat (gifted from Prof. Sasamoto, Tokyo University of Agriculture and Technology) at a dilution of 1:40,000 in 10 mM PBS including 0.5% casein. Dose-response study indicated that this dilution of the antibody gave optimal labelling results. Following this incubation the sections were rinsed with PBS and then treated with 0.5% biotinylated rabbit anti-goat secondary antibody (Vector Lab. Inc. ABC-peroxidase staining kit Elite) diluted in 10 mM PBS containing 0.5% casein for 30 min at room temperature. Sections were again washed in PBS and subsequently incubated with 2% avidin-biotin complex (Vector Lab. Inc. ABC kit Elite) in 10 mM PBS for 60 min at room temperature. Avidin and biotin were prepared at least 30 min before applied to the sections to allow the complex to form. The sections were again washed in PBS, and the bound antibody was visualized with 0.05% 3,3′-diaminobenzidine tetrachloride (Sigma Chemical Co.) in 10 mM Tris-buffered saline (Sigma Chemical Co.) and 0.01% H_2O_2 for 4 min.

Controls included (a) replacing the primary antibody with normal goat serum, (b) using the primary antibody that had been pre-incubated overnight at 4°C with 1 μg/ml porcine inhibin-α subunit (1–32) (Peninsula Lab. Inc.) before this mixture was applied to the section in order to check the specificity of the primary antibody and (c) omitting the primary antibody to check the specificity of the secondary antibody.

RESULTS

Specificity of antibody

Preparations which were stained with the antibody to inhibin, with the immunoneutralized antibody, and with normal goat serum were shown in Fig. 1. Inhibin antibody stained the immature rat Sertoli cells on PD 21, but the neutralized antibody or normal goat serum did not stain any cells. Therefore, these results showed that this polyclonal antibody specifically stained inhibin-containing cells, because Sertoli cells might be regarded as the major source of inhibin in the immature male rat [see reviews].

Immunohistochemical localization

The immunohistochemical localizations of inhibin-α subunit in developing gonads were summarized in Table 1. The first positive staining was gained in most of the Sertoli cells on GD 14 (Fig. 2. A) and this sign was also seen in a few Sertoli cells on GD 15. At the second, the Leydig cells were positively stained from GD 17 to PD 5. The intensity of staining was marked on GDs 17 (Fig. 2. B) and 18 and gradually decreased with development. The number of the Leydig cells with positive reaction was also decreased after GD 20. However, female gonads and mesonephric tubules, Müllerian and Wolffian ducts in both

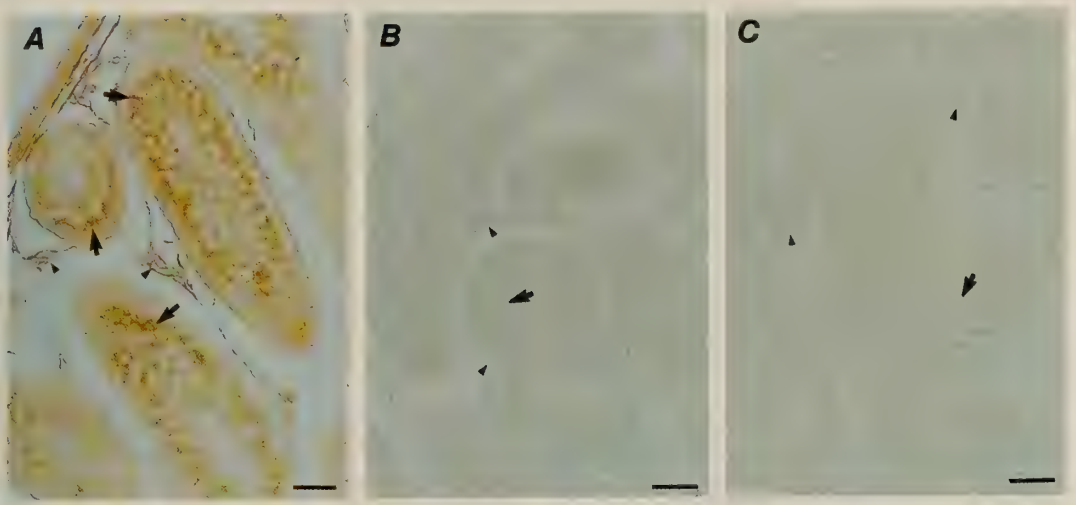

FIG. 1. Demonstration of staining specificity. Male gonads on PD 21 incubated with the inhibin-α antibody (A), with the neutralized antibody (B) or with normal goat serum (C). Staining is seen in the Sertoli cells (arrow) and the Leydig cells (arrow head) of A, but not those of B or C. Bars: 50 μm.

TABLE 1. Immunohistochemical localization of inhibin-α in the developing rat gonads

	Male							Female						
	Gonad				Duct		MT	Gonad				Duct		MT
	G	S	P	L	W	M		G	Gr	T	I	W	M	
GD 13	-	-			-		-	-				-		-
14	-	++			-	-	-	-	-		-	-	-	-
15	-	+		-	-	-	-	-	-		-	-	-	-
16	-	-		-	-	-	-	-	-		-	-	-	-
17	-	-		+++	-		-	-	-		-	-	-	-
18	-	-	-	+++	-		-	-	-		-	-	-	-
19	-	-	-	++/+	-			-	-		-		-	
20	-	-	-	++	-			-	-		-		-	
21	-	-	-	+/-	-			-	-		-		-	
PD 5	-	-	-	+/-	-			-	-	-	-		-	
11	-	-	-	-	-			-	-	-	-			
21	-	++	-	+/-	-			-	+++	-	-			

GD: Gestational day, PD: Postnatal day, G: Germ cell, S: Sertoli/supporting cell, P: Peritubular cell, L: Leyding cell, W: Wolffian duct, M: Müllerian duct, MT: Mesonephric tubule, Gr: Granulosa/supporting cell, T: Theca cell, I: Interstitial/stromal cell, Grade, −: No detectable, +: Slight but above background levels, ++: Moderate, +++: Marked staining, Shade box was shown that the cells or tissues were not found in that day.

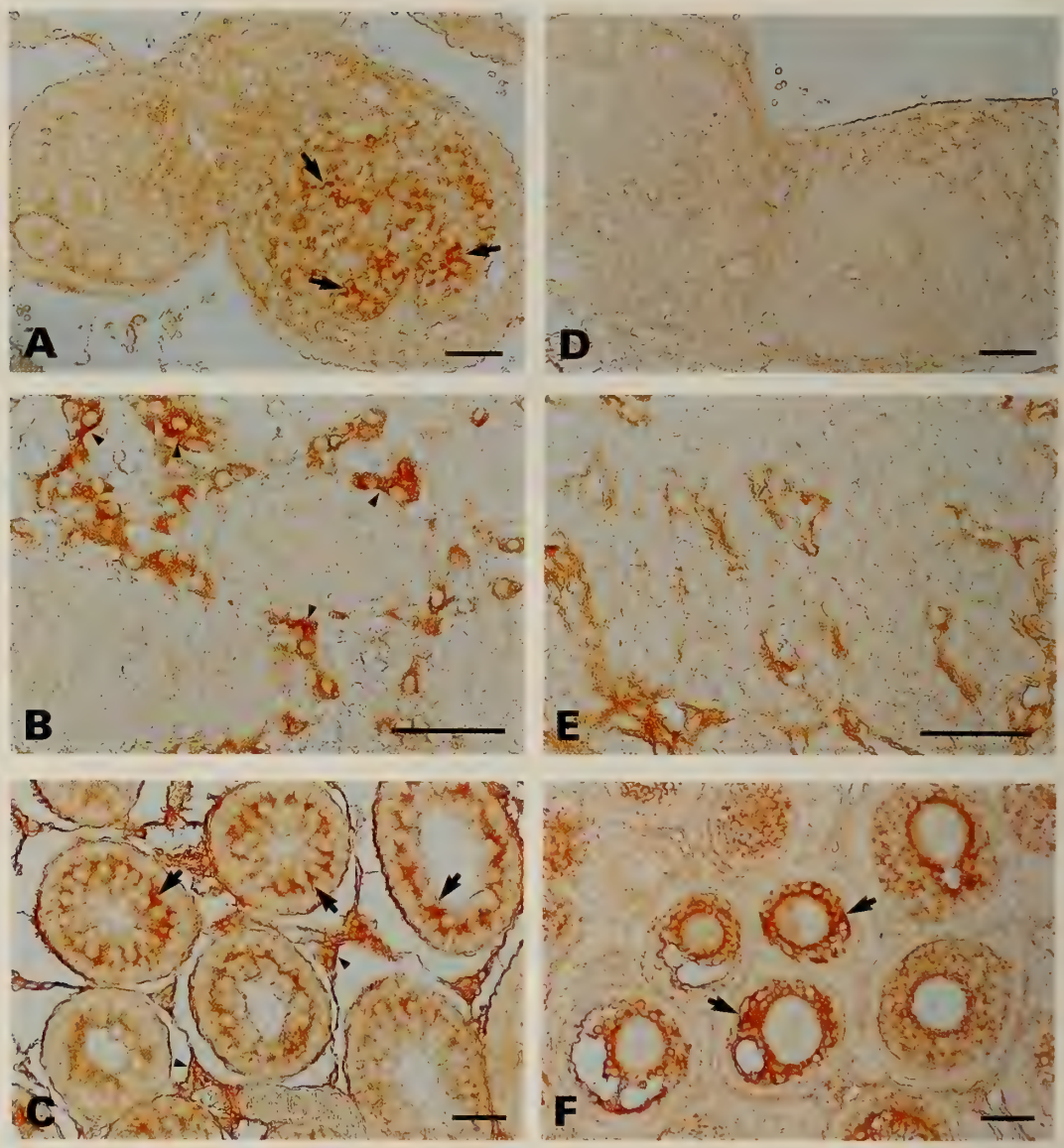

FIG. 2. Immunohistochemical localizations of inhibin-α in the perinatal gonads. (A) Male gonad on GD 14 shows the moderate staining in the Sertoli cells (arrow). (B) Male gonad on GD 17 expresses the marked staining in the Leydig cells (arrow head). (C) Male gonad on PD 21 is stained moderately in the Sertoli cells (arrow) and weakly in the Leydig cells (arrow head). (D) and (E) Female gonads on GDs 14 and 17, respectively, do not express any positive sign. (F) Female gonad on PD 21 expresses the marked reactivity in the granulosa cells (arrow). Bars: 50 μm.

sexes were negative during prenatal period (Fig. 2. D and E).

During postnatal period, positive staining was observed in most of the Sertoli cells for male gonads and the granulosa cells for female gonads on PD 21 (Fig. 2. C and F), and the intensity of staining was moderate or marked. The slight and/or faint staining was found in the Leydig cells on PDs 5 and 21. However, there were no detectable staining to the antibody in any other cells.

DISCUSSION

Pattern of immunohistochemical expression of inhibin-α subunit was partially consistent with the *in situ* identification of its mRNA [22]. Inhibin-α mRNA was localized in the tubular and interstitial tissues of male gonads during the third trimester gestational period from GD 14 to GD 21. Ogawa et al. [20] reported that inhibin-immunoreactivity was seen in the tubular and interstitial cells for males and the germ cells for females on GD 18.5. But in this experiment, inhibin-α subunit protein was only expressed in Sertoli cells on GDs 14 and 15, and in Leydig cells from GD 17. This inconsistency might be depend on the applicaiton of different types of antibodies, because antigens used were [Tyr^{20}] inhibin-α subunit (1–20) by Ogawa *et al.* [20] but [Tyr^{30}] porcine inhibin α-chain (1–30)NH_2 in our experiment.

Positive reactions in Sertoli cells on GDs 14 and 15 suggest that inhibin might be related to the testicular differentiation of the gonad, especially to the formation of seminiferous tubules and aggregation of the Sertoli cells around the germ cells like activin-A and -B, the homodimers of inhibin-βA and -βB subunits, in immature rat testis [13] because the sexual differentiation of gonad begins from the late GD 13 [11, 12, 17]. However an elucidation of the exact role of inhibin and/or inhibin-α subunit for the seminiferous tubule formation or other developmental events will require further investigation.

This is the first report of the positive staining in the fetal Leydig cells from GD 17. Immunoreactivity in purified Leydig cells which prepared from adult rats had been shown by Sharpe *et al.* [25] and Risbridger *et al.* [21]. Sharpe et al. [25] reported that Leydig cells in adult rats made little contribution to the intratesticular and blood levels of inhibin. However, inhibin modulates LH-induced androgen biosynthesis by testicular cells [9]. Leydig cells have synthetic ability of steroid hormones during the late gestation period. Therefore, inhibin expression in the fetal Leydig cells after GD 17 indicates that inhibin might modulate to the steroidogenesis in the fetal Leydig cells. Further study is needed to elucidate the role of inhibin on steroidogenesis and/or other physiological roles in the fetal Leydig cells.

Postnatal expression of inhibin in the Sertoli and granulosa cells was consistent with many previous works [see reviews and 18]. Inhibin contributes to negative feedback loop of FSH secretion from the pituitary in the immature rats. And also inhibin is concerned with the paracrine roles for testicular and ovarian functions: steroidogenesis in the Leydig and thecal cells, increase in the number of follicles, and germ cell-Sertoli cell interaction in immature and mature rats [see reviews and 6, 26].

Recently, Matzuk *et al.* [15] reported that inhibin-α was a tumor-suppressor gene of the gonadal stromal tumors by using inhibin-α-deficient mice. Mice homozygous for the deleted α-subunit gene were susceptible to the development of differentiated gonadal stromal tumors as early as 4 weeks of age, but were normal for the development of the gonads and external genitalia before tumor development by histological examination. Therefore, it is suggested that other factors may be participated in the sexual differentiation of the gonads.

ACKNOWLEDGMENTS

We are very grateful to Prof. S. Sasamoto, Tokyo University of Agriculture and Technology, for supplying us with a polyclonal antibody against porcine inhibin α-chain.

REFERENCES

1 Agelopoulou R, Magre S, Patsavoudi E, Jost A (1984) Initial phases of the rat testis differentiation in vitro. J Embryol Exp Morph 83: 15–31

2 Bardin CW, Morris PL, Chen C-L, Vogl-mayr J, Rivier J, Vale, WW (1987) Testicular inhibin: structure and regulation by FSH, androgens and EGF. In "Inhibin-Non-Steroidal Regulation of Follicle Stimulating Hormone Secretion" Ed by HG Burger, DM de Kretser, JK Findlay, M Igarashi, Raven Press, New York, Serono symposia Publications, 42: 179–190

3 Campen CA, Vale W (1988) Interaction between purified ovine inhibin and steroids on the release of gonadotropins from culture rat pituitary cells. Endocrinology 123: 1320–1328

4 de Jong FH, Grootenhuis AJ, Klaij IA, van Beurden WMO (1990) Inhibin and related proteins: Localization, regulation, and effects. In "Circulating Regulatory Factors and Neuroendocrine Function"

Ed by JC Porter, D Jezova, Plenum Press, New York, pp 271–293

5 Esch FS, Shimasaki S, Cooksey K, Mercado M, Mason AJ, Ying S-Y, Ueno N, Ling N (1987) Complementary deoxyribonucleic acid (cDNA) cloning and DNA sequence analysis of rat ovarian inhibins. Mol Endocrinol 1: 388–396

6 Fauser BCJM, Hsueh AJW (1988) Growth factors: Intragonadal regulation of differentiated functions. In "Progress in Endocrinology 1988 Vol 1" Ed by H Imura, K Shizume, S Yoshida, Elsevier Science Publishers, Amsterdam, pp 451–456

7 Findlay JK, Clarke IJ, Luck MR, Rodgers RJ, Shukovski L, Robertson DM, Klein R, Murray JF, Scaramuzzi RJ, Bindon BM, O'Sea T, Tsonis CG, Forage RG (1991) Peripheral and intragonadal actions of inhibin-related peptides. J Reprod Fert, Suppl 43: 139–150

8 Fukuda M, Miyamoto K, Hasegawa Y, Nomura M, Igarashi M, Kanagawa K, Matsuo H (1986) Isolation of bovine follicular fluid inhibin of about 32 kDa. Mol Cell Endocrinol, 44: 55–60

9 Hsueh AJW, Dahl KD, Vaughan J, Tucker E, Rivier J, Bardin CW, Vale W (1987) Heterodimers and homodimers of inhibin subunits have different paracrine action in the modulation of luteinizing hormone-stimulated androgen biosynthesis. Proc Natl Acad Sci USA 84: 5082–5086

10 Knight PG (1991) Identification and purification of inhibin and inhibin-related proteins. J Reprod Fert, Suppl 43: 111–123

11 Magre S, Jost A (1980) The initial phases of testicular organogenesis in the rat. Arch Anat Microsc Morphol Exp 69: 297–318

12 Magre S, Jost A (1991) Sertoli cells and testicular differentiation in the rat fetus. J Elect Microsc Tech 19: 172–188

13 Mather JP, Attie KM, Woodruff TK, Rice GC, Phillips DM (1990) Activin stimulates spermatogonial proliferation in germ-Sertoli cell cocultures from immature rat testis. Endocrinology 127: 3206–3214

14 Mather JP, Woodruff TK, Krummen LA (1992) Paracrine regulation of reproductive function by inhibin and activin. Proc Soc Exp Biol Med 201: 1–15

15 Matzuk MM, Finegold MJ, Su J-GJ, Hsueh AJW, Bradley A (1992) α-inhibin is a tumour-suppressor gene with gonadal specificity in mice. Nature 360: 313–319

16 McCullagh GR (1932) Dual endocrine activity of the testes. Science 76: 19–20

17 Merchant-Larios H, Villalpando I, Taketo-Hosotani T (1991) Gonadal morphogenesis in mammals. In "Reproduction, Growth and Development" Ed by A Negro-Vilar, G Perez-Palacios, Raven Press, New York, Serono Symposia Publications 71: 1–11

18 Merchenthaler, I, Culler MD, Petrusz P, Negro-Vilar A (1987) Immunocytochemical localization of inhibin in rat and human reproductive tissues. Mol Cell Endocrinol 54: 239–243

19 Miyamoto K, Hasegawa Y, Fukuda M, Nomura M, Igarashi M, Kanagawa K, Matsuo H (1985) Isolation of porcine follicular fluid inhibin of 32 k deltons. Biochem Biophys Res Commun 129: 396–403

20 Ogawa K, Kurohmaru M, Shiota K, Takahashi M, Nishida T, Hayashi Y (1991) Histochemical localization of inhibin and activin α, βA and βB subunits in rat gonads. J Vet Med Sci 53: 207–212

21 Risbridger GP, Clements J, Robertoson DM, Drummond AE, Muir J, Burger HG, de Kretser DM (1989) Immuno- and bioactive inhibin and inhibin α-subunit expression in rat Leydig cell culture. Mol Cell Endocrinol 66: 243–247

22 Roberts V, Vale W (1991) Expression of inhibin/activin subunit messenger ribonucleic acids during rat embryogenesis. Endocrinology 128: 3122–3129

23 Robertson DM, Foulds LM, Leversha L, Morgan FJ, Hearn MT, Burger HG, Wettenhall RE, de Kretser DM (1985) Isolation of inhibin from bovine follicular fluid. Biochem Biophys Res Commun 126: 220–226

24 Schwartz NB, Channing CP (1977) Evidence of ovarian "inhibin": suppression of the secondary use in serum follicle stimulating hormone levels in proestrous rats by injection of porcine follicular fluid. Proc Natl Acad Sci USA 71: 5721–5724

25 Sharpe RM, Kerr JB, Maddocks S (1988) Evidence for a role of Leydig cells in the control of the intratesticular secretion of inhibin. Mol Cell Endocrinol 60: 243–247

26 Skinner MK (1991) Cell-cell interactions in the testis. Endocr Rev 12: 45–77

27 Vale W, Rivier C, Hsueh A, Campen C, Meunier H, Bicsak T, Vaughan J, Corrigan A, Bardin W, Sawchenko P, Petraglia F, Yu J, Plotsky P, Spiess J, River J (1988) Chemical and biological characterization of the inhibin family of protein hormones. Rec Prog Horm Res 44: 1–38

28 Vale W, Hsueh A, Rivier C, Yu J (1991) The inhibin/activin family of hormones and growth factors. In "Peptide Growth Factors and Their Receptors II" Ed by MB Sporn, AB Roberts, Springer-Verlag, New York, pp 211–248

29 Ying S-Y (1987) Inhibins and activins: Chemical properties and biological activity. Proc Soc Exp Biol Med 186: 253–264

30 Ying S-Y (1988) Inhibins, activins, and follistatins: Gonadal proteins modulating the secretion of follicle-stimulating hormone. Endocr Rev 9: 267–293

ZOOLOGICAL SCIENCE 10: 455–466 (1993)

The Development of the Hermaphroditic Gonad in Four Species of Dicyemid Mesozoans

Hidetaka Furuya, Kazuhiko Tsuneki
and Yutaka Koshida

Department of Biology, College of General Education, Osaka University, Toyonaka 560, Japan

ABSTRACT—The development of the functionally hermaphroditic gonad, the infusorigen, in four dicyemid species, *Dicyema orientale, D. acuticephalum, D. japonicum,* and *D. misakiense,* was studied in fixed materials with the aid of a light microscope. After an agamete (axoblast) undergoes the first division and excludes a paranucleus, the resulting cell undergoes the second division. Afterwards, three different types of cell lineage can be identified. (1) In *D. orientale,* the first oogonium is produced by the second division, and the axial cell of an infusorigen and the first spermatogonium are produced by the third division. (2) In *D. acuticephalum,* the first oogonium is produced by the second division, the axial cell is produced by the third division, and the spermatogonium is produced by the fourth division. The fourth division also produces the first oogonium of another egg line. (3) In *D. japonicum* and *D. misakiense,* the first spermatogonium is produced by the second division, and the axial cell and the first oogonium are produced by the third division. In all species examined, oogonia occupy the outer surface of the axial cell and spermatogonia are incorporated into the axial cell. In this way, the spermatogenesis proceeds within the cytoplasm of the axial cell. Mature infusorigens of these four species consist of about twenty cells. The respective numbers of oocytes and spermatozoa produced in each infusorigen are roughly equal in these four species.

INTRODUCTION

Dicyemid mesozoans are found in the renal sac of benthic cephalopod molluscs. The bodies of dicyemids consist of only 20 to 40 cells and they are organized very simply [12, 14]. It has long been debated whether dicyemids are truly primitive multicellular animals [2, 7, 8, 11, 17], or whether they are actually organisms that have degenerated as a result of parasitism [5, 12, 14, 19].

As well known, two kinds of adult forms, nematogens and rhombogens, are found in dicyemids. Asexual reproduction occurs within the axial cell of a nematogen, while sexual reproduction takes place within the axial cell of a rhombogen. The features of the sexual reproduction are unique [12, 15]. A hermaphroditic gonad, which is called an infusorigen, is formed within the axial cell of a rhombogen, and fertilization occurs around the infusorigen. The zygote undergoes cleavages and develops into an infusoriform larva within the axial cell. The process of the fertilization and embryogenesis of infusoriforms have been described in detail [1, 3, 18], but the development of infusorigens has been studied only sporadically [10, 12, 14]. No research on the patterns of development of infusorigens has been performed from a systematic perspective. We examined the development of the infusorigens of *Dicyema orientale, D. acuticephalum, D. japonicum,* and *D. misakiense,* and found three different types of cell lineage. In this report, these three different cell lineages that can be followed during the development of infusorigens are described. In addition, we provide an estimate of the numbers of gametes that are produced and of the numbers of embryos that are generated in one infusorigen, and we discuss the reproductive capacity of infusorigens.

Accepted April 13, 1993
Received March 13, 1993

MATERIALS AND METHODS

Seventeen individual octopuses, *Octopus vulgaris,* and three cuttlefish, *Sepioteuthis lessoniana,* were purchased or collected by the authors in the waters off the western coast of Japan. *Dicyema orientale* from *Sepioteuthis lessoniana* and three species of dicyemids, namely, *D. acuticephalum, D. japonicum,* and *D. misakiense,* from *Octopus vulgaris* were examined in the present study.

After the host cephalopods had been sacrificed, their renal sacs were taken out and smeared directly on glass slides. Smeared dicyemids were immediately fixed with Carnoy's fixative or with alcoholic Bouin's solution (a mixture of absolute ethanol saturated with picric acid, formalin and acetic acid, 15:5:1, v/v). Specimens fixed with Carnoy's fixative were stained with Feulgen's stain or by the PAS method and were poststained with Ehrlich's hematoxylin and light green. Specimens fixed with alcoholic Bouin's solution were stained with Ehrlich's hematoxylin and light green only. The development of infusorigens in the axial cells of rhombogens was observed with the aid of a light microscope under an oil-immersion objective at a final magnification of 2000 diameters.

RESULTS

Dicyema orientale
(Figs. 1, 2, 7, and Table 1)

At the stage of the transition from the nematogen to the rhombogen, a number of agametes (axoblasts) degenerate. The remaining agametes, that number about 10 to 20, grow larger and

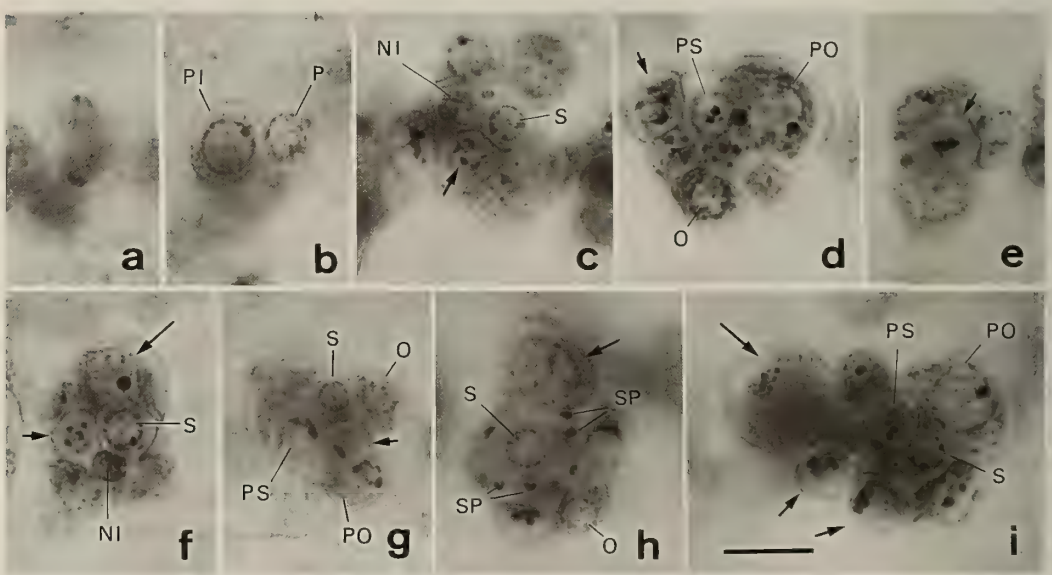

Fig. 1. Light micrograghs of developing infusorigens within the axial cells of rhombogens of *D. orientale.* Photographs were taken at a magnification of 2000 diameters under an oil-immersion objective. Scale bar represents 10 μm. (a): An agamete undergoing an unequal first division. (b): A progenitor cell of an infusorigen (PI) and a paranucleus (P) being produced after the first division. (c)-(i): Infusorigens. (c): The arrow indicates the zygotene stage of a primary spermatocyte. (d): The arrow indicates the zygotene stage of a primary oocyte. (e): The arrow indicates the metaphase of a primary spermatocyte. (f): The short arrow indicates the metaphase of a secondary spermatocyte viewed from the pole and the long arrow indicates the pachytene stage of a primary oocyte. The nucleolus is conspicuously large in the primary oocyte at the pachytene stage. (g): The arrow indicates the metaphase of a secondary spermatocyte viewed from the side. (h): The arrow indicates the diplotene stage of a primary oocyte. (i): The short arrows indicate the bouquet stage of a primary oocyte and the long arrow indicates the anaphase of a primary oocyte.
NI, axial cell nucleus of infusorigen; O, oogonium; PO, primary oocyte; PS, primary spermatocyte; S, spermatogonium; SP, spermatozoon.

undergo an unequal division (Fig. 1a). Each smaller daughter cell loses its cytoplasm and becomes just a nucleus, known as a paranucleus, and it lies near the cell from which it arose (Fig. 1b). The paranucleus stays within the axial cell of the rhombogen and grows to the same size as the axial cell nucleus of the rhombogen. The larger daughter cell, namely, the progenitor of the infusorigen,

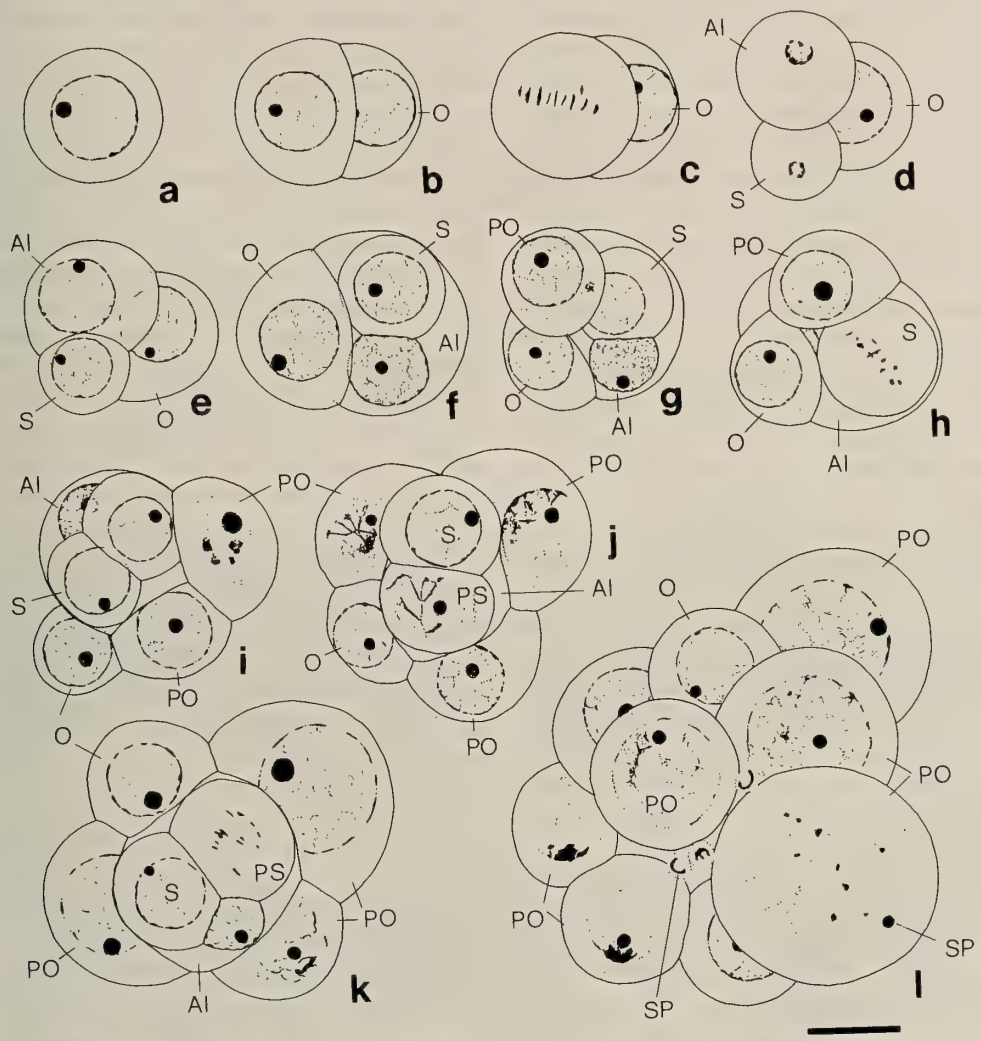

FIG. 2. Sketches of the development of the infusorigen of *D. orientale*. Bar represents 5 μm. (a): A progenitor cell of infusorigen. (b) and (c): Two-cell stage. In (c), the metaphase of the third division is seen. (d)-(f): Three-cell stage. In (d) and (e), both the axial cell (AI) and the first spermatogonium (S) produced after the third division are shown. In (f), the first spermatogonium (S)is embedded in the axial cell (AI). (g): Four-cell stage. (h): Five-cell stage. The metaphase of the first spermatogonium (S)is seen. (i): Six-cell stage in optical section. (j): Eight-cell stage in optical section. Primary oocyte (PO) at the upper right corner is in the zygotene stage. (k): Nine-cell stage in optical section. The anaphase of the primary spermatocyte (PS) is seen. (l): The infusorigen. A primary oocyte (PO) at the beginning of anaphase is seen in the lower right corner. This oocyte contains a spermatozoon (SP) in the cytoplasm. Spermatozoa (SP) in the center are emerging from the axial cell of the infusorigen.

AI, axial cell of infusorigen; O, oogonium; PO, primary oocyte; PS, primary spermatocyte; S, spermatogonium; SP, spermatozoon.

undergoes a nearly equal division to the two-cell stage (Figs. 2b and c). One of these cells becomes the first oogonium. The other cell undergoes an equal division and produces the first spermatogonium and an axial cell of the infusorigen (Figs. 2c-e). The axial cell of the infusorigen does not divide further, but it increases in size and incorporates the spermatogonium into its cytoplasm (Fig. 2f). The first oogonium remaining on the periphery of the infusorigen divides equally to generate a second oogonium and a primary oocyte (Fig. 2g). In the same way, the second oogonium produces a third oogonium and a primary oocyte. Very early primary oocytes can be distinguished from oogonia since the nucleolus in the former is larger than that in the latter (Figs. 2g and h). In primary oocytes, at the prophase of the first meiotic division, the chromatin becomes aggregated on one side of the nucleus and the nuclear membrane becomes indistinct on the side opposite the aggregation of chromatin (Figs. 1i and 2l). These features are characteristic of the so-called "bouquet stage" of the prophase of the meiotic division. The primary oocytes gradually become larger and chromosomes become visible as thick threads in the nuclei, features that characterize the zygotene stage. At this stage, both ends of the chromosomes are attached to the nuclear envelope (Figs. 1d and 2j). During the pachytene stage, the chromosomes become indistinct and the nucleus becomes similar in appearance to the interphase nucleus. At this stage, the nucleus includes a very large nucleolus (Figs. 1f and 2k-l). When primary oocytes have grown to about 7 μm in diameter, bead-like chromosomes appear in the nucleus. These oocytes are at the diplotene stage of meiotic prophase (Fig. 1h). The primary oocytes finally reach about 12 μm in diameter (Fig. 1i).

The first spermatogonium within the axial cell of the infusorigen undergoes an equal division and produces a spermatogonium and a primary spermatocyte (Figs. 2h-j). The prophase of the first meiotic division of the primary spermatocyte proceeds similarly to that of the primary oocyte, but the size of the primary spermatocyte does not change throughout the prophase (Figs. 1c, 1d, 2j, and 2k). After the first meiotic division, a pair of secondary spermatocytes enters interkinesis. At this stage, no chromosome structures can be seen. Within the axial cell of maturing infusorigen, usually two secondary spermatocytes are observed in addition to a spermatogonium and an axial cell nucleus. Soon after the second meiotic division, transformation of spermatids into spermatozoa occurs. Mature spermatozoa are composed of a small amount of deeply stained chromatin and a surrounding small clear area, interpreted as cytoplasm. The cell membrane is hardly visible. The entire spermatozoon is about 2 μm in diameter. The chromatin is usually horseshoe-shaped, but sometimes it is irregularly ring- or dot-shaped (Figs. 1h and 2l). After emerging from the axial cell of an infusorigen, the spermatozoon enters the primary oocyte (Fig. 2l). Fertilized oocytes remain adhering to the axial cell up to the time at which the first polar bodies are produced. Spermatozoa often adhere to the outer surface of the axial cell, to the oogonia, or to the primary oocytes, or they may appear between the oocyte and the axial cell (Fig. 2l). The spermatozoon within the oocyte lies at the periphery of the metaphase plate of the first meiotic division of the oocyte (Fig. 2l). The first polar bodies are composed of a mass of chromatin and a clear cytoplasmic area that is surrounded by a delicate membrane. They become detatched from the oocytes and often remain intact, but finally they degenerate.

The numbers of spermatogonia and primary spermatocytes, the number of spermatozoa within and on the surface of the infusorigen, and the numbers of oogonia and primary oocytes per infusorigen are shown in Table 1. *D. orientale*, being relatively long, has a large number of infusorigens and infusoriform embryos in the axial cell of a rhombogen (Table 1).

Dicyema acuticephalum
(Figs. 3, 4, 7, and Table 1)

One or rarely two agametes become larger and undergo an unequal division at the beginning of the rhombogen stage (Figs. 3a and 4a). The larger daughter cell is the progenitor of an infusorigen, while the smaller cell becomes a paranucleus (Fig. 3b). The progenitor cell of the infusorigen undergoes an equal division, which results in the two-cell

TABLE 1. The numbers of infusorigens, gametes, and embryos within the axial cells of rhombogens

Species	Body length of rhombogens (mm)	No. of infusorigens per rhombogen	No. of spermatogonia and primary spermatocytes per infusorigen[1)]
Dicyema orientale[2)]	~3.5	7–25	3.27±0.71
D. acuticephalum	~0.8	1– 2	3.38±0.86
D. japonicum	~1.0	1– 2	4.06±1.28
D. misakiense	~1.0	1– 2	4.04±1.24

Species	No. of spermatozoa per infusorigen[1)]	No. of oogonia and primary oocytes per infusorigen[1)]	No. of infusorform embryos per rhombogen
D. orientale[2)]	11.78±5.21	10.26±2.30	~250
D. acuticephalum	12.67±4.70	9.25±1.43	~ 20
D. japonicum	10.00±3.91	13.43±3.47	~ 35
D. misakiense	11.59±4.70	12.04±3.76	~ 35

[1)] Values represent means±S.D. and are based on results from 50 mature infusorigens.
[2)] *D. orientale* was described only with nematogens [16] and no rhombogens have been reported.

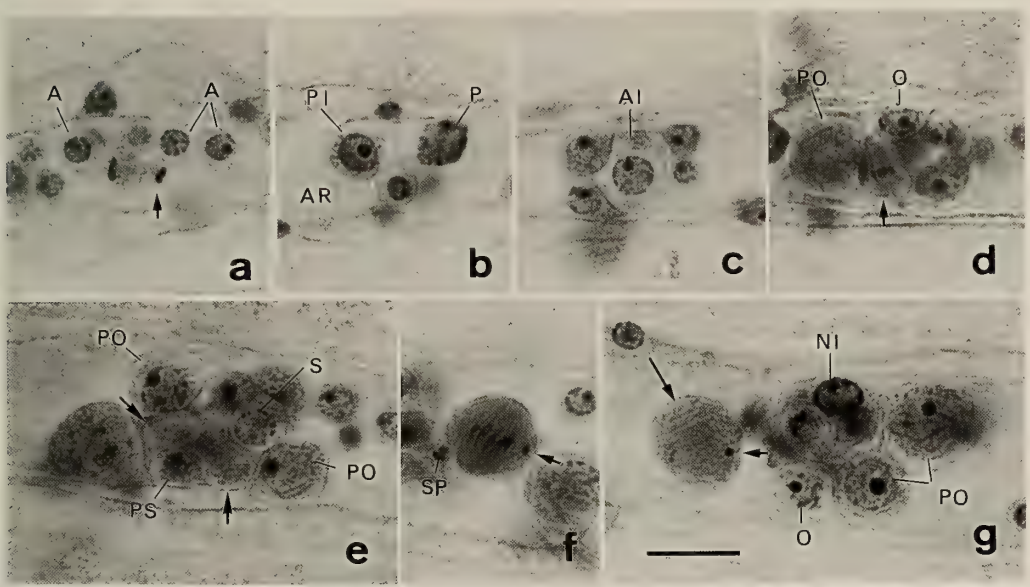

FIG. 3. Light micrographs of developing infusorigens within the axial cells of rhombogens of *D. acuticephalum*. Bar represents 10 μm. (a): Agametes (A). A telophase figure of the first unequal division is seen in the center. The arrow indicates a smaller daughter cell that becomes a paranucleus. (b): A progenitor cell of an infusorigen (PI) and a paranucleus (P) within an axial cell (AR) of a rhombogen. (c): Five-cell stage. (d)-(g): Infusorigens. (d): The arrow indicates the metaphase of a primary spermatocyte viewed from the side. (e): The arrows indicate the interkinesis stage of the secondary spermatocytes. (f): The metaphase of a primary oocyte viewed from the side. The arrow indicates a sperm within the oocyte. (g): The large arrow indicates the anaphase of a secondary oocyte. The short arrow indicates a sperm within it. The primary oocyte (PO) is at the pachytene phase.
AI, axial cell of infusorigen; NI, axial cell nucleus of infusorigen; O, oogonium; PO, primary oocyte; PS, primary spermatocyte; S, spermatogonium; SP, spermatozoon.

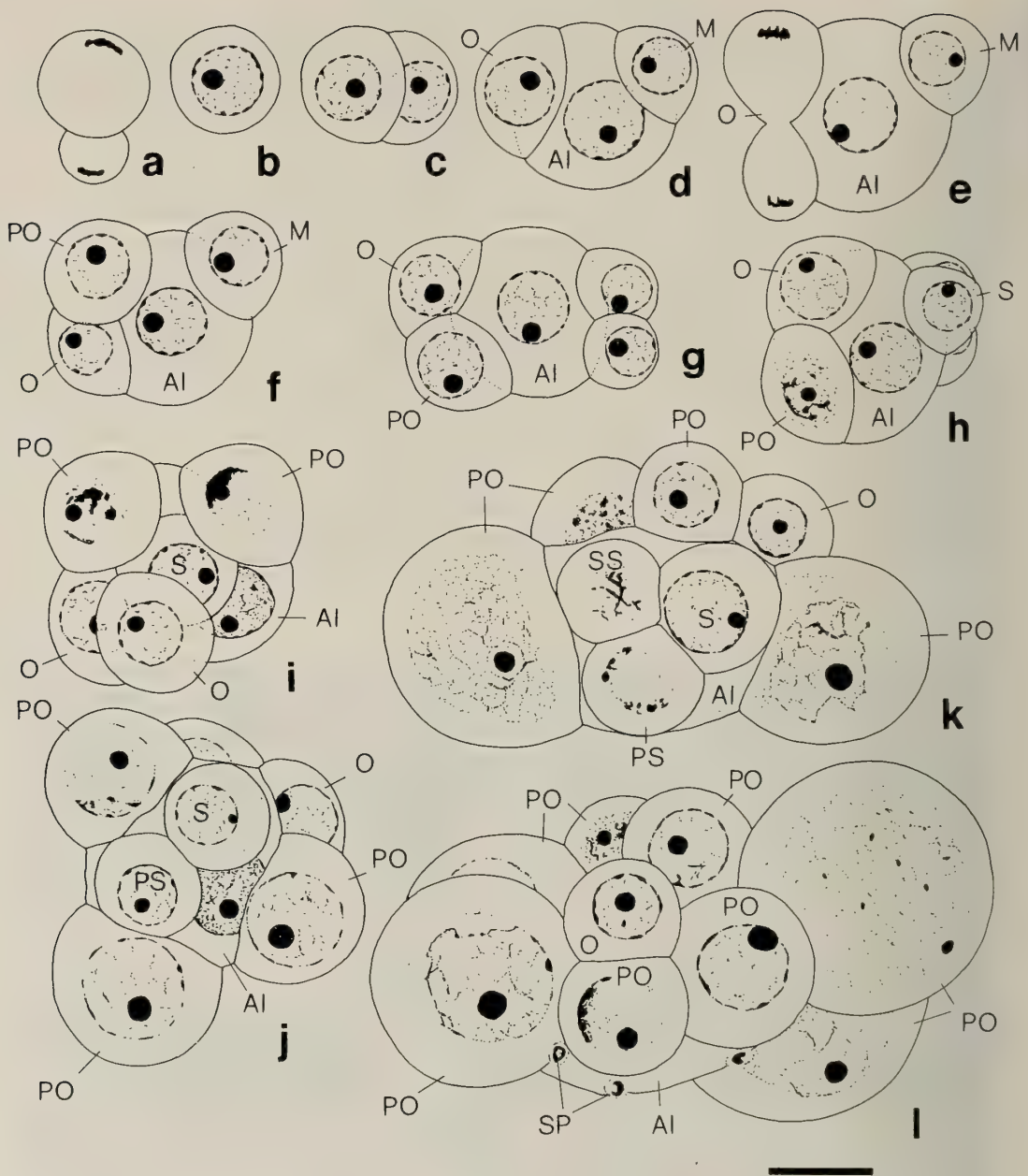

FIG. 4. Sketches of the development of the infusorigen of *D. acuticephalum*. Bar represents 5 μm. (a): The telophase of the first division of the agamete. The smaller cell becomes a paranucleus. (b): The progenitor cell of an infusorigen. (c): Two-cell stage. (d)-(e): Three-cell stage. In (e), the telophase of an oogonium (O) is seen. The cell marked M is a mother cell of an oogonium and a spermatogonium. (f): Four-cell stage. (g): Five-cell stage. Two cells on the right side of the axial cell, produced by the division of the mother cell (M in e and f), become the first spermatogonium and the oogonium of one egg line, respectively. (h)-(i): Six-cell stage. In (i), the first spermatogonium (S) is embedded in the axial cell (AI) and the primary oocytes (PO) are at the bouquet stage. (j): Eight-cell stage in optical section. (k): An infusorigen in optical section. A secondary spermatocyte (SS) is seen in the axial cell (AI). (l): An infusorigen (surface view). The anaphase of a primary oocyte (PO)is seen in the upper right corner.

AI, axial cell of infusorigen; M, mother cell of the first spermatogonium and the oogonium; O, oogonium, PO, primary oocyte; PS, primary spermatocyte; S, spermatogonium; SP, spermatozoon; SS, secondary spermatocyte.

stage (Fig. 4c). One of these cells becomes the first oogonium, and the other cell increases in size and divides unequally. The larger cell, the axial cell of the infusorigen, undergoes no further divisions (Fig. 4d), while the smaller cell divides equally and produces both the first spermatogonium and an oogonium (Fig. 4g). Both cells are so similar in size and appearance that they cannot be distinguished until one of them enters the mitotic phase on the periphery of the infusorigen or is embedded in the axial cell (Fig. 4i). *D. acuticephalum* has two egg lines (Fig. 7B). The oogonium of each egg line further divides and generates an oogonium and a primary oocyte (Figs. 4e-i). At around the six-cell stage, the first spermatogonium is incorporated into the axial cell of the infusorigen (Fig. 4i). The process of spermatogenesis is similar to that observed in *D. orientale*. The chromatin of spermatozoa usually forms a horseshoe or an irregular ring (Fig. 4l). The numbers of spermatogonia and primary spermatocytes, and other numerical data, are shown in Table 1.

Dicyema japonicum and *Dicyema misakiense* (Figs. 5–7 and Table 1)

The developmental pattern of the infusorigen is the same in *D. japonicum* and *D. misakiense*. One or rarely two of the agametes become larger and undergo an unequal division at the beginning of the rhombogen stage. The smaller cell is transformed into a paranucleus, while the larger cell becomes the progenitor of an infusorigen (Fig. 5a). This latter cell divides unequally and produces two cells (Figs. 5b and 6a). The smaller cell often undergoes an equal division (Fig. 6b), but one of the daughter cells soon degenerates. The remaining cell is the first spermatogonium (Fig. 6c). The larger cell divides equally and, thus, produces the first oogonium and an axial cell of the infusorigen (Figs. 5c and 6d). The axial cell undergoes no further divisions and increases in size. The first spermatogonium is incorporated into the cytoplasm of the axial cell (Fig. 6e) and its nucleus increases in size (Fig. 6f). The oogonium gives rise

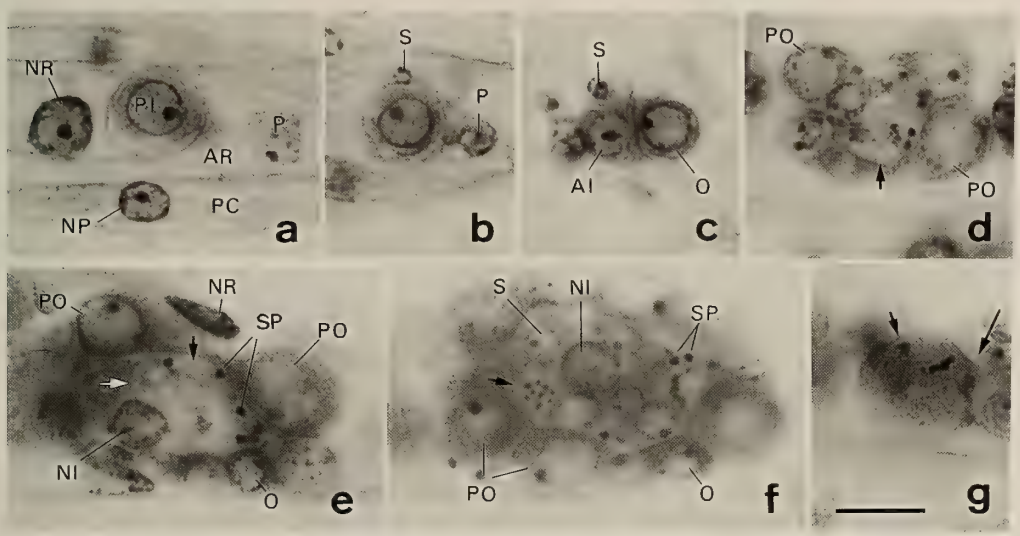

FIG. 5. Light micrographs of developing infusorigens within the axial cells of rhombogens of *D. japonicum*. Bar represents 10 μm. (a): A progenitor cell of an infusorigen (PI), the axial cell of a rhombogen (AR), a peripheral cell nucleus (NP), an axial cell nucleus of a rhombogen (NR), a paranucleus (P), and peripheral cell cytoplasm (PC) can be seen. (b): Two-cell stage. (c): Three-cell stage. (d)-(f): Infusorigens. (d): The arrow indicates the metaphase of the primary spermatocyte. (e): The arrows indicate the interkinesis stage of a secondary spermatocyte. (f): The arrow indicates the metaphase of a secondary spermatocyte viewed from the pole. (g): The telophase of a primary oocyte. The long arrow indicates the first polar body. The short arrow indicates the sperm within the primary oocyte.
AI, axial cell of infusorigen; NI, axial cell nucleus of infusorigen; NR, axial cell nucleus of rhombogen; O, oogonium; P, paranucleus; PO, promary oocyte; S, spermatogonium; SP, spermatozoon.

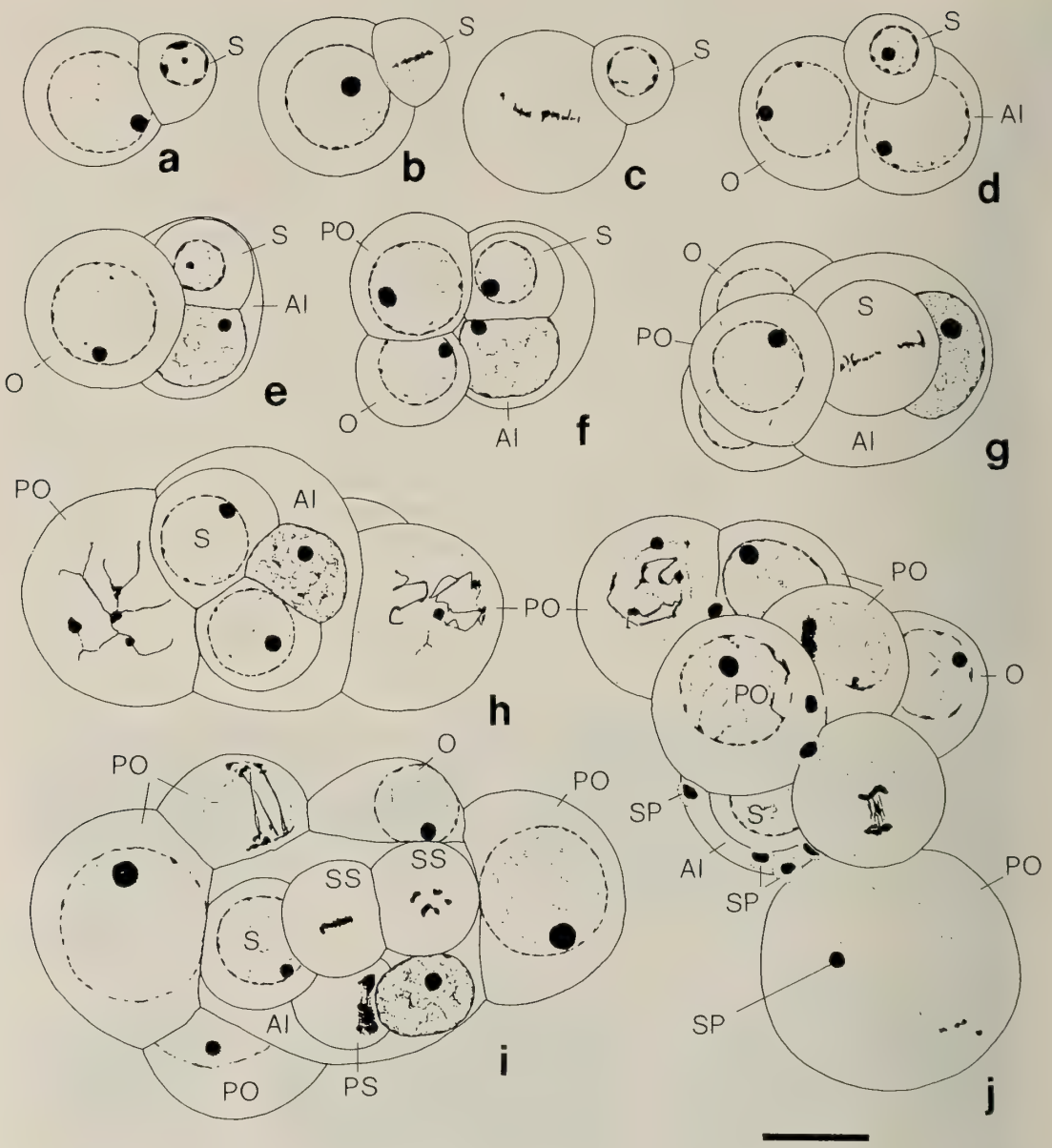

Fig. 6. Sketches of the development of infusorigens of *D. misakiense*. Bar represents 5 μm. (a)-(c): Two-cell stage. As seen in (b), the first spermatogonium (S) often divides quite early. In (c), the mother cell of both the first oogonium and the axial cell is in metaphase. (d)-(e): Three-cell stage. In (e), a spermatogonium (S) is embedded in the axial cell (AI). (f): Four-cell stage. (g): Five-cell stage. The metaphase of a spermatogonium (S) is seen. (h): Eight-cell stage in optical section. The primary oocytes (PO) at the zygotene stage are seen. (i): The infusorigen in optical section. The primary oocytes (PO at the left and right) at the pachytene stage and another oocyte (PO at the upper left corner) at the zygotene stage are seen. The metaphases of the secondary spermatocytes (SS) are also seen from the side (center) and from the pole (right). (j): The infusorigen (surface view). Some spermatozoa (SP) are emerging from the axial cell.
AI, axial cell of infusorigen; O,oogonium; PO, primary oocyte; PS, primary spermatocyte; S, spermatogonium; SP, spermatozoon; SS, secondary spermatocyte.

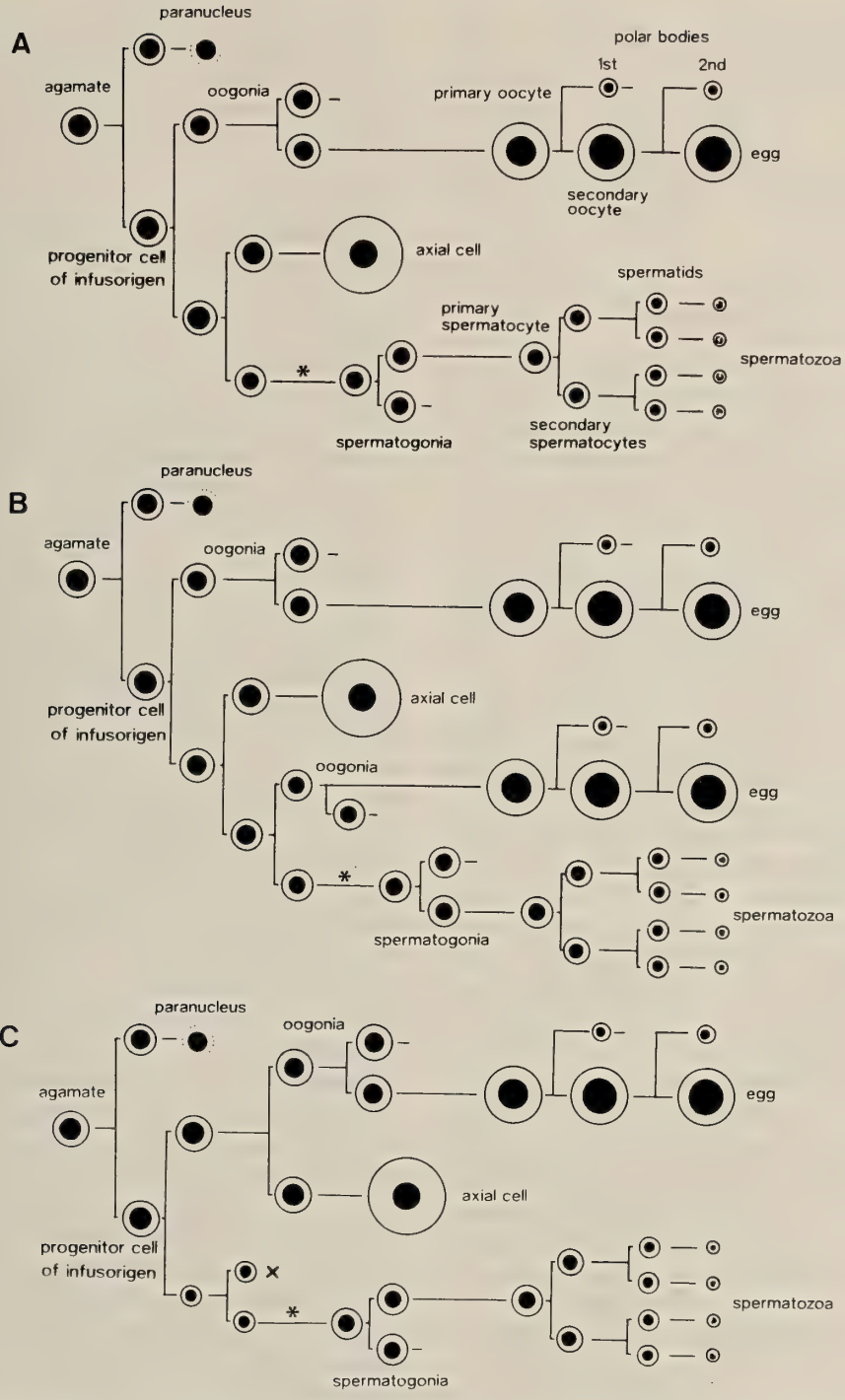

FIG. 7. The cell lineage of an infusorigen. (A): *D. orientale*. (B): *D. acuticephalum*. (C): *D. japonicum* and *D. misakiense*. The circle represents the cell and the central black area represents the nucleus. They are nearly scaled. The dotted circle means that the cytoplasm degenerates. At the site of the asterisk (*), the first spermatogonium is embedded in the axial cell. Short horizontal lines on right side of cells indicate that the cells proliferate further. In (c), the cross (x) means that the cell does not proliferate but degenerates.

to a new oogonium and a primary oocyte. Subsequent oogenesis and spermatogenesis proceed in the same manner as in *D. orientale* and *D. acuticephalum*. The nucleus of the spermatozoa is horseshoe- or dot-shaped, and the spermatozoa often aggregate (Figs. 5e, 5f, and 6j). The number of spermatozoa and other numerical data are shown in Table 1.

DISCUSSION

In the four species of dicyemid mesozoans studied herein, an agamete enlarged at the beginning of the rhombogen stage. In other species of dicyemids, Nouvel [14] and McConnaughey [12] also reported that an agamete enlarges at the very early stage of the rhombogen. This enlargement is interpreted as a sign of the beginning of the development of infusorigens. Then the agamete undergoes an unequal division and the smaller daughter cell becomes a paranucleus without contributing to the formation of an infusorigen. Although we can offer no explanation for the formation of a paranucleus, it is a constant feature and may, thus, be essential to the development of infusorigens.

Several differences were apparent in the cell lineage of the infusorigens of the four species (Fig. 7). Nevertheless, two common features were apparent; one is that the first spermatogonium is incorporated into an axial cell, in which spermatogenesis proceeds; and the other is that the oogonium remains at the periphery of the axial cell, where oogenesis occurs. The distinctive differences occur early in the development in the various species. Two patterns of cell lineage are distinguishable. One pattern is characterized by a second division that produces the first oogonium, and the other is characterized by a second division that produces the first spermatogonium. The former is seen in *D. orientale* and *D. acuticephalum*, and the latter in *D. japonicum* and *D. misakiense* (Fig. 7). In *D. orientale*, *D. japonicum*, and *D. misakiense*, all types of cell differentiate up to the third division. In *D. acuticephalum*, by contrast, spermatogonia are generated only after the fourth division (Fig. 7B). In spermatogenesis, all four species examined have only one sperm line. In oogenesis, *D. acuticephalum* has two egg lines, while the other three species have only one (Fig. 7). However, *D. acuticephalum* has a rather small number of oogonium and oocytes (Table 1). The body size may be a factor that limits the number of oocytes.

The development of infusorigens was reported by Lameere [10], Nouvel [14], and McConnaughey [12]. Lameere studied *D. typus*, while McConnaughey did not specify the species that he studied. However, both these authors observed that the first oogonium is produced by the second division and the first spermatogonium and axial cell are generated after the third division. This previously reported cell lineage is, thus, the same as that observed in *D. orientale*. Nouvel [14] traced the development of the infusorigen of *D. schulzianum*. His findings are identical to ours in *D. japonicum* and *D. misakiense* in that the first spermatogonium is produced after the second division and the oogonium and axial cell are produced after the third division. However, the first spermatogonium of *D. schulzianum* is relatively large compared to that of *D. japonicum* and *D. misakiense*. In *D. orientale*, *D. japonicum*, and *D. misakiense*, the first spermatogonia, formed by unequal divisions, are relatively small before they are incorporated into an axial cell. They increase in size until they are as large as oogonia after having been incorporated into an axial cell. In *D. acuticephalum*, the first spermatogonium is also a small-sized cell. The third division in this species proceeds unequally and generates a larger axial cell and a smaller cell. This smaller cell is the mother cell of both the first spermatogonium and the oogonium of one egg line. Thus, the differentiation of the first spermatogonium occurs later in *D. acuticephalum* than in the other species (Fig. 7). The pattern of cell lineage observed in *D. acuticephalum* has not been reported in the earlier literature. Although previous reports dealing with a few species [10, 12, 14] did not pay any attention to species-specific differences in the cell lineages of infusorigens, a distinct difference does exist and could be a criterion for classification of dicyemid species.

In *D. japonicum* and *D. misakiense*, the presumptive first spermatogonium often undergoes equal division before being incorporated into the

axial cell. However, one of the daughter cells degenerates soon without differentiating into an oogonium, in contrast to the case in *D. acuticephalum*. This paticular division might be an "extra" cell division because it does not occur consistently in all infusorigens examined.

In *D. aegira*, which is about 1.5 mm in total length and has one or two infusorigens, two to three times as many spermatozoa are produced as oocytes [1, 13]. Among the species studied herein, *D. orientale* is a relatively large dicyemid, reaching 3.5 mm in length, and it has 7 to 25 infusorigens. *D. acuticephalum*, which is small, and *D. japonicum* and *D. misakiense*, which are medium-sized, have usually one, or sometimes two infusorigens [4, 16]. In the four species that we examined, the numbers of spermatozoa and the numbers of the oogonia and primary oocytes were roughly equal (Table 1). The numbers of oogonia and primary oocytes were 2.7 to 3.3 times those of spermatogonia and primary spermatocytes. If spermatogenesis and oogenesis proceed at the same rate during the germ cell division and maturation, the number of spermatozoa can be estimated to be 13 to 16 (3.27 to 4.06×4). These values are 1.2 to 1.5 times the values for oocytes. This discrepancy may be attributed to a possibly lower rate of spermatogenesis than of oogenesis [1]. The apparently small number of spermatozoa might be due to the limited space within the axial cell of the infusorigen. A large number of spermatozoa may not be necessary in dicyemids, which perform self-fertilization within the axial cells of rhombogens. However, it is still unclear why the present four species have much smaller numbers of spermatozoa than *D. aegira*. It is apparent that the size of rhombogens and the number of infusorigens per rhombogen do not affect the number of gametes produced.

In the nematode *Caenorhabditis elegans*, the cell lineage of the gonad has been studied in detail [6, 9]. Dicyemids have very simple gonads that are composed of a very small number of cells, and thus, they may also prove to useful as model systems for studies of the differentiation of gametes.

REFERENCES

1 Austin CR (1964) Gametogenesis and fertilization in the Mesozoan *Dicyema aegira*. Parasitology 54: 597–600

2 Eernisse DJ, Albert JS, Anderson FE (1992) Annelida and Arthropoda are not sister taxa: a phylogenetic analysis of spiralian metazoan morphology. Syst Biol 41: 305–330

3 Furuya H, Tsuneki K, Koshida Y (1992) Development of the infusoriform embryo of *Dicyema japonicum* (Mesozoa: Dicyemidae). Biol Bull 183: 248–257

4 Furuya H, Tsuneki K, Koshida Y (1992) Two new species of the genus *D.* (Mesozoa) from octopuses of Japan with notes on *D. misakiense* and *Dicyema acuticephalum*. Zool Sci 9: 423–437

5 Ginetsinskaya TA (1988) Trematodes, Their Life Cycles, Biology and Evolution. Amerind Publishing Co. Pvt. Ltd., New Delhi. (Translation of the original Russian edition, 1968)

6 Hirsh D, Oppenheim D, Klass M (1976) Development of the reproductive system of *Caenorhabditis elegans*. Dev Biol 49: 200–219

7 Hyman L (1940) The Invertebrates, Vol I, McGraw Hill, New York

8 Hyman L (1959) The Invertebrates, Vol V, McGraw Hill, New York

9 Kimble J, Hirsh D (1979) The postembryonic cell lineages of the hermaphrodite and male gonads in *Caenorhabditis elegans*. Dev Biol 70: 396–417

10 Lameere A (1918) Contributions à la connaissance des dicyémides (2e partie). Bull Biol Fr Belg 51: 347–390

11 Lapan EA, Morowitz HJ (1974) Characterization of mesozoan dispersal larva. Exp Cell Res 94: 277–282

12 McConnaughey BH (1951) The life cycle of the dicyemid Mesozoa. Univ Calif Publ Zool 55: 295–336

13 McConnaughey BH, Kritzler H (1952) Mesozoan parasites of *Octopus vulgaris*, Lam. from Florida. J Parasitol 38: 59–64

14 Nouvel H (1948) Les Dicyémides. 2e partie: infusoriforme, tératologie, spécificité du parasitisme, affinités. Arch Biol 59: 147–223

15 Nouvel H (1947) Les Dicyémides. 1e partie: systématique, générations vermiformes, infusorigène et sexualité. Arch Biol 58: 59–220

16 Nouvel H, Nakao Y (1938) Dicyémides du Japon. Bull Soc Zool Fr 63: 72–80

17 Ohama T, Kumazaki T, Hori H, Osawa S (1984) Evolution of multicellular animals as deduced from 5S ribosomal RNA sequences: a possible early emergence of the Mesozoa. Nucleic Acids Res 12: 5101–5108

18 Short RB, Damian RT (1967) Oogenesis, fertilization, first cleavage of *Dicyema aegira* (Mesozoa: Dicyemidae). J Parasitol 53: 185–195

19 Stunkard HW (1954) The life history and systematic relations of the Mesozoa. Quart Rev Biol 29: 230–244

ZOOLOGICAL SCIENCE 10: 467–471 (1993)

Hormonal Deficiency Causing Albinism in *Locusta migratoria*

Seiji Tanaka

Department of Insect Physiology and Behavior, National Institute of Sericultural and Entomological Science, Tsukuba, 305, Japan

ABSTRACT—Hoppers of an albino strain in the migratory locust, *Locusta migratoria*, are uniformly creamy white when reared under crowded conditions. Implantation of corpora cardiaca taken from a normal hopper caused some albino hoppers to turn grey, reddish, brown, or dark brown like the colors of normal isolated solitary individuals, and others to develop the black and orange coloration like that of normal gregarious hoppers. Other organs such as brain and thoracic ganglia also induced various colors. Therefore, the albinism of this locust is caused by deficiency of some hormonal factor(s) present in the corpora cardiaca, brain and other ganglia. Implantation of some organs obtained from 7 other species also caused albino locusts to develop dark body colors, suggesting that some hormonal factor(s) commonly present in different insects can promote dark pigmentation in albino locusts.

INTRODUCTION

Genetic albinism appears to be caused by lack of the enzyme tyrosinase, which is required to produce the black pigment, melanin [6]. In the desert locust, *Schistocerca gregaria*, both enzyme and substrate for melanin formation are present, but melanization does not occur in albino individuals [10]. In the migratory locust, *Locusta migratoria*, the albino mutation is not uncommon and laboratory lines have been established to study the genetic and behavioral aspects of the albinism [5, 14, 21]. However, no information is available on the underlying mechanism causing this phenomenon. I present here evidence suggesting that albinism in *L. migratoria* is caused by deficiency of some hormonal factor(s) normally present in the brain, corpora cardiaca and thoracic ganglia of this species, and that a similar factor(s) inducing the dark coloration in albino locusts also exists in other insects including a katydid, crickets and moths.

MATERIALS AND METHODS

A colony of albino locusts of *L. migratoria* was maintained under crowded conditions at a 14 h (14L : 10D) photoperiod and 30°C since its establishment from albino individuals which appeared in a stock culture originating from Okinawa, Japan. The details of the rearing and handling methods have already been described [4, 20]. Various endocrine and nervous organs were removed from 1-day-old 5th instar hoppers, and transplanted with a small quantity of saline solution (3 μl; 0.9% NaCl) into 1-day-old 4th albino instars. A small incision was made between the 2nd and 3rd abdominal sternites of the recipients, and implants were injected into the body cavity using a micropipette. All hoppers were chilled on ice for 10–20 min before the operation and almost no mortality was observed in the recipients which were continusouly kept as groups. Four or 5 days after operation, they ecdysed to the 5th instar, and the body color of each individual was recorded 10 days after the operation. The same procedure was followed for transplantation of organs from other insects into albino locusts, and whether the recipients turned darker (+) or not (−) was recorded 10 days after operation. The donor species used included *Gryllus bimaculatus, Teleogryllus occipitalis, Modicogryllus confirmatus, Metriptera hime, Leucania separata, Bombyx mori*, and *Cephanodes hylas*.

Accepted March 10, 1993
Received December 29, 1992

RESULTS AND DISCUSSION

When various endocrine organs and ganglia

were taken from normal crowded hoppers, and transplanted into 4th-instar albino hoppers reared under crowded conditions, all implants except for suboesophageal ganglia (SG) promoted pigmentation in the albino hoppers (Table 1). However, the body color obtained was dependent upon the kind of organ implanted. Albinos implanted with a pair of corpora allata (CA) turned green (Fig. 1E). They looked like normal solitary hoppers except that the ventral side of their body remained whitish. This is consistent with the previous findings that implantation of extra CA or administration of juvenile hormone (JH) or JH analogues, to crowded hoppers induce the green solitary color [1, 2, 7, 8, 9, 15, 18, 19]. Implanted brains and thoracic ganglia induced various shades of grey, dark brown and straw yellow, the coloration being associated with normal non-green (="homochrome") solitary hoppers [16]. A similar color change was observed when albinos were implanted with CC, but in this case some developed the black patterns as well as the orange background color and became indistinguishable from the normal gregarious hoppers (Fig. 1 B, H). The black component of this gregarious coloration is attributed mostly to cuticular melanins [8, 16]. After

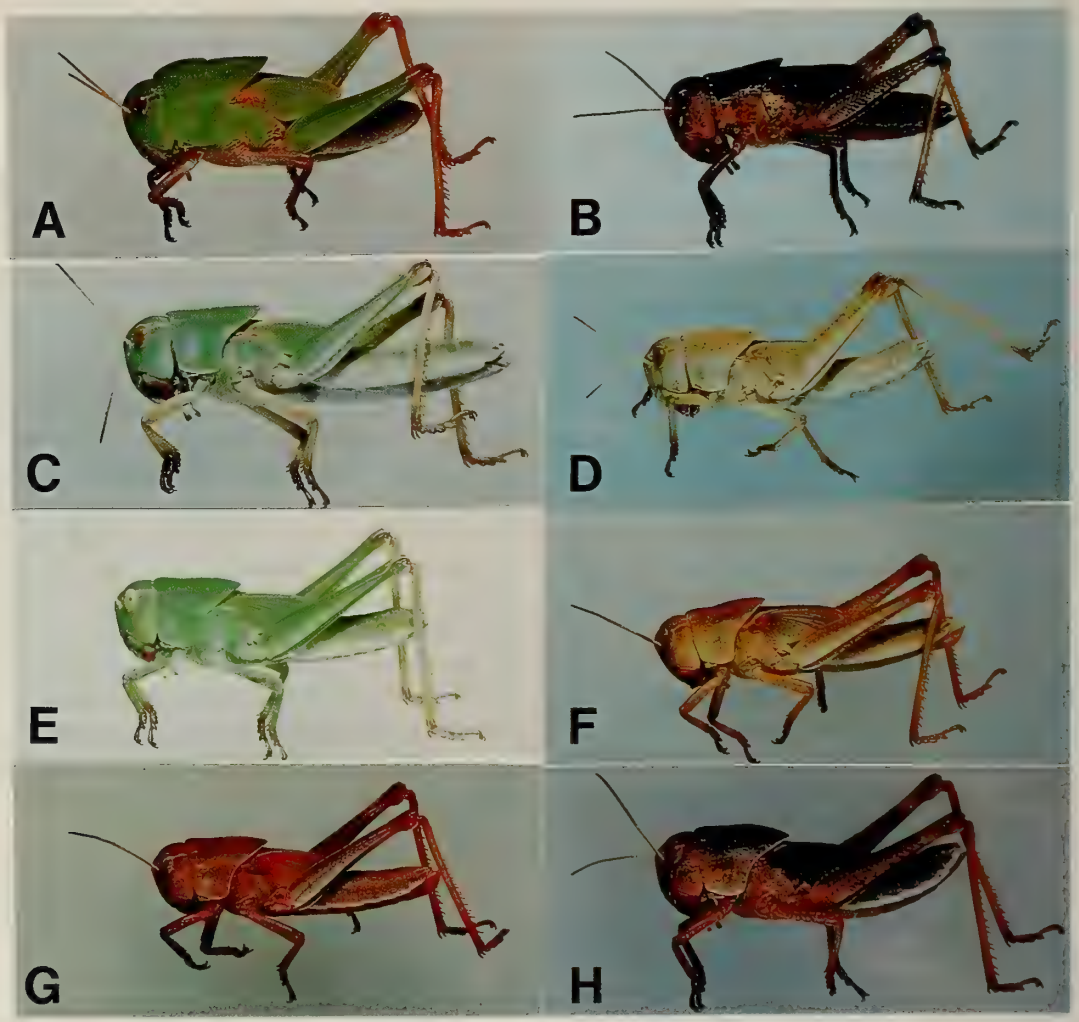

FIG. 1. Photographs of 5th instar hoppers of *L. migratoria*; normal solitary (A), normal crowded (gregarious)(B), albino isolated (C), albino crowded hopper without implantation (D) and albino crowded hoppers implanted with normal corpora allata (E), brains (F), or corpora cardiaca (G and H).

ecdysis, the melanins remain in the exuviae, while the pigments associated with the solitary form are mainly ommochromes, bile pigments and carotenoids [16] and do not remain in the exuviae. When a similar experiment was carried out with organs derived from field-collected green solitary hoppers, almost the same results were obtained ($\chi^2=1.37$; df=2; $P>0.05$; Table 1). This indicates that the factor promoting the gregarious black/orange coloration exists even in the CC of green solitary hoppers, although it either is not released or, if released, is inactive in the solitary

Table 1. Effects of implantation of various organs from 5th instar hoppers on the body color of albino hoppers in *L. migratoria*

Donors and Organs implanted	Color obtained in albino recipients				
	Solitary coloration				Greqarious coloration
	White	Green	Light homochromy	Dark homochromy	Black/orange
Normal (*Crowded in lab*)					
corpora allata (2)		10			
brain (1)			10	5	
corpora cardiaca (2)			3	7	5
thoracic ganglia (3)			9		
suboesophageal ganglia (3)	5				
Normal (*Field-collected solitary*)					
corpora cardiaca (2)			1	8	7
Albino (*Crowded in lab*)					
corpora allata (2)	1	9			
brains (1–2)	8				
corpora cardiaca (4–12)	15				
Albino (*Crowded in lab*)					
Control	20				

Donors were field-collected as 4th instars and reared individually in an outdoor insectary until used on the day after molting to the 5th instar. Numbers in the table indicate the numbers of individuals with the color indicated. Numbers in parentheses indicate the number of organs implanted. Controls included 10 intact crowded albino hoppers and 10 sham operated ones which were treated in the same way as the other operated hoppers except that no organ was implanted. Light homochromy includes straw yellow and brown, and dark homochromy reddish brown and dark brown.

Table 2. Effects of implantation of various organs from different insects on pigmentation in albino hoppers of *L. migratoria*

Donor species (Stage)	Organs impanted			
	Brain	Brain-SG	CC	SG
Gryllus bimaculatus (adult)	+		+	
Teleogryllus occipitalis (adult)	+		+	
Modicogryllus confirmatus (adult)	+		+	
Metriptera hime (larva)	+		+	
Leucania separata (larva)	+		+	−
Bombyx mori (pupa)		+		
Cephanodes hylas (larva)	+		+	−

The recipients either turned darker (+) or remained whitish (−) (N=3−10).

hoppers. By contrast, when CC or brains were taken from albino hoppers and implanted into other albino individuals, no color change occurred in the latter, although CA taken from albinos induced the green color (Table 1). From these results, it is concluded that genetic albinism in *L. migratoria* is due to a deficiency of some hormonal factors normally present in the CC, brain and other nervous ganglia.

The brown or black coloration could also be induced in albino hoppers by implantation of CC, brain or other nervous organs from other insects (Table 2). Melanization in the common armyworm, *L. separata*, is known to be induced by a hormone (the melanization and reddish coloration hormone) secreted from the brain-CC-CA complex or the SG [11, 17]. Albino hoppers developed brown pigments when implanted with a brain-CC complex from the armyworm, but no pigmentation was elicited by implantation of even 6 SG. In the cricket, *G. bimaculatus*, melanization is suppressed by the juvenile hormone produced by the CA, but the factor causing melanization has not been identified [2]. Implantation of CA from three species of crickets into albino locusts turned the recipients green (data not shown) while that of CC induced strong melanization in the albino locusts (Table 2). These results suggest that some hormonal factor(s) commonly present in different insects can promote dark pigmentation in albino locusts.

In this study, the gregarious coloration was obtained only in those albinos which had been implanted with CC from normal locusts, but whether the factor responsible for this coloration occurs only in CC or not remains uncertain. The involvement of CC and brain in the induction of dark pigments has been suggested using normal individuals of *L. migratoria* [3, 12, 13]. But, the substance(s) leading to the expression of the gregarious black color and/or the solitary black homochromy has not been identified chemically. The major obstacles to such a study include (i) difficulty in obtaining a large number of solitary hoppers for a bioassay and (ii) inability to remove the underlying background color or homochromy from such solitary individuals. The albino strain may provide an excellent bioassay system for endocrinological studies on phase polychromism in locusts.

ACKNOWLEDGMENTS

I thank Noriko Kenmochi, Matsuji Kaneko, and Eishi Hasegawa for assistance in rearing insects, and Hiroshi Shinbo and Masatoshi Nakamura for giving me *L. separata* and *B. mori*. Thanks are also due to M. Paul Pener (Hebrew University) and Lynn Riddiford (University of Washington) for helpful discussions and review of the manuscript.

REFERENCES

1 Fuzeau-Braesch S (1971) Contribution à l'etude de rôle de l'hormone juvénile dans la pigmentation. Arch Zool Exp Gen 112: 625–633

2 Fuzeau-Braesch S (1985) Colour changes. In "Comprehensive Insect Physiology, Biochemistry and Pharmacology Vol 9 Behaviour" Ed by GA Kerkut, LI Gilbert, Pergamon Press, Oxford, pp 549-589

3 Girardie A, Cazal M (1965) Role de la pars intercerebralis et des corpora cardiaca sur la melanisation ches *Locusta migratoria* (L.). CR hebd Seanc Acad Sci 261: 4525–4527

4 Hakomori T, Tanaka S (1992) Genetic control of diapause and other developmental traits in Japanese strains of the migratory locust, *Locusta migratoria* L.: Univoltine vs. bivoltine. Jpn J Ent 60: 319–328

5 Hunter-Jones P (1957) An albino strain of desert locust. Nature 180: 236–237

6 Hsia D Y-Y (1964) Inborn errors of metabolism. In "Diseases of Metabolism". Ed by GG Duncan, Saunders, Philadelphia, pp 301–448

7 Joly L (1954) Résultats d'implantations systématiques de corpora allata à de jeunes larves de *Locusta migratoria* L. CR Seanc Soc Biol 148: 579–583

8 Joly P, Joly L (1954) Résultats de greffes de corpora allata chez *Locusta migratoria*. Ann Sci Natur Zool Ser 11, 15: 331–345

9 Joly P, Meyer AS (1970) Action de l'hormone juvenile sur *Locusta migratoria* (Orthoptere) en phase gregaire. Arch Zool Exp Gen 111: 51–63

10 Malek SRA (1957) Sclerotization and melanization: two independent processes in the cuticle of the desert locust. Nature 180: 237.

11 Matsumoto S, Isogai A, Suzuki A, Sonobe H (1981) Purification and properties of the melanization and reddish colouration hormone (MRCH) in the armyworm, *Leucania separata* (Lepidoptera). Insect Biochem 11: 725–733.

12 Nickerson B (1954) A possible endocrine mechanism controlling locust pigmentation. Nature 174: 357–358

13 Nickerson B (1956) Pigmentation of hoppers of the desert locust (*Schistocerca gregaria* Forskåi) in relation to phase coloration. Anti-Locust Bull 24: 1–34

14 Nolte DJ (1971) Two pleiotropic albino mutations. Proc 4th Cong SA Genet Soc (Pretoria 1970), pp 36–38

15 Fridman-Cohen S, Pener MP (1980) Precocenes induce effect of juvenile hormone excess in *Locusta migratoria*. Nature 289: 711–713

16 Pener MP (1991) Locust phase polymorphism and its endocrine relations. Adv Insect Physiol 23: 1–79

17 Ogura N (1975) Hormonal control of larval colouration in the armyworm, *Leucania separata*. J Insect Physiol 21: 559–576

18 Roussel JP (1975) Action juvénilisante, chromatotrope, gonadotrope, et cardiotrope de-JHIII sur *Locusta migratoria*. J Insect Physiol 21: 1007–1015

19 Roussel JP (1976) Activité comparee des hormones juvéniles en C-18 (JH I) et en C-16 (JH III) chex *Locusta migratoria*. J Insect Physiol 22: 83–88

20 Tanaka S (1992) The significance of embryonic diapause in a Japanese strain of the migratory locust, *Locusta migratoria* (Orthoptera: Acrididae). Jpn J Ent 60: 503–520

21 Verdier M (1965) Mutation albinos de *Locusta migratoria* I. Origine et description (C.S.). Bull Soc Zool France 90: 493–501

ZOOLOGICAL SCIENCE 10: 473–480 (1993)

Use of Primary Cultures of Salmon Hepatocytes for the Study of Hormonal Regulation of Insulin-like Growth Factor I Expression *In Vitro*

Cunming Duan[1], Naoto Hanzawa, Yasuhiro Takeuchi,
Eisuke Hamada, Shigetoh Miyachi,
and Tetsuya Hirano[2]

Kamaishi Laboratories, Marine Biotechnology Institute, Heita, Kamaishi, Iwate 026 and [2]Ocean Research Institute, University of Tokyo, Minamidai, Nakano, Tokyo 164, Japan

ABSTRACT—Hepatocytes isolated from sockeye salmon (*Oncorhynchus nerka*) were seeded on an uncoated plastic dish with a positively charged surface, and cultured in hormone-free defined medium. Initially single cells began to aggregate and became flat after being attached to the dish. After approximately 6 days in culture, hepatocytes formed a monolayer sheet with cells in side-by-side contact, and remained in this form for at least 2 weeks. Hepatocytes in multicellular spheroids were also observed. The viability of the cells remained high (85–90%) during culture as judged by trypan blue exclusion. The cells actively incorporated [^{3}H]leucine into cellular and secreted proteins. Salmon and bovine insulins stimulated the leucine incorporation in a dose-dependent manner, suggesting that the cells remained responsive to hormones during culture. The basal IGF-I mRNA level in cultured hepatocytes was much lower than that of *in vivo* status. Salmon GH increased the level of IGF-I mRNA, whereas salmon prolactin had no effect. These findings suggest that the primary culture system of salmon hepatocytes can be used for the *in vitro* study of hormonal regulation of IGF-I gene expression in salmon.

INTRODUCTION

It has been well-documented that insulin-like growth factor I (IGF-I), which is a polypeptide with structure similarity to proinsulin, mediates many of the growth-promoting actions of growth hormone (GH) in mammals [7]. In teleosts, studies concerning the physiological functions of IGF-I has also been reviewed recently [3]. The nucleotide sequences of IGF-I cDNAs have been determined from coho salmon, Atlantic salmon, masu salmon, rainbow trout, and chinook salmon [2, 5, 14, 31, 32]. Mammalian IGF-I is highly active in stimulating cartilage sulfation or body growth in teleost species [10, 11, 15, 23, 24]. IGF-I-like bioactivity in serum and liver extract, and tissue responsiveness to IGF-I have also been found to be GH-dependent in some teleosts [10, 11, 13, 15, 24]. All of these findings strongly suggest that the GH-IGF-I axis is well conserved throughout evolution from teleost fishes to mammals.

In mammals, the major synthesis site of circulating IGF-I is liver, and GH directly stimulates the hepatic IGF-I mRNA expression and IGF-I peptide production [7, 27]. In teleosts, Cao *et al.* [5] reported that injections of bovine GH increased hepatic IGF-I mRNA levels. Duan and Hirano [11] showed that hypophysectomy reduced, and injection of eel GH restored, IGF-I mRNA content in the liver of the eel. They also reported that fasting significantly reduced hepatic IGF-I levels in the eel. Sakamoto *et al.* [30] reported that transfer of rainbow trout from fresh water to seawater increased IGF-I mRNA levels in liver, kidney and gill. In spite of some *in vivo* studies, detailed

Accepted March 16, 1993
Received January 18, 1993

[1] Present address and address correspondence to: School of Fisheries HF-15, University of Washington, Seattle, WA 98195 USA.

knowledge concerning the regulation of IGF-I production in teleosts is still scarce. To further examine the regulatory mechanism of IGF-I in teleosts, an *in vitro* model has been called for.

Short-term culture of isolated hepatocytes from salmonid species has been extensively explored for their utility in toxicologic and metabolic studies [4, 25]. Long-term culture of salmon or trout hepatocytes, however, has not been studied as extensively. The purpose of the present study was to establish a long-term primary culture system of salmon hepatocytes and to examine the effect of GH on IGF-I mRNA expression *in vitro*.

MATERIALS AND METHODS

Animals

Sockey salmon (350–600 g body weight) were obtained from Sunlock, Ltd., Kamaishi, Iwate. The fish were held in seawater in a flow-through 1,000 *l* aquarium and maintained at 15–17°C under natural photoperiod. They were fed once per day with commercial pellets.

Hormones

Bovine insulin (24 U/mg) was purchased from Sigma. Salmon insulin was provided by Dr. Erika Plisetskaya, University of Washington, Seattle, WA. Recombinant chum salmon GH was provided by Kyowa Hakko Kogyo, Co, Ltd.,Tokyo, and chum salmon prolactin was a gift from Dr. Hiroshi Kawauchi, Kitasato University, Sanriku, Iwate, Japan.

Isolation of hepatocytes

Fish were anesthetized by immersion in 0.02% MS222 prior to handling. A polyethylene cannula, connected to the perfusion reservoir, was inserted into the intestinal vein. The liver was perfused with an initial flow rate of 2 ml/min with 30 ml Ca^{2+}-free Krebs-Ringer. Then, the liver was perfused with 50 ml of the perfusion medium containing collagenase (Wako Pure Chemical Industries, 0.3 mg/l) for 25 to 30 min. The liver was removed from the fish and minced with scissors. The minced tissue was transferred to a beaker with 50 ml Ca^{2+}-free Krebs-Ringer containing collagenase, and mixed by stirring with a magnetic bar for 30 min. The suspension was filtered through a filter unit (150-mesh screen) and centrifuged at 50 $\times g$ for 2 min. The supernatant was discarded and the cells were resuspended in Krebs-Ringer and centrifuged for 2 min. The washings were repeated three more times. The final pellet was suspended with culture medium to a volume of 20 ml. Cells were counted in a Thoma haemacytometer.

Cell culture

Cells were suspended in William's E medium (Sigma) with 5% of fetal bovine serum (Sigma) and plated at 3×10^6 cells/60-mm Falcon Primaria dish. After about 12 hr, non-adherent cells were discarded, and the medium was replaced with serum-free William's E medium after washing 3 times by Dulbecco's phophate buffered saline (PBS). The cells were incubated in 5%CO_2/95% air at 15°C. Cells cultured for 5 or 6 days were used for the experiments.

Cell morphology

Morphology of the cells was examined by phase-contrast microscope and scanning electron microscope. For scanning electron microscope, the cells were fixed with 1% glutaraldehyde, postfixed with 1% OsO_4, dehydrated through a graded series of ethanol, and finally soaked in isoamyl acetate. The cells on the plate were dried with a critical point dryer (Hitachi, HPC-1), coated with Pt-Pd using an Eiko Ion Coater, and then observed with a JSM-U3 scanning electron microscope.

Incorporation of [^{3}H]leucine

After washing with PBS without Ca^{2+} and Mg^{2+} 3 times, the cells were incubated in 2 ml fresh William's E medium with or without hormone for 16 hr. Then, 2 μCi [^{3}3H] leucine (NEN) was added and incubated for 4 hr. Four to five dishes/group were used in each treatment. The measurement of incorporation of [^{3}H]leucine into hepatocyte as well as into the secreted proteins was performed as described by Plisetskaya *et al.* [28] with some modification. Briefly, the cells were separated from the medium by centrifugation for 5 min at 300$\times$g. The cell pellets were resuspended in ice-cold water and sonicated. The proteins from

both the sonicated cells and the medium were precipitated by ice-cold 5% trichloroacetic acid (TCA). The TCA precipitates were washed twice with 5% TCA. Then, the pellets were dissolved in 1 ml 0.1 M NaOH. The radioactivity was measured in a scintillation counter (Packard TRI-CARB 300) after adding 6 ml scintillation fluid (Aquasol-2, NEN). The radioactivity in the cell fraction was expressed as intracellular protein, and that in medium fraction was expressed as extracellular or secreted protein. The results were presented as DPM/10^6 cells viable at the beginning of the tracer experiment.

RNA isolation and Northern blot analysis

The hepatocytes cultured for 6 days were incubated in 2 ml fresh William's E medium with or without hormone for 24 hr. After removal of the culture medium, cells were washed twice with Ca^{2+}/Mg^{2+}-free PBS. Total RNA was isolated with a single-step extraction method using acid guanidium thiocyanate [6]. Poly [A^+] RNA was purified by oligo(dT)-latex using a commercial kit (Oligotex-dT30, Takara). A 1.1 kb cDNA probe encoding the entire coding sequence for coho salmon IGF-I (provided by Dr. Stephen J. Duguay, University of Washington, Seattle, WA) and a chicken β-actin cDNA probe (Sigma) were labelled with [^{32}P] by a multiprime DNA labelling kit (Amersham).

Poly [A^+] RNA was denatured by 2.2 M formaldehyde, electrophoresed on 1% agarose gels, and bound to a nylon filter (Hybond^{TM}) by capillary transfer in 20×SSC. The hybridization was performed as previously described [11]. Autoradiography was performed by exposing the filters to Kodak X-Omat AR film at −70°C.

Statistical analysis

The results were expressed as means ± SE, and differences among groups were evaluated statistically by ANOVA followed by the Fisher Protected Least Significant Difference Test (PLSD) using the Statview 512+ [8].

RESULTS

Changes in hepatocytes morphology during primary culture

The yield of liver cells obtained by the present method was about 1×10^8 cells/g liver. Parenchymal cells (hepatocytes) were the major cell type (more than 98%). The viability was usually greater than 90% as judged by trypan blue exclusion test. Figure 1a shows the typical spherical shape of freshly isolated salmon hepatocytes. Isolated salmon hepatocytes were single, round and large cells.

The attachment of salmon hepatocytes was incomplete in ordinary non-coated culture dishes. The plating efficiency in these ordinally non-coated culture dishes was usually lower than 20%. Preliminary experiments showed that coating the dish with bovine fibronectin improved the attachment to some extent, but bovine collagen or gelatin was ineffective (data not shown). Subsequent results showed that salmon hepatocytes attached firmly to Falcon Primaria culture dishes (Fig. 1b), which have positively charged surface, after overnight incubation (plate efficiency higher than 85%). Thus, cells were cultured in Primaria culture dishes in subsequent experiments.

Salmon hepatocytes showed significant morphological changes after attachment to the dish surface. Initially, single, round hepatocytes began to aggregate to each other, and became flat in 3–5 days (Fig. 1b). After being cultured for 6 days, cells spread and formed typical monolayer (Fig. 1c). The boundaries between cells became clear, and nuclei were clearly observed. They remained in this form for up to 3 weeks. Thereafter, they began to die, and more fibroblast-like cells appeared in the culture dishes (Fig. 1d). The multicellular spheroids with highly packed cells were observed sometimes (Fig. 2 a, b).

Protein synthesis and effect of insulin

Cultured hepatocytes actively incorporated [^{3}H] leucine into intracellular and extracellular proteins. Actinomycin D, which is an inhibitor of RNA synthesis and can affect protein synthesis via inhibition of RNA synthesis, decreased the [^{3}H]

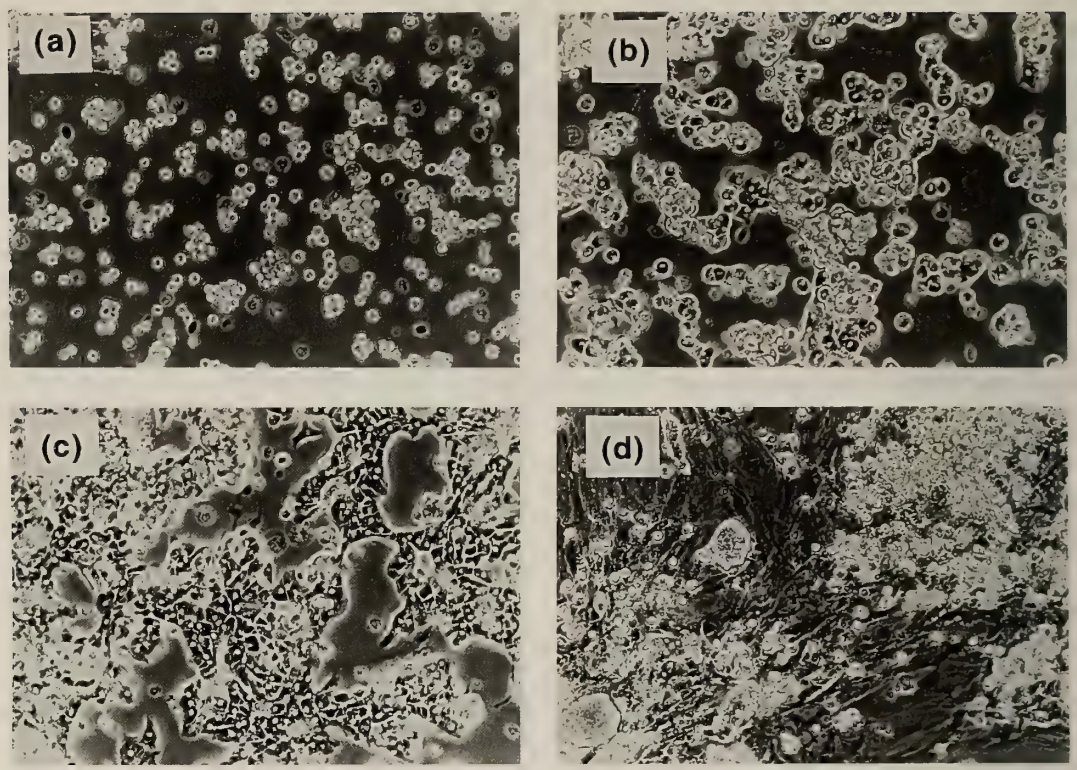

FIG. 1. Phase-contrast microscopy of salmon hepatocytes in primary culture. Cells at day 0 (a); day 3 (b); day 10 (c); day 30 (d). All magnification are ×200.

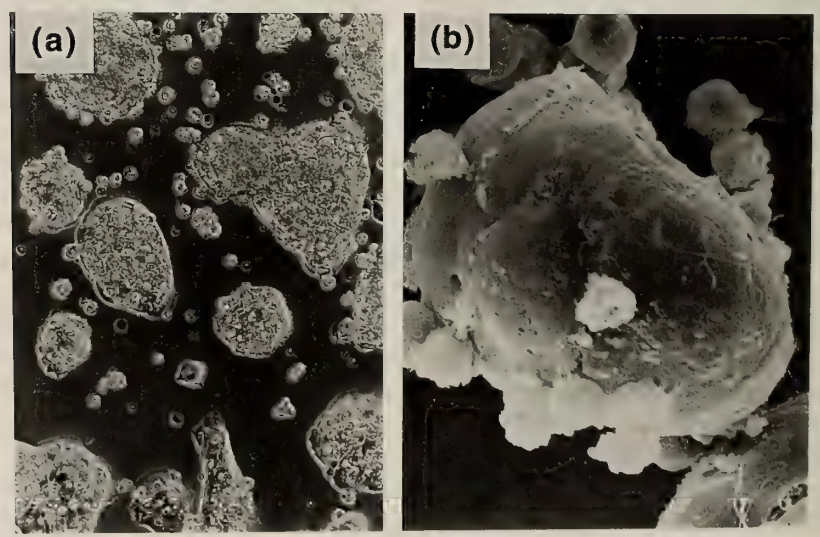

FIG. 2. Multicellular spheroids of salmon hepatocytes. (a) Phase-contrast microscopy (magnification, ×200); (b) scanning electron microscopy (magnification, ×1,000).

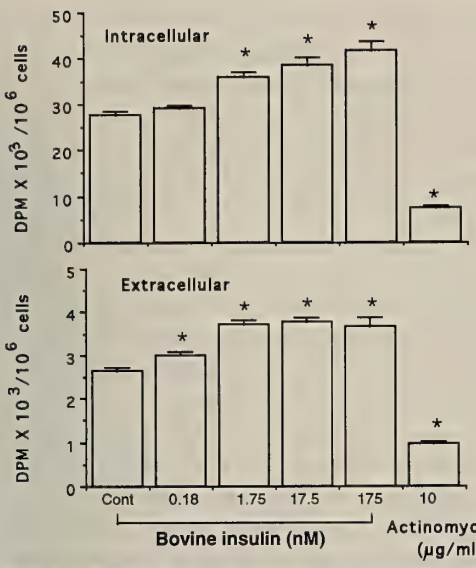

FIG. 3. Effect of insulin on the incorporation of [^{3}H] leucine into intracellular and extracellular proteins in primary cultures of salmon hepatocytes. Data are means ± SE (n=5). *Significantly different from the control ($p<0.05$).

leucine incorporation into proteins in a dose-dependent manner. At a dose of 10 μg/ml, it significantly reduced the incorporation of labelled leucine into intracellular and extracellular proteins (26 and 36% of the control levels, respectively) (Fig. 3), indicating that most of the [^{3}H] leucine measured was indeed incoporated into newly synthesized proteins in this system.

As shown in Figure 3, bovine insulin stimulated the [^{3}H] leucine incorporation into both intracellular proteins and extracellular proteins in a dose-dependent manner. The minimum effective dose was 1.75 nM for intracellular protein synthesis, and 0.18 nM for protein secretion. Similar dose-dependent stimulation was also obtained with homologous salmon insulin (data not shown).

IGF-I mRNA expression and effect of GH

Figure 4 shows the results of a Northern blot with 15 μg of poly [A$^+$] RNA isolated from intact salmon liver or hepatocytes cultured without any hormone for 6 days. Both liver and hepatocyte RNA showed a major class of IGF-I mRNA (approximately at 3.9 kb). The signal of hepatocyte RNA was much weaker than liver RNA so

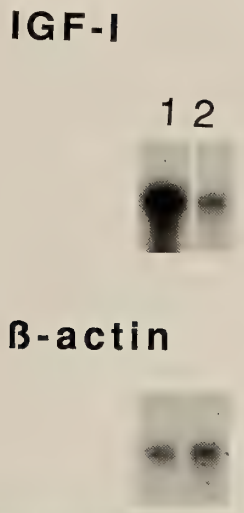

FIG. 4. Northern blot analysis of RNA. Fifteen micrograms of poly [A$^+$] RNA isolated from salmon liver (land 1) and six-day-old cultured salmon hepatocytes (lane 2) were used. (a) IGF-I mRNA. The exposure time was 2 days for liver RNA (lane 1) and 7 days for hepatocyte RNA (lane 2). (b) β-Actin mRNA. The same blot was rehybridized with chicken β-actin cDNA. The exposure time was 2 days.

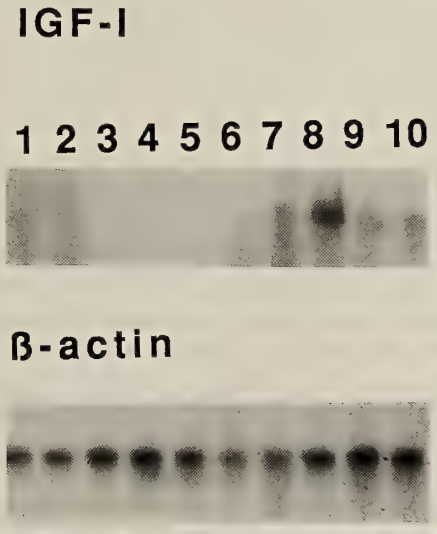

FIG. 5. Effects of salmon GH and prolactin on IGF-I mRNA levels in primary cultures of salmon hepatocytes. Lanes 1–2: prolactin 1,000 ng/ml; lanes 3–4: prolactin 100 ng/ml; lanes 5–6: control; lanes 7–8: GH 100 ng/ml; lanes 9–10: GH 10 ng/ml. Approximately two microgram of poly [A$^+$] RNA was used for each lane. The exposure time was 7 days for both IGF-I and β-actin mRNA.

that the blot had to be exposed for longer time (7 days as compared to 2 days of liver RNA), suggesting low expression level of IGF-I mRNA in hormone-free culture condition *in vitro*.

The effect of chum salmon GH and prolactin on IGF-I mRNA expression was then examined in primary cultures of salmon hepatocytes. Approximately 2 μg poly [A^+] RNA were obtained from each dish, and used for Northern blot analysis. Clear hybridization signals of IGF-I mRNA were obtained in GH-treated group (Fig. 5a, lanes 7–8, GH 100 ng/ml), whereas no apparent hybridization signal of IGF-I mRNA was seen in the control group or prolactin-treated groups after 7 days of exposure (Fig. 5a, lanes 1–6). When rehybridized the same blot with a β-actin cDNA probe, similar levels of clear β-actin mRNA signal were obtained with all groups (Fig. 5b, lanes 1–10).

DISCUSSION

In this study, salmon hepatocytes were cultured in a serum-free medium for up to several weeks. The cultured cells were responsive to insulins in term of stimulation of protein synthesis. GH stimulated IGF-I mRNA expression in primary cultures of hepatocytes, whereas prolactin had no effect.

There are many reports on culture of fish hepatocytes [25, 4]. To date, most of the studies used freshly isolated liver cells in suspension or primary culture cells over very short periods (within 24 h), whereas few studies were carried out with long-term primary culture system in a defined medium. This is in sharp contrast to the extensive studies on long-term cultures of mammalian hepatocytes [26]. This was partly because the attachment of fish hepatocytes to the surface of culture plate was slow and remained relatively weak, making it difficult to manipulate the cultures without disrupting of the cells [17, 22]. To solve this problem, efforts have been made to coat the culture plate various extracellular matrix components such as mammalian fibronectin, collagen, gelatin and fish serum or fish skin extract [4, 16, 18, 20, 22]. While some of the matrix components such as mammalian and fish fibronectins improved the efficacy of attachment [18], it is time-consumimg to prepare the coated plates. In this study, we have shown that salmon hepatocytes attached to Primaria dishes firmly without any treatment, and survived well up to several weeks.

The freshly isolated salmon hepatocytes seemed undamaged when viewed under phase-contrast microscope and scanning electron microscope (data not shown). The viability of the cells was approximately 90%. During the culture, cells reaggregated, became flat, and spread to form a monolayer. While most cells were in the monolayer form, some spheroids were also observed. In mammals, two distinct features of primary culture of adult hepatocytes are observed when the cells are cultured in Primaria dishes: monolayer culture with proliferative activity and multicellular spheroids with poor proliferative activity and high albumin-producing ability [21]. It is not clear whether the biochemical and physiological properties of these two forms of salmon hepatocytes in culture are similar to those of mammalian hepatocytes.

It has been well documented in teleosts that insulin stimulates protein synthesis both *in vivo* and *in vitro* [1, 19, 28]. In the present study, a dose-dependent stimulation was obtained with mammalian and salmon insulins. The minimum effective dose was 1.75 nM, which is within the physiological range of circulating insulin salmonids [29]. The dose dependency and minimum effective dose of insulins are consistent with previous findings obtained in intact animals, cultured liver slices, and suspension of isolated liver cells [1, 19, 28], suggesting our primary culture system is suitable for study of hormone action.

Although some *in vivo* studies have indicated the GH-regulated hepatic IGF-I mRNA expression in teleosts [5, 11, 9, 30], there was no published *in vitro* information to date. In the present study, Northern blot analysis revealed a major band of 4 kb with cultured hepatocyte RNA, which was identical to that obtained with intact liver RNA. A longer exposure time, however, was necessary to visualize the hybridization signals with hepatocyte RNA (7 days) than with liver RNA (2 days), indicating a lower level of IGF-I mRNA expression *in vitro* as compared to that of *in vivo*. The lower expression level is likely due to the lack of

hormone stimulation, because the cells were cultured in hormone-free medium. Addition of salmon GH to the medium at a concentration of 100 ng/ml markedly increased the IGF-I mRNA levels. There was no apparent signal in the control and prolactin-treated groups. Since β-actin mRNA levels were all similar, the absence of IGF-I mRNA in the control and prolactin-treated groups is most likely to be due to low expression levels of IGF-I mRNA. These results suggest that GH has a direct effect on hepatic IGF-I mRNA expression in salmonid species, and that our primary culture system can be used as an *in vitro* model to study the hormonal regulation of IGF-I expression.

While our study demonstrated for the first time that GH stimulates hepatic IGF-I mRNA expression *in vitro* in a teleost species, the accurate quantitation of the results was difficult due to the low sensitivity of Northern blot and the low expression level of IGF-I. As mentioned above, using Northern blot, we were unable to detect IGF-I mRNA in poly [A^+] RNA (2 μg) prepared from hepatocytes of the control groups even after a long exposure unless using larger amount of RNA sample. Thus, a more sensitive and reliable assay is necessary for further study of hormonal regulation of IGF-I mRNA expression *in vitro* in salmonids. RNA dot blot or slot blot is a simpler version of Northern blot technique, and is slightly more sensitive and semi-quantitative. However, results of dot-blot or slot blot can be misinterpreted if the RNA samples are contaminated by DNA. In comparison, another technique, solution hybridization/RNase protection assay, is more sensitive, specific and fully quantitative. Recently, we have developed a solution hybridization/RNase protection assay for salmon IGF-I mRNA [9]. Quantitative data obtained by this assay confirmed the finding of the present study: GH but not prolactin stimulates IGF-I mRNA expression in primary cultures of salmon hepatocytes. Studies concerning the detailed regulation mechanism of IGF-I mRNA expression in salmon are in progress using the primary culture system of hepatocytes established in the present study.

ACKNOWLEDGMENTS

We are grateful to Mr. Takeshi Yamanome, Sunlock, Ltd., for providing the experimental fish. We thank Drs. Erika M. Plisetskaya and Stephen J. Duguay, School of Fisheries, University of Washington, for their critical reading of the manuscript. Thanks are also due to Mr. Yoji Kikuchi, Kamaishi Laboratories, Marine Biotechnology Institute, for his technical assistance. This work was supported in part by grants from the Ministry of Education, Science and Culture and also from Fisheries Agency, Japan to T.H., and a grant from the Association for Overseas Technical Scholarship (AOTS) of Japan to C.D.

REFERENCES

1 Ablett RF, Sinnhuber RO, Selivonchick DP (1981) The effect of bovine insulin on ^{14}C-glucose and ^{3}H-leucine incorporation in fed and fasted rainbow trout (*Salmo gairdneri*). Gen Comp Endocrinol 43: 211–217

2 Aoyagi K, Kojima T, Tanabe Y, Soma G, Saneyoshi M (1993) Total nucleotide sequence and expression in *E. coli* of cDNA encoded insulin-like growth factor I (IGF-I) from cherry salmon, *Oncorhynchus masou*. Mol Marine Biol Biotech (in press)

3 Bern HA, McCormick SD, Kelley KM, Gray ES, Nishioka RS, Madsen SS, Tsai PI (1991) Insulin-like growth factors 'under water': Role in growth and function of fish and other poikilothermic vertebrates. In "Modern Concept of Insulin-like Growth Factors" Ed by EM Spencer, Amsterdam, Elsevier, pp 85–96

4 Blair JB, Miller MR, Pack D, Barnes R, Teh SJ, Hinton D (1990) Isolated trout liver cells: Establishing short-term primary cultures exhibing cell-to-cell interactions. In vitro Cell Dev Biol 26: 237–249

5 Cao QP, Duguay SJ, Plisetskaya EM, Steiner DF, Chan SJ (1989) Nucleotide sequence and growth hormone-regulated expression of salmon insulin-like growth factor I mRNA. Mol Endocrinol 3: 2005–2010

6 Chomczynski P, Sacchi N (1987) Single-step method of RNA isolation by acid guanidium thiocyanate-pheno-chloroform extraction. Anal Biochem 162: 156–159

7 Daughaday WH, Rotwein P (1989) Insulin-like growth factor I and II. Peptide, messenger ribonucleic acid and gene structures, serum, and tissue concentrations. Endocrine Rev 10: 68–91

8 Dowdy S, Wearden S (1989) "Statistics for Research". John Wiley & Sons, New York, pp 303–305

9 Duan C, Duguay SJ, Plisetskaya EM (1993) Insulin-like growth factor I (IGF-I) mRNA expression in coho salmon, *Oncorhynchus kisutch*: Tissue dis-

tribution and effects of growth hormone/prolactin family proteins. Fish Physiol Biochem (in press)

10 Duan C, Hirano T (1990) Stimulation of ^{35}S-sulfate uptake by mammalian insulin-like growth factor I and II in cultured cartilages of the Japanese eel, *Anguilla japonica*. J Exp Zool 256: 347–350

11 Duan C, Hirano T (1992) Effects of insulin-like growth factor-I and insulin on the in vitro uptake of sulphate by eel branchial cartilage: evidence for the presence of independent hepatic and pancreatic sulphation factors. J Endocrinol 133: 211–219

12 Duan C, Inui Y (1990) Effects of recombinant eel growth hormone on the uptake of [^{35}S] sulfate by ceratobranchial cartilages of the Japanese eel, *Anguilla japonica*. Gen Comp Endocrinol 79: 3220–325

13 Duan C, Inui Y (1990) Evidences for the presence of a somatomedin-like plasma factor(s) in the Japanese eel, *Anguilla japonica*. Gen Comp Endocrinol 79: 326–331

14 Duguay SJ, Park LK, Samadpour M, Dickhoff WW (1992) Nucleotide sequence and tissue distribution of three insulin-like growth factor I prohormones in salmon. Mol Endocrinol 6: 1202–1210

15 Gray ES, Kelley KM (1991) Growth regulation in the gobiid teleost, *Gillichthys mirabilis*: roles of growth hormone, hepatic growth hormone receptors and insulin-like growth factor-I. J Endocrinol 131: 57–66

16 Haschemeyer A, Mathews R (1983) Temperature dependency of protein synthesis in isolated hepatocytes of Antarctic fish. Physiol Zool 56: 78–87

17 Hayashi S, Ooshiro Z (1985) Primary culture of the freshly isolated liver cells of the eel. Nippon Suisan Gakkaishi 51: 765–771

18 Hayashi S, Ooshiro Z. (1986) Primary culture of the eel hepatocytes in the serum-free medium. Nippon Suisan Gakkaishi 52: 1641–1651

19 Inui Y, Ishioka H (1983) Effects of insulin and glucagon on amino acid transport into the liver and opercular muscle of the eel *in vitro*. Gen Comp Endocrinol 51: 213–218

20 Kocal T, Quinn BA, Smith IR (1988) Use of trout serum to prepare primary attached monolayer cultures of hepatocytes from rainbow trout (*Salmo gairdneri*). In Vitro Cell Dev Biol 24: 304–308

21 Koide N, Sakaguchi K, Koide Y, Asano K, Kawaguchi M, Matsushima H, Takenami T, Shinji T, Mori M, Tsuji T (1990) Formation of multicellular spheroids composed of adult rat hepatocytes in dishes with positively charged surface and under other nonadherent environments. Exp Cell Res 186: 227–235

22 Maitre JL, Valotaire Y, Guguen-Guillouzo Z (1986) Estradiol-17β stimulates of vitellogenin synthesis in primary culture of male rainbow trout hepatocytes. In vitro Cell Dev Biol 22: 337–343

23 McCormick SD, Kelley KM, Young G, Nishioka RS, Bern HA (1992) Stimulation of coho salmon growth by insulin-like growth factor I. Gen Comp Endocrinol 86: 398–406

24 McCormick SD, Tsai PI, Kelley KM, Nishioka RS, Bern HA (1992) Hormonal control of sulfate incorporation in branchial cartilage of coho salmon: Role of IGF-I. J Exp Zool 262: 166–171

25 Moon TW, Walsh PJ, Mommsen TP (1985) Fish hepatocytes: A model metabolic system. Can J Fish Aquat Sci 42: 1772–1782

26 Nakamura T (1987) "Methodology of Primary Culture of Hepatocytes", Jap Sci Soc Press, Tokyo, pp 5–53 (in Japanese)

27 O'Neill IE, Houston B, Goddard C (1990) Stimulation of insulin-like growth factor-I production in primary cultures of chicken hepatocytes by chicken growth hormone. Mol Cell Endocrinol 70: 41–47

28 Plisetskaya E, Bhattacharya S, Dickhoff WW, Gorbman A (1984) The effect of insulin on amino acid metabolism and glycogen content in isolated liver cells of juvenile of coho salmon, Oncorhynchus kisutch. Comp Biochem Physiol 78A: 773–778

29 Plisetskaya EM, Dickhoff WW, Paquette TC, Gorbman A (1986) The assay of salmon insulin by homologous radioimmunoassay. Fish Physiol Biochem 1: 35–41

30 Sakamoto T, McCormick SD, Hirano T (1992) Mode of action of growth hormone in salmonid osmoregulation: Mediation by insulin-like growth factor I. Fish Physio Biochem (in press)

31 Shamblott, MJ, Chen, TT. Identification of a second insulin-like growth factor in a fish species. Proc Natl Acad Sci USA 89: 8913–8917

32 Wallis AE, Devlin RH (1993) Duplication insulin-like growth factor-I genes in salmon display alternative splicing pathways. Mol Endocrinol 7: 409–422

ZOOLOGICAL SCIENCE 10: 481–488 (1993)

Metabolism of Androgens by the Mouse Submandibular Gland and Effects of Their Metabolites

KAZUHIKO SAWADA AND TETSUO NOUMURA

Department of Regulation Biology, Faculty of Science, Saitama University, Urawa, Japan

ABSTRACT—In the mouse submandibular gland, sexual difference becomes evident on day 30, when the granular convoluted tubules (GCT) of the gland rapidly grow in response to drastically increased levels of circulating testosterone and 5α-dihydrotestosterone (DHT) in the male. We studied the *in vitro* metabolism of both androgens by the mouse gland and the effects of their metabolites on the gland.

By the glands on days 20 and 30, ^{3}H-testosterone was not further converted to any derivatives. In contrast, ^{3}H-DHT used as a substrate was metabolized partly to ^{3}H-5α-androstane-3α,17β-diol (3α-diol) and ^{3}H-5α-androstane-3β,17β-diol (3β-diol) in both sexes (approximately 9 and 1%, respectively). On the basis of the metabolites identified, the gland contained both 3α- and 3β-hydroxysteroid dehydrogenase activities, which were not sexually different.

Neonatally-castrated mice were given daily injections of 3α-diol, 3β-diol, testosterone and DHT for 1–10 days from day 20. The relative occupied area (ROA) of GCT in the gland increased in both sexes by treatment with 3α-diol or DHT for 4 days, or by 3β-diol or testosterone for 10 days. The order of ROA gain after 4–10 days was DHT>3α-diol>testosterone>3β-diol. The mitotic activity of GCT increased in both sexes by treatment with 3α-diol or DHT for 4 days, but in only males by 3β-diol or testosterone for 10 days.

The results suggest that in the mouse gland testosterone exerts its effects without any intraglandular conversion, and that DHT primarily acts in its form, whereas its intraglandular metabolite, 3α-diol may be supplementary as a stimulant.

INTRODUCTION

In rodents, the male submandibular gland is larger than the female one and has a more complex morphology. The glandular contents of biologically active polypeptides, including nerve growth factor, epidermal growth factor, renin and proteases, are higher in the male than in the female, being responsive to androgens [3, 6, 12, 14, 16, 19, 28]. By histological, ultrastructural and morphometrical studies, both sexes experience a similar morphogenesis of the gland during perinatal development, and then the sexual difference arises at 3–4 weeks of age, when the granular convoluted tubules (GCT) grow more rapidly in the male than in the female [10, 11, 13, 21]. In a completely androgen-independent state (e.g., neonatal castration or androgen-insensitive Tfm mutation), the glands carry out the feminine development [21, 22]. The masculine development of the gland is caused by circulating androgens, testosterone and 5α-dihydrotestosterone (DHT), the latter being more effective [23]. In male mice, their circulating levels are drastically increased between days 20 and 30 [23], when sexual difference of the gland occurred morphologically.

Therefore, in order to determine how testosterone and DHT exert their effects on the mouse submandibular glands, we examined *in vitro* metabolism of these androgens by the glands, and the effects of the resulting metabolites on the glands by morphometry.

Accepted April 17, 1993
Received March 2, 1993

MATERIALS AND METHODS

Animals

CD-1 mice were obtained from Charles River Japan Co. and maintained by randomly mating in

our laboratory. The animals were given a commercial diet (CRF-1: Charles River Japan Co.) and tap water *ad libitum* and were kept at 23±1°C under 12-hr artificial illumination (from 8:00 to 20:00).

In vitro androgen metabolism by the mouse submandibular gland

Both male and female mice were killed on days 20 and 30. Approximately 50 mg tissue of the submandibular glands were minced into about 2 mm-fragments. Minced tissues were incubated with 10 nM [1, 2, 6, 7-^{3}H]testosterone and [1, 2, 4, 5, 6, 7-^{3}H]5α-dihydrotestosterone (DHT) (specific activity, 70 and 117 Ci/mmol, respectively; Amersham) in 2 ml Hanks' solution (Nissui Pharmaceutical Co., Ltd., Tokyo, Japan) containing 4 mM glucose-6-phosphate-2NA (Boehringer Mannheim GmbH, Germany) for 1 hr at 37°C in an atmosphere of 95% air and 5% CO_2. After 1 hr, the incubation was stopped with 3 ml ethyl acetate, containing each 100 μg of the following non-radioactive reference steroids: 4-androstene-3,17-dione (androstenedione), 5α-androstane-3,17-dione (5α-androstanedione), 5α-androstan-3α-ol-17-one (androsterone), 4-androsten-17β-ol-3-one (testosterone), 5α-androstan-17β-ol-3-one (5α-dihydrotestosterone, DHT), 5α-androstane-3α,17β-diol (3α-diol) and 5α-androstane-3β,17β-diol (3β-diol) (Sigma Chemical Co., St. Louis, Mo, U.S.A.). After shaking, the ethyl acetate fractions were transferred to a new set of glass tubes, and the water phase was reshaken twice each time with 3 ml ethyl acetate. The resulting 9 ml ethyl acetate fraction was washed with 1 ml saturated $NaHCO_3$ and twice with 1 ml distilled water, and was evaporated. The extracted steroids were redissolved in 20 μl methanol-dichloromethane (1:1, vol/vol), and applied to TLC Silica gel plate 60 $HF_{254+366}$ (Merck, Darmstadt, Germany). The plates were developed in the solvent system, dichloromethane-diethyl ether (4:1, vol/vol), and were scanned to detect the areas of radioactivity by Chromatoscaner (Aloka, Tokyo, Japan). The radioactive areas were scraped off and steroids were extracted from the Silica gel three times with 2 ml methanol-dichloromethane (1:1, vol/vol) each time. The dried residues of radioactive steroids, except for 5α-androstanediols, were transferred to scintillation vials. After adding 4 ml scintillation fluid (6 g DPO, 0.3 g POPOP in 1,000 ml toluene), radioactivity was measured in a Packard Liquid Scintillation Counter, model 3255 with an efficiency of 50% for ^{3}H. The fraction of 5α-androstanediols was acetylated by dissolving in equal volumes of pyridine and acetic anhydride (0.2 ml, total volume) and allowing the mixture to stand overnight at room temperature. The mixture was evaporated and redissolved in 20 μl methanol-dichloromethane (1:1, vol/vol), applied to the TLC plates and developed twice in dichloromethane. The results were expressed as the percentages of total radioactivity. The protein content of each sample was determined by BCA protein assay reagent (Pierce, Rockford, IL, USA) and enzyme activities of 3α- and 3β-hydroxysteroid dehydrogenases were expressed as f mol of 3α- and 3β-diols produced from DHT per hour per mg protein, respectively. Each datum was the mean of 2–4 independent experiments. The procedure losses were less than 10% after first chromatography and less than 20% after acetylation and second chromatography (for separation of 3α- and 3β-diols), and the results were corrected for these losses.

Morphological studies

Mice of both sexes were castrated on day 0 and were subcutaneously given daily treatments with each 100 μg of 3α-diol, 3β-diol, testosterone and DHT, and the vehicle alone (0.1 ml sesame oil) for 1, 4 and 10 days starting on day 20, and they were killed on days 21, 24 and 30, respectively. All animals were subcutaneously given a single injection of colchicine (5 μg/g body weight) dissolved in 0.9% NaCl, 5 hr before they were killed to arrest cell division at metaphase. Submandibular glands were weighed and fixed in Bouin's solution, embedded in paraffin and sectioned at 8 μm. Sections were stained with Delafield's hematoxylin and eosin.

The sectional figures of submandibular glands in the microscopic enlargements (×400) were traced by the camera lucida, and the area of GCT was measured by the picture analyzer (Logitec K-510, Kantou Denshi Co., Japan) connected with a

microcomputer (NEC PC-9801DA). The area was expressed as percentages of the total area of the gland (the relative occupied area, ROA). Cell height of GCT was measured in randomly chosen five sections.

Cells in division per 500–1,000 cells were counted in the GCT of the gland. Mitotic rate was estimated by counting the cells at metaphase per 5 hr in 100 cells.

Statistical analysis

Data were statistically analyzed by Student's *t*-test or by Cochran-Cox test.

RESULTS

In vitro androgen metabolism by the mouse submandibular gland

The results in Table 1 are expressed as the percentage conversion of each substrate to metabolites/hr/mg of wet tissue, and a proposed metabolic pathway of androgens in the mouse submandibular gland is shown in Figure 1. By the glands on days 20 and 30, ^{3}H-testosterone was not further converted *in vitro* to any radioactive metabolites, including DHT, and its recovery was

TABLE 1. *In vitro* androgen metabolism by the mouse submandibular gland

substrate	animals	age in days	% recovery			
			testosterone	DHT	3α-diol	3β-diol
testosterone	male	20	98.8	ND	ND	ND
		30	96.1	ND	ND	ND
	female	20	96.7	ND	ND	ND
		30	95.6	ND	ND	ND
DHT	male	20	—	79.4	9.6	1.1
		30	—	83.5	9.0	1.4
	female	20	—	78.9	8.2	1.2
		30	—	79.3	8.7	1.4

The results are expressed as the percentage conversion of each substrate to metabolites/hr/mg wet tissue. Values are the mean of 2–4 independent experiments. DHT=5α-dihydrotestosterone, 3α-diol=5α-androstane-3α,17β-diol, 3β-diol=5α-androstane-3β,17β-diol, ND=not detected.

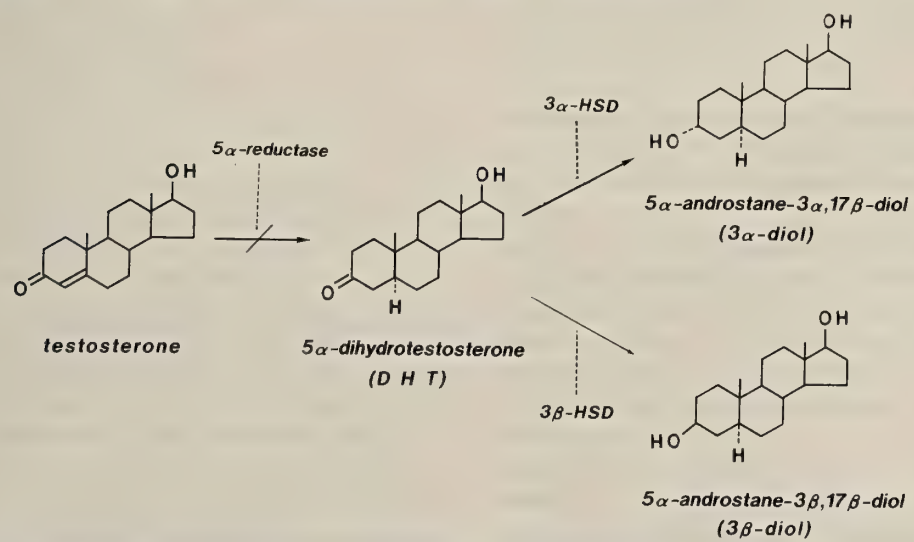

FIG. 1. A proposed metabolic pathway of androgens in the mouse submandibular gland. HSD=hydroxysteroid dehydrogenase.

TABLE 2. 3α- and 3β-Hydroxysteroid dehydrogenase activities in the mouse submandibular gland

animals	age in days	enzyme activity (fmol·mg^{-1} protein·hr^{-1})	
		3α-HSD	3β-HSD
male	20	369.8	43.4
	30	645.4	98.1
female	20	314.3	47.6
	30	574.6	93.2

Values are the mean of 2–4 independent experiments.
HSD = hydroxysteroid dehydrogenase.

more than 95% (Table 1). On the other hand, ^{3}H-DHT was metabolized in limited amounts to tritiated 3α- and 3β-diols (approximately 9 and 1%, respectively). The amounts of metabolic products from DHT did not differ between sexes at each age (Table 1). On the basis of the metabolites identified, the gland contained both 3α- and 3β-hydroxysteroid dehydrogenase (HSD) activities. The activities of these enzymes increased between 20 and 30 days, but were not sexually different at both ages (Table 2).

Effects of 5α-androstanediols on the mouse submandibular gland

By the mouse glands, some amounts of 3α- and 3β-diols could be converted *in vitro* from DHT. Therefore, the effects of 3α- and 3β-diols on the glands were examined morphometrically at 30 days of ages, and were compared with those of testosterone and DHT. In 30-day-old mice, the male glands were superior to the female glands in all morphometric parameters used: the weight, the ROA of GCT, the cell height of GCT, and the mitotic activity of GCT. By neonatal castration, these sex differences were abolished, and the intraglandular structures in the males resembled to those in the normal females, showing lower values in all four parameters [21]. In females, castration could not induce any changes in their glands [21].

The net weight of the glands in castrated males gradually increased and became significantly heavier by 10 daily treatments with all four androgens, although the effects of DHT were greater than those of other three androgens (Fig. 2). In castrated females the gland weight gain was

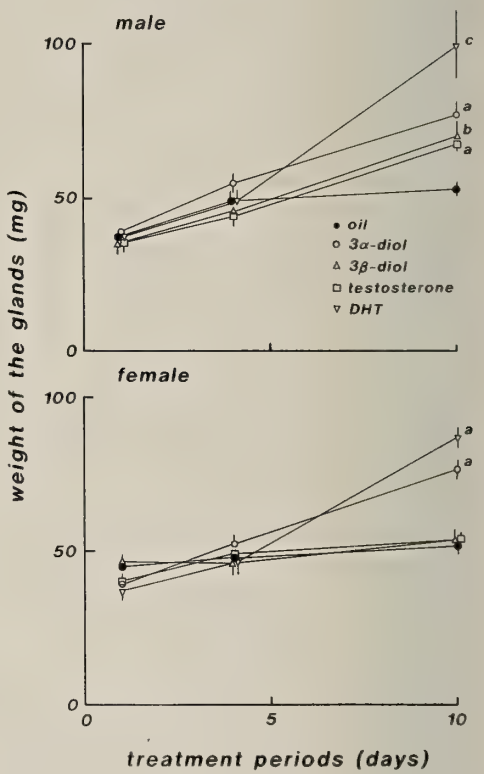

FIG. 2. Change in the weight of the submandibular glands of neonatally-castrated male and female mice, treated with each 100 μg of 5α-androstane-3α,17β-diol (3α-diol), 5α-androstane-3β,17β-diol (3β-diol), testosterone and 5α-dihydrotestosterone (DHT), and the vehicle alone for 1, 4 and 10 days from day 20. Values are mean ± S.E.M., n = 4–5 per group. a: $P<0.001$ *vs* oil control (Student's *t*-test), b: $P<0.05$, c: $P<0.02$ *vs* oil control (Cochran-Cox test).

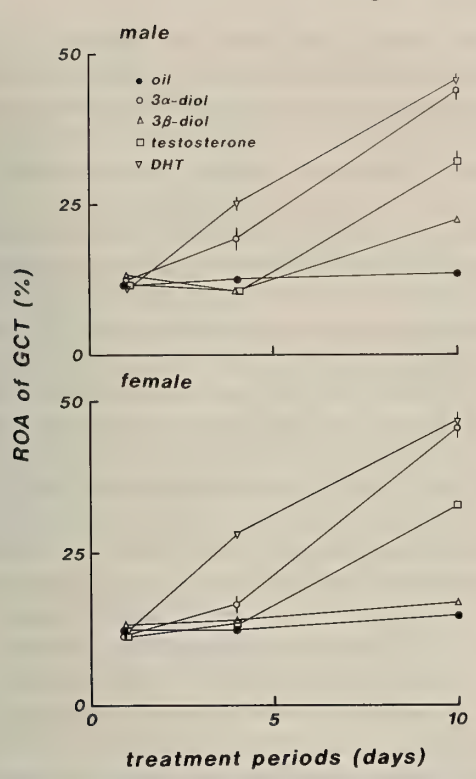

FIG. 3. Change in the relative occupied area (ROA) of the granular convoluted tubules (GCT) of the submandibular glands of neonatally-castrated male and female mice, treated with each 100 μg of 5α-androstane-3α,17β-diol (3α-diol), 5α-androstane-3β,17β-diol (3β-diol), testosterone and 5α-dihydrotestosterone (DHT), and the vehicle alone for 1, 4 and 10 days from day 20. Values are mean $\pm$ S.E.M., n=8–10 per group.

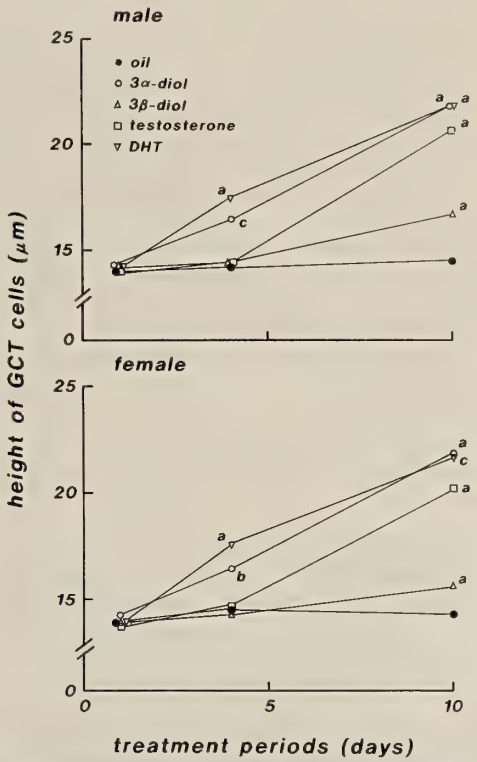

FIG. 4. Change in the cell height of the granular convoluted tubules (GCT) of the submandibular glands of neonatally-castrated male and female mice, treated with each 100 μg of 5α-androstane-3α,17β-diol (3α-diol), 5α-androstane-3β,17β-diol (3β-diol), testosterone and 5α-dihydrotestosterone (DHT), and the vehicle alone for 1, 4 and 10 days from day 20. Values are mean $\pm$ S.E.M., n=8–10 per group. a: $P < 0.001$ *vs* oil control (Student's *t*-test), b: $P < 0.005$, c: $P < 0.001$ *vs* oil control (Cochran-Cox test).

caused only by treatment with 3α-diol or DHT after 10 days (Fig. 2).

Both the ROA and the cell height of GCT in castrated animals were increased by 4 daily treatments with 3α-diol or DHT and by 10 daily treatments with 3β-diol or testosterone (Figs. 3 and 4). After 10 daily treatments, 3α-diol and DHT were nearly equal to increase both the ROA and the cell height of GCT, but the former was slightly inferior to the latter after 4 days of treatments (Figs. 3 and 4). The effects of 3β-diol on these two parameters were less effective than those of testosterone, and were sexually different, the male GCT being more responsive than the female GCT (Figs. 3 and 4). Both 3α- and 3β-diols could not cause any increases in the ROA of other three regions, the acini, the intercalated ducts and the excretory striated ducts, in both the male and female glands (data not shown).

3α-Diol induced to increase the mitotic activity of GCT in both sexes in a manner similar to DHT, that is, the mitotic activity was significantly increased after 4 days, and then gradually decreased to the control levels by 10 days (Fig. 5). By treatment with 3β-diol or testosterone for 10 days, the mitotic activity of GCT increased somewhat in castrated males (Fig. 5). In castrated females, these two androgens failed to increase the mitotic activity of GCT (Fig. 5). Neither 3α- nor 3β-diol had effects on the mitotic activities of other three

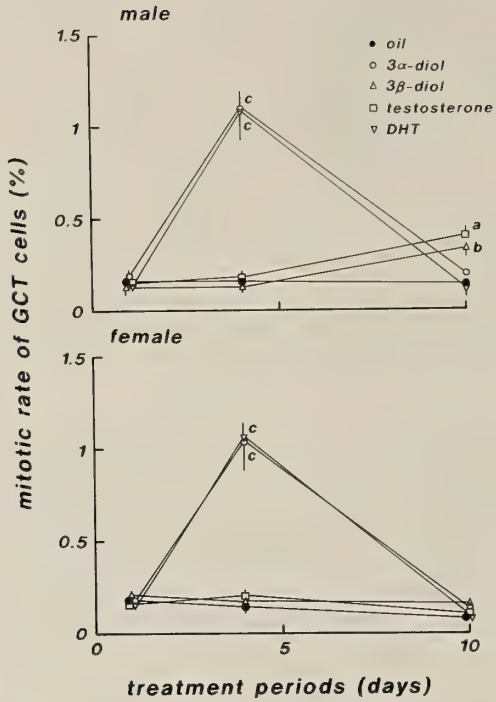

FIG. 5. Change in the mitotic rate of the granular convoluted tubules (GCT) of the submandibular glands of neonatally-castrated male and female mice, treated with each 100 μg of 5α-androstane-3α,17β-diol (3α-diol), 5α-androstane-3β,17β-diol (3β-diol), testosterone and 5α-dihydrotestosterone (DHT), and the vehicle alone for 1, 4 and 10 days from day 20. Values are mean$\pm$S.E.M., n=8–10 per group. a: $P<0.001$, b: $P<0.002$ *vs* oil control (Student's *t*-test), c: $P<0.001$ *vs* oil control (Cochran-Cox test).

regions in the gland of either sex (data not shown).

DISCUSSION

The mouse submandibular glands contain both cytosolic and nuclear androgen receptors [15, 17, 20, 26, 27]. The cytosolic receptor in the male glands increases during postnatal development and attains adult levels by day 20 [17, 26], while circulating levels of androgens (testosterone and DHT) begin to rise on day 20 [17, 23]. In our male mice on day 30 [23], circulating DHT levels (1.0$\pm$0.21 ng/ml), which is produced by testes [24] and metabolized from testosterone in the peripheral tissues [1, 9] including liver, prostate, epididymis, seminal vesicle and phallus, are approximately 4-fold over and the serum DHT/testosterone ratio (1:3 in the ratio) is 2-fold higher, compared with those of pubescent rats reported [8]. We have reported that administration of both testosterone and DHT to neonatally-castrated mice for 20 days from day 20 causes to increase all the gland weight, the ROA of GCT, the cell height of GCT, and the mitotic activity of GCT, and that DHT is more effective in comparison with testosterone [23]. In the present study, testosterone was not further converted *in vitro* to its derivatives, including DHT, by the submandibular glands of mice on days 20 and 30 (Table 1), suggesting that testosterone itself acts without intraglandular conversion to DHT and other metabolites, whereas DHT used as a substrate could be converted partly to 3α- and 3β-diols in amounts of less than 10% (Table 1). Daily injections of these two metabolites to neonatally-castrated mice for 10 days from day 20 caused to increase all four parameters in the gland (Figs. 2–5). The morphometrical changes in the gland induced by 3α-diol were nearly as much as those by DHT, but both the ROA and the cell height of GCT were slightly lower by treatment with 3α-diol than by DHT after 4 days (Figs. 3 and 4). On the other hand, 3β-diol was less effective than testosterone (Figs. 3 and 4). Thus these DHT metabolites produced by the gland have also androgenic effects on the gland growth, and particularly 3α-diol has a potency similar to DHT. These results indicate that, *in vivo,* DHT itself acts primarily, and that its metabolites, 3α-diol may act secondarily on the gland.

As described before [23], by treatment with DHT, the ROA and cell height of GCT in the glands of both sexes are increased for 7–20 days of treatments, whereas the mitotic activity is increased for 2–7 days only. Similar results were obtained by treatment with 3α-diol (Figs. 3–5). These androgens primarily affect the cell nucleus to initiate the mitosis, followed by the sequence of cellular events in GCT. In contrast, the mitotic activity was increased slightly and only in males by treatment with 3β-diol or testosterone for 10 days (Fig. 5). Although ample time may be allowed for peripheral conversion of the latter androgens to active mitogenic androgens and for accumulation

of their effects, different effects among these four hormones can be explained solely as a consequence of different binding affinities to the androgen receptor.

Metabolism of testosterone by the submandibular salivary glands has been reported in some mammalian species. By the domestic boar glands, testosterone is converted *in vitro* to its 5α-reduced products, a large amount of DHT and 3α-diol, and lesser amounts of 3β-diol [4]. Androstenedione is produced as the main metabolite by the rat glands *in vitro* [2] and by the canine glands *in vivo* [29]. In the present study, testosterone was not further converted *in vitro* to its derivatives by the mouse glands, corresponding to the results from the homogenate of the adult murine gland [7]. Therefore, it is suggested that androgen pathway in the submandibular glands may be different among mammalian species.

We demonstrated that the murine glands contained 3α- and 3β-HSD activities (Table 2). By histochemical study, the steroid metabolizing enzymes, including 3α- and 3β-HSDs, are mainly found in the excretory striated ducts (SD) in human [25] and pig [5]. In these two species, the GCT are absent in their glands [18]. The SD of the rodent gland are transformed to the GCT during puberty [10, 11, 13, 18, 21]. Therefore, the SD in human and pig have been considered to be identical with both the GCT and SD in rodents. In our mice, the ROA of GCT plus SD are superior in the males to those in the females on days 30–90 [21], but the activities of 3α- and 3β-HSDs were not sexually different on day 30 (Table 2). In order to solve these inconsistent results, further research is required to examine the histochemical localization of these enzymes in the glands of our mice.

REFERENCES

1 Albert J, Geller J, Stoeltzing W, Loza D (1978) An improved method for extraction and determination of prostate concentrations of endogenous androgens. J Steroid Biochem 9: 717–720

2 Baldi A, Charreau EH (1972) 17β-Hydroxysteroid dehydrogenase activity in rat submaxillary glands. Its relation to sex and age. Endocrinology 90: 1643–1646

3 Barka T (1980) Biologically active polypeptides in submandibular glands. J Histochem Cytochem 28: 836–859

4 Booth WD (1977) Metabolism of androgens *in vitro* by the submaxillary salivary gland of the mature domestic boar. J Endocr 75: 145–154

5 Booth WD, Hay MF, Dott HM (1973) Sexual dimorphism in the submaxillary gland of the pig. J Reprod Fert 33: 163–166

6 Byyny RL, Orth DN, Cohen S (1972) Radioimmunoassay of epidermal growth factor. Endocrinology 90: 1261–1266

7 Coffey JC (1973) Steroid metabolism by mouse submaxillary glands. I. *In vitro* metabolism of testosterone and 4-androstene-3,17-dione. Steroids 22: 247–257

8 George FW, Johnson L, Wilson JD (1989) The effect of a 5α-reductase inhibitor on androgen physiology in the immature male rat. Endocrinology 125: 2434–2438

9 Goldstein JL, Wilson JD (1972) Studies on the pathogenesis of the pseudohermaphroditism in the mouse with testicular feminization. J Clin Invest 51: 1647–1658

10 Gresik EW (1980) Postnatal developmental changes in submandibular glands of rats and mice. J Histochem Cytochem 28: 860–870

11 Gresik EW, MacRae EK (1975) The postnatal development of the sexually dimorphic duct system and of amylase activity in the submandibular glands of mice. Cell Tissue Res 157: 411–422

12 Gresik EW, Schenkein I, van der Noen H, Barka T (1981) Hormonal regulation of epidermal growth factor and protease in the submandibular gland of the adult mouse. Endocrinology 109: 924–929

13 Jayasinghe NR, Cope GH, Jacob S (1990) Morphometric studies on the development and sexual dimorphism of the submandibular gland of the mouse. J Anat 172: 115–127

14 Kasayama S, Yoshimura M, Oka T (1989) The regulation by thyroid hormones and androgen of epidermal growth factor synthesis in the submandibular gland and its plasma concentrations in mice. J Endocr 121: 269–275

15 Kyakumoto S, Kurokawa R, Ohara-Nemoto Y, Ota M. (1986) Sex difference in the cytosolic and nuclear distribution of androgen receptor in mouse submandibular gland. J Endocr 108: 267–273

16 Michelakis AM, Yoshida H, Menzie J, Murakami K, Inagami T (1974) A radioimmunoassay for the direct measurement of renin in mice and its application to submaxillary gland and kidney studies. Endocrinology 94: 1101–1105

17 Minetti CASA, Valle LBS, Fava-De-Moraes F, Romaldini JH, Oliveira-Filho RM (1986) Ontogenesis of androgen receptors in the mouse submandibular gland: correlation with the develop-

mental profiles of circulating thyroid and testicular hormones. Acta Endocr 112: 290–295

18 Pinkstaff CA (1980) The cytology of salivary glands. Int Rev Cytol 63: 141-261

19 Roberts ML (1974) Testosterone-induced accumulation of epidermal growth factor in the submandibular salivary glands of mice, assessed by radioimmunoassay. Biochem Pharmacol 23: 3305–3308

20 Sato N, Nemoto T, Baba R, Ota M (1985) Dialysis-induced transformation of mouse submandibular androgen-receptor. Biochem Int 10: 771–776

21 Sawada K, Noumura T (1991) Effects of castration and sex steroids on sexually dimorphic development of the mouse submandibular gland. Acta Anat 140: 97–103

22 Sawada K, Noumura T (1992) Sexually dimorphic duct system of the submandibular gland in mouse with testicular feminization mutation (Tfm/Y). Acta Anat 143: 241–245

23 Sawada K, Noumura T (1992) Differential effects of testosterone and 5α-dihydrotestosterone on growth in mouse submandibular gland. Zool Sci 9: 803–809

24 Sheffield JW, O'Shaughnessy PJ (1988) Testicular steroid metabolism during development in the normal and hypogonadal mouse. J Endocr 119: 257–264

25 Sirigu P, Cossu M, Perra, MT, Puxeddu P. (1982) Histochemistry of the 3β-hydroxysteroid, 17β-hydroxysteroid and 3α-hydroxysteroid dehydrogenases in human salivary glands. Arch Oral Biol 27: 547–551

26 Takuma T, Nakamura T, Hosoi K, Kumegawa M. (1977) Binding protein for 5α-dihydrotestosterone in mouse submandibular gland. Biochim Biophys Acta 496: 175–181

27 Verhoeven G (1979) Androgen binding proteins in mouse submandibular gland. J Steroid Biochem 10: 129–138

28 Walker P, Weichsel ME Jr, Hoath SB, Poland RE, Fisher DA (1981) Effect of thyroxine, testosterone, and corticosterone on nerve growth factor (NGF) and epidermal growth factor (EGF) concentrations in adult female mouse submaxillary gland: dissociation of NGF and EGF responses. Endocrinology 109: 582–587

29 Weiner AL, Ofner P, Sweeney EA (1970) Metabolism of testosterone-4-^{14}C by the canine submaxillary gland *in vivo*. Endocrinology 87: 406–409

ZOOLOGICAL SCIENCE 10: 489–496 (1993)

Binding of Thyroid Hormone to Freshwater Perch Leydig Cell Nuclei-rich Preparation and its Functional Relevance

Nihar R. Jana and Samir Bhattacharya[1]

Department of Zoology, Visva-Bharati University, Santiniketan-731 235, W. Bengal, India

ABSTRACT—Leydig cells were isolated from the testis of a freshwater perch, *Anabas testudineus*, belonging to the prespawning stage of reproductive cycle. Cells were sonicated and a pure nuclei preparation was obtained for binding assay. Under optimum assay conditions of pH 7.4 at 30°C and 90 min incubation binding of [^{125}I] 3,5,3′-triiodothyronine (T_3) to Leydig cell nuclei was saturable at 1.7 nmol/l concentration. A Scatchard analysis of T_3-binding exhibited a Kd of 26.8×10^{-9} mol/l and a maximum binding capacity (B_{max}) as 1.66 pmol/mg DNA. Competitive inhibition studies demonstrated that binding of T_3 to Leydig cell nuclei is analogue specific. Biological relevance of T_3 binding to perch Leydig cell was evaluated by adding varied concentrations of T_3 to Leydig cell incubation (1×10^6 cells/incubation). Twenty five ng to 100 ng of T_3 resulted in a dose dependent increase in androgen release while 200 ng of T_3 had no additional effect over 100 ng under present incubation system. Stimulation of androgen release by T_3 was significantly inhibited ($p<0.01$) by cycloheximide. T_3 (100 ng/ml) increased protein synthesis in Leydig cell (70% as compared to control) which was significantly inhibited ($p<0.01$) by cycloheximide. Results indicate that binding of T_3 to Leydig cell of perch testis triggers the synthesis of a protein (or proteins) which in turn stimulates androgen release.

INTRODUCTION

Thyroid has long been implicated in the reproduction of fish [11, 13–16, 20, 26, 29]. Annual cycles of thyroid activity in teleostean fish have been found to be correlated with the gonadal maturation [6, 8, 17]. Experimental hypothyroidism in teleosts effected retardation of ovarian development [23] and administration of thyroid hormone resulted in the maturation of oocytes in stellate sturgeon [10], goldfish [16] and freshwater perch [30]. All these reports clearly indicate an influence of thyroid hormone on teleostean gonadal function, but how it does so is still unclear.

Recent reports from this laboratory demonstrated high affinity and low capacity triiodothyronine (T_3) binding sites in the ovarian nuclei of perch [7, 22]. These information indicate a direct involvement of thyroid hormone in piscine ovarian function. However, report regarding the influence of thyroid hormone on male reproductive function in fish is lacking. The aim of this paper is to show T_3 binding to Leydig cell nuclei isolated from the testis of a freshwater perch, *Anabas testudineus* and also to demonstrate that the addition of T_3 to Leydig cell incubation *in vitro* causes significant increase in androgen release.

Accepted April 17, 1993
Received August 19, 1992
[1] To whom correspondence should be addressed.

MATERIALS AND METHODS

Aniaml

Anabas testudineus is a freshwater perch predominantly found in Eastern India. It breeds during the monsoon and its reproductive cycle can be divided into four phases [6]. Perch belonging to prespawning stage were used for the present experiment as thyroid hormone level in plasma remains high during this phase [6]. Adult male perch (25–30 g) length (10–12 cm) were acclimatized in laboratory aquaria at 28°–30°C for at least 7 days prior to experiment. They were fed *ad libitum* with commarcial fish food (Shalimar Fish Food, Bird and Fish food Manufacturers, Bombay, India).

Testis weight varied from 200–300 mg.

Preparation of Leydig cells from perch testis

The testis of the perch is encapsulated by tunica albuginea, a thin delicate membrane which envelopes the fibrous connective tissue. The connective tissue fiber from the peripheral stroma divides the lumen of testis into a large number of seminiferous tubules of varied shape and size. Each tubule contains germ cell at different developmental stages and Sertoli cell. Germ cell can be categorised as primary and secondary spermatogonia, spermatocyte, spermatid, and spermatozoa. Perch testis has discrete interstitial cell or Leydig cell between the seminiferous tubules. In histological section of perch testis stained with haematoxylin and eosin, interstitial or Leydig cells appear as a large cell with oval nuclei. Plenty of Leydig cells from perch testis could be observed under microscope. This is in contrast to other freshwater teleosts like the Indian catfish, *M. vittatus* and murrel, *C. gachua* where testis are devoid of true interstitium and characterised by possession of tubule boundary cells. In these fishes it is difficult to identify the Leydig cell. Since this perch, *Anabas testudineus* contains clearly defined Leydig cell in considerable number, the testes were collected by killing the perch, sliced with a surgical blade and then subjected to the preparation of Leydig cell according to the method described by Yu *et al.* [36] and Yu and Wang [37] which is a modification of the procedure reported by Dufau *et al.* [12] and Van Damme *et al.* [32]. Briefly small pieces of testis from perch were transferred to Erlenmyer flask containing preincubation medium (MEM with 25 mM HEPES, 0.1% BSA, 0.1% sodium bicarbonate, pH 7.4; penicillin 1000 U/ml; streptomycin 50 μg/ml). The testis pieces were gently dispersed for 10 min with a magnetic stirrer placed on ice bath and a completely homogeneous sunpension was obtained. The cell suspension was then filtered through a fine nylon mesh and preincubated for one hr at 30°C with shaking at 50 cycles/min. This was then cooled under ice and centrifuged at 400 g for 10 min at 4°C. Pelleted Leydig cells were suspended in the incubation medium which was a preincubation medium with 0.125 mM xanthine plus sodium heparin, 0.5% (v/v). It appears that testicular Leydig cells of perch differs from that of mammalian Leydig cells as the latter could be harvested by centrifugation at 250 g [37].

Purity of Leydig cells

To examine the purity of the Leydig cell preparation, histochemical staining for 3β-hydroxysteroid dehydrogenase (3β-HSD) enzyme was performed by a modification of the method of Wiebe [35]. The reaction mixture contained 0.1 M Na-K phosphate buffer, pH 7.2, 0.14 μmol 5α-androstan 3β-ol-17-one, 0.6 μmol nitroblue tetrazolium, 7 μmol NAD. 500 μl of reaction mixture was added to 1×10^6 cells and the suspension was incubated for one hr at 30°C. We have described earlier that 30°C was the optimum temperature for incubating the tissues from this fish [7, 8, 29]. 5α-A-3β-ol-17-one was omitted from control incubation. A drop of the cell suspension was placed on a glass slide and allowed to dry. After embedding in gelatin, positively stained cells was estimated by counting a minimum of six field under the light microscope. Approximately more than 85% cells were found to be 3β-hydroxysteroid dehydrogenase positive indicating them to be Leydig cells.

Binding incubation

T_3 binding to nuclear preparations from Leydig cells was performed by following the description reported earlier from this laboratory [7]. Leydig cells were lysed by ultrasonication (Labsonic 2000, B. Braun, West Germany) at 150 KHz and nuclei were isolated according to our earlier procedure [7, 22] adopted from the description of Lawson *et al.* [19]. To determine the optimum binding conditions of [^{125}I]-T_3 to Leydig cell nuclear preparations, incubations were performed at different temperatures pHs and time intervals. It was found that 90 min of incubation at pH 7.4 and temperature 30°C were optimum conditions of radiolabelled T_3 binding (data not shown). 30 μg of DNA was incubated in a final volume of 500 μl with varying concentrations of [^{125}I]-T_3 (0.26–2.2 nmol/l) in the absence (total binding) or presence of 500 fold excess of unlabelled T_3 (nonspecific binding) at pH 7.4 and 30°C for 90 min in a shaking water bath. After termination of incubations, free

and bound radioactivity were separated by the addition of ice cold 40% polyethylene glycol (PEG-mol. wt. 6000) and by centrifugation at 3000 g in a refrigerated centrifuge. The supernatant was aspirated and radioactivity of the pellet was measured in a Gamma Counter (1282 Compugamma CS, LKB, Sweden).

Incubation of Leydig cells

For *in vitro* incubation, Leydig cells were suspended in MEM (300 μl, containing 1×10^6 cells) and was added to each well of multiwell module (NUNC, Denmark). Incubations were performed at 30°C with gentle shaking under an atmosphere of oxygen. Cells were allowed to incubate for 2 hr and at 2 hr hormone and other chemicals were added, incubation was then continued for another 3 hr. Hence total incubation period was 5 hr. A 2 hr preincubation time was necessary for the recovery of cells. Viability of cells were determined at the beginning and at the end of incubation by Trypan blue (0.1%) dye exclusion method which showed 90–80% viability of the cells. For each experiment, functional ability of isolated Leydig cells in *in vitro* incubation was checked by the addition of purified carp gonadotropin [2], which released androgen in the medium. T_3 was added in increasing concentrations (25–200 ng/ml) to the Leydig cell incubation. T_3 was dissolved by the addition of 10 μl of NaOH (1N) to 1 ml of T_3 solution (distilled water). 10 μl volume was fixed for each concentration of T_3 which was added to 300 μl of Leydig cell incubation. Same concentration and volume of NaOH was added to control incubation (without T_3) as vehicle. Since MEM contained 25 mM HEPES, there was no changes of pH due to this addition. After termination of incubation, each incubate was centrifuged at 500 g, medium was collected and stored at −20°C until androgen RIA.

Protein synthesis in Leydig cells

To monitor the protein syunthesis in Leydig cells in response to T_3, cells (1×10^6/well) were incubated with [^{14}C]-leucine (specific activity −300 mCi/mmole) in MEM supplemented with 1 mM of eighteen different amino acids except leucine. The pH was adjusted to 7.4. Protein synthesis of Leydig cells were determined according to the procedure previously described from this laboratory [7]. Briefly, cells were incubated in the presence of T_3 (100 ng/ml) alone or T_3 (100 ng/ml) plus cycloheximide (50 μg/ml) or in the absence of either chemicals (control). The cells were then separated from the medium by centrifugation, resuspended in distilled water and subjected to ultrasonication at 150 KHz. Amount of protein in the lysed preparation was determined by following the method of Lowry *et al.* [21] taking bovine serum albumin as the standard. The sonicated material was precipitated with a final concentration of 10% TCA. The pellet obtained after centrifugation at 3000 g in a refrigerated centrifuge was first washed with 10% TCA followed by another wash with 5% TCA containing cold leucine (1 mM). 7% TCA was then added to the pellet and the sample was heated for 30 min at 95°C to denature nucleic acids. After centrifugation at 3000 g and two subsequent washes with ethanol : ether (1 : 1), the final precipitate was dissolved in 500 μl of 1(N) NaOH and counted in a Liquid Scintillation Counter (LSS 20, ECIL) in 10 ml of toluene based cocktail containing PPO, POPOP and methyl cellosolve and TCA precipitable radioactivity is expressed as dpm/mg protein.

Radioimmunoassay of androgen

RIA of androgen was carried out according to the procedure described by Yu and Wang [37] which was a modification of a method reported earlier [1]. The medium collected after Leydig cell incubation was subjected to androgen RIA. It was found that androgen values were similar with or without extraction by diethylether. The antiserum used (provided by Dr. John Y. L. Yu, Academia Sinica, Taiwan, batch no. ASIZ-T-3-02) had 100% crossraction with testosterone, 74% with 5α-dihydrotestosterone, 1.23% androstenedione, 0.59% androstenediol and very negligible crossreactions with other steroids. Sample, [^{3}H]-testosterone and antitestosterone serum were added and the samples were incubated for 18 hr at 4°C. Dextran coated charcoal was used to separate bound from free steroid. After centrifugation at 3000 g, supernatant containing the bound hormone was counted in a Liquid Scientillation Counter. The sensitivity

of the androgen RIA was 5.0 pg and the linear range of standard curve was 5–300 pg. The interassay co-efficient of variation was less than 10%.

Statistics

Data were analysed by one way analyses of variance (ANOVA). Where F value indicated significance means were compared by post hoc multiple range test. All values are expressed as mean ± standard error of the mean (SEM).

RESULTS

T_3 binding to perch Leydig cell nuclei

Nuclear preparation from Leydig cells were incubated at 30°C for 90 min at pH 7.4 and T_3 binding was one half maximal by 45 min and maximal at 90 min under these conditions. To obtain the specific binding of T_3, 30 μg of DNA were incubated with increasing concentrations of [^{125}I]-T_3 (from 0.26 nmol/l to 2.2 nmol/l). Figure 1 shows that specific binding of T_3 increased linearly from 0.26 nmol/l to 1.7 nmol/l and then reached a plateau indicating saturation of binding sites. Specific binding data were analysed by Scatchard plot which showed a Kd of 26.8×10^{-9} mol/l and maximum binding capacity (B_{max}) was 1.66 pmol/mg DNA (Fig. 2). Competitive binding experiments were conducted at optimal assay conditions with variation in T_3, TRIAC (3,3′,5-triiodothyroacetic acid), T_4 and carp GtH (cGtH-Banerjee *et al.* [2]) concentrations. Results clearly indicate that T_3 binding sites in Leydig cell nuclei are analogue specific (Fig. 3). T_3 inhibited the binding of [^{125}I]-T_3 very efficiently but less competitively than TRIAC while T_4 was a poor competitor. cGtH did not inhibit [^{125}I]-T_3 binding. Tissue specificity of T_3 binding was observed by incubating nuclear preparations of testis, liver, tail kidney and small intestine. Maximum specific binding occurred with liver nuclei followed by testis. Binding was negligible with small intestine and tail kidney nuclei (Fig. 4).

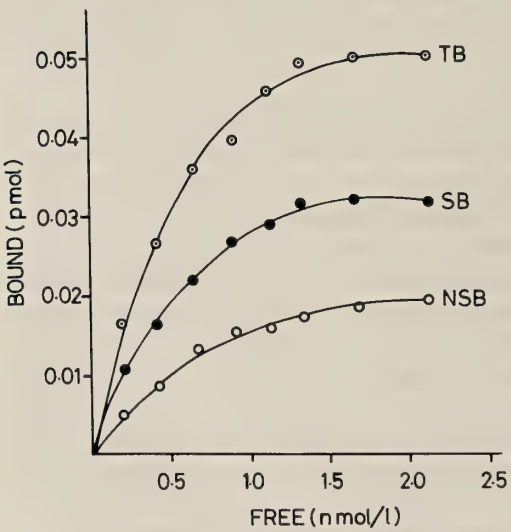

FIG. 1. Saturation curve of T_3 binding to Leydig cell nuclei. 30 μg of DNA from the Leydig cell nuclei were incubated with 0.26–2.2 nmol/l of [^{125}I]-T_3 for 60 min at 30°C. Non-specific binding (NSB) is in the presence of 500 fold excess cold T_3. Specific binding (SB) is the difference between total binding (TB) and non-specific binding. Data represents the mean ± SEM of six determinations.

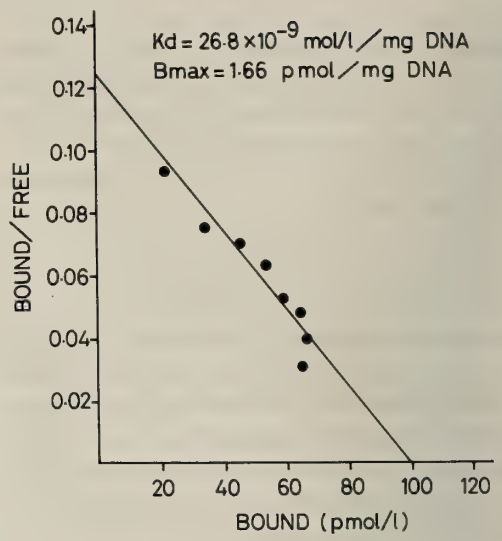

FIG. 2. Scatchard analysis of the data obtained from Fig. 1. The X axis represents p mol/l concentration of bound T_3 and Y axis represents bound to free ratio. Kd: Dissociation constant. B_{max}: Maximum binding capacity.

Effect of T_3 on androgen release from Leydig cells

Addition of increasing concentrations of T_3 to

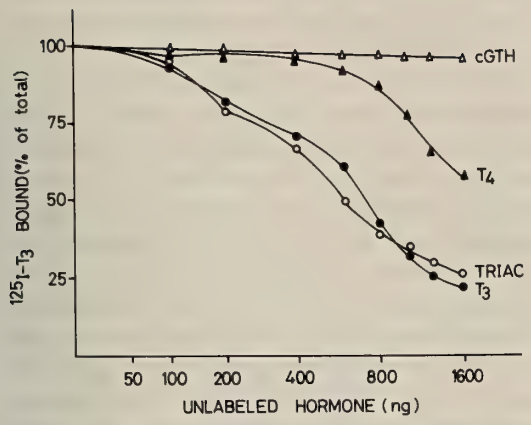

FIG. 3. Competitive inhibition of [^{125}I]-T_3 binding to perch Leydig cell nuclei by TRIAC, T_3, T_4, and cGTH. All values are mean ± SEM of six determinations.

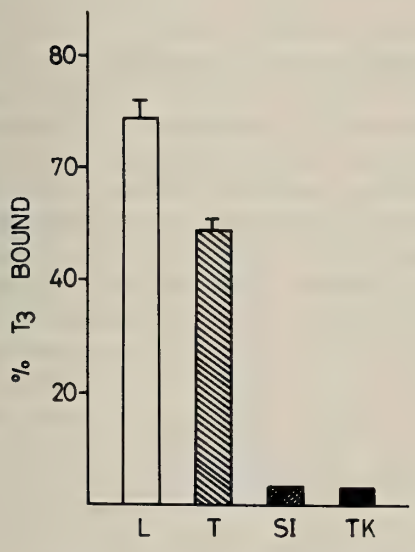

FIG. 4. [^{125}I]-T_3 binding to nuclei obtained from different tissues. Liver (L), Testis (T), Small intestine (SI), Tail kidney (TK). All values are mean ± SEM of six determinations.

Leydig cell incubation resulted in dose dependent increase of androgen release. Increase of androgen release was observed from 25 ng to 100 ng, further increase in dose had no additional effect in the present incubation system (Fig. 5).

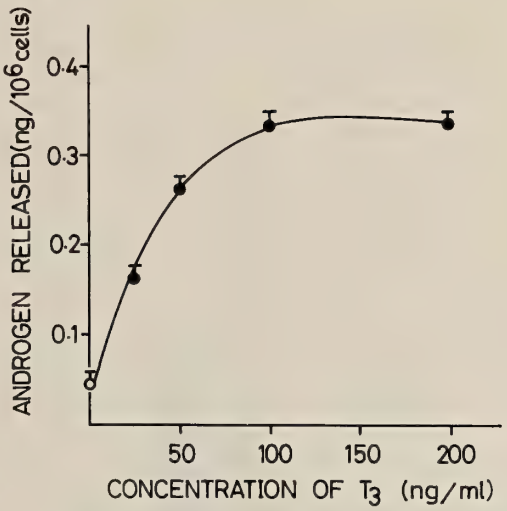

FIG. 5. Effect of T_3 on androgen release by Leydig cell of perch. After a preincubation of 2 hr the cells were incubated for another 3 hr in the absence of T_3 (control) or in the presence (increasing concentrations) of T_3. Data represents the mean ± SEM of six determinations.

TABLE 1. Inhibition of T_3-stimulated androgen release by cycloheximide

System	Androgen released (pg/1×10^6 cells)
Control	49.9 ±6
T_3 (100 ng/ml)	345* ±9.8
T_3 (100 ng/ml)+ Cycloheximide (50 μg/ml)	40** ±2.1

P*<0.01 as compared to control.
P**<0.01 as compared to T_3 added experiment.
Values are mean ± SEM of six determinations.

This stimulation of androgen release by T_3 was inhibited by cycloheximide (Table 1).

Stimulation of Leydig cell protein synthesis by T_3

Incubation of Leydig cell with [^{14}C]-leucine and T_3 resulted in a significant ($p<0.01$) increase in TCA precipitable radioactivity which was cycloheximide sensitive (Fig. 6). T_3 caused about 70% increase in protein synthesis as compared to control while cycloheximide inhibited this stimulation to about 53%.

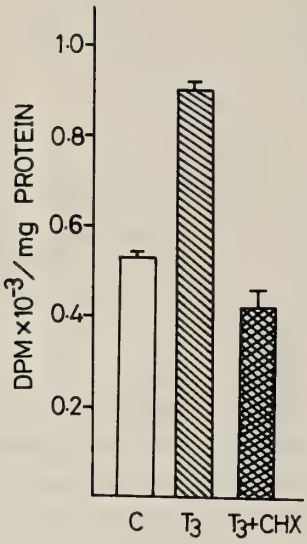

FIG. 6. Protein synthesis in the Leydig cell in reponse to T_3. Incubation of [^{14}C]-leucine into TCA precipitable protein was determined in presence (100 ng/ml) or in the absence of (control) of T_3 or T_3 (100 ng/ml) with 50 μg/ml cycloheximide (CHX). Data represents the mean ± SEM of six determinations.

DISCUSSION

The present study demonstrates that nuclear T_3 binding sites are present in Leydig cell of perch testis. Binding of T_3 to teleostean Leydig cell nuclei is a new report and suggests an influence of thyroid hormone on testicular function. This freshwater perch breeds once a year *i.e.* during monsoon or rainy season and its annual reproductive cycle consists of four stages [6]. We have selected prespawning stage male fish because gonadal metabolic activity is in peak during this stage. Standardisation of T_3 binding assay showed maximum binding at 30°C with pH 7.4. These two characteristics clearly coincided with the natural environment of prespawning stage (April–May) when water temperature varied between 28°–32°C and pH of the water is weakly alkaline (7.3–7.5). This indicates that optimal binding conditions may have physiological relevance.

Liver is the conventional binding site for thyroid hormone and commonly used for thyroid hormone receptor assay in teleost. The Scatchard plot analysis of our data shows that T_3 binding affinity to perch Leydig cell nuclei is comparable to hepatic nuclei of the same fish. $Ka = 0.041 \times 10^9\ M^{-1}$ in perch Leydig cell nuclei and $Ka = 0.06 \times 10^9\ M^{-1}$ in the hepatic nuclei of the same fish [7]. These values are closer to the affinity of hepatic nuclei of rainbow trout ($Ka = 0.22 \times 10^9\ M^{-1}$) [33] while hepatic nuclei of coho salmon has much higher affinity ($Ka = 1.03 \times 10^9\ M^{-1}$) [9]. Surprisingly T_3 binding affinity of perch ovarian nuclei is much higher ($Ka = 0.11 \times 10^9\ M^{-1}$) as compared to Leydig cell nuclei [7]. Occupation of receptor site by T_3 shows considerable variation. T_3 binding capacity was considerably higher in perch ovarian nuclei ($B_{max} = 4.312$ pmol/mg DNA) [7] as compared to Leydig cell nuclei ($B_{max} = 1.66$ pmol/mg DNA). Hepatic nuclei of perch showed five fold greater T_3 binding capacity ($B_{max} = 8.882$ pmol/mg DNA) [7] in comparison to Leydig cell nuclei. However T_3 binding to Leydig cell nuclei of perch is analogue and tissue specific.

Specific binding of T_3 is believed to result in the initiation of at least some of the effect of thyroid hormone [24]. Oppenheimer *et al.* [25] detected low concentration of nuclear T_3 binding sites within rat brain, spleen and testis, these tissues are supposed to be unresponsive to thyroid hormone. Unresponsiveness has been defined as a failure of thyroid hormone in increasing O_2 consumption. But in testis with relatively low thyroid hormone binding sites a small change in O_2 consumption induced by thyroid hormone may not be detectable [28]. Recently T_3 binding sites have been detected in rat testis Sertoli cell nuclei and a role of thyroid hormone in the regulation of growth and maturation of Sertoli cell has been suggested [18]. A novel C-erb-A gene encodes a protein which is a receptor for thyroid hormone and this gene has also been isolated from human testis library [3, 27, 34]. The binding of T_3 to perch Leydig cell nuclei is therefore not entirely unexpected but it obviously raises a question whether perch testis is functionally responsive to thyroid hormone or not.

To answer this question perch Leydig cells were incubated *in vitro*. Addition of T_3 to Leydig cell incubation resulted in androgen release. Increasing concentrations of T_3 causes a dose dependent

increases in androgen release indicating a biological response. Although it appears to be a very unusual effect of thyroid hormone, earlier report shows that thyroid hormone treatment may lead to a 1.5–2.5 fold increase in *in vitro* testicular testosterone synthesis in rat [28]. However what is more surprising in the present investigation is the inhibition of T_3 stimulated androgen release from the Leydig cell by cycloheximide. This suggests involvement of protein synthesis in the increased release of androgen. Role of thyroid hormone in protein synthesis is well known. It has been shown that T_3 specifically interacts with nuclear binding sites, triggering metabolic events which lead to the modulation of nuclear activity and results in stimulation of protein synthesis [4, 5, 31]. The above mentioned finding prompted us to observe T_3 effect on Leydig cell protein synthesis. Results clearly showed 70% increase in protein synthesis in Leydig cell by T_3 which is effectively inhibited by cycloheximide.

Our findings therefore show that a freshwater perch testicular Leydig cell nuclei contains a single species of high affinity and low capacity T_3 receptors which are saturable and analogue specific. These T_3 binding sites are possibly physiologically active as T_3 stimulates androgen release from Leydig cells. This stimulation appears to be not a direct effect of T_3 but mediated by a protein(s) induced by thyroid hormone. It is indeed a very interesting aspect and requires further validation in other teleosts.

ACKNOWLEDGMENTS

This work was supported by a grant from the Department of Sceince and Technology, Ministry of Science and Technology, New Delhi, India (SP/SO/CO3/88). The authors wish to express their sincere gratitude to Dr. John Y. L. Yu, Academia Sinica, Taipei, Taiwan for the generous gift of antiserum for androgen RIA.

REFERENCES

1 Anderson PH, Fukushima K, Schiller HS (1975) Radioimmunoassay of plasma testosterone with use of pollyethylene glycol to separate antibody bound and free hormones. Clin Chem 21: 708–714

2 Banerjee PP, Bhattacharya S, Nath P (1989) Purification and properties of pituitary gonadotropic hormone from Indian teleosts: Freshwater murrel (*Channa punctatus*) and carp (*Catla catla*). Gen Comp Endocrinol 73: 118–128

3 Benbrook D, Pfatl M (1987) A novel thyroid hormone receptor encoded by a C-DNA clone from a human testicular library. Science 238: 788–791

4 Bernal J, Coleoni AH, Degroot LJ (1978) Triiodothyronine stimulation of nuclear protein synthesis. Endocrinology 102: 452–459

5 Bernal J, Degroot LJ (1980) Mode of action of thyroid hormones. In "The thyroid gland" Ed by M De Vesseher, Raven Press, New York, pp 123–143

6 Chakraborti P, Bhattacharya S (1984) Plasma thyroxine levels in freshwater perch: Influence of season gonadotropins and gonadal hormones. Gen Comp Endocrinol 53: 179–186

7 Chakraborti P, Moitra G, Bhattacharya S (1986) Binding of thyroid hormone to isolated ovarian nuclei from a freshwater perch, *Anabas testudineus*. Gen Comp Endocrinol 62: 239–246

8 Chakraborti P, Rakshit DK, Bhattacharya S (1983) Influence of season gonadotropins and gonadal hormones on the thyroid activity of freshwater perch *Anabas testudineus* (Bloch). Can J Zool 61: 359–364

9 Darling DS, Dickhoff WW, Gorbman A (1982) Comparison of thyroid hormone binding to hepatic nuclei of the rat and a teleost (*Oncorhynchus kisutch*). Endocrinology 111: 1936–1942

10 Dettlaff TA, Davydova SI (1979) Differential sensitivity of cells of follicular epithelium and oocytes in the stellate sturgeon to unfavourable conditions and correlating influence of triiodothyronine. Gen Comp Endocrinol 39: 229–232

11 Dodd JM (1975) The hormones of sex and reproduction and their effects in fish and lower chordates twenty years on. Am Zool 15 (suppl 1): 127–171

12 Dufau ML, Mendelson CR, Catt KJ (1974) A highly sensitive *in vitro* bioassay for luteinizing hormone and chorionic gonadotropin: testosterone production by dispersed Leydig cells. J Clin Endocrinol Metab 39: 610–613

13 Eales JG (1979) Thyroid hormones in cyclostomes and fishes. In "Hormones and Evolution Vol 1" Ed by EJW Barington, pp 341–346

14 Fontaine YA (1975) Hormones in fishes. In "Biochemical and Biophysical perspective in marine biology Vol 2" Ed by DC Malins and JR Sargents, Academic Press, Orlando, Fla, pp 139–212

15 Gorbman A (1969) Thyroid function and its control in fishes. In "Fish Physiology Vol 2" Ed by WS Hoar and DJ Randal, Academic Press, New York, Vol 2: pp 241–274

16 Hurlburt ME (1977) Role of thyroid gland in ovarian maturation of the goldfish, *Carassius auratus*. L Can J Zool 55: 1906–1913

17 Ichikawa M, Mori T, Kawashima S, Ueda K, Shira-

hata S (1974) Histological changes in the thyroid and interrenal tissue of kokanee (*Oncorhynchus nerka*) during sexual maturation and spawning. J Fac Sci Univ Tokyo, 4: 175–182

18 Jannini AE, Olivieri M, Francavilla S, Gulino A, Ziparo E, D'armienoto M (1990) Ontogenesis of the nuclear 3,5,3′-triiodothyronine receptor in the rat testis. Endocrinology 126: 2551–2526

19 Lawson GM, Tsai MJ, Tsai SY, Minghetti PP, McClure ME, O'Malley BW (1982) In "Laboratory Methods Manual for Hormone action and Molecular Endocrinology". Ed by H Ballin and BW O'Malley, 6th Ed Houston Biological Assn Inc, pp 5–7

20 Leatham J (1972) Role of Thyroid. In "Reproductive Biology" Ed by H Ballin and S Glasser, Experta Medica, Amsterdam, pp 857–876

21 Lowry OH, Rosebrough NJ, Farr AL, Randall RJ (1951) Protein measurement with folin phenol reagent. J Biol Chem 193: 265–275

22 Maitra G, Bhattacharya S (1989) Seasonal changes of Triiodothyronine binding to piscine ovarian nuclei. Zool Sci 6: 771–775

23 Matty AJ (1960) Thyroid cycles in fish. Symp Zool Soc London, 2: 1–15

24 Oppenheimer JH (1979) Thyroid hormone action at the cellular level. Science 203: 971–979

25 Oppenheimer JH, Schwartz HL, Surks MI (1974) Tissue differences in the concentration of triiodothyronine nuclear binding sites in the rat: liver, kidney, pituitary, heart, brain, spleen and testis. Endocrinology 95: 897–903.

26 Sage M (1973) The evolution of thyroidal function in fishes. Am Zool 13: 899–905

27 Sap J, Munoz A, Damm K, Goldberg Y, Ghysdael J, Leutz A, Beug H, Vennstrom B (1986) The C-erb-A protein is a high-affinity receptor for thyroid hormone. Nature 324: 635–640

28 Schneider G, Kopach K, Ohanian H, Bonnefond V, Mittler JC, Ertel NH (1979) The hypothalamic-pituitary-gonadal axis during hyperthyroidism in the rat. Endocrinology 105: 674–679

29 Sen S, Bhattacharya S (1981) Role of thyroid and gonadotropin on the mobilization of cholesterol in a teleost, *Anabas testudineus* (Bloch). Indian J Exp Biol 19: 408–412

30 Sen S, Bhattacharya S (1982) Hormonal influence of perch ovarian 17β-hydroxysteroid dehydrogenase activity in *in vitro* system. Indian J Exp Biol 20: 664–667

31 Tata JR, Widnell CC (1966) Ribonucleic acid synthesis during early action of thyroid hormones. Biochem J 98: 604–620

32 Van Damme MP, Robertson DM, Diczfalusy E (1974) An improved *in vitro* bioassay method for measuring luteinizing hormone (LH) activity using mouse Leydig cell preparations. Acta Endrocrinol 77: 655–671

33 Vander Kraak JG, Eales JG (1980) Saturable 3,5,3′-triiodothyronine binding sites in liver nuclei of rainbow trout (*Salmo gairdneri*). Gen Comp Endocrinol 42: 437–448

34 Weinberger C, Thompson CC, Ong SE, Lebo R, Gruol JD, Evans MR (1986) The C-erb-A gene encodes a thyroid hormone receptor. Nature 324: 641–646

35 Wiebe PJ (1978) Steroidogenesis in rat Leydig cells: Effect of gonadotropin on the activity of 5-Ane and 5-Ene 3α- and 3β-hydroxysteroid dehydrogenases during sextual maturation. Endocrinology 102: 765–784

36 Yu JYL, Chang TY, Hsu HK, Liao CF, Wan WCM (1981) Androgen/testosterone synthesis by the dissociated testicular cells from mice of different ages in response to rat LH stimulation *in vitro*. Bull Inst Zool Acad Sin 20: 57–65

37 Yu JYL, Wang LM (1987) Comparative effect of diverse vertebrate gonadotropins on androgen formation *in vitro* from testes of roosters and mice. Biol Reprod 36: 816–824

ZOOLOGICAL SCIENCE 10: 497–504 (1993)

Developmental Changes of Testicular Gonadotropin Receptors and Serum Gonadotropin Levels in Two Strains of Mice

Koichi Shiraishi, Tippawan Singtripop, Min Kyun Park and Seiichiro Kawashima[1]

Zoological Institute, School of Science, University of Tokyo Tokyo 113, Japan

ABSTRACT—The relationship between testicular gonadotropin receptors and serum gonadotropin concentrations during sexual maturation was studied in two inbred mouse strains (BALB/cAJcl and ICR/Jcl strains). The specific binding of [^{125}I]iodo-FSH per unit testicular weight was the highest at 21 days of age in the BALB/cAJcl strain and 7 days in the ICR/Jcl strain, followed by a rapid decrease thereafter. The total FSH binding in the ICR/Jcl strain was significantly decreased at 35 days from the level at 28 days and remained low thereafter. However, such decrease was not observed in the BALB/cAJcl strain. Scatchard plot analyses showed that the changes in FSH binding were due to the changes in the number of binding sites and not in the affinity of binding. The specific binding of [^{125}I]iodo-LH per unit testicular weight reached a peak around puberty , and the total LH binding tended to remain constant after puberty in both strains. During early testicular developmental stages, the increase in the serum FSH levels was well correlated with the number of FSH receptors. Prepubertal increase in LH binding sites occurred after the rise in the serum FSH levels. To conclude, we found a strain difference in the regulation of the number of FSH receptors, indicating that down-regulation is not unique to the C57BL/6NCrj strain, but that it is not universal among strains of mice.

INTRODUCTION

The action of gonadotropins on the gonad is mediated by specific gonadotropin receptors localized in the plasma membrane of target cells. For example, follicle-stimulating hormone (FSH) first binds to the plasma membrane receptors of Sertoli cells [2, 8] and elicits various biochemical responses after stimulation of adenylyl cyclase [5, 12]. Therefore, the number of FSH receptors is one of the most important factors determining the sensitivity of Sertoli cells. Tsutsui [19] recently suggested that FSH and testosterone acted synergistically to induce FSH receptors during testicular development in the rat.

In immature and adult male rats, exogenous administration of large amount of FSH was effective in decreasing the number of FSH receptors in Sertoli cells [4, 10]. In male C57BL/6NCrj mice, endogeneous FSH was effective in decreasing its own receptors after puberty, and hypophysectomy when adult induced a significant increase in the number of FSH receptors in Sertoli cells [17]. This is the discovery showing that physiological level of FSH is effective in inducing down-regulation of FSH receptors. As the mechanism for this down-regulation of FSH receptors, internalization of FSH-FSH receptor complexes was claimed by autoradiographic and kinetic studies [13–15]. These findings in the mouse point out that the mouse testis serves as a suitable model for the study of down-regulation and the relationship between gonadotropin receptors and gonadotropin levels.

The present study was designed first to examine whether the down-regulation of FSH receptors found in male C57BL/6NCrj mice is unique to this strain or general phenomenon among various strains of mice, and secondly to afford fundamental knowledge on the developmental changes of gonadotropin receptors and serum gonadotropin concentrations in male mice of

Accepted April 26, 1993
Received April 6, 1993

[1] To whom requests of reprints should be addressed.

strains other than C57BL/6NCrj.

MATERIALS AND METHODS

Animals

Male mice of the BALB/cAJcl and ICR/Jcl strains maintained in this laboratory were used. They were housed in a temperature-controlled room($25 \pm 0.5^{\circ}C$) under daily photoperiods of 12-hr light and 12-hr dark cycles (lights on at 0600 h), and were given laboratory chow and tap water *ad libitum*.

Preparation of serum and receptor samples

Intact mice of various ages during testicular development were sacrificed by decapitation between 1000–1200 h. Trunk blood was collected and allowed to clot at room temperature for one hour. After centrifugation at $1,800 \times g$ for 20 min, serum was stored at $-20^{\circ}C$ until radioimmunoassay (RIA) for FSH and LH. In order to secure sufficient volume of serum for assay in younger mice, serum from one to six animals was pooled. Immediately after the blood collection, the testes were taken out and weighed. The testes from one to six mice were pooled (the number of pooled testes differed according to the weight). The testes were homogenized in 0.04 M Tris-HCl buffer (pH 7.4) containing 0.005 M $MgSO_4$ and 0.1% BSA. The concentration of the homogenates was adjusted to contain 40 mg fresh testes per 100 μl in each age group. The homogenates were centrifuged at $11,000 \times g$ for 20 min at $4^{\circ}C$. The resulting pellets were resuspended in cold Tris-HCl buffer and adjusted to contain 20 mg original tissue/100 μl. The suspension was instantaneously frozen on dry ice-ethanol and stored at $-70^{\circ}C$ until the binding assay was performed. For the binding assay, the frozen samples were quickly thawed and diluted in cold Tris-HCl buffer. The final receptor preparations were adjusted to contain 5 mg equivalent original tissue/100 μl.

Hormone preparations

NIDDK-rat FSH(rFSH)-I-7 and NIDDK-rat LH(rLH)-I-7 were radioiodinated for the assay of FSH and LH receptors, respectively. Unlabeled ovine FSH (oFSH) and ovine LH (oLH) (Bio-Active Chem. Lab.,Tokyo) were used to correct for non-specific binding throughout the assays of FSH and LH receptors, respectively. NIDDK-rat FSH-RP-2 and NIDDK-rat LH-RP-3 were used as reference preparations in RIA of FSH and LH, respectively. These hormone preparations were the gifts from Dr. S. Raiti the National Institute of Arthritis, Diabetes and Digestive and Kidney Diseases, NIH, and Dr. A. F. Parlow, Pituitary Hormone and Antisera Center, University of Maryland School of Medicine.

Binding assay

For the assays of FSH and LH receptors highly purified FSH (NIDDK-rFSH-I-7) and LH (NIDDK-rLH-I-7) were radioiodinated with ^{125}I in the presence of lactoperoxidase and hydrogen peroxide using the method described previously [16]. The specific activities of [^{125}I]iodo-FSH and [^{125}I]iodo-LH were 50 and 40 μCi/μg, respectively.

In radioreceptor assay (RRA) of FSH, receptor preparation and [^{125}I]iodo-FSH (1.0 ng) were incubated at $35^{\circ}C$ for 2.5 hr with or without unlabeled oFSH. For RRA of LH, receptor preparation and [^{125}I]iodo-LH (1.0 ng) were incubated at $35^{\circ}C$ for 2.5 hr with or without unlabeled oLH. At the end of incubation, the reaction tubes were centrifuged at $11,000 \times g$ for 20 min at $4^{\circ}C$ and washed three times by adding 1 ml Tris-HCl buffer containing 0.1% BSA to each tube and centrifuged. Radioactivity of resulting pellets was counted in an auto-well gamma counter. Specific binding was calculated by total binding minus non-specific binding. In Scatchard plot analysis, saturation binding experiments were performed, where the receptor preparation (100 μl) and labeled ligand were incubated with or without different amount (0.2–256 ng) of unlabeled ligand. Final volume of reaction mixture for saturation-binding experiments was adjusted to 400 μl. The equilibrium constant of dissociation (Kd) was determined with the Scatchard plots, constructed from the data obtained from the saturation-binding experiments.

RIA of FSH and LH

Serum FSH and LH were measured by RIA

using a double antibody method [18]. Concentrations of FSH and LH (both being assayed in 100 μl serum) were expressed in terms of ng NIDDK-rat FSH-RP-2 and NIDDK-rat LH-RP-3 per ml serum, respectively.

Statistical analysis

Differences between testicular weights, FSH and LH bindings, and serum FSH and LH concentrations were analyzed by Student's *t*-test.

RESULTS

Changes in testicular weight

Male mice of the BALB/cAJcl strain were sacrificed at 14, 21, 28, 35, 42, 56 and 77 days of age. Fig. 1 shows the changes in the testicular weight. The testicular weight steadily increased from 14 to 42 days ($P<0.001$). After 42 days the testicular weight continued to increase much slowly (Fig. 1, upper panel).

In ICR/Jcl strain, mice were killed at 7, 14, 21, 28, 35, 42, 56 and 77 days. The testicular weight increased progressively from 7 to 42 days ($P<0.001$), and after that the weight of testes showed no significant increases (Fig. 1, lower panel).

Changes in FSH binding during testicular development

In BALB/cAJcl mice, the specific binding of [^{125}I]iodo-FSH /5 mg tissue equivalent was the greatest at 14 or 21 days (Fig. 2, upper panel). It rapidly decreased from 21 to 35 days, followed by a gradual decrease until 77 days of age. The specific binding of [^{125}I]iodo-FSH per two testes increased rapidly from 14 to 21 days ($P<0.001$), and then continued to increase slowly until 42 days of age. The levels at 56 and 77 days were almost the same as the level at 42 days (Fig. 2, lower panel).

In ICR/Jcl mice, the level of specific binding of [^{125}I]iodo-FSH/5 mg tissue was the highest at 7 days of age. A rapid decrease was observed between 7 and 21 days of age ($P<0.001$). The

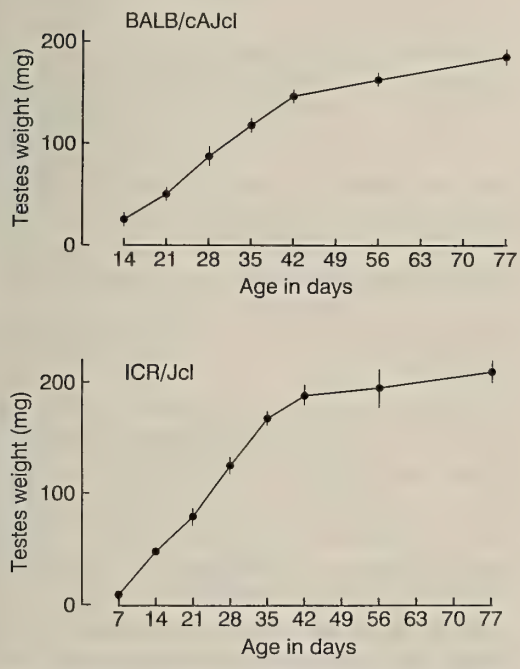

Fig. 1. Changes with age in the testicular weight in BALB/cAJcl (upper panel) and ICR/Jcl mice (lower panel). Each point represents the mean ± SEM (n =4).

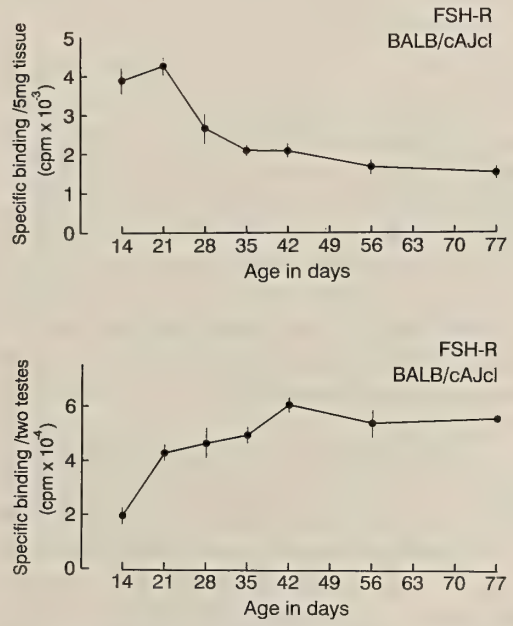

Fig. 2. Changes with age in specific binding of [^{125}I]iodo-rat FSH per 5 mg testicular tissue (upper panel) and specific binding of [^{125}I]iodo-rat FSH per two testes (lower panel) in BALB/cAJcl mice. Each point represents the mean ± SEM (n=4). Incubation of 2.5 hr at 35°C.

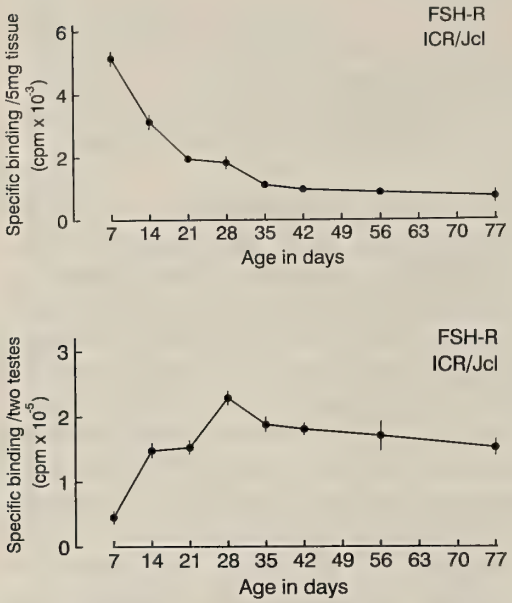

FIG. 3. Changes with age in specific binding of [^{125}I]iodo-rat FSH per 5 mg testicular tissue (upper panel) and specific binding of [^{125}I]iodo-rat FSH per two testes (lower panel) in ICR/Jcl mice. Each point represents the mean±SEM (n=4). Incubation for 2.5 hr at 35°C.

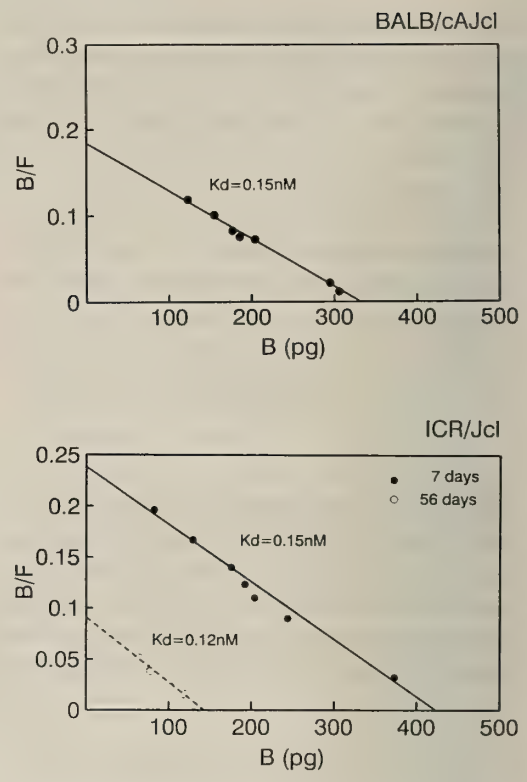

FIG. 4. Scatchard plots of the binding of [^{125}I]iodo-rat FSH to the receptor preparations of mice at 21 days of age in BALB/cAJcl mice (upper panel) and at 7 and 56 days of age in ICR/Jcl mice (lower panel).

level at 77 days was not significantly different from the level at 35 days (Fig. 3, upper panel). The specific binding of [^{125}I]iodo-FSH per two testes markedly increased from 7 to 14 days ($P<0.001$) and from 21 to 28 days ($P<0.001$), followed by a rapid decrease at 35 days ($P<0.05$). Thereafter, it tended to show a slow decrease between 35 and 77 days of age (Fig. 3, lower panel). In contrast to the marked changes in the specific binding, the non-specific binding on unit weight basis was low and almost constant regardless of age and strain (data not shown).

In order to calculate the number of binding sites, Scatchard plot analysis of the specific binding of FSH was carried out in testicular preparations from BALB/cAJcl mice at 21 days of age and ICR/JcL mice at 7 and 56 days of age. Scatchard plots showed straight lines in all groups, indicating the presence of one kind of binding sites. Kd calculated from the fitted lines of the plots in the testis from BALB/cAJcl mice at 21 days of age was 0.15 nM and those from ICR/Jcl mice at 7 and 56 days of age were 0.15 nM and 0.12 nM, respectively. The number of binding sites in the testis of 21-day BALB/cAJcl mice was 2.09 fmol/mg tissue and 7- and 56-day-old ICR/Jcl mice were 2.48 fmol and 0.91 fmol/mg tissue respectively (Fig. 4).

Changes in LH binding during testicular development

In BALB/cAJcl mice, the specific binding of [^{125}I]iodo-LH /5mg tissue equivalent slightly increased until 28 days of age, followed by a rapid increase at 35 days, and thereafter the high level was kept constant (Fig. 5, upper panel). Total binding per two testes continuously increased from 14 to 56 days ($P<0.01$) (Fig. 5, lower panel).

In ICR/Jcl mice, the specific binding of [^{125}I]iodo-LH /5 mg tissue slightly increased from 7 to 14 days, followed by a rapid increase between 14 to 28 days of age ($P<0.05$, 14 days vs. 28 days) (Fig. 6, upper panel). Then, the level tended to

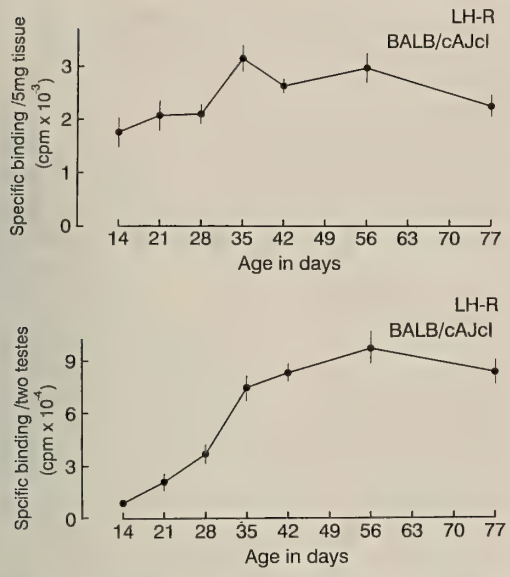

FIG. 5. Changes with age in specific binding of [^{125}I]iodo-rat LH per 5 mg testicular tissue (upper panel) and specific binding of [^{125}I]iodo-rat LH per two testes (lower panel) in BALB/cAJcl mice. Each point represents the mean±SEM (n=4). Incubation for 2.5 hr at 35°C.

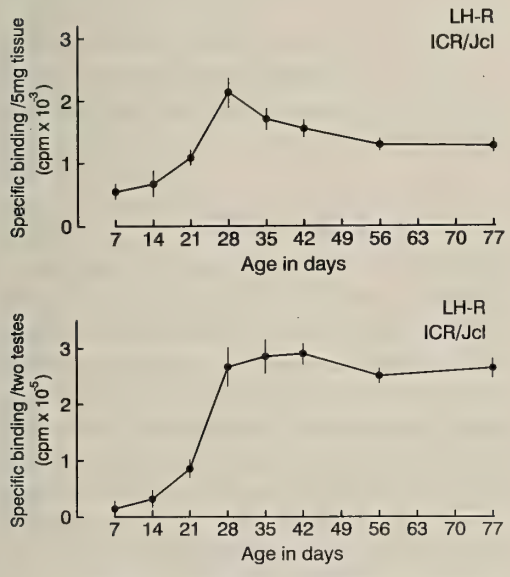

FIG. 6. Changes with age in specific binding of [^{125}I]iodo-rat LH per mg testicular tissue (upper panel) and specific binding of [^{125}I]iodo-rat LH per two testes (lower panel) in ICR/Jcl mice. Each point represents the mean±SEM (n=4). Incubation for 2.5 hr at 35°C.

decrease until 77 days. The specific binding per two testes gradually increased from 7 to 21 days ($P<0.01$), followed by a marked increase during 21 and 28 days ($P<0.05$) (Fig. 6, lower panel). During 28 and 77 days the high level was maintained.

Changes in serum FSH level in male mice

In BALB/cAJcl mice, the serum FSH level increased rapidly until 28 days of age ($P<0.05$, 7 days vs. 28 days). Thereafter, the serum FSH concentrations were almost constant (Fig. 7, upper panel). The period of rapid increase in the serum FSH level coincided well with the period of increase in the total binding shown as a broken line adopted from Fig. 2 (lower panel).

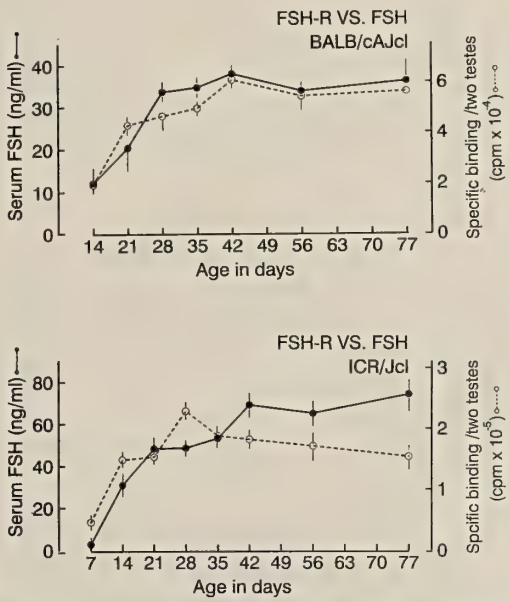

FIG. 7. Age-related changes in serum FSH levels (solid line with redrawn profile of specific binding of [^{125}I]iodo-rat FSH per two testes (broken lines) in BALB/cAJcl (upper panel) and in ICR/Jcl (lower panel). Concentrations of serum FSH are expressed as nanograms of NIDDK-rat FSH-RP-2 per ml. Each point represents the mean±SEM (n=4).

In ICR/Jcl mice, the serum FSH concentrations rapidly increased from 7 to 21 days of age ($P<0.001$) (Fig. 7, lower panel). Gradual increase was observed during 21 to 42 days. After that the serum FSH level was almost constant until 77 days

of age (Fig. 7, lower panel). The period of rapid increase in the serum FSH level fitted well with the period of increase in the total FSH binding (Fig. 7 lower panel). Increase in the serum FSH level was preceded by the increase in the total FSH binding at prepubertal period in ICR/Jcl strain, and the curve for the serum FSH level and that for FSH binding were roughly mirror-imaged between 21 and 35 days (Fig. 7, lower panel). Increase in the total LH binding occurred after the increase in the serum FSH at prepubertal period in both strains (Fig. 8).

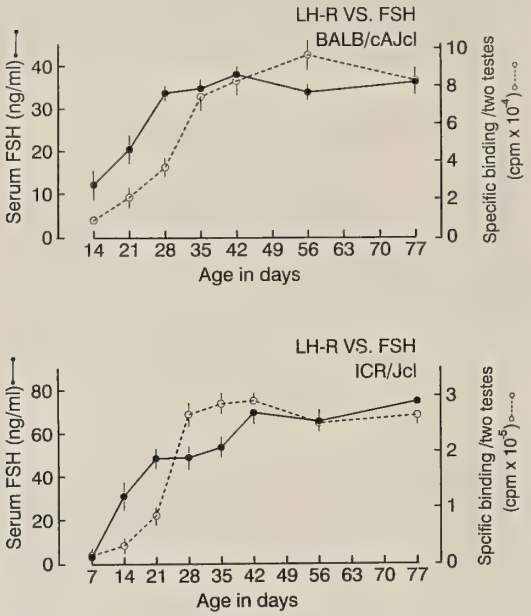

FIG. 8. Age-related changes in serum FSH levels (solid line) with redrawn profile of specific binding of [^{125}I]iodo-rat LH per two testes (broken lines) in BALB/cAJcl (upper panel) and in ICR/Jcl (lower panel). Concentrations of serum FSH are expressed as nanograms of NIDDK-rat FSH-RP-2 per ml. Each point represents the mean±SEM (n=4).

Changes in serum LH level in male mice

The serum LH levels were generally variable in both strains. In BALB/cAJcl mice, the serum LH concentration was high at 14 days of age and suddenly declined at 21 days. Thereafter, it tended to increase until 56 days of age (Fig. 9, upper panel). In ICR/Jcl mice, the serum LH level steadily increased during 7 to 28 days of age, and

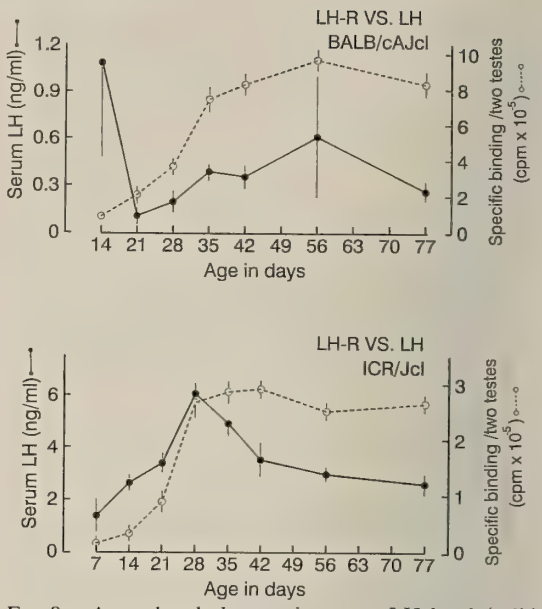

FIG. 9. Age-related changes in serum LH level (solid line) with redrawn profile of specific binding of [^{125}I]iodo-rat LH per two testes (broken line) in BALB/cAJcl (upper panel) and in ICR/Jcl (lower panel). Concentrations of serum LH are expressed as nanograms of NIDDK- rat LH-RP-3 per ml. Each point represents the mean±SEM (n=4).

gradually decreased from 28 to 77 days of age ($P<0.05$) (Fig. 9, lower panel). In accordance with the increase in the total LH binding the serum LH tended to increase.

DISCUSSION

Tsutsui *et al.* [17] have reported that down-regulation of testicular FSH receptors was a physiological phenomenon during sexual maturation in C57BL/6NCrj mice. In other species, such as Japanese quail [16] and photostimulated hamster [18], it is suggested that the increase in FSH levels stimulates the induction of its own receptors (up-regulation). In latter species the total number of FSH receptors is closely related to the plasma FSH levels. First aim of the present study was to examine whether the down-regulation of FSH receptors is unique to male C57BL/6NCrj mice or general phenomenon among various strains of mice. We found that the specific binding of [^{125}I]iodo-FSH per unit tissue weight decreased at

28 days of age from the level at 21 days in BALB/cAJcl strain. However, the highest specific binding per unit tissue was observed as early as at 7 days of age in the ICR/Jcl strain. Total FSH binding per two testes was closely correlated with the increase in circulating FSH levels in both strains of mice. Scatchard plot analyses showed that the increase in FSH binding was due to the increase in the number of binding sites rather than the increase in the affinity of binding in ICR/Jcl mice. The present results were in conformity with the findings of Ketelslegers *et al.* [7] who reported that the early development of testicular FSH receptors was accompanied by a prominent rise in the plasma FSH. However, after the attainment of a peak in the total specific binding of [^{125}I]iodo-FSH, it decreased significantly in ICR/Jcl mice. Whereas, significant decrease in the total specific binding was not observed in BALB/cAJcl mice. These results clearly show a difference in the two strains of mice. For the decrease from the pubertal level in the ICR/Jcl strain, down-regulatory effects of endogenous FSH might be a possible cause, because the serum level of FSH was much higher in the ICR/Jcl strain than BALB/cAJcl strain. We may conclude that down-regulation seems to be not unique to the C57BL/6NCrj strain, but it is not universal among strains of mice.

The present study showed that the specific binding of [^{125}I]iodo-LH per two testes increased until 56 days of age in BALB/cAJcl mice and 42 days in ICR/Jcl mice. After these days the high levels were maintained. These results are in accord with the findings of Pahnke *et al.* [11] who reported that the specific binding of [^{125}I]iodo-hCG increased with age until 60 days in rats and that during this period the number of Leydig cells increased. Similar results have been reported by Mori *et al.* [9] in mice. Mori *et al.* [9] showed that total LH binding markedly increased during 19 to 40 days, when the number of Leydig cells rapidly increased.

Ketelslegers *et al.* [7] found that the development of testicular LH receptors coincided with the phase of rise in the plasma FSH. In the present study, the specific binding of [^{125}I]iodo-LH per two testes increased rapidly in the prepubertal period in male mice in two strains, accompanied by an increase in the serum FSH levels. This finding indicates that the serum FSH is an important factor for the induction of LH receptors. In contrast to the serum FSH, the level of serum LH failed to show a good correlation with the number of LH receptors. In this conjunction, stimulatory effects of Sertoli cells to Leydig cell function have been well documented [1, 3, 6]. However, factors secreted from Sertoli cells by the stimulation of FSH and inducing LH receptors in Leydig cells have not yet been identified.

ACKNOWLEDGMENTS

This study was supported by a Grant-in-Aid for Scientific Research from the Ministry of Education, Science and Culture, Japan and a Research Grant from Zenyaku Kogyo Ltd. to S.K. The authors are grateful to Dr. S. Raiti and Pituitary Hormone Distribution Program, National Institute of Arthritis, Diabetes, and Digestive and Kidney Diseases (NIDDK) for the supply of rat gonadotropins, and to Dr. A. F. Parlow, Pituitary Hormone/Antisera Center, University of Maryland School of Medicine for the supply of RIA kits.

REFERENCES

1 Benahmed M, Reventos J, Tabaone E, Saez J M (1985) Cultured Sertoli cell-mediated FSH stimulatory effect on Leydig cell steroidogenesis. Am J Physiol 248: E176–E181

2 Castro AE, Alonso A, Mancini RE (1972) Localization of follicle-stimulating and luteinizing hormones in the rats testis using immunohistological tests. J Endocrinol 52: 129–136

3 Chen YD, Payne AM, Kelch RP (1976) FSH stimulation of Leydig cell function in the hypophysectomized immature rat. Proc Soc Exp Biol Med 153: 473–475

4 Francis GL, Brown TJ, Bercu BB (1981) Control of Sertoli cell response to FSH: Regulation by homologous hormone exposure. Biol Reprod 24: 955–961

5 Fritz IB (1978) Sites of action of androgens and follicle stimulating hormone on cells of the seminiferous tubule. In "Biochemical Actions of Hormones Vol 5" Ed by G Litwack, Academic Press, New York, pp 249–281

6 Janecki A, Jakubowiak A, Lukaszyk, A (1985) Stimulatory effect of Sertoli cell secretory products on testosterone secretion by purified Leydig cells in primary culture. Mol Cell Endocrinol 42: 235–243

7 Ketelslegers JM, Hetzel WD, Sherins RJ, Catt KJ (1977) Developmental changes in testicular gonadotropin receptor: plasma gonadotropins and plasma testosterone in the rat. Endocrinology 103: 212–

222

8 Mancini RE, Castro AE, Seiguer AC (1976) Histologic localization of follicle-stimulating hormone in the rat testis. J Histochem Cytochem 15: 516–525

9 Mori H, Tsutsui K, Kawashima S (1985) Developmental changes in testicular luteinizing hormone receptors and Leydig cell number in mice with reference to change in plasma gonadotropins and testosterone. J Sci Hiroshima Ser B, Div 1, 32: 143–156

10 O'Shaughnessy P J, Brown P S (1978) Reduction in FSH receptors in the rat testis by injection of homologous hormones. Mol Cell Endocrinol 12: 9–15

11 Pahnke VG, Leinberger FA, Kunzig HJ (1975) Correlation between hCG (LH)-binding capacity, Leydig cell number and secretory activity of rat testis throughout pubescence. Acta Endocrinol 79: 610–618

12 Risbridger GP, Hodgson YM, de Kretser DM (1981) Mechanism of action of gonadotropins on the testis. In "Testis" Ed by H Burger and D. de Kretser, Raven Press, New York, pp 195–212

13 Shimizu A, Tsutsui K, Kawashima S (1987) Autoradiographic study of binding and internalization of follicle-stimulating hormone in the mouse testis minces in vitro. Endocrinol Japon 34: 431–442

14 Shimizu A, Kawashima S (1989a) Kinetic study of inter-nalization and degradation of ^{131}I-labeled follicle-stimulating hormone in mouse Sertoli cells and its relevance to other systems. J Biol Chem 264: 13632–13638

15 Shimizu A, Kawashima S (1989b) Derivation and application of mathematic model for kinetics of ^{131}I-follicle-stimulating hormone bound to receptors. J Biol Chem 264: 13639–13641.

16 Tsutsui K, Ishii S (1978) Effects of follicle-stimulating hormone and testosterone on receptors of follicle-stimulating hormone in the testis of the immature Japanese quail. Gen Comp Endocrinol 36: 297–305

17 Tsutsui K, Shimizu A, Kawamoto K, Kawashima S (1985) Developmental changes in the binding of FSH to the testicular preparations of mice and the effects of hypophysectomy and administration of FSH on the binding. Endocrinology 117: 2534–2543

18 Tsutsui K, Kawashima S, Masuda A, Oishi T (1988) Effects of photoperiod and temperature on the binding of follicle-stimulating hormone (FSH) to testicular preparations and plasma FSH concentration in the Djungarian hamster, *Phodopus sungorus*. Endocrinology 122: 1094–1102.

19 Tsutsui K (1991) Pituitary and gonadal hormone-dependent and -independent induction of follicle-stimulating hormone receptors in the developing testis. Endocrinology 128: 477–487

ZOOLOGICAL SCIENCE 10: 505–509 (1993)

The Behavioral Reactions of a Snake and a Turtle to Abrupt Decreases in Gravity

RICHARD WASSERSUG[1] and AKEMI IZUMI-KUROTANI[2]

[1]*Department of Anatomy and Neurobiology, Faculty of Medicine, Sir Charles Tupper Medical Building, Dalhousie University, Halifax, Nova Scotia, B3H 4H7, Canada, and* [2]*Space Utilization Research Center, Institute of Space and Astronautical Science, 3-1-1, Yoshino-dai Sagamihara, Kanagawa 229, Japan*

ABSTRACT—We report here on the behavioral reaction of two reptiles to abrupt decreases in gravity. One striped rat snake, *Elaphe quadrivirgata*, and three striped-neck pond turtles, *Mauremys japonica*, were exposed to microgravity (μ-G) on parabolic flight, during the filming of a documentary for the NHK television station in Japan. The video films revealed that the snake reflexively responded to the shift from hyper- to hypogravity by taking up a defensive posture—on the first parabola, the snake struck at itself. The turtles actively extended their limbs and hyper-extended their neck in μ-G, a posture which is identical to that displayed during their contact "righting reflex", when placed upside-down in normal gravity. The aggressive display of the snake was unexpected, although the righting response of the turtles was consistent with that shown by other vertebrates, including fish and mammals, exposed to μ-G. An implication of these observations is that the afferent signal for the righting reflex of vertebrates in normal gravity must be the unloading of ventral receptors in the sensory system, rather than the loading of dorsal receptors. These are the first behavioral records for any reptiles exposed to hypogravity.

INTRODUCTION

In the nearly half century that man has been exploring space, a plethora of organisms have been exposed to microgravity (μ-G) either briefly, on parabolic flights, or for longer periods, on orbital missions. Several birds, reptiles, amphibians and fishes, as well as a large variety of mammals have all been exposed to μ-G [2]. Most of this work has focused on the physiological consequences of reduced gravity. Surprisingly little attention has been given to the reflexive behaviors of these organisms upon their initial exposure to microgravity. It is not known, for example, whether there are consistent patterns in the reflexive responses of animals to abrupt changes from hyper- to hypo-G. Do the responses of various vertebrates correlate with their phylogenetic relationships or way of life? Can we predict how any animal will react, for example, in freefall?

Early work with teleost fishes [e.g. 5, 6] suggests that aquatic vertebrates reflexively pitch downward in μ-G and that this leads to looping (forward somersaults). More recent studies, however, with a larger variety of aquatic species (Wassersug, unpublished data) suggest that such forward looping is not characteristic of all lower vertebrates exposed to μ-G. Some amphibian larvae, for example, make forward somersaults (e.g. *Xenopus*), whereas others make backward somersaults (e.g. *Bufo*). Others (e.g. *Rana*) float freely and still others twist and roll along their long axis while swimming forward in short dashes [3, 7, 9, 10]. Clearly, more animals will have to be examined before systematic patterns in the behavioral responses of vertebrates to decreased gravity can be revealed. Ultimately, if behavioral research in gravitation biology is to become a predictive science, such patterns should exist and be identifiable.

As a step towards producing a broader data base on the behavioral responses of vertebrates to de-

Accepted March 16, 1993
Received October 28, 1992

creased gravity, we report here on the behavior of a snake and three turtles exposed to changing gravity in parabolic flight. The behavior was videotaped in the early spring of 1992 by the Japanese television station NHK, in preparation for their April 6th, 1992 television program "Kurabete Mireba" (Comparative Ethology for the General Public). Although the film sequences discussed here were not used in the final production of the documentary, they were graciously made available to us for study.

To the best of our knowledge, there are no other records of the behavior of reptiles in parabolic flight. The great morphological difference between a snake and a turtle and their dramatically different responses, as noted below, emphasize how different the responses of organisms to decreased gravity can be.

MATERIALS AND METHODS

The snake used in this experiment was a single specimen of the common striped rat snake of Japan, *Elaphe quadrivirgata.* This an active, semi-arboreal snake. The turtles used were specimens of the Japanese striped-neck pond turtle *Mauremys* [*Clemmys*] *japonica.* All specimens were on loan to NHK from a local pet store in Nagoya, Japan, and were returned to that store at the end of the mission. Species identifications were confirmed by the supplier, but regrettably no other information on the specimens was recorded. Judging from the size of the containers holding the animals during the flight, we estimated that the snake was 75 cm long. The carapace lengths for the three turtles were similarly estimated at 6–8 cm, 10–12 cm and 13–15 cm respectively. All animals were active and in clearly good health.

The behavior of an additional turtle of the same species and size of the largest turtles exposed to μ-G was examined in the laboratory at the Biology Department of Shimane University, Matsue, Japan.

The snake was flown alone; the three turtles were flown together. For flight the animals were housed in a simple, smooth-sided aquarium without water. The maximum and minimum dimensions of their containers were on the order of half a meter to a third of a meter respectively. The aquarium was braced in the pressurized, temperature-controlled cabin of a Mitsubishi MU 300 aircraft. A fix-mounted Sony Hi 8 video camera continuously filmed the animals throughout their parabolic flights. The snake and turtles were each exposed to eight parabolas. The parabolic maneuvers were performed between 6.6 and 8.5 km elevation and provided in excess of 15–18 sec of μ-G (i.e. $G<10^{-3}$), with intervening hyper-G episodes of approximately 2-G.

RESULTS

Snake

Before the first parabola, the snake was actively exploring its cage. The animal had climbed the vertical edge with the front half of its body and was probing an upper corner with its head, as if searching for a crack or crevice to enter. As the aircraft entered μ-G on the first parabola, the snake immediately retracted its head into three tight curves. The animal thrashed about violently, twisting and rolling. Three seconds into μ-G, a mid-portion of the snake's body came within approximately 10 cm of its head. At that moment the snake struck at itself (Fig. 1). As soon as the head hit the body, it was withdrawn. The action was so fast that we could not confirm from the video images (only alternate ones of which are shown in Fig. 1) whether the mouth was open during this snout-body contact or whether teeth were planted in the skin.

For the remainder of the parabola the snake's head stayed cocked, as if prepared to strike again. At the initiation of reduced gravity on each subsequent parabola, the snake immediately cocked its head into the pre-strike posture just described. Additional strikes, however, were not observed. On the 3rd, 4th and 6th parabolas, the animal successfully braced a portion of its body between the top and bottom of its aquarium and stayed in contact with the container throughout μ-G. This bracing eliminated most of the chaotic twisting and rolling seen in the earlier parabolas.

The snake's response to the hyper-G phase of the parabolic trajectory before its first and subse-

quent exposure to μ-G was, in contrast, subdued. Whenever G increased from <1 to >1 the snake was, understandably, forced toward the bottom of its container. When the animal had a portion of its body elevated during hyper-G, it could be seen straining to maintain its posture. However, at no time in hyper-G did it respond either hyperactively or aggressively, as it did during the shift from hyper-G to hypo-G on the first parabola.

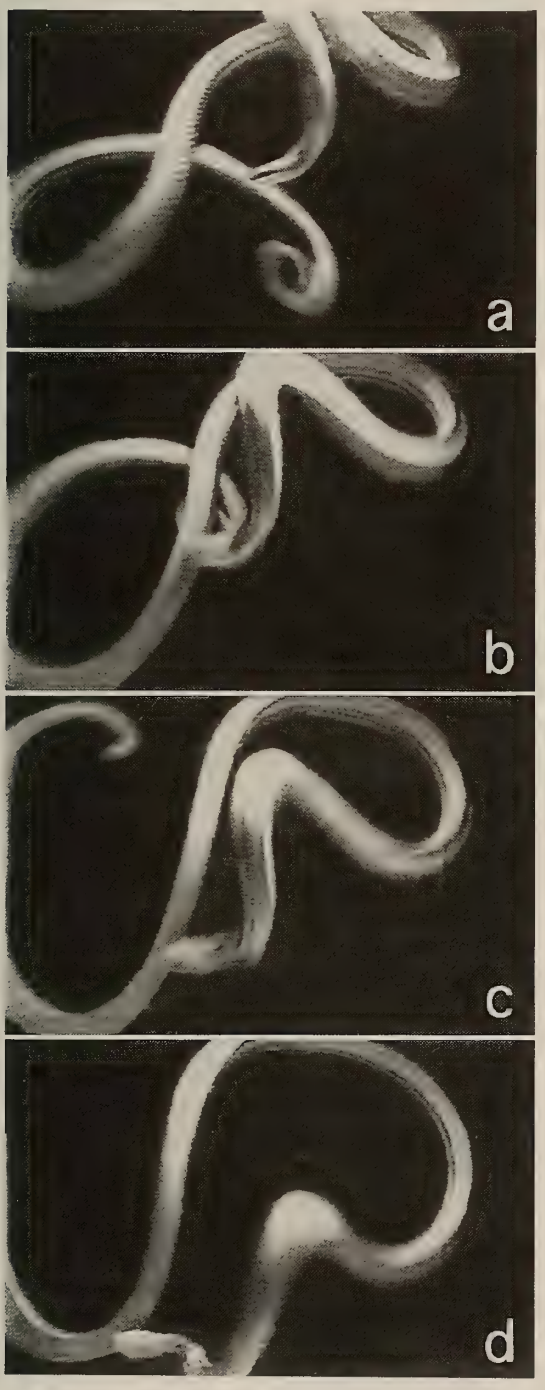

FIG. 1. Four sequential video frames of the rat snake, *Elaphe quadrivirgata,* in microgravity. In the first frame (a) the snake's head is in the middle of the field. In the subsequent two frames (b, c), the snake's snout strikes its body then descends to the bottom left of the field (d). The frames are separated by 20 msec. The video images have been computer enhanced to remove extraneous reflections from the container's walls.

Turtles

The reaction of the turtles to reduced G, in contrast to that of the snake's, was slower and more subdued. At the onset of μ-G, the turtles either stayed in contact with a substrate or were thrown between surfaces due to fluctuation in their acceleration relative to that of the aircraft. The turtles had no control over their trajectory in μ-G and tumbled until they hit a wall or one another. They did not withdraw into their shells. On the contrary, they extended their necks and raised their heads while at the same time fully extending and elevating their limbs (Fig. 2). The digits, most notably on the hind limbs, were spread while the foot was rotated along the long axis of the limb,

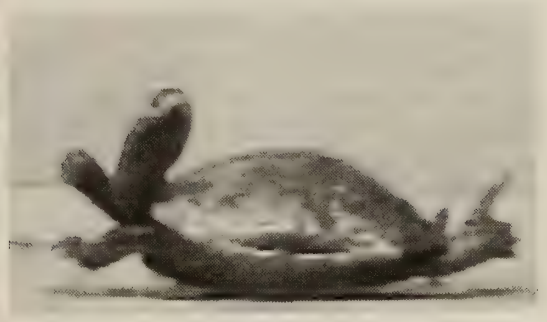

FIG. 2. A video image of a pond turtle, *Mauremys japonica,* in microgravity. Note the hyper-extension of the neck and the asymmetric dorsal deviation of the extended limbs. The same hyper-extension of head and limbs is used by *M. japonica* in normal gravity to generate torque through its long axis and thus to right itself when upside-down by rolling over. The video image has been computer enhanced as in Fig. 1.

bringing the anterior, leading edge upward. The impression created was one of the animal trying to reach or contact, with its head and limbs, objects dorsal to it. The limbs on both sides were not extended or elevated equally; that is, the maneuver was not performed symmetrically.

The dorsal extension just described was exhibited by a turtle during normal gravity in the aircraft when it "landed" upside-down. The posture was used by the turtle specifically to right itself. If was completely duplicated by *M. japonica* in the laboratory at Shimane University by simply putting the turtle upside-down on a styrofoam sheet. In that position, the turtle was able to contact the surface with its extended snout and claws and hold itself in place, such that it could quickly flip over, i.e. "roll" in aviation parlance. On the smooth surface of the flight container, the maneuver was futile except in one case involving the smallest turtle.

The turtles showed little response to either the initial or subsequent episodes of hyper-G. If they were free floating when G shifted from <1 to >1, they were propelled toward the bottom of their aquarium. They did not, however, retreat into their shells or exhibit other signs of undue stress in hyper-G. No progressive changes in the behavior of the turtles were seen as they went through the multiple parabolas.

DISCUSSION

The behavior of reptiles in decreasing G can be readily understood as a manifestation of behaviors that they show in 1-G under special circumstances. There is nothing in their behavioral repertoire during parabolic flight that can be said to be either G or "space specific." The behavior that the snake exhibited was, however, quite different from that of the turtle.

The cocked neck and strike shown by *E. quadrivirgata* as G decreased was clearly of a defensive sort. The writhing and twisting, particularly in early parabolas, is indistinguishable from that of the normal frightened and threatened *E. quadrivirgata*. The fact that the snake actually struck at itself suggests that the animal suffered loss of proprioceptive clues about body position in μ-G. On the other hand, *Elaphe* snakes are naturally preyed upon by hawks in Japan and they occasionally experience aerial suspension when captured. In this situation, it is in the snake's best interest to strike, even to strike blindly! Such a response may have been demonstrated by *E. quadrivirgata* during the shift from hyper- to hypo-G.

Snakes vary greatly in their response to tilting in 1-G, depending on whether they are terrestrial or arboreal [4]. In this regard, it would be particularly interesting to see whether other snakes that are more or less arboreal than *Elaphe* show the same defensive response in μ-G and parabolic flight.

The turtles responded to μ-G as if they were upside-down [1]. This has implications to understanding the stimulus for their righting reflex in 1-G. Specifically, the afferent signal for the hyper-extension of the neck and limbs used in the righting maneuver cannot be the *loading* of dorsal sensory receptors. Rather it must be *un*loading of ventral receptors.

Hyper-extension of the axial skeleton with asymmetrical limb movements has been observed in other vertebrates in μ-G. The combined limb and axial movements lead to long-axis rotation, or rolling. In 1-G this appears to be an important part of a righting reflex best known in arboreal and semi-arboreal vertebrates, such as the cat. The same maneuver is seen, however, in a variety of less arboreal animals in μ-G. These range from aquatic animals, such as the adult clawed frog (*Xenopus*) and salamander larvae [3, 8], to strictly terrestrial mammals, such as the rabbit (on the NHK video film, unpublished data). What distinguishes these behaviors in μ-G from the 1-G situation is that they are more repetitive and protracted in freefall, simply because they are not effective. The ability to duplicate these displays in turtles and many other animals by simply inverting them supports the conclusion that they are manifestations of a natural righting reflex.

ACKNOWLEDGMENTS

We thank Dr. M. Yamashita and NHK television for facilitating access to videofilms of animals in microgravity. Laboratory space at Shimane University was graciously provided by Dr. T. Naitoh. Drs. R. Marlow and

B. Young helped us access relevant literature. Mr. S. Pronych and Ms. M. Fejtek prepared the illustrations. Dr. H. Lillywhite, Mr. S. Pronych and Ms. M. Fejtek reviewed drafts of the manuscript. This work was supported by Canada's Space Agency and its Natural Science and Engineering Research Council, as well as a grant from the Japan Science and Technology Fund.

REFERENCES

1 Ashe V (1970) The righting reflex in turtles: a description and comparison. Psychon Sci 20: 150–152

2 Ballard RW, Mains RC (1990) Animal experiments in space: a brief overview. In "Fundamentals of Space Biology" Ed by M Asashima and G Malacinski, Japan Scientific Societies Press, pp 21–41

3 Izumi-Kurotani A, Wassersug RJ, Yamashita M, Naitoh T, Nagaoka S (1992) Frog behavior under microgravity. 9th ISAS Space Utilization Symp, pp 112–114

4 Lillywhite H (1987) Circulatory adaptations of snakes to gravity. Amer Zool 27: 81–95

5 Scheld HW, Baky A, Boyd JF, Eichler VB, Fuller PM, Hoffman RB, Keefe JR, Kuchnow KP, Oppenheimer JM, Salinas GA, von Baumgarten RJ (1976) Killifish hatching and orientation (Experiment MA-161), Apollo-Soyuz Test Project Preliminary Science Report. In "NASA Technical Memorandum X-58173" Washington DC, pp 281–305

6 Von Baumgarten RJ, Baldrighi G, Shillinger Jr GL (1972) Vestibular behavior of fish during diminished G-force and weightlessness. Aerospace Med 43: 626–631

7 Wassersug RJ (1992) The basic mechanics of ascent and descent by anuran larvae (*Xenopus laevis*). Copeia 1992: 890–894

8 Wassersug RJ, Izumi-Kurotani A, Yamashita M, Naitoh T (1993) Motion sickness in amphibians. Behav Neural Biol: in press

9 Wassersug RJ, Pronych SP, Schofield SM, Schmidt GK (1991) On the way of life of aquatic vertebrates and their behavioral responses to reduced gravity. ASGSB Bull 5: 42

10 Wassersug RJ, Pronych SP, Souza KA (1991) Studying the effects of microgravity on lower vertebrate development and behavior: a progress report. Proceedings Spacebound 91, CSA Publication No. 5891, pp 146–150

ZOOLOGICAL SCIENCE 10: 511–519 (1993)

Differences in the Responses of Two Mudskippers to Terrestrial Exposure

Yuen K. Ip, Chee Y. Lee, Shit F. Chew[1], Wai P. Low and Kah W. Peng

Department of Zoology, National University of Singapore, 10 Kent Ridge Crescent, Singapore 0511, Republic of Singapore

ABSTRACT—The concentration of NH_4^+ in the plasma and muscles of *Periophthalmodon schlosseri* and *Boleophthalmus boddaerti* increased significantly after exposure to terrestrial conditions for 24 hr. Such increases in NH_4^+ concentrations in *B. boddaerti* were not accompanied by any significant increase in urea concentrations. However, significant increases in urea concentrations occurred in the plasma, liver and muscle of *P. schlosseri* kept away from water. Results obtained indicate that the liver may be a major organ involved in urea production in this mudskipper. In addition, there were significant increases in the concentrations of total free amino acids in the plasma, liver and muscle of *P. schlosseri,* but not in those of *B. boddaerti,* after 24 hr of terrestrial exposure. Terrestrial exposure also affected the aminating and deaminating activities of glutamate dehydrogenase from the liver of *P. schlosseri*, leading to a significant increase in the aminating/deaminating ratio. It is concluded that *P. schlosseri*, having developed a greater affinity to land than *B. boddaerti,* has also acquired a greater capacity to detoxify ammonia.

INTRODUCTION

Mudskippers are gobioid teleosts usually found in mangrove swamps in the estuaries of rivers. They are amphibious and spend a substantial part of their lives out of water. In Singapore, *Boleophthalmus boddaerti* and *Periophthalmodon schlosseri* inhabit mud flats which are periodically inundated by the tide. The former makes burrows on the lower regions of the intertidal zone while the latter burrows on higher ground. At low tide, both are found on the mudflats. At high tide, *B. boddaerti* stays in its water-filled burrows and resurfaces only when the tide ebbs while *P. schlosseri* often swims with its snout and eyes above water along the water's edge.

Recent studies by low *et al.* [17, 18] reveal that the gills of *P. schlosseri* are better adapted to a terrestrial than an aquatic environment. It has relatively fewer and shorter gill filaments, and its gills exhibit intrafilamentary secondary lamellar fusions which reduce coalescence of the respiratory surfaces upon terrestrial exposure. However, such fusions would render branchial gaseous exchange in water *via* the counter-current mechanism inefficient. In contrast, the gills of *B. boddaerti* are better adapted for aquatic respiration as they exhibit relatively longer gill filaments, and most of their secondary lamellae are aligned to the respiratory water current.

In general, the nature of the major nitrogenous end-product of a species is correlated with that species's environment: aquatic species are ammonotelic, whereas terrestrial species are either ureotelic or purinotelic [3, 21]. Gordon *et al.* [9] first demonstrated that the Madagascan mudskipper, *Periophthalmus sobrinus*, might have a potential for the transition to ureotelism while it was out of water. Similar results were obtained for the Chinese mudskipper, *Periophthalmus cantonensis* [10]. However, Morii *et al.* [22, 23] and Morii [21] showed that NH_4^+ was mainly accumulated, and its conversion to urea was hardly performed, in the bodies of *P. cantonensis* and *Boleophthalmus pecti-*

Accepted March 29, 1993
Received December 7, 1992

[1] Present address: Biology Division, School of Science, National Institute of Education, Nanyang Technological University, 469 Bukit Timah Road, Singapore 1025, Republic of Singapore

nirostris during the period out of water. Iwata *et al.* [15] obtained results, similar to those of Morii [21] and Morii *et al.* [22, 23], on *P. cantonensis* in a separate study.

To date, whether mudskippers have a potential for the transition towards ureotelism during a terrestrial excursion is still disputable. This is mainly due to the lack of knowledge on their differences in terrestrial affinities. It would appear that *P. schlosseri* is a more important candidate to be examined in this regard because its gills show the highest degree of adaptation, amongst the mudskippers, to respire terrestrially. Since no such information on this mudskipper is available, the present study was undertaken to elucidate the mechanisms by which ammonia was detoxified in *P. schlosseri* when exposed to a terrestrial environment. Experiments were also performed on the relatively more aquatic species, *B. boddaerti,* for comparison. During the course of the study, it was observed that, different from *B. boddaerti, P. schlosseri* accumulated in its tissues not only urea and NH_4^+, but also significantly higher concentrations of total free amino acids (TFAA) after 24 hr of terrestrial exposure. Therefore, the possible involvement of glutamate dehydrogenase (GDH) in ammonia detoxification in the latter mudskipper was also examined.

MATERIALS AND METHODS

Collection and maintenance of mudskippers

P. schlosseri and *B. boddaerti* were collected along the estuarine canal at Pasir Ris, Singapore. They were maintained in 50% (15‰ salinity) seawater (SW) at 25°C in the laboratory and the SW was changed daily. The aquaria were tilted slightly, so that the fish were free to be in or out of water. No attempt was made to separate the sexes. *P. schlosseri* and *B. boddaerti* were fed small guppies and a manufactured product (Goldfish and Staple Flake, Everyday Co., Singapore), respectively.

Exposure of mudskippers to experimental conditions

Fish were exposed to terrestrial conditions at 25°C for 24 hr in aquaria lined with one layer of cotton wool and two layers of Whatman no. 1 filter paper steeped with 50% SW at the bottom. After 24 hr, fish were anaesthetized for 10 min in an atmosphere saturated with diethylether.

Fish submerged in aerated 50% SW at 25°C for 24 hr were used as controls for comparison. After 24 hr in the SW, fish were anaesthetized by the introduction of 3-aminobenzoic acid ethyl ester (MS222) at a final concentration of 0.005%.

Sample preparation for the analyses of NH_4^+, urea and free amino acids (FAA)

Anaesthetized fish were killed immediately by pithing. The lateral muscle and the liver were quickly excised. No attempt was made to separate red and white muscles. The excised tissues and organs were immediately freeze-clamped in liquid N_2 with precooled tongs [6]. The whole procedure was completed within 30 s. Frozen samples were kept at −80°C until analysis.

The frozen samples was weighed, ground to a powder under liquid N_2 and placed in either 5 vol (w/v) (for urea and NH_4^+ analyses) or 15 vol (w/v) (for FAA analyses) of ice-cold 6% trichloroacetic acid (TCA). The sample was homogenized thrice using an Ultra-Turrax homogenizer (Janke and Kunkel Gmbh & Co., Germany) at maximum speed for 20 sec each with 10 sec off intervals. The sample was then centrifuged at 10,000×*g* at 4°C for 10 min using a Kokusan H251 refrigerated centrifuge (Kokusan Enshinki Co., Japan). The supernatant fluid obtained was analyzed for NH_4^+, urea and FAA.

A separate group of fish exposed to similar conditions was used for the collection of blood samples. The caudal peduncle of the anaesthetized fish was severed and blood exuding from the caudal artery was collected in heparinized capillary tubes. The tubes were centrifuged at 4,000×*g* at 4°C for 10 min to obtain the plasma. The collected plasma was deproteinized in 2 vol (v/v) of ice-cold 6% TCA and centrifuged at 10,000×*g* at 4°C for 15 min. The resulting supernatant fluid was kept at −80°C until analysis.

Determinations of NH_4^+, urea and FAA

For the analysis of NH_4^+, the pH of the depro-

teinized sample was adjusted to 5.5–6.0 with 5 M $KHCO_3$. The NH_4^+ content was determined according to the method of Kun and Kearney [16]. The reaction medium, in a total of 2.7 ml, contained 100 mM Tris-HCl (pH 8.0), 10 mM α-ketoglutarate ($\propto$KG), 0.19 mM NADH, 24.3 IU GDH (Sigma Chemical Co., MO) and 0.2 ml sample. Freshly prepared NH_4Cl solution was used as the standard for comparison.

For the determination of urea, the pH of the sample was neutralized with 5 M K_2CO_3. To 0.2 ml of this neutralized sample, analysis was performed using a Sigma Urea Assay Kit Procedure 535 (Sigma Chemical Co., MO). To another 0.2 ml of the same sample, similar analysis was performed after incubating for 15 min at 30°C with 0.2 ml of 20 mM imidazole buffer (pH 7.0) containing 2 IU urease (Sigma Chemical Co, MO). The difference in absorbance obtained from samples with and without urease treatment was used for the estimation of the urea concentration in the sample. Urea obtained from Sigma Chemical Co. (USA) was used as a standard for comparison.

For the analysis of FAA, the sample was adjusted to pH 2.2 with 4 M LiOH and diluted appropriately with 0.2 M lithium citrate buffer (pH 2.2). FAA were analyzed using a Shimadzu LC-6A Amino Acid Analysis System with a Shim-pack ISC-07/S1504 Li type column. Since taurine was found to be present in much greater concentrations than other FAA in the various tissues and organs of these two mudskippers (except in the muscle of *B. boddaerti*) and since terrestrial exposure had no significant effect on its concentrations, the authors decided not to take it into account in the calculation for the concentration of TFAA to better reflect the overall changes in the concentrations of other FAA.

Results were expressed as μM/g for muscles and livers, and μM/ml for plasma.

Preparation of samples for enzymatic analyses

Samples for GDH assays were prepared according to Chew and Ip [4] with some modifications. The excised muscle was homogenized in 5 vol (w/v) of an ice-cold buffer, which contained 300 mM sucrose, 0.1 mM EDTA and 3 mM Tris-HCl (pH 7.4), using an Ultra-Turrax homogenizer at minimum speed for 10 sec. The liver sample was homogenized three strokes in 10 vol (w/v) of the same buffer using a teflon-glass homogenizer. The homogenized sample was centrifuged at $600 \times g$ for 15 min at 4°C in a Beckman J2-21 M/E refrigerated centrifuge (Beckman Instruments, USA) to remove any unbroken cells and nuclei. The supernatant fluid obtained was further centrifuged for 15 min at $10{,}000 \times g$ to obtain the mitochondria. The mitochondria were washed twice by resuspension and resedimentation in the same buffer and sonicated before assaying of GDH activity.

Enzyme assays

Enzyme assays were performed by monitoring changes of absorbance at 25°C using a Shimadzu UV-160A spectrophotometer.

Activity of GDH in the aminating direction was determined according to the method of Iwata *et al.* [15] with some modifications. The reaction mixture in a total volume of 2.8 ml contained 200 mM triethanolamine-HCl (pH 7.8), 0.1 mM NADH, 0.12 mM ADP, 10 mM αKG and 250 mM ammonium acetate. A control assay was conducted without αKG. The oxidation of NADH was monitored at 340 nm. Specific activities were expressed as μmol NADH oxidized/mg protein per min.

Activity of GDH in the deaminating direction was assayed using a modified colorimetric method of Beutler and Michal [2]. The absorbance change was monitored at 492 nm. The reaction medium, in a total volume of 1.3 ml, comprised 200 mM glycine-NaOH (pH 8.8), 0.4 mM NAD, 0.12 mM ADP, 0.8 mM iodonitrotetrazolium chloride, 0.17 IU/ml diaphorase (Sigma Chemical Co., USA) and 100 mM glutamate. The specific activity was expressed as μM formazan formed/mg protein per min.

Protein content of the sample was determined according to the method of Bradford [1]. Bovine gamma globulin (Sigma Chemical Co., USA) dissolved in 25% glycerol was used as the standard for comparison.

Determination of LT_{50} for mudskippers exposed to various concentrations of NH_4Cl

Because of the great difference in ammonia tolerance between the two mudskippers, different

concentrations of NH_4Cl were used to obtain the respective LT_{50} values. Ten *B. boddaerti* (20–30 g) were exposed individually at 25°C to 3.7 liter of aerated SW containing 20 or 50 mM of NH_4Cl (Merck Chemical Co., Germany). Similarly, 10 *P. schosseri* (90–120 g) were exposed to 150 mM NH_4Cl. The time of mortality for each group was recorded. The LT_{50} values were determined graphically.

Statistical analyses

Results were presented as mean ± SE. Student's *t*-test was used to compare differences between means. Differences with $P<0.05$ were regarded as statistically significant.

RESULTS

The concentrations of NH_4^+ in the plasma and muscles of *P. schlosseri* and *B. boddaerti* increased significantly after exposure to terrestrial conditions for 24 hr (Table 1). Under both the submerged and terrestrial conditions, the NH_4^+ concentrations in the liver of *P. schlosseri* were approximately 4 times higher than those of *B. boddaerti*. The increases in NH_4^+ concentrations in the plasma and muscle of *B. boddaerti* were not accompanied by any significant increase in urea concentrations. However, significant increases in urea concentrations occurred in the plasma, liver and muscle of *P. schlosseri* kept away from water (Table 1). The increase in the concentration of urea, without an accompanying increase in that of NH_4^+, in the liver of *P. schlosseri* exposed terrestrially led to a significant increase in the urea/NH_4^+ ratio in this organ.

The liver of *P. schlosseri* contained a significantly greater concentration of TFAA than that of *B. boddaerti* (Table 2). However, the TFAA concentration in the muscle of the latter was significantly higher than that of the former (Table 3). This was due to the presence of approximately 20 times more glycine in the muscle of *B. boddaerti* compared to that of *P. schlosseri*. The taurine concentrations in the liver (Table 2) and muscle (Table 3) of *P. schlosseri* were significantly higher than those of *B. boddaerti*.

After exposure to terrestrial conditions for 24 hr, there were significant increases in the concentrations of TFAA in the liver (Table 2), muscle (Table 3) and plasma (Table 4) of *P. schlosseri*, but not in those of *B. boddaerti*. In the latter

Table 1. Concentrations (μM/ml plasma and μM/g liver or muscle) of urea and ammonia and their ratios (urea/ammonia) in the plasma, liver and muscle of *B. boddaerti* and *P. schlosseri* fully submerged in 50% SW or exposed to terrestrial condition for 24 hr[1]

Fish	Tissues	Conditions	Urea	Ammonia	Urea / Ammonia
B. boddaerti	Plasma	Submerged	1.34±0.09	0.44±0.03	2.90±0.32
		Terrestrial	1.61±0.13	0.72±0.05*	2.09±0.27
	Liver	Submerged	0.55±0.07	0.64±0.07	0.91±0.17
		Terrestrial	0.59±0.15	0.88±0.09	0.66±0.13
	Muscle	Submerged	0.81±0.05	0.88±0.07	0.93±0.12
		Terrestrial	0.79±0.12	1.46±0.20*	0.59±0.11
P. schlosseri	Plasma	Submerged	1.14±0.16	0.54±0.06	2.17±0.29
		Terrestrial	2.34±0.32*	0.92±0.05*	2.19±0.33
	Liver	Submerged	0.61±0.13	2.54±0.21	0.23±0.05
		Terrestrial	1.66±0.21*	3.46±0.54	0.50±0.08*
	Muscle	Submerged	0.89±0.14	0.96±0.13	1.05±0.31
		Terrestrial	1.47±0.13*	1.64±0.09*	0.90±0.08

[1] Results represent means ± SE of three of five determinations on separate preparation from different animals.
* Significantly different from the corresponding value of the submerged fish.

TABLE 2. Concentrations (μM/g) of various free amino acids (FAA) and total FAA (TFAA) in the livers of *B. boddaerti* and *P. schlosseri* fully submerged in 50% SW or exposed to terrestrial condition for 24 hr[1]

FAA	*B. boddaerti*		*P. schlosseri*	
	Submerged	Terrestrial	Submerged	Terrestrial
Ala	0.22 ±0.02	0.15 ±0.03	1.17 ±0.12	4.13±0.74*
Arg	0.020±0.002	0.020±0.002	0.18 ±0.03	0.19±0.04
Asp	0.26 ±0.04	0.24 ±0.03	0.27 ±0.03	0.43±0.04*
Glu	1.96 ±0.32	3.10 ±0.47	4.20 ±0.29	5.39±0.31*
Gly	1.09 ±0.08	0.61 ±0.15*	1.04 ±0.12	0.68±0.09*
His	0.17 ±0.02	0.16 ±0.03	0.26 ±0.02	0.33±0.04
Ile	0.040±0.006	0.039±0.005	0.080±0.007	0.16±0.01*
Leu	0.130±0.020	0.094±0.014	0.21 ±0.02	0.37±0.02*
Lys	0.15 ±0.01	0.14 ±0.03	0.39 ±0.02	0.98±0.30
Phe	0.038±0.007	0.052±0.003	0.21 ±0.02	0.22±0.04
Pro	0.24 ±0.05	0.28 ±0.05	0.36 ±0.03	0.59±0.08*
Ser	0.17 ±0.01	0.13 ±0.02	0.10 ±0.01	0.18±0.02*
Thr	0.040±0.004	0.042±0.007	0.94 ±0.10	0.39±0.05*
Tyr	0.17 ±0.05	0.13 ±0.009	0.09 ±0.02	0.16±0.02
Val	0.18 ±0.04	0.22 ±0.04	0.24 ±0.02	0.60±0.11*
TFAA	5.13 ±1.06	5.59 ±0.80	10.3 ±0.8	15.5±1.4*
Tau	7.54 ±0.34	7.23 ±1.47	22.2 ±3.4	20.2±2.3

[1] Results represent means±SE of six to seven determinations on separate preparations from different animals.

* Significantly different from that of the corresponding value of the submerged fish.

TABLE 3. Concentrations (μM/g) of various free amino acids (FAA) and total FAA (TFAA) in the muscles of *B. boddaerti* and *P. schlosseri* fully submerged in 50% SW or exposed to terrestrial condition for 24 hr[1]

FAA	*B. boddaerti*		*P. schlosseri*	
	Submerged	Terrestrial	Submerged	Terrestrial
Ala	1.95±0.09	2.94±0.26*	1.30±0.12	2.99±0.32*
Arg	0.49±0.05	0.28±0.01*	0.18±0.02	0.33±0.03*
Asp	0.33±0.05	0.12±0.02*	0.13±0.01	0.11±0.02
Glu	0.42±0.06	0.31±0.02	0.23±0.05	0.22±0.03
Gly	22.6±1.0	23.0±1.3	1.07±0.13	1.30±0.16
His	0.71±0.13	1.03±0.03*	0.25±0.02	0.32±0.03
Ile	0.22±0.02	0.20±0.01	0.12±0.01	0.35±0.03*
Leu	0.41±0.04	0.36±0.01	0.27±0.02	0.66±0.05*
Lys	2.17±0.07	2.08±0.11	1.16±0.14	1.63±0.14
Phe	0.07±0.01	0.11±0.03	0.17±0.03	0.24±0.02
Pro	0.19±0.01	0.27±0.02*	0.10±0.02	0.24±0.01*
Ser	0.90±0.07	0.92±0.02	0.23±0.01	0.44±0.05*
Thr	0.32±0.06	0.54±0.04*	0.31±0.02	0.42±0.04*
Tyr	0.25±0.01	0.17±0.02*	0.10±0.03	0.18±0.02
Val	0.28±0.03	0.26±0.02	0.21±0.02	0.51±0.04*
TFAA	31.6±0.8	32.2±1.3	5.99±0.33	9.93±0.78*
Tau	7.40±0.49	9.05±1.93	19.4±1.9	19.1±2.9

[1] Results represent means±SE of five to six determinations on separate preparations from different animals.

* Significantly different from that of the corresponding value of the submerged fish.

Table 4. Concentrations (μM/ml) of various free amino acids (FAA) and total FAA (TFAA) in the plasma of *B. boddaerti* and *P. schlosseri* fully submerged in 50% SW or exposed to terrestrial condition for 24 hr[1]

FAA	*B. boddaerti*		*P. schlosseri*	
	Submerged	Terrestrial	Submerged	Terrestrial
Ala	0.043 ±0.002	0.071 ±0.004*	0.140 ±0.018	0.242 ±0.019*
Arg	0.023 ±0.002	0.025 ±0.007	0.044 ±0.019	0.056 ±0.003
Asp	0.0070±0.0012	0.0067±0.0006	0.0041±0.0001	0.0034±0.0002
Glu	0.013 ±0.002	0.014 ±0.002	0.014 ±0.001	0.012 ±0.003
Gly	0.248 ±0.013	0.260 ±0.020	0.076 ±0.008	0.078 ±0.009
His	0.019 ±0.001	0.021 ±0.005	0.022 ±0.004	0.027 ±0.003
Ile	0.051 ±0.005	0.047 ±0.001	0.063 ±0.004	0.156 ±0.006*
Leu	0.115 ±0.012	0.103 ±0.005	0.109 ±0.009	0.256 ±0.015*
Lys	0.020 ±0.003	0.056 ±0.007	0.057 ±0.019	0.139 ±0.031*
Phe	0.023 ±0.002	0.022 ±0.004	0.034 ±0.004	0.049 ±0.007*
Pro	0.0090±0.0006	0.0110±0.0010	0.018 ±0.001	0.036 ±0.008*
Ser	0.016 ±0.001	0.017 ±0.001	0.024 ±0.002	0.025 ±0.003
Thr	0.020 ±0.001	0.025 ±0.004	0.072 ±0.008	0.069 ±0.009
Tyr	0.022 ±0.003	0.024 ±0.001	0.021 ±0.002	0.036 ±0.005*
Val	0.073 ±0.007	0.066 ±0.003	0.121 ±0.007	0.195 ±0.026*
TFAA	0.721 ±0.030	0.762 ±0.041	0.886 ±0.075	1.359 ±0.088*
Tau	8.26 ±1.21	9.14 ±0.98	10.0 ±2.5	12.2 ±1.4

[1] Results represent means±SE of five to six determination on separate preparations from different animals.
* Significantly different from that of the corresponding value of the submerged fish.

Table 5. Specific enzyme activities of glutamate dehydrogenase in the amination (μM NADH oxidized/mg protein per min) and deamination (μM formazan formed/mg protein per min) directions, and their ratios (amination/deamination) from the livers and muscles of *B. boddaerti* and *P. schlosseri* fully submerged in 50% SW or exposed to terrestrial condition for 24 hr[1]

Fish	Tissues	Conditions	Amination	Deamination	Amination / Deamination
B. boddaerti	Liver	Submerged	0.18 ±0.03	0.0072±0.0008	21.8±2.2
		Terrestrial	0.25 ±0.03	0.0068±0.0006	28.2±2.7
	Muscle	Submerged	0.028±0.001	0.0022±0.0001	12.8±0.8
		Terrestrial	0.025±0.001	0.0022±0.0001	11.7±0.7
P. schlosseri	Liver	Submerged	1.62 ±0.21	0.0372±0.0060	58.1±12.0
		Terrestrial	0.85 ±0.06*	0.0088±0.0014*	116 ±21*
	Muscle	Submerged	0.13 ±0.03	0.0075±0.0015	17.7±0.6
		Terrestrial	0.20 ±0.03	0.0098±0.0018	19.3±2.0

[1] Results represent means±SE of five to six determinations on separate preparations from different animals.
* Significantly different from the corresponding value of the submerged fish.

mudskipper, only the concentration of alanine in the plasma was significantly increased after terrestrial exposure. However, similar exposure increased the concentrations of alanine, isoleucine, leucine, lysine, phenylalanine, proline, tyrosine and valine in the plasma of *P. schlosseri* (Table 4). There were significant decreases in glycine concentrations in the livers of both *B. boddaerti* and *P. schlosseri* exposed to terrestrial conditions (Table 2). On the other hand, the concentrations of alanine, aspartate, glutamate, isoleucine, leucine, proline, serine and valine increased significantly in the liver of only *P. schlosseri* after 24 hr of terrestrial exposure (Table 2). Terrestrial exposure significantly decreased (arginine, aspartate and tyrosine) and increased (alanine, histidine, proline and threonine) the concentrations of several FAA in the muscle of *B. boddaerti* (Table 3). In comparison, only significant increases in the concentrations of 8 FAA (alanine, arginine, isoleucine, leucine, proline, serine, threonine and valine) were observed in the muscle of *P. schlosseri* exposed to terrestrial conditions (Table 3). Terrestrial exposure had no significant effect on the concentrations of taurine in the liver (Table 2), muscle (Table 3) and plasma (Table 4) of both mudskippers.

The specific activities of GDH, in the aminating and deaminating directions, in the liver and muscle of *P. schlosseri* were significantly higher than those of *B. boddaerti* (Table 5). Terrestrial exposure had no significant effect on the aminating and deaminating activities of the GDH from the liver and muscle of *B. boddaerti.* In contrast, similar exposure decreased the aminating and deaminating activities of the GDH from the liver of *P. schlosseri*, but the amination/deamination ratio was significantly increased (Table 5).

The LT_{50} of *P. schlosseri* for 150 mM NH_4Cl was 13 hr. For *B. boddaerti*, the LT_{50} for 20 and 50 mM NH_4Cl were 75 and 36 min, respectively.

DISCUSSION

Since branchial NH_4^+ excretion would be inefficient when no external water current is available to irrigate the gills during terrestrial exposure, the plasma and muscles of *P. schlosseri* and *B. boddaerti* exposed terrestrially for 24 hr accumulated significantly greater quantities of NH_4^+ compared to those of the respective fish submerged in water. Similar to *P. cantonensis* and *B. pectinirostris* [21–23], terrestrial exposure had no significant effect on the urea concentrations in the plasma, liver and muscle of *B. boddaerti.* Hence, the accumulated NH_4^+ does not seem to be channelled into urea production in *B. boddaerti.* In contrast, *P. schlosseri* accumulated significantly greater concentrations of urea in the plasma, liver and muscle after being kept away from water for 24 hr. Thus, a conversion of NH_4^+ into urea might have occurred in this mudskipper during terrestrial exposure. The authors speculate that the liver may be the major organ involved in urea production in *P. schlosseri,* because this organ exhibited the greatest increase (2.5 fold) in urea content but without any significant accumulation of NH_4^+ after 24 hr of terrestrial exposure, leading to a significantly greater urea/NH_4^+ ratio compared to that of the submerged fish.

The pathway involved in the increased urea synthesis in *P. schlosseri* during terrestrial exposure is not elucidated in this study. Some teleosts can synthesize urea through purine catabolism in their liver [5, 8, 20]. Gregory [11] detected urate oxidase, allantoicase and allantoinase, which are involved in converting uric acid through allantoin and allantoic acid to glyoxylate and urea, in the mudskippers, *Periophthalmus expeditionium* and *Periophthalmus gracilis.* Glyoxylate could lead to the formation of glycine through transamination reactions. Since the glycine level in the liver of *P. schlosseri* exposed to 24 hr of terrestrial conditions was significantly lower than that of the submerged ones, it can be deduced that the increased urea production in this fish during terrestrial exposure may not be due to the degradation of uric acid. The ornithine-urea cycle is an alternative pathway for urea synthesis in some other teleosts [13, 20, 24]. However, Gregory [11] was able to detect only two (arginase and ornithine carbamoyltransferase) out of five enzymes of the ornithine-urea cycle in the liver extracts from the mudskippers, *P. expeditionium, P. gracilis* and *Scartelaos histophorus.* Since no information concerning this aspect is available for *P. schlosseri,* we are currently investigating if all the enzymes of this cycle are present in

this mudskipper.

Iwata *et al.* [15] reported that the muscle of *P. cantonensis* accumulated FAA, especially the non-essential ones, after terrestrial exposure. However, in *P. schlosseri,* accumulations of some essential amino acids, e.g. the branched-chain FAA, also occurred. Hence, there might be an increase in the mobilization of protein as carbon and energy sources in *P. schlosseri* exposed to terrestrial conditions. Such a shift in metabolic pathways may be related to the high terrestrial affinity of this mudskipper. It may be metabolically more active under the terrestrial condition as its gills are better adapted to respire on land than in water [17, 18]. Indeed, it is the only fish known to exhibit bradycardia when submerged in water ([7]; Ip, unpublished results).

A closer examination of the FAA profiles reveals that the major FAA accumulated in the tissues of *P. schlosseri* exposed to terrestrial conditions was alanine. The percentages of increases in TFAA which could be accounted for by the respective increases in alanine contents in the liver, muscle and plasma of *P. schlosseri* exposed terrestrially were approximately 57%, 22% and 56%, respectively. Such a phenomenon was not observed in *P. cantonensis* [15]. It has been demonstrated that most of the amino acids released by proteolysis in the white muscle of the spawning salmon during migration are collected and transported to other tissues as alanine [19]. Therefore, it is possible that a similar strategy is adopted by *P. schlosseri* during terrestrial exposure. According to our current understanding of pathways of amino acid metabolism, most of the free amino acid pool can be converted to alanine [12]. The overall quantitative energetics of these processes in white muscles appear to be quite favorable; the net conversion of glutamate to alanine would yield 10 mol ATP per mole alanine formed, and this value can be even higher for proline and for arginine conversion to alanine [12]. Since this favourable ATP yield from partial amino acid catabolism is not accompanied by a net release of NH_4^+, it would be advantageous to *P. schlosseri* which is confronted with the problem of NH_4^+ excretion when it moves away from water. For such a system to work, the NH_4^+ released from the partial catabolism of various FAA must be incorporated into glutamate, which can then undergo transamination to transfer the amino group to pyruvate, leading to the formation of alanine. It would appear that a portion of the NH_4^+ produced by *P. schlosseri* during the 24 hr of terrestrial exposure could be shuttled to the liver, and be converted into glutamate through amination of αKG. Although the specific activities (approaching V_{max}) of GDH obtained do not necessarily reflect the enzyme activities *in vivo*, the amination/deamination ratio in the liver of this mudskipper significantly increased after 24 hr of terrestrial exposure, which correlates well with the significant increase in glutamate content in this organ.

Contrary to *P. chrysospilos* [15] and *P. schlosseri, B. boddaerti* did not exhibit any increase in the TFAA and branched-chain FAA contents in its tissues when exposed terrestrially. Since there was no change in the glutamate level and the specific activities of GDH, in the aminating and deaminating directions, in the liver of *B. boddaerti* after 24 hr of terrestrial exposure, the formation of alanine in the muscle of this fish might not involve the amination of αKG through GDH in the liver as in *P. schlosseri.* Instead, the formation of alanine from certain FAA in the muscle of *B. boddaerti* during terrestrial exposure might involve transamination reactions within this tissue.

That the increases in concentrations of urea and FAA in the tissues of *P. schlosseri* exposed to terrestrial conditions indeed signal a greater capacity to detoxify ammonia, and not merely an increase in the mobilization of protein and amino acids, is reflected by the high tolerance of this mudskipper to NH_4^+ added to the ambient SW. Although it is generally accepted that fish are especially intolerant of dissolved ammonia [3], *P. schlosseri* could survive for at least 10 days in 100 mM NH_4Cl (Ip, unpublished results), and its LT_{50} for 150 mM NH_4Cl was 13 hr. To the best of the authors' knowledge, *P. schlosseri* exhibits one of the highest tolerance to NH_4^+ amongst teleosts, and even amongst mudskippers [14].

Hence, it can be concluded that, even though both are mudskippers, *P. schlosseri* and *B. boddaerti* have developed different degrees of adapta-

tion to survive in a terrestrial environment. The former mudskipper has acquired a greater capacity to detoxify ammonia than the latter. Thus, NH_4^+ excretion would be less of a problem to *P. schlosseri* than *B. bodaerti* during a terrestrial excursion.

REFERENCES

1 Bradford MM (1976) A rapid and sensitive method for the quantitation of microgram quantities of protein utilizing the principle of protein-dye binding. Anal Biochem 72: 248–259

2 Beutler HO, Michal G (1974) L-Glutamate: Determination with glutamate dehydrogenase, diaphorase and tetrazolium salts. In "Methods of Enzymatic Analysis Vol. 4" Ed by HU Bergmeyer, K Gawehn, Academic Press, New York, 2nd ed, pp 1708–1713

3 Campbell JW (1973) Nitrogen excretion. In "Comparative Animal Physiology "Ed by L Prosser, Saunders College Publishing, Philadelphia, 3rd ed pp 279–316

4 Chew SF, Ip YK (1990) Differences in the response of two mudskippers, *Boleophthalmus boddaerti* and *Periophthalmus chrysospilos* to changes in salinity. J Exp Zool 256: 227–231

5 Cvancara VA (1969) Distribution of liver allantoinase and allanatoicase activity in freshwater teleosts. Comp Biochem Physiol 29: 631–638

6 Faupel RP, Seitz HJ, Tarnowski W, Thiemann V, Weiss CH (1972) The problem of tissue sampling from experimental animals with respect to freezing technique, anoxia, stress and narcosis. Arch Biochem Biophys 148: 509–522

7 Gary WF (1962) Cardiac responses of fishes in asphyxial environments. Biol Bull 122: 362–368

8 Goldstein L, Forster RP (1970) Nitrogen metabolism in fishes. In "Comparative Biochemistry of Nitrogen Metabolism, Vol. 2" Ed by JW Campbell, Academic Press, New York, pp 495–518

9 Gordon MS, Boetius I, Evans DH, McCarthy R, Oglesby LC (1969) Aspects of the physiology of terrestrial life in amphibious fishes. I. The mudskipper *Periophthalmus sobrinus*. J Exp Biol 50: 141–149

10 Gordon MS, Ng WWS, Yip AYW (1978) Aspects of the physiology of terrestrial life in amphibious fishes. III. The Chinese mudskipper *Periophthalmus cantonensis*. J Exp Biol 72: 57–75

11 Gregory RB (1977) Synthesis and total excretions of waste nitrogen by fish of the *Periophthalmus* (mudskipper) and *Scartelaos* families. Comp Biochem Physiol 57A: 33–36

12 Hochachka PW, Guppy M (1987) Metabolic Arrest and the Control of Biological Time. Harvard University Press, London

13 Huggins AK, Skutsch G, Baldwin E (1969) Ornithine-urea cycle enzymes in Teleostean fish. Comp Biochem Physiol 28: 587–602

14 Iwata K (1988) Nitrogen metabolism in the mudskipper, *Periophthalmus cantonensis*: Changes in free amino acids and related compounds in various tissues under conditions of ammonia loading, with special reference to its high ammonia tolerance. Comp Biochem Physiol 91A: 499–508

15 Iwata K, Kakuta M, Ikeda G, Kimoto S, Wada N (1981) Nitrogen metabolism in the mudskipper, *Periophthalmus cantonensis*: A role of free amino acids in detoxification of ammonia produced during its terrestrial life. Comp Biochem Physiol 68A: 589–596

16 Kun E, Kearney EB (1974) Ammonia. In "Method of Enzymatic Analysis, Vol. 4" Ed by HU Bergmeyer, K. Gawehn, Academic Press, New York, 2nd ed, pp 1802–1806

17 Low WP, Ip YK, Lane DJW (1990) A comparative study of the gill morphometry in three mudskippers-*Periophthalmus chrysospilos, Boleophthalmus boddaerti* and *Periophthalmodon schlosseri*. Zool Sci 7: 29–38

18 Low WP, Lane DJW, Ip YK (1988) A comparative study of terrestrial adaptations of the gills in three mudskippers-*Periophthalmus chrysospilos, Boleophthalumus boddaerti* and *Periophthalmodon schlosseri*. Biol Bull 175: 434–438

19 Mommsen TP, French CJ, Hochachka PW (1980) Sites and patterns of protein and amino acid utilization during the spawning migration of salmon. Can J Zool 58: 1785–1799

20 Mommsen TP, Walsh PJ (1991) Urea synthesis in fishes: evolutionary and biochemical perspectives. In "Biochemistry and Molecular Biology of Fishes, 1. Phylogenetic and Biochemical Perspectives" Ed by PW Hochachka, TP Mommsen, Elsevier, New York, pp 139–163

21 Morii H (1979) Changes with time of ammonia and urea concentrations in the blood and tissue of mudskipper fish, *Periophthalmus cantonensis* and *Boleophthalmus pectinirostris* kept in water and on land. Comp Biochem Physiol 64A: 235–243

22 Morii H, Nishikata K, Tamura O (1978) Nitrogen excreton of mudskipper fish, *Periophthalmus cantonensis* and *Boleophthalmus pectinirostriis* in water and on land. Comp Biochem Physiol 69A: 189–193

23 Morii H, Nishikata K, Tamura O (1979) Ammonia and urea excretion from mudskipper fishes *Periophthalmus cantonensis* and *Boleophthalmus pectinirostris* transferred from land to water. Comp Biochem Physiol 63A: 23–28

24 Read LJ (1971) The presence of high ornithine-urea cycle enzyme activity in the teleost *Opsanus tau*. Comp Biochem Physiol 39B: 406–413

ZOOLOGICAL SCIENCE 10: 521–527 (1993)

Photoperiodic Responses of the Linden Bug, *Pyrrhocoris apterus*, under Conditions of Constant Temperature and under Thermoperiodic Conditions

HIDEHARU NUMATA[1], AIDA H. SAULICH[2] and TATYANA A. VOLKOVICH[2]

[1]*Department of Biology, Faculty of Science, Osaka City University, Sumiyoshi, Osaka 558, Japan, and* [2]*Laboratory of Entomology, Biological Research Institute, St. Petersburg University, St. Petersburg, 198904 Russia*

ABSTRACT—Photoperiodic responses were examined in the linden bug, *Pyrrhocoris apterus* (L.) (Heteroptera, Pyrrhocoridae), from Belgorod, Russia, under conditions of constant temperature and under thermoperiodic conditions with a 12-hr cryophase and a 12-hr thermophase. The critical daylength for the induction of adult diapause was longer at lower mean temperatures. The induction of diapause under thermoperiodic conditions was determined principally by the mean temperature of the thermoperiod, although thermoperiodic conditions enhanced the induction of diapause somewhat in the threshold zone. Development under thermoperiodic conditions was more rapid than at constant temperatures that were equivalent to the mean temperature under thermoperiodic conditions. Developmental retardation was observed under photophases a little shorter than the critical value for the induction of diapause, both at constant temperatures and under thermoperiodic conditions.

INTRODUCTION

Insects in the wild develop under conditions of daily and seasonal fluctuations in temperature and these fluctuations, together with changes in the photoperiod, regulate the seasonal life cycles of insects [7, 8, 21]. In some insects, the thermoperiod has been shown to influence the parameters of photoperiodic responses by amplifying or reducing the tendency to enter diapause, or by changing the critical daylength [2]. We must consider this influence in discussions of seasonal adaptation in insects, in particular in species that live in a continental climate with large daily changes in temperature. However, photoperiodic responses of insects have usually been studied at constant temperature in the laboratory.

The linden bug, *Pyrrhocoris apterus,* has an adult diapause that is controlled by a long-day photoperiodic response [12, 18, 22]. Saunders [18] showed that photoperiod also affects the developmental rate. Hodek [13] described the induction of diapause by brief exposure (2–4 days) to low temperatures in *P. apterus*. Furthermore, Honěk [14] reported that the fecundity of this species is higher under natural alternating temperatures than at a constant temperature in the laboratory. However, no experiments under thermoperiodic conditions have been performed to examine the photoperiodic response in *P. apterus*. In this study, we examined the photoperiodic response in *P. apterus,* from an inland region of Russia, at constant temperatures and under thermoperiodic conditions, and we discuss the effects of temperature on this response.

Accepted March 29, 1993
Received March 4, 1993

MATERIALS AND METHODS

Adults of *P. apterus,* after overwintering, were collected from the field in the reservation "Forest on the River Vorskla" (50°N, 36°E) which is located in the forest-steppe zone in the Belgorod Region, Russia. Their eggs were used for the experiments. The insects were reared in the laboratory by the method by Schlagbauer [19].

Nymphs were reared in 500-ml glass bottles. The density of the nymphs was kept at 100–150 for early instars and was reduced to 50–75 for the final (fifth) instar. Seeds of the linden tree *Tilia cordata,* strewn on the ground were collected and served as food. Puparia of the blue meat fly, *Calliphora vicina* were also supplied to late-instar nymphs and adults. Water was provided in test tubes with cotton plugs. Food and water were replaced every two or three days. Zigzag-folded strips of filter paper were used to increase the inner surface area. After adult emergence, the insects were kept in male and female pairs in Petri dishes. Thirty days after adult emergence, the females that had not laid eggs were dissected. The stage of their ovaries was examined, and the females with immature ovaries were judged as being in diapause [12].

Experiments were performed in boxes in which both temperature and photoperiod were controlled [5]. The light intensity in the boxes ranged between 180 and 250 lx and was supplied by 20 W fluorescent lamps. The deviation from the set temperatures was not more than 1.0°C. The humidity fluctuated between 50 and 70%. Photoperiodic conditions from a photoperiod with a 12-hr photophase and a 12-hr scotophase (12L-12D) to 18L-6D were used; the longest photophase corresponds to the maximum daylength in the region in which insects were collected, including civil twilight.

A square-wave type of thermoperiod was made by transferring the rearing bottles between temperatures at 9:00 and 21:00 every day. Thus, the thermoperiod was composed of a 12-hr cryophase and a 12-hr thermophase (12C-12T). The thermophase coincided with the photophase, and the cryophase with the scotophase. Under 12L-12D the thermoperiod and photoperiod were completely synchronized, whereas longer photophases extended into the cryophase (Fig. 1).

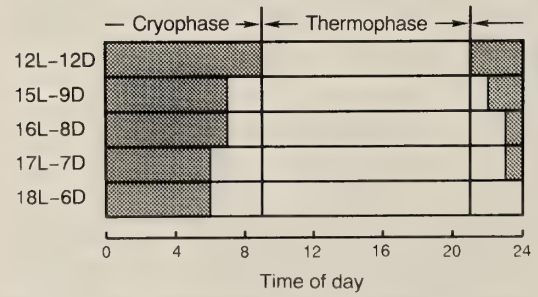

FIG. 1. The combinations of thermoperiod and photoperiod used in the experiments. Shaded bars, scotophase; open bars, photophase, in 24-hr cycles.

RESULTS

Induction of diapause at constant temperatures

First, we compared the photoperiodic response

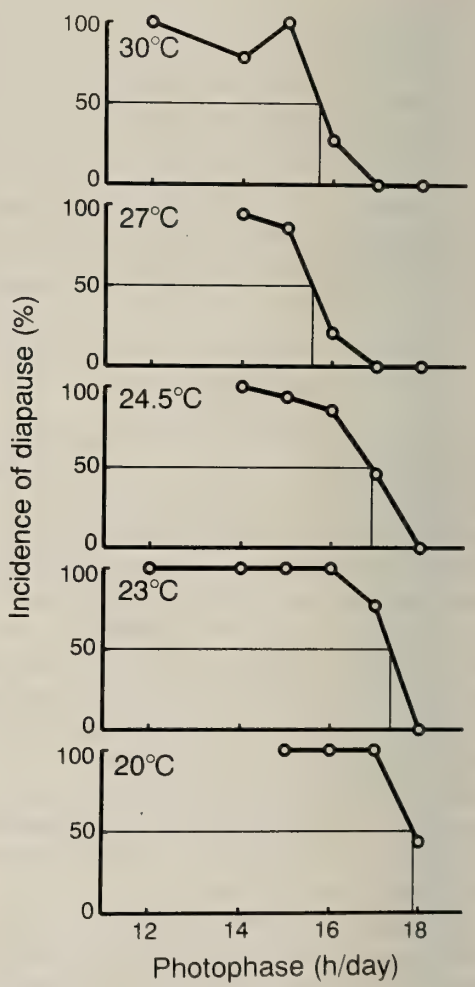

FIG. 2. The photoperiodic response curves for the induction of adult diapause at various constant temperatures in *Pyrrhocoris apterus.* n=20–32 (20°C), n=7–61 (23°C), n=154–190 (24.5°C), n=17–36 (27°C), n=14–39 (30°C).

with respect to induction of diapause for five constant temperatures: 20, 23, 24.5, 27 and 30°C. At each temperature, the insects showed a long-day photoperiodic response. As the temperature was raised from 20°C to 27°C, the critical daylength was shortened from about 18 hr to about 15.5 hr. However, the critical daylength was about 15.5 hr both at 27°C and at 30°C, even though at 30°C some females laid eggs even under 14L-10D (Fig. 2).

Induction of diapause under thermoperiodic conditions

Next, we examined the photoperiodic response under three sets of thermoperiodic conditions: a thermoperiod with a 13°C cryophase and a 27°C thermophase (abbreviated as 13–27°C; mean, 20°C); 13–33°C (mean, 23°C); and 20–32°C (mean, 26°C). The former two conditions are similar to the natural temperatures in the summer days in the native habitat of *P. apterus*. Under 13–27°C conditions, all adults entered diapause with any photoperiod other than 18L-6D, as they do at a constant temperature of 20°C, which is equivalent to the mean temperature under the thermoperiodic conditions (Fig. 3). However, under 18L-6D, the proportion of adults in diapause was significantly higher under 13–27°C conditions than at a constant 20°C ($P<0.05$ by Fisher's exact probability test). Furthermore, the preoviposition period was significantly shorter in nondiapause females reared under 13–27°C conditions (n=8, median=18, range=14–24 days) than in those reared at a constant 20°C (n=12, median=23, range=17–34 days; $P<0.01$ by Mann-Whitney U test, $U=13.0$). The photoperiodic response curve under 13–33°C conditions coincided with that at a constant 23°C, which is equivalent to the mean temperature under the thermoperiodic conditions. The proportion of diapause adults in 17L-7D was a little higher under 13–33°C conditions than at a constant 23°C (Fig. 3), but the difference was not significant ($P>0.3$ by Fisher's exact probability test). Although we did not examine the photoperiodic response at a constant 26°C, which is equivalent to the mean temperature of 20–32°C conditions, the insects showed an intermediate response between constant temperatures of 24.5°C and 27°C (Fig. 3).

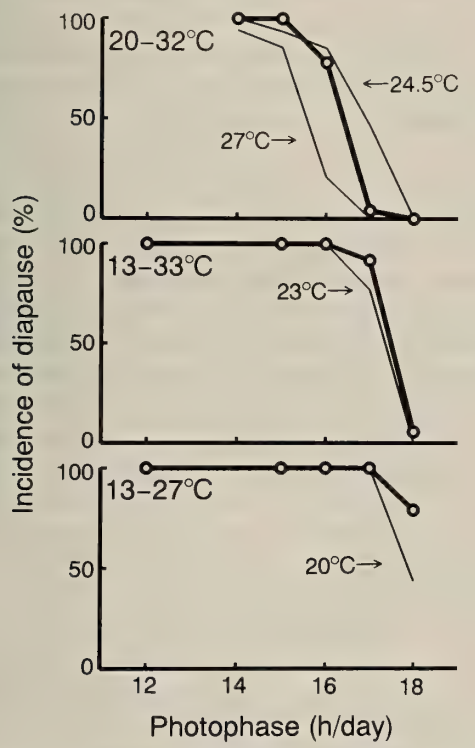

FIG. 3. The photoperiodic response curves for the induction of adult diapause under thermoperiodic conditions (12C-12T) in *Pyrrhocoris apterus*. n=31–56 (13–27°C), n=37–53 (13–33°C), n=13–24 (20–32°C). The photoperiodic response curves at constant temperatures equivalent to the means of the thermoperiodic conditions are shown by thin lines.

Thus, photoperiodic response curves for induction of diapause under thermoperiodic conditions were similar to those obtained at constant temperatures equal to the mean temperatures of the thermoperiods, although there was a little difference under 18L-6D. Next we examined the induction of diapause in 18L-6D under six other thermoperiodic conditions: 13–24.5°C, 15–27°C, 15–33°C, 20–27°C, 20–33°C and 27–33°C. At a cryophase temperature of 13°C, the number of diapause adults varied from 5.7 to 100% of the total depending on the temperature of the thermophase. At a cryophase temperature of 15°C the percentage of diapause adults varied from 0 to 56.5%, depending again on the temperature of the thermophase. At a thermophase temperature of

TABLE 1. Effects of thermophase and cryophase temperatures on the induction of adult diapause under 18L-6D and 12C-12T* in *Pyrrhocoris apterus*

Temperature (°C)			Incidence of diapause (%)	n
Cryophase	Thermophase	Mean		
13	24.5	18.75	100	21
13	27	20	78.9	38
13	33	23	5.7	53
15	27	21	56.5	23
15	33	24	0	15
20	27	23.5	0	22
20	32	26	0	13
20	33	26.5	0	15
27	33	30	0	19

* See text for details.

27°C, the percentage of diapause adults varied from 0 to 78.9% depending on the temperature of the cryophase (Table 1). Therefore, neither the temperature of the cryophase nor that of the thermophase independently defined the photoperiodic response. By contrast, the insects entered diapause at lower mean temperatures and failed to do so at higher mean temperatures both at constant temperatures and under thermoperiodic conditions. However, the threshold temperature was about 21°C under thermoperiodic conditions, and was a little higher than at constant temperatures (Fig. 4).

From the results at constant temperatures and under thermoperiodic conditions, we can conclude that the mean of the day and night temperatures defines for the most part the parameters of the photoperiodic response in *P. apterus*, although thermoperiodic conditions enhanced the induction of diapause to a slight extent near the critical daylength.

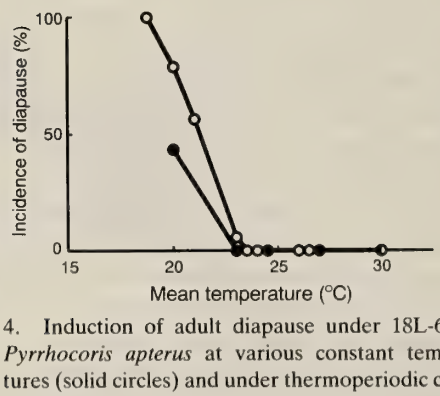

FIG. 4. Induction of adult diapause under 18L-6D in *Pyrrhocoris apterus* at various constant temperatures (solid circles) and under thermoperiodic conditions (12C-12T) (open circles).

Developmental rate

Then we compared the duration of egg and nymphal stages under various photoperiodic conditions at three constant temperatures (20, 24.5, 27°C) and under two sets of thermoperiodic conditions (13–27°C, 13–33°C). Under all conditions, the females developed a little more rapidly than the males, although the results are combined in Figure 5. Both at constant temperatures and under thermoperiodic conditions, retardation of development took place near the critical daylength for the induction of diapause. The insects developed most slowly under a photophase that was a little shorter than the critical value under all temperature conditions (Fig. 5). Apart from the developmental retardation in the threshold zone, the insects developed much more rapidly under 13–27°C conditions than at a constant 20°C, and more rapidly under 13–33°C conditions than at a constant 24.5°C (Fig. 5). Thus, development under thermoperiodic conditions was much more rapid than that estimated from the mean temperature of the thermoperiod. Figure 6 shows the developmental rate, designated as the reciprocal of the duration of egg and nymphal stages, under

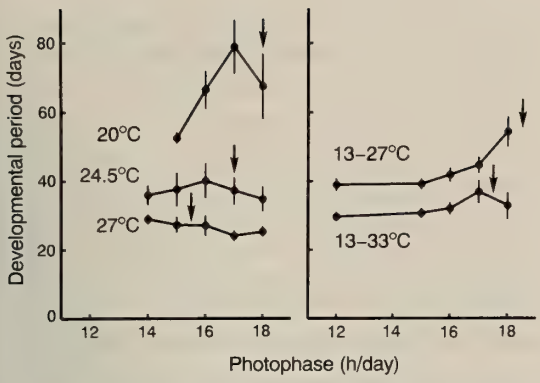

FIG. 5. Effects of photoperiod on the developmental period in *Pyrrhocoris apterus* at various constant temperatures and under thermoperiodic conditions (12C-12T). Solid circles with vertical lines, duration of the period from oviposition to adult emergence (mean±S.D., n=31–112). Arrows, photoperiods that induced adult diapause in 50% of insects.

15L-9D, which was not very much affected by the developmental retardation in the threshold zone. In Figure 6, we show the simple linear regression lines for the developmental rate at constant temperatures and under thermoperiodic conditions. The lower threshold temperature for development, shown as the intercept on the abscissa, was 12.5°C and 9.0°C at constant temperatures and under thermoperiodic conditions, respectively. However, there was only a slight difference in the accumulation of heat required for complete development, which is indicated by the reciprocal of the slope. It was 416 and 429 degree-days at

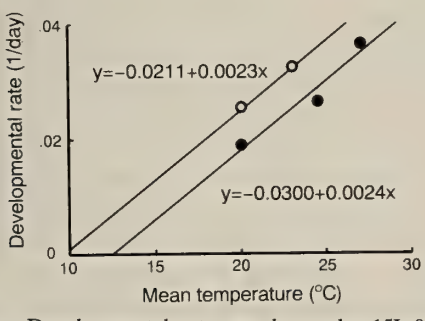

FIG. 6. Developmental rate per day under 15L-9D in *Pyrrhocoris apterus* at various constant temperatures (solid circles) and under thermoperiodic conditions (12C-12T) (open circles). Lines, simple linear regressions.

constant temperatures and under thermoperiodic conditions, respectively (Fig. 6). Thus, under thermoperiodic conditions the insects developed as rapidly as at a constant temperature that was higher by about 3.5°C than the mean temperature under the thermoperiodic conditions.

DISCUSSION

In *P. apterus* from Belgorod, the photoperiodic response for the induction of adult diapause depended on temperature (Fig. 2). At lower temperatures, the critical daylength was longer, as it is in many other insects with a long-day photoperiodic response [7, 8, 21]. However, increasing the temperature above 27°C had no effect on the critical daylength (Fig. 2). The critical daylength was found to be about 15 hr both at 20°C and at 25°C in *P. apterus* from Erevan, Armenia (40°N) [22]. Thus the dependence on temperature of the critical daylength varies between geographic populations within a species.

In many insects with a long-day photoperiodic response, thermoperiodic conditions enhance the photoperiodic induction of diapause under the natural phase relationship, i.e., when the cryophase is concurrent with the scotophase and the thermophase coincides with the photophase [1, 4, 6, 9, 10]. These results have been explained by the hypothesis that scotophase temperatures strongly influence the induction of diapause [2, 8, 10, 21]. However, experimental results obtained in recent years indicate that scotophase temperatures do not always determine the induction of diapause. For example, in the predatory bug *Podisus maculiventris* (Heteroptera, Pentatomidae, Asopinae), thermoperiodic conditions with a cool scotophase slightly reduce the incidence of diapause under short-day conditions but do not affect the critical daylength [11]. In another species in the same subfamily, *Perillus bioculatus*, thermoperiodic conditions with a cool scotophase reduce the incidence of diapause under near-critical photoperiods and, consequently, the critical daylength becomes shorter and equivalent to that at the temperature of the photophase [23]. Here we provide another example to contradict the view that the scotophase temperature has stronger effects on the induction

of diapause than the photophase temperature [2, 8, 10, 21].

In *P. apterus,* diapause under thermoperiodic conditions was determined principally by the mean temperature of the thermoperiodic conditions, although such conditions increased the incidence of diapause only slightly in the threshold zone (Figs. 3, 4). This weak enhancement of diapause induction in the threshold zone may be due to the low temperature in the scotophase as shown in other species [1, 4, 6, 9, 10]. However, we cannot deny the possibility that the 12C-12T theroperiod itself showed a short-day effect because in the present experiments the duration of thermophase did not coincide with that of photophase except 12L-12D (Fig. 1).

P. apterus developed under thermoperiodic conditions much more rapidly than at constant temperatures equivalent to the mean temperatures of the respective thermoperiods (Fig. 4). This response does not agree with the classic law of temperature summation but has been demonstrated in some other insects [2]. With respect to the rate of the development, thermoperiodic conditions corresponded to a higher temperature than the mean value, in contrast to the induction of diapause. In the European corn borer *Ostrinia nubilalis,* in which the effect of thermoperiodic conditions has been studied most intensively, thermoperiodic conditions produce essentially the same rate of larval development as do the appropriate mean temperatures [3, 17], although a low temperature in the scotophase increases the incidence of diapause [1, 4]. Thus, in both species, day and night temperatures are integrated in different ways for the development and for the modification of the photoperiodic response.

Saunders [18] reported that *P. apterus* from Prague, Czechoslovakia (50°N), developed more slowly around the critical photoperiod for the induction of diapause than under short-day or long-day conditions at a constant temperature of 25°C. Our present experiments confirmed these findings not only at various constant temperatures but also under thermoperiodic conditions. Furthermore, the peak of retarded development moved along the photoperiodic axis in a temperature-dependent manner, together with the critical daylength for the induction of diapause. Consequently, insects developed most slowly under a photophase a little shorter than the critical value for the induction of diapause under all temperature conditions (Fig. 5). Saunders [18] suggested that this developmental retardation promotes the seasonal synchronism in the univoltine population of *P. apterus* in Prague. Kidokoro and Masaki [16] showed a similar retardation of nymphal development near the critical photoperiod for the induction of egg diapause in both univoltine and bivoltine populations of the band-legged ground cricket, *Dianemobius nigrofasciatus,* and they attributed the main function of this response to a fine tuning of the growth rate so that the diapause stage would be reached at the appropriate time. Our field observations indicate that the Belgorod population of *P. apterus,* which lives at the same latitude as Prague, produces two generations, at least in warmer years (unpublished). Even in Czechoslovakia, *P. apterus* is not always univoltine [15, 20]. The developmental retardation in *P. apterus* must have an ecological significance even in bivoltine life cycles, as in *D. nigrofasciatus.*

Development under thermoperiodic conditions was more rapid than that estimated from the mean temperature of the thermoperiod (Figs. 5, 6). Furthermore, nymphs of *P. apterus* select warmer habitats and, therefore, their body temperature is sometimes much higher than the air temperature [15]. Therefore, under natural conditions, *P. apterus* may develop much more rapidly than in experiments at constant temperatures that were equivalent to the mean air temperatures. It is not appropriate to use the developmental parameters obtained from experiments at constant temperatures for predicting the seasonal development under natural conditions in *P. apterus.*

Furthermore, in *P. apterus* photoperiodic response for the induction of diapause depended much on temperature (Fig. 2), and the temperature is variable from year to year in Belgorod region. Therefore it is difficult to discuss the seasonal adaptation of this local population based only on the present results. We now plan to make further observations in the field and to perform experiments under natural conditions in an effort to determine the ecological significance of the

effect of photoperiod and temperature on diapause and development in *P. apterus*.

REFERENCES

1 Beck SD (1962) Photoperiodic induction of diapause in an insect. Biol Bull 122: 1–12

2 Beck SD (1983) Insect thermoperiodism. Annu Rev Entomol 28: 91–108

3 Beck SD (1983) Thermal and thermoperiodic effects on larval development and diapause in the European corn borer, *Ostrinia nubilalis*. J Insect Physiol 29: 107–112

4 Beck SD (1985) Effects of thermoperiod on photoperiodic determination of larval diapause in *Ostrinia nubilalis*. J Insect Physiol 31: 41–46

5 Braun VA, Goryshin NI (1978) Climate chambers with programming of photoperiodic and temperature rhythms for ecological research. Vestn Leningrad State Univ 3: 26–34 (in Russian)

6 Chippendale GM, Reddy AS, Catt CL (1976) Photoperiodic and thermoperiodic interactions in the regulation of the larval diapause of *Diatraea grandiosella*. J Insect Physiol 22: 823–828

7 Danks HV (1987) Insect Dormancy: An Ecological Perspective. Biological Survey of Canada, Ottawa, p 439

8 Danilevsky AS (1961) Photoperiodism and Seasonal Development of Insects, Leningrad State Univ, Leningrad, p 243 (in Russian)

9 Danilevsky AS, Kuznetsova IA (1968) The intraspecific adaptations of insects to the climatic zonation. In "Photoperiodic Adaptations in Insects and Acari" Ed by AS Danilevsky, Leningrad State Univ, Leningrad, pp 5–51 (in Russian)

10 Goryshin NI (1964) The influence of diurnal light and temperature rhythms on diapause in Lepidoptera. Entomol Obozr 43: 86–93 (in Russian)

11 Goryshin NI, Volkovich TA, Saulich AH, Vagner M, Borisenko IA (1988) The role of temperature and photoperiod in the control over development and diapause of the carnivorous bug *Podisus maculiventris* (Hemiptera, Pentatomidae). Zool Zh 67: 1149–1161 (in Russian)

12 Hodek I (1968) Diapause in females of *Pyrrhocoris apterus* L. (Heteroptera). Acta Entomol Bohemoslov 65: 422–435

13 Hodek I (1971) Induction of adult diapause in *Pyrrhocoris apterus* L. by short cold exposure. Oecologia 6: 109–117

14 Honěk A (1986) Enhancement of fecundity in *Pyrrhocoris apterus* under alternating natural conditions (Heteroptera, Pyrrhocoridae). Acta Entomol Bohemoslov 83: 411–417

15 Honěk A, Šrámková K (1976) Behavioral regulation of developmental cycle in *Pyrrhocoris apterus* L. (Heteroptera: Pyrrhocoridae). Oecologia 24: 277–281

16 Kidokoro T, Masaki, S (1978) Photopeiriodic response in relation to variable voltinism in the grownd cricket, *Pteronemobius fascipes* Walker (Orthoptera: Gryllidae). Jpn J Ecol 28: 291–298

17 Matteson JW, Decker GC (1965) Development of the European corn borer at controlled and variable temperatures. J Econ Entomol 58: 344–349

18 Saunders DS (1983) A diapause induction-termination asymmetry in the photoperiodic responses of the linden bug, *Pyrrhocoris apterus* and an effect of near-critical photoperiods on development. J Insect Physiol 29: 399–405

19 Schlagbauer N (1966) Eine Methode zur Massen- und Dauerzucht der Feuerwanze *Pyrrhocoris apterus*. Beitr Entomol 16: 199–202

20 Socha R, Šula J (1992) Voltinism and seasonal changes in haemolymph protein pattern of *Pyrrhocoris apterus* (Heteroptera: Pyrrhocoridae) in relation to diapause. Physiol Entomol 17: 370–376

21 Tauber MJ, Tauber CA, Masaki S (1986) Seasonal Adaptations of Insects. Oxford Univ. Press, New York, p 411

22 Volkovich TA, Goryshin NI (1978) Evaluation and accumulation of photoperiodic information in *Pyrrhocoris apterus* L. (Hemiptera, Pyrrhocoridae) during the induction of oviposition. Zool Zh 57: 46–55 (in Russian)

23 Volkovich TA, Kolesnichenko LI, Saulich AH (1990) The role of thermal rhythms in the development of *Perillus bioculatus* (Hemiptera, Pentatomidae). Zool Zh 69: 70–81 (in Russian)

ZOOLOGICAL SCIENCE 10: 529–536 (1993)

Phylogenetic Position of Acoel Turbellarians Inferred from Partial 18S rDNA Sequences

Tomoe Katayama[1], Masamichi Yamamoto[1], Hiroshi Wada[2] and Noriyuki Satoh[2]

[1]*Ushimado Marine Laboratory, Faculty of Science, Okayama University, Ushimado, Okayama 701-43, and* [2]*Department of Zoology, Faculty of Science, Kyoto University, Kyoto 606-01, Japan*

ABSTRACT—Primitive platyhelminths, especially Acoel turbellarians, are thought to be key to understanding the origin and evolution of metazoa. In order to infer their phylogenetic position within the phylum Platyhelminthes, we determined and compared the complete nucleotide sequence of a region of about 750 base pairs in the central part of an 18S rDNA for ten turbellarians, including two species of the group Acoela, six species of the group Polycladida, and two species of the group Tricladida. The deduced phylogenetic tree suggests that the three groups examined form discrete and separate entities. In addition, the tree suggests an earlier emergence of the Acoel turbellarians than the other platyhelminths. This animal may not be derived by means of secondary reduction from advanced acoelomates but may be nearest to its metazoan ancestors.

INTRODUCTION

The origin and evolution of multicellular animals (metazoans) have received considerable attention over the years [4, 9–11, 14, 26]. It is generally accepted that the metazoa arose from protozoa, perhaps 700–1000 million years ago. Models of the metazoic origin suggest that either colonial flagellates [10] or syncytial ciliates [9, 11] became acoel flatworm-like creatures (phylum Platyhelminthes), from which various modern metazoans have diverged. Current debate concerns whether the metazoa are monophyletic or polyphyletic and what the ancestral metazoa were like. Recent studies of the molecular phylogeny of invertebrates have suggested that the metazoa are polyphyletic (Cnidarians arose from a protist ancestry different from the Bilateria) [5, 8] and within the Bilateria, an early split gave rise to Platyhelminthes and the coelomate lineage [8, 13], although a monophyletic origin of the metazoa has also been proposed [16]. Regardless of route, primitive platyhelminths, especially Acoel turbellarians, are key animals in understanding the origin and evolution of modern metazoans.

In the present investigation, we compared molecular sequence data derived from 18S rDNAs to estimate the phylogenetic position of Acoel turbellarians. The 18S rRNA or its gene (18S rDNA) is ideally suited for phylogenetic studies of distantly related organisms because it is rich in information and the sequencing methodology permits the rapid accumulation of very large databases. According to Pace *et al.* [18], these molecules are conservative in overall structure and constitute a single gene family, so that problems of establishing homology among paralogous genes are avoided. The rRNA gene seems to be free of artifacts of lateral gene transfer between phylogenetically distant organisms. This and the absence of paralogous genes mean that 18S rRNA sequences accurately reflect phylogenetic relationships among the organisms from which the rRNA were prepared. The rRNA are present in large amounts in all organisms and are easily isolated. The conservative nature of the rRNA structure extends to the nucleotide sequence. Some regions of the molecule are highly conserved among distantly related species. Using these uni-

Acctpted March 5, 1993
Received November 9, 1992

versally conserved regions, direct rapid sequencing of 18S rRNA (DNA) was achieved. Enough data were accumulated from 18S rRNA sequences for statistically significant comparisons. Since each of the 1000 or so sequenced nucleotides constitutes a characteristic state, the evolutionary information content of rRNA sequences is very high.

Here we determined the complete nucleotide sequence of a region of about 750 base pairs (bp) in the central part of the 18S rDNA for ten turbellarian species consisting two species of Acoela, six of Polycladida and two of Tricladida. The phylogenetic relationship among these turbellarians was analyzed by sequence comparison. Our primary interest was in determining whether the acoel turbellarian is a primitive platyhelminth or a secondary reduction from advanced acoelomates.

MATERIALS AND METHODS

Animals

The nine turbellarian species examined included two species of the order Acoela, *Convoluta naikaiensis* (Yamasu) and *Amphiscolops* species (Yamasu), six species of the order Polycladida, *Notoplana koreana* (Kato), *Planocera multitentaculata* (Kato), *Stylochus orientalis* (Bock), *Pseudostylochus obscurus* (Stimpson), *Stylochoplana pusilla* (Bock), and *Thysanozoon brocchii* (Risso), and two species of the order Tricladida, *Dendrocoelopsis lactea* (Ichikawa et Okugawa) and *Dugesia japonica* (Yeri et Kaburaki). Whole animals were frozen in liquid nitrogen and kept at −80°C until use.

DNA isolation

Frozen and powdered samples were lysed in TE buffer (10 mM Tris-HCl, 0.1 M EDTA, pH 8.0) that contained 0.5% sodium dodecyl sulfate. After digesting samples with proteinase K (100 μg/ml) at 50°C for 3 hr, DNA was extracted with phenol and precipitated in ethanol and an equal volume of 5.0 M ammonium acetate. Samples resuspended in TE buffer were further purified by RNase A (20 μg/ml) digestion at 37°C for 1 hr followed by ethanol precipitation.

Adults of *Convoluta naikaiensis* have symbiotic alga. To avoid contamination of algal DNA, that of the turbellaria was extracted from embryos.

Amplification of the central region of 18S rDNA and sequencing

A region of about 1000 bp from the central part of 18S rDNA was amplified by the polymerase chain reaction (PCR) [20] in a Perkin Elmer Cetus thermal cycler. Amplifications were performed in 100 μl of 50 mM KCl, 1.5 mM $MgCl_2$, Tris-HCl (10 mM, pH 9.0), 0.1% Triton X-100, with 0.2 mM each dNTP, 100 pM primer, template DNA (10–100 μg) and 2 U *Taq* DNA polymerase (Promega). Primer-1 [5′-CAG(CA)CCCGCGGTAAT(TA)C-3′] and primer-2 [5′-ACGGGCGGTGTGT(AG)C-3′], the latter being identical to Primer C of Field *et al.* [8], were used for amplification. One of the primers was kinased prior to PCR at the 5′ terminal phosphate. The temperature regimen for 30 cycles was 1 min at 92°C, 2 min at 55°C, and 3 min at 72°C.

According to the method described by Higuchi and Ochman [12], single-stranded DNA was obtained by digesting the amplified product with lambda exonuclease. The nucleotide sequence of the single-stranded PCR products was directly determined by dideoxy chain-termination [22] using Sequenase ver 2.0 (USB) and [^{35}S]-dATP (Amersham). In addition to primer-1 and -2, primer-3 (5′-TTGGCAAATGCTTTCGC-3′), primer-4 (antisense of primer-3), primer-5 [5′-ATTCCTTT(AG)AGTTTC-3′] and primer-6 (antisense of primer-5) were used in sequence determination.

Comparison of sequences and inferences about phylogeny

Sequences were aligned on the basis of maximum nucleotide similarity. Using the aligned sequences, evolutionary distance values were calculated pairwise as described by Jukes and Cantor [15]. The phylogenetic tree was inferred from an analysis of results by the neighbor-joining method of Saitou and Nei [21]. The degree of support for internal branches of the tree was further assessed by bootstrapping [7].

The corresponding sequences of *Saccharomyces*

cerevisiae [17] and *Neurospora crassa* [17] provided data of outgroup organisms.

RESULTS

Partial nucleotide sequences of the 18S rDNAs from ten turbellarians

The complete nucleotide sequences of a region of about 750 bp in the central part of the 18S rDNA of ten species of turbellarians are summarized in Figure 1. The sequences correspond to positions 910–1646 in the sequence of human 18S rRNA [17]. Alignment of the nucleotide sequences from the ten planarian species revealed some key features. In some regions, the nucleotide sequences were highly conserved. For example, among the ten species, few changes were evident in the sequences from positions 277 to 380. In contrast, the nucleotide sequences of other regions, such as positions 214–267 and 543–614, were highly variable. Sequences of yet another region varied only moderately. These regional differences may reflect differences in the functional constraints upon the regions in the 18S rRNA.

The sequence alignment showed that the six species of the order Polycladida share common nucleotide sequences, as do the two species of the order Tricladida. However, the nucleotide sequences of these two groups are very different, suggesting their discrete separation. In addition, the nucleotide sequence of the two acoela species *Convoluta* and *Amphiscolops* differed from those of Polycladida and Tricladida so much that almost the entire region of the 18S rDNA we examined was changed. This suggests a large evolutionary divergence of the acoel turbellarians from the two other groups of planarians.

Phylogenetic relationships among the ten species of turbellarians

Structural similarity and evolutionary distance values were calculated pairwise as described [15] between the sequences aligned in Figure 1. The results are summarized in Table 1. A phylogenetic tree was constructed by the neighbor-joining method [21], by reference to the distance values of Table 1. The phylogenetic tree shown in Figure 2 indicated that the ten turbellarians can be subdivided into three groups, which correspond to the orders Acoela, Polycladida and Tricladida, and that the acoel group emerged first among the three. The internal branches of the tree were supported by the high bootstrapping values. Among the six species of Polycladida, the branching of *Thysanozoon* belonging to suborder Cotylea from the five species of Acotylea was evident (Fig. 2).

The phylum Platyhelminthes is subdivided into four major groups, Turbellaria (planarians), Monogenea (monogenetic flukes), Trematoda (digenetic flukes), and Cestoda (tapeworms) [4, 14]. Recent studies of the phylogenetic relationships among several parasitic platyhelminths by comparison of partial 18S rRNA sequences [2, 17] support the hypothesis that platyhelminths are monophyletic; that planarians emerged first, then flukes and finally tapeworms evolved. Together with the results of the present study, we constructed a phylogenetic tree to examine the position of acoel turbellarians within the phylum Platyhelminthes (data not shown). The tree suggests that *Convoluta* and *Amphiscolops* are more primitive members within Platyhelminthes.

Phylogenetic position of acoel turbellarians in the animal kingdom

The complete or partial nucleotide sequences of 18S rRNA (or DNA) of various phyla, including *Artemia salina* [17], *Caenorhabditis elegans* [17], *Ciona savignyi* [19], *Xenopus laevis* [17], and *Homo sapiens* [17] have been reported. The phylogenetic tree (Fig. 3) shows our positioning of the Acoel turbellarians, Polycladida and Tricladida in the animal kingdom. It is evident that these three groups of turbellarians are not interrupted by any other animal groups. Also, the branching point of the acoel turbellarians is earlier than those of the other turbellarians compared in this study.

DISCUSSION

In this investigation, we determined and compared the complete nucleotide sequence of a region of about 750 bp in the central portion of the 18S rDNA from ten species of turbellarians. The

```
                    ...,....+....,....+....,....+....,....+....,....+....,....+....,....+....,...70
 1. Stylochus       TTGTTGGTTTTCGGAACA-----TGAAGTAATGATTAAGAG---GGACAGAC-GGGGGCATTCGTATTGC
 2. Planocera             -
 3. Pseudostylochus
 4. Notoplana
 5. Stylochoplana
 6. Thysanozoon                                C
 7. Dendrocoelopsis             -                    A     A   T C          AT    GCT
 8. Dugesia                   A   -                  A     A     C-         AT    GCT
 9. Convoluta           AAC CGG G CTGTT    GCTCG  G      G A      A    G          T
10. Amphiscolops       A C      C TACCG AGTTTCCCTCAG  T GC  A  CTT A    G A        TC

    ....,....+....,....+....,....+....,....+....,....+....,....+....,....+....,....+....,..160
 1. -GGTGGG-AGAGGTGAAATTCTTGGATCATCGCAAGAC-GCCCTAC---AGCGAAAGCATTTGCCAAGAATGTTTCCATTAATCAAGAAC
 2.                                 -
 3.
 4.
 5.
 6.                     A               G  A
 7.      T             A A       AGC     AAA       T                        T
 8.      CT             GA  C    AGC    GAAA       T                        T
 9.  TAC TT                   G G        AAA       T                        T
10.  TAG TTC                  C A        AAA    TACT                        T

    ....,....+....,....+....,....+....,....+....,....+....,....+....,....+....,....+....,..250
 1. GAAAGTCAGAGGTTCGAAGACGATCAGATACCGTCCTAGTTCTGACCATAAACGATGCCAACTGGCAA-TCCGTTGCGATTGCAAGTTCG
 2.                                                                                    G
 3.
 4.
 5.
 6.                                                       CTG    C CG
 7.           A                                          T          A  G  TA CGAA G AATT CAATA
 8.      T    A                                          T      T   A G G TA CGAA GA ATT-TAATC
 9.           TA TA    G   T       C  G  A    A         TT A      TA G   TT  CC TG CC --TC
10.           TA T     G   T       C  G  A       T     T  A      TA G  CTT CCAAAG CAT- CCAT

    ....,....+....,....+....,....+....,....+....,....+....,....+....,....+....,....+....,..340
 1. ATCCAACGGGCAGCCT-CCGGGAAACCAAAGTCTTTGGGTTCCGGGGGAAGT-ATGGTTGCAAAGCTGAAACTTAAAGGAATTGAC-GGA
 2.                                                                                      T
 3.
 4.
 5.
 6.                                  AT
 7. TC TTG TA A  T A                 A
 8.    TTG TA A  T A                 A                G
 9.  CTGGG AA A TTTAA                T A T                        ATC
10.  CTTGG AA A  TTAA                T A T                        AT

    ....,....+....,....+....,....+....,....+....,....+....,....+....,....+....,....+....,..430
 1. AAGGCACCACAAGGAGTGGAGCCTGCG-CTTAATTTGACTCAACACGGGAAAACTCTACCCGGCCCGGACACTGTGAGGATTGACAGATT
 2.       -                  G                          -
 3.                                                     -
 4.                          G                          -
 5.                -                                    -
 6.                -   -  - C                           -          -      G  T
 7.  G        C                                      T   -      T
 8.  G        C       -   -   -                      TT  -C     T
 9.  G        C                                   G      -   A  T  A    TCT A              A
10.  G        C                                          -   G  T  A    TCT A
```

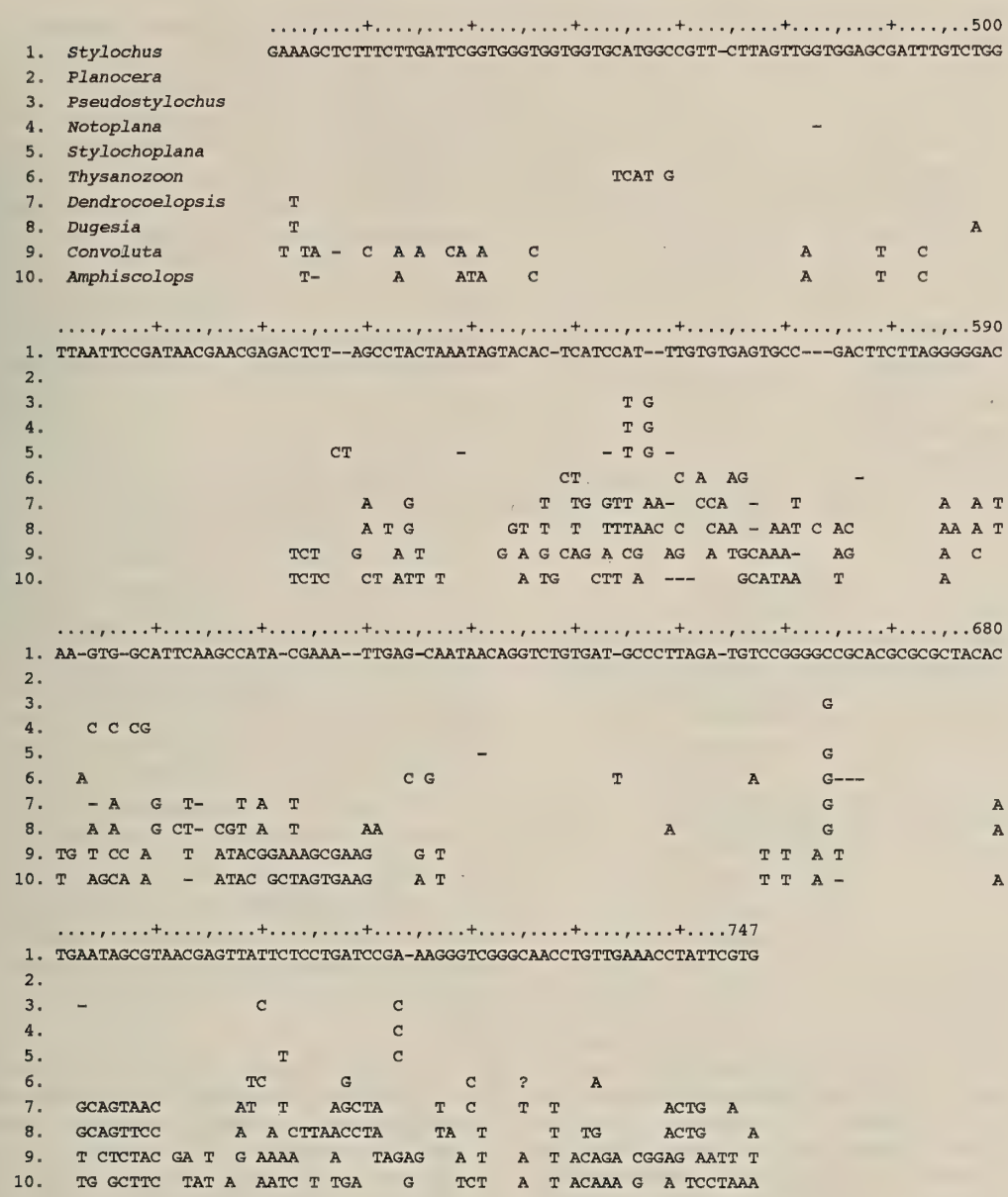

FIG. 1. Alignment of the central regions of the 18S rDNAs from ten Turbellarians. All the bases are shown for *Stylochus orientalis* and only bases different from these are shown for other species. Bars indicate deletions.

TABLE 1. Structural similarity and evolutionary distance data for turbellarian 18S rDNA sequences

Genera	1.	2.	3.	4.	5.	6.	7.	8.	9.	10.	11.	12.
1. *Stylochus*		0.000	0.004	0.002	0.005	0.048	0.100	0.131	0.221	0.214	0.184	0.188
2. *Planocera*			0.004	0.002	0.005	0.048	0.100	0.131	0.221	0.214	0.184	0.188
3 *Pseudostylochus*				0.002	0.002	0.048	0.100	0.131	0.223	0.219	0.188	0.191
4. *Notoplana*					0.004	0.049	0.102	0.134	0.221	0.216	0.186	0.188
5. *Stylochoplana*						0.049	0.098	0.134	0.223	0.216	0.188	0.188
6. *Thysanozoon*							0.134	0.170	0.270	0.248	0.228	0.231
7. *Dendrocoelopsis*								0.049	0.231	0.209	0.177	0.173
8. *Dugesia*									0.250	0.228	0.205	0.200
9. *Convoluta*										0.117	0.236	0.245
10. *Amphiscolops*											0.233	0.238
11. *Saccharomyces*												0.067
12. *Neurospora*												

The values are average numbers of nucleotide substitutions per sequence position determined by the Jukes and Cantor formula [15].

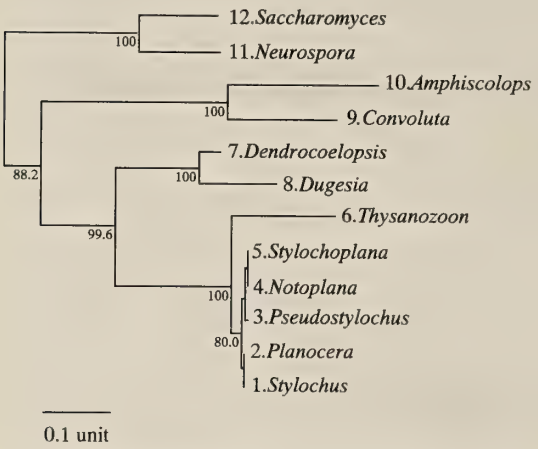

FIG. 2. The phylogenetic tree of ten turbellarians, as deduced by the neighbour-joining method using the fraction of observed substitution difference over all sites. The scale bar indicates an evolutionary distance of 0.1 nucleotide substitution per sequence position. Numbers at each branch indicate the percentage of times a node was supported in 500 bootstrap pseudoreplications by the neighbour-joining method.

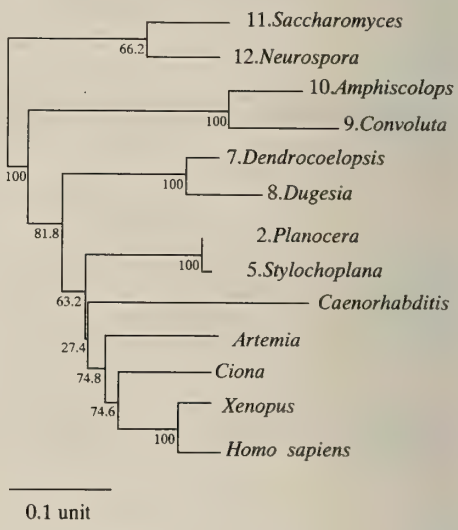

FIG. 3. Phylogenetic relationships of the turbellarians with other organisms (*Neurospora crassa, Saccharomyces cerevisiae, Caenorhabditis elegans, Artemia salina, Ciona savignyi, Xenopus laevis* and *Homo sapiens*). The tree was constructed by the neighbour-joining method. The scale bar indicates an evolutionary distance of 0.1 nucleotide substitution per sequence position. Numbers at each branch indicate the percentage of times a node was supported in 500 bootstrap pseudoreplications by the neighbour-joining method.

phylogenetic tree (Fig. 2) indicated that the ten species can be subdivided into three groups, which correspond to the orders Acoela, Polycladida and Tricladida. In addition, together with the phylogenetic tree including other groups of the animal kingdom (Fig. 3), early emergence of the acoel turbellarians in metazoic evolution is evident. Therefore, they might be some of the closest multicellular animals to their metazoan ancestors. The early emergence of acoel turbellarians will be substantiated further by investigating with other

molecular probes such as 28S rDNA.

A phylogenetic tree constructed from the 5S rRNA sequences suggested that the branching points of *Dugesia japonica* (Tricladida) and nematodes (eg, *Caenorhabditis elegans*) are slightly earlier than those of other metazoans, including *Planocera reticulata* (Polycladida) [9]. That means turbellarians including Tricladida and Polycladida are polyphyletic. However, that view was not supported in the present study (see Figs. 2 and 3). Even when nematodes are included in the 18S rRNA (DNA) tree (Fig. 3), Tricladida and Polycladida are categorized into one larger group, or Turbellarians.

It seems a consensus that all platyhelminths except for the lower turbellarians, including Acoela, Catenulida and Nemertodermatida, are of monophyletic origin [1–3, 6, 23, 24]. However, the relationships among the Catenulida, the Nemertodermatida-Acoela and the other orders of Platyhelminthes, are problematic [1, 3, 6, 23, 24]. Most views of the relationships within the Platyhelminthes support the hypothesis that a primary acoelomate condition is derived from an acoel-type worm, and as the phylum evolved, the gut became more elaborate and the division into distinct germ layers more pronounced. The Acoela, which are virtually solid with a ventral mouth and central 'syncytial' area acting as the gut, have many primitive features, and have been considered nearest to the ancestral group within the phylum [11]. Catenulida and Nemertodermatida, with fully a developed gut and more distinct mesodermal matrices, are assumed to represent the next level of sophistication. Recently, however, several investigators have argued that Catenulida and Nemertodermatida, the latter, in particular, may be more primitive [24, 26]. Acoela are unusual in having modified cilia, in lacking any intercellular matrix [24], and in showing a peculiar form of 'duet' cleavage similar to that of gastrotrichs and nematodes (cf. [26]). They might therefore be a derived group, an example of secondary reduction. The present 18S rDNA sequence analysis, however, did not support this view, namely the branching point of *Convoluta* was much earlier than those of other turbellarians. Further studies of the molecular phylogeny of Catenulida and Nemertodermatida will offer more conclusive evidence of turbellarian evolution.

ACKNOWLEDGMENTS

We are very grateful to Dr. Takashi Miyata and Mr. Naruo Niko, Department of Biophysics, Kyoto University for their help in constructing the phylogenetic trees. We also thank Dr. Sachiko Ishida, Department of Biology, Hirosaki University for providing us *Dendrocoelopsis lactea* species, Dr. Terufumi Yamasu, Department of Biology, Ryukyu University for his kind help in collecting acoel species, and Dr. Ken-ichi Tajika, Department of Biology, Nihon University School of Medicine for identifying the three species of Polycladida (*Notoplana, Planocera* and *Stylochus*). This research was supported in part by grants from the Research Institute of Marine Invertebrates (Tokyo) to N.S. and by the Narishige Zoological Science Award to M.Y.

REFERENCES

1 Ax P (1985) The position of the Gnathostomulida and Platyhelminthes in the phylogenetic system of the Bilateria. In "The Origins and Relationships of Lower Invertebrates". Eds. by SC Morris, JD George, R Gibson, HM Platt, Clarendon Press, Oxford, pp 168–180

2 Baverstock PR, Fielke R, Johnson AM, Bray RA, Beveridge I (1991) Conflicting phylogenetic hypotheses for the parasitic platyhelminths tested by partial sequencing of 18S ribosomal RNA. Intern J Parasitol 21: 329–339

3 Brooks DR (1989) A summary of the database pertaining to the phylogeny of the major groups of parasitic platyhelminths, with a revised classification. Can J Zool 67: 714–720

4 Brusca RC, Brusca CJ (1990) Invertebrates. Sinauer, Sunderland

5 Cristen R, Ratto R, Baroin A, Perasso R, Grell KG, Adoutte A (1991) An analysis of the origin of metazoa, using comparisons of partial sequences of the 28S RNA, reveals an early emergence of triploblasts. EMBO J 10: 499–503

6 Ehlers U (1986) Comments on a phylogenetic system of the Platyhelminths. Hydrobiologia 132: 1–12

7 Felsenstein J (1985) Confidence limits on phylogenesis: an approach using the bootstrap. Evolution 39: 783–791

8 Field KG, Olsen GJ, Lane DJ, Giovannoni ST, Gheselin MT, Raff EC, Pace NR, Raff RA (1988) Molecular Phylogeny of the animal kingdom. Science 239: 748–753

9 Hadzi J (1963) The Evolution of Metazoa. Perga-

mon Press, Oxford

10 Haeckel E (1874) The gastraea-theory, the phylogenetic classification of the animal kingdom and the homology of the germ-lamellae. Quart J microsc Sci 14: 142–165

11 Hanson ED (1977) The Origin and Early Evolution of Animals. Pitman, London

12 Higuchi RG, Ochman H (1989) Producing of single-stranded DNA templates by exonuclease digestion following the polymerase chain reaction. Nucleic Acids Res 17: 58–65

13 Hori H, Osawa, S (1987) Origin and evolution of organisms as deduced from 5S ribosomal RNA sequences. Mol Biol Evol 4: 445–472

14 Hyman LH (1951) The Invertebrate Vol 2. McGraw-Hill, New York

15 Jukes TH, Cantor RC (1969) Evolution of protein molecules. In "Mammalian Protein Metabolism". Ed. by HN Munro, Academic Press, New York, pp 21–132

16 Lake JA (1990) Origin of the metazoa. Proc Natl Acad Sci USA 87: 763–766

17 Neefs J-M, Van de Peer Y, Hendriks L, De Wachter R (1990) Compilation of small ribosomal subunit RNA sequences. Nucleic Acids Res 18: 2237–2317

18 Pace NR, Stahl DA, Lane DJ, Olsen GJ (1985) Analyzing natural microbial populations by rRNA sequences. Amer Soc Microbiol News 51: 4–12

19 Rieger RM (1985) The phylogenetic status of the acoelomate organization within the Bilateria. In "The Origins and Relationships of Lower Invertebrates". Eds. by S C Morris, JD George, R Gibson, HM Platt, Clarendon Press, Oxford, pp 101–122

20 Saiki RK, Gelfand DH, Stoffel S, Scharf SJ, Higuchi R, Horn GT, Mullis KB, Erlich HA (1988) Primer-directed enzymatic amplification of DNA with a thermostable DNA polymerase. Science 239: 487–491

21 Saitou N, Nei M (1987) The neighbor-joining method: a new method for reconstructing phylogenetic trees. Mol Biol Evol 4: 406–425

22 Sanger F, Nicklen S, Coulson AR (1977) DNA sequencing with chain-terminating inhibitors. Proc Natl Acad Sci USA 74: 5463–5467

23 Smith JPS, Teyler S (1985) The acoel turbellarians: kingpins of metazoan evolution or a specialized offshoot? In "The Origins and Relationships of Lower Invertebrates". Eds. by SC Morris, JD George, R Gibson, HM Platt, Clarendon Press, Oxford, pp 123–142

24 Smith JPS, Teyler S, Rieger RM (1986) Is the turbellaria polyphyletic? Hydrobiologia 132: 13–21

25 Wada H, Makabe KW, Nakauchi M, Satoh N (1992) Phylogenetic relationships between solitary and colonial ascidians, as inferred from the sequence of the central region of their respective 18S rDNAs. Biol Bull 183: 448–455

26 Willmer P (1990) Invertebrate Relationships. Cambridge Univ. Press, Cambridge

ZOOLOGICAL SCIENCE 10: 537–542 (1993)

[RAPID COMMUNICATION]

The Pattern of Volatile Compounds in Incubated and Fresh Preputial Fluid of Male Mice

Kyoko Ninomiya[1], Isao Nohara[2], Takaaki Toyoda[2] and Takeji Kimura[1]

[1]*Department of Biology, College of Arts and Sciences, University of Tokyo, Komaba, Tokyo 153, and* [2]*Central Research Center, Takasago International Corporation, Kamata, Tokyo 144, Japan*

ABSTRACT—The volatile compounds from incubated and fresh preputial fluid of male mice were analyzed by capillary gas chromatography-mass spectrometry. We found quantitative and qualititative changes in the volatile compounds of preputial fluid after incubation. These chemical changes in the incubated preputial fluid seem to be necessary for female attraction.

INTRODUCTION

Both androgen-dependent compounds in the urine and androgen-independent compounds from preputial glands which are found in excreted urine of male mice have been shown to be necessary for female attraction [4, 5]. We have also demonstrated that, when mixed with preputialectomized male urine, incubated preputial gland fluid, which may have been processed by oxidation, bacterial action or other chemical changes after excretion, is significantly more attractive to females than fresh preputial fluid [4], but the chemical nature of the male's preputial attractant factor remains unknown. Lipid extracts of the preputial gland secretions of male mice contain a number of long-chain alkyl acetates which are testosterone dependent [7]. Recently Novotny's group reported that the two major compounds in the fresh preputial fluid of male mice are *E,E*-α-farnesene and *E*-β-farnesene. These compounds are found at high levels in the urine of dominant male mice and are aversive to subordinate males [6].

In the present study, the major volatile compounds of both fresh and incubated preputial fluid from male mice were analyzed by capillary gas chromatography-mass spectrometry(GC-MS) and the distribution of these compounds was compared.

Accepted April 21, 1993
Received March 19, 1993

MATERIALS AND METHODS

Fluid was taken directly from the preputial glands of 11 male ICR/JCL mice at 8 weeks of age. These mice were purchased from Nihon Clea Co. (Tokyo) at 4 weeks of age and housed in groups of 5 or 6 in 24×17×12 cm plastic cages in a room which was maintained at about 23°C and kept on a 14 hr L: 10 hr D photoperiod. They received OA-1 mice chow (Nihon Clea Co.) and water ad libitum. Mice were anesthetized with sodium pentobarbital (Abbott) and their preputial glands were surgically removed. The glands were then cut open and the fluid was stored in glass vials. Half of the preputial fluid was incubated at 37°C for two days, and the other half was kept at minus 80°C until being analyzed.

Volatile compounds of incubated and frozen preputial fluid were analyzed using the head space technique, which employed a porous polymer (Tenax TA) as a collection medium. The volatiles were sparged from 0.1-ml preputial samples at room temperature with purified nitrogen gas, and absorbed onto a precolumn packed with Tenax TA

for 2 hr. The volatiles were desorbed by heating Tenax TA at 250°C for 6 min with herium gas, and then retrapped in the portion of the capillary column, which was cooled by dry ice acetone, to concentrate the vapor before GC-MS analysis. A chemical bonded PEG-20M column (0.25 mm ID $\times$50 m) was used as a analytical column. Column temperature was programmed from 70° C to 220°C at a rate of 4°C per min. Volatile constituents were identified with a Hitachi M-80B mass spectrometer connected to a gas chromatograph (Hewlett Packard HP-5790GC), using electron impact ionization at 20 eV.

RESULTS AND DISCUSSION

The major volatile compounds found in incubated and fresh preputial fluid are compared in Figure 1. The initial part of each chromatogram is enlarged in Figures 2 and 3 in order that each peak can be clearly labelled. Identified compounds, listed in Table 1, were categorized into three groups: those common to both incubated and fresh preputial fluid (Group C), those found only in incubated preputial fluid (Group I) and those found only in fresh preputial fluid (Group P). The C-14 peak of fresh preputial fluid in Figure 1 was contaminated with an unidentified compounds. The C-20 peak of fresh preputial fluid in Figure 1 was contaminated with benzyl acetate. The I-39 peak appears to be an isomer of tetradecenyl acetate. It seems possible that diethyl phthalate (I-41), benzoic acid (C-37) and dibutyl phthalate (C-38) originated from the porous polymer used as the collection medium.

The first of the two major peaks in the incubated preputial fluid (C-21) was identified as *E*-β-farnesene, and the second (C-24) as *E*,*E*-α-farnesene. Although these sesquiterpenic compounds are also known to be elevated in the urine of dominant male mice [1], there are several reasons why it does not seem likely that they are necessary for female attraction. First, although these two compounds were found in incubated and fresh preputial fluid at almost the same concentration, fresh preputial fluid is not effective for female attraction [4]. Second, Jemiolo *et al.* [2] demonstrated that these compounds must be presented at 50 to 100 times higher in concentration than their natural level to attract virgin females. Such high concentrations should not be necessary for female attraction because sex attractant factors work at a natural low concentration. Third, we found these compounds also in female preputial (clitoral) glands (unpublished data). Although the experimental analysis is not yet completed, it seems that these sesquiterpenes may not be important for female attraction because they are found in both male and female preputial glands. These facts suggest that compounds other than *E*-β-farnesene and *E*,*E*-α-farnesene must play an important role in producing the female attractant factors of male preputial glands.

In some of the compounds in Group C, we found quantitative changes between incubated and fresh preputial fluids. For example, the concentration of hexadecyl acetate (C-36), which is reported as a major constituent in lipid extracts of preputail glands [7], was greatly increased after incubation. Other compounds including some aldehydes (heptanal, octanal, *E*-2-heptenal, etc), terpene (cymene, limonene, etc), alkyl acetates (amyl acetate, hexyl acetate, etc) are found only in incubated preputial fluid. The highest peak (I-7) in these compounds was identified as limonene. Limonene (I-7, I-8) has been identified as an alarm pheromone of termites [2], but the behavioral effects of limonene in mice have not been investigated.

The present study provides several possible ways that preputial factor may influence female attraction. First, the new compounds which are produced after incubation (Group I) might be effective. Second, the quantitative changes in volatile compounds during the process of incubation might be important. Moreover, the combination of the quantitative changes as those observed in C-28, C-35, C-36 and the aforementioned qualitative changes might be necessary for female attraction. We are presently comparing the volatile compounds of the urine of preputialectomized males with those of intact males to explore these possibilities.

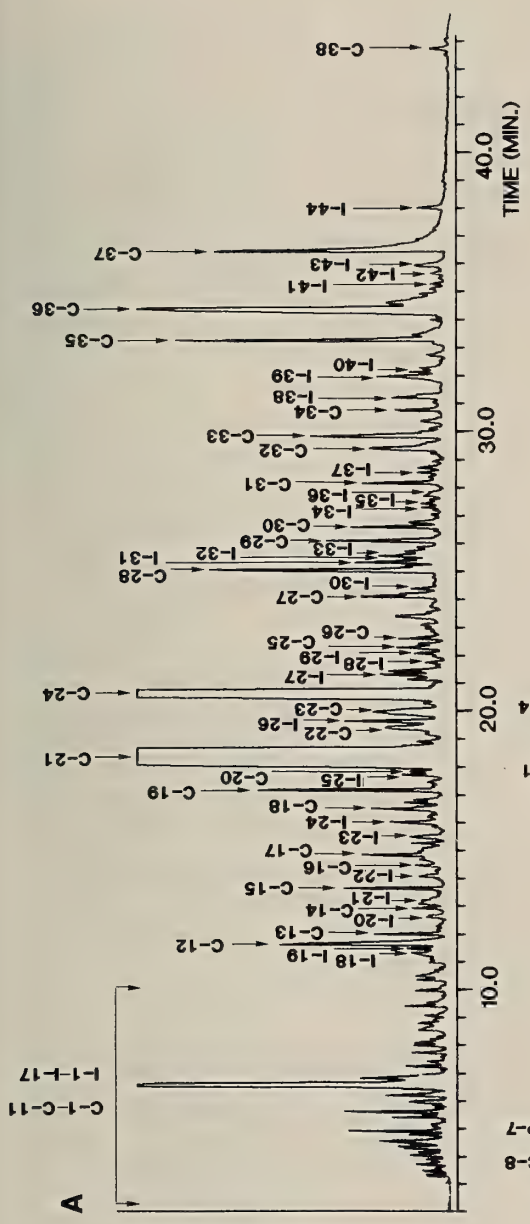

FIG. 1. Gas-chromatographic profiles of (A) preputial fluid from male mice following 2 days of incubation, and (B) fresh preputial fluid from male mice. The section between the arrows are enlarged in Fig. 2 and 3. Peak numbers refer to Table 1. For details see text.

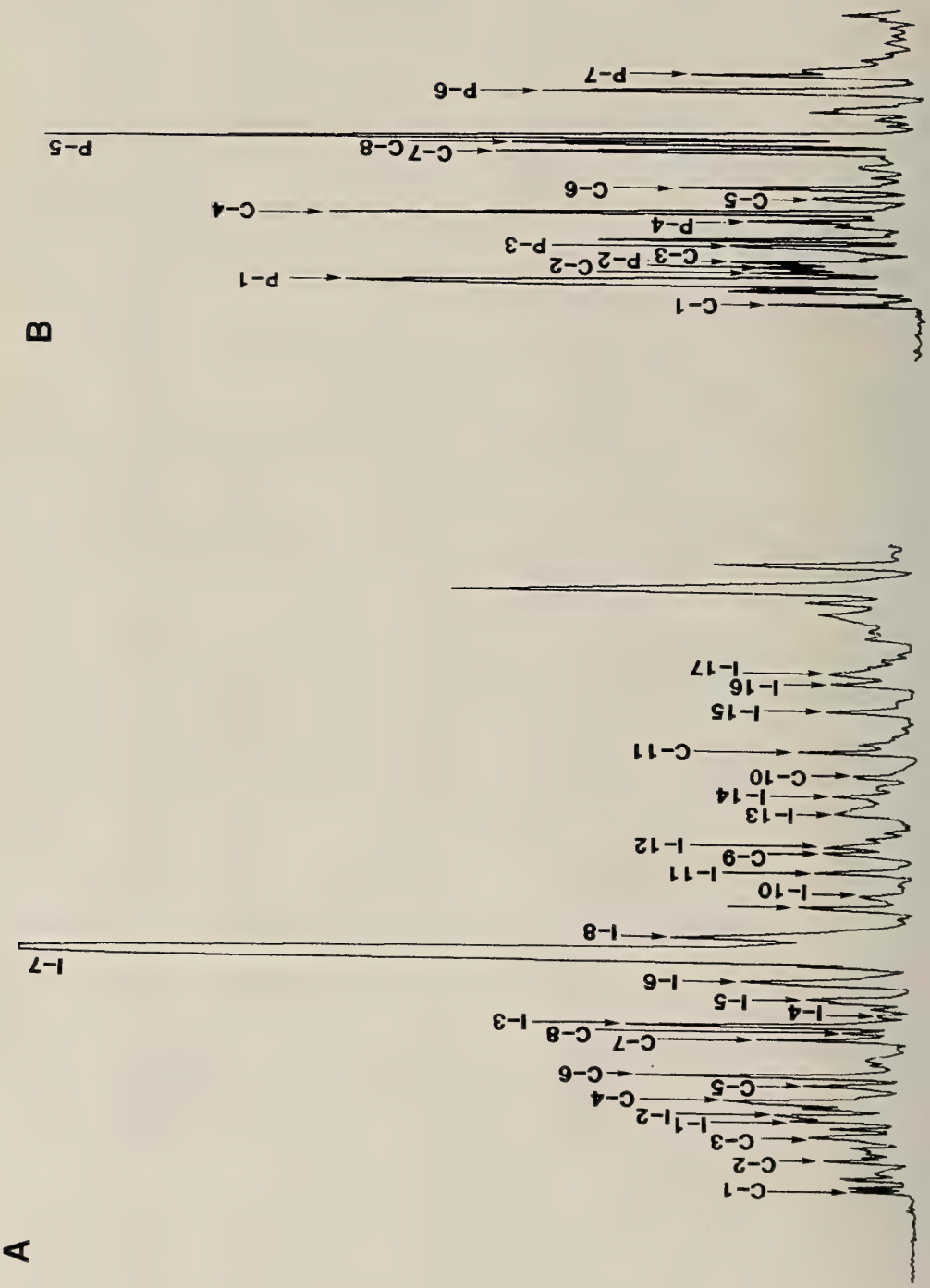

FIG. 2. Enlarged portion of (A) incubated preputial fluid in Figure 1.

FIG. 3. Enlarged portion of (B) fresh preputial fluid in Figure 1.

TABLE 1. Compounds found in both incubated and fresh preputial fluid (Group C), only in incubated preputial fluid (Group I) or only in fresh preputial fluid (Group P)

Group C Peak Compounds	Group I Peak Compounds	Group P Peak Compounds
C-1 octane	I-1 chroloform	P-1 methanol
C-2 nonane	I-2 decane	P-2 ethanol
C-3 *is*-pentanal	I-3 butanol	P-3 1-buten-3-one + benzene
C-4 toluene	I-4 myrcene	P-4 propanol + 2-methyl-3-buten-2-ol
C-5 *is*-butylacetate	I-5 amyl acetate	P-5 3-xylene
C-6 hexanal	I-6 heptanal	P-6 2-xylene
C-7 4-xylene	I-7 limonene	P-7 3-methyl-2-buten-2-ol
C-8 ethylbenzene	I-8 limonene	P-8 4-cymene
C-9 octan-2-one	I-9 amyl alcohol	P-9 *Z*-3-hexenyl acetate
C-10 6-methyl-5-hepten-2-one	I-10 styrene	P-10 1,4-dichlorobenzene
C-11 hexanol	I-11 hexyl acetate	P-11 valeric acid
C-12 acetic acid	I-12 octanal	P-12 geraniol
C-13 heptanol + furfural	I-13 tridecane	P-13 ethyl laurate
C-14 2-ethylhexanol	I-14 *E*-2-heptanal	P-14 β-ionone
C-15 benzaldehyde	I-15 heptyl acetate	P-15 diethyleneglycol
C-16 linalool + ?	I-16 nonan-2-one	P-16 nerolidyl formate
C-17 octanol	I-17 nonanal	
C-18 butan-1,4-olide	I-18 tetradecane	
C-19 acetophenone	I-19 4-*is*-propenyltoluene	
C-20 cyclohexyl *is*-thiocyanate	I-20 octyl acetate	
C-21 *E*-β-farnesene	I-21 2-decanone	
C-22 dodecanal	I-22 propionic acid	
C-23 *Z*,*E*-α-farnesene	I-23 nonyl acetate	
C-24 *E*,*E*-α-farnesene	I-24 2-undecanone	
C-25 tridecanal	I-25 nonanol	
C-26 caproic acid	I-26 carvone	
C-27 dodecyl acetate	I-27 pentan-1,5-olide	
C-28 tetradecanal	I-28 *E*,*E*-2,4-decadienal	
C-29 dodecanol	2I-9 2-tridecanone	
C-30 phenol	I-30 octan-1,4-olide	
C-31 capryic acid	I-31 benzothiazole	
C-32 tetradecyl acetate	I-32 enathic acid	
C-33 tetradecenyl acetate	I-33 10-undecanol	
C-34 nonanoic acid	I-34 nonan-1,4-olide	
C-35 capric acid	I-35 cinnamaldehyde	
C-36 hexadecyl acetate	I-36 pentadecanal	
C-37 benzoic acid	I-37 4-cresol	
C-38 dibutyl phthalate	I-38 tetradecanol	
	I-39 tetradecenyl acetate?	
	I-40 decanoic acid	
	I-41 diethyl phthalate	
	I-42 undecanoic acid	
	I-43 hexadecanol	
	I-44 lauric acid	

ACKNOWLEDGMENTS

We wish to thank Dr. Richard E. Brown and Ms. Heather Schellinck, Dalhousie University, for their helpful comments on the manuscript. KN is the recipient of a JSPS Research Fellowship. This study was partly supported by Grants-in Aid (Nos. 63540597 and 02640579) from the Japan Ministry of Education, Science and Culture.

REFERENCES

1 Harvey S, Jemiolo B, Novotny M (1989) J Chem Ecol 15: 2061–2072

2 Jemiolo B, Xie TM, Novotny M (1991) Physiol Behav 50: 1119–1122

3 Lindström M, Norin T, Valterová I, Vrkoc J (1990) Naturwissenshaften 77: 134–135

4 Ninomiya K, Kimura T (1988) Physiol Behav 44: 791–795

5 Ninomiya K, Kimura T (1990) Naturwissenschaften 77: 586–588

6 Novotny M, Harvey S, Jemiolo B (1990) Experientia 46: 109–113

7 Spener F, Mangold HK, Sansone G, Hamilton JG (1969) Biochim Biophys Acta 192: 516–521

ZOOLOGICAL SCIENCE 10: 543–546 (1993)

[RAPID COMMUNICATION]

Neural Control of Muscle Differentiation in the Leg of the Fleshfly *Sarcophaga bullata*

Pakkirisamy Sivasubramanian

Department of Biology, University of New Brunswick, Fredericton, Canada E3B 6E1

ABSTRACT—The tubular leg muscles of an adult fly differentiate from embryonic adepithelial cells present within the leg imaginal discs. Transection of the disc stalk from the ventral ganglion in a prepupa results in the formation of an externally normal looking leg that lacks locomotor muscles. The absence of motor axons in the nerve of in the experimental leg is suggestive of the importance of motor innervation in the development of leg muscles.

INTRODUCTION

Several studies using both *in vitro* and *in vivo* procedures have demonstrated the importance of innervation in the differentiation of vertebrate muscles [3, 6, 9, 14, 15, 19]. Among invertebrates insects have received special attention in this regard. The influences of nerves on insect muscle differentiation was first demonstrated by Kopec [8]. When he removed thoracic ganglia from gypsy moth caterpillars the resulting adults were devoid of thoracic muscles. Similar results were also obtained for silkmoths [11, 21]. By a more refined procedure Sivasubramanian and Nässel [18] recently demonstrated the role of mesothoracic larval nerve in the differentiation of thoracic flight muscles in the fly, *Sarcophaga bullata*. Although these studies did indicate the importance of innervation for the differentiation of flight muscles, additional information can be obtained from examining leg muscle differentiation in holometabolous insects such as flies which arise *de novo* from bags of embryonic cells called imaginal discs [4, 13, 20]. This is in contrast to the thoracic flight muscles that differentiate using the histolysing larval muscles as templates [5]. Further, the imaginal discs are attached to the larval ventral ganglion by means of stalks which also contain nerves that apparently act as guides for the growing adult axons between the legs and the ventral ganglion [1]. In larger species of flies these disc stalks along with their guiding pioneer axons can be surgically severed. The present study examines the legs developed from stalk transected imaginal discs of the fleshfly, *Sarcophaga bullata*. The results strongly suggest the importance of motor innervation for leg muscle differentiation.

Accepted April 12, 1993
Received February 4, 1993

MATERIALS AND METHODS

The fleshfly *Sarcophaga bullata* was reared in the laboratory under constant conditions of temperature (25°C) and photoperiod (16L:8D). Adults were fed with ample supply of sugar and water. Larvae were raised in fresh beef liver. Post-feeding, mature third instar larvae were collected from culture containers and used for experiments. All operations were performed on freshly formed prepupae (1–2 hr post pupariation). Mesothoracic legs lacking motor innervation were produced according to the method of Sivasubramanian and Nässel [17]. Since the stalk of the leg disc contains axons that presumably act as pioneers to guide the adult nerves disconnecting the stalk deprives the growing motor neurons from finding their targets. A "V" shaped incision was made on the anterior

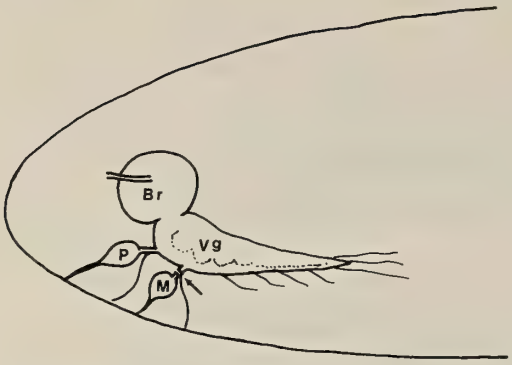

FIG. 1. Schematic diagram showing the lateral view of the larval brain (Br) and ventral ganglion (Vg). M and P are, respectively, mesothoracic and prothoracic leg imaginal discs. The arrow depicts the location of stalk transection.

ventral side (on segments 5 and 6, i.e., 2nd and 3rd segments after anterior spiracles) of freshly formed prepupa. The triangular flap was lifted up and the exposed stalk of left mesothoracic leg disc was transected. The site of transection is shown in Figure 1. The flap was left back on the slit and the dried hemolymph closed twe wound. The operated specimens kept in humid chambers at 25°C. metamorphosed into normal looking flies in 12 days.

Twenty experimental (left mesothoracic) legs were examined histologically and compared with normal, right mesothoracic legs. The femurs of the legs were embedded in epon and 2 μm thick plastic sections were stained with toluidine blue.

RESULTS AND DISCUSSION

Morphologically, the legs developed from stalk transected imaginal discs appear quite normal like the control legs (Fig. 2A and C) with full complement of segments, bristles etc. However, these experimental legs exhibit very little movement. The flies simply drag these legs while walking. Examination of histological sections reveal the reason for the absence of motor function in these legs. A cross section of the femur of a normal (right) mesothoracic leg is shown in Figure 2B. It is filled with tibial levator and depressor muscles. Compared to this the experimental leg is devoid of both sets of these muscles (Fig. 2D). There is a nerve bundle in the operated leg (Fig. 2D, arrow). Our previous study of horseradish peroxidase fillings of such stalk transected legs [17] as well as the absence of any movement in these legs suggest that this nerve is probably composed mostly sensory axons. However, these histological and behavioral observations cannot rule out the presence of few, albeit, nonfunctional motor axons in the nerve bundle.

Within the imaginal discs there are irregular shaped adepithelial cells which are the progenitors of adult leg muscles [13]. During metamorphosis, these cells organize themselves into columns, become multinucleate and eventually differentiate into the tubular muscles of the leg [16]. Are these adepithelial cells dependent on motor innervation for their differentiation?

The results of earlier studies were ambiguous about the role of innervation on leg muscle differentiation. When *Drosophila* mesothoracic leg discs were cultured *in vivo* muscle specific enzymes were expressed in the transplanted leg discs [20]. However, when the discs were cultured *in vitro* muscles failed to differentiate in the otherwise morphologically normal looking legs [9]. The present study used a different approach to examine the same problem. Here an *in situ* leg disc was deprived of motor innervation by transecting the disc stalk prior to metamorphosis [17]. When the stalk was selectively severed leaving the disc's attachment with the epidermis an externally normal looking leg developed. It is quite conceivable that the absence of muscle in the stalk transected legs is due to the lack of motor axons in the nerves of these legs.

Myogenesis is dependent on motor innervation in chick embryos [3]. Destruction of motor neurons by bungarotoxin inhibits myotube formation in rat skeletal muscles [6]. Presumably, the motor neuron terminals have some trophic or inductive influence on myogenic cells [15]. In grasshopper embryos motor neurons contact muscle pioneers very early in development [2] and perhaps this contact influences them from the very beginning. Precisely what stage of leg muscle differentiation in flies is controlled by motor innervation is not clear at the moment. However, preliminary screening of histological preparations

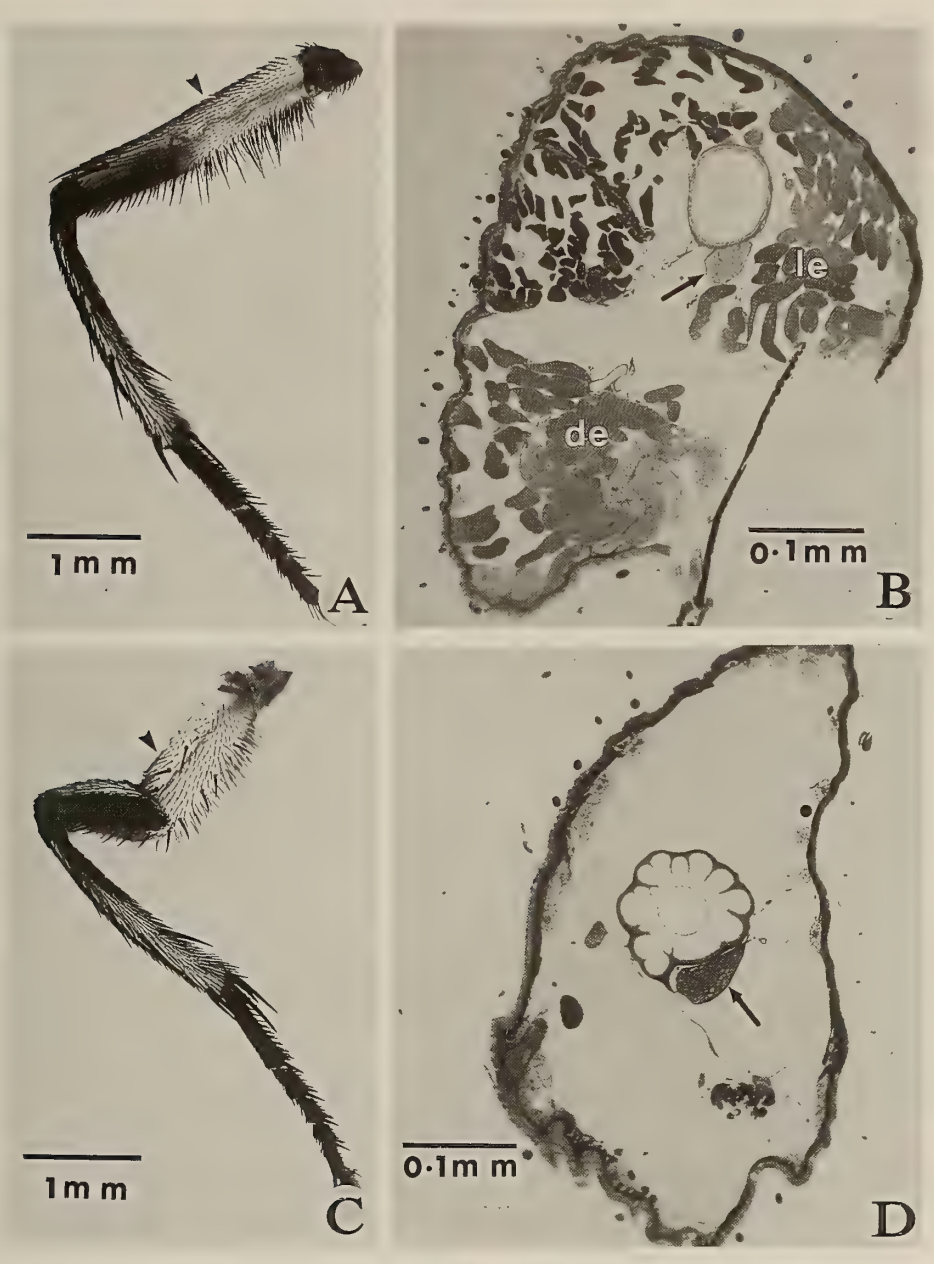

FIG. 2. Control (A) and stalk transected (C) legs indicating the approximate site of cross section (arrow heads). B. Cross section of a normal leg with levator (le) and depressor (de) muscles. D. Cross section of a stalk transected leg. Note the leg is completely devoid of muscles. Both legs have a leg nerve (arrow).

of developing stalk transected legs indicates that the proliferation of adepithelial cells (myoblast precursors) is unaffected implying the post mitotic events of myogenesis to be highly dependent on motor innervation.

ACKNOWLEDGMENTS

This research was supported by a grant from the Natural Sciences and Engineering Research Council of Canada.

REFERENCES

1 Auerbach C (1936) Trans Roy Soc Edin 58: 787–815

2 Ball EE, Ho RK, Goodman CS (1985) J Neurosci 5: 1808–1819

3 Bonner PH, Adams TR (1982) Develop Biol 90: 174–184

4 Crossley AC (1978) In "The Genetics and Biology of *Drosophila* Vol 2b" Ed by M Ashburner, TRF Wright, Academic Press, pp 499–560

5 Fernandes J, Bate M, Vijayraghavan K (1991) Development 113: 67–77

6 Harris AJ (1981) Phil Trans Roy Soc Lond Ser B. 293: 257–277

7 Jan YN, Ghysen A, Christoph I, Barbel S, Jan LY (1985) J Neurosci 5: 2453–2464

8 Kopec C (1923) J Exp Zool 37: 15–25

9 Mandaron P (1970) Develop Biol 22: 298–320

10 McLennan IS (1983) Develop Biol 98: 287–294

11 Nässel DR (1983) In "Functional Neuroanatomy" Ed by NJ Strausefeld, Springer Verlag, pp 44–91

12 Nüesch H (1985) In "Comprehensive Insect Physiology, Biochemistry and Pharmacology Vol 2" Ed by G Kerkut, LI Gibert, Pergamon Press, pp 425–452

13 Poodry CA, Schneiderman HA (1970) Roux's Arch Dev Biol 166: 1–44

14 Popiela H (1978) Exp Neurol 62: 404–416

15 Popiela H, Ellis S (1981) Develop Biol 83: 266–277

16 Reed CT, Murphy C, Fristrom D (1975) Roux's Arch Dev Biol 178: 285–302

17 Sivasubramanian P, Nässel DR (1989) Develop Growth Diff 31: 341–349

18 Sivasubramanian P, Nässel DR (1990) Zool Sci 7: 223–228

19 Sohal GS, Holt RK (1980) Cell Tiss Res 210: 383–393

20 Ursprung HM, Conscience-Egli M, Fox DJ, Wallimann T (1972) Proc Nat Acad Sci USA 69: 2812–2813

21 Williams CM, Schneiderman HA (1952) Anat Rec 113: 560–561

Development
Growth & Differentiation

Published Bimonthly by the Japanese Society of Developmental Biologists
Distributed by Business Center for Academic Societies Japan, Academic Press, Inc.

Papers in Vol. 35, No. 3. (June 1993)

Development, Growth and Differentiation (ISSN 0012–1592) is published bimonthly by The Japanese Society of Developmental Biologists. Annual subscription for Vol. 35 1993 U. S. $ 191,00, U. S. and Canada; U. S. $ 211,00, all other countries except Japan. All prices include postage, handling and air speed delivery except Japan. Second class postage paid at Jamaica, N.Y. 11431, U. S. A.

Outside Japan: Send subscription orders and notices of change of address to Academic Press, Inc., Journal Subscription Fulfillment Department, 6277, Sea Harbor Drive, Orlando, FL 32887–4900, U. S. A. Send notices of change of address at least 6–8 weeks in advance. Please include both old and new addresses. U. S. A. POSTMASTER: Send changes of address to *Development, Growth and Differentiation,* Academic Press. Inc., Journal Subscription Fulfillment Department, 6277, Sea Harbor Drive, Orlando, FL 32887–4900, U. S. A.

In Japan: Send nonmember subscription orders and notices of change of address to Business Center for Academic Societies Japan, 16–9, Honkomagome 5-chome, Bunkyo-ku, Tokyo 113, Japan. Send inquiries about membership to Business Center for Academic Societies Japan, 16–9, Honkomagome 5-chome, Bunkyo-ku, Tokyo 113, Japan.

Air freight and mailing in the U. S. A. by Publications Expediting, Inc., 200 Meacham Avenue, Elmont, NY 11003, U. S. A.

The Ultimate Name in Micromanipulation
Ease of operation, and the most advanced

Can be combined with
New WR & MX series

Model MX-1
3-D Micromanipulator

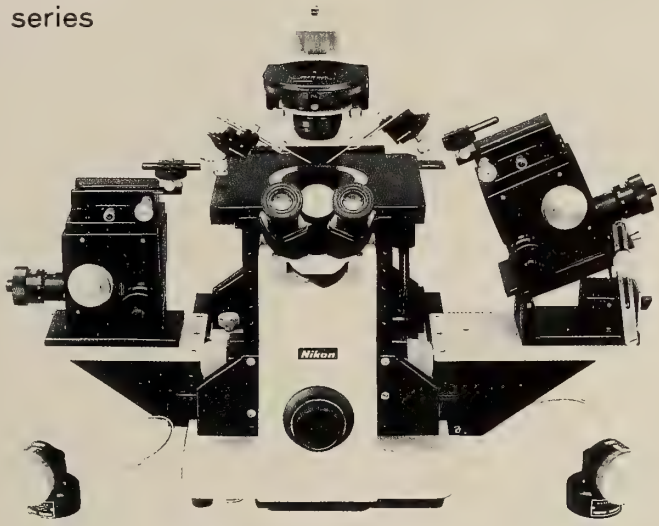

Model MX-2
3-D Micromanipulator

Model WR-87
One Dimensional
Aqua Purificate
Micromanipulator

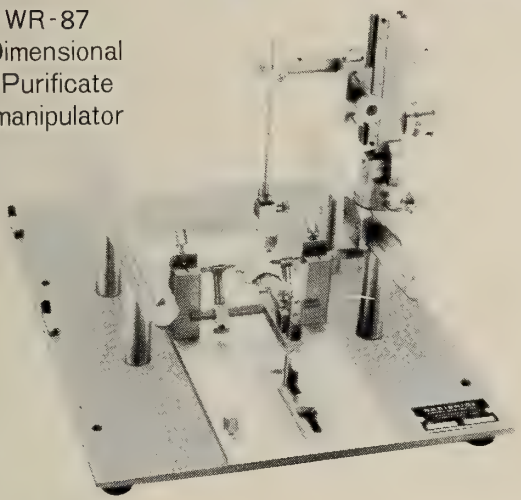

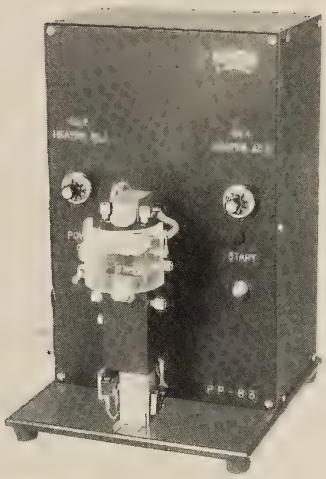

Model SR-6
Stereotaxic Instrument for Rat

Model PP-83
Glass Microelectrode Puller

* * * Send enquiries for request for MODIFICATIONS or IMPROVEMENTS * * *
Physiological, Pharmacological, Zoological & Neurosciences Research Equipments

---

NARISHIGE JAPAN

NARISHIGE SCIENTIFIC INSTRUMENT LAB.

9-28 KASUYA 4-CHOME SETAGAYA-KU, TOKYO 157, JAPAN
PHONE(INT-L)81-3-3308-8233, FAX(INT-L)81-3-3308-2005
CABLE:NARISHIGE LABO, TELEX, NARISHIGE J27781

(*Contents continued from back cover*)

Enviromental Biology

Systematics and Taxonomy

ZOOLOGICAL SCIENCE

VOLUME 10 NUMBER 3 JUNE 1993

CONTENTS

(*Contents continued on inside back cover*)

INDEXED IN:
Current Contents/LS and AB & ES,
Science Citation Index,
ISI Online Database,
CABS Database, INFOBIB

Issued on June 15
Printed by Daigaku Letterpress Co., Ltd.,
Hiroshima, Japan